scnat
akademie der naturwissenschaften
académie des sciences naturelles
swiss academy of sciences
accademia di scienze naturali

Abstract Volume
21st Swiss Geoscience Meeting

17–18 November 2023 · Mendrisio

Scuola universitaria professionale
della Svizzera italiana
SUPSI

ABOUT THIS PUBLICATION

PUBLISHER AND CONTACT
Swiss Academy of Sciences (SCNAT) • Platform Geosciences
House of Academies • Laupenstrasse 7 • P.O. Box • 3001 Bern • Switzerland
+41 31 306 93 25 • info@geosciences.scnat.ch • geo.scnat.ch

ORGANISATION SGM 2023
Institute of Earth Sciences of the University of Applied Sciences and Arts of Southern Switzerland (SUPSI)

PATRONNAGE
Swiss Academy of Sciences (SCNAT) • Platform Geosciences

LOCAL ORGANISING COMMITTEE
Camilla Capelli, IST-SUPSI – aquatic ecology (Co-president)
Filippo Schenker, IST-SUPSI – geology (Co-President)
Christian Ambrosi, IST-SUPSI – institute director
Rodolfo Perego, IST-SUPSI – hydrogeology
Maurizio Pozzoni, IST-SUPSI – hydrology
Annalisa Rollandi, IST-SUPSI – urban planning
Ilaria Sandrini, IST-SUPSI administration
Cristian Scapozza, Competence centre climate change and territory-SUPSI
Nicola Storelli, IST-SUPSI – microbial ecology
Daniele Strigaro, IST-SUPSI – geomatics
Daniele Albisetti, Fondazione Monte San Giorgio
Marco Antognini – Museo cantonale di storia naturale

COORDINATION
Pierre Dèzes, SCNAT
Caroline Reymond, SCNAT

PARTICIPATING SOCIETIES AND ORGANISATIONS
Commission for the Swiss Journal of Paleontology
Commission on Atmospheric Chemistry and Physics
Swiss Association for Geography ASG
Swiss Association of Geologists CHGEOL
Swiss Commission for Phenology and Seasonality CPS
Swiss Commission on Remote Sensing
Swiss Committee for Stratigraphy SKS/CSS
Swiss Geocomputing Centre
Swiss Geodetic Commission
Swiss Geological Society
Swiss Geological Survey swisstopo
Swiss Geomorphological Society SGmS
Swiss Hydrogeological Society SGH
Swiss Hydrological Commission CHy
Swiss Paleontological Society SPG/SPS
Swiss Snow Ice and Permafrost Society
Swiss Society for Hydrology and Limnology SGHL
Swiss Society for Quaternary Research CH-QUAT
Swiss Society of Mineralogy and Petrology
Swiss Soil Science Society
Swiss Tectonics Studies Group

COVER PHOTO
Fieldwork for permafrost measurements with the Adula peak in the background. Credits: SUPSI

21st
swiss
geoscience
meeting
2023 Mendrisio

Table of contents

01 Structural Geology, Tectonics and Geodynamics

Sandra Borderie, Paul Tackley, Vénice Akker

Swiss Tectonics Studies Group of the Swiss Geological Society

TALKS:

1.16 Rime V., Foubert A., Gebru E., Kidane T.: The formation of a magma-rich margin: structure and kinematics of the Danakil Depression, Afar, Ethiopia

1.17 Sonmez S.U., Moritz R., Keskin S., Turlin F., Ulianov A., Chiaradia M., Aydin U.: Investigating Oligocene Magmatic Evolution in the Artvin District, Easternmost Eastern Pontides: Insights from the Yanıklı Prospect

1.18 Tokle L., Hirth G., Behr W.M.: Characterization of disGBS in quartz through load-stepping experiments

1.19 Toussaint G., Gunatilake T., Miller S.A., Valley B.: Aftershock sequences in Greece studied by non-linear high pressure fluid diffusion models

1.20 Truttmann S., Diehl T., Herwegh M.: Hypocenter-Based 3D Imaging of Active Faults: Unravelling Seismogenic Faults at Depth

1.21 Zambrano M., Mazzoli S., Mosar J.: Styles of deformation at the eastern termination of the Jura fold and thrust belt: new insights from 3D seismic interpretation

1.22 Zhan W., Nevskaya N., Niemeijer A., Berger A., Spiers C., Herwegh M.: Experimental Brittle-Viscous Transition of Granitoid Gouges by Mixed Dissolution Precipitation Creep and Frictional Granular Flow

1.23 Zwaan F., Brune S., Glerum A., Vasey D.A., Naliboff J., Manatschal G., Gaucher E.C.: Natural H2 potential in rift-inversion orogens

POSTERS:

P 1.1 Akker I.V., Behr W.M., Morales F.G., Braden Z., Rast M., Hinshaw E., Helper M.: Deformation styles and timing of underplating sediment sequences in the Chugach accretionary prism, southern Alaska

P 1.2 Amrein A., Nibourel L., Galfetti T., Heuberger S.: Rapid extraction of 3D orientation and stratigraphic thickness for a mineral occurrence map

P 1.3 Arrigoni F., Pigazzi E., Colzada G., Marinoni A., Tantardini D., Toffolon G., Apuani T., Tartarotti P.: The geology of Valchiavenna in the frame of the Central Alps: recent insights from the CARG project Sheets 038 “Chiavenna”, 021 “Passo dello Spluga”, 022 “Madesimo” and 037 “Bodengo”

P 1.4 Balazs A., Oravecz E., Gerya T.: Long-term surface processes and tectonics interactions: insights from numerical modelling

P 1.5 Basilici M., Borderie S., Marro A., Nussbaum C., Mosar J.: High-Resolution Tectonic Map of the southwestern sector of the Delémont Basin area, Jura Fold-and-Thrust Belt (Switzerland)

P 1.6 Behnen K., Hertrich M., Maurer H., Giardini D.: Investigating S-wave anisotropy in the Rotondo granite by crosshole seismic surveys

P 1.7 Borderie S., Mosar J., Marro A., Basilici M., Clerc N., Meyer M.: Sensitivity analysis of stress field in the Geneva Basin and adjacent Jura fold-and-thrust belt

P 1.8 Candioti L.G., Schmalholz S.M., Duretz T.: Controls on exhumation velocities for an Alpine-type burial-exhumation cycle: a combined deterministic and statistical analysis

P 1.9 Cardello G.L., Bernasconi S.M., Fellin M.G., Rahn M., Rosskopf R., Mancktelow N.S.: Deciphering carbonate deformation through the Brittle-Ductile Transition: new methodological and regional insights from the SW Helvetic nappes, Switzerland

P 1.10 Chatelain Y., Ruch J., Panza E.: Structural analysis of a highly oblique rift zone influenced by a transform fault in southwest Iceland

P 1.11 Diehl T., Heidbach O., Heilig J., Schönball M., Giger S., Reinecker J., Schnellmann M., Wiemer S.: Stress Orientations in northern Switzerland: New Insights from Focal Mechanisms and Borehole Data

P 1.12 Gray T., Gerya T., Tackley P.: Tracking surfaces in global scale geodynamic models

P 1.13 Halter W.R., Kulakov R., Duretz T., Schmalholz S.M.: Viscous strain localization by multi-scale anisotropy development: Numerical modelling and upscaling

P 1.14 Heilig J., Diehl T., Herwegh M., Truttmann S., Wiemer S.: Revisiting the Stress Field of Switzerland with Focus on the South-Western Alps: Insights from an updated Focal-Mechanism Catalog

P 1.15 Hetényi G., Baron L., Scarponi M., Subedi S., Michailos K., Dal F., Gerle A., Petri B., Zwahlen J., Langone A., Greenwood A., Ziberna L., Pistone M., Zanetti A., Müntener O.: Would you like to (help) constrain the subsurface structure of the Balmuccia peridotite body?

P 1.16 Hinshaw E., Behr W., Zappone A., Ceccato A., Tewksbury-Christle C.: Geological constraints on the seismic anisotropy of Rotondo granite within the Bedretto Tunnel

P 1.17 Hufford L.J., Tokle L., Behr W.M., Morales L.F.G., Madonna C.: Constraining the mechanical properties of glaucophane deformed via dislocation-controlled mechanism(s) with experiments in the general shear geometry

P 1.18 Lanza F., Diehl T., Eberhart-Phillips D., Herwegh M., Fäh D., Wiemer S.: Tomography of P- and S-wave attenuation of Switzerland and surrounding regions: imaging seismotectonic processes in the Central Alps

P 1.19 Lemke K., Hetényi G.: Thermal properties of the lower continental crust of high-grade metamorphic rocks from the Ivrea-Verbano Zone (project DIVE)

P 1.20 Maino M., Corvo S., Schenker F. L., Perozzo M., Seno S., Langone L.: Deformation-induced changes in the metamorphic record along rheologically contrasted boundaries: inferences from Cima di Gagnone (Cima Lunga unit, Central Alps)

P 1.21 Marro A., Borderie S., Mosar J.: Kinematic study of inherited normal faulting in the internal Jura fold-and-thrust belt.

P 1.22 Moccetti Bardi N.: Numerical Investigation of Ocean-World Mantle Dynamics under a Low-Efficiency Eruption Limit

P 1.23 Neuenschwander T., Truttmann S., Schwichtenberg B., Herwegh M.: The Téné Fault: Architecture of a Seismogenic Carbonate Fault System

P 1.24 Pigazzi E., Morandi S., Tagliaferri A., Arrigoni F., Schenker F.L., Tartarotti P.: An analysis of the peak-temperature recorded by the meta-sedimentary covers of the Central Alps using Raman spectroscopy

P 1.25 Rahn M.: The thermal and exhumation history of northern Switzerland from Variscan to present

P 1.26 Ritter S., Balázs A., Gerya T.: The Influence of Strain-Rate Weakening on Strain Localization during Transform Fault Evolution

P 1.27 Oestreicher N., Ruch J., Serrano N., Luo X., Saemundsson T., Helgason J.K., Aaron J., Leva P., Maissen J., Manconi A., Derron M.H., Geirsson H., Mc Ginnis D., Panza E., Chatelain Y., Arlaud F., Hohl M.: Volcano deformation and landslide monitoring on an unresting caldera (Askja, central Iceland)

P 1.28 Serrano N., Ostreicher N., Derron M., Ruch J.: Landslide and structural analysis of an unresting volcano using drone imagery and field observations at Askja caldera (Central Iceland).

P 1.29 Tokle L., Schmalholz S.M., Ruh J.: Grain size evolution in necking calcite layers: The role of energy fraction stored in the microstructure

P 1.30 van Agtmaal L., Balàzs A., Gerya T.: 4D metamorphic evolution of collisional orogens from the Alps to the Himalayas: insights from numerical modelling

P 1.31 Zhou X., Coltice N., Tackley P.: Developing the global network of plate boundaries in 3D mantle convection models

1.1
Fault damage zones in oceanic crust revealed: **An extent and permeability assessment**

Alannah C. Brett[1], Larryn W. Diamond[1]

[1] *Institute of Geological Sciences, University of Bern, Baltzerstrasse 3, CH-3012 Bern (alannah.brett@geo.unibe.ch)*

The distribution of permeability in the upper oceanic crust controls heat and chemical flux between the crust and the oceans. The most spectacular manifestations of this flux are hydrothermal vents on the seafloor. Previous work has shown that such vents are located along seafloor faults, which are typically flanked by broad damage zones made up of fracture networks. Numerical thermal–hydraulic simulations are often used to assess the character and magnitude of the large-scale chemical fluxes, but obtaining realistic input values of the permeability of faults and their damage zones has proved to be difficult in studies of the modern seafloor. In the upper crust of the Oman ophiolite we have found well preserved damage zones in which the fracture fillings prove that they formed during subseafloor hydrothermal activity. In order to estimate the extent and permeability of these zones, we have mapped the fracture networks at various scales in outcrop. Based on statistical characterisation of our measured fracture apertures, lengths and attitudes, we used *DfnWorks* software to numerically generate discrete fracture networks and upscale them to represent the ~150 m wide damage zones. We then determined the permeability of the damage zones by performing hydraulic simulations of the upscaled fracture networks using *PFLOTRAN*. Our field-based simulations confirm and constrain the expected high permeability of fault-damage zones and provide quantitative estimates suitable for input into coupled thermal–hydraulic–chemical models.

1.2
High-pressure metamorphism in the Adula Nappe during the Alpine Orogeny: A Comparative Study with Cima Lunga Unit

Djordje Grujic[1], Svieda Ma[1], Luiz F. G. Morales[2,3], Mattew A. Coble[4]

[1] Department of Earth and Environmental Sciences, Dalhousie University, Halifax, Canada (dgrujic@dal.ca)
[2] Structural Geology and Tectonics Group, Department of Earth Sciences, Geological Institute, ETH Zürich, Zürich, Switzerland
[3] Scientific Center for Optical and Electron Microscopy (ScopeM), ETH Zürich, Zürich, Switzerland
[4] Department of Geological and Environmental Sciences, Stanford University, Stanford, USA

The mafic-ultramafic rocks within the Adula Nappe and its western extensions—the Alpe Arami and Cima Lunga units (collectively referred to as Cima Lunga)—retain the sole regional record of high- to ultrahigh-pressure metamorphism (~13-35 kbar) in the Central Alps. These rocks are enveloped by felsic gneissic country rocks that exhibit peak-pressure conditions up to 25 kbar lower. Traditionally, the Adula-Cima Lunga Nappe has been interpreted as a tectonic mélange composed of the European continental basement, Valais Ocean-derived metasediments and metavolcanics, as well as mantle-derived ultramafic rocks. The mechanics underlying the exhumation and emplacement of ultrahigh-pressure (UHP) rocks into lower-pressure units remain a subject of debate, as does the subduction of a large section of continental crust to mantle depths.

Our study explores the kinematics of (U)HP eclogite and the adjacent country rocks in the Cima Lunga unit through structural mapping and microstructural and textural analyses. Structural mapping has enabled a reinterpretation of the lower boundary of the Cima Lunga Nappe. Supported by structural, textural, and geochemical observations, we present the mafic-ultramafic (U)HP rocks as a separate lithological nappe rather than as lenses within a unified basement nappe.

We employed electron backscatter diffraction to analyse the lattice preferred orientation in omphacite, and other eclogite facies minerals, aiming to identify the deformation regime operative under (U)HP conditions. Our microstructural findings reveal scant evidence for simple shear; rather, the textural attributes of the eclogite rocks suggest a pure shear strain. Comparative analysis of our textural data with previously published studies on both the Cima Lunga and the main Adula Nappe reveals a persistent contrast in omphacite texture between these areas. In line with this, existing geochronological and thermobarometric data demonstrate that the main Adula Nappe has undergone two orogenic cycles of (U)HP subduction and exhumation, while Cima Lunga has experienced only one such cycle during the Alpine orogeny.

U-Pb and REE analyses of metamorphic zircon inclusions within garnets from Alpe Arami eclogite rocks yield U-Pb spot ages of approximately 40-30 Ma and consistently display typical eclogite facies REE patterns. Additionally, Ti-in-zircon temperatures from the same analytical spots appear to increase temporally. Zircons from two separate eclogite samples from Cima di Gagnone, processed using traditional methods, produced similar though more variable results. In contrast, zircons from granitoid gneisses both below and above the mafic and ultramafic layer show highly consistent rim ages, with mean and lower intercept ages centred around 31.6 Ma. Age depth-profiling on zircon prism faces yielded ages between 30-33 Ma on the outermost one μm.

Major and trace-element whole-rock analyses from the majority of the mafic eclogite samples from the Adula and Cima Lunga units suggest a MORB origin. Although samples from Cima Lunga and Alpe Arami units exhibit a high degree of similarity, they consistently differ from samples derived from the Adula Nappe, implying different geodynamic settings for the protoliths. In summary, divergences in structural position, age, and composition between the main Adula Nappe and the Cima Lunga unit lead us to propose that these tectonic units underwent distinct geodynamic histories.

1.3
Large-scale make-up of a deep subduction shear zone: observations from the Cycladic Blueschist Unit on Syros, Greece

Dominic Hildebrandt[1], Whitney M. Behr[1], Jesus Muñoz-Montecinos[1], Leif Tokle[1]

[1] *Structural Geology and Tectonics Group, Geological Institute, ETH Zurich, Sonneggstrasse 5, 8092 Zurich (dominic.hildebrandt@icloud.com)*

Geological and geophysical observations characterize deep subduction shear zones as heterogeneous and structurally complex fluid-rich environments. Slow Slip and Tremor (SST) are transient slip events with strain rates between regular earthquakes and plate convergence observed in such deep portions of modern subduction zones. Although studies suggest that stress and fluid transfers may link the deep SST zone with the up-dip megathrust as source region of hazardous regular earthquakes, the processes underlying SST are poorly understood. A major problem is that the large-scale anatomy of deep subduction shear zones with their multi-scale heterogeneities is not well characterized and therefore not available for assessing their rheological behavior. Here we report such data from the iconic HP-LT metamorphic rock record of the Cycladic Blueschist Unit exposed on Syros, Greece. Our study relies on field mapping, high-resolution drone surveys, 3D visualization and microscopic methods.

The Kampos Belt in the north of Syros is a ~ 3 km long and up to 1 km thick rock pile inferred to represent a fossil deep subduction interface formed at blueschist to eclogite facies conditions. In the west, it consists of meta-basic lenses in a matrix of meta-volcaniclastic schists, Tr-Chl schists and serpentinites. In the east, weak matrix rocks are sparse and more coherent metabasite bodies dominate. Substantial heterogeneity in terms of rock types, grain sizes, mineralogy and structures is inherited from the pre-subduction rifted passive margin setting. Five ductile thrust faults mapped along the eastern coastline and the repetition of an inherited rifted passive margin stratigraphy in the central and western part suggest that tectonic underplating is another major heterogeneity source leading to across-strike variations on scales of 10s to few 100s of m. Moderate tectonic dismemberment and metasomatism further modified these heterogeneities and their length scales. Along-strike rheological variability occurs on scales of 1 to 2 km and might be controlled by different slicing depths during underplating. Block-in-matrix associations in the western and central part are the major source of mechanical contrasts, as highlighted by dm-wide high-strain and metasomatic zones along block-to-matrix interfaces. Block sizes range from a few dm up to several 100s of m, with typical sizes between 1 and 5 m. Two clusters with elevated spatial block densities show along-strike lengths of ~ 600 m, consistent with calculated sizes of tremor-sourcing patches in modern subduction zones.

For the first time this study provides quantitative and qualitative geological constraints for multi-kilometer-scale heterogeneities of a fossil subduction complex. These data help to attribute observed seismic behaviors to fault characteristics and to refine and calibrate numerical simulations of SST.

1.4
Long-period noise in GPS displacement time series data, and its effect on uncertainty estimates of tectonic velocities

Roland Hohensinn[1,2] and Yehuda Bock[2]

[1] *International Space Science Institute (ISSI), Bern*
[2] *Scripps Institution of Oceanography; University of California, San Diego*

For almost three decades, thousands of GPS stations worldwide monitor ground motions at mm-level precision, giving unprecedent insights into geophysical phenomena observable on the solid Earth. Obtaining reliable trends from these data is crucial for monitoring long-term geophysical processes, such as plate tectonics, glacial isostatic adjustment, or sea level variations. To study the motion of the solid Earth, the functional models fitted to these data typically account for periodic motions, co-seismic and post-seismic displacements, and linear station velocities (trends). Other effects, such as non-tidal atmospheric, non-tidal oceanic and hydrological loading are either accounted for by geophysical forward models or are modeled as noise processes in the stochastic model, together with other random variations, such as GPS sensor noise.
In this contribution we present recent advances in the modeling of long-period (low-frequency) GPS noise, which has a main influence on the magnitude of trend uncertainties. Combination of different stochastic models, such as random-walk and/or flicker-noise processes, are crucial for deriving realistic uncertainties for trends observed from these data. On the example of GPS data from continental Europe and the Western U.S., we show that based on a proper choice of functional and stochastic time series models, trend uncertainties down to the level of few tenths of mm/year can be derived. To the end, we also strive the importance of detecting and modeling transients and artifacts (such as earthquakes or equipment changes), as they can strongly influence the derived station velocity as well as their uncertainties.

1.5
Impact of basement structures on thin-skinned tectonics in the Molasse Basin

Thomas Krayenbühl[1], Fiammetta Mondino[1], Yasin Makhloufi[1], Niels Giroud[2], Andrea Moscariello[3]

[1] *Geneva Earth Resources SA, Rue Jean Jaquet 10, 1201 Geneva (thomas.krayenbuhl@geneva-er.com)*
[2] *GEOOL SA, Place Chauderon 27, 1003 Lausanne*
[3] *Geo-Energy Group, Department of Earth Sciences, University of Geneva, Rue des Maraîchers 13, 1205 Geneva*

The Swiss Molasse Basin extends over the Swiss Plateau between the Jura Mountains and the Alps. The basin has been mapped carefully in context of the the Swiss GeoMol project (swisstopo) on the base of the available deep wells and legacy 2D seismic. The concept of the detachment of Mesozoic and Cenozoic sediments of the Molasse Basin and the Jura onto Triassic evaporites was proposed by Buxtorf in 1907 and 1916 (‘Fernschub or ‘distant-push’ hypothesis also known as thin skin mechanisms). This concept, which would be responsible of the formation of the informally so called ‘*Molasse Nappe*’ in the Swiss Plateau, is now widely accepted and observed in other foreland thrust belt settings across the world.

In the Jura and Swiss Plateau settings, a maximum displacement of ca. 30 km is commonly reconstructed and modeled. However, based on the review of recent publications, limited thoughts have been given to the impact of the basement top geometry on the internal structuration of the so called *‘Molasse Nappe*’.

In this paper, we propose a model of how deep seated structures, i.e. structures existing below the pre-Triassic evaporites sequences, may have affected the Mesozoic cover in the Molasse Basin as the nappe moved from its depositional realm to its present-day position. We suggest that the geometry of the detachment level at the base of the Keuper evaporite has led to fracturation of the Mesozoic and Cenozoic cover including some spectacular features such as the strike-slip fault of La Sarraz (Canton de Vaud). Recognizing the role of these features in the context a larger regional kinematic reconstruction, will have an impact on modeling fracture network in the context of the geothermal projects being developed over the Swiss Plateau. The principal difficulty in assessing our proposed model lays in the moderate quality of the currently available legacy 2D reflection seismic.

1.6
Topographic signatures and statistics of different tectonic regimes and application to terrestrial planets

Diogo L. Lourenço[1], Michael Manga[2], Paul J. Tackley[1]

[1] *Institute of Geophysics, Department of Earth Sciences, ETH Zürich, Switzerland (diogo.lourenco@erdw.ethz.ch)*
[2] *Department of Earth and Planetary Science, University of California Berkeley, Berkeley, CA, USA*

A tectonic regime is the surface expression of interior dynamics in a planet. With the help of numerical models, different tectonic regimes have been proposed. Some of these are: (1) plate tectonics or mobile lid, (2) stagnant lid, (3) episodic lid, (4) plutonic-squishy lid, (5) and heat pipe (e.g., Lourenço et al. 2020). Over time, a tectonic regime shapes the surface of a planet, including its surface topography. Using the numerical models, we can compute the topographies associated with different tectonic regimes including spatial and temporal measures of variations. In this study, we compute statistics for the topography formed by different tectonic regimes in numerical models and compare with the statistics of observed topography of different terrestrial planets, with the aim of linking a planet to a tectonic regime at the present-day. Venus' topography is better matched by topography distributions obtained for plutonic-squishy lid models than those for stagnant- or episodic-lid models, while Earth's oceanic topography is best matched by mobile-lid models.

REFERENCES

Lourenço, D. J., Rozel, A. B., Ballmer, M. D., & Tackley, P. J. 2020: Plutonic-squishy lid: A new global tectonic regime generated by intrusive magmatism on Earth-like planets. Geochemistry, Geophysics, Geosystems, 21, e2019GC008756. https://doi.org/10.1029/2019GC008756

1.7
Tracking magma pathways in the Southwest Rift Zone and the Koaʻe fault system (Kīlauea volcano) using photogrammetry and structural observations

Stefano Mannini[1], Joël Ruch[1], Richard W. Hazlett[2], Drew T. Downs[3], Carolyn E. Parcheta[4], Steven P. Lundblad[2], James L. Anderson[2], and Nicolas Oestreicher[1]

[1] *Department of Earth Sciences, University of Geneva, Rue des Maraîchers 13, 1205, Geneva, Switzerland*
[2] *Department of Geology, University of Hawaiʻi at Hilo, Hilo, HI 96720, USA*
[3] *U.S. Geological Survey, Hawaiian Volcano Observatory, Hilo, HI 96720, USA*
[4] *Alaska Earthquake Center, University of Alaska Fairbanks, Fairbanks, AK 99775, USA*

Normal faults, monoclines and graben structures are key surface features for tracking magma pathways beneath basaltic volcanoes. However, the relation between magma propagation and faulting at the surface is still not well understood. Kīlauea volcano is characterized by a summit caldera associated with two rift zones (East and Southwest Rift Zones) and has a south flank that is prone to recurrent instability. The Southwest Rift Zone (SWRZ) and the connecting Koaʻe fault system are major structures controlling magma propagation and the volcano flank instability. SWRZ has been affected by dozens of magmatic intrusions in the last few centuries. The connection between surface faulting and magma intrusion at depth is poorly studied, despite the faults' importance in controlling magma pathways and better forecasting the location of future eruption.

In March 2022, we completed five helicopter photogrammetric surveys in the south flank of the Kīlauea volcano, acquiring high-resolution images (~4–5 cm ground resolution). We generated a high-resolution DEM (~8 cm) and orthomosaic images (~4 cm). We also performed ground measurements, as strike and opening direction of extensional fractures and field observation to better understand the overall fault kinematics. Results of a detailed structural map combined with ground observation show in great details small interconnected grabens, monoclines, rollover structures and en-echelon fractures that were previously unnoticed. We infer that part of these structures are the surface expressions of past magma intrusions, with direct implications for understanding the location of future magma transports and eruptions. We further estimate the cumulative displacement across the Koae fault zone, during the last 600 years, corresponding to the age of the lava flows affected by normal faults. We found an average of 6 cm and 3 cm per year for vertical and horizontal, respectively. These measurements are consistent with GNSS data.

Finally, we propose a kinematic model constrained by structural data and morphotectonic features. It shows different magmatic pathways that are distributed in the SWRZ and very localized in the ERZ, suggesting that the SWRZ is moving too fast to the south due to the flank instability to become a mature system. Using fracture opening kinematics, we also suggest that the Koaʻe fault zone have been rotating clockwise and that it exists a direct structural connection between the Koaʻe fault zone and the ERZ, part of the Koae having been intruded by dikes during the 1970's. This suggests a complex reactivation of tectonic faults by dike intrusions when the stress field change due to the flank motion become favourable for magma intrusions.

1.8
The effects of intrusive magmatism and water on the tectonic regime of Venus

Marla Metternich[1,2], Paul J. Tackley[1], Diogo L. Lourenço[1], Cedric Thieulot[2]

[1] Institute of Geophysics, Department of Earth Sciences, ETH Zürich, Switzerland (m.a.metternich@gmail.com)
[2] Department of Earth Sciences, Faculty of Geosciences, Utrecht University, the Netherlands

Venus has many commonalities with Earth in terms of size, density and composition. Yet, the two sister planets have very different surface expressions and tectonics at present. Melting processes, composition, rheology, intrusive and extrusive magmatism are important factors and processes in the thermal evolution of a planet. Since water has a first order effect on the rheology and melting processes (Karato 2015), and Venus and Earth have likely been formed with similar water inventories (Raymond et al. 2006), it is key to take into account the potential effects of water while studying the thermal evolution and tectonic regime. This study aims to expand our understanding of the thermo-magmatic evolution and tectonic regime of Venus by considering intrusive magmatism, a “weak” plagioclase crustal rheology and water using the thermo-magmatic numerical convection code, StagYY (Tackley 2008). This study presents the first global geodynamical circulation models with water for Venus.

The dry models with a weak crustal rheology are generally characterised by global lithospheric overturns, regional overturns, basaltic drippings and continuously high surface mobility. Wet model results show that increasing outgas fractions cause local stiffening of the crust and lithosphere due to the depletion of water with time. A stronger effect of water on viscosity combined with outgassing also yields local stiffening. Given there is sufficient magmatism and outgassing, delamination of the stiffer crust is more efficient and global lithospheric overturns are replaced by more local delaminations and basaltic drippings (Fig.1). Towards the last billion years, a shift in tectonic regime towards a more subduction-like lid may occur due to sufficient cooling of the planet in combination with the more rigid lid upon water depletion. The subduction is often initiated by impingement of rising mantle plumes, a process suggested to happen around coronae on Venus, possibly even at present (Gerya 2014; Gülcher et al. 2020).

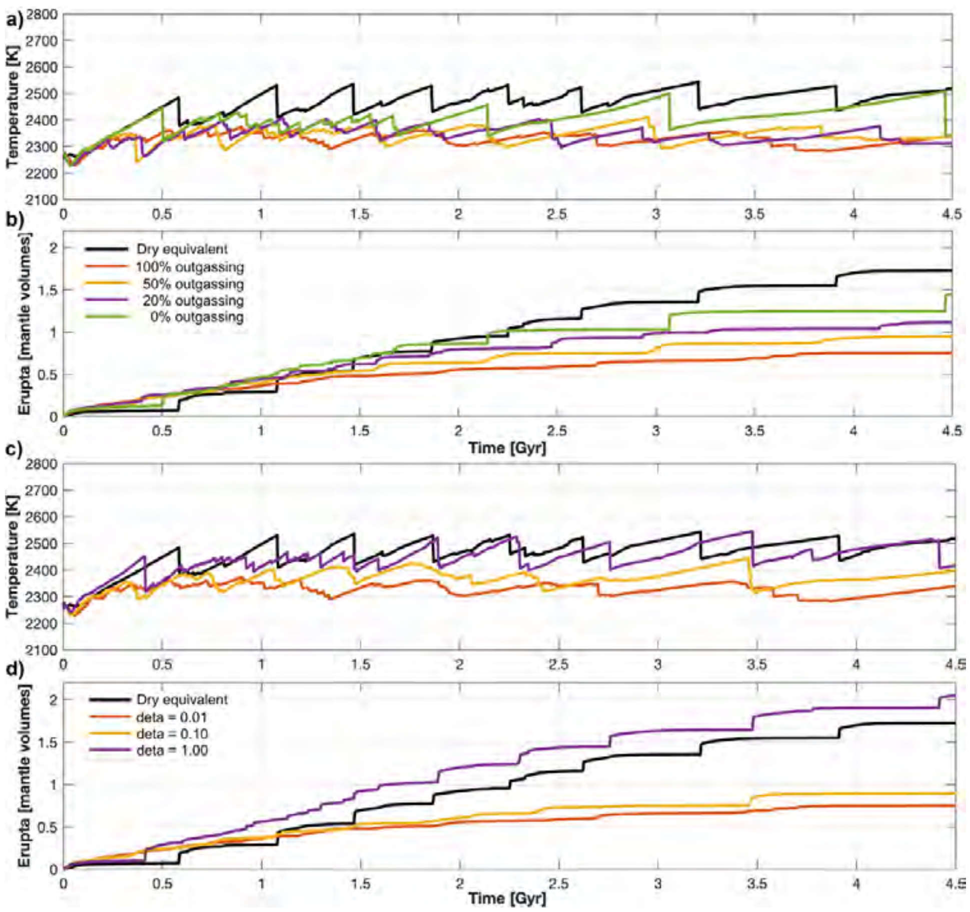

Fig.1: Globally averaged temperature (a,c) and erupted volumes (b,d) of models with varying outgas fraction (top two panels) and effect of water on viscosity (bottom two panels), in which a lower deta factor represents a stronger effect of water on viscosity.

REFERENCES

Gerya, T. 2014. Plume-induced crustal convection: 3D thermomechanical model and implications for the origin of novae and coronae on Venus. Earth and Planetary Science Letters, 391:183-192.

Gülcher, A. J., Gerya, T. V., Montési, L. G., and Munch, J. 2020. Corona structures driven by plume-lithosphere interactions and evidence for ongoing plume activity on Venus. Nature Geoscience, 13(8):547-554.

Karato, S. I. 2015. Water in the evolution of the Earth and other terrestrial planets. Treatise on Geophysics, 9, 105-144.

Raymond, S. N., Quinn, T., and Lunine, J. I. 2006. High-resolution simulations of the final assembly of Earth-like planets I. Terrestrial accretion and dynamics. Icarus, 183(2):265–282.

Tackley, P. J. 2008. Modelling compressible mantle convection with large viscosity contrasts in a threedimensional spherical shell using the yin-yang grid. Physics of the Earth and Planetary Interiors, 171(1-4):7–18.

1.9
Laboratory Observations linking Fault Surface Characteristics to Preparatory Earthquake Processes and Fault Stability

Sofia Michail[1], Paul Antony Selvadurai[1], Markus Rast[2], Antonio Felipe Salazar Vásquez[1,3], Patrick Bianchi[1], Sara Beth Cebry[4], Claudio Madonna[2], Stefan Wiemer[1]

[1] *Swiss Seismological Service, ETH Zurich, Sonnegstrasse 5, CH-8092 Zurich (sofia.michail@sed.ethz.ch)*
[2] *Structural Geology and Tectonics, Geological Institute, Department of Earth Sciences, ETH Zurich, Sonnegstrasse 5, CH-8092 Zurich*
[3] *School of Architecture, Civil Engineering, Landscape Architecture, Spatial Planning, Eastern Switzerland University of Applied Sciences, Oberseestrasse 10, CH-8640 Rapperswil*
[4] *School of Civil and Environmental Engineering, Cornell University, 220 Hollister Hall, USA-14853 Ithaka*

Preparatory earthquake processes, such as slow preparatory slip (preslip), exhibit complex relationships with spatial variations in frictional strength that are evident throughout the Earth›s crust. Our study investigates the role of fault surface characteristics such as roughness in initiating dynamic slip, which can introduce heterogeneity in slip. We performed a triaxial loading experiment at sequentially increasing confining pressure steps (Pc = 60, 80, 100 MPa) on a saw-cut sample of Carrara marble in dry and unlubricated conditions. We analyzed the quasi-static deformation associated with spatial and temporal frictional responses using fiber-optic Distributed Strain Sensing (DSS) for high spatial resolution monitoring of a) fault-parallel and b) axial strain. Simultaneous differential stress evolution was tracked to unravel the dynamics of frictional weakening and strengthening. In the first confining pressure step (Pc = 60 MPa), a single stick-slip event was observed with an associated static stress drop of 43 MPa. In the subsequent confining pressure steps of Pc = 80 and 100 MPa, although the normal stress on the fault was increased, no subsequent stick-slip events were observed. This suggests that a change in the frictional nature of the interface occured during the initial rupture at Pc = 60 MPa. The DSS array revealed a) a complex distribution of fault-parallel strain b) extensional axial strain closer to the leading and trailing edge of the fault. Local deviations from the expected elastic response due to inelastic processes were revealed. Measurements of heterogeneous contact pressure and roughness of the fault surface were made before and after the experiment, using a pressure sensitive film and optical profilometry, respectively. Results obtained before the experiment showed sections of the fault with lower normal stress, which coincided with regions on the DSS strain analysis that experienced more extensional response in the axial parts. This extensional response deviates from the numerical strain calculation for perfectly flat and mated saw-cut interfaces. These results were confirmed using a finite element model that showed the effect of the geometry of the fault on the strain response. Post-mortem measurements of contact pressure and surface roughness revealed distinct changes in normal stress distribution consistent with visual damage associated with surface wear. Fault surface heterogeneities identified by post mortem examination can be categorized into two groups: Sections exhibiting wear and sections characterized by similar surface features to the original fault interface. This heterogeneity in fault surface characteristics and hence frictional properties could have contributed to the inability to lock and mitigate dynamic rupture at higher confining pressures as the fault surface has changed after the stick-slip event. This study contributes to the understanding of frictional heterogeneity resulting from localized frictional weakening, which ultimately influences non-uniform preslip. Our laboratory observations provide insight into preparatory earthquake processes and their impact on fault stability by providing a bridge between fault surface characteristics and their changes, preslip distribution, and seismic behavior.

1.10

Fluid-Driven Shear Instabilities in the Subducted Oceanic Mantle at Intermediate Depths: Insights from the Rock Record

Jesús Muñoz-Montecinos[1], Samuel Angiboust[2,3], Clothilde Minnaert[2,4], Alberto Ceccato[1], Luiz F. G. Morales[1,5], Julien Gasc[6], Whitney Behr[1]

[1] *Structural Geology and Tectonics Group, Geological Institute, Department of Earth Sciences, ETH Zürich, Sonneggstrasse 5, 8092, Zürich, Switzerland (jesus.munozmontecinos@gmail.com)*
[2] *Laboratoire de Géologie de Lyon (LGL-TPE), Ecole Normale Supérieure de Lyon, F-69007 Lyon, France*
[3] *Institut Universitaire de France (IUF)*
[4] *Université Paris Cité, Institut de Physique du Globe de Paris, F-75005 Paris, France*
[5] *Scientific Centre for Optical and Electron Microscopy (ScopeM), ETH Zürich. Otto-Stern-Weg 3, 8093, Zürich, Switzerland*
[6] *Laboratoire de Géologie, Ecole Normale Supérieure, F-75005 Paris, France*

Serpentinites are a major carrier of fluids in deep subduction environments and release most of their fluid content when subducted in the 500-650°C temperature window. However, the mechanical conditions and processes by which this release occurs remains elusive despite fundamental implications on volatile transfer, elemental recycling and seismicity. We herein perform a petro-structural analysis of metamorphic olivine-rich veins widespread in the Western Alps meta-ophiolite high-pressure serpentinites. These veins are ubiquitously present in the entire km-thick serpentinite sole and associated slivers, with local variations in volumetric abundance. Some of these veins formed through static dehydration, with little to no significant shear-related deformation. Nevertheless, field and microstructural observations reveal that a vast amount of these veins experienced substantial shearing coeval with dilational veining. Dehydration and dilational vein systems prevail towards the nappe core (away from major tectonic boundaries), whereas hybrid and shear-dominated vein networks are predominant approaching the high-strain upper and lower tectonized bounds of the serpentinite bodies. These lateral variations in deviatoric shear component point to the key role of the local stress regime during serpentinite dehydration in the downgoing slab.

1.11
4D geodynamic evolution of the Aar Massif during the late-stage Alpine collision

Ferdinando Musso Piantelli [1], Lukas Nibourel[2], Alfons Berger[3], Marco Herwegh [3]

[1] *Swiss Geological Survey, Federal Office of Topography swisstopo, Seftigenstrasse 264, 3084 Bern, Switzerland*
[2] *ETH Zürich, Dep. of Earth Sciences, Sonneggstrasse 5, 8092 Zürich, Switzerland*
[3] *Institute of Geological Sciences University of Bern, Baltzerstrasse 1+3, 3012 Bern, Switzerland*

The inversion of crystalline units of former passive continental margins is a typical feature during late-stage collision. In this work, we selected the Aar Massif, the easternmost of the External Crystalline Massifs of the European Alps, to investigate how the 3D geometry of the passive margin, inherited structures, and crustal density variations influenced the late stage continent-continent collision. Explicit three-dimensional geological modelling, cross-section restoration coupled with metamorphic peak temperature data, allowed us to construct a 4D geodynamic evolution of the Aar Massif during the late-stage Alpine orogeny. Our results show that: (i) The Aar Massif results from the inversion of the former passive European margin, consisting of spatially complex 3D rifting structures. These outlined variable distribution of local half graben basins and a topographic high from the Permian to the Mesozoic. (ii) The reconstruction shows that at the onset of Alpine deformation (22 Ma), peak metamorphism was reached by burial at depths between -8 and -18 km with a horizontal geothermal gradient of 26°C/km. (iii) Exhumation of the basement units occurred in a distinct in-sequence deformation style. Inherited along-strike variations in the thickness and density of the basement units induced a non-cylindrical exhumation of the massif by activation of dense networks of reverse, thrust and strike-slip faults. Complex 3D interactions between these fault networks resulted in the present day shape of the massif. The in-sequence non-cylindrical exhumation of the basement units was controlled by an interplay between deep crustal dynamics and structural inheritance in the middle to the upper crust of the former European passive continental margin as well as surface erosion.

1.12
Lithospheric Strength: Does quartz really dominate the mid-crustal rheology?

Natalia Nevskaya[1], Alfons Berger[1], Holger Stünitz[2,3], Weijia Zhan[1], Markus Ohl[4], Oliver Plümper[4], Marco Herwegh[1]

[1] *Institut für Geologie, University of Bern, Baltzerstrasse 1+3, CH-3012 Bern (natalia.nevskaya@unibe.ch)*
[2] *Department of Geology, Tromsø University, Dramsveien 201, 9037 Tromsø, Norway*
[3] *Institut des Sciences de la Terre d›Orléans (ISTO), Université d›Orléans, 1A rue de la Férollerie, 45100 Orléans, France*
[4] *Department of Earth Sciences, Utrecht University, Princetonlaan 8a, 3584 CB Utrecht, Netherlands*

The movements of Earth's continental plates create different stress regimes in the Earth's crust, which leads to stress buildup and release in fault zones. The strength of the crust is defining whether this release of energy is fast or slow, and thereby controls if e.g., eathquakes or slow slip events will occur. Therefore, it is important to understand the strength of the Earth's crust. The mid-crustal rheology is usually inferred through extrapolation of experiments on monomineralic aggregates. At mid-crustal conditions, quartz is believed to be the weakest and rheologically dominant phase. Consequently, its rheological parameters are used in various numerical models to represent the Earth's middle crust. Field studies show, however, viscous deformation mostly localizes in mylonitic shear zones composed of fine-grained polymineralic mixtures rather than in monomineralic quartz bands. Hence, nature suggests fine-grained polymineralic granitoid rocks to be weaker than quartz. In this study, we conduct experiments to test these indications from field studies. Cylindrical, fine-grained, solid, natural, granitoid ultramylonite samples, composed of qtz + ab + K-fsp + bt + ep, with grain sizes of 125-15 μm are deformed in a Grigg's type apparatus at T=650°C, confining P=1.2 GPa, strain rates=10^{-3} to $10^{-5}s^{-1}$, and 0.2 wt% H_2O added.

By combining light microscope, SEM, TEM, and quantitative image analysis with mechanical data, microstructures are linked to stress and strain evolution. In the experimentally deformed samples, extreme strain localization and up to 1000x grain size reduction occurs.The measured strength, as compared to monomineralic studies, is one to four times weaker. We propose that fine-grained polymineralic rocks deform through different processes than predicted for monomineralic quartz aggregates at mid-crustal pressure and temperature conditions. We demonstrate that the samples deform through an interplay of fracturing, grain boundary sliding, and solution-precipitation. Nucleating new grains and keeping a small grain size below 50 nm, is possible because of a combination of mineral reactions and pinning processes in a polymineralic mixture only. As a result, the combination of deformation processes in small gain sizes makes deformation of polyphase mixtures very efficient and, most importantly, substantially weaker than quartz, impacting crustal rheological profiles.

1.13
Large-scale semi-automatically generated thickness maps: toward a faster identification of potential mineral resources

Lukas Nibourel [1], Anja Amrein[1], Thomas Galfetti [2], Stefan Heuberger [1]

[1] *Georesources Switzerland Group, Department of Earth Sciences, ETH Zurich, Sonneggstrasse 5, 8092 Zurich, Switzerland (lukas.nibourel@erdw.ethz.ch)*
[2] *Swiss Geological Survey, Federal Office of Topography Swisstopo, Seftigenstrasse 264, 3084, Wabern, Switzerland*

We present a large-scale geospatial data set of the true stratigraphic thickness of hardrock-bearing lithostratigraphic units of Switzerland such as the Helvetic Kieselkalk, the Garschella Formation or the North-Helvetic Flysch Group. These maps have been developed as part of a Switzerland-wide mineral resource mapping project using a combined Python, MATLAB and GIS approach (Nibourel et al., 2023). The used thickness data were automatically extracted from geological vector data sets (GeoCover) and manually compiled from cross-sections.
Our results highlight gradual thickness variations within different Helvetic nappes and discrete thickness jumps across nappe contacts (Figure 1). Based on these results, sufficiently thick hardrock occurrences can be identified rapidly. These can possibly be considered in land use or resource safeguarding plans. The thickness maps also indicate distinct paleogeographic basin geometries and/or tectonic thickness variations. This highlights the potential of the approach also for the creation of large-scale tectonic or paleogeographic reconstructions.

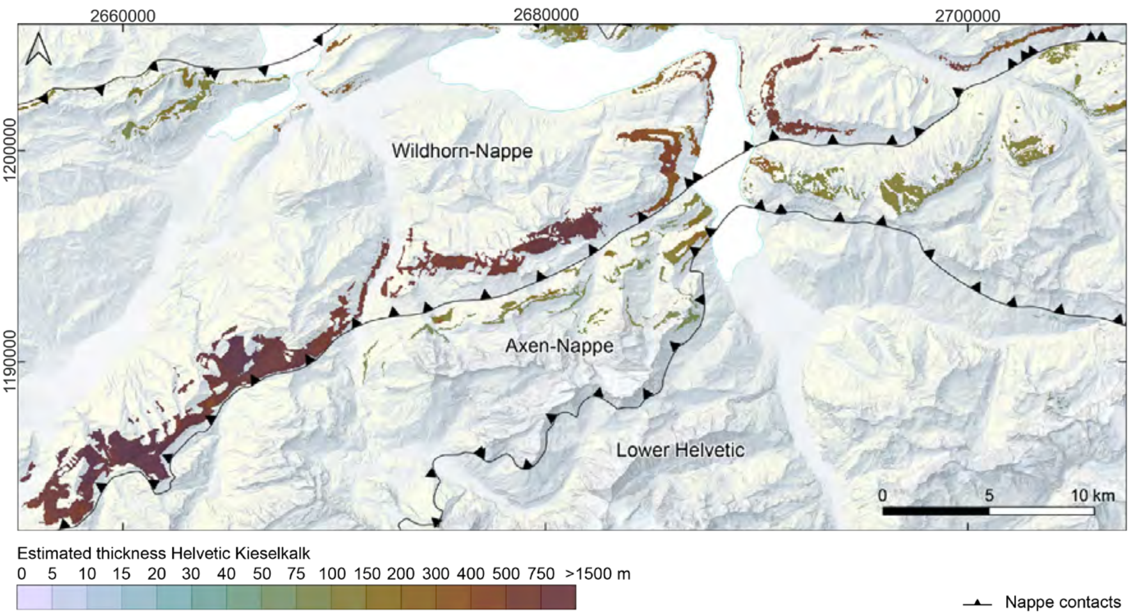

Figure 1. Example of modeled stratigraphic thickness of the Helvetic Kieselkalk in Central Switzerland.

REFERENCES

Nibourel, L., Morgenthaler, J., Grazioli, S., Schumacher, I., Schläfli, S., Galfetti, T., & Heuberger, S. (2023): Automated extraction of orientation and stratigraphic thickness from geological maps, Journal of Structural Geology, 172, 104865.

1.14
Rift obliquity in the North Volcanic Zone in Iceland using UAV-based structural data

Elisabetta Panza[1], Joël Ruch[1], Nicolas Oestreicher[1]

[1] *Department of Earth Sciences, University of Geneva, Rue des Maraîchers 13, CH-1205 Genève (elisabetta.panza@unige.ch)*

Iceland is one of the two locations on Earth (together with the Afar region, Ethiopia) where a Mid-Ocean Ridge, with its rift obliquity and structural developments, is directly observable onland. Rift obliquity has been observed through seismicity, InSAR and ground observations during volcano-tectonic events, however, the involved structural processes are still poorly understood.

Here we focus on structural analysis of rift obliquity of past events in the North Volcanic Zone of Iceland. In the summers of 2019, 2020, and 2021, we performed an extensive UAV survey (~33 km^2) in four areas of the active rift and obtained ~3 cm/px DEMs and ~2 cm/px orthomosaics. The imagery was the base for detailed structural and morphological mapping, aimed at analysing fracture orientations, opening obliquity, and their spatial variation along the rift segments. While plate motion data indicate an overall ~N104 opening in all the examined rift segments, spanning over ~200 km along the plate boundary, the overall strike of the rift structures goes from approximatively N-S in the North (Fjallagjá graben), bending to NNE-SSW towards the South.

We found that the obliquity changes from a dominant normal opening of the structures in the North (Fjallagjá) to a southward increase of a left-lateral shear component (2014-2015 Holuhraun graben). After a detailed morphotectonic analysis, we found that reccurent rifting events reactivate pre-existing structures (e.g., graben, volcanic vent), influencing the direction of fracture opening during a magmatic intrusion. We further discuss the origins of this obliquity and suggest that inherited structures and mantle plume provide weakness zones that can channel deformation and magma intrusions, and that topography influences the propagation of both fractures and magma intrusions. Their combination can have an impact on the missmatch between rift opening direction and the far field strain.

We conclude that obliquity can be inferred for past rifting events from surface data where the orientations of rift opening and inherited structures do not perfectly match. It is fundamental to take into account the existing structural pattern and its (re) activation history in active rift zones to avoid missing out on possible and preferential magma propagation ways and eruption sites during the monitoring of ongoing events.

1.15

Influence of water-clay interactions on the stress state and frictional properties of clay-rich rocks

Markus Rast[1], Claudio Madonna[1], Paul A. Selvadurai[2], Antonio Salazar Vásquez[2,3], Quinn Wenning[4], Jonas B. Ruh[5]

[1] *Geological Institute, ETH Zürich, Zürich, Switzerland (markus.rast@erdw.ethz.ch)*
[2] *Swiss Seismological Service, ETH Zürich, Zürich, Switzerland*
[3] *Eastern Switzerland University of Applied Sciences, Rapperswil, Switzerland*
[4] *Institute of Geophysics, ETH Zürich, Zürich, Switzerland*
[5] *Institute of Marine Sciences, CSIC, Barcelona, Spain*

Clay-rich rocks occur in various tectonic settings, such as the shallow subduction zone, and are also of great interest for natural barriers in nuclear waste deposits or for subsurface caprocks of CO_2 storage facilities. The interaction between clay minerals and polar fluids (such as water) may lead to swelling or, under confined conditions, build-up of swelling stress. The extent of both depends on the clay mineralogy and the pore water chemistry (Wagner, 2013). Many studies have focused on the closure of cracks in clay-rich rocks due to swelling, also referred to as 'self-sealing' (e.g., Zhang, 2011, Wenning et al., 2021). However, it remains unclear whether water-clay reactions may induce slip along pre-existing faults due to changes of the stress state (i.e., swelling stress) or alteration of the frictional properties. In the present study, this question will be addressed based on triaxial friction experiments.

The experiments are performed using oblique saw-cut cylindrical samples, with the upper half consisting of a clay-rich rock (Opalinus claystone) and the lower half consisting of a permeable sandstone (Berea sandstone). The friction slip envelope of the dry sandstone-claystone interface is estimated based on experiments at 4 to 25 MPa confining pressure and a constant axial loading rate of 0.1 mm/min. Fluid injection friction experiments are performed at 10 and 25 MPa confining pressure, constant piston position (axial loading rate of 0 mm/min), and an initial differential stress of about 70% of the expected yield stress. We applied a stepwise increase in fluid pressures by injection of decan (non-polar fluid) and, in a second experiment, deionized water (polar fluid). To estimate the effect of water-clay interactions on the stress-state, we compare the fluid pressures required to initiate slip when a non-polar fluid is injected (no water-clay interactions are expected) and when a polar fluid is injected (water-clay interactions will occur). We also derive wet friction slip envelopes of the sandstone-claystone interface in the presence of water and decane. In one decane and one water injection experiment each, we equipped the sample assemblage with fibre optic strain sensors glued to the sample surface (Salazar Vásquez et al., 2022). This allowed us to identify poroelastic deformation of the matrix, deformation due to water-clay interaction, and elastic relaxation due to slip along the saw-cut.

The friction slip envelope based on the injection experiments with a non-polar fluid (decane) is within the uncertainty of the dry friction slip envelope. In contrast, the water injection experiments show a weakening of the frictional interface with respect to the dry state. We interpret this weakening to be due to the transition of the claystone from a solid rock to a mud close to the saw-cut surface. Another observable difference when injecting a polar fluid compared to a non-polar fluid is that slip along the saw-cut already occurs when the water initially reaches the sandstone-claystone interface (at ambient fluid pressure of about 0.1 MPa), although the apparent stress state is below the yielding criteria of the friction slip envelope. This suggests that the swelling stress should be considered to describe the stress state at initial water injection. In summary, our data suggest that water-clay interactions may initiate slip due to (1) the alteration of the friction slip envelope and (2) the build-up of swelling stress.

REFERENCES

Salazar Vásquez, A., Rabaiotti, C., Germanovich, L. N., and Puzrin, A. M. (2022). Distributed fiber optics measurements of rock deformation and failure in triaxial tests. Journal of Geophysical Research: Solid Earth, 127.

Wagner, J.-F. (2013). Mechanical Properties of Clays and Clay Minerals. In Bergaya, F. and Lagaly, G., editors, Developments in Clay Science, volume 5, pages 347–381. Elsevier.

Wenning, Q. C., Madonna, C., Kurotori, T., Petrini, C., Hwang, J., Zappone, A., Wiemer, S., Giardini, D., and Pini, R. (2021). Chemo-Mechanical Coupling in Fractured Shale With Water and Hydrocarbon Flow. Geophysical Research Letters, 48(5).

Zhang, C. L. (2011). Experimental evidence for self-sealing of fractures in claystone. Physics and Chemistry of the Earth, 36(17-18):1972–1980.

1.16
The formation of a magma-rich margin: structure and kinematics of the Danakil Depression, Afar, Ethiopia

Valentin Rime[1], Anneleen Foubert[1], Ermias Gebru[1], Tesfaye Kidane[2,3]

[1] *Department of Geosciences, University of Fribourg, Ch. Du Musée 6, 1700 Fribourg (valentin.rime@unifr.ch)*
[2] *School of Agricultural, Earth and Environmental Sciences, University of Kwazulu-Natal, Durban, South Africa*
[3] *Department of Environmental Science and Geology, Wayne State University, Detroit, Michigan*

The Danakil Depression is situated in the northern part of the Afar Depression in Ethiopia and Eritrea and is in an advanced phase of rifting. It forms the equivalent of a magma-rich margin. As it is currently active and emerged, it offers a unique opportunity to study the processes of formation of these types of passive margins.
We combine field data, remote sensing and seismic reflection data to constrain the structure and kinematics of this basin. Seismic data reveal the formation of Seaward Dipping Reflectors (SDRs). Surprisingly, field data show that these SDRs are dominated by clastic sediments and only contain relatively minor amount of magmatic material. Paleoshorelines and other proxies allow to quantify uplift and subsidence rates across the basin. These data highlight high spatial variability and allow to better understand the structure and evolution of older, deeply buried passive margins.

1.17
Investigating Oligocene Magmatic Evolution in the Artvin District, Easternmost Eastern Pontides: Insights from the Yanıklı Prospect

Şafak Utku Sönmez[1], Robert Moritz[1], Serdar Keskin[,2], François Turlin[1], Alexey Ulianov[3], Massimo Chiaradia[2], Ümit Aydın[2]

[1] Department of Earth Sciences, University of Geneva, Rue des Maraîchers 13, 1205 Geneva, Switzerland (safak.soenmez@unige.ch)
[2] General Directorate of Mineral Research and Exploration of Turkey, Department of Mineral Research and Exploration, Ankara 06520, Turkey
[3] Institute of Earth Sciences, University of Lausanne, 1015 Lausanne, Switzerland

The Eastern Pontides (EPs) is one of the remarkable segments within the Tethyan orogenic belt with a wide range of magmatic rocks. During the Mesozoic, the EPs were an active magmatic arc with a predominant magmatic activity during the Late Cretaceous, resulting from the northward subduction of the northern branch of the Neotethys and the convergence of the Tauride-Anatolide block (TAB) with the Eurasian margin. The Cenozoic magmatism is predominantly Eocene and Miocene in age. So far, no magmatism has been reported during the Oligocene in the EPs, except by Karsli et al. (2020), who published U-Pb zircon ages at ~29.8 ± 0.3 Ma for the small Tepebaşı dacitic stock in the easternmost part of the EPs.

During recent field and geochronological investigations, we have discovered a variety of Oligocene dikes within the Yanıklı mineral prospect of the Artvin district, easternmost EPs, approximately 10 km northwest of the Tepebaşı dacitic stock. These new findings of Oligocene dikes provide evidence of considerably more important and widespread Oligocene magmatic activity in the EPs than concluded previously.

Three different NW-oriented Oligocene dikes have been identified and characterized by their composition and age. One dike type named ODike-1 has yielded U-Pb zircon ages of 31.04±0.19 Ma, and exhibits non-adakitic compositions. Two other dike types with adakite-like characteristics, named ODike-2 and ODike-3, have yielded, respectively, U-Pb zircon ages of 31.05±0.20 to 29.73±0.31 Ma and 29.21±0.31 Ma. These dikes originated from the low-degree partial melting of a thickened juvenile lower crust during asthenospheric mantle upwelling. $^{143}Nd/^{144}Nd_i$ and $^{87}Sr/^{86}Sr_i$ ratios, respectively, of 0.512742-0.512784 and 0.704714-0.706164 indicate a deep melt origin related to asthenospheric mantle upwelling.

We conclude that the asthenospheric upwelling was a significant heat source, while the lower portion of the delaminated crust continued sinking vertically into the underlying mantle. This initiated partial melting of the overlying lithospheric mantle during the Oligocene in Yanıklı. Additionally, the rollback of the Southern Neotethys during the Oligocene may have provided additional heat flow, influencing magmatic activity in the EPs to the north.

Comparisons between the EPs Oligocene magmatism in Yanıklı and other regions in the Tauride-Anatolide Block (TAB) and South Armenian block (SAB) reveal distinct characteristics, suggesting that the magmatic activity in Yanıklı is not linked to the same tectonic history observed in the TAB and SAB.

This study significantly contributes to our understanding of magmatic processes and tectonic dynamics in the EPs, and constrains the geodynamic framework of the central Tethyan orogenic belt.

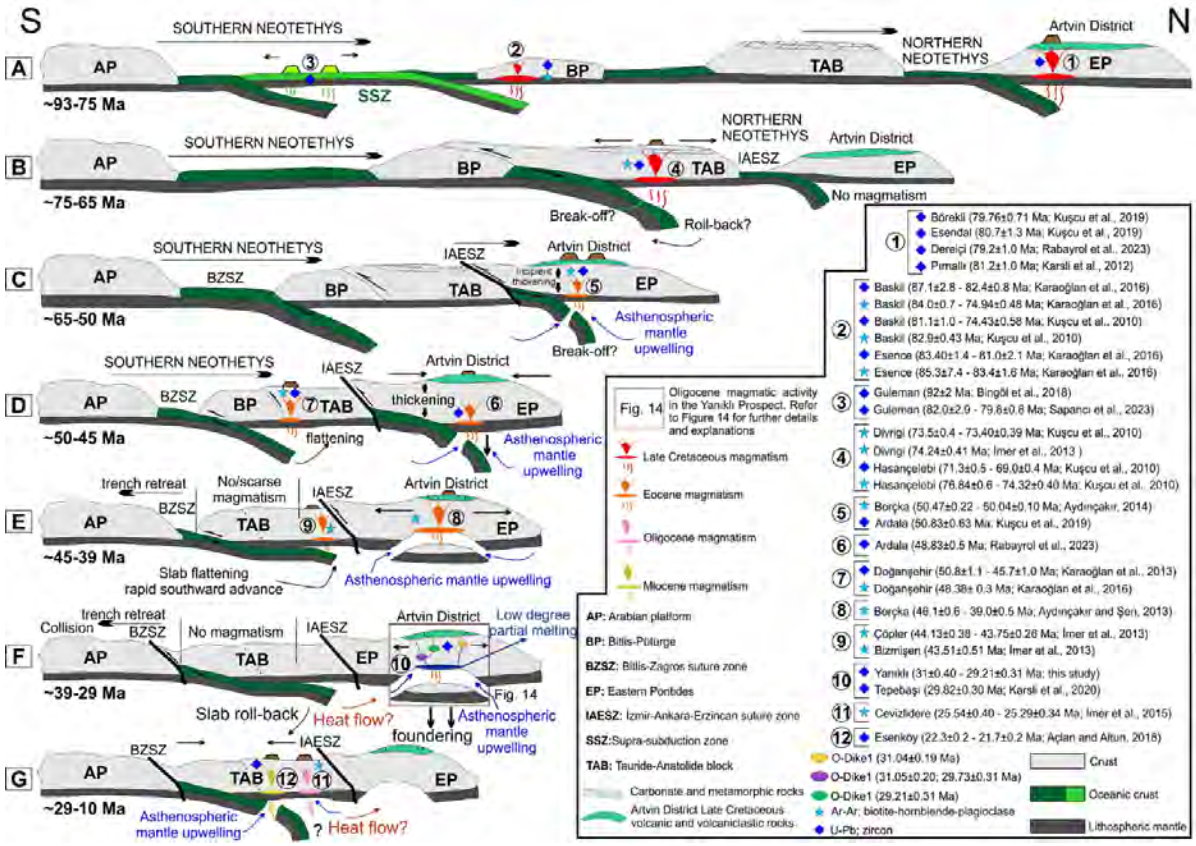

Figure 1. Late Cretaceous to early Miocene geodynamic and magmatic evolution of the Neotethys Oceans.

REFERENCES

Karsli, O., Caran, Ş., Çoban, H., Şengün, F., Tekkanat, O., Andersen, T. 2020: Melting of the juvenile lower crust in a far-field response to roll-back of the southern Neotethyan oceanic lithosphere: the Oligocene adakitic dacites, NE Turkey. Lithos 370-371, 105614

1.18
Characterization of disGBS in quartz through load-stepping experiments

Leif Tokle[1], Greg Hirth[2], Whitney M. Behr[1]

[1] Structural Geology and Tectonics Group, Geologic Institute, ETH Zurich (leif.tokle@erdw.ethz.ch)
[2] Department of Earth, Environmental, and Planetary Sciences, Brown University, RI, USA

Due to the abundance of quartz in the continental crust, quartz rheology is fundamental to our understanding of many geodynamic processes. Quartz rheology is commonly characterized using a dislocation creep flow law with a stress exponent equal to 4; however, several recent studies indicate that the stress exponent for quartz aggregates can be as low as 2 at conditions where it has been proposed to deform by a combination of dislocation creep and grain boundary sliding (GBS), known as dislocation accommodated grain boundary sliding (disGBS). To address these differing hypotheses, we conducted axial compression load-stepping experiments in a Griggs apparatus at 800°C, 1.5 GPa, and stresses ranging from ~50 MPa to ~1430 MPa. Quartz samples were prepared with different grain sizes of 3, 5, and 10 μm. For each experiment ~25 load steps were conducted during which the strain rate achieved a mechanical steady state. At the lowest stresses the mechanical data for the different grain size samples plot together, implying a grain size insensitive rheology, while with increasing stress the mechanical data show a clear grain size sensitivity. At the highest stresses the mechanical data converge again, suggesting a switch back to a grain size insensitive rheology. The grain size sensitive region has a slope of ~2 in log stress versus log strain rate space while both the lowest and highest stress mechanical data have slopes of ~3.0; however, additional experiments are required to further constrain these values. We interpret the highest stress data deformed by dislocation creep, while at lower stresses quartz deformed by disGBS, where dislocation creep and GBS act in series. We estimate the grain size exponent for the GBS regime to be 0.92 +/- 0.06. Microstructurally, we observe minimal variation in the starting and final grain sizes, suggesting that the grain size was nominally constant throughout the experiments. Additional experiments will be conducted at larger grain sizes (15, 30, 60 μm) and higher temperatures (900, 1000°C). These results will have an important impact on how we interpret quartz rheology at experimental and geologic conditions.

1.19 Aftershock sequences in Greece studied by non-linear high pressure fluid diffusion models

Gaëlle Toussaint[1], Thanushika Gunatilake[2], Stephen A. Miller[1], Benoît Valley[1]

[1] *Centre for Hydrogeology and Geothermics (CHYN), University of Neuchâtel, Neuchâtel, Switzerland (gaelle.toussaint@unine.ch)*
[2] *Swiss Seismological Service (SED), ETH Zürich, Zürich, Switzerland*

High-pressure fluids play a critical role in fault stability and seismogenesis. In natural systems, deeply trapped and internally generated high-pressure fluids diffuse along permeable pathways, reactivating faults and triggering extensive aftershock sequences. High-pressure fluids are also the common denominator in many engineering applications, including enhanced geothermal systems, where understanding the complex behavior between fluid injection and seismic activity is essential. Hence, numerical models are needed to simulate the coupling between fluid pressure propagation and seismogenesis in the crust.

We used a non-linear diffusion model that incorporates dynamic fault permeability and a source term accounting for direct fluid input from thermal decomposition to simulate three seismic sequences in Greece: I) the 2020-2021 Thiva sequence (Beotia, Central Greece), II) the 2021 Damasi-Tyrnavos sequence (Thessaly, Central Greece), and III) the 2012-2014 Florina sequence (North Greece). Despite different aftershocks characteristics, all sequences occurred in a similar geological context with numerous normal faults generated in carbonates by the extensive tectonic regime.

Model results show strong correlations between the calculated fluid pressure field and the location of thousands of relocated hypocenters. The model also accurately reproduces the temporal evolution of the sequences in terms of cumulative aftershock rates, supporting the hypothesis that the observed large aftershock series are fluid driven. The origin of these fluids is likely a combination of fluids released through dehydration of the subducting oceanic slab coupled with thermal decomposition of carbonates, explaining the non-Omori type behavior observed for these aftershock sequences.

This study exposes the role of high-pressure fluids in aftershock dynamics and provides valuable insights into the complex seismicity patterns observed in Greece. The developed model also holds promise for understanding aftershocks sequences in other tectonic environments.

1.20
Hypocenter-Based 3D Imaging of Active Faults: Unravelling Seismogenic Faults at Depth

Sandro Truttmann[1], Tobias Diehl[2], Marco Herwegh[1]

[1] *Institute of Geological Sciences, University of Bern, Baltzerstrasse 1+3, CH-3012 Bern (sandro.truttmann@unibe.ch)*
[2] *Swiss Seismological Service, ETH Zürich, Sonneggstrasse 5, CH-3092 Zürich*

Earthquakes commonly nucleate along pre-existing faults. However, the extent, geometry, and location of such subsurface faults often remain ambiguous due to the limited resolution of currently available geophysical methods. Acquiring knowledge about such attributes is however crucial, since even small-scale geometric variations can significantly impact the seismic fault reactivation processes.

In this study, we introduce an innovative approach called “hypocenter-based 3D imaging of active faults” that exploits seismogenic faults at depth based on high-precision, relatively relocated hypocenter catalogs. Applied on various earthquake sequences in the Swiss Alps, we successfully uncover the 3D geometrical and kinematic properties of recently active fault systems. Analyzing the spatiotemporal evolution of these sequences, we document the interplay between fault architecture, slip tendency and the migration patterns of the seismicity along faults with complex small-scale geometric variations.

The provided open-source Python toolbox is readily deployable for additional high-quality earthquake catalogs, offering the potential to reveal the detailed 3D architecture of further active faults. Such knowledge about the small-scale 3D properties of active faults in the subsurface contributes to the refined assessment of the regional seismic hazards.

1.21
Styles of deformation at the eastern termination of the Jura fold and thrust belt: new insights from 3D seismic interpretation

Miller Zambrano[1], Stefano Mazzoli[1], Jon Mosar[2]

[1] *Geology Division, School of Science and Technology, University of Camerino, 62031 Camerino MC (miller.zambrano@unicam.it)*
[2] *University of Fribourg, Department of Geosciences, Ch. du Musée 6, 1700 Fribourg, Switzerland*

The Jura fold and thrust belt is characterised by dominant thin-skinned thrusting and variable interaction with inherited structures and deep-seated (i.e., sub-detachment) faults (e.g., Laubscher, 1986; Schori et al., 2021). Using 3D seismic data, the styles of deformation at the eastern termination of the fold and thrust belt are documented in the area comprised between Schöfflisdorf and Eglisau. The investigated seismic cube (Nördlich Lägern) includes two major, ENE trending deformation zones involving the Triassic-Jurassic epicontinental platform succession and the stratigraphically overlying Cenozoic Molasse Basin deposits. The location of both deformation zones appears to be controlled by variable interaction between the detachment level hosted in the Triassic evaporites of the Muschelkalk Group and faults linked to an underlying Permo-Carboniferous half-graben. The northern deformation zone (NDZ), manifested at the surface by the Siglisdorf anticline, consists of a ~ 2 km wide pop-up produced by thin-skinned thrusting. Although this structure is located above a step produced by an antithetic fault of the underlying Permo-Carboniferous half-graben, the integrity of the detachment appears to be preserved along the entire along-strike extension of this structure. The southern deformation zone (SDZ, aka Baden-Irchel-Herdern Lineament) is located above a detachment segment of degraded quality due to salt mobility and associated salt weld development. The salt weld formed above the N-dipping master fault of the Permo-Carboniferous half-graben, in an area of strong interaction between the evaporite detachment level and the underlying inherited fault (most likely reactivated during mild basin inversion). The overlying SDZ consists of multiple thrusts and backthrusts forming a series of fish-tail structures arranged in a narrow, steep belt involving the Triassic-Jurassic series. Here, the Aalenian shales allow significant decoupling of the deformation between Triassic-Lower Jurassic formations and the overlying post-Aalenian succession.
In conclusion, different degrees of interaction between the salt detachment and underlying inherited faults produced a marked contrast in structural style between the detachment-dominated NDZ and the attachment-dominated SDZ.

REFERENCES

Laubscher, H.P. 1986: The eastern Jura: Relations between thin-skinned and basement tectonics, local and regional, Geol. Rundsch., 75, 535-553.

Schori, M., Zwaan, F., Schreurs, G., & Mosar, J. 2021: Pre- existing Basement Faults Controlling Deformation in the Jura Mountains Fold-and-Thrust Belt: Insights from Analogue Models, Tectonophysics, 814, 228980.

1.22
Experimental Brittle-Viscous Transition of Granitoid Gouges by Mixed Dissolution Precipitation Creep and Frictional Granular Flow

Weijia Zhan[1], Natalia Nevskaya[1], André Niemeijer[2], Alfons Berger[1], Chris Spiers[2], Marco Herwegh[1]

[1] *Institute of Geological Sciences, University of Bern, Baltzerstrasse 1+3, CH-3012 Bern (weijia.zhan@unibe.ch)*
[2] *Faculty of Geosciences, HPT Laboratory, Utrecht University, Princetonlaan 4, 3584 CB Utrecht, Netherlands*

Granitoid gouges play a central role as non-cohesive fault rock in the continental crust, affecting the crustal strength and constraining the lower limit of abundant seismic activities. Previous experiments suggested a brittle-viscous transition at around 350°C. However, these experiments were limited to short distances and low-resolution microscopic investigations, leaving a gap in our understanding of the detailed deformation processes in these fine-grained rocks that dominates the crustal rheology.

To overcome these limitations, we conducted a series of experiments on granitoid gouge subjected to constant sliding velocities (*V* = 0.1, 1, 100 μm/s) and substantial displacements (~15 mm), followed by systematic microstructural analysis. Deformation temperatures ranged from *T* = 20-650°C, with an effective normal stress and pore fluid pressure kept at 100 MPa. For experiments conducted at *V* = 100 μm/s, the steady-state shear stresses are overall high (= 73-82 MPa) and insensitive to temperature changes. In contrast, experiments with slower *V* = 1 and 0.1 μm/s showed a notably weakening in shear stresses as temperature increases, especially beyond 450°C. The lowest observed shear stress was = 37 MPa at *T* = 650°C, *V* = 0.1 μm/s. Microstructural analysis revealed that gouges in fast experiments exhibited homogeneous cataclastic microstructures, dissected by pervasive intergranular fracture arrays, such as R-shears and Y-shears. These features are typical of gouges that deform primarily through frictional granular flow. At slow V and elevated T, deformation becomes highly localized into principal slip zones, where grains were dramatically reduced to nm-size and tightly packed. Some pores were filled with newly precipitated biotite, or trapped within larger minerals as fluid intrusions, indicating the operation of dissolution-precipitation creep.

Our results highlight a gradual shift from frictional granular flow to dissolution precipitation creep as temperatures increase and velocities decrease, defining the brittle-viscous transition in our experiments. The most recent microphysical model of fault strength, incorporating mechanisms (e.g. dislocation creep) that activate at higher temperatures overestimates the weakening of granitoid gouge at this transition. Understanding dissolution-precipitation creep helps to improve the models and their extrapolations to natural faults.

1.23
Natural H_2 potential in rift-inversion orogens

Frank Zwaan[1,2], Sascha Brune[1,3], Anne Glerum[1,2], Dylan A. Vasey[4], John Naliboff[5], Gianreto Manatschal[6], Eric C. Gaucher[7]

[1] *GFZ German Research Centre for Geosciences, Telegrafenberg, 14473 Potsdam, Germany (frank.zwaan@gfz-potsdam.de)*
[2] *Department of Geosciences, University of Fribourg, 1700 Fribourg, Switzerland*
[3] *Institute of Geosciences, University of Potsdam, Potsdam, Germany*
[4] *Department of Earth and Climate Sciences, Tufts University, Medford, MA 02155, USA*
[5] *Department of Earth and Environmental Science, New Mexico Institute of Mining and Technology, Socorro, NM 87801, USA*
[6] *University of Strasbourg, CNRS, ENGEES, ITES UMR 7063, Strasbourg, France*
[7] *Lavoisier H2 Geoconsult, 74400 Chamonix, France*

Naturally occurring hydrogen gas (H_2) represents a potentially major source of clean energy but has been relatively understudied so far. The most promising mechanism for large-scale natural H_2 generation is serpentinization of mantle material as it reacts with water while brought into the "serpentinization window" (i.e., T = 200-350˚C) during mantle exhumation. We study such serpentinization-related natural H_2 generation during rifting and subsequent rift-inversion by means of numerical geodynamic models. In these models we trace how, when, and where mantle material enters the serpentinization window, and when active deformation along shear zones in mantle bodies may allow for water circulation and serpentinization to occur there. Although serpentinization-related natural H_2 generation is best known from rifted margins and spreading ridges, we find that volumes of natural H_2 generated during inversion may be up to 20 times higher than during rifting, due to the colder thermal regime. Moreover, suitable reservoirs and seals are readily available in rift-inversion orogens, whereas they may not be present when serpentinization occurs in rift settings. Our model results thus provide a first-order motivation to turn to rift-inverted orogens, rather than rifts and rifted margins, for natural H_2 exploration, as supported by indications of natural H_2 generation in the Western Alps, Pyrenees, and Caucasus.

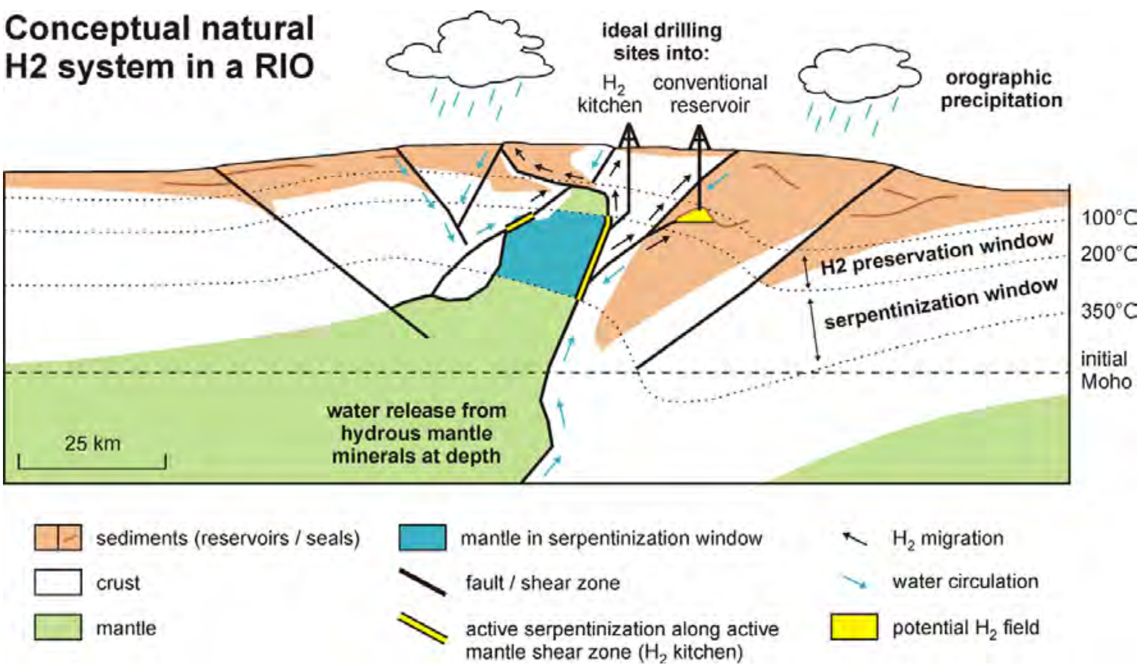

Fig. 1. Conceptual depiction of a natural H_2 system in a rift-inversion orogen (RIO). Water, originating from the deep or the surface, can flow along (active) fault zones towards those parts of the mantle that are in the serpentinization window (200-350˚C), where natural H_2 is being produced ("natural H_2 kitchen"). The natural H_2 can subsequently migrate towards the surface along fault zones, and may accumulate in reservoirs capped by seals of impermeable layers within sedimentary units. Ideally, such natural H_2 accumulation occurs within the 100-200˚C window, in which H_2 is relatively inert, so that a natural H_2 field may develop that can be exploited.

P 1.1
Deformation styles and timing of underplating sediment sequences in the Chugach accretionary prism, southern Alaska

Ismay Vénice Akker[1], Whitney M. Behr[1], Luiz F.G. Morales[1], Zoe Braden[1,2], Markus Rast[1], Emily Hinshaw[1], Mark Helper[3]

[1] *Department of Earth Sciences, Geological Institute, ETH Zürich, Zürich, Switzerland*
[2] *School of Public Policy and Global Affairs, Faculty of Arts, The University of British Columbia, Vancouver, Canada*
[3] *Jackson School of Geosciences, The University of Texas at Austin, USA*

The Chugach accretionary complex in southern Alaska records several hundred million years of subduction along active Alaskan-Aleutian margin. The McHugh Complex, displays low-grade (prehnite-pumpellyite facies) conditions representative of underplating at ~15-20 km depth, and consists of deformed basalts, cherts, argillites and greywackes. The McHugh Complex has been referred to as a 'mega-melange'. However, the timing of underplating/accretion and deformation history of the McHugh are both poorly constrained. Here we present detrital zircon ages (U-Pb geochronology), temperature estimates from Raman spectroscopy on carbonaceous material, and structural data along two cross-sections separated by ~65 km through the McHugh complex. Maximum depositional ages measured thus far show a progressive younging with increasing structural depth from 174 to 162 Ma. Temperature estimates thus far range from 218 to 290 ºC, with higher temperature domains interpreted to represent deeper levels of tectonic underplating. Our structural data shows that different underplating-related structural styles developed as a function of subducting lithology: 1) Thick basalt sequences and greywacke lenses each show discrete faults that define, meter-to-decameter-spaced, lenticular thrust slices. 2) Chert sequences show tight chaotic folds between branching thrust ramps that sole into bedding-parallel decollements, forming classic duplexes; and 3) Areas with sufficient argillite form wider (m-scale) block-in-matrix melange belts that incorporate other rock types (basalt, greywacke, chert) as blocks. Microstructural work on samples from both dated cross-sections allows us to infer the grain-scale deformation mechanisms. These results indicate that subducting rock type strongly influences deformation patterns during underplating along the subduction interface, supporting previous suggestions that lithology can indeed modulate megathrust seismic style and interface dynamics.

P 1.2
Rapid extraction of 3D orientation and stratigraphic thickness for a mineral occurrence map

Anja Amrein[1], Lukas Nibourel[1], Thomas Galfetti[2], Stefan Heuberger[1]

[1] *Georesources Switzerland Group, Department of Earth Sciences, ETH Zurich, Sonneggstrasse 5, 8092 Zurich, Switzerland (anja.amrein@erdw.ethz.ch)*
[2] *Swiss Geological Survey, Federal Office of Topography swisstopo, Seftigenstrasse 264, 3084 Wabern, Switzerland*

We present a novel Python, MATLAB and GIS-based approach to automatically extract the 3D orientation (dip direction/dip) and the stratigraphic thickness of a geological unit from a geological vector data set. It has been developed in the frame of a project mapping the hardrock-bearing lithologies in Switzerland (Nibourel et al. 2023).
The approach was applied to the bedrock polygons of the 1:25'000 geological vector dataset Geocover for the extraction of the layer orientation. For the extraction of the stratigraphic thickness, both the modelled orientation and the field orientation measurements from Geocover were used. Both orientation information types lead to modelled thickness data in good agreement with more than 1700 thickness compiled data from published cross-sections (Figure 1). Nearby (500 m) cross-section and modelled thickness data have a misfit which is mostly lower than 50%. Reliable, efficient filters and corresponding thresholds have been developed that also work for complex structural geometries such as isoclinal folds or overturned stratigraphy. Thickness extraction is followed by interpolation processing using the ordinary Kriging method to produce the thickness map in raster format.
Using this approach, large-scale tectonic or stratigraphic reconstructions can be performed without time-consuming digitisation of bedrock contacts or 3D models, and inconsistencies in non-topography-corrected vector datasets are easily found.

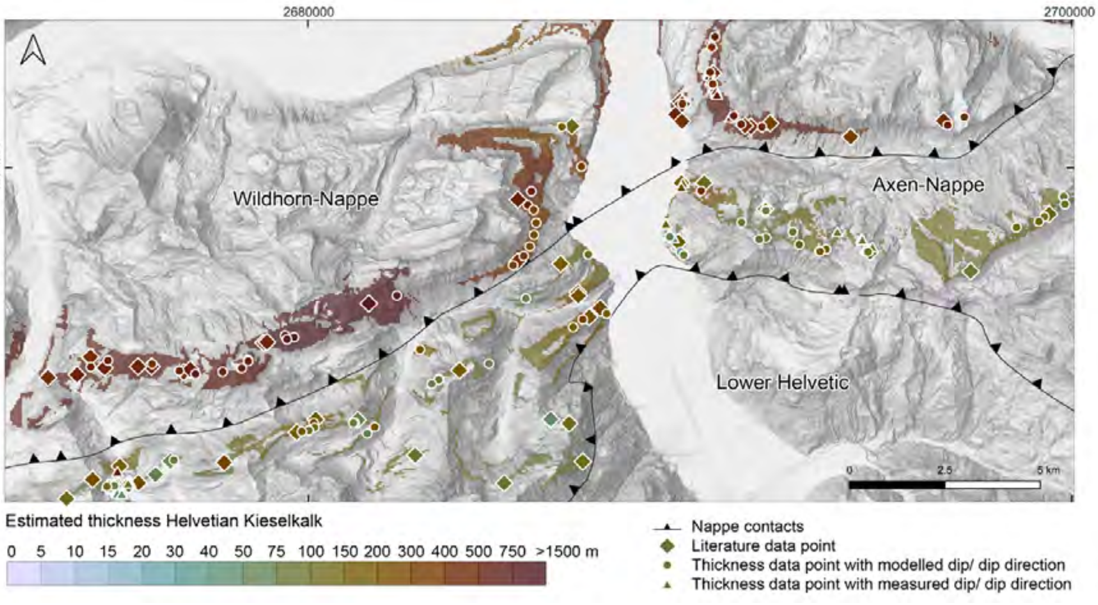

Figure 1. Map section of modelled stratigraphic thickness raster of the Helvetic Kieselkalk in Central Switzerland with modelled thickness data point and literature data points.

REFERENCES

Nibourel, L., Morgenthaler, J., Grazioli, S., Schumacher, I., Schläfli, S., Galfetti, T., & Heuberger, S. (2023): Automated extraction of orientation and stratigraphic thickness from geological maps, Journal of Structural Geology, 172, 104865.

P 1.3
The geology of Valchiavenna in the frame of the Central Alps: recent insights from the CARG project Sheets 038 “Chiavenna”, 021 “Passo dello Spluga”, 022 “Madesimo” and 037 “Bodengo”

Francesco Arrigoni[1], Enrico Pigazzi[1], Giuseppe Colzada[1], Alessia Marinoni[1], Davide Tantardini[1], Giovanni Toffolon[1], Tiziana Apuani[1], Paola Tartarotti[1]

[1] *Dipartimento di Scienze della Terra “A. Desio”, Università degli Studi di Milano (UNIMI), via Luigi Mangiagalli 34, IT-20133 Milano (francesco.arrigoni@unimi.it)*

The study and comprehension of the geodynamic history and tectonic structure of the Central Alps has always represented a key to unravel the emplacement of the whole Alpine structure and to better understand a great range of pre-alpine magmatic and metamorphic events. The extreme geological complexity of this area still presents several unsolved problems, both at local and regional scale. For this reason, a great number of past works focused on this portion of the Alpine chain, trying to address a wide range of problematics and providing interesting insights for the review and understanding of the Alpine orogeny.

New lymph on Central Alps geology has been recently provided by the beginning of new geological surveys in the area of Valchiavenna, lower Valtellina and Alto Lario, in the frame of the CARG Project (Carta Geologica d’Italia alla scala 1:50.000, geological sheets 038 “Chiavenna”, 021 “Passo dello Spluga”, 022 “Madesimo”, 037 “Bodengo”). Four geological sheets are underway in this province, that falls in the middle of the axial zone of the Central Alps, along the Italy-Switzerland national border. It comprehends a predominant mountain area of approximately 770 km^2, characterized by a hostile topography with altitudes ranging from 200 to 3300 m a.s.l.

Most of the territory sees the exposition of different poly-metamorphic basements belonging to the Penninic nappe stack (Adula, Tambo and Suretta Nappes) (Schmid et al., 2004), divided by slices of metasedimentary covers and/or tectonic mèlanges and intruded by some pre-Alpine granitoid bodies (e.g. Truzzo Granite and Roffna Porphyry Complex). The nappe stack is juxtaposed by some structural and paleogeographic uncertain units, as in the case of the Chiavenna Unit, a mafic-ultramafic complex, and the Gruf Complex, that represents one of the less studied units of the Central Alps. Due to the presence of unique high-grade rocks as sapphirine granulites, charnokites and migmatites (Galli et al., 2013), this unit has represented an enigma for its tectonic attribution and it could play a key role in the geological comprehension of the Central Alps. Two tertiary magmatic bodies, the Bergell Pluton and the Novate Granite, emplaced in the south-eastern part of the study area (Berger et al., 1996), surrounded by a multitude of tardive aplitic and pegmatitic swarms, the source of which is still to be definitely identified. Several lineaments cross the study area: the Forcola Line, westward, divides Adula Nappe from Tambo Nappe, while the Engadine Line, eastward, runs alongside the contact between the Chiavenna Unit, the Tambo Nappe and the Gruf Complex. The Insubric Line, to the south, divides the Penninic and Asutroalpine domains from the Southalpine domain.

This work aims at introducing the study area involved in the production of the four geological sheets of the CARG project Valchiavenna, and to present the advances on the field work, through several examples on the main geological features of the area, with the aid of traditional and innovative survey techniques, as digital mapping and drone photogrammetry.
The research on a great number of previous bibliographical works, joined to field work and laboratory analyses, could be a chance to reconsider and solve the main issues of this portion of the Central Alps, providing a starting point for more in-depth studies that can finally shed light on the complex tectonic structure of the Alps

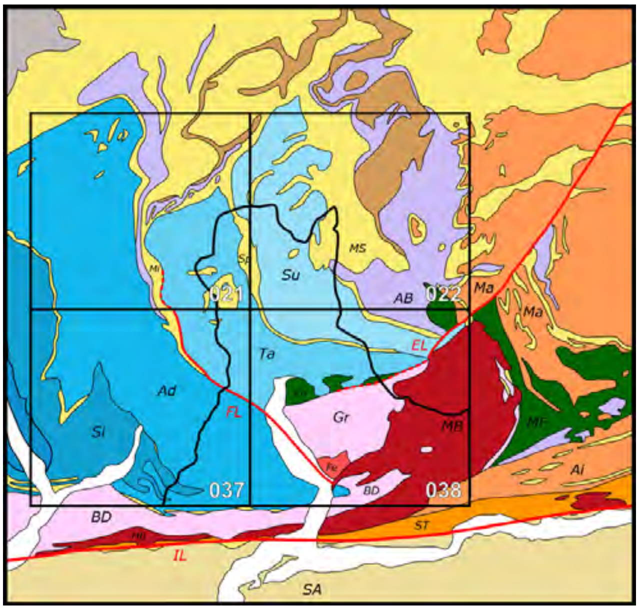

Figure 1. Tectonic map of the Central Alps (redrawn from Spicher, 1980). Abbreviations: AB = Avers Bundnerschiefer; Ad = Adula Nappe; Ai = Indistinct Austroalpine; BD = Bellinzona-Dascio Zone; C = Chiavenna Unit; EL = Engadine Line; Fe = Novate Granite; FL = Forcola Line; Gr = Gruf Complex; IL = Insubric Line; Ma = Margna Nappe; MB = Bergell Pluton; MF = Malenco-Forno Nappe; Mi = Misox Zone; MS = Suretta Cover; SA = Central Alps Southalpine; Si = Simano Nappe; Sp = Splugen Zone; Su = Suretta Nappe;

REFERENCES

Berger, A., Rosenberg, C. & Schmid, S.M. 1996: Ascent, emplacement and exhumation of the Bergell pluton within the Southern Steep Belt of the Central Alps, Schweiz. Mineral. Petrogr. Mitt., 76, 357-382.

Galli, A., Le Bayon, B., Schmidt M.W., Burg, J., Reusser, E, Sergeev, S.A. & Larionov A. 2013: U–Pb zircon dating of the Gruf Complex: disclosing the late Variscan granulitic lower crust of Europe stranded in the Central Alps, Contrib. Mineral. Petrol., 163, 353-378.

Schmid, S.M., Fügenschuh, B., Kissling, E., Schuster, R. 2004: Tectonic map and overall architecture of the Alpine Orogen, Eclogae geol. Helv., 97, 93-117.

Spicher, A. 1980: Tektonische Karte der Schweiz 1:500000; 2.Ausgabe, Schweiz. Geol. Komm., Kümmerly & Frey, Bern.

P 1.4
Long-term surface processes and tectonics interactions: insights from numerical modelling

Attila Balazs[1], Eva Oravecz[1,2], Taras Gerya[1]

[1] Institute of Geophysics, ETH Zurich, Sonneggstrasse 5, CH-8092 Zurich (attila.balazs@erdw.ethz.ch)
[2] Institute of Geography and Earth Sciences, Eotvos Lorand University, Budapest, Hungary

The links between crustal tectonics, mantle dynamics and surface processes such as erosion, sediment transportation and deposition coupled to climatic variations have been long recognized as the main drivers for the evolution of orogens and sedimentary basins. Understanding their complex interactions is challenging because of their wide range of spatial and temporal scales.

In this study, we analyze the surface fingerprints of distinct crustal and mantle processes that are linked to the specific stages of the Wilson cycle, and we will particularly focus on the drivers of surface evolution, in terms of subsidence and uplift patterns. We aim to better understand the feedback mechanisms between tectonics, mantle melting and surface processes during the Wilson-cycle, including the evolution of continental rifts, crustal breakup, structural inversion, oceanic subduction and collision.

Our method is based on conducting and analyzing a series of 2D and 3D thermo-mechanical models by 2D/3D ELVIS and compare the model results with geological and geophysical observational data from orogen-sedimentary basin systems. Tectonics primarily control the main sedimentary transport routes and alters the lithospheric stress field by sediment re-distribution. Sedimentation contributes to increased confining pressure leading to brittle strengthening of the crust, at same time driven by sediment blanketing it increases the crustal thermal gradients leading to ductile weakening effects. Depending on the rate of tectonic processes and the mantle thermal properties different surface processes rates alter the timing and flux of mantle melting, and by that primarily modify the style and further rates of tectonic processes (Balazs et al. 2023).

The topographic evolution of subduction zones is also governed by the links between surface and deep Earth processes. Enhanced sediment subduction lubricates the subduction interface and by water release weakens the overlying mantle. Forearc and back-arc sedimentary basins are sensitive proxies for variable plate and interface rheology. Lower surface processes rates enable a more efficient stress transfer between the plates facilitating back-arc extension. Whereas higher sediment subduction fluxes contribute to enhanced melting leading to arc rifting. The competition between the slab-pull force, upper plate strength and melt-induced weakening are all linked to variations of the subduction velocity and topography (Balazs et al. 2022).

REFERENCES

Balazs A., Faccenna C., Gerya T., Ueda K., Funiciello F., 2022: The dynamics of forearc - backarc basin subsidence: numerical models and observations from Mediterranean subduction zones. Tectonics, 41, e2021TC007078, https://doi.org/10.1029/2021TC007078

Balazs A., Gerya T., May D., Tari G., 2023: Contrasting transform and passive margin subsidence history and heat flow evolution: insights from 3D thermo-mechanical modelling. Geol. Soc. London Special Pub. 524, https://doi.org/10.1144/SP524-2021-94

P 1.5
High-Resolution Tectonic Map of the southwestern sector of the Delémont Basin area, Jura Fold-and-Thrust Belt (Switzerland)

Basilici M.[1], Borderie S.[1], Marro A.[1], Nussbaum C.[2], Mosar J.[1]

[1] *University of Fribourg, Department of Geosciences, Ch. du Musée 6, 1700 Fribourg, Switzerland.*
[2] *Federal Office of Topography Swisstopo, Swiss Geological Survey, Seftigenstrasse 264, 3084 Wabern, Switzerland.*

The arc-shaped, detached Jura fold-and-thrust belt represents the northwestern deformation of the Alpine foreland. It extends from SW to NE for ca. 370 km for a maximum width of 75 km, and is one of the best-studied orogenic arcs in the world. The Jura chain consists of Mesozoic and Cenozoic sandstones, evaporites, marls and mostly limestones deposited in an epicontinental, continental to marine environment, that were folded and faulted since the late Miocene as a consequence of the exhumation of external crystalline massifs due to the Alpine collision. The sedimentary succession is detached from the undeformed Lower Triassic sandstone series of the Buntsandstein unit and the Paleozoic basement, both of which are considered as parts of the mechanical basement (Becker, 2000; Sommaruga et al., 2017). However, inherited basement topography, as well as, late Pliocene reactivation of basement structures interfered with the present geometric configuration of the entire chain (Ustaszewski and Schmid, 2007; Schori et al., 2021). Presently, the Jura fold-and-thrust belt is subdivided into three contrasting tectonic domains from the most deformed to the least deformed areas at the outer arc: the Internal Jura, the external Plateaux and Faisceaux Jura, and the Avants-Monts (Sommaruga et al., 2017).

The study area is located in the detached foreland unit known as Faisceaux, in the External Jura, in the prolongation of the southern Rhine Graben. The dominant structure is the SW-NE oriented Caquerelle anticline which here meets the E-W oriented anticline bordering the southern side of the Delémont Basin. The tectonics of this region is influenced by inherited basement structures associated with the Paleogene intra-continental rifting phase, which corresponds here to the Upper Rhine Graben (Schumacher, 2002). Furthermore, the currently active seismicity appears to be associated with both sedimentary cover (e.g., Saint-Ursanne seismic sequence, 2000, M_L = 3.2) and crystalline basement (e.g., Biel sequence, 2014, M_L = 3.2), but with different orientations of the stress field (Diehl et al., 2015; Lanza et al., 2022). In this southern area, boreholes analysis revealed a contemporaneous horizontal stress field oriented N-S (Becker, 2000).

Gaining a comprehensive understanding of the complex tectonic setting in this area is of primary importance. Notably, this zone encompasses two crucial sites: the Mont Terri underground rock laboratory, offering a platform for studying the functionality of a geological repository, and the Haute-Sorne site, currently under evaluation for a potential deep geothermal project. In this study, we produce a high-resolution tectonic map of the area to provide new insights into the structural setting. The used dataset consists in: (i) a high-resolution field-work in the study area based on the 'National Swiss Map Raster 10' (1:10,000; Federal Office of Topography Swisstopo) which involved the integration of classical field methodologies with digital mapping and drone surveys (this approach was particularly employed for the Glovelier Quarry), (ii) published geological maps 'GeoCover' (Federal Office of Topography Swisstopo), (iii) a 0.5 m cell size digital elevation model 'swissALTI3D' (Federal Office of Topography Swisstopo), (iv) the available earthquakes catalogue (Swiss Seismological Service), and (V) all journals publications related to the geology of the study area and its surroundings.

The resulting map allowed us to investigate the tectonic kinematic development of the Caquerelle anticline and its link to others anticlines bordering the Delémont Basin. Inherited basement structures are a key aspect of the complex tectonic setting yielding structures with very different orientations. We compared stress field orientation with local and region transport direction, determined that the Caquerelle anticline is a transpressive oblique structure with respect to the regional E-W trend and the main transport direction, fact attributed to steps over a basement fault.

REFERENCES:

Becker, A. (2000). The Jura Muntains – and active foreland fold-and-thrust belt? Tectonophysics 321, 381-406. https://doi.org/10.1016/S0040-1951(00)00089-5

Schumacher, M. E. (2002). Upper Rhine Graben: Role of preexisting structures during rift evolution. Tectonics 21(1), 1006. https://doi.org/10.1029/2001TC900022

Ustaszewski, C. & Schmid, M. (2006). Control of preexisting faults on geometry and kinematics in the northernmost part of the Jura fold-and-thrust belt. Tectonics 25, TC5003. https://doi.org/10.1029/2005TC001915

Diehl, T., Deichmann, L., Clinton, J., Kästli, P., Cauzzi, C., Kraft, T., Behr, Y., Edwards, B., Guilhem, A., Korger, E., Hobiger, M., Haslinger, F., Fäh, D., Wiemer, S. (2015). Earthquakes in Switzerland and surrounding regions during 2014. Swiss Journal of Geosciences 108, 425-443. https://doi.org/10.1007/s00015-015-0204-1

Sommaruga, A., Mosar, J., Schori, M., Gruber, M. (2017). Chapter 20 - The Role of the Triassic Evaporites Underneath the North Alpine Foreland. In: Permo-Triassic Salt Provinces of Europe, North Africa and the Atlantic Margins (Eds: Soto, J. I.,

Flinch, J. F., Tari, G.), Elsevier, 447-466. https://doi.org/10.1016/B978-0-12-809417-4.00021-5
Schori, M., Zwaan, F., Schreurs, G., Mosar, J. (2021). Pre-existing Basement Faults Controlling Deformation in the Jura Mountains Fold-and-Thrust Belt: Insights from Analogue Models. Tectonophysics 814, 228980. https://doi.org/10.1016/j.tecto.2021.228980
Lanza, F., Diehl, T., Deichmann, N., Kraft, T., Nussbaum, C., Schefer, S., Wiemer, S. (2022). The Saint-Ursanne earthquakes of 2000 revisited: evidence for active shallow thrust-faulting in the Jura fold-and-thrust belt. Swiss Journal of Geosciences 115(2). https://doi.org/10.1186/s00015-021-00400-x

P 1.6
Investigating S-wave anisotropy in the Rotondo granite by crosshole seismic surveys

Kathrin Behnen[1], Marian Hertrich[1], Hansruedi Maurer[1], Domenico Giardini[1]

[1] *Institute of Geophysics, ETH Zürich, Sonneggstrasse 5, CH-8092 Zürich (kathrin.behnen@erdw.ethz.ch)*

Introduction

The BedrettoLab is an open and extendable research infrastructure of ETH Zurich. It is located in the Bedretto tunnel in the Swiss Alps. Its primary mission is to advance transdisciplinary research in geoenergy applications, such as deep geothermal reservoir development in crystalline rocks, and in frontier geoscience research, such as earthquake physics and predictability. Laboratories in the deep underground bridge the gap between natural scales (kilometres and above) and the research-lab scale (centimetres). This facility is extremely valuable to Earth scientists for hypothesis driven, fundamental research as well as for technology demonstrations. In a natural and realistic setting, experiments such as inducing micro-earthquakes or reservoir stimulation at the scale of tens to hundreds of meters can be conducted under controlled and repeatable conditions, observed closely by hundreds of multi-parameter sensors. Currently, about 50 scientists, engineers and technicians are part of the core BedrettoLab Team.

In the present project we aim at testing the hypothesis of stress induced anisotropy by the ambient state-of-stress in the volume of investigation. We present the initial results of comprehensive crosshole seismic surveys in three adjacent boreholes and discuss novel approaches of analysis and data acquisition to exploit a maximum information content of the recorded wavefields.

Field data

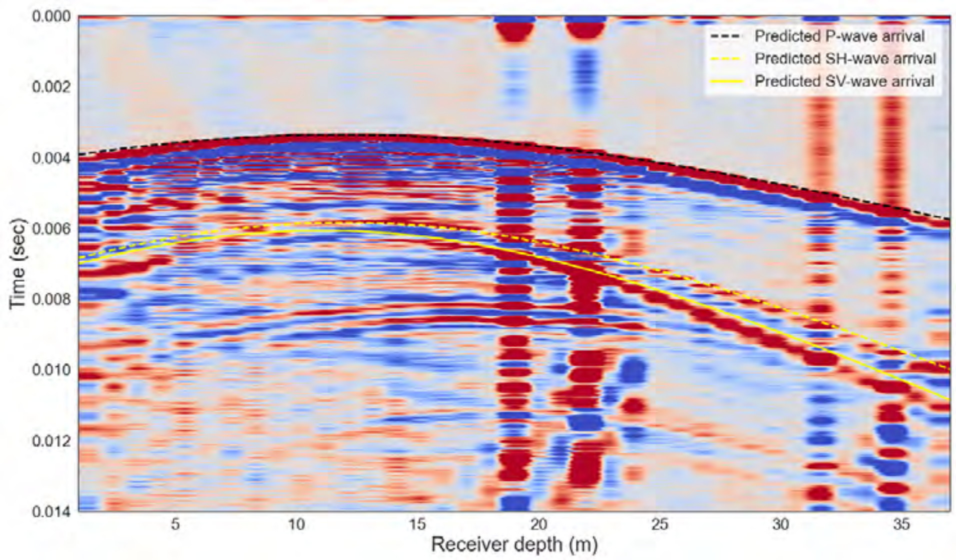

Figure 1 Shot gather of a sparker shot in borehole SB2.3 at a depth of 8m and the hydrophone chain in borehole SB2.1 from 1-37m. Synthetic traveltimes for P-, SV-, and SH-waves arrivals are based on manually adopted Thomsen parameters.

We acquired several comprehensive crosshole seismic surveys in a set of three boreholes of 30-40m length at dips of 0°, 20°, and 30°, oblique to each other. This setup allows us to cover many different ray orientations, which is crucial for seismic anisotropy analyses.

We used different sparker sources and recorded the signals either on hydrophones or 3-component geophones to determine the traveltimes of the different wave types. A typical shot gather of a hydrophone string is shown in figure 1. It clearly shows the P-wave arrivals and S-wave splitting, verifying the presence of seismic anisotropy in the test volume. The arrival times can be explained by synthetic traveltimes based on manually adopted Thomsen parameters, describing a tilted transverse isotropic medium (TTI).

The 3C geophone data enable a better separation of the different S-wave arrivals by rotating the different components to maximize the amplitude of the individual wavefield components. This approach allows us to pick the arrival time of both, the faster SH- and slower SV-waves.

In figure 2 we plot the measured apparent velocities of the different wave types (dots in the foreground) together with the synthetic velocities (transparent I the background). The velocities are shown as stereo plot with rays at 0° dip (horizontal) plotted at the outer rim and steeper ray paths plotted further to the centre. The observed data of P- and SH-waves show a clear pattern of tilted anisotropy. However, the SV-wave velocities still show inconsistencies with the assumed symmetry.

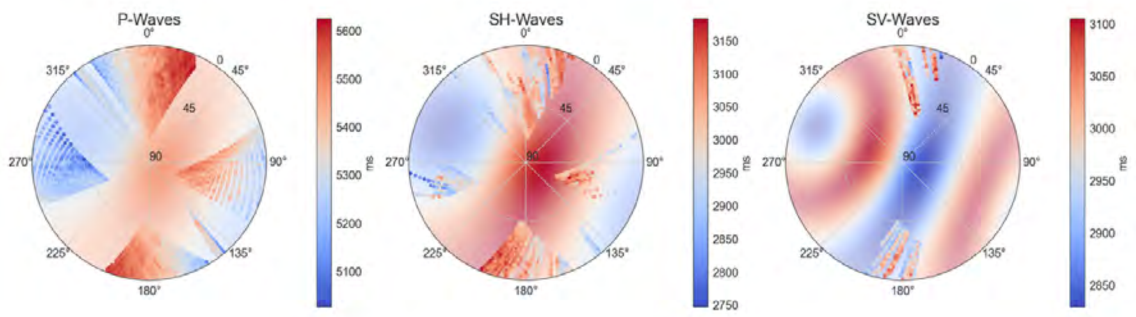

Figure 2 Comparison of the observed velocities (top layer) with the optimized TTI velocity model (background). Each ray path is plotted as a point in the stereo net representation as a function of its dip and azimuth.

Conclusions

The crosshole survey provides a very rich dataset, including prominent shear wave arrivals and partially indications of shear wave splitting, as predicted for an anisotropic medium. In our analysis we carefully investigate the ambiguity of anisotropy estimates and borehole trajectories, novel approaches of wavefield decomposition by oriented borehole sources and three-component geophones and application of sweep/chirp sources. We support our analysis by theoretical investigations of stress-induced anisotropy (Maitra 2021) and laboratory measurements on core samples with state-of-the-art laboratory machines (www rpmlab.ethz.ch).

REFERENCES

Maitra, M., & Al-Attar, D. 2021: On the stress dependence of the elastic tensor, Geophysical Journal International, 225(1), 378–415.

Thomsen, L. 1986: Weak elastic anisotropy, Geophysics, 51(10), 1954–1966.

P 1.7
Sensitivity analysis of stress field in the Geneva Basin and adjacent Jura fold-and-thrust belt.

Sandra Borderie[1], Jon Mosar[1], Adeline Marro[1], Matteo Basilici[1], Nicolas Clerc[2] and Michel Meyer[3]

[1] *Departement of Geosciences, University of Fribourg, Chemin du Musée 6, CH-1700 Fribourg (sandra.borderie@unifr.ch)*
[2] *Office cantonal de l'environnement, Service de géologie, sols et déchets, Quai du Rhône 12, CH-1205 Genève*
[3] *Services Industriels de Genève, Chemin du Château-Bloch 2, CH-1219 Le Lignon.*

The stress field at depth is an important parameter influencing the design of subsurface structures, particularly in the context of geothermal energy installation. The distortion of the regional stress field due to local-scale features such as sedimentary and tectonic structures or topography remains often insufficiently characterized.

Findings from previous studies in the Geneva Basin show the significance of the tectonic wedge's shape in localising deformation and on the resultant stress field. These studies also emphasize the role of friction coefficients along pre-existing faults on future deformation and stress distribution.

To go further, we conduct a sensitivity analysis on the stress field along a balanced cross-section extending from the Salève Anticline (Geneva Basin) to the front of the Jura fold-and-thrust belt. Notably, this section relies on new interpretations of seismic lines and on a new structural map of the Geneva Basin. The study area is detached from the basement by a basal Triassic *décollement* in which the main structures are rooted.

For the modelling, mechanical properties of rocks are estimated using available log data from well Humilly-2. Friction coefficients are calculated using the Lal Vp correlation method (Lal, 1999). The main tested parameter for the modelling is the effective friction along the pre-existing faults.

We expect the results to give a better understanding of the stress conditions in the study area and to estimate the impact of the local-scale features such as basement topography, surface topography, and existing faults.

REFERENCES

Lal, M. (1999, April 20). *Shale Stability: Drilling Fluid Interaction and Shale Strength*. SPE Asia Pacific Oil and Gas Conference and Exhibition. https://doi.org/10.2118/54356-MS

P 1.8
Controls on exhumation velocities for an Alpine-type burial-exhumation cycle: a combined deterministic and statistical analysis

Candioti L. G., Schmalholz S. M., Duretz T.

Ultra-high pressure (UHP) mineral assemblages have been found in exhumed continental crustal rocks of the European Western Alps. Geochronological and metamorphic studies on some tectonic units like the Brossasco-Isasca unit (Dora Maira massif) suggest exhumation velocities as fast as or even faster than subduction velocities. The dynamics that drive such fast UHP-rock exhumation remain debated.

To evaluate the processes that govern the exhumation velocities, we perform two-dimensional petrological thermo-mechanical deterministic models. The models simulate the burial-exhumation cycle of continental and oceanic units under Alpine-type orogenic conditions. We conducted 39 simulations with differences in (i) the strength of the continental plates, (ii) the thickness of the plate interface, (iii) frictional softening, (iv) the presence of heterogeneities in the continental upper crust, and (v) pre-existing shear zones inherited from passive margin formation. We statistically analyze the simulations by evaluating results that are recorded by 270,000 continental and oceanic marker points per simulation. During burial and exhumation, the markers record quantities like maximum exhumation velocity and burial depth, as well as peak pressure and temperature. We statistically analyze the marker data set to find correlations between exhumation velocities and quantities such as crustal strength or maximum buoyancy of buried rock units. We compare the numerically generated data sets to data recorded by characteristic Alpine structural units.

Individual markers show that oceanic units can be exhumed from shallow depths with up to 6 cm/yr. Continental units can be exhumed with up to 2-3 cm/yr from depths of up to 150 km. Individual markers of these units record a peak temperature of ca. 600-650 °C and a peak pressure greater than 40 kbar.

P 1.9
Deciphering carbonate deformation through the Brittle-Ductile Transition: new methodological and regional insights from the SW Helvetic nappes, Switzerland

Giovanni Luca Cardello[1], Stefano M. Bernasconi[2], Maria G. Fellin[2], Meinert Rahn[3], Riccarda Rosskopf[2], Neil Mancktelow[2]

[1] *Department of Chemistry, Physics, Mathematics, and Natural Sciences, Sassari University, Via Piandanna, 4, I-07100 Sassari (glcardello@uniss.it)*
[2] *Department of Earth Sciences, ETH, Zürich, Sonneggstrasse 5, CH-8092 Zürich*
[3] *Swiss Federal Nuclear Safety Inspectorate, Industriestrasse 19, CH-5201 Brugg*

The exhumation across the brittle-ductile transition (BDT) within the SW-Helvetic nappe-stack has been investigated using a new multimethological approach that integrates optical observations, thermochronology, stable isotopes, and clumped-isotope thermometry. This approach aims to constrain the time and temperature history of BDT deformation processes in carbonates. Our results show that single grain (U-Th)/He zircon and apatite fission track ages support new modelled burial/exhumation curves from different nappes, allowing to infer also the thermal path of the Wildhorn Nappe within the Rawil Depression. The latter is a prominent doubly plunging hinge zone in between the External Crystalline Massifs of SW Switzerland, whose post-nappe faulting development during the Tortonian-Early Pliocene is hereby related to the exhumation of the Aar Massif with differential exhumation rates from its most depressed area to its eastern side of about 0.2 km/Myr. By calculating and modelling the rock-buffered clumped-isotope temperatures (ranging from 216° C to 55 °C) from the Wildhorn Nappe, we indirectly date the occurrence of BDT processes. To do that we take the well-studied Rezli (Gasser and Mancktelow, 2010) fault as an example. Selected modelled microstructural types show that mylonitization related shear heating is indirectly dated as Early Miocene, while progressive embrittlement involving cataclasis started in the Late Miocene. Our results improve the understanding of the thermal evolution, tectonic activity and exhumation path of carbonates through the BDT in the Rawil Depression and shed light on analogous seismogenic carbonate-rich crustal sections.

REFERENCE

Gasser, D., & Mancktelow, N. S. (2010). Brittle faulting in the Rawil depression: field observations from the Rezli fault zones, Helvetic nappes, Western Switzerland. Swiss Journal of Geosciences, 103(1), 15-32.

P 1.10
Structural analysis of a highly oblique rift zone influenced by a transform fault in southwest Iceland

Yohann Chatelain[1], Joël Ruch[1], Elisabetta Panza[1]

[1] *Department of Earth Sciences, University of Geneva, Rue des Maraîchers 13, CH-1205, Genève (yohann.chatelain@etu.unige.ch)*

The South-Iceland-Seismic Zone and the Reykjanes Peninsula (southwest Iceland) are part of an active shear zone and of the plate boundary that separates the North American from the Eurasian plates. The Reykjanes Peninsula is a highly oblique rift zone with well-developed volcanic and hydrothermal systems. To the East, the SISZ corresponds to a transform fault zone with historical large earthquakes of up to M_w7, without noticeable volcanic activity.

These two regions are affected by a broad left-lateral shear zone oriented N070, dissected by NS right lateral strike-slip faults forming a bookshelf system suggesting a common tectonic driver. The connection between the two regions remain poorly understood by lack of integrative structural analysis that would help for for a better understanding of the complex tectonic setting.

Here we used photogrammetry with extensive drone mapping to identify and analyse several main NS fault system in both areas, along an EW sector of 140 by 25 km. This allow performing a robust fault population analysis and detailed structural maps. Using drone imagery, we obtained high-resolution DEMs (Digital Elevation Map) and orthophotos (3-4 cm GSD). We collected also structural field observations for fracture opening kinematics. We further complemented our dataset with earthquake catalogues to look for ongoing seismic activity, looking at seimic swarm orientations and earthquake event depths.

We worked on 20 NS fault across Reykjanes and the SISZ. All of them show multiple scales of en-echelon pattern with fractures, arrays, fault segments and compressional push-ups. We estimate that the direction and geometry of structures strongly suggest a structural continuity between the SISZ and the Reykjanes Peninsula. We also observe a decrease of the length of the NS fault segments, together with a decrease of the earthquake magnitudes and epicenter depth toward West. We further discuss that the presence of magma and hydrothermal systems in Reykjanes could increase the geothermal gradient, impending the occurences of large earhtquakes due to broaden ductile areas. This has direct implication when assessing seismic hazards in this populated area.

P 1.11
Stress Orientations in northern Switzerland: New Insights from Focal Mechanisms and Borehole Data

Tobias Diehl[1], Oliver Heidbach[2], Julia Heilig[3], Martin Schönball[4], Silvio Giger[4], John Reinecker[5], Michael Schnellmann[4], Stefan Wiemer[1]

[1] Swiss Seismological Service, ETH Zurich, 8092, Switzerland (tobias.diehl@sed.ethz.ch)
[2] Helmholtz Zentrum Potsdam, Deutsches GeoForschungsZentrum GFZ, 14473 Potsdam, Germany
[3] Department of Earth Sciences, ETH Zurich, 8092, Switzerland
[4] Nagra (National Cooperative for the Disposal of Radioactive Waste), Wettingen, Switzerland
[5] Geostress Consultant, Untere Höhbergstr 5, 72074 Tübingen, Germany

The orientation of the present-day stress field within the crust is an important parameter to assess the potential for reactivation of pre-existing faults. Past studies comparing stress data from borehole logs and earthquakes focal mechanisms revealed differences in parts of the northern Alpine foreland. While borehole data mainly sample the Mesozoic sediments, the majority of the earthquakes occur in the Paleozoic basement. The results of earlier studies based on compilations of a limited number of boreholes indicated a change of stress orientation with depth and a possible mechanical detachment between the sediments and the basement due to an evaporitic horizon in the Muschelkalk. In particular, studies reported a 15°25° counter-clockwise rotation of the maximum horizontal stress orientation S_{Hmax} in the basement with respect to Mesozoic sediments e.g. in the boreholes Sonnengarten and Schafisheim.

We revisit these interpretations and integrate in our new stress data compilation the results of a comprehensive re-analysis of old borehole image logs as well as a significant number of new data from recently drilled deep boreholes that cross the sedimentary infill and also touch the upper parts of the basement. We also integrate new earthquake focal mechanisms from the past ten years that have not been used for such a study.

In general, we see in both datasets a large-scale counter-clockwise rotation of the S_{Hmax} orientation from East to West. We still see in a few boreholes an abrupt change of the S_{Hmax} orientation in the Muschelkalk layers and will discuss if this re-orientation is also reflected in the S_{Hmax} orientation derived from the focal mechanisms taking into account the inherent uncertainties of these data. Furthermore, we will present a revised seismological analysis of the hypocenter location and the focal mechanism of the M_L 3.2 Eglisau event that occurred on September 12, 1999 and discuss these results in the context of the regional stress field from our new stress-data compilation.

P 1.12
Tracking surfaces in global scale geodynamic models

Timothy Gray[1], Taras Gerya[1], Paul Tackley[1,2]

[1] *Institute of Geophysics, ETH Zürich, Sonneggstrasse 5, 8048 Zürich (timothy.gray@erdw.ethz.ch)*

The study of coupled Earth systems, and in particular the coupled interactions between the lithosphere, atmosphere, and biosphere, have received greater attention in recent years (Gerya et al. 2020). Interactions between these systems occur primarily at the surface, and are driven on the large scale by topographic and bathymetric evolution controlled by deep mantle processes. However, due to the large difference in length scales between the mantle and the surface, it is difficult to capture topographic evolution to a high degree of accuracy in existing global mantle convection models including a free surface boundary condition.

Many global mantle convection models that model a free surface use a marker-in-cell technique with a layer of "sticky air" (i.e. material with the density of the air and very low viscosity, which is still much higher than that of real air) to represent the surface. However, this method requires a high number of markers near the surface to capture the topographic changes accurately. This increases the computational cost and motivates alternative methods of tracking the interface between the air and rock layers, as is done often in existing multiphase fluid flow codes. A volume of fluid method with piecewise-linear interface reconstruction is a suitable method for tracking a surface in an efficient way with the sub-grid level topographic resolution that is needed for coupling geodynamic models to models of other Earth systems.

We present benchmarks of an implementation of a volume of fluid method within the existing advanced mantle convection code StagYY (Tackley, 2008) using the unsplit volume of fluid library gVOF (López & Hernández, 2022). Moreover, we compare the results of these VOF methods with Lagrangian methods of tracking free surfaces. The method works for both 2D and 3D geometries, and on both Cartesian and non-Cartesian grids. Models of global scale topography and evolution produced using StagYY may later be used as a tool for further studies on the coupling of mantle dynamics with modelling of the landscape, and the evolution of the atmosphere and biosphere.

REFERENCES

Gerya, T., Stern, R., Pellissier, L., & Stemmler, D. (2020). Bio-geodynamics of the Earth: State of the art and future directions. EGU2020, EGU2020-10657.

López, J., & Hernández, J. (2022). gVOF: An open-source package for unsplit geometric volume of fluid methods on arbitrary grids. Computer Physics Communications, 277, 108400.

Tackley, P. J. (2008). Modelling compressible mantle convection with large viscosity contrasts in a three-dimensional spherical shell using the yin-yang grid. Physics of the Earth and Planetary Interiors, 171(1), 7–18.

P 1.13
Viscous strain localization by multi-scale anisotropy development: Numerical modelling and upscaling

William R. Halter[1], Roman Kulakov[2], Thibault Duretz[1,2], Stefan M. Schmalholz[1]

[1] *ISTE, Université de Lausanne, Géopolis, CH-1015 Lausanne (william.halter@unil.ch)*
[2] *Institut für Geowissenschaften, Goethe-Universität Frankfurt, DE-60438 Frankfurt a. M.*

Viscous strain localization and associated softening mechanisms are important for subduction initiation and the generation of tectonic nappes. Many strain localization and softening mechanisms have been proposed as being important during the viscous, creeping, deformation of rocks, such as thermal softening, grain size reduction, reaction-induced softening, or anisotropy development. However, which localization mechanism is the controlling one and under which deformation conditions remains debated. In this contribution, we focus on strain localization in viscous rock due to the generation of anisotropy. Particularly, we focus on multi-scale anisotropy evolution in shear zones with many strong or weak inclusions, representing for example porphyroclasts. The shape change and relative alignment of the inclusions during shearing generates an anisotropy on the scale of the inclusions, termed here macroscale. We spatially resolve this macroscale anisotropy in the numerical simulations. Additionally, we consider the evolution of a microscale anisotropy in the shear zone matrix, representing the formation of a mylonitic foliation. We do not spatially resolve this microscale anisotropy but model it with an anisotropic flow law that involves different normal and tangential viscosities. We calculate the finite strain ellipse during shearing and use its aspect ratio as proxy for the anisotropy that governs the ratio of normal to tangential viscosity. To track the orientation of the anisotropy during deformation we apply a director method.
We perform numerical simulations to evaluate the impact of micro- and macroscale anisotropy on strain softening and localization. We further discuss the quantification of effective anisotropies that can be used for upscaling, for example for lithospheric scale numerical models.

REFERENCES
Duretz T., R. de Borst and P. Yamato (2021), Modeling Lithospheric Deformation Using a Compressible Visco-Elasto-Viscoplastic Rheology and the Effective Viscosity Approach, Geochemistry, Geophysics, Geosystems, Vol. 22 (8), e2021GC009675

P 1.14
Revisiting the Stress Field of Switzerland with Focus on the South-Western Alps: Insights from an updated Focal-Mechanism Catalog

Julia Heilig[1], Tobias Diehl[2], Marco Herwegh[3], Sandro Truttmann[3], Stefan Wiemer[2],

[1] *Department of Earth Sciences, ETH Zürich, Sonneggstrasse 5, CH-8092 Zürich (jheilig@student.ethz.ch.ch)*
[2] *Swiss Seismological Service SED, Sonneggstrasse 5, CH-8092 Zürich*
[3] *Institute of Geological Science, University of Bern, Baltzerstrasse 1+3, CH-3012 Bern*

The state of stress of a region plays an important role in seismic hazard assessment. Especially the evaluation of the reactivation susceptibility of pre-existing faults is thus a crucial component of the hazard assessment of natural and anthropogenic seismicity. In addition, mapping the stress field also helps to understand regional seismotectonic processes. A common procedure to assess the state of stress and its regional variations is the analysis of earthquake focal mechanisms (FMs). In this study, we aim to update the regional stress field of Switzerland and improve its spatial resolution with a special emphasis on the Rawil Fault Zone (RFZ) located in southwestern Switzerland. This is achieved by performing stress inversions of FM solutions calculated by the Swiss Seismological Service (SED). For this study, the existing FM catalog of the SED was updated and the final catalog contains 471 FMs, which represents a significant improvement over previous studies in Switzerland (e.g., Kastrup et al. 2004). The stress inversions are performed with the MATLAB package MSATSI by Martinez-Garzon et al. (2014). We grouped the FM data with different methods in order to get the best possible spatial resolution, while maintaining the stability of the inversions. In many places we achieved a higher spatial resolution compared to previous studies. However, the FMs are highly clustered in space, which required a zonation approach in order to get meaningful results. In the internal parts of the Alps, the resulting stress field describes a stress regime dominated by strike-slip faulting with a tendency to a transtentional regime north and a normal-faulting regime south of the Penninic Thrust. At regional scales, our results confirm the tendency of counterclockwise rotation of the P- and T- axis and a clear change in orientation between the mean stress field in the foreland and the Alpine belt. An in-depth analysis of the RFZ's stress field provides new insights into the complexity of the RFZ with predominatly strike-slip mechanisms in the crystalline basement and predominantly transtensional tendencies in the shallower parts and the sedimentary cover. Interactions between the stress field in the basement and the pre-existing faults in the sedimentary layer, in combination with possible vertical changes in the stress regime, might explain the observed complexity of the RFZ.

REFERENCES

Martinez-Garzon, P., Kwiatek, G., Ickrath, M., & Bohnhoff, M. 2014: MSATSI: A MATLAB Package for Stress Inversion Combining Solid Classic Methodology, a New Simplified User-Handling, and a Visualization Tool, Seismological Research Letters, 85(4), 896–904. https://doi.org/10.1785/0220130189

Kastrup, U., Zoback, M. L., Deichmann, N., Evans, K. F., Giardini, D., & Michael, A. J. 2004: Stress field variations in the Swiss Alps and the northern Alpine foreland derived from inversion of fault plane solutions: STRESS FIELD IN SWITZERLAND, Journal of Geophysical Research: Solid Earth, 109(B1). https://doi.org/10.1029/2003JB002550

P 1.15
Would you like to (help) constrain the subsurface structure of the Balmuccia peridotite body?

György Hetényi[1],Ludovic Baron[1], Matteo Scarponi[1], Shiba Subedi[1], Konstantinos Michailos[1], Fergus Dal[2], Anna Gerle[3], Benoît Petri[4], Jodok Zwahlen[1], Antonio Langone[5], Andrew Greenwood[6], Luca Ziberna[7], Mattia Pistone[8], Alberto Zanetti[5], Othmar Müntener[1]

[1] *University of Lausanne, Switzerland (gyorgy.hetenyi@unil.ch)*
[2] *MSc of Geomatics, ETH Zurich, Switzerland*
[3] *Independent*
[4] *University of Strasbourg, France*
[5] *University of Pavia & CNR, Italy*
[6] *Montanuniversität Leoben, Austria*
[7] *University of Trieste, Italy*
[8] *University of Georgia, USA*

The Balmuccia peridotite body (Fig. 1, Quick et al. 2003) has been studied since decades, and is a future target of the Drilling the Ivrea-Verbano zonE (DIVE) drilling project (www.dive2ivrea.org). There is currently disagreement about the subsurface structure of this peridotite body: while former geological models suggest a lenticular shape with no root (Quick et al., 2003), more recent geophysical studies point at the peridotite outcrop being the tip of a “mantle-berg”, the apex of a high-density and high-seismic-velocity anomaly reaching the surface (Scarponi et al., 2020, 2021; Ryberg et al., 2023).

We here propose to further constrain the subsurface continuation of the outcropping Balmuccia peridotite by building and inverting for a 3D density model. To avoid our own personal bias in model construction hypotheses and the inversion, we propose a modelling challenge that is OPEN to any researcher or group of researchers. In this frame, we will make the input data listed below freely available, and expect colleagues to return their structural model(s). All submitted and documented model solutions, including assumptions and uncertainties, will be compared during a dedicated workshop, ultimately resulting in a joint publication.

The shared dataset is composed of the following:

- 150 new gravity data points on and around the Balmuccia peridotite,
- contours of 4 main lithologies and structural dip indicators at the surface,
- related rock densities based on in situ samples (both literature and new),
- a 10-metre resolution digital elevation model.

Altogether, this pre-processed dataset provides a common basis to set up a 3-D model, and to constrain its structure and density distribution at depth.

Interested researchers and groups are invited to contact the authors to obtain a copy of the dataset.

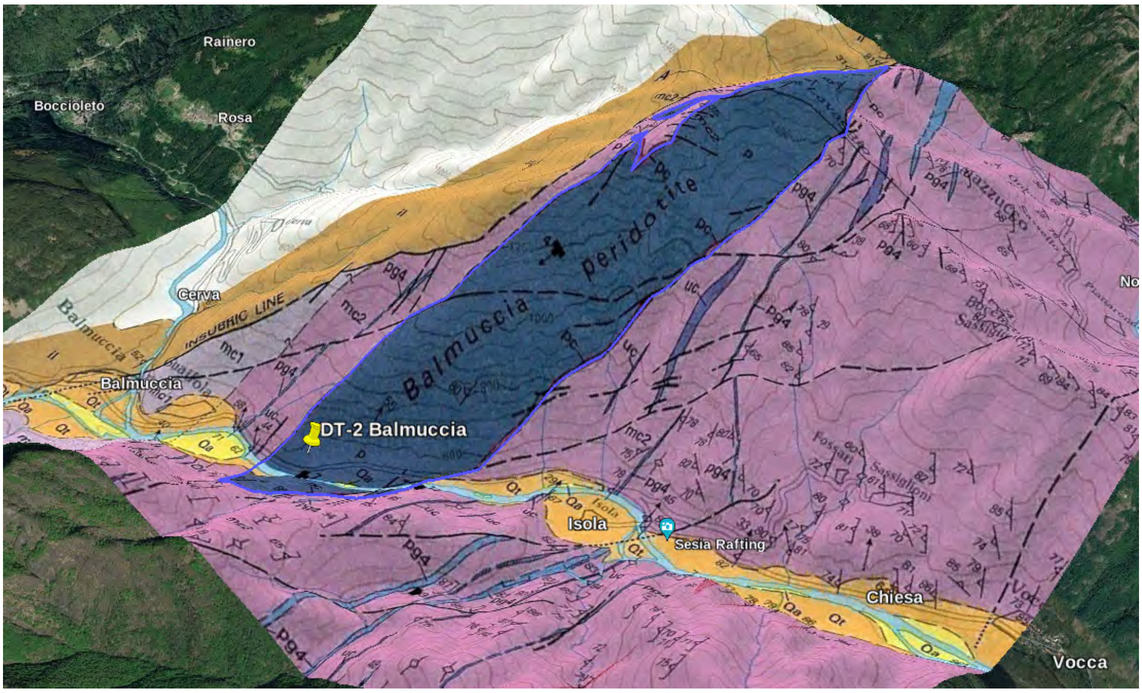

Figure 1. Geological map of Quick et al. (2003) draped over GoogleEarth© topography, with the exposed Balmuccia peridotite body in purple. The centre of the ca. 4.4 km long peridotite outcrop is at ca. 45.84°N, 8.16°E, and North is approximately towards the upper right corner of the figure.

REFERENCES

Quick, J. E., Sinigoi, S., Snoke, A. W., Kalakay, T. J., Mayer, A., and Peressini, G. 2003: Geologic map of the Southern Ivrea-Verbano Zone, Northwestern Italy, U.S. Geological Survey, Reston, Virgina, VA.

Ryberg, T., Haberland, C., Waverzinek, B., Stiller, M., Bauer, K., Zanetti, A., Ziberna, L., Hetényi, G., Müntener, I., Weber, M. H., and Krawczyk, C. M. 2023: 3-D imaging of the Balmuccia peridotite body (Ivrea–Verbano zone, NW-Italy) using controlled source seismic data, Geophys. J. Int., 234, 1985–1998.

Scarponi, M., Hetényi, G., Berthet, T., Baron, L., Manzotti, P., Petri, B., Pistone, M., and Müntener, O. 2020: New gravity data and 3D density model constraints on the Ivrea Geophysical Body (Western Alps). Geophys. J. Int., 222, 1977–1991.

Scarponi, M., Hetényi, G., Plomerová, J., Solarino, S., Baron, L., and Petri, B. 2021: Joint seismic and gravity data inversion to image intra-crustal structures: the Ivrea geophysical body along the Val Sesia Profile (Piedmont, Italy), Front. Earth Sci., 9, 671412.

P 1.16
Geological constraints on the seismic anisotropy of Rotondo granite within the Bedretto Tunnel

Emily R. Hinshaw[1], Whitney M. Behr[1], Alba Zappone[2], Alberto Ceccato[1], Carolyn Tewksbury-Christle[3]

[1] *Geological Institute, Department of Earth Sciences, ETH-Zürich, Sonneggstrasse 5, CH-8092 Zürich (ehinshaw@erdw.ethz.ch)*
[2] *Institute of Geophysics, Department of Earth Sciences, ETH-Zürich, Sonneggstrasse 5, CH-8092 Zürich*
[3] *Geosciences Department, Fort Lewis College, 1000 Rim Drive, Durango, CO, 81301, USA*

Within the Gotthard massif of the Swiss Alps, the 5km Bedretto Tunnel provides a unique opportunity to study geothermal techniques and related seismicity at high resolution with dense monitoring capabilities. Multi-scale geological characterization of rock bodies and structures within the tunnel can help with interpretation of seismic wave propagation patterns and can provide insights into how small-scale features aggregate to produce seismic anisotropy at the kilometric lengthscale. The tunnel is primarily composed of Rotondo granite, which is commonly assumed to be isotropic; however, this granite also exhibits abundant faults, compositional variations, and tectonitic to mylonitic shear zones, which may affect seismic anisotropy within the massif.

In this study, we investigate the geological constraints on seismic anisotropy of the Rotondo granite by characterising macro-structural compositional domains, faults, and shear zones. These data are used to constrain the seismic velocity and seismic anisotropy, which we calculate using the Matlab Seismic Anisotropy Toolbox (MSAT).

At the kilometer-scale, the Bedretto Tunnel internally exposes ~1km of Prato and Tremola series (amphibolite-facies schists and gneisses) and ~4 km of Rotondo granite. The Rotondo granite is compositionally 25-35% Quartz, 20-40% K-Feldspar, 10-25% Plagioclase, 3-8% Biotite, and <5% accessory minerals. Fault densities vary at the 10-meter scale from >40 to 0 measurable faults. Fault planes are generally steeply dipping (70-80°) towards 330°– some are decorated by chlorite and others contain clay gouge (in some cases fluid-saturated). Several distributed brittle and ductile shear zones (1-10 m width) also occur with minimal compositional variation from the typical granite and similar orientations to discrete faults (70-80°/330-340). A small volume percentage (<2%) of ductile shear zones are 60% Quartz and 40% Biotite, representing sheared lamprophyre dikes. At the micro-scale, mineralogical percentages and degree of alignment between crystallographic preferred orientations control the anisotropy, with biotite being the most anisotropic and most well-aligned mineral.

For each of the structural elements (undeformed/isotropic, fractured media, ductile shear zone) observed in the tunnel, we report the maximum anisotropy in percent. The undeformed granitic bulk rock estimates Vp/Vs = 1.76. In the end-member case where individual minerals are assumed to be 100% aligned in uniform orientation, quartz-biotite shear zones produce greater anisotropy (~37% Vp, ~57% Vs, Vp/Vs = 1.53) while granitic shear zones have a lower anisotropy (~26% Vp, ~33% Vs, Vp/Vs = 1.49) but higher absolute velocities. However, granitic shear zones have a higher impact on overall tunnel anisotropy, in comparison with quartz-biotite shear zones, because they comprise a greater percentage of the total tunnel volume.

When the anisotropic contribution of shear zones and faults is calculated for an averaged volume in the tunnel, without spatial context, the resulting anisotropy is <1%. However, when structural fabrics are spatially-contextualized in both fabric orientation and relative distribution, the total Vp anisotropy instead reaches between 3-10% (depending on the medium for fracture gouge material) and Vp/Vs is well below expected values for a typical granitic rock. Future work will include a more accurate understanding of how fracture gouge and permeability impact the overall seismic anisotropy calculation. We also plan to explore the directional dependence of seismic anisotropy and velocity on horizontal and vertical incidence waves within the Bedretto Tunnel.

P 1.17
Constraining the mechanical properties of glaucophane deformed via dislocation-controlled mechanism(s) with experiments in the general shear geometry

Lonnie J. Hufford[1], Leif Tokle[1], Whitney M. Behr[1], Luiz F. G. Morales[1,2], Claudio Madonna[1]

[1] *Structural Geology and Tectonics Group, Geological Institute, Department of Earth Sciences, ETH Zürich, Zürich, Switzerland (lonnie.hufford@erdw.ethz.ch)*
[2] *Scientific Center for Optical and Electron Microscopy (ScopeM), ETH Zürich, Otto-Stern-Weg 3, 8093, Zürich, Switzerland*

Glaucophane is a primary strain-accommodating mineral in subducted oceanic crust at blueschist facies conditions and important for our understanding of subduction dynamics. Dislocation-related mechanisms are attributed to glaucophane deformation in naturally deformed rocks, providing a need to constrain its mechanical properties. We present constant rate, strain rate stepping and load stepping experiments in a Griggs apparatus in the general shear geometry to investigate the mechanical properties of glaucophane deforming via dislocation-controlled mechanism(s). The starting material consists of glaucophane powder separated from MORB-affinity blueschists from Syros, Greece with grain size ranges of 63-355 μm (constant rate, strain rate stepping), 75-90 μm (constant rate) and ~30 μm (constant rate, load stepping). All experiments were conducted at 1.0 GPa between 650 and 750°C. Constant rate experiments were deformed to γ~2, while load stepping experiments had ~7 steps and strain rate stepping experiments had 4-5 steps. Mechanically, the stress exponents range from 2.2-3.9. Microstructurally, strain in the load stepping experiments is homogeneously distributed across the sample width, while strain is more localized in the constant rate and strain rate stepping experiments. Undulose extinction is observed in most grains, consistent with dislocation activity; however, subgrain development exists only to a minor extent with little to no evidence for subgrain rotation, suggesting limited dislocation climb at deformation conditions. Kinking is observed in all the samples and is the primary mechanism for grain size reduction in the constant load experiments while the constant rate and strain rate stepping experiments display evidence of a brittle mechanism responsible for early grain size reduction before reaching mechanical steady-state. Based on our observations we interpret the samples to have deformed by a glide-controlled mechanism at mechanical steady-state. We fit our load stepping mechanical data to an exponential flow law representative of glide-controlled creep. We find an activation enthalpy of 359 +/- 31 kJ/mol. Extrapolating this flow law to geologic conditions, it predicts viscosities greater than dislocation creep in quartz and less than dislocation creep in eclogite.

P 1.18
Tomography of P- and S-wave attenuation of Switzerland and surrounding regions: imaging seismotectonic processes in the Central Alps

Federica Lanza[1], Tobias Diehl[1], Donna Eberhart-Phillips[2], Marco Herwegh[3] , Donath Fäh[1] & Stefan Wiemer[1]

[1] *Swiss Seismological Service, Swiss Federal Institute of Technology, ETH Zurich, Sonneggstrasse 5 CH-8092 Zurich (federica.lanza@sed.ethz.ch)*
[2] *GNS Science, Private Bag 1930, Dunedin 9054, New Zealand*
[3] *University of Bern, Institut für Geologie, Baltzerstrasse 1+3 CH-3012 Bern*

We present 3-D Qp and Qs attenuation models of the crust for Switzerland and surrounding regions. The 3-D inversions derive the quality factor Q (1/attenuation) using path attenuation t^* observations for > 5000 distributed earthquakes recorded on permanent and temporary stations for the period 2002-2023. We followed a procedure of gradational inversions, in which a series of inversions are performed on decreasing size grids and varied size autolinking patterns based on the grid nodes' derivative-weight sum values. This method allows to obtain a reasonable Q model everywhere despite the spatially varying data distribution and to resolve deeper parts of the model thanks to including longer distances phases. The resulting Qs and Qp models show large and small-scale features in the upper crust, which are consistent with a recently improved high-resolution velocity models of the same region and serve to refine the interpretations of crustal structures from Vp and Vs. In the shallower layer (depths up to 2 km) low Qp and Qs values in the Alpine foreland correlating well with the sediments of the Molasse Basin. In addition, very low Qp (Q < 50) is likely linked to the Permo-Carboniferous sediments, deposited in troughs in the Pre-Mesozoic basement beneath northern Switzerland. At depths ranging between 2.0 - 6.5 km, low Q is also imaged along the Rhone valley in the Valais region in southwest Switzerland. This region locates in the transition zone between the Central and Western Alps, hosts a few of the presently seismically most active fault zones and, based on historical activity, it represents one of the seismically most hazardous areas within the Alpine Arc. As the attenuation of fractured rock volume is enhanced by fluids, the low Q values observed in this area may relate to distributed microfractures that produce greater fracture connectivity and permeability in a relatively higher strain-rate zone. Resulting enhanced fluid circulation is also manifest by the numerous thermal springs in the region. The European crystalline basement is well imaged by Qp and Qs both in the northern foreland and the External Crystalline Massifs (e.g., Aar massif). Relatively high Qp are also observed in the Penninic nappes possibly reflecting their high-grade metamorphism.
With this study, we show how such 3-D attenuation models, in combination with recently published Vp and Vs velocity models, may advance our understanding of seismotectonic processes in Switzerland. Furthermore, the attenuation models provide additional constraints in terms of composition and physical properties of the uppermost crust of the central Alps and thus they may contribute to the next generation seismic hazard models of Switzerland by improving physics-based ground motion models.

P 1.19
Thermal properties of the lower continental crust of high-grade metamorphic rocks from the Ivrea-Verbano Zone (project DIVE)

Kim Lemke[1], György Hetényi[1] and project DIVE Team

[1] *Insitut des Sciences de la Terre, University of Lausanne, CH-1015 Lausanne (kim.lemke@unil.ch)*

Transferred thermal energy also known as “heat” from the Earth’s interior is an important factor that determines the thermal state of our planet and governs important geological processes. Therefore, it is crucial to quantify the Earth’s thermal budget and the variability of the geotherm in order to understand its dynamics.
The distribution and flow of heat in the Earth’s lithosphere is dependent on the thermal properties of rocks, such as thermal conductivity (TC), thermal diffusivity (TD), specific heat capacity (Cp), and internal (primarily radiogenic) heat production (A). Thus, these properties are fundamental for any thermal study of the Earth’s lithosphere, and – in particular for this project – for the lower continental crust (LCC). Data on thermal properties of rocks that are representative for the LCC are rare and comprise mainly granulites (Ray et al., 2015).
The targets of our study are: (1) to gain new data on thermal properties of LCC rocks; (2) to track their variation within each lithology on a centimetre to a few metre scale and relate them to other geophysical and petrological properties; (3) to calculate the heat flow, compare the effects of sparse vs. continuous TC data sampling, and to determine the consequences for heat flow uncertainties; (4) to assess TC anisotropy of rock samples and its possible consequences when upscaling models.

The Ivrea-Verbano-Zone (IVZ, northern Italy) offers a great opportunity to study the thermal properties of LCC rocks, because it represents a nearly intact and time resolved archetypal lower continental crust to mantle transition zone (Brack et al., 2010). In the IVZ high-grade metamorphic rocks of amphibolite to granulite facies are exposed at and close to the surface. Because of its significance to the scientific community, the ICDP project DIVE (Drilling the Ivrea-Verbano ZonE) has been launched, which comprises projects of various disciplines such as geophysics, microbiology, petrology, etc. So far, the drilling of the first borehole DT-1b could be successfully completed (578.5 m depth) and provides continuous drill cores of mainly felsic and metamafic rocks of the LCC. The drilling of the second borehole is planned for autumn 2023 and should bring up rocks representative of the lower crust to upper mantle.

We perform TC and TD measurements with an optical thermal conductivity scanner (OTCS, Popov et al., 2016) on DIVE half-cores from borehole DT-1b and later DT-1a, and surface samples collected close to the boreholes. Furthermore, we measure the concentrations of heat producing elements (U, Th and K) with a Canberra gamma spectrometer (U. Lausanne) with a high-purity Ge-detector to calculate A. Cp will be measured using a calorimeter.
The first results show that it is possible to get a resolution of TC measurements on a mineral scale within a lithology, and that the spatial variability of TC is quite important. The variability of A is clearly related to lithological changes, with a decreasing trend towards more mafic rocks.

REFERENCES

Brack, P., Ulmer, P., Schmid, S. 2010: A crustal magmatic system from Earth mantle to the Permian surface: Field trip to the area of lower Valsesia and Val d’Ossola (massiccio dei Laghi, Southern Alps, Northern Italy). Swiss Bull. Angew. Geol., 15, 3-21.

Popov, Y., Beardsmore, G., Clauser, C., Roy, S. 2016: ISRM Suggested Methods for Determining Thermal Properties of Rocks from Laboratory Tests at Atmospheric Pressure. Rock Mech. Rock. Eng., 49, 4179-4207.

Ray, L., Förster, H-J.,Förster, A., Fuchs, S., Naumann, R., Appelt, O. 2015:Tracking the thermal properties of the lower continental crust: Measured versus calculated thermal conductivity of high-grademetamorphic rocks (Southern Granulite Province, India). Geothermics, 55, 138-149.

P 1.20
Deformation-induced changes in the metamorphic record along rheologically contrasted boundaries: inferences from Cima di Gagnone (Cima Lunga unit, Central Alps)

Maino M.,[1], Stefania Corvò[1], Filippo L. Schenker[2], Michele Perozzo[1], Tagliaferri[2] A., Silvio Seno[1] and Antonio Langone[1]

[1] *Department of Earth and Environmental Sciences, University of Pavia, Via Ferrata 1, Pavia, Italy (matteo.maino@unipv.it)*
[2] *University of Applied Sciences and Arts of Southern Switzerland (SUPSI), Institute of Earth Sciences, Via Flora Ruchat-Roncati 15, CH-6850 Mendrisio*

The Cima Lunga unit shows one of the best-preserved record of the deformation and metamorphic history of the Central Alps. Here, the occurrence of ultrahigh-pressure and/or high-temperature rocks embedded within significantly lower grade metamorphic rocks rises a major challenge for developing a consistent geodynamic model for exhumation of such deep-seated rocks. Subduction zones are, in fact, efficient player driving material from the surface down into the Earth's mantle. However, the mechanisms to exhume part of this material (and particularly the denser oceanic rocks) back to the shallow crust are still highly debated. Scientists generally invoke either mechanical decoupling within a tectonic mélange or variable metamorphic re-equilibration during the retrograde path. These interpretations are based on the common assumption that the mineral assemblages form under lithostatic pressure and near-equilibrium regional geothermal gradients. Hence, the resulting metamorphic histories based on the estimation of the pressure and temperature conditions represent the major tool for tectonic reconstruction as proxies of the burial and exhumation history of the rocks during subduction-exhumation phases. Alternative explanations highlight the role of deformation in promoting the coexistence of multiple local equilibria, which cease to correlate with lithostatic conditions and thus burial depths. In this view, the non-hydrostatic stress and the local temperature deviations are accounted as important components potentially modifying the metamorphic system.

In this contribution, we show new structural, petrological and geo- and thermos-chronometric data from the Cima Lunga units. The dataset comprises new field mapping covering the entire nappes extension (several hundred square kilometres) and structural, petrological analyses and monazite-zircon U-Pb dating. Our results show the highly variable pressure-temperature-time-deformation paths experienced by the compositionally heterogeneous rocks of the Cima Lunga and Adula nappes. We present evidence of contrasting metamorphic records among the rocks of these nappes, providing arguments to discuss pros and cons of the tectonic models proposed to explain these contrasting metamorphic records. New findings argue in favour of an exhumation history where deformation and fluids promote local P-T equilibria.

P 1.21
Kinematic study of inherited normal faulting in the internal Jura fold-and-thrust belt.

Adeline Marro[1], Sandra Borderie[1], Jon Mosar[1]

[1] *Earth Sciences Unit, Department of Geosciences, University of Fribourg, Chemin du musée 6, 1700 Fribourg. (adeline.marro@unifr.ch)*

The Internal Jura is the highest and most deformed part of the Jura Fold-and Thrust Belt (FTB). Together with the Molasse Basin, they are part of the Northern Alpine Foreland Basin. This foreland basin was initiated as a flexural basin due to the arrival of the Alpine Orogenic wedge and was subsequently detached along Triassic evaporites to form a detached wedge-top basin. The detachment initiated the folding and thrusting of the Jura FTB in Miocene times. Prior to its detachment and transport of some 30km to the NW, the Mesozoic cover has been dissected by rather steep faults associated either with the rifting of the European Cenozoic Rift system and/or due to the flexural bending of the lithosphere (Bradley and Kidd 1991; Bourgeois et al. 2007; Schori 2021). According to analogue models, normal faulting in the basement induced decoupling structures within the overlying Mesozoic cover in a presence of salt-rich evaporite layer (Withjack and Callaway 2000; Zwaan, 2022; Schori 2021). Furthermore, forward and analogue modelling demonstrate that these decoupling structures are passively displaced and remain intact during the Jura thrusting and folding (Schori et al., 2021). This suggests potential presence of inherited normal structures in the present-day Internal Jura FTB.

In the External Jura FTB, to the North of the Internal Jura FTB, the Heute and the Quingey faisceaux present normal faulting in the detached cover. In this area, the normal faulting can most likely be associated with the Bresse graben, thus predating the Jura FTB thrusting. These extensional structures currently observed on the Mesozoic cover have been displaced by as much as 10 km. Thus, the normal faults in the basement that induced these latter structures are located several kilometres to the SE. These normal faults in the External Jura provide good examples to assess potential inherited normal structures in the Internal Jura.

Conspicuous, large, steep, and straight normal faults parallel to the crest of the Reculet and Crêt de la Neige summits in the Internal Jura appear to be candidates of inherited and transported features. Detailed field investigation, re-assessment of the geological map and the hillshade from the digital elevation model have allowed us to elaborate a new tectonic map with refined details of the different structures associated with the Crêt de la Neige-Reculet ramp-related anticline. Thus, small scale folds and steep bedding are found all along the southern limb of the anticline, while the meridional part of the crest is cut by a graben-like structure affecting an important part of the sedimentary package. In addition, along-strike structural style change reveals a transition from a fold-propagation fold type to a fault-bend fold type anticline from SW- toward NE.

Combined with kinematic forward modelling, we can demonstrate that these normal structures and the small-scale folds can be linked to inherited tectonics occurring in an extensional setting above a basement fault, prior to transport and deformation associated with the Jura FTB.

REFERENCES

Bourgeois, O., Ford, M., Diraison, M., Le Carlier de Veslud, C., Gerbault, M., Pik, R., Ruby, N., & Bonnet, S. (2007). Separation of rifting and lithospheric folding signatures in the NW-Alpine foreland. *International Journal of Earth Sciences*, 96(6), 1003–1031.

Bradley, D. C., & Kidd, W. S. F. (1991). Flexural extension of the upper continental crust in collisional foredeeps. *Geological Society of America Bulletin*, 103(11), 1416.

Schori, M. (2021). *The Development of the Jura Fold-and-Thrust Belt: pre-existing Basement Structures and the Formation of Ramps*. (Doctoral dissertation, University of Fribourg). Geofocus, 50,200.

Withjack, M. O., & Callaway, S. (2000). Active normal faulting beneath a salt layer: an experimental study of deformation patterns in the cover sequence. *American Association of Petroleum Geologists Bulletin*, 84(5), 627–651.

Zwaan, F., Schreurs, G., Madritsch, H. & Herwegh, M. (2022). Influence of rheologically weak layers on fault architecture: insights from analogue models in the context of the Northern Alpine Foreland Basin. *Swiss J Geosci* 115, 26.

P 1.22
Numerical Investigation of Ocean-World Mantle Dynamics under a Low-Efficiency Eruption Limit

Paul Tackley[1], Diogo Louro Lourenço[1], Nickolas Moccetti Bardi[1]

[1] *Institut für Geophysik, ETH Zürich, Rämistrasse 101, CH-8092 Zürich (paul.tackley@erdw.ethz.ch, diogo.lourolourenco@erdw.ethz.ch, nmoccetti@ethz.ch)*

As exoplanetary research expands, there is a mounting focus on ocean worlds – planetary bodies with masses ranging from 3ME to 10ME featuring surfaces adorned by liquid or partially frozen oceans - for their potential to nurture life and intricate habitable systems. To comprehensively understand the dynamics of the icy layers on such ocean worlds, it becomes imperative to establish robust constraints on mantle behaviour, from the formation of these planets to the moment observations are performed. This undertaking is pivotal in characterizing vital parameters such as heat flux across the mantle-ice interface, melting intensity, chemical transport within the mantle, and tectonic regimes acting on the “lithospheric plates/the icy surface”.

By employing a state-of-the-art multigrid solver for mantle dynamics, initial insights are garnered into both mantle and crust reactions as external pressures intensify for scenarios characterized by minimal resurfacing efficiency. The investigation spans a comprehensive range of parameters encompassing mass and water mass fractions.

Noteworthy alterations arise within the viscosity and mobility fields. Concentrated melting near the 24GPa boundary emerges as a prominent phenomenon, distinctly lowering the viscosities of the upper mantle within a specific pressure window. This occurrence fosters escalated convective velocities, ultimately raising the average temperature of the mantle, and reinforcing azimuthal stresses exerted on the crust. This amalgamation culminates in more effective subduction. Consequently, there is an increase in surface heat fluxes at relatively weak surface pressures, while a reduction is observed for moderate to very high pressures where subduction is rather inhibited. This trend holds significant implications, such as varying the intensity of localized melting at the mantle-ice interface, and therefore chemical transport upwards. Internal differentiation is observed to occur at low masses where iron-rich material is constantly being fed to the CMB boundary. Higher masses, on the other hand, present elevated viscosities in their lower mantle which impedes the segregation of material and leads to a more homogeneous system. Crustal thickness also shows opposing trends for planets with and without surface oceans, which strongly dictates a shift from a mobile lid regime towards an episodic one at very high pressures depending on the mass.

Further work will aim at constraining the dynamics of cases where resurfacing occurs unimpeded. Once mantle behavior is correctly encapsulated, the next steps could aim to simulate the response of the overlaying ice layers to the results obtained from these simulations.

P 1.23
The Téné Fault: Architecture of a Seismogenic Carbonate Fault System

Teo Neuenschwander[1], Sandro Truttmann[1], Berit Schwichtenberg[1], Marco Herwegh[1]

[1] *Institut für Geologie, Universität Bern, Baltzerstraße 1+3, CH-3012 Bern (teo.neuenschwander@students.unibe.ch)*

The increasing quality of relocated earthquake hypocenters allows the subsurface tracking of seismically active fault zones and their time-dependent propagation. However, the spatial resolution of seismic data is insufficient to resolve structures at the metre scale and beyond, and information on interseismic creep is also lacking. This is where comprehensive studies of exhumed faults come into play. We are studying the Téné fault system (SW Swiss Alps), which has recently emerged beneath a retreating glacier, providing exceptional outcrop conditions. This fault system is located in the Valais region, the most seismically active area in Switzerland. The Téné fault system is an 860 m long, NE-SW trending, subvertical, dextral strike-slip system that has developed in the same stress field as the recent seismicity. The fault system has been studied using multiscale remote sensing, field mapping, meso- to microscale structural analysis, and quantitative analysis of fault rocks and their spatial distribution. A highly localised (few cm to 2 m wide) major central fault strand is located between divergent fault linkage and horse-tail structures which are up to 150 m wide. These structures have evolved over a long period, undergoing strain localisation during progressive exhumation and cooling. The system (i) formed at depth under a dominant viscous regime, (ii) progressed through cycles of hydrofracturing and highly brittle faults to (iii) a final stage of unhealed, non-cohesive fault rocks. Fluid was present at all stages of deformation, indicating the importance of fluid-assisted deformation and the influence of reduced effective pressures. We show that large dilatative domains at fault intersections and pull-apart structures represent major vertical fluid pathways separated by dense planar fault strands in the fault core. In particular, razor-sharp en-echelon fault segments and their association with injection breccias support a seismic origin. The Téné fault thus is an ideal field laboratory to study alternating cycles of seismic rupturing and interseismic creep, and provides a unique opportunity to study their spatial and temporal variations during exhumation.

P 1.24
An analysis of the peak-temperature recorded by the meta-sedimentary covers of the Central Alps using Raman spectroscopy

Enrico Pigazzi[1], Sabrina Morandi[1], Alessia Tagliaferri[2,3], Francesco Arrigoni[1], Filippo Luca Schenker[2], Paola Tartarotti[1]

[1] *Earth Science Department "A. Desio", Università degli Studi di Milano (UNIMI), via Luigi Mangiagalli 34, IT-20133 Milano (enrico.pigazzi@unimi.it)*
[2] *Institute of Earth Sciences, University of Applied Sciences and Arts of Southern Switzerland (SUPSI), via Flora Ruchat-Roncati 15, CH-6850 Mendrisio*
[3] *Institute of Earth Sciences, University of Lausanne (UNIL), Bâtiment Géopolis, CH-1015 Lausanne*

The Penninic nappes of the Swiss-Italian Central Alps are wrapped by layers of meta-sedimentary covers of Mesozoic to Cenozoic age that were involved in the Alpine orogeny. These meta-sedimentary rocks contain high amounts of carbonaceous material (CM). Its crystallinity has the peculiarity of recording the peak temperature to which CM has been subjected (e.g. French 1964). By analyzing this material through Raman spectroscopy it is possible to obtain such temperatures (e.g. Beyssac et al. 2002), which are then correlated with the geological evolution of the host rocks.
With this focus, we collected and analyzed samples within the meta-sediments of the Swiss Misox Zone (Mesozoic sediments pinched between Adula and Tambò nappes) and of the Italian Splügen Zone (Tambò nappe autochthonous and para-autochthonous cover; Figure 1).

This sector of the Alps underwent several deformation phases, ranging from subduction-related high pressure (HP) - low temperature (LT) conditions up to Barrovian conditions, followed by the subsequent more or less pervasive greenschist facies re-equilibration.

The temperatures obtained were compared with the peak metamorphic conditions evaluated for the basement and for other portions of the nearby meta-sedimentary units (Wiederkehr et al. 2011), then validated through micro-structural and field observations for a better comprehension of the geological evolution of this portion of the Alps.

Due to the complexity of the Alpine history, the recorded peak temperatures could relate to different stages of the orogeny, as already shown in the work of Wiederkehr et al. (2011) in nearby areas. Therefore, it is critical to compare these results with structural and petrographic analysis to attribute them to the correct geodynamic stage.

An interesting observation that emerged during the Raman analyses concerns the response of CM material. In many samples from the two areas, two distinct spectra morphologies are often detected, apparently indicating two different recorded temperatures, even within the same centimetric sample. Although not yet clarified, this evidence leads to (at least) two possible interpretations: 1) CM grains recording lower temperatures originated in a different environment with respect to the higher temperature ones and were then mixed together in a later stage; 2) the same peak temperature could have induced different CM responses, reflecting an intrinsic difference in the source CM material, as already observed for various synthetic materials. Despite this work does not provide an unambiguous solution to this question, we believe that this situation may occur in different study areas and should be taken into consideration to avoid misinterpretation of recorded peak temperatures.

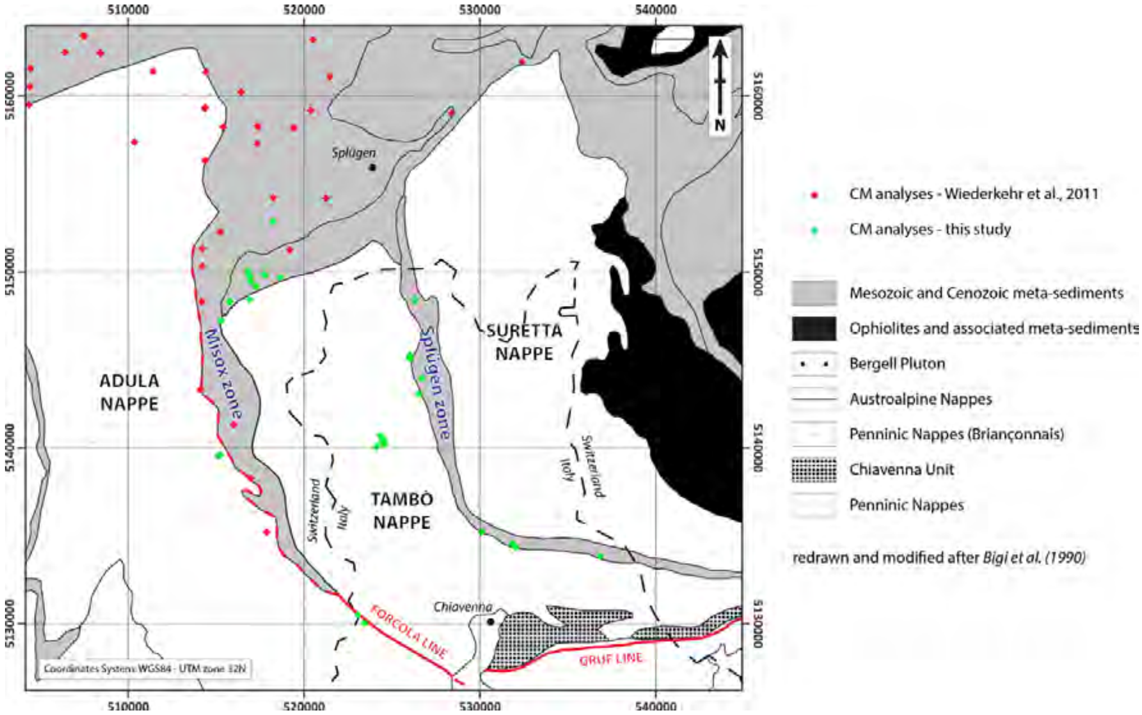

Figure 1. Tectonic sketch of the Central Alps with the position of CM samples (samples from this study and from Wiedekehr et al. (2011)).

REFERENCES

Beyssac, O., Goffé, B., Chopin, C., & Rouzaud, J. N. 2002: Raman spectra of carbonaceous material in metasediments: a new geothermometer. Journal of metamorphic Geology, 20(9), 859-871.

Bigi, G., Castellarin, A., Coli, M., Dal Piaz, G. V., Sartori, R., Scandone, P., & Vai, G. B. 1990: Structural Model of Italy, sheets 1-2: CNR. Progetto Finalizzato Geodinamica.

French, B. M. 1964: Graphitization of organic material in a progressively metamorphosed Precambrian iron formation. Science, 146(3646), 917-918.

Wiederkehr, M., Bousquet, R., Ziemann, M. A., Berger, A., & Schmid, S. M. 2011: 3-D assessment of peak-metamorphic conditions by Raman spectroscopy of carbonaceous material: an example from the margin of the Lepontine dome (Swiss Central Alps). International Journal of Earth Sciences, 100, 1029-1063.

P 1.25
The thermal and exhumation history of northern Switzerland from Variscan to present

Meinert Rahn[1]

[1] *Swiss Federal Nuclear Safety Inspectorate (ENSI), Industriestrasse 19, 5201 Brugg (meinert.rahn@ensi.ch)*

Siting a repository for radioactive waste requires knowledge on the site-specific thermal and latest burial and exhumation history. In the Swiss site selection process, all remaining sites under investigation are located in northern Switzerland. The proposed host rock is the middle Jurassic Opalinus clay, located within a Triassic to uppermost Jurassic sediment sequence that covers Variscan crystalline basement or Permocarboniferous trough filling sediments. The Mesozoic sequence is covered by minor Eocene and Neogene Molasse sediments. Significant hiatus in sedimentation include the uppermost Jurassic to lower Palaeogene, the late Eocene to early/middle Miocene and the late Miocene to early Quaternary on the other.

Based on the stratigraphic record, on thermochronology and vitrinite reflectance data, the thermal history of northern Switzerland was investigated in several studies to gain information on the large time gaps existing in the stratigraphic record. Aspects not yet fully resolved include (a) the impact of any potential Jurassic hydrothermal activity, well known in the Black Forest and affecting basement and sedimentary cover, (b) the role of a Cretaceous (and perhaps up to Palaeogene) sedimentary cover, and most importantly (c) the onset and amount of a late Neogene exhumation event.

Samples from the crystalline basement rocks of the southernmost Black Forest were collected and combined with crystalline basement samples from northern Switzerland boreholes. 11 new apatite FT ages ranging from 5 to 101 Ma indicate a fully to partially annealed status, offering the possibility to model the thermal history since the Variscan orogeny with the FT data. In line with previous thermochronological data and modelling results, we infer substantial burial underneath Cretaceous (but not Palaeogene) sediments. Our modelling data suggest that the onset of exhumation was diachronous with earlier start in the E, but later towards the W. Late exhumation of the rock column started in a time window bracketed between 10 and 4 Ma. Late Miocene exhumation reached several km in areas proximal to the Alpine front, while slightly more than 1 km close to the siting areas.

P 1.26
The Influence of Strain-Rate Weakening on Strain Localization during Transform Fault Evolution

Sandrine Ritter[1], Attila Balazs[1], Taras Gerya[1]

[1] *Institute of Geophysics, ETH Zurich, Sonneggstrasse 5, CH-8092 Zurich (sandrine.ritter@erdw.ethz.ch)*

Plate tectonics shape the surface of the Earth by dividing it into a mosaic of plates. The boundary between two tectonic plates is lubricated by weak zones. Ductile and brittle weakening mechanisms thereby, play an important role in facilitating subduction, orogeny or seafloor spreading along these weak zones. Such lithospheric damages can be prominently observed along transform faults and rift zones. A well-studied natural example of this is the Romanche transform fault zone in the equatorial Atlantic Ocean. However, the role of rheological weakening processes in the evolution of such a transform fault zone is still unclear.

We aim to model the evolution of a transform fault zone from continental rifting to seafloor spreading using rheological weakening processes. Therefore, we conducted a series of high-resolution 3D petrological-thermomechanical rifting models (I3EVLIS) that include visco-elasto-plastic rheology, mantle partial melting, oceanic crust growth, thermal contraction and mantle grain size evolution. Here we present modelling results of transform fault evolution, focusing on strain-rate weakening. Subsequently, we analyse the evolution and stability of transform faults and compare it with geophysical observations from the Atlantic Ocean.

P 1.27
Volcano deformation and landslide monitoring on an unresting caldera (Askja, central Iceland)

Nicolas Oestreicher[1], Joël Ruch[1], Nicolas Serrano[1], Xingjun Luo[1], Thorsteinn Saemundsson[2], Jón Kristinn Helgason[3], Jordan Aaron[4], Patricia Leva[4], Jasmin Maissen[5], Andrea Manconi[6], Marc Henri Derron[7], Halldór Geirsson[2], Daniel Mc Ginnis[8], Elisabetta Panza[1], Yohann Chatelain[1], Frédéric Arlaud[1] & Michael Hohl[6]

[1] *Department of Earth Sciences, University of Geneva, Rue des Maraîchers 13, 1205 Geneva (joel.ruch@unige.ch)*
[2] *Faculty of Life and Environmental Sciences, University of Iceland, Reykjavik, Iceland*
[3] *Icelandic Meteorological Office, Reykjavik, Iceland*
[4] *Department of Earth Sciences, ETH Zürich*
[5] *Berner Fachhochschule, Bern, Switzerland*
[6] *WSL-Institute for Snow and Avalanche Research SLF, Davos*
[7] *University of Lausanne, Geopolis – Quartier Mouline, Lausanne*
[8] *Department F.-A. Forel for environmental and aquatic sciences, University of Geneva*

Since the summer of 2021, the Askja caldera has been experiencing a new phase of unrest. The caldera floor has risen by more than 60 cm in two years with a slight increase of the background seismicity. These signs point to the presence of magma upwelling, which could be followed by an eruption in the months or years to come. It is therefore essential to install a monitoring system to better understand the period of activity that potentially precedes an eruption. This new activity goes with an increased risk of landslides on the already highly unstable slopes of the eastern part of the caldera. In 2014, a major landslide had already occurred, causing a tsunami that flooded the lakeshore several tens of meters above its pre-event level. The monitoring systems currently in place to track deformation are virtually non-existent, and are therefore not sufficient to understand the evolution of the magmatic system and correctly define the hazards associated with volcanic activity and landslides.

During the summer 2023, we installed a dense monitoring network with three time lapse cameras to track groud motion on the unstable eastern caldera rim, three corner reflectors to acquire InSAR signal even during snow-rich winter and a continuous GNSS instrument to analyse ground displacement. We also repeated drone flights above the entire caldera to compare them with flights acquired in 2020 and 2021 and analyse ground displacement over years using digital image correlation, combined with InSAR time series. We performed a detailed structural mapping using high-resolution drone imagery, combined with extensive field structural observations and a detailed mapping on several landslide events that occurred in the past decades or centuries. Furthermore, we installed a pressure sensor in the Oskuvatn lake to see potential correlation between lake level change, seismicity and possibly volcanic activity.

This integrative monitoring approach is the fruit of collaborations between swiss and icelandic institutions and will allow to study in unprecedented details an unresting volcano that may lead to an eruption and is subject to large deformation and landslide activity. This multi-monitoring approach could serve as a model for other unresting caldera worldwide.

P 1.28
Landslide and structural analysis of an unresting volcano using drone imagery and field observations at Askja caldera (Central Iceland).

Nicolás Serrano[1], Nicolas Oestreicher[1] , Marc Henri Derron[2], Joël Ruch[1]

[1] *Department of Earth Sciences, University of Geneva, Rue des Marichers 13, 1205 Geneva, Switzerland. (nicolas.serrano@etu.unige,ch)*
[2] *University of Lausanne, Geopolis – Quartier Mouline 1015, Lausanne.*

Large volcanoes are often prone to flank instabilities and structural failure. Faulting, dyke intrusion, rock weathering and seismicity are some of the factors that could lead to catastrophic landslides and eruptions. Due to the complexity of these interacting factors, volcano instabilities are still poorly understood.

Here we analyze the Askja volcano (central Iceland), currently in a state of unrest since 2021. Askja is affected by significant rock alteration due to hydrothermal processes. Together with intense weathering and gravitational processes, it constitutes a great oportunity to understand flank instabilites at volcanoes. We used high-resolution orthophotos and DEM (~4cm/pixel) captured on the eastern portion of the Öskjuvatn caldera during drone flight campaigns in 2020 and 2021 to analyze and map different volcanic, tectonic and gravitational structures that influence the slope stability. We also went in the field for three weeks in August 2023 to collect structural data and to validate previously mapped structures for a better characterization of the fracture system.

Our results for the structural analysis show an E-W structural trend (± 20°) for more than 3500 mapped fractures. We evidenced in the field several families of fractures that are not persistent or are confined to certain rock layers preventing the analysis of the slope as an homogeneous formation. We also observed dip slip motion affecting the main caldera ring fault that could favour planar sliding. A 3D analysis of the main scarps will allow to identify the potential slope movements associated to the diferent portions of the slope. Our field observations are key as they showed additional features that contribute to the overall flank instability. We observed several types of structures, with graben-like structures related to superficial creeping of the slope, high aperture cracks on the top of the caldera, complex networks of pumice-filled fractures, etc. We also observed evidences of permafrost melting that generate secondary widespread superficial ground displacement. In addition, we identified several overlapping old landslide deposits, supporting the recurrent pattern of great magnitude events, that is key for assessing landslide hazards in the area.

Due to the unrest conditions of this volcano, our preliminary structural and morphotectonic study proves to be a valuable contribution for the understanding of volcano instabilities by identifying the driving factors.

1.29
Grain size evolution in necking calcite layers: The role of energy fraction stored in the microstructure

Leif Tokle[1], Stefan Markus Schmalholz[2], Jonas Ruh[3]

[1] *Structural Geology and Tectonics Group, Geologic Institute, ETH Zurich (leif.tokle@erdw.ethz.ch)*
[2] *Institute of Earth Sciences, University of Lausanne, CH-1015 Lausanne (stefan.schmalholz@unil.ch)*
[3] *ICM - CSIC*

Grain size reduction plays a key role in strain localization during viscous rock deformation; therefore, understanding the parameters that influence grain size evolution in such localization processes is crucial. The paleo-wattmeter model (e.g. Austin and Evans, 2007), which considers the balance between grain growth and grain size reduction, offers valuable insights into grain size evolution. One key parameter in this model, λ, represents the fraction of total energy input during dislocation creep that is not dissipated as heat. We study the influence of λ on grain size evolution during the necking of calcite layers, generating a pinch-and-swell structure. We compare natural pinch-and-swell structures with structures predicted by mathematical models. Prior mathematical models of necking calcite layers have commonly adopted λ values of 0.1 (e.g. Austin and Evans, 2007; Peters et al., 2016; Schmalholz and Duretz, 2017). While these mathematical models are able to reproduce the first-order distribution of grain size in natural calcite pinch-and-swell structures, they also show a discrepancy wherein the grain size in the swells initially reduces during the early stages of necking and subsequently increases during the advanced stages. These considerable temporal variations in grain size within the swells are not supported by observations. We test the hypothesis that a reduced value of $\lambda < 0.1$ can lead to a more realistic grain size evolution, with the grain size in the swells remaining essentially constant during necking. Recent analysis of laboratory experiments with quartz (Tokle and Hirth, 2021) have supported the use of a lower value of $\lambda = 0.015$ for grain size evolution, prompting us to explore a similar applicability to calcite. We apply both 1D semi-analytical and 2D numerical models to study the grain size evolution during necking. By employing a comparison of mathematical models with natural data, we aim to assess whether reduced values of $\lambda < 0.1$ are also reasonable for the grain size evolution in calcite and which λ value provides the best fit between model results and observations.

REFERENCES

Austin, N.J. & Evans B. 2007: Paleowattmeters: A scaling relation for dynamically recrystallized grain size, Geology, 35, 343-346.

Peters, M., Berger A., Herwegh M. & Regenauer-Lieb K. 2016: Strain localization in ductile rocks: A comparison of natural and simulated pinch-and-swell structures, Tectonophysics, 680, 140-154.

Tokle, L., & Hirth J. 2021: Assessment of quartz grain growth and the application of the wattmeter to predict quartz recrystallized grain sizes, Journal of Geophysical Research, 126, e2020JB021475.

Schmalholz, S.M. & Duretz T. 2017: Impact of grain size evolution on necking in calcite layers deforming by combined diffusion and dislocation creep, Journal of Structural Geology, 103, 37-56.

1.30
4D metamorphic evolution of collisional orogens from the Alps to the Himalayas: insights from numerical modelling

Luuk van Agtmaal[1], Attila Balàzs[1], Taras Gerya[1]

[1] *Geophysical Fluid Dynamics group, Department of Earth Sciences, ETH Zurich, Sonneggstrasse 5, CH-8092 Zurich (luuk.vanagtmaal@erdw.ethz.ch)*

Reconstructing the pressure (P) and temperature (T) conditions of natural rocks through time (t) reveals the burial and exhumation cycle(s) - PT-t paths - that they experienced. Along with peak metamorphic conditions, these are major constraints on conditions within continental collision and subduction zones. Through decades of work, such data are now available for many collision zones, such as the Himalayas (e.g. Chakraborty et al., 2016)metabasites and a sheared granite gneiss – the Lingtse gneiss and the European Alps (e.g. Bousquet et al., 2008). Although common in 2D thermomechanical modelling studies, scarce attempts have been made to compare metamorphic evolution of markers in 3D continental collision models with natural PT-t paths. Here we present the metamorphic evolution through time of a 3D numerical model of a corner collision similar to the India-Asia collision. We highlight multiple ways of visualising and analysing the metamorphic evolution, e.g. conventional "2D" slices of PT-t paths and laterally stacked PT-t paths (Figure 1). In addition, we plan to use peak pressure and temperature conditions of markers to generate a metamorphic facies map for our 3D model, similar to what has been done recently in 2D (Vaughan-Hammon et al., 2022). We propose that with our new method, 3D modelling results can be compared better with observations which could improve the overall interpretability of complex, threedimensional, numerical models of subduction and continental collision.

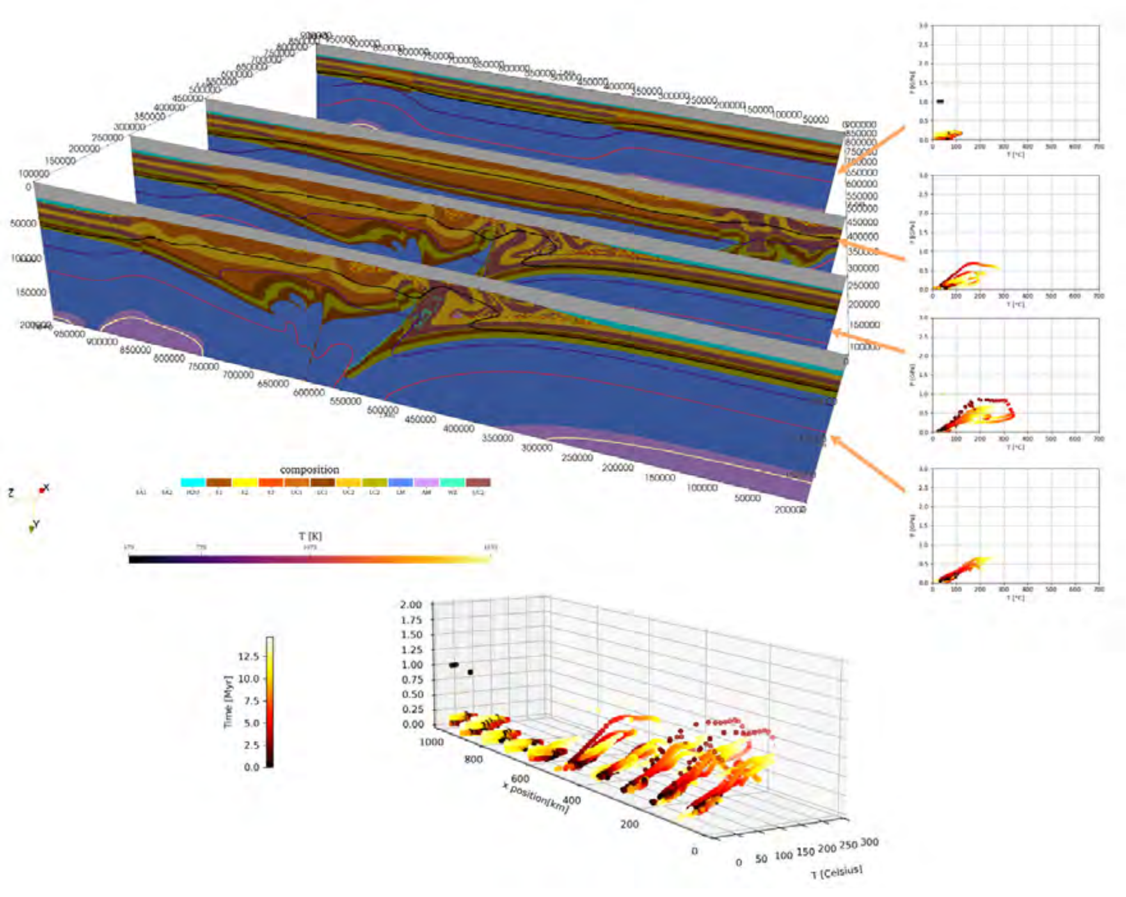

Figure 1. An example of visualising PT-t evolution in our 3D model at *t~15* Myrs. Top panels: four cross-sections of rock composition at *x*=100,300,500, and 900 km, overlain with temperature contours at 300, 500, 800, and 1300°C. bottom panels: an x,P,T-t diagram combining the PT-t paths grouped by starting lateral position, such that lateral displacements become visible.

REFERENCES

Bousquet, R., Oberhänsli, R., Goffé, B., Wiederkehr, M., Koller, F., Schmid, S. M., Schuster, R., Engi, M., Berger, A., & Martinotti, G. (2008). Metamorphism of metasediments at the scale of an orogen: A key to the Tertiary geodynamic evolution of the Alps. *Geological Society, London, Special Publications*, *298*(1), 393–411.

Chakraborty, S., Anczkiewicz, R., Gaidies, F., Rubatto, D., Sorcar, N., Faak, K., Mukhopadhyay, D. k., & Dasgupta, S. (2016). A review of thermal history and timescales of tectonometamorphic processes in Sikkim Himalaya (NE India) and implications for rates of metamorphic processes. *Journal of Metamorphic Geology*, *34*(8), 785–803. https://doi.org/10.1111/jmg.12200

Vaughan-Hammon, J. D., Candioti, L. G., Duretz, T., & Schmalholz, S. M. (2022). Metamorphic Facies Distribution in the Western Alps Predicted by Petrological-Thermomechanical Models of Syn-Convergent Exhumation. *Geochemistry, Geophysics, Geosystems*, *23*(8), e2021GC009898. https://doi.org/10.1029/2021GC009898

P 1.31
Developing the global network of plate boundaries in 3D mantle convection models

Xin Zhou[1], Nicolas Coltice[2], and Paul Tackley[1]

[1] *Institute of Geophysics, Department of Earth Sciences, ETH Zurich, Switzerland*
[2] *Département de Géosciences, Ecole Normale Supérieure, France*

The beginning of plate tectonics is when the single lid Earth was broken into a mosaic of plates, separated by high strain localized plate boundaries with horizontal displacement. The establishment of this global plate boundary network was primarily driven by local subduction zones. However, the transition from local subduction zones to a fully interconnected global network of plate boundaries remains poorly understood and is often overlooked. To elucidate the timescale and strain localization mechanisms over these tectonic regime transitions, we investigate the role of different physical parameters that may control the development of global plate boundary networks using 3D mantle convection models. We quantify the evolution of plate sizes, length of different plate boundaries and mobility of tectonic plates. We find that with stronger lithosphere, longer time is needed to develop the global plate boundary network. The layout of tectonic plates gradually evolves to a statistical steady distribution, while their size also highly depends on the strength of lithosphere. Our studies also demonstrate how the local subduction zones merge and interconnect to form the global plate boundary network. By comparing numerical results with geological proxies of plate tectonics, we assess key parameters that could contribute to the development and evolution of plate tectonics.

2 Mineralogy, Petrology and Geochemistry

Julien Allaz, Charline Lormand, Jacob Forshaw

Swiss Society of Mineralogy and Petrology

TALKS:

2.1 Bonnet G., Chopin C., Locatelli M., Kylander-Clark A.R.C., Hacker B.: Protracted Subduction of the European Hyperextended Margin Revealed by Rutile U-Pb Geochronology Across the Dora-Maira Massif (Western Alps)

2.2 Castellanos Melendez M.P., Szymanowski D., Bachmann O.: Petrochronological heterogeneities within a large pluton: from assembly to porphyry copper deposit formation

2.3 Dietrich J., Hermann J., Pettke T.: Magmatic genesis, hydration and subduction of the eclogite-facies Allalin gabbro (Western Alps, Switzerland)

2.4 Gennaro I., Tsay A., Schirra M., Zajacz Z.: Experimental determination of cation exchange coefficients to facilitate the prediction of Fe and Ca abundances in primary magmatic fluids

2.5 Gies N.B., Konrad-Schmolke M., Hermann J.: Modelling the global water cycle – the effect of Mg- sursassite and phase A on deep slab dehydration and the global subduction zone water budget

2.6 Gillespie J., Moore J., Escrig S., Müntener O., Baumgartner L.P.: Controls on compositional zoning of zircon from the Catedral granite, Torres del Paine

2.7 Jordan M., Pilet S., Brenna M.: Alkaline and arc-related magmas association in a subduction environment (Alexandra Volcanic Group, New Zealand): The role of melts at lithosphere-asthenosphere boundary

2.8 Jorgenson C., Caricchi L., Stuckleberger M., Fevola G., Weber G., Giordano G., Lubbers J.: 3D melt inclusion geometries help quantify eruption triggers at Colli Albani (Italy)

2.9 Lacroix B., Trap P., Durand C., Vennamann T., Goncalves P., Marquer D.: The Clumped-isotope geochemistry of exhumed carbonate shear zones: Examples from the Torngat Orogen (Canada)

2.10 Magnin K., Nitsche C., Serneels V.: An astonishing choice: First petrological examination of Neolithic axe heads from Düdingen, Fribourg

2.11 Marxer F., Almeev R., Holtz F.: A general approach to quantify phase equilibria and silicate mineral stability fields in calc-alkaline basaltic systems

2.12 Mateo I., Pachon E., Zajacz Z., González Rodríguez C., Schirra M., Tsay A., Li W., Miranda M.: Redox state, sulfur and chalcophile element budgets during magma differentiation in thick continental crust: a case study on the Parinacota volcano

2.13 Mazzucchelli M.L., Moulas E., Schmalholz S.M., Kaus B., Speck T.: Fluid-mineral equilibrium under stress investigated through molecular dynamics

2.14 Renggli C.J., Stojic A.N., Morlok A., Berndt J., Weber I., Klemme S., Hiesinger H.: Sulfur enrichment on the surface of Mercury

2.15 Scherzer S., Schwarzenbach E.M., Scicchitano M.R., Dragovic B., Kiczka M., John T.: Tracking fluid sources in the slab: Evidence from HP metabasalts from the Tianshan, NW China

2.16 Schirra M., Zajacz Z., Müller D.: The gold endowment of alkaline melts: Insights from LA-ICP-MS analysis of silicate melt inclusions

2.17 Ulrich M., Vesin C., Rubatto D., Hermann J., Scambelluri M.: Different formation processes for metamorphic olivine in Erro Tobbio unit, Italy

2.18 Vesin C., Ulrich M., Rubatto D., Hermann J., Scambelluri M.: Preserved conditions of oceanic serpentinization in a subducted slice of lithospheric mantle

POSTERS:

P 2.1 Coray M., Fulda D., Galli A., Guillong M., Nievergelt P., Heuberger S.: Lithostratigraphic characterisation of the Paleozoic units of the Suretta Nappe, Eastern Swiss Alps: insights from U-Pb dating of zircons and geological mapping in Val Madris (Grisons)

P 2.2 Degen S., Hermann J., Rubatto D., Secrétan A.: Distribution of C-bearing phases in the Ivrea lower continental crust (Ossola Valley, Italy)

P 2.3 Dominguez H., Lanari P., Tamblyn R., Riel N.: A multi-method approach to investigate pluton formation and melt production in the deep crust: case study of the El Oro Complex in Ecuador

P 2.4 Forshaw J.B., Riel N., Miron G.D., Lanari P.: Thermodynamic calculations of fluids in the deep crust

P 2.5 Krattiger N., Driesner T.: Numerical simulations of gold deposition by boiling in epithermal systems

P 2.6 Lormand C., Humphreys M.C.S., Coumans J.P., Chelle-Michou C., Li W.: Volatile budgets and evolution in porphyry-related magma systems, determined using apatite

P 2.7 Lueder M., Hermann J., Tamblyn R., Rubatto D., Lanari P., Markmann T.: Intra-Grain Variability of Trace Elements in Rutile

P 2.8 Markmann T., Lanari P.: Modelling fluid recycling and fluid fluxes during subduction

P 2.9 Pacchiega L., Rubatto D.: P-T conditions and timing of melting in the Ivrea lower continental crust

P 2.10 Popkhadze N., Şafak Utku Sönmez, Natsvlishvili M., Moritz R.: The structural and lithological control on mineralization at the Upper Cretaceous Sakdrisi epithermal deposit, Bolnisi district, Lesser Caucasus, Georgia

P 2.11 Robyr M.: Evidence for a pre-Himalayan metamorphism in the High Himalayan Crystalline of the Miyar Valley (NW India)

P 2.12 Secrétan A., Degen S., Pacchiega L., Hermann J., Müntener O.: Bulk rock composition and variability of continental lower crust (DIVE project DT-1b, Ornavasso, Val d'Ossola, Italy)

P 2.13 Sonmez S.U., Paul A., Popkhadze N., Moritz R.: Is Apatite a Reliable Mineral for U-Pb TIMS Dating in the Context of Complex Magmatic Regions in the Absence of Zircon?

P 2.14 Sun Y., Galli A., Szymanowski D., Guillong M., Simon J., Shipandeni A., Bachmann A.: Tectono-magmatic origin of aligned intrusions in the Damaraland igneous province, Namibia: new evidence from high-precision zircon dating and geochemistry

P 2.15 Tagliaferri A., Moulas E., Schmalholz S.M., Schenker F.L.: Garnet multi-component diffusion modelling reveals local heat sources affecting the cooling history of the Lepontine dome

P 2.16 Teller M., Franz L., Wetzel A.: Petrologic and sedimentological investigations on boulders of the river Dreisam (Black Forest, FRG)

P 2.17 Zappatini A., Hofmann B.A., Eggenberger U., Gnos E., Kruttasch P.M., Al-Ghafri H., Al Zakwani A., Sansom E.K., Devillepoix H.A.R., Cupák M., Lindemann S., Booz.B.: Recovery of the first camera-observed meteorite fall in Oman

P 2.18 Zelano I., Prud'Homme C., Virgone A., Verrecchia E., Souquet P., Hedacq R., Ferry J.-N.: The overlooked role of tropical trees in supporting biotic and abiotic Ca carbonate precipitation

2.1
Protracted subduction of the European hyperextended margin revealed by rutile U-Pb geochronology across the Dora-Maira massif (Western Alps)

Guillaume Bonnet[1,2], Christian Chopin[3], Michele Locatelli[4], Andrew R.C. Kylander-Clark[1], Bradley R. Hacker[1]

[1] *Department of Earth Science, University of California, Santa Barbara, USA*
[2] *Institut des Sicences de la Terre de Paris, Sorbonne Université, Paris, France*
[3] *Laboratoire de Géologie, Ecole Normale Supérieure, Paris, France*
[4] *Dipartimento di Scienze della Terra Ambiente e Vita, Università di Genova, Genova, Italy*

The Dora-Maira massif is an archetypal nappe stack of subducted and exhumed upper crust. Slices of continental crust experienced metamorphism at upper blueschist to ultrahigh-pressure (UHP) eclogite- facies conditions. While the timing of peak metamorphism in the UHP unit has been extensively studied, little is known about the other units. In order to constrain the timing and conditions of high-pressure metamorphism, U-Pb-trace element analyses of rutile and titanite were carried out across the nappe stack. The data reveal Alpine peak metamorphic ages younging downwards in the stack, from ~40 to ~33 Ma. Greenschist-facies retrogression of the whole massif occurred at ~32–31 Ma, after high-pressure metamorphism of the lowermost unit (Sanfront-Pinerolo Unit). Tectonic implications include (a) continuous and fast exhumation of subducted continental crust, (b) long-lived subduction from ~π60 to ~33 Ma of the distal European margin, reconstructed to be a hyperextended margin spread over ~130 km for the Dora-Maira massif alone, and (c) the initiation of continental collision synchronous with the end of high-pressure metamorphism.

2.2
Petrochronological heterogeneities within a large pluton: from assembly to porphyry copper deposit formation

Maria Paula Castellanos Melendez[1], Dawid Szymanowski[1], Olivier Bachmann[1]

[1] Institute of Geochemistry and Petrology, ETH Zürich, Clausiusstrasse 25, CH-8092 Zürich (maria.castellanos@erdw.ethz.ch)

Long magmatic histories and large volumes of magma may be key factors needed to form large porphyry copper deposits. However, the extent to which these factors, together with intrinsic parameters of the melt, might be fundamental for porphyry copper deposit formation is still highly debated. The Yerington porphyry Cu district, with its unique exposures of a tilted magmatic and hydrothermal upper crustal system (from ~ 3 to 1 kbar), has provided a natural laboratory to study different parameters important for ore formation. The composite batholith is made up of three consecutively emplaced plutons, the McLeod Hill quartz monzodiorite, the Bear quartz monzonite and the Luhr Hill granite, where mineralizing porphyry dikes were extracted from the latter.

Of the three, the McLeod quartz monzodiorite, with its volume in excess of 1000 km^3, forms the main intrusion, and its zircon cargo predates mineralization in the district by 1-2 Myr. High-precision zircon petrochronology indicates a continuum in zircon crystallization ages and geochemistry from the McLeod Hill to the Luhr Hill, suggesting that the magmatic system remained active and evolving for more than 3 Myr with coeval volcanism in its early stages. Geochemical variations within the Bear and the Luhr Hill are restricted to the more evolved compositions and lower crystallization temperatures. In contrast, the zircon population of the McLeod Hill shows a protracted history of pluton assembly accompanied by notable chemical variations that can be traced in time. Trace element compositions in the zircon population of different magma batches that made up the McLeod Hill intrusion suggest that the melt from which zircons crystallized was evolving from hotter and drier magmas with little to no fertility indicators for Cu mineralization towards more evolved (wetter, cooler) and more fertile magmas over almost 2 Myr. During this timespan, reaching compositional maturation needed to form porphyry copper deposits was allowed by magma chamber growth in the upper crust through frequent magma injection from deeper in the system but without extensive volcanism.

2.3
Magmatic genesis, hydration and subduction of the eclogite-facies Allalin gabbro (Western Alps, Switzerland)

Julia Dietrich[1], Jörg Hermann[1], Thomas Pettke[1]

[1] *Institute of Geological Sciences, University of Bern, Baltzerstrasse 1+3, CH-3012 Bern (julia.dietrich@unibe.ch)*

The Allalin gabbro of the Zermatt-Saas meta-ophiolite consists of variably metamorphosed Mg to Fe-Ti gabbros, troctolites, and anorthosites which are crosscut by basaltic dykes. Field relationships of the various rock types and petrographic studies together with mineral and bulk rock chemical composition data allow the reconstruction of the complete geological history of the Allalin gabbro.

The gabbroic body intruded as a tholeiitic magma in a slow spreading MOR environment. Magmatic differentiation is recorded by clinopyroxene compositions, which show a Mg# and compatible element content decrease, and an incompatible element content increase from Mg to Fe-Ti gabbro. Exhumation to shallower depths let to subsolidus deformation and cooling of the gabbro that was followed by the intrusion of fine-grained basaltic dykes that display chilled margins. Bulk rock data of these dykes reveal strong similarities to tholeiitic pillow basalts of the Zermatt-Saas and nearby meta-ophiolites.

Subduction of the Allalin gabbro resulted in different mineral assemblages in the Mg-gabbros as a function of hydration degree. In partially hydrated metagabbros magmatic mineralogy (olivine + clinopyroxene + plagioclase) is preserved together with disequilibrium textures in the form of reaction coronae surrounding mineral boundaries. Fully hydrated metagabbros display eclogite-facies mineral assemblages, documenting the complete gabbro-eclogite transformation. Magmatic olivine is pseudomorphically replaced by omphacite + talc + chlorite + chloritoid + garnet, magmatic clinopyroxene by omphacite + garnet, and magmatic plagioclase by omphacite + zoisite + kyanite + chloritoid. The locally variable extents of hydration took place near the sea floor, as recorded by the chemical zonation patterns of metamorphic garnet coronae, the presence of Cl-apatite, and an increase in B concentrations of the pseudomorphic olivine domains.

The Allalin gabbro therefore represents a classical example of an oceanic gabbro formed in a slow spreading setting in the mid Jurassic that experienced heterogeneous hydration near the sea floor. Paleogene subduction of the gabbro to some 90 km depth produced variably equilibrated gabbroic eclogites. In eclogite-facies Mg-gabbros, the water-rich minerals chlorite, talc and chloritoid pseudomorphing magmatic olivine remained stable to these depths, revealing the potential relevance of hydrated Mg-gabbros as a fluid source at subarc depths in subduction zones.

2.4
Experimental determination of cation exchange coefficients to facilitate the predicition of Fe and Ca abundances in primary magmatic fluids

Ivano Gennaro[1], Alexandra Tsay[1], Michael Schirra[1], Zoltan Zajacz[1]

[1] *Departement des Sciences de la Terre, Université de Genève, Rue des Maraîchers 13, CH-1205 Genève (ivano.gennaro@unige.ch)*

Aqueous fluids exsolved from magmas can cause extensive alteration of the country rocks and often precipitate ore-grade accumulations of economically important base and precious metals. While the fluid-melt partitioning of ore metals between silicic melts and magmatic-hydrothermal fluids has been extensively studied, the fluid-melt exchange of major elements (Na, K, Fe, Ca, H), perhaps with the exception of Na and K, is not well understood despite the important role these elements play in controlling host rock alteration and ore metal precipitation. To bridge this gap in knowledge, a series of experiments were conducted in René41 alloy pressure vessels at 800 °C and 1750 bar to simulate conditions apparent in upper-crustal magma reservoirs. Experiments used AuAgCu-alloy capsules containing a synthetic starting glass of rhyolitic composition, a starting fluid calculated to be in equilibrium with the melt at experimental conditions and an intact quartz cylinder. The latter was thermally fractured *in situ* during the experiment after the attainment of equilibrium to sample the fluid phase in the form of synthetic fluid inclusions (SFI). The starting fluids were used to vary Cl content and impose variation in the aluminosity of the silicate melt through changing the amounts and ratios of chloride salts (NaCl, KCl, $FeCl_2$, $CaCl_2$) and HCl or NaOH. Run product glasses were analysed using electron probe microanalysis and laser ablation inductively coupled plasma mass spectrometry (LA-ICP-MS), and the SFI were also analysed by using LA-ICP-MS.

Run product fluid and melt compositions were used to calculate exchange coefficients with regards to Na ($K^{f/m}{}_{i,Na}$), the most abundant element in magmatic-hydrothermal fluids. All exchange coefficients show essentially no change as a function of fluid chlorinity. In the case of K-Na and Fe-Na exchange, this is consistent with previous studies (Dolejs & Zajacz, 2018; Frank et al., 2003; Holland, 1972; Student & Bodnar, 1999). The Ca-Na exchange coefficient was expected to increase with increasing Cl concentration in the fluid (Holland, 1972); however, this is not apparent likely due to the non-ideal behaviour of $CaCl_2$ in solution. Considering the effect of melt aluminosity, expressed here as melt ASI (molar Al / [Na + K + 2Ca]), the Ca exchange coefficient decreases (0.75 to 0.25) while the Fe exchange coefficient increases (2 to 6) in a stepwise manner just below the transition from peralkaline to metaluminous melt at an ASI of ~0.95. The value of $^*K^{f/m}{}_{Fe,Na}$ further shows a sharp increase at an ASI of ~1.15, increasing from 5 to 20. The data indicate that peralkaline melts tend to release more Ca, whereas metaluminous and especially peraluminous melts release more Fe to the fluid in addition to Na and K.

Model calculations using the newly constrained exchange coefficients suggest that all fluids derived from metaluminous to slightly peraluminous melts typical for porphyry ore-forming systems will have sufficient Fe to precipitate abundant pyrite in addition to Cu-rich sulphide minerals. Therefore, the initial S/Fe ratio and average S redox state will determine if significant Au can be held dissolved in the fluid until the epithermal stage (e.g. Heinrich, 2004). Significant anhydrite precipitation without sourcing Ca from the country rock is, however, only likely from hypersaline brines, either directly exsolved from the magma or condensed during the ascent of initially low- to intermediate salinity single phase magmatic fluids.

REFERENCES

Dolejs, D., & Zajacz, Z. 2018: Halogens in Silicic Magmas and Their Hydrothermal Systems. In: The role of halogens in terrestrial and extraterrestrial geochemical processes (Ed. by Harlov, D. & Aranovich, L.). Springer International Publishing, 431–544.

Frank, M.R., Candela, P.A., & Piccoli, P.M. 2003: Alkali exchange equilibria between a silicate melt and coexisting magmatic volatile phase: An experimental study at 800°C and 100 MPa, Geochimica et Cosmochimica Acta 67(7), 1415–1427.

Heinrich, C.A., Driesner, T., Stefansson, A., Seward, T.M. 2004: Magmatic vapor Contraction and the transport of gold from the porphyry environment to Epithermal ore deposits, Geology 32(9), 761–764. formation, Reviews in Mineralogy and Geochemistry, 65, 363–378.

Holland, H.D. 1972: Granites, solutions, and base metal deposits, EconomicGeology 67, 281–301.

Student, J.J. & Bodnar, R.J. 1999: Synthetic fluid inclusions XIV: Coexisting silicate melt and aqueous fluid inclusions in the haplogranite–H_2O–NaCl–KCl system, Journal of Petrology 40(10), 1509–1525.

2.5
Modelling the global water cycle – the effect of Mg-sursassite and phase A on deep slab dehydration and the global subduction zone water budget

Nils B. Gies[1], Matthias Konrad-Schmolke[2], Jörg Hermann [1]

[1] *Institute of Geological Sciences, University of Bern, Baltzerstrasse 1+3, 3012 Bern, Switzerland*
[2] *Department of Earth Sciences, University of Gothenburg, Guldhedsgatan 5a, 41320 Gothenburg, Sweden*

The abundance, distribution, and transport of water between the Earth›s surface and the Earth›s interior on our planet are crucial for numerous geological, petrological and geophysical processes. Of particular importance is the role of the hydrated lithospheric mantle in cold subduction zones, where the amount of water transported into the deeper mantle is determined by the stability of the hydrous phases. These are controlled by the chemical composition, initial hydration intensity and the thermal structure of the subducting slab, as well as the thermodynamic properties of the hydrous phases in the subducting slab.

We implement different published thermodynamic data for the two dense hydrous magnesium silicates (DHMS) phase A [$Mg_7Si_2O_8(OH)_6$] and Mg-sursassite [$Mg_5Al_5Si_6O_{21}(OH)_7$] in a global set of 56 subduction zone thermal patterns (Syracuse et al., 2010) in a gridded two-dimensional thermodynamic forward model, taking the migration of fluids within the slab into account. The model uses a combination of MATLAB and Perple_X, which uses Gibbs energy minimization to calculate stable phases and amounts of coexisting fluid. This allows to quantify and benchmark the effects of different thermodynamic databases, thermal and geometric patterns of subduction zones, and chemical compositions on the water budget in the subducting slab.

Our results show that, beyond the breakdown of Lawsonite, sedimentary and mafic rocks play a minor role for the globally subducted water budget. The absolute amount of deeply subducted water in subducted ultramafic rocks as well as the different dehydration patterns and the migration of fluids within the plate strongly depends on the depth and intensity of the initial slab mantle hydration and the Clapeyron slopes of the dehydration reactions of phase-A and Mg-sursassite. The global amount of deeply subducted water for different investigated models varies between 8 x 10^8 Tg/Ma and 1.4 x 10^9 Tg/Ma. In subduction zones with an intermediate temperature structure, the differences span several orders of magnitude. Depending on the choice of the thermodynamic dataset the globally subducted water modelled with a 2 wt.% H_2O hydrated 12 km slab mantle is equal to subduction of the entire Earth’s surface water in 1 to 1.7 billion years.

REFERENCES

Syracuse, E.M., van Keken, P.E. and Abers, G.A., 2010. The global range of subduction zone thermal models. Physics of the Earth and Planetary Interiors, 183(1-2), pp.73-90.

2.6
Controls on compositional zoning of zircon from the Catedral granite, Torres del Paine

Jack Gillespie[1], Jo Moore[1,2], Stéphane Escrig[3], Othmar Müntener[1], Lukas P. Baumgartner[1]

[1] *Institute of Earth Sciences, Faculty of Geosciences and Environment, University of Lausanne, Lausanne CH-1015, Switzerland (jack.gillespie@unil.ch)*
[2] *Institut für Geologische Wissenschaften, Freie Universität Berlin, Berlin, Germany*
[3] *Laboratory for Biological Geochemistry, School of Architecture, Civil and Environmental Engineering, École Polytechnique Fédérale de Lausanne (EPFL), Lausanne, CH-1015, Switzerland*

The internal zoning of crystals record the conditions of their growth, and these patterns are used to understand the evolution of the host magmatic system. However, it remains uncertain to what extent these zoning patterns are the result of equilibrium or non-equilibrium crystallisation growth processes. Understanding which of these processes dominantly controls the crystal composition is critical to our ability to accurately link textural, chemical, and isotopic data obtained from these crystals to the evolution of the wider system.

This study focusses on zircon crystals from the Catedral granite of the 12.6-12.45 Ma Torres del Paine laccolith in Patagonia, which is remarkable due to the spectacular exposure of the intrusive complex. This has allowed for detailed three-dimensional field characterisation of the architecture of the magmatic system, which comprises an early mafic feeder zone, three distinct granitic sills, and a late mafic sill complex that underlies the granitic units. Previous high-resolution U-Pb zircon geochronology places good controls on the timespans of magmatism across the entire system, with CA-ID-TIMS dates of 12.50 ± 0.01 and 12.49 ± 0.02 Ma obtained from samples of the Catedral granite (Michel et al., 2005). Here we integrate these existing geochronological and field data with textural and chemical characterisation of internal zoning of zircon crystals to constrain numerical zircon crystal growth models.

EPMA elemental mapping, NanoSIMS trace element transects, and high-resolution CL imaging of zircon from the Catedral granite reveal distinct textural populations which attest to evolving conditions over the history of the laccolith. Periodic truncation features that disrupt oscillatory growth zoning are interpreted as resorption interfaces indicating periods of zircon dissolution and growth hiatuses likely driven by an external forcing mechanism (e.g. temperature, composition, pressure). These features belie the apparently short-lived and simple crystallisation history implied by the zircon dates obtained from the Catedral granite. Intrusions interpreted to have crystallized late in the history of the Torres del Paine sytem contain zircons with continuous oscillatory growth zoning. NanoSIMS trace element transects reveal changes in concentration of a magnitude and wavelength that are challenging to explain via equilibrium processes. These conditions and the roles of external vs internal factors will be explored through numerical models of zircon growth from a felsic melt.

REFERENCES
Michel, J., Baumgartner, L., Putlitz, B., Schaltegger, U., Ovtcharova, M., 2008. Incremental growth of the Patagonian Torres del Paine laccolith over 90 k.y. Geology 36, 459-462.

2.7
Alkaline and arc-related magmas association in a subduction environment (Alexandra Volcanic Group, New Zealand): The role of melts at lithosphere-asthenosphere boundary

Maud Jordan[1], Sébastien Pilet[1], Marco Brenna[2]

[1] *Institute of Earth Sciences, University of Lausanne, 1015 Lausanne, Switzerland (maud.jordan@unil.ch)*
[2] *Department of Geology, University of Otago, Duniden 9054, New Zealand*

Alkaline magmatism is frequently linked to intraplate settings, although it can also be observed in rift zones or in association with subduction zones. This is the case on New Zealand›s North Island, where alkaline and arc-related magmas are spatially and temporally linked. This association raises questions about the mechanisms of formation of these two magma suites that are generally considered to be the outcome of distinct melting processes: ‹flux melting› for arc-related magmas and ‹decompression melting› for alkaline ones.

New Zealand›s North Island constitutes the eastern border of the Australian Plate, beneath which the Pacific Plate is subducting. This Island features two distinct active volcanic zones: the Taupō Volcanic Zone in the centre, representing the current arc front associated with the subduction of the Pacific Plate; and the Auckland Volcanic Field to the northwest, which consists of an alkaline monogenetic volcanic field considered as unrelated to subduction. Nonetheless, these two types of volcanism have not always been confined to separate geographical regions. Subduction of the Pacific Plate initiated during the late Eocene period (40-30 Ma) north of the present-day Northland Peninsula. Since then, subduction has propagated southward with the resulting arc front migrating from Northland (~24-16 Ma) through the Coromandel Peninsula (~16-4 Ma) to its present location in the Taupō Volcanic Zone (2-0 Ma; Seebeck et al., 2014). During the Plio-Pleistocene (3-1.5 Ma), arc-related volcanism was active on the west coast in the Waikato region (approx. 300-400 km away from the trench). Interestingly, alkaline magmatism started during this period, in the form of a monogenetic volcanic field (Okete Volcanics) embedded within these arc-related composite volcanoes. Together, these two volcanic associations constitute the Alexandra Volcanic Group (McLeod et al., 2022).
This specific intercalation suggests a petrogenetic relationship between the genesis of these two types of magma, raising questions about the processes behind the formation of alkaline melts within such a context.

The arc-related series is composed of coarse-grained to ankaramitic basalt/andesite showing high silica (46-47 wt.% for Mg#65), low titanium (0.6-1.5 wt.%), and characteristic low Nb/La ratio (< 1). In contrast, the alkaline Okete Volcanics show fine-grained olivine alkali basalt to basanite with lower silica (43-44 wt.% for Mg#65), higher titanium (1.5-2.7 wt.%), and higher Nb/La ratio (> 1). However, intermediate compositions are also observed suggesting some mixing. Geochemical modelling of peridotite melting indicates that the alkaline Okete Volcanics can result from low-degree melts produced near the garnet-spinel transition, i.e. close to the base of the lithosphere. The presence of these low-degree melts at the lithosphere-asthenosphere boundary is in agreement with geophysical studies. Melt accumulation at the base of the lithosphere is inferred in various tectonic contexts to account for seismic and electrical anomalies observed at depths of 70-100 km (e.g. Hua et al., 2023). The existence of such melts is consistent with petrological constraints if the role of volatiles in nominally anhydrous minerals is considered (Dasgupta, 2018). Trace amounts of H_2O and CO_2 lower the solidus, generating small melt fractions in the upper asthenospheric mantle without requiring any external melting factors. These parcels of melt can then migrate and accumulate at the base of the lithosphere. Geochemical modelling suggests that the chemistry and volume of the Okete alkaline magmas are consistent with the extraction of these naturally occurring low-degree melt ponding at the base of the lithosphere. We interpret the association of arc-related and alkaline magmas by the juxtaposition of two distinct mechanisms. Localised pulses of Pacific slab-derived fluids cause induce melting of the overlying mantle, generating the arc-related magmas that can either make their way to the surface or mix with some of the accumulated low-degree alkaline melt present at the lithosphere-asthenosphere boundary. We further propose that during intervals between these fluid pulses, these alkaline melts ascend to the surface using melt extraction channels created by arc-related magmas and surface faults, thus producing the Okete monogenetic volcanic field.

New Zealand›s particular tectonic setting highlights the importance of melting processes in shallow environments in the production of alkaline magmas. In addition, it could explain the presence of the Auckland volcanic field further north, which is not associated with a mantle plume. In a broader context, this approach opens up new perspectives on the production of alkaline magmas in general, which are widespread in a large number of different geological contexts.

REFERENCES

Dasgupta, R. (2018). Volatile-bearing partial melts beneath oceans and continents-where, how much, and of what compositions? American Journal of Science, 318(1), 141–165. https://doi.org/10.2475/01.2018.06

Hua, J., Fischer, K. M., Becker, T. W., Gazel, E., & Hirth, G. (2023). Asthenospheric low-velocity zone consistent with globally prevalent partial melting. Nature Geoscience, 16(2), 175–181. https://doi.org/10.1038/s41561-022-01116-9

McLeod, O. E., Brenna, M., Briggs, R. M., & Pittari, A. (2022). Slab tear as a cause of coeval arc-intraplate volcanism in the Alexandra Volcanic Group, New Zealand. Lithos, 408–409, 106564. https://doi.org/10.1016/j.lithos.2021.106564

Seebeck, H., Nicol, A., Giba, M., Pettinga, J., & Walsh, J. (2014). Geometry of the subducting Pacific plate since 20 Ma, Hikurangi margin, New Zealand. Journal of the Geological Society, 171(1), 131–143. https://doi.org/10.1144/jgs2012-145

2.8
3D melt inclusion geometries help quantify eruption triggers at Colli Albani (Italy)

Corin Jorgenson[1], Luca Caricchi[1], Micheal Stuckleberger[2], Giovanni Fevola[2] , Gergor Weber[3], Guido Giordano[4], Jordan Lubbers[5]

[1] Department of Earth Sciences, University of Geneva, Rue de Maraîchaire 13, CH-1205 Genève, corin.jorgenson@etu.unige.ch
[2] German Electron Synchrotron DESY, Notkestraße 85, DE-22607 Hamburg
[3] Department of Earth Sciences, University of Oxford, 3 S Parks Rd UK- OX1 3AN Oxford
[4] Department of Earth Sciences, University of Roma Tre, Via Ostiense, 133B, IT- 00154, Rome
[5] U.S. Geological Survey, 4230 University Dr Suite 100, US-99508, Anchorage

Melt inclusions, small droplets of magma trapped in phenocrysts prior to an eruption, may record volatile content of the magma before degassing, thus are a key tool for volcanologists to gain a view of the pre-eruptive state of magma. In recent years, research surrounding the feasibility of using melt inclusions for constraining true pre-eruptive volatile contents of magma has revealed the complex nature of these inclusions. Here we present 3D tomographic scans of over 2000 melt inclusions from 35 crystals from Colli Albani volcano (Italy), a low viscosity complex which makes large volume explosive eruptions. A large 3D dataset of inclusions allows for us to gain a holistic view of the evolution of a melt inclusion in the context of the mineral host (leucite versus clinopyroxene), mineral zoning, and the surrounding inclusions. We define six categories to classify melt inclusions based on shape, crystallinity, and vapour phase (glassy bubble free, glassy with a single bubble, glassy with multiple bubbles, glassy with irregular bubbles, microcrystalline, and tube shaped). This new classification allows us to make inferences about how the melt inclusion was trapped from the textural context alone. Furthermore, we investigate the validity of the often-assumed ellipsoidal shape of both melt inclusions and vapour bubbles for recalculating the volume from microscope images and find that while vapour bubbles are commonly spherical, melt inclusions are frequently irregular shapes and thus assuming an ellipsoidal shape can lead to large errors. Lastly, we use these results to investigate the saturation state of the magma of Colli Albani Volcano (Italy) prior to eruption. We find that the melt inclusions record a wide range of vapour phase fractions, suggesting that crystal growth and trapping of melt inclusions may have occurred during several phases of volatile exsolution (i.e., before and after degassing). Approximately 40% of melt inclusions with vapour bubbles have a volume fraction of >10% vapour bubble, and this can extend up to 78%. This high vapour content is indicative of a volatile enriched magma at the time of melt inclusion trapping and may reveal the trigger mechanism for the rapid ascent of the magma at Colli Albani.

2.9
The Clumped-isotope geochemistry of exhumed carbonate shear zones: Examples from the Torngat Orogen (Canada)

Brice Lacroix[1], Pierre Trap[2], Cyril Durand[3], Torsten Vennamann[4] , Philippe Goncalves[2] , Didier Marquer[2]

1. Department of Geology, Kansas State University, USA
2. UMR 6249 Chrono-Environnement, Université de Franche-Comté, France
3. EA 4515 LGCgE, University of Lille, France
4. IDYST, University of Lausanne, Switzerland

Clumped isotope thermometry is a technique that ideally recovers the temperature of carbonate formation without any assumptions regarding the composition of precipitating water and/or oxygen isotope composition of another mineral phase, such as required for conventional stable isotope thermometry. However, applications of this technique to high-grade metamorphic marbles remain limited. Here, we present clumped- ($\Delta47$), stable O and C isotope compositions measured across sheared high-grade marbles from the Torngat orogen, Canada, to explore the role of retrograde metamorphic reactions and deformation on $\Delta47$ values. The petrography shows that shear zones are associated with local dissolution of carbonate grains and the appearance of retrograde minerals. Both metamorphic assemblages and C-isotope equilibrium between carbonate and graphite support that the shear zones formed from peak-temperature conditions and during retrograde conditions at temperatures in the range 550-590 ˚C. Clumped isotope compositions of the host dolomitic marbles record apparent peak metamorphic equilibrium temperatures of 300-500˚C. Although these temperatures are significantly lower compared to regional peak temperatures derived from metamorphic reactions (about 750 ˚C), and C-isotope equilibrium between carbonate and graphite (about 730 ˚C), they are higher than other apparent $\Delta47$ temperatures of dolomitic marbles elsewhere (e.g., metamorphic core-complex of Naxos, Notch Peak aureole). In calcitic marbles, temperatures recorded by $\Delta47$ are between 151˚C and 260 ˚C, consistent with apparent temperature measured in other calcitic marbles. Within the shear zone, measured $\Delta47$ temperatures along the shear zones are inconsistent, giving very low values (even lower than 0 ˚C). Our results suggest that $\Delta47$ does not record the absolute peak temperature experienced by marbles. However, the abrupt changes in $\Delta47$ values across the shear zone suggest $\Delta47$ disequilibrium during CO2-rich aqueous fluid-rock interactions.

2.10 An astonishing choice: First petrological examination of Neolithic axe heads from Düdingen, Fribourg

Kolia Magnin[1], Christoph Nitsche[1], Vincent Serneels[1]

[1] *Department of Geosciences, University of Fribourg, Chemin du Musée 6, CH-1700 Fribourg (christoph.nitsche@unifr.ch)*

Switzerland possesses a rich catalogue of Neolithic archaeological sites that have been extensively excavated and documented by cantonal services and universities. Among the most important artefacts of this time are axeheads, carved from various crystalline rocks, which were used both as ordinary tools and as representative objects for high-ranking members of these past societies. Especially from the 6th to the 3rd millennium BC, findings of green axeheads made from eclogites and jadeitites from Alpine sources appear in archaeological sites all over Europe, indicating that trade and exchange networks over thousands of kilometres were already in place at the time. In addition to the study of production techniques, it is especially the potential of tracing these artefacts along sites that defines their invaluable scientific value.
However, the petrographic study of the artefacts has long been restricted to non-invasive, macroscopic examination. Fortunately, a recent change in conservation policies of several collections now permits the application of classical petrographic methods that provide much more detailed insights into the materials that were chosen by the artisans.
For this first pilot study, a total of 17 samples of broken axeheads and percussive tools from the site of Düdingen-Schiffenengraben (ca. 4000 BC), Canton of Fribourg, were analysed. The results show that a large part of the sampled axeheads were made from surprisingly unusual and rare rocks, such as epidotitites showing complex corona textures around garnet. Percussive tools, macroscopically resembling normal coarse-grained gabbros, turned out to be completely transformed, leaving unique pseudomorph structures. None of those rocks have been mentioned in previous literature yet and their unique composition indicates a specific material choice that cannot be explained by simple collection of river gravel around the site. While making the samples difficult to study and define, the unusual nature of these rocks is a promising indicator for future provenance attempts, given the proposed scarcity of the observed rock types in the field. This paper aims to showcase the potential of classical petrography applied on Neolithic artefacts which, while being invasive, adds a whole array of new data that can be used to better understand interconnectivity of early societies. It also counts on the support of the petrological community, whose expertise is crucial to trace potential primary sources of the raw material encountered in the archaeological record and refine the reconstruction of Neolithic exchange networks all over the European continent.

2.11
A general approach to quantify phase equilibria and silicate mineral stability fields in calc-alkaline basaltic systems

Felix Marxer[1], Renat Almeev[1], François Holtz[1]

[1] *Institute of Mineralogy, Leibniz University Hannover, Callinstrasse 3, 30167 Hannover, Germany (f.marxer@mineralogie.uni-hannover.de)*

As the “in-situ” study of magmatic processes is only possible to a very limited extent at some active volcanoes, igneous petrology predominantly relies on the analysis and interpretation of solidified magmatic products and their crystal cargo. As a consequence, a huge variety of petrological tools has been developed over the last years that have been widely applied to igneous rocks to reconstruct magmatic processes (e.g. thermobarometers or crystallisation algorithms like rhyolite-MELTS and COMAGMAT). However, most thermobarometers are frequently of only limited validity due to significant uncertainties and model interdependencies, while thermodynamic models suffer from severe limitations (especially for H_2O-bearing systems) complicating the application of these tools to natural rocks.

The prediction of phase equilibria is particularly complex for calc-alkaline systems, because water and oxygen fugacity vary over wide ranges. This study is an attempt to fill this gap by providing new experimental data exploring systematically the effects of temperature, pressure, magma composition, H_2O, and fO_2 on phase equilibria in calc-alkaline basaltic systems. Our experimental program was designed to extend existing high-pressure experimental datasets (400-900 MPa) on a high-Mg basalt from the Adamello Batholith (Italy) and a high-Al basalt from the Cascades (U.S.) to upper crustal pressures. Experiments were run in internally heated pressure vessels (IHPV) at 200 and 400 MPa and varying H_2O contents (0-9 wt.%) with fO_2 conditions buffered between NNO-1 and NNO+2.3. Additional experiments at 500 MPa were performed on a high-Mg basalt from Klyuchevskoy volcano in Kamchatka (Russia) to extend the range of investigated starting material compositions and pressures.

Beside changes in mineral assemblages, we established the influence of different crystallisation parameters on silicate mineral chemistry (e.g. for olivine, clinopyroxene, and plagioclase). We combined our new data with high-quality experimental data from literature to formulate empirical mineral saturation models for plagioclase and clinopyroxene predicting the saturation of these phases as a function of bulk system composition, pressure, temperature, H_2O, and fO_2. Furthermore, employing our experimental data compilation, we tested existing mineral-based thermobarometers to provide some general insight on their limitations and present some recommendations for their application to natural rocks.

2.12
Redox state, sulfur and chalcophile element budgets during magma differentiation in thick continental crust: a case study on the Parinacota volcano

Iván Mateo Espinel Pachón[1], Zoltan Zajacz[1], Cristóbal González Rodríguez[2], Michael Schirra[1], Alexandra Tsay[1], Weikai Li[1] and Mara Miranda[1]

[1] Department of Earth Sciences, University of Geneva, Rue des Maraîchers 13, 1205 Geneva, Switzerland (Ivan.espinelpachon@unige.ch)
[2] Millenium Institute on Volcanic Risk Research- Ckelar Volcanoes, Chile

Porphyry-type ore deposits form via metal sulfide precipitation from magma-derived fluids at convergent plate boundaries. The potential of a magma to generate porphyry ores depends on the availability of volatile elements and ore metals, as well as the apparent redox conditions throughout the course of magma differentiation. The redox state of the magma controls magmatic sulfide stabiltiy and therefore chalcophile metals sequestration and potential re-mobilization. Furthermore, it controls the speciation of sulfur in the magmatic volatile phase and thus the temperature range and spatial focusing of sulfide precipitation in the associated hydrothermal system. The evolution of volatile element and chalcophile metal budgets and magma redox state during magma genesis and differentiation in continental arcs is still a matter for scientific debate.
To address this problematic, we studied the Parinacota volcano in the Central Volcanic Zone of the Andes, which is characterized by particularly large crustal thickness (up to 70 km). We used silicate melt inclusions (SMI) from all major eruptive units to decipher chalcophile metal, volatile and redox systematics as a function of pre-eruptive magma storage depth and degree of differentiation. The combination of SMI data with mineral textures, phase equilibrium constraints and geothermobarometric calculations allowed the identification of at least three distinct components within four separate magma storage zones. Magmas at Partinacota are invariably oxidized, and notably the most primitve basaltic to basaltic andesitic magmas have the highest oxidation state. In addition, the most primitive melts have the highest Sr/Y ratios and also display highly elevated sulfur concentrations reaching up to about 7000 ppm, well above typical arc magma values (500 – 2500 ppm). These findings suggest that the high oxidation state of the magmas at Parinacota is imposed in the mantle soruce by the influx of slab derived fluids, or with a smaller likelyhood, during very early stages of magma differentaition in the mid- to lower crust. Positive correlations between Sr/Y and S, as well as Sr and Ba indicate that Sr, S and Ba are donated by slab-derived fluids along with other fluid mobile elements, and that extensive magma differentiation at deep crustal levels is not always a prerequisite for the generation of high-Sr/Y, S and Cl-rich chalcophile metal-bearing fertile magmas.

REFERENCES

Chiaradia M (2022) Distinct magma evolution processes control the formation of porphyry Cu–Au deposits in thin and thick arcs. Earth Planet Sci Lett 599:. https://doi.org/10.1016/j.epsl.2022.117864
Grondahl C, Zajacz Z (2022) Sulfur and chlorine budgets control the ore fertility of arc magmas. Nat Commun 13:. https://doi.org/10.1038/s41467-022-31894-0
Wörner G, Mamani M, Blum-Oeste M (2018) Magmatism in the central andes. Elements 14:237–244. https://doi.org/10.2138/gselements.14.4.237

2.13
Fluid-mineral equilibrium under stress investigated through molecular dynamics

Mattia L. Mazzucchelli[1], Evangelos Moulas[2], Stefan M. Schmalholz[1], Boris Kaus[2], Thomas Speck[3]

[1] *Institute of Earth Sciences, University of Lausanne, Lausanne, Switzerland (mattia.mazzucchelli@unil.ch)*
[2] *Institute of Geosciences and Mainz Institute of Multiscale Modelling (M3ODEL), Johannes-Gutenberg University of Mainz, Mainz, Germany*
[3] *Institut für Theoretische Physik IV, University of Stuttgart, Stuttgart, Germany*

The interpretation of phase equilibria and reactions in geological materials relies on standard thermodynamics. This thermodynamics assumes that the stress in the systems is hydrostatic and homogeneous, which means it is the same for all the phases involved. However, stress gradients and non-hydrostatic stresses are typical in rocks. Even in porous rocks with fluids, non-hydrostatic stress can arise in the solid matrix because the solid grains are in contact with the fluid and with other grains with varying contact areas. Such a condition casts doubts on the predictive power and accuracy of existing hydrostatic multiphase thermodynamic models. However, there is still no accepted theory to evaluate the thermodynamic effect of non-hydrostatic stress on reactions (e.g. Hobbs & Ord, 2015; Tajčmanová et al., 2015; Wheeler, 2014).

We have investigated the direct effect of a homogeneous non-hydrostatic stress on the solid-fluid equilibrium with molecular dynamics simulations (Mazzucchelli et al., submitted). With such simulations the energy of the system, the pressure of the fluid, the stress of the solid, as well as the overall melting and crystallization process can be monitored until the stressed system reaches the equilibrium conditions. Our results show that for simple systems at the stress range expected in the lithosphere, the shift of the pressure of the fluid-solid equilibrium is small, consistent with theoretical predictions (Frolov & Mishin, 2010). On the contrary, the mean stress of the solid is significantly affected by the applied non-hydrostatic stress and can deviate substantially from the pressure of the fluid. In the presence of large non-hydrostatic stresses, the stressed system becomes unstable and a rim of hydrostatically-stressed solid eventually crystallizes around the initial high-stressed solid core. The overall differential stress of the solid phase decreases while preserving the total stress balance, until the solid-fluid system reaches a new stable equilibrium. These results suggest that phase equilibria can be accurately predicted by taking the fluid pressure as a proxy of the equilibration pressure. Moreover, models used to describe equilibria and reactions in minerals and rocks under stress should not use the pressure of the fluid as a proxy of the mean stress of the solid, and should therefore not equate the thermodynamic pressure of the reaction to the mean stress of the solid.

REFERENCES

Frolov, T., & Mishin, Y. 2010: Effect of nonhydrostatic stresses on solid-fluid equilibrium. I. Bulk thermodynamics. Physical Review B - Condensed Matter and Materials Physics, 82(17), 1–14.
Hobbs, B. E., & Ord, A. 2015: Dramatic effects of stress on metamorphic reactions. Geology, 43(11), e372.
Mazzucchelli M., Moulas E., Kaus, B., Speck T. submitted: Fluid-mineral equilibrium under stress: insight from molecular dynamics. American Journal of Science.
Tajčmanová, L., Vrijmoed, J., & Moulas, E. 2015: Grain-scale pressure variations in metamorphic rocks: Implications for the interpretation of petrographic observations. Lithos, 216–217, 338–351.
Wheeler, J. 2014: Dramatic effects of stress on metamorphic reactions. Geology, 42(8), 647–650.

2.14
Sulfur enrichment on the surface of Mercury

Christian J. Renggli[1], Aleksandra N. Stojic[2], Andreas Morlok[2], Jasper Berndt[1], Iris Weber[2], Stephan Klemme[1], Harald Hiesinger[2]

[1] *Institute for Mineralogy, University of Münster, Corrensstr. 24, D-48149 Münster (renggli@uni-muenster.de)*
[2] *Institute for Planetology, University of Münster, Wilhelm-Klemm-Str. 10, D-48149 Münster*

The NASA MESSENGER probe to Mercury observed unexpectedly high abundances of S on the surface of the planet (Nittler et al. 2011; Weider et al. 2015)). The observations suggest that sulfides on Mercury's surface include CaS (oldhamite) and MgS (niningerite), at extremely reducing conditions, several logfO_2 units below the Iron-Wüstite buffer (IW), at IW-5 to IW-7 (Zolotov 2011; Namur et al. 2016). We propose that these sulfides are not magmatic phases, but formed by sulfidation of silicates with S-rich volcanic or fumarolic gases (Renggli et al. 2022). For example, diopside reacts with $CS_{2(g)}$ to form CaS, MgS, and quartz:

Here, we present mid-infrared spectral observations of experimentally sulfidized silicates, which will allow us to directly test the sulfidation hypothesis. The Mercury Radiometer and Thermal Infrared Spectromenter (MERTIS) onboard ESA/JAXA BepiColombo mission to Mercury will map the planet's surface in the mid-IR (Hiesinger et al. 2022). We conducted the experiments in sealed and evacuated silica glass ampules at temperatures from 800 to 1200 °C. Experimental run products were measured by micro FTIR with a Bruker Hyperion 3000 using a MCT detector. We report observations over the spectral range from 800-1300 cm^{-1} at a spectral resolution of 2 cm^{-1}.
The silicated minerals reacted with the reduced S-rich gas to form the Ca- and Mg-rich sulfides and quartz, as predicted by the chemical reaction above. The extent of sulfidation of the silicates depends on reaction temperature, reflected in the mid-IR spectra. We do not observe sulfide features in the FTIR spectra. However, the sulfidation reaction is identified by the formation of quartz, with strong shifts in the spectral features.

In summary, we argue that on Mercury, reduced S-rich fumarolic and volcanic gases rapidly react with silicate minerals and glasses to enrich the surface in S by generating sulfides and quartz. According to MESSENGER data, quartz is not expected to be present in the most Mercury terranes (Namur & Charlier, 2017). Therefore, BepiColombo's finding of quartz with the MERTIS instrument in areas with significant S enrichment, would be consistent with our theory that Mercury's surface silicates have undergone sulfidation. Importantly, less reducing conditions would be needed for the surface basalts if the sulfides are not magmatic phases. Sulfidation of silicates at the planet's surface would follow substantial S degassing as a result of oxidation of melts from IW-7 to IW3 from the mantle source to the surface of Mercury.

REFERENCES

Hiesinger, H., Helbert, J., Alemanno, G., et al., 2022: Studying the Composition and Mineralogy of the Hermean Surface with the Mercury Radiometer and Thermal Infrared Spectrometer (MERTIS) for the BepiColombo Mission: An Update, Space Sci. Rev. 216, 110.
Namur, O., Charlier, B., Holtz, F., Cartier, C., McCammon, C. 2016: Sulfur solubility in reduced mafic silicate melts: Implications for the speciation and distribution of sulfur on Mercury, Earth Planet. Sc. Lett. 448, 102-114.
Namur, O. & Charlier, B. 2017: Silicate mineralogy at the surface of Mercury, Nat. Geosci. 10, 9-13.
Nittler, L. R., Starr, R.D., Weider, S.Z., et al., 2011: The major-element composition of Mercury's surface from MESSENGER X-ray spectrometry, Science 333, 1847-1850.
Renggli, C.J., Klemme, S., Morlok, A., Berndt, J., Weber, I., Hiesinger, H., King, P.L., et al. 2022: Sulfides and hollows formed on Mercury's surface by reactions with reducing S-rich gases, Earth Planet. Sc. Lett. 593, 117647.
Weider, S., Nittler, L.R., Starr, R.D., et al., 2015: Evidence for geochemical terranes on Mercury: Global mapping of major elements with MESSENGER's X-Ray Spectrometer, Earth Planet. Sc. Lett. 416, 109-120.
Zolotov, M. 2011: On the chemistry of mantle and magmatic volatiles on Mercury, Icarus 212, 24-41.

2.15
Tracking fluid sources in the slab: Evidence from HP metabasalts from the Tianshan, NW China

Sophie Scherzer*[1,2], Esther M. Schwarzenbach[1,2], Maria Rosa Scicchitano[3], Besim Dragovic[4], Mirjam Kiczka[5], Timm John[2]

[1] *Department of Geosciences, University of Fribourg, Fribourg, Switzerland*
[2] *Institute of Geological Sciences, Freie Universität Berlin, Berlin, Germany*
[3] *German Research Centre for Geosciences (GFZ), Potsdam, Germany*
[4] *School of the Earth, Ocean and Environment, University of South Carolina, Columbia, SC, USA*
[5] *Institute of Geological Sciences, University of Bern, Bern, Switzerland*

** Corresponding author: sophie.scherzer@unifr.ch*

Slab fluids, which are released by the subducting oceanic lithosphere through compaction and dehydration processes, migrate within the slab upwards to the slab-mantle wedge interface. With that they represent an essential mechanism for the transfer of volatiles from the slab to the mantle wedge. Consequently, hydrophile volatiles can be used as tracers to determine intra-slab fluid flow processes. However, migration processes of slab dehydration fluids, particularly with regards to transport mechanism of redox sensitive elements like sulfur, as well as the evolution of fluid sources during metamorphism of the slab, are not yet understood well.

In this study we investigate an eclogite-facies metabasalt from the HP/LT Akeyazi Metamorphic Complex of the South Tianshan Orogen, NW China. The sample comprises several omphacite-dominated HP veins that crosscut the blueschist-dominated matrix and formed under peak metamorphic conditions. Using mineral chemical analyses combined with *in situ* $\delta^{34}S$ measurements of pyrite, as well as trace element and isotope analyses of C, Sr and Pb in mineral and vein separates, we track fluid sources and the transfer of the redox sensitive elements S and C and reconstruct the metamorphic evolution and the related intra-slab fluid flow of the studied sample.

All isotope systems provide evidence for multiple episodes of fluid-rock interaction with fluids derived from distinct sources. In particular, pyrite grains show patterns in *in situ* $\delta^{34}S$ values which record changes in fluid chemistry that are supported by Sr isotope and trace element compositions. Large pyrite grains recording microbially derived S reveal low temperature seafloor alteration affecting the protolith pillow basalt prior to subduction. This is supported by dolomite $\delta^{13}C$ values close to seawater-carbonate compositions. Based on chemical variations, the rock was infiltrated by a two stage intra-slab fluid-flow under peak to prograde metamorphic conditions during ongoing subduction, responsible for the formation of the omphacite-dominated HP-veins. MORB-like pyrite $\delta^{34}S$ signatures of around -0.75‰ as well as Sr-mixing lines between AOC and slightly altered basalt indicate that the first HP fluid originated from dehydrating ocean floor basalts. In contrast, negative pyrite $\delta^{34}S$ values of around -10.75‰ and Sr signatures correlating with the mixing of altered basalt with seawater$_{454Ma}$ and pelagic clays suggest that the second HP fluid originated from the basalt-seafloor sediment transition. Pathways formed by the first fluid were reused and enlarged by the second fluid, which however also formed new pathways. This sample provides detailed insights into intra-slab fluid flow and fluid-rock interaction processes at HP/LT metamorphic conditions and allows a better understanding of fluid transfer and changes in fluid sources during subduction zone processes.

2.16
The gold endowment of alkaline melts: Insights from LA-ICP-MS analysis of silicate melt inclusions

Michael Schirra[1], Zoltan Zajacz[1], Daniel Müller[2]

[1] *Department of Earth Sciences, University of Geneva, Rue des Maraichers 13, CH-1205 Geneva (michael.schirra@unige.ch)*
[2] *Independent Consultant, Las Condes, Santiago, Chile*

Alkaline magmatism can generate giant epithermal Au deposits (Jensen & Barton 2000). Prominent examples of this economically significant mineralization style are Ladolam (Papua New Guinea) and Cripple Creek (Colorado). The root causes determining ore fertility of alkaline melts remain enigmatic. Silicate melt inclusions (SMI) that entrapped primitive melts can be used to trace magma evolution and changes in ore-relevant element concentrations. Since alkaline melts are typically assumed to represent small magma volumes produced by low-degree partial melting, their Au content may be decisive for the formation of giant Au deposits such as Ladolam on Lihir Island (>1500 t of Au, Müller et al. 2001). We reconstructed the magmatic evolution of Lihir Island, Papua New Guinea, using SMIs, mineral geochemistry and oxy-thermobarometry calculations to identify key parameters that influence ore fertility and report the first Au concentrations for alkaline melts determined in-situ by LA-ICP-MS analysis of SMIs.

Our results indicate that alkaline melts evolved from ankaramitic (CaO/Al_2O_3 > 1, MgO > 8 wt.%) parental magmas. Experimental studies suggest that ankaramitic melt can be generated by high-degree partial melting of a clinopyroxene-rich source (Médard et al. 2006). Enrichment of fluid-mobile and depletion of fluid-immobile trace elements in SMIs indicate that the source lithology was metasomatically overprinted, in agreement with reported metasomatized mantle xenoliths found near Lihir Island (McInnes et al. 2001). Initial melts were highly oxidized (ΔFMQ +4), relatively dry (≤ 0.5wt.% H_2O), and metal-rich (~ 100 µg/g Cu). Sulfur and Cl concentrations in contrast are not particularly elevated. With subsequent crystal fractionation, dominated by clinopyroxene crystallization, alkali metal concentrations increased rapidly, producing the alkaline character of the melts. Similarly, water, volatile and metal concentrations also increased. A rapid decrease in S contents of SMIs with continuous fractionation was caused by exsolution of a low-density single-phase fluid, which is recorded by the presence of small vapor-rich fluid inclusions co-existing with SMIs.

Gold concentrations in SMI are variable but generally high (~ 1 to 100 ng/g) compared to typical calc-alkaline arc magmas (< 5 ng/g, Grondahl & Zajacz 2022). However, Au concentrations are not correlated with any other analysed element concentrations and are often recorded in time-integrated LA-ICP-MS signals as high-intensity single readings (i.e., “spikes”). The systematic association of these high Au intensity anomalies with the transient SMI signals indicates that these high Au intensities might be caused by ablation of nanometer-sized Au particles hosted in the SMIs. These Au nanoparticles may be inherited from the metasomatized cumulate source lithology and play an important role in the fertility of these melts for gold mineralization.

REFERENCES

Grondahl, C. & Zajacz, Z. 2022: Sulfur and chlorine budgets control the ore fertility of arc magmas, Nature Communications, 13, 4218.
Jensen, E.P. & Barton, M.D. 2000: Gold deposits related to alkaline mgmatism, Reviews in Economic Geology, 13, 279-314.
Médard, E., Schmidt, M.W., Schiano, P., Ottolini, L. 2006: Melting of amphibole-bearing wherlites: An experimental study on the origin of ultra-calcic nepheline-normative melts, Journal of Petrology, 47, 481-504.
Müller, D., Franz, L., Herzig, P.M., Hunt, S. 2001: Potassic igneous rocks from the vicinity of epithermal gold mineralization, Lihir Island, Papua New Guinea, Lithos, 57, 163-186.

2.17 Different formation processes for metamorphic olivine in Erro Tobbio unit, Italy

Michelle Ulrich[1], Coralie Vesin[1], Daniela Rubatto[1,2], Jörg Hermann[1], Marco Scambelluri[3]

[1] *Institut für Geologie, University of Bern, Baltzerstrasse 1+3, CH-3012 Bern (michelle.ulrich@unibe.ch)*
[2] *Institute Des Sciences de La Terre, University of Lausanne, Quartier Mouline, CH-1015 Lausanne*
[3] *Dipartimento di Scienze della Terra, Ambiente e Vita, University of Genova, C.so Europa 26, 16132 Genova, Italy*

The high-pressure antigorite-serpentinites from the Erro-Tobbio Massif (Italy) contain metamorphic olivine that is thought to have been produced by the antigorite + brucite dehydration reaction. However, the Erro-Tobbio Massif also contains subducted peridotites that are only partially serpentinized, and metamorphic olivine could also have been formed by recrystallization of relic mantle olivine (Scambelluri et al., 1991).

In this study we investigate the olivine formation process using in situ oxygen isotopes and trace elements (SIMS and LA-ICP-MS, respectively) in metamorphic olivine.

Among five olivine-bearing samples, ranging from static olivine to olivine in shear bands, fracture networks and veins, we found two distinct types of metamorphic olivine:

1. Olivine, that appears as porphyroblasts or as static olivine, overgrown by antigorite shards, has low Li, low B, relatively high Ni/Mn ratio and $\delta^{18}O$ values of ~5–5.5 ‰;
2. Olivine in shear bands, fracture networks and veins has variable Li, high B but low Ni/Mn, $\delta^{18}O$ values of ~4–5 ‰ and is in isotopic equilibrium with the antigorite.

The low Li and B olivine (i) overlaps with the composition of mantle olivine from the partially serpentinized peridotites of the Erro-Tobbio unit and has a Ni/Mn ratio that partially overlaps with the Ni/Mn ratio of mantle olivine. However, the high MnO content of 0.3–0.4 wt.% indicates that olivine (i) is metamorphic. We propose that this olivine is the product of recrystallization during subduction of relic mantle olivine (Ol_{rec})., in contrast to olivine (ii), which is the product of the antigorite + brucite dehydration reaction (Ol_{dehyd}). The results demonstrate that both types of metamorphic olivine, formed by different processes, can occur together within single samples of the same unit.

REFERENCES

Scambelluri, M., Hoogerduijin Strating, E.H., Piccardo, G.B., Vissers, R.L.M., Rampone, E., 1991: Alpine olivine- and titanian clinohumite-bearing assemblages in the Erro-Tobbio peridotite (Voltri Massif, NW Italy), Journal of Metamorphic Geology, 9, 1, 79-91

2.18
Preserved conditions of oceanic serpentinization in a subducted slice of lithospheric mantle

Coralie Vesin[1], Michelle Ulrich[1], Daniela Rubatto[1,2], Jörg Hermann[1], Marco Scambelluri[3]

[1] *Institute of Geological Sciences, University of Bern, Bern CH-3012, Switzerland (coralie.vesin@unibe.ch)*
[2] *Institut des Sciences de la Terre, University of Lausanne, Lausanne CH-1015, Switzerland*
[3] *Dipartimento di Scienze della Terra dell'Ambiente e della Vita, Università degli Studi di Genova, Corso Europa 26, 16132 Genova, Italy*

Serpentinization of ultramafic rocks and their recycling in the mantle via subduction is a major contributor to the element cycling in the Earth's interior, from the element uptake in the oceanic environment to the dehydration of serpentinites in subduction zones. The Erro-Tobbio Massif (Western Ligurian Alps) represents a slice of fossil oceanic lithosphere that was serpentinized during the opening of the Tethyan ocean in the late Jurassic and was later subducted to high-pressure conditions during the Alpine collision. We studied samples that preserve evidence of lizardite formation during shallow low-temperature hydration in the oceanic environment as well as samples that contain antigorite that formed during subduction after the lizardite-to-antigorite transition. The aim is to compare the isotopic and chemical characteristics achieved at the different conditions of serpentinization and to assess the extent of homogenization during metamorphism.

The oxygen isotopic composition of serpentine (analyzed in situ by SIMS) is used to constrain the temperature of hydration, while the trace element composition (measured by LA-ICP-MS) serves to estimate the fluid composition during hydration. Transition metals (Ni, Cr, V, Co, Sc, Mn, Zn) are immobile elements and their concentrations in serpentine should be indicative of the primary mantle minerals that serpentine has replaced. In the oceanic serpentinite samples, the transition metal compositions of lizardite remain distinct in the olivine and pyroxene sites. Antigorite can preserve a similar transition metal composition to the mantle mineral it replaces, but it can also exhibit a range of transition metal compositions between the olivine and orthopyroxene poles. This suggests that the lizardite-to-antigorite transition partly redistributes the trace element composition. Lizardite in oceanic serpentinite samples shows significant variations in $\delta^{18}O$, indicating a temperature range of 70-325°C during serpentinization considering seawater as fluid, but higher temperatures could be calculated for a hydrothermally evolved fluid. Conversely, antigorite shows a narrow range of $\delta^{18}O$ values (5.4–7.5‰). During low-temperature hydration, the fluid-mobile elements (Cl, B, Li, Sr) are sourced from the seawater and incorporated into serpentine. In particular, the Cl/B ratio can increase among the different lizardite textures during oceanic serpentinization, indicating a more saline fluid resulting from fluid-rock interaction. Antigorite is generally depleted in Cl and B compared to lizardite, likely due to the loss of fluid-mobile elements during the lizardite-to-antigorite transition.

The geochemical variability of lizardite suggests that it formed under varying temperature and water-rock ratio conditions during hydration in oceanic environments. This study demonstrates that the metastable oceanic serpentinization can persist during subduction. Furthermore, the Erro-Tobbio antigorite serpentinites reveal the homogenization of the major elements (especially oxygen), but the trace elements are either released to fluids (e.g., fluid-mobile elements) or distributed between olivine and orthopyroxene sites (e.g., transition metals). This implies that the fluid resulting from the antigorite-out dehydration reaction has a constant and defined composition with respect to the major element (especially $\delta^{18}O$), regardless of the hydration processes in the oceanic environment, while the trace element composition is more influenced by hydration and dehydration processes.

P 2.1
Lithostratigraphic characterisation of the Paleozoic units of the Suretta Nappe, Eastern Swiss Alps: insights from U-Pb dating of zircons and geological mapping in Val Madris (Grisons)

Maira Coray[1], Donat Fulda[1], Andrea Galli[2], Marcel Guillong[2], Peter Nievergelt[1], Stefan Heuberger[1]

[1] *Georesources Switzerland Group, Department of Earth Sciences, ETH Zurich, Sonneggstrasse 5, 8092 Zurich, Switzerland (coraym@student.ethz.ch)*
[2] *Institute of Geochemistry and Petrology, Department of Earth Sciences, ETH Zurich, Sonneggstrasse 5, 8092 Zurich, Switzerland*

We present a new lithostratigraphy of the Paleozoic units of the Suretta nappe based on field mapping and U-Pb dating of detrital zircons and of garnets in metasediments.

The Suretta nappe is part of the middle Penninic nappes in eastern Switzerland and consists of polymetamorphic basement rocks, Permian intrusions in the northern part and a Permo-Mesozoic cover (Scheiber et al., 2013).

In recent literature, a paleozoic metasedimentary unit has been mapped between an older basement and the Permo-Mesozoic cover. This unit has been referred to as “Permian”, “Late Palaeozoic” or “monocyclic unit” (Baudin et al., 1995). It has only been poorly defined and not yet dated.

To refine the lithostratigraphy and the evolution of the Suretta nappe, geological mapping in Val Madris, petrographic descriptions, whole-rock geochemical investigations, and uranium-lead (U-Pb) detrital zircon and garnet geochronology have been performed.

This study shows that we can distinguish two metasedimentary formations between the older basement and the Permo-Mesozoic cover. The new ages prove that the stratigraphically lower Valle di Lei Formation is pre-Permian. The upper Val Saenta Formation contains Permian detrital zircons and is probably late Permian (Figure 1). The Val Saenta Formation can be correlated with the Col de Chassoure Formation in the middle Penninic Mont Fort and Siviez-Mischabel nappes in the Western Alps (Sartori et al. 2006).

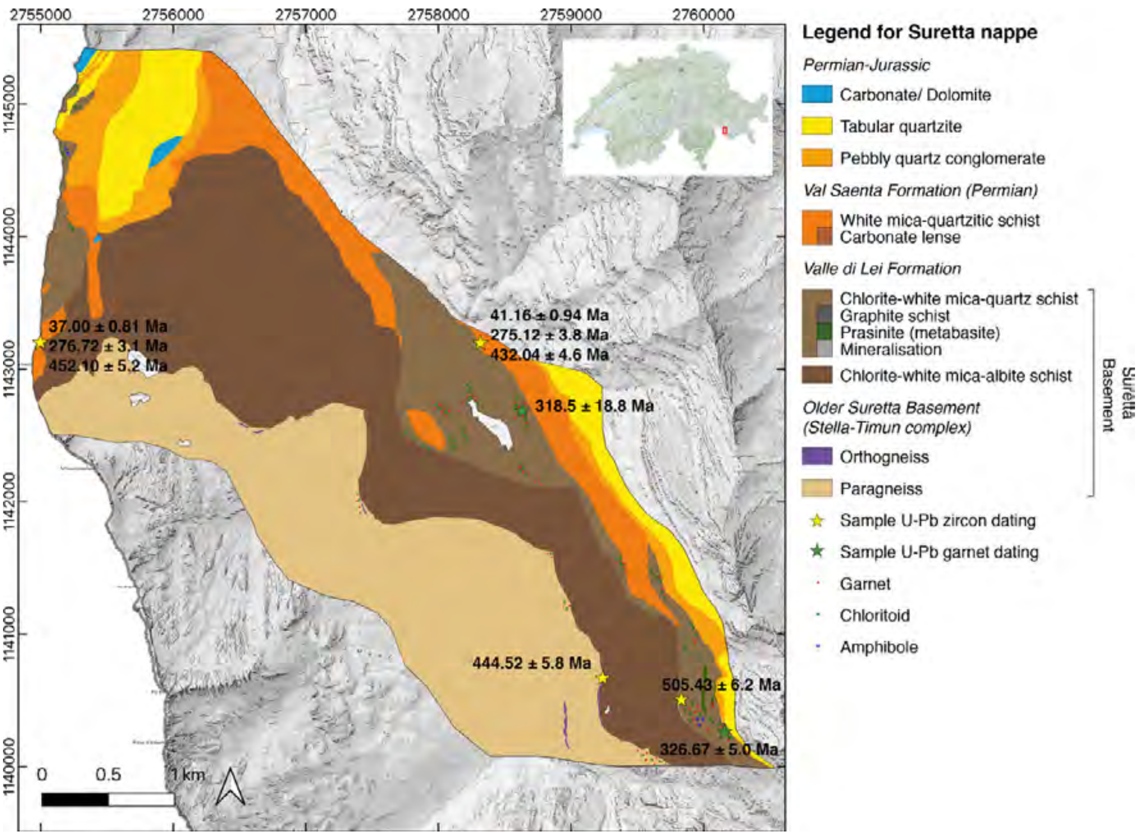

Figure 1. Our new geological map of the Val Madris with the dated samples.

REFERENCES

Baudin, T., Marquer, D., Barféty, J.-C., Kerckhove, C., & Persoz, F. 1995: Nouvelle interprétation stratigraphique de la couverture mésozoïque des nappes de Tambo et de Suretta: mise en évidence d'une nappe de décollement précoce (Alpes centrales suisses), Comptes rendus de l'Académie des sciences, 321(5), 401-408.

Sartori, M., Gouffon, Y., & Marthaler, M. 2006: Harmonisation et définition des unités lithostratigraphiques briançonnaises dans les nappes penniques du Valais, Eclogae geol. Helv., 99, 363–407.

Scheiber, T., Berndt, J., Heredia, B., Mezger, K., & Pfiffner, O. 2013: Episodic and long-lasting Paleozoic felsic magmatism in the pre-Alpine basement of the Suretta nappe (eastern Swiss Alps), International journal of earth sciences, 102(8), 2097-2115.

P 2.2
Distribution of C-bearing phases in the Ivrea lower continental crust (Ossola Valley, Italy)

Sarah Degen[1], Jörg Hermann[1], Daniela Rubatto[1,2], Alexia Secrétan[2]

[1] *Institute of Geological Sciences, University of Bern, Baltzerstrasse 1+3, CH-3012 Bern (sarah.degen@unibe.ch)*
[2] *Institut des Sciences de la Terre, University of Lausanne, CH-1015 Lausanne*

The Ivrea lower continental crust consists of underplated mafic as well as metasedimentary rocks. In the metasedimentary rocks, carbon in the form of residual carbonates and graphite can potentially be stored for millions to billions of years. Yet, the abundance of the carbon-bearing minerals is poorly quantified.

Rock samples from the Ossola valley collected from outcrops as well as drill cores obtained from the DIVE-project were studied regarding the distribution of C-bearing phases in the upper section of the lower continental crust. The drill core samples are mainly biotite schists (Qtz + Pl + Bt ± Grt ± Sil ± Kfs), amphibolites (Amp + Pl + Qtz ± Px ± Bt) and calcsilicates (Qtz + Pl + Grt + Px + Ttn ± Amp). Complementary marbles (Cb + Qtz + Px + Ttn + sulfides) and higher-grade metasediments (stronalites) were collected at outcrops. In most lithologies, varying degrees of partial melting has been observed. Graphite occurs in the matrix of biotite schists and as inclusions in garnet. Moreover, carbonates are present in relatively pure marble lenses and as interstitial grains in calcsilicates and to a lesser extent in amphibolites.

Total carbon analysis (TIC/TOC) revealed that the biotite schists contain between 0.01 and 1.21 wt.-% carbon whereas in case of amphibolites and calcsilicates, values range from 0.01 to 2.42 wt.-%. Furthermore, elemental carbon is dominant in the biotite schists whereas amphibolites and calcsilicates contain higher amounts of inorganic carbon.
An attempt to use apatite as a monitor for carbon mobilisation by quantification of the CO_2 content via ATR-FTIR (according to the method of Hämmerli et al., 2021) revealed that the mineral is CO_2-free in all rock types. This implies that apatite is either not a suitable monitor for carbon mobility in the investigated rocks or that mobilisation did not take place in the studied areas.

Garnets in C-bearing samples show compositional differences depending on the hosting lithology. The prevailing type of garnet in the biotite schist is composed of $Alm_{65}Grs_{11}Prp_{14}Sps_{8}Adr_{2}$. The Fe-component is lower and the Ca-component higher in the amphibolite ($Alm_{62}Grs_{15}Prp_{15}Sps_{5}Adr_{3}$). In calcsilicate rocks, this trend is even stronger, resulting in a composition of $Alm_{54}Grs_{29}Prp_{6}Sps_{9}Adr_{3}$. Therefore, garnet compositions can be used to distinguish between carbonate-rich protoliths for calcsilicates and carbonate-poor protholiths in case of the amphibolites.
Our study shows that felsic lithologies of the metasedimentary lower crust contain up to 2.42 wt.-% C and thus represent a reservoir that should be considered in the carbon budget of the crust.

REFERENCES

Hämmerli, J., Hermann, J., Tollan, P. & Naab, F. 2021: Measuring in situ CO_2 and H_2O in apatite via ATR-FTIR, Contributions to Mineralogy and Petrology, 176/12.

P 2.3
A multi-method approach to investigate pluton formation and melt production in the deep crust: case study of the El Oro Complex in Ecuador

Hugo Dominguez[1], Pierre Lanari[1], Renée Tamblyn[1], Nicolas Riel[2]

[1] *Institute of Geological Sciences, University of Bern, 3012 Bern, Switzerland*
[2] *Institute of Geosciences, Johannes Gutenberg University Mainz, J.-J.-Becher-Weg 21, D-55128, Mainz, Germany*

The El Oro Complex, in the southwestern part of Ecuador, is a tilted crustal section of metasediments from the Ecuadorian forearc. The lower segment of this complex underwent partial melting triggered by the intrusion of gabbroic magma over a relatively short period of 5 million years during the Triassic era. This event led to the formation of an S-type pluton known as the Marcabelí granitoid. Such a short-lived episode provides an excellent opportunity to gain a better understanding of the mechanisms underlying the formation and transport of melt in the continental crust, spanning deep to shallow regions.

We present a thermal model coupled with thermodynamics to simulate partial melting and melt extraction for different scenarios during the Triassic metamorphic history of the El Oro Complex. Temperature and assemblages are simulated at each timestep and melt is extracted from the model using a liquid percolation threshold. The findings of our simulations are compared with new field, geochemical and geochronological data. U-Pb geochronology and trace element compositions were performed on zircons from the granitoid and its source, allowing to have better constraints on the history and duration of the pluton emplacement. Combining these different approaches provide new insights into the melting processes of the deep continental crust.

This project has received funding from the European Research Council (ERC) under the European Union’s Horizon 2020 research and innovation programme (grant agreement No 850530).

P 2.4
Thermodynamic calculations of fluids in the deep crust

Jacob B. Forshaw[1], Nicolas Riel[2], George-Dan Miron[3], Pierre Lanari[1]

[1] *Institute of Geological Sciences, University of Bern, Switzerland*
[2] *Institute of Geosciences, Johannes Gutenberg University of Mainz, Germany*
[3] *Paul Scherrer Institute, Switzerland*

During orogenesis, metamorphic rocks devolatilise as they are subjected to an increase in Pressure and Temperature. The produced fluids exert a first-order control on metamorphic mineral assemblage development and enable mass transfer within the crust. Therefore, quantifying the chemical composition of fluids released by different rock types and lithologies at a range of Pressure-Temperature conditions is critical.

Current thermodynamic models simplify metamorphic fluids to three or fewer of their main components: H_2O, nonpolar gases, salts, and host-rock oxide components. We compare aqueous speciation calculations from different programs that use different models to investigate the effect on crustal mass transfer calculations. The dissolution of rock-forming minerals into aqueous species within a fluid is primarily determined by a fluid's density, dielectric constant, and chlorinity. Therefore, we examine how the thermodynamic properties of aqueous species vary due to different equations of state for H_2O, different electrostatic models, and different chlorinity values. The results of this study have wide-ranging implications for the thermodynamic modelling of complex crustal fluids.

This project has received funding from the European Research Council (ERC) under the European Union's Horizon 2020 research and innovation program (grant agreement No 850530).

P 2.5
Numerical simulations of gold deposition by boiling in epithermal systems

Nicolas Krattiger[1], Thomas Driesner[1]

[1] *Institute of Geochemistry and Petrology, ETH Zurich, Clausiusstrasse 25, CH-8092 Zurich (nicolas.krattiger@erdw.ethz.ch)*

Low-sulfidation epithermal deposits are an important source for gold and silver worldwide. They usually form in volcanic provinces in shallow crustal depths at temperatures between ~150 and 300°C. It is widely accepted that active geothermal systems are present-day analogues of systems which formed low-sulfidation epithermal deposits in the past. Previous studies on both active geothermal and fossil epithermal systems have revealed key aspects of low-sulfidation epithermal ore formation, e.g., that boiling is a main mechanism for high-grade gold precipitation (Simmons et al., 2005).

However, epithermal systems are characterized by a complex interplay between hydrological, geological, chemical, and physical processes, and key questions concerning the formation of economic gold deposits have not been answered yet. Especially, it is unclear how they have to interact such that boiling zones can efficiently form economic gold deposits. This question is of pivotal importance since many geothermal systems lack economic gold mineralization, as evidenced by active systems – there is no present-day geothermal area where active ore deposition has been recognized (Hedenquist & Lowenstern, 1994).

Computer simulations are a powerful tool to simulate deterministic systems showing complex emergent behaviour, as it is the case for geothermal systems (Ingebritsen et al., 2010). Assumptions based on field observations can be included as boundary conditions or input parameters and the behaviour of the system as a response to changes in these conditions can be investigated. Despite the great potential of numerical approaches, only some partial problems concerning the ore formation in epithermal systems have been modelled so far.

We perform 2D fluid flow simulations in a magmatic setting with a cooling pluton in the subsurface. The porous-media flow simulations are carried out using the modelling platform CSMP++ and coupled with a reactive-transport model for gold transport and precipitation in the crust, focusing on key aspects controlling gold solubility, mainly H_2S partitioning between the water vapor and liquid phase during boiling (Drummond & Ohmoto, 1985). The main focus of our study is (1) to investigate the role of host rock permeability on the distribution of gold precipitates in the system and (2) to estimate maximal gold grades that can ideally be achieved in a porous-media setting without fractures or other highly-permeable pathways focussing fluid flow.

REFERENCES

Drummond, S. E., & Ohmoto, H. 1985: Chemical evolution and mineral deposition in boiling hydrothermal systems, Economic Geology, 80, 126-147.

Hedenquist, J. W., & Lowenstern, J. B. 1994: The role of magmas in the formation of hydrothermal ore deposits, Nature, 370, 519-527.

Ingebritsen, S. E., Geiger, S., Hurwitz, S., & Driesner, T. 2010: Numerical simulation of magmatic hydrothermal systems, Reviews of Geophysics, 48.

Simmons, S. F., White, N. C., & John, D. A. 2005: Geological Characteristics of Epithermal Precious and Base Metal Deposits, Economic Geology 100th Anniversary Volume, 485-522.

P 2.6
Volatile budgets and evolution in porphyry-related magma systems, determined using apatite

Charline Lormand[1], Madeleine C. S. Humphreys[2], Jason P. Coumans[3], Cyril Chelle-Michou[4], Weiran Li[5]

[1] *Department of Earth Sciences, University of Geneva, Rue des Maraîchers 13, 1205 Geneva, Switzerland (charline.lormand@gmail.com)*
[2] *Department of Earth Sciences, Durham University, South Labs, Lower Mountjoy, South Rd, Durham DH1 3LE, United-Kingdom*
[3] *Natural Resources Canada, 580 Booth St, Ottawa, ON K1A 0E4, Canada*
[4] *Department of Earth Sciences, ETH Zürich, Clausiusstrasse 25, 8092 Zürich, Switzerland*
[5] *Department of Earth Sciences, The University of Hong Kong, Pokfulam Road, Hong Kong*

To what extent is the volatile evolution of mineralising systems, such as porphyry ore deposits, representative of volcanic plumbing systems? To answer this key question, melt and fluid inclusion compositions are commonly probed to constrain the volatile evolution near the magmatic-hydrothermal transition, as they capture a direct record of the dissolved or exsolved volatile phase. However, fluid inclusions are scarce, challenging to analyse, and melt inclusions may be affected by post-entrapment re-equilibration processes. We propose that in-situ analysis of apatite, which incorporates volatiles in its crystal lattice, may offer a superior alternative to melt and fluid inclusion analysis.

We use apatite as a recorder of the volatile budget of magmas and derive the volatile saturation state of magmatic systems. We model the volatiles in apatite following (Humphreys et al. 2021) but with the improvement that we integrate the temperature-dependent exchange coefficients that reflect the non-ideal mixing of F-Cl-OH in apatite (Li & Costa 2020). We model the apatite dataset of the Corrocohuayco porphyry-skarn Cu deposit, Peru (Chelle-Michou & Chiaradia 2017) which comprises early gabbrodiorites, mineralised hornblende(-biotite) porphyries, and later rhyodacite dykes. The modelling determines initial F, Cl and H_2O of each magma and allows us to estimate the timing of volatile saturation relative to crystal fractionation. Further, we are able to retrieve both the melt and fluid compositions (e.g., salinity) at the point of volatile saturation. Our modelling results fall within the range of direct measurements of melt and fluid compositions. This provides a new way to determine whether there are fundamental differences in magma crystallisation and fluid evolution in barren and mineralised systems.

REFERENCES

Chelle-Michou, C. Chiaradia, M. 2017: Amphibole and apatite insights into the evolution and mass balance of Cl and S in magmas associated with porphyry copper deposits, Contrib. Min. Petrol. 172:105.

Humphreys, M.C.S., Smith, V.C., Coumans, J.P., Riker, J.M., Stock, M.J., de Hoog, J.C.M., Brooker, R.A. 2021: Rapid pre-eruptive mush reorganisation and atmospheric volatile emissions from the 12.9 ka Laacher See eruption, determined using apatite, Earth and Planetary Science Letters 576:117198.

Li, W., Costa, F. 2020: A thermodynamic model for F-Cl-OH partitioning between silicate melts and apatite including non-ideal mixing with application to con-straining melt volatile budgets. Geochimica et Cosmochima Acta 269, 203–222.

P 2.7
Intra-Grain Variability of Trace Elements in Rutile

Mona Lueder[1], Jörg Hermann[1], Renée Tamblyn[1], Daniela Rubatto[1,2], Pierre Lanari[1], Thorsten Markmann[1]

[1] *Institute of Geological Sciences, University of Bern, Baltzerstrasse 1+3, CH-3012 Bern, Switzerland*
[2] *Institute of Earth Sciences, University of Lausanne, Géopolis, Quartier Mouline, 1015 Lausanne, Switzerland*

Rutile is one of the main accessory minerals in high grade metamorphic rocks and is frequently used as petrogenetic indicator mineral. Zr-in-rutile thermometry, U-Pb geochronology, and discrimination diagrams based on various trace elements are often used to infer formation processes of metamorphic host rocks or protoliths of detrital grains. Homogeneity of trace elements is often implicitely assumed. However, it has been shown that Zr-, Nb-, and Ta contents in rutile can vary from core to rim, but systematic studies of inter grain variability of trace elements in rutile are lacking.

We will present results from laser ablation inductively coupled plasma mass spectrometry (LA-ICP-MS) mapping on rutile grains from low-T – high-P metamorphic rocks, hydrothermal clefts, and pegmatites. Maps have been aquired by line scanning with spot sizes of 12–38 μm, depending on grain size, resulting in a spatial resolution of up to 12 μm. Data reduction was performed using the software *XMapTools*.

All samples are zoned in one or more trace elements, showing several different zoning patterns. Hydrothermal and pegmatitic rutile show predominantly sector zoning. Oscillatory trace element zoning within a sector are interpreted to indicate variability in fluid composition during rutile growth within these samples. Rutile from quartz veins in low-T eclogites show decreasing zirconium content from core to rim which is consistent with rutile growth during retrograde vein formation. Calculated Zr-in-rutile temperatures are in the range ~450–550 °C and decrease by ~20–30 °C from core to rim. Thus, Zr-in-rutile thermometry might be reliably appied in such cases. Contrarily, low-T metamorphic rutile shows irregular zoning patterns in Zr. This suggests that Zr contents depend on Zr activity or were modified by sample internal fractionation during rutile growth, rather than reflecting temperature variations. This result indicates that Zr-in-rutile temperatures should be used with caution to constrain the metamorphic evolution of low temperature rocks. Additionally, Nb and Ta are only partially correlated within a single grain, and Nb/Ta-ratios vary significantly between growth zones. Two processes can explain these variations (1) Nb and Ta fractionation during rutile growth, and (2) later modification during post-growth recrystallisation.

Rutile trace element contents have high intra-grain variabilities, with different behaviour depending on, lithology, P–T-conditions, or fluid availability. This has significant implications for using rutile as petrogenetic indicator mineral. Further investigation into understanding the processes responsible for observed trace element zoning are required.

P 2.8
Modelling fluid recycling and fluid fluxes during subduction

Thorsten Markmann[1], Pierre Lanari[1]

[1] *Institute of Geological Sciences, University of Bern, Baltzerstrasse, CH-3012 Bern (thorsten.markmann@geo.unibe.ch)*

Dissolution of hydrous minerals during prograde metamorphism, which releases aqueous fluids, is thought to play an important role in triggering subduction-related processes such as earthquakes or partial melting. Petrological models can simulate the release of metamorphic fluids by hydrated lithologies, and are used in this study to understand the fate of these fluids. An advanced petrological model based on Gibbs energy minimization was developed to simulate the fluid production and associated fluid fluxes in a multi-rock system during prograde metamorphism. Two scenarios are tested with (1) a fully hydrated mafic layer at the bottom of a stack of partly hydrated mafics and (2) a stack of mafics alternating between hydrated and partly hydrated material. Hydrated mafic lithologies typically lead to continuous fluid release due to the mineral decomposition. Relatively dry lithologies thus have the potential to consume such released fluids assuming pervasively infiltration. This internal fluid recycling may stabilize hydrous phases under blueschist to eclogite facies conditions and influence the fluid accumulation, migration and release from the subducted stack. As a consequently, the effective fluid release from the stack can be delayed by >10 km. We propose that this process results in the recycling of released fluids within the slab and might explain localized fluid releases in subduction zones, which are i.e. required to contribute to partial melting of the mantle wedge.

This project has received funding from the European Research Council (ERC) under the European Union’s Horizon 2020 research and innovation program (grant agreement No 850530).

P 2.9
P-T conditions and timing of melting in the Ivrea lower continental crust

Luca Pacchiega[1], Daniela Rubatto[1,2]

[1] *Institut für Geologie, Baltzelstrasse 1+3, CH-3012 Bern (luca.pacchiega@geo.unibe.ch)*
[2] *Institute of Earth Sciences (ISTE), Quartier UNIL-Mouline, Bâtiment Géopolis, CH-1015 Lausanne*

Partial melting plays a fundamental role in a wide range of geological processes including the formation and modification of the continental crust. In particular, the chemical differentiation and the thermal evolution of lower crustal terranes is strongly related to the production and upward migration of anatectic melts. In turn, the amount of melt that is produced through space and time is controlled by the protolith fertility and the P-T conditions attained during metamorphism.

The lower continental crust exposed in the Ivrea Zone is currently being investigated by DIVE, a scientific drilling project founded by ICDP. In this framework, this study focuses on the chronology and conditions of melting at the crustal depth of site DT-1b, the first borehole drilled in Val d'Ossola. The rock investigated are primarily migmatitic metasediments and amphibolites, which are the two main lithologies occurring in the drilled cores and the surrounding outcrops.

Thermodynamic modelling of selected samples constrains the P-T conditions attained during peak metamorphism to upper-amphibolite facies around 750 °C and 0.7 GPa. Additionally, we estimated melt productivity and the responsible melting reactions for both rock types. Zircon U-Pb dating of residual samples and of the corresponding leucosomes was used to constrain the timing of melting. In particular, metamorphic zircon domains in the leucosome from the amphibolite yield a single age at ~260 Ma. The latter might be related to melt crystallization and cooling following a thermal maximum, which occurred ~25 Ma after the emplacement of the Mafic Complex. Titanite has also been dated to ~265 Ma, in agreement with zircon, suggesting that melting and metamorphic recrystallization occurred within a few Ma.

Instead, zircons from a leucosome in the metasediments record a significantly larger spread of dates from ~300 Ma to ~260 Ma, without a clear statistical peak. This finding suggests that the metasediments at this crustal depth experienced a protracted melting history, occurring over a time interval of ~30 Ma and possibly starting prior the main regional magmatic event.

P 2.10
The structural and lithological control on mineralization at the Upper Cretaceous Sakdrisi epithermal deposit, Bolnisi district, Lesser Caucasus, Georgia

Nino Popkhadze[1,2], Şafak Utku Sönmez[3], Malkhaz Natsvlishvili[2], Robert Moritz[3]

[1] *Al. Janelidze Institute of Geology, Iv.Javakhishvili Tbilisi State University, Georgia*
[2] *RMG Rich metals Group (nino_popkhadze@yahoo.com)*
[3] *Department of Earth Sciences, University of Geneva, Rue des Maraîchers 13, 1205 Geneva, Switzerland*

The Bolnisi district is a part of the Lesser Caucasus and is located at its northern extremity. To the west, this ore district continues into the Eastern Pontides, Turkey. This favorable geotectonic location of the Late Cretaceous Bolnisi ore district (which is also part of the Arvin-Bolnisi Belt) between the Lesser Caucasus and the Eastern Pontides is reflected by its geological diversity, volcanism type and mineral deposit distribution. The Late Cretaceous (~87–71 Ma) bimodal volcanism in this region resulted in mafic and felsic rock types, the latter being a major host of the ore deposits and prospects, and being defined locally as the felsic Mashavera and Gasandami suites. The host rocks of the Bolnisi mining district are represented by Late Cretaceous volcanic and volcano-sedimentary rocks.

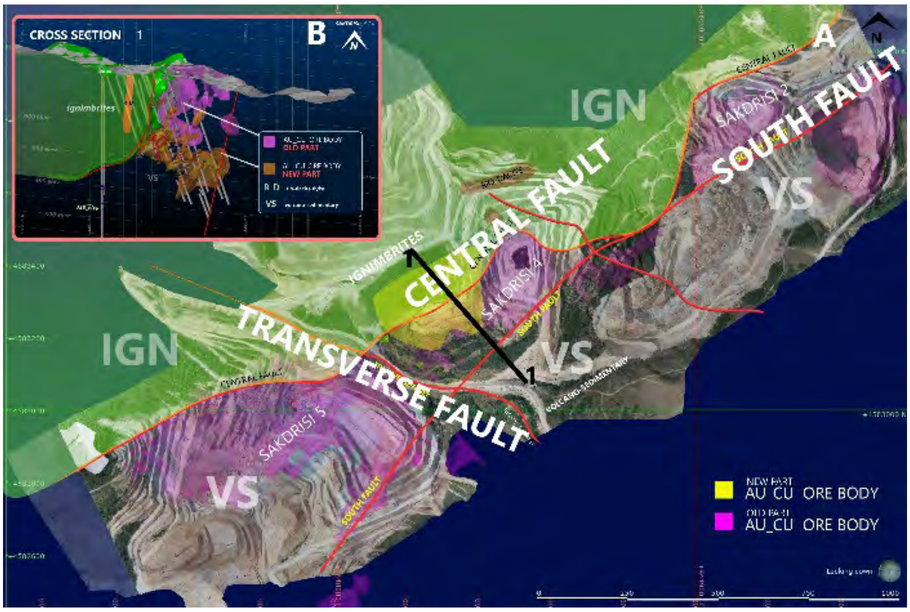

Fig.1 3D regional model of the Sakdrisi deposit, with modelled faults and lithology.

Our interpretations and mapping program were undertaken on Sakdrisi 4 and 5. Two complexes have been recognized in this deposit, and belong to the Mashavera suite. They include a lower mineralized volcano-sedimentary complex (LVSC) and an upper barren volcano-sedimentary (UVSC) (Fig.1) complex, which are separated by a NE oriented thrust. The lower mineralized complex is composed of the following lithological units: bedded sedimentary mudstone with tuff interlayers, pumice-bearing volcaniclastic rocks, slightly mineralized rhyolite and rhyolite tuff, and crosscutting explosive breccia, which is well expressed in the Sakdrisi 5 open pit (Fig.2). The upper non-mineralized complex consists of welded and non-welded ignimbrite, limestone lenses and crosscutting andesite-basaltic and rhyodacitic dykes. The mineralized zones are present in the LVSC at certain horizons, and consist mainly in quartz-sulfide and quartz veins, as it was discovered as a bonanza zone located just beneath the thrust zone at the Sakdrisi 4 open pit. Explosive breccia in the system creates a fracture system sometimes together with the regional faults where gold/copper gold bearing quartz and quartz-sulphide veins and stockworks are developing. Recent data from 400–600 m deep drill cores indicate enriched mineralized zones, which is a new discovery for this deposit.

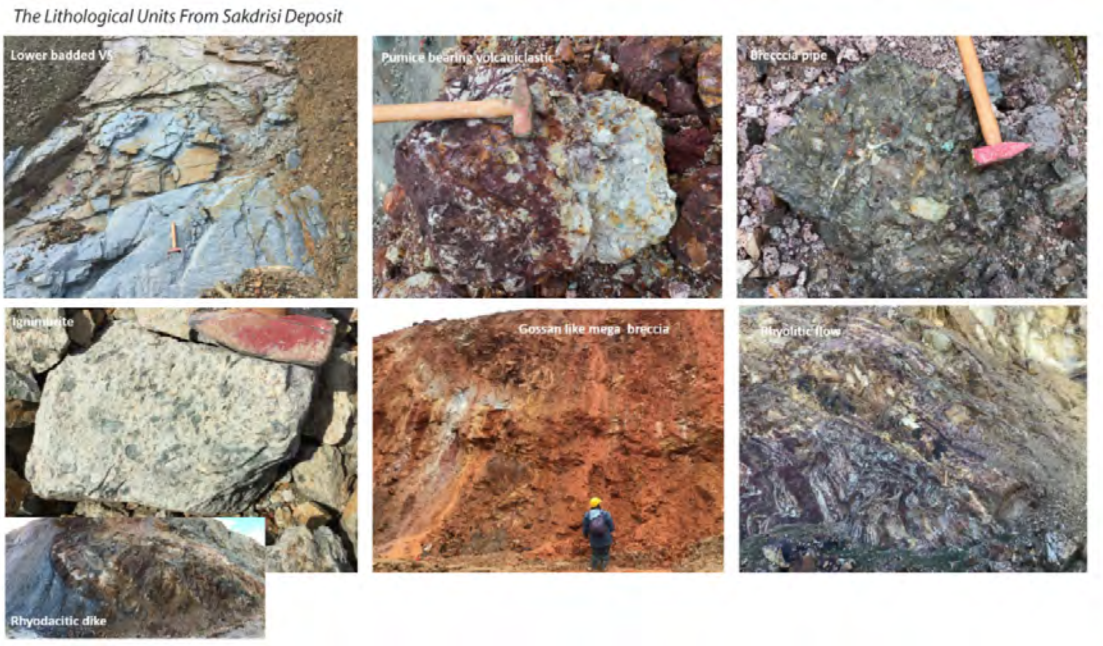

Fig.2 Lithological units from Sakdrisi deposit: lower badded volcano-sedimentary complex,pumice-bearing volcanoclastic, explosive breccia, welded ignimbrite, gossan like mega breccia, rhyolite flow.

On the Fig 1 is interpreted the 3D model of the Sakdrisi deposit with principal lithological units and main fault zones on Sakdrisi 4 and 5 deposits. The main fault is the central fault which is a thrust fault and also this zone separates the upper non-mineralized units from lower mineralized units. South fault is well outcropping in the Sakdrisi 5 and separates the greenish bedded volcano-sedimentary gypsum bearing horizon from strongly oxidized volcanoclastic pumice-bearing and fine-grained tuff horizons.

In conclusion, on Sakdrisi deposit there is both a structural and a lithological control on mineralization: the fault system created the fractures along which mineralized quartz, quartz-barite and quartz-sulfide and sulfide veins have been emplaced. The explosive breccia is mostly mineralized, even non-mineralized explosive breccia pipe in the close system created very fractured/permeable zones for fluid migration. Clastic/pumice-bearing rocks from Sakdrisi deposit is a good permeable rock, which here is strongly oxidized and mostly gold-bearing.

P 2.11
Evidence for a pre-Himalayan metamorphism in the High Himalayan Crystalline of the Miyar Valley (NW India).

Martin Robyr

Institute of Earth Sciences, University of Lausanne (martin.robyr@unil.ch), Geopolis, 1015 Lausanne

Most of the tectonic, metamorphic and geochronological data suggest that the Himalaya is essentially the consequence of a single orogenic cycle associated with the India-Asia collision during the Cenozoic era. Therefore, metamorphic assemblages and tectonic structures across the Himalayan range are systematically considered as post-collisional geological records. However, over the last decades, several observations arguing for geological events predating the continental collision have become increasingly recurrent in the literature. Nevertheless, although some of these arguments are thoroughly documented, they are unduly ignored in the construction of models drawing the tectono-metamorphic evolution of the Himalayan range. Yet, the occurrence of a pre-Himalayan history would have considerable consequences on the classical models for the building of the Himalaya.

The recent discovery of inclusions of staurolite crystals in greenschist facies garnets from the Miyar Valley in Upper Lahul region (Himachal Pradesh; NW India) revives the debate on the existence of a pre-Himalayan metamorphism. Indeed, the occurrence of high-temperature staurolites included in greenschist facies garnets suggests that the High Himalayan Crystalline rocks experienced an amphibolite facies metamorphism prior the predominant Himalayan greenschist facies metamorphism observed in this part of the range.

In this study, phase petrology, microtectonic investigations combined with preexisting geochronological data infer that the crystallization of the included staurolite predates the growth of Himalayan garnets. These original data bring new arguments to bear on the long lasting debate of the existence of a Pre-Himalayan orogenic cycle. They lead to the conclusion that the growth of staurolite predates the continental collision between India and Asia and reflects a metamorphic event that belongs to a pre-Himalaya orogenic cycle.

P 2.12
Bulk rock composition and variability of continental lower crust (DIVE project DT-1b, Ornavasso, Val d'Ossola, Italy)

Alexia Secrétan[1], Sarah Degen[2], Luca Pacchiega[2], Jörg Hermann[2] and Othmar Müntener[1]

[1] *Institut des Sciences de la Terre, University of Lausanne, CH-1015 Lausanne (alexia.secretan@unil.ch)*
[2] *Institute of Geological Sciences, University of Bern, Baltzerstrasse 1+3, CH-3012 Bern*

The Ivrea-Verbano zone, located in the Southern Alps, stands as one of the best studied archetypes of a continental crust-upper mantle section on Earth. Yet, mechanisms controlling the formation of the lower continental crust (LCC) remain enigmatic and highly debated. In the frame of the ICDP funded project DIVE (Drilling the Ivrea-Verbano Zone), questions regarding the formation, evolution and differentiation controlling the bulk chemical composition trough space and time are addressed. Knowledge of the bulk composition of the crust is one target for assembling data and testing key hypotheses.

Preliminary results from the Val d'Ossola DT-1b drill cores are presented with the goal to shed light on the compositional variability of lower crustal metasedimentary rocks. The nearly vertical drilling exposes intercalations of mafic and metasedimentary rocks. Both targeted and random sampling strategies along the 578.8-meter drill core were employed in order to minimize sampling bias. This should provide a ground truth for extrapolating the results towards more realistic assessments of the composition of the LCC. The collected dataset comprises 34 samples representative of felsic metasediments and 15 metamafic samples. Petrographic analyses disclose the predominant composition of felsic metasediments, characterized by biotite schists (Qtz + Pl + Bt ± Grt ± Sil ± Kfs), 28 samples, calc-silicates (Qtz + Pl + Grt + Px + Ttn ± Amp), 1 sample, and para-gneisses (Qtz + Pl ± Bt ± Kfs), 5 samples, while metamafic rocks encompass primarily amphibolites (Amp + Pl +Qtz ± Px ± Bt ± Grt). Note that protoliths of metamafics are not well defined yet and could be from both sedimentary and igneous origin.

Metasediments present a wide range of chemical variability (32 to 89 wt.% SiO_2; 5 to 19 wt.% Al_2O_3; 0.5 to 22 wt.% CaO; 1 to 14 wt.% FeO_{tot}; 0.35 to 0.54 Mg#), likely representative of different protoliths. Metamafic rocks cover a more restricted compositional range (43 to 57 wt.% SiO_2; 11 to 18 wt.% Al_2O_3; 5 to 17 wt.% CaO; 7 to 15 wt.% FeO_{tot}; 0.36 to 0.61 Mg#). Additional data, such as trace element, stable and radiogenic isotopes will further constrain LCC variability. DT-1b data are also compared to regional and global variations in continental and arc lower crust.

P 2.13
Is Apatite a Reliable Mineral for U-Pb TIMS Dating in the Context of Complex Magmatic Regions in the Absence of Zircon?

Şafak Utku Sönmez[1], André N. Paul[1], Nino Popkhadze[2,3], Robert Moritz[1]

[1] *Department of Earth Sciences, University of Geneva, Rue des Maraîchers 13, 1205 Geneva, Switzerland (safak.soenmez@unige.ch)*
[2] *Al. Janelidze Institute of Geology, Iv.Javakhishvili Tbilisi State University, Georgia*
[3] *RMG Rich metals Group*

The Bolnisi district in Georgia is a distinctive tectonic zone within the Lesser Caucasus, and it is a remarkable segment of the Tethyan orogenic belt with diverse magmatic rocks. Late Cretaceous bi-modal magmatism comprises low-K calc-alkaline to high-K rhyolitic rocks of the Mashavera and Gasandami Suites. They have yielded U-Pb LA-ICP-MS and TIMS zircon ages between 87.14±0.16 Ma and 81.64±0.94 Ma (Hässig et al., 2020; Moritz et al., 2020). High-K calc-alkaline to shoshonitic volcanic rocks of the Campanian Shorsholeti Suite, which represent a later magmatic event, and which stratigraphically overlie the Mashavera and Gasandami Suites. However, the precise age of Shorsholeti, consisting of shoshonitic porphyritic trachyte and trachyandesite remains uncertain due to the absence of dateable zircon. Subsidiary early Eocene adakite-like magmatism magmatism has also affected the Bolnisi district.

In this study, we investigate the U-Pb isotope composition of single crystals of apatite by ID-TIMS and *in-situ* analyses of major and trace elements by electron probe microanalyzer (EPMA). We want to understand if U-Pb ages of the investigated apatites are consistent with an age range of ca. 87.14±0.16 Ma to 81.64±0.94 Ma obtained on zircons in previous studies. This would mean that apatites could be considered as a geochronometer. Therefore, our primary objective is to determine whether apatite could serve as a reliable mineral for accurate dating in complex magmatic settings in the absence of zircon.

Samples were collected from four distinct areas in the Bolnisi district. Apatites from a trachyandesite sample (BR-1) display a dark blue color under optical cathodoluminescence, elevated La and Ce concentrations, and the highest Sr concentrations (EPMA) compared to the other apatites investigated in this study. Notably, the apatite grains from this site yielded the highest radiogenic Pb over common Pb ratio (Pb*/Pbc), yielding an U-Pb age of 80.04±2.0 Ma. Apatite grains from various rhyodacitic rocks (samples BEQ-2, LG-31, and LG-57) display a range of pale blue to dark yellow colors under optical cathodoluminescence. Apatites from these samples consistently exhibit lower Sr concentrations and a positive correlation between Ce and SiO_2 concentrations is a distinguishing feature compared to the apatites from the trachyandesite. These apatites yielded lower Pb*/Pbc ratios and the calculated dates are significantly younger than 80 Ma and imprecise. For apatites from samples LG-31 and LG-57, local overprints from Eocene magmatism are suggested. These apatites have higher La and Ce concentrations compared to sample BEQ-2, suggesting distinct local influences of post-mineralisation fluid alteration.

Our findings demonstrate that apatites from shoshonitic trachyandesite yield a reliable age with a moderate uncertainty of ~2.5%, indicating that they can be used as an alternative for dating magmatic rocks lacking zircons. The BR-1 date also coincides with the age of shoshonitic rocks in the Eastern Pontides, NE Turkey, which is considered as the western extension of the Bolnisi district (Moritz et al., 2020). Nonetheless, it is recommended to evaluate the data with caution, since apatite U-Pb isotopes could be disturbed or behaves as (partially) open systems during overprinting magmatic activity or the waning stages of fluid circulation. Depletion in Ce, La, and Sr indicates possible metamorphic or fluid alteration of the BEQ-2 samples, while higher Ce and La concentrations vs. Sr depletion might imply the influence of later stage Eocene magmatism for LG-31 and LG57 samples, that may have generated a compositionally different fluid percolating within the rocks studied in the Bolnisi district.

In conclusion, our study reveals significant differences in cathodoluminescence color and geochemical patterns between magmatic and hydrothermally altered apatites. This research substantially contributes to our understanding of utilizing apatites for U-Pb ID-TIMS dating in magmatic rocks lacking zircons. Furthermore, it enables dating a shoshonitic magmatic pulse within the Bolnisi District, Georgia, and is contributing to a better understanding of magmatic processes, tectonic dynamics, and constraining the geodynamic framework of the central Tethyan orogenic belt.

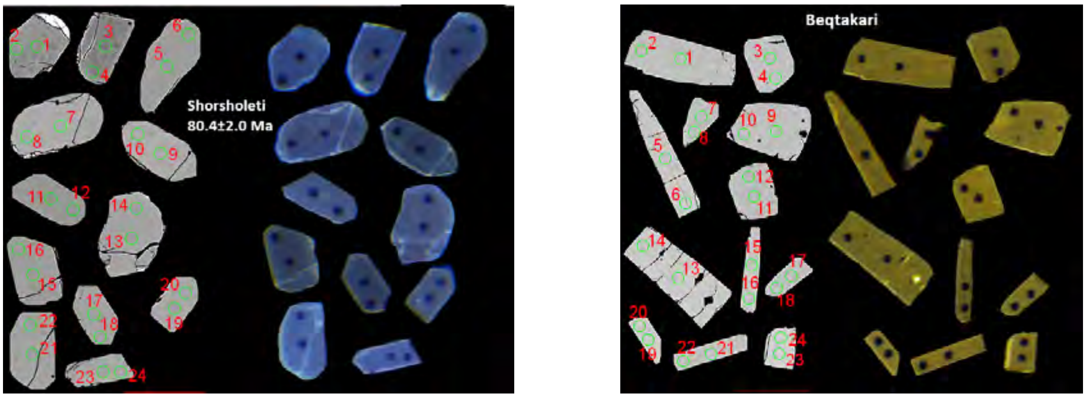

Figure 1. Apatite grains A) magmatic apatites from the shoshonitic trachy andesite of the Shorshorleti suite; B) altered apatites from rhyodacite of the Gasandami suite.

B

REFERENCES

Moritz, R., Popkhadze, N., Hässig, M., Golay, T., Lavoie, J., Gugushvili, V., Ulianov, A., Ovtcharova, A., Grosjean, M., Chiaradia, M., Dumitrica, P. 2020: At the crossroads of the Lesser Caucasus and the Eastern Pontides: Late Cretaceous to early Eocene magmatic and geodynamic evolution of the Bolnisi district, Georgia. Lithos 378-379, 105872.

Hässig, M., Moritz, R., Ulianov, A., Chiaradia, M., Popkhadze, N., Galoyan, G., Enukidze, O. 2020: Jurassic to Cenozoic magmatic and geodynamic evolution of the Eastern Pontides and Caucasus belts, and their relationship with the Eastern Black Sea Basin opening. Tectonics 39, e2020TC006336.

P 2.14
Tectono-magmatic origin of aligned intrusions in the Damaraland igneous province, Namibia: new evidence from high-precision zircon dating and geochemistry

Yi Sun[1], Andrea Galli[1], Dawid Szymanowski[1], Marcel Guillong[1], Jeremia Simon[2], Abraham Shipandeni[2], Olivier Bachmann[1]

[1] Institute of Geochemistry and Petrology, ETH Zürich, 8092 Zürich, Switzerland (yi.sun@erdw.ethz.ch)
[2] Geological Survey of Namibia, Ministry of Energy and Mines, Windhoek, Namibia

Early Cretaceous intrusions in the Damaraland igneous province (Namibia) display a SW-NE alignment. They are related to the Paraná-Etendeka Large Igneous Province (LIP), but their magmatic origin and timing of emplacement within the LIP evolution are still enigmatic. We use zircon geochronology, Hf isotope compositions, and bulk rock/zircon geochemistry of these intrusions to decipher the spatial pattern of magmatism and the mechanism(s) of magma formation and evolution. High-precision CA-ID-TIMS zircon ages show that the plutons were emplaced without clear spatial systematics over at least 1.4 My (133.2-131.8 Ma), around/after the 135-133 Ma volcanic activity peak in the southern Etendeka (Namibia) and the Paraná (Brazil). The youngest Damaraland zircon ages overlap with previously reported baddeleyite ages for highly evolved sills in the Southern Paraná, confirming that magmatism in the LIP continued beyond 132 Ma. In the whole Damaraland province, intrusive rocks follow two distinct evolution paths towards both the granite and the phonolite minima. Absence of spatial trends along the aligned complexes in both geochemistry and crystallization ages argues against plate movement over the Tristan-Gough plume as the origin of these complexes. Instead, lithospheric extension along reactivated lineaments led to near-synchronous melt generation across the province. Negative zircon εHf(t) values in silicic complexes (-5 to -12) likely arose from path contamination of melts from a +/- metasomatized mantle source(s) during ascent, while in average less negative εHf(t) in alkaline/carbonatitic intrusions (-2 to -6) reflect source contamination and stem from the preferential melting of mantle portions metasomatized by the Tristan-Gough plume.

P 2.15
Garnet multi-component diffusion modelling reveals local heat sources affecting the cooling history of the Lepontine dome

Alessia Tagliaferri[1,2], Evangelos Moulas[3], Stefan Markus Schmalholz[2], Filippo Luca Schenker[1]

[1] *Institute of Earth Sciences, University of Applied Sciences and Arts of Southern Switzerland (SUPSI), CH-6850 Mendrisio, Ticino, Switzerland (alessia.tagliaferri@supsi.ch)*
[2] *Institute of Earth Sciences, University of Lausanne (UNIL), CH-1015 Lausanne, Vaud, Switzerland (alessia.tagliaferri@unil.ch)*
[3] *Institute of Earth Sciences, Johannes Gutenberg-Universität Mainz, D-55128 Mainz, Deutschland*

The Lepontine dome (Central European Alps) is a metamorphic and structural dome formed by crystalline basement nappes accreted during the Alpine continental collision in the Eocene-Oligocene. The dome is characterized by a widespread Barrovian metamorphism. The peak amphibolite-facies conditions coincide with the final phase of nappe emplacement at ca. 31 Ma, dated via U-Pb zircon dating of syn-tectonic migmatites along the principal shear zone at the base of the Maggia-Adula nappe.

The duration of the cooling following the temperature peak is still not well contrained. Therefore, in this contribution we evaluate the apparent cooling rates of paragneisses within the Lepontine dome through inverse diffusion modelling in garnet. Our working procedure consists of: (i) analysis of garnet-rims compositional re-adjustment and (ii) comparison of the obtained cooling rates with 1-dimensional thermal models. We examined six garnet-paragneisses collected at different structural levels within the Lepontine nappe stack. The selected garnet crystals show at their rim a coupled Mg-decrease and Mn-increase, indicative of post-peak temperature retrograde modification. We applied geothermobarometry to determine the post-peak re-equilibration conditions and we obtained a cooling rate distribution which varies spatially within the study area.
The highest cooling rates are within the Maggia-Adula shear zone, whereas at the base of the footwall nappe the cooling rates are very low. In the migmatitic Southern Steep Belt which borders the Lepontine dome to the south, apparent cooling rates have intermediate values.

These results compared with thermal models permit to identify regional patterns related to geodynamic processes. The high cooling rates obtained within the main thrust cannot be explained by regional exhumation processes, but a transient local heat source has to be invoked. An additional spatially-confined heat source can be represented by hot fluids percolation or shear heating.

P 2.16
Petrologic and sedimentological investigations on boulders of the river Dreisam (Black Forest, FRG)

Manuel Teller[1], Leander Franz[1], Andreas Wetzel[1]

[1] *Department of Environmental Sciences, University of Basel, Bernoullistrasse 32, CH-4056 Basel (manuel.teller@stud.unibas.ch)*

In a larger study, the rivers of the Black Forest, their debris and their impact on the sediments of the Rhine River were investigated. In the framework of this project, petrologic and sedimentological studies on boulders carried by the river Dreisam and its headstreams were performed. For this purpose six different locations were sampled, from the headwaters in the Zartenbach to the western limits of the city of Freiburg im Breisgau (Baden-Württemberg, Germany).

The 29.7 km long river Dreisam flows along the border of the Central and Southern Black Forest. The bedrock in the Black Forest was originally deposited in the Precambrian or Early Paleozoic and underwent various metamorphic imprints as well as magmatic processes (Metz & Rein 1958). The main metamorphism took place 330–335 Ma ago during the Variscan orogeny (Kalt et al. 1994). Thus, mainly metamorphic and magmatic boulders were expected. The samples were investigated by thin sections and Raman spectroscopy to analyze the mineral composition and to decipher their origin. Sedimentologically, the roundness and sphericity of the boulders were determined as well as the evolution of these measures along the course of the river and related geomorphological features.

At the first sampling point in the headstream Zartenbach, almost exclusively paragneisses were detected. Due to the strong weathering and strain, a macroscopic identification of the boulders was often challenging. Thin sections revealed a distinct compositional banding with mafic hornblende- and biotite-rich layers as well as felsic sections with minor to intermediate anatectic features. According to the geological map (Groschopf et al. 1996) the paragneisses constitute a large complex in the source region of the river.

At the second sampling site (Ravennaschlucht), the large majority of boulders could also be assigned to the paragneisses. However, a certain amount of distinctly migmatic meta- and diatexites occurred showing fluent petrographic transitions. These rocks often contained prominent amounts of cordierite and sometimes garnet.

At the third sampling site (Höllental), boulders of meta- and diatexites with a marked increase in the degree of melting dominated. One sample with a very high degree of melting even showed nebulitic features.

At the fourth sampling site, where Höllen- and Wagensteigbach unite to the river Dreisam, felsic igneous rocks appeared for the first time forming well-rounded and spherical blocks. Very quartz-rich, fine-grained aplites, microgranites and a rhyolite were found. These magmatites very probably originated from small dikes in the vicinity of the Höllenbach (Groschopf et al. 1996). Besides minor paragneisses and diatexites, an augengneiss was also detected.

At the fifth sampling point in the eastern suburbs of Freiburg, in addition to the various crystalline rocks (para- and orthogneisses, rhyolites and aplites), fine-grained amphibole gneisses to amphibolites occured. Thin sections gave proof that three of the mafic rocks were retrograde eclogites displaying symplectitc intergrowths of albite and diopside replacing primary omphacite. Furthermore, relic garnets were mantled by coronitic aggregations of tschermakite and plagioclase.

The sixth sampling point in the western outskirts of Freiburg mainly supplied paragneisses and migmatites as well as a few granitic rocks. There, the only small pebble of clay-rich sandstone occurred, which likely originated from the nearby outcrops of Mesozoic sediments (Groschopf et al. 1996).

Our investigations highlight the dominance of metamorphic rocks in the spectrum of boulders in the river Dreisam, which is due to the massive complexes of paragneisses and migmatites in the central Black Forest area. Magmatic rocks mainly originate from subsequent felsic dykes whereas sedimentary rocks almost lack completely. The crystalline rocks are often affected by a late, low-grade hydrothermal alteration leading to the formation of prehnite, chlorite and carbonate.

Downstream, a general trend of increasing sphericity (S) and roundness (R) is evident for the studied boulders and pebbles, from $S = 0.37$ and $R = 0.33$ in the source area to $S = 0.40$ and $R = 0.66$ close to the confluence with the Rhine River. The graph (Fig. 1) nearly follows the 'growth' curve reported in literature (e.g., Pettijohn, 1975). Isotropic granite pebbles slightly differ from anisotropic gneisses in these textural measures. Deviations from the trend appear to be related to erosion of glacial terraces.

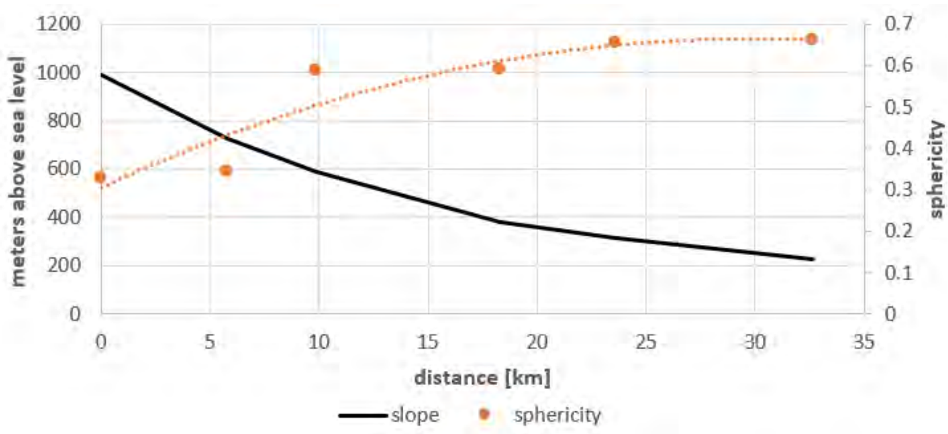

Figure 1. Trend line of the sphericity of gneisses and granites along the river.

REFERENCES

Groschopf, R., Kessler, G., Leiber, J., Maus, H., Ohmert, W., Schreiner, A. & Wimmenauer, W. 1996: Geologische Karte von Baden-Württemberg 1:50‘000, Blatt Freiburg i. Br. und Umgebung. Geologisches Landesamt Baden-Württemberg, Freiburg i. Br..

Kalt, A., Grauert, B. & Baumann, A. 1994: Rb-Sr and U-Pb isotope studies on migmatites from the Schwarzwald (Germany): constraints on isotopic resetting during Variscan high-temperature metamorphism. J. metamorphic Geol., 12, 667-680.

Metz, R. & Rein, G. 1958 all citations within: Geologisch – petrographische Überichtskarte des Südschwarzwaldes 1:50’000. Lahr.

Pettijohn, E.J. 1975: Sedimentary Rocks. Harper, New York, 628 pp.

P 2.17
Recovery of the first camera-observed meteorite fall in Oman

Anna Zappatini[1], Beda A. Hofmann[1,2], Urs Eggenberger[1], Edwin Gnos[3], Pascal M. Kruttasch[1], Hussain Al-Ghafri[4], Abdulmunaim Al Zakwani[4], Eleanor K. Sansom[5], Hadrien A. R. Devillepoix[5], Martin Cupák[5], Sebastian Lindemann[6], Beat Booz[7]

[1] *Institute of Geology, University of Bern, Baltzerstrasse 3, CH-3012 Bern (anna.zappatini@unibe.ch)*
[2] *Naturhistorisches Museum Bern, Bernastrasse 15, CH-3005 Bern*
[3] *Muséum d'histoire naturelle, Route de Malagnou 1, CH-1208 Genève*
[4] *Ministry of Heritage and Tourism, Al Khuwair, Muscat, Oman*
[5] *School of Earth and Planetary Sciences, Curtin University, Perth, Australia*
[6] *Physikalisches Institut, Universität Freiburg, Freiburg, Germany*
[7] *Department for meteor and fireball calculations, Fachgruppe Meteorastronomie (FMA), CH-5070 Frick*

In recent years, meteor cameras which scan the night sky for fireball events have yielded numerous observations all over the world. As the landing site of a meteorite can be modelled based on the fireball trajectory, a number of freshly fallen meteorites were retrieved thanks to those camera systems. Freshly fallen meteorites with camera observations are of particular importance to meteorite science. For instance, the orbit of the meteoroid around the sun can be calculated from the camera data. This helps to establish a link between a specific meteorite material and a location in the solar system.

Four sky observation cameras were installed in the desert of Oman in 2022 as a part of a collaboration between Swiss and Australian researchers and the Ministry of Heritage and Tourism in Oman. During the first year of observation, 19 fireballs were observed by the cameras in Oman. Of those, 13 were observed by two or more cameras, effectively enabling the triangulation of the falling meteorite. In a field campaign in February 2023, two promising target areas were searched. This led to the recovery of two fresh-looking meteorite pieces near Al-Khadhaf. The temporal link between camera observations and the recovered meteorites was established by gamma spectrometry. The presence of the short-lived cosmogenic nuclides ^{54}Mn ($t^1/_2$ = 312 d) and ^{22}Na ($t^1/_2$ = 2.6 a) confirmed the young (~1 a at the time of find) terrestrial age of the meteorite. The meteorite is an ordinary chondrite containing clasts of differing metamorphic degree, classified as a H5-6 breccia. The calculated trajectory indicates that the meteorite derived from the inner part of the asteroid belt. At the time of submission of this abstract, the meteorite is awaiting official recognition by the meteorite nomenclature committee. At the conference, we will present the recovery of the meteorite and discuss the results of the petrography, gamma spectrometry as well as the orbit and possible origin of the meteorite in the solar system.

REFERENCES

Devillepoix, H. A. R. et al. 2020: A Global Fireball Observatory, Planetary and Space Science, 191, 105036.

P 2.18
The overlooked role of tropical trees in supporting biotic and abiotic Ca carbonate precipitation

Isabella Zelano[1,2], Charlotte Prud'Homme[1], Aurelien Virgone[3], Eric Verrecchia[1], Pierre Souquet[3], Remy Hedacq[3], Jean-Noel Ferry[3]

[1] Institut of Earth Surface Dynamics, Université de Lausanne, CH-1015 Lausanne, Switzerland (isabella.zelano@unil.ch)
[2] Insitut of Chemistry, Université de Neuchatel, CH-2000 Neuchatel, Switzerland
[3] TOTAL S.A., CSTJF, 64000 Pau, France

The formation of pedogenic carbonates (PC) occurs via abiotic and biotic processes leading to the formation of minerals with various morphologies and isotopic composition (δ13C), depending on the local environmental factors (Zamanian et al 2016). The oxalate-carbonate pathway (OCP) is a peculiar biogeochemical succession of reactions leading to the accumulation of PC species in tropical acidic soils, where there is no geogenic carbonate rocks. The OCP develops in specific plant-soil systems where biological activity promotes the accumulation of Ca_2+ ions, e.g., in plant cells and the rhizosphere, and where the oxalate species i) is formed as by-product of photosynthesis, ii) accumulates in different plant parts, and iii) is subsequently oxidized by oxalotrophic bacteria and fungi associated to plant wounds or during leaf litter degradation. The accumulation of bicarbonate ions in the local environment, as a byproduct of the bacterial metabolism, induces an increase in alkalinity, and consequently of pH values, promoting mineral precipitation when supersaturation conditions with respect to $CaCO_3$ are reached (Pons et al. 2018).

The iroko tree (Milicia excelsa) in Ivory Coast has been reported to present calcite-cemented sandstones associated to wounds on trunks and in the rhizosphere where the soil pH can locally rise to 8, while the surrounding ferralitic soil displays pH between 4 and 6 (Pons et 2018). The presence of Ca-carbonate in this ecosystem has attracted increasing attention as a potential underestimated sink for inorganic C (up to 6 kg of C/year in soil) Cailleau et al 2011). However, the complex array of abiotic and biotic reactions underpinning the carbonate precipitation process leading to various types of mineral facies are not yet well understood.

In this study, we propose a systematic investigation of few soil-iroko systems in Ivory Coast, with the aim of elucidating the link between different types of $CaCO_3$ facies associated to the trees and their specific precipitation processes. To this purpose, soil samples were collected to quantify pH, oxalate and carbonate contents, as well as the cation exchange capacity at different depth and distances from the studied plants. Macro-samples (from 1 cm to 50 cm long) of plant materials and petrified wood were collected in the aerial parts of the plant and in the rhizosphere (e.g., trunk and roots). Standard petrographic analyses (associated to cathodoluminescence, UV light and Scanning Electron Microscopy) were used to observe the different types of $CaCO_3$ facies. Powders of such macro-samples were collected using a microdrill to determine the $\delta^{13}C$ values of the organic material and the carbonate phases to calculate Δ^{13}Ccarbonate-org values.
Obtained results show unequivocally that the carbon in the carbonate phases mainly derives from organic molecules synthetized through the photosynthesis, i.e., from atmospheric CO_2, and that carbonates are mainly associated to the rhizosphere or directly replace plant material. However, several different forms of carbonate are present in a same soil-plant system (i.e., micrites and sparites). Isotopic and petrographic investigations suggest that $CaCO_3$ precipitation occurs concomitantly through abiotic and biotic processes (e.g., climatic effects and biomineralization induced by natural CO_2 degassing). Additionally, the large window of Δ^{13}Ccarbonate-org values indicates the occurrence of carbonate precipitations outside the range of equilibrium conditions (Prud'Homme et al 2018) suggesting the presence of consecutive dissolution/reprecipitation phenomena (early diagenesis) due to microclimate effects, as well as a mix of organic molecule precursors leading to a range of carbon sources in carbonates (e.g., oxalate, latex, acetate associated to termite activity). Overall, this work shows that the iroko tree is an overlooked reactor permitting the CO_2 transformation, first in biomass, and later, in an alkalinity/$CaCO_3$ engine.

REFERENCES

Zamanian, K.; Pustovoytov, K.; Kuzyakov, Y. Pedogenic Carbonates: Forms and Formation Processes. Earth-Science Rev. 2016, 157, 1–17.
Pons, S.; Bindschedler, S.; Sebag, D.; Junier, P.; Verrecchia, E.; Cailleau, G. Biocontrolled Soil Nutrient Distribution under the Influence of an Oxalogenic-Oxalotrophic Ecosystem. Plant Soil 2018, 425 (1–2), 145–160.
Cailleau, G.; Braissant, O.; Verrecchia, E. P. Turning Sunlight into Stone: The Oxalate-Carbonate Pathway in a Tropical Tree Ecosystem. Biogeosciences 2011, 8 (7), 1755–1767.
Prud'homme, C.; Lécuyer, C.; Antoine, P.; Hatté, C.; Moine, O.; Fourel, F.; Amiot, R.; Martineau, F.; Rousseau, D. D. Δ13C Signal of Earthworm Calcite Granules: A New Proxy for Palaeoprecipitation Reconstructions during the Last Glacial in Western Europe. Quat. Sci. Rev. 2018, 179, 158–166.

3 Stable and radiogenic isotope geochemistry

Nicolas David Greber, Johanna Marin-Carbonne, Andres Rüggeberg, Benjamin Zachary Klein, Isabelle Baconnais, Sylvie Bruggmann

Swiss Society of Mineralogy and Petrology

TALKS:

3.1 Aquila G., Galili N., Hemingway J.: Clay-mineral extraction and purification for reconstructing silicate weathering

3.2 Bastías-Silva J., Burton-Johnson A., Chew D., Riley T., Jara W., Chiaradia M.: Spatial and temporal isotopic changes in Cordilleran magmatism: The Antarctic Peninsula, an alternative case

3.3 Blattmann F.R., Vennemann T., Schneebeli-Hermann E., Bucher H., Magill C.R.: A detailed look at organic carbon cycling across the Early Triassic (Smithian – Spathian) using compound specific n-alkane carbon isotope compositions

3.4 Chatterjee S., Ravindran A., Ahmad Q., Pandey O.P., Wille M., Mezger K.: Formation of sub continental lithospheric mantle was enabled by subduction driven recycling of surface derived material in the Paleoarchean

3.5 Gilliard D., Janssen D.J., Jaccard S.L., Haley B.: Dissolved chromium concentrations and stable isotopes in marine pore waters from the equatorial Pacific Ocean

3.6 Naumenko-Dèzes M., Kloppmann W., Blessing M., Mayer B.: Natural gas of radiolytic origin : Insigts from carbon isotopes

3.7 Timmerman S., Stachel T., Chinn I., Pearson G.: Use of Rb-Sr and Sm-Nd isotope systems in determining diamond crystallisation ages

POSTERS:

P 3.1 Jakobsson V., Spikings R.: Assessing mechanisms of argon isotope redistribution in muscovite: Preliminary results from the Black Hills, South Dakota

P 3.2 Toro Vivanco D., Timmerman S., Hermann J., Stracke A.: Resolving Earth's Lead Paradox

P 3.3 Webster R., Timmerman S., Jaques L., Storck J-C.: Constraining oceanic lithosphere depletion through non-traditional stable isotope analyses

P 3.4 Volante S., Scicchitano M.R., Barrote V., Kempf J., Torres García M.F., Dziggel A.: Tracing the source of fluids in the Archean crust factory: an example from the Lewisian Gneiss Complex (NW Scotland)

P 3.5 Adams A., Cisneros-Lazaro D., Vennemann T., Baumgartner L., Daval D., Bernard S., Stolarski J., Baronnet A., Meibom A.: Optimizing Experimental Conditions for Accurate Oxygen Diffusion Measurements in Biominerals

P 3.6 Bruggmann S., Blaser P., Martinez-Garcia A., Crosta X., Jaccard S.: Productivity changes from the Holocene to the Last Glacial Maximum evidenced by chromium isotopes

P 3.7 Jaimes-Gutierrez R., Wilson D.J., Pogge von Strandmann P., Puceat E., Musajo C., Adatte T., Castelltort S.: Stable and radiogenic isotopes as weathering regime proxies: The source-to-sink response to the Paleocene-Eocene Thermal Maximum in the Spanish Pyrenees

3.1
Clay-mineral extraction and purification for reconstructing silicate weathering

Giorgia Aquila[1], Nir Galili[1], Jordon Hemingway[1]

[1] *Geological Institute, ETH Zürich, Sonneggstrasse 5, CH-8006 Zürich (giorgia.aquila@erdw.ethz.ch)*

By serving as a negative feedback mechanism capable of attenuating climate and carbon-cycle perturbations, silicate weathering has acted as a major driver of global climate stability throughout Earth's history. However, it is currently not possible to accurately describe silicate weathering responses to past climate changes, primarily due to a lack of direct observations regarding temperature and hydrologic conditions at which the process took place. In this context, we suggest that triple-oxygen isotope compositions ($\Delta'^{17}O$ and $\delta'^{18}O$) of pedogenic clays can provide such direct paleotemperature and paleohydrology constraints.

To harness this proxy effectively, the initial step necessitates extraction of high-purity clay-mineral fractions from soils and sediments. Indeed, sample purity is critical to the precise determination of $\Delta'^{17}O$ and $\delta'^{18}O$, since the presence of other oxygen-bearing phases, whether organic or inorganic, may significantly shift measured isotope compositions, thereby leading to potentially erroneous interpretations. In this respect, we developed a clay purification protocol that combines different chemical and physical steps. Chemical steps aim to remove organic matter, carbonates, soluble sulfates, salts, and iron oxides, whereas physical steps are indispensable for the elimination of micro quartz particles. We place particular emphasis on the removal of oxides and quartz; we adopt and subsequently compare three distinct techniques for oxide removal and two for quartz removal.

This protocol successfully separates clays with high purity from soils and sediments samples, as confirmed by petrographic techniques (i.e., XRD). Such an achievement will contribute to more precise and accurate triple-oxygen isotope analysis of clays from natural samples, thus substantially mitigating the potential for misinterpretations and enhancing our capacity to ascertain the temperature and hydrological conditions governing silicate weathering events in Earth›s geologic past. Finally, we will present preliminary clay triple-oxygen isotope results from well constrained modern soil samples.

3.2
Spatial and temporal isotopic changes in Cordilleran magmatism: The Antarctic Peninsula, an alternative case

Joaquin Bastías-Silva[1,2,3*], Alex Burton-Johnson[4], David Chew[1], Teal Riley[4], Wuidad Jara[2], Massimo Chiaradia[3].

[1] Department of Geology, Trinity College Dublin, College Green, Dublin 2, Ireland
[2] Escuela de Geología, Facultad de Ingeniería, Universidad Santo Tomás, Santiago, Chile
[3] Department of Earth Sciences, University of Geneva, Geneva 1205, Switzerland
[4] British Antarctic Survey, High Cross, Madingley Road, Cambridge CB3 0ET, United Kingdom

Spatial and temporal changes in the radiogenic isotopic composition of arc magmatism is a fundamental tool for studying the interactions between the crust and the lithosphere in convergent margins (e.g. Ducea and Barton, 2007; Chapman et al., 2017). These changes have been used to interpret diverse tectonic phenomena including continental subduction (e.g. Bouilhol et al., 2013), subduction erosion (Kay et al., 2005), delamination (Kay et al., 1994), changes in crustal thickness (Haschke et al., 2002), and lithospheric extension (DePaolo and Daley, 2000) among others. Spatial trends in the radiogenic isotopic composition of arc magmatism have been interpreted as an intrinsic feature of Cordilleran-style orogenic systems (Chapman et al., 2017) and likely imply a fundamental change in the dynamics governing the formation of their igneous rocks. A consistent trend has been observed in arc magmas from the Central Andes, U.S. Cordillera and Tibet, whereby more isotopically juvenile compositions are encountered near the trench (i.e. radiogenic or enriched $^{176}Hf/^{177}Hf$ and $^{143}Nd/^{144}Nd$) and increasingly evolved landward (unradiogenic or depleted $^{176}Hf/^{177}Hf$ and $^{143}Nd/^{144}Nd$; Chapman et al., 2017). Furthermore, these Cordilleran systems are well-studied examples of both modern and ancient active margins, which suggest that this spatial-compositional trend is long-lived and persists throughout the life of a given continental arc. Additionally, these spatial trends are observed in a broad spectrum of geochemical compositions. These spatial isotopic trends for Cordilleran magmatism have been explained by the mantle lithosphere thinning towards the trench due to sub-lithospheric processes, such as delamination or subduction erosion, allowing the magmas to be sourced from isotopically juvenile asthenospheric mantle with minimal lithospheric interaction. Conversely, isotopically evolved arc magmas are founded landward, where the absence of lithospheric thinning permits the development of a thicker continental mantle lithosphere, producing isotopically evolved arc magmas.
The Antarctic Peninsula represents the southern continuation of the Andes convergent margin and although difficult access has partially hindered its understanding and characterisation, a plethora of recent data now permits a more robust characterisation of this Mesozoic-Cenozoic continental margin (e.g. Bastias et al., 2021, 2022; Riley et al., 2020, 2022; Burton-Johnson et al., 2023). The Antarctic Peninsula thus makes an excellent natural laboratory for both testing and revising the dynamics in Cordilleran convergent margins. We combine these existing datasets with newly presented geochemistry (elemental and isotopic) and geochronology from the Cenozoic arc record, providing key information for a poorly constrained period of the Antarctic Peninsula. We use these combined datasets to test the model proposed for other Cordilleran-active margins and examine the magmatic and tectonic history of the Antarctic Peninsula in comparison with the Central Andes, U.S. Cordillera and Tibet (*cf* Chapman et al., 2017).

REFERENCES

Ducea, M. N., & Barton, M. D. 2007:. Igniting flare-up events in Cordilleran arcs. Geology 35(11), p.1047-1050.
Chapman, J. B., Ducea, M. N., Kapp, P., Gehrels, G. E., & DeCelles, P. G. 2017: Spatial and temporal radiogenic isotopic trends of magmatism in Cordilleran orogens. Gondwana Research 48, p.189-204.
Bouilhol, P., Jagoutz, O., Hanchar, J. M., & Dudas, F. O. 2013: Dating the India–Eurasia collision through arc magmatic records. Earth and Planetary Science Letters 366, p.163-175.
Kay, S.M., Coira, B., Viramonte, J. 1994: Young mafic back arc volcanic rocks as indicators of continental lithospheric delamination beneath the Argentine Puna plateau, central Andes. Journal of Geophysical Research - Solid Earth 99, p.24323–24339.
Kay, S.M., Godoy, E., Kurtz, A. 2005: Episodic arc migration, crustal thickening, subduction erosion, and magmatism in the south-central Andes. Geological Society of America Bulletin 117, p.67–88.
Haschke, M., Siebel, W., Günther, A., Scheuber, E. 2002: Repeated crustal thickening and recycling during the Andean orogeny in north Chile (21°–26°S). Journal of Geophysical Research - Solid Earth 107, ECV-6.
DePaolo, D.J., Daley, E.E. 2000: Neodymium isotopes in basalts of the southwest basin and range and lithospheric thinning during continental extension. Chemical Geology 169, p.157–185.
Bastías, J., Spikings, R., Riley, T., Chew, D.; Grunow, A., Ulianov, A., Chiaradia, M., Burton-Johnson, A. 2022: Cretaceous arc magmatism in the Antarctic Peninsula and its tectonic implications. Journal of the Geological Society 180 (1): jgs2022–067. doi: https://doi.org/10.1144/jgs2022-067
Bastías, J., Spikings, R., Riley, T., Ulianov, A., Grunow, A., Chiaradia, M., Herve, F. 2021: A revised interpretation of the Chon Aike magmatic province: active margin origin and implications for the opening of the Weddell Sea. Lithos 386-387, 106013.

https://doi.org/10.1016/j.lithos.2021.106013.
Riley, T. R., Burton-Johnson, A., Flowerdew, M. J., Poblete, F., Castillo, P., Hervé, F., Leat, P., Millar, I., Bastías, J., & Whitehouse, M. J. 2023: Palaeozoic–Early Mesozoic geological history of the Antarctic Peninsula and correlations with Patagonia: Kinematic reconstructions of the proto-Pacific margin of Gondwana. Earth-Science Reviews 236, 104265.
Riley, T. R., Flowerdew, M. J., Millar, I. L., & Whitehouse, M. J. 2020: Triassic magmatism and metamorphism in the Antarctic Peninsula: identifying the extent and timing of the Peninsula orogeny. Journal of South American Earth Sciences 103, 102732.
Burton-Johnson, A., Bastias, J., & Kraus, S. 2023: Breaking the Ring of Fire: How ridge collision, slab age, and convergence rate narrowed and terminated the Antarctic continental arc. Tectonics, e2022TC007634.

3.3
A detailed look at organic carbon cycling across the Early Triassic (Smithian - Spathian) using compound specific n-alkane carbon isotope compositions

Franziska R. Blattmann*, Torsten Vennemann*, Elke Schneebeli-Hermann**, Hugo Bucher** & Clayton R. Magill***

** Institute of Earth Surface Dynamics, University of Lausanne, Quartier UNIL-Mouline, 1015 Lausanne, Switzerland (Franziska.Blattmann@unil.ch)*
*** Paläontologisches Institut und Museum, Universität Zürich, Karl-Schmid-Strasse 4, 8006 Zürich, Switzerland*
**** The Lyell Center, Heriot-Watt University, Research Avenue South, Edinburgh EH14 4AP, Scotland*

After the largest mass extinction in Earth's history at the Permian-Triassic boundary ca. 252 million years ago, the Early Triassic epoch is noted to have a series of dramatic carbon isotope excursions. The underlying factors driving these isotopic fluctuations remain a matter of contention consequent to limited data differentiating between terrestrial and marine carbon cycles. This study concentrates on the Smithian-Spathian boundary (SSB), around 2 million years after the commencement of carbon cycle disruptions at the Permian-Triassic boundary, which is marked by a global positive $\delta^{13}C_{bulk}$ excursion of approximately 5 ‰ (e.g., Widmann et al 2020). Our study focuses on analyses of organic-rich shales from Spitsbergen for n-alkane molecular distributions and their compound-specific carbon isotopic compositions ($\delta^{13}C_{n\text{-alkane}}$). Measured $\delta^{13}C_{n\text{-alkane}}$ values suggest that both marine and terrestrial systems were impacted by carbon cycle disturbances as evidenced by >6 ‰ fluctuations in associated biomarker n-alkane records. For the marine system, $\delta^{13}C$ values predominantly mirror variations in dissolved organic carbon $\delta^{13}C$, influenced by local fluvial influx, atmospheric carbon dioxide levels, primary productivity, and changes in temperature. Terrestrial ecosystems also experienced notable changes as vegetation shifted from lycophytes to gymnosperms (Hermann et al. 2011), influencing the overall carbon isotopic fractionation between vegetation and atmospheric CO_2. Overall, these findings shed light on the complex interplay between terrestrial and marine carbon cycle dynamics during the Smithian-Spathian in the Early Triassic.

REFERENCES
Hermann E., Hochuli P. A., Bucher H., Brühwiler T., Hautmann M., Ware D. and Roohi G. (2011) Terrestrial ecosystems on North Gondwana following the end-Permian mass extinction. Gondwana Research 20, 630-637.
Widmann P., Bucher H., Leu M., Vennemann T., Bagherpour B., Schneebeli-Hermann E., Goudemand N. and Schaltegger U. (2020) Dynamics of the largest carbon isotope excursion during the Early Triassic biotic recovery. Frontiers in Earth Science 8, 196.

3.4
Formation of sub continental lithospheric mantle was enabled by subduction driven recycling of surface derived material in the Paleoarchean

Sukalpa Chatterjee[1], Arathy Ravindran[2], Qasid Ahmad[1,3], Om Prakash Pandey[4], Martin Wille[1], Klaus Mezger[1]

[1] *Institut für Geologie, Universität Bern, Switzerland (sukalpa.chatterjee@unibe.ch)*
[2] *Institut für Geologie und Mineralogie, Universität zu Köln, Germany*
[3] *Université de Lorraine, National Centre for Scientific Research, Centre de Recherches Pétrographiques et Géochimiques, F-54000 Nancy, France*
[4] *Department of Earth Sciences and Engineering, King Abdullah University of Science and Technology (KAUST), Saudi Arabia*

Earth is unique among the rocky planets in the solar system in terms of having a bimodal distribution of thick felsic continental crust and thin mafic oceanic crust. Formation and stabilization of this thick felsic crust was a fundamental process in Earth's history as it lead to formation of a stable landmass on the early Earth. Coupled formation, evolution and stabilization of a thick sub continental lithospheric mantle (SCLM) was critical in ensuring the stability of the thick continental crust. Hence, a way to study the evolution of Archean felsic crust is to understand the co-evolution of the lithospheric mantle beneath it. Large-scale dyke swarms that intrude Archean cratons can provide information on the formation of the sub cratonic lithosphere and efficiently track its secular evolution (Bartels et al., 2015; Pandey & Paul, 2022). Dyke swarms that intruded the Paleoarchean felsic crustal nucleus of the Singhbhum Craton are of Neoarchean to Paleoproterozoic age. The parental magma of these mafic-ultramafic dykes were enriched in incompatible elements that indicate the presence of a "crustal component" in their source (Pandey et al., 2021). Mobility and stable isotope fractionation of the redox-sensitive element Mo combined with radiogenic isotopes (Nd, Hf), have the potential to track the petrogenesis of the different dyke swarms and the composition of their source(s) (Skora et al., 2017; Ahmad et al., 2022).

Four dyke swarms that intruded between 2.8 Ga and 1.765 Ga were studied to derive constraints on the chemical evolution of their mantle source region. Trace element abundance combined with stable Mo and radiogenic Hf and Nd isotope signatures of these primitive dyke swarms indicate that the crustal enrichment signature in the dykes' parental magma is not due to assimilation and fractional crystallization processes during magma emplacement, but rather due to mantle source enrichment. The covariation of ($\delta^{98/95}$Mo with immobile element ratios indicate the involvement of hydrous melts originating from surface-derived materials, in the metasomatism of dykes' parental magma source region in the lithospheric mantle. A redox dependent multicomponent element (Mo, Ce) and isotope (δMo, εHf, εNd) mixing model affirms that the metasomatism of lithosphere underlying the Singhbhum Craton was facilitated by low degree anoxic melts coming from sediments and hydrated mafic crust, during their subduction driven recycling. The mixing model further predicts that the Singhbhum cratonic lithosphere was metasomatized in the Paleoarchean around 3.44 Ga, which is coeval with the formation of Singhbhum granitoids.

REFERENCES

Ahmad, Q., Wille, M., Rosca, C., Labidi, J., Schmid, T., Mezger, K., & König, S. (2022). Molybdenum isotopes in plume-influenced MORBs reveal recycling of ancient anoxic sediments. Geochemical Perspectives Letters, 23, 43–48.

Bartels, A., Nielsen, T. F. D., Lee, S. R., & Upton, B. G. J. (2015). Petrological and geochemical characteristics of Mesoproterozoic dyke swarms in the Gardar Province, South Greenland: Evidence for a major sub-continental lithospheric mantle component in the generation of the magmas. Mineralogical Magazine, 79(4), 909–939.

Pandey, O. P., Mezger, K., Upadhyay, D., Paul, D., Singh, A. K., Söderlund, U., & Gumsley, A. (2021). Major-trace element and Sr-Nd isotope compositions of mafic dykes of the Singhbhum Craton: Insights into evolution of the lithospheric mantle. Lithos, 382–383.

Pandey, O. P., & Paul, D. (2022). Secular evolution of the subcontinental lithospheric mantle beneath Indian cratons: Insights from geochemistry and geochronology of the Precambrian mafic dykes. Lithos, 422–423, 106729.

Skora, S., Freymuth, H., Blundy, J., Elliott, T., & Guillong, M. (2017). An experimental study of the behaviour of cerium/molybdenum ratios during subduction: Implications for tracing the slab component in the Lesser Antilles and Mariana Arc. Geochimica et Cosmochimica Acta, 212, 133–155.

3.5
Dissolved chromium concentrations and stable isotopes in marine pore waters from the equatorial Pacific Ocean

Delphine Gilliard[1], David J. Janssen[2], Samuel L. Jaccard[1], Brian Haley[3]

[1] *Faculty of Geosciences and Environment, Institute of Earth Sciences (ISTE), 1015 Lausanne (delphine.gilliard@unil.ch)*
[2] *Eawag – Swiss Federal Institute of Aquatic Science and Technology, Seestrasse 79, 6047 Kastanienbaum*
[3] *College of Earth, Ocean, and Atmospheric Sciences, Oregon State University, US*

The interaction between pore water and sediments can result in the scavenging or release of elements, influencing sedimentary and water column chemistry. Therefore, pore water can play a significant role in the chemical composition of marine sediments and deep seawater, with potential implications for sediment proxies. Cr concentration ([Cr]) and stable isotope composition (δ^{53}Cr) have been used as a paleoproxy for atmospheric oxygen content from records in sedimentary deposits e.g. (Frei et al., 2009; Planavsky et al., 2018). This study focuses on the analysis of pore water to better understand the processes driving isotopic shifts and Cr dynamics in marine sediments to refine our understanding of Cr behavior as a paleoproxy.

Early water column-based studies suggested benthic fluxes of Cr play a significant role in shaping dissolved Cr distributions (e.g. Achterberg & Van den Berg, 1997; Jeandel & Minster, 1987; Murray et al., 1983), although pore water data to assess these suggestions are scarce. Recent pore water data, showing fluxes of Cr into deep waters (Bruggmann et al., 2023; Janssen et al., 2021) help to give direct constraints on the magnitude of benthic fluxes and their impact on the oceanic Cr cycle; however, these localized data cover only small sections of the global ocean. To address this knowledge gap, three sets of sediment cores paired with water column depth profiles were collected during the Kilo Moana expedition KM2012 in October and November 2020 in the equatorial Pacific. These sites were chosen to cover sedimentary regimes of high spatial significance in the global ocean.

Our preliminary results indicate that pore water [Cr] range from 5.0 to 7.3 nmol/kg and δ^{53}Cr varies from 0.43 ± 0.06 to 0.68 ± 0.08 ‰ (2SEM). These data indicate higher and isotopically lighter pore water [Cr] and δ^{53}Cr, respectively, compared to seawater, in agreement with limited avaiable field data (Janssen et al., 2021). These data, in combination with available literature data, give an opportunity to assess controls on benthic Cr fluxes as well as their significance across diverse sediment regimes. This provides new insights into the interactions governing Cr cycling between sediments, seawater, and pore water, contributing to a more comprehensive understanding of how Cr records are preserved in sedimentary rocks and helping improve future Cr paleoproxy applications.

REFERENCES

Achterberg, E. P., & Van Den Berg, C. M. G. (1997). Chemical speciation of chromium and nickel in the western Mediterranean. *Deep-Sea Research Part II: Topical Studies in Oceanography*, *44*(3–4), 693–720. https://doi.org/10.1016/S0967-0645(96)00086-0

Bruggmann, S., Severmann, S., & McManus, J. (2023). Geochemical conditions regulating chromium preservation in marine sediments. *Geochimica et Cosmochimica Acta*, *348*, 239–257. https://doi.org/10.1016/J.GCA.2023.03.003

Frei, R., Gaucher, C., Poulton, S. W., & Canfield, D. E. (2009). Fluctuations in Precambrian atmospheric oxygenation recorded by chromium isotopes. *Nature*, *461*(7261), 250–253. https://doi.org/10.1038/nature08266

Janssen, D. J., Rickli, J., Abbott, A. N., Ellwood, M. J., Twining, B. S., Ohnemus, D. C., Nasemann, P., Gilliard, D., & Jaccard, S. L. (2021). Release from biogenic particles, benthic fluxes, and deep water circulation control Cr and δ53Cr distributions in the ocean interior. *Earth and Planetary Science Letters*, *574*, 117163. https://doi.org/10.1016/J.EPSL.2021.117163

Jeandel, C., & Minster, J. F. (1987). Chromium behavior in the ocean: Global versus regional processes. *Global Biogeochemical Cycles*, *1*(2), 131–154. https://doi.org/10.1029/GB001i002p00131

Murray, J. W., Spell, B., & Paul, B. (1983). The Contrasting Geochemistry of Manganese and Chromium in the Eastern Tropical Pacific Ocean. In *Trace Metals in Sea Water* (pp. 643–669). Springer US. https://doi.org/10.1007/978-1-4757-6864-0_37

Planavsky, N. J., Cole, D. B., Isson, T. T., Reinhard, C. T., Crockford, P. W., Sheldon, N. D., & Lyons, T. W. (2018). A case for low atmospheric oxygen levels during Earth's middle history. In *Emerging Topics in Life Sciences* (Vol. 2, Issue 2, pp. 149–159). Portland Press Ltd. https://doi.org/10.1042/ETLS20170161

3.6
Natural gas of radiolytic origin : Insigts from carbon isotopes

Maria Naumenko-Dèzes[1], Wolfram Kloppmann[1], Michaela Blessing[1], Bernhard Mayer[3]

[1] French Geological Survey (BRGM), 3 Avenue Claude Guillemin, 45100 Orléans, France. marie@geosphere.ch
[2] Nicholas School of the Environment, Box 90227, Duke University Durham, North Carolina 27708, United States.
[3] Department of Earth, Energy & Environent, University of Calgary, Calgary, Alberta, Canada T2N 1N4

Natural gas is extracted from conventional and unconventional reservoirs, and the composition and isotopic signatures of gas components provide useful proxies of gas origin and maturity. Several types of gases have been distinguished so far: microbial (primary and secondary), thermogenic (early mature, oil-associated, late mature), and abiotic (Milkov et al., 2020). However, in many cases, assessing the origin may be hindered due to different post-sedimentary processes like mixing, migration, sorption, etc. (e.g., Bernard et al., 1976; Bernard et al., 1977; Chung et al., 1988; Milkov and Etiope, 2018).

Additionally, a recent irradiation laboratory experiment conducted by Silva et al. (2019) demonstrated the possibility of the production of measurable quantities of radiolytic gases including methane, ethane, and propane with very distinct $\delta^{13}C$ values. This leads to the question: Does the process of radiolysis create considerable amounts of radiolitic natural gases? For example, the Alum Shale formation (Mid-Cambrian to Tremadoc, Northern Europe) is a prominent example of uranium-rich black shales, that were formed ~500 Ma ago and where the radiation dose obtained by the organic matter is significant. The irradiation in the shale causes changes in the structure and properties of organic matter, such as an increase in aromaticity, condensation degree, vitrinite reflectance, and, to some extent, carbon isotope signatures. These changes are explained by radiation-initiated cross-linking of organic molecules that results in aromatization and polymerization in the kerogens (Schovsbo, 2002; Lewan& Buchardt, 1989; Yang et al., 2019).

Our study (Naumenko-Dèzes et al., 2022) investigated whether radiolytic methane, ethane, and propane constitute a previously overlooked component of natural gas, especially in organic-rich shale gas plays. We demonstrate that light alkanes derived from the irradiation of kerogen and oil make a non-negligible contribution to natural gas mixtures from unconventional hydrocarbon reservoirs. By using an isotopic maturation-mixing model on a large set of natural gas data we quantify the effect of the admixture of light alkanes of radiolytic origin to gases of thermogenic and microbial origin. We also demonstrate that the resulting isotope signatures can lead to misinterpretation of gas origin and maturation levels and we provide a novel explanation of the so-called isotope reversals in natural gas from unconventional hydrocarbon reservoirs. We conclude that radiolytic gas derived from organic matter constitutes a previously not recognized type of natural gas, that needs to be considered especially in organic-rich unconventional hydrocarbon reservoirs that frequently contain uranium (U) in substantial quantities

REFERENCES

Bernard, B.B., Brooks, J.M. and Sackett, W.M., 1976. Natural-gas seepage in gulf of mexico. Earth and Planetary Science Letters, 31(1): 48-54.

Bernard, B.B., Brooks, J.M. and Sackett, W.M., 1977. A Geochemical Model For Characterization Of Hydrocarbon Gas Sources In Marine Sediments, 9th Annual Offshore Technology Conference, Houston, Tex.

Chung, H.M., Gormly, J.R. and Squires, R.M., 1988. Origin of gaseous hydrocarbons in subsurface environments: Theoretical considerations of carbon isotope distribution. Chemical Geology, 71(1–3): 97-104.

Lanphere, M., & Pamic J. 1992: K-Ar and Rb-Sr ages of Alpine granite-metamorphic complexes in northern Croatia, Acta Geologica, 22, 5-22.

Lewan, M.D. and B. Buchardt, Irradiation of organic matter by uranium decay in the Alum Shale, Sweden. Geochimica et Cosmochimica Acta, 1989. 53(6): p. 1307-1322.

Milkov, A.V. and Etiope, G., 2018. Revised genetic diagrams for natural gases based on a global dataset of >20,000 samples. Organic Geochemistry, 125: 109-120.

Milkov, A.V., Faiz, M. and Etiope, G., 2020. Geochemistry of shale gases from around the world: Composition, origins, isotope reversals and rollovers, and implications for the exploration of shale plays. Organic Geochemistry, 143

Naumenko-Dèzes, M., Kloppmann, W., Blessing, M., Bondu, R., Gaucher, E.C. and Mayer, B., 2022. Natural gas of radiolytic origin: An overlooked component of shale gas. Proceedings of the National Academy of Sciences, 119(15), p.e2114720119.

Schovsbo, N.H., 2002. Uranium enrichment shorewards in black shales: A case study from the Scandinavian Alum Shale. Gff, 124(2): 107-115.

Silva, R.C., Snowdon, L.R., Huang, H., Nightingale, M., Becker, V., Taylor, S., Mayer, B., Pedersen, J.H., di Primio, R. and Larter, S., 2019. Radiolysis as a source of 13C depleted natural gases in the geosphere. Organic Geochemistry, 138

Yang, S.Y., Schulz, H.M., Schovsbo, N. and Mayanna, S., 2019. The organic geochemistry of “Kolm”, a unique analogue for the understanding of molecular changes after significant uranium irradiation. International Journal of Coal Geology, 209: 89-93

3.7
Use of Rb-Sr and Sm-Nd isotope systems in determining diamond crystallisation ages

Suzette Timmerman[1,2], Thomas Stachel[1], Ingrid Chinn[3] & Graham Pearson[1]

[1] *Institut für Geologie, University of Bern, Baltzerstrasse 1+3, CH-3012 Bern (suzette.timmerman@unibe.ch)*
[2] *Department of Earth and Atmospheric Sciences, University of Alberta, Earth Sciences Building 1-26, CA-T6G 2E3 Edmonton*
[3] *DeBeers Group Services Ltd, Private Bag X01, SA-2193 Johannesburg*

Diamonds and their inclusions provide rare, direct and unaltered insights into deep Earth geochemical and geodynamic processes. Diamond crystallisation ages are an essential tool in determining when such processes occur, as well as in better understanding how and why diamonds form. Dating the crystallisation of diamond relies on mineral/fluid inclusions, which are protected - by their inert diamond host - from isotopic exchange with the surrounding mantle. Yet, Rb-Sr and Sm-Nd isotope systematics of silicate inclusions in diamonds rarely yield consistent ages. Further, radiogenic $^{87}Sr/^{86}Sr$ ratios are often unsupported by their low Rb/Sr ratios (Smit et al. 2022 and references therein).

Here, we present Rb-Sr and Sm-Nd isotopic data of lherzolitic clinopyroxene and garnet inclusions of diamonds from Victor, Canada. The main inclusion population yields a Sm-Nd isochron age within error of the ~720 Ma Re-Os age of sulphide inclusions of diamonds from the same mine, indicating that diamond crystallisation was likely triggered by the Franklin magmatic event (Aulbach et al. 2018). Rb-Sr isotope systematics appear to suffer from various degrees of Rb loss and indicate a younger age. The cause of the Rb-Sr complexity and its implications will be discussed in the context of diamond exploration.

REFERENCES

Smit, K. et al. 2022: Geochronology of Diamonds, Rev. Mineral. Geochem. 88(1), 567-636.

Aulbach, S. et al. 2018: Diamond ages from Victor (Superior Craton): Intra-mantle cycling of volatiles (C, N, S) during supercontinent reorganisation. Earth. Planet. Sc. Lett. 490, 77-87.

P 3.1
Assessing mechanisms of argon isotope redistribution in muscovite: Preliminary results from the Black Hills, South Dakota

Vidar Jakobsson[1] and Richard Spikings[1]

[1] *Department of Earth Sciences, University of Geneva, 1205 Geneva, Switzerland*

Several key assumptions form the basis of extracting continuous thermal history information from the Ar isotopic compositions of minerals. Recent in-situ $^{40}Ar/^{39}Ar$ and geochemical analyses have shown that argon distributions are frequently a consequence of fluid-associated retrograde reactions, even in gem-quality mica (Naumenko-Dèzes et al., 2021). Mica can retain $^{40}Ar/^{39}Ar$ crystallisation ages at temperatures above 500°C (Airaghi et al., 2018), despite predicted closure temperatures. However, retrograde re-equilibration often occurs, rendering mica useful for hygrochronometry (Villa, 2016). We test the hypothesis that diffusion profiles in white mica can remain over geological timescales, despite the effects of partial retrograde re-equilibration.

A Mesoproterozoic metasedimentary sequence is intruded by a granitic core in the Black Hills. The metasedimentary rocks yield white mica $^{40}Ar/^{39}Ar$ total-fusion dates that increase with distance from the granite, span several 100 Ma and have been interpreted to record cooling (Dahl & Foland 2008). However, the role of fluid interaction on the Ar isotopic compositions has not been thoroughly assessed. To test the hypothesis, we have re-sampled the meta-sedimentary units and the Harney Peak Granite. White micas are initially classified using optical light petrology and QEMSCAN, before detailed characterisation using EPMA, EBSD, TEM, SIMS - $\delta^{18}O$ and in-situ Rb-Sr dating to add a petrographic and temporal context for the in-situ Ar isotopic data. In-situ Ar isotope analyses will be compared to Ar isotopic data acquired using furnace step-heating to assess the causes of inflexions in Arrhenius trajectories. By studying a range of textures to provide recommendations for interpreting $^{40}Ar/^{39}Ar$ mica ages.

REFERENCES

Airaghi et al., (2018) Journal of Metamorphic Geology, 36(7), 933-958.
Allaz et al., (2011). Journal of Petrology, 52(4), 691-716.
Dahl & Foland (2008). *American Mineralogist*, *93*(8-9), 1215-1229.
Naumenko-Dèzes et al., (2021). *Chemical geology*, *573*, 120215.
Popov et al., (2020. *Chemical Geology*, *556*, 119841.
Villa, I. M. (2016). Chemical Geology, 420, 1-10.

P 3.2
Resolving Earth's Lead Paradox

Diego Toro Vivanco[1], Suzette Timmerman[1], Jörg Hermann[1], Andreas Stracke[2]

[1] Institut für Geologie, University of Bern, Baltzerstrasse 1+3, CH-3012 Bern (diego.toro@unibe.ch)
[2] Institut für Mineralogie, University of Münster, Corrensstraße 24, D-48149 Münster

Following the accretion and differentiation of the Earth into core and silicate mantle, the formation of crust initiated a process of depletion in incompatible elements via partial melting of the mantle. With the posterior onset of plate tectonics, the mass exchange between geochemical reservoirs drives the continuous compositional evolution of the crust and mantle, and the bio-chemical cycles that ultimately control Earth's surface habitability.

Amongst the diverse isotope systems, the U-Th-Pb system has been widely employed to study our planet's differentiation and evolutionary history. Its key significance is based on the refractory and lithophile behaviour of U-Th and the volatile and chalcophile behaviour of Pb, their different oxidation states, and the different half-lives of the radioactive parent isotopes ($^{238}U \rightarrow ^{206}Pb$, $t_{1/2}$=4.468 Gyr; $^{235}U \rightarrow ^{207}Pb$, $t_{1/2}$=703.8 Myr; $^{232}Th \rightarrow ^{208}Pb$; $t_{1/2}$=14.05 Gyr).

Bulk Silicate Earth (BSE) should plot on the so-called Geochron (Patterson 1956) in a $^{206}Pb/^{204}Pb$ vs $^{207}Pb/^{204}Pb$ plot. However, the Pb isotope ratios of rocks from mantle and crustal reservoirs both lie on the right side of the Geochron. This skewed distribution was termed the 1st Pb Paradox (e.g., Hofmann, 2008; Burton et al., 2012).

Multiple solutions to this apparent paradox have been proposed throughout the years. The most straightforward solution would be the existence of a reservoir that counterbalances the radiogenic accessible reservoirs (e.g., Hofmann, 2008). Unradiogenic Pb (i.e., low $^{206}Pb/^{204}Pb$ and $^{207}Pb/^{204}Pb$) is found in abyssal and cratonic peridotites (e.g., Burton et al., 2012; Warren and Shirey, 2012; Aulbach et al., 2019), indicating that Earth asthenospheric or subcontinental lithospheric mantle may be significant repositories for unradiogenic Pb.

A review of Pb and U contents and Pb isotope ratios in mineral phases (silicates and sulphides) of mantle xenoliths and abyssal peridotites from the literature will be presented to assess - through mass balance modelling - the potential of the asthenospheric and lithospheric mantle as the unradiogenic Pb reservoir.

REFERENCES

Aulbach, S., Heaman, L. M., Jacob, D. E., & Viljoen, K. S. (2018). Ages and sources of mantle eclogites: ID-TIMS and in situ MC-ICPMS Pb-Sr isotope systematics of clinopyroxene. Chemical Geology.
Burton, K. W., Cenki-Tok, B., Mokadem, F., Harvey, J., Gannoun, A., Alard, O., & Parkinson, I. J. (2012). Unradiogenic lead in Earth's upper mantle. Nature Geoscience, 5(8), 570–573.
Hofmann, A. W. (2008). The enduring lead paradox. Nature Geoscience, 1(12), 812–813.
Patterson, C. (1956). Age of meteorites and the earth. Geochimica et Cosmochimica Acta, 10(4), 230–237.
Warren, J. M., & Shirey, S. B. (2012). Lead and osmium isotopic constraints on the oceanic mantle from single abyssal peridotite sulfides. Earth and Planetary Science Letters, 359-360, 279–293.

P 3.3
Constraining oceanic lithosphere depletion through non-traditional stable isotope analyses

Robert Webster[1], Suzette Timmerman[1], Lynton Jaques[2], Julian-Christopher Storck[1]

[1] *Institute For Geology, University of Bern, Baltzerstrasse 1+3, CH-3012 Bern (robert.webster@unibe.ch)*
[2] *Research School of Earth Sciences, Australian National University, Canberra 2600, Australian Capital Territory, Australia*

Archaean cratonic harzburgites are highly depleted in incompatible elements, a feature that resulted from major melt depletion creating the depleted, buoyant lithospheric mantle beneath Archaean cratonic nuclei. Yet, the mantle unit (harzburgites/dunites) of the Papua New Guinea (PNG) ophiolites are some of the most depleted rocks, but are only Cretaceous in age (Barrett et al., 2022). We look to isolate the contribution partial melting had to create such depleted rocks in a modern setting by presenting a model of Fe-Ti isotopic fractionation through two PNG ophiolite sequences.

The PNG ophiolites consist of the Marum Ophiolite (upper mantle unit + cumulates) and the Papuan Ultramafic Belt (upper mantle unit + cumulates + basalt) and record cogenetic sequences based on major and trace element compositions (Davies and Jaques, 1984). Based on known mineral modes and Fe-Ti concentrations, we develop a theoretical model for the expected Fe-Ti isotope fractionation and will test this against analyses of the natural rock record. As Ti isotope systematics readily record magmatic differentiation, we expect to see a correlation with typical differentiation indices (e.g. MgO) (Millet et al., 2016; Storck et al., 2023). Further, we expect heavier Fe isotope ratios with melt evolution, consequently becoming more enriched in Fe^{3+}, since earlier forming minerals favour Fe^{2+} and lighter isotopes (Williams et al., 2018).
Future work in the project will focus on how fluid activity may cause further depletion.

REFERENCES
Barrett, N., Jaques, A.L., González-Álvarez, I., Walter, M.J. and Pearson, D.G., 2022. Ultra-refractory peridotites of Phanerozoic mantle origin: The Papua New Guinea ophiolite mantle tectonites. Journal of Petrology, 63(3), p.egac014
Davies, H.L. and Jaques, A.L., 1984. Emplacement of ophiolite in Papua New Guinea. Geological Society, London, Special Publications, 13(1), pp.341-349.
Millet, M.A., Dauphas, N., Greber, N.D., Burton, K.W., Dale, C.W., Debret, B., Macpherson, C.G., Nowell, G.M. and Williams, H.M., 2016. Titanium stable isotope investigation of magmatic processes on the Earth and Moon. Earth and Planetary Science Letters, 449, pp.197-205.
Storck, J.C., Greber, N.D., Duarte, J.F.V., Lanari, P., Tiepolo, M. and Pettke, T., 2023. Molybdenum and titanium isotopic signatures of arc-derived cumulates. Chemical geology, 617, p.121260.
Williams, H.M., Prytulak, J., Woodhead, J.D., Kelley, K.A., Brounce, M. and Plank, T., 2018. Interplay of crystal fractionation, sulfide saturation and oxygen fugacity on the iron isotope composition of arc lavas: An example from the Marianas. Geochimica et Cosmochimica Acta, 226, pp.224-243.

P 3.4
Tracing the source of fluids in the Archean crust factory: an example from the Lewisian Gneiss Complex (NW Scotland)

Silvia Volante[1,2], Maria Rosa Scicchitano[3], Vitor Barrote[,4], Jonas Kempf[5], Maria Fernanda Torres García[2], Annika Dziggel[2]

[1] *Structural Geology and Tectonics Group, Geological Institut, Department of Earth Sciences, ETH Zürich, Switzerland (svolante@ethz.ch)*
[2] *Department of Tectonics and Resources, Institute of Geology, Mineralogy, and Geophysics, Ruhr-Universität Bochum*
[3] *Deutsches GeoForschungsZentrum GFZ, Potsdam D14473, Germany*
[4] *Paul Scherrer Institute, Villingen, 5232, Swityerland*
[5] *School of Earth and Planteray Sciences, the Institute for Geoscience Research (TIGeR). Timescales of Mineral Systems group, Curtin Univeristy, Bentley, Australia*

In the early Earth, significant production of sodic continental crust (i.e., trondhjemite–tonalite–granodiorite—TTG) occurred during the Archean eon by partial melting of basaltic (mafic) crust, at depth between 25 and 50 kilometres. Fluid-fluxed melting has recently been invoked as an important trigger for TTGs formation[1], but the geodynamic settings and processes involved are highly debated. Important questions about the source of the melt-triggering fluids and how they were transported to deeper crustal levels have remained difficult to ascertain.

In this contribution, we combine petrographic observations, major and trace element whole-rock geochemical data, in-situ oxygen isotope analysis, and U-Pb dating of zircon from TTG gneisses from the Lewisian Gneiss Complex (LGC), in NW Scotland, to highlight the differences between two distinct groups of TTGs present in this region: hornblende-bearing (i.e., central region of the LGC) and biotite-bearing (northern and southern regions) TTGs.

Our results show that hornblende-TTGs are commonly primitive, Na-rich tonalitic magmas derived from partial melting of low-K mafic rocks and yield $\delta^{18}O$ values of 5–6‰ indicating that these magmas were hydrated by mantle-derived fluids rather than from a sedimentary or hydrothermal source. By contrast, less sodic, more ‘’mature’’, biotite-TTGs reflect more evolved trondhjemite to granodiorite compositions. The biotite-TTGs yield $\delta^{18}O$ values that, in places, are slightly above that of the average mantle zircon (5.3 ± 0.6‰ 2SD)[2]. This may indicate that TTG magma production in the northern and southern regions of the Lewisian Gneiss Complex was triggered by mantle-derived fluids that were previously contaminated with a supracrustal source to account for the small positive O isotopic excursions. These results highlight the hybrid sources of fluids which play an important role in the evolution of intracrustal recycling and crust-mantle interaction during crust formation in the Archean.

REFERENCES

1. Pourteau, A. *et al.* TTG generation by fluid-fluxed crustal melting: Direct evidence from the Proterozoic Georgetown Inlier, NE Australia. *Earth and Planetary Science Letters* **550**, 116548 (2020).
2. Valley, J. W. *et al.* 4.4 billion years of crustal maturation: oxygen isotope ratios of magmatic zircon. *Contributions to Mineralogy and Petrology* **150**, 561–580 (2005).

P 3.5
Optimizing Experimental Conditions for Accurate Oxygen Diffusion Measurements in Biominerals

Arthur Adams[1*], Deyanira Cisneros-Lazaro[1], Torsten Vennemann[2], Lukas Baumgartner[2], Damien Daval[3], Sylvain Bernard[4], Jarosław Stolarski[5], Alain Baronnet[6], Anders Meibom[1]

[1] *Laboratory for Biological Geochemistry, School of Architecture, Civil and Environmental Engineering, École Polytechnique Fédérale de Lausanne (EPFL), CH-1015 Lausanne, Switzerland. (*arthur.adams@epfl.ch)*
[2] *Institute of Earth Surface Dynamics, University of Lausanne, CH-1009 Switzerland.*
[3] *Université Grenoble Alpes, Grenoble, France*
[4] *Sorbonne Université, Paris, France*
[5] *Polish Academy of Sciences, Warsaw, Poland*
[6] *Aix-Marseille Université, Marseille, France*

Oxygen isotope compositions from pristine biominerals are the foundational proxies for paleoseawater temperatures spanning from the Paleozoic to the present. Recent research; however, has identified potential temperature biases introduced by low-temperature oxygen solid-state diffusion, particularly in calcitic biominerals e.g., foraminifera (Cisneros-Lazaro, et al., 2022; Adams et al., 2023). The extent of this diffusion-related effect on the paleotemperature record remains incompletely assessed due to challenges in determining accurate diffusion coefficients in (bio)minerals at low temperatures, yet its significance even under ambient ocean burial conditions may be substantial.

In this study, we address the formidable challenges of measuring and understanding diffusive phenomena in mineral systems at low temperatures (≤ 300 °C). We incubated foraminifera tests in autoclaves in four oxygen isotope exchange mediums: (1) ^{18}O-labeled calcite-saturated liquid water between 30–190 °C, (2) ^{18}O-labeled Na_2CO_3 fluids at 190–300 °C, (3) 97 atom% $H_2{}^{18}O$ vapour at 190–300 °C, and (4) $C^{18}O_2$ gas at 190–300 °C. The resulting rates and ultrastructural patterns of isotope exchange in foraminifera tests were examined using bulk isotope measurements and NanoSIMS mapping.

At low temperatures no recrystallization took place and the results were consistent with a grain-boundry diffusion mechanism. However, at higher temperatures in aqueous fluids, biomineral nanocrystallites become prone to recrystallization despite calcite-saturated incubation fluids. In constract, foraminifera tests did not recrystallize at high temperatures in water-vapour or CO_2, but NanoSIMS mapping revealed isotope exchange patterns that differed from lower temperature experiments.

While the rates of diffusive processes have been conventionally considered too slow to be detectable at low temperatures, our experiments demonstrate their capacity to influence isotopic compositions in biocarbonate minerals even over short experimental timeframes. By exploring a range of experimental conditions, we illuminate the complexity of these processes and their implications for accurate paleoclimatic interpretations.

REFERENCES

Adams, A., Daval, D., Baumgartner, L. P., Bernard, S., Vennemann, T., Cisneros-Lazaro, D., Stolarski, J., Baronnet, A., Grauby, A., Guo, J., & Meibom, A. 2023: Rapid grain boundary diffusion in foraminifera tests biases paleotemperature records, Communications Earth & Environment, 4:144.

Cisneros-Lazaro, D., Adams, A., Guo, J., Bernard, S., Baumgartner, L. P., Daval, D., Baronnet, A., Grauby, O., Vennemann, T., Stolarski, J., Escrig, S., & Meibom, A. 2023: Fast and pervasive diagenetic isotope exchange in foraminifera tests is species-dependent, Nature Communications, 13:113.

P 3.6
Productivity changes from the Holocene to the ice age evidenced by chromium isotopes

Sylvie Bruggmann[1], Patrick Blaser[1], Alfredo Martinez-Garcia[2], Xavier Crosta[3], Samuel Jaccard[1]

[1] *Institute of Earth Sciences, University of Lausanne, Géopolis, Quartier UNIL – Mouline, CH-1015 Lausanne (sylvie.bruggmann@unil.ch)*
[2] *Max Planck Institute for Chemistry*
[3] *University of Bordeaux*

Chromium (Cr) and the processes controlling its stable isotope fractionation are sensitive to redox conditions and/or biological productivity in modern marine environments. However, there is an ongoing debate related to the preservation and interpretation of Cr isotope compositions ($\delta^{53}Cr$) in the sedimentary record. While the database on Cr isotope compositions in seawater, as well as in ancient sedimentary rocks is growing, the Cr isotope system has yet barely been applied to marine sediments from Earth's recent past. Such sedimentary records can provide useful archives to explore Cr isotope systematics across arguably well-characterised climate intervals of the past, such as the Last Glacial Maximum (LGM). Here, we provide a new data set on Cr isotope compositions in a marine sediment core from the Crozet Plateau (MD19-3580) to unravel the biogeochemical controls on the $\delta^{53}Cr$ values since the last ice age.

The downcore sedimentary leachate data show that $\delta^{53}Cr$ values generally follow sea surface temperatures (SST). The highest $\delta^{53}Cr$ values are found in sediments deposited during the Holocene, where the biogenic carbonate content is at its maximum. Samples deposited during the LGM, on the other hand, show the lowest $\delta^{53}Cr$ values. These data can be interpreted as primarily reflecting changes in biogenic productivity, rather than changes in deep ocean oxygenation, suggesting that changes in export production exert a strong control on the marine biogeochemical cycling of Cr in modern and past environments.

P 3.7
Stable and radiogenic isotopes as weathering regime proxies: The source-to-sink response to the Paleocene-Eocene Thermal Maximum in the Spanish Pyrenees

Jaimes-Gutierrez R., Wilson D.J., Pogge von Strandmann P., Puceat E., Musajo C., Adatte T., Castelltort S.

Global warming and the associated hydrological cycle variations are known to disrupt the weathering regime over geological timescales. Enhanced weathering and erosion, which constitute denudation, serve as feedback mechanisms for regulating Earth's temperature over multi-million-year timescales. Weathering can draw down CO_2 from the atmosphere, while enhanced physical transport of clay particles can accelerate organic carbon sedimentation and, hence, carbon sequestration. In this study, we aimed to uncover changes to the denudation regime accompanying a massive climatic disturbance in deep time, the Paleocene-Eocene Thermal Maximum (PETM). The global warming of 5-8 °C due to the PETM has been documented to have increased the magnitude and intensity of precipitation events in the Spanish Pyrenees. But how did weathering respond to such a climatic and hydrological disturbance?

We investigated the lithium (Li), hafnium (Hf), and neodymium (Nd) isotopic composition of the <2 μm clay size-fraction in three sections in the Spanish Pyrenees, from source to sink: the Esplugafreda, Campo, and Zumaia localities. The Li isotope record at Esplugafreda in the terrestrial domain shows a positive δ^7Li excursion during the onset and body of the event (syn-PETM) and a negative excursion during the recovery (post-PETM), with no variation in the $\Delta\varepsilon$Hf, the εHf corrected for provenance changes with the εNd record. The Campo transitional section shows a negative Li isotope excursion during the body of the event. In the Zumaia deep marine section, the body of the event was characterized by a positive δ^7Li excursion, coeval with a negative excursion in $\Delta\varepsilon$Hf.

Overall, these results suggest a relative decrease in weathering (W) to denudation (D = W+E, where E is erosion) from pre-PETM to syn-PETM. The terrestrial section (Esplugafreda) indicates a local decrease in clay formation relative to erosion (E). The transitional section (Campo) integrates over a larger catchment area and could reflect an absolute increase in weathering. Finally, the "sink" deep-marine (Zumaia) section could indicate a relative decrease in regional weathering to denudation (W/D), consistent with the positive Li isotope and negative $\Delta\varepsilon$Hf excursions. This source-to-sink approach suggests that, although weathering in the Pyrenees increased in absolute amounts during the PETM, the amount of physical erosion of sediments increased substantially more than the chemical weathering, controlling the denudation regime in the region. These changes imply a trend towards a kinetically-limited regime in the region, with local variations in the weathering efficiency. The next step in this project will aim to quantify the relative importance of weathering to erosion during the PETM and, therefore, the share of each of these denudational processes in the climate recovery.

4 Environmental Biogeochemistry of Trace Elements

Matthias Wiggenhauser, Montserrat Filella, Marie Marques, Adrien Mestrot, Andreas Voegelin

TALKS:

4.1 Dittrich M., Voegelin A.: Raman and X-ray fluorescence microspectrocopy analysis of deep-sea ferromanganese nodules

4.2 Fontanella M.C. (Keynote): Trace metals in Italian paddy soils and uptake by rice

4.3 Grigg A.R.C., ThomasArrigo L.K., Notini L., Schulz K., Kaegi R., Barmettler K., Wisawapipat W., Kretzschmar R.: Transformation of jarosite and Al-substituted jarosite in flooded acid sulfate soil

4.4 Haaf D., Nghiem A., Renard P., Berg M., Winkel L.H.E.: Investigating arsenic redistribution in pumping-influenced groundwater with machine learning approaches

4.5 Nenonen V., Kaegi R., Hug S.J., Mangold S., Göttlicher J., Winkel L.H.E., Voegelin A.: Effects of organic ligands on the structure, colloidal properties and PO4 uptake of Fe oxidation products

4.6 Notini L., Kubeneck L.J., ThomasArrigo L.K., Schulz K., Fantappiè G., Rothwell K.A., Barmettler K., Wisawapipat W., Grigg A.R.C., Kretzschmar R.: Role of Coexisting Goethite in Ferrihydrite Transformation: Field Study

4.7 Reusser J.E., Siegenthaler M.B., Winkel L.H.E., Wächter D., Kretzschmar R., Meuli R.G.: The geochemical soil atlas of Switzerland

4.8 Santos J., Garcia-Calleja J., Xue X., Trindade K., Amouroux D., Slaveykova V.: Impact of planktonic communities from two alpine lakes in the fate of inorganic and methyl mercury: a species-specific isotope tracer approach

4.9 Siegenthaler M.B., Tolu J., Meuli R.G., Winkel L.H.E.: Selenium associated with soil organic matter across land uses in Swiss soils

POSTERS:

P 4.1 Aquino N.J., Janssen D.: Trace Metals in Rivers of Southern Greenland: Distribution, Controls, and Reactivity

P 4.2 Blattmann T.M., Plötze M., Yoshimura T., Galili N., Usman M.O., Eglinton T.I.: Quantifying environmental reactivity of clay minerals: Progress and questions regarding cation exchange capacity and mineral surface area

P 4.3 Sukekava C., Filella M., Laglera L.M.: Redefining the role of humic substances in oceanic iron biogeochemistry using competitive ligand exchange

P 4.4 M. Filella, T. Matoušek, A. García-Figueroa, M. Barešová, M. Prokopová, M. Pivokonský: New state-of-the-art HG-ICP-MS/MS methods for (sub)ppt speciation analysis of some less studied technology-critical elements (Ge, Sb and Te) applied to contrasting freshwaters

P 4.5 Brito F., Espinoza A., Freisinger E., Wiggenhauser M.: Identification of a Cadmium (Cd) Isotope Fractionation for a Plant Metallothioneins

P 4.6 Lefebvre P., Kretzschmar R.: Impact of Ferrihydrite Transformation on incorporated Zinc in Field Conditions

P 4.7 Morgenthaler U., Viacava K., Tolu J., Mestrot A.: Antimony release upon soil flooding- identification and characterization of the underlying biogeochemical drivers

P 4.8 Pellegri G., Wiggenhauser M., Eriksen J., Sarret G., Tercier-Waeber M.-L., Winkel L.: The Role of Thiols in Trace Metal Cycling in Swiss agricultural Soils

P 4.9 Voegelin, A., Wick, S., Baeyens, B., Marques Fernandez, M.: Thallium adsorption onto soil clay minerals

P 4.10 Wiggenhauser M., Konrad L., Hug M., Hepner N. , Radmehr N. , Tolu J., Pestoni G., Kronenberg L., Herter-Aeberli I.: The potential of European wheat cultivars to close trace metal gaps in plant-based diets

4.1
Raman and X-ray fluorescence microspectrocopy analysis of deep-sea ferromanganese nodules

Maria Dittrich[1,2], Andreas Voegelin[2]

[1] *Biogeochemistry Group, DPES, University of Toronto Scaborough (m.dittrich@utoronto.ca).*
[2] *Eawag, Swiss Federal Institute of Aquatic Science and Technology, Ueberlandstrasse 133, CH-8600 Duebendorf, Switzerland.*

Recently, a great interest in deep-ocean resources has been turned again to iron-manganese nodules enriched in Cu, Co, Ni, Mo, Li, Ti, rare earth (REE) elements and others technology-critical elements (Hein et al. 2015). Detailed mineralogical studies revealed the minerals' disordered properties and low crystallinity. The nodules can be formed through abiotic and biotic reactions, involving hydrogenetic process (mineral precipitation from deep water), diagenesis (process in pore waters). The nodules growth rates is estimated between thousands and millions of years per mm. The formation mechanisms of nodules are still debated, especially the role of microbes (Molari et al., 2020). Combining Raman microscopy, XRF, and SEM-EDS techniques allows us to shed light on the mineralogical and microbial signatures of iron-manganese nodule.
s

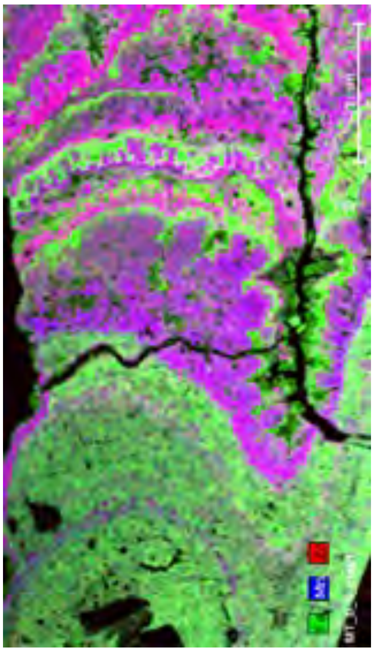

Figure 1. Nodule sample used for thin section (A). Exemplary XRF element map of Fe, Mn and Zn, showing close association of Zn with Mn.

REFERENCES
Hein JR, Koschinsky A (2014) Deep-ocean ferromanganese crusts and nodules. In: Holland HD, Turekian KK, Treatise on Geochemistry. (2nd edn), Oxford Elsevier, USA, 273.
Molari M., Janssen F., Vonnahme T.R., Wenzhöfer F., Boetius A (2020) The contribution of microbial communities in polymetallic nodules to the diversity of the deep-sea microbiome of the Peru Basin, Biogeosciences, 17,3203-3222.

4.2
Trace metals in Italian paddy soils and uptake by rice

Maria Chiara Fontanella[1]

[1] *Department for Sustainable Food Process, Catholic University of Sacred Heart of Piacenza, Piacenza 29100, Italy.*

Paddy soils in Italy can contain various trace metals, which are elements present in very small quantities but can have significant environmental and health implications due to their toxicity. Common trace metals of concern in soils include cadmium (Cd), arsenic (As) and others.

The uptake of trace metals by rice plants is influenced by several factors:
- Soil Characteristics: The concentration of trace metals in the soil, as well as its pH, organic matter content, micro/nano plastics and mineral composition, like silicium (Si) concetration, can influence the availability of these metals for uptake by rice plants.
- Water Management: The flooding of paddy fields affects the redox potential of the soil. This, in turn, can influence the mobility and availability of trace metals for uptake by rice. During the anaerobic conditions in soil, iron- bound As is released in solution. Moreover, arsenate (As^{5+}) is reduced to arsenite (As^{3+}), which is less strongly retained by several soil solid phases and can be absorbed by rice roots. Aerobic rice resulted in the lowest As content. But the dry period must be regolated, until the booting stage, to monitor the increase of another armful element like Cd.
- Rice Cultivar: Different rice cultivars can have varying abilities to accumulate trace metals. It is possible to recommend rice varieties based on the issues observed in previous years.
- Dietary: Different operations, like milling and parboiling, affect As fate and its chemical forms in grains, influencing harmuful elment intake.
- Sales target: Italian rice easily falls within the limits imposed for As and Cd in common rice, while there might be difficulties for the production of rice intended for the baby food market (0.10 mg/kg of maximum inorganic As level from EU 2015/1006; 0.040 mg/kg of total Cd from EU 488/2014)

REFERENCES

Tenni, D, et al. Total As and As speciation in Italian rice as related to producing areas and paddy soils properties. Journal of Agricultural and Food Chemistry, 2017, 65.17: 3443-3452.

Fontanella, M.C., et al. Effect of milling and parboiling processes on arsenic species distribution in rice grains. Rice Science, 2021, 28.4: 402-408.

Mamathaxim, N, et al. Effects of microplastics on arsenic uptake and distribution in rice seedlings. Science of The Total Environment, 2023, 862: 160837.

4.3
Transformation of jarosite and Al-substituted jarosite in flooded acid sulfate soil

Andrew R. C. Grigg[1,*], Laurel K. ThomasArrigo[1,2], Luiza Notini[1], Katrin Schulz[1], Ralf Kaegi[3], Kurt Barmettler[1], Worachart Wisawapipat[4], Ruben Kretzschmar.[1]

[1] *Institute of Biogeochemistry and Pollutant Dynamics, ETH Zurich, Universitätstrasse 16, CHN, 8092 Zurich, Switzerland (andrew.grigg@usys.ethz.ch)*
[2] *Institute of Chemistry, University of Neuchatel, Avenue de Bellevaux 51, 2000 Neuchatel, Switzerland*
[3] *Swiss Federal Institute of Aquatic Science and Technology (EAWAG), 8600 Dübendorf, Switzerland*
[4] *Department of Soil Science, Faculty of Agriculture, Kasetsart University, Bangkok 10900, Thailand*

Jarosite ($KFe_3(SO_4)_2(OH)_6$) is a common mineral in oxidised acid sulfate environments, such as active acid sulfate soils (ASS). In addition to being a major pool of Fe and S in ASS, jarosite has a capacity to sorb and incorporate trace elements, including toxic elements such as As and Pb, and major elements such as Al. As a result, the stability of jarosite may govern the cycles of nutrients and pollutants in ASS. In acid sulfate rice paddies, jarosite may be exposed to flooding for several weeks or months at a time. In this setting, microbial metabolism can lead to Fe reduction, driving the reductive dissolution, hydrolysis or Fe(II)-catalysed transformation of jarosite. Jarosite is known to transform into ferrihydrite, goethite and lepidocrocite under reducing conditions (Jones et al., 2009; Karimian et al. 2017, 2018). However, this understanding is largely based on mixed-suspension studies which only replicate selected biogeochemical properties of soils, and do not mimic the chemical complexity, diffusion limitations, microbiological diversity, and spatial heterogeneity of soils.

Here, we studied the transformation rates and products of synthetic unsubstituted and Al-substituted jarosite, using experimental designs that replicated the effect of 1) Fe(II) and pH conditions in flooded ASS 2) the full chemical complexity of the flooded ASS pore water and 3) contact between the mineral and the ASS matrix. The first experiment employed a mixed-suspension of unsubstituted or Al-substituted jarosite that was suspended in 50 mM MOPS buffer (pH 7) and 0.5 or 5 mM Fe(II) in glass bottles on a shaker in a glovebox. In the second experiment, unsubstituted and Al-substituted jarosite were incubated in mesocosms containing continuously flooded samples of acid sulfate topsoil from a rice paddy in Central Thailand. Mineral samples were incubated as pure phases for sixteen weeks at 30°C, using mesh bags made of PETE fabric (pore size of 52 µm). The transformation products in pure-mineral mesh bags were followed using X-ray diffraction. In the third experiment, using the same mesocosm design, mesh bags containing soil, enriched with ^{57}Fe-labelled jarosite and aluminium-jarosite, were incubated for sixteen weeks. The transformation products were measured using ^{57}Fe Mössbauer spectroscopy (Notini et al., 2023).

In the mixed-suspension experiment, jarosite transformation was complete within two to eight hours, with the products of ferrihydrite, lepidocrocite, and goethite. Aluminium substitution caused slower jarosite transformation, and hindered lepidocrocite formation in favour of goethite and ferrihydrite. In the soil mesocosms, the pure unsubstituted and Al-substituted jarosite took longer to react: the unsubstituted jarosite completely transformed to goethite and minor amounts of ferrihydrite within twelve to sixteen weeks, while partial transformation of Al-substituted jarosite to goethite and ferrihydrite occurred within sixteen weeks. In samples of ^{57}Fe-labelled jarosite that was mixed with soil, ^{57}Fe-Mössbauer spectroscopy also showed that jarosite was completely dissolved within sixteen weeks, but that the major products were non-mineral products (such as Fe(II) sorbed to the soil matrix) and highly disordered Fe phases. The contrasting results obtained from the three different experiments highlight the importance of complex matrices to understand jarosite transformation in the environment.

REFERENCES

Jones, A. M.; Collins, R. N.; Rose, J.; Waite, T. D. 2009: The effect of silica and natural organic matter on the Fe(II)-catalysed transformation and reactivity of Fe(III) minerals, Geochim. Cosmochim. Acta, 73(15), 4409–4422.

Karimian, N.; Johnston, S. G.; Burton, E. D. 2017: Antimony and arsenic behaviour during Fe(II)-induced transformation of jarosite, Environ. Sci. Technol., 51(8), 4259–4268.

Karimian, N.; Johnston, S. G.; Burton, E. D. 2018: Antimony and arsenic partitioning during Fe^{2+}-induced transformation of jarosite under acidic conditions, Chemosphere, 195, 515–523.

Notini, L., Schulz, K., Kubeneck, L. J., Grigg, A. R. C., Rothwell, K. A., Fantappiè, G., ThomasArrigo, L. K. and Kretzschmar, R. 2023: A new approach for investigating iron mineral transformations in soils and sediments using ^{57}Fe-labelled minerals and ^{57}Fe Mössbauer spectroscopy, Environ. Sci. Technol., 57(27), 10008–10018.

4.4
Investigating arsenic redistribution in pumping-influenced groundwater with machine learning approaches

David Haaf[1,2], Athena Nghiem[1,2], Philippe Renard[3], Michael Berg[2], Lenny H.E. Winkel[1,2]

[1] Inorganic Environmental Geochemistry Group, ETH Zürich, Rämistrasse 101, CH-8092 Zürich (david.haaf@eawag.ch)
[2] Department Water Resources and Drinking Water, Eawag, Überlandstrasse 133, CH-8600 Dübendorf
[3] Stochastic Hydrogeology, University of Neuchâtel, Rue Emile-Argand 11, CH-2000 Neuchâtel

Geogenic arsenic (As) contamination of groundwater poses a serious threat to human health, particularly in the river deltas of South-east Asia. The potential risk of As exposure and subsequent health effects may be especially concerning in large and rapidly growing cities within these deltas, which often rely on groundwater pumping to meet high domestic water demands. Extensive pumping in urbanized areas can affect regional As distribution in aquifers by altering groundwater flow, as demonstrated in Hanoi, Vietnam (van Geen et al., 2013). Multiple field studies at specific sites in and around Hanoi have identified different mechanisms for vertical and lateral As redistribution such as leaching of As and/or As-mobilizing solutes driving reducing conditions from organic-rich layers such as peat or river banks, and advection of As between and within Holocene and Pleistocene aquifers (e.g., Berg et al., 2008; Stopelli et al., 2021, 2020)elevated arsenic levels are present in both, the Holocene and Pleistocene aquifers. Family-based tubewells predominantly tap the Holocene aquifer, while the Hanoi water works extract more than 600,000 m3/day of groundwater from the Pleistocene aquifer. Detailed groundwater and sediment investigations were conducted at three locations exhibiting distinct geochemical conditions, i.e., i. These studies have provided valuable insights into the variety of As-mobilizing processes; however, it is not clear (i) how these mechanisms are transferable beyond these specific field sites to other areas with similar conditions, and (ii) how these processes can be generalized to large scales where multiple drivers of As redistribution may occur together.

In this study, the suggested hypotheses for As redistribution were investigated on a large scale, i.e., the greater Hanoi area (an area of 2000 km²), using a novel interpretable machine learning approach. This approach combines hydrochemical data available from existing studies with an improved 3D geological model and temporally resolved hydrological data to predict As contamination under different hydrochemical conditions based on geological parameters, i.e., lithology and layer thickness, quantified along groundwater flow paths affected by pumping.

Here we show how this novel approach, in combination with site-specific biogeochemical knowledge, can identify different As contamination mechanisms in the greater Hanoi area.

REFERENCES
Berg, M., Trang, P.T.K., Stengel, C., Buschmann, J., Viet, P.H., Van Dan, N., Giger, W., Stüben, D. 2008: Hydrological and sedimentary controls leading to arsenic contamination of groundwater in the Hanoi area, Vietnam: The impact of iron-arsenic ratios, peat, river bank deposits, and excessive groundwater abstraction, Chem. Geol., 249, 91–112. https://doi.org/10.1016/j.chemgeo.2007.12.007

Stopelli, E., Duyen, V.T., Mai, T.T., Trang, P.T.K., Viet, P.H., Lightfoot, A., Kipfer, R., Schneider, M., Eiche, E., Kontny, A., Neumann, T., Glodowska, M., Patzner, M., Kappler, A., Kleindienst, S., Rathi, B., Cirpka, O., Bostick, B., Prommer, H., Winkel, L.H.E., Berg, M. 2020: Spatial and temporal evolution of groundwater arsenic contamination in the Red River delta, Vietnam: Interplay of mobilisation and retardation processes, Sci. Total Environ., 717, 137143. https://doi.org/10.1016/j.scitotenv.2020.137143

Stopelli, E., Duyen, V.T., Prommer, H., Glodowska, M., Kappler, A., Schneider, M., Eiche, E., Lightfoot, A.K., Schubert, C.J., Trang, P.K.T., Viet, P.H., Kipfer, R., Winkel, L.H.E., Berg, M. 2021: Carbon and methane cycling in arsenic contaminated aquifers, Water Res., 200, 117300. https://doi.org/10.1016/j.watres.2021.117300

van Geen, A., Bostick, B.C., Thi Kim Trang, P., Lan, V.M., Mai, N.-N., Manh, P.D., Viet, P.H., Radloff, K., Aziz, Z., Mey, J.L., Stahl, M.O., Harvey, C.F., Oates, P., Weinman, B., Stengel, C., Frei, F., Kipfer, R., Berg, M., 2013: Retardation of arsenic transport through a Pleistocene aquifer, Nature, 501, 204–207. https://doi.org/10.1038/nature12444

4.5
Effects of organic ligands on the structure, colloidal properties and PO_4 uptake of Fe oxidation products

Ville Nenonen[1,2*], Ralf Kaegi[1], Stephan J. Hug[1], Stefan Mangold[3], Jörg Göttlicher[3], Lenny H.E. Winkel[1,2] & Andreas Voegelin[1]

[1] *Eawag, Swiss Federal Institute of Aquatic Science and Technology, Ueberlandstrasse 133, CH-8600 Duebendorf, Switzerland (*ville.nenonen@eawag.ch)*
[2] *Department of Environmental Sciences, Institute of Biogeochemistry and Pollutant Dynamics, ETH, Swiss Federal Institute of Technology, Zurich, Switzerland.*
[3] *Karlsruhe Institute of Technology, Institute of Synchrotron Radiation, Hermann-von-Helmholtz Platz 1, D-76344 Eggenstein-Leopoldshafen, Germany*

The oxidation of dissolved Fe(II) in natural waters leads to the precipitation of amorphous to poorly-crystalline Fe(III)-solids that can sequester dissolved phosphate (PO_4) and other nutrients or contaminants (Senn et al, 2015). In addition to inorganic solutes, also dissolved organic matter (DOM) can strongly affect the structure, transformation, colloidal properties, and PO_4 binding of Fe(III)-precipitates (Vindedahl et al., 2016).

For an improved understanding of the fate of PO_4 in aquatic environments, there is a need for a mechanistic insights into the effects of DOM on Fe(III)-precipitate formation induced by groundwater exfiltration and consequences for PO_4 and organic carbon (OC) sequestration. In this laboratory study, we examined the effects of model organic ligands (citrate, 3,4-dihydroxybenzoate (3,4-DHB), galacturonate, 2,4-dihydroxybenzoate (2,4-DHB), humate) on the formation and transformation of Fe(III)-precipitates in bicarbonate-buffered aqueous solutions at two PO_4 levels, with either Na or Ca as electrolyte cation. Changes in the structure and colloidal properties of the precipitates were probed with spectroscopic and microscopic techniques and related to changes in PO_4 retention.

The Fe(III)-precipitates formed in OC-free control experiments were mixtures of amorphous Fe(III)-phosphate and poorly-crystalline lepidocrocite. Increasing organic ligand concentrations led to less (and less crystalline) lepidocrocite and increasing ferrihydrite formation, resulting in more effective PO_4 and OC binding. In the Na electrolyte, above a certain concentration, strongly binding ligands effectively stabilized colloidal Fe(III) or complexed Fe(III), and thereby limited PO_4 removal. In the presence of Ca, these effects were strongly attenuated, leading to singificantly higher PO_4 and OC retention by filterable solids. The effects of the organic ligands decreased in the order citrate > 3,4-dihydroxybenzoate > galacturonate > 2,4-dihydroxybenzoate ≥ humate; along with decreasing strenght of Fe(III)-ligand complexation.

In conclusion, organic ligands can enhance the co-precipitation and retention of PO_4 and OC with Fe(III) at redox-interfaces via their effect on the structure of the Fe(III)-precipitates. On the other hand, organic ligands can also lead to more negatively charged and colloidally more stable Fe(III)-precipitates, and thereby enhance the transport of PO_4 and OC in environmental systems in colloidal form.

REFERENCES

Senn, A.-C., Kaegi, R., Hug, S. J., Hering, J. G., Mangold, S., Voegelin, A., Composition and structure of Fe(III)-precipitates formed by Fe(II) oxidation in near-neutral water: Interdependent effects of phosphate, silicate and Ca. Geochim. Cosmochim. Acta 2015, 162, 220–246.

Vindedahl, A. M., Strehlau, J. H., Arnold, W. A., Penn, R. L. Organic matter and iron oxide nanoparticles: aggregation, interactions, and reactivity. Environ. Sci. Nano 2016, 3, 494–505.

4.6
Role of Coexisting Goethite in Ferrihydrite Transformation: Field Study

Luiza Notini[1], L. Joëlle Kubeneck[1], Laurel ThomasArrigo[2], Katrin Schulz[1], Giulia Fantappiè [1], Katherine A. Rothwell[1], Kurt Barmettler[1], Worachart Wisawapipat[3], Andrew R. C. Grigg[1], and Ruben Kretzschmar[1]

[1] Institute of Biogeochemistry and Pollutant Dynamics, ETH Zurich, Universitätstrasse 16, CHN, 8092 Zurich, Switzerland (luiza.notini@usys.ethz.ch)
[2] Institute of Chemistry, University of Neuchatel, Avenue de Bellevaux 51, 2000 Neuchatel, Switzerland
[3] Department of Soil Science, Faculty of Agriculture, Kasetsart University, Bangkok 10900, Thailand

In redox-affected environments, electron transfer between aqueous Fe(II) and Fe(III)-minerals catalyzes iron mineral transformation and recrystallization processes. Minerals with lower crystallinity, such as ferrihydrite (Fh), tend to transform into more crystalline phases, while thermodynamically stable minerals, such as goethite (Gt), tend to undergo recrystallization rather than transformation. Laboratory experiments have demonstrated that the coexistence of Gt leads to more Fh transforming into Gt within 24 hours (Notini et al.,2022). However, little is known about how coexisting Gt will influence Fh transformation in natural environments, where minerals are in contact with a complex solid matrix, including other minerals, organic matter, and microorganisms. Here, we approached this question with three simultaneous field experiments in different regions of the world.

We used ^{57}Fe-labelled minerals and Mössbauer spectroscopy (Notini et al., 2023) to investigate the role of Gt during Fh transformation in situ. We installed PETE mesh bags filled with ^{57}Fh or ^{57}Fh+Gt into rice paddy soils (Thailand), intertidal flat sediments (Germany), and wetland soils (Iceland) for eight weeks. ^{57}Fh+Gt buried in paddy soils led to more Fh to Gt transformation than the pure ^{57}Fh. However, in intertidal sediments and wetland soils, Fh did not transform into Gt, even when Gt was added.

Our results suggest that coexisting minerals can change Fh transformation pathways in the natural environment. However, it also highlights that the complex composition of soil will control iron mineral transformation in different environments.

REFERENCES

Notini, L., ThomasArrigo, L. K. , Kaegi, R. and Kretzschmar, R. 2022: Coexisting Goethite Promotes Fe(II)-Catalyzed Transformation of Ferrihydrite to Goethite, Environ. Sci. Technol., 56 (17), 12723-12733.

Notini, L., Schulz, K., Kubeneck, L. J., Grigg, A. R. C., Rothwell, K. A., Fantappiè, G., ThomasArrigo, L. K. and Kretzschmar, R. 2023: A new approach for investigating iron mineral transformations in soils and sediments using ^{57}Fe-labelled minerals and ^{57}Fe Mössbauer spectroscopy, Environ. Sci. Technol., 57(27), 10008–10018.

4.7
The geochemical soil atlas of Switzerland

Jolanda E. Reusser[1,2], Maja B. Siegenthaler[1,3], Lenny H.E. Winkel[2,3], Daniel Wächter[4], Ruben Kretzschmar[2], Reto G. Meuli[1]

[1] *Research Division Agroecology and Environment, Agroscope, CH-8046 Zurich (jolanda.reusser@agroscope.admin.ch)*
[2] *Institute of Biogeochemistry and Pollutant Dynamics, ETH Zurich, CH-8092 Zurich*
[3] *Department of Water Resources and Drinking Water, Swiss Federal Institute of Aquatic Science and Technology, Eawag, CH-8600 Dübendorf*
[4] *Swiss Competence Center for Soil, Bern University of Applied Sciences, CH-3052 Zollikofen*

Broad-scale distributions of element concentrations in soils are presented in geochemical soil atlases (e.g. Reimann et al., 2014). So far no highly-resolved nationwide geochemical soil atlas existed for Switzerland. Our atlas will fill this gap by presenting the concentration ranges and spatial distributions of 20 elements (Fig. 1) in topsoils across Switzerland. The selection of elements includes both, essential and non-essential major and trace elements, some of which can also be potentially toxic contaminants. Our aim was to present 'ambient background' concentrations, which are defined as 'the sum of the natural background of an element and diffusive inputs in the past or present without anthropogenic point sources' (Reimann et al., 2018, ECHA, 2008). Based on the modeled maps, regions with potential deficiencies or soil contaminations can be assessed.

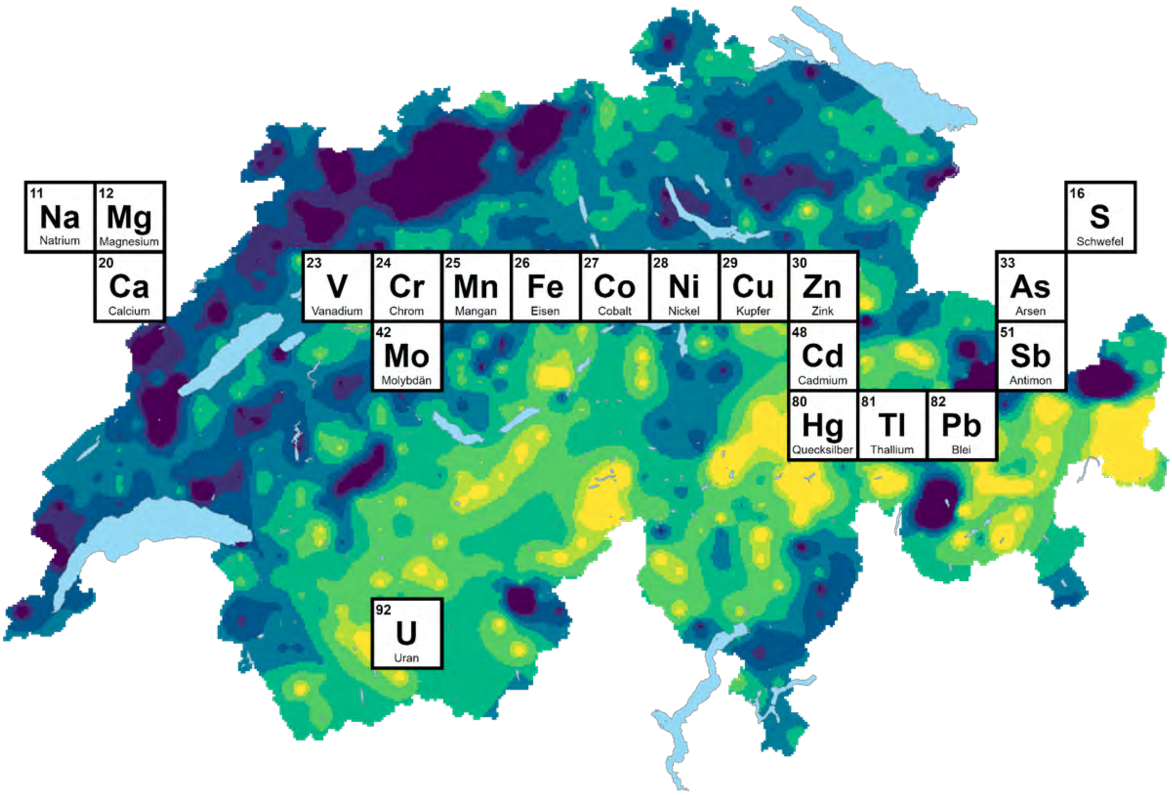

Figure 1. Elements of the geochemical soil atlas of Switzerland overlaying the map of interpolated chromium concentrations (mg/kg) in topsoil (0-20 cm). Reusser et al., in prep.

Between 2011 and 2015, in total 4'270 samples of the topsoil (0-20 cm) have been collected at 1'153 sampling sites along a regular 6 by 4 km grid within the framework of the Swiss Biodiversity Monitoring (BDM) program (Meuli et al., 2017). Element concentrations were measured in aqua regia digests of dried, sieved (<2 mm) and milled soil samples using ICP-MS. The exclusion of outliers

and sites within the perimeter of presumed anthropogenic point sources such as registered contaminated sites reduced the BDM dataset to 1'082 sampling sites. The BDM dataset was complemented with an additional dataset compiled by Stanisic et al. (2021) (279 sampling sites) and the soil database of the Swiss Soil Monitoring Network NABO (102 sampling sites).

Our results show that element concentrations vary greatly between regions, whereby comparatively high concentrations were often measured in the northwestern parts of Switzerland and in the eastern alpine regions (e. g. chromium, Fig. 1). In some of these regions, hotspots exist where defined threshold values are exceeded, especially for the potentially toxic elements arsenic, cadmium, chromium, copper, nickel and vanadium. In contrast to the hotspots, element concentrations in topsoils of the Midlands are generally low. These regions are important for agricultural production, where potential deficiencies of trace elements as well as main nutrients (i. e. sulphur) in the soil could negatively impact the quality of food and fodder. In addition, relationships between element concentrations and lithology, land use, as well as soil properties were assessed in order to identify possible drivers of the spatial distributions.

The geochemical soil atlas of Switzerland provides the base for further targeted in-depth studies of specific regions. Furthermore, the gained information on the spatial distributions and concentration ranges of elements in topsoils supports decision making of governmental and cantonal agencies. The atlas will be published in German, French, Italian and English at the end of 2023 resp. beginning of 2024.

REFERENCES

ECHA, 2008. Guidance on Information Requirements and Chemical Safety Assessment, Appendix R.7.13–2: Environmental Risk Assessment for Metals and Metal Compounds. European Chemicals Agency, Helsinki, Finland.

Meuli, R.G., et al., 2017. Connecting Biodiversity Monitoring with Soil Inventory Data – A Swiss Case Study. Bulletin BGS 38, 65-69.

Reimann, C., et al., 2014. Chemistry of Europe’s agricultural soils - Part A: Methodology and interpretation of the GEMAS data set. Geologisches Jahrbuch, Reihe B, Regionale Geologie Ausland Heft 102-103.

Reimann, C., et al., 2018. GEMAS: Establishing geochemical background and threshold for 53 chemical elements in European agricultural soil. Applied Geochemistry 88, 302-318.

Reusser, J. E., et al. The geochemical soil atlas of Switzerland. In preparation.

Stanisic, L., et al., 2021. Zusammenfassender Bericht über bestehende Studien und Untersuchungen zu geogenen Schadstoffgehalten in Böden und Gesteinen der Schweiz. Universität Bern, Bundesamt für Umwelt (BAFU), Bern.

4.8
Impact of planktonic communities from two alpine lakes in the fate of inorganic and methyl mercury: a species-specific isotope tracer approach

J.P.Santos[a], Javier Garcia-Calleja[b], Xujian Xue[a], Kevin Trindade[a], David Amouroux[b], Vera Slaveykova[a]

[a] *Faculty of Sciences, Earth and Environment Sciences, Department F.-A. Forel for Environmental and Aquatic Sciences, University of Geneva, 66 Bvd. Carl Vogt, 12*
[b] *Universite de Pau et des Pays de l'Adour, E2S UPPA, CNRS, IPREM, Institut des Sciences Analytiques et de Physico-chimie pour l'Environnement et les matériaux, Pau 64000, France*

Mercury is a persistent contaminant that can cause severe damage to human and environmental health. Despite the low concentration levels, mercury can bioaccumulate in aquatic organisms, and in the case of organic mercury, it can be biomagnified through the aquatic food web posing serious health issues to fish consumers.

In the present study, we investigated the sequestration and transformation capacity of inorganic and monomethylmercury in the photic zone by natural planktonic communities (ranging between 0.4 – 230 µm) from the mesotrophic Lake Geneva and the eutrophic Lake Greifensee, Switzerland. Sequestration and transformation were followed thanks to the species-specific approach used, where an enriched isotope mix of $^{199}Hg(II)$ and $^{201}MeHg$ (ratio 10:1) was spiked to the collected plankton. To fully comprehend the results obtained, qPCR assay analysis were used to explore the abundance of the functional genes of merA, merB and HgcAB responsible for mercury methylation, demethylation and mercury reduction.

Results highlighted clear differences in K*met* and K*deme* on the different lakes. Lake Grienfensee planktonic cultures, when incubated with mixed isotopes, promoted both methylation and demethylation, while in the case of Lake Geneva, that was not seen. However, when assessing the abiotic contribution in both Lakes, we could detect both methylation and demethylation in Lake Geneva, while no transformations were registered for Lake Greifensee. The current data highlighted the importance of different in situ communities and physicochemical parameters toward the Hg biogeochemical cycle.

Keywords: inorganic mercury, methylmercury, plankton communities, lake, freshwater system

4.9
Selenium associated with soil organic matter across land uses in Swiss soils

Maja B. Siegenthaler[1,2,3], Julie Tolu[1,3], Reto G. Meuli[2], Lenny H. E. Winkel[1,3]

[1] *Department of Water Resources and Drinking Water, Eawag, CH-8600 Dübendorf (maja.siegenthaler@eawag.ch)*
[2] *Agroecology and Environment, Agroscope, CH-8046 Zurich*
[3] *Institute of Biogeochemistry and Pollutant Dynamics, ETH Zurich, CH-8092 Zurich*

Selenium (Se) is a micronutrient for humans and animals but has a narrow range of safe intake levels (Combs et al., 2001). Insufficient Se intake is largely caused by low Se contents in crops, which result from generally low Se concentrations in soils combined with limited availability of Se for plant uptake (Gashu et al., 2021). Because soil Se losses (via leaching) and plant availability largely depend on the chemical form of Se (i.e., its speciation), it is crucial to understand the factors controlling soil Se speciation and how they are linked to agricultural management.

We investigated Se speciation in topsoils covering different land uses (i.e., croplands, grasslands, and forests) as well as gradients in soil properties, e.g. pH (3.2-7.5) and soil organic carbon (SOC; 1-16%). These soils were collected at 92 sites in Switzerland that are part of the Swiss Soil Monitoring Network. Dried and milled soils were extracted with NaOH to target organic and mineral-adsorbed Se. To determine Se speciation in NaOH extracts, we used a recently developed method based on size exclusion chromatography (SEC) coupled to UV and elemental mass spectrometry (ICP-MS/MS) with on-line Se isotope dilution (Tolu et al., 2022). Contrary to other methods, SEC-ICP-UV-MS/MS enables full recovery of Se species in NaOH extracts, through the quantification of Se associated with small (organo-)mineral nanoparticles, various organic Se fractions, and free Se oxyanions. Our aim was threefold: i) to quantify the NaOH-extractable Se oxyanions, a readily available source of Se for plants, and the organic Se pool, a potential source for plants in the long term; ii) to test the correlation between NaOH-extractable organic Se and SOC content reported for volcanic soils along a rainfall gradient (Tolu et al., 2022); and iii) to investigate the effects of land use and related soil properties on the types of organic Se.

Our results demonstrate that Se species can be quantified with SEC-UV-ICP-MS/MS across land uses and soil properties despite very low total soil Se concentrations, i.e., 0.07-0.93 mg kg^{-1}, on average 0.29 mg kg^{-1} (n=92). As observed for the volcanic soils (Tolu et al., 2022), the proportions of NaOH-extractable organic Se were positively correlated with SOC for grasslands and forests, however, not for croplands. In addition, croplands showed on average slightly higher proportions of Se oxyanions compared to grasslands and forests (33% versus 24% and 27%). A similar trend was observed for small hydrophilic organic Se (25% versus 22% and 19%). The improved knowledge on the organic Se variability across soil types will advance the understanding and predictive capabilities of soil Se speciation and plant availability, which will become more important for the agricultural management of Se considering decreasing atmospheric Se inputs (Feinberg et al., 2021) and SOC degradation (Crowther et al., 2015).

REFERENCES

Combs, G. F. 2001. Selenium in global food systems, British Journal of Nutrition, 85, 517-547.
Crowther, T.W., et al., 2016. Quantifying global soil carbon losses in response to warming, Nature, 540, 104-108.
Feinberg, A., et al., 2021. Reductions in the deposition of sulfur and selenium to agricultural soils pose risk of future nutrient deficiencies, Communications Earth & Environment, 2, 101.
Gashu, D., et al., 2021. The nutritional quality of cereals varies geospatially in Ethiopia and Malawi, Nature 594, 71–76.
Tolu, J., et al., 2022. Understanding soil selenium accumulation and bioavailability through size resolved and elemental characterization of soil extracts, Nature Communications, 13, 6974.

P 4.1
Trace Metals in Rivers of Southern Greenland: Distribution, Controls, and Reactivity

Norberto Jr Aquino[1], David J Janssen[1]

[1] *Aquatic Geochemistry Group, Department of Surface Water – Research and Management, EAWAG – Swiss Federal Institute of Aquatic Science and Technology, Seestrasse 79, 6047 Kastanienbaum (norbertojr.aquino@eawag.ch; david.janssen@eawag.ch)*

Trace metals (TMs) play a crucial role in Earth's biogeochemical cycle. They can be limiting and co-limiting nutrients in aquatic environments and, in elevated concentrations, can also act as environmental pollutants, adversely affecting aquatic organisms. The complex roles of TMs motivate study of their distribution, concentration, and transport, especially in regions more susceptible to climatic change such as the Arctic. Previous Arctic river data have indicated high natural levels of contaminant metals (e.g. Colombo et al., 2019; Hawkings et al., 2021) as well as important fluxes of macro- and micronutrients (e.g. Hawkings et al., 2015, 2020). Here we present trace metal and macronutrient data from 44 rivers in southern Greenland. These rivers cover a range of enviornmental settings, including glaciated and non-glaciated catchments, as well as areas subject to land use change. This study is the first of its kind, providing high spatial resolution on TM distributions in rivers of Greenland, where data are available in only a few catchments.

Anthropogenic controls from land-use changes (e.g. farming, mining) are negligible, and riverine TM distributions largely reflect geogenic controls. Proglacial rivers exhibit higher concentrations of particulate TMs (total and labile) compared to non-glaciated tundra rivers, reflecting the high suspended sediment content in proglacial rivers. Despite relatively low particle reactivity, these particles dominate total metal (particulate + dissolved) and potentially reactive metal (labile particulate + dissolved) concentrations in proglacial settings. In tundra rivers, average dissolved TM concentrations exceed those of proglacial rivers, and relative particulate metal lability is higher.

First order flux estimates based on annual discharge from tundra and glacial environments in Greenland show that proglacial rivers have a higher total flux of potentially reactive TMs (dissolved + labile particulate), predominantly driven by labile particulate phases. However, in terms of dissolved metal fluxes, tundra rivers may be a comparable or larger source of nutrients to the coastal ocean despite lower total discharge volumes. Furthermore, the spatial proximity of many tundra rivers to the open ocean compared to proglacial rivers, which are primarily found further within the fjords, may facilitate delivery of reactive nutrients from tundra rivers to the ocean, despite lower total reactive metal fluxes. Given the sensitivity of both glacial and tundra enviornments to climate change, and the potential different drivers of change in these distinct environments, the relative importance of these two settings may shift in the future. This underscores the importance of constraining controls on metal and nutrient distributions in both settings.

REFERENCES

Colombo, M., Brown, K. A., De Vera, J., Bergquist, B. A., & Orians, K. J. (2019). Trace metal geochemistry of remote rivers in the Canadian Arctic Archipelago. *Chemical Geology*, *525*, 479-491.

Hawkings, J., Wadham, J., Tranter, M., Lawson, E., Sole, A., Cowton, T., Tedstone, A., Bartholomew, I., Nienow, P., & Chandler, D. (2015). The effect of warming climate on nutrient and solute export from the Greenland Ice Sheet. *Geochem. Perspect. Lett*, *1*, 94-104.

Hawkings, J. R., Linhoff, B. S., Wadham, J. L., Stibal, M., Lamborg, C. H., Carling, G. T., Lamarche-Gagnon, G., Kohler, T. J., Ward, R., & Hendry, K. R. (2021). Large subglacial source of mercury from the southwestern margin of the Greenland Ice Sheet. *Nature Geoscience*, *14*(7), 496-502.

Hawkings, J. R., Skidmore, M. L., Wadham, J. L., Priscu, J. C., Morton, P. L., Hatton, J. E., Gardner, C. B., Kohler, T. J., Stibal, M., & Bagshaw, E. A. (2020). Enhanced trace element mobilization by Earth's ice sheets. *Proceedings of the National Academy of Sciences*, *117*(50), 31648-31659.

P 4.2
Quantifying environmental reactivity of clay minerals: Progress and questions regarding cation exchange capacity and mineral surface area

Thomas M. Blattmann[1,2], Michael Plötze[3], Toshihiro Yoshimura[2], Nir Galili[1], Muhammed O. Usman[4], Timothy I. Eglinton[1]

[1] *Geological Institute, ETH Zurich, Sonneggstrasse 5, CH-8092 Zurich (thomas. blattmann@erdw.ethz.ch)*
[2] *Biogeochemistry Research Center, Japan Agency for Marine-Earth Science and Technology (JAMSTEC), 2-15 Natsushima-cho, 237-0061 Yokosuka, Japan*
[3] *Institute for Geotechnical Engineering, ETH Zurich, Laura-Hezner Weg 7, CH-8093 Zurich*
[4] *Department of Earth and Environmental Sciences, University of Waterloo, 200 Unviersity Avenue West, 3G1 Waterloo, Canada*

Cation exchange capacity (CEC) and mineral surface area (MSA) of clay minerals are key for understanding the reactivity of clays in their environment and their impact on global biogeochemical cycles. We demonstrate a method for the determination of cation exchange capacity using the ammonium method delivering highly reproducible CEC quantities for a range of cation-exchanged clay minerals. While clay minerals homoionized with calcium largely showed a clear dominance of exchangeable calcium, sodium exchanged forms revealed that other cations (especially calcium) still dominate exchangeable sites, contrary to evidence from X-ray diffraction and expectations from what could be regarded as a rigorous cation exchange procedure. Additionally, we present a comparison of water and nitrogen-based MSA, both using the BET theory, for a variety of minerals and mineral matrices relevant for earth, environmental, and clay science. These datasets are used to discuss the overlay of multitude of effects influencing both nitrogen- and water-based MSA quantities. Recommendations are given to systematize MSA measurement strategies and provide guidance on the interpretation of complex MSA datasets. There is much we still need to learn to fully understand these fundamental parameters. Our state of progress will be presented.

P 4.3
Redefining the role of humic substances in oceanic iron biogeochemistry using competitive ligand exchange

Camila Sukekava[1], Montserrat Filella[2], Luis M. Laglera[1]

[1] *Departamento de Química, University of the Balearic Islands, Cra. de Valldemossa, km 7.5, ES-07122 Palma*
[2] *Department F.-A. Forel, University of Geneva, Boulevard Carl-Vogt 66, CH-1205 Geneva*

Organic complexation of iron is a critical factor in preventing its precipitation, facilitating its transport and influencing its reactivity and bioavailability in natural waters. Humic substance (HS) complexes are the main source of terrestrial iron reaching ocean waters. However, the transition from Fe-HS species to other forms of organic complexation with indigenous oceanic ligands has not been adequately described.

To explore this, we monitored the ligand exchange of iron-saturated Suwannee River fulvic and humic acids (SRFA and SRHA) after addition of deferoxamine B (DFOB) and protoporphyrin IX for comparison. We observed that Fe-HS concentrations gradually decreased to an apparent steady state, typical of a reversible reaction within 1 to 15 hours. The dissociation kinetics and species partitioning of the Fe-SRHS complexes at equilibrium challenged the current paradigm of HS-iron complexation. SRFA showed an iron binding affinity similar to that of DFOB, while the affinity of SRHA was even higher. The heterogeneity of the iron HS binding groups was confirmed, although experiments in NaCl solutions revealed that interference from major divalent ions caused most of the observed heterogeneity.

The different dissociation kinetics of the Fe-SRHS complexes obtained with various competing ligands and the absence of Fe-DFOB dissociation in the presence of iron-free SRFA indicate an intimate associative mechanism of ligand exchange. The ternary complex (SRHS-Fe-DFOB) does not form if the departing complex is Fe-DFOB.

We hypothesise that at SA and siderophore concentrations found in the open ocean, iron ligand exchange is limited, and organic iron speciation will be determined primarily on a first-come, first-served basis. Our findings reveal the complexity of cation-ligand interactions in seawater, with implications for the interpretation of recent iron speciation measurements and for understanding iron partitioning in the presence of ubiquitous HS.

P 4.4
New state-of-the-art HG-ICP-MS/MS methods for (sub)ppt speciation analysis of some less studied technology-critical elements (Ge, Sb and Te) applied to contrasting freshwaters

M. Filella[1], T. Matoušek[2], A. García-Figueroa[2], M. Barešová[3], M. Prokopová[3], M. Pivokonský[3]

[1] Department F.-A. Forel, University of Geneva, Boulevard Carl-Vogt 66, CH-1205 Geneva (montserrat.filella@unige.ch)
[2] Institute of Analytical Chemistry of the Czech Academy of Sciences, Veveří 97, CZ-602 00 Brno
[3] Institute of Hydrodynamics of the Czech Academy of Sciences, Pod Paťankou 30/5 CZ-160 00 Prague 6

The measurement of concentrations of chemical elements of proven toxicity such as lead, cadmium or arsenic in freshwaters has been considered solved for many years (with the exception, in some cases, of their chemical speciation). This view has changed recently with the development of new information technologies and, above all, with the need to reorient the current economic model towards decarbonisation. This combination has made much of the periodic table more topical. In this respect, it is worth noting that the fifth technical assessment (2023) of "critical raw materials" for the EU considers some 50 elements to be technologically critical! The various parties involved have realised that there are still many gaps in our ability to measure the concentrations of many of these elements and their species at the concentration levels needed to understand natural processes. We will present here the case of elements such as antimony, germanium and tellurium, which are present in natural waters at (sub)ppb or even ppt concentrations. Their analysis by ICP-MS, the standard technique in many laboratories, is further complicated by unfavourable properties such as high ionisation potential, isotopic number distribution of the elements, isobaric and polyatomic interferences, and intricate chemistry. The development of advanced methods based on the hydride generation (HG) technique, combined with state-of-the-art ICP-MS/MS detection, offers an answer to the challenge, but requires careful sampling, preservation and laboratory work and is hampered by the absence of certified reference materials and standards for some species. The new methods have been applied to natural waters of proven chemistry from drinking water reservoirs and the interesting results obtained will be shown.

ACKNOWLEDGEMENTS
The authors acknowledge the institutional support of the Czech Academy of Sciences [RVO: 68081715 and RVO: 67985874] and the Czech Academy of Sciences Premium Academiae, and thank Strategy AV21 of the Czech Academy of Sciences (VP20 – Water for life) for valuable support.

P 4.5
Identification of a Cadmium (Cd) Isotope Fractionation for a Plant Metallothioneins

Fernando Antônio Gomes Brito[1], Alejandro Marquez Espinoza[2], Eva Freisinger[2], Matthias Wiggenhauser[1]

[1] *Group of Plant Nutrition, ETH Zürich, Eschikon 33, CH-8315 Lindau (fgomes@ethz.ch)*
[2] *Department of Chemistry, University of Zurich, Winterthurerstrasse 190, 8057 Zürich*

Metallothioneins (MTs) are sulfur-rich proteins that bind to metal ions and are found in most living organisms. In plants, they may sequester trace metals in the cells of different organs, such as roots and leaves. Previous studies have found a systematic enrichment of heavy Cd isotopes in cereal grains, while light isotopes were retained in roots, stems, and leaves (Wiggenhauser et al., 2021). This isotope fractionation in plants could be related to the strong binding of light Cd isotopes to thiols, such as MTs. Based on theoretical calculations for small ligands, we expect MTs to preferably bind to light Cd (Zhao et al. 2021)knowledge of the equilibrium isotope fractionation of Cd with organic ligands is crucial to further advance Cd isotope source and process tracing in the field of biogeochemistry. In this study, we calculated reduced partition function ratios (103lnβ. However, to date, no experimental data has determined the isotope fractionation for Cd to thiols, neither for kinetic nor equilibrium fractionation.

We aim to determine the Cd isotope fractionation for an MT model, chickpea metallothionein (cicMT2). To achieve this goal, cicMT2 was recombinantly expressed in *E. coli* cells attached to a GST tag for purification, which was cleaved in a second step to obtain the native protein sequence. Metal-free cicMT2 were incubated with Cd(II) ions using different equilibration times to analyze the isotopic fractions of metals bound to cicMT2. After separating the unbound metal ions using size exclusion chromatography, the protein samples were measured for isotope ratios using a multi-collector ICPMS.

At the initial incubation time recorded (10 minutes), δ^{114}Cd isotope composition was -0.30 ± 0.2‰ in cicMT2. Whereas at the final incubation time (32 hours), the isotope composition was -0.15 ± 0.02‰. The isotopic equilibrium was reached at 6 hours of incubation. The binding of cicMT2 to Cd caused a strong isotope fractionation between the complexed and free Cd pool. At 10 minutes of incubation, the fractionation factor between free and complexed Cd was very strong ($\Delta^{114}Cd_{free\text{-}MT}$ = 1.20‰). The fractionation induced by cicMT2 remained significant at isotopic equilibrium ($\Delta^{114}Cd_{free\text{-}MT}$ = 0.53‰). The findings are consistent with the theoretical calculations and synchrotron X-ray studies (Wiggenhauser et al., 2021; Zhao et al., 2021). These studies provide evidence that the significant isotope fractionation towards lighter isotopes may be due to the average bond length between thiols and Cd. This bond length was longer than the bonds formed by Cd-O and Cd-N complexes. This is likely related to the enrichment of light isotopes in cicMT2 at equilibrium. This is the first time that experimental research evidenced that the lighter Cd isotope is enriched in Cd-cicMT2. Our findings foster the idea that the binding of Cd to thiols could be a main factor of Cd isotope fractionation in plants.

REFERENCES

Wiggenhauser, M., Aucour, A. M., Bureau, S., Campillo, S., Telouk, P., Romani, M. 2021: Cadmium transfer in contaminated soil-rice systems: Insights from solid-state speciation analysis and stable isotope fractionation. *Environ. Pollut.* 269, 115934.

Zhao, Y., Li, Y., Wiggenhauser, M., Yang, J., Sarret, G., Cheng, Q. 2021: Theoretical isotope fractionation of cadmium during complexation with organic ligands. *Chem. Geol.* 571, 120178.

P 4.6
Impact of Ferrihydrite Transformation on incorporated Zinc in Field Conditions

Pierre Lefebvre[1], Ruben Kretzschmar[1]

[1] *Soil Chemistry group, Institute of Biogeochemistry and Pollutant Dynamics, Department of Environmental Systems Science, ETH Zürich, Universitätstrasse 16, CH-8092 Zürich (pierre.lefebvre@usys.ethz.ch)*

In soils and sediments, iron (Fe) minerals play a major role in the cycling of many elements, including toxic or nutrient trace metals. In particular, ferrihydrite (noted Fh) is a poorly ordered metastable Fe-oxyhydroxide with high metal sorption capacity which can transform with time into more crystalline Fe minerals, a reaction that is catalysed by dissolved Fe(II) under reducing conditions such as that found in flooded soils and sediments. Although the impact of metals incorporated into (or adsorbed onto) ferrihydrite has been well described in model experiments with mineral suspensions, the applicability of these results to natural environments is still to be confirmed. In general, *in-situ* studies of iron (Fe) mineral recrystallization and transformation processes in soils are lacking compared to well-controlled laboratory-based experiments, especially because it is very challenging to detect poorly crystalline minerals in small quantities in a soil matrix. This challenge is being tackled with a new method developed within our group (Notini et al. 2023) by labelling Fe minerals with the ^{57}Fe isotope, enabling ^{57}Fe Mössbauer spectroscopy that specifically targets the minerals of interest diluted in soil material.

In this study, we focus on the impact of the Fe(II)-catalysed transformation of ferrihydrite on the mobility of zinc, as a proxy of divalent trace metals. We performed laboratory mesocosm experiments in order to compare the rates and products of transformation of Fh with coprecipitated Zn (Fh-Zn), in conditions as close as possible to natural environments. Sediments from the Wadden sea (Elbe River estuary, northern Germany) were flooded with artificial seawater until reducing conditions were established. Freshly synthesized Fh-Zn (with 0, 0.5 and 5 wt% Zn) labelled with ^{57}Fe was mixed with sediment and placed in porous meshbags that were inserted in the anoxic sediments. Fh-Zn samples were thereby incubated in presence of dissolved Fe(II) (from the sediment matrix) for more than three months, and we tracked the kinetics and products of the Fh transformation by Mössbauer spectroscopy, as well as the fate of incorporated Zn by bulk and micro-X-Ray Absorption Spectroscopy at the Zn *K*edge. Preliminary results show that Fh-Zn partly transformed under the established reducing conditions (Eh < 200 mV, dissolved Fe(II) at ~ 0.8 mM) to an ordered Fe(II) phase, without any new Fe(III) mineral such as goethite. Overall, the observed Fh-Zn transformation rate are unsurprisingly much slower than in mineral suspension experiments. Higher Zn concentrations do not appear to drastically slow down the Fh-Zn transformation rate compared to Zn-free Fh, as expected from the literature. These first results underline significant discrepancies between model experiments and natural environments.

REFERENCE

Notini, L., Schulz, K., Kubeneck, L. J., Grigg, A. R. C., Rothwell, K. A., Fantappiè, G., ThomasArrigo, L. K. and Kretzschmar, R. 2023: A New Approach for Investigating Iron Mineral Transformations in Soils and Sediments Using ^{57}Fe-Labeled Minerals and ^{57}Fe Mössbauer Spectroscopy. Environ. Sci. Technol. 57, 10008–10018.

P 4.7
Antimony release upon soil flooding- identification and characterization of the underlying biogeochemical drivers

Ursina Morgenthaler[1], Karen Viacava[1], Julie Tolu[2], Adrien Mestrot[1]

[1] *Institute of Geography, University of Bern, Hallerstrasse 12, 3012 Bern, Switzerland (ursina.morgenthler@unibe.ch)*
[2] *Eawag, Swiss Federal Institute of Aquatic Science and Technology, Department of Water Resources and Drinking Water (W+T), Überlandstrasse 133, 8600, Dübendorf, Switzerland*

Antimony (Sb) is used in a wide variety of everyday products, and its emissions to the environment are increasing severely. Due to its toxicity, elevated concentrations of Sb pose a significant risk to humans and the environment. Soil Sb can be very mobile under flooded conditions, a state which is expected to occur more frequently and more intensively in the future due to climate change. Sb could represent a danger for surrounding environments when mobilized from soil to porewater and thus (bio)available to (micro)organisms. Environmental concerns about Sb have emerged only recently, and many aspects of its complex biogeochemistry remain unclear.

Here, we incubated different Sb-contaminated soils under flooded conditions in mesocosms, which allowed for soil, porewater, surface water, and head-space sampling over an incubation time of three months. Soil porewater was analyzed for Sb speciation, Sb size fractionation, and a series of explanatory parameters. A new sequential extraction procedure, adapted for Sb, was applied to the soils.

Very high porewater Sb concentrations were observed shortly after flooding (hundreds of μgL^{-1}), which decreased sharply, presumably due to the reduction to Sb(III) and readsorption onto Iron(Fe) -oxides. Sequential extraction revealed that most Sb is bound to amorphous Fe –oxides or remains in the residual phase. This Fe-bound Sb was released upon reductive dissolution, as seen in a simultaneous increase in Sb and Fe concentration around three weeks after flooding. The size fractionation of porewater Sb revealed that most Sb is present as very small, purely dissolved ions, meaning that colloidal transport only plays a minor role in Sb mobility. Interestingly, trimethylated Sb was detected in soil porewater after a few weeks of flooding.

This study implemented new analytical methods for Sb characterization and, by including soil, water, and air, draws a more comprehensive picture of Sb geochemistry of flooded soils.

P 4.8
The Role of Thiols in Trace Metal Cycling in Swiss agricultural Soils

Geremia Pellegri[1,5], Matthias Wiggenhauser[1], Jørgen Eriksen[2], Géraldine Sarret[3], Marie-Louise Tercier-Waeber[4], Lenny Winkel[5,6]

[1] Institute of Agricultural Sciences, ETHZ, Eschikon 33, CH-8315 Lindau (geremia.pellegri@usys.ethz.ch)
[2] Department of Agroecology, University Aarhus, DK-8830 Tjele
[3] Institute of Earth Sciences, University of Grenoble Alpes, FR-38000 Grenoble
[4] Department of Inorganic and Analytical Chemistry, University of Geneva, CH-1211 Genève
[5] Institute of Biogeochemistry and Pollutant Dynamics, ETHZ, CH-8092 Zürich
[6] Department of Water Resources and Drinking Water, Eawag, CH-8600 Dübendorf

Low supply of the essential trace metals such as zinc (Zn) and copper (Cu) can impair crop yields and quality. Other trace metals like cadmium (Cd) are non-essential for plants and potentially detrimental for human health. Since the selectivity of plants to take up trace metals is limited, they inadvertently take up Cd. This is mainly due to the similarities of the biochemical characteristics of Cd, Zn, and Cu. Consequently, agricultural soils with elevated Cd concentrations can increase Cd accumulation in crops and potentially decrease the concentration of essential trace elements. To cope with trace metals, plants can synthesize organic molecules with reduced sulfur groups (thiols) that complex metals and detoxify them. Thiols form more stable complexes with soft metals such as Cd and Cu compared to less soft metals such as Zn. Hence, thiols may act as a metal filter in plants.

Although thiols are a minor fraction of all sulfur (S) forms in the soil, they seem to bind a significant fraction of trace metals (Karlsson & Skyllberg, 2007; Wiggenhauser et al., 2021). By forming complexes with metals and exhibiting a higher affinity for Cd in comparison to Zn, thiols could decrease the phytoavailability of Cd, thereby, acting as a metal filter in soil as observed in plant tissues. Hence, thiols may be a crucial player in decreasing the soil-to-plant transfer of Cd. However, the function of thiols in the soil-to-crop transfer of trace metals in arable soils is largely unexplored. In this project, the role of sulfur (S) and in particular thiols on the phytoavailability and the crop uptake of essential as well as toxic trace metals such as Zn, Cu, and Cd will be investigated in Swiss arable soils. To this end, a soil survey, soil incubation, and a pot experiment will be conducted. Speciation of S and metals will be determined using synchrotron X-ray techniques while the phytoavailability of trace metals will be determined by measuring dynamic trace metal concentrations in soil solution, using isotope dilution techniques, and by analyzing plant metal uptake. Thereby, we seek to improve the understanding of biogeochemical processes that govern the soil-to-crop transfer of trace metals. This is a prerequisite for developing agricultural strategies that improve food quality by optimizing the trace metal concentrations in crops.

REFERENCES
Karlsson, T., & Skyllberg, U. (2007). Complexation of Zinc in Organic SoilsEXAFS Evidence for Sulfur Associations. Environmental Science & Technology, 41(1), 119–124.

Wiggenhauser, M., Aucour, A.-M., Bureau, S., Campillo, S., Telouk, P., Romani, M., Ma, J. F., Landrot, G., & Sarret, G. (2021). Cadmium transfer in contaminated soil-rice systems: Insights from solid-state speciation analysis and stable isotope fractionation. Environmental Pollution, 269, 115934.

P 4.9
Thallium adsorption onto soil clay minerals

Andreas Voegelin[1]*, Silvan Wick[1], Bart Baeyens[2], Maria Marques Fernandez[2]

[1] *Eawag, Überlandstrasse 133, CH-8600 Dübendorf (*andreas.voegelin@eawag.ch)*
[2] *Paul Scherrer Institute, Forschungsstrasse 111, CH-5232 Villigen PSI*

Thallium (Tl) is a highly toxic trace element. In the environment, Tl mainly occurs as monovalent Tl(I). From contaminated soils, Tl may be taken up by plants or leach into groundwater, and thereby enter the food chain. The bioavailability and mobility of Tl in soils are controlled by sorption processes on soil minerals. Owing to its similar ionic radius and similarly low hydration enthalpy, the Tl^+ cation shows a similar geochemical reactivity as the alkali metal cations K^+, Rb^+, and Cs^+. Therefore, micaceous clay minerals have long been assumed to control the retention of Tl in soils. First spectroscopic evidence for predominent association of Tl with illite in soil was obtained in a study on the speciation of Tl in geogenically Tl-rich soils from the Swiss Jura mountains,[1] and emphasized the need to further study the adsorption of Tl(I) onto soil clay minerals. A laboratory study on the adsorption of Tl(I) onto illite confirmed that Tl^+ exhibits a very high adsorption affinity and that its uptake in the presence of competing cations (Ca^{2+}, Na^+, K^+, NH_4^+) can be quantified using a 3-site cation exchange model previously developed to quantify the highly specific adsorption of Cs^+ and Rb^+ at the frayed particle edges of illite.[2] Further work showed that this model also allowed to describe the solubility of exchangeable Tl in geogenically Tl-rich soils.[3] More recently, we studied the adsorption of Tl onto a suite of soil clay minerals - illite, smectite, muscovite and vermiculite – as well as onto a soil clay mineral assemblage.[4] Macroscopic adsorption data were combined with X-ray absorption spectroscopy results to assess the link between adsorption affinity and mode of Tl adsorption. The results showe that the complexation of Tl between two siloxane cavities at the frayed edges of illite or in the collapsed interlayers of vermiculite results in very strong Tl binding. Also Tl adsorbed onto single siloxane cavities on the planar surfaces of illite and muscovite was strongly retained. Overall, this study confirmed that the adsorption of Tl^+ onto clay minerals follows the same trends as observed for Cs^+ in extensive work on the fate of radiocesium in soils. Consequently, mechanistic insights gained from studies on the uptake of Cs by clay minerals and concepts for the quantification of the adsorption and retention of Cs in soils and sediments should be transferable to Tl(I).

REFERENCES

1. A. Voegelin, N. Pfenninger, J. Petrikis, J. Majzlan, M. Plötze, A.-C. Senn, S. Mangold, R. Steininger and J. Göttlicher, *Thallium speciation and extractability in a thallium- and arsenic-rich soil developed from mineralized carbonate rock*, Environ. Sci. Technol., **2015**, 49, 5390-5398.
2. S. Wick, B. Baeyens, M. Marques Fernandes and A. Voegelin, *Thallium adsorption onto illite*, Environ. Sci. Technol., **2018**, 52, 571-580.
3. S. Wick, B. Baeyens, M. Marques Fernandes, J. Göttlicher, M. Fischer, N. Pfenninger, M. Plötze and A. Voegelin, *Thallium sorption and speciation in soils: Role of micaceous clay minerals and manganese oxides*, Geochim. Cosmochim. Acta, **2020**, 288, 83-100.
4. A. Voegelin, S. Wick, N. Pfenninger, S. Mangold, B. Baeyens, M. Marques Fernandes, *Thallium adsorption onto phyllosilicate minerals*, Environmental Science: Processes & Impacts, 2022, 24, 1343-1359.

P 4.10
The potential of European wheat cultivars to close trace metal gaps in plant-based diets

Matthias Wiggenhauser[1], Lisa Konrad[1], Mikayla Hug[1], Naemi Hepner[2], Nina Radmehr[2], Julie Tolu[3], Giulia Pestoni[4], Lukas Kronenberg[5], Isabelle Herter-Aeberli[2]

[1] *Institute of Agricultural Sciences, Group of Plant Nutrition, ETH Zürich (wiggenh@ethz.ch)*
[2] *Laboratory of Human Nutrition, Institute of Food, Nutrition and Health, ETH Zürich, Switzerland*
[3] *Eawag, Department of Water Resources and Drinking Water (W+T) and ETH Zurich, Institute of Biogeochemistry and Pollutant Dynamics (IBP), Group of Inorganic Environmental Geochemistry*
[4] *Distance University of Applied Sciences, Switzerland*
[5] *John Innes Centre, Norwich, UK*

The FAO expects a shift towards plant-based diets in wealthy countries such as Switzerland due to environmental, health, and animal welfare concerns. This shift can critically reduce the intake of trace metals such as zinc (Zn), iron (Fe), and selenium (Se). As wheat could be a potential source to close this ‘micronutrient gap’, we screened for the first time the trace metal concentrations in European wheat elite genotypes that grew on a weakly alkaline soil within the years 2016 to 2019. We then calculated the contribution of high Zn and Fe wheat cultivars to plant-based diets using the menuCH food data set. The concentrations in the wheat grains ranged from 16 to 31 mg kg^{-1} for Zn and 25 to 56 mg kg^{-1} for Fe between the different genotypes. Compared to other countries, these concentrations are neither high nor low. Analyses of variance revealed that the genotypes and the year of sampling had significant effects on these concentrations. Phytate to trace metal molar ratios were high for Zn (> 15) and Fe (> 1), indicating a low bioavailability. The Se concentrations were low (> 11 ng g^{-1}) compared to other countries and not the genotype, but rather environmental factors controlled the variability of Se concentrations in wheat grains. These observations agree with further calculations that revealed that that there is a higher potential to breed high Fe and Zn cultivars compared to Se. Feeding the wheat grain concentration data into the menuCH data base revealed that using a high Zn and Fe wheat cultivar can increase the intake of these elements by around 5%, regardless of the diet groups. This proposes that wheat cultivars that are high in Fe and Zn could slightly improve the micronutrient intake of the Swiss population. However, more research is needed to investigate how far agricultural measures (breeding and fertilization) could further increase the trace metal concentrations in Swiss wheat grains and how efficiently they can be absorbed by the different diet groups.

5 Palaeontology

Allison Daley, Harriet Drage, Christian Klug, Torsten Scheyer

Schweizerische Paläontologische Gesellschaft,
Kommission des Swiss Journal of Palaeontology (KSJP)

TALKS:

5.1 Bastiaans D., Herbst E.C., Zanatta C., Scheyer T.M.: Adding a third dimension: exploring the functional ecology and evolution of Thalattosauriformes using digital reconstructions.

5.2 Benites-Palomino A., Aguirre-Fernandez G., Sanchez-Villagra M.: A Miocene sperm whale (Physeteroidea) from Peru expands the bounds of cranial asymmetry

5.3 Carrillo J.D., Silvestro D.: Contrasting diversity and disparity patterns in a continental radiation: diversification and morphological evolution in caviomorph rodents

5.4 Cooper J., Pimiento C.: Shark functional diversity throughout the Cenozoic

5.5 Corthésy N., Saleh F., Antcliffe J.B., Daley A.C.: Kaolinite stabilizes soft tissues through authigenic mineralization within days of marine shrimp decay

5.6 Drage H.B., Pates S.: Euarthropod horsehoe carapace convergence shaped by hydrodynamics?

5.7 Girard L.C., Lyson T.R., Hoganson J.W., Joyce W.G.: The cranial morphology of *Hutchemys rememdium* and its impact on the phylogenetic relationships of Plastomenidae (Testudinata, Trionychidae)

5.8 Greif M., Calandra I., Lautenschlager S., Kaiser T., Klug C.: Feeding behaviour and diet in Devonian ctenacanth chondrichthyans using tooth wear and finite element analysis

5.9 Gueriau P., Saleh F., Daley A.C.: Early Ordovician phyllocarid crustaceans from the South Pole

5.10 Hautmann M., Friesenbichler E., Bucher H.: A long-term perspective of the recovery from the end-Permian mass extinction

5.11 Hermanson G., Dziomber L., Girard L., Joyce W.G., Foth C., Evers S.W.: A phylogenetic comparative approach to turtle shell ecomorphological patterns

5.12 Jobbins M., Rücklin M., Sánchez Villagra M.R., Lelièvre H., Grogan E., Szrek P., Klug C.: Extreme lower jaw elongation in an alien-looking placoderm from Morocco

5.13 Kocáková K., Silvestro D., Pimiento C.: Age dependent extinction in modern sharks, rays and skates (Neoselachii)

5.14 Le Verger K., Ramstein N., Lonneux O., Ijspeert A.J., Scheyer T.M., Sánchez-Villagra M.R., Jusufi A.: New paleontological insights on the armor and weaponery of the mammalian knight: from anatomy to paleorobotics.

5.15 Lustri L., Gueriau P., Saleh F., Antcliffe J.B., Drage H.B., Lynch S., Potin G., Corthésy N., Daley A.C.: An exceptionally preserved ontogenetic series of horseshoe crabs from the Early Ordovician and the origin of chelicerates

5.16 Lynch S., Gueriau P., Drage H.B., Dutheil D.B., Charbonnier S., Daley A.C.: Moulting and development in a freshwater prawn from the Late Cretaceous of Morocco

5.17 Maridet O., Tissier J., Mennecart B., Coster P., Legal S., Costeur L.: New data on the Eocene-Oligocene mammalian turnover in south-eastern France: Red Queen or Court Jester, what evolutionary model for the “Grande Coupure”?

5.18 Mathes G., Silvestro D., Kocáková K., Gardiner A., Pimiento C.: Unraveling the role of temperature in Neoselachian extinction events

5.19 Menon J.C.L., Brinkman D.B., Joyce W.G., Evers S.W.: A three-dimensionally preserved fossil stem cholonioid from the Campanian of Alberta, Canada, provides insights into the evolutionary origin of sea turtles

5.20 Pimiento C., Kocáková K., Mathes G., Silvestro D.: Can species longevity predict extinction risk in the Anthropocene?

5.21 Pople J., Potin G.J.-M., Daley A.C.: Epibionts and trace fossils on arthropod carapaces from the Early Ordovician of Morocco

5.22 Potin G.J.-M., Gueriau P., Daley A.C.: Radiodont ecology and evolution: new oral cone data from the Fezouata Shale (Early Ordovician, Morocco)

5.23 Rollot Y., Zuber M., Hamann E., Joyce W.G.: A study of the carettochelyid turtle Allaeochelys crassesculpta from the Eocene (Early Lutetian) Messel Pit, Germany, using micro-computed laminography

5.24 Saleh F., Lustri L., Gueriau P., Potin G.J.-M., Pérez-Peris F., Laibl L., Jamart V., Vite A., Antcliffe J.B., Daley A.C., Nohejlová M., Dupichaud C., Schöder S., Bérard E., Lynch S., Drage H.B., Vaucher R., Vidal M., Monceret E., Monceret S., Lefebvre B.: The Cabrières Biota (France) provides insights into Ordovician polar ecosystems

5.25 Schneebeli-Hermann E., Kustatscher E.: Late Triassic palynomorphs from the Belchentunnel

5.26 Sciscio L., Meyer C.A., Belvedere M.: Late Jurassic sauropod trackway comparisons – examples from the Purgatoire Vaelly (USA) and Jura (Switzerland) tracksites

5.27 Tajika A., Landman N.H., Cochran J.K., Nishida K., Ishimura T., Shirai K., Klug C.: Selective extinction of cephalopods at the K-Pg mass extinction event

5.28 Torchet A., Shaw J., Scheyer T.: From Fossils to Food Webs – Reconstructing the trophic networks of the Middle Triassic Monte San Giorgio fossil Lagerstätte (Middle Triassic, Switzerland/Italy)

5.29 Vasilyan D., Goldin P., Lazarev S.: The life in the isolation: Serravalian-Tortonian (Middle – Late Miocene) marine verterbate fauna of Karagie, Kazakhstan, Eastern Paratethys

5.30 Yang X., Aguado M.T., Helm C., Zhang Z., Schmidt A.R., Bleidorn C.: Cambrian *Gaoloufangchaeta* was the earliest known pelagic annelid

5.31 Yang Zhao, Klug C., Cong P.: Systematics and palaeoecology of the Cambrian problematica dinomischids

POSTERS:

P 5.1 Cisneros-Lazaro D., Adams A., Otter L.M., Stołarski J., Bernard S., Daval D., Baronnet A., Grauby O., Baumgartner L.P., Vennemann T., Escrig S., Meibom A.: Shell shocked: PiFM imaging spills the beans- sugars more important than proteins during biocalcite diagenesis

P 5.2 Corthésy N., Saleh F., Antcliffe J.B., Thomas C., Daley A.C.: Clay minerals impact the microbial communities of decaying marine shrimps

5.1
Adding a third dimension: exploring the functional ecology and evolution of Thalattosauriformes using digital reconstructions.

Dylan Bastiaans[a], Eva C. Herbst[a], Chiara Zanatta[a], Torsten M. Scheyer[a]

[a] *Universität Zürich, Paläontologisches Institut und Museum , Karl-Schmid-Strasse 4, 8006 Zürich, Switzerland;*

The Middle Triassic UNESCO world heritage site of Monte San Giorgio has produced a wealth of exceptional remains of various vertebrate lineages. One of the most enigmatic and understudied clades are the Thalattosauriformes (sensu Nicholls 1999). This exclusively Triassic clade of secondarily aquatic reptiles shows a wide distribution across the northern hemisphere (Druckenmiller et al. 2020). Despite its relatively modest evolutionary timespan and taxonomic breadth, this group is characterized by exceptional morphological disparity. Thalattosaurs are characterized by a derived cranial architecture, most prominent is the considerable reduction or closure of the upper temporal fenestra (Druckenmiller et al. 2020; Nicholls 1999).

Their detailed cranial morphology and functional ecology is poorly understood because of a highly problematic fossil record historically composed of relatively rare isolated or fragmentary remains. Several virtually complete skeletons of at least three genera are known from Monte San Giorgio, representing both families of thalattosauriforms: the askeptosauroid *Askeptosaurus italicus* and the thalattosauroids *Hescheleria ruebeli* and *Clarazia schinzi*. Their preservation, as highly flattened slab specimens, makes them difficult to study even with modern approaches by reducing the effectiveness and fidelity of conventional radiographic approaches. To overcome problems concerning low-resolution output we used an integrative imaging approach, combining traditional high-resolution CT-scanning and angled radiography (CL). Segmentation, re-positioning, and retrodeformation was used to reconstruct the 'in vivo' cranial morphology of several thalattosaur genera. Subsequent quantitative and functional anatomical studies and comparison with contemporaneous marine reptile groups (e.g. sauropterygians) provide new insights in their ecology.

The crania of (derived) thalattosauroids are highly akinetic with complex interlocking, wedge-like elements, likely indicative of efficient force dissipation during feeding. Despite a degree of molarization of the dentition, the lack of visible tooth wear, highly infrequent tooth replacement, and low relative volumetric enamel contributions hint at limited durophagous capabilities. In contrast, askeptosauroids show more flexible skulls with potentially some degree of kinesis in the palate. Quantitative tooth shape analyses (3D GMM) show a limited morphospace occupation (i.e. relative homodonty) in askeptosauroids. Thalattosauroids encompass a greater dental morphospace compared to all other Mesozoic and extant marine amniote groups. Crown size and tooth occupation along the dental shelf is prominently reduced in thalattosauroids, while askeptosauroids merely show a decrease in relative crown height. The dental disparity and tooth distribution within thalattosauroids show the potential for a higher degree of oral processing and possibly a broader dietary range. Askeptosauroids with their mostly piercing dentition likely had a diet of softer prey items and perhaps small vertebrates. The new three-dimensional cranial reconstructions provide detailed morphological information for future phylogenetic work and form a basis for subsequent functional analyses.

REFERENCES

Druckenmiller, P. S., Kelley, N. P., Metz, E. T., & Baichtal, J. 2020: An articulated Late Triassic (Norian) thalattosauroid from Alaska and ecomorphology and extinction of Thalattosauria. Scientific reports, 10(1), 1746.

Nicholls, E. L. 1999: A reexamination of *Thalattosaurus* and *Nectosaurus* and the relationships of the Thalattosauria (Reptilia: Diapsida). PaleoBios 19:1-29.

5.2
A Miocene sperm whale (Physeteroidea) from Peru expands the bounds of cranial asymmetry

Aldo Benites-Palomino[1], Gabriel Aguirre-Fernandez[1], Marcelo Sanchez-Villagra[1]

[1] *Department of Paleontology, University of Zurich, Karl-Schmid-Strasse 4, 8006 Zurich, Switzerland*

Nasofacial asymmetry is a significant feature of toothed whales and dolphins (Odontoceti), related to their underwater breathing and dorsal migration of the nares (Churchill et al. 2018). One of the most extreme cases is seen in pygmy sperm whales (Kogiidae), as these retain a sole functional naris, and their skulls have been compartmentalized to house their greatly derived nasal organs (Benites-Palomino et al. 2020, 2021). A new fossil from Peru evidences one of the most extreme case of asymmetry known so far. The new fossil is characterized by a supracranial basin (region which houses the enlarged nasal organs) occupying most of the right facial region of the animal, a tubular rostrum and a left supraorbital region more anteriorly located than the right one. Particularly, the anterior displacement of the left supraorbital region shows a new pattern unknown for mammals and seen only in a handful of vertebrates. Additional characteristics present in the specimen such as the greatly ossified rostrum with many innervation rami suggest a specialized benthic ecology with particular sensory capabilities previously unknown in cetaceans.

REFERENCES

Benites-Palomino, A., Vélez-Juarbe, J., Collareta, A., Ochoa, D., Altamirano, A., Carré, M., et al. (2021). Nasal compartmentalization in Kogiidae (Cetacea, Physeteroidea): insights from a new late Miocene dwarf sperm whale from the Pisco Formation. Papers in Palaeontology, n/a(n/a). https://doi.org/10.1002/spp2.1351

Benites-Palomino, A., Vélez-Juarbe, J., Salas-Gismondi, R., & Urbina, M. (2020). Scaphokogia totajpe, sp. nov., a new bulky-faced pygmy sperm whale (Kogiidae) from the late Miocene of Peru. Journal of Vertebrate Paleontology, 39(6), e1728538. https://doi.org/10.1080/02724634.2019.1728538

Churchill, M., Geisler, J. H., Beatty, B. L., & Goswami, A. (2018). Evolution of cranial telescoping in echolocating whales (Cetacea: Odontoceti). Evolution, 72(5), 1092–1108. https://doi.org/10.1111/evo.13480

5.3
Contrasting diversity and disparity patterns in a continental radiation: diversification and morphological evolution in caviomorph rodents

Juan D. Carrillo[1], Daniele Sivestro[1]

[1] *Department of Biology, University of Fribourg, and Swiss Institute of Bioinformatics, Chemin du Musée 10, CH1700, Fribourg (juan.carrillo@unifr.ch)*

Understanding the relationship between diversification and morphological variation (disparity) in evolutionary radiations is a major challenge in macroevolution and the fossil record can shed light on the dynamics of evolutionary radiations (Foote & Miller, 2007). Sister clades can show an imbalance in species richness (diversity) and can also follow different patterns of morphological evolution, but the relationship between the imbalance in diversity and disparity remains unclear. Caviomorph rodents radiated in the Americas, and the sister clades Octodontoidea and Chinchilloidea diverged early in the caviomorph radiation (Vucetich et al. 2015). These clades today display drastically different diversity, with 195 extant species in the former and only six extant species in the latter. However, the fossil record documents a higher diversity and disparity in Chinchilloidea, including the largest rodent species that have ever lived (Engelman, 2022). Here, we combine data from extant and extinct species to infer their evolutionary history and evaluate how the diversification and morphological evolution dynamics shaped their contrasting patterns of diversity and disparity. We infer a total evidence, time-calibrated phylogeny including 149 extant and 52 extinct species, and use craniodental traits and body mass to study their morphological evolution. Our analyses indicate Chinchilloidea + Octodontoidea originated during the late Eocene (ca. 36.5 Ma) and the clades diverged shortly after. The inferred ancestral body mass was small (ca. 200 gr), but subsequently Chinchilloidea shows a higher body mass range through time, reaching its maximum in the Plio-Pleistocene. The rates of morphological evolution in Chinchilloidea were significantly higher than in Octodontoidea. The two clades had similar diversity trajectories until the beginning of the Miocene, when Octodontoidea shows a trend of increasing diversity until the present, whereas Chinchilloidea diversity stagnates, with drops in the late Miocene and Pleistocene. Late Neogene and Quaternary extinctions in Chinchilloidea significantly reduced the clade's disparity, reversing a pattern of relative higher disparity in comparison with Octodontoidea that appear since early in their origin. Our findings show a case of remarkable decoupling between species diversity and disparity, highlighting complex relationships between ecomorphological differentiation, species richness, and how they are affected by extinction events.

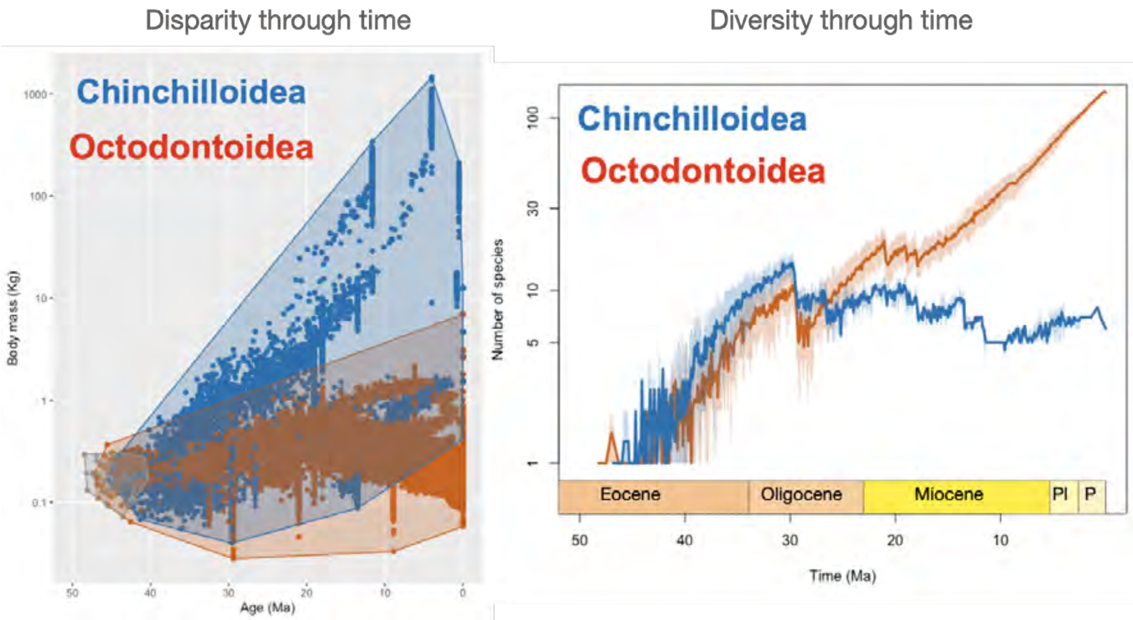

Figure 1. Contrasting patterns of morphological evolution and diversification dynamics in caviormorph rodents. *Disparity through time (left).* Body mass evolution of extinct and extant lineages. The shade areas show the range of body mass (log transformed) through time for each clade and the root (light gray), the dots represent the body mass of the tips (extinct and extant species) and nodes across a sample of 100 phylogenetic trees. The ancestral body mass was similar for both clades, but subsequently Chinchilloidea shows a higher body mass range through time, reaching the higher values in the Pliocene and Pleistocene and a decrease towards the present. *Diversity through time (right).* Lineage through time plot. The solid lines and the shaded areas represent the mean and the 95% credible interval, respectively, of the number of species (log transformed) trough time for the sample of 100 phylogenetic trees. The two clades had similar diversity trajectories until the beginning of the Miocene, when Octodontoidea shows a trend of increasing diversity until the present, whereas Chinchilloidea diversity stagnate and decrease after the Pleistocene.

REFERENCES

Engelman, R.K. 2022. Resizing the largest known extinct rodents (Caviomorpha: Dinomyodae, Neoepiblemidae) using occipital condyle width. Royal Society Open Science,9(6),220370.

Foote, M., & Miller, A.J. 2007: Principles of Paleontology, New York, Freeman and Company, 454 pp.

Vucetich, M.G. Arnal, M. Deschamps, C.M. Perez, M.E. Vieytes, E.C. 2015. A Brief History of Caviomorph Rodents as Told by the Fossil Record. In: Biology of Caviomorph Rodents: Diversity and Evolution. (Ed. by Vasallo, A.I. & Antenucci D).SAREM – Sociedad Argentina para el Estudio de los Mamíferos, p11-62.

5.4
Shark functional diversity throughout the Cenozoic

Jack Cooper[1], Catalina Pimiento[1,2,3]

[1] *Department of Biosciences, Swansea University, Swansea, UK (jackacooper33@gmail.com)*
[2] *Paleontological Institute and Museum, University of Zurich, Zurich, Switzerland*
[3] *Smithsonian Tropical Research Institute, Balboa, Panama*

Modern sharks have a long evolutionary history, during which they have persisted through numerous environmental changes, continuously playing key ecological functions such as apex predators. This longevity provides an opportunity to gauge how shark functional diversity has changed in deep time compared to the present. Here, we quantify shark functional diversity throughout the Cenozoic (66 million years ago to the present) using their teeth, which are well-preserved and abundant in the fossil record, and have been demonstrated to be good proxies of functional traits such as body size and feeding mechanism. To do so, we compiled a dataset of over 9,500 shark teeth from museum collections and scientific literature and took different dental measurements. We found that sharks maintained a relatively high functional diversity in the geological past, with 60-87% of the functional space occupied (functional richness) during the Cenozoic. However, functional diversity consistently declined since the Miocene, losing half of the functional space over time, reaching the lowest level (43%) in the Recent. Assessing species' contribution to functional diversity suggested that species turnover of benthic feeding specialists and the extinction of the largest apex predators were probable drivers of this recent decline. Today's sharks therefore have a distinctly narrower contribution to ecosystem functioning compared the past, indicating that future disturbances could be more ecologically damaging than previous species losses of at least the last 66 million years.

5.5
Kaolinite stabilizes soft tissues through authigenic mineralization within days of marine shrimp decay

Nora Corthésy[1], Farid Saleh[1], Jonathan B. Antcliffe[1], Allison C. Daley[1]

[1] *Institute of Earth Sciences, University of Lausanne, Géopolis, CH-1015 Lausanne (nora.corthesy@unil.ch)*

Decay experiments constrain the factors involved in the early stages of fossilization, when most labile anatomical information is either lost or retained (Allison, 1986; Hancy & Antcliffe, 2020; Plotnick, 1986)soft-bodied, and lightly skeletized animals display considerable resistance to skeletal damage during transport under experimental conditions. This resistance diminishes as decay advances. In addition, a high degree of decay-induced disarticulation may occur with minimal transport when carcasses are buoyed up from the sediment-water interface by decay gases. Decay, rather than nature or duration of transport, determines the completeness of fossil soft-bodied and poorly mineralized animals.”,”container-title”:”Geology”,”DOI”:”10.1130/0091-7613(1986. Experiments on the decay of animals buried in various clay minerals showed differing preservation profiles (Naimark et al., 2016; Wilson & Butterfield, 2014)places where soft-bodied organisms became mineralized, provide a substantial bulk of palaeobiological information, but the detailed mechanisms of how soft-tissue preservation takes place remain debatable. An experimental taphonomy approach, which allows for direct study of decay and mineralization, offers a means to study the preservational potential of different soft-bodied organisms under controlled conditions. Here we compare the preservational capacity of two types of clay (kaolinite and montmorillonite. However, the effect of clays on decaying animals placed on the surface of sediments without burial is still unknown. The decay of the marine shrimp *Palaemon varians* deposited on three clay types was assessed. Results show that kaolinite minerals slow decay rates. After 120 hours on kaolinite substrate, a fine black film forms on the carcass replicating the cuticle in microscopic detail and stabilizing the general morphology. Cryo-Scanning Electron Microscopy analysis shows that the film consists of newly formed aluminosilicate minerals, confirming silicification can occur rapidly after death on the seafloor. The other tested clay minerals do not show these effects, and with kaolinite they only took place at marine salinities and never in freshwater. Thus, kaolinite not only slows down decay, but it also facilitates the mineralization of soft parts even in the absence of complete burial. This questions whether rapid burial is necessary for soft tissue preservation.

REFERENCES

Allison, P. A. (1986). Soft-bodied animals in the fossil record: The role of decay in fragmentation during transport. *Geology*, *14*(12), 979. https://doi.org/10.1130/0091-7613(1986)14<979:SAITFR>2.0.CO;2

Hancy, A. D., & Antcliffe, J. B. (2020). Anoxia can increase the rate of decay for cnidarian tissue: Using Actinia equina to understand the early fossil record. *Geobiology*, *18*(2), 167–184. https://doi.org/10.1111/gbi.12370

Naimark, E., Kalinina, M., Shokurov, A., Boeva, N., Markov, A., & Zaytseva, L. (2016). Decaying in different clays: Implications for soft-tissue preservation. *Palaeontology*, *59*(4), 583–595. https://doi.org/10.1111/pala.12246

Plotnick, R. E. (1986). Taphonomy of a Modern Shrimp: Implications for the Arthropod Fossil Record. *PALAIOS*, *1*(3), 286. https://doi.org/10.2307/3514691

Wilson, L. A., & Butterfield, N. J. (2014). SEDIMENT EFFECTS ON THE PRESERVATION OF BURGESS SHALE-TYPE COMPRESSION FOSSILS. *PALAIOS*, *29*(4), 145–154. https://doi.org/10.2110/palo.2013.075

5.6
Euarthropod horsehoe carapace convergence shaped by hydrodynamics?

Harriet B. Drage[1], Stephen Pates[2]

[1] Institut des sciences de la Terre, Université de Lausanne, Batiment Géopolis, Lausanne, 1015-CH, (harriet.drage@unil.ch)
[2] Department of Zoology, University of Cambridge, Downing Street, Cambridge, UK, CB2 3EJ

Euarthropods with horseshoe-shaped carapaces have lived in the oceans near continuously for over 500 million years, with this carapace shape having evolved multiple times within the group; in horseshoe crabs, trilobites and radiodonts. The vaulted semi-circular carapace is considered an adaptation to a benthic marine lifestyle, which in horseshoe crabs facilitates positive lift avoidance, increases stability, and prevents overturning.

However, the extent to which the horseshoe-shaped carapaces of trilobites, radiodonts, and horseshoe crabs are similar in 2D and 3D has not yet been quantified. Thus, the extent to which this similarity represents convergence resulting from hydrodynamic pressures of a benthic mode of life remains unresolved.

We modelled the carapace morphology of these three groups in 2D and 3D using outline analysis and surface semi-landmark analysis respectively. The hydrodynamic importance of certain features, such as carapace brim width and angle, length of posterior projections (genal spines), and convexity of the carapace were then tested in isolation and together using Computational Fluid Dynamics simulations. We thereby quantify the extent of convergence between these groups, and determine the role of a horseshoe-shaped carapace morphology in facilitating a benthic life mode for euarthropods from the Cambrian to the present day.

Figure 1. Example simulation of water flow around a trilobite cephalon, produced using Ansys Fluent.

5.7
The cranial morphology of *Hutchemys rememdium* and its impact on the phylogenetic relationships of Plastomenidae (Testudinata, Trionychidae)

Léa C. Girard[1], Tyler R. Lyson[2], John W. Hoganson[3], Walter G. Joyce[1]

[1] *Department of Geosciences, University of Fribourg, 1700 Fribourg, Switzerland (lea.girard@unifr.ch)*
[2] *Department of Earth Sciences, Denver Museum of Nature & Science, Denver, Colorado 80205, U.S.A*
[3] *North Dakota Geological Survey, Bismarck, North Dakota 58505, USA.*

Trionychids (soft-shelled turtles) can easily be recognized by the unique morphology of their shell, which is highly reduced and covered with a thick leathery skin, rather than scales. Today this aquatic clade of turtles is spread across Africa, Asia, Australasia, and North America. Their origin can be traced back to the Early Cretaceous of Asia with forms that already resemble their living relatives closely. As a result, it is difficult to discerne phylogenetic relationships and the evolutionary history of the group is still poorly understood. Plastomenidae is an extinct subclade of North American trionychids whose content and inner relationships are still debated. Plastomenids are characterized, among others, by the secondary reossification of the plastron and a prolonged midline contact between the maxillae that forms a secondary palate. Here, we examine the cranial morphology of *Hutchemys rememdium*, a potential plastomenid, based on undescibed skulls and jaws from the Paleocene of North Dakota. 3D models were generated from X-ray micro-computed tomography scans. These models allow for a near-complete understanding of the cranial anatomy of this taxon. A phylogenetic analysis suggests an expanded Plastomenidae that is sister group to Cyclanorbinae.

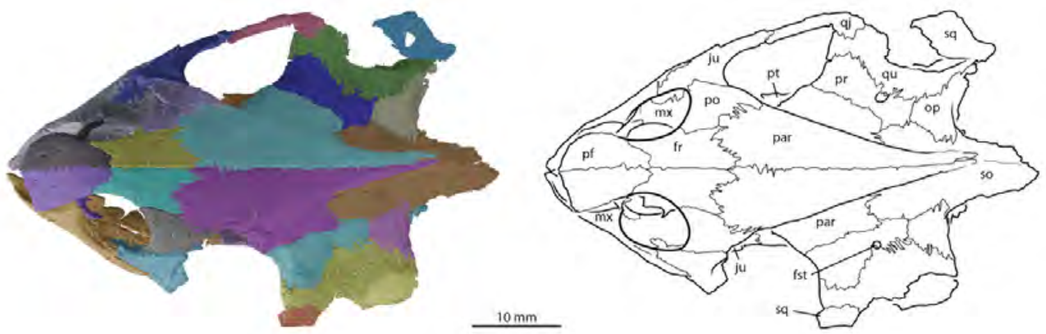

Figure 1. 3D model (left) and line drawing (right) of *Hutchemys rememdium* NDGS 10019 (left). Abbreviations: f: frontal; fst: foramen stapediotemporale; j: jugal; mx: maxillary; op: opisthotic; par: parietal; pf: prefrontal; po: postorbital; pr: prootic; pt: pterygoïd; q: quadrate; qj: quadratojugal; so: supraoccipital; sq: squamosal; v: vomer.

5.8
Feeding behaviour and diet in Devonian ctenacanth chondrichthyans using tooth wear and finite element analysis

Merle Greif[1*], Ivan Calandra[2], Stephan Lautenschlager[3], Thomas Kaiser[4], Christian Klug[1]

[1] *Department of Palaeontology, University of Zurich, Karl-Schmid-Strasse 4, 8006 Zurich, Switzerland (merle.greif@pim.uzh.ch)*
[2] *Imaging Platform at LEIZA (IMPALA), and Laboratory for Traceology and Controlled Experiments (TraCEr), MONREPOS Archaeological Research Centre, Leibniz-Zentrum für Archäologie, 56567 Neuwied, Germany*
[3] *School of Geography, Earth and Environmental Sciences, University of Birmingham, Edgbaston, Birmingham*
[4] *Centre for Taxonomy and Morphology, Leibniz Institute for the Analysis of Biodiversity Change (LIB), Martin-Luther-King-Platz 3, 20146 Hamburg*

Many modern sharks are known as dietary opportunists and their feeding behaviour and diet can be observed in many different ways. By contrast, the reconstruction of feeding behaviour and diet of their early ancestors is rather difficult. Direct evidence such as oesophagus, stomach or gut contents is scarce in early chondrichthyans (e.g. Kriwet et al., 2008; Chevrinais et al., 2017). Indirect evidence may be obtained from coprolites, tooth marks, tooth morphology or tooth wear (Weber et al. 2021). In many cases, only one of the latter is used to reconstruct feeding behaviour and diet. By combining Dental Microwear Texture Analyses (DMTA) and Finite Element Analysis (FEA), we use morphology as well as tooth wear of the cladodont teeth of the large Devonian chondrichthyan *Ctenacanthus concinnus* from Morocco in an attempt to reconstruct feeding behaviour and diet. These teeth show intense tooth wear as a result of a low tooth replacement rate (Williams, 2001; Botella et al., 2009). Additional information can be extracted from the fossil composition of the layer of origin. The Late Devonian *Gonioclymenia* limestone that yielded the teeth of *C. concinnus* is very rich in diverse species of ammonoids, other chondrichthyans and conodonts. Strikingly, with increasing chondrichthyan body size in the Devonian, also ammonoid body size increased and additionally they developed more complex sutures.
The combination of the results from all three approaches leads to a number of conclusions and assumptions. Most likely, *C.concinnus* was an opportunistic predator that was capable of crushing hard materials, puncturing and holding prey as well as cutting large prey using the sharp-edged main cusps of its teeth by shaking or spinning its head.

REFERENCES
Kriwet, J., Witzmann, F., Klug, S., & Heidtke, U. H. J. (2008). First direct evidence of a vertebrate three-level trophic chain in the fossil record. *Proceedings of the Royal Society B: Biological Sciences*, *275*(1631), 181–186.
Chevrinais, M., Jacquet, C., & Cloutier, R. (2017). Early establishment of vertebrate trophic interactions: Food web structure in Middle to Late Devonian fish assemblages with exceptional fossilization. *Bulletin of Geosciences*, *92*.
Weber, K., Winkler, D. E., Kaiser, T. M., Žigaitė, Ž., & Tütken, T. (2021). Dental microwear texture analysis on extant and extinct sharks: Ante- or post-mortem tooth wear? *Palaeogeography, Palaeoclimatology, Palaeoecology*, *562*, 110147.
Williams, M. E. (2001). Tooth Retention in Cladodont Sharks: With a Comparison between Primitive Grasping and Swallowing, and Modern Cutting and Gouging Feeding Mechanisms. *Journal of Vertebrate Paleontology*, *21*(2), 214–226.
Botella, H., Valenzuela-Ríos, J. I., & Martínez-Pérez, C. (2009). Tooth replacement rates in early chondrichthyans: A qualitative approach. *Lethaia*, *42*(3), 365–376

5.9
Early Ordovician phyllocarid crustaceans from the South Pole

Pierre Gueriau[1], Farid Saleh[1], Allison C. Daley[1]

[1] Institut des sciences de la Terre, Université de Lausanne, Geopolis, CH-1015 Lausanne (pierre.gueriau@hotmail.fr)

Phyllocarids are marine malacostracan crustaceans that possess a bivalved carapace covering the head, thorax and the anterior part of the abdomen, the latter ending in a telson generally bearing lateral caudal rami. They have extant relatives and an abundant and morphologically variable Palaeozoic fossil record (Rolfe 1969), which extends back to the late Cambrian (Collette and Hagadorn 2010). Phyllocarids diversified extensively during the 'Great Ordovician Biodiversification Event', participating significantly to the colonisation of midwater niches by arthropods, the construction of complex modern foodwebs, and also playing a crucial role in the 'Ordovician Plankton Revolution' (Vannier et al. 2003, Liu et al. 2022). In this contribution, we will present new Early Ordovician phyllocarids from the Tremadocian Fezouata Biota, Morocco (Van Roy et al. 2010), and from a newly discovered, exceptionally preserved upper Floian assemblage of southern Montagne Noire, France (Saleh et al. submitted). The particularity of these fossil assemblages is that they offer unique snapshots into high polar latitude ecosystems during the Ordovician, with Montagne Noire representing the closest Lagerstätte to the South Pole known for that period (Saleh et al. submitted). As such, more than just documenting taxa new to science that increase the known diversity of phyllocarids, these fossils also provide new insights into the early palaeogeographic distribution, dispersal and origin of the group.

REFERENCES

Collette, J.H., & Hagadorn, J.W., 2010: Three-dimensionally preserved arthropods from Cambrian Lagersta ̈tten of Quebec and Wisconsin. Journal of Paleontology, 84, 646-667.

Liu, Y.L., Fan, R.Y., Zong, R.W., & Gong, Y.M. 2022: The evolution and initial rise of pelagic caryocaridids in the Ordovician. Earth-Science Reviews, 231, 104097.

Rolfe, W.D.I. 1969: Phyllocarida, p. 296–331. In R. C. Moore (ed.), Treatise on Invertebrate Paleontology Part R, Arthropoda 4(1). Geological Society of America and University of Kansas Press, Lawrence.

Vannier, J., Racheboeuf, P.R., Brussa, E.D., Williams, M., Rushton, A.W., Servais, T., & Siveter, D.J., 2003: Cosmopolitan arthropod zooplankton in the Ordovician seas. Palaeogeography Palaeoclimatology Palaeoecology, 195, 173-191.

Van Roy, P., Orr, P.J., Botting, J.P., Muir, L.A., Vinther, J., Lefebvre, B., Hariri, K.E., & Briggs, D.E.G, 2010: Ordovician faunas of Burgess Shale type, Nature 465, 215-218.

5.10
A long-term perspective of the recovery from the end-Permian mass extinction

Michael Hautmann[1], Evelyn Friesenbichler[1], Hugo Bucher[1]

[1] *Paläontologisches Institut, University of Zurich, Karl-Schmid-Strasse 4, CH-8006 Zürich (michael.hautmann@pim.uzh.ch)*

Biotic recoveries from mass extinctions provide unique insights into macroecological and macroevolutionary processes at timescales that are not observable from studies of the Recent. However, most previous analyses of biotic recoveries have concentrated on their early phases and on the role of the inorganic environment for shaping ecological and evolutionary patterns. This presentation reviews the recovery from the greatest mass extinction in Earth history over a longer period of time, including the previously neglected main phase during the Middle Triassic. It is shown that a potential amelioration of the environmental conditions cannot explain sufficiently the rapid burst of diversity that is recorded for benthic marine ecosystems in the Middle Triassic (Fig. 1). Three main biological causes for this explosive diversification are identified: ecosystem engineering by reef-building and carbonate secreting organisms (Friesenbichler et al. 2021a, b), increase in the diversity and abundance of predators (Scheyer et al. 2014), and increasing intensity of interspecific competition (Hautmann et al. 2015). Acting in concert, these three factors led to a diversity-dependent increase in rates of diversification that resulted in a hyperbolic (rather than exponential) increase in diversity at the beginning of the Middle Triassic. It is suggested that the hyperbolic model is a better descriptor for most diversification events than the standard exponential model is, and that the biotic environment plays a much more important role in shaping large-scale diversity patterns than generally acknowledged.

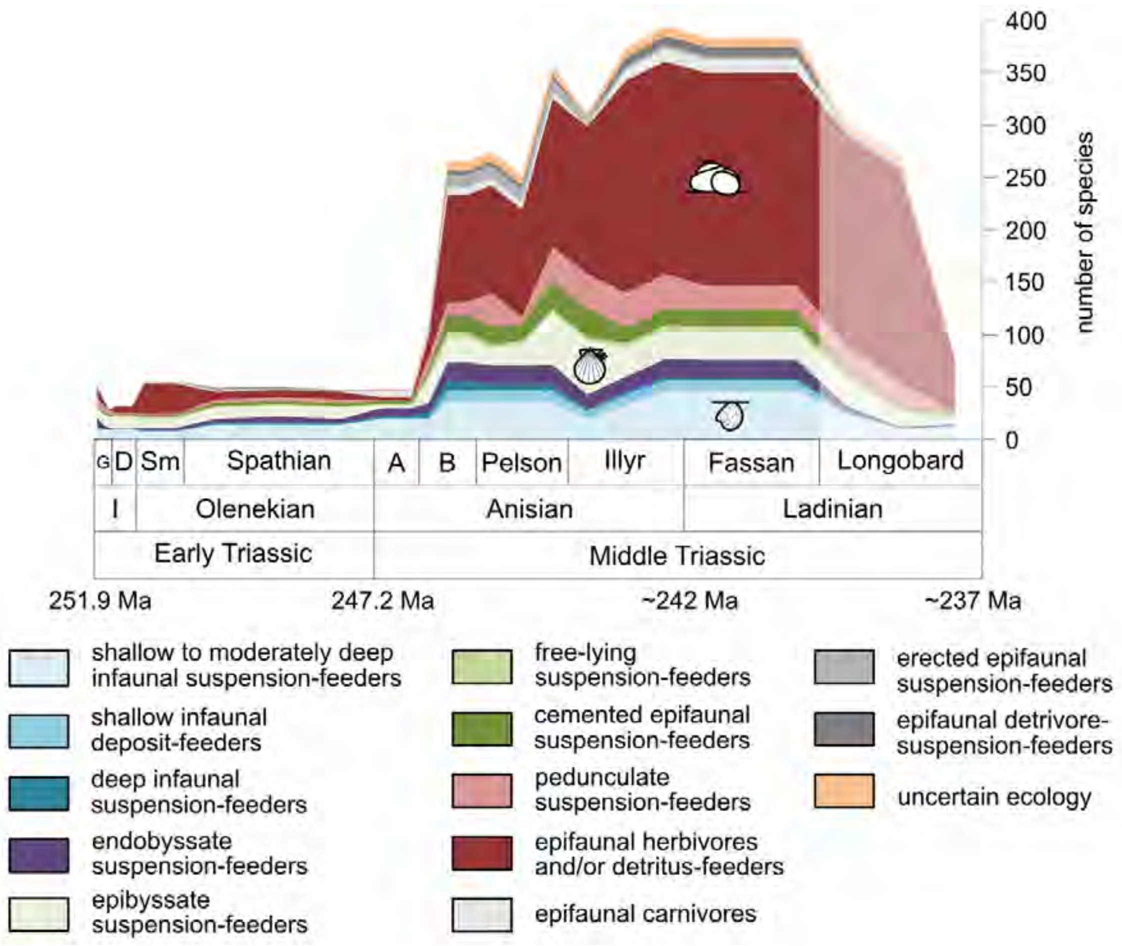

Figure 1. Maximum species richness for different guilds of benthic marine communities in the Early and Middle Triassic. From Friesenbichler et al. (2021b, fig. 1).

REFERENCES

Friesenbichler, E., Hautmann, M., Grădinaru, E., & Bucher, H. 2021a: A highly diverse bivalve fauna from a Bithynian (Anisian, Middle Triassic) Tubiphytes microbial buildup in North Dobrogea (Romania), Papers in Palaeontology, 7, 447-495. https://onlinelibrary.wiley.com/doi/full/10.1002/spp2.1286

Friesenbichler, E., Hautmann, M. & Bucher, H. 2021b: The main stage of recovery after the end-Permian mass extinction: taxonomic rediversification and ecologic reorganization of marine level-bottom communities during the Middle Triassic, PeerJ 9:e11654. http://doi.org/10.7717/peerj.11654

Hautmann, M., Bagherpour, B., Brosse, M., Frisk, Å., Hofmann, R., Baud, A., Nützel, A., Goudemand, N. & Bucher, H. 2015: Competition in slow motion: The unusual case of benthic marine communities in the wake of the end-Permian mass extinction, Palaeontology, 58, 871–901. https://onlinelibrary.wiley.com/doi/full/10.1111/pala.12186

Scheyer, T. M., Romano, C., Jenks, J., & Bucher, H. 2014: Early Triassic marine biotic recovery: the predators' perspective, PLoS One, 9(3), e88987. https://journals.plos.org/plosone/article?id=10.1371/journal.pone.0088987

5.11
A phylogenetic comparative approach to turtle shell ecomorphological patterns

Guilherme Hermanson[1], Laura Dziomber[2], Léa Girard[1], Walter G. Joyce[1], Christian Foth[1], Serjoscha W. Evers[1]

[1] *Department of Geosciences, University of Fribourg, Chemin du Musee 6, CH 1700 Fribourg (guilhermehermanson@gmail.com)*
[2] *Institute of Plant Sciences & Oeschger Centre for Climate Change Research, University of Bern, Hochschulstrasse 4*

Turtles are most noticeably characterized by the presence of the shell, a rigid osseous structure composed of the dorsal carapace and ventral plastron that encapsulate most of their body. Morphological variation of the shell is readily recognizable in the dimensions and aspect ratios of the carapace, relative plastron size, or shell decorations, all of which vary across distinct clades, but likely also ecologies (e.g., Claude et al. 2003; Stayton 2019). Habitat ecology has been hypothesized as the prevailing non-phylogenetic driver of turtle shell shape variation (e.g., Claude et al. 2003; Benson et al. 2011; Dziomber et al. 2020). However, other potential ecological or functional constraints on shell shape remain overlooked, such as an enlargement of the shell accommodating larger guts in herbivores (e.g., Bjorndal 1997), or self-righting ability (Stayton 2019). Previous research also attempted to use shell shape as a proxy to infer turtle palaeoecology (Benson et al. 2011; Dziomber et al. 2020), which is key to our understanding of ecological transitions throughout the evolutionary history of turtles. Some of these studies, however, did not or only incompletely account for phylogenetic autocorrelation of species data (Felsenstein 1985).

We expand a previously published 3D shape landmark dataset of turtle shells to include 155 extant turtle species (c. 50% of their species diversity) and eight fossils to characterize shell shape variation for turtles. Hereby, we use phylogenetic statistical comparative tools to assess the effects of size, ecology, as well as functional specializations on turtle shell shape variation. For the fossils (five stem-turtles, three extinct crown-turtles), we re-evaluate previous palaeoecology hypotheses. Additionally, we assess evolutionary rates of shell shape through time to understand how they vary across different clades and ecological groups.

We find that body size, habitat ecology, herbivory, and self-righting indices explain turtle shell shape variation, although phylogenetic relatedness also constrains shell morphospace. Evolutionary allometry shows that larger turtles have relatively small plastra, and longer, narrower and flatter carapaces than small turtles. Herbivores tend to exhibit taller carapaces than non-herbivorous taxa, irrespective of the habitat ecology. Increased self-righting indices also imply higher-domed carapaces, indicating that several ecological and functional traits linked to terrestriality influence shell doming. Highly aquatic turtles possess very streamlined carapaces, with broad nuchal regions, whereas more terrestrial turtles tend to increase shell height, especially in the mid-anterior region of the carapace, but mainly exhibit more developed plastra. We also detect rate heterogeneity across clades and ecologies. These show that stem-turtles had elevated evolutionary rates, whereas shell shape evolution decelerated by the time of the crown-group origin in the Jurassic.

Palaeoecological predictions for early testudinatans does not recover fully terrestrial habits unambiguously as the ancestral condition for shelled turtles. Instead, whereas the shell shape of the Triassic stem-turtle *Proterochersis robusta* support a terrestrial ecology for this taxon, *Proganochelys quenstedtii* exhibits an uncertain signal between terrestrial and generalized aquatic ecologies, partially contradicting depositional, osteohistological and forelimb anatomy data (Joyce & Gauthier 2004; Scheyer & Sander 2007). This may indicate high ecological plasticity at the dawn of shelled turtles, but could also indicate that the earliest Triassic stem-turtles were equipped with a mosaic of morphological traits that are now adaptations in extant terrestrial or aquatic forms.

REFERENCES

Benson, R.B.J., Domokos, G., Várkonyi, P.L. & Reisz, R.R. 2011. Shell geometry and habitat determination in extinct and extant turtles (Reptilia: Testudinata). Paleobiology, 37(4), 547-562.
Bjorndal, K.A. 1997. Fermentation in reptiles and amphibians. In: Gastrointestinal Microbiology. Volume 1: Gastrointestinal Ecosystems and Fermentations (Eds. Mackie, R.I. & White, B.A.), Chapman & Hall, New York, 199-230.
Dziomber, L, Joyce, W.G. & Foth, C. 2020. The ecomorphology of the shell of extant turtles and its applications for fossil turtles. PeerJ, 8, e10490.
Felsenstein, J. 1985. Phylogenies and the comparative method. The American Naturalist, 125(1), 1-15.
Joyce, W.G. & Gauthier, J.A. 2004. Palaeoecology of Triassic stem turtles sheds new light on turtle origins. Proceedings of the Royal Society of London. Series B: Biological Sciences, 271(1534), 1-5.
Scheyer, T.M. & Sander, P.M. 2007. Shell bone histology indicates terrestrial palaeoecology of basal turtles. Proceedings of the Royal Society B: Biological Sciences, 274(1620), 1885-1893.
Stayton, C.T. 2019. Performance in three shell functions predicts the phenotypic distribution of hard-shelled turtles. Evolution, 73(4), 720-734.

5.12
Extreme lower jaw elongation in an alien-looking placoderm from Morocco

Melina Jobbins[1], Martin Rücklin[2,3], Marcelo R. Sánchez Villagra[1], Hervé Lelièvre[4], Eileen Grogan[5], Piotr Szrek[6], Christian Klug[1]

[1] Palaeontological Institute and Museum, University of Zurich, Zurich, Switzerland (chklug@pim.uzh.ch)
[2] Naturalis Biodiversity Center, Leiden, The Netherlands
[3] University of Leiden, Leiden, The Netherlands
[4] St Guénolé Penmarch, France
[5] Saint Joseph's University, Philadelphia, Pennsylvania, USA
[6] Polish Geological Institute–National Research Institute, Warsaw, Poland

Placoderms are an equally diverse and enigmatic group of Devonian vertebrates, which gained fame for the fierce looking apex predator *Dunkleosteus* (Lehman 1956; Anderson & Westneat 2007; Rücklin et al. 2012) on the one side and, more importantly, for the evolution of jaws and teeth (Rücklin et al. 2012; Zhu et al. 2013, 2022) as well as the origin of life birth in vertebrates on the other side (Long et al. 2007). Excellently preserved placoderm fossils were discovered in, e.g., the Frasnian of Australia and Germany as well as the Famennian of Ohio and Morocco.

Morocco has vast outcrops of highly fossiliferous Devonian strata and hence, it is not surprising that new discoveries of Devonian 'fish' are published almost every year (e.g. Jobbins et al. 2022; Klug et al. 2023). Placoderms had a rather high diversity and disparity through time; their jaw form evolved in the course of the Devonian, showing adaptations to a range of diets and feeding strategies. Particularly in the Famennian, the giant *Dunkleosteus* had jaws of over 70 cm length that were built for shearing; the inferognathal of adult *Titanichthys* exceeded one meter and is adapted to filter feeding (Lehman 1956; Coatham et al. 2020).

Kulczycki was probably startled by the strange spine-like bone he discovered in the 1950s in the Polish Holy Cross Mountains. He correctly inferred its placoderm nature but described it as a spine. Accordingly, he introduced the new genus *Alienacanthus*, strange spine, for this form (Kulczycki 1957).

In the past decades, further specimens of *Alienacanthus* were discovered in Poland and in Morocco, i.e. on both sides of the former Palaeotethys ocean. These materials revealed that the presumed spine is actually a lower jaw of a placoderm, where the skull and upper jaw measure half the length of the lower jaw. We described the new materials, revised the taxon, analysed its phylogenetic position, assessed its possible ecology and discussed modularity of skull parts in this group (e.g. Jobbins et al. submitted).

REFERENCES

Anderson, P. S. L., & Westneat, M. W. 2007: Feeding mechanics and bite force modelling of the skull of *Dunkleosteus terrelli*, an ancient apex predator, Biology Letters, 3, 77–80.

Coatham, S. J., Vinther, J., Rayfield, E. J., & Klug, C. 2020: Was the Devonian placoderm Titanichthys a filter-feeder? Royal Society Open Science, 7: 200272, 1-10. http://dx.doi.org/10.1098/rsos.200272

Jobbins, M. E. M., Rücklin, M., Ferron, H. G., & Klug, C. 2022: A new selenosteid placoderm from the Late Devonian of the eastern Anti-Atlas (Morocco) with preserved body outline and its ecomorphology, Frontiers in Ecology and Evolution, 10:969158, 1-20. doi: 10.3389/fevo.2022.969158

Jobbins, M. E. M., Rücklin, M., Sánchez Villagra, M. R., Lelièvre, H., Grogan, E., Szrek, P., & Klug, C. submitted: Extreme lower jaw elongation in a 'placoderm' reflects high disparity and modularity in early vertebrate evolution Nature Communications.

Klug, C., Coates, M. I., Frey, L., Greif, M., Jobbins, M., Pohle, A., Lagnaoui, A., Bel Haouz, W., & Ginter, M. 2023: Broad snouted cladoselachian with sensory specialisation at the base of modern chondrichthyans, Swiss Journal of Palaeontology, 142, 1-28. https://doi.org/10.1186/s13358-023-00266-6

Kulczycki, J. 1957: Upper Devonian fishes from the Holy Cross Mountains (Poland), Acta Palaeontologica Polonica, 2(4), 285-380, 13 pls.

Lehman, J. P. 1956: Les Arthrodires du Dévonien supérieur du Tafilalt (Sud Marocain), Notes et Mémoires du Service Géologique du Maroc, 129, 1–70.

Long, J. A., & Trinajstic, K., & Johanson, Z. 2009: Devonian arthrodire embryos and the origin of internal fertilization in vertebrates, Nature, 457, 1124–1127. doi: 10.1038/nature07732

Rücklin, M., Donoghue, P. C. J., Johanson, Z., Trinajstic, K., Marone, F., Stampanoni, M. 2012: Development of teeth and jaws in the earliest jawed vertebrates, Nature, 491(7426), 748–51.

Zhu, M., Yu, X., Ahlberg, P. E., Choo, B., Lu, J., Qiao, T., Qu, Q., Zhao, W., Jia, L., Blom, H., & Zhu, Y. 2013: A Silurian placoderm with osteichthyan-like marginal jaw bones, Nature, 502(7470), 188–193. https://doi.org/10.1038/nature12617

Zhu, Y., Li, Q., Lu, J., Chen, Y., Wang, J., Gai, Z., Zhao, W., Wei, G., Yu, Y., Ahlberg, P. E., & Zhu, M. 2022: The oldest complete jawed vertebrates from the early Silurian of China, Nature, 609(7929), 954–958. https://doi.org/10.1038/s41586-022-05136-8

5.13
Age dependent extinction in modern sharks, rays and skates (Neoselachii)

Kristína Kocáková[1], Daniele Silvestro[2,3,4], Catalina Pimiento[1,5,6]

[1] *Department of Paleontology, University of Zurich, Karl-Schmid-Strasse 4, 8006 Zurich, Switzerland (kristina.kocakova@pim.uzh.ch)*
[2] *Department of Biology, University of Fribourg, Chem. du Musée 10, 1700 Fribourg, Switzerland*
[3] *Swiss Institute of Bioinformatics, Amphipôle, Quartier UNIL-Sorge, 1015 Lausanne, Switzerland*
[4] *Gothenburg Global Biodiversity Centre, Department of Biological and Environmental Sciences, University of Gothenburg, Carl Skottsbergs gata 22B, 413 19 Gothenburg, Sweden*
[5] *Department of Biosciences, Swansea University, Wallace Building, Singleton Park, Swansea SA2 8PP, United Kingdom*
[6] *Smithsonian Tropical Research Institute, Roosevelt Ave. Tupper Building – 401, Panama City 0843-03092, Panama*

Extinction is a selective process whereby some species are more prone to go extinct than others. It has been proposed that extinction selectivity can be determined by the age of a taxon (i.e. time elapsed since origination). Several studies have investigated this age-dependancy extinction, with some demostrating that age determines extinction in some lineages, while others have found no evidence for age-depenancy. However, our understanding of the role of age in extinction has been mainly based on marine invertebrates or terrestrial mammals, and on studies that have used high taxonomic ranks or narrow time periods. In this study, a novel neural network-based Age-Dependent Extinction model has been applied on an unprecedented collection of fossil occurrences of marine vertebrates identified to the species level. Specifically, we investigate the role of age in the extinction of neoselachians (modern extant sharks, rays and skates and their extinct relatives) over last 145 Myr. Our results suggest that throughout the entire timeframe explored in this study, extinction selectivity decreased with age, with younger species showing higher susceptibility to extinction than older species. Further exploration of the implications of these findings are still being carried out, however, our results overall shed light on a historically understudied aspect of extinction selectivity, opening new avenues for interpretation of the factors shaping neoselachian evolutionary history.

5.14
New paleontological insights on the armor and weaponery of the mammalian knight: from anatomy to paleorobotics.

Kévin Le Verger[1], Nicole Ramstein[1], Olivier Lonneux[2], Auke J. Ijspeert[2], Torsten M. Scheyer[1], Marcelo R. Sánchez-Villagra[1], Ardian Jusufi[1,3,4].

[1] *Department of Paleontology, University of Zurich, Karl-Schmid-Strasse 4, 8006 Zurich (kevin.leverger@pim.uzh.ch)*
[2] *Ecole Polytechnique Federale de Lausanne, Route Cantonale, 1015 Lausanne*
[3] *Locomotion in Biorobotic and Somatic Systems Group, Max Planck Institute for Intelligent Systems, Heisenbergstraße 3, 70569 Stuttgart*
[4] *Swiss Federal Laboratories for Materials Science and Technology, Ueberlandstrasse 129, 8600 Dübendorf*

The arms race is a central concept in biology, acting as a driving force behind synapomorphies and convergences. In most organisms, multiple anti-predator defense strategies can be defined (Kikuchi et al. 2023). Glyptodonts are the only known mammals that have evolved heavy armor and tail weaponry. While armor is an ancestral clade feature following a relatively stable general organization plan, tail weaponization followed a more complex evolutionary history (Fernicola & Porpino 2012). From an unarmed highly-armored tail to a spiked tail club, glyptodonts display a wide variety of tail anatomy, whose function remains highly debated. These herbivorous giants used these adaptations to defend themselves, however, the evolution of tail weaponry remains questioned between: (1) increasing protections against predators, notably due to synchronous acquisitions towards stronger armor/weaponry with the Great American Interchange; (2) intensified increase in intraspecific fighting; (3) or a subtle combination of these two factors. To preliminary investigate these three scenarios, we examined the anatomy of the four tail morphotypes of Pleistocene glyptodonts from the Santiago Roth Collection, housed at the Department of Palaeontology of the University of Zurich, in relation to body armor and size variation (Le Verger 2023), using eight morphological traits (Figure 1A). This approach enabled us to construct a spectrum from the most passive defense (*Glyptodon*), to the most active defense (*Doedicurus*). While in the first extreme, the anatomy of the tail functioned primarily to reinforce the armor, in the second, the weaponized tail anatomy alone does not allow to favor either hypothesis. We have therefore started to explore tail biomechanics in *Doedicurus*, using a combination of modeling and robotic approaches (Figure 1B). Preliminary investigations suggest a coordination of tail and body movements lead to notably higher impacts than tail movements alone, with a potentially high impact force (Figure 1C), in line with the suggestion of intraspecific combat in the literature (Alexander et al. 1999). Given the velocity of Pleistocene predators, the slow lifestyle of glyptodonts, and the potentially complex tail motion, we favor the hypothesis of an evolution toward tail weaponization for intraspecific fighting (2), although we cannot exclude its use against predators (1). The armor and weaponry are therefore probably the combined witnesses of a strong natural and sexual selection that brought glyptodonts to the pinnacle of mammalian protection until the late Pleistocene drastic climatic changes and their interaction with humans brought their history to the end (Carlini et al. 2022).

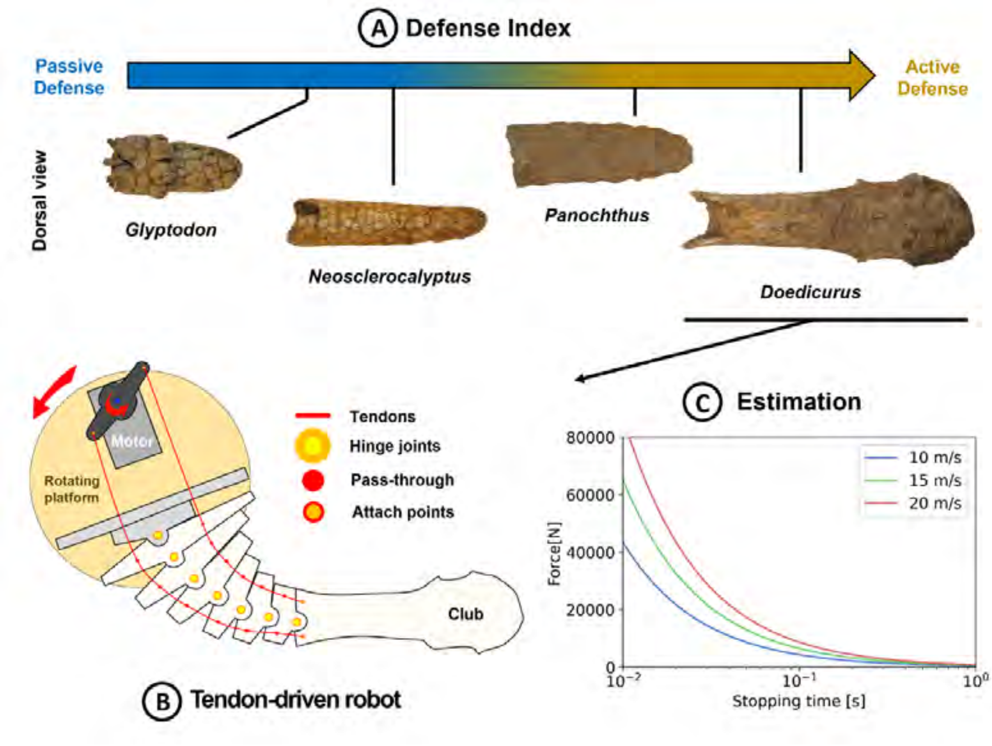

Figure 1. Schematic approach. First, we determined from the anatomy how the different glyptodont tails were distributed through a defense index (A). Then, we selected the glyptodont with the most active defense (= the most weaponized) in order to build a tendon-driven robot (B), from which we extracted the biomechanical components of interest for our hypotheses (C). Specimens are not to scale.

REFERENCES

Alexander, R. M., Fariña, R. A., & Vizcaíno, S. F. 1999: Tail blow energy and carapace fractures in a large glyptodont (Mammalia, Xenarthra), Zoological Journal of the Linnean Society 126, 41-49.

Carlini, A. A., Carrillo-Briceño, J. D., Jaimes, A., Aguilera, O., Zurita, A. E., Iriarte, J., & Sánchez-Villagra, M. R. 2022: Damaged glyptodontid skulls from Late Pleistocene sites of northwestern Venezuela: evidence of hunting by humans?, Swiss Journal of Palaeontology 141, 1-14.

Fernicola, J. C., & Porpino, K. D. O. 2012: Exoskeleton and systematics: a historical problem in the classification of glyptodonts, Journal of Mammalian Evolution 19, 171-183.

Kikuchi, D. W., Allen, W. L., ... & Exnerová, A. 2023: The evolution and ecology of multiple antipredator defences, Journal of Evolutionary Biology 36, 975-991.

Le Verger, K. 2023: Xenarthrans of the collection of Santiago Roth from the Pampean Region of Argentina (Pleistocene), in Zurich, Switzerland, Swiss Journal of Palaeontology 142, 1-39.

5.15
An exceptionally preserved ontogenetic series of horseshoe crabs from the Early Ordovician and the origin of chelicerates

Lorenzo Lustri[1], Pierre Gueriau[1], Farid Saleh[1], Jonathan B. Antcliffe[1], Harriet B. Drage[1], Sinéad Lynch[1], Gaëtan Potin[1], Nora Corthésy[1], Allison C. Daley[1]

[1] *Institut des sciences de la Terre, Université de Lausanne, Geopolis, CH-1015 Lausanne (lorenzo.lustri90@gmail.com; allison.daley@unil.ch)*

Horseshoe crabs (Xiphosurida) are a group of marine chelicerates (which also includes sea spiders, sea scorpions, spiders, mites and ticks), and are often considered as “living fossils” (Fisher 1984). The status as living fossils for the horseshoe crabs, as well as their origins and the origins of all chelicerates is still a matter of debate. Here, we describe the oldest juvenile and adult (Fig. 1B) representatives of Xiphosurida from the Early Ordovician Fezouata Biota (Morocco) (Van Roy et al. 2010) (Fig. 1A). An investigation of over 300 specimens allowed the recovery of unique anatomical features that were previously unknown in this group, including a prosoma bearing stalked eyes inserted dorsally and trilobitomorpha-like gills (Fig. 1C). Those features are proposed as potential homologies that support trilobite affinities for chelicerates; which contrasts with the hypothesis suggesting that trilobites are more closely related to crustaceans and insects (mandibulates). A phylogenetic analysis, using Bayesian methods, resolves the Fezouata Biota xiphosurid as the sister group of all other Xiphosurida and allows further comparative phylogenetic methods (PCMs) to analyze the evolution of development within the group. A morphometric analysis of 60 individuals was performed to assess the ontogenetic sequence. By including environmental data, a clear correlation between developmental growth patterns and the environment was found (Fig. 1D); allowing for a detailed comparison of the population dynamics of this new taxon with extant populations of Xiphosurida (Carmichael et al. 2003). Some of the intermediate and proximal depositional environments preserved in the Fezouata Shale may have acted as nursery habitats for this taxon. This study has taken a total evidence approach and finds novel anatomical, developmental, evolutionary, and ecological information concerning early xiphosurids. The weight of evidence provides a unique opportunity to reveal the origins of the chelicerate body plan and their deeper origins from Cambrian arthropods.

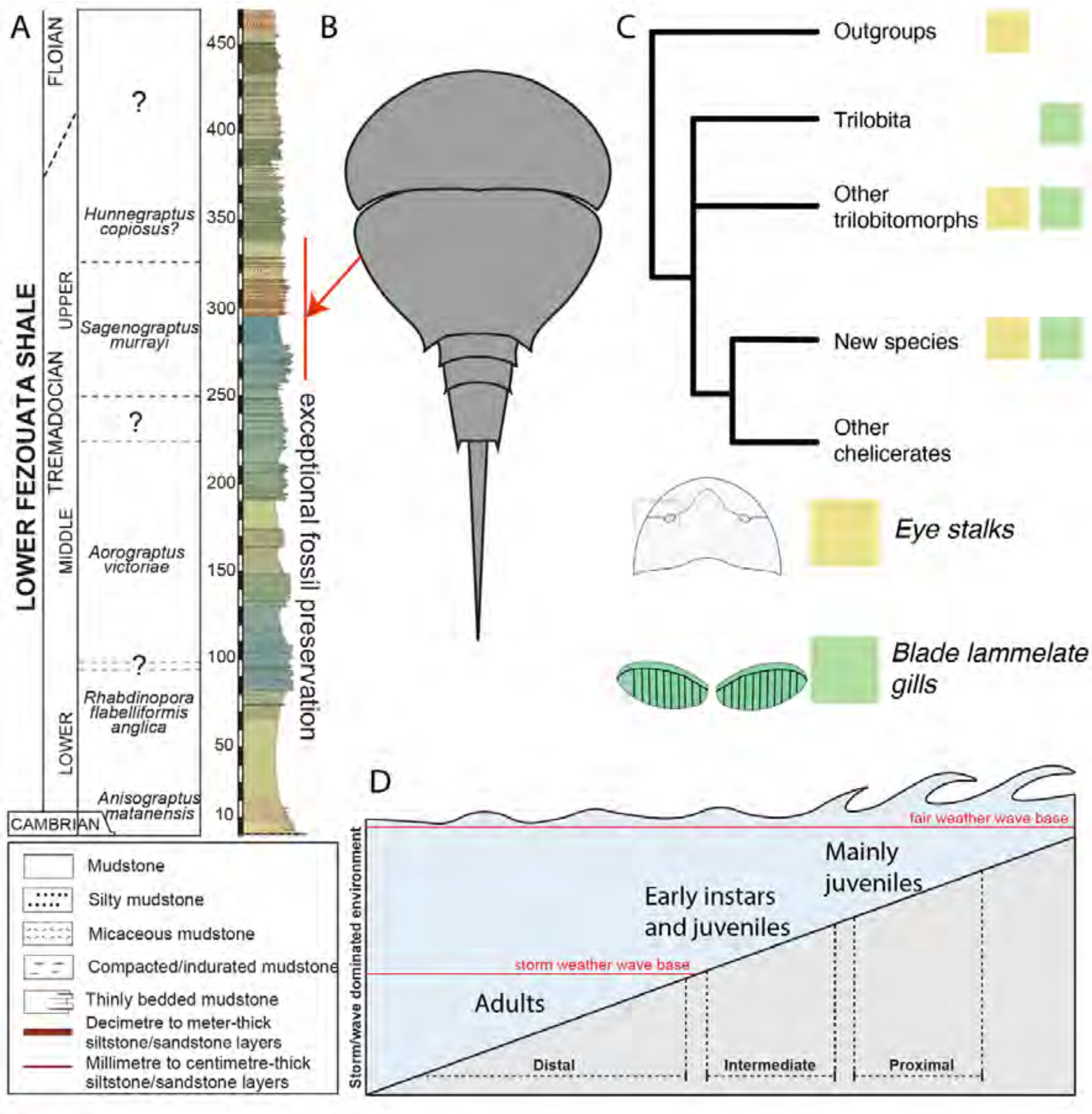

Figure 1. (A) Geological log of Fezouata Sahale showing zone of exceptional fossil preservation (modified from Saleh et al 2021); (B) schematic reconstruction of adult life stage of the new horseshoe crab taxon; (C) distribution of new anatomical characters with phylogenetic significance; (D) Fezouata Shale depositional environments and associated developmental stages of the new taxon (modified from Saleh et al 2021).

REFERENCES

Fisher, D.C., 1984: The Xiphosurida: archetypes of bradytely?. In Living fossils (pp. 196-213). New York, NY: Springer New York.

Van Roy, P., Orr, P.J., Botting, J.P., Muir, L.A., Vinther, J., Lefebvre, B., Hariri, K.E. and Briggs, D.E., 2010: Ordovician faunas of Burgess Shale type, Nature 465, 215-218.

Carmichael, R.H., Rutecki, D. and Valiela, I., 2003: Abundance and population structure of the Atlantic horseshoe crab Limulus polyphemus in Pleasant Bay, Cape Cod. Marine Ecology Progress Series, 246, pp.225-239.

Saleh, F., Vaucher, R., Antcliffe, J.B., Daley, A.C., El Hariri, K., Kouraiss, K., Lefebvre, B., Martin, E.L., Perrillat, J.P., Sansjofre, P. and Vidal, M., 2021: Insights into soft-part preservation from the Early Ordovician Fezouata Biota. Earth-Science Reviews, 213, p.103464.

5.16 Moulting and development in a freshwater prawn from the Late Cretaceous of Morocco

Sinéad Lynch[1], Pierre Gueriau[1], Harriet B. Drage[1], Didier B. Dutheil[2], Sylvain Charbonnier[2], Allison C. Daley[1]

[1] *Institute of Earth Sciences, University of Lausanne, Switzerland*
[2] *Centre de Recherche en Paléontologie, Sorbonne Université-MNHN-CNRS-Paris, France*

Cretapenaeus berberus Garassino, Pasini & Dutheil, 2006 is a freshwater prawn (Dendrobranchiata, Penaeidae) from the Upper Cretaceous (Cenomanian) Kem Kem Group of Morocco. *C. berberus* is the only known freshwater penaeid, among the uncommon freshwater-dwelling species in Dendrobranchiata (Garassino et al. 2006; Tavares & Martin 2010). A sample of ~100 specimens *C. berberus* enables us to analyse growth in this species.

Of the specimens of *C. berberus* examined, most are carcasses and few are moults. Moults can be recognized by their displaced cephalothorax, resulting from opening of an exuvial gape at the cephalothorax posterior to enable shedding of the old exoskeleton (Daley & Drage 2016). Exceptionally preserved muscles, found only in carcasses, provide additional evidence to distinguish moults from carcasses. Multispectral imaging and geochemical characterisation will be used to investigate further differences in carcass and moult composition.

Preliminary analysis shows a wide size range in the sample, with cephalothorax lengths measuring from ~2 to 23 mm. All moults are from fairly large specimens. Early larval stages appear to be absent, and the smallest specimens are either late larval or early juvenile stages. As in all decapods, no segments are added during post-larval growth. *C. berberus* provides Late Cretaceous evidence of typical modern decapod moulting mechanism and a unique case of dendrobranchiate growth in freshwater.

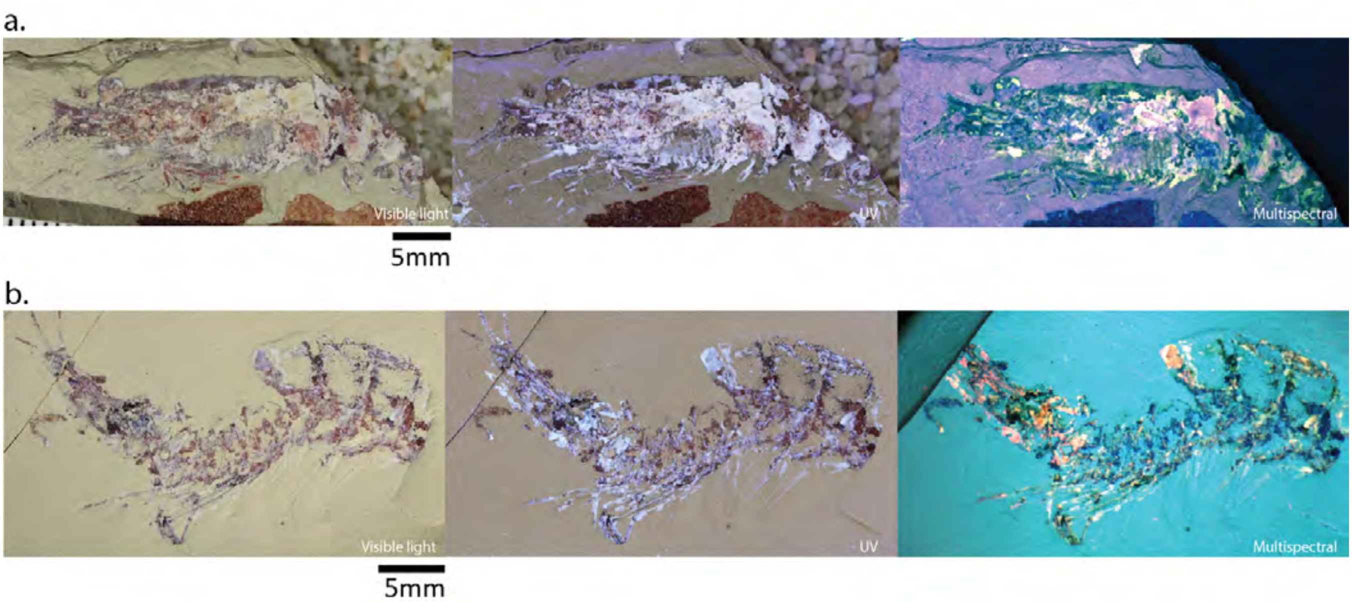

Figure 1. Examples of a carcass (a.) and moult (b.) of *C. berberus* in visible light (left); UV light (middle) and multispectral light (right).

REFERENCES

Daley, AC., & Drage, HB. 2016: The fossil record of ecdysis, and trends in the moulting behaviour of trilobites. Arthropod structure & development, 45(2), 71-96

Garassino, A., Pasini, G., & Dutheil, DB. 2006: *Cretapenaeus berberus* n. gen. n. sp. (Crustacea, Decapoda, Penaeidae) from the Late Cretaceous (Cenomanian) of southeastern Morocco, Atti della Società italiana di Scienza naturali e del Museo civico di Storia naturale, Milano, 147, 3–17

Tavares, C., & Martin, JW. 2010: Suborder Dendrobranchiata Bate, 1888, pp. 99-164. In Schram FR., & von Vaupel Klein JC. (eds.) Treatise on *Zoology-Anatomy, Taxonomy, Biology*. The Crustacea, 9A. Koninklijke Brill NV, Leiden, Netherlands.

5.17
New data on the Eocene-Oligocene mammalian turnover in south-eastern France: Red Queen or Court Jester, what evolutionary model for the "*Grande Coupure*"?

Olivier Maridet[1,2], Jérémy Tissier[1], Bastien Mennecart[3], Pauline Coster[4], Stéphane Legal[4], Loïc Costeur[3]

[1] *Jurassica Museum, Route de Fontenais 21, 2900 Porrentruy, Switzerland (olivier.maridet@jurassica.ch)*
[2] *Department of Geosciences, University of Fribourg, Chemin du Musée 6, CH-1700 Fribourg, Switzerland*
[3] *Natural History Museum Basel, Basel, Switzerland, Augustinergasse 2, CH-4001 Basel, Switzerland*
[4] *Réserve Naturelle Nationale Géologique du Luberon, Parc naturel régional du Luberon, 60 Place Jean Jaurès, F-84400 Apt, France*

About a century ago, in 1909, the paleontologist Hans Georg Stehlin described, based on the European mammalian fossil record, "the greatest and most sudden change known so far during the tertiary times". He underlined the correlation of this terrestrial faunal event with the Eocene/Oligocene boundary and named it "*Grande Coupure*". This event was characterized in Europe by the extinction of numerous endemic mammals immediately replaced by new immigrants of Asian origin. This apparently brutal replacement has led many authors to assume that biotic competition between endemic taxa and immigrants was the main driving factor of this major turnover. Such a scenario would fit the Red Queen evolutionary model (Van Valen 1973).

During the past seven years, new excavations in the Early Oligocene of Murs (Luberon, south-eastern France) have led to a much better knowledge of the regional mammalian fossil record following the "*Grande Coupure*". Altogether 21 mammal species were discovered from this locality making it one of the richest stratified locality in the early Oligocene of south-eastern France. The locality of Murs is of particular interest as it yielded numerous remains of *Plagiolophus huerzeleri,* the last representative of one of the few genera of endemic Palaeotheriidae that survived the "*Grande Coupure*" in Europe.
These new data from Murs associated with a compilation of other mammalian localities from the same region (71 taxa over 43 localities from the late Eocene to the mid Oligocene) allow a new and more detailed analysis of the Eocene-Oligocene transition in south-eastern France. Results show drastic turnovers of both generic and familial richness at the Eocene-Oligocene transition, involving taxonomic groups that cannot be in direct competition due to different ecological requirements. In contrast, species richness started to decrease before the arrival of immigrant taxa due to asynchronous appearances and disappearances. These observations indicate that appearances and disappearances are not correlated at species level thus suggesting a progressive shift of habitats from the late Eocene onward. This shift is driven by long-lasting climatic changes thus showing that abiotic interactions better explain the mammalian turnover than biotic ones alone. Such an evolutionary process better corresponds to the Court Jester model (Barnosky 1999; Benton 2009). In the future, similar analyses will be necessary in other regions to test if the evolutionary model observed in south-eastern France can be generalised for the "*Grande Coupure*" at the scale of the whole Europe.

REFERENCES

Barnosky A. 2001: Distinguishing the effects of The Red Queen and Court Jester on Miocene mammal evolution in the northern Rocky Mountains. Journal of Vertebrate Paleontology, 21(1), 172–185.

Benton M.J. 2009: The Red Queen and the Court Jester: Species diversity and the role of biotic and abiotic factors through Time. Science, 323, 728-732.

Van Valen L. 1973: A new evolutionary law. Evolutionary Theory, 1, 1–30.

5.18
Unraveling the role of temperature in Neoselachian extinction events

Gregor Mathes[1], Daniele Silvestro[2], Kristína Kocáková[1], Amanda Gardiner[1], Catalina Pimiento[1,3]

[1] *Department of Paleontology, University of Zurich, Karl-Schmid-Strasse 4 8001 Zurich, Switzerland (gregor.mathes@pim.uzh.ch)*
[2] *Department of Biology, University of Fribourg, Av. de l'Europe 20, 1700 Fribourg, Switzerland*
[3] *Department of Biosciences, Swansea University, Swansea, UK*
[4] *Smithsonian Tropical Research Institute, Panama*

Neoselachians (comprising modern sharks, rays, and skates) make up one of the most ecologically diverse marine vertebrate lineages in modern oceans. However, causes and mechanisms of extinction events during their long evolutionary history are poorly constrained. Following recent calls in Palaeontology for the application of causal inference approaches to the fossil record, we applied a Bayesian causal inference model within a structural equation modelling framework to a novel compilation of fossil neoselachian occurrences, aiming to move beyond documenting patterns towards processes of extinction. We show that the severity of extinction in neoselachians is strongly tied to global temperatures. Specifically, we found extinction risk to increase as global temperatures decrease, with extinction risk being 66% higher during hypothermals than during periods of substantial warming. This negative temperature-extinction relationship was consistent for 150 million years and across various temporal and taxonomic scales and can be linked to metabolic strategies of individual species. We additionally find that species highly susceptible to temperature changes in the geological past are less at risk of extinction in modern oceans based on the IUCN Red List. We therefore provide a particularly compelling example of unbiased extinction processes inferred from the fossil record that can be informative for modern conservation efforts.

5.19
A three-dimensionally preserved fossil stem cholonioid from the Campanian of Alberta, Canada, provides insights into the evolutionary origin of sea turtles

Juliette C. L. Menon[1], Donald B. Brinkman[2,3], Walter G. Joyce[1], Serjoscha W. Evers[1]

[1] Department of Geosciences, University of Fribourg, Chemin du Musée 6, CH-1700 Fribourg (juliette.menon@unifr.ch)
[2] Department of Preservation and Research, Royal Tyrrell Museum of Paleontology, Drumheller, Alberta, Canada
[3] Department of Biological Sciences, University of Alberta, Edmonton, Alberta, Canada

Early sea turtle (chelonioid) evolution is poorly understood, especially because of phylogenetic uncertainties regarding the earliest members of the lineage. Although late Early Cretaceous protostegids have repeatedly been placed as early stem sea turtles (Hirayama 1998; Evers & Benson, 2019), this is debated (e.g., Joyce 2007; Cadena & Parham 2015; Gentry et al., 2019). Molecular divergence time analyses place the origin of crown sea turtles somewhere between the second part of the Late Cretaceous and the early Paleogene (e.g., Joyce et al., 2013; Thomson et al. 2021). The earliest unambiguous stem sea turtles are toxochelyids, which consist of a range of taxa from the Late Cretaceous of North America (Zangler 1953; Nicholls 1988; Brinkman et al. 2006; Matzke 2009). However, most toxochelyid material is poorly preserved and severely crushed, prohibiting the acquisition of informative morphological data that could help elucidate phylogenetic relationships. Here, we provide a new description of the Campanian fossil turtle *Nichollsemys baieri* based on 3D models derived from high-resolution micro-computed tomography (CT) scanning. This fossil turtle is nearly perfectly preserved in three dimensions, showing details of the internal and external anatomy of the cranium and mandible. Systematic comparisons and phylogenetic analysis show that *Nichollsemys baieri* is a toxochelyid-grade stem sea turtle. Thus, *Nichollsemys baieri* is one of the best-preserved early sea turtle fossils and provides unique new insights into the early morphological evolution of the group. In addition, our systematic work shows that as many as five toxochelyids lived during the Campanian and that some crown sea turtles already existed during the Late Cretaceous. This suggests a Campanian diversification of stem sea turtles and potentially a relatively early origin of crown sea turtles around the same time, thus at the earlier end of the range of possibilities proposed by molecular divergence time estimates (Joyce et al., 2013; Thomson et al., 2021).

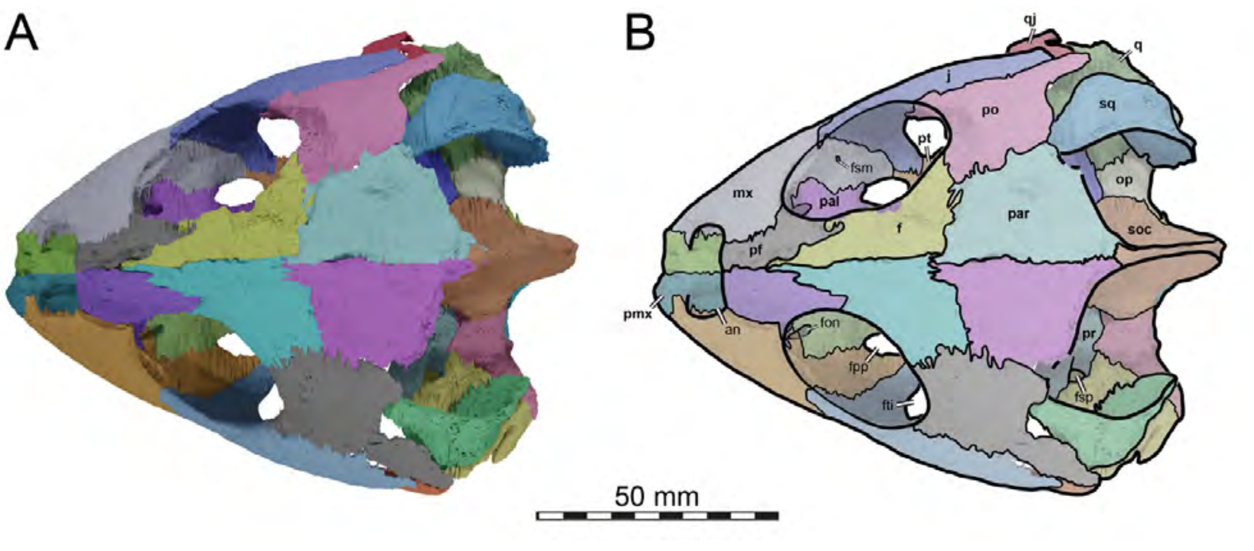

Figure 1. Three-dimensional renderings of the cranium of the holotype specimen of Nichollsemys baieri (TMP 97.99.01): A. dorsal view; B. interpretative diagram of the dorsal view. an. apertura naris; f. frontal; fon. foramen orbito-nasale; fpp. foramen palatinum posterius; fsm. foramen supramaxillare; fsp. foramen stapedio-temporale; fti. inferior temporal fossa; j. jugal; mx. maxillar; op. opisthotic; pal. palatine; par. parietal; pf. prefrontal; pmx. premaxillar; po. postorbital; pr. prootic; pt. pterygoid; qj. quadratojugal; q. quadrate; soc. supraoccipital; sq. squamosal; v. vomer.

REFERENCES

Brinkman, D., Hart, M., Jamniczky, H., & Colbert, M. 2006: Nichollsemys baieri gen. et sp. nov, a primitive chelonioid turtle from the late Campanian of North America, Paludicola, 5(4), 111-124.

Cadena, E. A., & Parham, J. F. 2015: Oldest known marine turtle? A new protostegid from the Lower Cretaceous of Colombia; PaleoBios, 32(1).

Evers, S. W., & Benson, R. B. 2019: A new phylogenetic hypothesis of turtles with implications for the timing and number of evolutionary transitions to marine lifestyles in the group, Palaeontology, 62(1), 93-134.
Gentry, A. D., Ebersole, J. A., & Kiernan, C. R. 2019: *Asmodochelys parhami*, a new fossil marine turtle from the Campanian Demopolis Chalk and the stratigraphic congruence of competing marine turtle phylogenies, Royal Society Open Science, 6(12), 191950.
Hirayama, R. 1998: *Mesodermochelys* (Testudines; Chelonioidea; Dermochelyidae) from the Late Cretaceous of Nakagawa-cho, Hokkaido, North Japan, Bulletin of the Nakagawa Museum of Natural History, 1, 69-76.
Joyce, W. G. 2007: Phylogenetic relationships of Mesozoic turtles, Bulletin of the Peabody Museum of Natural History, 48(1), 3-102.
Joyce, W. G., Parham, J. F., Lyson, T. R., Warnock, R. C., & Donoghue, P. C. 2013 : A divergence dating analysis of turtles using fossil calibrations: an example of best practices, Journal of Paleontology, 87(4), 612-634.
Matzke, A. T. 2009: Osteology of the skull of Toxochelys (Testudines, Chelonioidea), Palaeontographica Abteilung A, 93-150.
Nicholls, E. L. 1988: New material of Toxochelys latiremis Cope, and a revision of the genus Toxochelys (Testudines, Chelonioidea), Journal of Vertebrate Paleontology, 8(2), 181-187.
Thomson, R. C., Spinks, P. Q., & Shaffer, H. B. 2021: A global phylogeny of turtles reveals a burst of climate-associated diversification on continental margins, Proceedings of the National Academy of Sciences, 118(7), e2012215118.
Zangerl, R. 1953: The vertebrate fauna of the Selma Formation. Part IV. The turtles of the family Toxochelyidae, Fieldiana, Geology Memoirs, 3, 136-227.

5.20 Can species longevity predict extinction risk in the Anthropocene?

Catalina Pimiento[1,2,3], Kristína Kocáková[1], Gregor Mathes[1], Daniele Silvestro[4]

[1] *Department of Paleontology, University of Zurich, Karl-Schmid-Strasse 4 8001 Zurich, Switzerland (catalina.pimientohernandez@pim.uzh.ch)*
[2] *Department of Biosciences, Swansea University, Swansea, UK*
[3] *Smithsonian Tropical Research Institute, Panama*
[4] *Department of Biology, University of Fribourg, Av. de l'Europe 20, 1700 Fribourg, Switzerland*

Species are going extinct at an accelerated rate. Yet, some species are more prone to extinction than others. How this selectivity operates is crucial to address species loss because in its answer lies great predictive power. Existing conservation efforts are largely based on the IUCN Red List of Threatened Species, which categorizes species according to observed population declines. Even though these strategies can help diminish the severity of extinctions, they cannot prevent the decline of species too poorly known to be identified as threatened. The fossil record could aid conservation strategies by providing fundamental information on extinction selectivity and predictability. Palaeontological research has shown that the extent to which species are prone to extinction is largely linked to their intrinsic traits such as geographic range, body size, and thermoregulation. Another trait potentially related with extinction selectivity, but that has received less attention, is species' longevity (i.e., time from origination). Early studies have suggested species' longevity has no relation with extinction, whereas more recent works suggest that extinction rates are higher for short-lived species. Here, we assess the role of species' longevity in extinction susceptibility using the fossil record of extant elasmobranchs (sharks, rays and skates), a highly threatened clade today. Indeed, ~10% of living elasmobranchs have a fossil record that can go deep in geological time. We use a new comprehensive dataset of fossil occurrences and use a deep learning approach to test the extent to which species' longevity can be used to predict IUCN status. Our results have the potential to complement current conservation schemes, potentially allowing them to become more proactive.

5.21
Epibionts and trace fossils on arthropod carapaces from the Early Ordovician of Morocco

Jonathan Pople[1], Gaëtan J.-M. Potin[1], Allison C. Daley[1]

[1] *Institut des Sciences de la Terre, Université de Lausanne, Quartier UNIL-Mouline, Bâtiment Géopolis, CH-1015 Lausanne (jonathan.pople@unil.ch)*

The Early Ordovician Fezouata Shale is a Burgess Shale-type Lagerstätte providing a unique record of soft-bodied organisms during the transition from the Cambrian Explosion to the Ordovician Radiation (Van Roy et al. 2015a). Stem- and crown-group euarthropods are highly diverse in the Fezouata Shale and include several species of giant suspension-feeding radiodonts (Van Roy et al. 2015b; Potin et al. 2023). A survey of hundreds of specimens has revealed that arthropod carapaces, especially those of radiodonts, attracted sessile epifauna, the most abundant of which is an indeterminate brachiopod species (fig. 1) interpreted as an ectosymbiont of living giant nektonic radiodonts based on its exclusive association and implied long development. Less common epibiotic taxa include the conulariid *Eoconularia*, the brachiopod *Nanorthis*, and the tubular fossil *Sphenothallus*. Non-biomineralized arthropod carapaces from Fezouata are also associated with abundant burrows preserved as positive and negative relief structures (fig. 2). This feature is common in Cambrian-aged Burgess Shale-Type Lagerstätten but was considered to be generally absent from later strata (Mikuláš et al. 2012). Traces on carapaces from the Fezouata Shale are simple, shallow-tier structures that sometimes form dense assemblages, and are interpreted to represent the activity of small endofauna grazing on microbial mats growing on decaying carapaces. A preservational model for these traces is proposed, whereby bioturbation-driven deformation of lithification surfaces associated with carapaces is preserved by cementation and differential compaction. Traces from the Fezouata Shale are comparable to those in Cambrian assemblages (Mikuláš et al. 2012; Mángano et al. 2019), but reach much larger sizes, reflecting the increased size of substrate carapaces; complex trace morphologies are less abundant in Fezouata but may have been negatively affected by preservational biases.

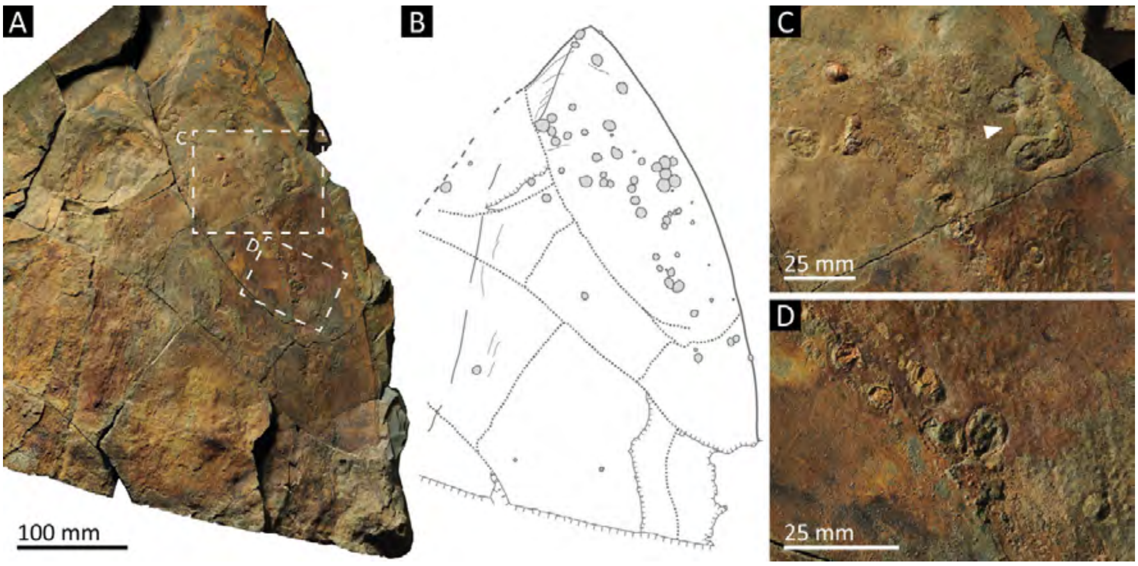

Figure 1. Giant radiodont carapace from the Fezouata Shale with abundant epibiotic brachiopods, MGL 108071-1. (A) Natural light photograph of the whole specimen. (B) Interpretative drawing; brachiopods shown with a light gray fill. (C-D) Closeups of (A); white arrow in (C) shows a brachiopod cluster.

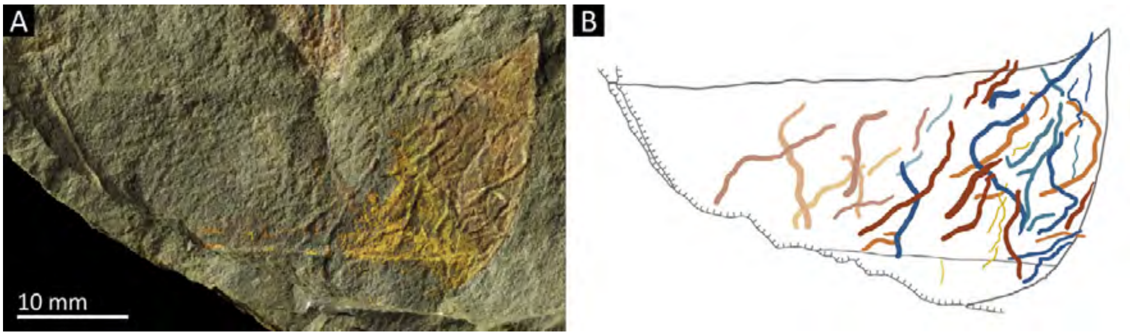

Figure 2. High density simple unbranched traces on the non-biomineralized carapace of a bivalved arthropod from the Fezouata Shale, MGL 104583. (A) Natural light photograph. (B) Interpretative drawing; warm colors represent positive relief bioturbations, cool colors represent negative relief bioturbations.

REFERENCES

Mángano, M. G., Hawkes, C. D., & Caron, J.-B. 2019: Trace fossils associated with Burgess Shale non-biomineralized carapaces: Bringing taphonomic and ecological controls into focus. Royal Society Open Science, 6, 172074. https://doi.org/10.1098/rsos.172074.

Mikuláš, R., Fatka, O., & Szabad, M. 2012: Paleoecologic Implications of Ichnofossils Associated with Slightly Skeletonized Body Fossils, Middle Cambrian of the Barrandian Area, Czech Republic. Ichnos, 19, 199-210. https://doi.org/10.1080/10420940.2012.703626.

Potin, G. J.-M., Gueriau, P., & Daley, A. C. 2023: Radiodont frontal appendages from the Fezouata Biota (Morocco) reveal high diversity and ecological adaptations to suspension-feeding during the Early Ordovician. Frontiers in Ecology and Evolution, 11, 1214109. https://doi.org/10.3389/fevo.2023.1214109

Van Roy, P., Briggs, D., & Gaines, R. 2015a: The Fezouata fossils of Morocco; an extraordinary record of marine life in the Early Ordovician. Journal of the Geological Society, 172, 541–549. https://doi.org/10.1144/jgs2015-017.

Van Roy, P., Daley, A. C., and Briggs, D. E. G. 2015b: Anomalocaridid trunk limb homology revealed by a giant filter-feeder with paired flaps. Nature 522, 77–80. https://doi.org/10.1038/nature14256.

5.22
Radiodont ecology and evolution: new oral cone data from the Fezouata Shale (Early Ordovician, Morocco)

Gaëtan J-M Potin[1], Pierre Gueriau[1], Allison C Daley[1]

[1] *Institute of Earth Sciences, University of Lausanne, Lausanne, Switzerland (gaetan.potin@unil.ch)*

Radiodonts are an emblematic group of the Cambrian Explosion, including apex predatory species such as the iconic *Anomalocaris canadensis* (Whiteaves 1892, Briggs 1989). In the Early Ordovician, abundant radiodont remains are found in the Fezouata Shale (Morocco). So far, 3 species have been described (Van Roy et al. 2015, Potin et al. 2023), to which we can add at least 3 other unpublished morphotypes. Those descriptions are based only on frontal appendages, the most commonly preserved part of the animal, however other anatomical parts can be preserved, such as the mouthpart (Potin & Daley 2023, Potin et al. 2023). The radiodont mouthpart, called oral cone, has a peculiar morphology because of the circular shape organized with typically 28 plates of different sizes around a central opening. Their rarity in the fossil record makes identifications difficult, in terms of taxonomy and feeding-strategy. Two almost complete but isolated radiodont oral cones have been found in the Fezouata Biota (Fig.1). The larger oral cone specimen shows a unique morphology of only 24 plates, in tetraradial arrangement and bearing prominent nodes on just two of the larger plates. There is also the smallest oral cone ever found in the fossil record so far, with a more typical 28 plates in tetraradial arrangement. Their combinations of features are unique and neither oral cone can be attributed to radiodont taxa known from appendages with any certainty. Multivariate statistics have been employed to identify the likely feeding mode of these oral cones, while their incorporation into phylogenetic trees reveals complexities associated with radiodont evolutionary relationships.

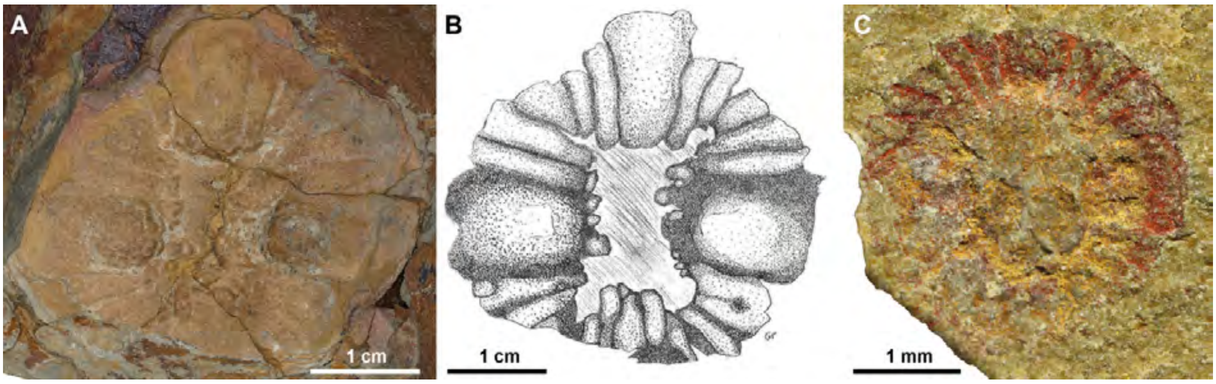

Figure 1. Radiodont oral cones from the Fezouata Shale Formation, *Sagenograptus murrayi* biozone, Morocco. (A/B) Almost complete specimen MGL 108045a, (A) picture with keyence macroimaging system under natural light, (B) *camera lucida* hand drawing. (C) YPM IP 517066, picture under polarized filter. Image credit: G. Potin.

REFERENCES

Briggs, D. E. G. (1979). Anomalocaris, the largest known Cambrian arthropod. Palaeontology 22 (3), 631–664.

Potin, G.J.-M., Gueriau, P., Daley, A.C. 2023. Radiodont frontal appendages from the Fezouata Biota (Morocco) reveal high diversity and ecological adaptations to suspension-feeding during the Early Ordovician. Frontiers in Ecology and Evolution, 11. doi: 10.3389/fevo.2023.1214109

Potin, G.J.-M., Daley, A.C. 2023. The significance of Anomalocaris and other Radiodonta for understanding paleoecology and evolution during the Cambrian Explosion. Frontiers in Earth Science, 11. doi: 10.3389/feart.2023.1160285

Van Roy, P., Daley, A. C., and Briggs, D. E. G. (2015b). Anomalocaridid trunk limb homology revealed by a giant filter-feeder with paired flaps. Nature 522 (7554), 77–80.doi: 10.1038/nature14256

Whiteaves, J. F. (1892). Description of a new genus and species of phyllocarid crustacea from the middle Cambrian of Mount Stephen, B.C. Can. Rec. Sci. V (4), 205–208.

5.23 A study of the carettochelyid turtle *Allaeochelys crassesculpta* from the Eocene (Early Lutetian) Messel Pit, Germany, using micro-computed laminography

Yann Rollot[1], Marcus Zuber[2, 3], Elias Hamann[2], Walter G. Joyce[1]

[1] *Department of Geosciences, University of Fribourg, Chemin du Musée 6, CH-1700 Fribourg (yann.rollot@unifr.ch)*
[2] *Institute for Photon Science and Synchrotron Radiation, Karlsruhe Institute of Technology, Hermann-von-Helmholtz-Platz 1, 76344 Eggenstein-Leopoldshafen, Germany*
[3] *Laboratory for Applications of Synchrotron Radiation, Karlsruhe Institute of Technology, Kaiserstrasse 12, 76131 Karlsruhe, Germany*

Carettochelyidae is a clade of aquatic, hidden-neck turtles, of which the pig-nosed turtle *Carettochelys insculpta*, which lives as a relict in New Guinea and Australia, is the only extant representative. The fossil record of this clade is relatively poor with only 14 valid species that range from the Early Cretaceous to the Miocene. The early evolutionary history of the clade, which is inferred to have taken place during the Middle to Late Jurassic, is still a mystery. One of the most emblematic fossil turtles ever found is the carettochelyid *Allaeochelys crassesculpta* from the Eocene Messel Pit of Germany. This taxon is not only remarkable because of the extraordinary richness of material recovered, but also because it represents the first record of fossilized copulating tetrapods. Despite the uniqueness of this turtle, most aspects of its anatomy remain poorly known, as only preliminary descriptions were provided more than 100 years ago.
As *Allaeochelys crassesculpta* is the only carettochelyid turtle for which the entire anatomy is preserved in the fossil record, the description of the available material is a crucial step towards a better understanding of carettochelyid anatomy and evolution. Two issues that affects these remains is their crushing and their preservation in epoxy resin plates, which prevents full-body, three-dimensional descriptions using standard x-ray computed tomography. Here, we use x-ray computed laminography to scan a selection of complete fossils, with a specific focus on skulls, forelimbs, and hindlimbs, and then document the anatomy of *Allaeochelys crassesculpta* in detail for the first time. Preliminary descriptive insights and 3D imaging results are presented herein.

5.24
The Cabrières Biota (France) provides insights into Ordovician polar ecosystems

Farid Saleh[1*], Lorenzo Lustri[1], Pierre Gueriau[1,2], Gaëtan J.-M. Potin[1], Francesc Pérez-Peris[1,3], Lukáš Laibl[4,5], Valentin Jamart[1], Antoine Vite[1,6], Jonathan B. Antcliffe[1], Allison C. Daley[1], Martina Nohejlová[7], Christophe Dupichaud[6], Sebastian Schöder[8], Emilie Bérard[8], Sinéad Lynch[1], Harriet B. Drage[1], Romain Vaucher[1,9], Muriel Vidal[10], Eric Monceret[11], Sylvie Monceret[11], and Bertrand Lefebvre[6]

[1]*Institute of Earth Sciences, University of Lausanne, Géopolis, CH-1015, Lausanne, Switzerland*
[2]*Université Paris-Saclay, CNRS, ministère de la Culture, UVSQ, MNHN, Institut photonique d'analyse non-destructive européen des matériaux anciens, 91192, Saint-Aubin, France*
[3]*Department of Earth and Environmental Sciences, 115 Trowbridge Hall, University of Iowa, Iowa City, Iowa, 52242, USA*
[4]*Czech Academy of Sciences, Institute of Geology, Rozvojová 269, 165 00 Prague 6, Czech Republic*
[5]*Institute of Geology and Palaeontology, Faculty of Science, Charles University, Albertov 6, Prague, 12843, Czech Republic*
[6]*Université de Lyon, Université Claude Bernard Lyon 1, École Normale Supérieure de Lyon, CNRS, UMR5276, LGL-TPE, Villeurbanne, France*
[7]*Czech Geological Survey, Prague 11821, Czech Republic*
[8]*Synchrotron SOLEIL, L'Orme des merisiers, 91192, Gif-sur-Yvette, France*
[9]*Department of Earth Sciences, University of Geneva, Geneva, Switzerland*
[10]*Univ Brest, CNRS, Ifremer, Geo-Ocean, UMR 6538, Place Nicolas Copernic, F-29280, Plouzané, France*
[11]*Independent*

*corresponding author (farid.nassim.saleh@gmail.com)

Early Palaeozoic sites with exceptional fossil preservation are predominantly found in Cambrian rocks and tend to capture past tropical and temperate ecosystems. In this study, we describe the diversity and preservation of the Cabrières Biota, a newly discovered Early Ordovician Konservat-Lagerstätte from Montagne Noire, southern France. The Cabrières Biota showcases a diverse polar assemblage of both biomineralised and exceptionally preserved soft-bodied organisms predominantly preserved in iron oxides. Echinoderms are extremely scarce, while sponges and algae are abundantly represented. Non-biomineralised arthropod fragments are also preserved, along with elements reminiscent of Cambrian Burgess Shale-type ecosystems, such as armoured lobopodians. The taxonomic diversity observed in the Cabrières Biota mixes Early Ordovician Lagerstätten taxa with Cambrian forms. The Cabrières Biota, being the closest Konservat-Lagerstätte to the Ordovician South Pole, likely served as a biotic refuge amid the high-water temperatures of the Early Ordovician, and shows comparable ecological structuring to modern polar communities.

5.25
Late Triassic palynomorphs from the Belchentunnel

Elke Schneebeli-Hermann[1], Evelyn Kustatscher[2,3,4],

[1] *Department of Paleontology, University of Zurich, Karl Schmid-Strasse 4, 8006 Zurich, Switzerland (elke.schneebeli@pim.uzh.ch)*
[2] *Museum of Nature South Tyrol, Bindergasse/Via Bottai 1, 39100 Bozen/Bolzano, Italy*
[3] *Department für Geo- und Umweltwissenschaften, Paläontologie und Geobiologie, Ludwig-Maximilians-Universität, Richard-Wagner-Straße 10, 80333 München, Germany*
[4] *Bayerische Staatssammlung für Paläontologie und Geobiologie, Richard-Wagner-Straße 10, 80333 München, Germany*

More than fifty years ago Bernhard Scheuring studied Late Triassic palynomorphs in samples collected during the construction of the first Belchentunnel (Scheuring, 1970). Modern studies on Carnian (Late Triassic) palynomorphs are rare in Switzerland, despite sediments include one of the important plant fossil localities, Neue Welt near Basel. Here, we present the results of the re-study of the famous Belchentunnel samples that Bernhard Scheuring studied and published in 1970. The most concerning result is the state of preservation of slides: more than 60% of the slides are degraded. On the other hand, well-preserved slides showed an unexpected number of algae, acritarchs, and spore taxa not described so far (Schneebeli-Hermann & Kustatscher, 2023). Spores give further insight into vegetation composition and allow for the correlation with biostratigraphic schemes established for the Germanic Basin. Especially the significance of the distribution of the spore *Porcellispora longdonensis* for facies interpretation increases as it might suggest the presence of ephemeral ponds. Its distribution throughout the Belchentunnel succession culminates in an acme just below the Schilfsandstein.

REFERENCES

Scheuring, B.W. 1970: Palynologische und palynostratigraphische Untersuchungen des Keupers im Bölchentunnel (Solothurner Jura). Schweizerische Paläontologische Abhandlungen 88, 1-119.

Schneebeli-Hermann, E., & Kustatscher, E. 2023: Triassic palynology of the Swiss Belchentunnel : a restudy of the Scheuring samples. Swiss Journal of Palaeontology, 2. https://doi.org/10.1186/s13358-023-00278-2

5.26
Late Jurassic sauropod trackway comparisons - examples from The Purgatoire Valley (USA) and Jura (Switzerland) tracksites

L. Sciscio[1, 2*], C. A. Meyer[3], M. Belvedere[4]

[1] *Jurassica Museum, Rte de Fontenais 21, 2900, Porrentruy, Switzerland (lara.sciscio@jurassica.ch)*
[2] *Department of Geosciences, University Fribourg, Chemin du Musée 6, 1700, Fribourg, Switzerland*
[3] *Department of Environmental Sciences, University of Basel, Bernoullistrasse 32, CH-4056, Basel, Switzerland*
[4] *Dipartimento di Scienze della Terra, Università di Firenze, Via G. La Pira 4, 50121 Firenze, Italy*

Late Jurassic track sites often share similar ichnofaunas dominated by sauropod and theropod trackmakers. This study delves into two geographically distinct Late Jurassic tracksites that exhibit comparable ichnofauna and proposed ichnotaxa. The research takes a comprehensive approach by analyzing sauropod tracks and trackways from two specific sites: Purgatoire Valley (Lower Morrison Formation; Colorado, U.S.A) and the Jura Mountains (Reuchenette Formation; Canton Jura, NW Switzerland). Notably, recent fieldwork at the Purgatoire tracksite, involving advanced techniques like photogrammetry and sedimentological analyses, has enabled a fresh evaluation of the *Parabrontopodus mcintoshi* holotype track surface, along with an extensive *in situ* examination of the paratype of *Parabrontopodus*. Through descriptive and quantitative analyses of trackway data collected from both sites, along with the application of statistical methods, the study uncovers potential differences between the reported ichnotaxa at these locations. Additionally, factors such as the movement of the trackmakers and the properties of the substrate they traversed are considered to shed light on potential morphological disparities. Of particular focus is the ichnogenus *Parabrontopodus*, which holds significance in the ichnotaxonomy of Late Jurassic sauropods. While many trackways from the Jura are informally described as cf. Parabrontopodus, only a limited number have undergone rigorous examination. Our research not only highlights morphological resemblances among cf. *Parabrontopodus* tracks and trackways but also underscores statistical distinctions in the ichnofauna between the different sites. Our preliminary findings underscore the intricate nature of sauropod ichnotaxonomy, especially when foot morphology appears similar despite variations in overall trackway attributes. Such differences could potentially be attributed to factors like the age and locomotion abilities of the trackmaker, its behavior, and even abiotic elements such as the substrate and surrounding environment.

5.27
Selective extinction of cephalopods at the K-Pg mass extinction event

Amane Tajika[1,2,3], Neil H. Landman[2], J. Kirk Cochran[2,4], Kozue Nishida[5], Toyoho Ishimura[6], Kotaro Shirai[7], Christian Klug[1]

[1] *Paleontological Institute, University of Zurich, Zurich, Switzerland, CH-8001 Zurich (atajika@amnh.org)*
[2] *Division of Paleontology, American Museum of Natural History, Central Park West 200, NY 10024, USA*
[3] *University Museum, University of Tokyo, Hongo 7-3-1, 113-0033 Tokyo, Japan*
[4] *School of Marine and Atmospheric Sciences, Stony Brook University, NY 11790, Stony Brook, USA,*
[5] *Graduate School of Life and Environmental Sciences, University of Tsukuba,Tenno-dai 1, 305-0006 Tsukuba, Ibaraki, Japan*
[6] *Graduate School of Human and Environmental Studies, Kyoto University, Yoshida Nihonmatsu-cho, Sakyo-ku, Kyoto 606-8316, Japan*
[7] *Atmosphere and Ocean Research Institute, University of Tokyo, Chiba 277-8564, Japan*

Understanding the mechanism of selective extinction is of utmost importance to predict the impact of current anthropogenic environmental changes on the ecosystem. The Cretaceous-Paleogene (K-Pg) mass extinction event has attracted the attention of both the general public and researchers due to its selective nature. In the marine realm, ammonoids and nautiloids, both of which possessed an external shell, are an iconic example of selective extinction: although ammonoids were more diverse and much more abundant than nautiloids during the Late Cretaceous, the former became extinct. The mechanism of the selective extinction of externally shelled cephalopods at the K-Pg mass extinction is still debated. In this study, we test the hypothesis that nautiloids possessed a metabolic rate lower than ammonoids, which resulted in selective extinction.

We used a new metabolic proxy—the fraction of metabolic carbon in the stable carbon isotopic ratio of the shell (C_{meta}). Results reveal significant differences in Cmeta among different modern cephalopod taxa (nautilids [*Nautilus* spp.], internally shelled coleoids [*Sepia officinalis*, *Spirula spirula*], gladius-bearing coleoids [*Dosidicus gigas*], and octopod with eggcase [*Argonauta argo*]). This is consistent with our knowledge about their metabolic rate estimated from oxygen consumption. When comparing extinct cephalopods, the nautilid *Eutrephoceras*, which survived the K-Pg mass extinction event, possessed a lower metabolic rate than all examined Maastrichtian ammonoids.

We conclude that the difference in metabolic rate was one of the contributing factors to the extinction selectivity in cephalopods at the K-Pg boundary; the lower metabolic rate in nautiloids was an advantage during a time of environmental perturbation (surface water acidification and resulting decrease in plankton) following the asteroid impact.

REFERENCE

Tajika, A., Landman NH., Cochran JK., Nishida, K., Shirai, K., Ishimura, T., Murakami-Sugihara N., & Sato, K. 2023: Ammonoid extinction and nautiloid survival: Is metabolism responsible? Geology, 51(7), 621-625.

5.28
From Fossils to Food Webs: Reconstructing the trophic networks of the Middle Triassic Monte San Giorgio fossil Lagerstätte (Middle Triassic, Switzerland/Italy)

Alexandre Torchet[1], Jack Shaw[2], Torsten Scheyer[1]

[1] *Paläontologisches Institut und Museum, Universität Zürich, 8006 Zürich, Switzerland*
[2] *Department of Geology and Geophysics, Yale University, CT 06520 New Haven, United States of America*

Since its discovery, the Monte San Giorgio (MSG) lagerstätte near Meride (Canton Ticino, Switzerland) has revealed an abundance of exceptionally preserved fossils, offering a unique window into the ecology of marine fauna after the recovery from the End-Permian Mass Extinction Event. While distinct changes in faunal composition have been identified over the 3-million-year span of the MSG environment, there has never been a detailed study on the network of trophic interactions among the organisms of the MSG faunas. In this study, we present the most complete paleoecological analysis to date on the MSG Lagerstätte by reconstructing the trophic networks of the fossil assemblages from the MSG Lagerstätte.

To assemble the most complete database on MSG fossils, we documented every fossil species with a set of ecological parameters. Our study focused on three fossil assemblages: the Middle Besano, Upper Besano, and Cava inferiore. The trophic networks of those successive faunas were reconstructed by using the R package Paleo Food Web Inference Model (PFIM), a new R package designed for such reconstructions.

This approach revealed for the first time a visualisation of a food web from a Middle Triassic marine fauna, as well as a quantification of the trophic level of each and every species in the food web based on their corresponding set of ecological parameters.

Our results have significant implication for the understanding of extinct ecosystem complexities and organizations, and how these evolve through deep time. By adding a new element to the growing list of fossil faunas studied for trophic network reconstruction, we open up new research opportunities for understanding the intricacies of ancient food webs. Moreover, our study marks a new benchmark for the paleoecology of the MSG Lagerstätte.

5.29
The life in the isolation: Serravalian-Tortonian (Middle – Late Miocene) marine vertebrate fauna of Karagie, Kazakhstan, Eastern Paratethys

Davit Vasilyan[1,2], Pavel Goldin[3], Sergei Lazarev[1,2]

[1] *Jurassica Museum, Route de Fontenais 21, CH-2900 Porrentruy (davit.vasilyan@jurassica.ch)*
[2] *University of Fribourg, Chemin du Musée 5, CH-1700 Fribourg*
[3] *Schmalhausen Institute of Zoology, Bogdana Khmelnytskogo 15, UA-01054, Kyiv*

The Paratethys Sea has been formed during Eocene-Oligocene times as a result of the isolation of the northern part of the former Tethys Ocean by landmasses forming present-day mountainous chains from the Alps, Balkans, Anatolia, to Zagros and Tien-Shan mountains. During its largest extension, the Paratethys covered vast territories, from present-day Eastern France to Western China. Active orogeny caused a gradual break-up of the sea and resulted formation of three “subbasins”. Among them, the Eastern Paratethys was the largest, which stretched from modern-day Romania to Kazakhstan. Progressive Alpine-Hymalian orogeny increased the uplift and formation of larger landmasses, between which the basin was connected to the global ocean via gateways. During the Miocene, most of these gateways have been unreversably closed and the basin experienced an isolated evolution from the global ocean. Undergoing an endorheic phase of its history between 12.6-6.1 Ma, the base level of the basin was controlled by, i.e. became extremely sensitive to the climatic fluctuations.

Having been connected to the global ocean, the Easter Paratethys was populated by fish and mammalian species known from other regions outside of Paratethys. However, at 12.6 Ma when it became hydrologicaly isolated from the global ocean, the fauna underwent a remarkable evolution. From this point on, a local (endemic) fauna of marine vertebrates (fishes, whales, dolphins, seals etc.) evolved. Many forms show a number of peculiar adaptations most probably developed as a result of the changes in the water chemistry.

In the present work, we have studied the fish and marine mammalian remains from the Karagie section, western Kazakhstan, which represents the most eastern part of the Eastern Paratethyan Basin. The section has a well-constrained age model using several methods such as magnetostratigraphy and biostratigraphy of foraminifera, ostracods, mollusks etc. Karagie section covers time period from 13.2 Ma to 7.5 Ma. Our preliminary data analysis suggests fully marine conditions during the Konkian (13.2-13 Ma), where sharks, whales (an undescribed taxon, possibly related to cf. *Imerocetus* sp. from the southern Caucasus), dolphins (?Eurhinodelphidae), marine teleost fishes (Sciaenidae indet., ?Sparidae indet., Perciformes indet.) have been found. Among fishes, forms of very large sizes (over 2 meter large) are found. During the Volhynian (12.4-12 Ma Ma), the basin became isolated together with its sister basin Central Paratethys from the global ocean. We could identify a large number of similar taxa across both basins, which include marine teleost fish (sciaenids), dolphin (*Kentriodon fuchsii, Sophianacetus commenticius,* cf. *Imerodelphis thabagarii,* Kentriodontidae indet., *Pachyacanthus suessi*), whale (*Otradnocetus virodovi*, Cetotheriidae indet.) and seal (*Praepusa*) taxa. The marine mammal fauna of the Konkian and Volhynian shows most similarities to that of the Eastern Paratethys of Caucasus but also has common elements with the Vienna basin and other Paratethyan areas. The following Bessarabian time (11.9-9.8 Ma), we could detect (during early Bessarabian 11.9-~10 Ma) a fauna of seals (*Praepusa* sp., *?Pachyphoca* sp.), dolphins (*Kentriodon fuchsii*) and few whales (all of family Cetotheriidae, including an undescribed taxon). Here the fishes are represented by rather rare finds of at least three groups (Sciaenidae indet., Sparidae indet and an unknown Teleostei). An unknown Teleostei shows so far not known bone hyperossification. From the second half of the Bessarabian (10 Ma) until the top of the studied section (Maeotian, 7.5 Ma), no macroremains of marine vertebrates have been found. This period coincides with the onset of numerous base level drops, which most probably caused the extinction of many marine vertebrates in the basin or at least in this part of the basin.

As a next step of the studies, we aim to compare the rich microremain record of fishes, represented by otoliths, with the record of the skeletal elements. It will allow to complement the fish record and obtain a better picture of the ichthyofauna.

FUNDING: The study has been supported by the Swiss National Science Foundation project Nr. 200021_197323.

5.30
Cambrian *Gaoloufangchaeta* was the earliest known pelagic annelid

Xiaoyu Yang[1,2], M. Teresa Aguado[2], Conrad Helm[2], Zhiqian Zhang[3], Alexander R. Schmidt[4], Christoph Bleidorn[2]

[1] *Yunnan Key Laboratory for Palaeobiology, Institute of Palaeontology, Yunnan University, Waihuan South Road, 650500 Kunming (xyyang0917@gmail.com)*
[2] *Animal evolution and Biodiversity, Georg-August-Universität Göttingen, Untere Karspüle 2, 37073 Göttingen*
[3] *School of Fine Arts, Yunnan Normal University, Juxian Street 768, 650500 Kunming*
[4] *Department of Geobiology, Georg-August-Universität Göttingen, Goldschmidtstraße 3, 37077 Göttingen*

Annelida is a phylum of segmented worms with around 20,000 described recent species showing a great diversity of morphology and lifestyles (Capa & Hutchings 2021). Molecular clock estimates reveal the origin of Annelida back to the Ediacaran period (Erwin 2020), which is in discordance with the first appearance of this clade in the early Cambrian evidenced by the fossil records of stem-group and basally branching annelids (Parry et al. 2019). In this study, using new material from the early Cambrian Guanshan biota, we re-interpret *Gaoloufangchaeta bifurcus* Zhao, li and Selden, 2023 as the earliest known pelagic errantian annelid. *Gaoloufangchaeta* has a big prostomium bearing three pairs of head appendages, a pair of eyes and a muscular eversible pharynx with papillae, and well-developed parapodia with aciculae and capillary chaetae. This character combination affiliates *Gaoloufangchaeta* with the Phyllodocida (Annelida: Errantia), extending the fossil record of Errantia back to the early Cambrian. This study provides further support to the Ediacaran hypothesis for the origin of Annelida, and indicates both morphological and ecological diversification of annelids in the early Cambrian, in accordance with the ‘Cambrian Explosion’.

REFERENCES

Capa, M. & Hutchings, P. 2021: Annelid Diversity: Historical Overview and Future Perspectives. Diversity 13, 129.

Erwin, D.H. 2020: The origin of animal body plans: a view from fossil evidence and the regulatory genome. Development 147, dev182899.

Parry, L., Eriksson, M. & Vinther, J. 2019: 3. The Annelid Fossil Record. In: Volume 1: Annelida Basal Groups and Pleistoannelida, Sedentaria I (Ed. by Purschke, G., Böggemann, M. & Westheide, W.). Berlin, Boston: De Gruyter. 69-88.

Zhao, J., Li, Y.J. & Selden, P.A. 2023: A new primitive polychaete with eyes from the lower Cambrian Guanshan biota of Yunnan Province, China. Front. Ecol. Evol. 11, 1128070.

5.31 Systematics and palaeoecology of Cambrian problematic dinomischids

Yang Zhao[1], Christian Klug[1], Peiyun Cong[2]

[1] *Paläontologisches Institut und Museum, Universität Zürich, Karl-Schmid-Strasse 4, CH-8006 Zürich (yang.zhao@pim.uzh.ch)*
[2] *Institute of Palaeontology, Yunnan University, 650500 Kunming, China*

The rapid radiation of metazoan body plans during the Ediacaran-Cambrian period includes many problematic fossils that normally have morphologies disparate from modern animals. These problematic fossils, in the best cases, can be assigned to the total group of a particular living phylum, or, in some cases, are interpreted as extinct, evolutionary dead-end clades. Dinomischidae is one of these problematic fossil groups, which is argued to provide crucial information on the morphology and palaeoecology of early basal metazoans. Dinomischids were previously treated as a paraphyletic group, with the three genera *Xianguangia*, *Daihua* and *Dinomischus* arranged along the stem of the ctenophore clade (Zhao *et al.*, 2019). Here, we present an updated interpretation of the morphology of *Xianguangia* and assgin an additional problematic taxon, *Calathites spinalis*, as a new member of the Dinomischidae based on newly collected soft-bodied fossils. Now, four genera are recovered as a monophyletic group in our phylogenetic analysis (Figure 1). Dinomischids possess similar architectures in their tentacle-sheath complex that features a sclerotized tentacle fringed with pinnules and enveloped with the smooth sheath externally. Functional comparison of the ciliated pinnules suggests that dinomischids were suspension-feeders that likely sieved organic matters down to 21 µm, corresponding well to the size range of micro-plankton (Zhao et al., 2023). However, members of Dinomischidae have different attachement structures with varying shape and size, which allow them to occupy lower and middle epifaunal tiers. We suggest that dinomischids might stabilize their body upright on the seafloor by embedding the base into the firm Proterozoic-style substrate, an attachment strategy widely employed by co-occurring basal metazoans. The substrate changes and the rising ecological competition during this period probably have shaped the taxonomic diversity pattern and the mode of life of dinomischids.

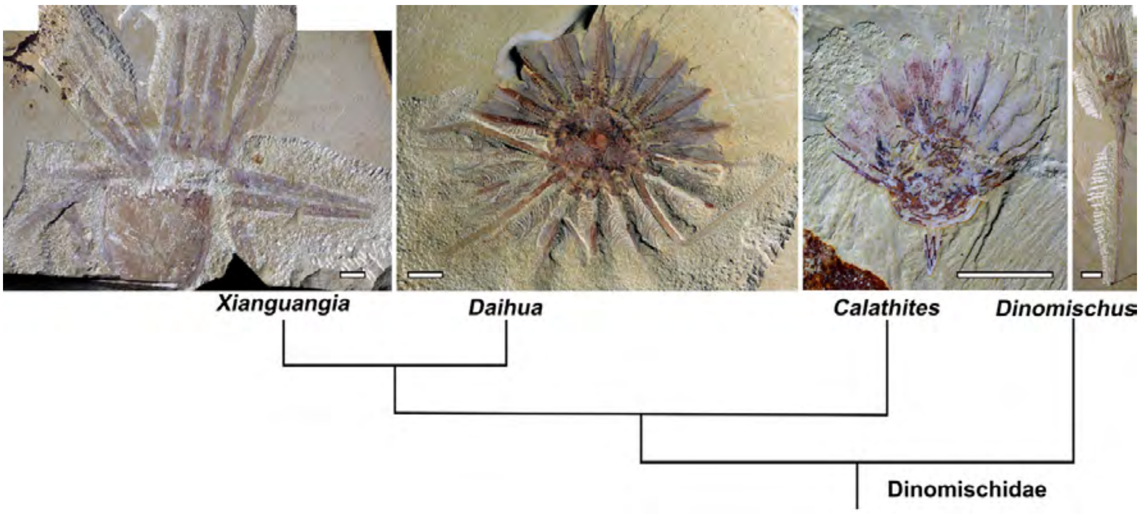

Figure 1. The updated in-group relationship of Dinomischidae. Scale bars: 5 mm

REFERENCES

Zhao, Y., Vinther, J., Parry, L. A., Wei, F., Green, E., Pisani, D., Hou, X., Edgecombe, G. D. & Cong, P. 2019: Cambrian sessile, suspension feeding stem-group ctenophores and evolution of the comb jelly body plan, Current Biology, 29, 1112-1125. e2.

Zhao, Y., Hou, X.-G. & Cong, P.-Y. 2023: Tentacular nature of the ‘column’ of the Cambrian diploblastic *Xianguangia sinica*, Journal of Systematic Palaeontology, 21, 2215787.

P 5.1
Shell shocked: PiFM imaging spills the beans- sugars more important than proteins during biocalcite diagenesis

Deyanira Cisneros-Lazaro[1], Arthur Adams[1], Laura M. Otter[2], Jaroslaw Stołarski[3], Sylvain Bernard[4], Damien Daval[5], Alain Baronnet[6], Olivier Grauby[6], Lukas P. Baumgartner[7], Torsten Vennemann[8], Stéphane Escrig[1] and Anders Meibom[1,7]

[1] *Laboratory for Biological Geochemistry, School of Architecture, Civil and Environmental engineering, Ecole Polytechnique Fédérale de Lausanne, Lausanne, CH-1015 Switzerland (deyanira.cisneroslazaro@epfl.ch)*
[2] *Research School of Earth Sciences, Australian National University, Canberra, ACT 2601, Australia*
[3] *Institute of Paleobiology, Polish Academy of Sciences, PL-00-818 Warsaw, Poland*
[4] *Museum National d'Histoire Naturelle, Sorbonne Université, CNRS UMR 7590, IMPMC, 75005 Paris, France*
[5] *ISTerre, Univ. Grenoble Alpes, Univ. Savoie Mont Blanc, CNRS, IRD, IFSTTAR, 38041, Grenoble, France*
[6] *CNRS, CINaM, Aix-Marseille Université, 13009 Marseille, France*
[7] *Center for Advanced Surface Analysis, Institute of Earth Science, University of Lausanne, CH-1015 Lausanne, Switzerland*
[8] *Institute of Earth Surface Dynamics, University of Lausanne, CH-1015 Lausanne, Switzerland*

The fossilized remains of marine calcifiers are essential to reconstructing both deep-water and sea-surface temperatures going back millions of years, but these paleoclimate records can be biased by the effects of diagenesis. In our previous works (Cisneros-Lazaro et al. 2022, Adams et al. 2023), we experimentally simulated the effects of fluid-mediated isotopic exchange on modern foraminifera tests using ^{18}O-labeled artificial seawaters in controlled experiments. We attribute significant differences in the amount of oxygen isotope exchange across different species to species-specific variations in the amount and distribution of organo-mineral interfaces. To understand the role organic matter plays during biocalcite diagenesis, we expand our work to include the calcitic layer of bivalves and investigate the composition and distribution of organic matter in foraminifera and bivalves using photo-induced force microscopy (PiFM). PiFM is a new cutting-edge technique that has the necessary spectral (~1 cm^{-1}) and spatial resolution (~5 nm) needed to chemically fingerprint and map intracrystalline organic matter (Otter et al. 2021). We find that proteins are limited to the interprismatic organic walls of bivalves but that intracrystalline sugars are abundant in both bivalves and foraminifera and link their distribution to sites of preferential ^{18}O-exchange in associated calcite. These results not only shed light on the biomineralization process of bivalves and foraminifera but also highlight the key role intracrystalline sugars have to play during the diagenesis of biocalcites.

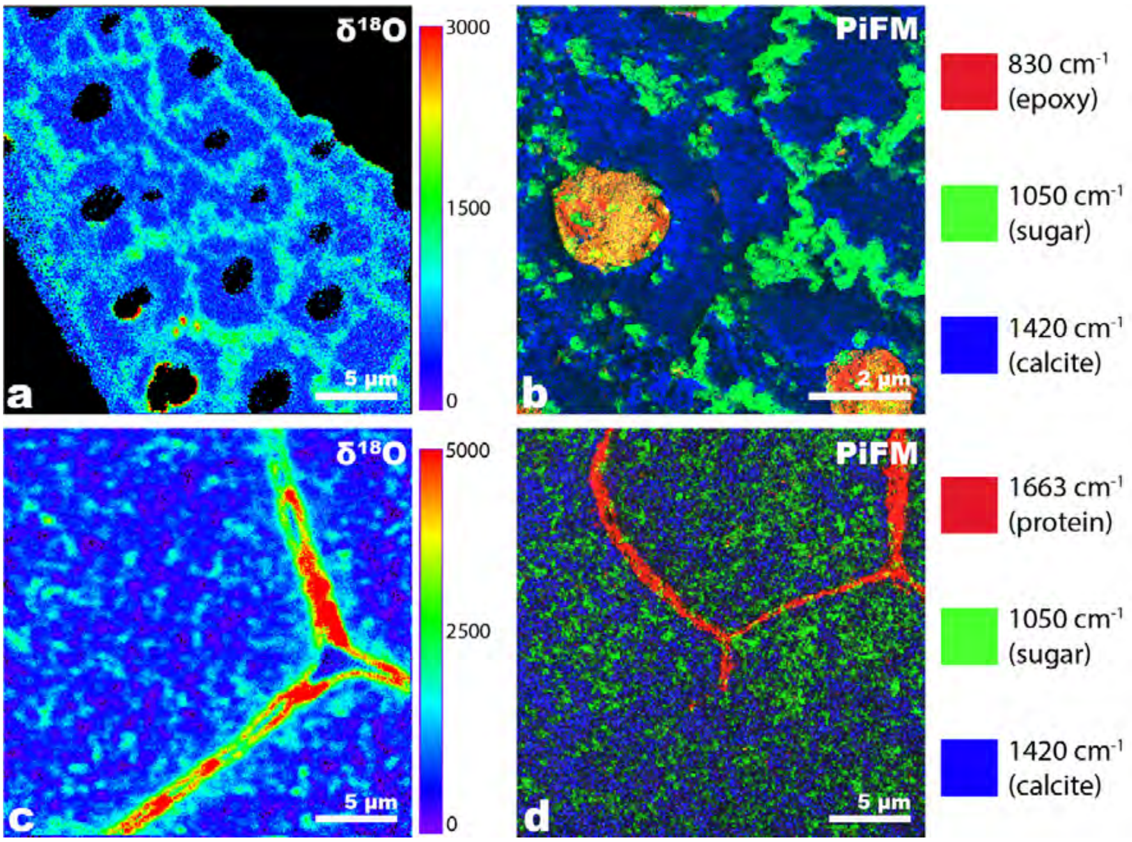

Figure 1. NanoSIMS and PiFM maps of foraminifera *Ammonia confertitesta* (a and b) and *Pinctada margartitifera* (c and d). Preferential ^{18}O-enrichment within biocalcites is clearly linked to the presence of intracrystalline sugar-rich organic matter.

REFERENCES

Cisneros-Lazaro, D. et al. 2022: Fast and pervasive diagenetic isotope exchange in foraminifera tests is species-dependent. Nature Communications 13, 1–11.

Adams, A. et al. 2023: Rapid grain boundary diffusion in foraminifera tests biases paleotemperature records. Communications Earth and Environment 4, 1-11.

Otter, L. M. et al. 2021: Nanoscale Chemical Imaging by Photo-Induced Force Microscopy: Technical Aspects and Application to the Geosciences. Geostandards and Geoanalytical Research 45, 5-27.

P 5.2
Clay minerals impact the microbial communities of decaying marine shrimps

Nora Corthésy[1], Farid Saleh[1], Jonathan B. Antcliffe[1], Camille Thomas[2], Allison C. Daley[1]

[1] *Institute of Earth Sciences, University of Lausanne, Géopolis, CH-1015 Lausanne (nora.corthesy@unil.ch)*
[2] *Department of Earth Sciences, University of Geneva, 13 Rue des Maraîchers, CH-1205 Geneva*

Fossilization favors the preservation of mineralized structures over soft tissues, which are rarely retained in deep time. To understand exceptional fossil preservation, experimental taphonomy is essential to identify biotic and abiotic factors influencing the fossilization potential (Parry et al., 2018; Purnell et al., 2018)autolysis and microbial decay, authigenic mineralization, diagenesis, metamorphism, and finally weathering and exhumation. Determining which tissues are preserved and how biases affect their preservation pathways is important for interpreting fossils in phylogenetic, ecological, and evolutionary frameworks. Although laboratory decay experiments reveal important aspects of fossilization, applying the results directly to the interpretation of exceptionally preserved fossils may overlook the impact of other key processes that remove or preserve morphological information. Investigations of fossils preserving non-biomineralized tissues suggest that certain structures that are decay resistant (e.g., the notochord. Of the biotic factors involved in preservation, bacteria are known to play a major role in carcass recycling and degradation. Bacterial growth can be limited in the presence of certain clays (McMahon et al., 2016). However, the impact of clays on bacterial community composition during animal decay is unknown. The microbial communities of marine shrimps decaying on three different clays were identified using 16S ribosomal RNA sequencing. Marine shrimps decaying on kaolinite minerals were the least degraded as kaolinite not only limits bacterial growth but also favors the growth of Proteobacteria over Firmicutes, with the latter being more efficient in recycling the polysaccharides that are the principal component in shrimp cuticle. This highlights that the primary observation of kaolinite limiting bacterial growth (McMahon et al., 2016) may not be as important as which specific bacteria it inhibits. Thus, kaolinite promotes the growth of bacteria that are less efficient in recycling complex organic compounds present in exoskeletal elements of many animal groups, which increases soft tissue preservation potential.

REFERENCES

McMahon, S., Anderson, R. P., Saupe, E. E., & Briggs, D. E. G. (2016). Experimental evidence that clay inhibits bacterial decomposers: Implications for preservation of organic fossils. *Geology*, *44*(10), 867–870. https://doi.org/10.1130/G38454.1

Parry, L. A., Smithwick, F., Nordén, K. K., Saitta, E. T., Lozano-Fernandez, J., Tanner, A. R., Caron, J.-B., Edgecombe, G. D., Briggs, D. E. G., & Vinther, J. (2018). Soft-Bodied Fossils Are Not Simply Rotten Carcasses – Toward a Holistic Understanding of Exceptional Fossil Preservation. *BioEssays*, *40*(1), 1700167. https://doi.org/10.1002/bies.201700167

Purnell, M. A., Donoghue, P. J. C., Gabbott, S. E., McNamara, M. E., Murdock, D. J. E., & Sansom, R. S. (2018). Experimental analysis of soft-tissue fossilization: Opening the black box. *Palaeontology*, *61*(3), 317–323. https://doi.org/10.1111/pala.12360

6 Stratigraphy and Sedimentology: processes and deposits through time

Alain Morard, Alicia Fantasia, Nina Zeyen, Oliver Kempf

Swiss Committee for Stratigraphy (SKS/CSS)
Swiss Palaeontological Society (SPG/SPS)
Swiss Geological Survey – swisstopo

TALKS:

6.1 Baumgartner P.O., Andjić A., Kuoč D., Diserens M.-O.: Direct radiolarian biochronologic correlation between the Oceanic Anoxic Event 3 (OAE 3, Coniacian-Santonian) and the main phase of the Caribbean Large Igneous Province (CLIP).

6.2 Baumgartner P.O., Bernoulli D., Ferràndez-Cañadell C., Baumgartner-Mora C., Epard J.-L., Stockar R., Lorenzo V.: Gravity-flow deposits derived from middle to upper Eocene thrust-top carbonate shoals in accretionary wedges N and S of the paleo-Alps (Ultrahelvetic Sex Mort Nappe and South-Alpine Ternate Formation).

6.3 Cirelli S., Schaad E., Grosjean M., Chiaia-Hernández A.: Current-use pesticides as a threat to alpine regions.

6.4 Crinière A., Moscariello A.: The Cretaceous-Paleogene Transition of the Western Swiss Plateau: new insight from subsurface and outcrops data.

6.5 Eruteya O.E., Moscariello A.: Discovery of paleokarsts and erosional morphologies along the Cretaceous-Paleogene Transition in the Geneva Basin, Western Switzerland.

6.6 Fabbri S.C., Sabatier P., Paris R., Falvard S., Feuillet N., Lothoz A., St-Onge G., Gailler A., Cordrie L., Arnaud F., Biguenet M., Coulombier T., Mitra S., Chaumillon E.: Combining sedimentary imprints with numerical modeling of paleo-tsunamis: a case from the Lesser Antilles (Saint Martin).

6.7 Lazarev S., Stoica M., Mandic O., Coric S., Vasilyan D.: From restricted marine basin to a mega-lake: Sarmatian s.l. integrated stratigraphy of the Eastern Paratethys from the perspective of the Caspian Basin (Karagiye, Kazakhstan).

6.8 Mertens C., Paradis S., Hemingway J.: Reinterpreting the Phanerozoic $\delta^{34}S$ record: identifying key environmental drivers of pyrite isotopic composition in marine sediments.

6.9 Meyer C.A., Salazar C.A., Hippler D., Yurac M., Mendez J., Gesualdi V., Hurem N., Belvedere M.: A new look at the ichnology, sedimentology and geochemistry of the Majala and Chacarilla Formation (Late Jurassic/Early Cretaceous) of the Atacama Desert Northern Chile).

6.10 Samsoondar S., Knappertsbusch M.: Archival research for shell evolution in *Globorotalia praescitula-archeomenardii-praemenardii* lineage at famous Oligocene-Miocene Cipero Coast type section, Trinidad and Tobago, SE Caribbean.

6.11 Schaad E., Fahrni N., Gosain N., Grosjean M., Chiaia-Hernàndez Aurea C.: Sedimentary records of plant protection products in small lake systems in Switzerland under anthropogenic pressure.

6.12 Vaucher R., Musajo C., Spangenberg J.E., Poyatos-Moré M., Zeeden C., Puigdefàbregas C., Castelltort S., Adatte T.: Sediment supply controls on Early Eocene delta sequences (South Pyrenean Foreland Basin, Spain).

6.13 Walde M.: The geology of the Suldtal area, with focus on the stratigraphy and detrital geochronology of the flysch units.

6.14 Zimmerli G.N., Wohlwend S., Deplazes G., Jaeggi D., Wetzel A., Foubert A.: Petrographical and geochemical facies correlation of Opalinus Clay (Switzerland).

POSTERS:

P 6.1 Fantasia A., Thibault N., Adatte T., Spangenberg J.E., Mattioli E., Regelous M., Bodin S.: Driving mechanisms of organic carbon burial in the aftermath of the Toarcian hyperthermal event.

P 6.2 Wohlwend S., Bernasconi S.M., Mazurek M., Deplazes G.: New insights from a combined C-isotope analysis of calcite and siderite in the Opalinus Clay – another step towards unravelling early diagenesis.

P 6.3 Nakajima K., Wacker L., Welte C., Heusser C., Haghipour N., Eglinton T.I.: Pollen separation with flow cytometry: an emerging method for radiocarbon dating.

P 6.4 Soria J.L., Lloren R., Yap W., Haas M., Gallentes A., Navarosa J., Guatno M.R., Pelesco C., Dubois N., Siringan F.P., Switzer A.: Preservation potential of the 2013 Super Typhoon Haiyan overwash deposits in Leyte island, Philippines.

6.1
Direct radiolarian biochronologic correlation between the Oceanic Anoxic Event 3 (OAE 3, Coniacian-Santonian) and the main phase of the Caribbean Large Igneous Province (CLIP)

Peter O. Baumgartner, Goran Andjić[1], Duje Kuoč[,2], Marc-Olivier Diserens[1]

[1] *Institut des Sciences de la Terre, Université de Lausanne, Géopolis, CH-1015 Lausanne (peter.baumgartner@unil.ch)*
[2] *Department of Geology, Croatian Geological Survey, Zagreb, Croatia*

The CLIP, among other large igneous provinces, such as the Madagascar LIP, have classically been regarded as the principal cause of the late Cenomanian/Turonian Boundary Event (CTBE), or Oceanic Anoxic event 2 (e.g. Takashima et al. 2006). However, the main CLIP phase (95–69 Ma) is too young to have significantly contributed to the climate change of the CTBE (~94 Ma) as already noted by Jones and Jenkyns (2001, p. 136). More recently, the High Arctic Igneous Province has been shown to influence the CTBE, particularly by massive methane release contributing to rapid global warming.

CLIP-OAE3 correlation. Here we synthesize radiolarian biostratigraphic work of the last two decades that allows us to correlate radiolarian-bearing sediments interbedded with or directly overlying basalts and intrusives of the CLIP with well-calibrated pelagic sections of the OAE3 (Coniacian–Santonian) in Europe and elsewhere. Although a standard Late Cretaceous low latitude radiolarian zonation remains to be established, we can correlate characteristic radiolarian assemblages from sediments interbedded or overlying CLIP basements from Costa Rica, Panama, and the Dominican Republic with those preserved in pelagic sections spanning the upper Turonian to Santonian interval in Central Italy (Gubbio), Greece (Argolis Peninsula) and Romania (Deva Beds). These sections are primarily calibrated by planktonic foraminifera, nannofossils and carbon isotope stratigraphy.

The OAE3 period is characterized worldwide by increased biogenic silica preservation in pelagic paleoenvironments, especially during the late Turonian–early Santonian time interval. Enhanced organic carbon burial is regarded as regionally restricted to the Atlantic and adjacent basins (e.g. Wagreich & Mansour, 2022).

Loma Chumico Formation. The Coniacian–lower Campanian Loma Chumico Formation (S-Nicoya Peninsula, NW-Costa Rica, AndjiĆ et al. 2019) encroaches directly on the Manzanillo Terrane representing the main CLIP phase dated by $^{40}Ar/^{39}Ar$ geochronology as 96–89 Ma. This formation consists of a lower, organic-rich Chumico Shale Member and an arc-derived volcano-pelagic Berrugate Member. The Chumico Shale Mb. is an accumulation of organic carbon along the Pacific Margin of Central America clearly assignable to OAE3 and directly in stratigraphic contact with CLIP basalts. Well-preserved radiolarian assemblages extracted form green cherts and tuffaceous siliceous mudstones between the CLIP basement and the organic-rich shales yielded a radiolarian assemblage of which nearly all species occur in Coniacian strata of the Deva Beds (Romania). AndjiĆ et al. (2019) recorded *Archaeospongoprunum venad*oensis Pessagno, *Pseudoaulophacus putahensis* Pessagno, and *Pseudodyctiomitra tiara* (Holmes, not *sensu* Dumitrica 1975) that have their last occurrence in the Coniacian. On the other hand, samples from the organic-rich Chumico Mb. and the higher, volcano-pelagic Berrugate Mb. can be dated as Coniacian-Santonian by the presence of *Annikaella omanensis* De Wever et al., *Eostichomitra perapedhia* (Bragina), *Pseudodictyomitra crassa* Bragina, either restricted to or not ranging above the Santonian.

Nicoya Complex and Azuero Plateau. In the Nicoya Complex s. str. (N-Nicoya Peninsula) ferruginous radiolarites interlayered with CLIP-phase basalts dated as 92–83 Ma, and radiolarites in stratigraphic contact with CLIP-related basalts of the Azuero Plateau yielded similar Coniacian–Santonian assemblages (Baumgartner et al. 2008, etc.).
Hispaniola. In the Dominican Republic we described a Turonian–Coniacian radiolarian assemblage from the Tireo Group which is stratigraphically placed between the Duarte Complex (early Cretaceous CLIP phase) and the Siete Cabezas Formation (Campanian CLIP phase).

Globally enhanced silica burial. Beyond the regional (Atlantic and Eastern Pacific margin) occurrences of organic-rich shales attributed to OAE3, the late Turonian–Santonian time interval is recognised by us as a time of enhanced silica burial with frequent preservation of radiolarians. We have studied well-preserved radiolarians from bio-siliceous samples of this interval from DSDP Sites in the Indian Ocean (Site 258 N-flank of Naturaliste Plateau) tropical Pacific (Sites 61, 163, 452, 585 Mariana Basin), Central Atlantic (Site 389 Galicia Bank, 603 Hatteras Abyssal Plain), as well as from land sections in Greece (S-Argolis Peninsula) and the Gubbio sections in the Central Apennines (Contessa quarry and Bottacione).

Silica events and positive ∂^{13}C-excursions. The Gubbio sections have been correlated by carbon isotope stratigraphy to the English Chalk sections (Jarvis et al. 2006). The positive ∂^{13}C-excursions recognized and correlated between both areas are fingerprinted by flint levels in the English Chalk, and also by peak abundances of visible chert in the Central Apennine sections. For our upcoming work towards a standard Late Cretaceous radiolarian biochronology we count on the recognition of these positive $\partial^{13}C$-excursions to obtain a <my resolution for the calibration of radiolarian biochronologic events.

Project funded by: SNF, No. 200020-162670, granted to P.O.Baumgartner

REFERENCES

Andjić, G., Baumgartner, P.O., Baumgartner-Mora, C., 2019. Collision of the Caribbean Large Igneous Province with the Americas: earliest evidence from the forearc of Costa Rica. GSA Bulletin, 131 (9-10), 1555–1580.

Baumgartner, P. O., Flores, K., Bandini, A. N., Girault, F., Cruz, D., 2008. Late Triassic to Cretaceous Radiolaria from Nicaragua and Northern Costa Rica -The Mesquito Oceanic Terrane. Ofioliti, 33, 1–19.

Jarvis, I., Gale, A., Jenkyns, H.C., Pearce, M.A., 2006. Secular variations in the Late Cretaceous carbon isotopes: a new $\partial^{13}C$ carbonate reference curve for the Cenomanian-Campanian (99.6-70.6 Ma). Geological Magazine 143, 561–608.

Mansour, A., Wagreich, M., 2022. Earth system changes during the cooling greenhouse phase of the Late Cretaceous: Coniacian-Santonian OAE3 subevents and fundamental variations in organic carbon deposition. Earth-Science Reviews 229.

Takashima, R., Nishi, H., Huber, B.T., Leckie, R.M., *2006*. Greenhouse world and the Mesozoic Ocean. *Oceanography 19*(*4*), 82–92.

6.2
Gravity-flow deposits derived from middle to upper Eocene thrust-top carbonate shoals in accretionary wedges N and S of the paleo-Alps (Ultrahelvetic Sex Mort Nappe and South-Alpine Ternate Formation)

Peter O. Baumgartner[1], Daniel Bernoulli[2], Carles Ferràndez-Cañadell[3], Claudia Baumgartner-Mora[1], Jean-Luc Epard[1], Rudolf Stockar[4], Valentin Lorenzo[1]

[1] *Institut des Sciences de la Terre, Université de Lausanne, Géopolis, CH-1015 Lausanne (peter.baumgartner@unil.ch)*
[2] *Department of Earth Sciences, ETH, CH-8032 Zürich*
[3] *Departament Dinàmica de la Terra i de l'Oceà, Facultat de Ciències de la Terra, Universitat de Barcelona, Martí Franquès s/n, 08028 Barcelona (Spain)*
[4] *Museo Cantonale di Storia Naturale, Viale Carlo Cattaneo 4, CH-6900 Lugano*

Here we compare two occurrences of deep-water clastic carbonate mass-flow deposits that contain middle to late Eocene shallow-marine bio- and lithoclats derived from now eroded, short-lived carbonate shoals evolving on top of advancing thrust sheets. Both occurrences are of similar age, contain a mixture of penecontemporaneously displaced shallow-water carbonates, older lithoclastic components and siliciclastics, and show comparable sedimentary structures. The time of sedimentation, constrained for the South-Alpine example as late Priabonian/?earliest Rupelian (35-34 Ma), roughly coincides with the transition from subduction of the European Plate to its collision with the Adriatic Plate, resulting in a certain symmetry of accretionary wedges N and S of the Eocene Alps.

Sex Mort Nappe. In the relatively internal Ultrahelvetic Sex Mort Nappe (VS/BE, Pointe de la Plaine Morte, and Sex Mort areas) deep-water mass-flow deposits rest unconformably on often deeply brecciated or massive, cherty Upper Jurassic limestones. The lowermost boulder breccias contain mainly angular limestone clasts derived from the underlying formations, set in a brownish-yellow, coarse sandy matrix containing *Nummulites* spp. In places, these breccias are polymictic and contain also clasts of eroded Cretaceus formations (radiolarian and calpionellid-bearing limestone, "Gault"-sandstone, globotruncanid-bearing limestone of the Seewen and Wang formations). These up to 15 m thick boulder breccias represent Eocene debris flows or rock avalanches derived from unstable submarine outcrops of tectonic imbricates of the Ultrahelvetic realm. The rare occurrence of *Nummulites* in the matrix may indicate erosion of coeval carbonate shoals. The Sex Mort Flysch consists of yellowish-brown, cm- to dm-bedded sandstone-shale alternations, sometimes with turbiditic structures, interbedded with debris-flow deposits. It encroaches in places directly on the grey, brecciated Upper Jurassic formations. Up-section, after several tens of m of flysch, occur the "*Lithothamnium* limestone beds". We studied these 5-10 m thick channel-fill sequences in the area recently uncovered from below the ice of the Plaine Morte Glacier. At the bottom of these sequences lenticular bodies of debris flow breccias show a clast composition similar to the lowermost boulder beds. Up-section, a fining- and thinning-upward series of smaller debris flow deposits and turbidites follows, in which the proportion of Eocene bioclastic material increases rapidly up-section. Rhodophycaean algae and larger benthic foraminifera (LBF) are the most dominant bioclasts. LBF include: (1) Taxa restricted to the late Priabonian Shallow Benthic Zone (SBZ) 20, such as *Heterostegina gracilis*. (2) Taxa with a Priabonian range, such as *Sanetschella indeprensa* and *Rotorbinella epardi* (Ferràndez-Cañadel et al. 2023). (3) Taxa restricted to the early-middle Priabonian, such as *Virgasterocyclina ferrandezi ferrandezi* (SBZ 18c-19). Hence, this assemblage can be assigned to the SBZ 19-20, but clearly shows reworking of material of sligthly older Priabonian age.

We estimate that there are at least two to three stratigraphically superposed channel-fill complexes; however, this is difficult to ascertain, since the whole flysch sequence is isoclinally folded. The beds are also laterally thinning and may be replaced by sandy, bioclast-bearing turbidites only.

Ternate Formation. The tectonic setting of the Ternate Formation (Bernoulli, 1980) is difficult to evaluate, because of a thick Quaternary cover in the area. Seismic profiles in the S-Alpine foreland of the Po Basin and deep exploration wells (Lisanza 1) suggest that the Ternate Formation is probably thrust to the north along a major backthrust ("Gonfolite backthrust"). The formation is exposed for about 150 m, without a contact with over- or underlying formations. The formation includes calcareous mass-flow deposits including chanellized rubble beds, pebbly mudstones and limestone turbidites interbedded with minor hemipelagic marls, deposited in a submarine fan of low-transport capacity. The redeposited limestone beds include both penecomporaneously displaced shallow-water bioclasts and lithoclastic material derived from Mesozoic formations of the Southern Alps, probably eroded from submarine canyons, testifying to pre-late Eocene thrusting and submarine erosion. Herb (1976) considered the Bartonian material from the matrix of pebbly mudstones as reworked hemipelagics and, based on planktonic foraminifera, argued for a late Priabonian sedimentation age for the bulk of the Formation. The reworked shallow water LBF include middle Bartonian to late Priabonian species: *Heterostegina gracilis* (SBZ 20, documented by Herb in photographs), *Virgasterocyclina ferrandezi ferrandezi* (SBZ 19), and *Heterostegina reticulata helvetica* (SBZ 18C) and *H. r.*

tronensis (SBZ 18B) in Ternate blocks at Prella/TI

We conclude that the source areas of carbonate bioclasts in both examples were short-lived, undifferentiated, shallow carbonate banks of Bartonian to Late Priabonian age associated with active thrusts. Frequent seismicity and/or high river discharge from the late Eocene Alpine hinterland may have triggered gravitational mass transport into the deeper marine foreland basin. The onset of continent-continent collision may have caused the incorporation of the Ternate Formation into the South-Alpine accretionary wedge soon after its deposition.

Project funded by: SNF, No. 200021-185067 granted to Claudia Baumgartner

REFERENCES

Bernoulli D. 1980. The Ternate Formation, a Late Eocene bioclastic submarine fan. In: R. Trümpy (Ed.) Geology of Switzerland, Part B: Geological Excursions, pp. 204–205.

Ferràndez-Cañadell C., Baumgartner-Mora C., Baumgartner P.O., and Epard J.L. 2023. Priabonian (upper Eocene) larger foraminifera from the Helvetic Nappes of the Alps (Western Switzerland): new markers for Shallow Benthic zones 19–20. Micropaleontology, vol. 69, nos. 4-5, pp. 401–449.

Herb, R. 1976. Das Alter der eozänen Sedimente im südwestlichen Varesotto (Norditalien). Eclogae Geol. Helv., vol. 69, pp. 821–825.

6.3
Current-use pesticides as a threat to alpine regions

Sergio Cirelli[1*], Emmanuel Schaad[1], Martin Grosjean[1], Aurea C. Chiaia-Hernández R.[1]

[1] *University of Bern, Institute of Geography and Oeschger Center for Climate Change Research, Hallerstrasse 12, 3012, Bern, Switzerland (sergio.cirelli@unibe.ch)*

The rapid expansion and diversification of synthetic chemicals outpace known agents of global change, such as CO2 emissions, global population growth, agricultural expansion, and biodiversity loss. However, they nonetheless receive relatively minor consideration in planetary change discussions (Bernhardt, E.S. et al., 2017). The processes governing the transportation of synthetic chemicals, such as current-use pesticides (CUPs), through the atmosphere and their potential impact on health and the environment still need to be fully understood.

Contemporary chemicals are designed to be non-persistent, non-bioaccumulative, and non-toxic. However, several studies have documented that due to their physical-chemical characteristics (e.g., low water solubility, strong bond to particulate matter, persistence, and volatility), CUPs may be deposited in pristine environments and mountain regions far from their initial emission sources (Zhong, G. et al., 2012; Balmer, J.E. et al., 2019). These studies have demonstrated that specific atmospheric processes must play a crucial role, given that these areas are not in direct contact with potential contamination sources.

Thus, it is surprising that until now, there is still scarce information on the fate of CUPs and their transformation products in the atmospheric compartment.

The present study employed a novel multi-proxy workflow incorporating paleolimnology tools and chemical analysis, enabling the exploration of historical CUP records in lake sediment dating back to the mid-20th century (Chiaia-Hernández, A. et al., 2020). This methodology was utilized to detect and quantify CUPs in sediment cores obtained from Lake Oberstockensee, situated at 1665 meters above sea level. The selected lake stands in a region characterized by abundant precipitation, consistent sedimentation rates, and an absence of direct exposure to potential sources of contamination from agricultural or urban environments. Hence, any contamination detected in the sediment will derive from long-range atmospheric transport and deposition.

The results show the unbiased presence of CUPs (e.g., fungicides) and unknown anthropogenic contaminants characterized by different time series and clusters. Of relevance, these findings suggest a relatively recent atmospheric anthropogenic contamination of Alpine lakes.

This study provides a fundamental building block to gain a comprehensive overview of the intricate pathways and transformations of CUPs throughout the environment, as well as their ultimate fate. Moreover, the persistence of organic chemicals offers a means to reconstruct environmental changes, providing signatures of the Anthropocene.

REFERENCES

Bernhardt, E.S. et al. 2017: Synthetic chemicals as agents of global change. Frontiers in Ecology and the Environment, Volume 15, (2), 84-90.

Balmer, J.E. et al. 2019: Levels and trends of current-use pesticides (CUPs) in the arctic: An updated review, 2010-2018, Emerging Contaminants, Volume 5, Pages 70-88

Chiaia-Hernández, A. et al. 2020: High-Resolution Historical Record of Plant Protection Product Deposition Documented by Target and Nontarget Trend Analysis in a Swiss Lake under Anthropogenic Pressure, Environmental Science & Technology, 54 (20), 13090-13100

Zhong, G. et al. 2012: Distribution and Air-Sea Exchange of Current-Use Pesticides (CUPs) from East Asia to the High Arctic Ocean, Environmental Science & Technology, 46, 1, 259-267

6.4
Cretaceous-Paleogene Transition in the Western Swiss Plateau: New insight from subsurface and outcrops data

Aurélia Crinière[1], Andrea Moscariello[1]

[1] *Geo-Energy Group, Department of Earth Sciences, University of Geneva, Rue des Maraîchers 13, 1205, Geneva, Switzerland*

This study provides new insight on the sedimentary record known as Siderolithic deposited in correspondence of a large regional unconformity marking the Cretaceous-Paleogene Transition. In this work we investigate the results of the geothermal exploration campaign carried out in the Geneva Basin, to characterise the texture, composition, provenance, and environmental conditions of deposition unexpected 160 m thick heterogenous sedimentary sequence representing a karst infill. Petrography, mineralogy (bulk and clay), geochemistry (major, trace, and rare earth elements) and petrophysical analysis were conducted on overall 115 samples. Six sub-units were identified indicating a clear sequence of depositional events which allow the reconstruction of the karst evolution from its formation, infill and subsequent diagenetic processes. Evidence of karst formation (dissolution and wall collapse) associated with both hypogenic and epigenic processes are provided by the occurrence of Upper Cretaceous lithologies no longer present in the Geneva Basin. A considerable thickness of quartz-rich sandstone made of medium to coarse well rounded and fine sub-angular grains with a variable matrix component predominantly made of siderite, kaolinite and chlorite fill the upper part of the karst (116 m). The latter is interpreted as being originate from a mixed source likely fluvial and aeolian in origin and could represent good candidate for geothermal energy use. Geochemical data and clay mineralogy indicate humid climate condition which together with analogue deposits biostratigraphically constrained in the Swiss Plateau, suggest a deposition during the Middle Eocene Climatic Optimum, making this study one of few accounts of continental record of the MECO in Western Europe.

6.5
Discovery of Paloekarsts and Erosional Morphogies along the Cretaceous-Paleogene Transition in the Geneva Basin, Western Switzerland

Ovie Emmanuel Eruteya[1] and Andrea Moscariello[1]

[1] *Geo-energy, Reservoir Geology and Basin Analysis Group, Department of Earth Sciences, University of Geneva, Rue de Maraîchers 13, 1205 Geneva*
(Ovie.Eruteya@unige.ch and Andrea.Moscariello@unige.ch)

Analysis of the new 3D seismic reflection dataset acquired by Services industriels de Genève (SIG) in the Geneva Basin revealed an astonishing and unexpected view on a new deeply buried landscape whose nature, extension and variety was unknown until now (Figure 1). This interval is known as the CPT: the Cretaceous-Paleogene Transition and is related to the ca 95-Ma unconformity between the Lower Cretaceous carbonates and the Oligocene Molasse clastic succession.

The detailed seismic interpretation of the 3D cube revealed a clear tectono-geomophological partioning (zonation) (Figure 1a). Zone 1 in the vicinity of the GEo-01 borehole is charcterized by faults systems and relatively smooth morphology (Figure 1a). However, zone 2 in the vicinity of the GEo-02 borehole is characterized by perversavie paleo-karst morphologies. Importantly, the GEo-02 borehole penetrating these karsts revealed a siderolithic infill characterized by exotic well sorted, almost pure quartz sandstone (Figures 1a and b). Zone 3 is characterized by an extensive incised valley systems, all converging to the deepest point of a narrow and structurally controlled trench corresponding to the foreland foredeep of the Molasse Basin (Figure 1c). Importantly, a prominent SW-NE trending mounded morphology in the vicinity of the Thonex-1 borehole exist around the deepest point of Zone 3 (Figure 1a).

The preliminary findings from this study opens an unexpected “new chapter” in the geological history of the Western Swiss Plateau where the interplay between erosional processes, surface drainage development and tectonic evolution resulted in this fascinating and yet poorly known landscape.

Actually, the unprecedented sheer extension and pervasiveness of these features across the study area likely formed during the subaerial exposure of the Lower Cretaceous carbonates during the early phase of the Alpine build-up (Paleocene-Eocene?). The formation processes, depositional environment (continental vs marine ? marginal vs deep marine ?) and age of these paleo canyons are indeed the big open questions which will keep the geoscientist community busy for a while in the next foreseeable future. Also, is the implication of these features on the ongoing geo-energy exploration in these segment of the Swiss Molasse Basin.

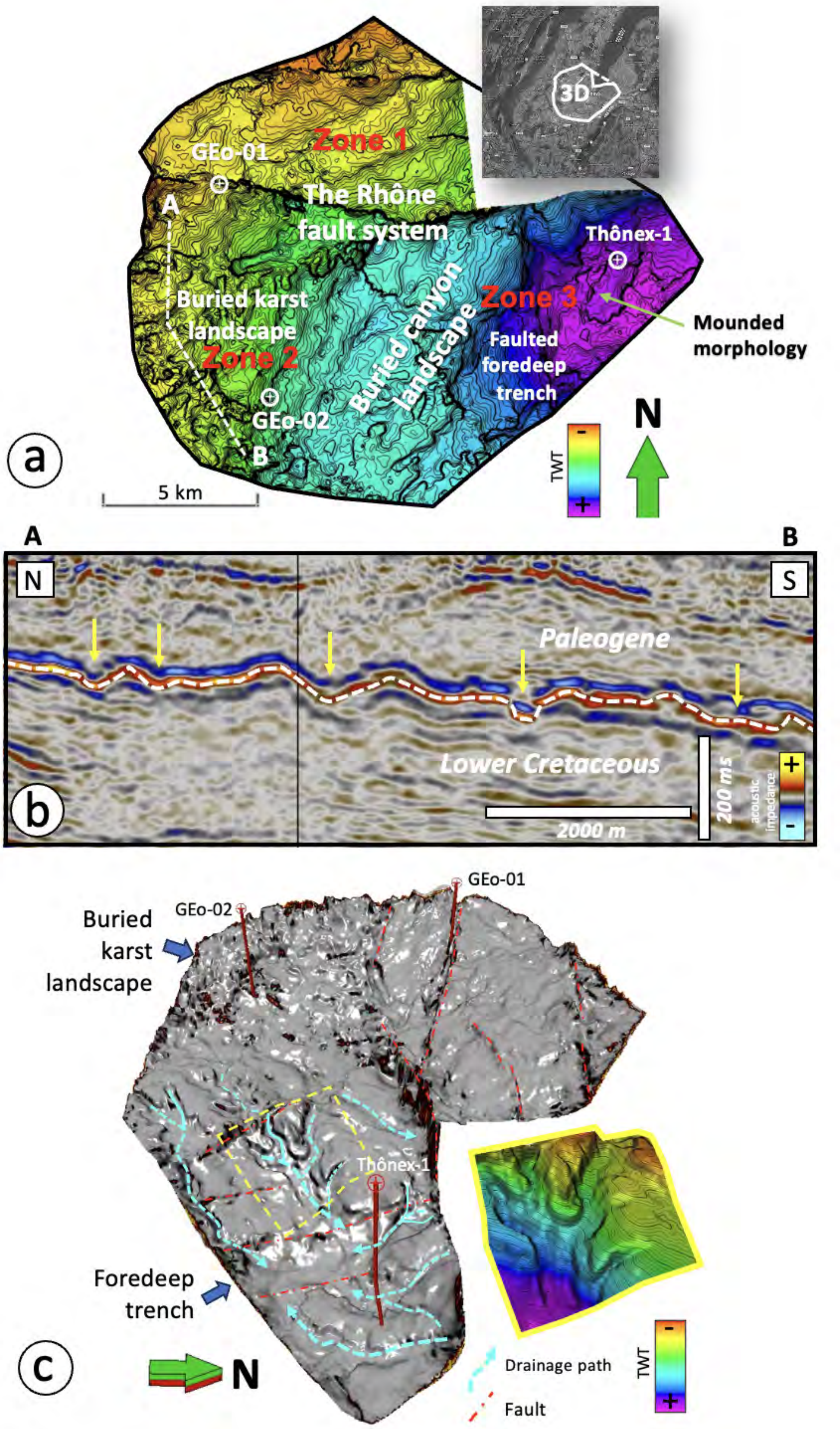

Figure 1.(a) Structural map of the Cretaceous-Paleogene Transition (CPT) in the Geneva Basin showing the three main geomorphologic zones (see text for description). (b) Seismic profile showing depressions interpreted as paleokarst morphologies (yellow arrows) along the CPT (location of profile is shown in Figure 1a). (c) Variance atrribute map of the CPT showing the buried karstified landspace and network of drainage system.

6.6
Combining sedimentary imprints with numerical modeling of paleo-tsunamis: A case from the Lesser Antilles (Saint Martin)

Stefano C. Fabbri[1,2,3], Pierre Sabatier[1], Raphaël Paris[4], Simon Falvard[4], Nathalie Feuillet[2], Amélie Lothoz[1], Guillaume St-Onge[3], Audrey Gailler[5], Louise Cordrie[2], Fabien Arnaud[1], Maude Biguenet[1,6], Thibault Coulombier[6], Saptarshee Mitra[4], Eric Chaumillon[6]

[1] EDYTEM, Université Savoie Mont-Blanc, CNRS, Le Bourget du Lac, France (stefano.fabbri@unibe.ch)
[2] IPGP, Géosciences Marines, CNRS, Paris, France
[3] Institut des sciences de la mer de Rimouski (ISMER), UQAR, Rimouski, Canada
[4] Université Clermont Auvergne, CNRS, IRD, OPGC, Laboratoire Magmas et Volcans, Clermont-Ferrand, France
[5] CEA, DAM, DIF, F-91297 Arpajon Cedex, France
[6] LIENS, Université de la Rochelle, CNRS, La Rochelle, France

In this study, we investigated sedimentary records to identify extreme-wave events (EWEs), specifically hurricanes and paleo-tsunamis, in a coastal lagoon located at Saint Martin Island (Lesser Antilles) in the Caribbean Sea. The study aimed to differentiate between tsunami and storm deposits through sediment-logical, geochemical, and radiocarbon dating analyses, complemented by X-ray computed microtomography (micro-CT) for sediment fabric examination, which further allowed for the determination of paleo-flow directions, facilitating the comparison of event dynamics within its landscape.

This multiproxy approach was applied to a transect of three oriented short sediment cores (sites 1-3, Fig. 1). We were able to identify sediment layers brought during both tsunami- and hurricane-triggered EWE, making our study site extremely valuable as a natural archive. Thanks to geochemical (Ca/Fe ratios) and sedimentary signatures (coarse-grained sandy deposits), we identified six out of seven EWEs as paleo-tsunamis. The most recent event deposit (EWE I) marks the occurrence of the unprecedented powerful Category 5 Hurricane Irma in 2019, whose landscape impact is well documented through satellite imagery and direct observations. Deposit thickness and frequency variations were evident across the transect. Six paleo-tsunamis were successfully dated, with ^{14}C ages from bottom to top of ~3400 yr cal BP, ~2900 yr cal BP, ~2500 yr cal BP, and ~2100 yr cal BP, including the well-studied Pre-Columbian tsunami ~1400 yr CE (EWE III) and the transatlantic Lisbon tsunami 1755 CE (EWE II) previously recorded in this region (Biguenet et al., 2021). Comparisons with other sites and neighboring islands in the Caribbean Sea reveal good agreement with our events. This leads us to a tentative local tsunami chronology of six well-documented paleo-tsunami events over the last 3500 years BP with a recurrence interval of 400 to 500 years.

Furthermore, the micro-CT-based sediment analysis provided intricate sediment fabric insights, potentially serving to formulate universal event-type criteria in the future. However, a deeper comprehension of the relationship between sediment fabric and tsunami wave dynamics is needed to fully understand the linkage between them. We therefore used the deposits of the Pre-Columbian tsunami and compared paleo-flow directions from micro-CT-derived flow directions to numerical models. The results that best explain the Pre-Columbian tsunami deposit emplacement are in line with a Mw 8.5–8.7 megathrust earthquake source located on the subduction interface at the Puerto Rico Trench, north of Anegada Island, in accordance with Cordrie et al. (2022) study on Scrub, Anguilla, Anegada and St Thomas islands. Ultimately, integrating deposits of EWEs with numerical models remains pivotal for devising effective hazard mitigation strategies tailored to the vulnerable coastal communities.

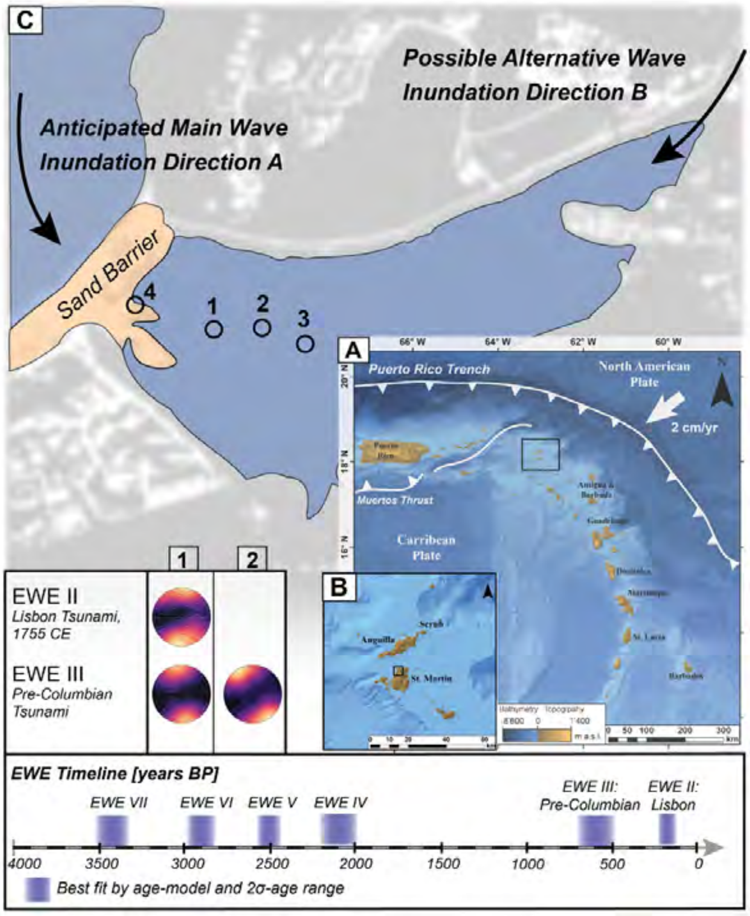

Figure 1A: Overview of the Lesser Antilles including major tectonic plates. B: Overview of Saint Martin and neighboring islands with the location of the cored coastal lagoon indicated. C: Simplified aerial photograph of the lagoon with the location of the core transect (sites 1-3) and the cored storm washover deposit (site 4), including the timeline of discovered EWE deposits and micro-CT-derived sedimentary fabrics (stereograms) for the transatlantic Lisbon tsunami and the Pre-Columbian tsunami, indicative for tsunami paleo-flow direction.

REFERENCES

Cordrie, L., Feuillet, N., Gailler, A., Biguenet, M., Chaumillon, E., Sabatier, P., 2022. A Megathrust earthquake as source of a Pre-Colombian tsunami in Lesser Antilles: Insight from sediment deposits and tsunami modeling. Earth-Science Reviews 228.

Biguenet, M., Sabatier, P., Chaumillon, E., Chagué, C., Arnaud, F., Jorissen, F., Coulombier, T., Geba, E., Cordrie, L., Vacher, P., Develle, A.L., Chalmin, E., Soufi, F., Feuillet, N., 2021. A 1600 year-long sedimentary record of tsunamis and hurricanes in the Lesser Antilles (Scrub Island, Anguilla). Sedimentary Geology 412.

6.7
From restricted marine basin to a mega-lake: Sarmatian s.l. integrated stratigraphy of the Eastern Paratethys from the perspective of the Caspian Basin (Karagiye, Kazakhstan)

Sergei Lazarev[1,2], Marius Stoica[3], Oleg Mandic[4], Stjepan Coric[5], Davit Vasilyan[2,1]

[1] *Department of Geosciences, University of Fribourg, Chemin du Musée 6, 1700 Fribourg, Switzerland (sergei.lazarev@unifr.ch)*
[2] *JURASSICA Museum, Route de Fontenais, 21, 2900 Porrentruy, Switzerland*
[3] *Faculty of Geology and Geophysics, University of Bucharest, Balcescu Bd. 1, 010041 Bucharest, Romania*
[4] *Geological-Paleontological Department, Natural History Museum Vienna, Burgring 7, 1010, Vienna, Austria*
[5] *Geological Survey Austria, Neulinggasse 38, 1030 Vienna, Austria*

The Eastern Paratethys is a former epicontinental sea that occupied large territories of West Eurasia during the Cenozoic – from the Carpathian foreland in the west to Central Asia in the east. Comprising three major subbasins - the Dacian (Carpathian foreland), the Euxinian (Black Sea), and the Caspian basins, the Eastern Paratethys played a crucial role in Eurasian climate, paleobiogeography, and ecosystem sustainability.

During the so-called Sarmatian s.l. Stage (12.6–7.65 Ma), the Eastern Paratethys underwent a series of paleohydrological changes that gradually transformed this sea into a megalake. Accompanying changes in water chemistry led to a high level of aquatic ecosystem endemism and later to their extinction.

Despite relatively good documentation of the Sarmatian s.l. faunal trends, aspects such as comprehensive age constraints, biozonation, and sedimentological characteristics of strong water-level fluctuations are still missing, thus complicating interregional paleobiogeographic, tectonic, and paleoenvironmental studies of this 5 million-year-long portion of West Eurasian history.

Here, we present our integrated stratigraphic constraints of the Sarmatian s.l. from the easternmost part of the Eastern Paratethys – the Caspian Basin. The 135-meter-thick outcrop in the Karagiye Depression (Kazakhstan) exposes Konkian-Sarmatian s.l.-Maeotian deposits that were studied using a combination of magnetostratigraphy, sedimentology, micropaleontology (ostracods and foraminifers), mollusc fauna, and nannoplankton.

The Konkian interval (incomplete, 13.2–13 Ma) consists of various bioturbated marlstones deposited in lagoon settings and comprises rich foraminifera and ostracod fauna. The mollusc fauna has been assigned to the Limacina konkensis zone, and the nannoplankton assemblage belongs to the NN6 zone.

The Sarmatian s.l. consists of three substages (Volhynian, Bessarabian, and Khersonian): Volhynian (incomplete, 12.4–12.0 Ma) is represented by bioturbated marlstone interbedded with frequent coquina beds deposited in shallow water lagoons. Here, two foraminifera zones (*Varidentella reussi* and *Elphidium reginum*), one ostracod zone (*Euxinocythere turpe*), and one mollusc zone (*Sarmatimactra eichwaldi–Abra reflexa*) were documented. The nannoplankton assemblage is also representative of the NN6 zone.

The Bessarabian interval (11.9–9.8 Ma) begins with a large transgression that established offshore-offshore transition settings with claystones and occasional tempestite beds that gradually transition into shallow lagoon settings with serpulid framestones, wackstones, and grainstones. The end of the Bessarabian is marked by a remarkable water-level drop that brought subaerial depositional settings. Here, two ostracod zones (*Euxinocythere graveodosoensis* and *Loxoconcha subcrassula*), two mollusc zones (*Plicatiformes plicatofittoni–Sarmatimactra vitaliana* and *P. fittoni–S. fabreana*), and two foraminifera zones (*Porosononion aragviensis* and *P. hyalinum*) were documented.

The Khersonian substage (9.8–7.5 Ma) consists of two intervals (9.8–9.4 Ma and 8.0–7.5 Ma) separated by a large gap within the stage (9.4–8.0 Ma). The lower interval was deposited in shoreface-barrier settings with remarkable *Chersonimactra* rudstones, while the upper one formed on the foreshore (coastal plain)–upper shoreface settings represented by alternation of wave-rippled mudstones, microbiolites, and pedogenically modified mudstones. Neither foraminifera nor nannoplankton were detected in the Khersonian. There are two mollusc zones (*Chersonimactra balcica* and *C. bulgarica*) and two ostracod zones (*Euxinocythere immutata* and *E. dilecta*).

The Maeotian begins as a transgression that terminated Khersonian coastal plain environments and established shallow water nearshore settings with oolithic barriers, algae bioherms, and microbiolites (stromatolites). The mollusc fauna here belongs to the zone *Loripes pseudoniveus–Ervilia minuta*.

The new integrated stratigraphic constraints from Karagiye provide new insights into the paleoenvironmental evolution of the Caspian branch of the Eastern Paratethys during the Konkian-Maeotian time.

Funding: The study has been supported by the Swiss National Science Foundation project Nr. 200021_197323.

6.8
Reinterpreting the Phanerozoic $\delta^{34}S$ Record: Identifying Key Environmental Drivers of Pyrite Isotopic Composition in Marine Sediments

Cornelia Mertens[1], Sarah Paradis[1], Jordon Hemingway[1]

[1] *Geologisch Institut, ETH Zurich, Sonneggstrasse 5, CH-8092 Zürich (cornelia.mertens@erdw.ethz.ch)*

The most important sulfur sink from a global redox-perspective is diagenetic pyrite produced in marine sediments. The amount and isotopic composition of this pyrite is thought to reflect environmental and physical properties of the ocean. This includes sulfate reduction rate, sulfate concentration, sedimentation rates, organic carbon and reactive iron concentrations and reactivities, porosity of the sediment among other factors.

Our goal is to identify the main drivers that can explain the majority of observed sulfur isotopic composition in pyrite. To this end, we use a diagenetic model and calculate theoretical profiles for organic carbon, reactive iron, and a number of sulfur species and their isotopes in marine sediments. We calibrate our model using 216 sedimentary cores from a wide range of environmental conditions and locations from across the world.

The model allows us to calculate burial rates and isotopic composition of pyrite in marine sediments on a global scale as well as infer drivers of the Phanerozoic pyrite $\delta^{34}S$ record. We show that isotopic composition of pyrite is determined by a limited number of environmental variables. Based on this, we reinterpret Phanerozoic $\delta^{34}S$ trends as recording a shift in the locus and environmental conditions where pyrite is formed, rather than a change in microbial sulfate reducer fractionation.

6.9
A new look at the ichnology, sedimentology and geochemistry of the Majala and Chacarilla Formation (Late Jurassic/Early Cretaceous) of the Atacama Desert Northern Chile)

Christian A. Meyer[1*], Christian A. Salazar[2], Dorothee Hippler[3], Marko Yurac[4], Javiera Mendez[2], Vincenzo Gesualdi[5], Nejla Hurem[3], Matteo Belvedere[5,6]

[1] *Departement Umweltwissenschaften, University of Basel, Bernoullistrasse 32, CH-4056 Basel (chris.meyer@unibas.ch)*
[2] *Escuela de Geología, Facultad de Ciencias Universidad Mayor, 7500000 Providencia, Santiago de Chile, Chile*
[3] *Graz University of Technology, Institute of Applied Geosciences, 8010 Graz, Austria*
[4] *Unidad de Patrimonio Paleontológico, Consejo de Monumentos Nacionales, 7500000 Providencia, Santiago de Chile, Chile*
[5] *Dipartimento di Scienze della Terra, Università degli Studi di Firenze, 50121 Firenze, Italy*
[6] *NBFC, National Biodiversity Future Center, Piazza Marina 61, Palermo 90133, Italy;*

The skeletal record of dinosaurs in Chile consists of non-avian dinosaurs such as sauropods, theropods and thyreophorans (e.g., Soto-Acuña et al., 2015). The track record however consists only of isolated reports from the Late Jurassic/Early Cretaceous (e.g., Rubilar-Rogers et al. 2000).

In 2022 a field campaign explored the area of the Quebrada de Huatacondo (Tarapacá Basin) where an ornithopod trackway and isolated theropod tracks had been registered previously (loc. cit.) . First results indicate the presence of 12 different tracklevels in the Late Jurassic Majala and Early Cretaceous Chacarilla Formations. We recorded minute, intermediate sized and large theropod tracks, as well as sauropods and many trampled surfaces; the reported large ornithopods however show long metatarsal impressions and are therefore assigned to theropods (Yurac Diaz et al., 2021). The tracks are recorded in a sedimentary succession made up of more than 800 m of cross-bedded fine sand- and siltstones with mud cracks, ripple marks and occasional invertebrate traces (e.g. (*Ophiomorpha*) that we interpreted as deposits of a distal flood plain.

The same formations have been explored in a campaign in 2023 further south in the Quebrada de Arcas (Calama Basin), where we had only two location reports from Rubilar-Rogers and Otero (2008) and, more recently, by mapping geologists. Although the Majala Fm did not yield any tracksites, we could detect 20 new tracklevels in the overlaying Chacarilla Fm. These levels yield tracks and trackways of medium- and large-sized theropods as well as medium sized sauropods. Occasionally, surfaces display invertebrate burrows of crayfish and bivalves. The Chacarilla Fm consists of a more than 300m thick stack of thickening upward cycles of fine-grained sandstones and siltstones with mud cracks and ripple marks that have likely been deposited on a distal alluvial plain under arid conditions.

Preliminary mineralogical and geochemical results indicate that most of the fine-grained sandstones and siltstones can be classified as litharenites mainly consisting of quartz with minor to accessory contributions of alkali feldspar, illite and chlorite with calcite and/or quartz as main cementing phases. The geochemical composition of the sampled sedimentary rocks equals an almost upper crustal composition with distinct formation-specific differences between sand- and siltstones of the Majala and Chacarilla Formations. the base and the top part.

Figure 1: Large theropod footprint from the Chacarilla Formation (Quebrada de Huatacondo; Scales 25 cm).

Figure 2: Steeply inclined surface with sauropod trackways from the Chacarilla Formation (Quebrada de Arcas; Geologists for scale).

REFERENCES

Galli, C. & Dingman, R. 1962 Cuadrángulos Pica, Alca, Matilla y Chacarilla. Carta Geológica de Chile. Instituto de Investigaciones Geológicas, Carta Geológica de Chile No 7-10, escala 1:50.000. 125 pp.

Rubilar-Rogers,D., K. Moreno, K. & Blanco, N. 2000: Grandes huellas de dinosaurios ornitópodos en la Formación Chacarilla (Jurásico Superior-Cretácico Inferior), Región de Tarapacá, Chile, Actas del IX Congreso Geológico Chileno. Puerto Varas, 550–554.

Soto-Acuña, S., Otero, R.A., Rubilar-Rogers, D. & Vargas, A.O. 2015: Dinosaurios no avianos de Chile, Publicación Ocasional del Museo Nacional de Historia Natural, Chile, 63: 209-26.

Yurac Diaz, M., Salazar, C., Meyer, C.A., Suárez, M.E. & Belvedere M. 2021: The dinosaur ichnological record of Northern Chile: A review ans its potential development. Abstracts Meeting European Vertebrate Palaeontologist, Benevento. p. 223.

6.10
Archival research for shell evolution in *Globorotalia praescitula-archeomenardii-praemenardii* lineage at famous Oligocene-Miocene Cipero Coast type section, Trinidad and Tobago, SE Caribbean

Sadie Samsoondar[1] and Michael Knappertsbusch[1]

[1] *Department of Geology, Natural History Museum Basel, Augustinergasse 2, 4051 Basel, Switzerland; sadie.samsoondar@bs.ch; michael.knappertsbusch@bs.ch*

Globally important microfossil type samples are sometimes only accessible within unique museum collections like those within Hans G. Kugler´s Legacy at Natural History Museum Basel, Switzerland (NMB). Kugler (1893-1986), the Father of Trinidad´s Geology, was a Swiss petroleum geologist. Cenozoic planktonic foraminiferal biozonations orginiated largely in Trinidad (1930s-1970s) by renowned micropalaeontologists like A. Senn, H.H. Renz, J. Cushman, P.W. Jarvis, R.M. Stainforth, P. Brönnimann, B. Carr-Brown, H.M. Bolli, and J.B. Saunders. Their efforts were economically driven within oil companies. Less known to the micropalaeontological community was that these pioneering works were orchestrated by Dr. Hans G. Kugler, the Chief Petroleum Geologist. Kugler prioritized the use of microfossils while drilling for oil in Venezuela and Trinidad to great success (Samsoondar et al., 2020).Type sections in Trinidad soon became international standards for worldwide biostratigraphy and are today integrated in global biogeochronological schemes for geological age determination and worldwide correlation. Kugler preserved copious amounts of type and co-type samples and literature within today´s world´s largest Trinidad collection housed at the NMB. Since Kugler´s time, urbanization and overwhelming vegetation of tropical Trinidad has rendered most type sections inaccessible, a great tragedy to the micropalaeontological community. Our recent investigations into Kugler´s archive at NMB, however, revealed unprecedented documentation for many of these unique samples. Kugler's collection is thus today of immense scientific value and of great international interest.

The Cipero Coast [Oligo-Miocene Cipero Formation], Trinidad, is the first location, globally, where planktonic foraminiera were used for the establishment of plankton biostratigraphic zonal- and correlational- schemes and taxonomy in the tropics. Continued research on the Cipero Coast, rendered it a standard and classical type section, so earning it a significant role in the erection of Neogene geological time scales. Today, the Cipero Coast is tragically inaccessible. Given this section`s importance on taxonomy, integrated biogeochronology and geological time scales, micropalaeontologist today must dig out isolotaed historical slides from different institutions around the world, often without sufficient documentation for precise sample reconstruction. As a pilot study, we chose samples (raw sediment and archives) from the famous Cipero Coast. These unique archives, which are key to world distributed Trinidad samples, are extremely rare and can only be found at the NMB. We here exploit archival studies and highly endorse its irreplaceable role in restoring scientific context to historical samples and to allow new analysis to be conducted on them. This deep archival investigations enabled our Cipero Coast samples to be newly georeferenced. We then generate its first numerical age-depth model. Such a numerical age model forms a prerequisite for quantitative studies of geological and palaeontological processes such as shell evolution of planktonic foraminifera. We apply our age model for a morphometric study of ancestral *Globorotalia praescitula-archeomenardii-praemenardii* from that area into to the descendent Neogene tropical *Globorotalia menardii*. The evolution of the latter has been intensively investigated on a global scale and recently refined at Ceara Rise in the tropical West Atlantic (Knappertsbusch, 2023). By re-investigating the Cipero Coast section in Trinidad, we re-experienced the difficulty of the old veterans in biostratigraphy, who, while studying plankton evolution and its potential for biostratigraphy and long-distance correlation, were faced with a tectonically chopped geology and strong facies changes over short distance. These difficulties and shortcomings in the development of biostratigraphic concepts came to light after intensively studying the materials preserved and stored in the archives and collections at the NMB. On preliminary note we confirm, and for the first time quantify, a rather slow size increase of these ancestral menardiforms into their younger descendents confirms our perception that *G. menardii* was an evolutionary rather conservative species. This observation supports the suspicion that the enigmatic singular but widespread rapid size increase in *G. menardii* that occurred throughout the tropical Atlantic during the late Pliocene, rather represents immigration than interpunctated evolution.

For the advancement of biostratigraphic practices, archival and collection material studies, like ours, are paramount. Archival studies allow critically reassessment of the conditions and pitfalls under which biostratigraphic zonal and correlation schemes once were erected. Such ancillary materials gives us information about the quality of samples, their composition, preservation and richness in marker species initially used for defining zonal schemes, but also inform about strategy and concepts for sampling, the resolution of samples in an outcrop or well section, as well as former methods of sample preparation. All such information is necessary if one wishes to re-use original material for new scientific analysis and comparing this new data with that of the original publications. Often, these details about distributed museum samples are difficult to access even though it is necessary for standardizing taxonomy or biostratigraphy. We here attempt to rectify this problem with at least the Legacy of

Hans G. Kugler at the NMB.

In this broader context, our study serves to scientifically better understand the fascinating evolutionary processes in this important and climatic relevant group of marine, shell secreting planktonic protists, but also is exemplary of how to exploit hidden information from museum archives and collections for improvement of taxonomy and integrated biogeochronology and geological time scales.

REFERENCES

Knappertsbusch, M. 2023. Morphological cladogenesis and terminal dwarfing in extinct Late Miocene through Pliocene menardiform globorotalids: New complementary data to “Evolutionary prospection in the Neogene planktic foraminifer Globorotalia menardii and related forms from ODP Hole 925B (Céara Rise, western tropical Atlantic): evidence for gradual evolution superimposed by long distance dispersal ? Swiss J. Palaeontology, 135:205-248”. Data archive and report published on https://doi.org/10.5281/zenodo.7812050

Samsoondar, S., Wilson, B. and Farfan, P. 2020. Early Neogene Stratigraphy and Oceanography of Trinidad – A Fresh Perspective. Nova Science Publishers. https://novapublishers.com/shop/early-neogene-stratigraphy-and-palaeoceanography-of-trinidad-west-indies-a-fresh-perspective/

More info at:
https://micropal-basel.unibas.ch/Research/TRINIDAD/KUGLER_ARCH_COLL.html
https://micropal-basel.unibas.ch/Research/TRINIDAD/CIPERO.html
https://micropal-basel.unibas.ch/

6.11
Sedimentary records of plant protection products in small lake systems in Switzerland under anthropogenic pressure

Emmanuel Schaad[1], Nicole Fahrni[1], Nayan Gosain[1], Martin Grosjean[1], Aurea C Chiaia-Hernàndez[1]

[1] *Institute of Geography and Oeschger Center for Climate Change Research, University of Bern, Hallerstrasse 12, CH-3012 (emmanuel.schaad@unibe.ch)*

Plant protection products (PPPs), commonly termed “pesticides”, are currently a topic of high concern due to their ubiquitous presence in different environmental compartments. Mitigation measures and monitoring regarding PPP contamination in freshwater ecosystems have almost exclusively focused on large lakes and rivers (Chiaia-Hernández et al., 2020; Moschet et al., 2014). At the same time, smaller water bodies such as ponds have only rarely been included in monitoring studies as well as in the general regulatory framework of Switzerland. Smaller water bodies could be under exceptionally high pressure from PPP contamination, as they are often located near agricultural fields and have a lower dilution potential than lakes due to their reduced size.

In this work, a novel multiproxy-workflow that combines chemical analysis (LC-MS/MS) and paleolimnology methods (e.g., chronology, hyperspectral measurements of sedimentary green pigments, and µXRF) was used to characterize sediment cores from three ponds located on the Swiss Central plateau in the Canton of Bern.
Our study reveals that PPPs are very stable under anaerobic conditions and PPPs can provide a historical deposition of chemical contamination since the 1960s. Furthermore, up to 50% of the studied compounds (~40 PPPs) were detected in the pond sediments, and distinct clustering between banned PPPs and current-use PPPs is evident. Moreover, a cumulative risk assessment deemed sediment quality insufficient in all three lakes.

In addition, our work reveals that PPP fluxes are not related to sedimentary processes such as soil erosion (Ti counts, µXRF scans), lake biogeochemistry (calcite precipitation, microscope analysis), or lake productivity (green pigments, HSI). Therefore, post-depositional processes or variations in sediment binding do not majorly influence PPP fluxes over time, and PPP behavior can be predominantly related to sales (used as a proxy for PPP application) or bans.

The obtained results are of great concern given that ponds outnumber lakes by about 100 to 1 in Switzerland, and they serve as habitats and spawning grounds for many organisms and often are key habitats for many rare and endangered species, contributing enormously to a rich biodiversity (Williams et al., 2004). Furthermore, lake systems like those studied here are abundant in the Swiss Plateau and Central Europe. Therefore, our findings likely represent many small European lakes influenced by agriculture.

REFERENCES

Chiaia-Hernández, A. C., Zander, P. D., Schneider, T., Szidat, S., Lloren, R., & Grosjean, M. (2020). High-Resolution Historical Record of Plant Protection Product Deposition Documented by Target and Nontarget Trend Analysis in a Swiss Lake under Anthropogenic Pressure. *Environmental Science and Technology*, *54*(20), 13090–13100. https://doi.org/10.1021/acs.est.0c04842

Moschet, C., Wittmer, I., Simovic, J., Junghans, M., Piazzoli, A., Singer, H., Stamm, C., Leu, C., & Hollender, J. (2014). How a complete pesticide screening changes the assessment of surface water quality. *Environmental Science and Technology*, *48*(10), 5423–5432. https://doi.org/10.1021/es500371t

Williams, P., Whitfield, M., Biggs, J., Bray, S., Fox, G., Nicolet, P., & Sear, D. (2004). Comparative biodiversity of rivers, streams, ditches and ponds in an agricultural landscape in Southern England. *Biological Conservation*, *115*(2), 329–341. https://doi.org/10.1016/S0006-3207(03)00153-8

6.12
Sediment supply controls on Early Eocene delta sequences (South Pyrenean Foreland Basin; Spain)

Romain Vaucher[1,2], Claire Musajo[2], Jorge E. Spangenberg[3], Miquel Poyatos-Moré[4], Christian Zeeden[5], Cai Puigdefàbregas[6], Sébastien Castelltort[1], Thierry Adatte[2]

[1] Department of Earth Sciences, University of Geneva, Rue des Maraîchers 13, 1205 Geneva, Switzerland (romain.vaucher@unige.ch)
[2] Institute of Earth Sciences (ISTE), University of Lausanne, Geopolis, 1015 Lausanne, Switzerland
[3] Institute of Earth Surface Dynamics (IDYST), Géopolis, University of Lausanne, 1015 Lausanne, Switzerland
[4] Departament de Geologia, Universitat Autònoma de Barcelona, Barcelona, Spain
[5] Leibniz Institute for Applied Geophysics (LIAG), Geozentrum Hannover, Hannover, Germany
[6] Department of Earth and Ocean Dynamics, University of Barcelona, C/ Martí i Franquès, s/n, 08028 Barcelona, Spain

Accommodation changes are often emphasized in interpreting depositional sequences, regardless of scale, despite evidence demonstrating that sediment supply can also play a key role as a sequence builder. Here, we focus on the coastal environments of a temporally well-constrained source-to-sink system in the South Pyrenean Foreland Basin (SPFB) to provide evidence for supply-driven delta sequences during the Early Eocene.

The Early Eocene Climate Optimum (49.14 to 53.26 Ma) was characterized by high atmospheric CO_2 concentrations, elevated global temperatures, and ice-free poles. Additionally, this period was marked by several hyperthermal events involving abrupt and significant releases of isotopically depleted carbon into the atmosphere, leading to notable negative carbon isotope excursions (CIEs) in sedimentary records globally. These hyperthermal events were associated with rapid temperature increases and likely intensified precipitation, potentially resulting in increased erosion and chemical weathering on land. These factors could have amplified clastic sediment production and flux to the ocean, promoting the normal regression of the sedimentary systems. Concurrently, in this particular case study, uplift associated with the Pyrenean orogeny occurred in the hinterland, contributing to enhanced the accommodation creation in the foreland basin and sediment supply due to the expanded drainage area.

Our study analyzed the paleoenvironmental record of the Castigaleu sequence (Early Eocene; Ypresian; 52-50.2 Ma), exposed in the SPFB near Navarri, Spain. A 643.5 m thick mixed siliciclastic-carbonate section was logged and sampled (n = 301). Sedimentary facies studies were complemented by geochemical analysis (organic carbon stable isotopes: $\delta^{13}C_{org}$) and organic matter characterization (Rock-Eval pyrolysis analysis). This approach aimed to determine what triggered the successive deltaic progradation.

The onset and progradation of this deltaic system along this section are characterized by the sudden appearance of delta-front environments defined by meter-thick cross-stratified medium-grained sandstones, coinciding with the first recorded negative CIE in the stratigraphic section. Subsequent pulses of progradation/aggradation correlate with subsequent negative CIEs, while positive CIEs correspond to more distal pro-delta and offshore environments, indicating a backstepping of the deltaic system.

In turn, this study demonstrates that during the deposition of the Castigaleu sequence, the main triggering mechanism generating sequences was the climate-induced high-frequency variation in sediment supply rather than the changes in accommodation.

6.13
The geology of the Suldtal area, with focus on the stratigraphy and detrital geochronology of the flysch units

Michel Walde

Dep. of Earth Sciences, ETH Zürich, Sonneggstrasse 5, CH-8092 Switzerland (mwalde@ethz.ch)

Melanges and broken formations of the Alps have been studied since the 19th century by numerous authors with different backgrounds, each one contributing to the overall knowledge about their dynamic genesis. However, the lack of agreement and their definition leads to confusion and inconsistency. The Suldtal, being a sparsely studied area, contains undiscovered geologic records about the sin-tectonic sedimentation of the early alpine orogeny. To disentangle the sequence of events from the Late Cretaceous to the Paleogene, a structural and stratigraphic approach combined with detrital dating are taken in this project. The centre of attention was drawn onto the Wildflysch Formation in the Suld Valley, located south of Lake Thun. Macroscopic to microscopic observations on geologic relationship and geometries suggest a progressing accretionary wedge from the Late Cretaceous to the Oligocene. The Helvetic and Penninic units from the Cretaceous to Paleocene are proposed to be thrusted and exposed by the accretionary wedge during the Wildflysch formation in the Eocene. These units are most likely olistoliths transported by gravitational mass wasting processes and deposited in the alpine foredeep together with turbiditic deposits of the Taveyannaz and the Stad Formation from the Helvetic ramp. The horizontal and undeformed nature of these contemporary units, suggest that the post-sedimentary tectonic deformation has played only a minor role in the Wildflysch.

6.14
Petrographical and geochemical facies correlation of Opalinus Clay (CH)

Géraldine Nicole Zimmerli[1], Stephan Wohlwend[2], Gaudenz Deplazes[3], David Jaeggi[4], Andreas Wetzel[5], Anneleen Foubert[1]

[1] *Department of Geosciences, University of Fribourg, Chemin du Musée 6, CH-1700 Fribourg (geraldine.zimmerli@unifr.ch)*
[2] *Geological Institute, ETH Zurich, Sonneggstrasse 5, CH-8092 Zürich*
[3] *Nagra, Hardstrasse 73, CH-5430 Wettingen*
[4] *Federal Office of Topography swisstopo, Seftigenstrasse 264, CH-3084 Wabern*
[5] *Department of Environmental Sciences, University of Basel, Bernoullistrasse 30/32, CH-4056 Basel*

The Opalinus Clay, a silty to sandy claystone formation of Toarcian to Aalenian (Early/Middle Jurassic) age, is known in Switzerland as the selected host rock for deep geological disposal of radioactive waste. Since more than thirty years, various geotechnical, mineralogical and sedimentological studies have addressed the Opalinus Clay within the framework of the Nagra (National Cooperative for the Disposal of Radioactive Waste) by initiating deep drilling campaigns and the Mont Terri Project.

The aim of the present study is to understand the lateral and vertical facies variability within the Opalinus Clay in Central Northern Switzerland using petrographical, mineralogical (X-ray diffraction, multi-mineral interpretation) and geochemical (X-ray fluorescence, hierarchical clustering analysis, non-metric multidimensional scaling) data. Petrographic descriptions performed on thirteen drill cores let to a revised subfacies classification scheme, which is based on texture (colour, grain-size, sedimentary structures) and composition (mineralogy). The new subfacies classification scheme for the whole Opalinus Clay in Switzerland and its potential application to other mudstone formations around the world is presented.

Subfacies descriptions are significant to assess and understand the lateral and vertical facies variability at regional scale. Small-scale vertical facies variations as well as marker horizons (timemarkers) are identified, which can be correlated at regional scale. The observed complex lateral and vertical facies variability requires to revise and to develop a new depositional model for the Opalinus Clay at regional and basin scale. An ongoing study concerning grain-size analysis to reconstruct current velocities can create answers.

P 6.1
Driving mechanisms of organic carbon burial in the aftermath of the Toarcian hyperthermal event

Alicia Fantasia[1,2], Nicolas Thibault[3], Thierry Adatte[4], Jorge E. Spangenberg[5], Emanuela Mattioli[6], Marcel Regelous[7], Stéphane Bodin[2]

[1] *Department of Geosciences, University of Fribourg, 1700 Fribourg, Switzerland (alicia.fantasia@unifr.ch)*
[2] *Department of Geoscience, Aarhus University, 8000 Aarhus C, Denmark*
[3] *Department of Geosciences and Natural Resource Management, University of Copenhagen, 1350 Copenhagen K, Denmark*
[4] *Institute of Earth Sciences, University of Lausanne, 1015 Lausanne, Switzerland*
[5] *Institute of Earth Surface Dynamics, University of Lausanne, 1015 Lausanne, Switzerland*
[6] *Univ. Lyon, UCBL, ENSL, CNRS, LGL-TPE, F-69622, Villeurbanne, France*
[7] *GeoZentrum Nordbayern, Universität Erlangen-Nürnberg, Erlangen, Germany*

Carbon cycle-climate dynamics were nonlinear through Earth's history, driven by changes in internal and external forcing processes acting on various geological timescales. This study focuses on determining the relationship between volcanism, orbital parameters, and organic carbon burial during the Aalenian (Middle Jurassic) - a pivotal time at the dawn of the Mesozoic Marine Revolution, marked by a disruption of the carbon cycle and major climate shifts. Here, new high-resolution magnetic susceptibility and trace elements data are combined with previously published organic carbon isotopes and total organic carbon data from two sites in France and Chile. Our dataset shows for the first time a temporal coincidence between the major carbon cycle perturbation during the middle–late Aalenian and the onset of enhanced volcanic activity, suggesting a causality link. We propose that volcanic activity triggered a transient warming episode within the long-term Middle Jurassic coldhouse and played a key role in shifting organic carbon burial from the ocean to terrestrial settings. This period therefore contrasts with other Mesozoic carbon cycle perturbations, which generally record enhanced marine organic matter burial in oxygen-depleted environments during volcanism-triggered warming events.

P 6.2
New insights from a combined C-isotope analysis of calcite and siderite in the Opalinus Clay – another step towards unravelling early diagenesis

Stephan Wohlwend[1], Stefano M. Bernasconi[1], Martin Mazurek[2], Gaudenz Deplazes[3]

[1] *Geologisches Institut, ETH Zürich, Sonneggstrasse 5, 8092 Zürich (stephan.wohlwend@erdw.ethz.ch)*
[2] *Institut für Geologie, Universität Bern, Baltzerstrasse 1+3, 3012 Bern*
[3] *Nagra, Hardstrasse 73, 5430 Wettingen, Switzerland*

The sedimentary succession of the Opalinus Clay predominantly comprises silty claystone, with varying amount of a siliciclastic fraction, and a minor presence of carbonates. In this study, 31 bulk rock samples taken from the Bülach1 drill core in northern Switzerland were analysed. Within the two lower sub-units, known as the «Clay-rich sub-unit» and «Mixed clay-silt-carbonate sub-unit», the total carbonate content is rather consistent at around 10 wt.%. Moving upwards into the uppermost two sub-units, the overall carbonate content increases, reaching slightly higher average values of up to 15 wt.%. Detailed XRD-analysis shows that the Opalinus Clay not only contains calcite; a significant amount of siderite is also present. Other carbonate minerals such as dolomite and ankerite are negligible. Siderite was shown to be a valuable diagnostic mineral for the Opalinus Clay and is a product of early diagenetic processes. In contrast, calcite could be derived from a combination of bioclastic components as well as from diagenetically precipitated micritic calcite. The XRD-analysis further demonstrates that the siderite content ranges from 2 to 4 wt.% across the entire Opalinus Clay. Consequently, the ratio of calcite to siderite within the lower two sub-units is roughly 2:1.

Previous measurements of carbon-isotopes in bulk rock samples have indicated that the «Mixed clay-silt-carbonate sub-unit» exhibits higher fluctuations in the $\delta^{13}C_{carb}$ in bulk carbonates. These values not only shift towards more negative values, but some also exhibit a shift towards more positive values. We present a new analytical approach that allows measuring $\delta^{13}C$ from the calcite fraction ($\delta^{13}C_{cal}$) by reaction with phosphoric acid in a first step at low temperature, and subsequently from the siderite fraction ($\delta^{13}C_{sid}$) at 70°C. This approach provides a new possibility to investigate the distinct behaviour of different carbonates during early diagenesis. The XRD-analysis enable a direct validation of the newly calculated calcite and siderite contents derived from the isotope analysis, showing that during the chosen reaction time, the siderite reacted almost completely with the phosphoric acid. Comparison of $\delta^{13}C_{cal}$ with $\delta^{13}C_{sid}$ data, shows that different intervals within the Opalinus Clay exhibit distinct trends. Specifically, the «Mixed clay-silt-carbonate sub-unit» shows more positive $\delta^{13}C_{sid}$ values, reaching up to 4.4 ‰, while the uppermost sub-unit displays more negative values of up to -6.0 ‰ Consequently, the variations in the Cisotopic compositions of both calcite and siderite offer a promising avenue for gaining insights into early diagenetic processes.

P 6.3
Pollen separation with flow cytometry: an emerging method for radiocarbon dating

Kai Nakajima[1,2], Lukas Wacker[2], Caroline Welte[1,2], Christian Heusser[1,2], Negar Haghipour[1,2], Timothy I. Eglinton[1]

[1] Geological Institute, ETHZ, Sonnegstrasse 5, 8092 Zurich
[2] Laboratory of Ion Beam Physics, ETHZ, Otto-Stern Weg 5, 8093 Zurich
(knakajima@phys.ethz.ch)

Radiocarbon (^{14}C) dating of pollen is an emerging method for establishing chronologies of lacustrine sediment records that are scarce in macrofossils. Pollen are ubiquitously abundant in lacustrine sediments and represent atmospheric ^{14}C concentrations at the time of formation. Further, because pollen are established markers for terrestrial ecosystem variability, pollen-based ^{14}C data can generate ideal, proxy-specific ^{14}C-chronologies for palynological research. Traditional approaches for pollen separation from sedimentary matrices for the purpose of ^{14}C analysis were limited by a costly trade-off between purity, processing time, and yield (Porch & Kershaw 2010), rendering them unsuitable for routine application. Only in recent years, a novel approach of utilising flow cytometry in combination with physical and chemical preprocessing proved efficient for the rapid separation of pollen from terrestrial sediments at high purity suitable for ^{14}C dating (Tennant 2013).
We examine the robustness of this approach with a dedicated flow cytometer (BD Influx Cell Sorter, BD Biosciences, US) by conducting a comprehensive blank assessment and producing pollen-^{14}C data for two lake records for comparison with previously acquired data based on terrestrial macrofossils and tephra layers. The ^{14}C blank assessment conducted for the entire pollen isolation process indicates our protocol is suitable for microscale (< 20 µg C) pollen-^{14}C dating. This will enable future dating of sediments previously limited by the amount of pollen or the lack of other datable material. Our pollen-^{14}C data for two lake records from different environments are each in agreement with macrofossil-^{14}C data (Engels 2021) and tephra dates (Jones 2018) respectively. With our newly established protocol and a dedicated instrument for routine application, pollen-^{14}C dating will provide a versatile and attractive alternative to traditional dating approaches for terrestrial records.

REFERENCES

Engels, S. (2021). The influence of Holocene forest dynamics on the chironomid fauna of a boreal lake (Flocktjärn, northeast Sweden). Boreas, 50(2), 519-534.

Jones, G., Lane, C. S., Brauer, A., Davies, S. M., De Bruijn, R., Engels, S., ... & Wagner-Cremer, F. (2018). The Lateglacial to early Holocene tephrochronological record from Lake Hämelsee, Germany: a key site within the European tephra framework. Boreas, 47(1), 28-40.

Porch, N., & Kershaw, A. P. (2010). Comparative AMS 14C dating of plant macrofossils, beetles and pollen preparations from two late Pleistocene sites in southeastern Australia. Altered Ecologies: Fire, Climate and Human Influence on Terrestrial Landscapes, Terra Australis, 32, 395-403.

Tennant, R. K., Jones, R. T., Brock, F., Cook, C., Turney, C. S., Love, J., & Lee, R. O. B. (2013). A new flow cytometry method enabling rapid purification of fossil pollen from terrestrial sediments for AMS radiocarbon dating. Journal of Quaternary Science, 28(3), 229-236.

P 6.4
Preservation potential of the 2013 Super Typhoon Haiyan overwash deposits in Leyte island, Philippines

Janneli Lea Soria*[1], Ronald Lloren[2,3], Wenshu Yap[4], Mischa Haas[5], Adonis Gallentes[6], Jodivine Navarosa[7], Mark Russel Guatno[8], Clyde Pelesco[9], Nathalie Dubois[2,3], Fernando Siringan[6], and Adam Switzer[4]

[*1] *Institute of Environmental Science and Meteorology, University of the Philippines, Diliman, Quezon City 1101 (lea.soria@gmail.com)*
[2] *Department of Earth Sciences, ETH Zürich, Sonneggstrasse 5, CH-8006 Zürich*
[3] *Department of Surface Waters Research and Management, Eawag, Überlandstrasse 133, CH-8600 Dübendorf*
[4] *Earth Observatory of Singapore, 50 Nanyang Avenue, 50 Nanyang Ave, Block N2-01a-15, Singapore 639798*
[5] *Kanton Luzern, Dienststelle Umwelt und Energie, Libellenrain 15, 6006 Luzern*
[6] *Marine Science Institute, University of the Philippines, Diliman, Quezon City 1101*
[7] *Philippine Science High School - Central Visayas Campus, Argao, Cebu 6021*
[8] *Guatno Surveying Services, Sevilla, Bohol*
[9] *Baybay, Leyte*

The onslaught of the 2013 Super Typhoon (ST) Haiyan storm surge in the Philippines left overwash sediments mostly as sand sheets blanketing the coastal landscape along its path. Notably, being the most documented modern overwash deposit in the Philippines, the Haiyan overwash sediments facilitate the discovery of similar marine flood events in the past across the country. In June 2023, we revisited one of the well-studied sites in Leyte Island. This aims to examine whether the storm overwash deposits are still preserved and could still reflect the original depositional conditions or whether post-depositional processes have altered the sedimentary evidence, a decade after the event. The sedimentology profile and microfossil assemblage conducted within the six months after the 2013 ST Haiyan (Pilarczyk et al., 2016, Soria et al., 2017) will serve as the reference data to assess post-depositional changes. Recognition of post-depositional processes is equally crucial in assessing the preservation potential of modern overwash deposits. Both information will help to minimise uncertainties in interpreting paleo overwash deposits.

In Leyte island, variations in the preservation potential of ST Haiyan overwash deposits were observed: a. Overwash deposits near the beach have been disturbed and removed due to persistent coastal erosion and building of a coastal embankment as compared to the previously mapped and documented in 2014. b. Further inland, auger and shallow trenches in the mangrove and marsh environments, less disturbed by human activities, revealed that the ST Haiyan overwash sand deposit remained recognizable from the pre-Haiyan soil (Figure 1). A distinct organic-rich mangrove soil that represents post-Haiyan deposition now sits on top of the ST Haiyan overwash deposit. While the sandy textural signature of the ST Haiyan overwash deposit is generally preserved, the internal sedimentary structures such as laminations in some instances are now nearly obscured.
A few exploratory longer sediment cores also revealed anomalous sand layers below the pre-Haiyan soil, which could possibly correspond to an older marine flooding event. An additional seven sediment push cores were collected along a transect covering ~1.2 km within the inundation distance of the ST Haiyan storm surge. The sediments will be subjected to geochemical, biological, and molecular analyses for the potential development of new novel proxies that will complement the prevailing multi-proxy toolkit for paleotempestology or paleotsunami studies (e.g., Bellanova, et al., 2020; Yap et al., 2021). New proxies are particularly useful when sedimentary profile and microfossil evidence are compromised. Coupled with accurate and robust age-dating methods, we aim to generate a high-resolution, multi-century analysis of coastal flooding recurrence intervals for the region.

Figure 1. A shallow trench (TAN0623-02) revealed a preserved ST Haiyan overwash sand deposit sandwiched in between the organic-rich pre- and post-Haiyan mangrove soils.

REFERENCES

Bellanova, P., Frenken, M., Reicherter, K., et al. 2020: Anthropogenic pollutants and biomarkers for the identification of 2011 Tohoku-oki tsunami deposits (Japan). Marine Geology, 422, 106117.

Pilarczyk, J.E., Horton, B.P., Soria, J.L.A., et al. 2016: Micropaleontology of the 2013 Typhoon Haiyan overwash sediments from the Leyte Gulf, Philippines. Sedimentary Geology 339, 104–114.

Soria, J.L.A., Switzer, A.D., Pilarczyk, J.E., Siringan, F.P., Khan, N.S., Fritz, H.M. 2017: Typhoon Haiyan overwash sediments from Leyte Gulf coastlines show local spatial variations with hybrid storm and tsunami signatures. Sedimentary Geology 358, 121–138.

Yap, W., Switzer, A.D., Gouramanis, C. et al. 2021: Environmental DNA signatures distinguish between tsunami and storm deposition in overwash sand. Commun Earth Environ 2, 129. https://doi.org/10.1038/s43247-021-00199-3

7 Seismic Hazard and Risk in Switzerland: From Science to Mitigation +

23 Alpine Hazards: Early Detection, Monitoring, Warning, Modelling, Mitigation

Donat Fäh, Blaise Duvernay, Savvas Saloustros.
Andrea Manconi, Yves Bühler, Elisabeth Hafner, Cristina Pérez-Guillén, Antonio Abellán, Michel Jaboyedoff, Virginia Ruiz-Villanueva, Saskia Gindraux.

TALKS:

7.1 Amini A., Van Mol R.N.H.M., Hunzinger L., De Cesare G.: Enhancing Flood Resilience: Sediment Management in Le Bez Torrent

7.2 Bergamo P., Chieppa D., Panzera F., Fäh D.: Ongoing work for the study of site amplification phenomena in the Swiss alpine valleys and their implication for the Swiss building code

7.3 Bijelić N., Lignos D.G.: Recent Advancements in Data-Centric Machine Learning in Earthquake Engineering and Surrogate Modellig of Steel Moment Resisting Frames

7.4 Dallo I., Schnegg L.N., Marti M., Fulda D., Papadopoulos A.N., Bergamo P., Wenk S.R., Valenzuela N., Roth P., Danciu L., Haslinger F., Fäh D., Kästli P., Wiemer S.: The transdisciplinary design of user-centered seismic risk maps

7.5 De Pedrini A., Pozzoni M., Ambrosi C., Ghezzi S., Spataro A., Osculati L., Uggeri A.: Monitoring and evolutionary analysis of the Cadegliano Viconago landslide between Switzerland and Italy

7.6 Elmorsy M., Vassiliou M.F.: An Experimental Framework for Statistical Validation of System Level Assumptions in Seismic Analysis of RC Structures

7.7 Hafner E.D., Heisig H., Zesiger M., Bühler Y.: Comparing three avalanche periods mapped from optical remote sensed imagery around Davos, Switzerland

7.8 Häusler, M., Glüer, F., Fäh, D.: An Update from the Seismic Monitoring of the Brienz/Brinzauls rock slope instability

7.9 Imtiaz A., Papadopoulos A., Bergamo P., Fäh D.: A scenario-based earthquake loss assessment for Basel, Switzerland

7.10 Inzunza-Araya E., Saloustros S., Beyer K.: Experimental investigation of the size effect on the seismic behaviour of unreinforced masonry walls

7.11 Janusz P., Bonilla L.F., Bergamo P., Fäh D.: Assessing the possibility of nonlinear soil response in the Lucerne area

7.12 Jones N., Strozzi T., Caduff R., Inderbitzin L., Hodel M., Stadlin S.: Early detection of ground motion using satellite radar interferometry (InSAR) – Gwalpeten rockslope instability (Bisistal, Kanton Schwyz)

7.13 Katsamakas A., Vassiliou M.F.: Shake-table response of a bridge-like model with rocking piers and restraining tendons

7.14 Koroni M., Bergamo P., Ermert L., Roten D., Fäh D.: Long-period waveform modelling in sedimentary basins using spectral-element simulations to estimate ground motion in the Rhône Valley and Swiss Molasse basin

7.15 Korre E., Yang H., Jeremic B., Anastasopoulos I.: Response of structures on shallow foundations under conditions of earthquake induced liquefaction

7.16 Roth P., Papadopoulos N., et al.: ERM-CH23: New Perspectives on Earthquake Risk Assessment and Management in Switzerland

7.17 Ruttner-Jansen P., Glaus J., Voordendag A., Wieser A., Bühler Y.: Setup for monitoring snow depth changes in an avalanche prone area

7.18 Shynkarenko A., Kremer K., Lontsi A.M., Bergamo P., Fäh D.: Results of the seismological and geotechnical investigations of submerged slopes in Lake Lucerne

7.19 Stojadinović B., Blagojević N., Bodenmann L., Arslantürkoglu S.: From the Swiss Earthquake Risk Model to the Swiss Earthquake Resilience Model

POSTERS:

P 7.1 Dallo I., Böse M., Hetényi G., Roduit R.: Seismo@School – A Swiss-wide initiative to bring current earthquake knowledge to schools

P 7.2 Ermert L., Boschi L., Obermann A.: Towards surface wave attenuation monitoring with ambient seismic noise

P 7.3 Panzera F., Bergamo P., Danciu L., Fäh D.: On the selection of design-compatible waveforms for structural-analysis purpose in Switzerland

P 7.4 Lightfoot A.K., Strupler S., Wiemer S.: Continuous Measurements of Radon and Other Dissolved Gas Species in Groundwater: A Crucial Step in Earthquake Precursor Research?

P 7.5 Schierjott J., Strupler M., Kremer K., Vendettuoli D., Bürgler M., Vetsch D.: A workflow for assessing lake tsunamis that are generated by various types of mass movements

P 23.1 Halter T., Lehmann P., Bast A., Staehli M.: Combining climate and soil moisture information in statistical modelling for landslide early warning

P 23.2 Shastri R.P., Brönnimann S.: Numerical Investigation of High Impact Foehn storm in February 1925 using WRF and PALM model

7.1
Enhancing Flood Resilience: Sediment Management in Le Bez Torrent

Azin Amini[1], Romain Van Mol[1], Lukas Hunzinger[2], Giovanni De Cesare[1]

[1] *Platform of Hydraulic Constructions (PL-LCH), Ecole Polytheqnique Fédérale de Lausanne (EPFL), CH - 1015 Lausanne (azin.amini@epfl.ch)*
[2] *Flussbau AG SAH, CH - 3007 Bern*

INTRODUCTION

In the canton of Bern, Switzerland, the “Le Bez” torrent is known for its flash floods, causing sediment and wood debris buildup in Villeret village settled on the alluvial fan. To mitigate this issue, a sediment/wood trap system is being implemented upstream. This system comprises two retention basins with a sill and vertical rack to retain wood debris, alongside a filter check dam equipped with hydraulic/mechanical controls to retain debris during major floods. The objective is to provide enough capacity to retain sediment during floods with over five years’ return period, striking a balance between effective retention and maintaining sediment transport during smaller discharges to prevent downstream bedload depletion. This study aims to find an efficient design of these basins using physical modelling.

METHODOLOGY

A physical model, scaled at 1:10 using Froude’s similarity rules and Shields’ bedload transport correspondace (see Saugy et al. 2022), is constructed to assess the system’s behavior (Figure 1). Various flood scenarios, from 5 to 300-year return periods, are tested by establishing flow, sediment and debris wood discharges at the upstream boundary, while the downstream boundary models the check dam. Continuous sediment measurements at the model’s outlet provide data on sediment transport dynamics and the system’s effectiveness. The check dam is designed based on the findings of Schwindt et al. (2017).

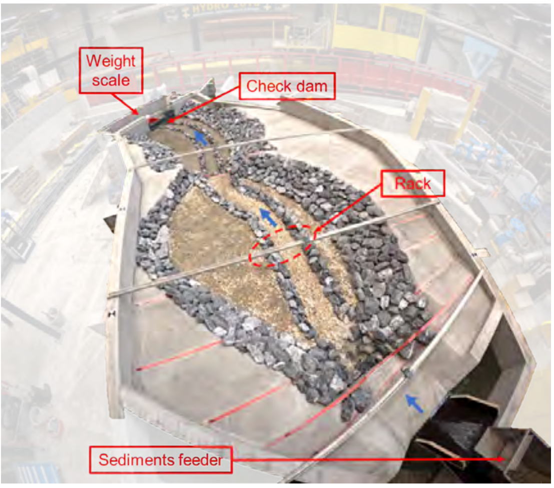

Figure 1. Downstream view of the physical model representing the sediment trap composed by two basins and two weirs upstream of each of them.

RESULTS

The results are relevant to two main issues that need to be addressed within this study: 1) ensuring adequate sediment transport and 2) effectively retaining wood debris. The first series of tests showed that the optimal vertical clearance of the grid i.e., the distance between the channel bottom and the check dams’s vertical bars is 1.8*d_{90} (d_{90}: particle diameter representing the 90% cummulative percentile value), as shown in Figure 2. This configuration facilitates sediment transport during minor floods while effectively retaining sediment for major events (Van Mol et al. 2023).

Figure 2. Check dam with the optimal bottom clearance of the vertical bars

Two different wood rack configurations have been tested in a second series of tests. The rack is situated in the middle of the upper basin. In the first step, a linear rack with small bar spacing was placed over the entire cross-section (Figure 3, left). This configuration led to sediment depletion downstream of the rack, as it retains the sediment particles as well. Consequently, a second configuration with a L-shaped rack, larger bar spacing and minor curve effect was tested. Additionally, the main channel was slightly widened to allow bedload bypassing the rack (Figure 3, right). The second configuration leads to better results, retaining only the wood debris, while sediment can be transported through the bars and the widened section. Further tests are ongoing to finalize the rack's design.

Figure 3. Two different rack configutraions to retain wood debris

REFERENCES

Saugy, J.-N., Amini, A. & De Cesare, G. 2022: Flow structure and grain motion assessments of large river widening in a physical model using ultrasonic Doppler velocity measurements. Experiment in Fluids, 63 (7). https://doi.org/10.1007/s00348-022-03430-9

Schwindt, S., Franca, M.J., De Cesare, G., & Schleiss, A.J. 2017: Analysis of mechanical-hydraulic bedload deposition control measures. Geomorphology, 295, 467–479. https://doi.org/10.1016/j.geomorph.2017.07.020

Van Mol, R. N. H. M., Schaller, N., Amini, A., Hunzinger, L. & De Cesare, G. 2023: Physical modeling of sediment trap for Le Bez River, Switzerland. Proceedings of the 40th IAHR World Congress, August 2023, Vienna, Austria

7.2
Ongoing work for the study of site amplification phenomena in the Swiss alpine valleys and their implication for the Swiss building code

Paolo Bergamo[1], Dario Chieppa[1], Francesco Panzera[2], Donat Fäh[1]

[1] *Swiss Seismological Service (SED) at ETH Zürich, Sonneggstrasse 5, CH-8092 Zürich (paolo.bergamo@sed.ethz.ch)*
[2] *Dipartimento di Scienze Biologiche, Geologiche e Ambientali, Università di Catania, Corso Italia, 57 - 95129 - Catania*

The same earthquake can affect with significantly different damage levels settlements located only few hundred meters apart. The reason is the local seismic response, which is mainly related to the geophysical properties of the soil layers in the subsurface, but also to their geometry (e.g. a large plain or a 2D/3D sedimentary basin). Therefore, alluvial valleys, and in particular deeply-incised alpine valleys, represent peculiar geological environments, as the thickness of their sedimentary infill increases from few to hundreds of meters and then decreases back to few meters along the cross-section of the valley bottom. This morphological setting causes distinctive earthquake local response effects (e.g. Bard & Bouchon 1985). Furthermore, valleys are not marginal from the risk point of view, as they can be densely populated and host critical transport and industrial infrastructures.

On this basis, in 2019 the Earthquake working group of the SIA commission 261 recommended a basic study on the topic of local earthquake response in alpine valleys, later included in the federal measures for seismic risk management (BAFU, 2020). The ongoing “Alpine Valleys” research project, carried out by the Swiss Seismological Service (SED), directly addresses this recommendation. The aim of the project is twofold: i) a systematic investigation of the amplification effects of seismic waves in the alpine valleys of Switzerland and ii) developing a proposal for their consideration in the forthcoming revision of the building code SIA 261. For these purposes, we have compiled a joint dataset of:

- Geological, topographic and morphological data, including – among others – i) a depth-to-bedrock model covering almost all Switzerland and surrounding areas (obtained collating different models, Mey et al. 2016, Swisstopo 2019 and references therein, see Fig. 1a); ii) an automatic identification and classification of the valley bottoms (Fig. 1b); iii) the national map of SIA 261 soil classes, itself a collation of various cantonal maps (BAFU, 2016, see Fig. 1c).
- Local amplification factors empirically extracted at SED (urban) free-field stations by means of empirical spectral modelling technique (ESM; Edwards et al., 2013, see Fig. 1c).

As the “Alpine Valleys” project is about to enter in its final phase, we present our current results, obtained by cross-referencing the geological/topographic/morphological datasets with the site amplification factors mentioned above. The main outcomes are the following:

- topographic amplification effects (Maufroy et al., 2015) can be observed at low frequency (≤ 1.67 Hz) on the valley beds of narrow (< 1000 m wide) alpine valleys or at the edges of wider valleys;
- amplification phenomena (in the band 1 – 10 Hz) related to 2D/3D local response effects can be observed on the bed of wide (> 2 km wide) valleys, particularly in the alpine area where the thickness of the sedimentary infill is larger.

Future work is related to correlating the 2D/3D soil response to geometrical parameters of the underlying sediments (width, depth, shape ratio) and to assessing whether the current Swiss building code (SIA 261, 2020) already includes a conservatism allowing for 2D/3D soil response phenomena in the alpine valleys, or modifications should be recommended.

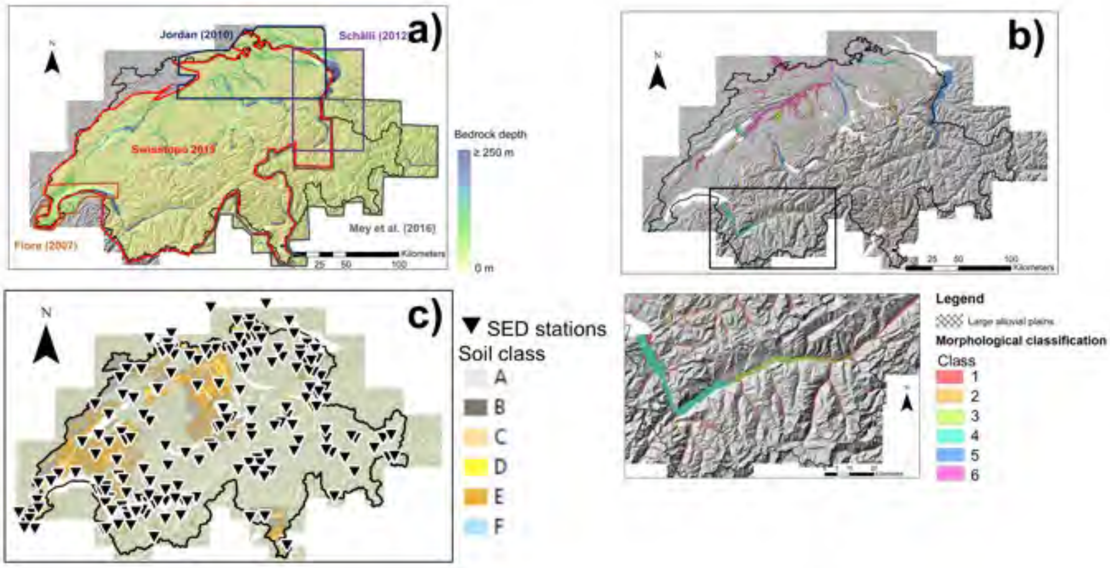

Figure 1. a) Bedrock-depth model for Switzerland, obtained collating several geological models. b) Top: morphological classification of Swiss valleys into 6 categories. Bottom: close-up on the Rhône valley. c) SED stations for which empirical amplification factors were computed, superimposed with the SIA soil class map (BAFU, 2016).

REFERENCES

Bard P. Y. and M. Bouchon,1985. The two-dimensional resonance of sediment-filled valleys. BSSA, 75(2), 519-541.

Bundesamt für Umwelt, BAFU, 2016. Karte der seismischen Baugrundklassen nach der Baunorm SIA 261.

Bundesamt für Umwelt, BAFU, 2020. Erdbebenrisikomanagement - Massnahmen des Bundes. Bericht an den Bundesrat. Standbericht und Planung für den Zeitraum 2021 bis 2024.

Edwards B., et al., 2013. Determination of site amplification from regional seismicity: application to the Swiss national seismic networks. SRL, 84(4), 611-621.

Maufroy E. et al., 2015. Frequency-scaled curvature as a proxy for topographic site-effect amplification and ground-motion variability. BSSA,105(1): 354.

Mey et al., 2016. Glacial isostatic uplift of the European Alps. Nat Commun 7, 13382 (2016).

Società svizzera degli ingegneri e degli architetti, SIA, 2020. SIA 261 Azioni sulle strutture portanti. Copyright © 2020 by SIA Zurich

Swiss Federal Office for Topography, Swisstopo, 2019. Mächtigkeitsmodell des Lockergesteins.

7.3
Recent Advancements in Data-Centric Machine Learning in Earthquake Engineering and Surrogate Modellig of Steel Moment Resisting Frames

Nenad Bijelić[1], Dimitrios G. Lignos[1]

[1] *Resilient Steel Structures Laboratory, Civil Engineering Institute, École polytechnique fédérale de Lausanne (EPFL), Lausanne, Switzerland (nenad.bijelic@epfl.ch)*

While the performance-based earthquake engineering (PBEE) approach is increasingly being utilized by practicing engineers, one of the major impediments to its widespread adoption is the heavy burden of the underlying nonlinear simulations. In that sense, data-driven machine learning (ML) approaches have been gaining research interest in the earthquake engineering domain including efforts to sidestep the nonlinear response history analyses while maintaining their predictive power. However, most of the past research efforts focused on algorithmic developments or contrasting of the performance of different ML tools – i.e., the so-called “model-centric” approach – while putting less emphasis on the most effective use of data. In contrast, this talk discusses a “data-centric” approach to seismic collapse risk assessment.

The specific objective herein is to demonstrate the opportunity for reducing the required number of physics-based simulations to trace structural collapse by leveraging domain-specific data augmentation. To this end, two recent methodological advancements are presented: 1) a surrogate-agnostic data engineering methodology for seismic collapse risk assessment, termed the automated collapse data constructor (ACDC) technique, and 2) a novel approach for seismic collapse fragility and risk estimation termed the data-driven collapse classification (D2C2) method (Bijelić et al. 2023a, 2023b).

In a nutshell, the ACDC technique leverages the training set of collapse capacity data to generate statistically similar realizations of the ground motion intensity measures (IMs) and the associated collapse capacities. The ACDC uses the conditional spectrum methodology (Baker, 2011) or its extension, the generalized conditional intensity measure (Bradley, 2010) approach, to model the distributions of the ground motions conditioned on the increasing values of the collapse capacities. The weights for the contribution of individual motions from the training set to the conditional intensity measure distributions are obtained using kernel smoothing. Note that no further physics-based analyses are required for the ACDC approach. Hence, the numerical cost of the analyses is not increased due to using data augmentation. Additionally, the ACDC approach is model agnostic, i.e., it does not depend on the specific ML or statistical tool that will be trained on the augmented data.

Once the training data is available and potentially augmented using ACDC, the D2C2 methodology is leveraged to establish the link between the input ground motion and the corresponding collapse response. The D2C2 approach is inspired by the way collapse capacities are computed using numerical response history analyses in the incremental dynamic analysis (IDA) method (Vamvatsikos & Cornell, 2002). Particularly, the response of a structure to a single ground motion is analyzed by amplitude scaling of that ground motion to a set of intensities which are typically represented by the spectral acceleration at the fundamental period of the structure. Subsequently, the numerical value of the collapse capacity in IDA procedure is effectively determined by bisection between collapse and non-collapse responses, while the precision to which the collapse capacity is determined is controlled by the choice of intensities at which to perform the response history analysis. In that sense, the collapse response is a binary variable. This allows posing of the collapse capacity prediction as a classification problem. Given this context, a practical advantage of D2C2 is that it can be directly used in the PBEE framework in the same way that IDA is used. The only difference is that a data-driven surrogate is used instead of a physics-based numerical simulation.

The utility of the proposed methodologies is demonstrated through examples from extensive case studies of seismic collapse risk estimation of steel MRF structures ranging from four to twenty stories in height. In particular, the results suggest that the ACDC and D2C2 methodologies allow dramatic improvements in the predictive capability of data-driven surrogates while at the same time significantly reducing data requirements. Moreover, a major implication and finding demonstrated in this talk is that “big data” is not paramount to effectively leverage ML tools for assessment of earthquake-induced collapse risk.

REFERENCES

Baker, J. 2011: Conditional Mean Spectrum: Tool for Ground-Motion Selection, Journal of Structural Engineering, 137, 322-331.

Bijelić, N., Lignos D.G. & Alahi, A. 2023a: The automated collapse data constructor technique and the data-driven methodology for seismic collapse risk assessment, Earthquake Engineering and Structural Dynamics, 52, 2452-2479.

Bijelić, N., Skiadopoulos, A. & Lignos D.G. 2023b: Surrogate modelling for seismic collapse risk assessment of steel moment resisting frames, Proceedings of the Canadian Conference – Pacific Conference on Earthquake Engineering 2023,

Vancouver, British Columbia, Canada.
Bradley, B.A. 2010: A generalized conditional intensity measure approach and holistic ground-motion selection, Earthquake Engineering and Structural Dynamics, 39, 1321-1342.
Vamvatsikos, D. & Cornell, C.A. 2002: Incremental dynamic analysis, Earthquake Engineering and Structural Dynamics, 31, 491-514.

7.4
The transdisciplinary design of user-centered seismic risk maps

Irina Dallo[1], Laura Noemi Schnegg[2], Michèle Marti[1], Donat Fulda[3], Athanasios N. Papadopoulos[1], Paolo Bergamo[1], Simon Ramon Wenk[1], Nadja Valenzuela[1], Philippe Roth[1], Laurentiu Danciu[1], Florian Haslinger[1], Donat Fäh[1], Philipp Kästli[1], and Stefan Wiemer[1]

[1] *Swiss Seismological Service at ETH Zurich, Switzerland (irina.dallo@sed.ethz.ch)*
[2] *Department of Environmental System Science, ETH Zurich, Switzerland*
[3] *Georesources Switzerland Group, Department of Earth Sciences, ETH Zurich, Switzerland*

Maps are a widely used tool to communicate spatial hazard and risk information to the public, with the aim of increasing individual risk awareness. The use of maps is triggered by scientific evidence that maps are the format most preferred by the public. However, past studies have shown that maps are often misinterpreted if not well designed, and can trigger wrong attitudes. Thereby, the different elements, such as the icons on the map, the chosen layers, the legend, or the used colour scale, influence the comprehension of the information on the map. In the context of natural hazards, and more precisely earthquakes, research has so far mainly focused on the design of hazard maps, and little has been studied about the effective design of risk maps. We thus assessed how to design understandable, helpful, and action-oriented seismic risk maps for the public.

To this end, we – an interdisciplinary group at the Swiss Seismological Service at ETH Zurich – applied a transdisciplinary study in Switzerland. First, we co-designed different versions of the seismic risk map, varying the colour scale and legend type. Second, we tested these versions with a public survey (between-subjects experiment) in December 2022, representative of the German- and French-speaking parts of Switzerland. We assessed which map version performed best regarding the correct interpretation, perceived usefulness, risk perception, and motivation to take protective action. Further, we analysed whether certain social groups (e.g., house owners) have specific preferences, risk perceptions, or intentions to take action.

Our findings, among others, revealed that i) a legend with the combination of qualitative and quantitative labels leads to more accurate interpretations and is preferred by the public; ii) the colour scale mainly determines how people perceive the spatial risk; and iii) personal factors influence people's interpretation skills, risk perception, and intention to take action. The insights from the survey led to the final earthquake risk map of Switzerland (see Figure 1).

At the conference, we will present this study and provide recommendations on how to best design user-centered earthquake risk maps to ensure their effective use by societies.

This project has received funding from the Federal Office for the Environment (FOEN), the Federal Office for Civil Protection (FOCP), and the Swiss Federal Institute of Technology Zurich (ETH Zurich).

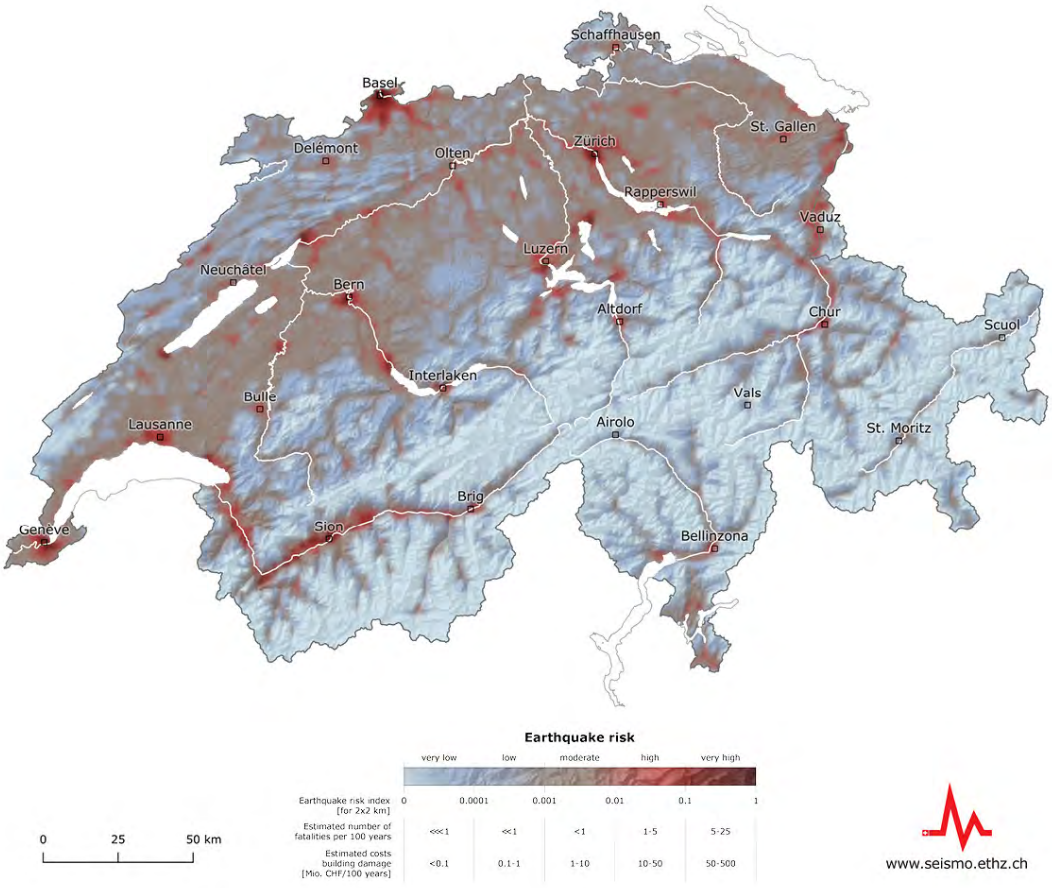

Figure 1. The earthquake risk map of Switzerland, which is based on an index that combines the expected number of fatalities with the estimated financial losses due to building damage [seismo.ethz.ch].

7.5
Monitoring and evolutionary analysis of the Cadegliano Viconago landslide between Switzerland and Italy

Alessandro De Pedrini[1,2], Maurizio Pozzoni[1], Christian Ambrosi[1], Simone Ghezzi[1], Alessio Spataro[1], Luca Osculati[3], Alessandro Uggeri[3]

[1] *Institute of Earth Sciences, University of Applied Sciences and Arts of Southern Switzerland, Via Flora Ruchat-Roncati 15, CH-6850 Mendrisio (alessandrio.depedrini@supsi.ch)*
[2] *Department of Earth Sciences, Swiss Federal Institute of Technology, Sonneggstrasse 5, CH-8092 Zürich*
[3] *Idrogea Servizi S.r.l., Via C. Rovera 26, IT-21026 Gavirate*

The landslide of Cadegliano Viconago in the province of Varese (IT) has been for over twenty years a danger to the population and infrastructures located along the course of the Tresa river, at the border between Italy and Switzerland. The landslide leads to the accumulation of debris which has caused flows in several events on the provincial road passing at the foot of the landslide. The slope even shows traces of deep damage which manifests with the exposure of scarps and traction fractures, with even centimeter displacements during the most intense rainfall events. A catastrophic collapse would lead to the partial or total interruption of the road system, a barrage of the Tresa river with the possible formation of a basin and the destruction of a well field for drinking water use in Switzerland.

Even though in recent years of monitoring it was observed a trend towards smaller displacements, intense and prolonged rains could drastically influence the dynamic behavior of the landslide and cause a catastrophic failure.

For this reason, thanks to the financing of an Interreg project with the involvement of the Interregional Agency for the Po River and the Canton Ticino Land Department, two DMS (Differential Monitoring of Stability) columns were installed in March 2021 to investigate the landslide activity and to define alert thresholds. DMS multiparameter columns provide continuous data with detailed displacement, accelerometric, and piezometric measurements. The deep monitoring data joined by geodetic measurements since 2006, provide information on the landslide's dynamics. The monitoring, the cores from the drilling, and the in-situ surveys provide a basis to set a numerical stability model to understand the slope kinematics and the response to the water table changes.

Although the first years of monitoring with the DMS columns were devoid of intense and prolonged rains, the rainfall/displacement relation is appreciable analyzing the most intense rain events recorded in autumn 2002 and 2014. In that period, the humidity status identified by the Standard Precipitation Index (SPI) showed a very high value and coincided with the opening or extension of tensile fracture.

Regarding the volume affected by the disruption, our analysis suggests a slip surface at a depth of about thirty meters which can plausibly lead to the detachment of a volume mass ranging from 70'000 to over 2'000'000 m^3.
The numerical stability model was followed by expansion models of the unstable mass which produced scenarios with possible consequences also in Swiss territory.

Figure 1. Net in adherence stretched by the movement of the slope

Figure 2. On-situ installation of the DMS column

7.6
An Experimental Framework for Statistical Validation of System Level Assumptions in Seismic Analysis of RC Structures

Medhat Elmorsy[1,2], Michalis F. Vassiliou[1]

[1] *Chair of Seismic Design and Analysis, Institute of Structural Engineering (IBK), ETH Zürich Stefano-Franscini-Platz 5 CH-8093 Zürich, Switzerland (medhat.elmorsy@ibk.baug.ethz.ch)*
[2] *Structural Engineering Department, Mansoura University, Mansoura, Egypt*

Structural response to earthquakes is an inherently stochastic problem. Therefore, numerical model validation at all levels (material, component, and system level) should be statistic. Such a statistical procedure (Bachmann et al. 2018) is possible at a material and a component level, but it is currently impossible at a system level due to the prohibitive cost of performing multiple shake table tests with virgin identical specimens. Therefore, there is a need to develop a methodology to perform low cost system-level seismic testing of RC structures, so that it can be performed multiple times and increase the available datasets for model calibration. It is also worth noting that the lack of such test datasets has led to very different modeling approaches proposed in the literature.

To this end, testing of multiple small-scale RC models (on the order of 1:30-1:40) in a geotechnical centrifuge is proposed. The tests will be used to validate the global level assumptions for given component level behavior, experimentally obtained cyclic tests performed at the component level. Figure 1 depicts the proposed framework.

The geotechnical centrifuge preserves similitude of stresses and is used in lieu of the "Artificial Mass Simulation" method in which nonstructural masses are added to preserve similitude (Moncarz & Krawinkler 1981). As it is ineffcient to manufacture such small scale reinforcing cages by hand, the scaled reinforcement will be manufactured with a metal 3D printer, to make the construction of multiple specimens more efficient and timewise feasible – something that was not possible before 3D printing.

This paper discusses material and component level tests performed at the model scale (Elmorsy et al. 2023a, 2023b). The tests reveal that (a) the mechanical properties of 3D printed submillimeter rebars can be adjusted by modulating the printing parameters, (b) concrete mechanical properties that are suitable for the discussed framework can be achieved using gypsum as a binder, (c) reasonable (compared to full scale rebars) bond behavior between the rebars and the concrete can be acieved by adjusting the mix design and the rebar surface ribs, and (d) upon testing RC columns under cyclic loading, similar (to full scale cylic tests RC columns) failure mode, stiffness, strength, and ductility could be achieved.

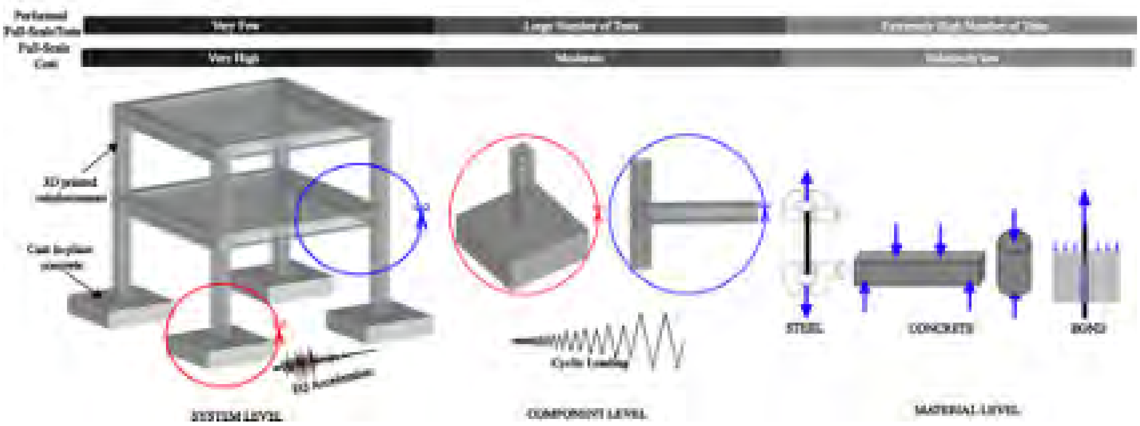

Figure 1. Ilustration of the three levels of the framework; System level, Component level, and material level.

REFERENCES

Bachmann, J., Strand M., Vassiliou, M.F., Broccardo, M., & Stojadinovic, B. 2018: Is rocking motion predictable?, Earthquake Engineering & Structural Dynamics, 47(2), 535-552.

Elmorsy, M., Wrobel, R., Leinenbach, C., & Vassiliou, M.F. 2023: Material Testing of Micro-Concrete and 3D-Printed Reinforcement for Use in Small-Scale Seismic Testing of RC Structures, 9th ECCOMAS Thematic Conference on

Computational Methods in Structural Dynamics and Earthquake Engineering (COMPDYN 2023), Athens, Greece.
Elmorsy, M., Wrobel, R., Leinenbach, C., & Vassiliou, M.F. 2023: Additively Manufactured Steel Reinforcement for Small Scale Reinforced Concrete Modeling: Tensile and Bond Behavior, Materials and Design (under review).
Moncarz, P. & Krawinkler, H. 1981: Theory and Application of Experimental Model Analysis in Earthquake Engineering, John A Blume Earthquake Engineering Center, Department of Civil Engineering, Stanford, California.

7.7 Comparing three avalanche periods mapped from optical remote sensed imagery around Davos, Switzerland

Elisabeth D. Hafner[1,2,3], Holger Heisig[4], Mathias Zesiger[4], Yves Bühler[1,2]

[1] *WSL Institute for Snow and Avalanche Research SLF, Davos Dorf, 7260, Switzerland (elisabeth.hafner@slf.ch)*
[2] *Climate Change, Extremes, and Natural Hazards in Alpine Regions Research Center CERC¸ Davos Dorf, 7260, Switzerland*
[3] *EcoVision Lab, Photogrammetry and Remote Sensing, ETH Zurich, Zurich, 8092, Switzerland*
[4] *Federal Office of Topography swisstopo, Wabern, 3084, Switzerland*

Avalanche warning, hazard zoning, hazard mitigation measures, forestry and risk management profit from accurate and relibale documentation to better understand past avalanche periods. In recent years the systematic mapping of avalanches over large areas with remote sensing has been shown to be reliable (Hafner at al., 2021) and relying on machine learning also time-effective (i.e., Hafner et al., 2022). In a case study around Davos, Switzerland, we analyze three avalanche periods (in 1999, 2018, 2019) with very high avalanche danger (level 5) and compare them to large scale hazard indication simulations of avalanches with a 100 year return period (LSHIM; Bühler et al., 2022). For the avalanche period in 1999 we relied on imagery acquired by airplane on the 25th of February after three distinct periods with approximately 3 m of new snow in 30 days (SLF, 2000). The greyscale data was acquired with a scale of 1:30 000 and processed by swisstopo (Federal office of Topography) this year to orthophotos with a spatial resolution of 0.5m. For 2018 and 2019 SPOT 6/7 satellite data with a spatial resolution of 1.5m and information in the channels red, green, blue and near-infrared was tasked after periods with high and very high avalanche danger (for details see Bühler et al., 2019). The avanches were in all cases manually mapped with the methodology described in Bühler et al., 2019. For comparison we have chosen the warning region of Davos, covering approx. 176km^2, 81.2% of it classified as potential avalanche terrain according to the LSHIM.

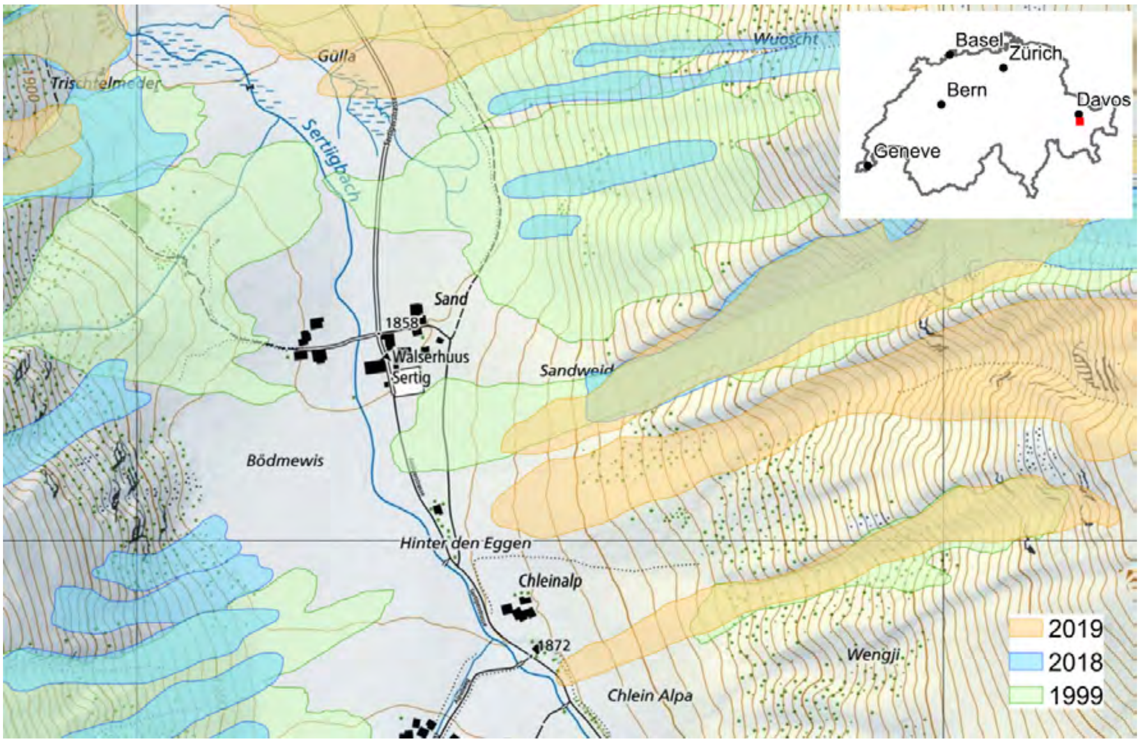

Figure 1. Comparison of the avalanches mapped from optical remote sensing data after periods with very high avalanche danger in 1999, 2018 and 2019 around Sertig Sand, Davos, Switzerland (map source: Federal Office of Topography).

REFERENCES

Bühler, Y*., Hafner, E. D*., Zweifel, B., Zesiger, M., and Heisig, H. 2019: Where are the avalanches? Rapid SPOT6 satellite data acquisition to MAP an extreme avalanche period over the Swiss Alps, The Cryosphere, 13, 3225–3238, https://doi.org/10.5194/tc-13-3225-2019. * these authors contributed equally

Bühler, Y., Bebi, P., Christen, M. (2022). Large Scale Hazard Indication Simulations for avalanches, canton of Grisons. *EnviDat.* https://www.doi.org/10.16904/envidat.316.

SLF:Eidg. Institut für Schnee- und Lawinenforschung (Ed.). (2000). Der Lawinenwinter 1999. Ereignisanalyse. Davos: Eidg. Institut für Schnee- und Lawinenforschung.

Hafner, E. D., Techel, F., Leinss, S., and Bühler, Y.2021: Mapping avalanches with satellites – evaluation of performance and completeness, The Cryosphere, 15, 983–1004, https://doi.org/10.5194/tc-15-983-2021.

Hafner, E. D., Barton, P., Daudt, R. C., Wegner, J. D., Schindler, K., and Bühler, Y. 2022: Automated avalanche mapping from SPOT 6/7 satellite imagery: results, evaluation, potential and limitations, The Cryosphere Discussions, 2022, 1–20, https://doi.org/10.5194/tc-2022-80.

7.8
An Update from the Seismic Monitoring of the Brienz/Brinzauls rock slope instability

Mauro Häusler[1,2], Franziska Glüer[1], Donat Fäh[1]

[1] *Schweizerischer Erdbebendienst SED, Institut für Geophysik, ETH Zürich, Sonneggstrasse 5, CH-8092 Zürich (mauro.haeusler@sed.ethz.ch)*
[2] *Spektrum Geophysik AG, Florastrasse 18, 4600 Olten*

Ensuring a reliable monitoring of unstable rock slopes is imperative for the effective mitigation of landslide risks. We present a study on the partial collapse of the Brienz/Brinzauls landslide in Switzerland that occurred in June 2023, utilizing seismic techniques. Our investigation involves the analysis of ambient vibration data acquired prior to, during, and subsequent to the collapse, aiming to uncover insights into the mechanisms driving the landslide with the ultimate goal to detect seismic precursors that could be used for early warning.

Employing automated frequency tracking techniques over a span of five years (2018 – 2023), we monitored parameters such as resonance frequencies, wavefield polarization, amplitudes, and seismic activity rate. These seismic observables are compared to surface deformation rates measured by Global Navigation Satellite System. In this study, we update already published findings (2018 – 2020; Häusler et al., 2022) until July 2023 including the partial collapse of the “Insel” compartment.

Our findings uncover noteworthy alterations in seismic parameters leading up to the collapse, which correlate with high intensity of rock fall, a reduction in resonance frequency, and shifts in wavefield polarization. Importantly, the seismic data exhibits an immediate response during and after the event, gradually reverting to values similar to pre-event levels within two weeks following the failure. This study enriches our understanding of landslide dynamics, thus improving the development of potential early-warning systems.

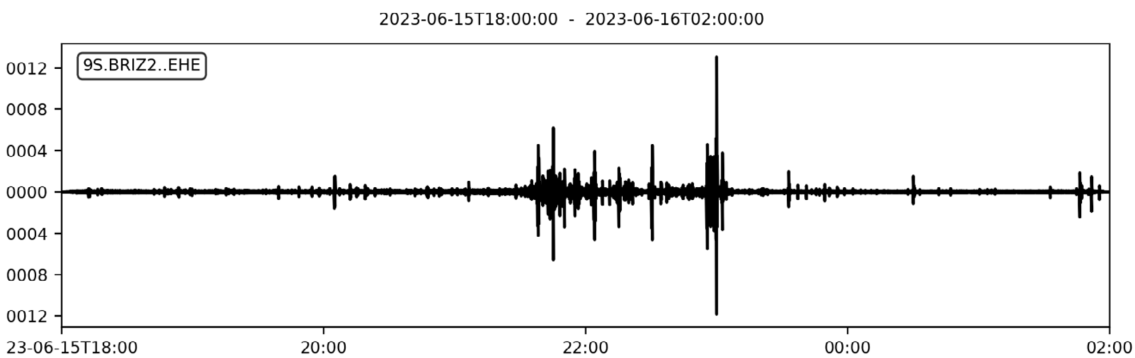

Figure 1. Seismic trace (East-component) of the night of 15 / 16 June 2023. The partial collapse occurred between 21:30 and 00:00 (UTC).

REFERENCES
Häusler, M. et al. 2022. Monitoring the changing seismic site response of a fast-moving rockslide (Brienz/Brinzauls, Switzerland), *GJII*, 2022 https://doi.org/10.1093/gji/ggab473

7.9
A scenario-based earthquake loss assessment for Basel, Switzerland

Afifa Imtiaz[1], Athanasios Papadopoulos[1], Paolo Bergamo[1], Donat Fäh[1]

[1] *Swiss Seismological Service (SED), ETHZ, Switzerland (afifa.imtiaz@sed.ethz.ch)*

Scenario-based earthquake loss assessment plays a pivotal role in understanding the potential impacts of earthquakes on communities and infrastructures. It provides valuable insights for disaster preparedness, emergency planning, and risk reduction policy-making. In this work, we present results of loss assessments for the building stocks of canton Basel-Stadt based on the strongest historical earthquake (Mw=6.6) that occurred in 1356.

We followed the general framework established in the recently released Earthquake Risk Model of Switzerland (ERM-CH23; Wiemer et al., 2023). Figure 1 summarizes the components considered in the process. The seismic hazard is based on the latest update of the national hazard model (SUIhaz2015, Wiemer et al., 2016). To represent the ground shaking properties, two ground motion models were considered: a macrosesmic intensity-based model (MIM) and a spectral acceleration-based model (SAM). A set of four Intensity Prediction Equations (IPEs) was used. As a first step, we used the spectral period-dependent national amplification model developed under ERMCH-23 (Wiemer et al., 2023). It will be replaced by local models in the next stage. The national model is based on the empirically observed site response cross-referenced with a lithological classification, thickness of quaternary sediments, and topographical slope. It also provides the estimation of site-to-site variability and single-site within-event variability, which were used to estimate the intra-event variability. Amplification maps have been derived for Peak Ground Velocity (PGV) and pseudo-spectral acceleration (PSA) at 0.3, 0.6, and 1 s. The building inventory of the area has been retrieved from the extensive geo-referenced database assembled by the Federal Office for the Environment (FOEN). It has been classified according to a specifically developed building taxonomy for Switzerland and a set of fragility curves was obtained for them. The consequence model was developed based on international models and adapted to Swiss practices. The fragility models and consequence models are convolved to derive vulnerability functions, which relate ground shaking intensity to loss ratio. In order to propagate all the recognized uncertainties, a logic tree approach was used as in ERM-CH23 (see Wiemer et al., 2016).

We performed the scenario simulation for individual buildings by using the OpenQuake engine (Pagani et al., 2014). The EMS98 damage scale of buildings (Grünthal et al., 1998) has been used to characterize five damage grades: slight, moderate, substantial, very heavy (partial collapse), and destruction (complete collapse) as DG1 to DG5. Figure 2 shows a summary of total damages (DG2 to DG5) and losses from the scenario by residential quarters. We observe that half of the building damages occur mostly in masonry buildings, the highest being in the historical quarter, the central part of the canton comprised of old masonry building structures. It indicates that building vulnerability influences damage distribution more than ground motion amplification in Basel.

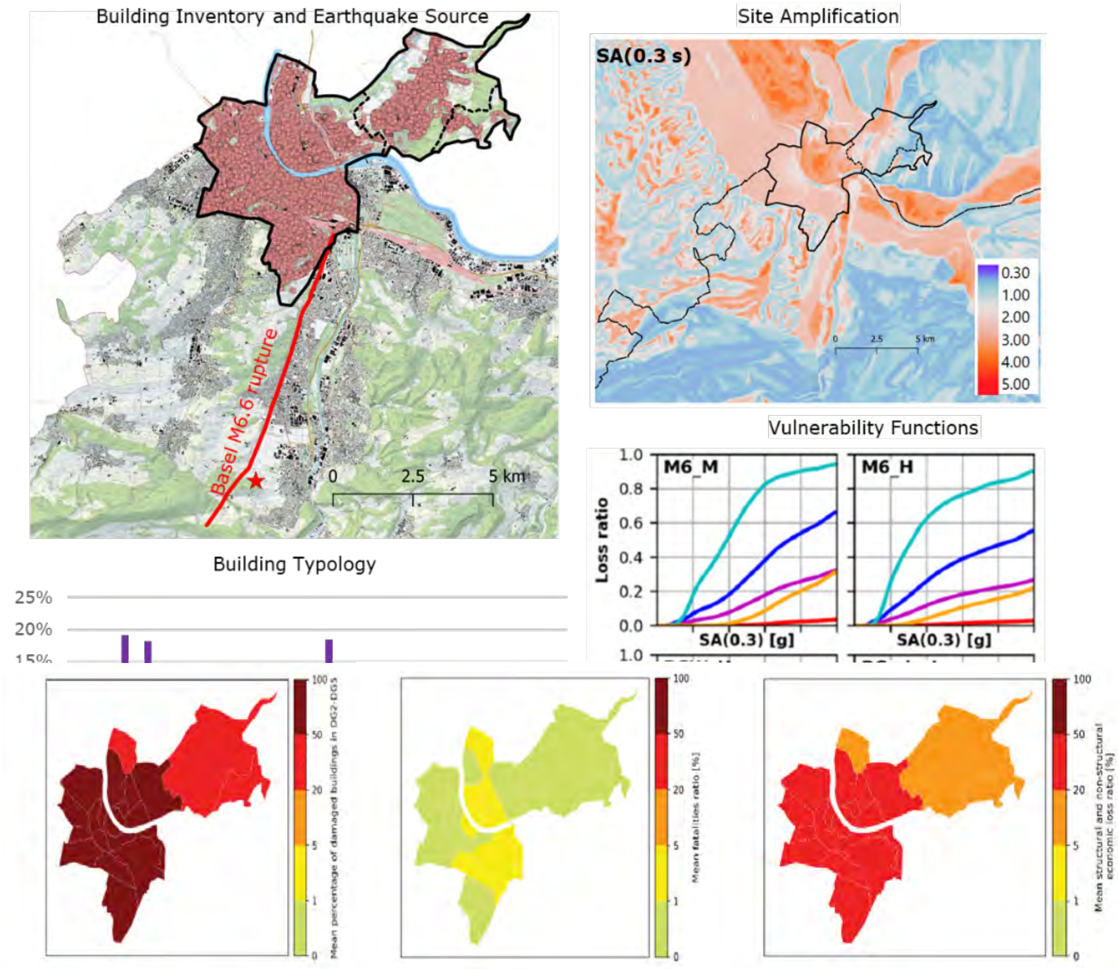

Figure 2. Results (DG2 to DG5) from the scenario as mean percentage of each residential quarter – damaged buildings (left), fatalities (middle), and economic loss from building damages (right).

REFERENCES

Grünthal, G., Musson, R. M. W., Schwartz, J., & Stucchi, M. 1998. European Macroseismic Scale 1998 (Vol. 15). Luxembourg: Cahiers du Centre Européen de Géodynamique et de Séismologie.

Pagani, M., Monelli, D., Weatherill, et al. 2014. OpenQuake Engine: An Open Hazard (and Risk) Software for the Global Earthquake Model. Seismological Research Letters, 85(3), 692–702. doi: 10.1785/0220130087

Wiemer, S., Papadopoulos, A., Roth, P., Danciu, L., Bergamo, P., Fäh, et al. 2023: Earthquake Risk Model of Switzerland (ERM-CH23), Swiss Seismological Service, ETH Zurich. doi: https://doi.org/10.12686/a20

Wiemer, S., Danciu, L., Edwards, B., et al. 2016: Seismic Hazard Model 2015 for Switzerland (SUIhaz2015), Swiss Seismological Service (SED) at ETH Zurich, 164 pp., 2016.

7.10
Experimental investigation of the size effect on the seismic behaviour of unreinforced masonry walls

Ernesto Inzunza Araya[1], Savvas Saloustros[1], Katrin Beyer[1]

[1] *Earthquake Engineering and Structural Dynamics Laboratory (EESD), School of Architecture, Civil and Environmental Engineering (ENAC), École Polytechnique Fédérale de Lausanne (EPFL), 1015 Lausanne (ernesto.inzunza@epfl.ch)*

The drift capacity of URM walls is a significant parameter not only for assessing existing structures, but also for seismic design of masonry structures. In fact, the new version of Eurocode Part 1-1 includes guidelines to account on the inelastic behaviour of structures, where the deformation capacity is a necessary variable. To address this task, empirical drift capacity models based on experimental evidence are currently used. These models include the influence of some wall features, like failure mode, but they are still limited to the available experimental data. Although there are data sets of URM walls coming from various test campaigns, there is no precedent of an experimental campaign specifically studying the effect of wall size on displacement capacity. This paper presents an experimental study of the size effect on the drift capacity of URM masonry walls built with hollow clay bricks and standard cement mortar. A total number of 6 quasi-static cyclic tests have been performed for 3 different wall sizes (heights of 2.8 m, 2.0 m and 1.4 m) and 2 different levels of compression load (axial load ratios of 0.10 and 0.20). All the specimens had the same aspect ratio (L/H) of 0.75 and were tested under double bending boundary conditions to observe a shear-controlled behaviour. By means of this work is possible to identify the principal mechanical phenomena controlling the size effect (important for extending analytical formulations) and to provide with valuable experimental data to validate some further numerical studies. Indeed, the evidence obtained from this campaign it is a valuable contribution to previous numerical studies developed on the size effect of URM walls (Dolatshahi et al. 2018, Lourenço 1997). Furthermore, this research also provides a reference for how small test specimens can be for obtaining drift capacity values in storey-high walls.

REFERENCES

Dolatshahi, K. M., Nikoukalam, M. T., & Beyer, K. 2018: Numerical study on factors that influence the in-plane drift capacity of unreinforced masonry walls. Earthquake Engineering & Structural Dynamics, 47 (6), 1440-1459.

Lourenço, P. B. 1997: Two aspects related to the analysis of masonry structures: Size effect and parameter sensitivity, Tech. rep., Faculty of Engineering, TU Delft, Netherlands.

7.11
Assessing the possibility of nonlinear soil response in the Lucerne area

Paulina Janusz[1], Luis Fabian Bonilla[2], Paolo Bergamo[1], Donat Fäh[1]

[1] Swiss Seismological Service, ETH Zürich, Sonneggstrasse 5, 8092 Zürich, Switzerland (paulina.janusz@sed.ethz.ch)
[2] Université Gustave Eiffel, 14-20 Boulevard Newton, Cité Descartes, 77447 Marne-la-Vallée Cedex 2, France

In areas of low or moderate seismic hazard like central Switzerland, the influence of nonlinear soil behaviour on seismic risk is often unknown; however, it becomes important when large return periods are considered. In the case of strong earthquakes, some areas like the city of Lucerne are especially vulnerable to nonlinear response and related liquefaction because of their location on soft, water-saturated deposits that are prone to severe site effects (Janusz et al., 2022).

We have developed a procedure to study nonlinear soil response in areas such as Lucerne, where recordings of strong ground motions are not available. First, we calibrate the soil column parameters using CPT (Cone Penetration Test), and measured ground motion amplification and velocity profiles from active and passive seismic data. We simulate wave propagation in complex media using a fully-nonlinear finite-difference code NOAH (Bonilla et al., 2005). As we perform a simulation with effective stress analysis, soil dilatancy parameters (Iai et al., 1990) that describe the development of pore pressure excess in the used constitutive model are required. For this, we use the inversion procedure introduced by Roten (2014) based on CPT data and the Neighbourhood algorithm (Sambridge, 1999). As input ground motions, we use sets of 11 scaled waveforms (Panzera et al., 2021) that are compatible with soil class "A" and match the elastic response spectrum for return periods of 475 and 975 years used for buildings of importance class I and III in the Swiss building code SIA261 (2020). The waveforms are corrected to Swiss rock reference (Poggi et al., 2011), and deconvolved to remove the surface effect and define the incident wavefield (Hallo et al., 2022).

The results show a high possibility of strong nonlinear behaviour (Figure 1), soil cyclic mobility, and liquefaction for some tested scenarios and sites; however, we observe a variability that depends on the input ground motion and location. The response is highly influenced by the occurrence of strong pore pressure effects in the soil that can happen even in very thin sandy layers. As we cannot verify the simulations using strong motion observation recorded in Lucerne, we compare them to empirical data from other areas concluding that we predict reasonable levels of nonlinearity. Furthermore, we also test the sensitivity of the method to the model parameters, including soil dilatancy parameters, assessing the epistemic uncertainty.

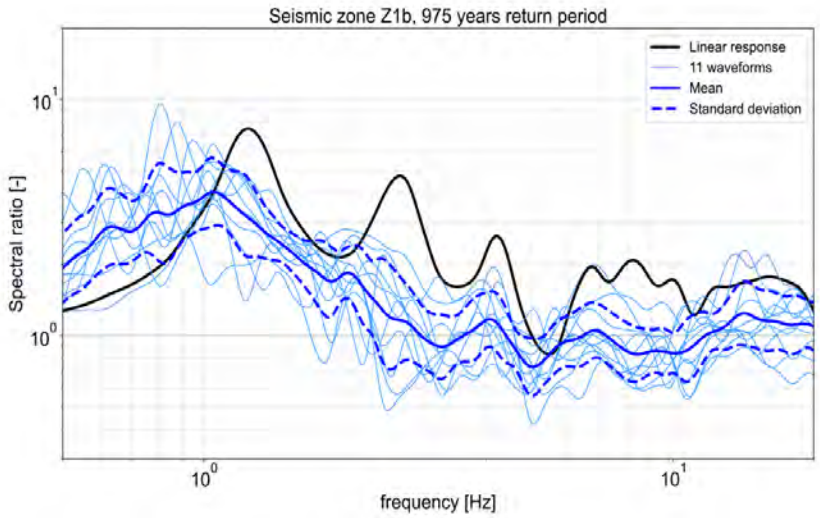

Figure 1. Comparison of Fourier spectral ratios with respect to the Swiss rock profile (Poggi et al., 2011) for linear and nonlinear simulations using 11 waveforms compatible with the elastic response spectrum for seismic zone Z1b (SIA261, 2020) and building importance class III corresponding to about 975 years return period in the seismic hazard.

REFERENCES

Bonilla, L. F., Archuleta, R., & Lavallée, D. 2005: Hysteretic and dilatant behavior of cohesionless soils and their effects on nonlinear site response: Field data observations and modeling. Bulletin of the Seismological Society of America, 95, 2373–2395.

Hallo, M., Bergamo, P., & Fäh, D. 2022: Stochastic Model to Characterize High-Frequency Ground Motion at Depth Validated by Kik-Net Vertical Array Data. Bulletin of the Seismological Society of America. https://doi.org/10.1785/0120220038

Iai, S., Matsunaga, Y., & Kameoka, T. 1990: Parameter Identification for a Cyclic Mobility Model (Report of the Port and Harbour Research Institute Vol. 29, No. 4, pp. 57–83).

Janusz, P., Perron, V., Knellwolf, C., & Fäh, D. 2022: Combining Earthquake Ground Motion and Ambient Vibration Recordings to Evaluate a Local High-Resolution Amplification Model—Insight From the Lucerne Area, Switzerland. Frontiers in Earth Science, 10. https://doi.org/10.3389/feart.2022.885724

Panzera, F., Bergamo, P., Laurentiu, D., Fäh, D. 2021:Worldwide Strong motion metadata inspection to select design-compatible waveforms for Switzerland: Preliminary results. 37th General Assembly of the European Seismological Commission, 2021.

Roten, D. 2014: Documentation of tools for analysis of nonlinear soil behavior.

Sambridge, M. 1999: Geophysical inversion with a neighbourhood algorithm—I. Searching a parameter space. Geophysical Journal International, 138(2), 479–494. https://doi.org/10.1046/j.1365-246X.1999.00876.x

SIA261. 2020: Actions on Structures, SIA 261. Swiss Standards, Swiss Society of Engineers and Architects.

7.12
Early detection of ground motion using satellite radar interferometry (InSAR) - Gwalpeten rockslope instability (Bisistal, Kanton Schwyz)

Nina Jones[1], Tazio Strozzi[1], Rafael Caduff[1], Lukas Inderbitzin[2], Markus Hodel[2], Sonja Stadlin[2]

[1] *GAMMA Remote Sensing AG, Worbstrasse 225, CH-3073 Gümligen (jones@gamma-rs.ch)*
[2] *Umweltdepartement Kanton Schwyz, Amt für Wald und Natur, Abteilung Naturgefahren, Bahnhofstrasse 9, CH-6431 Schwyz*

The Gwalpeten rockslope instability was located at the very back of the Bisistal valley in the Canton of Schwyz at approximately 2’708’415 / 1’194’530. The instable rock face was about 120 m high, 130 m wide and on average 30 m deep. On Sunday 30 July 2023 it collapsed in two phases resulting in a rock avalanche; first, an initial fall of about 150,000 cubic metres occurred, followed by a second collapse of about 330,000 cubic metres. Due to the surrounding talus and mountain pasture landscape, the collapse caused no loss of life or damage to key buildings and infrastructure.

Prior to the event, we analysed the displacement rate of the rockslope instability with Satellite Radar Interferometry (InSAR). This analysis was commissioned due to the known instable nature of the area and occurrence of repeated rock falls in past years. For our study we considered 41 ERS-1/2 images acquired between 04.06.1992 - 29.10.2000 from descending orbit 480, 35 ENVISAT images acquired between 19.10.2003 - 17.10.2010 from descending orbit 480, 36 ENVISAT images acquired between 20.06.2003 - 01.10.2010 from ascending orbit 251, 68 Radarsat-2 images acquired between 09.05.2011 - 23.11.2019 from descending orbit 16 and 382 Sentinel-1 images acquired between 26.01.2015 - 09.03.2023 from descending orbit 66. To determine slow (mm-cm per year), continuous slope movements from 1992 to 2013, standard Persistent Scatterer Interferometry (PSI) was applied on multi-annual stacks of radar images. Due to higher velocities starting in 2014, a mean seasonal movement rate for the summer months was then determined using advanced PSI and InSAR methods based on Radarsat-2 and Sentinel-1 SAR data.

Time series from the PSI and InSAR analysis with annually (up to and including 2013) and seasonally (in summer, from 2014) averaged displacements (e.g., Figure 1) show a clear increase in movement from about 1-3 cm/a in the 1990’s and 2000’s to more than 5 cm/a from 2014 to 2018 and up to 10 cm/year in 2019 and 2020. A further clear acceleration up to 20 cm/year was then observed in 2021, with a subsequent deceleration to 15 cm/yr in summer 2022. Due to snow cover and low coherence, no data from the winter months could be considered for a continuous time series evaluation. Seasonal changes in movement could therefore not be determined. Nevertheless, individual coherent interferograms are available from which we can visually assume that the displacement in the Gwalpeten instability was generally faster in summer and slower in winter.

An analysis with Sentinel-1 and SAOCOM images acquired in 2023 during the snow-free period prior to the collapse of 30 July 2023 is ongoing to inspect the potential and limits of InSAR in early warning. This analysis also aims to identify gaps and define useful procedures for a systematic displacement monitoring programme involving radar images acquired from various current and future missions.

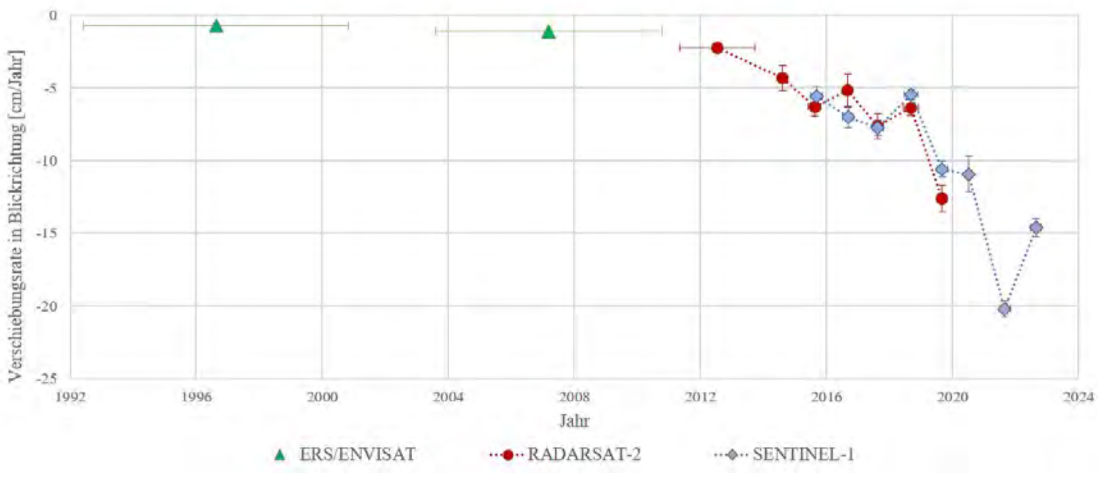

Figure 1. Time series of the displacement rate in the satellite line-of-sight direction from the PSI analysis with annually (up to and including 2013) and seasonally (in summer, from 2014) averaged displacements. Horizontal bars show the measurement interval, vertical bars the estimated errors of the measurements.

7.13
Shake-table response of a bridge-like model with rocking piers and restraining tendons

Antonios A. Katsamakas[1], Michalis F. Vassiliou[1]

[1] *Chair of Seismic Design and Analysis, Institute of Structural Engineering (IBK), ETH Zürich, Stefano-Franscini-Platz 5, CH-8093 Zürich (katsamakas@ibk.baug.ethz.ch)*
[2] *Chair of Seismic Design and Analysis, Institute of Structural Engineering (IBK), ETH Zürich, Stefano-Franscini-Platz 5, CH-8093 Zürich (vassiliou@ibk.baug.ethz.ch)*

Rocking structures are the ones that uplift from their base when they are subjected to sufficiently strong ground motion excitation. Uplift works as a mechanical fuse, limiting the seismic forces transmitted to the structure. Therefore, rocking can be used as a seismic design strategy for buildings and bridges. This study presents the shake-table response of a bridge-like model under 170 ground motion excitations. The model represented a simplified bridge in 1:5 scale. It comprised four cylindrical rocking columns capped with a thick concrete slab. The columns were connected to the concrete slab with steel tendons (one tendon per column). The tendons were fixed at the top of the slab and at the base of the column.The axial stiffness of the tendons provided positive post-uplift stifness to the system. The columns were allowed to rock and wobble, whereas steel restrainers prevented the columns from sliding out-of-position. After subjected to 170 design-level ground motions, the specimen demostrated zero damage and minimal residual displacements. The peak displacements were below 250 mm (in model scale), thus compatible to the ones expected in seismically-isolated structures. The maximum force recorded at the tendons was below 70% of their maximum strength. The accelerations transmitted to the superstructure were below 0.2 g. The slab rotations were moderate and below 0.04 rad. The above confirm the efficiency of rocking as a seismic design strategy, especcially when combined with steel tendons to provide positive lateral stiffness to the system. The experimental results promote the understanding and designing of rocking systems and provide an extensive dataset for the calibration of numerical models.

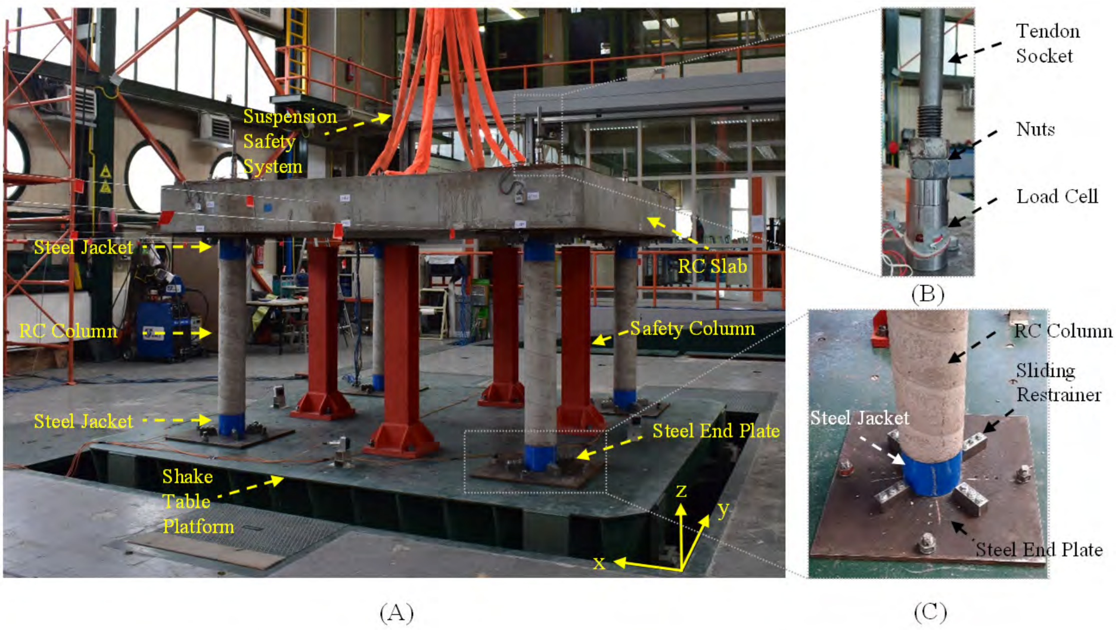

Figure 1. (A) Side view of the tested structure, (B) Detail of the fixation of the tendon on top of the concrete slab, (C) Detail at the base of the rocking column.

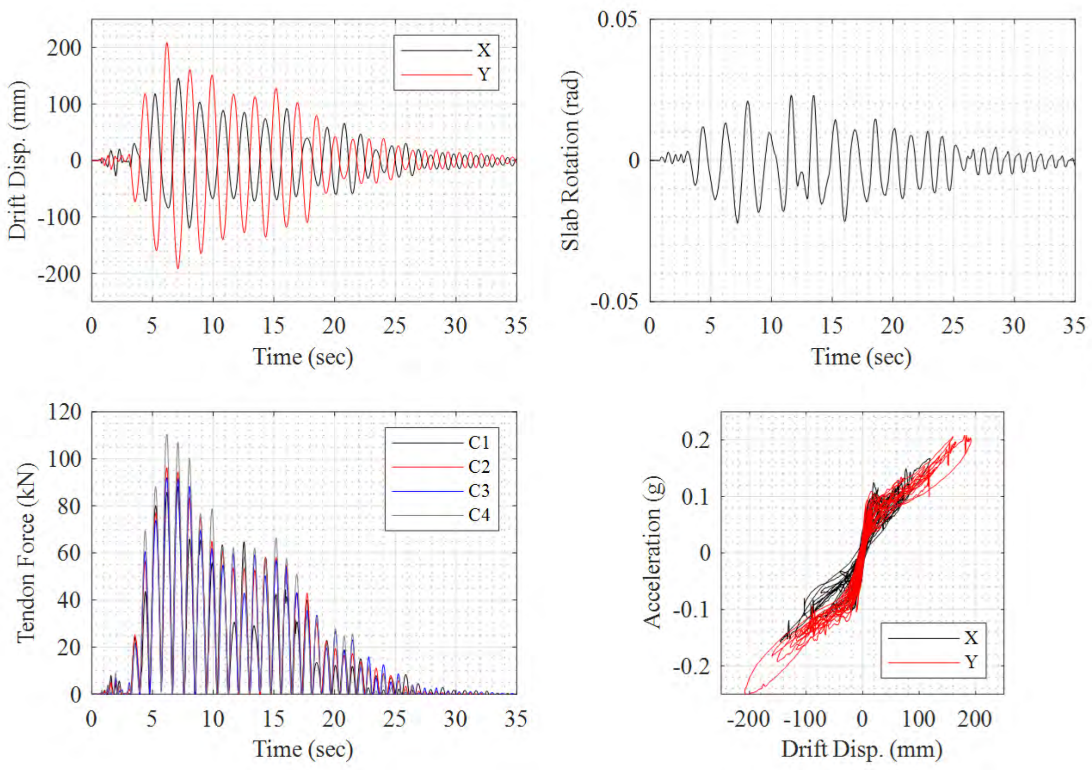

Figure 2. Indicative structural response under the 1971 San Fernando ground motion (Los Angeles, USA), as recorded in Hollywood Stor station.

REFERENCES

Reggiani Manzo, N., Vassiliou, M.F., Mouzakis, H., Badogiannis, E. 2022: Shaking table tests of a resilient bridge system with precast reinforced concrete columns equipped with springs, Earthquake Engineering & Structural Dynamics, 51, 213-239.

Katsamakas, AA., Vassiliou, M.F. 2022: Finite element modeling of free-standing cylindrical columns under seismic excitation, Earthquake Engineering & Structural Dynamics, 1-20.

7.14
Long-period waveform modelling in sedimentary basins using spectral-element simulations to estimate ground motion in the Rhône valley and Swiss Molasse basin

Maria Koroni[1], Paolo Bergamo[1], Laura Ermert[1], Daniel Roten[2], Donat Fäh[1]

[1] Swiss Seismological Service, ETH Zürich, Sonneggstrasse 5, CH-8092 Zürich (maria.koroni@sed.ethz.ch)
[2] University of California San Diego, 9500 Gilman Drive, La Jolla CA 92093

In this study 3D simulations of seismic waveforms with resolvable periods up to *2 seconds* are performed, using 1D velocity models of two geologically significant areas in Switzerland: the Rhône valley and the Swiss Molasse Basin (SMB). Understanding the seismic response of these sedimentary basins is important because of the high seismic hazard in the Sion area (Swiss Hazard Model, *SUIhaz2015, Wiemer, et al., 2016*), and the existence of Swiss nuclear facilities mainly situated within SMB, respectively.

The seismic modelling introduced in our study has two main objectives. The first is to validate existing models of seismic velocity, address their spatial characteristics, and provide insights on necessary improvements by comparing synthetic to existing data from recorded events with magnitudes larger than M_w4. The second is to develop a methodology for simulating scenario earthquakes. This will help to improve our understanding of long-period ground shaking by generating high-fidelity synthetic ground motion data.

The simulations are performed using state-of-the-art spectral-element methods as implemented in the commercial software Salvus (*Afanasiev et al., 2019*; *Hapla et al., 2021*). In our simulations, the surface topography is fully accounted for, important for Swiss areas surrounded by high mountains that may affect wave propagation quite significantly. The velocity profiles used in this study are taken from existing studies of the Rhône valley (*Roten et al., 2008)* and the 1D velocity profile of SMB (*Campus & Fäh, 1997*). We run synthetic simulations of the 2005 Vallorcine event (FR) with M_w4.4 for the Rhône valley (CH) and for the SMB, the 2017 Urnerboden event with M_w4.1 is used.

The synthetics are compared in terms of displacement and velocity waveforms to observed data recorded on stations of the permanent Swiss seismic network that exist within the computational domain of our study. With the comparisons, we aim to validate the 1D velocity models used for simulating synthetics. The goodness of fit assessed at all stations will also indicate areas that need improvements in subsurface velocity modelling.

Spectral-element methods allow for increasing complexity of the mesh. Some important features of sedimentary basins such as crossing boundaries between the geological layers can thus be properly implemented. This will gradually lead to more accurate modelling of past and scenario earthquakes that may occur at long return periods in and affect areas in Switzerland where critical infrastructure is located or seismic hazard is high.

REFERENCES
Roten, D., Fäh, D., Olsen, K.B. & Giardini, D. 2008: A comparison of observed and simulated site response in the Rhône valley, Geophysical Journal International, 173, 958-978.
Campus, P. & Fäh, D. 1997: Seismic monitoring of explosions, a method to extract information on the isotropic component of the seismic source, Journal of Seismology, 1, 205-218.
S. Wiemer, L. Danciu, B. Edwards, M. Marti, D. Fäh, S. Hiemer, J. Wössner, C. Cauzzi, P. Kästli, K. Kremer 2016: Seismic hazard model 2015 for Switzerland (SUIhaz2015), Swiss Seismological Service (SED) at ETH Zurich, Zurich, Switzerland.
Hapla, V., Knepley, M.G., Afanasiev, M., Boehm, C., van Driel, M., Krischer, L. & Fichtner A. 2021: Fully parallel mesh I/O using PETSc DMPlex with an application to waveform modelling. SIAM Journal on Scientific Computing, 43(2): C127–C153.
Afanasiev M. and others, Modular and flexible spectral-element waveform modelling in two and three dimensions, Geophysical Journal International, Volume 216, Issue 3, March 2019, Pages 1675–1692, https://doi.org/10.1093/gji/ggy469

7.15
Response of structures on shallow foundations under conditions of earthquake induced liquefaction

Eva Korre[1], Han Yang[2], Boris Jeremic[3], Ioannis Anastasopoulos[1]

[1] Institute for Geotechnical Engineering, ETHZ, Stefano-Franscini-Platz 5, CH-8093 Zurich (evkorre@ethz.ch)
[2] School of Civil Engineering, Tianjin University, 43-C220, Peiyang Park Campus: No.135 Yaguan Road, Haihe Education Park, Tianjin, 300350, China
[3] Department of Civil and Environmental Engineering, University of California, Davis, 3147 Ghausi Hall One Shields Avenue Davis, CA 95616

Earthquake-induced liquefaction can occur during an earthquake in loose sandy soils below the ground water table. Liquefaction is associated with rising pore water pressures,leading to partial or total loss of the soil's shear strength and to the soil behaving similar to a viscous fluid. Experience from previous earthquakes has revealed its disastrous consequences, including excessive settlement and rotation up to complete toppling,especially in dense urban environments.

The complexity of this phenomenon calls for advanced and highly specialized constitutive models, able to accurately capture the soil response under liquefied conditions. The advanced constitutive model SANISAND (Dafalias & Manzari, 2004) was utilized in this work, since it allows full hydromechanical coupling between the solid and fluid phase in the soil, allowing thus the phenomenon of earthquake-induced liquefaction to be properly simulated. Calibration of the constitutive model was materialized by taking advantage of the extensive database of soil element tests (cyclic and monotonic triaxial compression tests, as well as constant volume direct simple shear tests, CVDSS), performed in the laboratory facilities of the Chair of Geotechmical Engineering at ETHZ.

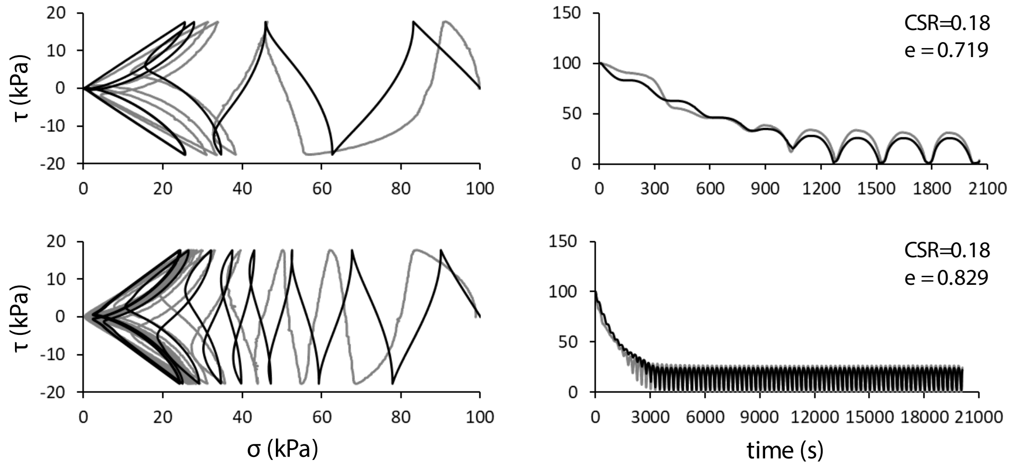

Figure 1 Comparison between numerical and experimental results for CVDSS tests, performed at two different void ratios, for a different number of cycles.

After confirming that on a soil element level the response was consistent to the one experimentally observed (Fig. 1), the next step was to validate the FE model against existing centrifuge experiments performed by Adamidis & Madabhushi, (2017, 2018).

Six numerical models were generated in total corresponding to the six different centrifuge experiments performed by Adamidis & Madabhushi, (2017, 2018). The centrifuge models tested a rigid structure resting on shallow strip foundations, of width . Two different assumptions were made regarding the structure's weight: light, applying of overburden pressure to the underlying soil and heavy, applying of overburden pressure to the underlying soil. In total, three soil profiles with and varying thickness , so that / were investigated.

For the Finite Element (FE) simulations, the open source numerical analysis code Real-ESSI (REAListic modeling and simulation of Earthquakes, and/or Soils, and/or Structures and their Interaction), developed at UC Davis (http://sokocalo.engr.ucdavis.edu/~jeremic/Real_ESSI_Simulator/) was utilized. Real-ESSI offered the comparative advantage of being an open source software, with four key novelties which contributed to tackiling the complexity of this problem:

(a) The u-p-U element formulation, which to the authors' knowledge has not been applied to any 3D finite element (FE) analysis for soil liquefaction so far.
(b) The fully coupled interface, taking into account the interaction between the fluid phase of the soil material with the solid phase of the structure.
(c) The DRM (Domain Reduction Method) boundaries, which allow accurate simulation of "free field boundaries" and realistic wave propagation in dynamic problems.
(d) FE simulation of the soil liquefaction problem with the possibility of large complex models via parallel processing.

The overall response of the models showed that for shallow soil profiles (/) there were discrepancies between the numrical prediction and the exprimental results in terms of excess pore water pressure and settlement, as well as the structure's response in terms of acceleration and settlements. For deeper liquefiable layers (/) the numerical prediction was significantly improved. This improvement was attributed to the combined effect of the comparatively higher effective stresses being developed inside the soil and the larger distance of the bottom soil boundary. The former reduced numerical issues, providing increased robustness to the analysis, while the latter reduced the effect of reflections and refractions of seismic waves.
The best comparison between the FE analyses and the experimental results was achieved with the deep model (both with the light and the heavy structure). However, the response in the area below the structure where soil-structure interaction is more prominent, was not fully consistent with the experimental results, overestimating the generated excess pore water pressure.

ACKNOWLEDGMENTS
This work was supported by an ETH Zurich Postdoctoral Fellowship.

REFERENCES

Dafalias, Y. F., & Manzari, M. T. 2004: Simple Plasticity Sand Model Accounting for Fabric Change Effects, Journal of Engineering Mechanics, 130(6), 622–634. doi: 10.1061/(asce)0733-9399(2004)130:6(622)
Adamidis, O., & Madabhushi, S. P. G. 2017: Deformation mechanisms under shallow foundations on liquefiable layers of varying thickness, Géotechnique, 1–12. doi: 10.1680/jgeot.17.p.067
Adamidis, O., & Madabhushi, S. P. G. 2018: Experimental investigation of drainage during earthquake-induced liquefaction, Géotechnique,68(8), 655–665. doi: 10.1680/jgeot.16.p.090

7.16
ERM-CH23: New Perspectives on Earthquake Risk Assessment and Management in Switzerland

P. Roth[1], A. N. Papadopoulos[1], L. Danciu[1], P. Bergamo[1], F. Panzera[5], D. Fäh[1], B. Duvernay[2], A. Khodaverdian[3], P. Lestuzzi[3], O. Odabasi[4], E. Fagà[4], P. Bazzurro[4], N. Schmid[1], P. Kästli[1], N. Valenzuela[1], M. Marti[1], I. Dallo[1], F. Haslinger[1], S. Wiemer[1]

[1] *Swiss Seismological Service, ETH Zurich, Switzerland*
[2] *Federal office for the environment, Bern, Switzerland*
[3] *École Polytechnique Fédérale de Lausanne, Switzerland*
[4] *RED Risk Engineering + Development, Pavia, Italy*
[5] *Department of Biological, Geological and Environmental Sciences, University of Catania, Italy*

Effective seismic risk mitigation requires a thorough understanding of the risks at both the national and sub-national levels. In Switzerland, earthquakes can occur throughout the country and are considered to be the natural hazard with the potential for causing the greatest damage. In this context, we present insights from the development of the first national earthquake risk model of Switzerland, known as ERM-CH23, developed under the coordination of the Swiss Seismological Service. ERM-CH23 advances the understanding of earthquake risk in Switzerland as it incorporates the latest science, updated datasets, and local expertise. The model features a high-resolution site amplification model, an exposure model based on an extensive geo-referenced database of building objects across the country, and a complex logic tree that allows a comprehensive consideration of different sources of uncertainty. The OpenQuake engine developed by the Global Earthquake Model was used to execute event-based probabilistic risk analyses, as well as loss and damage assessment for selected historical and synthetic earthquake scenarios. ERM-CH23 assesses several types of loss, including economic losses due to damage to building components and contents, as well as human losses such as deaths, injuries, and displacement. We give an overview of the model and its results as well as of various downstream products and applications. Overall, ERM-CH23 provides valuable insights into seismic risk in Switzerland and is expected to serve as a valuable tool for seismic risk management in the country.

This project has received funding from the Federal Office for the Environment (FOEN), and the Federal Office for Civil Protection (FOCP)

7.17
Setup for monitoring snow depth changes in an avalanche prone area

Pia Ruttner-Jansen[1,2,3], Julia Glaus[1,2], Annelies Voordendag[3,4], Andreas Wieser[3], Yves Bühler[1,2]

[1] *WSL Institute for Snow and Avalanche Research SLF, Flüelastrasse 11, CH-7260 Davos Dorf (pia.ruttner@slf.ch)*
[2] *Climate Change, Extremes, and Natural Hazards in Alpine Regions Research Center CERC, CH-7260 Davos Dorf*
[3] *Institute of Geodesy and Photogrammetry, ETH Zurich, Stefano-Franscini-Platz 5, CH-8093 Zurich*
[4] *Department of Atmospheric and Cryospheric Sciences (ACINN), University of Innsbruck, Innrain 52f, A-6020 Innsbruck*

Avalanches are a threat to people and infrastructure in mountainous areas. There are different protection measures, with road closures being a temporary measure decided by a committee of local experts if a safe passage on traffic lines cannot be guaranteed. The decisions of the local experts are based on the avalanche bulletin, the weather forecast, data from autonomous weather stations and most importantly, personal experience. However, accurate and timely information about the current snow conditions on the slopes are often missing. A major driver influencing the avalanche danger level, especially after new snow, is the wind. Wind drifted snow causes inhomogeneities in the snow depth, leading to local accumulations that are more prone to avalanching. Information on the snow depth variations would be a valuable input for the experts, aiding their decisions on road closures or openings.

To fill in that gap, we propose an experimental setup to map and monitor the snow depth distribution in avalanche release areas. A low-cost LiDAR sensor and a photo camera, accompanied by several meteorological sensors measure the changes of snow depth at high spatiotemporal resolution. A first realization of the setup will be installed close to the skiing resort at Jakobshorn in Davos and is designed to operate autonomously for the upcoming winter seasons. The system is controlled remotely, and the data is available in (near-) real time. This enables an insight into the on-site conditions, without taking any risks in entering dangerous terrain in critical situations.

The newly acquired snow depth database, together with the recorded meteorological parameters will be the basis for different modelling and simulation approaches. These enable the possibility to extrapolate from the first study site and transfer the approach to other regions. Finally, all data will be provided to the local experts that need to take decisions on road safety measures.

7.18
Results of the seismological and geotechnical investigations of submerged slopes in Lake Lucerne

Anastasiia Shynkarenko[1], Katrina Kremer[1,2], Agostiny Marrios Lontsi[1,3], Paolo Bergamo[1], Donat Fäh[1]

[1] *Swiss Seismological Service, ETH Zurich, Sonneggstrasse 5, CH-8092 Zurich, Switzerland (a.shynkarenko@sed.ethz.ch)*
[2] *Institute of Geological Sciences and Oeschger Centre for Climate Change Research, Baltzerstrasse 1+3, CH-3012 Bern, Switzerland*
[3] *Faculty of Engineering and Technology, University of Buea, PO Box 63 Buea, Cameroon*

Unstable slopes pose a major natural hazard both in the offshore and onshore environments. In addition to the primary danger related to sediment sliding, offshore slope failures can trigger tsunamis. Such slope failure-triggered tsunamis occurred in Swiss lakes (e.g., in 563 in Lake Geneva and 1601 in Lake Lucerne; Hilbe et al. 2011; Kremer et al. 2012). Nowadays, the shores of Swiss lakes are densely populated and occupied by important infrastructures. Therefore, it is crucial to investigate and monitor the submerged lake slopes to assess and mitigate the risks related to their potential failure.

The triggers of submerged slope failures can be of seismic or aseismic nature and call for the investigation of the structure, sediment properties, and seismic response of the slopes. To test a multi-disciplinary approach to investigate the submerged slopes using seismological and geotechnical methods, we have selected Lake Lucerne in Central Switzerland (Fig. 1a).

The seismological methods – ambient vibration and earthquake-based – were used to (i) resolve the subsurface slope structure and shear-wave velocity profiles down to depths of more than 100 meters (Fig. 1b) and (ii) assess the seismic response of investigated slopes in terms of resonance frequencies and amplification functions (Shynkarenko et al. 2023). The geotechnical methods – in-situ Cone Penetration Tests with pore pressure measurement (CPTu) and laboratory tests – allowed us to assess the index properties of the sediments, the undrained shear strength (Fig. 1c), the consolidation state, etc. The thickness of the sediments and topography of the slopes was resolved using the existing reflection seismic and multibeam bathymetry data, respectively (Shynkarenko 2023 and references therein). Collected information allowed us to (i) perform a 1D static stability analysis and identify the locations with the highest failure potential (Shynkarenko et al. 2022), (ii) back-analyze past subaqueous slope failures in Swiss lakes and evaluate the threshold for the failure triggering in terms of earthquake magnitude and epicentral distance, macroseismic intensity, and ground motion intensity measures (Fig. 1d).

In summary, the combination of the applied methods provides a comprehensive characterization of the structure, seismic response, and sediment properties of subaqueous lake slopes at complementing scales, depths, and resolution. For future studies, obtained information constitutes the input for numerical modelling of submerged slope behavior under static or dynamic loading.

REFERENCES

Hilbe, M. et al. 2011: Subaqueous morphology of Lake Lucerne (Central Switzerland): implications for mass movements and glacial history, Swiss Journal of Geosciences, 104, 425–443, doi: 10.1007/s00015-011-0083-z
Kremer, K. et al. 2012: Giant Lake Geneva tsunami in AD 563, Nature Geoscience, 5(11), 756–757, doi:10.1038/ngeo1618
Shynkarenko, A. et al. 2021: Investigating the subsurface in a shallow water environment using array and single-station ambient vibration techniques, Geophysical Journal International, 227(3), 1857-1878, doi:10.1093/gji/ggab314
Shynkarenko, A. et al. 2022: Geotechnical characterization and stability analysis of subaqueous slopes in Lake Lucerne (Switzerland), Natural Hazards, 113, 475-505, doi:10.1007/s11069-022-05310-1
Shynkarenko, A. 2023: Characterization of structure and stability of subaqueous lake slopes using seismological and geotechnical data, PhD Thesis #28929, ETH Zürich, doi:10.3929/ethz-b-000602257
Shynkarenko, A. et al. 2023: On the seismic response and earthquake-triggered failures of subaqueous slopes in Swiss lakes, Geophysical Journal International, 235(1), 566–588, doi:10.1093/gji/ggad240

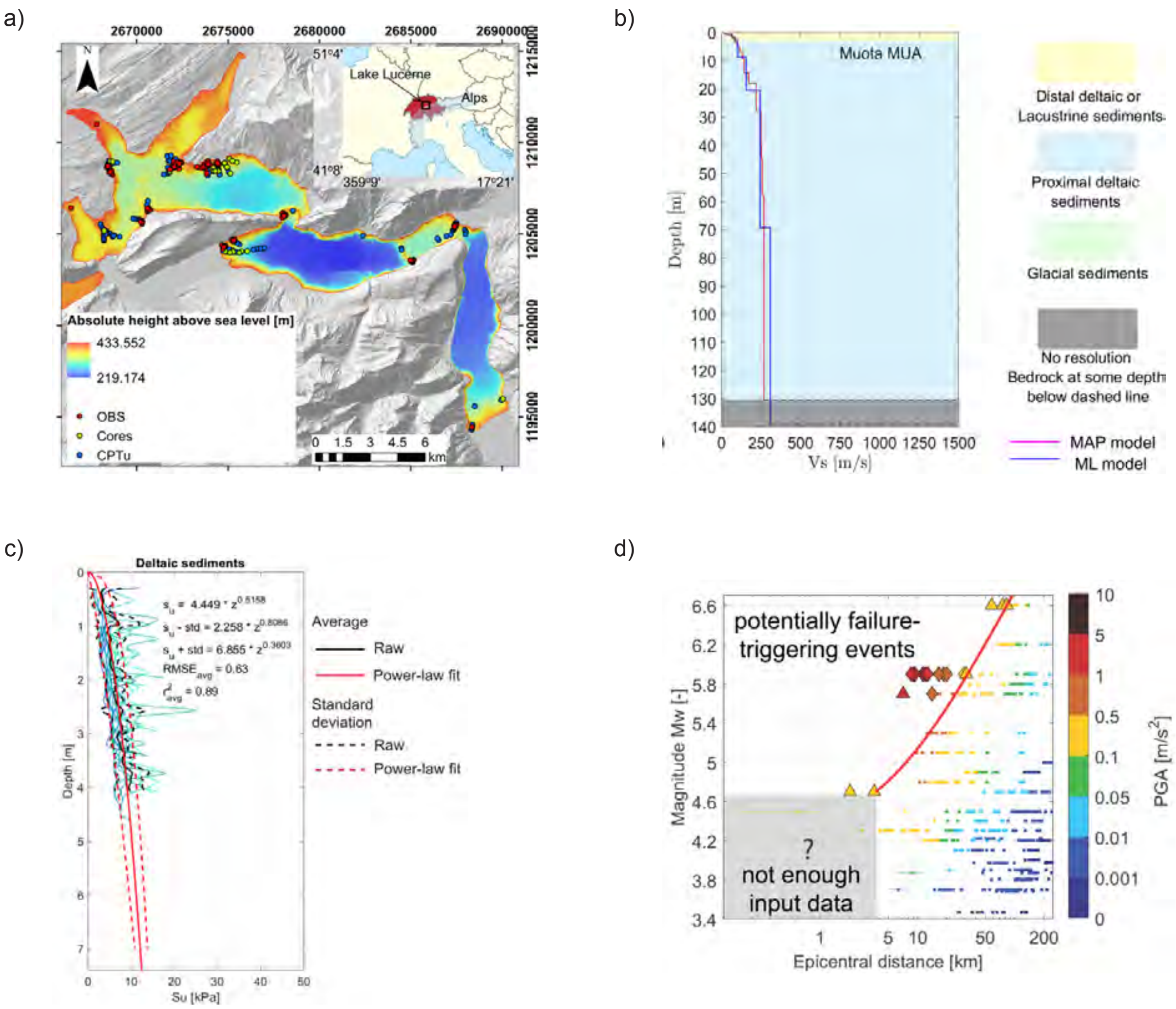

Figure 1. a) Locations in Lake Lucerne that were investigated with seismological (OBS) and geotechnical (cores, CPTu) methods (Shynkarenko 2023); b) Maximum a posteriori (MAP) and maximum likelihood (ML) shear-wave velocity profiles with assigned lithological units for deltaic site Muota (Shynkarenko et al. 2021); c) Undrained shear strength profile for deltaic sediments fitted with the power-law equation (Shynkarenko et al. 2022); d) Moment magnitude (M_w) vs epicentral distance (R_e) plot for each earthquake-site pair in our dataset; the points' shape represents the type of failure evidence (Shynkarenko et al. 2023).

7.19
From the Swiss Earthquake Risk Model to the Swiss Earthquake Resilience Model

Božidar Stojadinović[1], Nikola Blagojević[1], Lukas Bodenmann[1], Safak Arslantürkoglu[1]

[1] *Chair of Structural Dynamics and Earthquake Engineering, Institute of Structural Engineering (IBK), Department of Civil, Environmental and Geomatic Engineering (BAUG), ETH Zürich, Stefano-Franscini-Platz 5, CH-8093 Zürich*

The recently completed Swiss Earthquake Risk model represents a significant step forward for the seismology, earthquake engineering and earthquake risk management communities. This model builds on the Swiss Earthquake Hazard model and focuses on the earthquake risk exposure of the buildings in Switzerland. While maintenance and periodic updating of Swiss Earthquake Risk model is an important future task, the next, new, step is the development of the Swiss Earthquake Resilience model.

Earthquake resilience comprises three processes: the two processes of earthquake occurrence and quantification of its consequences are already included in an earthquake risk model; the process of post-earthquake recovery of the affected built environment and society is key to extending an earthquake risk model to the earthquake resilience model. The principal dimensions of an earthquake resilience model are its duration (time) and its regional (spatial) nature.

Post-earthquake risk assessment is a regional effort. It goes beyond the seismic risk assessment for individual structures prescribed in the SIA 269/8 code for seismic evaluation and retrofit of structures, both in detail and quantity. The specifics of the Swiss building inventory require specific and more detailed damage state assessment (Arslantürkoglu 2023) than that inherent to the risk models based of a more generic EMS-98 approach. Early-arriving data on a few buildings inspected after an earthquake can, crucially, help to increase the accuracy of the risk assessment of all buildings in the entire affected region using, for example, Bayesian techniques (Bodenmann 2023a). Finally, the very measure of risk needs to be adapted to the regional nature of the problem (Bodenmann 2023b).

Post-earthquake recovery is a regional problem, too. Sheltering the population of the affected region requires regional coordination among the less damaged buildings and designed temporary or permanent shelter facilities. Re-establishing the basic societal functions, such as healthcare, education and commerce, requires functional buildings. This entails the provision of power, water, transportation and communication services provided by the regional infrastructure systems, and engenders interdependencies.

Post-earthquake recovery is a long process, compared to the very short earthquake occurrence and somewhat longer post-earthquake risk assessment processes. The repair and return to function of buildings in the affected region requires coordination of planning, financing, design and construction efforts on a regional scale. The engineering aspects of the recovery process (Blagojević 2023), together with multiple interdependencies, go well beyond the REDI framework, but can be modelled using modern and comprehensive reginal resilience quantification frameworks, such as iRe-CoDeS (Blagojević 2022).

Extending the Swiss Earthquake Risk model to the Swiss Earthquake Recovery model is possible. However, these initial steps need to be completed:

- Repair and functional recovery modelling of the buildings. This step requires active engagement of the Swiss earthquake engineering community to develop repair and functional recovery models specific to the typical Swiss buildings as well as to the typical Swiss repair and recovery strategies and actions.
- Modelling of the damage, repair and functional recovery of the civil infrastructure systems. This step requires a collaborative effort of seismologists and earthquake engineers with the infrastructure system operators, businesses and cantonal and federal governments to understand the operations of the infrastructure systems and priorities for the re-establishment of their functions.
- Modelling of the societal consequences of an earthquake, extending beyond the repairs to restoration of societal functions, such as healthcare, education and commerce, and management of the funding and other resources, such as manpower, machinery and materials on a reginal scale. This step requires collaboration with the insurance industry and cantonal and federal policy makers.

REFERENCES

Arslantürkoglu, S. and Stojadinovic B. 2023. Seismic Fatality Risk Evaluation Framework for Existing Buildings in Switzerland, Bulleting of Earthquake Engineering, https://doi.org/10.1007/s10518-022-01558-x

Bodenmann, L., Reuland Y. and Stojadinovic B. 2023a. Dynamic Post-Earthquake updating of Regional Damage Estimates using Gaussian Processes, Reliability Engineering and System Safety, https://doi.org/10.1016/j.ress.2023.109201

Bodenmann, L., Broccardo M., Galanis P. and Stojadinovic B. 2023b. The Role of Risk Measures in Relating Earthquake Risks at Buildings and Portfolio Levels, Earthquake Engineering and Structural Dynamics, https://doi.org/10.1002/eqe.3878

Blagojevic, N. and Stojadinovic B. 2022. A Demand-Supply Framework for Evaluating the Effect of Resource and Service Constraints on Community Disaster Resilience", Resilient Cities and Structures, https://doi.org/10.1016/j.rcns.2022.03.001

Blagojevic, N., Terzic V. and Stojadinovic B. 2023. F-RecN + iRe-CoDeS: Computational Framework for Regional Recovery simulation using Advanced Building Recovery Models, Engineering Structures, https://doi.org/10.1016/j.engstruct.2023.116156

P 7.1
Seismo@School – A Swiss-wide initiative to bring current earthquake knowledge to schools

Irina Dallo[1], Maren Böse[1], György Hetényi[2], and Romain Roduit[3]

[1] *Swiss Seismological Service at ETH Zurich, Switzerland (irina.dallo@sed.ethz.ch)*
[2] *University of Lausanne, Switzerland*
[3] *Centre Pédagogique Prévention Séismes, Switzerland*

At the beginning of the twentieth century, floods and droughts were the natural hazards that caused the most fatalities around the world. However, today the highest death tolls are mainly due to large earthquakes. In Switzerland, earthquakes are the natural hazard with the highest damage potential. Earthquake education and preparedness are key to mitigating earthquake risk. Recent studies, however, have shown that the awareness of seismic hazard and risk and knowledge about earthquakes in general are low in Switzerland. On the other hand, there is a strong interest to learn more about natural hazards and to participate in citizen science activities.

Children and teenagers are an ideal target group for educational efforts, because of their natural sense of curiosity and wonder for science. By talking to parents and friends, key messages can be easily spread across society. Further, students learn which protective actions they can take and, once older, they can support mitigation policies and measures since they have fundamental knowledge about earthquakes and their risks. Despite several institutions having already developed information on earthquakes for the general public, there is a lack in providing access to dedicated materials making it attractive and easy for teachers and students to learn more about this topic, especially in an explorative and interactive way.

In a two-year project "*Increasing Earthquake Awareness in Switzerland*" funded by the Swiss National Science Foundation, we will build on past and current efforts to develop educational materials and activities for secondary schools (12-18 years old), allowing students to jointly explore earthquake-related topics and to increase their awareness and (practical) knowledge (Figure 1). To this end, we will help teachers to prepare their educational activities most efficiently, and will also install low-cost, but efficient, seismometers in a network of schools. The ultimate goal is a Swiss-wide seismo@school program in several languages, with a network of teachers, regular activities, and links with international seismo@school projects including fostering cross-border activities, e.g. with Nepal.

At the conference, we will present the current status of the project, provide an overview of teachers' needs for informational materials and school activities, and share our plans for expanding the network of seismometers in schools.

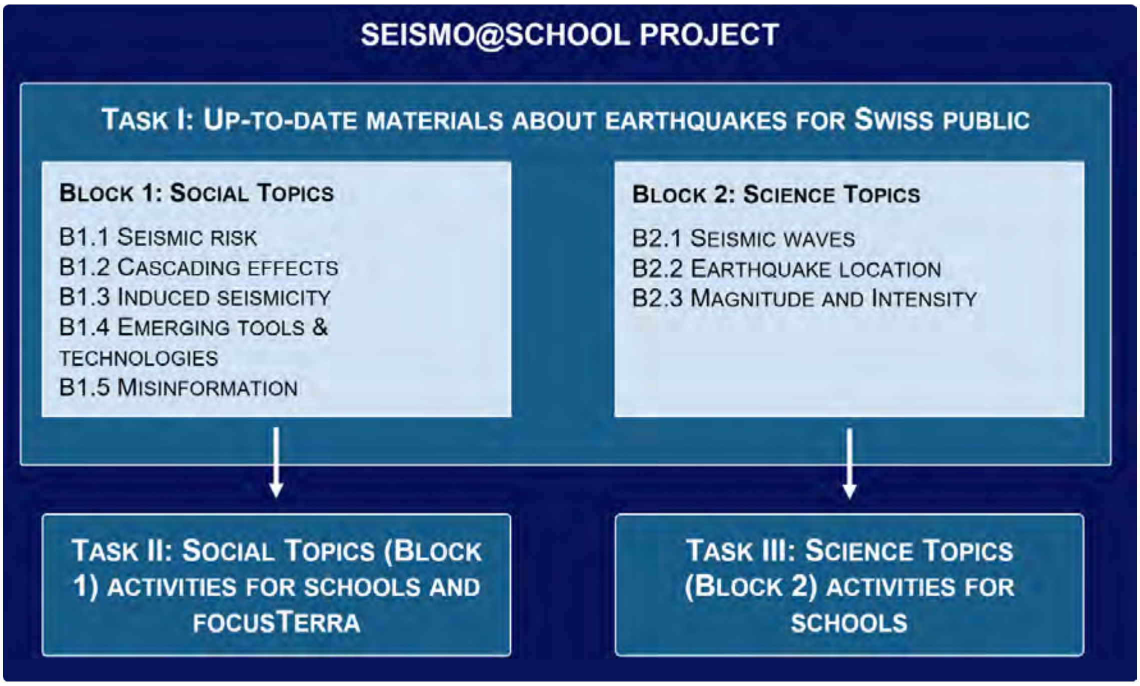

Figure 1. Overview of the three tasks and defined social and science topics of the seismo@school project *Increasing Earthquake Awareness in Switzerland*

P 7.2
Towards surface wave attenuation monitoring with ambient seismic noise

Laura Ermert[1], Lapo Boschi[2], Anne Obermann[1]

[1] Schweizerischer Erdbebendienst, ETH Zürich, CH-8092 Zürich, Switzerland (laura.ermert@sed.ethz.ch)
[2] Dipartimento di Geoscienze, Università degli Studi di Padova, 2-35122 Padova, Italy

Ambient seismic vibrations, often called ambient seismic noise, allow us to continuously monitor Earth's crust. In particular, measurements of velocity changes performed on station-station ambient noise correlations by coda wave interferometry can contribute important data to the near real-time observation of natural hazards (Cubuk-Sabuncu et al., 2022). While attenuation changes would be an immensely useful complement to velocity-based monitoring, it is unclear what effect the strong spatio-temporal variability of ambient noise sources has on attenuation measurements. So far, attenuation measurements on the ballistic surface waves as well as the coda of ambient noise correlations have only been successful after spatial or temporal averaging of observations along with strict quality control. This significantly reduces the amount of interpretable data and the temporal and spatial resolution of the results (e.g. Soergel et al. 2020). Therefore, it is currently not possible to conduct attenuation monitoring at satisfactory spatial and temporal resolution, e.g. at a scale of tens of kilometers and a temporal resolution of days to weeks.

Our goal in the current project is to address this issue by explicitly considering noise source effects. The strongest sources of natural ambient seismic noise are the so-called ocean microseisms. In fact, these provide a well-measurable signal whose amplitude is not random, but depends on ocean wave activity (Hasselmann, 1963). Its frequency band (~0.05 – 0.25 Hz) is well suited to monitor the crust. Time-dependent power spectral densities of ambient seismic vibrations at single stations (such as in Fig. 1, left panel) have previously been successfully simulated using ocean wave data and seismic wave propagation models (e.g. Gualteri et al. 2014). Here, we propose to simulate station-station correlations with a similar approach, i.e., by considering ocean wave data as inputs to the seismic wave propagation. We aim to reproduce the envelopes of observed ambient noise correlations averaged over several days to weeks. Such a model might allow us to account for the influence of ocean microseism sources on ambient noise correlation envelopes, and thus to take steps towards ambient noise-based attenuation monitoring.

In this presentation, we will first illustrate the problem we are aiming to solve by showing time-dependent ambient-noise based surface wave attenuation measurements at pairs of selected broadband stations in Switzerland and Iceland. Using the method of Magrini & Boschi (2020) to extract surface wave attenuation from ambient noise, we find clear seasonal variations in the retrieved attenuation parameter α (Fig. 1, right panel), which may be caused by noise source variations.
We will compare the results obtained from ballistic surface waves (Fig. 1) to measurements of coda-Q following the approach of Soergel et al. (2020) to determine whether both types of measurements are affected by the source variability. Finally, we will show first results of modeled time-dependent correlation envelopes based on ocean wave hindcasts, and evaluate how well they reproduce the observed data. From this, we will derive recommendations for the next steps towards ambient noise-based surface wave attenuation monitoring.

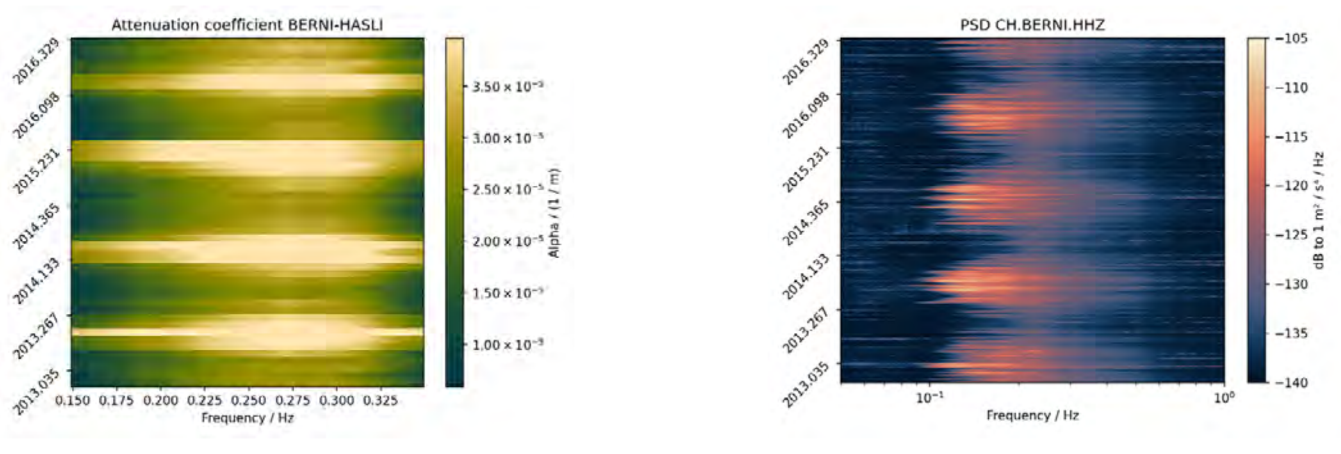

Figure 1. Time-dependent power spectral density of three years of observed ambient seismic noise at station BERNI at Berninapass, Eastern Switzerland (left) and time-dependent surface wave attenuation parameter α for surface waves propagating between Hasliberg and Berninapass (right). During summer, there is less energetic secondary microseismic noise between 0.1 and 0.2 Hz (left). This coincides with an increase in apparent surface wave attenuation (right). Ambient noise source effects may be the cause of the apparent increase. Our goal in this study is to construct a numerical model of time-dependent ambient noise correlations to determine whether this is the case, and if so, to correct for the source effects to reveal any variation in crustal attenuation.

REFERENCES

Cubuk-Sabuncu, Y., Jónsdóttir, K., Caudron, C., Lecocq, T., Parks, M. M., Geirsson, H., & Mordret, A. (2021). Temporal Seismic Velocity Changes During the 2020 Rapid Inflation at Mt. Þorbjörn-Svartsengi, Iceland, Using Seismic Ambient Noise. Geophys Res Lett, 48(11), e2020GL092265. https://doi.org/10.1029/2020GL092265

Soergel, D., Pedersen, H. A., Stehly, L., Margerin, L., Paul, A., & AlpArray Working Group. (2020). Coda-Q in the 2.5–20 s period band from seismic noise: Application to the greater Alpine area. Geophys J Int, 220(1), 202–217. https://doi.org/10.1093/gji/ggz443

Hasselmann, K. (1963). A statistical analysis of the generation of microseisms. Rev Geophys, 1(2), 177-210. https://doi.org/10.1029/RG001i002p00177

Gualtieri, L., Stutzmann, E., Capdeville, Y., Ardhuin, F., Schimmel, M., Mangeney, A., & Morelli, A. (2013). Modelling secondary microseismic noise by normal mode summation. Geophys J Int, 193(3), 1732–1745. https://doi.org/10.1093/gji/ggt090

Magrini, F., & Boschi, L. (2021). Surface-Wave Attenuation From Seismic Ambient Noise: Numerical Validation and Application. J Geophys Res: Solid Earth, 126(1), e2020JB019865. https://doi.org/10.1029/2020JB019865

P 7.3
On the selection of design-compatible waveforms for structural-analysis purpose in Switzerland

Francesco Panzera[1,2], Paolo Bergamo[1], Laurentiu Danciu[1], Donat Fäh[1]

[1] Swiss Seismological Service (SED) at ETH Zurich, Sonneggstrasse 5, CH-8092 Zürich (paolo.bergamo@sed.ethz.ch)
[2] Biological, geological and Environmental department at University of Catania, Corso Italia 57, IT-95126 Catania

Using the collected database of waveforms derived for the project “Database for design-compatible waveforms” (Panzera et al., 2022), financed by Federal Office for the Environment (FOEN), for each seismic zone and soil class in SIA261 a set of eleven three-component, scaled waveforms was selected for application in structural analysis of buildings of importance class III in SIA261. To comply with SIA 261 rules, elastic response spectra are multiplied with a factor 1.5, thus corresponding to about 975 years return period in the seismic hazard. Our selection is made for structural analysis purpose, then we choose three period ranges for the selection: 0.02-1.0 s, 0.1-2.0 s, and 0.25-4.0 s (Fig. 1). These three period ranges were chosen to cover the fundamental periods of most of the Swiss building stock, in agreement with the definition of period range in the EC8 rules ($0.2T_0$-$1.5T_0$). Using these period ranges we expect to cover building periods 0.10-0.66 s, 0.50-1.33 s and 1.25-2.66 s respectively. The search is made using the geometric mean of the two horizontal components, and scaling in amplitude the waveforms to improve the final fit with the target (minimum scaling factor = 0.5, maximum scaling factor = 2.0 if possible). The vertical components is not included in the search, but the same scaling is applied, although we do not expect to match the vertical ground motion design spectrum defined in SIA261. Therefore, 75 spectrum compatible sets of waveforms are selected (see e.g. in Fig. 1). For soil classes A, B, C and D we selected only real accelerograms applying all EC8 rules. For soil class E, we release some restrictions and we add synthetics for some spectral periods and zones. Moreover, sometimes we increased also the scaling factor up to 3. We should also mention that no selection code so far implements all proposed EC8 criteria (e.g. neither Rexel by Iervolino et al. (2009) nor Search & Match by Youngs et al. (2007)). The selection criteria in the EC rules are very restrictive causing a number of challenges in the selection procedure.

ACKNOWLEDGEMENTS
This work is made in the frame of the project Database for design-compatible waveforms financed by Federal Office for the Environment (FOEN).

REFERENCES

Bergamo P., Panzera F., Danciu L., Fäh D., 2022. Disaggregation of the seismic hazard at return period 975 years. SED report for the BAFU project “Database for design-compatible waveforms”. https://doi.org/10.3929/ethz-b-000579218

Eurocode 8, 2004, Design of structures for earthquake resistance, General rules, seismic actions and rules for buildings, European Standard, European Committee for Standardization.

Iervolino I., Galasso C., Cosenza E., 2009. REXEL: computer aided record selection for code-based seismic structural analysis. Bulletin of Earthquake Engineering, 8:339-362. DOI 10.1007/s10518-009-9146-1

SIA261 (Società svizzera degli ingegneri e degli architetti), 2020. Azioni sulle stritture portanti. Società svizzera degli ingegneri e degli architetti, Zurigo, 2020.

Panzera F., Bergamo P., Danciu L. Fäh D., 2022. On the selection of design-compatible waveforms for microzonation purpose in Switzerland. 20th Swiss Geoscience Meeting, Lausanne, Switzerland. Symposium 7: Seismic hazrd and risk in Switzerland: from science to mitigation.

Youngs, R. R., Power, M. S., Wang, G., Makdisi, F. I., and Chin, C. C., 2007. Design ground motion library (DGML) - Tool for selecting time history records for specific engineering applications, in SMIP Seminar on Utilization of Strong-Motion Data.

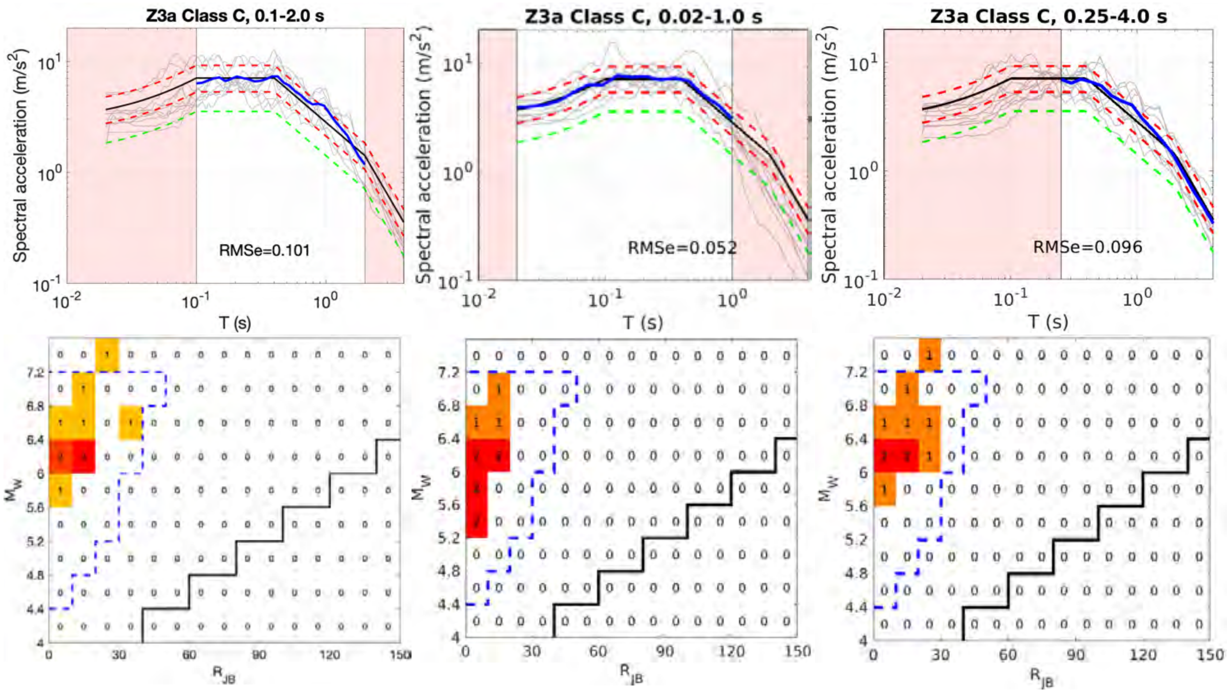

Figure 1. Upper panels: extracted sets of n=11 geometric means of two-components, scaled response spectra (gray lines) for Z3a zone using as target the SIA261 elastic response spectra (black line) for soil class C. The blue line is the mean of the spectra. Red dashed lines indicate the 1.3 and 0.75 ratio threshold; the green dashed line indicates the 0.5 ratio threshold. Shadowed red areas highlight the period range not considered for the selection. Lower panels corresponding number of selected recordings subdivided by bin of Joyner-Boore distances (10 km width) and M_w (0.4 unit) for the period ranges 0.1-2.0s (left panel), 0.02-1.0 s (central panel) and 0.25-4.0 s (right panel). The dashed blue lines indicate the areas where probability of exceedance (over all IMTs) is significant for the five SIA261 zones for return period 975 years, following the approach illustrated in Bergamo et al. (2022). The black continuous lines indi-cate our limit for the first selection of waveforms.

P 7.4
Continuous Measurements of Radon and Other Dissolved Gas Species in Groundwater: A Crucial Step in Earthquake Precursor Research?

Alexandra Lightfoot[1], Michael Strupler[1], Stefan Wiemer[1]

[1] *Swiss Seismological Service (SED) at ETH Zurich, Sonneggstrasse 5, 8092 Zurich, Switzerland (alexandra.lightfoot@sed.ethz.ch)*

The ArtEmis project is focused on improving the understanding of the relationship between radon (Rn) concentration fluctuations in groundwater and earthquakes. The initial phase of the project entails measuring Rn concentrations at selected study sites by employing already available techniques, while in parallel developing a new Rn sensor, with increased sensitivity and at low-cost. In order to measure Rn concentrations at a high spatial resolution, further development and deployment of over 100 sensors is needed. Additional observables, such as groundwater temperature and acidity levels and other dissolved gas species will also be analysed.

In preparation and to validate data to be obtained from the newly developed sensors, Rn analysis will be performed in advance and later in parallel utilising the currently available standard for analysing continuous Rn gas concentrations in groundwater (i.e., the Rad8). One location for pilot testing such continuous Rn analysis will be at the Bedretto tunnel and laboratory in Ticino, Switzerland, where groundwater channels are connected to existing fault lines. The Bedretto tunnel is located specifically around 1.5 km below the Swiss Alps, extending ~5 km in length between Bedretto (Ticino) and the Furkapass in Switzerland. Due to its well-documented geological, seismo-tectonic and geochemical properties, and the fact that experiments on induced seismicity are already conducted, the Bedretto site is ideal for real-time monitoring of continuous Rn concentrations in groundwater.

In addition to Rn, other dissolved gas species will simultaneously be analysed with a portable mass spectrometer, which is proceeded by a gas-permeable membrane-inlet system. Such additional efforts are made given the observations that other dissolved gas species may also provide insight into the relationship between seismic events and dissolved gas concentration changes in groundwater[†]. First results of snapshot Rn concentrations from several boreholes and fissures within the Bedretto tunnel are presented.

REFERENCES

†Giroud, S., Tomonaga, Y., Brennwald, M. S., and Kipfer, R. (2022). “Monitoring dissolved gases in thermal water to assess the potential relation between fluid evolution and seismicity,” in Goldschmidt 2022 Abstract. doi: 10.46427/gold2022.8935

P 7.5
A workflow for assessing lake tsunamis that are generated by various types of mass movements

Jana Schierjott[1], Michael Strupler[2], Katrina Kremer[2,3], Daniela Vendettuoli[3], Matthias Bürgler[1], David Vetsch[1]

[1] VAW, ETH Zurich, Hönggerbergring 26, 8093 Zürich (schierjott@vaw.baug.ethz.ch)
[2] Swiss Seismological Service at ETH Zurich, Sonneggstrasse 5, 8092 Zürich
[3] Institute of Geological Sciences and Oeschger Centre for Climate Change Research, Baltzerstrasse 1+3, 3012 Bern

Due to their glacial history, the related bathymetric-topographic expression and sediment-mechanical characteristics, lakes in the alpine and peri-alpine settings in Switzerland result in prime conditions for mass movements that can occur either on subaqueous slopes, or on the subaerial lake-bordering steep topography (e.g. Strupler et al. 2020). Both of these mechanisms can generate tsunami-like waves when interacting with the water body and cause fatalities as well as economic loss in communities along the shore. In Canada, a disastrous subaerial landslide impacted Lake Chehalis and caused run-up heights of up to 38 m (e.g. Roberts et al. 2013). A subaqueous mass movement in a peri-alpine setting generated a tsunami with wave heights of more than 5 m in Lake Lucerne, Switzerland in 1601 (e.g. Hilbe and Anselmatti, 2014). Such tsunamis can become particularly devastating to communities and infrastructure when they lead to overtopping of natural or artificial dam structures and subsequently affecting downstream areas. Hence, a detailed hazard assessment is an essential tool in order to mitigate the outcome of or prevent such events from happening.

We present a workflow that addresses this particular hazard in the peri-alpine setting in a holistic way. GPU-accelerated numerical simulations using the freely available software BASEMENT allow for a rapid calculation of various inundation parameter distributions, considering uncertainties in landslide parameters. We demonstrate the workflow designed to be applied by consulting firms using examples of reconstructed subaqueous and subaerial mass movement-triggered tsunami events that occurred on Lake Lucerne, central Switzerland.

REFERENCES (IN ORDER OF OCCURRENCE)
Strupler, M., Evers, F. M., Kremer, K., Cauzzi, C., Bacigaluppi, P., Vetsch, D. F., Boes, R. M., Fäh, D., Anselmetti, F. S., & Wiemer, S. 2020: A Simplified Classification of the Relative Tsunami Potential in Swiss Perialpine Lakes Caused by Subaqueous and Subaerial Mass-Movements. *Frontiers in Earth Science*, **8**,1–14.

Roberts, N. J., R. J. McKillop, M. S. Lawrence, J. F. Psutka, J. J. Clague, M.-A. Brideau, & Ward, B. C. 2013: Impacts of the 2007 landslide-generated tsunami in Chehalis Lake, Canada. *Landslide science and practice*, **6**, 133–140.

Hilbe, M., Anselmatti, F. S. 2014: Signatures of slope failures and river-delta collapses in a perialpine lake (Lake Lucerne, Switzerland). *Sedimentology*, **61,** 1883-1907.

P 23.1
Combining climate and soil moisture information in statistical modelling for landslide early warning

Tobias Halter[1], Peter Lehmann[2], Alexander Bast[3], Manfred Stähli[1],

[1] *Swiss Federal Institute for Forest, Snow and Landscape Research WSL, Birmensdorf, Switzerland*
[2] *Department of Environmental Systems Science, ETH Zurich, Zurich, Switzerland*
[3] *WSL Institute for Snow and Avalanche Research SLF, Davos, Switzerland*

Shallow landslides events triggered by rainfall events pose a serious threat to people and infrastructure in mountainous areas. Regional landslide early warning systems (LEWS) have proven to be a cost-efficient tool to inform the public about the imminent landslide danger (Stähli, et al., 2015). Previous studies have demonstrated the efficacy of using landslide inventories from Switzerland to effectively forecast periods of increased landslide danger by considering rainfall characteristics (Leonarduzzi, et al., 2017) or relative changes in volumetric water content measured at soil moisture measurement stations across the country (Wicki, et al., 2020). In this study, we build upon the knowledge gained from these investigations and combine antecedent soil moisture information (including soil water potential data) with climatic data (starting with rainfall and temperature) to establish dynamic thresholds that enable the prediction of landslide probability in both time and space. To achieve this objective and to separate between critical and non-critical rainfall events, we explore machine learning approaches. We apply these models to different subsets of data and test them for different combinations of input variables. We aim to: 1) evaluate the effectiveness of different statistical models in predicting landslide hazards, 2) assess the significance of various climatic and soil moisture variables, and 3) evaluate the benefits of integrating soil moisture and climatic information within LEWS. By accomplishing these objectives, we aim to enhance the accuracy and reliability of landslide forecasting, contributing to improved landslide risk management in areas with steep slopes.

REFERENCES

Leonarduzzi, E., Molnar, P., McArdell, B. W. (2017). Predictive performance of rainfall thresholds for shallow landslides in Switzerland from gridded daily data. *Water Resources Research, 53(8)*, 6612-6625.

Stähli, M., Sättle, M., Huggel, C., McArdell, B., Lehmann, P., Van Herwijnen, A., . . . Kos, A. (2015). Monitoring and prediction in early warning systems for rapid mass movements. *Natural Hazards and Earth System Science 15*, 905-917.

Wicki, A., Lehmann, P., Hauck, C., Seneviratne, S., Waldner, P., & Stähli, M. (2020). Assessing the potential of soil moisture measurements for regional landslide early warning. *Landslides 17*, 1881-1896.

P 23.2
Numerical Investigation of High Impact Foehn storm in February 1925 using WRF and PALM model.

Renuka P. Shastri, Stefan Brönnimann

Institute of Geography and Oeschger Centre for Climate Change Research, University of Bern, Switzerland

One of the most hazardous windstorms was observed on 15th February 1925 in Switzerland. The storm is categorized as a ‚High impact Foehn Storm' that affected all foehn regions of (German-)Switzerland, all communities, stables, and houses were partially or completely damaged in the canton of Glarus. In the previous work, by Stucki et al. 2015 the WRF downscaling (from 20CRv2 with a 220 km grid width of 3 km) was done for this storm. The wind speeds remained in the valleys below the expected values. The question arose whether with LES high gust peaks also would occur at the bottom of the valley. It motivates to verify the ability of the PArallelized Large-eddy simulation Model (PALM) to simulate the Wind Field intensity. This storm was analyzed by the PALMv6.0 and Weather Research and Forecasting Model (WRFv4.1.2). In the first stage, WRFv4.1.2 was downscaled to a resolution of 1x1 km^2 by using the „Twentieth Century Reanalysis" (20CRv3) as a boundary condition. Three nested domains with resolutions 25km, 5 km, and 1 km were set up for the simulation experiment. The second stage involves downscaling of PALMv6.0 to a resolution of 20 meters by using the output of WRFv4.1.2 as a boundary condition. The simulation shows a strong wind field between Netstal and Näfels. Peak gusts of 40 m/s and more hit the valley floor south of Näfels. A vertical section in the main valley in the south-north direction shows strong turbulence fields reaching the ground with velocities of 30 to 40 m/s and more. In total, the simulation shows good agreement with the damage described and the simulated peak gusts easily reach the measured maxima of extreme storms.

8 Deep geothermal energy, CO_2-storage and energy-related exploration of the subsurface

Benoît Valley, Daniela van den Heuvel, Christophe Nussbaum, Marie Violay

TALKS:

POSTERS:

P 8.1 Köpping J., Driesner T.: Magmatic hydrothermal fluid flow in caldera settings – Insights from 3D numerical simulations

P 8.2 Solms T., Driesner T., Bachmann O., Chambefort I.: Magmatic-hydrothermal fluid flow related to silicic intrusions: implications for supercritical geothermal systems

P 8.3 Vontobel M., Sohrabi R., Valley B.: Fracture network characterization for hydrothermal projects: Application to the AGEPP project in Lavey-les-Bains, Switzerland

P 8.4 Mhlambi S., van Bever Donker J., Eruteya E.O., Moscariello A., Samankassou E.: Feasibility of CO2 Storage in Depleted Gas Reservoirs: A Case Study of the F-O Gas Field, Bredasdorp Basin, offshore South Africa

P 8.5 Rangel Jurado N., Cervelli M., Games F., Kong X.-Z.: Investigating the chemical reactivity of the Gipskeuper and Muschelkalk formations to wet CO2 injection: A case study towards the first Swiss CCS pilot project

P 8.6 Stopelli E., Heuberger S., Lupi N., Galfetti T.: Critical raw materials from deep geothermal fluids – how to sample and what to analyse?

8.1
GEOBEST2020+: A program and workflow for handling the risk of induced seismicity associated with deep geothermal projects in Switzerland

Verónica Antunes[1], Toni Kraft[1], Vanille A. Ritz[1], Philippe Roth[1], Tania Toledo[1], Pascal R. Graf[1], Stefanie Zeller[1], Stefan Wiemer[1]

[1] Swiss Seismological Service at ETH Zurich, Switzerland (geobest-team@sed.ethz.ch)

Deep geothermal energy is a clean and renewable source of energy that can assist Switzerland in reaching its energy and climate objectives. Worldwide, numerous geothermal projects have been successfully operated for decades. Unfortunately, several projects were also aborted due to unexpected levels of induced seismicity. Therefore, adequate risk governance is essential to establish safe and economically viable geothermal projects.

Within the GEOBEST2020+ project, funded by the Federal Office of Energy (SFOE) in the framework of the SwissEnergy program, the Swiss Seismological Service (SED) supports cantonal authorities in adequately handling the risk of induced seismicity associated with deep geothermal projects in Switzerland. In this framework, GEOBEST2020+ provides operator-independent seismological expertise and baseline seismic monitoring services to the cantons at no extra costs for them.

In terms of seismological consulting, the SED experts support the cantonal authorities in: 1) defining induced-seismicity-related requirements for the mandatory authorizations; 2) reviewing seismological aspects of permit and concession requests submitted by project operators; and 3) providing independent, project-specific information on geothermal energy and seismicity to the public.

Regarding seismic monitoring and earthquake alarming, the SED provides: 1) customized seismological monitoring networks; 2) automatic real-time earthquake analyses, manually reviewed by experienced seismologists; 3) earthquake alerting via SMS and email to specific stakeholders; 4) rapid preliminary assessment of the natural or human-made origin of the events; 5) public-access archival of the recorded seismological data; and 6) public, project-specific web-pages with background and real-time earthquake information.

8.2
Insights on pre-failure strain localization from physics-based numerical and laboratory techniques

Patrick Bianchi[1,*], Paul Antony Selvadurai[1], Antonio Salazar Vásquez[1,2], Luca Dal Zilio[3], Taras Gerya[3], Claudio Madonna[4], Stefan Wiemer[1]

*[1] Swiss Seismological Service, ETH Zurich, Sonneggstrasse 5, CH-8092 Zurich (*patrick.bianchi@sed.ethz.ch)*
[2] University of Applied Sciences of Eastern Switzerland, Rapperswil, CH-8640 Rapperswil
[3] Institute of Geophysics, ETH Zurich, CH-8092 Zurich
[4] Geological Institute, ETH Zurich, CH-8092 Zurich

How porous rock volumes deform in response to variations of loading stress or pore pressure is a key feature that significantly influences the localization of strain before catastrophic failure. Investigating the factors governing this phenomenon at the pore scale becomes crucial, since the overall deformation response of a rock formation corresponds to the superposition of processes related to multiple single pores. This plays a significant role in reservoir system applications (e.g., enhanced geothermal systems, subsurface CO_2 storage, etc.), since the dynamics caused by the injection or extraction of fluids are controlled by the interplay between a fluid and a rock phase. The implementation of poro-elasto-visco-plastic constitutive relations in numerical frameworks is thus crucial to correctly simulate physical processes that couple these phases. However, the validation of these numerical codes remains essential and, due to the opportunity to collect extensive data sets, laboratory experiments offer suitable conditions to perform such numerical validations.

We present the results of a failure test on a dry sample of Berea sandstone confined at 20 MPa (Bianchi et al., 2023). Fully calibrated piezoelectric transducers (PZTs, Selvadurai et al., 2022) are employed both passively and actively to continuously monitor acoustic emissions (AEs) and to construct a time-varying homogeneous velocity model, respectively. This combination of techniques allows us to locate the AEs with an accuracy of ±2.5 mm and to determine their moment tensor solutions. Two typologies of optical fibers (polymide and acrylate) are glued on the sample surface and, by using distributed strain sensing (DSS) technologies (Salazar Vásquez et al., 2022), we can measure surface strain with a sampling frequency of 0.1 Hz and a spatial resolution of 5 mm. This data is further employed to validate simulations conducted with H-MEC (Dal Zilio et al., 2023) – a fully coupled continuum-based seismo-hydro-mechanical poro-elasto-visco-plastic numerical code.

The laboratory results show two AE clusters developing at the top and bottom of the sample throughout almost the entire test and these events predominantly display compressive source mechanisms. Numerical simulations reinforce these observations, as pore visco-plastic compaction is found in the same sample regions. As the experiment proceeds toward the main failure, we observe a transition of the source mechanisms that is representative of the development of shear bands. This process is confirmed by the computational observations, which display a structure of multiple shear bands developing within the sample before the peak stress. During the second half of the experiment, the tomographic results show an overall decrease in seismic velocity that, combined with the absence of AEs in central regions of the rock specimen, suggests that deformation occurs inelastically. A macrofracture is also nucleated during the simulations, even though this is not pre-imposed as initial condition. The circumferential DSS data highlights spatio-temporal localization of surface strain before the peak stress and the region experiencing higher extension correlates with a volume of rock with high seismic activity that precedes the macrofracture nucleation. A correlation with the numerical results is found also here, since the rock volumes found in the proximity of the macrofracture source region show to deform towards the specimen surface – a behavior that causes local extension. This combination of physics-based numerical and laboratory techniques allows us to better capture strain localization before catastrophic failure and it sets a fundamental validation basis for future upscaling efforts at the reservoir and field scales.

REFERENCES
Bianchi, P., Selvadurai, P. A., Salazar Vásquez, A., Dal Zilio, L., Madonna, C., Gerya, T., & Wiemer, S. 2023: Unraveling Pre-Failure Strain Localization in Siliclastic Rocks: Laboratory and Numerical Investigations. *Manuscript submitted for publication to Rock Mechanics and Rock Engineering*.

Dal Zilio, L., Hegyi, B., Behr, W., & Gerya, T. 2022: Hydro-mechanical earthquake cycles in a poro-visco-elasto-plastic fluid-bearing fault structure. Tectonophysics, 838, 229516.

Salazar Vásquez, A., Rabaiotti, C., Germanovich, L. N., & Puzrin, A. M. 2022: Distributed fiber optics measurements of rock deformation and failure in triaxial tests. Journal of Geophysical Research: Solid Earth, 127, e2022JB023997.

Selvadurai, P. A., Wu, R., Bianchi, P., Niu, Z., Michail, S., Madonna, C., & Wiemer, S. 2022: A Methodology for Reconstructing Source Properties of a Conical Piezoelectric Actuator Using Array-Based Methods. Journal of Nondestructive Evaluation 41, 23.

8.3
Fluid effect in the critical interpretation of compressive failure in Berea sandstone, insights from Distributed Strain Sensing

Hao Chen[1], Paul Antony Selvadurai[1], Antonio Salazar Vasquez[1,2], Patrick Bianchi[1], Sofia Michail[1], Rast Markus[3], Claudio Madonna[3] and Stefan Wiemer[1]

[1] Swiss Seismological Service, ETH Zurich, Sonneggstrasse 5, CH-8092 Zürich (hao.chen@sed.ethz.ch)
[2] University of Applied Sciences of Eastern Switzerland, Oberseestrasse 10, 8640 Rapperswil
[3] Geological Institute, Department of Earth Science, ETH Zurich, Sonneggstrasse 5, CH-8092 Zürich

The last decades have shown growing interest in the use of deep georeservoirs in the context of geothermal energy or carbon sequestration. In fact, the fluid injection used to improve the georeservoirs permeability may induce a large increase of seismicity, which could result in a vast negative socio-economic consequences (Duboeuf et al. 2020). Despite many efforts, understanding the link between fluid and seismicity is unclear. Improved models may eventually mitigate or predict induced earthquakes associated with injection.

Clear examples of the critical phenomena associated with earthquakes are the Gutenberg-Richter law and Omori law. In such a case, the scale-free statistics describing properties of the earthquake sequences provide important insight for the investigation of precursory activity in terms of phase transitions of the rock volume (Bak et al. 2002). A clearer understanding of the relationship between these seismic statistics and progressive damage evolution of the rock have been also evaluated in laboratory rock fracture experiments (Kandula et al. 2019). This study aims at characterizing the precursory deformation by accounting for the effect of fluid under pressure. Predictability of catastrophic failure was investigated in the framework of criticality in systems. We studied the evolving surface strain fields of Berea sandstones in a triaxial configuration and under dry and wet conditions using distributed strain sensing (DSS) technology. This allows us to detect the evolution of damage dynamics.

During triaxial deformation, the differential stress was applied at a constant displacement rate of 0.02 mm/min under a constant confinement of 20 MPa. For the wet experiment, a pore pressure kept constant at 5 MPa was applied on an initially saturated specimen with the effective confining pressure of 20 MPa. The criticality of the system refers to the dynamics of observables that change abruptly, when the control parameter defined as the normalized time to failure ($\Delta = (t_f - t) / t_f$) approaches a critical value. In this study, the evolution of damage rate defined as rate of cumulative volumetric strain and incremental volumetric strain were tracked in terms of a control parameter to test the nature of criticality.

For the dry experiment, the damage rate initially exhibited a steep increase, bending toward a shallower slope in a power law near the failure. In comparison, the largest strain increment diverged following a power law with a higher exponent after an initial fluctuation (Figure 1(a) and (b)). This implies that the physics governing the damage dynamics are different, and it favors the growth of largest cluster in localization region. Thus, the growth of largest damage cluster provides a more reliable precursor of the timing of failure than the acceleration of global deformation. In contrast, under wet conditions, the increase of damage rate showed a preference for an exponential model, thus an acceleration of damage could be more abrupt, when the fault spanned the system resulting in macro-failure. In this case, the largest strain increment still exhibited a power law divergence when approaching failure, but with a lower slope than that observed in a dry sample (Figure 1(c) and (d)). This suggests that the behavior of Berea sandstone remains consistent with critical phase transition between intact and failed state at low fluid pressure condition, but the effect of fluid makes the failure process unstable as it promotes the localization process. These results have significant implications for forecasting failure under fluid pressure by tracking the evolving strain field and precursory behavior.

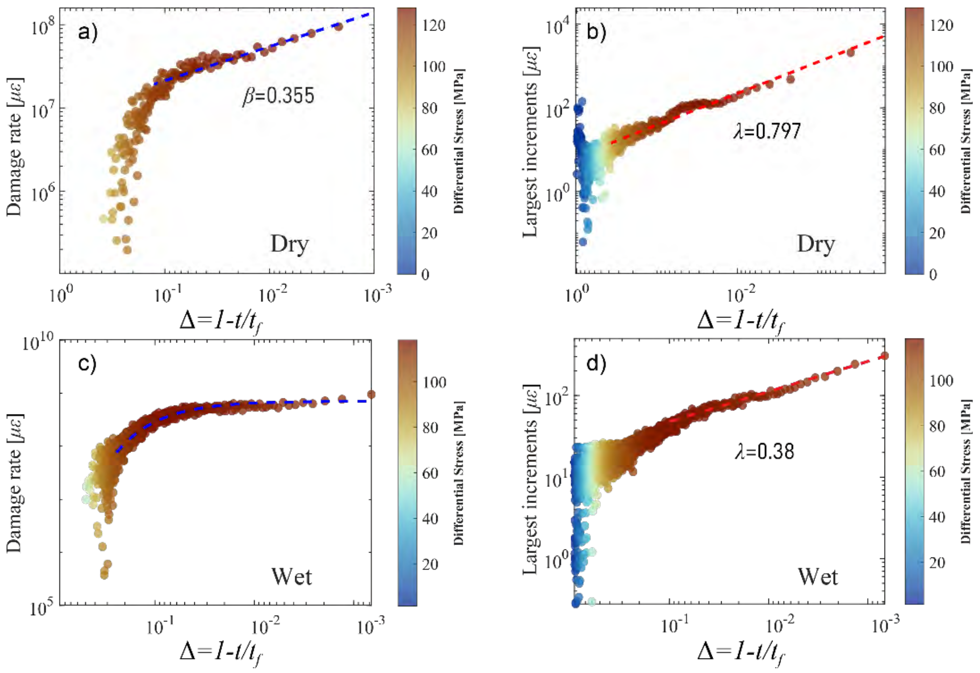

Figure 1. Top: evidence for the power law acceleration of (a) damage rate (b) and largest volumetric strain increment under dry condition. Bottom: (c) exponential increase of damage rate and (d) power law divergence of largest strain increment under fluid saturated and pressurized condition.

REFERENCES

Bak, Per, Kim Christensen, Leon Danon, and Tim Scanlon. 2002: Unified Scaling Law for Earthquakes, Physical Review Letters 88 (17): 178501.

Duboeuf, Laure, Louis De Barros, Maria Kakurina, Yves Guglielmi, Frederic Cappa, and Benoit Valley. 2020: Aseismic Deformations Perturb the Stress State and Trigger Induced Seismicity during Injection Experiments, Geophysical Journal International 224 (2): 1464–75.

Kandula, Neelima, Benoît Cordonnier, Elodie Boller, Jérôme Weiss, Dag Kristian Dysthe, and François Renard. 2019: Dynamics of Microscale Precursors During Brittle Compressive Failure in Carrara Marble, Journal of Geophysical Research: Solid Earth 124 (6): 6121–39.

8.4
Using elementary slip solutions to solve for displacement in complexly fractured rock

Giulia Conti[1], Stephan Matthai[2], Patrick Jenny[1]

[1] Institute of Fluid Dynamics, ETH Zürich, Sonneggstrasse 3, CH-8052 Zürich (gconti@ethz.ch)
[2] Department of Infrastructure Engineering, The University of Melbourne, Victoria VIC 3010, Australia

Geomechanical simulations of fractured rock are challenging and computationally expensive, but indispensable to investigate aperture changes in enhanced geothermal systems (EGS). Since shear displacement due to fluid injection is an especially important mechanism for permeability enhancement in EGS, we focus on fractures subjected to shearing while assuming linear elasticity for the rock matrix.

Analytical solutions exist for simple test cases of isolated fractures, and approximations from far field stresses calculate the local shear and normal stress on the fracture with Cauchy's equation. However, we expect that using these leads to wrong results in complicated fracture patterns, because the interaction between fractures is neglected. This is the main reason why mechanical solvers like boundary element methods, extended finite element methods (XFEM) and extended finite volume methods (XFVM), all of which resolve the mechanics locally by solving for stress equilibrium, were developed.

We developed a very efficient framework which also takes into consideration fracture interaction. For single fractures with elliptic slip profiles there exist analytical solutions, and due to the linear relationship between maximum slip and induced stress field, these single fracture solutions serve as basis functions in our framework. The total stress field simply is the superposition of the far field and all slip induced stress fields. We determine the maximum slip value of each fracture using a local force balance constraint. Hence, the number of degrees of freedom can be dramatically reduced as compared with existing mechanical solvers, so that more realistic fracture patterns can be handled.

8.5
Seasonal energy storage through geo-methanation: suitability of the Swiss Molasse Basin

Larryn W. Diamond[1], Ferdinando Musso Piantelli[1,2], Philippos Garefalakis[1], Daniela B. van den Heuvel[1],

[1] *Institute of Geological Sciences, University of Bern, Baltzerstrasse 1+3, CH-3012 Bern (daniela.vandenheuvel@unibern.ch)*
[2] *Bundesamt für Landestopografie swisstopo, Seftigenstrasse 264, 3084 Bern*

Geo-methanation is a process whereby green H_2, which is produced from excess renewable energy through electrolysis of water, is mixed with industrial waste CO_2 and injected into a reservoir formation in the subsurface. There, in-situ methanogenic organisms thrive and convert the gases to renewable CH_4 which can be produced and utilised when needed, thereby acting as a CO_2-neutral form of seasonal energy storage. Proof of concept has been achieved in a reservoir formation in Austria, with gas conversion within weeks to months.

In this study, we assessed the suitability of sediments in the Swiss Molasse Basin (SMB) for geo-methanation. We first derived criteria to evaluate potential reservoir formations: whether they likely have (1) sufficient porosity and permeability to allow injection/extraction of gases, (2) the capacity to retain gases at the same site over weeks to months (seal and trapping structures) and (3) *P–T* conditions conducive to microbial methanation. In a second step we applied these criteria to known Tertiary, Mesozoic and Palaeozoic aquifer formations within the SMB, based on geological and petrophysical data in the literature. This led to the following ranking of the formations with respect to their apparent suitability for geo-methanation (1 being highest, 3 being lowest):

1. Dinkelberg Fm. (“Buntsandstein aquifer”)
   Stamberg Mb./Schinznach Fm. (“Muschelkalk aquifer”)
2. Klettgau Fm. (“Keuper aquifer“)
   Hauptrogenstein
   Lower Freshwater Molasse (USM)
   Upper Marine Molasse (OMM)
   Upper Freshwater Molasse
3. (Pre-)Weitenau Fm.
   Beggingen Mb./Staffelegg Fm. (“Lias aquifer”)
   Jurassic Reef Complex/Etoillets Fm.

We then utilised the 3D geological model GeoMol and the associated underground temperature model to identify areas where these formations fall within the correct depth–temperature interval (~ 600 m, 30 to 60 °C) for geo-methanation. The resulting maps show depth to top of formation and formation thickness. In addition, potential gas trapping structures (anticlines, large-scale faults) were included as they represent prime targets for exploration.

In a final step, the individual formation maps were combined into a single map which indicates geographic areas where one or more potentially suitable reservoirs for geo-methanation can be found. While this “suitability map” helps to guide possible exploration efforts, it does not quantify the potential for geo-methanation. To estimate the potential, more data on petrophysical properties of the aquifers of interest, their volume and distribution as well as the quality of trap structures and sealing formations would be needed.

8.6
Exploration of the Lower Freshwater Molasse and Quaternary glaciogenic deposits around Bern (Switzerland) using the public cantonal drilling database

Guilhem Amin Douillet[1], Daniela Van den Heuvel[1], Ahathian Manikkapoody[1], Veerle Verhoeven[1], Déborah Harlet[1], Pierre Dietrich[1,2], Werner Leu[3], Andre El-Alfy[4], Peter Meier[4], Fritz Schlunegger[1], Larryn Diamond[1]

[1] *Institut für Geologie, Universität Bern, Baltzerstrasse 1+3, Bern, CH 3012, Switzerland (guilhem.douillet@unibe.ch)*
[2] *Univ Rennes, CNRS, Géosciences Rennes, UMR 6118, 35000 Rennes, France*
[3] *Geoform AG, Av. Général-Guisan 28 I CH-1800 Vevey*
[4] *Geo-Energie Suisse AG, Reitergasse 11 CH-8004 Zürich SwitzerlandInstitut, University of Basel, Bernoullistrasse 32, CH-4056 Basel (anna.karenina@unibas.ch)*

Interest is increasing in developing geological reservoirs for heat and gas storage in near-urban areas. The Mittelland region around Bern (Switzerland) is formed by Tertiary Molasse sediments recording the evolution of the Northern foreland basin of the European Alps with subsequent incision by glaciogenic overdeepened valleys from the Quaternary glaciation. Here, we explore the publicly available borehole dataset from the Bernese canton (https://www.map.apps.be.ch/) and shed new light on both units. A collection of ca. 800 selected sediment profiles were extracted from borehole data, in order to characterize the 3D architecture of the subsurface for future reservoir exploration.

The subsurface Tertiary deposits around Bern consist of a thick Group of alluvial to fluvial sediments: the Lower Freshwater Molasse (German abbreviation USM, Chattian to Aquitanian, ca. 30-20 Ma). It contains conglomerates in the proximal zones near the Alps that evolve into a meandering paleo-fluvial system in the lowlands around Bern. Surface outcrops allow to identify coarse-sand fluvial channels, silt-dominated overbank levees, and weathered mudstone paleosols. The surface image depicts sharp and unpredictable lateral changes in lithofacies associations, and a dominant lateral amalgamation of sandstone beds as meander belts.

The molasse unit is cut by a major glacial incision restricted to a branching overdeepened valley with steep flanks and a pathway approximately mimicking the current-day Aare valley. Around Bern, a complex pattern emerged from repeated glacial advances and retreats at what is thought to be the former confluence of the Vallais and Aare glaciers. It contains conglomerates to marl lithologies organized in complex patches.

The USM is characterized from 683 logs covering a ca. 20x20 km^2 zone around Bern (Fig. 1, 2), whereas 115 logs >50 m depth were used to constrain the glacial deposits in a zone ca. 5x4 km^2 below Bern (Fig. 3).

The main spatial and time patterns of lithologies emerging from the USM data are as follow (Fig. 2):

1. On the large scale, a large coarsening upward sequence is represented by an increase in the ratio of sandstone/mudstone layers (from ca. 7.8 % sandstones to ca. 19.1 % sandstone between 300 and 700 m.a.s.l.). Below, a possible fining upward sequence might also be present between 140 and 300 m.a.s.l (from 7.8 to 10.3 % sandstones).
2. Directly below Bern and approximately following the current Aare/Wohlensee valley, a very high sandstone/mudstone ratio (ca. 52.5 % sandstones) is present.
3. In contrast, the region of Berserk (Fribourg/Bern limit) is made up of a very low sandstone/mudstone series (ca. 2.2 % sandstones).

The sedimentological interpretation of these different signals is challenging and may be linked to three factors: 1) a stratigraphic response to relative sea level fluctuations, 2) autogenic reorganization of the main drainage system of the molasse basin, and 3) the configuration and evolution of the alpine megafan systems.

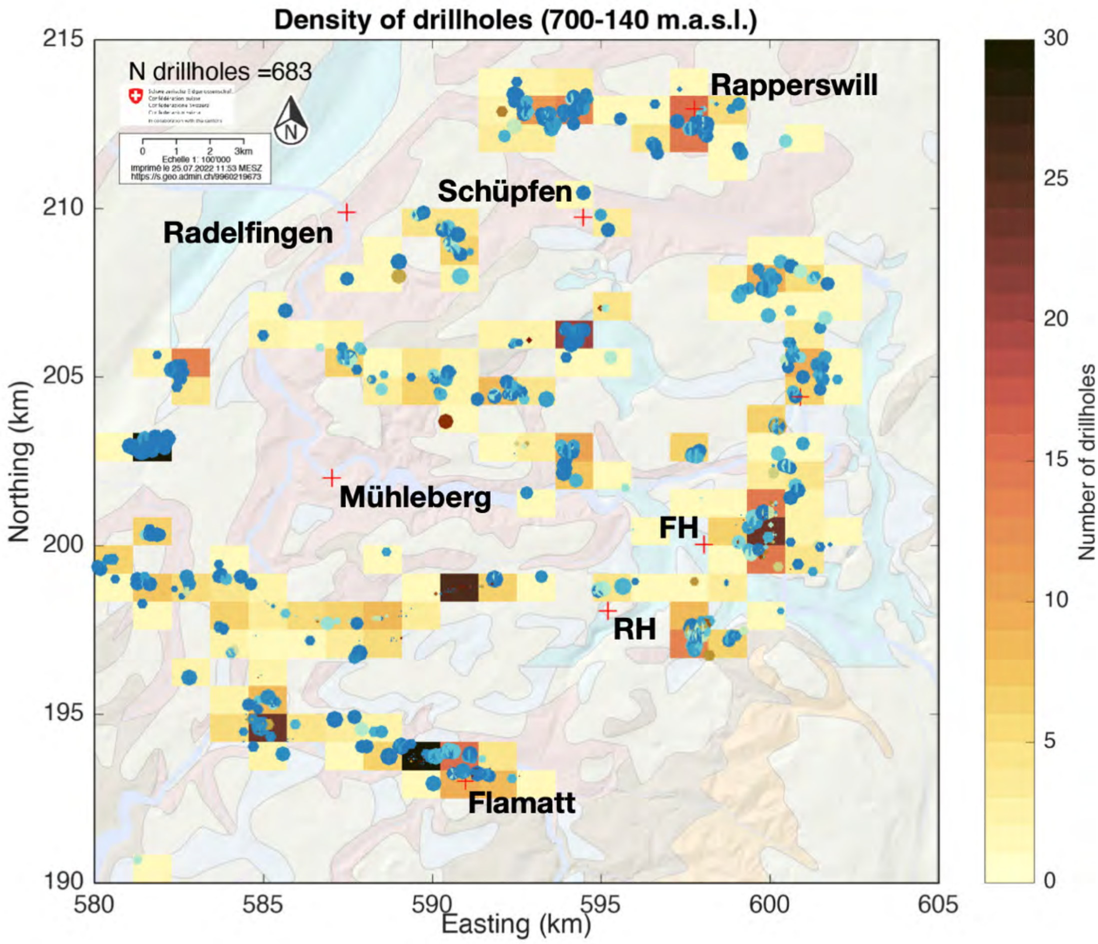

Figure 1. Location of drillholes for the USM study (radius of dots represents the length of the logs) with density of drillholes in a boxplot view (yellow-red colour-scale).

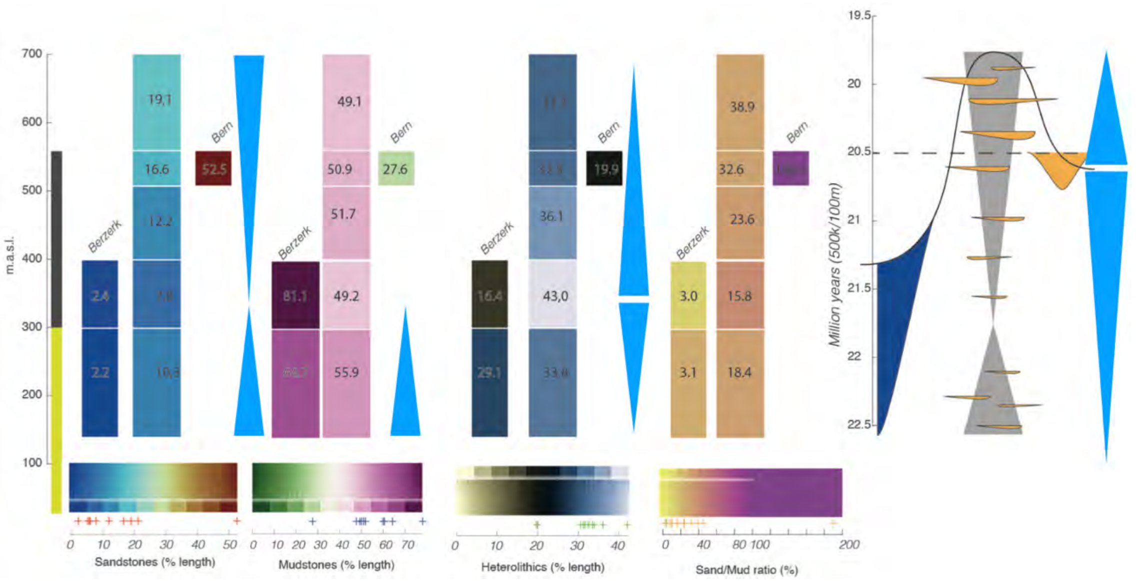

Figure 2. Statistical distribution of sandstones, mudstones and heterogenous units in the study region by depth.

The sedimentary infill within the Quaternary incisions is dominated by steeply-dipping gravel layers (7 to 24% slope) that are organized as relatively small (ca. 1 km radius) fan systems protruding from the valley flanks and prograding towards the valley axis (Fig. 3). Several fan systems were recognized, emanating from morphological “embayments” whose presence is deduced in available maps of Quaternary deposits. It is envisioned that the local fans were fed by glaciofluvial material from narrow and short-lived side-catchments after glacial retreat from the main valley. The source material would have been derived from glacial deposits left at the surface by the retreat of the main Aare and Saane glaciers.

This new view implies that at the large-scale, correlations based on lithology should be avoided as individual fan systems are small and their emplacement is potentially diachronous. Therefore, architectural discontinuities are considered to be more reliable markers. At the local scale, correlations should instead be based on lithologies and models based on depth-equivalence should be avoided since correlative layers are steeply dipping and local features.

Both the USM and Quaternary units contain restricted coarse-grained sediment bodies encapsuled in mudstones and thus they have a potential as future reservoirs. A good understanding of their characteristics and predictability are thus key for future exploratory drillings.

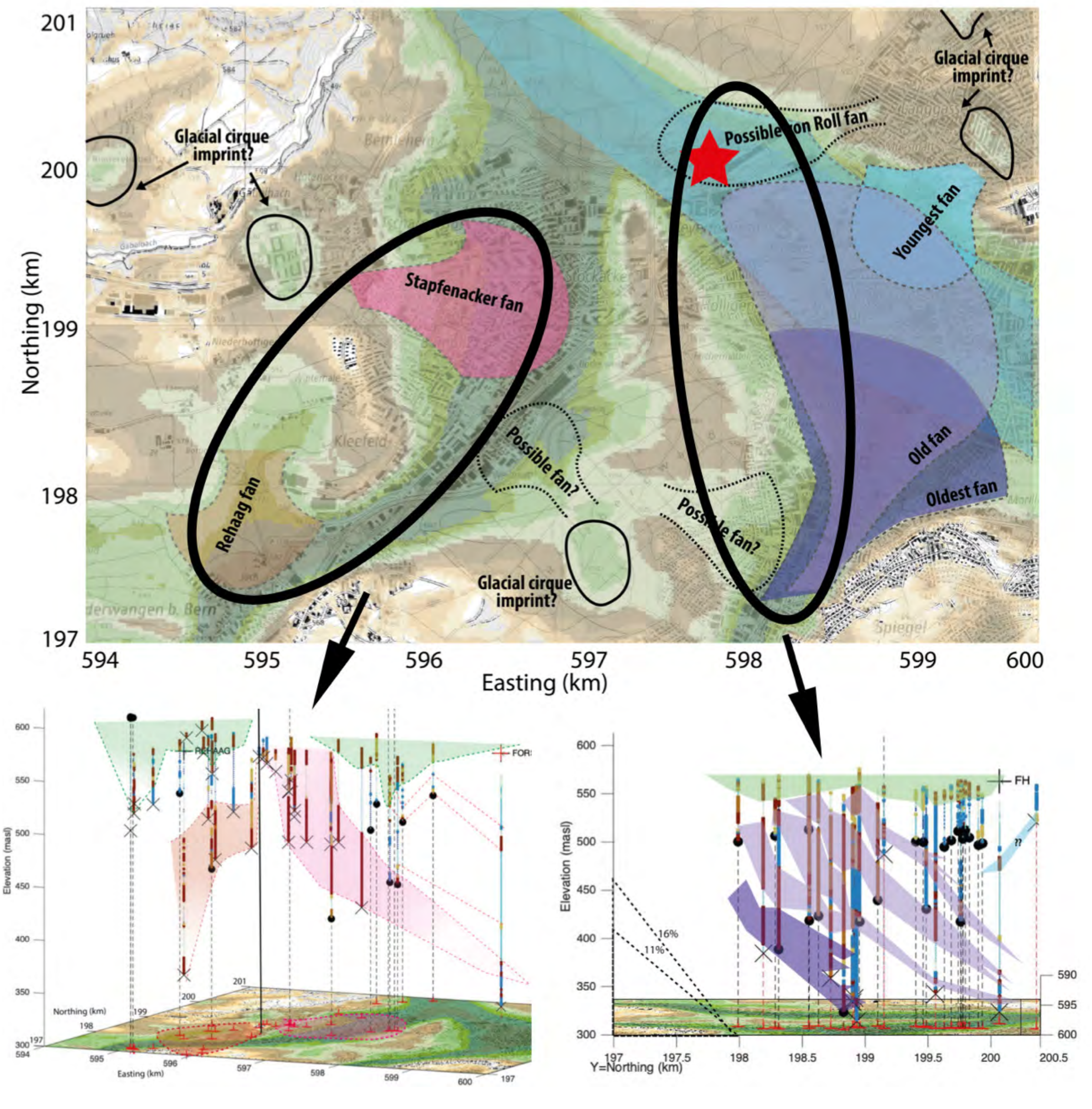

Figure 3. Distribution of local fans within the Quaternary infill beneath Bern. Top: Map, bottom: Pseudo-3D view of the borehole data with highlight on gravel beds for two fan systems.

8.7
Estimating fracture aperture in naturally fractured reservoirs via ensemble-based data assimilation

Michael Liem[1], Giulia Conti[1], Stephan Matthai[2], Patrick Jenny[1]

[1] *Institute of Fluid Dynamics, ETH Zürch, Sonneggstrasse 3, CH-8092 Zürich (liemm@ethz.ch)*
[2] *Department of Infrastructure Engineering, University of Melbourne, Victoria, Australia*

Reservoir rocks targeted by geothermal, hydrocarbon, geo-sequestration or nuclear waste applications are often fractured. Where these fractures dominate flow and transport, their properties and aperture, in particular, need to be characterised so that performance and risks can be assessed with confidence. However, their direct measurement is challenging. Usually, such data becomes available only for certain well intervals. All other data are interpretations of geophysical measurements. This makes indirect methods such as the study of outcrop analogues or interpretation of production data appealing.

In this computational study, we assume that fracture geometry is known *a priori*. A pattern of 4000 individual fractures mapped in aerial photographs of an outcrop (Odling, 1997) serves as an input. Subjected to far-field stress, some of these fractures experience shearing and dilatation. The exact values of the ensuing aperture are unknown, yet an initial guess can be obtained.

Data assimilation is a widely used technique in reservoir simulation, helping to match production history, reduce uncertainty associated with certain model parameters, and improve simulation results. Recently, ensemble-based methods such as the ensemble smoother with multiple data assimilation (ESMDA, Emerick & Reynolds 2013) are gaining popularity. We use ESMDA based on synthetic flow and transport data to reduce the uncertainty of fracture aperture, studying the influence of the prior ensemble on the performance of the data assimilation framework.

Using a geomechanical simulator for generating more realistic realisations of fracture aperture for the prior ensemble is desirable but computationally expensive. A purely stochastic approach on the other hand is cheap but fails to incorporate all available geologic data. Combining the benefits of both methods, we generate prior ensembles based on geomechanical far-field stress approximations (FFSA). This does not rely on geomechanical simulations. Geological knowledge still gets incorporated informing reasonable prior realisations at low computational costs. The posterior ensemble after the ESMDA updates improves the estimate of the fracture aperture and the flow and transport behaviour. Compared to the naïve stochastic approach, fewer realisations and ESMDA iterations are required, creating confidence and lowering computational costs considerably.

REFERENCES

Emerick, A. A. & Reynolds, A. C. 2013. Ensemble smoother with multiple data assimilation. Computers & Geosciences. DOI: https://doi.org/10.1016/j.cageo.2012.03.011

Odling, N. E. 1997. Scaling and connectivity of joint systems in sandstones from western Norway. Journal of Structural Geology. DOI: https://doi.org/10.1016/S0191-8141(97)00041-2

8.8
Searching for hot rocks & water with lukewarm results: Lessons learnt from 30 years of geothermal E&P activity in Switzerland.

Andrea Moscariello[1] and Ladislaus Rybach[2]

[1] Geo-Energy Group, Department of Earth Sciences, University of Geneva, Rue de Maraîchers 13, 1205 Geneva
[2] Institut für Geophysik ETHZ, Sonneggstrasse 5, CH-8092 Zürich
(andrea.mooscariello@unige.ch)

Switzerland enjoys an exceptional favorable social and political support on energy transition policies aimed at eliminating 12 million tons of CO_2 per year in order to meet the 2050 objectives and thus maintaining the target of zero carbon emissions. Geothermal energy is indeed considered by society and both the federal and cantonal governments as one of the viable ways to meet that ambitious target.

If from one side Switzerland is a world's leader in installation of heat pumps which have contributed greatly to reduce the consumption of fossil fuels for heating both for domestic, industrial and agricultural use, the quest for high temperature rocks and water in the deep Swiss subsurface over the last 30 years has somehow not provided the expected results.

The outcomes of wells such as Thônex drilled 30 years ago (1993), followed by Basel (2006), Triemli (2009), St Gallen (2013) and more recently Lavey-les-Bains (2022), Venzel/La Côte and Yverdon (2023) have clearly demonstrated that the Swiss subsurface geothermal potential is still not been exploited as initially hoped. Unexpected success such as the one of the GEo-01 (2018) well in the Geneva Basin and the repurposing of some of the deep wells such as Triemli and Thônex have however demonstrated that the geothermal potential exists and that providing a successful second life to initially disappointing results is a viable option.

Overall, the last 30 years of deep geothermal industry projects in Switzerland offer a large number of lessons learnt which will analyzed and presented in this paper. Will the Swiss industry and regulatory agencies learn from these past experiences ? Will these lessons learnt be taken into account ? Only the future will tell.

Two important lessons seems however to stand out:1) A successful geothermal energy industry, similarly to other business dealing with natural geo-resources exploitation, requires a consolidated and experienced geo-energy exploration mind set supported by courageous large upfront investments; 2) As per the hydrothermal potential, the Swiss subsurface is not yet known well enough to be able to take a stand. Like for the hydrocarbon industry, the understanding of the main controls on porosity and permeability needs to be worked out properly both at basin and reservoir scale. This is only possible with a thorough regional exploration approach and it is not possible when dealing with a 'one shot approach' in a spatially limited area.

8.9
De-Risking geothermal exploration in the Swiss Plateau: A workflow combining the petroleum system modelling (PSM) and common potential/ risk segment (CPS-CRS) mapping workflow

Silvia Omodeo-Salé[1], Yasin Makhloufi[1], Ovie Emmanuel Eruteya[1], Andrea Moscariello[1]

[1] *Geo-Energy Group, Department of Earth Sciences, University of Geneva, Rue de Maraîchers 13, 1205 Geneva (silvia.omodeosale@unige.ch)*

The Swiss Plateau (Switzerland) is characterized by a widespread occurrence of hydrocarbon seepages which are evidence of a complex active petroleum system characterized by multiple plays. Geothermal wells drilled over the last 20 years have also encountered both oil and gas (e.g. Schlattingen-1; St Gallen GT-1; etc.), which in some occasions have had negative short- and long term social perception and economic impact on the geothermal projects at local and national scale. Therefore, in order to assess the risk associated with the presence of oil and/or gas in areas of the Swiss Plateau with potential for geothermal energy exploration, it is critical to first evaluate the hydrocarbon potential of the basin. To achieve this goal, we adopted a robust workflow involving petroleum system modelling (PSM) and Common Potential Segment (CPS) maps. The PSM allows to re-constructing the thermal maturity of the potential source rocks, the timing of the hydrocarbon generation and expulsion, and to delineating the areas in the basin where migration and accumulations are most likely to occur. 2D PSM modelling was applied to five regional transects, representative of the stratigraphic and structural geometry of the basin throughout its extension.

The results obtained by the petroleum system modelling were used to produce Common Potential Segment (CPS) maps, which evaluate the petroleum potential of an area, by considering the following variables: presence and maturity of a source rock; presence and quality of a reservoir; presence and integrity of a seal; presence of a trap presence and the petroleum accumulation and saturation. These maps where then used to produce Common Risk Segment (CRS) maps, which define the risk of hydrocarbon occurrence in an area. The CPS & CRS approach is applied to each level of the identified hydrocarbon Play.

Several uncertainties in the final result must be considered, mostly related to poor data availbility. However, we acknowledge that the final maps produced by the workflow proposed herein can be an essential basis for assessing the risk of encountering hydrocarbons, when drilling for geothermal exploration and production in the Swiss Plateau.

8.10
Modelling natural and induced seismicity in the Hengill geothermal field, SW Iceland

Vanille A. Ritz[1], Antonio P. Rinaldi[1], Leila Mizrahi[1], Sigríður Kristjánsdóttir[2], Raymi Castilla[3], Victor Clasen Repollés[1], Pengliang Yu[4], David Dempsey[5], Vala Hjörleifsdóttir[6], Stefan Wiemer[1]

[1] *Swiss Seismological Service at ETH Zurich, Sonneggstrasse 5, 8092 Zürich, Switzerland (vanille.ritz@sed.ethz.ch)*
[2] *Veðurstofa Íslands / Icelandic Met Office, Bústaðavegur, Reykjavík, Iceland*
[3] *Geo-Energie Suisse AG, Reitergasse 11, 8004 Zürich, Switzerland*
[4] *Penn State University, University Park, United States of America*
[5] *University of Canterbury, 20 Kirkwood Avenue, Upper Riccarton, Christchurch 8041, New Zealand Aotearoa*
[6] *Orkuveita Reykjavíkur / Reykjavik Energy, Bæjarháls 1, Reykjavík, Iceland*

The Hengill Geothermal Field is located in southwest Iceland and hosts the Hellisheiði and Nesjavellir power plants. The area is characterized by a complex triple junction between tectonic features: the Reykanes Peninsula rifting, the South Iceland Volcanic Zone and the West Volcanic Zone. The geothermal field comprises 60+ production wells and 17 injection wells. Significant seismicity, both natural and induced has been recorded since the 1990s and the start of homogeneous national seismic records in Iceland.

The beginning of the reinjection in the Húsmúli area in 2011 was associated to a seismic crisis. A high resolution catalogue covering the first nine months of injection allows us to have a look at the dynamics of the seismicity and to characterise the fractures and state of stress of the area. We model this onset of induced seismicity using a hybrid coupled hydro-geomechanical model (TOUGH2-Seed).

In the framework of the Geothermica project COSEISMIQ (http://www.coseismiq.ethz.ch/en/home/), a dense temporary network was installed to monitor the seismicity in the Hengill region between December 2018 and August 2021. With this enhanced network, novel analysis and relocation techniques, a high resolution relocated catalogue was curated and comprises around 8500 events in the Hengill area.

We use a Seismogenic index type model and different flavours of Epidemic Type Aftershock Sequence (ETAS) to model the natural and induced seismicity during the two and a half year period. Using a pseudo-forecasting approach, the performance of the models is compared to assess the strengths and weaknesses of the different models.

8.11
Structural characterisation of hydrothermal fluid pathways: Preliminary results from the GeoTex project, Rhône Valley, Switzerland

Timothy C. Schmid[1], Marco Herwegh[1], Alfons Berger[1], Daniela B. Van den Heuvel[1], Christoph Wanner[1], Larryn W. Diamond[1]

[1] Institute of Geological Sciences, University of Bern, Baltzerstrasse 1+3, CH-3012 Bern (timothy.schmid@unibe.ch)

Meteoric water commonly infiltrates deeply into high-elevation mountain ranges. Along its subsurface circulation path the water heats up according to the background geothermal gradient and eventually emerges at lower elevation as thermal springs. Whether such topographically-driven circulation establishes or not depends on the host rock's permeability. In this context, fault zones play an important role as they can provide excellent flow paths for fluids. This is particularly the case when fault zones are active, since their deformation counteracts clogging by mineral precipitation. Thus, the investigation of 4D fault and fracture geometries and their kinematics is a means to understand the locations and dynamics of geothermal systems in orogenic belts. Here, we present preliminary results from the ongoing GeoTex research project, which aims at better defining the geothermal potential of the Rhône Valley, an area of rugged topography in SW Switzerland. The Rhône Valley represents a geothermally active zone within an orogen, which is characterised by numerous thermal springs, regional-scale faults and enhanced seismic activity. It is therefore a promising setting to explore further for geothermal energy.

Based on structural data from fieldwork and quantitative remote sensing, we are characterising fault geometries (i.e., spatial orientation, relationship of intersecting fault families as well as kinematics) in the vicinity of five known thermal springs: Lavey-les-Bains, Saillon, Leukerbad, Brigerbad and Grimsel Pass. The circulation paths at these key sites are linked to major Alpine structures in the Aiguilles Rouges and Aar Massifs, such as strike-slip faults (Saillon, Brigerbad, Grimsel Pass) or the axial planes of folds within the massifs (Lavey-les-Bains, Leukerbad). Our results suggest spatial correlations between the locations of the sites and the 3D structure of the host massifs, their vicinity to basement–cover contacts, and faults that have created permeability via their kinematics. Specifically, fold hinges and/or limbs of the massifs near basement–cover contacts exert geometric and lithologic control at some sites, whereas dilatant domains along strike-slip faults and intersections of NE-SW and NW-SE striking faults focus flow at other sites. We are also using observable paleofluid pathways marked by veins and rock alteration as analogues for recent geothermal circulation at the key sites. Through the above approach we have derived conceptual models for fluid flow at the key sites, which may help to predict the locations of blind active geothemal systems elsewhere in the Rhône Valley.

8.12
Geostorage – storing heat for the winter

Urs Spring[1], Andre El-Alfy[2], Peter Meier[2,] David da Silva[3], Werner Leu[4], Raymi Castilla[2]

[1] Energie Wasser Bern, Monbijoustrasse 11, CH-3001 Bern
[2] Geo-Energie Suisse AG, Reitergasse 11, CH-8004 Zürich (a.el-alfy@geo-energie.ch)
[3] TBF + Partner AG, Beckenhofstrasse 35, CH-8042 Zürich
[4] Geoform AG, Av. Général-Guisan 28l, CH-1800 Vevey

At the Forsthaus energy centre (Energiezentrale Forsthaus), Energie Wasser Bern operates a waste incineration plant, a wood-fired power plant and a combined gas and steam power plant. These plants generate electricity and heat. The heat produced is supplied to the district heating network of Energie Wasser Bern.

Particularly in summer, the heat from waste incineration cannot be fully utilised. In winter, on the other hand, this heat would be in great demand. This is where the «Geostorage» pilot project comes in.

In summer, the sandstone layers of the lower sweet water molasses, at a depth between 200 and 500 metres are to be heated with surplus heat. The sandstone underground would be heated with 90-degree hot water. In the winter months, the stored energy could then be recovered and fed into the district heating network - precisely when demand is high.
In this way, Energie Wasser Bern could build up a «seasonal energy stock» of 12 to 15 gigawatt hours.

Both the City of Bern 2035 energy plan and the federal government›s 2050 energy strategy envisage savings and efficiency improvements. In this context, the intermediate storage of energy plays a central role. The Geostorage facility is intended to take on such a function. It would further increase the efficiency of the Energiezentrale Forsthaus, reduce the need for raw materials and cut greenhouse gas emissions.

At the 21st Swiss Geoscience Meeting in Mendrisio, the Forsthaus Geostorage project will be presented - the status of the work, the geological findings and an outlook.

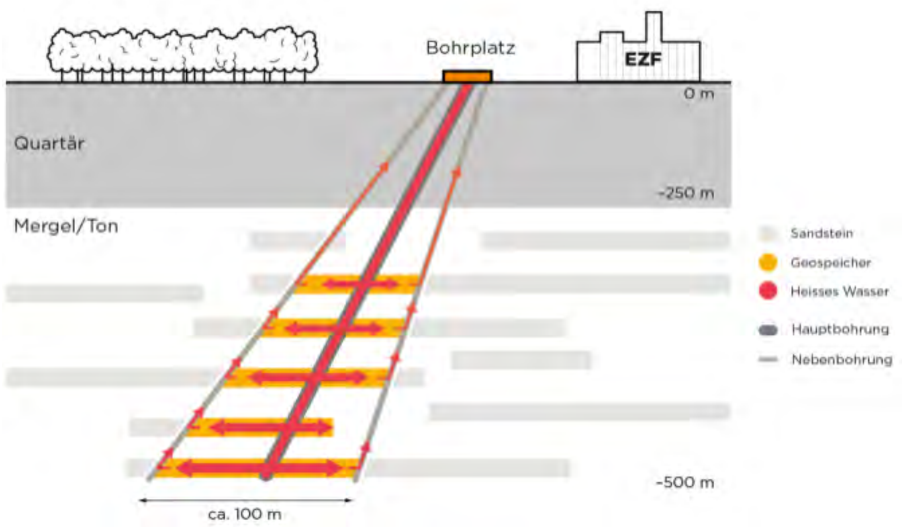

Functional principle of a Geostorage

8.13
Calibration of Basel (BS-1) stress-strength profiles using borehole failure geometry and stress measurements

Farid Zabihian[1], Reza Sohrabi[1], Andrés Alcolea[2], Peter Meier[2], Benoît Valley[1]

[1] *Centre for Hydrogeology and Geothermics (CHYN), University of Neuchâtel, Neuchâtel, Switzerland (farid.zabihian@unine.ch)*
[2] *Geo-Energie Suisse AG, Zürich, Switzerland*

Geothermal reservoirs are developped to exploit the heat and/or energy stored in the earth crust. These reservoirs are inherently heterogeneous in terms of both stress and strength, which impacts their productivity and sustainability. Deep geothermal boreholes of an Enhanced Geothermal System (EGS), like BS-1 in Basel, are most often drilled in the crystalline basements into the hot and low-permeable rocks. The key to success of a deep geothermal project is to address many technical challenges, risks and costs associated with deep drilling and stimulation of the EGS. These challenges include, amongst many others, high stress conditions resulting in borehole instability and impacting in induced seismicity risk.

Borehole stability is an important concern throughout both the drilling and operational phases of deep geothermal projects. One way to improve stability, thus preventing costly delays in drilling, is to deviate the well along the most favorable orientation relative to the in-situ state of stress. Such trajectory does not often coincide with that intersecting sufficient pre-existing fractures, i.e., the actual targets for stimulation, or those intersected are not prone to hydroshearing stimulation. Additionally, maintaining a smooth (in the sense of regular) borehole wall is essential for facilitating subsequent well completion activities, such as the installation of multi-packers for multi-stage hydraulic stimulation and operation.

Reducing the aforementioned risks involves characterizing in-situ state of stress and strength and assessing wellbore failure before and, especially, while advancing the borehole in order to optimise and update the drilling parameters, e.g., its trajectory, radius, etc. Borehole failure including borehole breakouts and Drilling-Induced Tensile Fractures (DITFs) can be imaged after interpreting, e.g., acoustic televiewer logs (as shown in Figure 1).

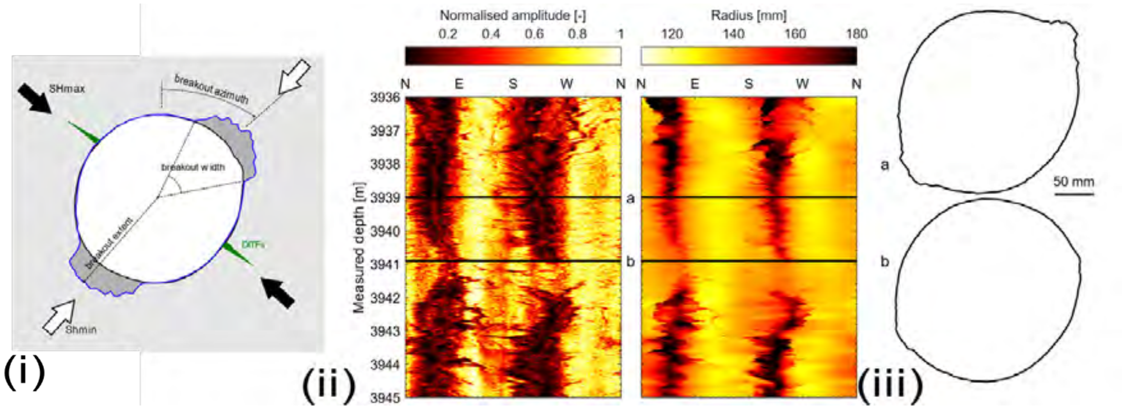

Figure 1. (i) Geometry of borehole breakouts and DITFs along a vertical borehole, (ii) image-logs of an interval along borehole BS-1 in Basel (Switzerland); (iii) interpreted cross-sections of the borehole, showing the small scale heterogeneity of breakout geometry over short distances.

On the other hand, the analysis of failure observations, i.e., breakouts and DITFs, provides remarkable insights into the rock›s strength, the in-situ state of stress, and their interplay at the closest vicinity of the borehole. Unlike many other primarily point-like stress measurement methods, e.g., mini-frac tests, the analysis of borehole failure profiles enables the characterization of stress and strength along uninterrupted 1D profiles along the drilled borehole. This allows to characterise stress variability occurring sometime over short distances, as shown in Figure 1(iii).

We enhanced a workflow initially developed by Dahrabou et al. (2022) for interpreting borehole failure information, and applied it to the crystalline section of the BS-1 borehole in Basel. Measurements were logged and interpreted shortly after drilling of the borehole and the variables in Figure 1(i) (i.e., breakout width, extent and orientation, and existence of DITFs) were employed to estimate model parameters. Main outcomes are borehole profiles including, amongst others, the heterogeneous distributions (1) of the principal components of the stress tensor with corresponding directions, and (2) of rock strength properties such as cohesion and friction.

The computationally efficient implemented semi-analytical solution, based on the Kirsch analytical solution for wellbore failure, enables the systematic estimation of model parameters and the corresponding uncertainties. Parameter estimation is carried out by the Regularized Pilot Points Method (Alcolea et al., 2006), following a two-step process taking advantage of the software package PEST (Doherty et al., 2010). Initially, consistent depth-related trends for the parameters are obtained (so-called 1st order characterisation), and next, deviations from these trends, which represent heterogeneity, are estimated (2nd order characterisation). This approach enables the generation of many equally-probable stress and strength profiles along the borehole.

An issue is the ill-posedness of the related inverse problem (aka. model calibration), which manifests in a broad range of calibrated stress and strength profiles leading to a similar solution in terms of borehole failure. To tackle this problem, the workflow readily accommodates direct measurements of the parameters being calibrated (e.g., S3 out of a mini-frac tests or cohesion/friction out of lab tests). Including such measurements greatly reduces the posterior, i.e., calibrated, parameter space, thus reducing the uncertainty of the calibrated models.

The findings from this investigation illustrate credible combinations of stress and strength parameters that more accurately replicate the intricate breakout distribution along BS-1 borehole. Furthermore, it highlights the advantages of refining parameter estimates based on robust empirical measurements or prior estimates.

REFERENCES

Alcolea A., Carrera J., Medina A. 2006: Pilot points method incorporating prior information for solving the groundwater flow inverse problem, Advances in Water Resources, 29, 1678–1689.

Dahrabou A., Valley B., Meier P., Brunner Ph., Alcolea A. 2022: A systematic methodology to calibrate wellbore failure models, estimate the in-situ stress tensor and evaluate wellbore cross-sectional geometry, International Journal of Rock Mechanics & Mining Sciences, 149, https://doi.org/10.1016/j.ijrmms.2021.104935.

Doherty, J.E., Hunt, R.J., and Tonkin, M.J., 2010, Approaches to highly parameterized inversion: A guide to using PEST for model-parameter and predictive-uncertainty analysis: U.S. Geological Survey Scientific Investigations Report 2010–5211, 71 p.

P 8.1
Magmatic hydrothermal fluid flow in caldera settings – Insights from 3D numerical simulations

Jonas Köpping[1], Thomas Driesner[1]

[1] *Department of Earth Sciences, ETH Zürich, Clausiusstrasse 25, CH-8092 Zürich (jonas.koepping@erdw.ethz.ch)*

Fracture systems and fault zones can locally enhance the effective rock permeability and as such create preferential fluid flow pathways. In magmatic hydrothermal systems, hot and buoyant fluids may exploit these faults and fracture networks to migrate to shallower depths. Understanding how magma-driven fluid flow evolves within faults and fractures and exploring potential boiling zones can help to further our knowledge on geothermal reservoirs in shallow-level volcanic complexes as well as on the formation of vein-type ore deposits.

Numerical simulations are a powerful tool to explore subsurface heat and fluid transport on the kilometre-scale and over geological timescales. It is important to conduct simulations in three dimensions (3D) as this will allow to resolve the intra-fault flow dynamics and the interplay between fluid flow within the fault plane and the host rock. Here, we present 3D numerical simulations of a simplified conceptual caldera setting, where a cone-shaped, high-permeability ring fault is located above an oblate magma body emplaced at 3–4 km depth. We use the Complex Systems Modelling Platform (CSMP++) to conduct multi-phase, pure-water fluid flow simluations in a porous rock. To explore the first-order behaviour of hydrothermal fluids in both the ring fault and the caldera, we systematically vary the permeability of the host rock, the fault, and the solidified intrusion, as well as the brittle-ductile-transition temperature (T_{BDT}).

Reference simulations without a high-permeability ring fault suggest that higher hydrothermal plume temperatures occur in systems with relatively high T_{BDT} (i.e., 460 ºC) and intermediate host rock and intrusion permeability (10^{-15} m^2). Simulations with a high-permeability ring fault promote rapid transport of hot fluids via the fault plane, which effects the large-scale hydrothermal system by (1) delaying the formation of a hydrothermal plume above the magma chamber; (2) deflecting the plume tips towards the fault plane and therefore modifying the plume geometry; and (3) reducing the temperature of the central plume (by up to 50 ºC at 500 m depth).

The three-dimensionality of our simulations allows us to explore fluid convection at various scales and, importantly, within the fault plane. Large-scale convection and the recharge of meteoric fluids from the surface to the intrusion occurs in all simulations independent of the presence of a high-permeability fault. We observe complex three-dimensional flow patterns along the contact of the fault and both the hangingwall and footwall, resulting in fluid flow into and out of the fault plane. Additional intra-fault convection occurs when the permeability contrast between the fault and the host rock is at least two orders of magnitude and the fault permeability is $\geq 10^{-14}$ m^2. Intra-fault convection is an efficient mechanism to transport cold meteoric fluids to greater depths, allowing for enhanced heat mining. When fault permeabilities are $<10^{-14}$ m^2, meteoric recharge via the fault is not significant enough, resulting in flat to slightly undulating thermal fronts migrating upwards along the fault plane.

Our results clearly indicate the effect of high-permeability ring faults on the thermal evolution of the large-scale hydrothermal system around a cooling intrusion, and thus they highlight the need to include all spatial dimensions when modelling hydrothermal fluid flow that involves faults and/or fracture networks. By exploring convective fluid flow patterns along the fault plane and within the caldera, our findings have direct implications for better assessing the potential of geothermal reservoirs associated with shallow-level volcanic complexes and the formation of vein-type hydrothermal ore deposits.

P 8.2
Magmatic-hydrothermal fluid flow related to silicic intrusions: implications for supercritical geothermal systems

Thierry Solms[1], Thomas Driesner[1], Olivier Bachmann[1], Isabelle Chambefort[2]

[1] *Institut für Geochemie und Petrologie, ETH Zürich, Clausiusstrasse 25, 8092 Zürich (thierry.solms@erdw.ethz.ch)*
[2] *GNS Science, Wairakei Research Centre, Private Bag 2000, Taupō 3352, New Zealand*

The Taupo Volcanic Zone (TVZ) in Aotearoa New Zealand is a unique magmatic arc regarding the magnitude of its Quaternary silicic magma flux, producing 25 caldera-forming eruptions within an area of 120 x 60 km. The magnitude of magmatic activity is joined by an equally impressive geothermal heat output (~4200 MW), which is harnessed via numerous geothermal wells drilled into the extensional rift basin (Wilson & Rowland 2016; Bibby et al. 1995).

Because of potential decreases in economic and ecological costs, many future geothermal projects worldwide aim at tapping supercritical hydrothermal resources (T > 373.946 °C, P > 220.64 bar for pure H_2O). Supercritical resources occur in proximity to their magmatic heat sources, especially when hosted in silicic rocks (Scott et al. 2016), which feature relatively low brittle-ductile transition temperatures (T_{BDT}) and thus possibly low permeabilities at supercritical conditions.

It is currently assumed that hydrothermal systems in the TVZ are the product of meteoric water percolating down through the fractured basement to the upper crustal mush zone (7-8 km), before ascending where permeable pathways permit it. Because current wells only reach around 3 km, numerical modelling is an important tool to understand magma-driven hydrothermal fluid flow at supercritical conditions.

We used the modelling platform CSMP++ to simulate hydrothermal fluid flow applied to a conceptual cross-section of the TVZ, which includes cooling intrusions at different depths in the crust, representing different views of potential magmatic heat sources. Systematic variation of relevant geological parameters in our models (e.g. intrusion geometry and depth, melt temperature, host rock permeability, T_{BDT}, volatile content of melt) allows us to investigate which set-up reproduces hydrothermal fluid temperatures observed in geothermal wells in the TVZ, and to study the thermal evolution over geological time scales. Furthermore, by adding code functionality which allows to model magmatic volatile phase (MVP) transport in and around hydrous intrusions (Lamy-Chappuis et al. 2020), we can study the effects of MVP degassing on the dynamics of hydrothermal systems above silicic intrusions.

We find that large, deep-seated (at 7-10 km depth), cooling silicic intrusions cannot reproduce TVZ reservoir temperatures unless the basement's permeability is locally increased. For smaller, and more shallow-seated (4 km) intrusions, we find that they can produce geothermal fluid temperatures, matching observations in the wells (>300°C), by triggering a focussed up-flow plume which persists long after the intrusion has cooled below solidus temperatures.

Our results can help inform future exploration efforts for supercritical geothermal resources in silicic volcanic terranes and extend our understanding of hydrothermal systems beyond geothermal reservoirs, down to the magmatic-hydrothermal transition zone.

REFERENCES

Bibby, H. M., Caldwell, T. G., Davey, F. J., & Webb, T. H. (1995). Geophysical evidence on the structure of the Taupo Volcanic Zone and its hydrothermal circulation. Journal of volcanology and geothermal research, 68(1-3), 29-58.

Lamy-Chappuis, B., Heinrich, C. A., Driesner, T., & Weis, P. (2020). Mechanisms and patterns of magmatic fluid transport in cooling hydrous intrusions. Earth and Planetary Science Letters, 535, 116111.

Scott, S., Driesner, T., & Weis, P. (2016). The thermal structure and temporal evolution of high-enthalpy geothermal systems. Geothermics, 62, 33-47.

Wilson, C. J., & Rowland, J. V. (2016). The volcanic, magmatic and tectonic setting of the Taupo Volcanic Zone, New Zealand, reviewed from a geothermal perspective. Geothermics, 59, 168-187.

P 8.3
Fracture network characterization for hydrothermal projects: Application to the AGEPP project in Lavey-les-Bains, Switzerland

Martin Vontobel, Reza Sohrabi, Benoît Valley

Centre for Hydrogeology and Geothermics (CHYN), University of Neuchâtel, Emile-Argand 11, 2000 Neuchâtel (martin.vontobel@unine.ch)

In the Paris Climate Agreement, Switzerland committed to reducing its greenhouse gas emissions by 2030 to 50 % of the emission levels in 1990 (BFE, 2020). To this end, the generation of renewable energies must be expanded quickly and consistently (BFE, 2023). The production of electricity and heat from deep geothermal energy has considerable potential (BFE, 2017). However, one of the biggest obstacles in the development of medium-depth to deep geothermal energy is the subsurface, which is often only poorly known (BFE, 2022).

This work proposes an approach to characterising fracture networks for hydrothermal projects that aim to explore the subsurface with a directional well profile. The approach focuses on finding a wellbore deflection for which the number of intersected productive fractures is maximised, thereby increasing the chances for a required production rate to be met. As part of the characterisation, the fracture network's connectivity is studied, which constitutes a key component for both the hydrogeological and the mechanical behaviour of the fractured rock. In the present case, the characterisation approach is applied to the Aiguilles Rouges Massif in Lavey-les-Bains (VD, Switzerland), which was targeted by the AGEPP hydrothermal project.

A Discrete Fracture Network (DFN) type model was used for the characterisation. DFN model parameters were derived from lineament maps, fracture trace maps and borehole fracture intercepts. To investigate differences that arise during fracture picking as a result of the subjective perception of the interpreter, independent data sets by two interpreters (picking 1 and 2) were analysed.

The results of the fracture network characterisation show that the fracture size distribution of the Aiguilles Rouges Massif can be described by a global power-law function with an exponent of 3.54. The spatial distribution of lineaments and fracture traces and the spatial distribution of borehole intercepts only show a slight or no fractal scaling. A comparison between borehole pickings 1 and 2 shows that increases and decreases in fracture frequency along the 2′958 m TVD deep borehole coincide well. However, in some cases, the two data sets show substantial differences in the absolute values of fracture frequency. A positive aspect that was identified is that the orientation distributions of the picked fractures are often similar.

Regarding the prediction of wellbore deflections that are favourable in terms of fracture frequency, the task remains challenging when the analysis is based on fracture data from above the kick-off point alone. However, a combined examination based on the criteria of fracture frequency and borehole stability showed that the prediction of favourable wellbore deflections is possible. For the realised wellbore deflection it was shown that it is one of the more favourable deflections for inclinations up to 40°. This is true when the closed fractures are included in the analysis or when only the open fractures are considered. Based on the two pickings, two different wellbore deflections were found to be the most favourable ones with respect to the fracture frequency and borehole stability criteria.

With regard to the connectivity study, it can be said that it is possible, even if not for all studied parameter setups, to generate fracture networks that show a connectivity. The critical threshold was often found in the range of P32 fracture densities that correspond to the P10 values of picked partially open and open fractures. As a result, at most a few connections can be expected to exist in the Aiguilles Rouges fracture network. A change in the maximum diametres of modelled fractures from lmax = 800 m to 100 m has shown that, in most cases, the fracture network changes from possibly connected to unconnected. Knowing that the fracture network in Lavey-les-Bains is connected, and assuming that the DFN model applied in this work is valid, this could be interpreted to suggest that larger discontinuities such as faults play a role in the rising of the geothermal water.

REFERENCES

BFE (2017). Potentiels, coûts et impact environnemental des installations de production d'electricité - Synthèse. URL: https://www.admin.ch/gov/fr/accueil/ documentation/communiques.msg-id-68703.html (accessed: 2023.08.29).

BFE (2020). Qu'est-ce que la Stratégie énergétique 2050? URL: https://www.bfe.admin.ch/bfe/fr/home/politique/strategie-energetique-2050/qu-est-ce-que-la-strategie-energetique-2050.html (accessed: 2023.08.29).

BFE (2022). Page d'accueil / Approvisionnement / Energies renouvelables / Géothermie. URL: https://www.bfe.admin.ch/bfe/fr/home/approvisionnement/energies-renouvelables/geothermie.html (accessed: 2023.08.29).

BFE (2023). Loi fédérale relative à un approvisionnement en electricité sûr reposant sur des énergies renouvelables. URL: https://www.bfe.admin.ch/bfe/fr/home/approvisionnement/approvisionnement-en-electricite/loi-federale-approvisionnement-electricite-renouvelables.html (accessed: 2023.08.29).

P 8.4
Feasibility of CO_2 Storage in Depleted Gas Reservoirs: A Case Study of the F-O Gas Field, Bredasdorp Basin, offshore South Africa

Sanelisiwe Mhlambi[1,2] Jan van Bever Donker[1], Ovie Emmanuel Eruteya[2], Andrea Moscariello[2] and Elias Samankassou[2]

[1] *Earth Sciences Department, University of Western Cape, Robert Sobukwe Road, Bellville, 7535*
[2] *Department of Earth Sciences, University of Geneva, Rue de Maraîchers 13, 1205 Geneva (3555622@myuwc.ac.za)*

As global climate change mitigation efforts intensify, repurposing depleted oil and gas reservoirs for CO_2 storage becomes increasingly vital. The Bredasdorp Basin, host to South Africa's only oil- and gas-producing fields, offers a pivotal focal point for this research. This study investigates the potential for CO_2 storage in the depleted gas reservoirs of the F-O Gas Field, located 400 km southeast of Cape Town, offshore South Africa, within the complex geological framework of the Bredasdorp Basin.

The F-O Gas Field is characterized by its Valanginian-age upper shallow marine tidal dune field, nestled at a depth of 3700 m. The field showcases a 3-way dip closure with a fault trap and features a compartmentalized reservoir. Reservoir properties exhibit variation, with thickness spanning the range of 80 to 160 m. The field presents a distinctive challenge due to its low porosity (ranging from 2 to 16%, averaging at 9%) and low permeability (0.01 mD to 10 mD, with an average of 1 mD), which are characteristic of very tight and heterogeneous sand reservoirs. These attributes necessitate a meticulous reservoir delineation and a thorough assessment of its fluid flow capacity over an extended economic horizon.

The application of advanced reservoir characterization workflow, involving 3D seismic data and well-log analysis provides indispensable insights into the structural complexities, reservoir properties, and CO_2 storage potential of the F-O Gas Field. The seamless integration of these datasets enables the development of a high-fidelity static reservoir model, an indispensable tool for assessing CO_2 storage scenarios and identifying optimal injection sites.

In conclusion, this study underscores the paramount importance of data-driven assessments in advancing the feasibility of carbon capture and storage within gas reservoirs. Through the integration of 3D seismic and well-log data, it offers a comprehensive examination of the F-O Gas Field's suitability for CO_2 storage. Structural elements and fluid flow dynamics surface as critical considerations for the formulation of effective CO_2 injection and containment strategies.

P 8.5
Investigating the chemical reactivity of the Gipskeuper and Muschelkalk formations to wet CO_2 injection: A case study towards the first Swiss CCS pilot

Nicolás Rangel Jurado[1], Martina Cervelli[2], Federico Games[2], Xiang-Zhao Kong[1]

[1] *ETH Zürich, Sonneggstrasse 5, 8092 Zurich (nrangel@ethz.ch)*
[2] *Ad Terra Energy, Chemin des Vergers 4, 1208 Geneva*

INTRODUCTION

Over the past two centuries, global population growth has driven a dramatic increase in primary energy demand, predominantly met by fossil fuels, leading to a substantial and unprecedented rise in atmospheric carbon dioxide (CO_2). As Switzerland aims for net-zero emissions by 2050, carbon capture and storage (CCS) within subsurface formations has emerged as an important technology to address the issue (Swiss Federal Office of Energy 2020). In order to accelerate the adoption of this technology and ensure its long-term safety, a comprehensive understanding of how the injected CO_2 will interact with *in situ* fluids and rocks in geological reservoirs is paramount (Figure 1).

CASE STUDY: ÉCLÉPENS

The Éclépens area, located in the Western part of the Swiss Molasse Basin, has been recently identified as a potential site for geological sequestration of CO_2 (Hau et al. 2022) with a prospective CO_2 storage capacity ranging from 2 to 6 million tons. If successful, Éclépens would be the first full-chain CCS project of its kind in Switzerland. Two rock specimens from the Muschelkalk and the Gipskeuper formations were selected based on their favorable petrophysical attributes to represent the reservoir and caprock samples, respectively, in the laboratory experiments further explained in the following section.

METHODS

In order to investigate the chemical reactivity of CO_2-rich mixtures towards the potential storage formations in Éclépens, we conducted core-scale batch experiments under reservoir conditions. The specimens from the Muschelkalk and Gipskeuper formation were subjected to interactions with water-saturated CO_2 under elevated pressure and temperature conditions (35 MPa, 150 ºC) for approximately 500 hours. A wide range of high-resolution techniques, including scanning electron microscopy (SEM) and X-ray diffraction (XRD), among others, were employed before and after the fluid-mineral interactions occurred. These analyses were utilised to characterise the evolution of the morphology, petrophysical properties, and chemical composition of the samples. Upon termination of the experiment, the fluid effluents, both in aqueous and gas phase, were also analysed using inductively coupled plasma atomic emission spectroscopy (ICP-AES) to determine the extent of the associated ion dissociation reactions triggered by the water-saturated CO_2 and the aqueous solution.

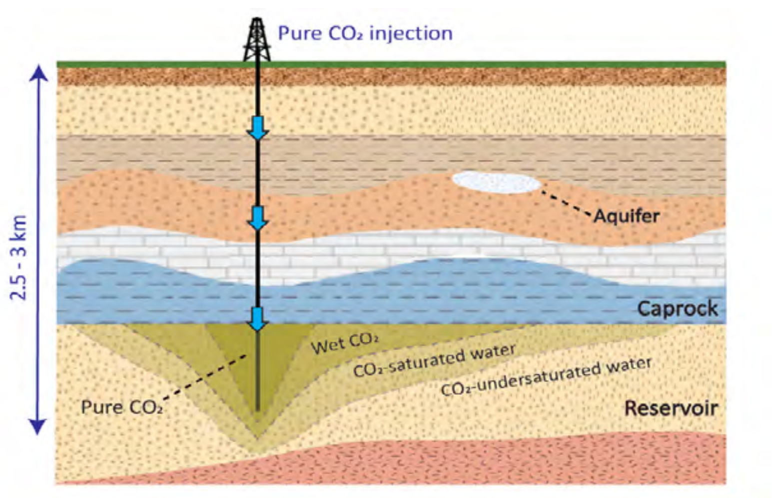

Figure 1. Schematic showing CO_2 injection in a deep reservoir. Carbon dioxide injection creates regions that exhibit the full spectrum of mutual CO_2-H_2O solubility. Dry sCO_2 and wet sCO_2 are less dense than the aqueous phase for nearly all PT ranges in subsurface reservoirs, resulting in the upward migration of the CO_2-rich phase towards the caprock.

RESULTS AND DISCUSSION:

Comparison of the pre- and post-experiment XRD analysis confirms a significant amount of mineral dissolution as well as the absence of new mineral phases caused by the interaction with water-saturated (wet) CO_2. However, these results alone are not conclusive, as this dissolution could have been caused by the water-saturated CO_2 during the 500-hour experiment, by the CO_2-saturated water that condensed out of CO_2 due to depressurization during experiment termination, or a combination of both processes. However, the results from ICP-AES analysis of major elements (Ca, Mg, and K) indicate that the residual aqueous phase located at the bottom of the batch reactor contains notably higher concentrations of dissolved ions compared to those present in the wet CO_2 phase. The difference in ion concentration levels is significant, typically ranging from 0.5 to 2 orders of magnitude. This suggests that the condensed aqueous solution is the primary medium for dissolution. Additionally, pre-, and post-experiment SEM scans suggest that accessory minerals like sodium were readily dissolved and mobilized by the wet CO_2 phase.

CONCLUSIONS:

Our experimental investigation shows that fluid-mineral interactions involving CO_2-rich supercritical fluids are less severe than those caused by aqueous solutions. Nonetheless, the existence of dissolved ions in the wet CO_2 samples is clear evidence of ion dissociation caused by the gaseous phase that warrants further investigation. The experimental characterization of CO_2-rich mixtures reacting with reservoir and seal rocks represents a critical step in ensuring the reliability, long-term security, and technical feasibility of deploying CCS globally.

REFERENCES

Hau, K., F. Games, R. Lathion, M. Brehme, and M. O. Saar. 2022. On the feasibility of producing geothermal energy at an intended CO_2 sequestration field site in Switzerland. European Geothermal Congress 2022.

Swiss Federal Office of Energy (2020). Energieperspektiven 2050+. Tech. rep. United Nations. 2015. Paris Agreement to the United Nations Framework Convention on Climate Change. Govt. publication.

P 8.6
Critical raw materials from deep geothermal fluids - how to sample and what to analyse?

Emiliano Stopelli[1], Stefan Heuberger[2,*], Nicole Lupi[3], Thomas Galfetti[4,*]

[1] *Nagra, National Cooperative for the Disposal of Radioactive Waste, Hardstrasse 73, CH-5430 Wettingen (emiliano.stopelli@nagra.ch)*
[2] *Georesources Switzerland Group, Department of Earth Sciences, ETH Zurich, Sonneggstrasse 5, CH-8092 Zurich*
[3] *Swiss Federal Office of Energy, Pulverstrasse 13, CH-3063 Ittigen*
[4] *Swiss Geological Survey, Federal Office of Topography swisstopo, Seftigenstrasse 264, CH-3084 Wabern*

**presenting authors*

As the european countries are committed to achieve climate neutrality by 2050, the transition to a clean energy economy is expected to generate a massive demand of electric cars, solar panels, wind turbines, batteries, superconductors and other green tech components. Since certain elements, labeled as Critical Raw Materials (CRMs) by the European Commission (2023), are the building components for the development of this technology, the demand for these materials is projected to increase exponentially in the next decades.

Geothermal fluids are known to represent a potentially-promising source of some CRMs and especially lithium, a crucial component for the manufacturing of batteries (Goldberg et al., 2021). Mandated by the Swiss Geological Survey and the Swiss Federal Office of Energy, the Georesources Switzerland Group recently performed an evaluation of the available hydrochemical data obtained from deep drilling projects in Switzerland (Heuberger and Morgenthaler, 2023). The investigation showed that Switzerland still lacks a comprehensive hydrochemical dataset to assess, whether or not the Swiss deep aquifers are of economic interest for a potential extraction of strategic metals, like for instance the Upper Rhine Graben (Frey et al., 2022).

As research and development in this field is still in its early stage, there is still no standard best practice, or an internationally-recognized protocol on (1) how to sample fluids from deep wells and (2) what kind of analytical programme and methodology is necessary. The authors intend to close this gap by bridging the expertise of Nagra in deep groundwater characterisation, the mineral and geothermal exploration community as well as geological surveys of the neighbouring countries. The final aim is to produce a technical guideline that will assist the permitting authorities and planners in ensuring that future geothermal exploration projects will sample and analyze the deep fluids encountered according to state-of-the-art techniques. By doing so, the gap in the current hydrochemical knowledge will shrink along with the growing adoption and development of geothermal energy in Switzerland.

You are kindly invited to share your thoughts and advice on this novel subject at our poster booth.

REFERENCES
European Commission 2023: European Critical Raw Materials Act. Proposal for a regulation of the European Parliament and of the Council establishing a framework for ensuring a secure and sustainable supply of critical raw materials and amending Regulations (EU) 168/2013, (EU) 2018/858, 2018/1724 and (EU) 2019/102.

Frey, M., Bär, K., Stober, I., Reinecker, J., van der Vaart, J. & Sass, I. 2022: Assessment of deep geothermal research and development in the Upper Rhine Graben. Geothermal Energy 10, 18.

Goldberg, V., Winter, D., Nitschke, F., Rath, M., Held, S., Spitzmüller, L., Budach, I., Pavez, M., Morata, D., Koschikowski, J., Kohl, T. 2021. The potential of raw material extraction from thermal brines – Successful milestones of the BrineMine project. Oil Gas European Magazine 47, 26-33.

Heuberger, S. & Morgenthaler, J. 2023: Lithium in geothermal brines - Status report on the current situation in Switzerland and in neighbouring countries. Technical report, Georesources Switzerland Group, ETH Zurich, 43 p.

10 Quaternary environments: landscapes, climate, ecosystems and human activity during the past 2.6 million years

Sandra Bruegger, Marius Buechi, Catharina Dieleman, Loren Eggenschwiler, René Löpfe, Marc Luetscher, Tobias Schwestermann, Bigna Steiner

Swiss Society for Quaternary Research (CH-QUAT)

TALKS:

10.1 Ajallooeian F., Ladd S.N., Dubois N., Schubert C.J., Lever M.A., Eglinton T.I., De Jonge C.: Testing Temperature Sensitivity of brGDGTs across various timescales: Days to Centuries

10.2 Baumann P., Nieberle M., Wegmüller F., Turck R.: Geophysics at Steigelfadbal (Vitznau, LU): Approach to Non-Invasive Archaeological Cave Research

10.3 Bollen M., Blaser P., Bruggman S., Müller J., Gutjahr M., Jaccard S.: Unveiling Glacial Retreat Dynamics through Mulit-faceted Analysis of a Weddell Sea Sediment Core across Termination 1

10.4 Buechi M.W., Anselmetti F.S., Bros E., Deplazes G., Gegg L., Ivy-Ochs S., Kober F., Landgraf A., Madritsch H., Mueller D., Preusser F., Spillmann T., Tomonaga Y.: Overdeepened glacial basins as archives for Quaternary glaciations and subglacial processes: A detailed study from the Swiss Northern Alpine foreland

10.5 Cook D.L., Ivy-Ochs S., Monegato G., Scardia G., Dieleman C., Christl M., Vockenhuber C., Akçar N.: Reconstructing the lower/middle Pleistocene transition in the western sector of the Garda end-moraine system using $^{26}Al/^{10}Be$ cosmogenic burial dating

10.6 Courtney-Mustaphi C., Steiner E., von Fumetti S., Heiri O.: Quaternary assemblages of aquatic invertebrate mandibles and other sclerotized remains

10.7 Eglinton T., Graven H., Hagedorn F., Szidat S., Brunmayr A., Duborgel M., Geissbuehler D., Laemmel T., Minich L., Mittelbach B., Rhyner T., White M.: The Radiocarbon Inventories of Switzerland (RICH) project: an integrated approach to understand the changing carbon cycle

10.8 Girardclos S., Gastineau R., Kremer K., Anselmetti F.S.: Human-initiated autocyclic delta failures

10.9 Hajdas I., Crann C., DeLong K., Fiałkiewicz-Kozieł B., Ju Ivar Do Sul J., Kaiser J., McCarthy F., Turner S., Stenger M.A., Waters C.,Zinke J.: Detection of the bomb peak ^{14}C for the onset of the Anthropocene

10.10 Held F., Cheng H., Edwards R.L., Tüysüz O., Fleitmann D.: Hydrological and temperature variations in the Black Sea region during the last 650’000 years recorded by speleothem fluid inclusions

10.11 Kamleitner S., Ivy-Ochs S., Salcher B., Reitner J.M.: Subglacial landforms and basal ice flow patterns of the LGM Rhine glacier

10.12 Lapellegerie P., Millet L., Rius D., Heiri O.: Summer temperature reconstruction fo the LGM in Central Europe based on chironomids

10.13 Lleshi K., Jouvet G., Cook S.J., Herman F.: Retrieving climates form the last glacial maximum using an invert glacier model

10.14 Mathes N., Luetscher M., Ivy-Ochs S., Dieleman C., Christl M., Vockenhuber C., Akçar N.: The Jura ice cap and Alpine ice sheet interface: Insights from burial dating exogenic cave sediments

10.15 Santos M., Bröder L., Hernández-Almeida I., Lattaud J.: Investigating the evolution of Holocene sea ice and primary production in the Beaufort Sea, Canadian Arctic using lipid biomarkers

10.16 Schaller S., Schuster S., Beraus S., Buechi M.W., Buness H., Anselmetti F.S.: New insights into the Basadingen Through: An overdeepened valley in Northern Switzerland

10.17 Wheen L.: Exploring the link between Earth’s orbital parameters and glacial cycles

POSTERS:

P 10.1 Binaghi M., Ivy-Ochs S., Yeşilyurt S., Christl M., Akçar N.: Post-LGM glacier fluctuations in the northern Valaisian Alps

P 10.2 Broś E., Ivy-Ochs S., Kober F., Grischott R., Vockenhuber C., Christl M., Gautschi P., Maden C., Nørgaard J., Knudsen M.F., Pollhammer T., Salcher B., Ylä-Mella L., Jansen J.D., Buechi M.W., Deplazes G., Synal H.-A.: Timing and patterns of Early to Middle Pleistocene outwash deposition derived from study of the Deckenschotter

P 10.3 Bucher G., Dieleman C., Ivy-Ochs S., Aaron J., Vockenhuber C., Akçar N.: Reconstruction of postglacial mass movements in the Lurnigalp

P 10.4 Camenzind L., Deline P., Ivy-Ochs S., Aron J., Christl M., Akçar N.: Evolution of the Polygenetic le Pont Cone, The Ferret Valley, Mont Blanc Massif

P 10.5 Devillet G., Damber M., Lappellegerie P., Brügger S., Heiri O.: Impact of recent climate change and human impact on Cladocera populations inferred from high-resolution cores of Swiss mountain lakes

P 10.6 Dieleman C., Deline P., Ivy Ochs S., Hug P., Aaron J., Christl M., Akçar N.: Reconstructing the evolution of the Frébouge polygenetic cone in the Italian Ferret Valley, Mont Blanc Massif

P 10.7 Felder M.H., Gilli A., Dubois N., Anselmetti F.S., Hanselmann K., Eglinton T.I.: Reconstruction of high-alpine paleoenvironment using lake sediments of the Jöri Lakes, Graubünden, Switzerland

P 10.8 Hofmeister E., Kipfer T., Fleitmann D., Cheng H., Häuselmann A., Affolter S.: Central Europe temperature snapshots over the last 300’000 years derived from speleothem fluid inclusion water isotopes from Milandre Cave, Switzerland

P 10.9 Kipfer T., Affolter S., Hofmeister E., Häuselmann A., Lütscher M., Cheng H., Fleitmann D.: Alpine lapse rate in drip waters and speleothem fluid inclusions

P 10.10 Kremer K., Sullivan E., Luyet E., Annan P., Rast D., Zimmerli M., Fabbri S.C., Gastineau R.: Spatial and temporal distribution of microplastics in lake sediments in Switzerland

P 10.11 Lattaud J., Burrough S., Walsh E., Vogel H., De Jonge C.: A paleolake in the desert: environmental reconstruction using organic and inorganic proxies

P 10.12 Melo Velasco V., Ivy-Ochs S., Akçar N., Christl M., Vockenhuber C., Reitner J.: Reconstructing the Lateglacial and Holocene glacial history at the Leg Grevasalvas catchment (Graubünden)

P 10.13 Morgan A., Cheng H., Edwards L.R., Matter A., Hofmeister E., Tüysüz O., Fleitmann D.: Late Holocene speleothem-reconstruction from SW Asia

P 10.14 Rubin A., Ivy-Ochs S., Schlüchter C., Binaghi M., Jordan A., Vockenhuber C., Akçar N.: Integrated analysis of the Sierre Landslide, Rhone Valley

P 10.15 Scherer S., Ivy-Ochs S., Kamleitner S., Inderbitzin L., Vockenhuber C., Christl M.: Reconstructing the final phase of the Last Glacial Maximum Reuss glacier at Blattiswald and the timing and extent of the prehistoric Steinerberg (Rubenen) landslide in the region of Goldau, Schwyz

P 10.16 Schmidt C., Oehler S., Niyonzima P., Herman F., King G.: Continental temperatures since the Last Glacial Maximum inferred from luminescence palaeothermometry

P 10.17 Studer A.S., Wörmer L., Vogel H., Dubois N., Hinrichs K.-U., Lehmann M.F.: First lacustrine application of the diatom-bound nitrogen isotope paleo-proxy reveals coupling of denitrification and N2 fixation in a hyper-eutrophic lake

10.1
Testing Temperature Sensitivity of brGDGTs Across Various Timescales: Days to Centuries

Fatemeh Ajallooeian[1], S. Nemiah Ladd[2], Nathalie Dubois[1,3], Carsten J. Schubert[1,3], Mark A. Lever [4],Timothy I. Eglinton[1], Cindy De Jonge[1]

[1] Geological Institut, ETH Zurich, Switzerland (fatemeh.ajallooeian@erdw.ethz.ch)
[2] Department of Environmental Science, University of Basel, Switzerland
[3] Swiss Institute of Aquatic Science and Research (Eawag), Switzerland
[4] Marine Science Institute, University of Texas at Autstin, USA
Correspondonce: Fatemeh Ajallooeian

Based on global datasets, changes in the degree of methylation of bacterial membrane-spanning lipids (branched Glycerol Dialkyl Glycerol Tetraethers (brGDGTs)), have been used as a quantitative proxy for mean annual (or growth season) temperature changes in different environmental settings (Loomis et al., 2014, Russell et al., 2018, Martinez-Sosa et al., 2019). However, existing freshwater calibrations still contain significant uncertainty, and the potential impact of other parameters such as water chemistry, anoxia and bacterial community changes on the temperature dependency are not well-constrained.

To shed light into these uncertainties, we study the environmental drivers of brGDGTs in Lake Rot (Rotsee), a shallow (16 m), subalpine, eutrophic lake in Switzerland that is characterized by a seasonal mixing regime (Naeher et al., 2014). To understand the mechanisms behind the variability in brGDGT distributions on different timescales, we combine laboratory mesocosms at different temperatures, high-temporal resolution sampling in surface (oxic) and deep (suboxic) water layers, and the study of long-term variability across a Holocene-spanning, 10-long sediment core. Extracted brGDGTs were analyzed using HPLC-MS and HPLC-HRMS. Water chemistry parameters (including water pH, dissolved oxygen, conductivity, and concentration of cations/anions) were measured in the experimental mesocosms and seasonal variability tests. Last but not least, 16S rRNA gene amplicon sequencing on a subset of samples was performed to outline potential brGDGT producing communities and their role in brGDGTs variability.

Based on the mesocosm work (n=180), we present a disparate and seasonally non-uniform response of brGDGT lipids to varying temperatures on the timescale of days to weeks. A limited impact of temperature on the degree of methylation (summarized as the MBT'_{5ME} proxy) is observed, and a potential impact of inorganic water parameters such as conductivity on the production of 6-methyl brGDGTs. Although the seasonal suspended particulate matter (SPM) samples (n=20) exhibit a correlation with water temperature, specifically within the surface oxic layer, the distribution of GDGTs in bottom waters is notably influenced by mixing regimes and the availability of oxygen. Lastly, in the paleo-record, substantial variations in the MBT'_{5ME} (0.14-0.42, n = 60) are observed (Fig. 1), allowing us to distinguish between the period of warming since the last glacial maximum (4 °C) and a stable Holocene temperature range (8-10 °C). This highlights that the temperature dependency on longer timescales is different, possibly because the change in our seasonal mesocosms experiment can be averaged out over longer timescales, allowing long-term temperature changes to be reconstructed.

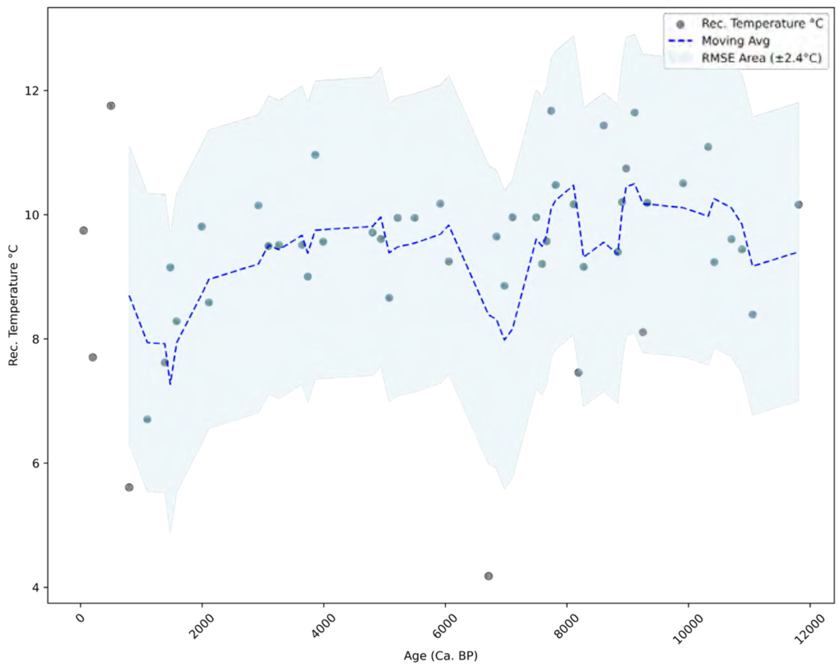

Figure 1. provides an illustration of the Holocene reconstructed temperature for Lake Rot. The shaded area represents the calibration error window as determined by the root mean square error (RMSE). Additionally, the dashed blue line portrays the moving average of the reconstructed temperature, with a window size of 5.

REFERENCES

1: Loomis, S. E., Russell, J. M., Heureux, A. M., D'Andrea, W. J., & Damsté, J. S. S. (2014). Seasonal variability of branched glycerol dialkyl glycerol tetraethers (brGDGTs) in a temperate lake system. Geochimica et Cosmochimica Acta, 144, 173-187.

2: Russell, J. M., Hopmans, E. C., Loomis, S. E., Liang, J., & Damsté, J. S. S. (2018). Distributions of 5-and 6-methyl branched glycerol dialkyl glycerol tetraethers (brGDGTs) in East African lake sediment: Effects of temperature, pH, and new lacustrine paleotemperature calibrations. Organic Geochemistry, 117, 56-69.

3: Martínez-Sosa, P., & Tierney, J. E. (2019). Lacustrine brGDGT response to microcosm and mesocosm incubations. Organic Geochemistry, 127, 12-22.

4: Naeher, S., Peterse, F., Smittenberg, R. H., Niemann, H., Zigah, P. K., & Schubert, C. J. (2014). Sources of glycerol dialkyl glycerol tetraethers (GDGTs) in catchment soils, water column and sediments of Lake Rotsee (Switzerland)–Implications for the application of GDGT-based proxies for lakes. Organic Geochemistry, 66, 164-173.

10.2
Geophysics at Steigelfadbalm (Vitznau, LU): Approach to Non-Invasive Archaeological Cave Research

Philipp Baumann[1], Matthias Nieberle[2], Fabio Wegmüller[1], Rouven Turck[1]

[1] *Institut für Archäologie, Universität Zürich, Karl-Schmid-Strasse 4, CH-8006 Zürich (philipp.baumann6@uzh.ch)*
[2] *Kantonsarchäologie Aargau, Industriestrasse 3, CH-5200 Brugg*

The Steigelfadbalm cave above Vitznau, LU on Lake Lucerne is an important archaeological site belonging to the Middle Palaeolithic Mousterian. The cave was formed by the erosion of layers of sandstone and marl (Mergel), which lie between the Nagelfluh forming the main share of Mt. Rigi (Fig. 1). The cave was then further eroded by glacial processes (Rabeder et. al. 2017).


Figure 1. Aerial view of the cave location (red dot) (Kantonsarchäologie Luzern)

Excavations were carried out between 1913 and 1937 by a team lead by Wilhelm Amrein, then director of the Gletschergarten of Lucerne. These excavations yielded an abundance of animal bones as well as stone tools. The animal bones, initially thought to belong to the extinct cave bear species *ursus spelaeus,* were later found to belong to *ursus ingressus*, a cave bear species found mainly in Styria (A). The Steigelfadbalm cave represents the westernmost site of *ursus ingressus.* A radiometric AMS dating of a cave bear bone was carried out and resulted in a calibrated age of 31’177 years BP. The analysis of the animal bones carried out by Frischauf et. al. (2017) however also disproved Amrein’s theory that there were worked bone tools amid the assemblage.

The knapped stone tools indicate a presence of hominins during the Pleistocene. Altough the precise stratigraphic context remains unclear, they probably belong to the Mousterian. They would therefore be the first evidence of this techno-complex in central Switzerland (Frischauf et. al. 2017).

Besides these Palaeolithic finds, the excavation yielded some other finds of later periods, such as a Neolithic flint blade, a Bronze Age arrowhead and a lead bullet. This suggests that the cave was used as a shelter by hunters and shepherds during much of recorded time.

To further study the cave, several factors needed to be known. The first was to locate the old excavation areas, as many of the plans and drawings made at the time have been lost or cannot be accurately located. The second was to find out how much sediment lay between the modern walking level and the Nagelfluh cave floor, and to locate possible areas for future excavation. The natural sediments in the cave consist of loamy sand, in which disturbed and undisturbed sections could not be identified.

This led to the idea of a project in which geophysical survey equipment would be used in the cave to answer some of the questions raised. In a first phase, three pseudo ERT sections were carried out using a TAR-3 (Frobisher)(Fig. 2). A small area was also surveyed with a single sensor Fluxgate 256 magnetometer (Geoscan).
Although conditions in the cave were not optimal for this type of survey, promising results were obtained. The results of this research will be presented at SGM 2023.

Figure 2. Setting up electrodes for the ERT lines. (Fabio Wegmüller)

REFERENCES

Frischauf, C., Nielsen, E. & Rabeder, G. 2017: The cave bears (Ursidae, Mammalia) from Steigelfadbalm near Vitznau (Canton of Lucerne, Switzerland). Acta Zoologica Cracoviensia 60 (2), S. 35–57. DOI: 10.3409/azc.60_2.35.

Rabeder, G., Frischauf, C. & Nielsen, E. 2017: Steigelfadbalm, eine fossilführende Bärenhöhle in der Nagelfluh der Rigi bei Luzern (Zentralschweiz). Die Höhle 68,1, 2017, 124–133.

10.3
Unveiling Glacial Retreat Dynamics through Mulit-faceted Analysis of a Weddell Sea Sediment Core across Termination 1

Bollen M., Blaser P., Bruggman S., Müller J., Gutjahr M., Jaccard S.:

In the pursuit of understanding Earth's complex climate system, the examination of paleoceanography through the analysis of sediment cores using multiple proxies is of great significance. The Southern Ocean is globally important due to its significant role in influencing atmospheric CO_2, and additionally with great effects on the stability of the Antarctic Ice Sheet (AIS). Studying the dynamics of deglaciation in this region, here with a specific focus on the Filchner-Ronne Ice Shelf, provides crucial insights into past climatic changes, contributing to our understanding of current and future trends. The integration of these observations into global climate models will also help better our ability to resolve anticipated behavior of the AIS under anthropogenic climate change.

In this study, we report findings from an investigation of the 5 meter long sediment core PS111_53-2, obtained near the modern calving front Ronne Ice Shelf in the Weddell Sea. Sedimentological observations indicate that the core preserves the full deglacial transition from sub-ice sheet to open marine conditions. Radiogenic isotopes of neodymium and lead target both the authigenic and detrital phases of the sediment, and are coupled with redox-sensitive trace element concentrations to better understand environmental change in the region. Further insight was gained through the study of organic carbon composition, environmental magnetism, and SEM imagery.

This sediment archive provides a unique insight into the timing and nature of glacial retreat across Termination 1 in the Weddell Sea Embayment. Our results illustrate a hugely dynamic environment that is reflective of the complexities expected at the interface of the cryosphere, atmosphere, and oceans across a period of global climate reorganization.

10.4
Overdeepened glacial basins as archives for Quaternary glaciations and subglacial processes: A detailed study from the Swiss Northern Alpine foreland

Marius W. Buechi[1], Flavio S. Anselmetti[1], Ewelina Bros[2], Gaudenz Deplazes[3], Lukas Gegg[4], Susan Ivy-Ochs[2], Florian Kober[3], Angela Landgraf[3], Herfried Madritsch[3,5], Daniela Mueller[4], Frank Preusser[4], Thomas Spillmann[3], Yama Tomonaga[6]

[1] *Institute of Geological Sciences & Oeschger Centre for Climate Change Research, University of Bern, 3012 Bern (marius.buechi@unibe.ch)*
[2] *Laboratory of Ion Beam Physics, ETH Zurich, 8093 Zürich*
[3] *NAGRA - Nationale Genossenschaft für die Lagerung radioaktiver Abfälle, 5430 Wettingen*
[4] *Institute of Earth and Environmental Sciences, University of Freiburg, Albertstr. 23b, 79104 Freiburg (D)*
[5] *now at: Swiss Geological Survey, swisstopo, 3084 Wabern*
[6] *Eawag, Swiss Federal Institute of Aquatic Science and Technology, 8600 Dübendorf & Department of Environmental Sciences, University of Basel, 4056 Basel*

Overdeepened glacial basins are typical, yet poorly understood, elements of glacial landscapes. The 10s to 100s of meters of unconsolidated sediment filling the overdeepenings are a largely untapped terrestrial archive for Quaternary environmental change and landscape evolution.

We present the results of a detailed study on Quaternary overdeepenings in the Swiss northern Alpine foreland that were eroded under the Rhine paleoglacier and its adjacent lobes. Seismic data and drill cores (c.1800 m in total from 11 sites) acquired by Nagra allowed us to reconstruct the geometry and the depositional evolution of these overdeepenings and the connected downstream fluvial channels. Our analysis shows that the overdeepened basin fills are composed of a limited number of architectural elements and genetic basin sequences. When mapped out, these elements and sequences help to understand when and how overdeepenings were eroded and infilled. In addition, a multi-method dating approach is tested to help constraining the timing of erosion and infill in response to extensive glaciation of the Alpine foreland.

Overall, the results contribute to a more complete reconstruction of the repeated extensive glaciation of the Alpine forelands and a better understanding of landscape evolution in response to global climatic changes during the Quaternary.

10.5
Reconstructing the lower/middle Pleistocene transition in the western sector of the Garda end-moraine system using $^{26}Al/^{10}Be$ cosmogenic burial dating

Dylan L. Cook[1], Susan Ivy-Ochs[2], Giovanni Monegato[3], Giancarlo Scardia[4], Catharina Dieleman[5], Marcus Christl[2], Christof Vockenhuber[2], Naki Akçar[5]

[1] Department of Earth Sciences, ETH Zurich, Sonneggstrasse 5, CH-8092 Zurich (dycook@student.ethz.ch)
[2] Laboratory of Ion Beam Physics, ETH Zurich, Otto-Stern-Weg 5, CH-8093 Zürich
[3] CNR-IGG, Via Giuseppe Moruzzi, 1, 56124 Pisa PI, IT
[4] Instituto de Geociências e Ciências Exatas, Universidade Estadual Paulista, Av. 24 A, 1515 - Bela Vista, Rio Claro - SP, 13506-700, Brazil
[5] Institute of Geological Sciences, University of Bern Baltzerstrasse 3, CH-3012 Bern

The Lake Garda region in Northern Italy hosted repeated glaciations by the Adige-Sarca glacier during the Pleistocene, forming Lake Garda, the Garda end-moraine system, and an extensive suite of glacial and glaciofluvial deposits. Uplift to the west of Lake Garda shifted glacier advances eastward over the course of the Pleistocene, preserving pre-Last Glacial Maximum (LGM) deposits in the western Garda end-moraine system. Reconstructing the timeline and extent of these pre-LGM glaciations has been made difficult by the limited availability of exposures and challenges in determining absolute ages for pre-LGM deposits. This study provides the first absolute age of emplacement of the outermost moraine of the western Garda end-moraine system through the application of cosmogenic burial dating. A cut-and-cover railway construction project briefly exposed Pleistocene deposits at the Calcinato moraine in the spring of 2022, allowing for stratigraphic description and sampling of crystalline clasts from the exposed units for $^{26}Al/^{10}Be$ burial dating. Burial age calculations were performed using P-PINI (Particle-Pathway Inversion of Nuclide Inventories), which incorporates source-to-sink based simulations of burial and exposure to calculate a burial age (Norgaard et al., 2023). Prior paleomagnetic investigations indicated the exposed moraine may be in the range of MIS 22 – MIS 16 in age. The results of dating these briefly exposed moraine sediments provide an independent temporal constraint for paleomagnetic data, builds upon ongoing research examining pre-LGM glaciations in the Garda end-moraine system, and furthers understanding of the evolution of Alpine glaciations in the southern Alps during the Pleistocene.

REFERENCES

Norgaard, J., Jansen, J. D., Neuhuber, S., Ruszkiczay-Rudiger, Z., & Knudsen, M. F. (2023). P-PINI: A cosmogenic nuclide burial dating method for landscapes undergoing non-steady erosion. Quaternary Geochronology, 74.

10.6
Quaternary assemblages of aquatic invertebrate mandibles and other sclerotized remains

Colin Courtney-Mustaphi[1], Enrica Steiner[1], Stefanie von Fumetti[1], Oliver Heiri[1]

[1] *Geoecology, Department of Environmental Sciences, University of Basel, Klingelbergstrasse 27, 4056 Basel, Switzerland (colin.courtney-mustaphi@unibas.ch)*

Chitinous remains can persist for years to hundreds of thousands of years as subfossils or fossils in sediments. Remains of aquatic invertebrates found in lacustrine sediments are useful palaeoenvironmental indicators to reconstruct environmental changes (Frey, 1964; Smol et al., 2001) that include variations to lake depth, nutrient availability, trophic status, salinity, and climate (for example, Verschuren and Marnell, 1997; Korhola et al., 2000; Heiri et al., 2011; Vondrák et al., 2019). Strongly scleroticized chitinous body parts from the exoskeleton of invertebrates are often the most resistant to degradation during syn- and post-depositional processes. Some identification guides, catalogues and atlases are available for the identification of remains for several invertebrate groups, such as chironomids, cladocerans, and ostracods, among others (Uutala, 1990; Brooks et al., 2007; Szeroczyñska and Sarmaja-Korjonen, 2007). Mandibles, claw-like remains, and pygopodia observed in sieved Quaternary lacustrine, palustrine, and deltaic sediments sediments, are infrequently recognised, reported and interpreted. Aquatic invertebrate remains of several ecologically important taxonomic invertebrate groups continue to be underused in paleoenvironmental studies, in part, because there are few summarising visual keys or accessible documentation sources.

We present an overview over a project to i) document the aquatic invertebrate remains, ii) create reference microscope slides, iii) plans to further develop the catalogue, iv) discuss the potential for its application to paleoenvironmental studies, and v) present example studies that apply the catalogue to understand past environmental changes in lakes. The study has assembled >150 digital photomicrographs of pre-identified aquatic invertebrate specimens collected from streams and lakes that have been chemically cleared to resemble remains found in sieved lake sediment samples, commonly in the >100 μm size fraction. The photograph keys document an overview of mandibles, mouthparts, head remains, and claw-like appendages from several of the key taxonomic groups sensitive to aquatic environmental changes. We present taxa that include Crustacea (Amphipoda, Isopoda, Ostracoda, and Notostraca) and Insecta (Coleoptera, Diptera, Ephemeroptera, Hemiptera, Odonata, Lepidoptera, Megaloptera, Plecoptera, and Trichoptera). We present lake sediment records that show how these invertebrate remain assemblages can be used to reconstruct past environmental changes and anthropogenic influences (Tóth et al., 2019; Ursenbacher et al., 2020). The compilation of aquatic invertebrates observed in European lake sediments is a companion tool for the analysis of assemblages of invertebrate remains for paleoecologists interested in the late Quaternary and recent lake sediment deposits (Courtney-Mustaphi et al., in press).

REFERENCES

Brooks, S., Langdon, P., Heiri, O. 2007: The identification and use of Palaearctic Chironomidae larvae in palaeoecology. Quaternary Research Association Technical Guide 10. QRA, London, UK.

Courtney-Mustaphi, C., Steiner, E., von Fumetti, S., Heiri, O. in press 2023: Aquatic invertebrate mandibles and sclerotized remains in Quaternary lake sediments. Journal of Paleolimnology.

Frey, D.G. 1964: Remains of animals in Quaternary lake and bog sediments and their interpretation. Ergebnisse der Limnologie, 2, 1–114.

Heiri, O., Brooks, S.J., Birks, H.J.B., Lotter, A.F. 2011: A 274-lake calibration data-set and inference model for chironomid-based summer air temperature reconstruction in Europe. Quaternary Science Reviews, 30, 3445–3456.

Korhola, A., Olander, H., Blom, T. 2000: Cladoceran and chironomid assemblages as quantitative indicators of water depth in subarctic Fennoscandian lakes. Journal of Paleolimnology, 24, 43–54.

Smol, J.P., Birks, H.J.B., Last, W.M. 2001: Zoological indicators in lake sediments: An introduction. In: Smol, J.P., et al (eds.) Tracking Environmental Change Using Lake Sediments Volume 4 Zoological Indicators. Kluwer Academic Publishers, Dordrecht, pp 1–4.

Tóth, M., van Hardenbroek, M., Bleicher, N., Heiri, O.: 2019. Pronounced early human impact on lakeshore environments documented by aquatic invertebrate remains in waterlogged Neolithic settlement deposits. Quaternary Science Reviews, 205, 126–142.

Ursenbacher, S., Stötter, T., Heiri, O.: 2020. Chitinous aquatic invertebrate assemblages in Quaternary lake sediments as indicators of past deepwater oxygen concentration. Quaternary Science Reviews, 231, 106203.

Uutala, A.J. 1990: *Chaoborus* (Diptera: Chaoboridae) mandibles—paleolimnological indicators of the historical status of fish populations in acid-sensitive lakes. Journal of Paleolimnology, 4, 139–151.

Verschuren, D., & Marnell, L.F. 1997: Fossil zooplankton and the historical status of westslope cutthroat trout in a headwater lake of Glacier National Park, Montana. Transactions of the American Fisheries Society, 126, 21–34.

Vondrák, D., et al. 2019: Postglacial succession of caddisfly (Trichoptera) assemblages in a central European montane lake. Biologia, 74, 1325–1338.

10.7
The Radiocarbon Inventories of Switzerland (RICH) project: An integrated approach to understand the changing carbon cycle

Timothy Eglinton[1], Heather Graven[2], Frank Hagedorn[3], Soenke Szidat[4], Alex Brunmayr[2], Margaux Duborgel[3], Dylan Geissbuehler[4], Thomas Laemmel[4], Luisa, Minich[3], Benedict Mittelbach[1], Timo Rhyner[1], Margot White[1]

[1] *Geological Institute, ETH Zurich, Sonneggstrasse 5, CH-8092, Zurich (timothy.eglinton@erdw.ethz.ch)*
[2] *Department of Physics, Imperial College London, Prince Consort Rd, London SW7 2BW, UK*
[3] *Swiss Federal Institute for Forest, Snow and Landscape Research WSL*
Zuercherstr. 111, 8903 Birmensdorf,
[4] *Departement für Chemie, Biochemie und Pharmazie, Universitaet Bern, Freiestrasse 3, 3012 Bern*

Anthropocene climate change is directly linked with perturbations to the global carbon cycle brought on by emissions of greenhouse gases (GHGs) associated with fossil fuel combustion and land-use change. The turnover of carbon in terrestrial and aquatic ecosystems and rate of exchange with the atmosphere comprises a major source of uncertainty in predictions of how the global carbon cycle responds to, and contributes to climatic change.

Radiocarbon is a powerful tool for constraining sources of carbon, and its rate of turnover within carbon pools and exchange between carbon reservoirs in the Anthropocene. The absence of radiocarbon in fossil fuels and its depletion in other “pre-aged” C reservoirs (e.g., mineral soils, permafrost) provides constraints on carbon exchange with the atmosphere and surface biosphere on centennial or longer timescales, while the ^{14}C “bomb spike” resulting from above-ground nuclear weapons testing in the mid-20th Century serves as a tracer of carbon flow among more rapidly cycling pools. With recent advances in ^{14}C measurement capabilities, there is the opportunity to use ^{14}C as a crucial constraint on carbon cycle models, as well as to examine underlying processes, and detect (and quantify) the pace of carbon cycle change.

The SNF Sinergia “Radiocarbon Inventories of Switzerland” (RICH) project is a collaborative initiative that seeks to develop a first-of-its-kind, national-scale ^{14}C inventory spanning all major carbon pools and encompassing the five different Swiss ecoregions. The RICH team comprises three groups that focus on acquiring comprehensive ^{14}C measurements of carbon species in the atmosphere, soils and the hydrophere, together with a carbon cycle modeling group, and involves a large consortium of project partners and collaborators. This presentation will outline the goals and scope of the RICH project, and provide illustrations of the information that is now flowing from this highly collaborative undertaking. The information derived from the project will ultimately be used to assess vulnerability of, and interplay between, different C pools, as well as provide a crucial benchmark against which to gauge past and future changes in carbon stocks, and to constrain carbon-cycle models. The RICH project is envisioned to serve as a model that can be adopted and adapted, and used to assess the efficacy of efforts to reduce emissions as well as to sequester GHG on regional to global scales.

10.8
Human-initiated autocyclic delta failures

Stéphanie Girardclos[1], Renaldo Gastineau[2], Katrina Kremer[2] and Flavio S. Anselmetti[2]

[1] *Dept. of Earth Sciences and Institut des Sciences de l'Environnement, University of Geneva, Switzerland (Stephanie.Girardclos@unige.ch)*
[2] *Institute of Geological Sciences and Oeschger Centre for Climate Change Research, University of Bern, Switzerland*

River regulation has resulted in changes in the hydrology and particle budgets of fluvial systems. Significant rivers have been modified since the 19th century to control flood hazards, to gain land from swamp areas for agricultural purposes, and to stabilize river- and lake levels to facilitate navigation. Such dramatic changes in the river course have impacted the sediment distribution at the delta mouths and the grain-size dissemination along the river, which could lead to slope instabilities. Deposits of such catastrophic mass movements have been for instance observed in Lake Brienz, where thick (0.5 to 1.3 m) megaturbidites are stacked in the deep basin. This study uses sediment cores and seismic data to reconstruct the megaturbidites' history in Lake Brienz. Data reveal that megaturbidites, originating from the Aare Delta, have mean ages of 1854, 1906, 1942, and 1996 CE and that they were unprecedented in -at least- the past 500 years. The recurrent collapses are attributed to enhanced sediment accumulation in the proximal delta area due to increased sediment transport after Aare course straightening and channelization during the late 18th century. These findings indicate that river regulation can affect delta sedimentation, leading to autocyclic delta collapses. Those collapses, in turn, can potentially generate tsunami waves, representing an additional natural hazard for communities near shorelines.

10.9
Detection of the bomb peak ^{14}C for the onset of the Anthropocene

Irka Hajdas[1], Carley Crann[2], Kristine DeLong[3], Barbara Fiałkiewicz-Kozieł[4], Juliana Ivar Do Sul[5], Jerome Kaiser[5], Francine M.G. McCarthy[6], Simon Turner[7], M Allison Stenger[8], Colin Waters[9], Jens Zinke[9]

[1] Laboratory of Ion Beam Physics, ETH Zürich, Switzerland (hajdas@ethz.ch)
[2] André E. Lalonde AMS Laboratory, University of Ottawa, Canada
[3] Department of Geography and Anthropology and Coastal Studies Institute, Louisiana State University, USA
[4] Adam Mickiewicz University, Institute of Geoecology and Geoinformation, Poland
[5] Leibniz Institute for Baltic Sea Research Warnemünde, Germany
[6] Department of Earth Sciences, Brock University, Canada
[7] Environmental Change Research Centre, Department of Geography, University College London, London, UK
[8] Stanford University, USA
[9] School of Geography, Geology & The Environment, University of Leicester, UK

The unprecedented environmental changes resulting from anthropogenic activities initiated during the Great Acceleration of the mid-20th century can be traced using radiocarbon analysis. The cosmogenic isotope ^{14}C, which is produced in the atmosphere, is well-known as the geochronological tool applied to archives of the last 55 thousand years. However, during the last 200 years the natural signal of ^{14}C in the atmosphere and connected reservoirs (biosphere, ocean, soils etc.,) has been perturbed by human activities. Two anthropogenic effects are observed: a decreasing trend observed in ^{14}C concentration of the atmosphere (Suess effect) which has been temporarily reversed by aboveground thermonuclear tests of the 1950/60s.

The excess of the artificially produced ^{14}C (bomb pulse) is a useful time marker for the mid-20th century and the detection of the bomb peak in natural archives has thus been proposed as a tool to locate and date the onset of a proposed new epoch, the Anthropocene.

Here we present results of radiocarbon analysis conducted as a part of the research dedicated to establishing the Global boundary Stratotype Section and Point (GSSP) for the proposed Anthropocene. The studied sites include corals (Flinders Reef, AU and Flower Garden Banks, USA), peat (Śnieżka peatland, PL), lake sediment (Crawford Lake, CA and Searsville Lake, USA) and marine sediment (East Gotland Basin, Baltic Sea). The variety of records (different carbon reservoirs) required site and sample-specific treatment prior to analysis and site-specific interpretation of the measured ^{14}C. Nevertheless, the mid-20th century bomb peak, was detected at all but one site. In all records the observed onset of the ^{14}C bomb peak always postdates 1954, the year of the first atmospheric ^{14}C bomb increase. The specific reservoir effects and corrections will be discussed.

10.10
Hydrological and temperature variations in the Black Sea region during the last 650'000 years recorded by speleothem fluid inclusions

Frederick Held[1], Hai Cheng[2], R. Lawrence Edwards[3], Okan Tüysüz[4], Dominik Fleitmann[1]

[1] *Department Environmental Sciences, University of Basel, Bernoullistrasse 32, CH-4056 Basel (frederick.held@unibas.ch, dominik.fleitmann@unibas.ch)*
[2] *Institute of Global Environmental Change, Xi'an Jiaotong University, 710049 Xi'an, Shaanxi, China (xjtu.edu.cn)*
[3] *Department of Geology and Geophysics, University of Minnesota, 310 Pillsbury Drive SE, Minneapolis, Minnesota 55455-0231, USA (edwar001@umn.edu)*
[4] *Eurasia Institute of Earth Sciences, Istanbul Technical University, Maslak 34469 Istanbul, Turkey (tuysuz@itu.edu.tr)*

The Eastern Mediterranean including the Black Sea region is influenced by subtropical Mediterranean, temperate European, and continental Asian air masses which make paleoclimate archives from the Black Sea region a valuable source of information about past climatic changes in temperature and rainfall. On glacial interglacial time scales, most information on climate variability in the Black Sea region comes almost entirely from marine/lake sediment cores (e.g. Wegwerth et al., 2015, 2020; Shumilovskikh et al., 2012). In contrast to these paleoclimate archives, oxygen isotope ratios of speleothem calcite ($\delta^{18}O$) and water isotope ratios (δD_{FI} and $\delta^{18}O_{FI}$) of speleothem fluid inclusions from Sofular Cave in northern Turkey can provide direct information on the isotopic composition of rainfall and, therefore, potentially identify the sources of moisture at the Black Sea coast. During the last 650'000 years most of the δD_{FI} and $\delta^{18}O_{FI}$ values plot closer to the Local Meteoric Water Line (LMWL) than to the Eastern Mediterranean Water Line (EMWL). This indicates that the Black Sea was the dominant moisture source for Sofular Cave during glacial and interglacial periods (Fleitmann et al., 2009; Badertscher et al., 2011). In addition, isotope measurements on speleothem fluid inclusions enables us to reconstruct temperature changes. Holocene temperatures of ~15°C to ~20°C are within the range of modern cave air temperatures and proxy records from the Black Sea (Sanchi et al., 2014; Menot and Bard, 2012).

REFERENCES

Badertscher, S., Fleitmann, D., Cheng, H., Edwards, R.L., Göktürk, O.M., Zumbühl, A., Leuenberger, M., Tüysüz, O. 2011: Pleistocene water intrusions from the mediterranean and caspian seas into the Black Sea, Nature Geoscience, 4 (4), 236–239.

Fleitmann, D., Cheng, H., Badertscher, S., Edwards, R.L., Mudelsee, M., Goktürk, O.M., Fankhauser, A., Pickering, R., Raible, C.C., Matter, A., Kramers, J., Tüysüz, O. 2009: Timing and climatic impact of Greenland interstadials recorded in stalagmites from northern Turkey, Geophysical Research Letters, 36 (19), L19707.

Menot, G., & Bard, E. 2012: A precise search for drastic temperature shifts of the past 40,000 years in southeastern Europe, Paleoceanography, 27(2).

Sanchi, L., Ménot, G., & Bard, E. 2014: Insights into continental temperatures in the northwestern Black Sea area during the Last Glacial period using branched tetraether lipids, Quaternary Science Reviews, 84, 98-108.

Shumilovskikh, L. S., Tarasov, P., Arz, H. W., Fleitmann, D., Marret, F., Nowaczyk, N., Plessen, B., Schlütz, F. & Behling, H. 2012: Vegetation and environmental dynamics in the southern Black Sea region since 18 kyr BP derived from the marine core 22-GC3, Palaeogeography, Palaeoclimatology, Palaeoecology, 337, 177-193.

Wegwerth, A., Ganopolski, A., Ménot, G., Kaiser, J., Dellwig, O., Bard, E., Lamy, F. & Arz, H. W. 2015: Black Sea temperature response to glacial millennial-scale climate variability, Geophysical Research Letters, 42(19), 8147-8154.

Wegwerth, A., Kaiser, J., Dellwig, O., & Arz, H. W. 2020: Impact of Eurasian ice sheet and North Atlantic climate dynamics on Black Sea temperature variability during the penultimate glacial (MIS 6, 130–184 ka BP), Paleoceanography and Paleoclimatology, 35(8), e2020PA003882.

10.11
Subglacial landforms and basal ice flow patterns of the Last Glacial Maximum Rhine glacier

Sarah Kamleitner[1,2], Susan Ivy-Ochs[1], Bernhard Salcher[3], Jürgen M. Reitner[4]

[1] *Laboratory of Ion Beam Physics, ETH Zurich, Otto-Stern-Weg 5, CH-8093 Zurich*
[2] *Institute of Earth Surface Dynamics, University of Lausanne, Bâtiment Geopolis UNIL-Mouline, CH-1015 Lausanne (sarah.kamleitner@unil.ch)*
[3] *Department of Geography and Geology, Paris Lodron University of Salzburg, Hellbrunnerstrasse 34, A-5020 Salzburg*
[4] *GeoSphere Austria, Hohe Warte 38, A-1190 Vienna*

High-resolution (sub)glacial geomorphological mapping was applied to generate a first digital inventory of streamlined subglacial bedforms within the footprint of the Last Glacial Maximum Rhine glacier. 2460 drumlins were mapped across the former piedmont lobe on the Swiss-German Alpine foreland. Glacial lineations and subglacial ribs (ribbed/Rogen moraine) – the first record of this type of subglacial bedform on the Alpine foreland – were identified. Orientation and elongation data of mapped drumlins and glacial lineations build the basis for the reconstruction of paleo basal flow. Two flowsets, associated with the Schaffhausen stadial (LGM maximum) and the Stein am Rhein stadial (late LGM readvance), respectively, were discerned. Basal flow trajectories of the LGM maximum advance were interpreted visually and are limited to areas proximal to the former Rhine glacier margin. The flow field of the late LGM glacier readvance (to the Stein am Rhein stadial moraines) extends tens of kilometres upstream and was reconstructed by implementing a recently published kriging routine. The obtained basal flow patterns are paired with information on ice surface levels from mapped ice marginal deposits and combined with relative ice velocity differences inferred from spatial changes in subglacial landform elongation, thereby revealing detailed insights on ice flow geometries, particularly during the glacier readvance. Flow trajectories diverge around basal highs and converge in narrow valley section, where basal velocities, driven by topography, are higher. These results suggest that the basal flow patterns developed under thin ice effectively controlled by local topography. The gained basal flow patterns of the paleo Rhine glacier offer new insights on landscape evolution of the northern Alpine foreland and provide an evidence-based flow dataset for the validation of future physical modelling results.

10.12
Summer temperature reconstruction for the Last Glacial Maximum in Central Europe based on chironomids

Pierre Lapellegerie[1], Laurent Millet[2], Damien Rius[2], Oliver Heiri[1]

[1] *Geoecology, Department of Environmental Sciences, University of Basel, Klingelbergstrasse 27, CH-4056 Basel (pierre.lapellegerie@unibas.ch)*
[2] *CNRS UMR 6249, Laboratoire Chrono-Environnement, UFR des Sciences et Techniques, Université de Bourgogne-Franche-Comté, 16 route de Gray, FR-25030 Besançon*

The location of Bergsee (382m a.s.l.), close to the Black Forest and beyond the maximum extent of the Rhine glacier during the Würm glaciation, make the sediment of this lake a unique palaeoenvironmental archive that probably recorded the entire Last Glacial Period. Here we present a chironomid record from Bergsee covering ca. 35 ka including the period corresponding to the Last Glacial Maximum. The record is divided into 6 statistically significant biostratigraphical zones. Between ca. 45–30 ka taxa typical for the littoral of relatively warm lakes (*Parakiefferiella bathophila*-type, *Paratanytarsus* and *Tanytarsus pallidicornis*-type) are dominating. Then (ca. 30–23 ka) *Sergentia coracina*-type, a profundal and cold indicative taxon, becomes dominant alongside *P. bathophila*-type. Low diversity and high abundances of *S. coracina*-type suggest the most severe environmental conditions of the record. The third zone (ca. 23–20 ka) is largely dominated by *P. bathophila*-type and warmer indicative taxa replace *S. coracina*-type. In the fourth zone (ca. 20–17 ka) *Paratanytarsus* and *Tanytarsus pallidicornis*-type dominate and the presence of *Chironomus anthracinus*-type suggests slightly warmer conditions and more nutrients in the lake. In the next zone (ca. 17–11 ka), *Corynocera ambigua*, a taxon with uncertain distribution in respect to temperature, becomes the dominant chironomid. Changing abundances of *C. ambigua* match the climate variability of the Lateglacial, with high abundances corresponding to the cold phases of the Oldest and Younger Dryas interrupted by the warmer Bølling/Allerød. However, the high abundances of *C. ambigua* are not necessarily due to colder temperature but could also be explained by changes in the trophic conditions in the lake or other environmental changes. The last zone (ca. 11–9 ka, onset of the Holocene), shows the highest diversity and presence of warm indicative taxa such as *Microtendipes pedellus*-type and *Pseudochironomus*. The high abundances of *C. ambigua* make the temperature reconstruction challenging for the Lateglacial. A chironomid-temperature transfer function based on a Swiss-Norwegian training set reconstructs exceptionally cold values in this interval, which disagrees with reconstructions from other palaeoenvironmental archives in the region. To address this problem, temperature reconstructions using two additional transfer functions based on other training sets (Finnish and Russian), having different temperature optima for *C. ambigua*, were applied to the Bergsee chironomid record as well and the Swiss Norwegian model was also used without *C. ambigua*. The reconstructions with the Swiss-Norwegian (*C. ambigua* removed), Finnish and Russian training sets give more realistic temperatures for the Lateglacial. All these reconstructions indicate the coldest phase between 25–23 ka with July air temperature of ca. 11.5°C, which is consistent with estimates of the maximum extent of northern Alpine glaciers, the pollen record from Bergsee and other palaeoenvironmental records in the region.

10.13
Retrieving climates from the last glacial maximum using an invert glacier model

Kejdi Lleshi[1], Guillaume Jouvet[1], Samuel J. Cook[1], Frédéric Herman[1,2]

[1] IDYST, University of Lausanne, Bâtiment Géopolis , CH-1015 Lausanne. (kejdi.lleshi@unil.ch)
[2] University of Lausanne, Bâtiment Unicentre , CH-1015 Lausanne.

Climate change is a pressing issue globally, with temperatures predicted to rise >1.5 °C by the end of the century, leading to widespread changes in not just temperature but also precipitation patterns around the world, with concomitant effects on human societies and the natural environment. One way of exploring how our climate may change under temperature shifts of this order of magnitude is by looking at past natural climate change during the Quaternary period when glacial-interglacial shifts led to multi-degree temperature variations on geologically short timescales. During the Last Glacial Maximum (LGM) ~ 21000 years BP, the global climate was significantly colder and drier than today. An accurate assessment of the LGM climate and its driving factors is therefore a very good case study for comprehending climate change and CO_2 sensitivity, which is directly relevant to today’s predicted warming scenarios. In this study, we present a new machine-learning-based inversion technique that is capable of inverting the LGM glacier footprints reconstructed in the Alps to retrieve climate information. More specifically, we are aiming to reconstruct the glacier equilibrium line altitude (ELA), the altitude where the annual accumulation and ablation of ice due to precipitation and melt are zero. A glacier-evolution model is emulated by a machine-learning model, which is much faster than the conventional glacier-evolution model while maintaining a high level of fidelity. The emulator also offers the advantage of being applicable in a gradient-based inversion scheme. This method enables convergence towards a climate scenario that yields glacier footprints consistent with the reconstructed footprints, as shown in Figure 1. The climate scenario inferred in the ELA field presents a west-east and north-south gradient in the ELA field‘s position during the LGM in the European Alps. By reconstructing the climate for glacier footprints at different times, we can more accurately track the climatic shifts engendered by the multi-degree temperature changes occurring across the LGM and thus provide more accurate possibilities for the future of our warming world.

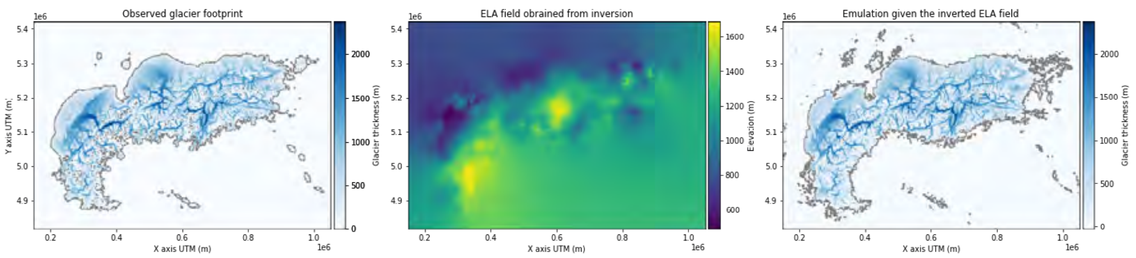

Figure 1. Left panel: ‘Observed’ glacier footprint from a glacier-evolution model simulation. Middle panel: The ELA field inferred from the inversion of the ‘Observed’ glacier footprint (on the left panel). Right panel: Prediction from the emulator given the ELA field inferred from the inversion (in the center panel). The inversion result is validated by the similarity of the left and right panels.

10.14
The Jura ice cap and Alpine ice sheet interface: Insights from burial dating exogenic cave sediments

Neal Mathes[1], Marc Luetscher[2], Susan Ivy-Ochs[3], Catharina Dieleman[4], Marcus Christl[3], Christof Vockenhuber[3], Naki Akçar[4]

[1] *Department of Earth Sciences, ETH Zurich, Sonneggstrasse 5, CH-8092 Zurich (nmathes@ethz.ch)*
[2] *Swiss Institute for Speleology and Karst Studies (SISKA), Rue de la Serre 68, CH-2300 La Chaux-deFonds*
[3] *Laboratory of Ion Beam Physics, ETH Zurich, Otto-Stern-Weg 5, CH-8093 Zurich*
[4] *Institute of Geological Sciences, University of Bern, Baltzerstrasse 1+3, CH-3012 Bern*

The central Jura Mountains have a complex glacial history that reflects the dynamic interactions between the Jura ice cap and Alpine ice sheet throughout the Pleistocene. They are home to many karstic features that trap and preserve sediments. These exogenic deposits are an important archive for paleoenvironmental information. This study investigates surface and exogenic deposits and determines burial ages to better understand the spatiotemporal relationship between the Jura ice cap and the Rhone glacier. The analyzed exogenic sediments were collected from Grotte aux Fées, the largest cave system in the Jura Mountains, and are of Alpine origin. Cosmogenic ^{10}Be and ^{26}Al ages were calculated based on simple burial dating, isochron-burial dating, and P-PINI age modeling techniques (Granger & Muzikar 2001; Erlanger et al. 2012; Nørgaard et al. 2023).

Preliminary results indicate that the upper Orbe Valley experienced a more complex LGM (Last Glacial Maximum) history than previously realized, with multiple advances of the Jura ice cap recorded in a thick sequence (>150m) of proglacial and subglacial sediments. Burial ages suggest that the Alpine glaciers extended into the Jura Mountains and reached Grotte aux Fées at least twice during the Middle and Early Pleistocene. These results have the potential to advance ongoing debates around the existence and timing of the earliest glaciations reaching the Alpine foreland (Nørgaard et al. 2023). Glacial extent along the Jura-Alpine ice contact was dependent on the relative climatic conditions in the different ice accumulation areas (Jouvet et al. 2017). Evidence of more extensive, pre-LGM, Alpine glaciations of the Jura Mountains provides insights into how the paleoclimate of the Alps and Jura may have varied between glacial cycles.

REFERENCES

Erlanger, E.D., Granger, D.E., & Gibbon, R.J. 2012: Rock uplift rates in South Africa from isochron burial dating of fluvial and marine terraces. Geology. 40, 1019-1022.
Granger, D.E. & Muzikar, P.F. 2001: Dating sediment burial with in situ-produced cosmogenic nuclides: theory, techniques, and limitations. Earth and Planetary Science Letters. 188, 269-281.
Jouvet, G., Seguinot, J., Ivy-Ochs, S., & Funk, M. 2017: Modelling the diversion of erratic boulders by the Valais Glacier during the last glacial maximum. Journal of Glaciology. 63, 487-498.
Nørgaard, J., Jansen, J.D., Neuhuber, S., Ruszkiczay-Rüdiger, Z., & Knudsen, M.F. 2023: P–PINI: A cosmogenic nuclide burial dating method for landscapes undergoing non-steady erosion. Quaternary Geochronology. 74, 101420.

10.15
Investigating the evolution of Holocene sea ice and primary production in the Beaufort Sea, Canadian Arctic using lipid biomarkers

Madeleine Santos[1*], Lisa Bröder[1], Iván Hernández-Almeida[2], and Julie Lattaud[3]

The Arctic’s Beaufort Sea region has experienced a remarkable decline in sea ice, wherein the loss of multi-year covered areas has increased fourfold from 1997 to 2021, with a current loss rate of 183,000 km2/yr−1 (Babb et al., 2022). The accelerated melting and retreat of sea ice have been identified as one of the main controlling factors of primary production in the Arctic Ocean and its adjacent shelf seas, due to elevated light availability and stratification (Ardyna et al. 2017). To place the rapid sea ice decline into geologic context, this study demonstrates the interconnected evolution of sea ice and primary production within the Beaufort Shelf over the Holocene epoch using lipid biomarkers.

Lipid biomarkers have been identified to come from specific organisms that are sensitive to changes in their growth environment. These biomarkers were reported to be relatively well preserved in marine sediments, thus making them particularly useful in reconstructing ancient environments. This study presents the outcomes of analyzing lipid biomarkers derived from two sediment cores (PCB9 and 11) obtained from the outer shelf and shelf break regions of the Beaufort Sea. The analytical techniques involved in this work are lipid extractions and subsequent characterization and quantification of biomarkers extracted using gas chromatography-mass spectrometry (GC-MS), gas chromatography-flame ionization detection (GC-FID), and high-performance liquid chromatography coupled with mass spectrometry (HPLC-MS).

Sea ice diatom-produced highly branched isoprenoids, namely IP_{25} and diene, exhibit increasing trends throughout the Middle to Late Holocene for both cores analyzed in the study, which signify increasing sea ice cover in the Beaufort Shelf. Meanwhile, phytoplankton biomarkers, namely brassicasterol and triene, have been used to infer shifts in primary productivity. The Middle Holocene emerged as a period of heightened variability in primary production, potentially linked to its relocation towards marginal ice zones (MIZ) and open water conditions that had existed in the Beaufort Sea during this time period. Afterwards, during the Late Holocene, there were prolonged ice conditions across the Beaufort Shelf, which was accompanied by a significant reduction in primary production levels. In summary, this research shows that there is an intricate relationship between sea ice evolution and primary productivity across the Holocene era in the Beaufort Sea.

10.16
New insights into the Basadingen Through: An overdeepened valley in Northern Switzerland

Sebastian Schaller[1], Bennet Schuster[2,1], Sarah Beraus[3], Marius W. Buechi[1], Hermann Buness[3], Flavio S. Anselmetti[1]

[1] *Institute of Geological Sciences and Oeschger Centre for Climate Change Research, University of Bern, Baltzerstrasse 1+3, 3012 Bern, Switzerland*
[2] *Institute of Earth and Environmental Sciences, University of Freiburg, Tennenbacher Str. 4, 79106 Freiburg, Germany*
[3] *Leibniz Institute for Applied Geophysics (LIAG), Stilleweg 2, 30655 Hannover, Germany*

The ICDP (International Continental Scientific Drilling Program) project «DOVE» (Drilling Overdeepened Alpine Valleys) comprises a series of drill holes into overdeepened glacial troughs around the Alps. The sedimentary fill of these troughs provides crucial information for the reconstruction of glaciation, climate, and landscape evolution of the Alps during the Mid- and Late Pleistocene. In the project›s frame, an over 250 m-thick sedimentary succession of unconsolidated Quaternary sediments was recovered from the Basadingen Trough. This trough belongs to a system of overdeepenings formed in the NE sector of the Rhine foreland glacier lobe along the SSE-NNW valley system that connects the present-day Thur Valley with the Rhine Valley – a connection that does not exist in the present surface morphology and that was probably active only during the Middle Pleistocene.

In our contribution, we show new results that correlate the recovered sediment core with the high-resolution 2D seismic site survey lines. This combination enables a refinement of the earlier interpretation and, further, allows a direct link between the seismic lines, the petrophysical properties of the core (from MSCL- and wireline-logging), and the sedimentological properties. Seismic stratigraphic interpretation (seismic sequence and seismic facies analysis) can be correlated to the sedimentologic ‹glacial› sequences encountered in the cores, allowing a more detailed reconstruction of the glacial advance and retreat history. Combining the two seismic interpretations on the two 2D seismic lines with the known local geological information (e.g., drill cores, bedrock map, topography, model of the Quaternary sediment cover) allows the creation of a 3D model of a part of the Basadingen Trough. The 3D model helps to visualize the likely shape of the bedrock incision and the architecture of the trough infill and the covering sediments. Expanding into the third dimension enables a view of the situation from different angles and perspectives. It can help to overcome 2D effects that may bias true geometries so that a local glaciation model for the Basadingen Trough and, eventually, a more general one for the Northern Alpine foreland can be developed. ← Use the «Abstract_body_text» pre-defined style in the «Styles Pane»

10.17
Exploring the link between Earth's orbital parameters and glacial cycles

Liam Wheen[1]

[1] *Engineering Mathematics, University of Bristol, Beacon House, Queens Rd, BS8 1QU Bristol, England (liam.wheen@bristol.ac.uk)*

We investigate the effect of Earth's orbitally varied solar radiation on the variation in global ice volume over the past 800,000 years. Despite this connection being known, the mechanisms through which this effect is realised are still unclear. We propose that solar radiation alone is able to explain the observed glacial cycles. To demonstrate this, we construct a linear model that takes the orbital parameters as inputs, fitting the coefficients to ice volume proxy data. We then propose a physical interpretation of this model, using bulk ocean and surface temperatures as intermediate mechanisms, which are shown to align well with the relevant proxy data. Our findings suggest that the majority of ice volume dynamics since the mid-Pleistocene transition can be explained by a simple linear model of the orbital parameters. We also compare the quality of our fit to similar conceptual models, finding comparable performance despite the uniquely linear nature of our model.

P 10.1
Post-LGM glacier fluctuations in the northern Valaisian Alps

Mattia Binaghi[1], Susan Ivy-Ochs[2,4], Serdar Yeşilyurt[3], Marcus Christl[4], Naki Akçar[1]

[1] Institute of Geological Sciences, University of Bern, Baltzerstrasse 1+3, CH-3012 Bern, (mattia.binaghi@students.unibe.ch)
[2] Department of Earth Sciences, ETH Zürich, Otto-Stern-Weg 5, CH-8093 Zürich
[3] Department of Geography, Ankara University, 06230 Ankara, Turkey
[4] Department of physics, ETH Zürich, Otto-Stern-Weg 5, CH-8093 Zürich

The northern Valaisian Alps are home to several glaciers today, such as the Great Aletsch glacier, the largest glacier in the Alps. The landscape in this region is glacially overprinted and often contains glacial sediments and well-preserved moraines, which were deposited by glacier fluctuations after the Last Glacial Maximum (LGM). The presence of glacial landforms in the tributary valleys raises the following questions: When and how large were the northern Valaisian glaciers during the post-LGM? and which climatic deteriorations caused their fluctuations? To answer these, the focus of our study is on the reconstruction of the glacier advances in two of the northern tributary valleys, the Belalp and Lüsgenalp valleys, of the Great Aletsch glacier.

For the detailed mapping of the study area, nine flight missions with an unmanned aerial vehicle (UAV) were employed to take aerial photographs. These photographs were subsequently processed using the photogrammetry program Agisoft Metashape® to generate high-resolution orthoimages and Digital Elevation Models (DEMs). We mapped the surficial geology of the Belalp and Lüsgenalp valleys in detail both in the field and remotely in QGIS®. To reconstruct the chronology of the glacier fluctuations of the Belalp and Lüsgenalp valleys, 14 samples in the Lüsgenalp valley for surface exposure dating with the cosmogenic ^{10}Be were collected and 21 exposure ages from the moraines in the Belalp valley from Schindelwig et al. (2012) were recalculated. In a further step the paleoglaciers of the Belalp and Lüsgenalp valleys will be modelled using GlaRe® and ELA® (toolboxes of ArcGIS®) to determine the equilibrium line altitudes and thus to calculate the paleotemperatures. Afterward, the regional paleoclimatic conditions of the northern Valaisian Alps will be reconstructed by comparing our results with the existing climate proxies in the Alps. The results will be presented.

REFERENCES

Schindelwig, I. et al. (2012) 'Lateglacial and early Holocene dynamics of adjacent valley glaciers in the Western Swiss Alps', Journal of Quaternary Science, 27(1), pp. 114–124. doi: 10.1002/jqs.1523.

P 10.2
Timing and patterns of Early to Middle Pleistocene outwash deposition derived from study of the Deckenschotter

Ewelina Broś[1], Susan Ivy-Ochs[1], Florian Kober[2], Reto Grischott[3], Christof Vockenhuber[1], Marcus Christl[1], Philip Gautschi[1], Colin Maden[4], Jesper Nørgaard[5], Mads F. Knudsen[5], Thomas Pollhammer[6], Bernhard Salcher[6], Lotta Ylä-Mella[7], John D. Jansen[7], Marius W. Buechi[8], Gaudenz Deplazes[2], Hans-Arno Synal[1]

[1] *Laboratory of Ion Beam Physics, ETH Zurich, Otto-Stern-Weg 5, CH-8093 Zurich (ewelinao@ethz.ch)*
[2] *NAGRA - Nationale Genossenschaft für die Lagerung radioaktiver Abfälle, Hardstrasse 73, CH-5430 Wettingen*
[3] *BTG Büro für Technische Geologie AG, Grossfeldstrasse 74, CH-7320 Sargans*
[4] *Institute of Geochemistry and Petrology, ETH Zurich, Clausiusstrasse 25, CH-8092 Zurich*
[5] *Department of Geoscience, Aarhus University, Høegh-Guldbergs Gade 2, DK-8000 Aarhus*
[6] *Department of Environment and Biodiversity, University of Salzburg, Kapitelgasse 4-6 AT-5020 Salzburg*
[7] *Institute of Geophysics, Czech Academy of Science, Boční II/1401, CZ-14100 Prague*
[8] *Institute of Geological Sciences & Oeschger Centre for Climate Change Research, University of Bern, Hochschulstrasse 4, CH-3012 Bern*

In this study we combine cosmogenic ^{10}Be - ^{26}Al burial dating with high-resolution digital topographic analysis to decipher the timing and depositional patterns of several Deckenschotter units. Deckenschotter are coarse gravels interbedded with sands and less frequently tills that were deposited in the forefield of glaciers that had expanded northwards from the Alps (Graf 1993, 2009). Understanding the timing of Deckenschotter deposition helps us to envision how the foreland looked during the Early to Middle Pleistocene, the configuration and behaviour of pre-overdeepening foreland-reaching glaciers and their outwash, as well as reconstruct the patterns and causes of post-Deckenschotter incision into the northern foreland.
We use cosmogenic ^{10}Be and ^{26}Al to date seven Deckenschotter units at six different sites in northern Switzerland and southwestern Germany. The studied sites are Tromsberg, Iberig, Feusi, Schwändihalden, Cholfirst and Hungerbol. ^{10}Be - ^{26}Al burial ages are calculated using the P-PINI (Particle Pathway Inversion of Nuclide Inventories) code, a new burial-dating model that applies a source-to-sink approach to the evolution of cosmogenic nuclide concentrations (Knudsen et al. 2020, Nørgaard et al. 2023). With the code a vast number of scenarios for sediment production in the source and deposition in the sink are calculated and compared to AMS-measured nuclide data. Final age determination is based on measured nuclide concentrations that match modelled scenarios.

To strengthen our understanding of the deposition of the studied Deckenschotter units, we perform an in-depth examination of their topographic relationships. This is facilitated by the methodology developed by Pollhammer (2019) for creating 2D profiles along paleo-river paths implied by the Deckenschotter outcrops. This extensive toolset allows for processing, statistical analysis and displaying of sediment bodies using R and Python in ArcGIS. Data from high-resolution DEM are projected orthogonally into 2D (paleo-) river long profiles together with unit attributions from existing geological maps. DEM data are displayed semi-transparently in the profile view making morphologic flat surfaces stand out, thus providing critical insights into drainage patterns to be scrutinized in concert with the dating results.

REFERENCES
Graf, H.R. 1993: Die Deckenschotter der zentralen Nordschweiz, Diss. ETH Zurich nr 10205, 151 pp.
Graf, H.R. 2009: Stratigraphie und Morphogenese von frühpleistozänen Ablagerungen zwischen Bodensee und Klettgau, E&G Quaternary Science Journal, 58, 12-54.
Knudsen, M.F., Nørgaard, J., Grischott, R., Kober, F., Egholm, D.L., Hansen, T.M., & Jansen, J.D. 2020: New cosmogenic nuclide burial-dating model indicates onset of major glaciations in the Alps during Middle Pleistocene Transition. Earth and Planetary Science Letters, 549, 116491.
Nørgaard, J., Jansen, J.D., Neuhuber, S., Ruszkiczay-Rüdiger, Z., & Knudsen, M.F. 2023: P–PINI: A cosmogenic nuclide burial dating method for landscapes undergoing non-steady erosion. Quaternary Geochronology, 74, 101420.
Pollhammer T. 2019: GIS-Kompilation und -Analyse glazialer und glaziofluvialer Sedimentkörper im Nördlichen Alpenvorland (DE-AT-CH). Masterarbeit Naturwiss. Fak. Uni. Salzburg, pp. 72.

P 10.3
Reconstruction of postglacial mass movements in the Lurnigalp

G. Bucher[1], C. Dieleman[1], S. Ivy-Ochs[2], J. Aaron[3], C. Vockenhuber[2], N. Akçar[1]

[1] *Institute of Geological Sciences, University of Bern, Baltzerstrasse 1-3, 3012 Bern (giacomina.bucher@students.unibe.ch)*
[2] *Laboratory of Ion Beam Physics, ETH Zurich, Otto-Stern-Weg 5, 8093 Zurich*
[3] *Department of Earth Sciences, ETH Zurich, Sonneggstrasse 5, 8092 Zurich*

The postglacial landscape in the Alps is shaped by large-scale mass movements. Rock avalanche deposits with volumes larger than 10^6 m^3 exist in several valleys. Whereas, only a few are known from the Bernese Alps. Consequently, our knowledge of the contribution of mass movements to the postglacial landscape evolution in this part of the Alps is limited. The focus of this study is on the bouldery deposit situated in the upper reaches of the Lurnigalp Valley, a U-shaped tributary valley located in the southwest of Adelboden. Although the boulder deposit was originally mapped as a till, we hypothesize that it could be the product of the collapse of the bedrock from the limestone cliff Bütschiflue.

We aim to test this hypothesis by combining detailed geomorphological field and remote mapping, photogrammetry, sedimentary petrology, surface exposure dating with cosmogenic ^{36}Cl, and runout modeling with DAN3D®. From aerial images taken with an unmanned air vehicle in the field, we generated a high-resolution digital elevation model (DEM) and orthoimage. In the field, we mapped the surficial geology and geomorphology, collected samples to investigate the facies of the boulder in thin sections, and took 15 rock surface samples for surface exposure dating with cosmogenic ^{36}Cl.

We found that the glacial deposits form a hummocky surface on the valley floor. Locally this hummocky topography is flattened by alluvial deposits or overlain by the bouldery deposit. The northwestern flanks of the valley are covered by slope debris. Whereas polygenetic cones were observed on the southeastern flanks. Based on the facies analysis, we argue that the bouldery deposit stems from a rock avalanche from the Bütschiflue. Our ^{36}Cl cosmogenic chronology suggests that this collapse happened at the end of Younger Dryas. We will model several runout scenarios in DAN3D® to explore whether the valley was occupied by a glacier at the time of the collapse or not. In addition, all the results will be incorporated into a landscape evolution model of the Lurnigalp Valley. Finally, the implications of this evolution model will be discussed in the Alpine context.

P 10.4
Evolution of the Polygenetic le Pont Cone, The Ferret Valley, Mont Blanc Massif

Lena Camenzind[1], Dr. Philip Deline[2], Prof. Dr. Susan Ivy-Ochs[3,4], Prof. Dr. Jordan Aron[4], Dr. Marcus Christl[3], PD Dr. Naki Akçar[1]

[1] *Institute of Geological Science, University of Bern, Baltzerstrasse 1+3, CH-3012 Bern (lena.camenzind@students.unibe.ch)*
[2] *EDYTEM Lab, Université Savoie Mont Blanc, bd de la mer Caspienne 5, F-73376 Le Bourget du Lac cedex*
[3] *Laboratory of Ion Beam Physics, ETH Zurich, Otto Stern-Weg 1, CH-8093 Zurich*
[4] *Department of Earth Sciences, ETH Zurich, Sonneggstrasse 5, CH-8092 Zurich*

The topography of the Mont Blanc Massif is characterized by a significant elevation gap between the valley floors and the mountain peaks. This gap, in combination with different processes such as the glacial, amplifies the recurrence of natural hazards in this deeply carved landscape. Not only the inhabitants of the valley but also tourism and the population in the region, are under the permanent threat of natural hazards such as the rock avalanches. By studying past mass movements in detail, return periods and the extent of gravitational processes can be determined (e.g. Deline et al., 2015). This can help make better predictions for natural hazards. For example, there are several polygenetic cones, a product of a complex interaction of slope, glacial and/or fluvial processes, in the northern slope of the Ferret Valley, Courmayeur, Italy. The Frébouge polygenetic cone is the largest and most well-preserved polygenetic cone in the valley. The complex development of this cone has been unraveled and is composed of rock avalanche, debris flow, and glacial deposits (Dieleman et al. *submitted*).

This study focuses on the second largest polygenetic cone in the valley, the Le Pont cone. Similar to the Frébouge cone, the Le Pone cone is also of polygenetic origin and built-up of rock avalanche, debris flow, and glacial deposits. However, the extent and timing of deposition of these sediments remain unknown. As a result, the main objective of this study is to reconstruct the evolution of the Le Pont cone and establish a timeline for the deposition events. During the reconnaissance fieldwork, we found that the Le Pont cone is mainly made up of rock avalanche and debris flow sediments. During the next steps, orthophotos and a digital elevation model (DEM) of the study area will be created using unmanned air vehicle photogrammetry. Subsequently, the geomorphology of the cone will be mapped in detail. Suitable boulders from the rock avalanche and debris flow deposits will be sampled for surface exposure dating with ^{10}Be. In addition, the rock avalanche will be reconstructed, and the failure will be modeled. Finally, all results, combined with existing studies, will be reconciled into a landscape evolution model of the Ferret Valley. Results will be presented.

REFERENCES

Dieleman, C., Deline, P., Ivy Ochs, S., Hug, P., Aaron, J., Christl, M., and Akçar, N.: Evolution of the Frébouge polygenetic cone during the Holocene (Val Ferret, Mont Blanc Massif), *submitted*. Earth Surface Dynamics (ESurf)

Deline P., Akçar N., Ivy-Ochs S., Kubik P.W., 2015. Repeated Holocene rock avalanches onto the Brenva Glacier, Mont Blanc massif, Italy: A chronology. Quaternary Science Reviews, 126, 186-200.

P 10.5
Impact of recent climate change and human impact on Cladocera populations inferred from high-resolution cores of Swiss mountain lakes

Ghéreint Devillet[1], Maja Damber[1], Pierre Lapellegerie[1], Sandra Brügger[1,2], Oliver Heiri[1]

[1] Geoecology Research Group, Department of Environmental Sciences, University of Basel, Klingelbergstrasse 27, CH-4056 Basel (ghereint.devillet@unibas.ch)
[2] Laboratory of Environmental Chemistry, Paul Scherrer Institute, Forschungsstrasse 111, CH-5232 Villigen

Mountain lakes are particularly sensitive to climate and environmental changes, and therefore they can provide early warning on ecosystem changes affecting alpine areas. Climate change can have various effects on these lakes: increases in temperature and reductions of glaciers in the catchment, increases in erosion, a rise in pH and alkalinity and eutrophication are some examples. Water fleas, or Cladocera (Arthropoda, Branchiopoda), are important zooplanktonic indicators found in mountain lakes. They potentially provide information on air temperature, pH, water level, impact of fish predation, and other environmental parameters. Moreover, their remains are usually well preserved in lake sediments, so they can be studied to reconstruct past changes in cladoceran assemblages in lakes as a consequence of past environmental change.

We will present an overview and first results from a project that aims to assess the impact of recent climate change and local human activities on Cladocera communities of high mountain lakes in the Swiss Alps. To do so, sediments from around 40 lakes, at an altitude between ~1700 and ~2800m a.s.l., are being sampled in the deepest part of the lake basin. They include the Macun lakes, in the Swiss National Park, the Jöri lakes, and several lakes in the Engadine, Bernese Alps, Central Switzerland and the Vaudois Alps. Some of the lakes have previously been sampled for cladoceran assemblages by Lotter et al. (1997) and Bigler et al. (2006) whereas others are sampled for the first time.

Cladoceran species - environment relationships and response to recent environmental change will be analysed in three separate approaches: For several lakes (e.g., the Macun and Jöri lakes), the Cladocera communities will be analysed at high-temporal resolution in downcore studies to assess the effect of the climate change and human activities on these ecosystems during the past 100-150 years. For several other lakes, the cladoceran species composition of the newly obtained surface sediments will be compared with the observations of Lotter et al. (1997) and Bigler et al. (2006), who sampled these lakes and analysed cladocerans in the surface sediments in the period 1993-2002. Our results will determine the response of these communities to environmental changes between these two time intervals and now, and at a broader scale. Moreover, the distribution of cladoceran remains in lake surface sediments in the 40 sampled lakes will provide an assessment of the present distribution of different cladoceran groups in Swiss mountain lakes. Finally, since most, if not all, of the lakes have been subject to fish introduction, Cladocera remains will also be analysed in order to spot any species composition changes typical for variation in predation pressure. This would potentially allow a reconstruction of changes in fish predation through time.

In separate subprojects, all the lakes will also be analysed for chironomids, pollen and diatoms in the sediments, allowing for a comparison of the cladoceran results with changes in these other indicators of past ecosystem change.

Overall, we expect that the project will provide important new information on how cladoceran assemblages in Swiss mountain lakes respond to recent environmental change. For example, they will allow a better understanding of Cladocera communities in an almost natural environment (Macun lakes in the Swiss National Park), how they react to long-term climate change, how they can be used to monitor mountain lakes, and finally how fishes impact cladocerans in these lakes through time.

REFERENCES

Bigler, C., Heiri, O., Krskova, R., Lotter, A. F., & Sturm, M. 2006: Distribution of diatoms, chironomids and cladocera in surface sediments of thirty mountain lakes in south-eastern Switzerland, Aquatic Sciences, 68(2), 154–171. https://doi.org/10.1007/s00027-006-0813-x

Lotter, A. F., Birks, H. J. B., Hofmann, W., & Marchetto, A. 1997: Modern diatom, cladocera, chironomid, and chrysophyte cyst assemblages as quantitative indicators for the reconstruction of past environmental conditions in the Alps. I. Climate, Journal of Paleolimnology, 18(4), 395–420. https://doi.org/10.1023/A:1007982008956

P 10.6
Reconstructing the evolution of the Frébouge polygenetic cone in the Italian Ferret Valley, Mont Blanc Massif

Catharina Dieleman[1], Philip Deline[2], Susan Ivy Ochs[3], Patricia Hug[4], Jordan Aaron[4], Marcus Christl[3], Naki Akçar[1]

[1] Institute of Geological Sciences, University of Bern, Baltzerstrasse 1+3, CH-3012 Bern (catharina.dieleman@geo.unibe.ch)
[2] EDYTEM Lab, University Savoie Mont Blanc, 5 bd de la mer Caspienne, F-73376 Le Bourget-du-Lac cedex
[3] Laboratory of Ion Beam Physics, ETH Zurich, Otto-Stern-Weg 5, 8093 Zurich
[4] Geological Institute, ETH Zurich, Sonneggstrasse 5, CH-8092 Zurich

Polygenetic landscapes are formed by complex multi-process interactions, which are often recorded in Alpine proglacial settings (e.g., Heckmann and Morche, 2019). Glacial, fluvial, and gravitational processes yield high sediment volumes in excess of the transportation capacity (Hallet et al., 1996). This causes sediment accumulation on the slopes, which is driven in part by sudden failures such as rock avalanches or debris flows (Hallet et al., 1996; Kamp and Owen, 2013). As these failures occur unexpectedly and can harm villages and infrastructure in the vicinity, the understanding of these mass movement processes is of great societal interest. The Italian Ferret Valley in the Mont Blanc Massif is characterized by steep valley flanks and is home to many polygenetic cones representing an exceptional field laboratory to investigate the interplay between glacial, fluvial, and gravitational processes.

This study investigates the Frébouge polygenetic cone, one of the active and well-preserved cones in the Ferret Valley, to decipher the geomorphic processes and their interaction forming the cone and to unravel its evolution (Dieleman et al., *submitted*). Therefore, we combined detailed geomorphological field and remote mapping, ^{10}Be surface exposure dating of different geomorphic landforms, and runout modeling with DAN3D. The geomorphological map revealed complex interactions of glacial, fluvial, and debris flow, as well as rock and snow avalanche, processes. The established chronology revealed that the debris flows represent the oldest deposits and therefore the onset of the cone formation. Afterwards, a rock mass with a volume of ca. 10 Mm^3 got detached from the Grandes Jorasses area, overran the Frébouge cone and traveled more than 100 m up onto the opposite valley slope. Moraines and striated boulders on the cone indicate several advances of the Frébouge Glacier, which reached its maximum extent during the Little Ice Age (LIA). This study illustrates the increasing importance of examining the formation processes and the evolution of polygenetic landscapes in Alpine valleys to assess the vulnerability of the settlements and infrastructure as well as to mitigate the hazards.

REFERENCES

Dieleman, C., Deline, P., Ivy Ochs, S., Hug, P., Aaron, J., Christl, M., and Akçar, N.: Evolution of the Frébouge polygenetic cone during the Holocene (Val Ferret, Mont Blanc Massif), *submitted*.

Hallet, B., Hunter, L. and Bogen, J. 1996: Rates of erosion and sediment evacuation by glaciers: A review of field data and their implications, *Global and Planetary Change*, 12(1), 213-235. https://doi.org/10.1016/0921-8181(95)00021-6

Heckmann, T. and Morche, D. 2019: Geomorphology of Proglacial Systems: Landform and Sediment Dynamics. In: T. Heckmann & D. Morche (Eds), *Recently Deglaciated Alpine Landscapes*, Springer.

Kamp, U. and Owen, L. A. 2013: 5.16 Polygenetic Landscapes. In J. F. Shroder (Ed.), *Treatise on Geomorphology* (pp. 370-393). San Diego: Academic Press.

P 10.7
Reconstruction of high-alpine paleoenvironment using lake sediments of the Jöri Lakes, Graubünden, Switzerland

Martin H. Felder[1], Adrian Gilli[1], Nathalie Dubois[2], Flavio S. Anselmetti[3], Kurt Hanselmann[1], Timothy I. Eglinton[1]

[1] *Geological Institute, ETH Zurich, Sonneggstrasse 5, CH-8092 Zurich (mafelder@student.ethz.ch)*
[2] *Department of Surface Waters Research and Management, Eawag, Überlandstrasse 133, CH-8600 Dübendorf*
[3] *Institute of Geological Sciences and Oeschger Centre of Climate Change Research, Univ. of Bern, Switzerland*

During the last decades, climate change has become an increasingly important issue. Elevated temperatures exert a profound impact on entire ecosystems. This can be observed very well in the melting of the Alpine glaciers. Understanding past glacial fluctuation holds immense value in projecting glacier melting under future climate change.

The Jöri area is a high-alpine plateau near Davos in eastern Switzerland. The dramatic retreat of the Jöri Glacier over the past 150 years has created new landscapes with numerous lakes and swamps. Geomorphological mapping indicates that the Jöri Glacier still reached the shore of the two largest Jöri Lakes I and III during the Little Ice Age (LIA) in the second half of the 19th century. Both lakes are located at an altitude approx. 2’500 m.a.s.l. Within this context, lake sediments can record glacial fluctuation in their catchment. As these two lakes are just outside the maximum ice extent, they potentially provide a record of environmental change spanning the entire Holocene.

In July 2022, a seismic survey in Lakes Jöri I and III was conducted with a 3.5 kHz pinger source to image the subsurface of both lakes. In the following month, multiple short and long sediment cores were recovered from Lake Jöri I with an UWITEC piston-coring system. A composite 3.7 m-long sediment core was retrieved reaching the underlying till layer.

The seismic profiles depict the moraine dividing Lake Jöri I into two basins. Structures within the moraine indicate that it was formed from at least two glacial advances, one predating the LIA. This indicates that a previous glacial advance, predating the LIA, exhibited a similar extent. Notably, the total thickness of the lake sediment is only 270 cm. The sediment core contains two contrasting parts. The lower part reveals a sediment rich in organic matter indicating a warm, biologically productive early and middle Holocene with little or no present glacier. The upper part of the sediment core is finely laminated pointing towards the presence of a glacier. The age model is so far based on bulk C^{14} dates, which are potentially influenced by mobilisation of old soils and/or organic material from melting permafrost. However, the preliminary age model points towards a high sedimentation rate around 3 ka BP when the Jöri Glacier advanced close to the shore of Jöri Lake I.

In this contribution, we will present the evidence for glacio-tectonic impact by the Jöri Glacier during the LIA and demonstrate how the Jöri Glacier might have fluctuated since the Younger Dryas. The ongoing measurements could also provide new insights into the carbon cycle and thereby help to understand bulk radiocarbon dating of Alpine lake sediments.

P 10.8
Central Europe temperature snapshots over the last 300’000 years derived from speleothem fluid inclusion water isotopes from Milandre Cave, Switzerland

Elisa Hofmeister[1], Timon Kipfer[1], Dominik Fleitmann[1], Hai Cheng[2], Anamaria Häuselmann[1], Stéphane Affolter[1]

[1] *Quaternary Geology, Department of Environmental Sciences, University of Basel, Basel, Switzerland*
[2] *Institute of Global Environmental Change, Xi’an Jiatong University, Xi’an, China*

Speleothems are secondary cave deposits that offer great potential for high-resolution and well-dated paleoclimate reconstructions. Speleothems contain minute amounts of water trapped in the stalagmite fabric in micrometric size fluid inclusions. The fluid inclusion water can be extracted to measure hydrogen (δ^2H_{fi}) and oxygen ($\delta^{18}O_{fi}$) isotopes. Previous studies conducted in Milandre Cave (Jura Mountains, Switzerland) have shown that $\delta^{18}O_{fi}$ and δ^2H_{fi} values of the trapped water are a key-proxy for paleotemperature reconstruction (Affolter et al., 2019). To reconstruct temperature, we use either the calcite-water oxygen isotope paleothermometer or an isotope- temperature transfer function. Biogenic proxies such as pollen and tree rings are essentially biased towards the warm season. In contrast, temperature estimates from speleothem fluid inclusions deliver information about the mean annual temperature and can be slightly biased towards the colder season. To date, stalagmites collected from Milandre Cave cover several interglacial and glacial periods, allowing us to reconstruct paleotemperatures for the Holocene and Younger Dryas as well as Marine Isotope Stages 5, 7, 8 and 9. Our preliminary results show that reconstructed absolute temperatures for MIS 5, 8 and 9 are between 2 and 5°C lower than Holocene temperatures of around 9°C.

These quantitative paleotemperature snapshots obtained from Milandre Cave, together with speleothems from neighboring caves in the Jura Mountains, will allow us to deliver robust temperature reconstructions for central Europe for several interglacial and glacial periods.

REFERENCE

Affolter et al. (2019), Sci. Adv. 5 eaav3809, doi.org/10.1126/sciadv.aav3809

P 10.9
Alpine lapse rate in drip waters and speleothem fluid inclusions

Timon Kipfer[1], Stéphane Affolter[1], Elisa Hofmeister[1], Anamaria Häuselmann[1], Marc Lütscher[2], Hai Cheng[3], and Dominik Fleitmann[1]

[1] *Quaternary Geology, Department of Environmental Sciences, University of Basel, Switzerland*
[2] *Swiss Institute for Speleology and Karst Studies (SISKA), Switzerland*
[3] *Institute of Global Environmental Change, Xi›an Jiatong University, Xi›an, China*

The modern stable isotope lapse rate for precipitation shows a gradient of -0.0019 ‰ per meter elevation for Switzerland, based on data from the Swiss National Network for Isotopes in the Water Cycle (ISOT) (Schotterer, 2010). Thus far, there is only scarce information about the isotope lapse rate in the past and it is usually assumed that the lapse rate remained similar to what it is today. Speleothems growing in karst caves incorporate precipitation water – via drip waters – in micrometric sized fluid inclusions (0.01 to 0.1 weight %). Therefore, they are an excellent natural archive of past precipitation and are well suited to investigate the lapse rate in the past. Using an improved speleothem fluid inclusion water extraction line, we target the hydrogen (δ^2H) and oxygen ($\delta^{18}O$) stable isotope analyses of released amounts down to 0.1 µl/g. This will allow us to obtain direct information on past precipitation and determine absolute paleotemperatures (Affolter et al., 2019).

To date, no monitoring program exists for stable isotopes in cave drip waters. That is why we have launched the Citizen Science project “Cave Drip Water” in collaboration with various caving clubs in Switzerland and France to collect drip water samples across Switzerland and in neighbouring regions (https://duw.unibas.ch/de/quartaergeologie/citizen-science/). The relationship of the isotopic composition of these drip waters from caves at different altitudes distributed throughout Switzerland will give us a modern drip water lapse rate. It will allow us to investigate the spatial distribution of water isotopes in karst systems and compare it with the most recent water isotope patterns in precipitation from Switzerland. Moreover, these observations will set a baseline for the use of water isotopes analyzed in speleothem fluid inclusion measurements.

Here we present preliminary results from the Citizen science project “Cave Drip Water” as well as a preliminary isotope lapse rate based on speleothem fluid inclusion water measured on stalagmites from the Holocene and past interglacials. Initial results tend to show a similar isotopic lapse rate trend in the past as it is today.

REFERENCES

Schotterer U., Schürch M., Rickli R., Stichler W. (2010). “Wasserisotope in der Schweiz: Neue Ergebnisse und Erfahrungen aus dem nationalen Messnetz ISOT“ Gas, Wasser, Abwasser 2010
Affolter et al. (2019), Sci. Adv. 5 eaav3809, doi.org/10.1126/sciadv.aav3809

P 10.10
Spatial and temporal distribution of microplastics in lake sediments in Switzerland

Katrina Kremer[1,2], Elizabeth Sullivan[1], Elisa Luyet[1], Prescilli Annan[2], Deborah Rast[1], Melina Zimmerli[2], Stefano C. Fabbri[1,3,4], Renaldo Gastineau[1]

[1] *Institute of Geological Sciences and Oeschger Centre for Climate Change Research, Baltzerstrasse 1+3, 3012 Bern (katrina.kremer@unibe.ch)*
[2] *Swiss Seismological Service, ETH Zurich, Sonneggstrasse 5, 8092 Zurich*
[3] *Université du Québec à Rimouski, Institut des sciences de la mer de Rimouski (ISMER), Rimouski, Canada*
[4] *Laboratoire EDYTEM, Université Savoie Mont Blanc, Le Bourget du Lac, France*

Lake sediments provide an excellent archive of our past and allow to reconstruct the impact of human activities on freshwater environments. Since the 1950s, plastics consumption has strongly increased across the globe and large amounts of this plastic is not recycled and end up in the environment. Through fluvial systems, plastics are transported and deposited in sediment sinks such as lakes and oceans where the plastics accumulate. Thus, sediments containing these plastic fragments can be used to assess their fate pathways, mass loads and accumulation rates in different environmental systems.
This study aims to assess the plastics contamination in lake sediments, particularly for the microplastic (MPs)-sized fraction (particles < 1mm) within different lakes in Switzerland. We aim to understand the temporal deposition and the accumulation areas of the plastics. For this purpose, we retrieved short sediment cores to study the deposition history of MPs. To establish the chronology, sediments are dated through varve counting and ^{137}Cs radioisotope dating, and by core-to-core correlation to previously dated sediment cores. In addition, surface sediment samples have been taken from different locations within lake basins to study the spatial distribution of plastics. We separated MPs from the sediments using density- and oil-based separation techniques before identification and characterization of MP particles.

In this contribution, we present a compilation of the temporal evolution and the spatial distribution of MPs contamination recorded in sediments of urbanized as well as remote lakes in Switzerland (e.g. Lakes Hallwil, Zurich, St. Moritz, Oeschienen). This compilation is based on several student's projects and thus is considered as a student-driven database of MPs contamination in Swiss lakes. We will present the workflow adopted to separate and characterize MPs, show the limitations of our approach and present the results of this dataset.

P 10.11
A paleolake in the desert: environmental reconstruction using organic and inorganic proxies.

Julie Lattaud[1,2], Sallie Burrough[3], Ella Walsh[3], Hendrik Vogel[4], Cindy De Jonge[1]

[1] Geological Insitute, ETHZ, Sonneggstrasse 5, 8092 Zurich (julie.lattaud@unibas.ch)
[2] Department of Environmental Sciences, University of Basel, Bernoullistrasse 32, 4056 Basel
[3] Department of Earth Sciences, University of Oxford, South Parks Road, OX1 3AN Oxford
[4] Institute of Geological Sciences & Oeschger Centre for Climate Change Research, University of Bern, Baltzerstrasse 1, 3012 Bern

There is genetic and archeological evidence for sustained periods of human occupation during the late Quaternary in southern Africa, more precisely in central Botswana (Burrough, 2016; Chan et al., 2019)"ISBN":"978-94-017-7519-9","note":"collection-title: Vertebrate Paleobiology and Paleoanthropology\nDOI: 10.1007/978-94-017-7520-5_9","page":"161-174","publisher":"Springer Netherlands","publisher-place":"Dordrecht","source":"DOI.org (Crossref. Their migration and dispersal out of the region is likely due to the influence of increasing humidity opening green corridors and landscape. However, few records exist that link local environmental changes to human migration, likely due to the scarcity of well-preserved records. Core SUA16DS3 recovered in the Sua Pan in central Botswana (Fig. 1) covers almost continuously the period 20-80 ky (MIS 4 to MIS 2), a time period that overlaps with major periods of human occupation in the region (McFarlane, 2001, Burrough, 2016). Bulk organic and inorganic analysis allowed for the reconstruction of the paleoenvironmental conditions in and around the area of a current salt pan. Starting around 70 ky, an increase in salinity and temperature (reconstructed from bacterial and archaeal biomarkers) in the lake reflects the transition from a dry lake (in agreement with Ringrose et al., 2005) when human archeological remnants are found within the lake (Burrough, 2016) to the highstand described above, when no remains are found anymore. From 80 to 60 ky, an increase in aquatic primary productivity, as shown by the $\delta^{13}C$ of organic matter and specific biomarkers (mid-chain alkanes) indicate a likely high lake level, that reaches a highstand around 64 ky (based on shorelines, Burrough et al., 2009). From 60 to 40 ky, very high sedimentation rates, indications of stratification in the lake water column, and high primary production indicate the potential for a highly productive lake. However, the coeval presence of human remains dated 40-35 ka (Early Stone Age factory site, McFarlane, 2001) in the lake area and lower reconstructed pH, likely point to the presence of several shallow productive ponds rather than a big and deep lake (Ringrose et al., 2005). From 40 to 20 ky, the lake seems to have the lowest sedimentation rate, present a high reconstructed pH and lower reconstructed salinity, as well as lower to absent primary production that can point towards an aridification of the lake and the formation of the salt pan.

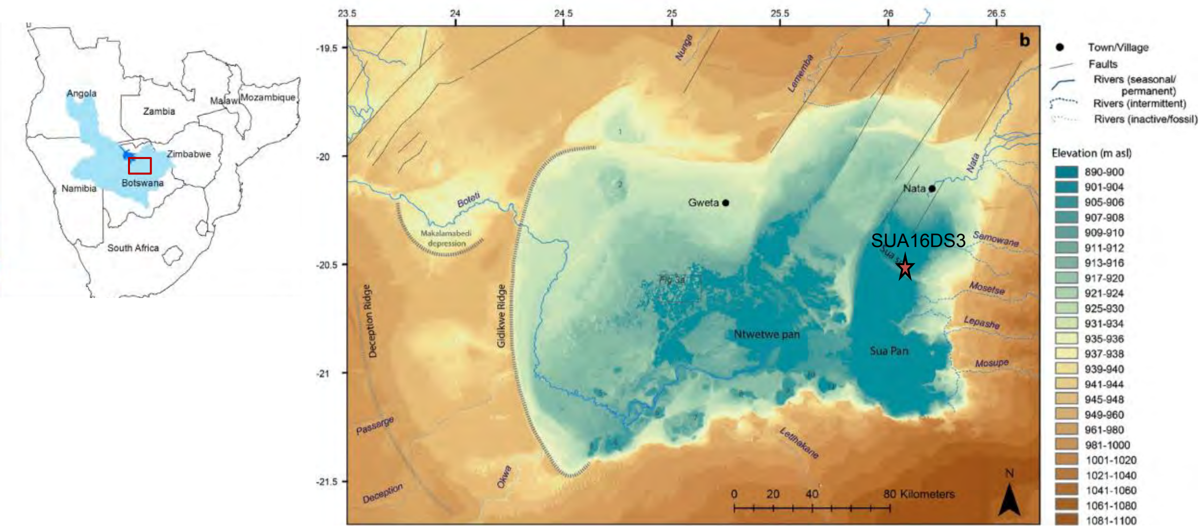

Figure 1. Location of the core within the wider Makgadikadi region, adapted from (Burrough, 2022).

REFERENCES

Burrough, S. L. 2016. Late Quaternary Environmental Change and Human Occupation of the Southern African Interior. In S. C. Jones & B. A. Stewart (Eds.), *Africa from MIS 6-2* (pp. 161–174). Springer Netherlands.

Burrough, S. L. 2022. The Makgadikgadi Basin. In F. D. Eckardt (Ed.), *Landscapes and Landforms of Botswana* (pp. 77–90). Springer International Publishing.

Burrough, S. L., Thomas, D. S. G., & Bailey, R. M. 2009. Mega-Lake in the Kalahari: A Late Pleistocene record of the Palaeolake Makgadikgadi system. *Quaternary Science Reviews*, *28*(15–16), 1392–1411.

Chan, E. K. F., Timmermann, A., Baldi, B. F., Moore, A. E., Lyons, R. J., Lee, S.-S., Kalsbeek, A. M. F., Petersen, D. C., Rautenbach, H., Förtsch, H. E. A., Bornman, M. S. R., & Hayes, V. M. 2019. Human origins in a southern African palaeo-wetland and first migrations. *Nature*, *575*(7781),

McFarlane, M. J. & Sedadika. P. 2001. Archaeological evidence for the reassessment of the ages of the Makgadikgadi paleolakes. *Botswana Notes & Records*, *33*(1), 83–90.

Ringrose, S., Huntsman-Mapila, P., Basira Kampunzu, A., Downey, W., Coetzee, S., Vink, B., Matheson, W., & Vanderpost, C. 2005. Sedimentological and geochemical evidence for palaeo-environmental change in the Makgadikgadi subbasin, in relation to the MOZ rift depression, Botswana. *Palaeogeography, Palaeoclimatology, Palaeoecology*, *217*(3–4), 265–287.

P 10.12
Reconstructing the Lateglacial and Holocene glacial history at the Leg Grevasalvas catchment (Graubünden)

Vicente Melo Velasco[1], Susan Ivy-Ochs[2], Naki Akçar[3], Marcus Christl[2], Christof Vockenhuber[2] and Jürgen Reitner[4]

[1] *Institute of Science and Technology Austria ISTA, Earth Science Faculty, Am Campus 1, 3400 Klosterneuburg, Austria. (jmelovel@ist.ac.at)*
[2] *Laboratory of Ion Beam Physics, ETH Zürich, Otto-Stern-Weg 5, 8093 Zürich, Switzerland*
[3] *Institute of Geological Sciences, University of Bern, Baltzerstrasse 1-3, 3012, Bern, Switzerland*
[4] *Geological Survey of Austria, Neulinggasse 38, 1030, Vienna, Austria*

This study investigates the glacial history during the Lateglacial and Holocene periods in the Leg Grevasalvas catchment. Although there is presently minimal glacial coverage, the abundance of (peri-)glacial landforms suggests a significant glacial influence in the past. Our research combines geomorphological mapping with exposure dating using cosmogenic ^{10}Be and ^{36}Cl, glacier and ELA reconstructions, and image feature tracking analysis. This comprehensive approach aims to unravel the evolution of glacial evolution in the catchment during the Lateglacial and Holocene.

The obtained exposure ages point to landform construction during the Egesen Lateglacial stadial and the early Holocene period. Through the reconstruction of paleo-glacier extents and analysis of their geomorphological characteristics, it was deduced that some of the linear depositional landforms are likely subglacial lineations. This challenges previous mapping that categorised them as lateral moraines. These lineations are thought to have formed due to a combination of processes similar to those that shape megaflutes, drumlins, and possibly medial moraines.

Our calculated ELA results are consistent with other reported values from the region. For comparative purposes and to explore broader paleoclimatic implications, we selected two glaciers in the Bedretto Valley (Ticino, Switzerland) and three glaciers in the Galitzen Valley (Lienz, Austria) for ELA reconstructions. Given the likelihood of significant debris coverage on the later glaciers, interpreting the determined Egesen Equilibrium Line Altitudes becomes complex.

The analysis of rock glacier activity in the Grevasalvas study area revealed that only two out of the five identified rock glaciers are presently active. The others are either entirely inactive or display some activity that might be attributed more to gravitational processes than periglacial creep.

During the early Holocene, glaciers in the area underwent rapid deterioration. Currently, a small glacierette is situated at the base of the northern slope of Piz Lagrev. In front of this glacierette, three frontal moraines are evident, with one of them having been dated. However, this dating resulted in an unreasonably old age, which is attributed to a long exposure on the rock wall before detaching and being incorporated in part of the moraine. Further studies are warranted to gain a more comprehensive understanding of the late Holocene to present-day evolution of the catchment.

P 10.13
Late Holocene speleothem-reconstruction from SW Asia

Alistair Morgan[1], Hai Cheng[2], Lawrence R. Edwards[3], Albert Matter[4], Elisa Hofmeister[1], Okan Tüysüz[5], Dominik Fleitmann[1]

[1] Department of Quaternary Geology, University of Basel, Bernoullistrasse 32, CH- 4056 Basel, Switzerland (alistair.morgan@unibas.ch, dominik.fleitmann@unibas.ch, elisa.hofmeister@unibas.ch)
[2] Institute of Glocal Environmental Change, Xi'an Jiaotong University, 710049 Xi'an, China (xjtu.edu.cn)
[3] Earth & Environmental Sciences, University of Minnesota, MN 55455 Minneapolis, USA (edwar001@umn.edu).
[4] Institute of Geological Sciences, University of Bern, CH-3012 Bern, Switzerland (amatter@geo.unibe.ch).
[5] Eurasia Institute of Earth Sciences and the Department of Geological Engineering, Istanbul Technical University, 34467 Istanbul, Turkey (tuysuz@itu.edu.tr).

NW Turkey is uniquely positioned between the climatic influences of the North Atlantic, Mediterranean and Eurasia. Variability in these systems through the Late Holocene is thought to influenced to major historical events, such as the 'Bronze Age Collapse', and periods including the 'Roman Climate Anomaly' and 'Little Ice Age'. The region is noteworthy considering it's geographical and historical significance over the last 4,000 years as the landscape for thriving Thracian tribes, Ancient Greece colonisation, the Roman Byzantine and Ottoman Empires. With the Eastern Mediterranean at risk from agricultural drought (Dabanlı et. al., 2017), which has proven to impact societies historically (Jones et. al., 2019), the region warrants the study of spatio-temporal human-climate interactions.

With no sub-decadal palaeoclimate records preceding 900-years regionally, and heterogeneity of Eastern Mediterranean climate generally (Jacobson et. al., 2021), Uzuntarla cave successfully fills this gap of paleoclimate reconstructions. Speleothem U-1 was dated using a combination of U/Th, ^{14}C and earthquake chronologies, facilitating the construction of a highly resolved multi-proxy record. Using the combined evidence of calcite fabric and growth axis changes, stable isotope ($\delta^{13}C$, $\delta^{18}O$) and trace elements (Mg/Ca, P/Ca), it is found that U-1 is highly sensitive to changes in regional precipitation amount and seasonality. The record presented, compared to meteorological, palaeoclimate and historical records, paints a picture of dynamic changes in regional precipitation since the Bronze Age coinciding with major societal transitions and events including drought, famine and flooding.

REFERENCES

Dabanlı, İ., Mishra, A.K. and Şen, Z., 2017: Long-term spatio-temporal drought variability in Turkey. Journal of Hydrology, 552, pp.779-792.

Jacobson, M.J., Flohr, P., Gascoigne, A., Leng, M.J., Sadekov, A., Cheng, H., Edwards, R.L., Tüysüz, O. and Fleitmann, D., 2021. Heterogenous late Holocene climate in the Eastern Mediterranean—the Kocain Cave record from SW Turkey. Geophysical Research Letters, 48(20), p.e2021GL094733.

Jones, M.D., Roberts, C.N., Leng, M.J., Turkes, M., 2006: A high-resolution late Holocene lake isotope record from Turkey and links to North Atlantic and monsoon climate. Geology 34, 361-364.

P 10.14
Integrated analysis of the Sierre Landslide, Rhone Valley

Anja Rubin[1], Susan Ivy-Ochs[2], Christian Schlüchter[1], Mattia Binaghi[1], Aaron Jordan[3], Christof Vockenhuber[2], Naki Akçar[1]

[1] *Geological Institute, University of Bern, Baltzerstrasse 1 + 3, CH – 3012 Bern (anja.rubin@students.unibe.ch)*
[2] *Laboratory of Ion Beam Physics, ETH Zurich, Otto-Stern Weg 5, CH - 8093 Zurich*
[3] *Geological Institute, Department of Earth Sciences, ETH Zurich, Sonneggstrasse 5, CH - 8001 Zürich*

Following the retreat of glaciers after the Last Glacial Maximum (LGM), there was an increase in large mass movement activity in the alpine valleys. Today, the danger of such a natural disaster poses a continuous threat to the urban areas in the alpine valleys (e.g., the Brienz Landslide in the Canton of Graubünden). Investigating past mass movements and assessing return periods has potential to enhance our ability to predict future hazards. The Sierre Landslide in the Rhone Valley (Canton of Valais) is one of the unexplored large alpine landslides. The Sierre Landslide extends over a length of 12 km in the valley and has a volume of 1.9 km^3 (Pedrazzini et al., 2013). The timing of its release is not yet known, only a minimum bound is indirectly set to ca. 9 ka based on the ^{14}C ages from two pieces of wood found in channelized debris flows (Schoneich et al., 1998).

The goal of this study is to use detailed Quaternary geomorphological mapping, surface exposure dating and modeling to constrain when, how, and why this landslide occurred. In the field, the landslide mass and release area will be mapped in detail. The timing of the Sierre landslide will be directly dated by surface exposure dating with cosmogenic ^{36}Cl. We have collected 16 rock surface samples, 13 from boulders and 3 from the bedrock within the scar area for the analysis of cosmogenic ^{36}Cl. Once the landslide timing and volume are constrained, the pre-landslide topography will be reconstructed and the runout will be modelled with DAN3D®. The results will be harmonized with the existing data and incorporated into a post-LGM landscape evolution history of the Rhone Valley. This study highlights the growing significance of investigating past movements and landscape evolution in the alpine valleys to better assess threats and mitigate future hazards.

REFERENCES

Pedrazzini, A., Jaboyedoff, M., Loye, A., & Derron, M. H. 2013: From deep seated slope deformation to rock avalanche: Destabilization and transportation models of the Sierre landslide (Switzerland). *Tectonophysics*, *605*, 149–168.

Schoneich, P., Dorthe-Monachon, C., Jaillet, S., Ballandras, S. 1998: Le retrait glaciaire dans les Préalpes et les Alpes au Tardiglaciaire. Bull. d'Ét. Préhist. et alpines de la vallée d'Aoste, IX, pp. 23-37.

P 10.15
Reconstructing the final phase of the Last Glacial Maximum Reuss glacier at Blattiswald and the timing and extent of the prehistoric Steinerberg (Rubenen) landslide in the region of Goldau, Schwyz

Sonja Scherer[1], Susan Ivy-Ochs[1], Sarah Kamleitner[1], Lukas Inderbitzin[2], Christof Vockenhuber[3], Marcus Christl[3]

[1] *Departement Erdwissenschaften, ETH Zurich, Otto-Stern-Weg 5, CH-8093 Zürich (sonjascherer@hispeed.ch)*
[2] *Fachbereich Naturgefahren, Canton Schwyz, Bahnhofstrasse 20, CH-6431 Schwyz*
[3] *Departement Physik, ETH Zurich, Otto-Stern-Weg 5, CH-8093 Zürich*

The Blattiswald region (Canton Schwyz, Switzerland) provides a unique opportunity to explore both glacial history and landslide processes. Employing a multi-method approach, we study deposits from Blattiswald and the Steinerberg (Rubenen) landslide. By extensive on-site landform mapping, GIS analysis, and cosmogenic nuclide surface exposure dating, we have revealed the features and timing of glacial deposition and the landslide event. During the latter part of the Last Glacial Maximum, a significant rockfall descended onto the Hüfi glacier, a tributary of the Reuss glacier. As the Hüfi glacier advanced westward, it converged with the Reuss glacier, which carried the boulders along its eastern side branch towards Lake Zug. Ultimately, during the earliest part of the phase of Early Lateglacial ice decay, when Lauerzersee potentially existed as an extensive dead-ice body, the erratics melted out of the ice and were deposited in Blattiswald after a supraglacial journey covering approximately 35 km.

Among the four major landslides on Rossberg's southern slope – Oberarth, Röthener, Goldau, - the Steinerberg (Rubenen) landslide is the oldest and smallest by volume at approximately 7.5 million m^3. Originating south of Wildspitz, its debis nearly reached the edge of Lauerzer Lake basin. The resulting deposits from this event partly covered the crystalline blocks at Blattiswald. The Steinerberg (Rubenen) landslide's inherent causal factors encompass the dip slope, existing lithologies, and prevailing joints in the Lower Freshwater Molasse Nagelfluh bedrock. Notably, glacier undercutting by the Reuss glacier's eastern side branch stands out as a siginifant preparatory factor contributing to the landslide's occurrence.

P 10.16
Continental temperatures since the Last Glacial Maximum inferred from luminescence palaeothermometry

Christoph Schmidt[1], Salome Oehler[1], Pontien Niyonzima[1], Frédéric Herman[1], Georgina King[1]

[1] *Institute of Earth Surface Dynamics, University of Lausanne, Quartier UNIL-Mouline, Géopolis, CH-1015 Lausanne (christoph.schmidt@unil.ch)*

Quantifying past surface air temperatures is crucial to understand the evolution of climate systems through time and benchmark climate models to accurately predict future climate scenarios. However, most of the temperature information originates from deep sea archives and ice cores, while continental climate archives are patchy and sparsely distributed. This lack of empirical temperature data applies also to the otherwise well-studied transition from the Last Glacial Maximum (LGM) to the present interglacial (Holocene).

Here we introduce a methodology to reconstruct absolute surface air temperatures based on the thermoluminescence (TL) of natural feldspar minerals in bedrock. Free electrons in these minerals are created through environmental radiation and localised at trapping sites (defects, impurities). Once (thermally) released from the trap, electrons can recombine with charge of opposite sign to produce luminescence. While the filling rate of the traps is constant through time, the depletion rate is a function of temperature and varies for different types of traps. In this way the relative trap filling of a range of traps with different thermal stability mirrors the thermal history of the rock (e.g., Ronca and Zeller, 1965). The trap filling is determined through TL measurements in the laboratory and inverse modelling is applied to translate these numbers into a probability distribution of time-temperature series by prescribing the shape of the temperature history (e.g., ^{18}O curve; Biswas et al., 2020).

In the course of a new project, we advance the methodology and apply it to a series of samples from the northern hemisphere to decipher the evolution of latitudinal and altitudinal temperature gradients since the LGM. We present initial results on the former aspect and on sampling strategy. Furthermore, different approaches are reviewed to translate reconstructed bedrock temperatures into surface air temperatures (due to the systematic offset between the two). Finally, we discuss the potential of the method in terms of spatial coverage and its applicability to sedimentary archives.

REFERENCES

Biswas, R. H., Herman, F., King, G. E., Lehmann, B., & Singhvi, A. K. 2020: Surface paleothermometry using low-temperature thermoluminescence of feldspar, Clim. Past, 16, 2075-2093, 10.5194/cp-16-2075-2020.

Ronca, L. B. & Zeller, E. J. 1965: Thermoluminescence as a function of climate and temperature, American Journal of Science, 263, 416-428, 10.2475/ajs.263.5.416.

P 10.17
First lacustrine application of the diatom-bound nitrogen isotope paleo-proxy reveals coupling of denitrification and N_2 fixation in a hyper-eutrophic lake

Anja S. Studer[1], Lars Wörmer[2], Hendrik Vogel[3], Nathalie Dubois[4], Kai-Uwe Hinrichs[2], Moritz F. Lehmann[1]

[1] Department of Environmental Sciences, University of Basel, Basel, Switzerland (anja.studer@unibas.ch)
[2] MARUM – Center for Marine Environmental Sciences, University of Bremen, Bremen, Germany
[3] Institute of Geological Sciences and Oeschger Centre for Climate Change Research, University of Bern, Bern, Switzerland
[4] Department of Surface Waters Research and Management, Eawag, Dübendorf, Switzerland

Past changes in the input/output, and internal cycling, of bioavailable nitrogen (N) in marine and lacustrine environments can be reconstructed by analyzing the N isotopic composition (i.e., the $^{15}N/^{14}N$ ratio, or $\delta^{15}N$) of organic matter in the sedimentary record. Bulk sedimentary $\delta^{15}N$ signatures, however, can be biased by secondary (i.e., post-burial) alteration and/or the admixture of external (e.g., terrestrial) organic and inorganic N inputs. Such a bias can be overcome by measuring the $\delta^{15}N$ of organic N trapped and protected in the mineral structure of (micro-)fossils, such as diatoms, foraminifera and corals, which is thought to record the pristine$\delta^{15}N$ signature of the dissolved inorganic N (generally nitrate) in the ambient water. While the diatom-bound N isotope paleo-proxy is widely used in the marine environment, it has not yet been applied to the lacustrine realm. This is the first study that validates the use of diatom fossil-bound N isotope proxy data in a lake. Firstly, through the comparison of bulk sedimentary and diatom-bound $\delta^{15}N$ records in a sediment core from eutrophic Lake Lugano (Switzerland), we demonstrate the differential effects changing redox/preservation conditions can have on the early diagenetic alteration of bulk $\delta^{15}N$ signatures. Secondly, combining our diatom-bound $\delta^{15}N$ measurements with X-ray fluorescence scanning and molecular biomarker analyses, we reconstruct nutrient cycling and paleoenvironmental conditions in the lake over the past ~130 years. Our sediment record indicates that primary productivity increased at the beginning of the 1960s, coeval with the period of severe eutrophication in Lake Lugano. At the same time, diatom-bound $\delta^{15}N$ values increased as well, which could either point to (i) a rise in the$\delta^{15}N$ of the nitrate input to the lake, e.g., through manure, (ii) enhanced nitrate utilization in the lakes' surface waters, or (iii) enhanced water-column denitrification in the hypolimnion. In order to differentiate among these possibilities, and to specifically assess the role of N_2 fixation as natural N input, we also determined the concentration of heterocyst glycolipids (HG) in the sediments, which is a diagnostic biomarker for N_2 fixing cyanobacteria. HG concentrations increased between the 1960s and the mid-1980s in parallel with diatom-bound $\delta^{15}N$ and several proxies that indicate increasing productivity, suggesting that N_2 fixation is closely coupled to water-column denitrification (and thus, N loss) in Lake Lugano. We argue that greater primary productivity during eutrophication led to anoxic conditions in the deeper water column as a result of enhanced organic matter remineralization, causing enhanced water-column denitrification in Lake Lugano. At the same time, the nitrogen-to-phosphorous (N:P) ratio in the lake declined due to the increased N loss and remobilization of P from the sediments under anoxic conditions, fostering N_2 fixation in surface waters. This study confirms the applicability of diatom-bound $\delta^{15}N$ to lake sediments and emphasizes the need for caution when interpreting bulk sedimentary $\delta^{15}N$ in paleolimnological studies.

11 Geomorphology

Christophe Lambiel, Cristian Scapozza, Dorota Czerski, Caroline Bolliger, Jonathan Bussard, Chantal Del Siro, Reynald Delaloye, Mauro Fischer, Isabelle Gärtner-Roer, Nikolaus Kuhn, Mario Kummert, Géraldine Regolini, Julie Wee

Swiss Geomorphological Society (SGmS)

TALKS:

11.1 Aarnink J., Rouge F., Fornari A., Ruiz-Villanueva V.: Five triple quad copter flights to better understand instream large wood dynamics during a flood

11.2 Droujko J., Molnar P.: Open-source, Low-cost turbidity sensor network: proof-of-concept hydropeaking study on the Spöl river

11.3 Duvanel T., Johns P., Lambiel C., Delaloye R.: Towards the first national rock glacier inventory in the Swiss Alps

11.4 Gevers M., Lane S., Miesen F., Mancini D., Jenkin M., Bouscary C., Perchanok F., Delaney I.: Identifying seasonal variations in sediment discharge from ice sheet terminus to proglacial forefield. A case study from Leverett glacier, Western Greenland.

11.5 Ligeza G., Bontognali T., Josset J.L., Kuhn N.: Optimizing ExoMars/CLUPI close-up imaging for investigating physical biosignatures and Martian surface processes.

11.6 Pascal I., del Hoyo J., Aarnink J., Finch B., de Graffenried B., Travaglini E., Theule J., Maino C., Abellán A., Ancey C., Ruiz-Villanueva V.: Sediment and large wood supply in proglacial streams: insights from the Upper Navisence catchment monitoring

11.7 Qie J., Favillier A., Ballesteros-Cánovas J.A., Stoffel M., Zhong Y., Lopez-Saez J., Guillet S., Corona C.: Supply-limited torrents do not feel the heat of climate change

11.8 Rowan A.V., Egholm D.L., Clark C.D.: Forward modelling of the completeness and preservation of Quaternary palaeoclimate signals recorded by ice-marginal moraines

11.9 Vendettuoli D., Strupler M., Anselmetti F.S., Fabbri S.C., Shynkarenko A., Kremer K.: Which deltas exhibit a higher vulnerability to slope failures within the Swiss perialpine lakes?

POSTERS:

P 11.1 de Palézieux L., Sutter E.: Automated quantification of variations in river sediment angularity in the vicinity of landslides using machine learning-assisted image segmentation

P 11.2 Delaney I., Al Alam E., Selitaj A., Hodel E., Huss M., Farinotti D., Dubois N.: Identifying changes to proglacial areas in the Swiss Alps over the past decade through systematic analysis repeated terrain models

P 11.3 Fankhauser J., Mair D., Ivy-Ochs S., Aaron J., Christl M., Akçar N.: Timing of the Poschiavo Rock Avalanche

P 11.4 Grischott R., Gischig V., Huwiler A., Thöny R., Aaron J.: Probabilistic runout modeling of giant earth flows in Brienz/Brienzauls GR

P 11.5 Lian T., Peleg N., Bonetti S.: Quantifying the effects of rainfall temporal variability on landscape evolution processes

P 11.6 Repnik L., Breillad A., Giovanardi A., Comiti F., Gianini M., Argentin A.-L., Pitscheider F., Lane S.: Bedload transport trends under rapid climate change: Understanding changes in the Turtmann valley at a decadal timescale

P 11.7 Schlatter D.M., Nissen M.: The northernmost sampled rocks (83.68407 N) and preliminary geological and geomorphological data from recently discovered “islands” located between North Greenland and the North Pole

P 11.8 Schmidt C., Schlunegger F., McArdell B., König L., Christl M., Akçar N.: Quantifying different erosion mechanisms in the Gürbe catchment using a 10Be tracing method

P 11.9 Vance G., Kirschner D., Willett S., Pellissier L.: Evaluating aquatic biodiversity in the Northern Apennines and Ligurian Alps (Italy) with environmental DNA (eDNA)

P 11.10 Wee J., Vivero S., Hauck C., Lambiel C.: Assessing the properties of ground ice and its influence on seasonal surface dynamics of glacitectonized frozen landforms in the Swiss Alps

11.1
Five triple quad copter flights to better understand instream large wood dynamics during a flood

Janbert Aarnink[1], Florent Rouge[1], Aldo Fornari[1], Virginia Ruiz-Villanueva[1,2]

[1] *Institute of Earth Surface Dynamics, University of Lausanne, Quartier Mouline, CH-1015 Lausanne (janbert.aarnink@unil.ch)*
[2] *Institute of Geography, University of Bern, Hallerstrasse 12, CH-3012 Bern*

River ecosystems benefit from large wood creating habitats for different species (Wohl et al., 2019). During floods the deposited pieces of wood can be entrained and transported downstream, and in some cases, when the river crosses infrastructure, the transported wood may cause damages. Wood buoyancy is controlled by density, and when wood floats, it generally follows the flow streamlines with a similar velocity. However, the dynamics of floating wood is complex, as wood interacts with the flow and its motion is affected by turbulence, gravitational and drag forces. In addition, local flow conditions and the contact with other wood pieces may affect the forces acting on the floating wood. As wood is primarily transported during floods, observations are scarce. We fill this gap by monitoring real-world wood movement during large scale environmental floods in the Spöl River.

The Spöl River is partially located in the Swiss National Park, and is regulated by two dams, the Punt dal Gal and Ova Spin. As part of a large restoration program, the hydropower company in charge of the dams´ operations releases environmental floods every year. In this study we monitored the transport of wood pieces during these releases by combining different approaches.

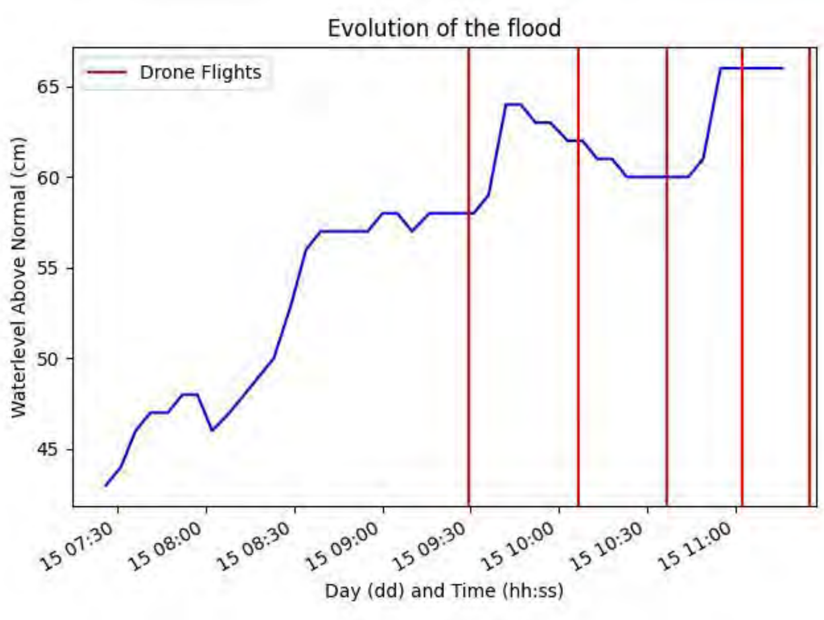

Figure 1: Water level evolution and timing of drone flights.

During the rising limb of the flood released in June 2023, 3 drones were flown simultaneously. Due to battery constraints, a maximum duration of 15 minutes per flight was performed 5 times between 09:30 and 11:45 in the morning (see Figure 1). Each drone recorded a 24 frames per second 4K video with a resolution of 3840x2160. With an average of 60 meters this resulted in an average pixel size of 2.3 centimetres. This means that a piece of large wood (1m in length minimally) has a minimum pixel length of 43.

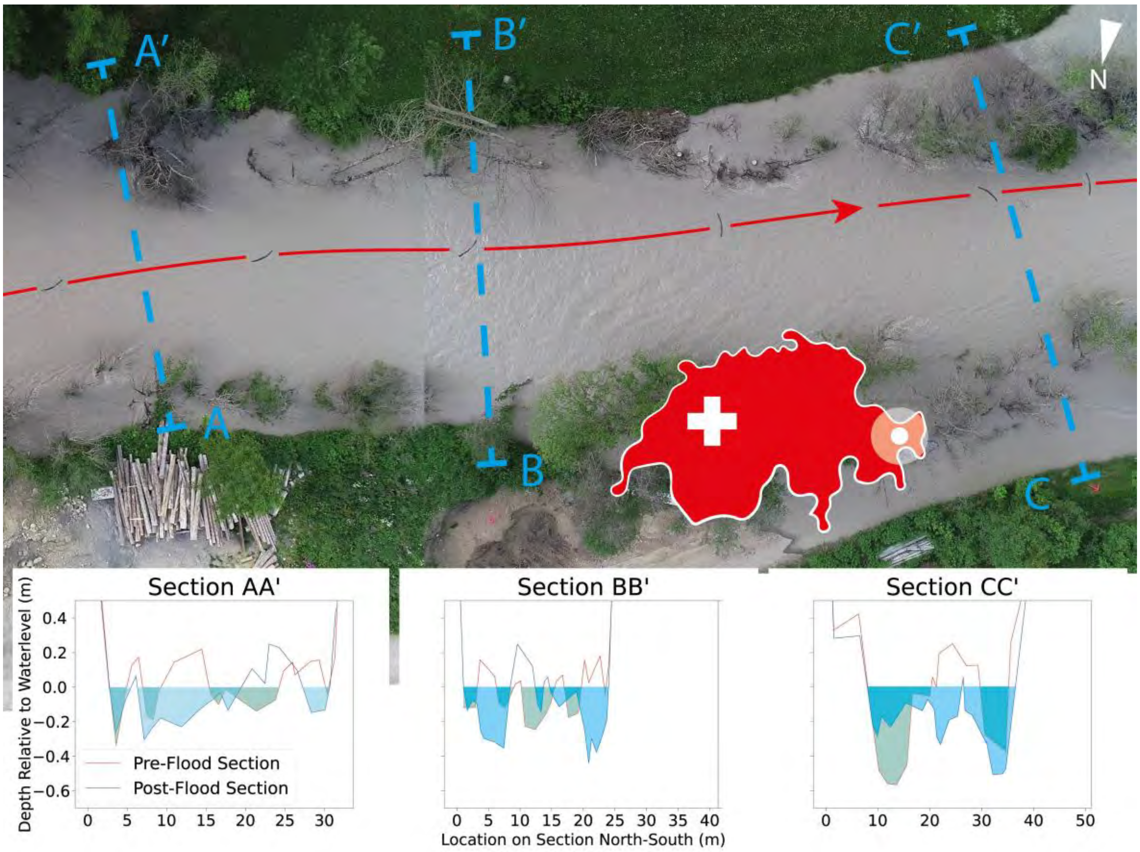

Figure 2: A sub-section of the 3 stitched drone recordings. A piece of wood is followed over time as it passes through 3 of the 6 measured cross-sections.

The video recordings contain approximately 100 pieces of instream large wood of which amongst others the size, trajectory and rotation were analysed (Figure 2). An analysis of the surface flow indicated the local velocities. Using 6 pre and post-flood measured cross-sections the evolution of the riverbed is analysed. The data from this study gives an insight into the wood transport behaviour of individual pieces floating during a flood. The results will be useful to compare with numerical models (e.g., Iber-Wood; Ruiz-Villanueva et al., 2014), and will help to validate whether our understanding of the process is translated into effective simulations.

Acknowledgements
This work is funded by the Swiss National Science Foundation project PCEFP2_186963, and supported by the University of Lausanne, the Swiss Academy of Sciences, the Swiss National Park, and the Engadiner Kraftwerke.

REFERENCES

Ruiz-Villanueva V., Bladé E., Sánchez-Juny M., Marti-Cardona B., Díez-Herrero A., Bodoque J.M. 2014: Two-dimensional numerical modeling of wood transport, Journal of Hydroinformatics, 16, 1077–1096. DOI: 10.2166/hydro.2014.026
Wohl, E., Kramer, N., Ruiz-Villanueva, V., Scott, D. N., Comiti, F., Gurnell, A. M., Piegay, H., Lininger, K. B., Jaeger, K. L., Walters, D. M., & Fausch, K. D. 2019: The natural wood regime in rivers, BioScience, 69, 259–273

11.2
Open-source, Low-cost turbidity sensor network: proof-of-concept hydropeaking study on the Spöl river

Jessica Droujko[1], Peter Molnar[1]

[1] *Institute of Environmental Engineering, ETH Zürich, Laura-Hezner-Weg 7, CH-8093 Zürich (droujko@ifu.baug.ethz.ch)*

Fine sediment transport in rivers is important for catchment nutrient fluxes, global biogeochemical cycles, water quality and pollution in riverine, coastal and marine ecosystems. Monitoring of suspended sediment in rivers with current sensors is challenging and expensive and most monitoring setups are restricted to few single site measurements. To meet these challenges, we have developed an open-source and low-cost sensor network for various applications: from identifying sediment source activation and transport in small streams, glacier networks and deltas, to environmental monitoring of maximum sediment concentration levels for the survival of fry fish, for prevention of river bed clogging, and for pollutant monitoring (binding to sediments). Our turbidity sensor is much cheaper than existing options of comparable quality. We conducted two proof-of-concept studies using the low-cost network on the Spöl river in Switzerland during an experimental flood (in 2021 and 2023). The collected data reveal sudden sediment concentration increases and decreases (pulsing) as the discharge increases steadily throughout the day. The highest concentration of sediment is much larger (4-5 g/L) than would be expected and appeared with the onset of the flood and again with the peak discharge. Our findings also reveal clockwise and counter-clockwise hysteresis loops in the stage-concentration relation, which point to a switch in the sediment supply between supply limited and unlimited conditions during the experimental flood. This study shows that high spatial- and temporal-resolution monitoring of suspended sediment is possible with a low-cost sensor network.

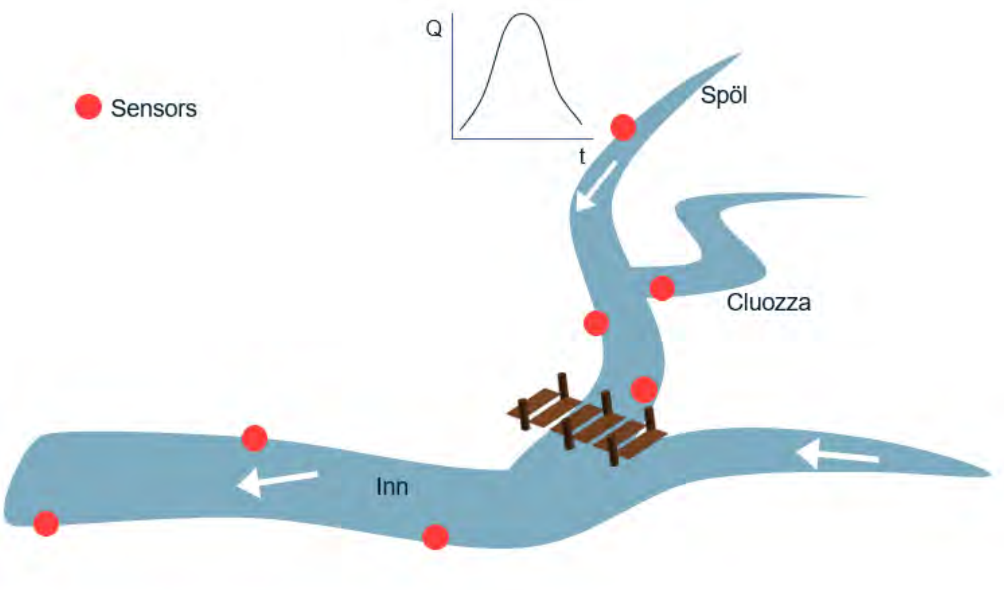

Figure 1. Depiction of sensor network during the experimental floods on the Spöl.

11.3
Towards the first national rock glacier inventory in the Swiss Alps

Thibaut Duvanel[1], Paula Johns[2], Christophe Lambiel[1], Reynald Delaloye[2]

[1] *Institute of Earth Surface Dynamics, University of Lausanne, Geopolis Building UNIL Mouline 1015 Lausanne (thibaut.duvanel@unil.ch)*
[2] *Department of Geosciences, University of Fribourg, Chemin du Musée 4, 1700 Fribourg*

Rock glaciers are debris landforms typical of high mountain environments. They can be identified in the landscape by their steep frontal and lateral margins, as well as their lobed surface with ridges and furrows (RGIK, 2022a). Their morphology is related to their downslope creeping movement. Over the past decades, the scientific community has highlighted the value of studying these landforms to improve our understanding of the impacts of climate change on high mountain regions.

Recently, a dedicated action group from the International Permafrost Association developed a standard methodology for rock glacier inventorying and mapping (RGIK, 2022a, b). It consists primarily of interpretating orthophotos to locate and outline rock glacier units, together with SAR interferometry or other optical techniques to assess their kinematics. The approach is currently tested and systematically applied in a various selected regions around the world within the framework of the ESA CCI Permafrost project.

The RoDynAlps research project, funded by the Swiss National Fundation and led by the Universities of Fribourg, Lausanne, Zurich and the WSL Institute for Snow and Avalanche Research, aims to better understand the dynamics of rock glaciers in the Swiss Alps. One of its main objectives, in the continuity of an initiative by Delaloye et al., 2019, is to establish an exhaustive inventory of rock glaciers in the Swiss Alps by following the RGIK methodology.

At present, relying on the new 0.5 m Swiss Surface 3D Lidar DEM hillshade and a dataset of interferograms derived from Sentinel 1 images 2020–2022, we have investigated a region of 1500 square kilometers between the Mont-Blanc massif and the Hérens valley, comprising several hundred rock glacier units, including relict, transitional, and active landforms. Special attention has been given to the identification and characterization of the destabilized rock glaciers (Johns P., 2023; Kolly O., 2019). To limit the subjectivity of the geomorphological interpretation, we used the consensus-based method promoted by RGIK (2022a, b) consisting in comparing the work of several operators on small control areas.

REFERENCES

Delaloye R., Barboux C., Gärtner-Roer I., Lambiel C., Pellet, C., Phillips, M. and Scapozza, C. (2019) *Toward the first national rock glacier inventory in the Swiss Alps (SwissRG2020)*. Abstract, 17th Swiss Geoscience Meeting, Fribourg 2019

RGIK (2022a). Towards standard guidelines for inventorying rock glaciers: baseline concepts (version 4.2.2). IPA Action Group Rock glacier inventories and kinematics, 13 pp.

RGIK (2022b). Towards standard guidelines for inventorying rock glaciers: practical concepts (version 2.0). IPA Action Group Rock glacier inventories and kinematics, 10 pp.

Johns P. (2023). Contribution to an Inventory of Destabilized Rock Glaciers in the Valais Alps. Unpublished bachelor thesis, Dept. Geosciences, Univ. Fribourg, Switzerland.

Kolly O. (2019). Contribution à l'inventaire des glaciers rocheux déstabilisés dans la partie occidentale des Alpes Valaisannes. Unpublished bachelor thesis, Dept. Geosciences, Univ. Fribourg, Switzerland.

11.4
Identifying seasonal variations in sediment discharge from ice sheet terminus to proglacial forefield. A case study from Leverett glacier, Western Greenland.

Marjolein Gevers[1], Stuart Lane[1], Floreana Miesen[1], Davide Mancini[1], Matthew Jenkin[1], Chloé Bouscary[1], Faye Perchanok[1], Ian Delaney[1]

[1] *Institute des dynamiques de la surface terrestre (IDYST), Université de Lausanne, Lausanne, Switzerland (marjolein.gevers@unil.ch)*

Increased melt of the Greenland Ice Sheet will affect the export of sediment from land-based outlet glaciers, as well as the transport of this sediment through its proglacial areas. Catchments in Greenland have a high baseflow, reduced diurnal variation in discharge, and different sediment supply compared to other glaciated (Arctic) catchments that have traditionally been monitored intensively. The response of sediment transport processes in the rivers fed by land terminating glacier outlets of the Greenland Ice Sheet remains uncertain.

Using two hydrological gauging stations and seismic stations in summers of 2022 and 2023, we present a record of sediment transport to locations in the proglacial area at Leverett glacier, a land terminating glacier located at the western margin of the Greenland Ice Sheet (Fig.1). The first station is located close to the current glacier terminus, while the second station is about 2 km from the current glacier terminus. The spacing of the two stations allows assesment of the movement of sediment through the proglacial area. Water level and suspended sediment concentration are used to evaluate seasonal fluctuations in suspended sediment export through the study area, while variations in bedload transport are evaluated using seismic data. Additionaly, two timelapse cameras were installed to monitor the evolution of the proglacial area over the summer season. One camera overlooks the whole proglacial area while the second one is installed to monitor one of the hydrological gauging stations.

With these datasets, we aim to establish the relationship between sediment transport and water level of the proglacial river from Leverett glacier over the summer season to estimate sediment availibility both subglacially and within the proglacial area. This will allow a better understanding of the role that proglacial areas have in sediment supply downstream, under a warming climate.

Figure 1. Fieldwork August 2023 in the proglacial area of Leverett glacier, West Greenland

11.5
Optimizing ExoMars/CLUPI close-up imaging for investigating physical biosignatures and Martian surface processes.

Gabriela Ligeza[1], Tomaso Bontognali[1,2], Jean-Luc Josset[2], Nikolaus Kuhn[1]

[1] *Department of Environmental Sciences, University of Basel, CH-4056 Basel (gabriela.ligeza@unibas.ch)*
[2] *Space Exploration Institute, 2000, Neuchâtel, Switzerland*

ExoMars is an astrobiology program led by the European Space Agency, with the primary goal of launching a rover to Oxia Planum to search for evidence of past life. While the mission's focus is astrobiology, it also includes several secondary objectives, such as investigating Martian geomorphology, aeolian phenomena, and volcanic processes to gain deeper insights into the planet's evolution and ancient climate. The CLUPI instrument (a close-up imager) will play a crucial role in this mission by capturing high-resolution images of rocks, geological formations, and drill cores, providing a comprehensive overview of Oxia Planum's geological context. Due to telemetry data limitations, only few CLUPI images can be sent to the science team per day, which is vital for assessing hypotheses and planning rover activities in subsequent cycles. Therefore, it is essential for CLUPI to capture relevant information and magnify mission-relevant features such as laminations, grain size particles, physical biosignatures, and other sedimentary structures.

In this context, we present a comprehensive image catalog for CLUPI, outlining the optimal conditions for image acquisition. Our findings illustrate the profound impact that varying illumination conditions (specifically, the orientation of the illumination axis and the ratio between direct and diffused light) may have on distinguishing rock textures and sedimentary structures within close-up imagery. We have demonstrated that by strategically capturing images at different times of the day, under specific lighting conditions, it becomes possible to increase the likelihood of detecting diverse rock textures and relevant structures. These findings hold the potential to expand the scope of collected data, contributing to a better understanding of the Oxia Planum's geomorphology and the surface processes on Mars.

11.6
Sediment and large wood supply in proglacial streams: insights from the Upper Navisence catchment monitoring

Ivan Pascal[1,2], Javier del Hoyo[1], Janbert Aarnink[1], Bryce Finch[1], Bob de Graffenried[2], Eric Travaglini[3], Joshua Theule[3], Carlo Maino[3,4], Antonio Abellán[3], Christophe Ancey[2], Virginia Ruiz-Villanueva[1,5]

[1] Institute of Earth Surface Dynamics, University of Lausanne, Quartier Mouline, CH-1015 Lausanne (ivan.pascal@unil.ch)
[2] Environmental Hydraulics Laboratory, Swiss Federal Institute of Technology Lausanne (EPFL), Station 18, CH-1015 Lausanne
[3] Centre de Recherche sur l'Environnement ALPin (CREALP), Rue de l'industrie 45, CH-1950 Sion
[4] EPSRC Centre for Doctoral Training in Modelling Heterogeneous Systems, University of Warwick, Coventry CV4 7AL, United Kingdom
[5] Institute of Geography, University of Bern, Hallerstrasse 12, CH-3012 Bern

Vegetation quickly takes root on the slopes of moraines and riverbanks in proglacial areas, leading to a gradual rise in the tree-line elevation (Cowie et al., 2014). Therefore, gravitational and fluvial processes, encompassing phenomena like debris flows, landslides, snow avalanches, and bank erosion, can convey significant quantities of sediment and wood into proglacial river networks (e.g. Wohl et al., 2019). The river morphodynamics is thus intricately controlled by the interaction among flow, sediment, and large wood regimes. Nevertheless, quantifying the magnitude and frequency of sediment and large wood supply to proglacial streams poses a formidable obstacle. This challenge primarily arises from the limited availability of data, which, in turn, is mainly attributed to the complexities involved in establishing comprehensive monitoring frameworks capable of capturing both sediment and wood supply dynamics. Still, such information is critical to better understand the evolution of river corridors under rapid glacier retreat. Moreover, it would help to adapt to the potential related hazards affecting populated mountain valleys.

Therefore, we recently designed and implemented a monitoring framework focused on identifying sources of sediment and instream large wood in the Upper Navisence catchment (Val d'Anniviers, Wallis, Switzerland) and on characterising their regimes. The Upper Navisence and *Torrent de l'Arpitettaz* are the two main streams that drain this catchment encircled by several 4000-m-high peaks. A glacio-nival hydrologic regime characterises these streams that are surrounded by conifer trees (mainly *Larix decidua*) combined with riparian species (mainly *Alnus* sp. and *Betula* sp.) up to around 2200 m asl. During the summer of 2023, water discharges were markedly increased by intense glacial melt and heavy, and short rainstorms. The resulting flood events caused significant geomorphic changes and wood recruitment, particularly along the Torrent de l'Arpitettaz (mid-august event).

The monitoring framework included RGB and multispectral Unmanned Aerial Vehicle (UAV) surveys for identifying geomorphic changes and temporal variations in the spatial distribution of instream wood accumulations and vegetation cover. A low-cost seismic station for monitoring the timing of bedload pulses was tested on the Torrent de l'Arpitettaz banks. Moreover, a time-lapse camera was installed for collecting image sequences on which a wood tracking tool based on machine learning (Aarnink et al., 2021) will be assessed. Dendrochronological sampling of both standing trees and instream wood is also being conducted. A GIS fuzzy logic approach (Steeb et al. 2023) was used to identify zones prone to wood supply in different scenarios. Subsequently, these predictions will be subjected to comparative analysis involving both field and remote-sensing observations.

Preliminary analyses of data collected during 2023 and analyses of archived data provided new insights into the sources of wood and sediment in this river corridor. These analyses have highlighted the primary supply processes accountable for these materials and some important feedback mechanisms. We found that the Torrent de l'Arpitettaz channel shifted across a forested area in 2019, driven by a large debris flow sequence (started in August) originated from recently exposed moraine deposits located on the north-facing valley flank. We observed that the stream is still progressively recruiting large wood pieces across the forest during the summer floods. This large-wood input temporarily and locally stabilises the channel bed and promotes a multithread planform, as the wood forms large jams with standing trees and boulders.
The understanding and prediction of the complex cascade processes that govern the transient morphodynamic evolution of proglacial streams present a formidable challenge within the current context of climate change. The monitoring framework introduced in this study will offer a more comprehensive and holistic understanding of these phenomena.

This work is supported by the CLIMACT UNIL-EPFL under the starting grant assigned to the 'NaviSedWood' project, and the Swiss National Science Foundation project PCEFP2_186963.

REFERENCES

J. Aarnink, M. Vuaridel, and V. Ruiz-Villanueva (2021): Monitoring instream large wood transport in rivers, using video cameras, deep learning and RFID, in Conference Proceedings of the 19th Swiss Geoscience Meeting, Geneva, Switzerland.

N. M. Cowie, R. D. Moore, and M. A. Hassan (2014): Effects of glacial retreat on proglacial streams and riparian zones in the Coast and North Cascade Mountains: Effects of Glacial Retreat on Proglacial Streams and Riparian Zones, Earth Surf. Process. Landf., vol. 39, no. 3, pp. 351–365. doi: 10.1002/esp.3453.

N. Steeb, V. Ruiz-Villanueva, A. Badoux, C. Rickli, A. Mini, M. Stoffel, and D. Rickenmann (2023): Geospatial modelling of large-wood supply to rivers: a state-of-the-art model comparison in Swiss mountain river catchments, Earth Surf. Dynam., vol. 11, pp. 487–509, https://doi.org/10.5194/esurf-11-487-2023.

E. Wohl, N. Kramer, V. Ruiz-Villanueva, D. N. Scott, F. Comiti, A. M. Gurnell, H. Piegay, K. B. Lininger, K. L. Jaeger, D.M. Walters, and K. D. Fausch (2019): The Natural Wood Regime in Rivers, BioScience, vol. 69, no. 4, pp. 259–273. doi: 10.1093/biosci/biz013.

11.7
Supply-limited torrents do not feel the heat of climate change

Jiazhi Qie[1,2], Adrien Favillier[1,2], Juan A. Ballesteros Cánovas[1,2,3], Markus Stoffel[1,2,3], Yihua Zhong[1,2], Jérôme Lopez-Saez[1,2], Sébastien Guillet[1,2], Christophe Corona[1,5]

[1] *Climatic Change Impacts and Risks in the Anthropocene (C-CIA), Institute for Environmental Sciences, University of Geneva, 66 Boulevard Carl Vogt, CH-1205 Geneva, Switzerland*
[2] *dendrolab.ch, Department of Earth Sciences, University of Geneva, 13 rue des Maraichers, CH-1205 Geneva, Switzerland*
[3] *National Museum of Natural Sciences, MNCN-CSIC, C/ Serrano 115bis, E-28006 Madrid, Spain*
[4] *Department F.-A. Forel for Environmental and Aquatic Sciences, University of Geneva, 66 Boulevard Carl Vogt, CH-1205 Geneva, Switzerland*
[5] *Geolab, UMR 6042 CNRS, Université Clermont Auvergne, F-63057, Clermont-Ferrand, France*

Debris-flows are water-laden masses of soil and rock with volumetric sediment concentrations that typically exceed 40% (De Haas et al., 2018). These masses of sediment move rapidly through channel networks and across alluvial fans, where they can devastate people and property (Dowling and Santi, 2014). Debris flows are typically triggered by intense precipitation and soil instability occurring in the same locations periodically (Imaizumi et al., 2006; Marchi et al., 2021). Debris flows are expected to change more than other landslide processes, presumably because of accelerate permafrost thawing and glacier retreat which lead to an increase in unstable sediments potentially mobilized by more frequent convective rainfalls. It has also been speculated that slope stabilization by vegetation and the reduced number of extreme summer rainfall projected over the Alps could significantly alter the frequency and magnitude of debris flows. Yet, the systematic lack of long-term observations of debris flows largely hampers an in-depth assessment of how activity may have been altered by a changing climate.

Here, we reconstruct the longest, continuous times series (1626-2020) of debris flow using growth-ring of trees damaged by past debris flow events at Multetta (Swiss Alps). Over the 1763-2020 period, we did not show clear link between extreme precipitation events and debris flow initiation nor detect significant anomalies in debris flow frequency or spatial patterns during e.g., the coldest periods of the Little Ice Age (LIA) or the warmest decades of the 21st century (Figure 1). This absence of climatic control on debris flow initiation is consistent with the clustered distribution of repose time patterns indicating a dependency between events in response to the cycle of sediment discharge and recharge (Figure 2). This major dichotomy between supply-limited and supply-unlimited basins have substantial implications on torrential hazard assessment and mitigation in the global warming context and offer support for further investigation of the decadal-scale to centennial-scale response of catchments to climate variability.

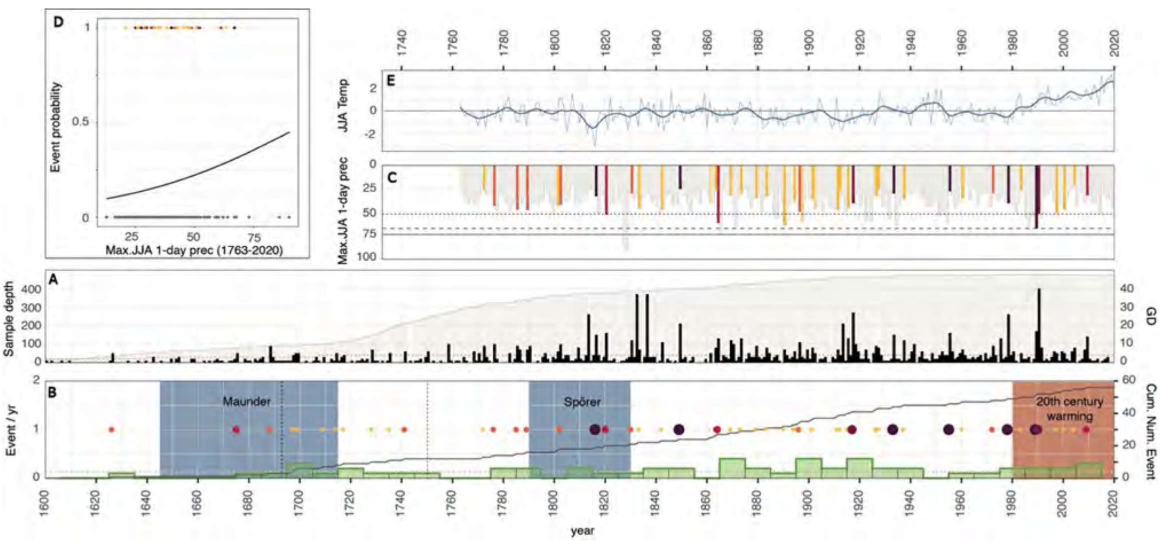

Figure 1. Debris flow activity, frequency and size, at Multetta does not show any clear trend related to climate fluctuations: (A) Annual number of living trees (sample depth, grey area) and growth disturbances (GD, black bars) over the period 1600–2020. (B) Reconstructed debris flow events (circles) of XS, S, M, L, XL and XXL sizes (yellow to black color gradient). According to the completeness analysis conducted on the reconstruction, the time series can be considered as free of bias since the late 17th-mid-18th century (vertical dotted lines). The dark line showing the cumulative number of events do not show any clear breakpoint that would indicate an increasing frequency of debris flows activity. This absence of anomalies is confirmed at the decadal scale (green bars) with a frequency of events ranging between 0 and 0.3 (mean=0.16, horizontal dashed line). (C) Over the 1763-2020 CE period, all reconstructed debris flow events (vertical bar, yellow to black

gradient) were triggered by JJA daily precipitation > 25 mm.day-1 but there is no dependence between debris flow occurrence or size and extreme precipitation events with return period exceeding 10 (horizontal dotted line), 50 (horizontal dashed line) or 100 (horizontal continuous line) years. (D) This absence of clear relation between debris flow events and precipitation is confirmed by the logistic regression which is significant ($p<0.05$) but poorly predictive ($R^2=0.025$) (E) No clear control of temperature fluctuations on debris flow activity is evidenced during the coldest period of the Little Ice Age or as a result of the accelerating warming climate.

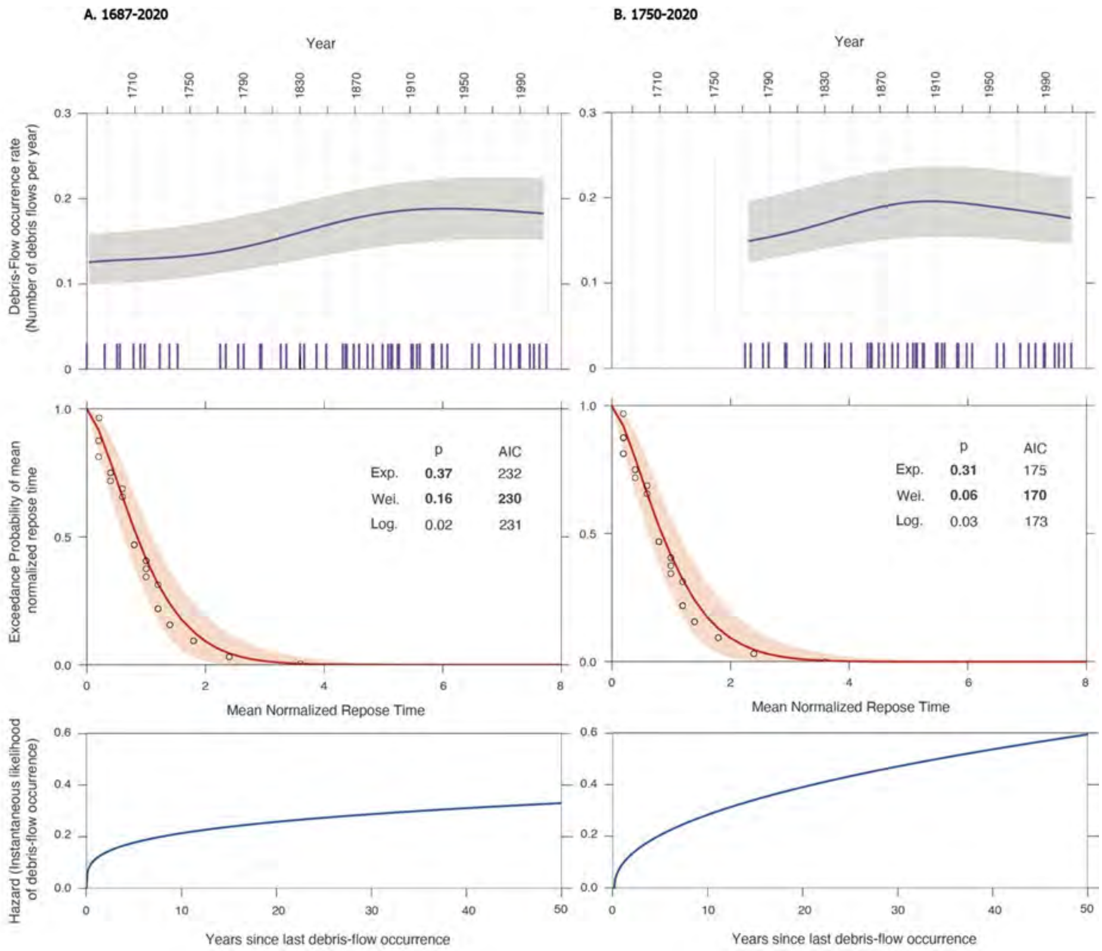

Figure 2. The best-fitting distributions of repose-time patterns at Multetta over the (A) 1687-2020 and (B) 1750-2020 periods are given by the Weibull distribution (p>0.05, lowest AIC), showing regular and dependent debris-flow repose times and supposing a supply-limited catchment. The upper and central panels show the estimated yearly debris-flow occurrence rate and corresponding estimated repose time distributions. All repose times were normalized by dividing by their mean value. The general suitability of the distributions was tested based on the p-value associated to a Monte Carlo version of the Kolmogorov–Smirnov test. The distribution with the lowest AIC value (Weibull in our case) is shown with a pointwise 95% confidence interval based on 1000 bootstrap samples. The bottom panel shows the describe the likelihood that a debris flow will occur at a certain time lag after the last debris-flow event based on hazard function of the Weibull distribution.

REFERENCES

De Haas, T. et al. Avulsions and the spatio-temporal evolution of debris-flow fans. Earth-Science Reviews 177, 53–75 (2018).

Dowling, C. A. & Santi, P. M. Debris flows and their toll on human life: a global analysis of debris-flow fatalities from 1950 to 2011. Nat Hazards 71, 203–227 (2014).

Imaizumi, F., Sidle, R. C., Tsuchiya, S. & Ohsaka, O. Hydrogeomorphic processes in a steep debris flow initiation zone. Geophys. Res. Lett. 33, L10404 (2006).

Marchi, L. et al. Debris flows recorded in the Moscardo catchment (Italian Alps) between 1990 and 2019. Nat. Hazards Earth Syst. Sci. 21, 87–97 (2021).

11.8
Forward modelling of the completeness and preservation of Quaternary palaeoclimate signals recorded by ice-marginal moraines

Ann V. Rowan[1], David L. Egholm[2], Chris D. Clark[3]

[1] *Department of Earth Science, University of Bergen and Bjerknes Centre for Climate Research, Bergen, Norway (ann.rowan@uib.no)*
[2] *Department of Geoscience, Aarhus University, Denmark*
[3] *Department of Geography, University of Sheffield, UK*

Glaciers and ice sheets fluctuate in response to climate change and often record these changes by building ice-marginal (terminal and lateral) moraines. Typically, a cooling climate causes glaciers to expand, and warming causes glaciers to shrink. However, the glacier response time and the influence of high-relief mountainous topography on glacier dynamics complicates this behaviour, such that ice-marginal moraines are not always a straightforward palaeoclimate indicator. We used a higher-order ice-flow model to simulate changes in glacier erosion, extent, and thickness in the response to change in mean annual air temperature (MAAT), and the resulting formation and preservation of moraines in a synthetic mountain landscape.

Our results show that the rate of change in MAAT relative to the glacier's response time determines the geometry, number and position of ice-marginal moraines. The interpretation of moraine sequences in the field may be challenging where the model results indicate that glaciers can also build distinct moraines in the absence of climate change, and the distance from the glacial maximum may not represent the chronological order of moraine formation. While moraines can be preserved despite erosion during subsequent glaciations, moraine sequences frequently contain gaps that could be misinterpreted as representing periods of stable climate. These results provide theoretical understanding for the interpretation of glacial landforms both in the field and from digital terrain models to understand Quaternary glacier evolution and palaeoclimate change.

11.9
Which deltas exhibit a higher vulnerability to slope failures within the Swiss perialpine lakes?

Daniela Vendettuoli[1], Michael Strupler[2], Flavio S. Anselmetti[1], Stefano C. Fabbri[1,3,4], Anastasiia Shynkarenko[2], Katrina Kremer[1]

[1] Institute of Geological Sciences and Oeschger Centre for Climate Change Research, Baltzerstrasse 1+3, 3012 Bern (daniela.vendettuoli@geo.unibe.ch)
[2] Swiss Seismological Service, ETH Zurich, Sonneggstrasse 5, 8092 Zurich
[3] Université du Québec à Rimouski, Institut des sciences de la mer de Rimouski (ISMER), Rimouski, Canada
[4] Laboratoire EDYTEM, Université Savoie Mont Blanc, Le Bourget du Lac, France

Significant lacustrine mass movements and the failure of deltas may serve as triggers for tsunamis. In light of the concurrent expansion of population and infrastructure in close proximity to the Swiss lake shores, we must assess the vulnerability of lake deltas to potential failure. Therefore, it is essential to conduct a thorough and inclusive evaluation and analysis of the Swiss perialpine lakes' deltas. Currently, the study of tsunamis in lakes caused by subaquatic slope failure is hampered by a lack of data on the physical characteristics of deltas and their probable evolution scenarios.

The primary objective of our research, which is supported by the Swiss Federal Office for the Environment, is to gain a deeper understanding of the specific characteristics of deltas that may exhibit a greater susceptibility to slope failure. To accomplish our objective, we classify the deltas based on their morphological, morphometric, and sedimentological characteristics using publicly available datasets. In this study, we propose a categorization approach to deltas that consists of two basic classes. Delta-Type 1 is characterised by gentle slope gradients, bathymetric profiles displaying outgoing changes in the horizontal distance along the slope in relation to minor variations in water depth, and the presence of notable bedforms. The rivers that flow into and out of these deltas are distinguished by their length and discharge rates. Delta-Type 2 is characterised by more pronounced variations in slope gradients and shorter rivers with reduced flow rates, resulting in the formation of relatively smaller subaquatic fans. Since the 17th century, newly developed deltas, such as the Kander Delta in Lake Thun, have formed as a consequence of human activities. The current method does not account for these deltas.
The findings of this study provide a basis for evaluating the potential hazard of tsunamis in the Swiss perialpine lakes, leading to a more comprehensive assessment of tsunami risks.

P 11.1
Automated quantification of variations in river sediment angularity in the vicinity of landslides using machine learning-assisted image segmentation

Larissa de Palézieux[1], Elia Sutter[1]

[1] Geologisches Institut, ETH Zurich, Sonneggstr. 5, 8092 Zurich (larissa.depalezieux@erdw.ethz.ch)

Within alpine river systems, landslides serve as stochastic point sources of sediment, that can abruptly chang key sediment properties within the river bed. While the amount of landslide-derived sediment contribution to river systems has been described and to a certain degree quantified, the precise properties necessary for a geotechnical classification of sediment are often not well known.

In this study we employ new technologies to quantify sediment angularity at different locations with respect to mapped channel-adjacent landslides. Based on high-resolution drone images (up to 5 mm resolution), we use machine learning-assisted image segmentation, to detect pebble outlines in the river sediment in drone images with high accuracy (Mair et al., 2022) and quantify sediment grain size distributions (Mair et al., submitted, Stringer and Pachitariu, 2021). In addition, we can use the pebble outlines to quantify angularity by deriving its Wadell index (Roussillon et al., 2009).

We find that both grain size distributions and angularity vary depending on the respective sample location to a given landslide. We observe on average decreased grain size distributions and increased angularity downstream of the landslides

REFERENCES

Mair, D., Henrique, A., Prado, D., Garefalakis, P., Witz, G., and Schlunegger, F. (submitted): Automated finding, segmenting, and measuring of grains in images of fluvial sediments – the potential of transfer learning in deep neural networks.

Roussillon, T., Piégay, H., Sivignon, I., Tougne, L., & Lavigne, F. (2009). Automatic computation of pebble roundness using digital imagery and discrete geometry. *Computers & Geosciences*, *35*(10), 1992-2000.

Stringer, C.A., Pachitariu, M., (2021). Cellpose: a generalist algorithm for cellular segmentation. Nat Methods 18, 100–106. https://doi.org/10.1038/s41592-020-01018-x.

P 11.2
Identifying changes to proglacial areas in the Swiss Alps over the past decade through systematic analysis repeated terrain models

Ian Delaney[1], Elias Al Alam[1], Adrijan Selitaj [1], Elias Hodel[2], Matthias Huss[2,3], Daniel Farinotti[2,3], Nathalie Dubois[4]

[1] Institut des dynamiques de la surface terrestre (IDYST), Université de Lausanne, Geopolis, CH-1022 Lausanne
[2] Laboratory of Hydraulics, Hydrology and Glaciology (VAW), ETH Zürich, Hönngerbergring 26, CH-8049 Zurich
[3] Swiss Federal Institute of Forest, Snow and Landscape Research (WSL), Züricherstrasse 111, CH-8903 Birmensdorft
[4] Swiss Federal Institute of Aquatic Science and Technology, Überlandstrasse 133, CH-8600 Dübendorf

Glacier retreat exposes expanses of land previously covered by glaciers, known as proglacial areas. These proglacial areas can often consist of unconsolidated sediment, not yet stabilized by vegetation and soil formation. Proglacial areas can both serve as a sediment source, as glacier meltwater mobilizes material in these areas, and a sediment sink, when sediment mobilized below the glacier is deposited there. While recent work has identified and quantified many of the key processes controlling sediment transport from proglacial areas, the manifestation of these processes across different catchments remains uncertain.

To better evaluate the changes to sediment dynamics across multiple proglacial areas, we leverage a set of digital elevation models collected at an annual resolution from seven glaciers in Switzerland across the last decade. These glaciers are monitored by GLAMOS and vary in glacier and catchment size, aspect, gradient and retreat rate. By differencing elevation models of these proglacial areas, we examine both the evolving volume and erosion rate of these proglacial areas. Furthermore, we identify locations in the proglacial areas where sediment mobilization and deposition occurs. These findings are placed in the context characteristics of their catchments to understand the response of proglacial areas as glaciers retreat.

Figure 1. Proglacial area of Findelngletscher in 2021.

P 11.3
Timing of the Poschiavo Rock Avalanche

Janine Fankhauser[1], David Mair[1], Susan Ivy-Ochs[2], Jordan Aaron[3], Marcus Christl[2], Naki Akçar[1]

[1] Institut für Geologie, University of Bern, Baltzerstrasse 1+3, CH-3012 Bern (janine.fankhauser@students.unibe.ch)
[2] Laboratory of Ion Beam Physics, ETH Zurich, Otto-Stern-Weg 5, 8093 Zurich
[3] Department of Earth Sciences, ETH Zurich, Sonneggstrasse 5, 8092 Zurich

Throughout the Quaternary, the Swiss Alps have been carved by repeated glaciations. This carving influences on the one hand the valley topography and on the other hand the stability of the bedrock. The removal of ice from the alpine valleys after the Last Glacial Maximum sparked the instabilities in the bedrock of the valley walls, thus the rock avalanche activity. For example, a large rock avalanche dammed the Poschiavino River and caused the formation of the Poschiavo Lake in Val Poschiavo, near Miralago (Motta di Meschino in Canton of Graubünden). In addition, an alternation of glacial and mass move movement sediments is found in the drill cores, which indicates that several mass movements occurred during the deglaciation. Based on the ^{14}C ages from the wood pieces found in a core, most of these layers were attributed to the Younger Dryas (Zwahlen, 2019). The size and timing of the Poschiavo rock avalanche are of utmost importance for the reconstruction of the landscape evolution of the valley.
Therefore, the aim of this study is to date and model the Poschiavo rock avalanche to reconstruct the sequence of events. The rock avalanche at Miralago will be mapped in detail in the field, in particular, large and suitable boulders will be identified for surface exposure dating with cosmogenic ^{10}Be. In addition, the boulder lithology will be determined with petrographical analysis to further narrow down the release area of the collapse. Furthermore, aerial images will be taken with an unmanned air vehicle to map the inaccessible outcrops such as the steep slopes of the Motta di Meschino. After the mapping and calibration of the timing of the rock avalanche, the runout of the collapse will be modeled with DAN3D®. The results will be presented.

REFERENCES

Zwahlen, P. (2019). Der Bergsturz von Miralago : Talgeschichte im Valposchiavo. *Swiss Bulletin Für Angewandte Geologie*, *1*, 69-.

P 11.4
Probabilistic runout modeling of giant earth flows in Brienz/Brienzauls GR

Reto Grischott*, Valentin Gischig**, Andreas Huwiler**, Reto Thöny*, Jordan Aaron**

** BTG Büro für Technische Geologie AG, Sargans*
***Engineering Geology, Department of Earth Sciences, ETH Zurich*
****Amt für Wald und Naturgefahren, Kanton Graubünden*

The landslide complex in Brienz/Brinzauls in Grisons is one of the most active in the Alps. A detailed study based on drilling campaigns paired with geophysical investigations revealed that it is composed of six distinct compartments with volumes ranging from 0.8 to 19 Mio m^3 are prone to slide down as major mass movement. The hazards are threatening the underlying village of Brienz, which has 84 inhabitants all year round as well as important infrastructure such as the Rhaetian railway lines, roads as well as electricity and gas lines. Lithologies such as brittle dolomites and carbonates have the potential sudden failure and propagate down as rock avalanche (Sturzstrom). However, silent witnesses of moderate to rapid flowlike landslides above Brienz indicate that another process has to be considered. The historic “Igl Rutsch”, which dates from the year 1877, reached velocities of m/ day and stopped right before the village Brienz. The deposits of “Igl Rutsch” are neighbored from deposits from further events such as “Armauns” and “Got da Laresch”. At 15th June 2023, the rock compartments, the so-called “Insel”, slid down as an flowlike landslide after several weeks of acceleration and stopped again right before the village Brienz.

Runout analysis is a key aspect of assessing the hazard potential of the six rock compartments. Therefore, detailed runout modelling is required to determine the reach probability and serve for further risk analyses. Runout modelling of rock avalanches have been routinely done with DAN3D (McDougall & Hungr, 2004) or RAMMS::Debrisflows (SLF). However, modelling slower flowlike landslides using these modelling programmes is inappropriate, as they cannot simulate velocities in the m/day range.

A simple and fast method to predict runout of landslides is the Fahrböschung method. The Fahrböschung of a landslide expresses the quotient of vertical and horizontal distance from the top release to the most distal runout point in the sense of flow. Already Heim 1932 observed a robust, but empirical anti-correlation of volume vs Fahrböschung of alpine landslides. The Fahrböschung for the three given earth flows “Armauns”, “Igl Rutsch” and “Got da Laresch” is decreasing with increase of their volume. These field observations indicate, that the Fahrböschung might serve as a local proxy for runout.

Since the Fahrböschung value of future moderate to rapid flowlike landslide events for the six rock compartments is not known a priori, a probabilistic approach was pursued. For each rock compartment, a Gauss-distribution within the regional limits of observed Fahrböschung values was established and the corresponding likelihoods were combined to a probabilistic map. The probabilistic map for the rock compartment “Insel” reveals very high likelihoods for rather short runout north of the village Brienz and low likelihoods for long runouts towards to the Albula river. Comparisons of the effective runout from the event of June 2023 with the probabilistic map will be shown on the conference. Further, reasons for the observed runout in terms of kinematic and flow behaviour and limits of the used method will be discussed.

REFERENCES

McDougall, S., & Hungr, O. (2004). A model for the analysis of rapid landslide motion across three-dimensional terrain. *Canadian Geotechnical Journal*, *41*(6), Article 6.

Heim, A. (1932) Der Bergsturz und Menschenleben. Fretz und Wasmuth Verlag, Zürich, 218 p.

P 11.5
Quantifying the effects of rainfall temporal variability on landscape evolution processes

Taiqi Lian[1], Nadav Peleg[2], Sara Bonetti[1]

[1] *Laboratory of Catchment Hydrology and Geomorphology, EPFL Valais Wallis, Route des Ronquos 86, CH-1951 Sion, Switzerland (taiqi.lian@epfl.ch)*
[2] *Institute of Earth Surface Dynamics, University of Lausanne, Quartier Centre, CH-1015 Lausanne, Switzerland*

Rainfall characteristics such as its intensity, duration, and frequency are key determinants of the hydro-geomorphological response of a catchment. The presence of non-linear and threshold effects makes the relationship between rainfall variability and geomorphological dynamics difficult to quantify. This is particularly relevant under predicted exacerbated erosion induced by an intensification of hydroclimatic extremes. In this study, we quantify the effects of changes in rainfall temporal variability on catchment morphology and sediment transport across a broad spectrum of grain size distributions and climatic conditions. To this purpose, multiple rainfall realizations are simulated using a rainfall generator, while geomorphic response and soil erosion dynamics are assessed by means of a landscape evolution model (CAESAR-Lisflood). A virtual catchment is used for the numerical experiments and simulations are run over centennial time scales. Preliminary results show that higher rainfall temporal variability increases the net sediment discharge as well as the domain erosion and deposition volume, with dry regions responding more actively to temporal rainfall variations and finer grain size configurations amplifying the observed response. Side channels developed longer and more in deeper in response to higher precipitation temporal variability. Such a quantification of the effects of predicted changes in rainfall patterns on catchment hydro-geomorphic response, as mediated by local soil properties, is crucial to forecast future changes in sediment and soil carbon fluxes.

P 11.6
Bedload transport trends under rapid climate change: Understanding changes in the Turtmann valley at a decadal timescale

Leona Repnik[1], Arnaud Breillad[3], Alessandro Giovanardi[1], Francesco Comiti[2], Mattia Gianini[1], Anne-Laure Argentin[2], Felix Pitscheider[2] and Stuart Lane[1]

[1] *Institute of Earth Surface Dynamics, University of Lausanne, Géopolis, CH-1015 Lausanne (leona.repnik@unil.ch)*
[2] *Fakultät für Agrar-, Umwelt- und Lebensmittelwissenschaften, University of Bolzano, Universitätsplatz 5, IT-39100 Bozen*
[3] *Ecole Nationale Sciences Geographiques (ENSG-Géomatique), 6-8 Av. Blaise Pascal, FR-77420 Champs-sur-Marne*

Climate change is resulting in rapidly increasing temperatures in the European Alps. This increase is faster than the global average. Many of the resulting consequences are well studied, including the retreat of glaciers and melting of permafrost. However, very little is known about the impacts of rising temperatures on bedoad transport (>2mm grain size). This is due to a lack of historical records and of continuous monitoring, explained by the complexity and difficulty in measuring bedload transport.

In this context, the objectives of the research are (1) to reconstruct historical sediment yield using unique records from hydropower stations and (2) to use a landscape analysis of erosion and deposition patterns and subglacial sediment supply to determine the drivers of these changing patterns. The latter involves photogrammetric reconstruction of erosion and deposition patterns from archival imagery, their combination with sediment routing algorithms that take into account sediment connectivity to the basin outlet and estimation of the subglacial sediment contribution from the differences between sediment yield and routed erosion/deposition. These analyses will be conducted for more than 60 river basins across Alpine Switzerland and northern Italy.

In this poster, we present this method for the Turtmann valley (Valais, Switzerland). Using aerial historical photogrammetry, a historical Digital Elevation Model (DEM) of the Turtmann valley was produced for the year 1977. A 2019 DEM was used as a reference to create a DEM of Difference (DoD), highlighting areas of erosion and deposition. A comparison to geomorphological maps allows for an understanding of the geomorphological processes that have taken place to result in these patterns. Routing of erosion and deposition using a mass balance treatment allows us to estimate yield to the basin outlet where we can compare this with records of sediment yield from the hydropower company. These analyses suggest that during a period of rapid climate warming the sediment yield from the system is dominated by subglacial sediment supply and with only relatively small and localized supply from hillslopes. As the glaciers in the system get smaller, we would expect this to switch as we pass through peak sediment.

P 11.7
The northernmost sampled rocks (83.68407° N) and preliminary geological and geomorphological data from recently discovered “islands” located between North Greenland and the North Pole

Denis M. Schlatter[1], Martin Nissen[2]

[1] *Helvetica Exploration Services GmbH, Carl-Spitteler-Strasse 100, CH-8053 Zürich (* denis.schlatter@helvetica-exploration.ch; http://www.helvetica-exploration.ch)*
[2] *Office for Earth Observation, Agency for Data Supply and Infrastructure Ministry of Climate, Energy and Utilities, Rentemestervej 8 2400 Copenhagen NV*

In North Greenland at 83.66249° N, Inuit Qeqertaat (Kaffeklubben Ø) is located in the Arctic Ocean, just north of Cape Morris Jesup (83.644699° N) which is the northernmost point of mainland Greenland and consequently the northernmost point on Earth. In proximity of Kaffeklubben Ø and located even further north, several islands have been reported, however it has been debated since a long time, which of them are real islands, which of them are apparently ephemeral “islands”, and which of them represents the northernmost “real” island on Earth (Bennike & Shea, 2019).

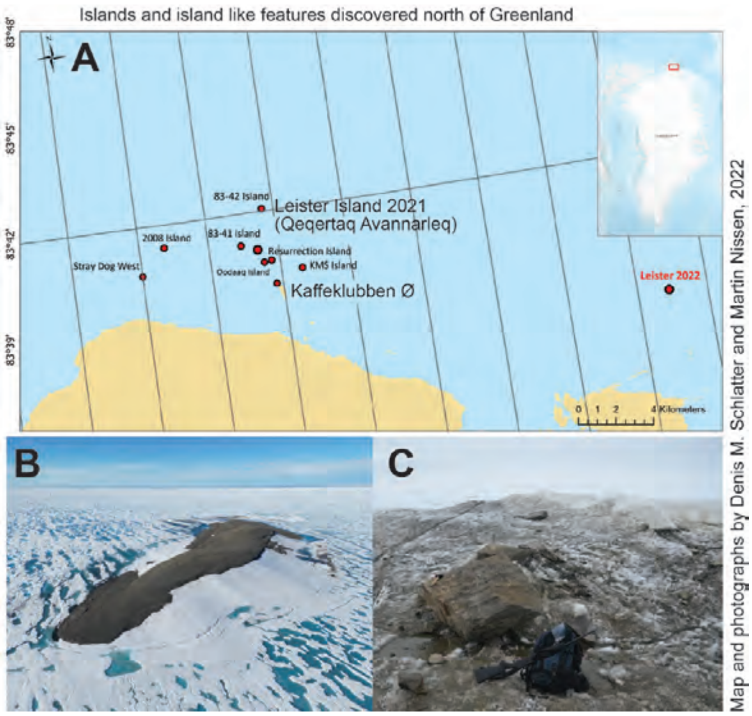

Figure 1. **A**: Map showing the location of Kaffeklubben Ø, Leister Island 2021 and other island-like features discovered in the area. Cape Morris Jesup is located about 40 km to the West of Kaffeklubben Ø and outside the map. The inset map shows the location of these “islands” with respect to Greenland. **B**: Kaffeklubben Ø is considered the northernmost island in the world. **C**: Sample 190893 collected on the Leister Island 2021 is an erratic glacial boulder of a metamorphic rock comprising mica schist and abundant quartz.

In this paper we discuss how to distinguish real islands from short-lived islets and we shed light into the formation of these features and finally we discuss results of the geochemical analyses of rocks that have been sampled from Kaffeklubben Ø (Fig. 1A and 1B) and from a recently discovered “island” informally named Leister Island 2021 (Qeqertaq Avannarleq) which is located just north of Kaffeklubben Ø at latitude 83.684070° N (Fig. 1A and 1C). During 2021 and 2022 extensive research was carried out by the Swiss Danish initiated research expeditions (Leister et al., 2023). During 2021 the “Around North Greenland” expedition resulted in the discovery of the northernmost “island”, whereas in the summer of 2022 the follow-up expedition “Go North” confirmed that this and previously discovered “islands” did not qualify as islands because of their non-permanent feature, and therefore demonstrated that the northernmost island of the world is Kaffeklubben Ø. Field work comprised airborne LIDAR surveys, geodetic measurements of previously reported islets, sea ice measurements, gravimetric measurements and measurement of the depth of the Arctic Ocean with an echosounder. The field work also comprised collecting of five rocks that were analysed for geochemistry. These surveys showed that the Leister 2021 Island and smaller "islands" in vicinity lack a rock basement, and are therefore debris-covered ice island fragments. By contrast, the Kaffeklubben Ø which is also of larger size shows continuity with a rock basement and is therefore classified as an island. The geological survey revealed that the surface of Kaffeklubben Ø is covered by large amount of glacial boulders comprising red andesite porphyry thus supporting a glacial push in west-east direction, likely from the Cape Washington area located about 100 km to the west where the same andesitic rocks occur. The four rocks from glacial boulders sampled from the Leister Island 2021 show a large variety of rock types which supports that these are glacial debris. The surface of the "island" also comprises sandy areas with mud cracks, and some patches of about 10x10 m of glacial moraine material. The erratic blocks have various sizes and are up to 1.2x1x1 m. The sampled rocks comprise boulders of (1) dark-greenish mica schist rich metamorphic rock, (2) blocks with a quartz vein hosted in mica schist with few specs of sulphide and 5 cm thick quartz veinlet in mica schist, (3) mica schist from large erratic blocks, (4) mica schist from large erratic block with abundant quartz. The geochemical analyses also show a large variety with different contents of e.g. Fe and Al. By contrast one rock sampled from Kaffeklubben Ø shows distinct differences in the geochemical contents compared to the four samples from the Leister Island 2021 by having elevated REE (up to 272 ppm Ce, and 124 ppm La) and interestingly also by a slight anomalous gold content of 16 ppb. The five rocks sampled from the extreme north of Greenland are now integrated in the more than 100 years old Greenland rock collection at the Geological Museum in Lausanne, together with many specimens from the "de Quervain expedition" of 1912. This outcome of these two Leister expeditions potentially have territorial consequences, because the Kaffeklubben Ø island was confirmed to be a real island, and consequently defines the northernmost boarder of Greenland and thus the extent of the realm of Denmark.

REFERENCES

Bennike, O. & Shea, J. 2019: Oodaaq Ø and other short-lived islets north of Greenland. Polar Record 55: 14–24

Leister Foundation (ed.) Leister, C., Lassen, H., Breum, M., Nissen, M., Thor, S., Rasch, M., Forsberg, R., Elberling, B., Primé, A., Schneider, T., Schlatter, D.M., Biersma, E., Rixen, C. & Charrière, J. 2023: Leister Expeditions 2021 and 2022, Discoveries and Explorations in North Greenland 268 pages, in print.

P 11.8
Quantifying different erosion mechanisms in the Gürbe catchment using a ^{10}Be tracing method

Chantal Schmidt[1], Fritz Schlunegger[1], Brian McArdell[2], Louis König[3], Marcus Christl[4], Naki Akçar[1]

[1] *Institute of Geology, University of Bern, Baltzerstrasse 1+3, CH-3012 Bern*
[2] *Swiss Federal Research Institute WSL, Zürcherstrasse 111, CH-8903 Birmensdorf*
[3] *Departement of Environmental Systems Science, ETH Zürich, Universitätsstrasse 16, CH8092 Zürich*
[4] *Laboratory of Ion Beam Physics, ETH Zurich, Otto-Stern-Weg 5, 8093 Zurich*

Quantifying the supply of material from different sediment sources in Alpine river catchments has remained a challenging task. Here, we conduct such an analysis for the Gürbe catchment situated at the northern margin of the Swiss Alps. We particularly apply a set of new methods to quantify the different erosion mechanisms and the transfer of sediment from the hillslope to the channel network in the headwaters and finally to the depositional fan at the downstream end of the catchment. The headwaters of the Gürbe catchment cover an area of approximately 12 km^2. The river originates at the foothill of the Gantrisch at an elevation of c. 1850 m above sea level (asl) and flows into the Aare River about 29 km farther downstream at an elevation of 509 m asl. The headwater reach itself is situated above 609 m asl and has a length of around 8 km. There, the sediment production occurs through three main mechanisms: (1) overland flow erosion producing sand and silt and thus suspension loads; (2a) shallow landslides connected to the main channel and (2b) deep-seated landslides, both of which supply a mixture of gravel, boulders, and silt/sand during floods, thus contribute to both the bedload and suspension load of the Gürbe River; and (3) incision of the river into glacial till in the upper part of the headwaters and into landslides. The lithology in the Gürbe catchment consists of Molasse, Flysch and Quaternary deposits, which renders the provenance tracing of the material a difficult task. However, previous research has shown that the cosmogenic ^{10}Be concentration differs for various sediment sources (Clapuyt et al. 2019; Cruz Nunes et al. 2015; Van den Berg et al. 2012). Based on the existing studies, we expect low concentrations of cosmogenic ^{10}Be in sediments produced by deep-seated landslides and incision, and high concentrations by overland flow erosion and shallow landslides. Therefore, we measure the ^{10}Be concentrations in the sand fraction, which we anticipate recording the signal of overland flow erosion and landslides. As a novel approach, we also determine ^{10}Be concentrations in gravels collected from the Gürbe channel as well as from the landslide tongues reaching into the Gürbe. The cascade of sediment from the various sediment sources through the channel network will then be quantified through tracing and sediment budget modelling. In addition, the ^{10}Be tracing and mixing modeling approach will be complemented by (1) turbidity measurements to quantify the transfer of the suspension load; (2) mapping of landslides; (3) detection of the landscape changes using UAV surveys, and (4) further paired-cosmogenic nuclide analysis like $^{10}Be/^{14}C$ ratio in quartz to collect information about transient material storage.

REFERENCES

Clapuyt, F., Vanacker, V., Chrsistl, M., Van Oost, K., & Schlunegger, F. 2019: Spatio-temporal dynamics of sediment transfer in landslide-prone Alpine catchments. Solid Earth, 10(5), 1489-1503.

Cruz Nunes, F., Delunel, R., Schlunegger, F., Akçar, N., & Kubik, P. 2015: Bedrock bedding, landsliding and erosional budgets in the Central European Alps. Terra Nova, 27(5), 370-378.

Van den Berg, F., Schlunegger, F., Akçar, N., & Kubik, P. 2012; 10Be-derived assessment of accelerate erosion in a glacially conditioned inner gorge, Entlebuch, Central Alps of Switzerland. Earth Surface Processes and Landforms, 37(11), 1176-1188.

P 11.9
Evaluating aquatic biodiversity in the Northern Apennines and Ligurian Alps (Italy) with environmental DNA (eDNA)

Gabrielle Vance[1], Dominik Kirschner[2], Sean Willett[1], Loïc Pellissier[2]

[1] *Department of Earth Sciences, ETH Zurich, Sonneggstrasse 5, CH-8092 Zurich (gabrielle.vance@erdw.ethz.ch)*
[2] *Department of Environmental Systems Science, ETH Zurich, Universitätstrasse 16, CH-8092 Zurich*

Mountain building reorganizes drainage networks, which can influence the speciation, evolution, extinction, and dispersal of aquatic species. In northern Italy, aquatic communities exhibit unique compositions, many endemic species, and spatial structure, which may relate to drainage reorganization driven by regional tectonics. Tectonic advection of topography and ensuing topographic asymmetry may lead to river capture, which can separate or connect ecological domains and thus isolate or mix aquatic populations. Here, we use environmental DNA (eDNA) collected from rivers in the Northern Apennines and Ligurian Alps to assess the influence of tectonic advection and subsequent drainage reorganization on aquatic biodiversity. We examine the distribution of native freshwater fish species and investigate the extent to which this data can identify spatial patterns of genetic diversity. Comparing species assemblages and richness shows differences in community composition across the water divide, but not between mountain ranges. We assess intraspecific variation on the Ligurian and Adriatic sides of the main drainage divide and between the older Ligurian Alps and younger Northern Apennines, where we observe a more random distribution in most, but not all species. Populations of primary fish species, such as the cyprinid Telestes muticellus (Italian vairone), which can not disperse through marine waters naturally, show some spatial structuring. This could suggest geological or anthropogenic drivers of its pattern of intraspecific diversity.

P 11.10
Assessing the properties of ground ice and its influence on seasonal surface dynamics of glacitectonized frozen landforms in the Swiss Alps

Julie Wee*, Sebastián Vivero*, Christian Hauck* & Christophe Lambiel**

** Department of Geosciences, University of Fribourg, Switzerland (julie.wee@unifr.ch)*
*** Institute of Earth Surface Dynamics, University of Lausanne, Switzerland*

The high alpine environment is characterized by glacial and periglacial landforms, which express varying degrees of sensitivities to the current warming trend. The morphodynamical response of these landforms to this trend is not uniform in space nor in time as the occurrence of ice in high mountain environments can be found under a wide spectrum of landform settings and assemblages. As geomorphological systems, environments in which glacier-permafrost interactions occurred result from a wide and interconnected spectrum of glacial, periglacial, gravitational and hydrological processes. Such interactions give rise to the co-existence of a diverse range of landforms in close proximity, such as glaciogenic debris, glacier ice masses, including debris-covered ice and buried dead glacier ice, but also thermally-controlled (permafrost-related), creeping debris-masses (rock glaciers, push-moraines) deformed and sometimes partly displaced by the loading of glacial-stress (glaciotectonic). Besides geometrical alteration, these glacitectonized frozen landforms may encompass sporadic embedding and burial of glacier ice (sedimentary ice) into frozen debris.

This contribution aims to understand the spatial and temporal complexity of relations and interactions between glacial and periglacial processes through the assessment of ground ice properties and their influence on surface dynamics measured at alpine sites where glacier-permafrost interactions have occurred or still occur. We base our analysis on long-term time series of ground surface temperature, together with in-situ geodetic and geophysical measurements, as well as archival aerial and recent uncrewed aerial vehicle surveys.

In the debris-covered glacier zones and contact zones, geodetic measurements document surface elevation changes often reaching a few decimetres to some meters per year due to ice melt-induced subsidence. Moreover, geophysical surveys point to isolated remains of buried surface ice embedded on top of deep-reaching permafrost. In contrast, geophysical surveys performed in the periglacial zones indicate ice-rich periglacial condition at depths of 5-7 meters (i.e. in the permafrost layer), causing vertical surface changes in the range of centimetres per year due to thaw-induced subsidence.

In complex contact zones, where both sedimentary and interstitial ice occur simultaneously and where interconnected processes take place, we can most often discriminate glacial from periglacial processes as their spatio-temporal patterns of surface change and geophysical signatures are (mostly) different.

12 Soil: Formation, Processes, and Conservation

Tobias Sprafke, Ophélie Sauzet

Bodenkundliche Gesellschaft der Schweiz (Swiss Soil Science Society)

TALKS:

12.1 Curatola Fernández G.F., Makowski Giannoni S., Delgado Florián E., Rengifo P., Rascón J., Chinchipe Vela E., Butrich C., Salas López R., Oliva-Cruz M., Scheske C.: Mapping peatlands in a jalca ecoregion to inform a community conservation strategy

12.2 Eichenberger, J.: Impact of soil map resolution on SWAT+ modelling, case study of Petite Glâne, Switzerland

12.3 Ingensand J., Lotfian M., Gressin A., Bron M., Gondret K., Matteodo M., Favre-Boivin F., Bullinger G., Raymondon G., Boivin P.: Assessing and managing soil quality with geodata: the IQS project

12.4 Minich L., Moreno Duborgel M., Geissbühler D., Udke A., Perez Rodriguez C., Wacker L., Gautschi P., Egli M., Hagedorn F.: The age and sources of respired CO_2 from soils of dominant land use types across Switzerland

12.5 Rowan.S., Luetscher.M., Szidat.S., Lechleitner.F: Unraveling Karst Critical Zone CO_2 Dynamics: Insights from Milandre Cave Monitoring

12.6 Walder M., Gallarotti N., Torres M.A., Eglinton T.I., Griepentrog M., Geirsdóttir Á., Haghipour N., Harning D., Plötze M.: Pedogenic trajectories of volcanic soils and implications for organic carbon storage: field evidence from Haukadalur (Iceland)

12.7 Wasner D., Xingguo H., Schnecker J., Frossard A., Zagal Venegas E., Doetterl S.: Biogeochemical drivers of soil bacterial community composition along a geoclimatic gradient

POSTERS:

P 12.1 Ceresa E., Velasquez L., Losapio G.: Investigating the Effects of Glacier Retreat on Soil Development and Ecosystem Fluxes

P 12.2 Udke A., Zehnder M., Rixen C., Egli M., Hagedorn F.: Soil organic carbon storage along three alpine elevation gradients from 1700m to 3100m a.s.l.

P 12.3 Moreno Duborgel M., Haghipour N., González-Domíngez B., Eglinton T., Hagedorn F.: How are soil carbon pools influenced by climate and mineralogy? Radiocarbon inventory of Swiss soils

P 12.4 Zou X., Buchmann N., Shekhar A., Singh K.A., Mo Y., Jiang X., Liu W.: Edaphic and meteorological controls over soil moisture dynamics and infiltration patterns in tropical rainforests

P 12.5 Zucha W., Blattmann T., Plötze M.: Influence of Fulvic and Humic Acids on the Undrained Shear Strength of Clayey Soils

P 12.6 Coudene M., Singer E., Bullinger G., Brunner P., Turberg P., Le Bayon R.-C.: Urban soils and ecosystem services in cities: assessing water and heat regulation potential

P 12.7 Grunder A., Bigalke M.: Micro Plastic Pollution: An efficient extraction protocol for MINAGRIS

12.1
Mapping peatlands in a jalca ecoregion to inform a community conservation strategy

Giulia F. Curatola Fernández[1,2], Sandro Makowski Giannoni[2,3], Ellen Delgado Florián[4], Piero Rengifo[2], Jesús Rascón[5], Elder Chinchipe Vela[5], Carolina Butrich[2], Rolando Salas López[5], Manuel Oliva-Cruz[5], and Christel Scheske[2]

[1] *Institute of Geography, University of Bern, Hallerstrasse 12, CH-3012 Bern (giulia.curatola@unibe.ch)*
[2] *Peruvian Society of Environmental Law, Prolongación Arenales 437, 15073 Lima (Peru)*
[3] *Competence Center in Sustainability, University of Lausanne, Vortex, CH-1015 Lausanne*
[4] *Department of Geography, University of Georgia, 210 Field Street, 30602 Athens, Georgia (USA)*
[5] *Instituto de Investigación para el Desarrollo Sustentable de Ceja de Selva, University of Toribio Rodrigo de Mendoza de Amazonas, Calle Universitaria 304, Chachapoyas (Peru)*

The *jalca* ecoregion is a high-Andean zone of northern Peru, where peat is expected to form, but its presence has rarely been recorded. The Gocta waterfall, one of the world›s 20 highest waterfalls, is located in this ecoregion, and its flow depends on the upper jalca›s hydrological function, especially the water regulation function of wetlands and peatlands. In the last decades, the local population has increasingly relied on tourism and is concerned about preserving the jalca area to maintain a year-round water flow. However, to develop a sound conservation strategy for this area, it is vital to generate information about the characteristics of the hydrological system upstream of the waterfall, the land use and its management, and the most common ecosystem types. For this, we applied GIS, remote sensing, and participatory mapping techniques to delineate Gocta›s drainage area, identify land tenure, and map the area covered by peatlands. We used multispectral, radar, and DEM data to classify peatland through a random forest machine learning algorithm. For the training and validation of the classification, soil samples were collected in the field and analysed in the laboratory to discriminate peat soil. The Gocta drainage area covered an area of ~3000 ha, of which ~18% was peatland. We obtained very accurate classification results (overall accuracy of 97.1%), showing that the method applied allowed us to detect peatlands in the jalca successfully. Land tenure was complex, including private, communal, and informal forms. We will present the results› implications in the context of peatland mapping and community-based conservation strategies at the local level and for research in other tropical mountain areas.

12.2
Impact of soil map resolution on SWAT+ modelling, case study of Petite Glâne, Switzerland

Joana Eichenberger

Centre for Development and Environment, University of Bern, Switzerland

When local or regional soil data are lacking, modelers using the Soil and Water Assessment Tool (SWAT) must rely on freely available but very coarse soil maps, such as the Digital Soil Map of the World (DSMW). Up to now, the significance of soil map resolution in SWAT modeling has been relatively neglected compared to the attention given to DEM resolution. The few studies conducted on the matter have demonstrated that the key impact of soil map resolution is the number and size of the Hydrologic Response Unit (HRU), ultimately affecting the results. However, as for the impact of the resolution on the model›s performance, opinions are divided as to whether the coarser or the finer resolution performs better.

This paper explores impact of soil map resolution on SWAT+ (a completely revised version of the SWAT model) modelling with the Contiguous object Connectivity Approach (COCOA) model se up. SWAT+ COCOA was developed within the Horizon2020 OPTAIN project and contrary to former SWAT/SWAT+ model setups, HRUs are not attributed internally by overlaying the input soil map and land use map but defined solely by the land use map. With this approach, each land use object is attributed with the dominant soil based on the soil input data, consequently, the influence of soil maps can be more thoroughly assessed.

Based on the Horizon2020 OPTAIN case study in Switzerland, the Petite Glâne watershed (100 km2), the SWAT+ COCOA model is used with three different soil maps: the DSMW with a resolution of 1:5’000’000, a soil map based on the Swiss Soil Suitability Map with a resolution of 1:200›000, and a high-resolution soil map based on local soil profile data (1m resolution). The assessment of the simulated flows with the three different soil maps is done by comparing them with measured runoff and water quality values before and after calibration.

12.3
Assessing and managing soil quality with geodata: the IQS project

Jens Ingensand[1], Maryam Lotfian[1], Adrien Gressin[1], Maximin Bron[1], Karine Gondret[2], Magali Matteodo[3], Fabienne Favre-Boivin[3], Géraldine Bullinger[3], Guillaume Raymondon[4], Pascal Boivin[2]

[1] Institut INSIT, University of Applied Sciences Western Switzerland (HEIG-VD), Route de Cheseaux 1, 1401 Yverdon-les-Bains (jens.ingensand@heig-vd.ch)
[2] Institut inTNE, University of Applied Sciences Western Switzerland (HEPIA), Route de Presinge 150, 1254 Jussy
[3] Institut iTEC, University of Applied Sciences Western Switzerland (heia-fr), Boulevard de Pérolles 80 1700 Fribourg
[4] Région Morges, Rue Dr. Yersin 1, 1110 Morges

Soil undergoes very long processes of formation. In Switzerland, large areas have been permanently sealed over the last 30 years. Despite the tightening of the Swiss Spatial Planning Act in 2014, high-quality soil continues to be destroyed. Soil is a non-renewable natural resource that fulfils a number of functions, such as biomass production, habitat for biodiversity and flood regulation. (Evans et al, 2021)

Switzerland does not have a complete soil map, and above all, soil quality addresses dynamic properties over time, which are therefore not easily put on maps. Soil quality is mainly determined by land use, and there is an urgent need to provide decision-makers with tools for visualising and managing land use from a soil quality perspective (Montanarella et al, 2016)

We have therefore created a method that estimates the quality of soil for different soil functions by taking into account several criteria such as its cover and its use. More specifically in a pilot project called IQS Morges, an estimate of soil quality was established on the basis of several existing reference datasets, such as orthoimages, digital terrain models, georeferenced soil data (soil maps) and spatial planning layers. Maps for the Morgian region showing both soil quality and estimation reliability were created. (See Figure 1)

Two complementary tools were developed on the basis of open-source software to adjust the estimated score and to simulate the impact of new development projects on soil quality. A semi-automatic process was implemented to model the input parameters, but also to render the results as maps.

At several workshops, the results of the project were communicated to the communes of the Morgian region and to soil experts. The maps and tools developed represent an added value for experts and decision-makers, for example in the context of new developments. The method and tools developed are designed to be used not only in the Morgian region, but throughout Switzerland.

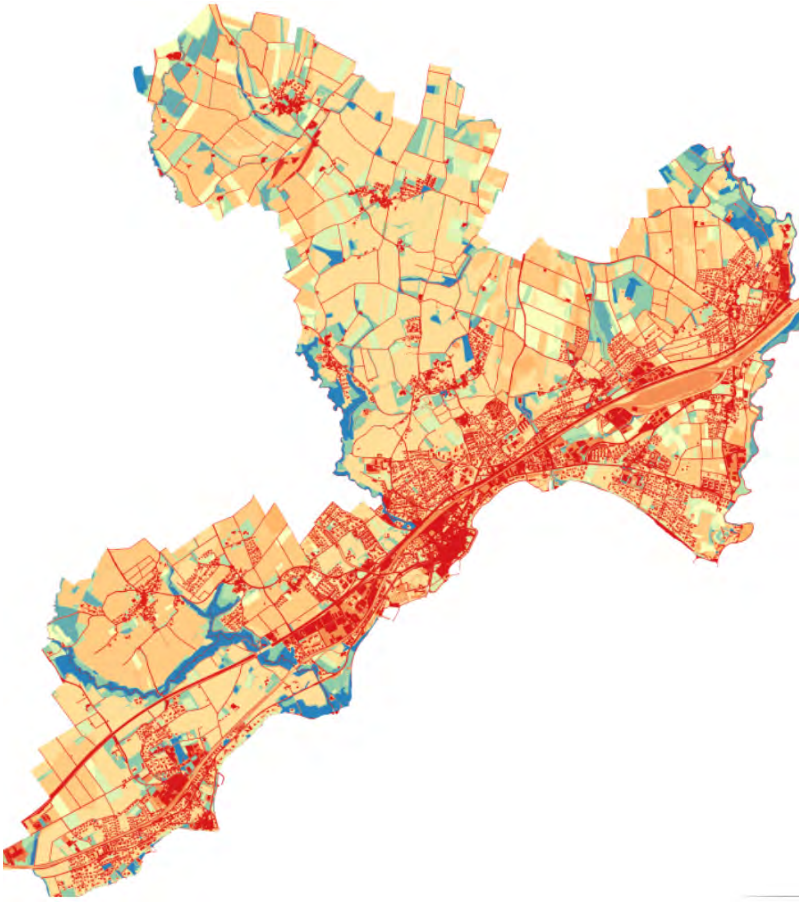

Figure 1.Generated map of the Morgian region that shows the estimated quality of the soil.

REFERENCES

Evans, D.L., Janes-Bassett, V., Borrelli, P., Chenu, C., Ferreira, C.S.S., Griffiths, R.I., Kalantari, Z., Keesstra, S., Lal, R., Panagos, P., Robinson, D.A., Seifollahi-Aghmiuni, S., Smith, P., Steenhuis, T.S., Thomas, A., Visser, S.M., 2021. Sustainable futures over the next decade are rooted in soil science. Eur J Soil Sci ejss.13145. https://doi.org/10.1111/ejss.13145

Federal Act on Spatial Planning (accessed 14.8.2023) https://www.fedlex.admin.ch/eli/cc/1979/1573_1573_1573/en

Montanarella, L., Pennock, D.J., McKenzie, N., Badraoui, M., Chude, V., Baptista, I., Mamo, T., Yemefack, M., Singh Aulakh, M., Yagi, K., Young Hong, S., Vijarnsorn, P., Zhang, G.-L., Arrouays, D., Black, H., Krasilnikov, P., Sobocká, J., Alegre, J., Henriquez, C.R., de Lourdes Mendonça-Santos, M., Taboada, M., Espinosa-Victoria, D., AlShankiti, A., AlaviPanah, S.K., Elsheikh, E.A.E.M., Hempel, J., Camps Arbestain, M., Nachtergaele, F., Vargas, R., 2016. World’s soils are under threat. SOIL 2, 79–82. https://doi.org/10.5194/soil-2-79-2016

12.4 The age and sources of respired CO_2 from soils of dominant land use types across Switzerland

Luisa Minich[1,2], Margaux Moreno Duborgel[1,2], Dylan Geissbühler[1,3], Annegret Udke[1,4], Ciriaco Perez Rodriguez[4], Lukas Wacker[5], Philip Gautschi[5], Markus Egli[4], Frank Hagedorn[1]

[1] Swiss Federal Institute for Forest, Snow and Landscape Research (WSL), Switzerland
[2] Biogeoscience, Department of Earth Sciences, ETH Zurich, Switzerland
[3] Laboratory for the Analysis of Radiocarbon with AMS, Department of Chemistry, Biochemistry and Pharmaceutical Sciences, University of Bern, Switzerland
[4] Geochronology, Department of Geography, University of Zurich
[5] Laboratory for Ion Beam Physics, Department of Physics, ETH Zurich, Switzerland

Land use regulates soil CO_2 fluxes through various factors such as vegetation type, root density, nutrient input, and management. Isotopic techniques using radiocarbon (^{14}C) or stable carbon (^{13}C) represent a powerful approach to identify the sources soil CO_2 fluxes. However up to now there has not been a systematic comparison of the age and sources of the soil CO_2 efflux between different land use types. In this study, we aim to investigate how land use across Switzerland affects the age and sources of soil-respired CO_2 by using radiocarbon and stable isotopic appraoches.

We measured *in situ* rates and isotopic signatures (^{14}C, ^{13}C) of soil-respired CO_2 from 18 sites of six dominant land use types in Switzerland: forests, croplands, managed peatlands (original and deposition), and grasslands (low-land and alpine). We further disentangled source contribution (autotrophic vs. heterotrophic respiration) to total soil respiration for each site by separating ^{14}C, and ^{13}C signatures of CO_2 derived from root and soil incubations.

We expect that the age of soil-respired CO_2 decreases from managed peatlands to crop- and grasslands due to a decrease in the mean age of soil organic matter. Similarly, we hypothesize that soil-respired CO_2 is younger in grasslands than in forests because of an increasing rhizosphere respiration along this trajectory. We further hypothesize that the contribution of autotrophic respiration increases from peatlands and croplands towards forests and grasslands due to an increase in fine root biomass. More specifically, we expect that original peatlands release “older” carbon than peatlands covered with mineral soil (deposition), and that alpine grasslands release “older” carbon than low-land grasslands because of slower turnover in alpine climates. First results show, that CO_2 fluxes decrease from grasslands to forests and from peatlands to croplands. More specificly, fluxes decrease from low-land to alpine grasslands and from original peatlands to peatlands with deposition. We are currently conducting an in-depth data analysis and will present the results at the conference.

12.5
Unraveling Karst Critical Zone CO_2 Dynamics: Insights from Milandre Cave Monitoring

Sarah Rowan[1], Marc Luetscher[2], Sönke Szidat[1], Franziska Lechleitner[1]

[1] *Oeschger Centre for Climate Change Research, Department of Chemistry, Biochemistry, and Pharmaceutical Sciences, University of Bern, Freiestrasse 3, 3012 Bern, Switzerland (sarah.rowan@unibe.ch)*
[2] *Swiss Institute for Speleology and Karst Studies. Rue de la Serre 68, 2300 La Chaux-de-Fonds, Switzerland.*

As almost all terrestrial life is sustained from the resources found in the critical zone, a sound understanding of how carbon cycles in these environments is crucial for predicting how these interactions will evolve in under future climate scenarios. The global unsaturated zone may host between 2 – 53 PgC of CO_2 globally (Baldini et al., 2018), a revervoir which is vulnerable to flux into the atmosphere via various mechanisms such as changes in water table height. We present results from a CO_2 monitoring campaign at Milandre cave, where concentration, ^{14}C and $\delta^{13}C$ of CO_2 were analysed along vertical cross sections with different land covers. Samples were taken of the external atmosphere, bore-hole wells tapping into soil and epikarst, and from the cave atmosphere. Differences are seen comparing the boreholes of different land coverage, with meadow wells showing a larger seasonal amplitude than forest wells. Similarly, CO_2 from the soil zone is clearly influenced by the seasonal cycle, in contrast to CO_2 from the deeper epikarst zone, which shows very high concentrations (up to 3.7%). The CO_2 concentration within the cave is strongly influenced by the seasonally enhanced ventilation regime, a product of temperature difference between the cave atmosphere and the outside atmosphere. The isotopic variation of cave CO_2 is also influenced by ventilation, with samples lying along a $\delta^{13}CO_2$ Keeling plot mixing line. The average Keeling plot intercept lies at -26‰, suggesting a dominant contribution of carbon in cave air from biological respiration and a minimal contribution of CO_2 degassing from dripwaters entering the cave. Interestingly, the cave $^{14}CO_2$ from samples not strongly influenced by atmospheric inflow are markedly more aged, typically attributed to the effects of degassing. However, due to the depleted $\delta^{13}CO_2$ a sole explanation due to degassing is unlikely and a further source, aged biological material, must be considered. These results have implications for the understanding of the critical zone carbon cycle, the export of carbon from the soil zone towards deeper reservoirs, and the interplay between ecosystem respiration and weathering intensity at the catchment scale.

REFERENCES

Baldini, J., Bertram R., & Ridley H. 2018: Groun air: A first approximation of the Earth's second largest reservoir of carbon dioxide gas, Science of the Total Environment, 616-617, 1007-1013.

12.6
Pedogenic trajectories of volcanic soils and implications for organic carbon storage: field evidence from Haukadalur (Iceland)

Matthias Walder[1], Nora Gallaroti[1], Mark A. Torres[2], Timothy I. Eglinton[1], Marco Griepentrog[3], Áslaug Geirsdóttir[4], Negar Haghipour[1], David Harning[5], Michael Plötze[6]

[1] *Geological Institute, ETH Zurich, Sonneggstrasse 5, 8092 Zurich (mwalder@student.ethz.ch)*
[2] *Department of Earth, Environmental, & Planetary Sciences, Rice University, 6100 Main Street MS-126, Houston, TX 77005*
[3] *Institute of Terrestrial Ecosystems, ETH Zurich, Universistätsstrasse 16, 8092 Zurich*
[4] *Faculty of Earth Science, University of Iceland, Sæmundargata 2, 102 Reykjavík*
[5] *David Harning, Institute of Arctic and Alpine Research, University of Colorado Boulder, 4001 Discovery Drive, Boulder, CO 80303*
[6] *Institute for Geotechnical Engineering, ETH Zurich, Stefano-Franscini-Platz 5, 8093 Zurich*

The spatial abundance and distribution of soil organic carbon is inherently linked to physiochemical properties of the ambient mineralogy. External stimuli can have a determining influence on chemical equilibria that govern mineral dissolution and precipitation, causing soil formation to proceed along a certain pedogenic trajectory. Lateral channel migration interrupts pedogenic episodes and entrains soil organic carbon in streamflow which, over several deposition and mobilization cycles, gets either oxidized and emitted to the atmosphere or stored in a downstream sink. The petrogenic carbon devoid Haukadalsá catchment in west Iceland is an ideal site to unbiassedly study transport and storage mechanisms by means of radiocarbon dating. Understanding pathways and distributions of organic carbon within soil profiles requires a closer examination of mineral-carbon interactions. Here we assess the spatially varying balance between degradation and stabilization of organic carbon by juxtaposing properties of terrestrial lipid biomarkers, iron/aluminum oxide concentrations and sedimentological parameters. Metal-humus complexes were found to preferentially form in an environment enriched in plant derived n-alkanes and characterized by less decayed, younger organic matter. In horizons where poorly crystalline mineral phases were more dominant, organic material tended to have undergone more biodegradation. Soil pH governs the predominance of one type of metal-humus association over another. Tephra deposition and precipitation are external forces that have opposing effects on pH evolution. Climatic shifts (changed rainfall intensity, wind patterns) might thus change current pedogenic trajectories, affecting carbon storage capacity and export fluxes.

REFERENCES

Arnalds, Ó. 2004: Volcanic soils in of Iceland, Catena, 56 (1-3), 3–20.
Buurman, P., Peterse, F, & Almendros M. G. 2007: Soil organic matter chemistry in allophanic soils: A pyrolysis-GC/MS study of a Costa Rican andosol catena. European Journal of Soil Science, 58 (6), 1330–1347.
Chadwick, O. A., & Chorover, J: 2001. The chemistry of pedogenic thresholds. Geoderma,100 (3-4), 321–353
Garrido, E., & Matus, F: (2012). Are organo-mineral complexes and allophane content determinant factors for the carbon level in chilean volcanic soils? Catena, 92, 106-112.
Geirsdóttir, Á., Miller, G. H., Thordarson, T., & Ólafsdóttir, K. B: 2009. A 2000 year record of climate variations reconstructed from Haukadalsvatn, West Iceland. Journal of Paleolimnology, 41 (1), 95–115.
Parfitt, R., & Childs, C: 1988. Estimation of forms of Fe and Al: A review, and analysis of contrasting soils by dissolution and Mossbauer methods. Soil research, 26 (1), 121–144
Shoji, S., Dahlgren, R., & Nanzyo, M: 1993. Genesis of volcanic ash soils. In: developments in soil science. Elsevier, 21, 101-143.
Shoji, S., & Fujiwara, Y: 1984. Active aluminum and iron in the humus horizons of andosols from northeastern Japan: Their forms, properties, and significance in clay weathering. Soil science, 137 (4), 216–226.
Torres, M. A., Kemeny, P. C., Lamb, M. P., Cole, T. L., & Fischer, W. W: 2020. Long-term storage and age-biased export of fluvial organic carbon: Field evidence from west Iceland. Geochemistry, Geophysics, Geosystems, 21 (4).

12.7 Biogeochemical drivers of soil bacterial community composition along a geoclimatic gradient

Daniel Wasner[1], Han Xingguo[2], Joerg Schnecker[3], Aline Frossard[2], Erick Zagal Venegas[4], Sebastian Doetterl[1]

[1] *Soil Resources, Department of Environmental Systems Science, ETH Zurich, Zurich, Switzerland (daniel.wasner@usys.ethz.ch)*
[2] *Forest Soil and Biogeochemistry, Swiss Federal Research Institute WSL, Birmensdorf, Switzerland*
[3] *Centre for Microbiology and Environmental Systems Science, University of Vienna, Vienna, Austria*
[4] *Department of Soil and Natural Resources, Faculty of Agronomy, University of Concepción, Concepción, Chile*

Soil bacteria are numerous and fulfil a plethora of crucial ecosystem functions. It is therefore a central question of soil biogeochemistry what determines soil bacterial community composition. One tool to study the distribution of soil bacteria across space are correlational studies along biogeochemical gradients. However, insights from large-scale correlative studies on community composition often come with two major limitations. First, most such studies only investigate (compositional) relative abundance data. Relative abundance data reflects the dominance of taxa, but it does not necessarily allow for insights on taxa-inherent traits. Second, most correlational studies are conducted with low taxonomic resolution (i.e. at the level of phyla, or classes at most). However, recent experimental research has suggested that functional coherence is only found at lower taxonomic levels. A third unknown at the large scale is the potential role of organic matter (OM) quality as a driver of soil bacterial community composition. While ecological theory suggests niche partitioning along the continuum of OM chemical composition, it remains untested whether this actually shapes community composition across large scales.

Here we sampled a set of 35 grassland topsoils (0 – 10 cm) along a 2300 km north-south transect in Chile ranging from arid steppe to tundra climate, thereby covering 6 USDA major soil groups with a wide range of OM quantity (0.6 – 18.7 % soil organic carbon) and quality. To obtain relative read abundances of soil bacteria across the gradient, we conducted Illumina barcoding of a region of the 16S rRNA gene. We further performed qPCR of the same primer region to obtain estimates of absolute gene abundances. In addition, we developed a new approach to investigate bacterial community composition at low taxonomic levels without having to discard abundance data of rare taxonomic groups. In order to investigate links between relative and absolute bacterial abundance patterns and biogeochemical variables, we measured relevant physico-chemical properties of the soils, compiled climatic data of the sites and characterized OM quality in depth. For this OM characterization, we employed RockEval Pyrolysis, isotopic measurements, diffuse reflectance infrared spectroscopy as well as UV-Vis spectroscopy. We used ordination methods to remove auto-correlation from the biogeochemical variables, and performed conservative correlation analyses.

We could explain 12-59% of relative abundances with biogeochemical variables. We were able to explain community composition of bacteria best in soils with high OM quantity (> 7 %) and low pH (< 5.5). Relative abundances of taxonomic groups were better predictable than absolute abundances, meaning that the dominance of individual taxa is more an emergent property of the community than based on taxa-specific inherent traits. This finding underscores that relative abundance data can not be used to infer preferences of individual taxa, as is often done inaccurately in literature. Further, we found clusters of functional coherence up to the taxonomic level of orders, but not at higher levels. Finally, consistent with previous studies, we found that pH was the most important single predictor of community composition. OM quality – as characterized in this study – did not constitute a quantitatively important driver of soil bacterial community composition across large scales. Instead, OM quantity explained a larger part of soil bacterial communities than the various aspects of OM quality.

P 12.1
Investigating the Effects of Glacier Retreat on Soil Development and Ecosystem Fluxes

Erica Ceresa[1,2], Laura Velasquez[1,2], Gianalberto Losapio[1,2]

[1] *Institute of Earth Surface Dynamics, University of Lausanne, UNIL-Mouline, CH-1022 Lausanne*
[2] *Department of Bioscience, University of Milan, via Celoria 26, IT-20133 Milan*

Driven by global warming, glaciers are retreating worldwide, significantly impacting high-altitude and polar ecosystems. Areas in front of retreating glaciers are rapidly colonized by microbes and vegetation in a process of primary succession which results in development of soil and accumulation of organic matter. When vegetation cover and plant productivity increases, more organic carbon is transferred to the soil, thus the older the soil the greater the content of organic matter. The soil with its properties tied to its developmental stage has a major role in the carbon accumulation process with its increasing potential for carbon release as the organic matter storage increases. Yet, the links among plant diversity, soil respiration and glacier retreat remain unclear.
This study examines glacier foreland ecosystem development, focusing on the accumulation of carbon resulting from vegetation colonization and soil respiration. The aim of this research is to better understand net ecosystem exchange (NEE) between atmosphere, biosphere, and soil, analyzing soil development, carbon emission and carbon uptake along the primary succession to elucidate potential correlations between ecosystem development and these pivotal factors.

P 12.2
Soil organic carbon storage along three alpine elevation gradients from 1700m to 3100m a.s.l.

Annegret Udke[1], Michael Zehnder[2], Christian Rixen[2], Markus Egli[3], Frank Hagedorn[1]

[1] Swiss Federal Institute for Forest, Snow and Landscape WSL, Zürcherstrasse 111, CH-8903 Birmensdorf, Switzerland
[2] WSL Institute for Snow and Avalance Research SLF, Flüelastrasse 11, CH-7260 Davos Dorf, Switzerland
[3] University of Zurich, Department of Geography, Geochronology, Winterthurerstrasse 190, CH-8057 Zurich, Switzerland

Soils in cold regions present the greatest soil organic carbon (SOC) reservoir globally. At the same time, cold regions experience stronger climate warming than any other regions of the world, triggering a cascade of changes that eventually will alter the carbon cycling in these systems. Two counteracting processes are of particular interest: i) the migration of plants into previously inaccessible regions, potentially increasing the carbon uptake and input into soils, and ii) warming induced increase of decomposition, releasing carbon into the atmosphere. Soils that accumulated large amounts of carbon under more favourable climatic conditions in the past could present a potentially high carbon source. Whereas previous studies mainly focused on the circum-Arctic region, where a substantial amount of (labile) SOC is stored in permafrost, mountain permafrost and soils in temperate climates remain little investigated.

Here, we assessed alpine SOC storage, soil organic matter (SOM) characteristics, and their potential response to a warmer climate by sampling three elevation gradients of alpine soils on calcareous, gneissic and amphibolitic bedrock from 1700 to 3100m a.s.l. near Davos, Grisons. The transects ranged from sub-alpine forests over grasslands to high elevation blockfields and encompassed 29 soil pits down to the bedrock. We measured SOC stocks, the isotopic signature of C and N in the soils, above- and belowground vegetation as well as *in situ* and laboratory soil respiration.

Across all elevation gradients, SOC stocks decrease with elevation, with a strong decline above 2700m a.s.l. paralleling the pronounced reduction in vegetation cover/biomass. At the same time, there was an increase in $\delta^{13}C$ values and a decline in CN values with increasing elevation, which suggests two main changes in SOC cycling along the gradients: i) SOC is more transformed at higher elevation and thus ii) the net input of fresh SOC increases towards lower elevation. Therefore, we expect older SOC ages at higher elevation, which still needs to be confirmed by bulk ^{14}C dates (awaiting results). In the high-alpine region of the amphibolitic transect above 3100m a.s.l., SOC was buried beneath an up to 1m stone cover. Although vegetation free, soils stored substantial amounts of SOC (0.8% OC, >1.4 kgC/m^2) which we attribute to periglacial processes burying soils that developed during past warmer periods. Colder conditions (possibly permafrost occurring at least for the last millennium) preserved SOC from decomposition. The buried OM had high $\delta^{13}C$ values of -23.2‰ and narrow CN ratios of 10.7. Despite its high transformation state and probably old age, these buried soils represent a CO_2 source during the snow-free period, releasing approximately 2.8 mg CO_2-C/m^{2}h. However, this is little soil respiration compared to lower elevation, i.e. around 75 mg CO_2-C/m^{2}h at 2350m a.s.l.

Stocks and characteristics of SOC strongly differed between the gradients on calcareous and siliceous bedrock. Calcareous soils showed a shallower SOC depth profile than the two silicious gradients, which likely results from faster turnover due to higher pH and lower reactivity of SOC-binding minerals. Also, CN values were narrower at lower elevation compared to the soils on siliceous bedrock, which indicates that SOC is more transformed as on siliceous bedrock suggesting a smaller stabilization of microbial metabolites by their interaction with mineral surfaces.

Overall, these first results suggest that the importance of buried (possibly old) carbon increases with higher elevation, while alpine sites (<2800 m) are dominated by cycling of fresh C from current vegetation. Future analysis of weathering indices, SOC characterisation, and ^{14}C ages will provide further insight into stabilisation processes of alpine SOM

P 12.3
How are soil carbon pools influenced by climate and mineralogy? Radiocarbon inventory of Swiss soils

Margaux Moreno Duborgel [1,2], Negar Haghipour[3], Sia Gosheva[1,5], Beatriz González-Domíngez[4], Timothy Ian Eglinton[2], Frank Hagedorn[1]

[1] *Swiss Federal Institute for Forest, Snow and Landscape Research (WSL), Zürcherstrasse 111, 8903 Birmensdorf, Switzerland (margaux.duborgel@wsl.ch)*
[2] *Department of Earth Sciences, ETH Zurich, Sonneggstrasse 5, 8092 Zurich, Switzerland*
[3] *Laboratory for Ion Beam Physics, Department of Physics, ETH Zurich, 8093 Zurich, Switzerland*
[4] *Department of Geography, Soil Science and Biogeochemistry Unit, University of Zurich, Winterthurerstrasse 190, 8057, Zurich, Switzerland*
[5] *Department of evolutionary Biology and environmental Studies, University of Zurich, Winterthurerstrasse 190, 8057, Zurich, Switzerland*

One key role of soils is carbon storage. Soils are the largest reservoir of organic carbon in terrestrial ecosystems. Despite numerous studies, the vulnerability of carbon pools is not yet fully understood. Especially in the context of global warming, the fate of soil carbon stocks and its feedback with climate change is unknown. In addition, the factors influencing the turnover of soil organic matter are difficult to disentangle.

The aim of our study was to identify the relative influence of climate and mineralogy on soil organic matter (SOM) turnover on a regional scale. We analysed C pools and ^{14}C contents in the organic layer, mineral soil (0-20cm) and its fractions from 56 sites across Switzerland, spanning along pronounced natural climatic and geological gradients. We fractionated the mineral soil (0-20 cm depth) into particulate organic matter (POM) and mineral-associated organic matter (MOM) according to density. In addition, the mineral-associated organic matter was oxidised with hydrogen peroxide to remove its labile fraction of carbon and retaining the residual ‘stable’ fraction. The stability of different soil C pools was assessed by looking at stable isotopes of C and N. Our ^{14}C dataset was analysed together with ancillary data comprising soil properties and climatic variables from the studied sites. A principle component analysis (PCA) was carried out to evaluate the influence of soil properties and climate conditions on the SOC stocks and on their ^{14}C signature. We hypothesised that POM would be climate sensitive whereas MOM would be influenced by soil chemical and physical properties.

Our results show that MOM, and especially its residual fraction, are enriched in $\delta^{13}C$ and $\delta^{15}N$ compared to the POM and the organic layer. This indicates that MOM and its residual fraction are composed of microbially-derived SOM that has been further processed than POM. In agreement, our ^{14}C data shows that the residual fraction of MOM is the oldest and most stable fraction and that MOM is a mixture of compounds that turn over on decadal time scale and very old carbon resisting the oxidation treatment. The results of our principle component analysis reveal no clear driver of SOC stabilisation. There seem to be only a small influence of temperature and precipitation on POM. The ^{14}C ages in MOM and its residual fraction increased towards low and very high pH values. This non-linear pattern suggests that SOM stabilization is driven by the interaction with minerals. While low pH values potentially promote SOM interactions with pedogenic oxides, high pH values foster the stabilization by calcium carbonate.

P 12.4
Edaphic and meteorological controls over soil moisture dynamics and infiltration patterns in tropical rainforests

Xin Zou[1, 2 3], Nina Buchmann[3], Ankit Shekhar[3] , Ashutosh Kumar Singh[1], Yuxuan Mo[1], Xiaojin Jiang[1], Wenjie Liu[1], *

[1] CAS Key Laboratory of Tropical Forest Ecology, Xishuangbanna Tropical Botanical Garden, Chinese Academy of Sciences, Menglun, Yunnan 666303, China.
[2] University of Chinese Academy of Sciences, Beijing 100049, China
[3] ETH Zurich, Department of Environmental Systems Science, 8092, Zurich, Switzerland

Tropical rainforests play a crucial role in regulating regional hydrological cycles and preserving numerous ecosystem services. However, our knowledge of soil hydrological functions in this biodiversity-rich ecosystem is limited. To address this gap, we conducted experiments in mountainous rainforests at various (flat 0°, moderate 10° and steep 30°) slopes. We aimed to analyze the spatiotemporal dynamics of soil moisture and uncover their infiltration patterns, while considering the effects of meteorological and edaphic factors. The results showed that soil moisture was significantly influenced by meteorological features (i.e., precipitation and air temperature) and slope gradients (Figure 1). Within the soils, soil physical properties (e.g., capillary holding capacity, bulk density, and sand content) were the major controls of soil moisture during the dry period, soil organic matters, fine root biomass and soil physical properties jointly controlled soil moisture during the transition and wet periods. Soil water flow (lateral, preferential and uniform flows) fractions varied greatly with precipitation levels and slopes, indicating the complex interplay between precipitation, slope, and edaphic factors in shaping the infiltration patterns (Figure 2). In comparison to the flat (SF) and steep-slope (SS) sites, the moderate-slope (SM) site demonstrated higher and rather stable levels of soil moisture, along with more balanced infiltration patterns in response to the changes in precipitation. These results appeared due to the favorable soil environment at the SM site, characterized by improved physical structure, and a higher abundance of organic matter and fine roots. Thus, our findings have important implications for the establishment of faster green capping on mountainous terrain, suggesting that moderate-slope sites the best location for restoration as it has a greater capability in storing sufficient soil water, and better drainage and groundwater recharge system.

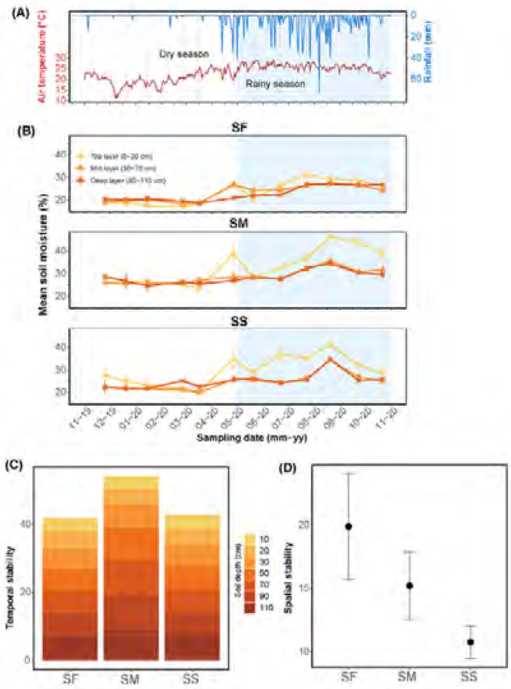

Figure 1. Daily mean air temperature and summed up precipitation (A), and monthly measured soil moisture from soil depths of 0-110 cm aggregated into three different depths – top layer, mid layer and deep layer at three study sites (B) from November 2019 to October 2020. Temporal stability of different soil layers (C) and spatial stability (D) of soil moisture across three sites. The stability is represented by coefficient of variation of soil moisture across time (temporal stability of 12 months) and across depth (spatial stability of 7 depths). The errorbars in (B) and (D) indicate the standard deviation. The white background shows the dry season and the blue background shows the rainy season. SF: flat site; SM: moderate-slope site; SS: steep-slope site.

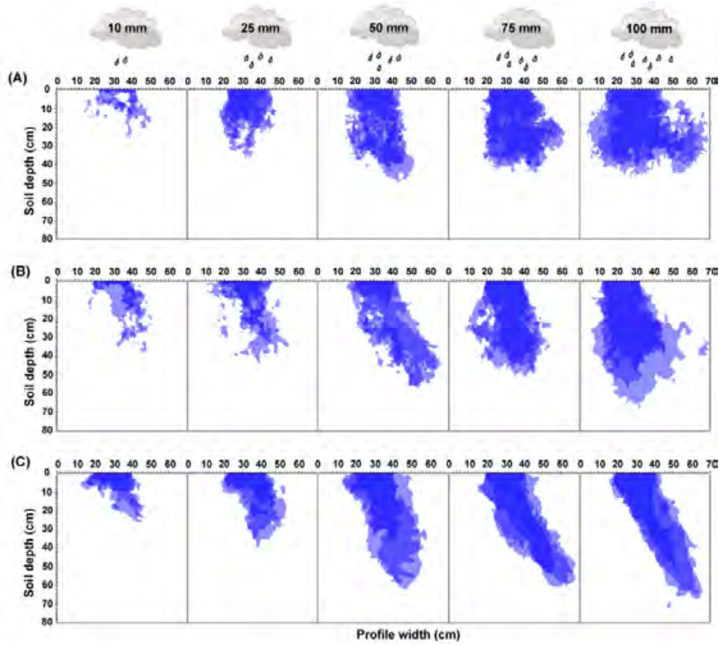

Figure 2. Infiltartion patterns visualized by dye-tracer under five simulated precipitation levels at flat (A), moderate-slope (B) and steep-slope (C) sites. Blue zone: dye-stained, white zone: non-stained. The photographs were taken 24 hours after the infiltration event, and the size of the soil profiles excavated for photographing is indicated by the profile width and soil depth.

P 12.5
Influence of Fulvic and Humic Acids on the Undrained Shear Strength of Clayey Soils

Wolfgang Jan Zucha[1], Thomas Blattmann[2], Michael Plötze[1]

[1] ClayLab, Institute for Geotechnical Engineering, ETHZ, Laura-Hezner-Weg 7, CH-8093 Zurich (wolfgang.zucha@igt.bauge.ethz.ch)
[2] Geological Institute, ETH Zurich, Sonneggstrasse 5, 8092 Zurich

In engineering, soil organic matter is considered detrimental for engineering properties. This is especially relevant in the case of clayey soils, as this challenging material shows unpredictable soil mechanical behavior. Although this issue has received little attention in the scientific community, recent studies showed that organic material alters indeed the soil mechanical properties (e.g. Varghese et al., 2021; Zeng et al., 2017). However, results are contradictory and difficult to interpret, because they focus purely on physical parameters, and they lack sample characterization of clay and organic used. In this study, the influence of organic matter on the shear strength of different clays was investigated. For the mixtures, commercial humic- (HA) and fulvic acid (FA) were mixed with the four different clays kaolinite, illite, Ca-, and Na-bentonite. HA and FA were chosen because they are the two most prominent proxies for soil organic matter and have been used for over two centuries. Results of the vane shear tests on organic-clay mixtures showed that the outcome strongly depends on the clay used. Overall, HA increases shear strength of Ca-bentonite and illite, while it decreases the shear strength of kaolinite and Na-bentonite. The addition of FA decreases the shear strength of all clay samples but to a different extent. This intuitively implies that the results depend very much on direct interaction between organic used and clay mineral type. However, further physicochemical investigations revealed that the influence of organic matter on the shear strength of clayey soils was not always a result of a direct reaction between organic and clay. More often, it is a secondary interaction which involves i.e. impurities (soluble cations) in the organic used or accessory mineral phase in the clay used. Such secondary interactions are often a result of an altered soil pH due to the mixing of clay and organic. This shows further that seemingly less important properties of clay or organic matter may be key parameters for the mechanical behavior of organic-rich clayey soils. But it also shows that even simplified organic-clayey soils are by no means a binary system. Future research should carefully assess its samples and consider a paradigm shift away from HA/FA towards more natural organic matter (Lehmann and Kleber, 2015).

REFERENCES

Varghese, R., Chandrakaran, S., & Rangaswamy, K. (2021). Influence of type of organic substances on the strength and consolidation behaviour of inorganic clay soil. *International Journal of Geotechnical Engineering*, *15*(9), 1165–1176. https://doi.org/10.1080/19386362.2019.1591739

Zeng, L. L., Hong, Z. S., & Gao, Y. F. (2017). One-dimensional compression behaviour of reconstituted clays with and without humic acid. *Applied Clay Science*, *144*(April), 45–53. https://doi.org/10.1016/j.clay.2017.04.025

Lehmann, J. and Kleber, M. (2015). The contentious nature of soil organic matter. *Nature*, *528,* 60-68. doi:10.1038/nature16069

P 12.6
Urban soils and ecosystem services in cities: assessing water and heat regulation potential

Marie Coudene[1,2], Eloïse Singer[2],Géraldine Bullinger-Weber[1], Philip Brunner[3], Pascal Turberg[4], Renée-Claire Le Bayon[2]

[1] *Institute of Construction and Environmental Technologies, School of Engineering and Architecture of Fribourg (HES-SO), Bd de Pérolles 80, CH-1700 Fribourg (marie.coudene@hefr.ch)*
[2] *Functional Ecology Laboratory, University of Neuchâtel, Emile-Argand 11, CH-2000 Neuchâtel*
[3] *The Centre for Hydrogeology and Geothermics, University of Neuchâtel, Emile-Argand 11, CH-2000 Neuchâtel*
[4] *ENAC IIE PERL, EPFL Ecole Polytechnique Fédérale de Lausanne, GR B2 387 (Bâtiment GR) Station 2, CH-1015 Lausanne*

Urban green spaces supply several ecosystem services (ESS) key to human well-being, especially in the context of increasing extension of cities. Soils in urban areas have multiple functions that are becoming more valued by urban communities. Among them, soils favor carbon storage and climate regulation, biomass provision for food and water flow regulation, and can lower temperatures locally. However, the potential to enhance these ESS via targeted urban soil management remains largely untapped. The main challenge is considering the variability of urban soils due to the inherent heterogeneity of urban environments, intensifying natural soil variability. For instance, due to management practices, urban soils have different degrees of compaction, soil structure alteration, and biological activities. These differences lead to fundamental comprehension gaps in water and heat soil pathways.

Our research aims to study urban soil properties to improve our knowledge of these highly managed environments that influence water and heat regulation. Large herbaceous areas, e.g. urban parks, are ideal research fields, as they allow sampling over large areas away from trees, limiting evapotranspiration effects. The city of Lausanne offers multiple park areas differing in their management and land use. The geographic and geological history of the town provides an excellent opportunity to analyze contrasting environments.

A prospecting campaign is currently made to discriminate and classify the soil types. We identify patterns and variables that help us a better understanding of soil water regulation function: soil depth, structure, porosity, texture, etc. Computer tomography analysis provides better insights into pore network. The preliminary findings highlight that urban soils exhibit expected heterogeneous features relative to their pedogenesis processes. As a complement, several experiments will quantify the links between infiltration and temperature dynamics to understand urban soils’ water and temperature dynamics.

P 12.7
Micro Plastic Pollution: An efficient extraction protocol for MINAGRIS

Adrian Grunder[1], Moritz Bigalke[2]

[1] *Geographisches Institut Universität Bern, Universität Bern, Hallerstrasse 12, CH-3012 Bern (adrian.grunderiub.unibe.ch)*
[2] *Institut für Angewandte Geowissenschaften, Technische Universität Darmstadt, Schnittspahnstrasse 9, DE-64287 Darmstadt*

The global production of plastic has been consistently increasing, with a significant share being mismanaged, especially at the end of life. Once plastic enters the environment, it undergoes degradation, being fragmented into smaller pieces through chemical and physical weathering.

While microplastics (particles with a diameter smaller than 5mm) in aquatic systems have received substantial attention, terrestrial systems have been inadequately studied. Given the widespread presence of diverse plastics, this knowledge gap is concerning. Soils, serving as pollutant sinks and sites of accumulation are particularly vulnerable due to the long-lasting nature of most plastics. With the ongoing fragmentation, ultimately polymers can penetrate cell walls, effectively entering our food chain and confronting us with currently unknown consequences.

As most food directly (food) or indirectly (fodder) depends on soils, MINAGRIS (Micro- and Nano-Plastics in Agricultural Soils) is conducting a comprehensive study in Europe, analyzing soil samples from over 200 agricultural fields. Twice five separate samples were taken on each field and mixed into two composite samples, improving the sample's representativeness for the whole field. The soils then got sieved down to a 5 mm grain size. From there, the MPs got extracted using density separation and different digestion steps. Once isolated, the particles were analyzed using FT-IR microscopes (FPA & MCT) to identify and characterize microplastics in terms of particle abundance, polymer type, shape, and size. The quality control protocols covering sampling, preparation, and extraction help harmonize the data and ensure comparability between the different countries, cultures, and cropping systems. Lab-created MP-free soils underwent the standardized sampling and preparation procedure to allow an assessment of the field and lab contamination alike. Spiked soils, spiked blanks, and chemical blanks are additionally processed with every batch. The Universities of Bern and Wageningen are replicating each other's work, helping to solidify the study. Based on the first results, additional back-to-the-field sampling will be conducted in 2025.

In order to assess how contaminated the pedosphere really is, comparability in results is needed. To ensure this, the development of a standardized method for plastic extraction from soils and its quantification was necessary. The present work aims at addressing this as part of the MINAGRIS project by unifying previous research and developing one harmonized protocol. The developed method is adapted based on earlier work by Bigalke & Scheurer (2018). It consists of a sequence of density separations and filtrations including an OM oxidation step resulting in the deposition of the particles on an aluminum oxide filter. NaBr 48% (ρ= 1.5g/cm^{-3}) was chosen as the density separation solution allowing for an extraction of most common polymers. To avoid an interference of $CaCO_3$ during the OM oxidation, small quantities of HCl 1% were added for a short time. A NaUT (Natriumhydroxide, Urea, Theourea) treatment coupled with an OM oxidation was implemented, substantially reducing OM content and thus greatly reducing background noise (Olson et al. 2020, Bigalke et al., 2022). In order to counter-balance an iron oxide triggered coloration of the sample, H_2SO_4 (2M) was applied on the filter removing residual iron oxides. Using this extraction protocol no significant alteration of the MPs was observed and a recovery rate of 100% is expected. This was tested using virgin PLA, PE and PVC polymers. Currently, 240 agricultural soils across 11 European countries are being analyzed using this protocol.

REFERENCES

Bigalke et al., 2022: Microplastics in agricultural drainage water: A link between terrestrial and aquatic microplastic pollution, Science of the Total Environment, 806.

Olson et al. 2020; Facilitating microplastic quantification through the introduction of a cellulose dissolution step prior to oxidation: Proof-of-concept and demonstration using diverse samples from the Inner Oslofjord, Norway, Marine Environment Research, 161.

Scheurer, M. & Bigalke, M. 2018: Microplastics in Swiss Floodplain Soils, Environmental Science & Technology, 52, 3591−3598.

13 Hydrology, Hydrogeology, and Limnology

Damien Bouffard, Sandra Pool, Michael Döring, Sanja Hosi, Daniel Hunkeler, Christophe Lienert, Peter Molnar, Michael Sinreich, Natacha Tofield-Pasche, Daniel Viviroli

Swiss Hydrological Commission CHy,
Swiss Society for Hydrology and Limnology SGHL,
Swiss Hydrogeological Society SGH

TALKS:

13.16 Salamin A., Renard P., Christe P., Favre G., Doucerain C.: A model of the evolution of the water resource availability at the Glarey karstic spring in the glaciated Tsanfleuron watershed

13.17 Seibert J., Blanco S., Scheller M., Schwarzenbach F., Goebel R., van Meerveld I.: Citizen-science observations made in Switzerland – Towards new horizons in regional hydrology

13.18 Viviroli D., Sikorska-Senoner A.E., Evin G., Staudinger M., Kauzlaric M., Chardon J., Favre A.-C., Hingray B., Nicolet G., Raynaud D., Seibert J., Weingartner R., Whealton C.: Estimating very rare floods at multiple sites in the Aare River basins with comprehensive hydrometeorological simulations

13.19 Wanner C., Camesi L., Waber H.N., Zimmermann S., Sinreich M.: Natural background concentrations in shallow Swiss aquifers

13.20 Wiersma P., Mariéthoz G.: From flow to snow: streamflow-based snow mass reconstruction using inverse hydrological modeling

POSTERS:

P 13.1 Abhervé R., Roques C., Aquilina L., Brunner P., de Dreuzy J.R., Longuevergne L.: Simulation and calibration of headwater stream intermittency using a groundwater flow model

P 13.2 Acciardo A., Gholizadeh N., Mesimeri M., Scarabello L., Hertrich M., Magnabosco C.: Detection of hydrogen peroxide after hydraulic stimulation of granitic bedrock at the Bedretto Tunnel

P 13.3 Bassani F., Fatichi S., Bonetti S.: Towards a metabolic theory of catchments: scaling of water and carbon fluxes with size

P 13.4 Belloni C., Valley B., Roques C.: Tidal characterization of the Liappey fractured aquifer, Bagnes (VS)

P 13.5 Bouffard D., Amadori M., Brescani M., Giardino C., Odermatt D., Irani Rahaghi A., Runnalls J., Toffolon M., Werther M.: ALPLAKES: Advancing Lake Research and Management through Integrative Remote Sensing and Hydrodynamic

P 13.6 Calvani G., Ruiz-Villanueva V., Schwarz M., Perona P.: On the scaling relationship between grain-size, riverbed slope and catchment area at the reach scale

P 13.7 Dubois E., Marshall M., Boukhreiss F., Cherif S.A., Mariéthoz G., Grossiord C., Perona P.: Tree planting as a nature-based solution for urban flooding in Nouakchott City, Mauritania

P 13.8 Engelhardt M., Hemingway J., De Clippele A., Ludjwera A., Haghipour N., Six J.: Lake archives from tropical Africa: Reconstructing the paleoclimate leading to the African Rainforest Crisis 3000 years ago

P 13.9 Fan X., Peterson T., Henley B., Arora M.: Quantifying the sensitivity of groundwater to climate variations in Australia

P 13.10 Feller K., Calvani G., Caponi F., Perona P.: Evaluating riparian vegetation removal due to morphodynamic processes in the river Thur

P 13.11 Halloran L., Mohammadi N., Figueroa R., Carron A., Gutierrez F., Hunkeler D., Brunner P., Arnoux M., Baumann H.: The RADMOGG Project (2023-2027): Resilience and Dynamics of Mountain Groundwater using Gravimetry

P 13.12 Horton P., Mosimann M., Kaderli S., Martius O., Zischg A.P.: A machine-learning approach to predict overland flow impacts

P 13.13 Humphrey V., Hüsler F., Oesch D., Bircher S., Sturm J., Scapozza C.: The Federal Drought Monitoring and Warning System

P 13.14 Janzing J., Wanders N., Brunner M.I.: The effect of an improved snow and glacier routine of a large-scale hydrological model on Alpine streamflow and extremes

P 13.15 Kayitesi N.M., Guzha A.C., Tonini M., Mariethoz G.: Impacts of Land Use Land Cover and Climate Changes on hydro-morphological processes of the African Great Lakes Regions. Case of Lake Kivu catchment.

P 13.16 Mettra F., Bouffard D., Reiss R.S., Lemmin U., Doda T., Blanckaert K., Barry D.A.: Effects of strong Wind-driven Currents on Winter Cascading in Lake Geneva during a cold Spell

P 13.17 Mhanna S., Brunner P., Halloran L.: Google Earth Engine Applications in Hydrology and Hydrogeology

P 13.18 Mittelbach B., White M., Rhyner T., Haghipour N., Dubois N., Eglinton T.: Radiocarbon Inventories of Switzerland: Insights from a year of sediment trap data in Lake Geneva

P 13.19 Moeck C.: Swiss Groundwater Network – CH-GNet

P 13.20 Müller T., Fischer M., Lane S.N., Schaefli B.: Separating snow and ice melt contributions based on water stable isotopes and a glacio-hydrological model in a highly glacierized catchment

P 13.21 Musy S., Currle F., Nakajima T., Tomonaga Y., Sano Y., Schilling O.S.: The hydrogeology of Mt. Fuji as a model for water resource management in tectonically active volcanic regions

P 13.22 Padoan F., Calvani G., De Cesare G., Perona P.: An improved definition of the Habitat Suitability Index for brown trout including the role of macroroughness

P 13.23 Pastore C., Luetscher M., Doumenc F., Sedaghaktish A., Weber E., Jeannin P.-Y.: Dispersion of artificial tracers in ventilated caves

P 13.24 Pedimina T., von Fumetti S.: Temporal and spatial comparison of springs in three different mountain regions in the Southern Swiss Alps

P 13.25 Pelzmann V., Leis A., Schuerch M., Reszler C.: Regionalization of Oxygen-18 and Deuterium in precipitation in Switzerland as a basis for hydrological and hydrogeological studies

P 13.26 Perego R., Pera S.: Characterization of river/groundwater interactions by signal processing of electrical conductivity time series

P 13.27 Rhyner T.M.Y., Mittelbach B.V.A., White M.E., Broeder L., Raymond O., Haghipour N., Brunmayr A., Storck F.R., Passera L., Schwab M.S., Hilton R., Zobrist J., Eglinton T.I.: Radiocarbon Inventories of Switzerland: What controls the radiocarbon signature of dissolved inorganic carbon in Swiss rivers?

P 13.28 Roques C., Halloran L., Louis C., Abhervé R., Illien L., Andermann C., Hovius N., Oestreicher N., Figueroas R., the CHYN team: Poschiavino Critical Zone Observatory: monitoring impacts of climate change on alpine cryo-hydrological systems

P 13.29 Rotta F., Gallitelli L., Roncoroni M., Capelli C., Leoni B., Marchini A., Lepori F.: Microplastic pollution in rivers: concentrations, environmental drivers and biological risks in Lake Lugano watershed

P 13.30 Sauter G., Bouffard D., Blanckaert K., Kremer K.: Monitoring of river-induced bottom currents in Swiss lacustrine deltas

P 13.31 Simonnot B., Dubois E., Marshall M., Grossiord C., Perona P.: Implementing a 3D groundwater model to simulate tree-planting scenarios against urban flooding in Nouakchott city, Mauritania

P 13.32 Van Hamel A., Brunner M.I.: Extreme water temperatures in mountain rivers

P 13.33 Wenyue Zou, Guanghui Hu, Wiersma P., Shuiqing Yin, Mariethoz G., Peleg N.: Multiple-point geostatistics-based spatial downscaling of heavy rainfall fields

P 13.34 White M.E., Mittelbach B.V.A., Rhyner T., Haghipour N., Wessels M., Dubois N., Eglinton T.I.: Radiocarbon Inventories of Switzerland: Sources and cycling of dissolved organic carbon in Swiss lakes

P 13.35 Zakeri F., Mariethoz G., Girotto M.: Reconstructing High-Resolution Snow Water Equivalent (SWE) Data for Improved Water Resource Management (1950-2100)

13.1
Multi-objective calibration for better simulation of flash floods

Paul C. Astagneau[1,2], François Bourgin[1], Vazken Andréassian[1], Charles Perrin[1], Manuela I. Brunner[2,3,4]

[1] *Université Paris-Saclay, INRAE, HYCAR Research Unit, Antony, France (paulastagneau123@yahoo.fr)*
[2] *WSL Institute for Snow and Avalanche Research SLF, Davos Dorf, Switzerland*
[3] *Institute for Atmospheric and Climate Science, ETH Zurich, Zurich, Switzerland*
[4] *Climate Change, Extremes and Natural Hazards in Alpine Regions Research Center CERC, Davos Dorf, Switzerland*

River floods characterized by quickly rising water levels, i.e., flash floods, cause large social and economic impacts worldwide. Rainfall-runoff models often have a limited ability to simulate such rapid catchment responses. While the structure of these models may be inadequate to reproduce the processes involved in quick runoff formation, parameter calibration also plays an important role in accurately simulating flash floods. The estimation of model parameters is particularly complex when threshold processes are triggered during flood formation on a small number of time steps. This results in increased uncertainty in model simulations, usually translating into low parameter identifiability and robustness. A single-objective calibration, relying on one standard metric (e.g. Kling-Gupta efficiency; KGE) calculated over the entire streamflow time series only, may limit model accuracy and parameter adequacy in such cases.

This study investigates the use of different objective functions, within a multi-objective calibration framework, for simulating flash floods. It is based on a large-sample dataset of 781 continental French catchments for which 43,019 flood events were selected. A state-of-the-art multi-objective optimiser (Monteil et al., 2020) was used to calibrate the GR5H-RI hourly rainfall-runoff model (Astagneau et al., 2022). Five objective functions placing varying degrees of emphasis on high flows and rapid flood rises were combined within the multi-objective framework resulting in four calibration options. These functions were calculated over the flood event set and vary depending on their emphasis on different periods of the streamflow time series (rising limbs, flash floods…). The four calibration options were compared to a single-objective calibration relying on the KGE criterion. The different calibration options were first evaluated in terms of model performance in simulating floods. Second, the robustness and identifiability of the parameters were assessed using Pareto front theory. Finally, the results were analysed with respect to the number of flood events used to build the objective functions.

Our results show that introducing flood performance criteria (e.g. criteria calculated over flood rise periods only) into the calibration process improves simulation performance for floods, particularly in the case of flash floods. Different trade-offs were found between increasing performance in simulating floods and improving parameter identifiability and robustness. We also find that the use of a classical metric (e.g. KGE calculated over the entire streamflow time series only) as a single objective function is not sufficient to accurately reproduce flood peaks and volumes in many cases. We argue that this shortcoming should be taken into account when calibrating a model for flood forecasting by using a composite single-objective criterion that combines a classical metric and a metric that places more emphasis on flash floods.

REFERENCES

Astagneau, P.C., Bourgin, F., Andréassian, V. & Perrin, C. 2022: Catchment response to intense rainfall: evaluating modeling hypotheses, Hydrological Processes, 36(8), e1467.

Monteil, C., Zaoui, F., Le Moine, N. & Hendrickx, F. 2020: Multi-objective calibration by combination of stochastic and gradient-like parameter generation rules – the caRamel algorithm, Hydrology and Earth System Sciences, 24, 3189–3209.

13.2
Proliferation of genus *Planktothrix* drives bacterioplankton community divergence and short-term losses of functional diversity in Lake Geneva

Anna Carratalà.

Environmental Chemistry Laboratory, EPFL

Planktothrix, a planktonic cyanobacteria genus, often leads to harmful blooms in temperate lakes undergoing recovery from eutrophication. These blooms pose public health challenges due to potential cyanotoxin production. While the effects of cyanotoxins are well-documented, limited knowledge exists about the influence of Planktothrix blooms on lake bacterioplankton communities. In this study, we conducted a 15-month investigation into Planktothrix dynamics and assessed corresponding shifts in bacterioplankton communities using 16S rRNA amplicon sequencing.

The analysis conducted in Lake Geneva revealed prevailing genera, including the CL500-29 marine group, Flavobacterium, Planktothrix NIVA-CYA15, CL500-3, hgcl clade, and Rhodoferax. Notably, Planktothrix NIVA-CYA15 and Flavobacterium emerged as primary drivers of community differentiation, as indicated by multidimensional scaling of Bray Curtis dissimilarities. Moreover, a strong correlation between Planktothrix and the abundance of predicted photosynthesis proteins underscored its importance in the lake's primary production.

Interestingly, an upsurge in Planktothrix reads corresponded with reduced bacterioplankton abundance (quantified via 16S rRNA gene qPCR), alongside diminished taxonomic and functional diversity. Restoration of diversity indices followed the decline in Planktothrix reads. Elevated Planktothrix abundance correlated with specific water column conditions: temperatures of 9-12 °C, pH of 7.8, solar irradiance at 50 W/m2, increased wind speeds, conductivity between 0.2-0.22 μS/cm, low turbidity (0.8 NTU), oxygen saturation of 90-100%, and dissolved oxygen levels of 10-11 mg/l.

In summary, this study enriches our comprehension of spatiotemporal bacterioplankton dynamics and the ecological role of Planktothrix in Lake Geneva. As the largest peri-alpine lake in western Europe, these findings contribute to the broader understanding of how cyanobacteria blooms impact microbial communities in recovering eutrophic ecosystems.

13.3
Tracing and quantifying microbes in riverbank filtration sites combining online flow cytometry and noble gas analysis

Friederike Currle[1], Théo Blanc[2], Yama Tomonaga[1], Rolf Kipfer[3,4,5], Daniel Hunkeler[2], Philip Brunner[2], Oliver S. Schilling[1,3]

[1] *Hydrogeology, Department of Environmental Sciences, University of Basel, Bernoullistrasse 32, CH-4056 Basel (friederike.currle@unibas.ch)*
[2] *Centre for Hydrogeology and Geothermics, University of Neuchâtel, Rue Emile-Argand 11, CH-2000 Neuchâtel*
[3] *Eawag, Swiss Federal Institute of Aquatic Science and Technology, Überlandstrasse 133, CH-8600 Dübendorf*
[4] *Institute of Biogeochemistry and Pollutant Dynamics, ETH Zurich, Universitätstrasse 16, CH-8092 Zurich*
[5] *Institute of Geochemistry and Petrology, ETH Zurich, Clausiusstrasse 25, CH-8092 Zurich*

Understanding microbial transport in surface water – groundwater systems is crucial for drinking water management. Particularly in the context of climate change, the quality of groundwater pumped near streams might be affected by high microbial loads after heavy rain, peak flow and spring snowmelt events. Dissolved noble gases have been shown to be conservative tracers and provide information on pathways and travel times of groundwater. Although it is known that due to size exclusion, microbes appear to travel faster than solutes, most hydrological tracer methods target groundwater movement and solute transport, while specific tracers for microbial transport are not yet considered for protection zone delineation of drinking water supply wells. Recently, online flow cytometry (FCM) has been shown to be a promising tool to track on site, continuously and in near-real time the movement of microbes in riverbank filtration settings (Besmer et al., 2016). Beyond direct cell counting, advanced computational tools enable to extract automatically relevant features from the multivariate FCM data describing the phenotypic diversity of the microbial community.

Aiming to understand microbial transport behavior in surface water – groundwater systems and develop tracer methods to track their movement, we combined online FCM with online (noble) gas analysis at a riverbank filtration site in the Emme valley, Switzerland (Schilling et al., 2022). Dissolved gas concentrations and microbial community patterns (measured using the gas equilibrium-membrane inlet portable mass spectrometer miniRUEDI (Brennwald et al. (2016), Gasometrix GmbH), the electronic radon detector Rad7 (DURRIDGE), and the online flow cytometer BactoSense (bNovate Technologies SA)) were monitored continuously over a period of several months of river restoration activity inside the river, a piezometer next to the river, and nearby riverbank filtration wells. Systematic changes in the microbial and dissolved gas patterns could be observed in reaction to a 2-year peak flow event, river restoration activities, and spring snowmelt events.

In summary, this combination of state-of-the-art analytical techniques allows to track and quantify microbial pathways from surface water into and through an alluvial aquifer. Furthermore, the setup increases understanding of reactive microbial transport compared to the transport of conservative dissolved gases and, highlights the potential of environmental DNA as a hydrological tracer technique.

REFERENCES

Besmer, M. D., Epting, J., Page, R. M., Sigrist, J. A., Huggenberger, P., & Hammes, F. (2016): Online flow cytometry reveals microbial dynamics influenced by concurrent natural and operational events in groundwater used for drinking water treatment. Sci. Rep., 6, Article 38462. https://doi.org/10.1038/srep38462

Brennwald, M. S., Schmidt, M., Oser, J., & Kipfer, R. (2016): A Portable and autonomous mass spectrometric system for on-site environmental gas analysis. Environ. Sci. Technol., 50, 13455-12463. https://doi.org/10.1021/acs.est.6b03669

Schilling, O. S., Partington, D. J., Doherty, J., Kipfer, R., Hunkeler, D., & Brunner, P. (2022): Buried paleo-channel detection with a groundwater model, tracer-based observations, and spatially varying, preferred anisotropy pilot point calibration. Geophys. Res. Lett., 49(14), e2022GL098944. https://doi.org/10.1029/2022GL098944

13.4
Tracking snow melt infiltration over alpine soils : Instrumental approach

Judith Eeckman[1], Brian De Grenus[2], Floreanna Miesen[2], Jean-Michel Fallot[1], Nadav Peleg[2]

[1] Lausanne University, Institute of Geography and Durability, Lausanne, Switzerland (judith.eeckman@unil.ch)
[2] Lausanne University, Institute of Earth Surface Dynamics, Lausanne, Switzerland

Alpine soils, generally poorly consolidated, can induce significant flow delays and significantly influence river flows during low water periods. In particular, the snowmelt flow is particularly conducive to a slow infiltration into soils. A better description of the link between snowmelt and infiltration processes in the soils can then lead to a better understanding of a drought risk induced by a lack of reserves in the soils. The Nant valley (Vaud, Switzerland), instrumented within the framework of various projects within the Faculty of Geosciences of the University of Lausanne, represents a case study for this work. An important instrumental set up has been locally deployed during two consecutives years. Infiltration processes in the soils are estimated through the installation of soil moisture sensors at different depths in areas of alpine meadows. The dynamics of the melt flow is described at one measurement point using a dedicated instrumentation. Infiltrometry tests are performed and soil samples are collected for further granulometry analysis, in order to better describe the infiltration capacity at different points of the catchment. The instrumental device as well as the results deduced from measurements are presented in this work. The results illustrate various possible dynamics of the snowmelt infiltration process. Behaviors at the beginning of winter or in spring are distinguished and the influence of diurnal melting is highlighted.

13.5
Non-canonical denitrification pathways in the anoxic benthic nepheloid layer of a seasonally stratified lake

Teresa Einzmann[1], Moritz F. Lehmann[1], Annie Bourbonnais[2], Jakob Zopfi[1], Claudia Frey[1]

[1] *Department of Environmental Sciences, University of Basel, Basel, Switzerland*
[2] *School of the Earth, Ocean and Environment, University of South Carolina, Columbia, SC, US*

Nitrous oxide (N_2O) is a strong greenhouse gas and ozone-destroying agent, with increasing atmospheric mixing ratios over the last few decades. Lakes play an uncertain role regarding their contribution to global N_2O emissions, in parts due to the lack of a better understanding of the environmental controls on N_2O production and consumption processes.
In this study, through natural-abundance isotope measurements and ^{15}N-label incubations, we investigated N_2O production pathways within the anoxic benthic nepheloid layer (BNL) forming in the South Basin of eutrophic Lake Lugano (Switzerland) during summer stratification. Short-termed accumulation of high N_2O concentrations (up to 800 nmol/L) was observed in near-bottom waters accompanied by a significant decline in $\delta^{15}N$ bulk values, and an increase in the N_2O site preference (SP) to +42 ‰. Incomplete heterotrophic denitrification is usually the main production mechanism for N_2O in low-oxygen environments, but N_2O from nitrate/nitrite reduction is generally characterised by a low SP signature of -5-0 ‰ (Sutka et al., 2006)however, requires a foundation in laboratory experiments in which individual production pathways can be isolated. Here we evaluate the site preferences of N2O produced during hydroxylamine oxidation by ammonia oxidizers and by a methanotroph, ammonia oxidation by a nitrifier, nitrite reduction during nitrifier denitrification, and nitrate and nitrite reduction by denitrifiers. The site preferences produced during hydroxylamine oxidation were 33.5 ± 1.2‰, 32.5 ±0. 6‰, and 35.6 ± 1.4‰ for Nitrosomonas europaea, Nitrosospira multiformis, and Methytosinus trichosporium, respectively, indicating similar site preferences for methane and ammonia oxidizers. The site preference of N2O from ammonia oxidation by N. europaea (31.4 ± 4.2‰, whereas high SP values suggest an oxidative N_2O production mechanism. First incubation experiments with ^{15}N-labelled NH_4^+ (to investigate oxidative N_2O production through nitrification) and ^{15}N-labelled NO_3^- (to investigate reductive N_2O production through denitrification) corroborated reductive N_2O production in the Lake Lugano BNL. Isotope fractionation during partial N_2O reduction can increase N_2O SP, but cannot explain the high values that we observed. Alternative denitrification pathways known to produce N_2O with a high SP, such as fungal denitrification (SP = >30 ‰, Rohe et al. 2014) and chemo-denitrificaiton (SP = 0-27 ‰, Li et al., 2022) were investigated in complementing incubation experiments involving bacterial and fungal inhibitors. These experiments confirmed that bacterial denitrification contributes significantly to N_2O production in the BNL, but also demonstrated the importance of fungal and chemo-denitrification.

REFERENCES

Li, S., Wang, S., Pang, Y., & Ji, G. 2022: Influence of Electron Donors (Fe, C, S) on N 2 O Production during Nitrate Reduction in Lake Sediments: Evidence from Isotopes and Functional Genes , ACS ES&T Water, 2(7), 1254–1264.

Rohe, L., Anderson, T.-H., Braker, G., Flessa, H., Giesemann, A., Lwicka-Szczebak, D., Wrage-Mönnig, N., & Well, R. 2014: Dual isotope and isotopomer signatures of nitrous oxide from fungal denitrification – a pure culture study, Rapid Communiciations in Mass Spectrometry, 28, 1893-1903.

Sutka, R. L., Ostrom, N. E., Ostrom, P. H., Breznak, J. A., Gandhi, H., Pitt, A. J., & Li, F. 2006: Distinguishing nitrous oxide production from nitrification and denitrification on the basis of isotopomer abundances, Applied and Environmental Microbiology, 72(1), 638–644.

13.6
Calcite precipitation in hardwater lakes: new insights into the link with picoplankton dynamics

Nicolas Escoffier[1], Gaël Many[1], Antonio Mucciolo[2], Romain Bedel[3], Marie-Elodie Perga[1]

[1] Institute of Earth Surface Dynamics, University of Lausanne, CH-1015 Lausanne (nicolas.escoffier@unil.ch)
[2] Electron Microscopy Facility, University of Lausanne, CH-1015 Lausanne
[3] Flow Cytometry Facility, University of Lausanne, CH-1015 Lausanne

In hardwater lakes fueled by carbonate weathering from surrounding catchments, calcite precipitation is a major process of the lacustrine carbon cycle by which alkalinity loss is coupled with primary production. While recent studies clarified the magnitude and biogeochemical conditions underlying calcite precipitation at fine scales, the mechanisms supporting the nucleation of calcite are poorly described. In the pelagic realm of deep oligotrophic lakes, calcite nucleation has often been associated with autotrophic picoplankton, however, direct observations remain scarce. Here, we focused on the largest hardwater lake of western Europe, Lake Geneva, and combined depth-resolved high-frequency data with discrete sampling to investigate the link between calcite precipitation and picoplankton dynamics. Calcite precipitation during periods of lake thermal stratification and high primary productivity coincided with increasing abundances of distinct picoplankton populations that were characterized by specific fluorescence signatures using spectral flow cytometry. Phycoerythrin rich picocyanobacteria constituted the dominant population whose maximum abundances in the water column occurred at depths of enhanced stability and alkalinity depletion. Moreover, the sorting of this population combined with imaging by SEM-EDX enabled to confirm that picocyanobacteria acted as nucleation sites for calcite and to analyze the diverse patterns of association between calcite crystals and picoplankton cells. These results provide a refined understanding of calcite nucleation mechanisms and allow inferring the relevance of this biologically mediated process for the lacustrine carbon cycle.

13.7
Exploring regional-scale hydrological processes that determine low young water fraction in mountainous catchments

Alessio Gentile[1], Davide Canone[1], Natalie Ceperley[2,3], Davide Gisolo[1], Maurizio Previati[1], Giulia Zuecco[4,5], Bettina Schaefli[2,3], Stefano Ferraris[1]

[1] *Interuniversity Department of Regional and Urban Studies and Planning (DIST), Politecnico and Università degli Studi di Torino, Viale Mattioli, 29, IT-10125 Torino, (alessio.gentile@polito.it)*
[2] *Institute of Earth Surface Dynamic (IDYST), Faculty of Geosciences and Environment (FGSE), University of Lausanne, CH-1015 Lausanne*
[3] *Institute of Geography (GIUB) and Oeschger Centre for Climate Change Research (OCCR), University of Bern, CH-3012 Bern*
[4] *Department of Land, Environment, Agriculture and Forestry (TESAF), University of Padova, Viale dell'Università 16, IT-35020 Legnaro (PD)*
[5] *Department of Chemical Sciences (DiSC), University of Padova, Via Marzolo 1, IT- 35131 Padova*

Mountains are vital regulators of global water resources, acting as natural water towers that supply freshwater to downstream regions. The age of water, referring to the time elapsed since its entry into the hydrological cycle, has emerged as a critical parameter in understanding the dynamics and the hydrological processes in mountainous catchments.

Natural tracers such as stable water isotopes are commonly used to track the movement of water through catchment. Specifically, the seasonal isotope cycles in precipitation and streamwater allow easy estimation of the portion of runoff younger than roughly 2-3 months, also known as young water fraction (F^*_{yw}). This metric is practical for catchment intercomparison studies, and hydrologists have been intrigued by low F^*_{yw} estimates in high-elevation, mountainous watersheds. Accordingly, such catchments are often assumed to produce a large amount of rapid surface or subsurface runoff due to steep bedrock slopes. This surprising result highlights the limited knowledge of hydrological processes in remote environments, and the challenge to conceptualize these processes.

This study investigates, at a regional scale, the relevance of some key hydrological variables and processes (groundwater storage potential, catchment storage contribution to the stream, low-flow duration, and snowpack ephemerality) that we consider to be the main drivers of F^*_{yw} variation according to elevation, by providing a framework for the interplay of these processes along elevation gradients. We use data from 27 study catchments located across Switzerland and Italy that span a wide range of underlying geology and hydro-climatic regimes.

On one hand, our results reveal that the extension of Quaternary deposits available in geological data sets is not a sufficiently good proxy of groundwater storage potential due to the unknown thickness of such deposits. On the other hand, our results reveal how the interconnection of the other variables/processes investigated in this work explains the F^*_{yw} variations along elevation gradients.

The low-flow periods over the hydrologic year indicate the time windows in which the stored (old) water predominantly contributes to the stream, thus reducing the average annual young water fraction. In mountain catchments, the proportion of low-flow periods over the year is strongly driven by the snowpack duration. At high elevations (> 1500 m a.s.l.), the persistence of winter snowpack causes the lack of a liquid water input to the catchment thus favouring a long (up to six months at the highest elevations) low-flow period dominated by (old) groundwater. The seasonal snowpack melts during the spring/summer seasons preferentially recharging the groundwater storage with old (i.e., > 2-3 months) meltwater and likely pushing out stored water. Conversely, ephemeral snowpacks at low elevations (< 1500 m a.s.l.) can intermittently melt during the winter season, both reducing the length of low-flow periods and providing young water to the stream due to the reduced elapsed time between snowfall and snowmelt and the critical role of soil freezing that inhibits infiltration.
Interestingly, we have also found that the average fraction of baseflow (F_{bf}), estimated by using the Duncan (2019) baseflow filter, roughly indicates the fraction of runoff older than a threshold age between 2 to 3 months (i.e., $F^*_{yw} + F_{bf} \approx 1$), that could be a valuable result for catchments in which stable water isotopes measurements are unavailable.
The framework that emerges from our results is a starting point for the development of hydrological models that want to consider and conceptualize the relevant processes in mountainous alpine catchments.

REFERENCES

Gentile A, Canone D, Ceperley N, Gisolo D, Previati M, Zuecco G, Schaefli B, Ferraris S. 2023: Towards a conceptualization of the hydrological processes behind changes of young water fraction with elevation: a focus on mountainous alpine

catchments. Hydrology and Earth System Sciences, 27 (12), 2301–2323.
Kirchner JW. 2016: Aggregation in environmental systems-Part 1: Seasonal tracer cycles quantify young water fractions, but not mean transit times, in spatially heterogeneous catchments. Hydrology and Earth System Sciences, 20 (1), 279–297.
von Freyberg J, Allen ST, Seeger S, Weiler M, Kirchner JW. 2018: Sensitivity of young water fractions to hydro-climatic forcing and landscape properties across 22 Swiss catchments. Hydrology and Earth System Sciences, 22 (7), 3841–3861.
Hayashi M. 2020: Alpine Hydrogeology: The Critical Role of Groundwater in Sourcing the Headwaters of the World. Ground Water, 58 (4), 498–510.
Duncan HP. 2019: Baseflow separation – A practical approach. Journal of Hydrology, 575, 308–313.

13.8
Modeling irrigation demand under increasing drought extremes

Malve Heinz[1,2,3], Bettina Schaefli[1,3], Christoph Raible[1,4], Annelie Holzkämper[1,2]

[1] *Oeschger Centre for Climate Change Research, University of Bern, Switzerland (malve.heinz@unibe.ch)*
[2] *Water protection and Substance Flows, Agroscope Reckenholz, Switzerland*
[3] *Hydrology, Institute of Geography, University of Bern, Switzerland*
[4] *Climate and Environmental Physics, Physics Institute, University of Bern, Switzerland*

Droughts are the leading cause of agricultural yield losses worldwide and play a significant role in yield variability for European agriculture (Bodner et al. 2015; Joint Research Centre 2023). Farmers may intensify irrigation or extend irrigated areas to prevent these losses and maintain quality. At the same time, water availability for irrigation in the vital summer months is decreasing due to shifted rainfall and streamflow regime patterns. Thus, the potential for water-use conflicts between agriculture, industry, and ecosystems will rise (Klein et al. 2013; Zarrineh et al. 2020; Holzkämper et al. 2020). Since irrigation alone might not be sufficient to mitigate the effects of droughts and heat in the future, solutions to minimize the dependencies are crucial. In this context, a key open question is to which extent management measures could alleviate drought impacts and how these measures impact catchment hydrology. In Switzerland, there is a lack of data on the current irrigation practices to analyze the regional or national irrigation water demand and supply. This data is needed as a basis for planning, both on the field scale regarding agricultural management, as well as on the regional scale regarding larger infrastructural projects like irrigation cooperatives. We are presenting a modeling approach to quantify the irrigation demand on the regional level through a case study in the Broye catchment in Western Switzerland. The region is characterized by intensive agricultural use and increased drought-related irrigation bans in summer (Zarrineh et al. 2020). In the first phase of our project, we quantify irrigation demand for the years 2021 and 2022, both with and without irrigation bans. Our study focuses on potatoes, which account for 50% of irrigation water consumption in the Broye region. For this purpose, we use the SWAP model, a field-scale agro-hydrological model that considers soil-water-atmosphere-plant interactions. SWAP simulates soil water and solute fluxes, as well as crop growth dynamics, by solving equations such as the Richards equations (Kroes et al. 2017). We employ latin hypercube sampling and sobol indices to discern the most influential parameters concerning both yield and irrigation demand. Subsequently, we calibrate the derived subset of parameters by optimizing an objective function linked to the fit with reference data on yield and irrigation demand. This calibration process is facilitated by a genetic algorithm, utilizing the DEoptim package in R. Using land use data, the areas where potato fields can be irrigated within the catchment are identified. We then apply the model for each grid cell containing irrigated potato fields. The irrigated demand is then summed up over all cells. The preliminary results show, that during the summer drought in 2022, only 1/3 of the irrigation demands could be satisfied due to the extensive irrigation bans. In contrast, in the cooler and wetter 2021, irrigation demand was only a fraction of that in 2022 and there were no restrictions on irrigation. Starting from this baseline of demand we now want to explore the potential of field-scale crop and soil management to reduce the reliance on irrigation. Possible measures are the cultivation of different varieties (or even species), reduced tillage, or the application of organic amendments. These measures directly impact plant properties (such as phenology) or soil physical properties that can be represented within the model. In future works, we plan to evaluate the impacts of such measures on runoff generation processes and how they can be represented in a catchment-scale rainfall-streamflow model.

REFERENCES

Holzkämper, A., Cochand, F., Rössler, O., Brunner, P., & Hunkeler, D. (2020). AgriAdapt – Modellgestützte Untersuchung der Einflüsse von Klima- und Landnutzungsänderungen auf Grundwasserressourcen im Berner Seeland, im Auftrag des Bundesamts für Umwelt BAFU

Joint Research Centre (2023). Crop monitoring in Europe - July 2023. JRC MARS Bulletin, European Commission, Joint Research Centre.

Kroes J.G. , v. D. J. C., Bartholomeus , Groenendijk P. , Heinen M., Hendriks R.F.A., Mulder H.M. , Supit I., van Walsum P.E.V. (2017). SWAP version 4. Theory description and user manual. Wageningen University & Research.

Michel, A., Brauchli, T., Lehning, M., Schaefli, B., & Huwald, H. (2020). Stream temperature and discharge evolution in Switzerland over the last 50 years: annual and seasonal behaviour. Hydrology and Earth System Sciences, 24(1), 115-142. https://doi.org/10.5194/hess-24-115-2020

Zarrineh, N., Abbaspour, K. C., & Holzkamper, A. (2020). Integrated assessment of climate change impacts on multiple ecosystem services in Western Switzerland. Sci Total Environ, 708, 135212. https://doi.org/10.1016/j.scitotenv.2019.135212

13.9 Trace metal and nutrient dynamics in the ferruginous Lake Poso, Indonesia

David J Janssen[1], Adrianus Damanik[2,3], Nicolas Tournier[2,3], Sri Yudawati Cahyarini[4], Hendrik Vogel[2,3]

[1] *Eawag – Swiss Federal Institute of Aquatic Science & Technology, Department Surface Waters, 6047 Kastanienbaum Switzerland*
[2] *Oeschger Centre for Climate Change Research, University of Bern, 3012 Bern Switzerland*
[3] *University of Bern, Institute of Geological Sciences, University of Bern, 3012 Bern Switzerland*
[4] *BRIN, Research Centre for Climate and Atmosphere, 40135 Bandung, Indonesia*

The tectonic, ancient Lake Poso is a deep meromictic lake in Central Sulawesi, Indonesia. The lake is near the Malili Lakes of Central Sulawesi, but is hydrologically disconnected (Vaillant et al., 2011), giving it unique potential for biogeochemical and ecological studies over wide temporal scales. While the lake has been studied for the diversity of its endemic species, relatively few geochemical data are available. Here we present data of trace metals and nutrients from the surface to a depth of 350 m from a depth profile collected in the center of the lake. Surface waters are highly depleted in dissolved nutrients, in agreement with recent reports of oligotrophic conditions (Sulawesty et al., 2022; Damanik et al., in rev.), and suggesting little anthropogenic chemical impact on the lake (Damanik et al., in rev.).

The chemical structure of the lake is broadly defined by a redox transition near 90 m, with oxic waters above and anoxic, iron-rich (ferruginous) waters below. Trace metal distributions are largely driven by scavenging onto Fe and Mn oxides near this redox transition as well as redox-driven changes in solubility, both direct and indirect. Scavenging-prone metals show mid-depth minima coinciding with the redox transition and concentrations increase in anoxic deep waters, while sulfide-insoluble metals decrease to near zero at the redox transition, despite only minor apparent SO_4 reduction in the anoxic zone. Given the age of the lake (>1 Ma), relatively low anthropogenic pressure, and the strong geochemical gradients, Lake Poso holds potential for paleoreconstructions and paleoproxy development. In particular, the high concentrations of nutrients in the anoxic zone indicate that deep mixing events could promote major changes in biological productivity, which will likely leave signals in the sediment record associated with enhanced carbon export and changes in O_2 availability in deep waters.

REFERENCES

Damanik, A., Janssen, D.J., Tournier, N., Stelbrink, B., von Rintelen, T., Haffner, G.D., Cohen, A., Cahyarini, S.., Vogel, H. Perspectives from modern hydrology and hydrochemistry on a lacustrine biodiversity hotspot: Ancient Lake Poso, Central Sulawesi, Indonesia. In review at the Journal of Great Lakes Research.

.Sulawesty, F., Triyanto, Haryani, G., Lukman, Samir, O., Ali, F., & Nafisyah, E. (2022). Trophic Status of Waters in Poso Watershed, Central Sulawesi. IOP Conference Series: Earth and Environmental Science, 950(1), 012039. doi: 10.1088/1755-1315/950/1/012039.

Vaillant, J.J., Haffner, G.D. and Cristescu, M.E., 2011. The ancient lakes of Indonesia: towards integrated research on speciation. Integrative and Comparative Biology, 51(4), pp.634-643. doi: 10.1093/icb/icr101.

13.10
Identifying the origin and distribution pattern of metalimnetic methane dynamics in Lake Geneva

Santona Khatun, Jasmine S. Berg, Didier Jézéquel, Nicolas Escoffier, Damien Bouffard, Abolfazl Irani Rahaghi, Carsten J. Schubert, and Marie-Elodie Perga

Although methane (CH_4) is mainly produced in anoxic sediments, a metalimnetic supersaturation of CH_4 has been repeatedly detected in many lakes even in Lake Geneva. Metalimnetic methane accumulation (MMA) has been concomitantly attributed to advective fluxes transporting CH_4 from methanogenic littoral sediments to the lake center, and to oxic methane production through different microbial metabolisms including the phosphonate-pathway by Cyanobacteria. We aimed to address the origin of MMA with an extensive sampling campaign across Lake Geneva in the summer of 2022. Methane advective transport was tracked using CH_4 $\delta^{13}C$ (delta13C) while the potential for aerobic methane production was assessed through molecular analysis. Surprisingly, dissolved CH_4 in Lake Geneva was negatively correlated with blue-green algae (BBE data, to be further confirmed by the targeted amplicon sequencing). Instead, dissolved CH_4 was closely associated with turbidity suggesting that the methane is transported by the interflow of the Rhône River across tens of km during the stratification period which was also confirmed in the isotopic analysis. We used a simple advection model to test the possibility of this hypothesis. In summary, the results suggest that metalimnetic methane peak in Lake Geneva is likely to result from the advection of CH_4 produced in sediments and remobilized by turbulences within the river inflow.

13.11
Zooplankton structure moderates eutrophication effects in a deep perialpine lake (Lake Lugano, Switzerland and Italy)

Fabio Lepori[1], Bianca Lucchini[2], Céline Spitzli[2], Moritz F. Lehmann[2]

[1] *Insitute of Earth Sciences, University of Applied Sciences and Arts of Southern Switzerland, Via Flora Ruchat-Roncati 15, CH – 6850 Mendrisio (fabio.lepori@supsi.ch)*
[2] *Department of Environmental Sciences, University of Basel, Bernoullistrasse 30/32, CH-4056 Basel*

In deep lakes recoverying from eutrophication, chemocline erosion or sporadic mixing after muliple years of stratification can lead to a sudden rise in surface-water phosphorus concentrations (SW-P), decreasing water quality as a result. A major concern is that, due to climate change, periods between mixing events are becoming longer, leading to extended P accumulation in the hypolimnion and, in turn, greater SW-P surges upon mixing. Here we investigated the eutrophication impact of a large SW-P surge in the northern basin of Lake Lugano. After partial recovery from eutrophication in the 1990s, this basin underwent a period of SW-P re-enrichment in the 2000s due to upward mixing of deep waters (Lehmann et al. 2015, Lepori & Roberts 2017). We were particularly interested in comparing two phases: 1984-1988 (Phase I), when SW-P was high (> 30 µg L^{-1}) due to high external P loadings, and 2003-2007 (Phase II), when SW-P was high due to high internal P loadings. Specifically, we assessed if these two phases differed in terms of surface-water nutrient chemistry, water transparency and plankton characteristics.

One important consideration in this study was that, at the end of Phase I (specifically in 1988-1999), the structure of the zooplankton grazer assemblage changed from dominance by small zooplankters (small *Daphnia* and other small cladocerans) to dominance by large zooplankters (large *Daphnia* and calanoid copepods).

We compared several variables between the two phases, including soluble reactive P: SRP, total P: TP, total nitrogen:TN, silicon: Si, Z_{SD}: Secchi depth, CHL: Chlorophyll *a*; PHYTO: phytoplankton biomass, ZOO: zooplankton biomass, and some of their ratios (CHL:TP, ZOO:CHL). We also explored changes in plankton composition using ordination techniques (PCA). Based on classic P-based eutrophication models, we expected that the two phases would cause similar eutrophication symptoms, i.e. similarly high CHL and low Z_{SD}.

Our results indicate that differences in average SW-P concentrations and nutrient ratios (SRP:TP, TN:TP, and Si:TP) between phases were small and usually non-significant. In contrast, the two phases showed different CHL and Z_{SD}, along with other plankton characteristics. During Phase I, CHL was high and Z_{SD} was low, indicating severe eutrophication. During Phase II, CHL remained substantially lower and Z_{SD} reached relatively high values. Differences in the ratios CHL:TP and ZOO:PHYTO were striking. On average, the CHL:TP ratio was approximately two times lower, and the ZOO:PHYTO ratio three times higher during Phase II compared to Phase I (Fig. 1). PCA analyses further indicated that Phase I was characterized by a lower biomass of cladocerans and copepods, a higher biomass of cyanobacteria and a lower biomass of green algae, whereas Phase II showed opposing characteristics.

Our findings demonstrate that the plankton community of the northern basin of Lake Lugano responded in different ways to similar SW-P enrichments, producing severe eutrophication symptoms during the first phase (Phase I) and little signs of eutrophication during the second phase (Phase II). We argue that our results are explained by the change in zooplankton grazer assemblage between phases and support the “consumer-dependent” eutrophication model, which posits that lakes dominated by large grazers are less prone to eutrophication compared to lakes dominated by small grazers (Mazumder & Lean 1994). Two implications in the context of lake management are that: (1) simple P-based models may be inadequate tools for predicting algal biomass, and (2) lake restoration measures that favour large (rather than small) zooplankters (e.g., through biomanipulation) may help reduce eutrophication symptoms alongside classical measures aimed at reducing phosphorus.

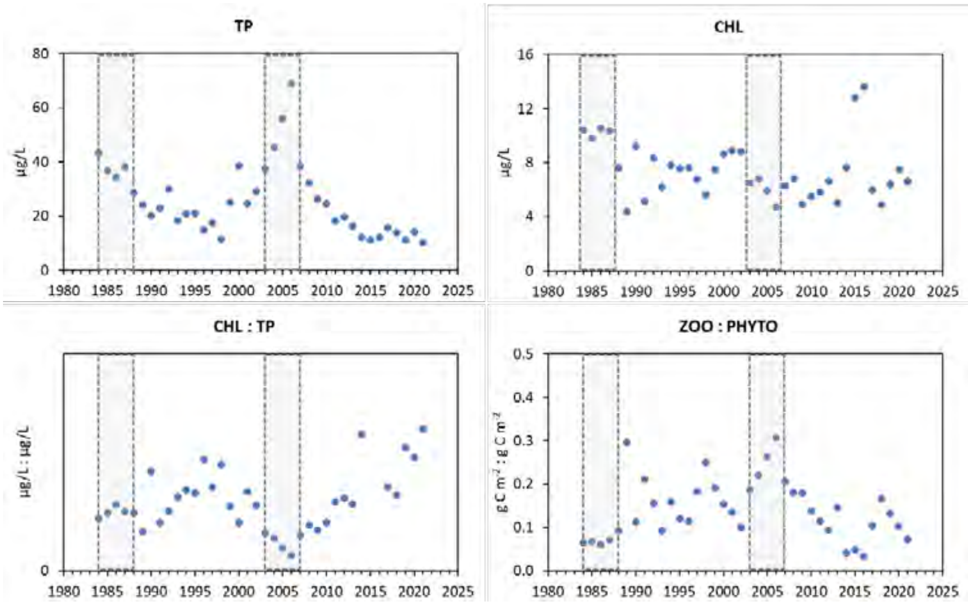

Figure 1. Comparison between P-enrichment phases I and II (indicated by the gray boxes).

REFERENCES

Lehmann, M.F., Simona, M., Wyss, S., Blees, J., Frame, C.H., Niemann, H., Veronesi, M. & Zopfi, J., 2015: Powering up the "biogeochemical engine": the impact of exceptional ventilation of a deep meromictic lake on the lacustrine redox, nutrient, and methane balances, Frontiers in Earth Science, 3, 45.

Lepori, F. & Roberts, J.J. 2017: Effects of internal phosphorus loadings and food-web structure on the recovery of a deep lake from eutrophication, Journal of Great Lakes Research, 43, 255-264.

Mazumder, A. & Lean, D.R., 1994: Consumer-dependent responses of lake ecosystems to nutrient loading. Journal of Plankton Research, 16, 1567-1580.

13.12
Soil-plant hydraulics and stomatal conductance: When do whole tree water dynamics matter?

Stefano Martinetti[1], Andrea Carminati[2], Peter Molnar[1], and Marius Floriancic[1,2]

[1] *Institute for Environmental Engineering, ETH Zurich, Zurich, Switzerland*
[2] *Institute of Terrestrial Ecosystems, ETH Zurich, Zurich, Switzerland*

When plants transpire they require to take up water from the soil through their roots in order to maintain a sustainable plant water status. During dry periods water can become limiting and cause closure of the stomata, the pores on leaves surface through which water and carbon dioxide diffuse between the atmosphere and the leaves interior. Other than water availability, further known factors that influence stomatal conductance are environmental stimuli such as light exposure and vapor pressure deficit. Also, species-specific hydraulic traits and rooting strategies can modify the magnitude and timing of stomatal closure during drought. The interplay between leaf water potential and stomatal conductance mainly characterizes the hydraulic functioning of different species under dry conditions. However, stem and roots properties influence the pathway of water from the soil to the leaf too. Therefore their hydraulic traits and functioning are likely factors influencing stomatal conductance.

Here we monitored water fluxes and potentials on leaves, stem and deep and shallow roots of beech and spruce, as well as nearby soil, at the "WaldLabor" study site near ETH Hönggerberg. We used the data to calibrate and test a soil-plant hydraulic model and to compare above-ground and below-ground water dynamics of a tree. Our results show the different water use strategies of beech and spruce, with spruce typically closing stomata earlier, i.e. at less negative water potentials than beech, and generally showing a looser link between above-ground transpiration proxies and below-ground root water uptake. Results from the soil-plant hydraulic model were well aligned with measurements for beech and correctly predict the point at which beech close stomata for different states of soil water availability (see Figure 1).

In hydrological modeling the role of stomatal conductance is increasingly gaining importance, given its direct control on the transpiration flux. Species-specific hydraulic traits andx water use strategies need to be considered when modeling stomatal conductance. As such, soil-plant hydraulic models offer a physically-based approach to predict stomatal conductance considering whole tree water dynamics.

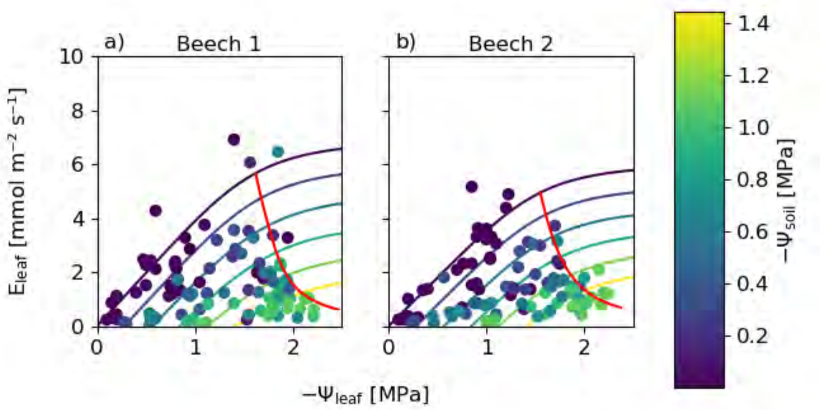

Figure 1. Leaf gas exchanges (y-axis) from stomatal conductance measurements and leaf water potential measurements(x-axis). The color of the dot represents soil water potential at the point of measurement. A soil-plant hydraulic model was calibrated (colored lines) and correctly predicts the point of stomatal closure (red curve) for beech.

REFERENCES

Martinetti, S., Carminati, A., Molnar, P. & Floriancic, M. 2023: Plant hydraulic traits and water use strategies modulate root water uptake and transpiration in beech and spruce, soon to be submitted.

13.13
Combined use of multiple tracers to idenity groundwater flow and pollutant transport in an urban area

Christian Moeck[1],Andrea Popp[1,2],Matthias S. Brennwald[1],Mario Schirmer[1,3,4], Rolf Kipfer[1,2,5]

[1] *Swiss Federal Insitute of Aquatic Science and Technology (Eawag), W+T, Dübendorf (Christian.moeck@eawag.ch)*
[2] *Department of Environmental Systems Science, ETH Zurich, Zurich, Switzerland*
[3] *Centre d'hydrogéology et géothermie (CHYN), University of Neuchâtel, Neuchâtel, Switzerland*
[4] *Département de géologie et de génie géologique, Université Laval, Quebec city, Canada*
[5] *Department of Earth Science, ETH Zurich, Zurich, Switzerland*

For our urban study site in Northern Switzerland, we used stable water isotopes, chlorinated solvents, dissolved gas concentrations, and ^{3}H and tritiogenic ^{3}He concentrations to assess water flow paths and mixing between artificially infiltrated surface water and groundwater. Especially, the recent developments of portable field-operated gas equilibrium membrane inlet mass spectrometer (GE-MIMS) systems provide a unique opportunity to measure dissolved gas concentrations, such as ^{4}He with a high temporal resolution at relatively low costs. Although the GE-MIMS are not capable of providing apparent water ages, ^{4}He accumulation rates are often obtained from $^{3}H/^{3}He$ ages and it has been shown that non-atmospheric ^{4}He concentrations determined in the laboratory (e.g., by static (noble gas) mass spectrometry) and by field-based (GE-MIMS) methods closely agree. This agreement allowed us to establishing an inter-relationship between $^{3}H/^{3}He$ apparent water ages and the non-atmospheric ^{4}He excess (e.g., calibrating the ^{4}He excess in terms of residence time).
We demonstrate that the ^{4}He excess concentrations derived from the GE-MIMS system serve as an adequate proxy for the experimentally demanding laboratory-based analyses. We combined the obtained water ages with hydrochemical data, water isotopes ($\delta^{18}O$ and $\delta^{2}H$), and PCE concentrations to understand water flow dynamics. Moreover, we explain the origin and spatial distribution of PCE contamination found at our study site with our multi-tracer approach.

13.14
Thirsty Earth: a multiplayer computer game for water resources education and research

Marc F. Müller[1,2], Lauren McGiven[2], Diogo Bolster[2], Matthew Noffsinger[3], Caleb Reinking[3]

[1] *Department of Systems Analysis, Integrated Assessment and Modelling, Eawag, Ueberlandstr 133, CH-8600 Dübendorf (marc.mueller@eawag.ch*
[2] *Department of Civil and Environmental Engineering and Earth Science, University of Notre Dame, Notre Dame, IN 46556, USA*
[3] *Center for Research Computing, University of Notre Dame, Notre Dame, IN 46556, USA*

The sustainable and management of water resources requires cooperative institutions whose development are rarely included in already overloaded engineering and earth sciences curricula. The resilience of such institutions in the context of climatic and demographic change is also poorly understood. We propose an open access online multiplayer simulation game to help address both of these education and research gaps. The game -- Thirsty Earth – assigns players to the roles of farmers within rural communities making annual decisions on the type of crop to plant and water sources to use to maximize their agricultural profits given random climate inputs. In doing so they experience key tradeoffs linked to climate variability, cooperative infrastructure management and sustainable water use that are at the heart of many of today's water management challenges.To address these challenges, players can purchase and share reliable information bits on the status and use of water resources, which can then be used to regulate behavior through collective action. In the talk or poster, we will (i) demonstrate the game, (ii) report on its integration as an experiential learning module within a University-level water resources engineering class and (iii) describe plans to use the game within an experimental research design. We will deploy the game massively online via the Mechanical Turk platform, where observing player's behavior will help understand the resilience of water management institutions to changing climate inputs.

13.15
Projecting future Swiss river temperatures on a National scale while maintaining local features

Love Råman Vinnå[1], Jannis Epting[1], Oliver Schilling[1,2]

[1] Applied and Environmental Geology, Hydrogeology, Department of Environmental Sciences, University of Basel, Basel
[2] Department Water Resources and Drinking Water, Eawag–Swiss Federal Institute of Aquatic Science and Technology, Dübendorf
Corresponding author: ramanvinna@unibas.ch

A key water quality indicator for both ecosystem and human water needs is river temperature, which is expected to change as climate warms. River temperatures are strongly controlled on regional to local scale by hydrological and atmospherical processes upstream. Therefore, when studying influencing factors on river temperatures it is desirable to use local-scale atmospheric data. Yet, climate change is a global phenomenon, usually studied with Global Circulation Models (GCMs), which sometimes are coupled to Regional Climate Models (RCMs), through the use of Representative Concentration Pathway (RCP) climate scenarios. This coupling produces climatic projections on a relatively coarse spatial scale. However, local biases are a huge problem for the use of thes projections in local-scale, especially in mountainous regions. For Switzerland, most biases have been removed by downscaling GCM-RCM coupled models to the local scale in the CH2018 project (2018). Switzerland's use and management of water resources is already impacted by a changing climate. As temperatures increase, glaciers recede and snow is present for fewer days each year, affecting both temperature and discharge of streams and rivers (FOEN (ed.), 2021). One important consideration for riverine temperature management is the tolerance threshold for aquatic life. The Swiss Water Protection Ordenance stipulates that river water may not be thermaly used once the temperature exceeds 25 °C, which is the critical temperature for the survival of the Brown Trout (FOEN (ed.), 2021).

To simulate river temperatures, one important process to include is river flow. Yet, the coupling of advanced discharge models with water temperature models and the consideration of a sufficient number of climate change projections is often unfeasible on the regional scale due to computational constraints. Here, we present a physically based, semi-empirical modelling approach with two surface water temperature models (air2stream and air2water) to provide regional projections of future river temperatures in Switzerland. Our method was first applied in Basel and has since been expanded to project future river temperature at all river stations where the Federal Office of the Environment monitores water temperature. Our approach simplifies the computation of river temperatures while maintaining local robustness by including the most important factors affecting river water temperature (i.e., air temperature, discharge variations, seasonality and river depth). We project river water temperatures based on locally downscaled climate forcings from 9 GCM, 8 RCM, 3 RCP scenarios and future river flows from 4 discharge models. Our results beeing presented spann a wide variety of river thermal types including alpine, regulated, groundwater springs, plateau, and downstream lake types.

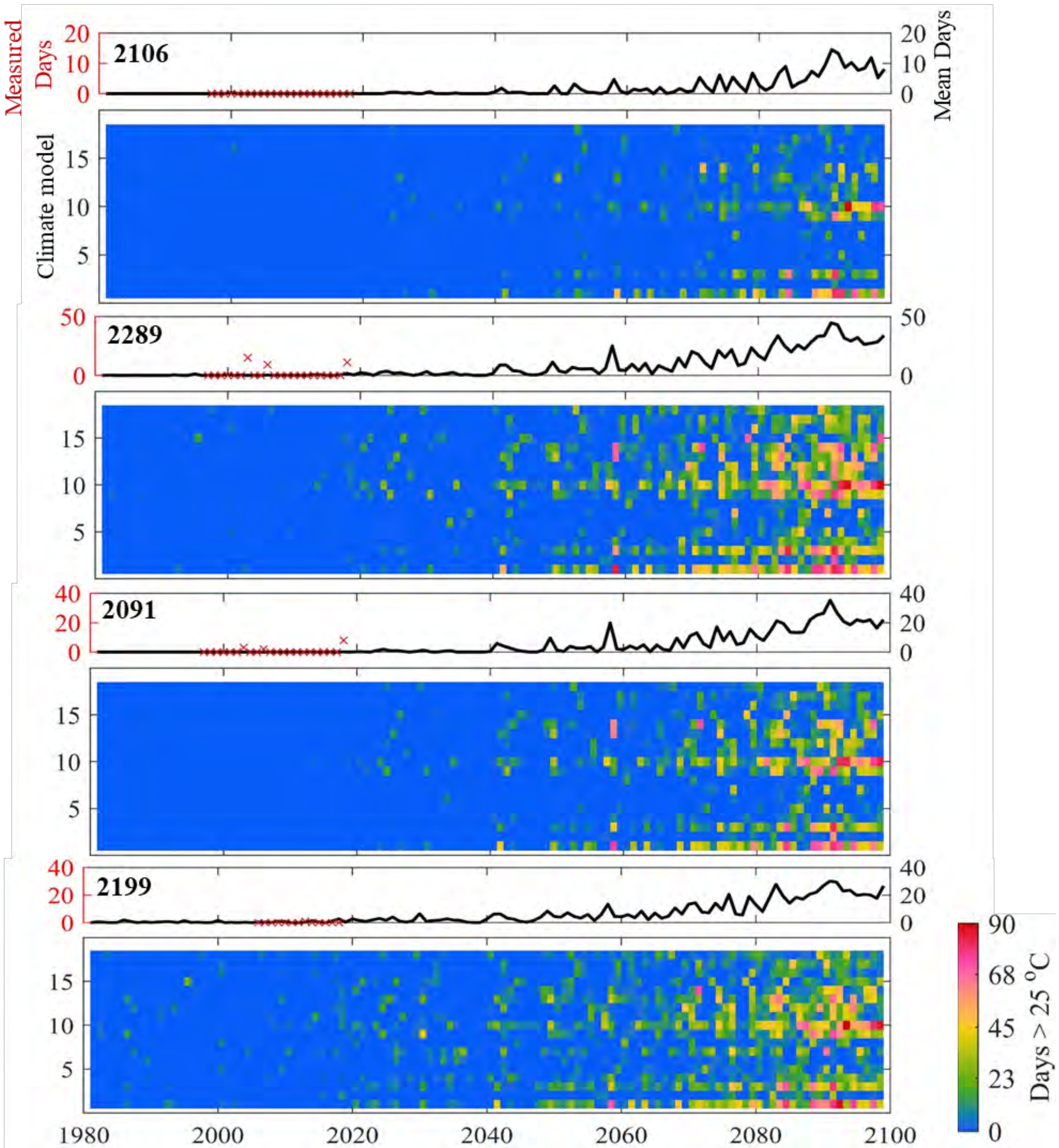

Figure 1. The total number of days per year during which river water temperatures exceed 25 °C at stations 2106 (Birs), 2289 (Rhein), 2091 (Rheinfelden) and 2199 (Wiese) for RCP8.5. Top figures: Mean threshold values from all climate models combined (black line) and from measurements (red crosses). Bottom figures: Simulation results from individual climate models (Epting et al., 2023).

REFERENCES

CH2018. 2018. CH2018 – Climate Scenarios for Switzerland, Technical Report, National Centre for Climate Services, Zurich, 271 pp. ISBN: 978-3-9525031-4-0.

Epting, J., Råman Vinnå, L., Annette, A., Stefan, S., & Schilling, O. S. 2023. Climate change adaptation and mitigation measures for alluvial aquifers - Solution approaches based on the thermal exploitation of managed aquifer (MAR) and surface water recharge (MSWR). Water Research, 238, 119988. https://doi.org/10.1016/j.watres.2023.119988

FOEN (ed.). 2021. Effects of climate change on Swiss water bodies. Hydrology, water ecology and water management. Federal Office for the Environment FOEN, Bern. Environmental Studies No. 2101: 125 p.

13.16
A model of the evolution of the water resource availability at the Glarey karstic spring in the glaciated Tsanfleuron watershed

Anthony Salamin[1,2], Philippe Renard[1], Pierre Christe[3], Gérald Favre[4], Carole Doucerain[1,5]

[1] Centre for Hydrogeology and Geothermics (CHYN), University of Neuchâtel, Rue Emile-Argand 11, 2000 Neuchâtel (philippe.renard@unine.ch)
[2] BEG - Géologie & Environnement SA, Route de la Printse, 1994 Aproz (anthony.salamin@unine.ch)
[3] Groundwater Group. Department of the Environment (SEN), Canton of Valais, Avenue de la Gare 25, 1950 Sion (pierre.christe@admin.vs.ch)
[4] Geologos SA, rte de Crassier 16, 1277 Borex (geologos@bluewin.ch)
[5] Laboratory of the ecology of natural and anthropised hydrosystems (LEHNA), Université Claude Bernard, 43 Boulevard du 11 novembre 1918, 69622 Villeurbanne Cedex (carole.doucerain@ens.psl.eu)

The Glarey spring is one of the main outlets of the Diablerets massif. The commune of Conthey in Valais taps it for its drinking water supply. This spring drains most of the Tsanfleuron lapiaz located at altitudes ranging from 2,000 to almost 3,000 meters. The upper part of the catchment is covered by a glacier that contributes to the flow of the spring. The region is subject to heavy precipitations, which can bring an annual equivalent water level of over three meters in the upper reaches of the basin. Much of this precipitation falls in the form of snow, causing high spring flow when the snowpack melts. However, this substantial snowfall cannot compensate the inexorable melting of the Tsanfleuron glacier. Its inevitable disappearance threatens to upset the hydrological and hydrogeological regime within the watershed. The objective of this work is therefore to evaluate the possible evolution of the water resources at the Glarey spring.

The research approach involves the collection of novel field data and the construction of a model able to forecast the impact of climate change scenarios. The model includes two main components (Figure 1). The hydrological component models the evolution of the Tsanfleuron glacier based on mass balance computations as a function of altitude. It uses the precipitation and temperature records measured in Sion. The hydrological model provides watershed-wide chronicles of liquid precipitation, snowmelt, and glacier melt. These chronicles are the input of the hydrogeological model that estimates the discharge rate at the Glarey spring. This component of the model includes a production function, representing the infiltration through the epikarst while taking into account the effects of evapotranspiration, and transfer function representing the hydraulic behavior of the endokarst with fast and slow flows. The model was calibrated using actual measurements and was then used to forecast future discharge using a broad range of Swiss CH18 climate scenarios. This allowed to obtain a range of possible evolutions from 2020 to 2090.

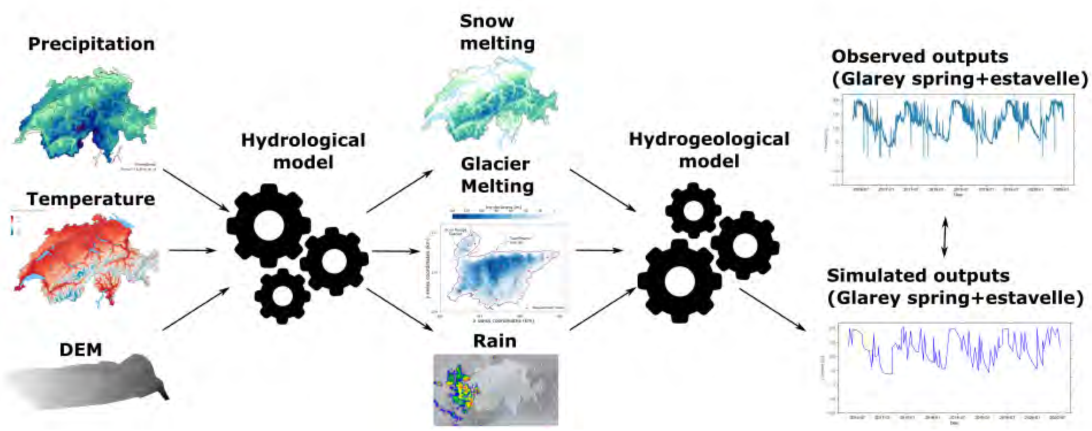

Figure 1. Illustration of hydrological and hydrogeological models used to simulate the evolution of the Glarey spring discharge.

The results show a large variability and uncertainty in the long term forecasts depending on the climate scenarios. All the models predict the complete melt of Tsanfleuron glacier. But the impact on the discharge rate at the Glarey spring is less drastic, most of the models indicate a change in the temporal distribution of the discharge:

- A reduction in summer induced by the disappearance of the glacier and the reduction of the amount of snow accumulated at high altitude.
- An increase in winter and spring due to more rain and earlier snowmelt.

But depending on the climate scenario, some models show a global reduction of the water availability while others show even an increase in water availabilty. Figure 2 shows one example of such results for the RCP8.5 scenario plotted with the MASH (Moving Average Shifted Horizon) technique.

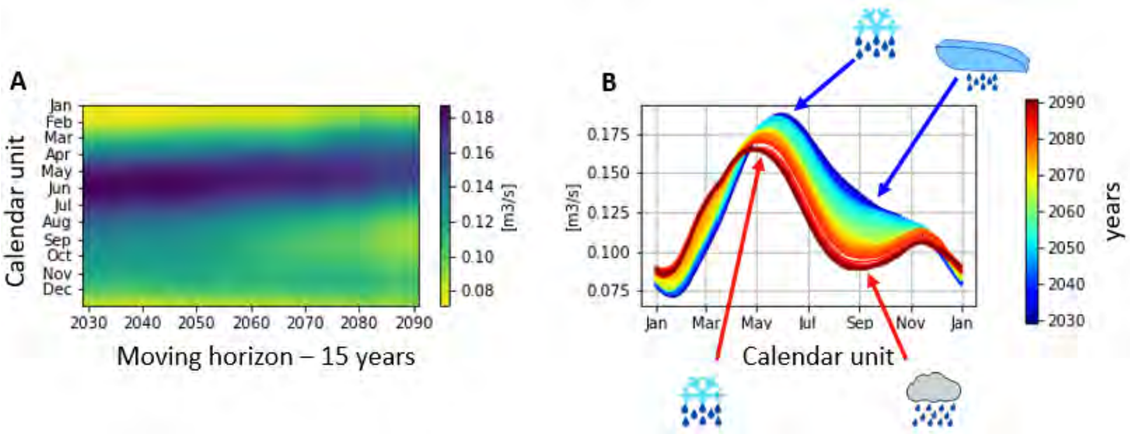

Figure 2. Example of predicted evolution of the Glarey spring discharge based on the average of the RCP8.5 scenarios. The graph B clearly shows an evolution from a nivo-glacial to a pluvio-nival groundwater regime.

13.17
Citizen-science observations made in Switzerland – Towards new horizons in regional hydrology

Jan Seibert, Sara Blanco, Mirjam Scheller, Franziska Schwarzenbach, Rieke Goebel, Ilja van Meerveld

Department of Geography, University of Zurich, Switzerland, jan.seibert@geo.uzh.ch

CrowdWater is a citizen science project in which we investigate how the public can be involved in collecting hydrological data, such as stream water levels, soil moisture conditions and the presence of water in temporary streams. Even in data-rich countries like Switzerland, these observations by the public can provide an important addition to the existing data. In CrowdWater, we also study the value of the collected data for hydrological modeling. Therefore, in several studies, we have evaluated the potential value of citizen science observations, which might be uncertain and spotty in time. The project's long-term goal is to collect many observations and thus improve the prediction of hydrological events, such as drought or flooding, by using data collected by the public in hydrological model calibration. Here, we present experiences from the CrowdWater project with regard to app-based data collection and evaluation of these data. We also highlight methods to ensure data quality, including a gamified approach and machine learning for analyzing the photos submitted through the app. Additionally, we will give an update on new activities in the CrowdWater project.

13.18
Estimating very rare floods at multiple sites in the Aare River basins with comprehensive hydrometeorological simulations

Daniel Viviroli[1], Anna E. Sikorska-Senoner[1,2], Guillaume Evin[3], Maria Staudinger[1], Martina Kauzlaric[4,5], Jérémy Chardon[6], Anne-Catherine Favre[6], Benoit Hingray[6], Gilles Nicolet[6], Damien Raynaud[6], Jan Seibert[1,7], Rolf Weingartner[4,5], Calvin Whealton[8]

[1] *Department of Geography, University of Zürich, Zürich, Switzerland*
[2] *now at: MeteoSwiss, Zürich, Switzerland & Center for Climate Systems Modeling ETH Zürich, Zürich, Switzerland*
[3] *Université Grenoble Alpes, INRAE, CNRS, IRD, Grenoble INP, IGE, Grenoble, France*
[4] *Mobiliar Lab for Natural Risks, University of Bern, Bern, Switzerland*
[5] *Oeschger Centre for Climate Change Research, University of Bern, Bern, Switzerland*
[6] *Université Grenoble Alpes, CNRS, IRD, Grenoble INP, IGE, Grenoble, France*
[7] *Department of Aquatic Sciences and Assessment, Swedish University of Agricultural Sciences, Uppsala, Sweden*
[8] *Paul Scherrer Institute, Villigen, Switzerland*

Rare to very rare floods (associated to return periods of 1000–100 000 years) can result in extensive human and economic damage. However, their estimation is limited by the comparatively short streamflow records available. Some of the limitations of commonly used estimation methods can be avoided by employing continuous simulation (CS), which considers many simulated meteorological configurations and a conceptual representation of hydrological processes. CS also avoids assumptions about antecedent conditions and their spatial patterns.

In this study, we implemented CS to estimate rare and very rare floods at 19 locations in the Aare River basin, covering an area of 17 700 km². To achieve this, we utilized exceedingly long simulations from a hydrometeorological model chain (Viviroli et al., 2022). The model chain consisted of three components: First, the multi-site stochastic weather generator GWEX produced 30 meteorological scenarios (precipitation and temperature) spanning 10 000 years each. Second, these weather generator simulations served as input for the bucket-type hydrological model HBV, run at an hourly time step for 80 catchments covering the entire Aare River basin. Third, runoff simulations from the individual catchments were routed for a representation of the entire Aare River system using the routing system model RS Minerve, including a simplified representation of main river channels, major lakes and relevant floodplains. The final simulation outputs spanned about 300 000 years at an hourly resolution, encompassing the Aare River outlet, critical points further upstream as well as the outlets of the catchments simulated with HBV. These simulation results were subsequently used to asses flood hazard and flood risk for critical infrastructure within the EXAR (Extreme flood events on the River Aare) project (Andres et al., 2021).

The comprehensive evaluation conducted over different temporal and spatial scales demonstrated that the main features of the meteorological and hydrological observations were well represented, enabling meaningful insights into low probability floods. While uncertainties were still considerable, the explicit consideration of important flood generating processes (snow accumulation, snowmelt, soil moisture storage) and routing (bank overflow, lake regulation, lake and floodplain retention) provided a substantial advantage compared to common extrapolation of streamflow records.

The suggested approach enables a comprehensive exploration of possible but unobserved spatial and temporal patterns of hydrometeorological behaviour (Figure 1). This is particularly valuable in a large river basin where the complex interaction of flows from individual tributaries and lake regulations are typically not well represented in the streamflow records. The framework is also suitable for estimating more common, i.e., more frequently occurring floods.

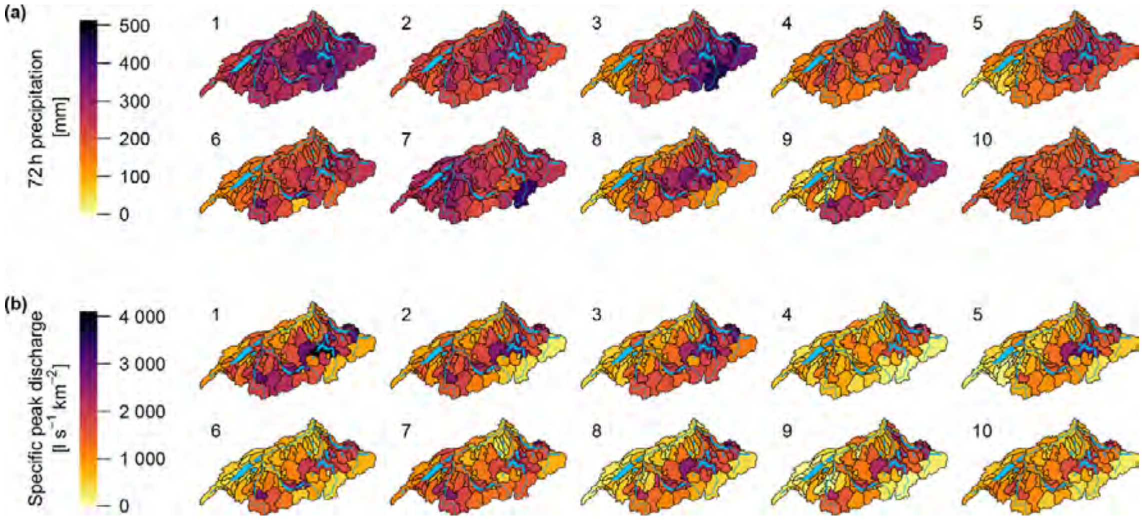

Figure 1. Patterns of cumulative precipitation (maximum 72 h sum) (a) and specific peak discharge (b) for the 10 largest peak flow events simulated at the outlet of the Aare River basin.

REFERENCES

Andres, N., Steeb, N., Badoux, A. & Hegg, C., 2021. Extremhochwasser an der Aare. Hauptbericht Projekt EXAR, Methodik und Resultate. WSL Berichte, 104. WSL, Birmensdorf. https://www.wsl.ch/de/projekte/exar-1.html

Viviroli, D., Sikorska-Senoner, A.E., Evin, G., Staudinger, M., Kauzlaric, M., Chardon, J., Favre, A.-C., Hingray, B., Nicolet, G., Raynaud, D., Seibert, J., Weingartner, R. & Whealton, C., 2022. Comprehensive space-time hydrometeorological simulations for estimating very rare floods at multiple sites in a large river basin. Natural Hazards and Earth System Sciences, 22(9), 2891–2920. https://doi.org/10.5194/nhess-22-2891-2022

13.19
Natural background concentrations in shallow Swiss aquifers

Christoph Wanner[1], Lola Camesi[1], H. Niklaus Waber[2], Stephanie Zimmermann[3], Michael Sinreich[3]

[1] *Rock-Water Interaction Group, Institute for Geological Sciences, University of Bern, Baltzerstrasse 3, CH-3012 Bern (christoph.wanner@unibe.ch)*
[2] *WaterGeoChem Consulting, CH-3013 Bern*
[3] *Federal Office for the Environment FOEN, Division Hydrology, Section Hydrogeological Basis, CH-3003 Bern*

The determination of geogenic background concentrations of dissolved constituents in groundwater is an important prerequisite to identify anthropogenic influences on the groundwater composition. In Switzerland, this is for instance accounted for by the water protection ordinance (GSchV). This ordinance defines exceptions for the numerical requirements for groundwater to be used as drinking water resource if the corresponding solutes (e.g. Cl, SO_4) originate from natural sources. Until recently, however, no systematic determination of background concentrations in shallow groundwater of Swiss aquifers has been carried out. Accordingly, in case of natural sources, the requirements for groundwater for use as drinking water could not be fully quantified.

In this contribution, we present the first nationwide determination of background concentrations for 32 inorganic parameters in shallow groundwater. The determination is based on groundwater collected in 2018 and 2019 at about 550 monitoring sites of the Swiss National Groundwater Monitoring (NAQUA), which is operated jointly by the Federal Office for the Environment (FOEN) and cantonal authorities. In a first step, the area of Switzerland was divided into 18 classes based on geographical, geological, hydrogeological and hydrogeochemical criteria. In a second step, background concentrations were determined individually for each of the 18 classes and for each of the 32 parameters using a statistical approach based on probability plots (Walter et al., 2012).

In most cases, the determined background concentrations probably correspond to the geogenic background concentrations. Exceptions include classes with a limited number of sampling locations. This is the case for the greater Geneva area, the upper Rhone and Rhine Valley, the western Jura, the main valleys in Ticino, and the crystalline parts of the Alps. For all these regions, no conclusive statement can be made about the representativeness of the determined background concentrations due to the low number of sampling locations. Furthermore, in the Swiss Molasse Basin characterized by a high population density and intensive agricultural activity, the determined background concentrations of Na, Cl, K, B, Cr, Cu, Pb, and Zn are overprinted by anthropogenic sources that cannot be separated from the geogenic background using the applied statistical method.

Despite the identified limitations, the determined background concentrations reflect the local geology very well. Since calcite occurs in all hydrogeochemical classes at least as trace mineral, Ca^{2+} and HCO_3^- are the dominating ions in almost all shallow groundwater. Depending on the mineralogical composition, however, large differences in the total mineralization and trace element concentrations occur in the different classes. NAQUA thus reflects well the chemical composition of shallow groundwater.

The determined background values are generally low and meet the requirements for groundwater to be used as drinking water resource in almost all aquifers. This also applies for the classes where an anthropogenic contribution to the background concentrations of Na, Cl, K, B, Cr, Cu, Pb, and Zn was identified. However, two potentially critical parameters remain. In aquifers of the crystalline parts of the Alps, the background concentration of arsenic locally exceeds the Swiss drinking water limit of 10 mg/L due to the natural occurrence of As-bearing minerals such as arsenopyrite. In addition, in consolidated sandstone aquifers in the western part of the molasse basin, the background concentration of Cr is locally close to the Swiss drinking water limit of 20 mg/L due to naturally occurring Cr-spinels. It follows that in these two regions, groundwater to be used as drinking water supply needs to by systematically analysed for arsenic or chromium.

To improve the representativeness of the determined background concentrations in the future, more data from the cantons and municipalities should be taken into account in addition to the data from NAQUA. Using more data from more sampling locations will also help to better separate between anthropogenic and geogenic contributions to the determined background concentrations. In any case, repeating the determination of background concentrations in the future is crucial to identify potential adverse effects of inorganic anthropogenic sources on the quality of Swiss shallow groundwater.

REFERENCE

Walter, T., Beer, A., Brose, D., Budziak, D., Clos, P., Dreher, T., Fritsche, H. G., Hübschmann, M., Marczinke, S., Peters, A., Poeser, H., Schuster, H., Wagner, B., Wagner, F., Wirsig, G., & Wolter R. 2012: Determining natural background values with probability plots. In: Groundwater Quality Sustainability Edition: IAH Selected Papers on Hydrogeology Chapter: Chapter 26. CRC Press. DOI: 10.1201/b12715-32.

13.20
From flow to snow: streamflow-based snow mass reconstruction using inverse hydrological modeling

Pau Wiersma[1], Grégoire Mariéthoz[1]

[1] *University of Lausanne, Faculty of Geosciences and Environment, Institute of Earth Surface Dynamics, Switzerland*

With climate change, rivers will contain more rainwater and less snow melt. This affects flood and drought risk, as well as the management of water resources. To quantify these changes in detail over the past decades, we need both runoff observations and daily estimates of snow melt, which in turn require spatial snow water equivalent (SWE) reconstructions. Methods to reconstruct SWE exist, but they depend on either remote sensing data or abundant in-situ observations, which limits their applicability in time (recent satellite timespans) and space (Global North) respectively. In addition, existing methods are often not assisted by or evaluated against streamflow observations, which contain valuable indirect information on the catchment-wide SWE. Without assessing whether the reconstructed SWE matches the streamflow after melting out there is limited guarantee that it respects the catchment›s mass balance.

In this study, we propose an inverse streamflow-based SWE reconstruction framework that can operate without remote sensing data or in-situ snow observations, allowing it to be applied far back in time and across different mountainous areas. As a basis, we use a distributed hydrological model with a temperature-index snow model at 1km resolution. On a year by year and catchment by catchment basis, we calibrate the inputs and parameters controlling the spatial SWE evolution (precipitation, temperature, spatially distributed melt rate) using streamflow observations. The calibration is done using the Robust Parameter Estimation (ROPE) algorithm, which narrows the parameter space across several stages of Latin Hypercube sampling and produces an ensemble of parameter sets with nearly equal likelihood rather than a single global optimum. This finally produces an ensemble of SWE scenarios that match the streamflow after melting out and therefore respect the water balance of the catchment as best as possible. As a proof of concept, we apply the framework on 5 Swiss catchments over the years 2000-2020 and evaluate it using in situ snow observations, MODIS snow cover and upstream streamflow observations. We expect the method to potentially be less efficient in simulating fine-scale variations but to be able to capture the SWE evolution well on the catchment scale at 1km resolution.

P 13.1
Simulation and calibration of headwater stream intermittency using a groundwater flow model

Ronan Abhervé[1], Clément Roques[1], Luc Aquilina[2], Philip Brunner[1], Jean-Raynald de Dreuzy[1], Laurent Longuevergne[1]

[1] *Centre for Hydrology and Geothermics (CHYN), Université de Neuchâtel, Neuchâtel, Switzerland (ronan.abherve@unine.ch)*
[2] *Univ Rennes, CNRS, Geosciences Rennes - UMR 6118, 35000 Rennes, France*

Recent research has highlighted the crucial role for ecological communities (1) and the significant prevalence of temporary streams: over 50% of the world›s rivers are temporary (2). However, the main parameters and processes involved in the stream intermittency remain poorly understood (3). The literature identifies several controlling factors, including meteorology, geology and land cover (4), but a major challenge remains: understanding the role of the subsurface, i.e. the effect of the aquifer›s hydraulic properties (5).

In line with the new definition of an intermittent river (6), "*a non-perennial river or stream with a considerable connection to the groundwater table, having variable cycles of wetting and flow cessation, and with flow that is sustained longer than a single storm event*", we use a 3D process-based groundwater flow model at the catchment-scale to simulate stream flow and the spatio-temporal extension/contraction of the hydrographic network. Focusing on two crystalline catchments in Brittany (northwest France), with a similar temperate climate, we explore the combined effect of hydraulic conductivity K (transmission capacity) and porosity θ (storage capacity). We propose a calibration approach with performance criteria based solely on surface information: 1) stream flow measured at the catchment outlet and 2) mapping of the observed hydrographic network (7) (for the low-water period: perennial streams and for the high-water period: perennial + intermittent streams).

The calibration results show that the methodology leads to an optimal aquifer model for the 2 catchments (Canut: $K = 4.5 \times 10^{-5}$ m/s, θ = 0.1% and Nancon:
$K = 1.5 \times 10^{-5}$ m/s, θ = 2.2%). For both catchments, the comparison of simulated versus observed stream flow, focusing on low flows, achieves an excellent $NSE_{log}>0.86$. At the same time, the model reproduces very well the hydrographic network observed during both high and low water periods (Figure 1), resulting in a very good success criterion. Finally, the models are validated using data from discrete visual monitoring of stream hydrological conditions (national ONDE network).

Based on these modelling results, we then discuss hydrogeological controls such as the role of aquifer storage capacity on headwater stream intermittency. We believe that the use of stream intermittency mapping, benefiting from innovations in crowdsourcing and remote sensing, will address the need for hydrological models and predictions for ungauged basins.

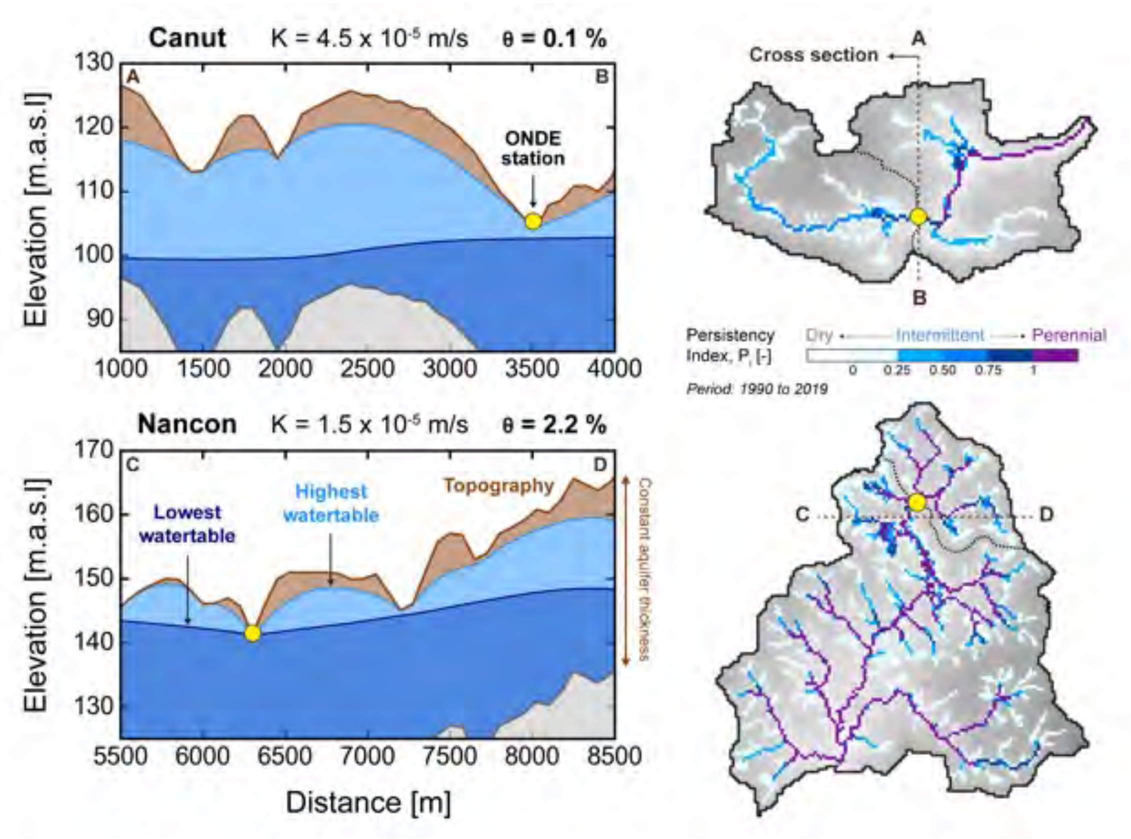

Figure 1. Simulation results for the calibrated model for the two catchments studied, the Canut and the Nancon. Left panels: cross-section of simulated maximum (high water) and minimum (low water) groundwater levels. Right panels: persistency index map (probability of water occurrence) calculated from simulation results between 1960 and 2019.

REFERENCES

1. Datry T, Larned ST, Tockner K. Intermittent rivers: A challenge for freshwater ecology. Bioscience. 2014;64(3):229–35.
2. Messager ML, Lehner B, Cockburn C, Lamouroux N, Pella H, Snelder T, et al. Global prevalence of non-perennial rivers and streams. Nature. 2021 Jun 17;594(7863):391–7.
3. Fovet O, Belemtougri A, Boithias L, Braud I, Charlier JB, Cottet M, et al. Intermittent rivers and ephemeral streams: Perspectives for critical zone science and research on socio-ecosystems. Wiley Interdiscip Rev Water. 2021;8(4):1–33.
4. Costigan KH, Jaeger KL, Goss CW, Fritz KM, Goebel PC. Understanding controls on flow permanence in intermittent rivers to aid ecological research: integrating meteorology, geology and land cover. Ecohydrology. 2016;9(7):1141–53.
5. Shanafield M, Bourke SA, Zimmer MA, Costigan KH. An overview of the hydrology of non-perennial rivers and streams. Wiley Interdiscip Rev Water. 2021;8(2):1–25.
6. Busch MH, Costigan KH, Fritz KM, Datry T, Krabbenhoft CA, Hammond JC, et al. What's in a Name? Patterns, Trends, and Suggestions for Defining Non-Perennial Rivers and Streams. Water. 2020;1–19.
7. Abhervé R, Gauvain A, Roques C, Longuevergne L, Louaisil S, Aquilina L, et al. Calibration of groundwater seepage on the spatial distribution of the stream network to assess catchment-scale hydraulic conductivity. Hydrol Earth Syst Sci Discuss. 2022;(Preprint):1–26.

P 13.2
Detection of hydrogen peroxide after hydraulic stimulation of granitic bedrock at the Bedretto Tunnel

Andrew Acciardo[1], Nima Gholizadeh[1], Maria Mesimeri[1], Luca Scarabello[1], Marian Hertrich[1], Cara Magnabosco[1]

[1] Department of Earth Sciences, ETH Zurich, Sonneggstrasse 5, CH-8092 Zurich (andrew.acciardo@erdw.ethz.ch)

Earthquakes and other seismicity-inducing events grind up and crush rocks in the subsurface. In the presence of water, this process can initiate a mechanoradical reaction that results in the formation of reactive oxygen species (ROS), including hydrogen peroxide. For the anaerobic microorganisms that live in the subsurface, exposure to these oxidants presents a potential threat to their existence, as ROS can cause cell damage that may eventually lead to cell death. Laboratory based experiments have demonstrated that H_2O_2 can be derived from this water-rock reaction, but field evidence is lacking. To evaluate whether cataclastic H_2O_2 production is observable in a deep groundwater reservoir, can be measured following induced seismicity, a hydraulic stimulation experiment was performed in the Bedretto Lab Deep Life Observatory (Ticino, Switzerland). In this experiment, 5.25m^3 of water was injected into a packer-isolated interval of a borehole, which led to measurable deformation in the surrounding reservoir and over 3,000 seismic events (maximum Magnitude -3.0) within a total volume of 26,000,000m^3. Fluorometric analysis of water samples taken from the flow-back of the interval indicate an increase in H_2O_2 concentrations relative to both baseline levels and levels after a less intense hydraulic stimulation experiment that produced an order of magnitude less seismic events. Peak H_2O_2 concentrations in flow-back fluids reached approximately 1.7μM during the stimulation. These experiments demonstrate that seismicity-related increases in H_2O_2 are able to be measured in-situ. Whether the observed change in H_2O_2 can be attributed directly to water-rock interactions will be verified with additional laboratory-scale experiments, which will also enable a more precise quantitative understanding of the amount of H_2O_2 produced during fracturing. The abiotic production of H_2O_2 in the deep subsurface, along with other molecules including H_2 and O_2, may have played an important role in the origin of life as well as in the ability of microorganisms to exist in such an energy-poor environment. These studies will help illuminate the influence of mechanoradical ROS production for life on Earth as well as potential life on planets and moons in our solar system and beyond.

P 13.3
Towards a metabolic theory of catchments: scaling of water and carbon fluxes with size

Francesca Bassani[1], Simone Fatichi[2], Sara Bonetti[1]

[1] *Laboratory of Catchment Hydrology and Geomorphology, EPFL Valais Wallis, Route des Ronquos 86, CH-1951 Sion, Switzerland (francesca.bassani@epfl.ch)*
[2] *Department of Civil and Environmental Engineering, National University of Singapore Institut, 1 Engineering Drive 2 Block, E1A #07-03, Singapore*

Catchments are heterogeneous ecosystems involving several abiotic and biotic processes, where the mutual interactions among water, vegetation, and biogeochemical fluxes take place at different scales.

Many biological processes in nature are characterized by allometric scaling relationships (Brown, 2004), which postulate that a biological variable B (e.g., the metabolic rate of an organism) scales with its mass M to the power of a scaling exponent ranging between 3/4 and 2/3 (West, 1997; da Silva, 2006).

Few studies adopted scaling laws to describe the metabolism of ecosystems including forests (Enquist, 2017) and river basins (Rodriguez-Iturbe, 2011), although at the catchment and regional scales these dynamics remain largely unexplored.

Our analysis goes towards this direction, with the aim of finding a feasible reduced-order framework relating key water and carbon fluxes to the catchment's physical and geometrical properties. Supported by hyper-resolution ecohydrological simulations covering the whole European Alps (Mastrotheodoros, 2020) and remote sensing data, we identify allometric scaling relationships linking water and carbon dynamics (e.g., transpiration, gross primary productivity, carbon use efficiency) to topographic catchment properties (e.g., contributing area), respectively acting as proxies for the catchment metabolic rate B and mass M.

These results reveal that drainage basins can be seen as complex biological systems whose dynamics follow similar scaling relations.

REFERENCES

Brown, J. H. (2004). Toward a metabolic theory of ecology. *Ecology*, 1771-1789.
da Silva, J. K. (2006). Allometric scaling laws of metabolism. *Physics of Life Reviews*, 229-261.
Enquist, B. J.-R. (2017). Assessing trait-based scaling theory in tropical forests spanning a broad temperature gradient. *Global Ecology and Biogeography*, 1357--1373.
Mastrotheodoros, T. a. (2020). More green and less blue water in the Alps during warmer summers. *Nature Climate Change*, 155-161.
Rodriguez-Iturbe, I. a. (2011). Metabolic principles of river basin organization. *Proceedings of the National Academy of Sciences*, 11751-11755.
West, G. B. (1997). A general model for the origin of allometric scaling laws in biology. *Science*, 122-126.

P 13.4
Tidal characterization of the Liappey fractured aquifer, Bagnes (VS)

Céleste Belloni[1], Benoît Valley[1], Clément Roques[1]

[1] *Centre for Hydrogeology and Geothermics, University of Neuchâtel, Rue Emile Argand 11, CH-2000 Neuchâtel (celbelloni@gmail.com)*

Solid Earth tides have had an increased use in hydrogeology to characterize aquifers and wells. The Liappey fractured aquifer has shown a strong response to tides through the CHA-1 well. The Earth tides strain cyclically closes and opens up the fractures, increasing and decreasing pore pressure. The increase in pore pressure causes higher discharge at the well.

The aquifer, a fractured ante-Permian gneiss, was the object of geothermal investigations by the Bagnes commune, and the artesian CHA-1 bore was drilled. This work's main focus is the use of tidal analysis to infer aquifer properties, fracture orientation and understand the flow dynamics. The goal is to explore different models and methods in tidal analysis and verify their use for the CHA-1 well. To this end, the discharge of the flowing well was continuously monitored for a 6-month duration (in addition to discharge data from 2017), and logging (optical and flow log) was performed in the well.

The logging exhibits a well with importantly damaged walls, as well as large collapses; and a general SE dip direction of the fracturation, with principally subvertical fractures. The tidal analysis reveals that there is a large discrepancy between the discharge response to tides in 2017 against 2023, including the phase shift going from negative to positive. In the end, the analysis leads to the interpretation that the flow in the Liappey well-aquifer system has evolved from a horizontally dominated permeability to a bi-directional permeability, with a sharp increase in vertical flow, probably associated with degradation of the cementing around the well, resulting in an increase in vertical exchanges between the waters of the Quaternary sediments and those of the fractured aquifer.

Moreover, the use of tidal analysis permitted the estimation of the orientation of the average hydraulic transmission in the aquifer, yielding results congruent with the fracturation analysis from the logging, demonstrating that this passive method is promising for fracture orientation estimation.

P 13.5
ALPLAKES: Advancing Lake Research and Management through Integrative Remote Sensing and Hydrodynamic

Damien Bouffard[1,2] , Marina Amadori[3], Mariano Brescani[3], Claudia Giardino[3], Daniel Odermatt[1], Abolfazl Irani Rahaghi[1,4] , James Runnalls[1], Marco Toffolon[5] , Mortimer Werther[1]

[1] *Eawag, Swiss Federal Institute of Aquatic Science & Technology, Surface Waters – Research and Management, Kastanienbaum, Switzerland*
[2] *Faculty of Geosciences and Environment, Institute of Earth Surface Dynamics, University of Lausanne, Lausanne, Switzerland*
[3] *Institute for Electromagnetic Sensing of the Environment (IREA), National Research Council of Italy (CNR), 20133 Milan, Italy*
[4] *Department of Geography, University of Zurich, 8057 Zurich, Switzerland*
[5] *Department of Civil, Environmental and Mechanical Engineering, University of Trento, Italy*

The ALPLAKES initiative aims at advancing in lake research and management, building upon the achievements of the previous Meteolakes (ESA SEOM S2-4Sci Land and Water, http://meteolakes.ch/) project. Meteolakes pioneered the integration of satellite Earth observation and hydrodynamic modeling, exemplified by the web-centric platform Meteolakes, which has engaged over 600,000 users since 2016. ALPLAKES progresses this approach, expanding from the foundational Meteolakes platform to encompass twelve Alpine lakes spanning altitudes from 60 to 1800 meters above sea level. Utilizing Sentinel-2 products, ALPLAKES combines remote sensing data with hydrodynamic models, enhancing the predictive capabilities of the models. Light penetration maps from Sentinel-2 play a crucial role in inputting solar radiation distribution on the hydrodynamic model and thereby impacting lake thermal evolution. Maps of total suspended matter (another Sentinel-2 product) provide visible space-borne patterns, which are incorporated into hydrodynamic models using particle tracking techniques. This method, initially developed for Sentinel-2's total suspended matter product, holds potential for various other products such as chlorophyll, oil spills, or RGB composites, provided constituent proliferation rates are negligible within the chosen timeframe. The outcomes are openly accessible through the new web-based platform (release date oct. 2023).

P 13.6
On the scaling relationship between grain-size, riverbed slope and catchment area at the reach scale

Giulio Calvani[1], Virginia Ruiz-Villanueva[2], Massimiliano Schwarz[3], Paolo Perona[1]

[1] *Platform of Hydraulic Constructions PL-LCH (IIC-ENAC), Ècole Polytechnique Fédérale de Lausanne, Lausanne, Switzerland (giulio.calvani@epfl.ch)*
[2] *Institute of Earth Surface Dynamics, University of Lausanne, Switzerland*
[3] *Forestry Department, Bern University of Applied Sciences, Zollikofen, Switzerland*

Since the 1950s, several authors have attempted to model the scaling relationships among geometrical and hydro-morphological characteristics of fluvial streams at different spatial scales (i.e., section, reach or catchment). For instance, flow discharge, water depth, river width, and channel slope have been related each other for gravel-bed (Parker et al., 2007) and sand-bed (Wilkerson & Parker, 2011) rivers in bankfull condition, based on a dimensionless approach at the cross-sectional scale. At a much larger scale (i.e., the catchment scale), relationships between drainage area, bed slope and mean grain size diameter have been proposed by several authors (e.g., Hack, 1957). However, the literature lacks proper explanation for such empirical formulations. In this work, we derived an equation relating catchment area, mean grain size and channel bed slope, based on physically-based formulations available in the literature and a flow discharge-catchment area relationship valid in bankfull conditions. As a result, the proposed model mathematically explains the existing link between geomorphological characteristics and hydrological quantities observable in mountain streams at equilibrium conditions. For the sake of comparison, we successfully tested the derived relationship against the dataset of river measurements of Hack (1957) and an additional dataset for different rivers (e.g., Wohl & Wilcox, 2005). The proposed relationship may be applied to infer catchment-scale characteristics based on local (reach-scale) measurements.

REFERENCES

Hack, J. T. (1957). Studies of longitudinal stream profiles in Virginia and Maryland (Vol. 294). US Government Printing Office.

Parker, G., Wilcock, P. R., Paola, C., Dietrich, W. E., & Pitlick, J. (2007). Physical basis for quasi-universal relations describing bankfull hydraulic geometry of single-thread gravel bed rivers. Journal of Geophysical Research: Earth Surface, 112(F4).

Wilkerson, G. V., & Parker, G. (2011). Physical basis for quasi-universal relationships describing bankfull hydraulic geometry of sand-bed rivers. Journal of Hydraulic Engineering, 137(7), 739-753.

Wohl, E. E., & Wilcox, A. (2005). Channel geometry of mountain streams in New Zealand. *Journal of hydrology*, *300*(1-4), 252-266.

P 13.7
Tree planting as a nature-based solution for urban flooding in Nouakchott City, Mauritania

Emmanuel Dubois[1], Montana Marshall[1], Fatimatou Boukhreiss[2], Saleck Ahmed Cherif[2], Grégoire Mariéthoz[3], Charlotte Grossiord[4], Paolo Perona[1]

[1] *Platform of Hydraulic Constructions (PL-LCH), Civil Engineering Department, Ecole Polytechnique Fédérale de Lausanne (EPFL), Station 18, 1015 Lausanne, Switzerland (emmanuel.dubois@epfl.ch)*
[2] *Région de Nouakchott, avenue Bacar Ould Soueid'Ahmed, B.P. 5203, Nouakchott, Mauritania*
[3] *Institute of Earth Surface Dynamics (IDYST), University of Lausanne, UNIL-Mouline, Geopolis, 1015 Lausanne, Switzerland*
[4] *Plant Ecology Research Laboratory (PERL), Civil Engineering Department, Ecole Polytechnique Fédérale de Lausanne (EPFL), Station 2, 1015 Lausanne, Switzerland*

Nouakchott City has been facing constant flooding for more than a decade, making part of the city inhabitable and posing long-term health threats. Within the city, a shallow groundwater table had relatively constant groundwater levels due to sea intrusion. However, the infiltration of most of Nouakchott's used water since the establishment of a new domestic water supply in 2010 has acted as artificial aquifer recharge, resulting in a rise of groundwater levels that reached the topographic surface in the low-lying parts of the city. This surge in groundwater, coupled with a decrease in already limited soil water storage, causes the city's flooded area to double during the rainy season spanning July to September. The goal of this project is to assess how tree planting could increase Nouakchott's resilience against urban flooding by lowering the water table level. This nature-based solution would be advantageously oriented toward sustainable development as it would be a low-cost and multi-benefit solution. An integrated tree planting strategy could enhance the provision of services for the people, the economy, and biodiversity (e.g., shade in the streets, potential fruit harvesting, livestock food production, green habitats...). Consequently, this work presents a joined interdisciplinary ecohydrology and plant physiology approach for monitoring and modelling the transpiration and dewatering capacity of diverse local tree species. Given the exceptionally challenging conditions for vegetation, characterized by a hot desert climate and an available shallow water table with brackish water, the annual dynamics of trees and transpiration remain highly uncertain. In order to quantify and simulate the impact of tree planting scenarios, five tree species found in Nouakchott were identified as salt-tolerant and selected as potential candidates for this nature-based solution. Since February 2023, the transpiration rates of the selected tree species have been monitored using sap flow meters. Furthermore, as knowledge regarding groundwater dynamics was limited, five observation wells have been equipped with automatic water depth sensors to facilitate long-term data collection and a spatio-temporal time series of the city's flooded areas was reconstructed using an innovative methodology based on remote sensing data. Based on these preliminary results, the proposed tree planting solution is being analyzed through a SWOT approach (strengths, weaknesses, opportunities, and threats). This holistic approach ensures comprehensive consideration of all transdisciplinary aspects associated with the endeavour, which we present and discuss in this work.

P 13.8
Lake archives from tropical Africa: Reconstructing the paleoclimate leading to the African Rainforest Crisis 3000 years ago

Michelle Engelhardt[1], Jordon Hemingway[1], Antoine de Clippele[2], Alfred Ludjwera[3], Negar Haghipour[1,4], Johan Six[2]

[1] *Geological Institute, ETH Zürich, Sonneggstrasse 5, 8092 Zurich, Switzerland (mengelhardt@erdw.ethz.ch)*
[2] *Department of Environmental Systems Science, ETH Zürich, Universitätsstrasse 2, 8092 Zurich, Switzerland*
[3] *Institut Supérieur des Techniques Appliqués (ISTA), 3930 Aérodrome, Kinshasa/N'dolo, Democratic Republic of Congo*
[4] *Ion beam Physics, ETH Zürich, Otto-Stern-Weg 5, 8093 Zurich, Switzerland*

The second largest rainforest biome on Earth lies in the Congo Basin in central Africa. However, due to slash-and-burn farming practices as well as climate change, the rainforest is quickly contracting. Interestingly, former studies have found evidence for a similar so-called "African Rainforest Crisis" taking place in the late Holocene around 3000 years ago (Brncic et al. 2009; Garcin et al. 2018). There are indicators assigning this crisis to the expansion of the Bantu people, who are believed to have migrated to this area to pursue extensive farming at this time. Pollen records, on the contrary, speak for a shift towards a drier climate as the primary mechanism inducing the crisis. Since data from this area are scarce, more information is needed to resolve the exact causes of the African Rainforest Crisis, especially as it is a likely analog for ongoing and future rainforest contraction.

To provide such information, we collected about 30 m of core from in sum 13 lakes along the rainforest-savannah boundary in the Kasaï Basin, Democratic Republic of Congo, which constitutes the southwest portion of the Congo Basin. We use bulk radiocarbon measurements to develop age models of the sediment records. Additionally, XRF data will offer insights on the underlying mineralogy. By using the mineralogy as an indicator of the weathering degree, we expect to draw conclusions on the hydrology and temperature throughout the late Holocene. To further constrain the paleoclimate reconstructions, XRD, pollen and triple-oxygen isotope analysis on the clay-size fraction are planned. A holistic interpretation will aim to reveal the role of climate change as a trigger of the African Rainforest Crisis.

This work is part of a larger project which is the first to study the erosion dynamics from source to sink in the Kasaï region. The ultimate goal is to combine data from the uplands, floodplains, rivers, and lakes to further constrain estimates of this ecosystem's net carbon balance through time and to better predict how the Congo rainforest will respond to today's land use- and climate-triggered challenges.

REFERENCES

Brncic, T. M., Willis, K. J., Harris, D. J., Telfer, M. W., & Bailey, R. M. 2009: Fire and climate change impacts on lowland forest composition in northern Congo during the last 2580 years from palaeoecological analyses of a seasonally flooded swamp, The Holocene, 19(1), 79–89.

Garcin, Y., Deschamps, P., Ménot, G., de Saulieu, G., Schefuß, E., Sebag, D., Dupont, L. M., Oslisly, R., Brademann, B., Mbusnum, K. G., Onana, J.-M., Ako, A. A., Epp, L. S., Tjallingii, R., Strecker, M. R., Brauer, A., & Sachse, D. 2018: Early anthropogenic impact on Western Central African rainforests 2,600 y ago, Proceedings of the National Academy of Sciences, 115(13), 3261–3266.

P 13.9
Quantifying the sensitivity of groundwater to climate variations in Australia

Xinyang Fan[1,6,7,8], Tim Peterson[2,1], Benjamin Henley[3,4,5,1], Meenakshi Arora[1]

[1] *Department of Infrastructure Engineering, University of Melbourne, 700 Swanston St, VIC 3053, Melbourne, Australia*
[2] *Department of Civil Engineering, Monash University, Wellington Rd, VIC 3800, Melbourne, Australia*
[3] *School of Earth, Atmosphere and Life Sciences, University of Wollongong, Northfields Ave, NSW 2522, Wollongong, Australia*
[4] *Securing Antarctica's Environmental Future, Monash University, Wellington Rd, VIC 3800, Melbourne, Australia*
[5] *ARC Centre of Excellence of Climate Extremes, Monash University, Wellington Rd, VIC 3800, Melbourne, Australia*
[6] *Institute of Applied Geosciences, Karlsruhe Institute of Technology, Adenauerring 20b, 76131, Karlsruhe, Germany*
[7] *now at Institute of Geography, University of Bern, Hochschulstrasse 6, 3012, Bern, Switzerland*
[8] *now at Faculty of Civil, Geo and Environmental Engineering, Technical University of Munich, Arcisstraße 21, 80333, Munich, Germany (xinyang.fan@tum.de)*

Climate change is projected to impact groundwater availability in many regions globally but the projections are highly uncertain. Quantifying the historic impact contributes to an improved understanding of the climate change impact but has been rarely studied, primarily because of limited groundwater records and influences of multiple drivers, such as pumping for agricultural irrigation and land use changes. This study aims to understand the risks to groundwater by estimating the sensitivity of groundwater level and recharge to climate variations across Australia. More than 4000 groundwater sites in the country were first modelled with a time-series groundwater modeling toolbox *HydroSight* to identify the sites, where >80% of the groundwater level fluctuations have been driven by climate variations alone. A multiple linear regression approach was then applied to quantify the groundwater level and recharge sensitivity to precipitation and potential evapotranspiration at the identified climate-dominated sites. Results show that groundwater level and recharge are around 8 times more sensitive to precipitation than to evapotranspiration variations. The head sensitivity shows to be higher at the sites located in the arid climates and porous media than those in the tropical climates and fractured media, and contrarily for the recharge sensitivity. Land use however shows a modest impact on the sensitivity. These findings allow for an essential first-order estimate of climate change impact on groundwater and understanding the governing factors of groundwater response.

P 13.10
Evaluating riparian vegetation removal due to morphodynamic processes in the river Thur

Kilian Feller[1,2], Giulio Calvani[1], Francesco Caponi[2], Paolo Perona[1]

[1] *Platform of Hydraulic Constructions PL-LCH (IIC-ENAC), Ècole Polytechnique Fédérale de Lausanne, Lausanne, Switzerland (kilian.feller@epfl.ch)*
[2] *Laboratory of Hydraulics, Hydrology and Glaciology, ETH Zurich, Zurich, Switzerland*

The dynamics of riparian vegetation in a fluvial environment are characterized by numerous both positive and negative feedbacks with the hydrology of the river. Vegetation influences the flow field, the sediment transport, and the morphodynamics, whereas the hydrology of the river has an influence on the vegetation growth and can cause flood-induced mortality due to either burial or uprooting. In this work, the applicability of the physically based stochastic uprooting model for riparian vegetation by Perona and Crouzy (2018) is discussed. The results of the uprooting model are compared to field studies performed in 2009 and 2010 by Pasquale et al. (2014) on a gravel island of the river Thur restored corridor. For this field study, willow cuttings were planted all across the island, and their evolution was systematically monitored over the growing season. We perform 2D morphodynamic simulations (with BASEMENT v2.8.2) of the seasonal floods occurring in the study reach, and use model's results to produce a comparison of the empirical statistics against the theoretical one predicted by Perona and Crouzy (2018). This model considers plant uprooting by flow occurring as a result of the stochasticity affecting the erosion process and the plant rooting depth. The uprooting model depends, aside from the erosion, on two input parameters that were not directly measured in the field study, the critical erosion depth and the variance of the erosion. The critical erosion depth had to be approximated from literature formulae, and the variance of the erosion was calibrated. The results of the morphodynamic simulation are sufficiently accurate for 2009, whereas substantial differences between the simulated and the measured bed level changes exist for 2010. This discrepancy between the simulation and the measurements is explained by the high number of floods that had to be simulated in 2010. The comparison of the uprooting model with the data from the field study shows a high model performance (R^2 = 0.68) for 2009, where the erosion input data is accurate, but almost no predictive power in 2010 with the inaccurate erosion input data (R^2 = 0.06). To this regard, the uprooting model by Perona and Crouzy (2018) is then compared to the performance of two additional simplified models (e.g., one purely deterministic and one conceptual). We show that the model by Perona and Crouzy (2018) still outperforms the simplified models for the accurate input data but displays predictive power in the same range as the simplified models in the case of the inaccurate morphodynamic simulation in 2010.

REFERENCES

Pasquale, N., Perona, P., Francis, R., & Burlando, P. (2014). Above-ground and below-ground Salix dynamics in response to river processes. Hydrological Processes, 28 (20), 5189–5203.

Perona, P., & Crouzy, B. (2018). Resilience of riverbed vegetation to uprooting by flow. Proceedings of the Royal Society A: Mathematical, Physical and Engineering Sciences, 474 (2211), 20170547.

P 13.11
The RADMOGG Project (2023-2027): Resilience and Dynamics of Mountain Groundwater using Gravimetry

Landon J.S. Halloran[1,*], Nazanin Mohammadi[1], Ronny Figueroa[1], Antoine Carron[1], Fernando Gutierrez[1], Daniel Hunkeler[1], Philip Brunner[1], Marie Arnoux[2] & Henri Baumann[3]

[1] *Centre d'hydrogéologie et de géothermie (CHYN), Université de Neuchâtel, Neuchâtel (NE).*
[2] *Centre de recherche sur l'environnement alpin (CREALP), Sion (VS).*
[3] *Federal Institute of Metrology (METAS), Bern-Wabern (BE).*
[*] *landon.halloran@unine.ch*

RADMOGG is a new SNSF-funded project that will strengthen the use of hydro-gravimetric methods in hydrogeology and will deepen our comprehension of hydrogeological processes in mountain catchments. Alpine catchments are increasing in importance for water supply, yet are also critically impacted by climate change. Groundwater in alpine catchments will progressively play a more critical role in ensuring perennial streamflow down-gradient, yet these catchments remain under-monitored. Furthermore, the data value of direct, single-point piezometric measurements is especially low in these catchments due to their inherent heterogeneity and extreme seasonal changes.

To address this knowledge and monitoring gap, RADMOGG will develop a numerical method for the assimilation of time-lapse gravimetry (TLG) data into groundwater models. Correspondingly, it will quantitatively evaluate the value of gravimetric data in reducing uncertainty in hydro(geo)logical models. Based on these methodological developments, it will quantify, in a spatially-resolved way, groundwater export from mountain catchments. Finally, it will use numerical methods to evaluate the role and limits of groundwater in ensuring hydrological resilience in the face of climatic stress.

RADMOGG is both a numerical- and field-focused project. It involves two field sites: *Tsalet* (VS), an alpine headwater catchment with hydrogeological heterogeneity where groundwater plays a crucial role in streamflow dynamics, and *Röthenbach* (BE), a subalpine basin characterised by substantial temporal variability in subsurface water storage within its alluvial aquifer. The outcomes of this project will provide quantitative insights that will inform future water management strategies in mountainous regions in the face of climate change.

P 13.12
A machine-learning approach to predict overland flow impacts

Pascal Horton[1], Markus Mosimann[1], Severin Kaderli[1], Olivia Martius[1], Andreas Paul Zischg[1]

[1] Mobiliar Lab for Natural Risks, Oeschger Centre for Climate Change Research (OCCR), Institute of Geography, University of Bern, Hallerstrasse 12, CH-3012 Bern (pascal.horton@unibe.ch)

While overland flow events are responsible for frequent and costly damages, they only recently became a focus for research and a target for insurance companies. Here, as a follow-up of the work of Bernet et al. (2019), we focus on an impact-based approach, using aggregated damage claims related to surface water floods recorded by the Mobiliar insurance company. Based on data-driven approaches, we aim to predict the probability of occurrence of such damages using precipitation data and features characterizing local conditions.

The CombiPrecip precipitation dataset, which is a combination of radar and gauges data at an hourly time step and with a 1 km^2 resolution, has been used to build a catalog of precipitation events for each of its pixels and over the period 2013-2022. Events were defined by a precipitation total above 10 mm separated by a period of at least 8 hours without precipitation (> 0.1 mm/h). The damage data were aggregated to the same resolution. In addition, static terrain properties were derived for each pixel and consist of the slope, aspect, plan, profile, and total curvature, flow accumulation, land cover (percentage of 12 land cover classes), and the percentage of the pixel covered by the national overland flow map. The terrain and flow accumulation features were computed at different resolutions (10, 25, 100, and 250 m) and aggregated to the 1 km^2 cells by computing the mean, median, minimum, maximum, and standard deviation of the values.

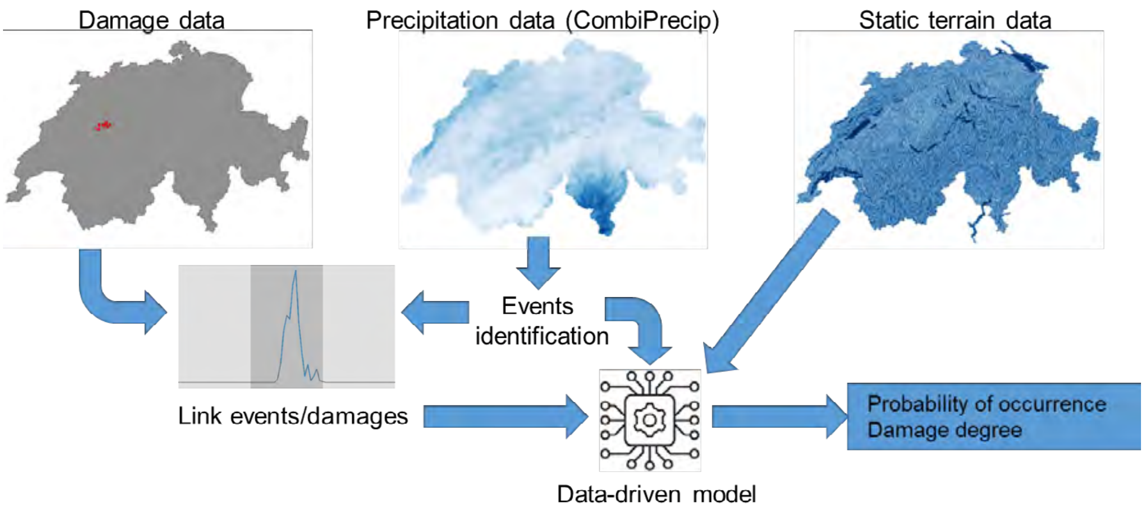

Figure 1. Illustration of the different components of the data-driven model for the prediction of damages related to overland flow.

A random forest model has been trained using these terrain features in addition to the event characteristics (mean and maximum intensity, precipitation sum, antecedent precipitation index, and three temporal properties). The most important features identified by the random forest model are related to the event properties, the number of contracts per cell, the urban land cover type, and to a minor extent some terrain properties. Although the random forest improves on previous work that was done in a similar context, we feel that we are limited by the tabular-type approach and are heading toward a model that better accounts for spatio-temporal patterns, such as a convolutional neural network (CNN).

REFERENCES

Bernet, D. B., Trefalt, S., Martius, O., Weingartner, R., Mosimann, M., Röthlisberger, V., & Zischg, A. P. 2019: Characterizing precipitation events leading to surface water flood damage over large regions of complex terrain. Environmental Research Letters, 14(6), 64010. https://doi.org/10.1088/1748-9326/ab127c

P 13.13
The Federal Drought Monitoring and Warning System

V. Humphrey[1], F. Hüsler[2], D. Oesch[3], S. Bircher[1], J. Sturm[3], C. Scapozza[2]

[1] *Federal Office of Meteorology and Climatology MeteoSwiss*
[2] *Federal Office for the Environment*
[3] *Federal Office of Topography swisstopo*

In May 2022, the Swiss Federal Council mandated the Federal Office for the Environment (FOEN), MeteoSwiss and swisstopo to jointly develop a national monitoring, early detection, and warning system for drought. This new platform is scheduled to first go into operation on January 1, 2025 and aims at providing comprehensive information on historical, current, and forecasted drought conditions in Switzerland. Within this project, a new web portal will be established integrating the "drought.ch" platform from the Swiss Federal Institute for Forest, Snow and Landscape Research (WSL). It will primarily support decision-making by cantonal and regional authorities, and provide relevant information to critically impacted economic sectors. The platform will be further developed and improved over the coming decades, in collaboration with the user community and Swiss research institutions. In this contribution, we provide an overview of the project organization and ongoing activities, including some of the envisaged new climatological and hydrological products, as well as satellite-based data streams, that are also expected to benefit research applications. FOEN is leading the program and coordinates efforts to establish the web platform and implement warnings. Furthermore, FOEN will be responsible for the hydrological monitoring and modeling, and the impacts on forestry. MeteoSwiss will develop a national soil moisture monitoring network, new climatological products to support drought monitoring, as well as extended-range meteorological forecasts required for hydrological modelling. Finally, swisstopo will provide a repository accessible via download and webservices of analysis-ready and postprocessed satellite imagery and vegetation indices from high-resolution satellites like Sentinel-2.

P 13.14
The effect of an improved snow and glacier routine of a large-scale hydrological model on Alpine streamflow and extremes

Joren Janzing[1,2,3], Niko Wanders[4] and Manuela Brunner[1,2,3]

[1] WSL Institute for Snow and Avalanche Research SLF, Davos Dorf, Switzerland. (joren.janzing@slf.ch)
[2] Climate Change, Extremes and Natural Hazards in Alpine Regions Research Center CERC, Davos Dorf, Switzerland.
[3] Institute for Atmospheric and Climate Science, ETH Zurich, Zurich, Switzerland.
[4] Department of Physical Geography, Utrecht University, Utrecht, The Netherlands.

To accurately study spatial patterns in streamflow and upstream-downstream relationships in Alpine regions, large-scale hydrological models are needed that exceed national boundaries. These large-scale models have increasingly higher resolutions, which are required to capture the complex topography of mountain regions. Therefore, process representations at smaller spatial scales become relevant. However, large-scale hydrological models do not always capture cryospheric processes well (Hou et al. 2023), which can affect simulations of discharge in Alpine regions through errors in timing, quantity and spatial patterns of snow and glacier melt. Here, we propose an improved snow and glacier routine for the PCR-GLOBWB 2.0 global hydrological model (Sutanudjaja et al. 2018; Hoch et al. 2023) and study their effects on simulations of discharge and hydrological extremes over the Alps.

We set up the PCR-GLOBWB 2.0 model over the Alps at a resolution of 30 arcsec (~1km). The existing model uses a simple constant degree-day factor to simulate snowmelt and does not explicitly represent glaciers. First, we implemented, tested, and compared different extensions of the existing temperature index model including a degree-day factor that varies seasonally or one that is dependent on snow albedo effects. Second, we added a new dynamic glacier component to the model. We calibrated the model against datasets of snow cover, glacier mass balances and discharge over Switzerland.

Our preliminary results show a limited improvement of discharge simulations through the new snowmelt routine. The glacier routine leads to strong increases in performance for glacierized catchments. Furthermore, the new snow and glacier modules address the issue of unrealistic snow accumulation across multiple seasons in PCR-GLOBWB 2.0. Our future work will specifically focus on the effect of cryospheric processes on historical floods and droughts by running the model over the larger Alpine domain including the headwater catchments of the Rhine, Rhone, Danube and Po rivers.

REFERENCES

Hoch, J. M., Sutanudjaja, E. H., Wanders, N., Van Beek, R. L., & Bierkens, M. F. 2023: Hyper-resolution PCR-GLOBWB: opportunities and challenges from refining model spatial resolution to 1 km over the European continent, Hydrology and Earth System Sciences, 27(6), 1383-1401.

Hou, Y., Guo, H., Yang, Y., & Liu, W. 2023. Global evaluation of runoff simulation from climate, hydrological and land surface models, Water Resources Research, 59(1), e2021WR031817.

Sutanudjaja, E. H., Van Beek, R., Wanders, N., Wada, Y., Bosmans, J. H., Drost, N., ... & Bierkens, M. F. 2018. PCR-GLOBWB 2: a 5 arcmin global hydrological and water resources model, Geoscientific Model Development, 11(6), 2429-2453.

P 13.15
Impacts of Land Use Land Cover and Climate Changes on hydro-morphological processes of the African Great Lakes Regions. Case of Lake Kivu catchment.

Kayitesi N.M., Guzha A.C., Tonini M., Mariethoz G.

Lake Kivu (LKV), bordering Rwanda, and Democratic Republic of Congo is one of the African Great Lakes, which are a series of Rift Valley lakes in and around the East African Rift. LKV catchment is highly susceptible to natural disasters, including floods, landslides, mass movement and soil erosion. This is a result of the catchment geologic formation, steep topography, and the loss of forest cover on fragile soils, coupled with the increased prevalence of extreme rainfall events. Over recent decades, the LKV catchment has undergone substantial Land Use Land Cover Changes (LULC), driven by a complex interplay of political, economic, and socio-demographic factors. Furthermore, climate change is intensifying these changes due to global warming and increased frequency of extreme events. These changes manifest in catchment hydro-morphological processes, such as alteration of rainfall- runoff patterns, and changes in the water balance. The LKV catchment represents a case of rapid landscape degradation, and prompt efforts are being made to implement reforestation schemes. However, there is a lack of detailed spatio-temporal analysis to understand the landscape changes, and their subsequent impacts on the hydro-morphological dynamics of the catchment.

This study aims at analyzing the LULC and Climate changes that occurred in the LKV catchment from 1980s, and subsequently forecast future scenarios, using remote sensing data and a predictive LULC model. The resultant changes in LULC and climate are then related to associated changes in catchment hydro-morphology. Preliminary findings indicate that during the 1980s and 1990s, the catchment encountered a forest decline of about 10% of the catchment area (340 km^2), with a 13% expansion in agricultural land. This trend reversed after the 2000s, marked by extensive reforestation that expanded total land cover by 8%, primarily driven by changes in bare land, grass land and intensified agricultural areas. Furthermore, the study applies a hydrological model to analyze the catchment responses to these landscape changes. It provides a foundation for prioritizing and implementing strategic measures to restore and maintain the integrity of LKV catchment.

P 13.16
Effects of strong Wind-driven Currents on Winter Cascading in Lake Geneva during a cold Spell

François Mettra[1], Damien Bouffard[2], Rafael Sebastian Reiss[1], Ulrich Lemmin[1], Tomy Doda[2], Koen Blanckaert[3], David Andrew Barry[1]

[1] *ECOL-IIE-ENAC, Ecole Polytechnique Fédérale de Lausanne (EPFL), 1015 Lausanne, Switzerland (current e-mail address: francois@meteomettra.ch)*
[2] *Eawag, Swiss Federal Institute of Aquatic Science and Technology, Surface Waters – Research and Management, 6047 Kastanienbaum, Switzerland*
[3] *Institute of Hydraulic Engineering and Water Resources Management, TU Wien, A-1040 Vienna, Austria*

Cooling-driven density currents, also known as winter cascading or thermal syphon, are important for horizontal littoral-pelagic exchange of heat and dissolved gases. They contribute to the erosion of the thermocline, deep mixing and sediment focusing. In the literature, they have been studied only in the case of weakly to moderate wind conditions (e.g., Doda et al., 2022; Ramón et al., 2022). Earlier studies in Lake Geneva related the dynamics of those cold density currents to the shelf width and the cooling intensity, and determined that they represent an important volume flushed from the shelf (Fer et al., 2001, 2002). Recently, it has been found by numerical simulation that they also significantly contributed to deep water renewal during the last bottom re-oxygenation in 2012 (Peng et al., submitted), which was caused by an extremely cold spell, accompanied by strong winds.

In this field study, we investigated winter cascading on the north-western shore of Lake Geneva during a strong and cold *Bise* (wind from North-East) event in February 2018 based on nearshore mooring data from two sites which are spaced 2-km in the alongshore direction. The wind direction was alongshore and favored coastal downwelling (Fer et al., 2002). One site, characterized by a wide shelf, is upwind of the second site, characterized by a narrow shelf.

During this cold wind event, strong differential cooling, with colder water in the shallow littoral zone (than in the pelagic zone), was observed, especially at the upwind site (as expected for a wide shelf). However, the upwind site did not show winter cascading during the strongest winds. Interestingly, the downslope flow was stronger at the narrow shelf than at the wide upwind shelf, whereas, during weaker winds, winter cascading was stronger at the wide shelf, as expected from the existing literature. The downslope velocity scale of winter cascading, ~5-10 cm s^{-1} (Fer et al., 2002), became occasionally smaller than the alongshore velocity scale (up to 20 cm s^{-1}). This means that alongshore advection dominated and that the cold water formed on the wide shelf caused winter cascading further downstream along the shore. In both situations, Ekman transport due to the coastal downwelling was significantly weaker than the observed downslope transport. This confirms that the main driving mechanism of this downslope transport is differential cooling, even during strong winds, although Ekman transport also contributes to the downslope flow.

In summary, we show that winter cascading occurs on both wide and narrow shelves, depending on background currents (resulting from wind) and cooling intensity. Differential cooling is always stronger on wide shelves, but due to the long initiation and propagation time scales of the subsequent cooling-driven flow (compared to background alongshore currents), winter cascading is generated downstream of the wide shelf. Overall, it points to the important effects of the wind direction (relative to the shore direction) and the nearshore bathymetry on the generation of winter cascading.

REFERENCES

Doda, T., Ramón, C. L., Ulloa, H. N., Wüest, A., & Bouffard, D. 2022: Seasonality of density currents induced by differential cooling. Hydrology and Earth System Sciences, 26(2), 331–353.

Fer, I., Lemmin, U., & Thorpe, S. A. 2001: Cascading of water down the sloping sides of a deep lake in winter. Geophysical Research Letters, 28(10), 2093-2096.

Fer, I., Lemmin, U., & Thorpe, S. A. 2002: Winter cascading of cold water in Lake Geneva. Journal of Geophysical Research: Oceans, 107(C6), 13-1.

Peng, N., Lemmin, U., Reiss, R. S., Mettra, F., & Barry, D. A. Heat Budget Decomposition: A Novel Approach to Identify and Quantify Density-Driven Deepwater Renewal Processes during Winter Cooling in a Large, Deep Lake (Lake Geneva), submitted to Water Resources Research.

Ramón, C. L., Ulloa, H. N., Doda, T. & Bouffard, D. 2022: Flushing the Lake Littoral Region: The Interaction of Differential Cooling and Mild Winds. Water Resourses Research, 58(3), e2021WR030943.

P 13.17
Google Earth Engine Applications in Hydrology and Hydrogeology

Saeed Mhanna[1*], Landon Halloran[1], Philip Brunner[1]

[1] *Center of Hydrogeology and Geothermics, Université de Neuchâtel *(saeed.mhanna@unine.ch)*

With the advancement of remote sensing and computing technology, cloud-based platforms, such as Google Earth Engine (GEE), have emerged as necessary tools for storing and processing large volumes of data. While it is well-known that remote sensing products can offer valuable insight into planetary processes, many in the hydrology and hydrogeological community are unaware of the power and relative simpilicy of open-access, cloud-based tools. Hydrological and hydrogeological studies that seek to monitor and understanding complex processes can often benefit by integrating extensive RS datasets. GEE enables access to a wealth of Earth observation data sources, providing opportunities for researchers to examine changes in total water storage, land cover, surface water availability, soil moisture, precipitation patterns, vegetation dynamics, and much more. In this presentation, we present an overview of current and future applications of GEE for the hydrology and hydrogeology community. We also demonstrate multiple practical examples showing how this tool can be used to rapidly provide valuable insight on a variety of hydrology research themes and discuss the caveats of the approaches.

P 13.18
Radiocarbon Inventories of Switzerland: Insights from a year of sediment trap data in Lake Geneva

Benedict V.A. Mittelbach[1], Margot E. White[1], Timo M.Y. Rhyner[1], Negar Haghipour[1,2], Nathalie Dubois[1,3], and Timothy I. Eglinton[1]

[1] Department of Earth Sciences, ETH Zürich, Switzerland (benedict.mittelbach@erdw.ethz.ch)
[2] Laboratory for Ion Beam Physics, ETH Zürich, Switzerland
[3] Department of Surface Waters Research & Management, EAWAG, Dübendorf, Switzerland

This study investigates the allochthonous and autochthonous contributions of organic and inorganic carbon to burial fluxes in Lake Geneva. By understanding these contributions, we aim to shed light on the broader implications for carbon sequestration in freshwater systems.

From July 2022 to July 2023, monthly samples were retrieved from sediment traps at two strategically selected sites: near the Rhone delta (river-proximal) and the deepest part of the lake (river-distal). These locations differed in their expected ability to capture river-derived (allochthonous) and lake-derived (autochthonous) sediment contributions. Initial findings indicate substantial temporal variations in sedimentation rates throughout the year. External inputs, evident from heightened levels of clastic sediment, were especially dominant at the river-proximal site. Further, autochthonous biogenic material, which can be linked to internal lake processes, displayed distinct seasonal patterns.

Subsequent analyses focussed on the carbon dynamics recorded by these sediment traps. Different carbon sources, such as atmospheric vs. rock-derived, can be distinguished by their isotopic composition. We thus used radiocarbon and stable carbon analyses as means of source identification of the different carbon pools entering the sedimentary reservoir in Lake Geneva. Future analyses will aim to understand and quantify the mechanisms of carbon deposition. This includes the transformation of dissolved inorganic carbon to organic carbon through in-situ primary production and to particulate inorganic carbon through calcite precipitation.

This exceptionally well-monitored lake and river system offers the ideal site for our in-depth analyses. When coupled with existing sediment and carbon budgets of the lake, this research provides a comprehensive perspective on the carbon dynamics of Lake Geneva and other hardwater lakes globally.

P 13.19
Swiss Groundwater Network – CH-GNet

Christian Moeck[1]

[1] Swiss Groundwater Network, CH-8600 Dübendorf (christian.moeck@eawag.ch)

The primary objective of CH-GNet is to raise awareness of existing research in the field of groundwater and related disciplines and to create a forum for exchange, information and networking.
More specifically, we make developed tools and gained information from science visible, promote practice-oriented research, compile scientific facts and identify groundwater-relevant problems as well as possible (voluntary) solutions. We are seeking to promote a smooth exchange between different organisations and provide advice and arrange contacts with research institutions. We are bundling practice-relevant research results and making them visible, through organized workshops and conferences and the development of documents, help promoting continuous competence building. CH-GNet wants to support the cooperation of various interest groups. In the present poster examples of the CH-GNet activities are shown.

Figure 1. Swiss Groundwater Network. More Information can be found on our webpage www.swissgroundwaternetwork.ch

P 13.20
Separating snow and ice melt contributions based on water stable isotopes and a glacio-hydrological model in a highly glacierized catchment

Tom Müller[1,2], Mauro Fischer[2,3], Stuart N. Lane[1], Bettina Schaefli[2,3]

[1] *Institute of Earth Surface Dynamics (IDYST), University of Lausanne, UNIL Mouline, CH-1015 Lausanne (tom.muller.1@unil.ch)*
[2] *Institute of Geography, University of Bern, Hallerstrasse 12, CH-3012 Bern*
[3] *Oeschger Centre for Climate Change Research, University of Bern, Hochschulstrasse 4, CH-3012 Bern*

Highly glacierized catchments are rapidly evolving with climate warming. Changes in annual glacier runoff leads to significant impacts on downstream ecosystems and water availability for human uses. Glacio-hydrological models have been developed to assess current or future changes in runoff but predictions are mainly based on statistical models using past or present observations which may simplify the physical processes responsible for runoff generation. In addition, detailed in-situ mass balance observations are sparse and uncertainties remain in the spatio-temporal interpolation of point mass balance measurements. Water stable isotopes are widely used in catchment hydrology to assess the main sources of water but application in snow dominated catchments remains challenging. In highly glacierized catchments, studies using water stable isotopes are still sparse.

Here, we develop a semi-distributed glacio-hydrological model and implement a simple, parsimonious isotope routine allowing to simulate the contribution and corresponding discharge signature of snow and ice melt isotopes. We compare our modelling results with two years of discharge and isotope measurements directly at the glacier portal of the Otemma glacier in southwestern Switzerland. We find a satisfying potential of the model to reproduce stream observations, but show that the use of isotopes to separate between snow and ice contributions appears very challenging. In particular, we show that the spatio-temporal variability of snow isotopes may lead to large uncertainties in the contribution of different water sources and thus challenges the use of mixing models using only isotopes for temperate mid-altitude glaciers. Although further research is needed, we provide guidelines and discuss the potential of combining isotopes within a glacio-hydrological modelling framework.

P 13.21
The hydrogeology of Mt. Fuji as a model for water resource management in tectonically active volcanic regions

Stéphanie Musy[1], Friederike Currle[1], Teresa Nakajima[2], Yama Tomonaga[1,3], Yuji Sano[2], Oliver S. Schilling[1,4]

[1] *Hydrogeology, Department of Environmental Sciences, University of Basel, Bernoullistrasse 32, CH-4056 Basel (stephanie.musy@unibas.ch)*
[2] *Center for Advanced Marine Core Research, Kochi University, Japan*
[3] *Entracers GmbH, Dübendorf, Switzerland*
[4] *Department Water Resources and Drinking Water, Eawag–Swiss Federal Institute of Aquatic Science and Technology, Dübendorf, Switzerland*

Mt. Fuji is the iconic centerpiece of a large, tectonically active volcanic watershed (100 km^2) which plays a vital role in supplying safe drinking water to millions of people through groundwater and numerous freshwater springs. Situated at the top of the sole known continental triple-trench junction, the Fuji watershed is characterized by a complex geology and significant tectonic instability.

Recently, the long-standing understanding of Mt. Fuji catchment being a conceptually simple, laminar groundwater flow system with three isolated aquifers was challenged. The combined use of noble gases, vanadium, and microbial eDNA as measured in different waters around Fuji revealed the presence of substantial deep groundwater water upwelling along Japan's tectonically most active fault system, the Fujikawa Kako Fault Zone[1].

These findings call for deeper investigations of the hydrogeology and the mixing dynamics within large-scale volcanic watersheds, which are typically characterized by complex geologies and extensive networks of fractures and faults. In our study, we approach these questions by integrating existing and emerging methodologies, such as continuous, high-resolution monitoring of dissolved gases (GE-MIMS;[2]) and microbes[3]we implemented a custom-built continuous staining device in combination with real-time flow cytometry (RT-FCM, eDNA, trace elements, and integrated 3-D hydrogeological modeling[4]the information content of the tracers can potentially be fully explored through the explicit simulation of an advection-dispersion transport equation, for example using integrated surface-subsurface hydrological models (ISSHMs.

The collected tracer time series, along with hydraulic and seismic observations, are used to develop an integrated SW-GW flow model of the Mt. Fuji watershed. Climate change projections will further inform predictive modeling and facilitate the design of resilient and sustainable water resource management strategies in tectonically active volcanic regions.

REFERENCES

[1] Schilling, O.S. et al., Revisiting Mt Fuji's groundwater origins with helium, vanadium and environmental DNA tracers, Nat. Water **1** 1 (2023) 60.
[2] Brennwald, M.S., Schmidt, M., Oser, J., Kipfer, R., A Portable and Autonomous Mass Spectrometric System for On-Site Environmental Gas Analysis, Environ. Sci. Technol. **50** 24 (2016) 13455.
[3] Props, R. Et al., Detection of microbial disturbances in a drinking water microbial community through continuous acquisition and advanced analysis of flow cytometry data, Water Res. **145** (2018) 73.
[4] Delottier H. et al., Explicit simulation of environmental gas tracers with integrated surface and subsurface hydrological models, Front. Water **4** (2022).

P 13.22
An improved definition of the Habitat Suitability Index for brown trout including the role of macroroughness

Francesca Padoan[1], Giulio Calvani[1], Giovanni De Cesare[1], Paolo Perona[1]

[1] *Platform of Hydraulic Constructions PL-LCH (IIC-ENAC), Ècole Polytechnique Fédérale de Lausanne, Lausanne, Switzerland (francesca.padoan@epfl.ch)*

The Habitat Suitability Index (HSI) is a quantitative measure that has been developed to help aquatic ecologists, river scientists and engineers identifying preferred habitats for a particular species (Raleigh et al., 1984; Shim et al., 2020, among others). To this aim, the quantification of the HSI usually considers several parameters, identifying food availability and environmental characteristics, and combines them in a comprehensive indicator. For the specific case of mountain river habitats and the brown trout (Salmo trutta L.), the HSI considers environmental variables such as water temperature, flow velocity, water depth, and substrate type (e.g., Raleigh et al., 1984). However, in mountain streams, the interaction between large bed materials (e.g., cobbles and boulders) and the flow field is responsible for the formation of local wake zones in the river reaches that fish can use as shelters to rest or feed, and its inclusion in the quantification of the HSI via manual surveys can be very time consuming. In this work, we build on a recent literature work to correct actual HSI in the low-flow range where the presence of macroroughness is particularly evident when the flow stage is in the order of the grain size of such large boulders (i.e., macroroughness regime). This technique is based on the derived distribution approach and is particularly useful to take the spatial distribution of large stones/obstacles into accounts (Niayifar et al., 2018). As a result, we provide the HSI as a function of the flow magnitude and show that the correction due to the role of macroroughness can generate an additional peak at low discharges thus making the HSI function bimodal. This more detailed definition of the HSI is particularly useful to refine hydrodynamic models and their use to better assess new habitat formation following renaturation measures.

REFERENCES

Niayifar, A., Oldroyd, H. J., Lane, S. N., & Perona, P. (2018). Modeling macroroughness contribution to fish habitat suitability curves. Water Resources Research, 54(11), 9306-9320.

Raleigh, R. F., Zuckerman, L. D., & Nelson, P. C. (1984). Habitat suitability index models and instream flow suitability curves: brown trout. Western Energy and Land Use Team, Division of Biological Services, Research and Development, Fish and Wildlife Service, US Department of the Interior.

Shim, T., Kim, Z., Seo, D., Kim, Y. O., Hwang, S. J., & Jung, J. (2020). Integrating hydraulic and physiologic factors to develop an ecological habitat suitability model. Environmental Modelling & Software, 131, 104760.

P 13.23
Dispersion of artificial tracers in ventilated caves

Claudio Pastore[1,2], Marc Luetscher[1], Amir Sedaghaktish[1,2], Frédéric Doumenc[3,4], Eric Weber[1], Pierre-Yves Jeannin[1]

[1] Swiss Institute for Speleology and Karst Studies (SISKA), Rue de la Serre 68, 2300 La Chaux-de-Fonds, Switzerland, (claudio.pastore@isska.ch)
[2.] Université de Neuchâtel, Avenue du 1er-Mars 26, 2000 Neuchâtel, Suisse
[3] Université Paris-Saclay, CNRS, FAST, 91405, Orsay, France
[4] Sorbonne Université, UFR 919, 4 place Jussieu, F-75252 Paris Cedex 05, France

The high permeability characterizing the karst vadose zone favours significant air circulation. Together with water fluxes, airflows are recognised to drive the transport of bacteria, fungi, pollens and airborne matter, but also hazardous gases and aerosols in general, into the deeper part of the network.

Therefore, ventilation is an efficient mode of transport for aerosols in caves, and there is a strong relationship between cave air motion, aerosol/gas transport, and subsequent deposition and spatial distribution in cave systems.
Modelling this airborne transport requires geometrical and physical parameters, including the conduit cross-section areas, the airflow, and more specifically the average air speed as well as the longitudinal dispersion coefficient () related to the advective fluxes. Longitudinal dispersion can be described as the spreading of a solute along the longitudinal axis of the flow.

Using punctual injection of artificial CO_2 in different cave and mine settings, we demonstrate that it is possible to infer reliable geometric information (average cross-sections) when compared to topographic survey, and a more accurate estimate of average air velocity (peak tracer velocity) otherwise difficult to estimate along conduits with complex geometries. Moreover, we estimate the longitudinal dispersion , fundamental to solving the 1-D advection-diffusion equation, using Chatwin's method (Chatwin, 1971)it is argued, has certain advantages over more usual methods. It is shown that Fischer's observations in an open channel were not made at a sufficient distance downstream from the point of injection for Taylor's theory to apply but that they are consistent with a description of the early stages of the dispersion process due to Sullivan (1968. This method is commonly used in hydrogeology to estimate the retardation of the tracer related to the tailing.

In caves, where conduits are far from smooth, the ratio (where d is the conduit diameter and U* is the friction velocity) is much higher than that predicted by Taylor's theory. According to Taylor's (1954) experiments, in smooth pipes, the ratio is constant and equal to 5.05. During our experiments, this ratio was three or more times higher.

We suggest also that the method could be used with opportune adjustments to similar breakthrough curves carried out for any aerosols moving along a ventilated pipe.

REFERENCES

Chatwin, P.C., 1971: On the interpretation of some longitudinal dispersion experiments. J. Fluid Mech. 48, 689–702. https://doi.org/10.1017/S0022112071001800
Taylor, G., 1954: The dispersion of matter in turbulent flow through a pipe. Proc. R. Soc. Lond. A 223, 446–468. https://doi.org/10.1098/rspa.1954.0130

P 13.24
Temporal and spatial comparison of springs in three different mountain regions in the Southern Swiss Alps

Tania Pedimina[1] & Stefanie von Fumetti[1]

[1] *Department of Environmental Sciences, Geoecology, University of Basel, Klingelbergstrasse 27, CH-4056 Basel (tania.pedimina@unibas.ch)*

Springs in the Alps are environmentally stable and biodiverse habitats, which are threatened by anthropogenic impacts. Due to their environmental stability they may function as refugia for species endangered by climatic changes. In this study springs in three distinct regions within the southern Alps of Switzerland were analyzed to gain a better understanding of how these sensitive habitats are being preserved or affected by environmental changes. Specifically, the study focuses on the springs of Monte Generoso, Monte Tamaro, and Monte Bar in the Canton Ticino. The aim was to conducted a) a spatial comparison of the three mountain summits and b) a temporal comparison of springs at the Monte Generoso, which have been sampled in 2012 for the first time (Bonta, 2012). The sampling of the springs took place in May 2023. Subsequently, an analysis of the ecological conditions (i.e. macroinvertebrate assemblages, ecomorphology, and physiochemistry) of the springs was carried out. The sampling followed standardized protocols set by the FOEN (Lubini et al., 2014). The chosen regions exhibit similar characteristics in terms of valley shape and altitude, but they differ in exposure and geology. Despite their geological dissimilarities, all three selected regions share comparable environmental conditions besides electrical conductivity, which is considerably higher in the Monte Generoso springs (Fig. 1).

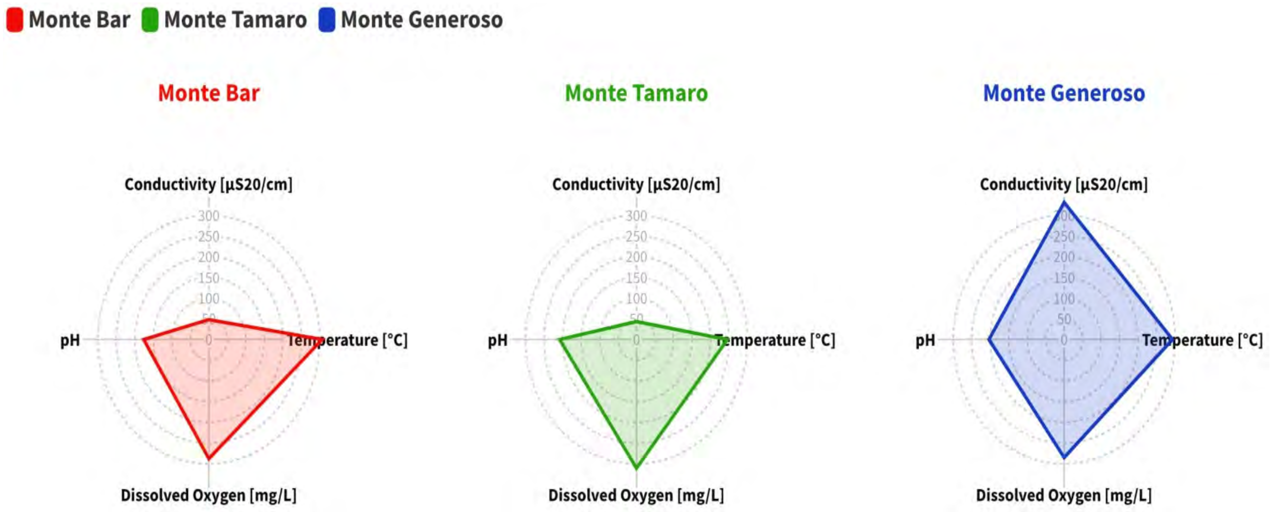

Figure 1: Schematic representation of average measurements (2023) for the 19 springs from Monte Bar (red), Monte Tamaro (green), and Monte Generoso (blue), depicting abiotic factors such as temperature (°C), pH, dissolved oxygen (mg/L), and conductivity (µS20/cm).

While the springs of Monte Bar and Monte Tamaro remain primarily in their natural states, the springs of Monte Generoso show a higher degree of human influence. Initial disparities are observed, particularly in the springs of Monte Generoso: they exhibit minimal presence of Ephemeroptera, Plecoptera and Trichoptera (EPT-Taxa). Other taxa such as Diptera, specifically Chironomidae, as well as Annelida and diverse Crustacea, were consistently abundant across all observed regions. The relatively low number of bioindicators such as EPT-Taxa in Monte Generoso could indicate the potential occurrence of significant eutrophication during these years. This is supported by the observation of numerous cows and signs of intensive pasturing near the sampled springs, particularly in the most impacted areas. The assumed degradation of the springs at Monte Generoso is further supported by the decrease in the number of EPT-Taxa from 2012 to 2023.

Conversely, Monte Bar and Monte Tamaro appear to host more diverse macroinvertebrate assemblages. Both areas seem to be better preserved or less affected by human impacts. As a result, they exhibit a lower number of individuals but a higher diversity. These differences in faunal composition might be due to various factors such as distinct exposures or varying geological characteristics of the regions as well as a different degree of anthropogenic influence. Another possible factor could be the exceptionally dry winter of 2022, during which snowfall was significantly reduced, potentially affecting the microclimate (Zhao et al., 2022) of the springs' soil. This, in turn, could have influenced the macroinvertebrate communities.

REFERENCES

Bonta, S. (2012): Natural characterization of springs and their Biocoenosis in the Canton Ticino (Southern Swiss Alps). MSc Thesis, University of Basel, 79 pp.

Lubini-Ferlin V., Stucki P., Vicentini H., Küry D. (2014): Ökologische Bewertung von Quell-Lebensräumen in der Schweiz. Entwurf für ein strukturelles und faunistisches Verfahren. Bericht im Auftrag des Bundesamtes für Umwelt (BAFU), 33 pp.

Zhao, Z., De Frenne, P., Peñuelas, J., Van Meerbeek, K., Fornara, D.A., Peng, Y., Wu, Q., Ni, X., Wu, F., Yue, K. (2022): Effects of snow cover-induced microclimate warming on soil physicochemical and biotic properties. Geoderma, Volume 423, 115983, ISSN 0016-7061. https://doi.org/10.1016/j.geoderma.2022.115983

P 13.25
Regionalization of Oxygen-18 and Deuterium in precipitation in Switzerland as a basis for hydrological and hydrogeological studies

Valentina Pelzmann[1], Albrecht Leis[1], Marc Schuerch[2], Christian Reszler[1]

[1] *JR-AquaConSol GmbH, Steyrergasse 21, 8010 Graz (valentina.pelzmann@jr-aquaconsol.at)*
[2] *Swiss Federal Office for the Environment (FOEN), Hydrology Division, Hydrogeological Basis Section, 3003 Bern, Switzerland*

The stable isotopes of the water molecule, oxygen-18 and deuterium, are conservative tracers and therefore widely used in hydrology and hydrogeology. The applications comprise, e.g, the determination of the catchment location and water travel times of springs, groundwater wells and surface waters, in the frame of water resources management and protection studies. Long-term data also allow insights into the effects of climate change on the atmospheric conditions (air moisture sources, temperature, evaporation). Crucial part of these studies is the knowledge of the "input" function for the particular catchment or point of interest. This presentation shows the developement and test of a method regionalizing, i.e. interpolating, stable isotope data in precipitation on a monthly basis. Data of the isotope observation network in Switzerland (ISOT), a module of the NAQUA National Groundwater Monitoring, are used as well as data of nearby stations in neighbouring countries. The main influencing variables (e.g., topographical and climate variables) are tested in a multi-regression framework, and the residuals are interpolated by the use of ordinary kriging. The tests are performed by cross-validation, also to provide information about regional differences of the interpolation quality. Monthly maps of oxygen-18 and deuterium, so-called "Isoscapes", in a 500 m raster has been generated for selected years. As an example, the Isoscape of oxygen-18 in January 2013 is shown in Figure 1. The figure illustrates the high spatial variability in this month due to the topography (e.g., differences between the Plateau and the Alps) as well as the different climate zones (e.g., higher values in the south).

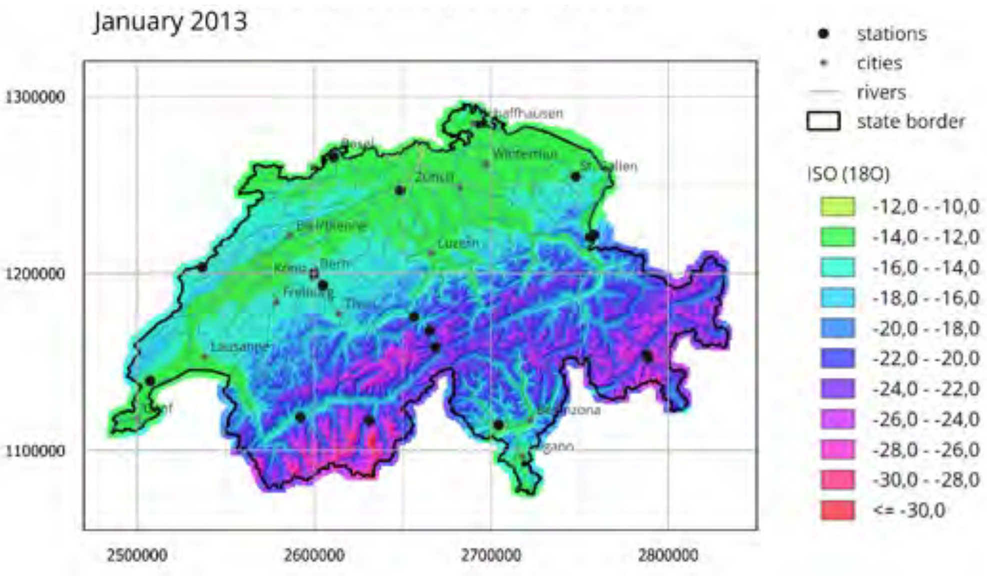

Figure 1. Calculated pattern of oxygen-18 in precipitation in January 2013 for Switzerland in a 500m raster (Swiss reference system: CH1903+ (LV95)).

As a further validation of the method, for particular monitoring sites of groundwater and surface water with known catchments, the "input" function is determined and compared to the measurements. Doing this, existing hydrological and hydrogeological information for the corresponding site could be improved. For example, in Figure 2, precipitation-weighted regional means of oxygen-18 extracted from the Isoscapes are compared to the measured oxygen-18 in groundwater stations, both averaged over seven years. The scatter plot shows that, for most of the catchments the regionalized data fit well to the measurements. Larger deviations are marked with red and blue colour. The red-marked samples/catchments represent an overestimation by the regionlized values. This indicates, that the real catchment of the sample point is located at higher elevation than the catchment polygon that was used to extract the data from the Isoscapes. This is plausible at the corresponding sample points, because they are groundwater wells influenced by a nearby large river with a catchment, that reaches very high altitudes and is dominated by snow and glacier meltwater (e.g., Rhone). At the blue-marked samples the measured data are underestimated by the regionalized data. This indicates larger uncertainties in the Isoscapes. The corresponding sample points are mainly located in the south and at the borders of different topography and climate zones.

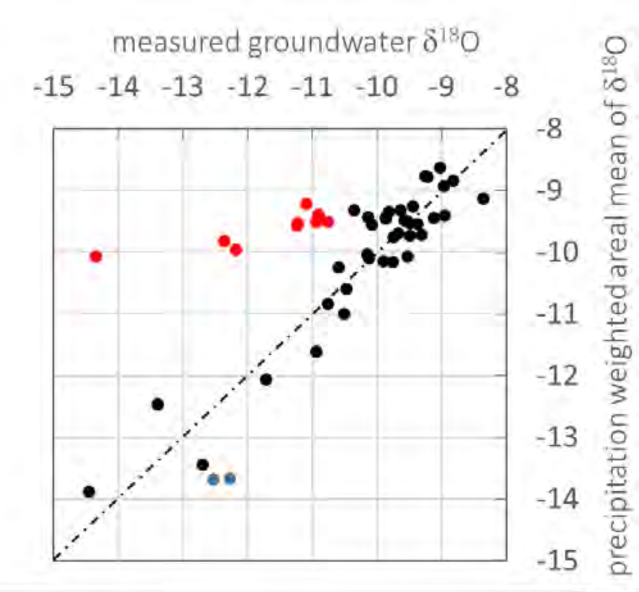

Figure 2. Precipitation-weighted regional mean of oxygen-18 against measured groundwater oxygen-18, both averaged over the period 2007-2013. Red: groundwater stations influenced by a river from the Alps; blue: stations in the south.

Monthly time series for every location can be extracted from the Isoscapes to be used as input in hydrological data analyses and modelling. Therby the data offer new possibilities in water movement and quality research by allowing spatially distinguished insights into the corresponding atmospheric and hydrological processes. By the well tested and validated method, monthly patterns of isotope data in precipitation (Isoscapes) are available at the Swiss Federal Office for the Environment (FOEN) for selected years (2013, and 2020).

P 13.26
Characterization of river/groundwater interactions by signal processing of electrical conductivity time series

Rodolfo Perego[1], Sebastian Pera[1]

[1] *Institute of Earth Sciences, University of Applied Sciences and Arts of southern Switzerland SUPSI - Campus Mendrisio, Via Flora Ruchat-Roncati 15 CH – 6850 Mendrisio (rodolfo.perego@supsi.ch)*

In the framework of climate change that leads to increased frequence of extreme events and to more frequent floodings, river restoration has become a fundamental nature-based solution to reduce the likelihood of flooding events and mitigate their damage on human structures and population.

Canton Ticino, southern Switzerland, currently hosts very important river restoration projects such as the one designed for river Vedeggio, which final part crosses the Vedeggio aquifer before flowing into lake Lugano. Vedeggio aquifer also hosts the two largest drinking water wells of the Canton in terms of pumping rate, Manno and Bioggio, which can provide up to 60 m^3/min of drinking water to the city of Lugano and are strategical to the Cantonal water supply framework. Due to their proximity to the river, it can be assumed that a significant fraction of water pumped by wells is exfiltrated river water.

Both the effectiveness of river restoration and the amount of river water exfiltrating in the aquifer can be studied in detail by designing and operating a high-frequency surface water/groundwater monitoring network.

This work proposes a time-series analysis of electrical conductivity signals, a natural tracer that is already present in the water, propagates fast and is subject to less smoothing than temperature, in order to better understand the correlations between surface water and groundwater. Electrical conductivity signals were treated (detrended, outliers removal) and different signal analysis techniques were applied (simple cross-correlation, optimized cross-correlation and non-parametric deconvolution). The methods converged in the estimate of the lag times between river and groundwater signals, allowing to understand the mutual interactions between surface water and groundwater and estimating the amount of river water flowing into the different piezometers and wells.

This has a double value: from one hand to assess the modifications induced by river restoration projects and from the other hand to improve the management of drinking water wells, understanding their connections to the river channel. The proposed method can be useful for similar cases where river exfiltrates into the aquifer and there is the need to assess how river restoration modifies the interactions between surface and groundwater.

REFERENCES

Vogt, T., Hoehn, E., Schneider, P., Freund, A., Schirmer, M., and Cirpka, O.A. 2010 Fluctuations of electrical conductivity as a natural tracer for bank filtration in a losing stream, Advances in Water Resources (33), pp. 1296-1308.

P 13.27
Radiocarbon Inventories of Switzerland: What controls the radiocarbon signature of dissolved inorganic carbon in Swiss rivers?

Timo M. Y. Rhyner[1*], Benedict V. A. Mittelbach[1], Margot E. White[1], Lisa Broeder[1], Olivier Raymond[1], Negar Haghipour[2], Alexander Brunmayr[3], Florian R. Storck[4], Lucas Passera[4], Melissa S. Schwab[5], Robert Hilton[6], Jürg Zobrist[7], Timothy I. Eglinton[1]

[1] Geologisches Institut, ETH Zürich, Sonneggstrasse 5, 8092 Zürich, Switzerland (timo.rhyner@erdw.ethz.ch)
[2] Department of Physics, Laboratory of Ion Beam Physics, Zürich, Switzerland
[3] Department of Physics, Imperial College London, London, UK
[4] Hydrology Division, Federal Office for the Environment FOEN, Bern, Switzerland
[5] Jet Propulsion Laboratory, California Institute of Technology, United States
[6] Department of Earth Sciences, University of Oxford, Oxford, United Kingdom
[7] Senior Eawag Emeritus, Herracherweg 103, Uster, Switzerland

Carbon transport through rivers represents a fundamental connection linking different reservoirs of the global carbon cycle. Yet the influence of natural and human-induced controls on sources and cycling of riverine carbon remains poorly understood and disentangling the relative importance of their drivers is challenging. Dissolved inorganic carbon (DIC), which typically represents the dominant carbon phase in rivers, derives from a complex array of physicochemical and biological processes. We explore radiocarbon (^{14}C) signatures of DIC carried by Swiss rivers from spatial, longitudinal, and temporal perspectives to assess different source contributions, delivery pathways and dynamics. A total of twenty-one rivers were explored, originating from the five distinct Swiss ecoregions: Jura, Swiss Plateau, Northern Alps, Central Alps, and Southern Alps. The sharp spatial contrasts in elevation, geomorphology, lithology, climatic controls, hydrological and cryospheric characteristics, as well as anthropogenic influences (Botter et al., 2019; Nussbaum et al., 2014) in their corresponding drainage basins allow for the assessment of regional-scale controls on DIC isotopic signatures. We observed marked variability in riverine $\Delta^{14}C$ of DIC with values ranging from -301‰ (2840 ^{14}C yr) to -41‰ (450 ^{14}C yr), indicating a large diversity in sources and processes contributing to fluvial DIC loads. In general, mean basin elevation correlated negatively with $\Delta^{14}C$ of DIC (i.e., older ages at higher elevation), however additional factors such as lithology and seasonal controls also exert a strong influence. The influence of the latter factors is exemplified by a closer look into the longitudinal variations along the Engadin Valley. Here, weathering processes in the upper and lower Engadin manifest themselves into differences in magnitude of longitudinal variability of fluvial radiocarbon signals, with seasonal modulation of $\Delta^{14}C$ values. To test whether this observation of the characteristic dependency of DIC on rock-weathering processes persists, we extend this longitudinal view onto the Upper Rhone Valley in Switzerland. This longitudinal perspective is complemented by a monthly time-series of the Sihl River, providing a temporal perspective and further insights into the complexity of seasonally changing source contributions to the DIC pool. We apply mass balance calculations using radiocarbon and supporting data to constrain petrogenic, biospheric, cryospheric and atmospheric sources of DIC in Swiss rivers. Our ultimate goal is to explore how carbon export from different drainage basins and ecoregions may evolve in the face of on-going regional climate and environmental change.

REFERENCES

Botter, M., Burlando, P., & Fatichi, S. (2019). Anthropogenic and catchment characteristic signatures in the water quality of Swiss rivers: A quantitative assessment. Hydrology and Earth System Sciences, 23(4), 1885–1904. https://doi.org/10.5194/hess-23-1885-2019

Nussbaum, M., Papritz, A., Baltensweiler, A., & Walthert, L. (2014). Estimating soil organic carbon stocks of Swiss forest soils by robust external-drift kriging. Geoscientific Model Development, 7(3), 1197–1210. https://doi.org/10.5194/gmd-7-1197-2014

P 13.28
Poschiavino Critical Zone Observatory: monitoring impacts of climate change on alpine cryo-hydrological systems

Clément Roques[1], Landon Halloran[1], Cyprien Louis[1], Ronan Abhervé[1], Luc Illien[2], Christoff Andermann[2,3], Niels Hovius[2], Nicolas Oestreicher[4], Ronny Figueroas[1], and the CHYN team[1]

[1] Centre for Hydrology and Geothermics (CHYN), Université de Neuchâtel, Neuchâtel, Switzerland.
[2] GFZ, German Research Centre for Geosciences, Potsdam, Germany
[3] Univ Rennes, CNRS, Geosciences Rennes, UMR 6118, 35000 Rennes, France
[4] Department of Earth Sciences, Institute of Geology, ETH Zürich, Zürich, Switzerland

Mountains are the “water towers” of the hydrological cycle, storing water as snow, ice, and groundwater which is progressively delivered to the valleys. The cryosphere is a key component of alpine hydrology, controlling groundwater storage and stream runoff dynamics. Recent observations have revealed long-term modifications in stream discharge and water quality which have been attributed to increasing degradation of the cryosphere due to climate change. Considering that the degradation of the cryosphere is likely to have an important impact on interdependent natural- and socio-ecosystem services, there is an urgent need to provide reliable predictions of future water availability in a changing climate perspective. However, quantifying and predicting the impact of cryosphere degradation on water resources availability remain major challenges for the Critical Zone community. This is a direct consequence of the difficulties in gathering relevant data at high elevations and a lack of fundamental understanding of the processes that need to be integrated in numerical tools at relevant spatiotemporal scales.

The University of Neuchâtel is currently developing a Critical Zone Observatory dedicated to the monitoring of cryo-hydrological systems. The catchment is located in the Swiss Alps, in the Bernina range of Canton Grisons (Figure 1). It is a unique infrastructure with 18 boreholes previously drilled for a hydroelectricity project (Lago Bianco Pump storage project, RePower). The boreholes are about 200 meters deep, and located at elevations ranging from 1’000 to 2’400 masl. Boreholes have been cored and logged with optical televiewer for lithological and fracture mapping, and tests have been performed to infer hydraulic properties of the bedrock. Variations in pore pressures have been recorded in all boreholes from 2010 to 2018. Since 2018, the monitoring setup has been maintained on eight selected boreholes. In addition, river gauge stations owned by the Swiss Federal Office of Environment, located on the Poschiavino river and one on the Val d’Ursé river, were installed in 2017. The sub-catchment of Val d’Ursé is the focus of active research, with a higher density of environmental sensors (Figure 1c). This catchment hosts a major rock glacier located on its north-east facing slope, which strongly contributes to spring and stream discharge dynamics through freezing/thawing cycles. Several perennial and non-perennial springs are currently monitored for water temperature and conductivity to quantify mixing. The catchment is also equipped with two passive seismic stations that were also deployed by the GFZ in 2022 to record ambient seismic noise.

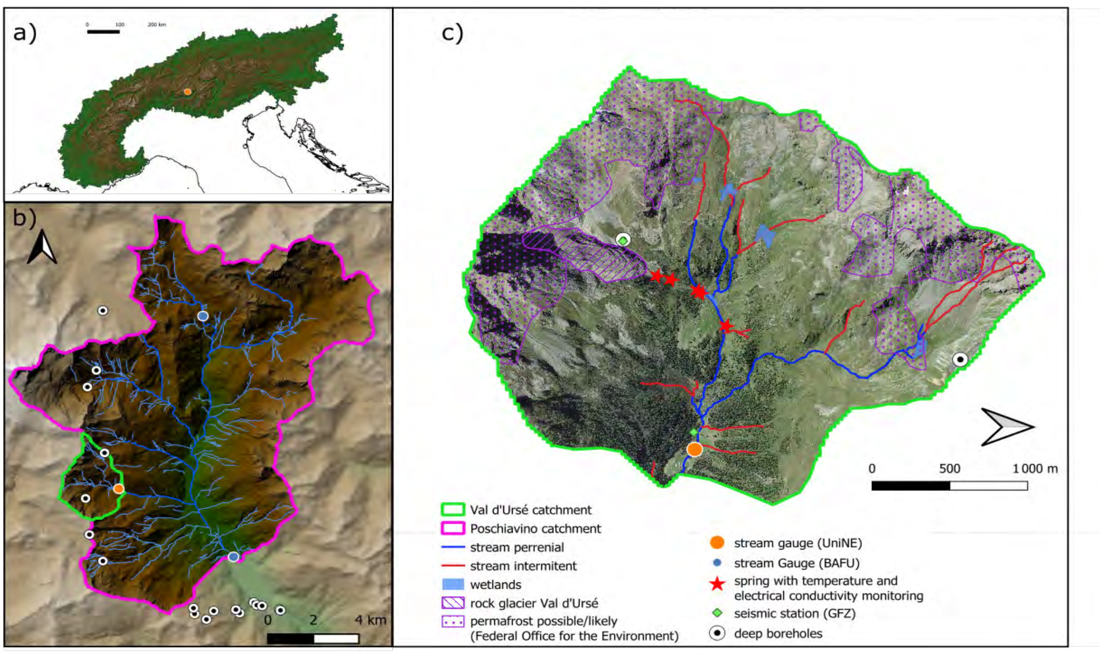

Figure 1. Location and monitoring setup of the Poschiavino Observatory (a-b) and overview of the Val d’Ursé sub-catchment and its monitoring settup (c).

The amount and quality of data provided by the Poschiavino CZO is rare for a high Alpine setting. In our presentation, we will provide an overview of: 1) the data that are currently available, 2) the current knowledge on the hydrological functioning of the site, 3) the hypotheses driving our work, and, 4) the perspectives for future multi-disciplinary collaboration.

P 13.29
Microplastic pollution in rivers: concentrations, environmental drivers and biological risks in Lake Lugano watershed

Federica Rotta[1,2], Luca Gallitelli[3], Matteo Roncoroni[1], Camilla Capelli[1], Barbara Leoni[4], Agnese Marchini[2], Fabio Lepori[1]

[1] *Institute of Earth Sciences, Department of Environment Constructions and Design, University of Applied Sciences and Arts of Southern Switzerland, Via Flora Ruchat-Roncati 15, CH-6850 Mendrisio, Switzerland (federica.rotta@supsi.ch)*
[2] *Department of Earth and Environmental Sciences, University of Pavia, Italy*
[3] *Department of Sciences, University Roma Tre, Italy*
[4] *Department of Earth and Environmental Sciences, University of Milano-Bicocca, Italy*

Since the Industrial Revolution, tons of plastic waste have been dispersed into the environment, of which approximately 10% have ended up in rivers, lakes and oceans (Mora-Teddy & Matthaei, 2020). Long exposure to environmental factors (e.g. UV radiation, wind and wave action) eventually weathers and breaks up of large plastics into particles below 5 mm, known as microplastics (MPs). Because of the large volumes involved, MPs have become one of the most widespread pollutants of the 21st century.

Rivers are an important component in the MP pathway, carrying approximately 70 - 80% of all plastic waste entering the marine environment (De Carvalho et al., 2021). In addition, recent research indicates that riverbeds retain high amounts of MPs and that riverine biota (e.g. macroinvertebrates and fish) frequently ingest MPs, potentially causing ecological impacts. However, research on the distribution and behavior of MPs within river ecosystems is still limited.

We present preliminary results from an ongoing study promoted and funded by the International Commission for the Protection of Italian-Swiss Waters (CIPAIS), which aims to assess MP pollution in small rivers located in Lake Lugano's catchment. Recent research has reported high concentration of MPs in the surface waters of this lake compared to other lakes in Switzerland and abroad (Nava et al., 2023). In contrast, no other studies have addressed the contamination of the rivers in the catchment, which comprise eight tributaries and the lake's outlet.

In this study, environmental samples of MPs were collected using nets (mesh: 0.25 mm) and a sediment sampler to (1) measure the abundance of MPs in the water column and sediments, further divided into coarse sediments and fine sediments; and (2) identify, through data analysis, the main environmental factors influencing MP pollution in rivers (e.g. water velocity, presence/absence of wastewater treatment plants upstream, percentage of urbanized land in the upstream catchment). In addition, the MPs in the gut of benthic macroinvertebrates (plastic burden) were analyzed with the objective to (3) examine ingestion levels by riverine biota.

MPs were found in all the studied rivers (mean: water column 8.4 MP m^{-3}, sediments 33.7 MP kg^{-3} dry weight), in concentrations comparable to those found in the water column and sediments of large urban rivers around the world (D'Avignon et al., 2022). Moreover, MP particles (< 50 μm) were found in approximately 80% of individual macroinvertebrates at all sites. The variability in MP concentration among rivers was not explained by any of the environmental factors considered, suggesting that MP pollution reflected unmeasured local point sources rather than large-scale catchment characteristics. In addition, the MP burden of macroinvertebrates was unrelated to the MP environmental concentration (cf. Windsor et al., 2019).

Our results support the idea that small rivers are both important pathways for MP transport and sites of high MP accumulation. In addition, the high MP burden observed in benthic macroinvertebrates indicates that plastic particles enter into riverine food webs, posing a risk to these organisms and, potentially, organisms at higher trophic levels.

This study, along with other ongoing research on MP in Lake Lugano's catchment, will provide a comprehensive basis to understand the spatial and temporal variability of MPs and reveal the complex dynamics that drive MP pollution in fresh-water ecosystems.

REFERENCES

D'Avignon, G., Gregory-Eaves, I., Ricciardi, A., 2022: Microplastics in lakes and rivers: an issue of emerging significance to limnology. Environmental Review 30, 228-244.

De Carvalho, A.R., Garcia, F., Riem-Galliano, L., Tudesque, L., Albignac, M., ter Halle, A., Cucherousset, J. 2021: Urbanization and hydrological conditions driven the spatial and temporal variability of microplastic pollution in the Garonne River. Science of the Total Environment 769, 144479.

Mora-Teddy, A.K. & Matthaei, C.D. 2020: Microplastic pollution in urban streams across New Zealand: concentrations, composition and implications. New Zealand Journal of Marine and Freshwater Research 54:2, 233-250.

Nava et al., 2023: Plastic debris in lakes and reservoirs. Nature 619, 317-322.

Windsor, F.M., Tilley, R.M., Tyler, C.R., Ormerod, S.J. 2019: Microplastic ingestion by riverine macroinvertebrates. Science of the Total Environment 646, 68-74.

P 13.30
Monitoring of river-induced bottom currents in Swiss lacustrine deltas

Gaétan Sauter[1], Damien Bouffard[2,3], Koen Blanckaert[4] Katrina Kremer[1,5]

[1] Institute of Geological Sciences and Oeschger Centre for Climate Change Research, Baltzerstrasse 1+3, CH-3012 Bern, Switzerland
[2] Swiss Federal Institute of Aquatic Science and Technology (EAWAG), Department Surface Waters – Research and Management, Kastanienbaum, Switzerland.
[3] Faculty of Geoscience and Environment, University of Lausanne, Lausanne, Switzerland
[4] TU WIEN Research Unit Hydraulic Engineering and Environmental Hydromechanics
[5] Swiss Seismological Service, ETH Zurich, Sonneggstrasse 5, CH-8092 Zurich, Switzerland

Slopes failures in deltas have the potential to induce underwater mass movements that can be tsunamogenic as shown in historical records. For instance, in 1687 AD, the spontaneous Muota Delta failure caused a 4-meter wave height (Hilbe and Anselmetti, 2015), while in 1996 AD, the triggered Aare Delta failure generated a 50-centimeter wave (Girardclos et al., 2007). The processes responsible for such delta failures remain unclear and notably the dynamic of erosion and deposition pattern of sediments in sublacustrine deltas. We propose to combine moored Acoustic Doppler Current Profilers (ADCPs) and repeated bathymetric mapping to advance in this research gap.

Here, we focus on two ADCPs measurement campaigns in the Aare delta in Lake Brienz in 2022 and the Muota Delta in Lake Lucerne in 2023. In both cases, two moorings with downward-looking ADCPs were deployed for a period of three months. Measured bottom currents are subsequently compared with other parameters, including river parameters from the Federal Office of Environment FOEN (discharge, temperature, turbidity), meteorological data from Meteoswiss (wind speed, wind directions, rainfall).

Our analysis highlights the large variability in bottom lake currents in submerged channels near river mouths and especially their linkage with wind and river discharge. The next steps will be to (i) fully characterize the triggers responsible for such currents in the deltaic area and (ii) to combine such hydrodynamic observations with repeated bathymetry mapping and finally better asses the origin and distribution of sediments related to these bottom currents.

REFERENCES

Girardclos S, Schmidt OT, Sturm M, Ariztegui D, Pugin A, Anselmetti FS (2007) The 1996 AD delta collapse and large turbidite in Lake Brienz. Marine Geology 241 (1-4):137-154

Hilbe M, Anselmetti FS (2015) Mass Movement-Induced Tsunami Hazard on Perialpine Lake Lucerne (Switzerland): Scenarios and Numerical Experiments. Pure and Applied Geophysics 172 (2):545-568. doi:10.1007/s00024-014-0907-7

P 13.31
Implementing a 3D groundwater model to simulate tree-planting scenarios against urban flooding in Nouakchott city, Mauritania

Barthelemy Simonnot[1], Emmanuel Dubois[1], Montana Marshall[1], Charlotte Grossiord[2], Paolo Perona[1]

[1] Platform of Hydraulic Constructions (PL-LCH), Civil Engineering Department, Ecole Polytechnique Federale de Lausanne (EPFL), Station 18, 1015 Lausanne, Switzerland
[2] Plant Ecology Research Laboratory (PERL), Civil Engineering Department, Ecole Polytechnique Federale de Lausanne (EPFL), Station 2, 1015 Lausanne, Switzerland

Despite its hot desert climate, parts of Nouakchott City, the capital of Mauritania, experience persistent flooding due to combined soil saturation excess and surface runoff, which causes damage to urban infrastructure and health issues. An investigation into the potential of tree planting as a solution to mitigate flooding is underway in Nouakchott. The city is located by the Atlantic Ocean that acts as a hydraulic boundary condition and contributes to the shallow aquifer that outcrops in the low-lying areas of the city. Another source of groundwater recharge lies in the infiltration of wastewater in the city. In the absence of a wastewater network, individual septic systems in households act as a diffuse artificial groundwater recharge system throughout the city.

By utilizing information provided by local stakeholders regarding the distribution system for domestic water (domestic water network and kart delivery), a conceptual map of artificial groundwater recharge was created, estimating recharge volumes for each neighborhood. As well, groundwater levels have been intermittently measured since 2015 across a network of 13 observation wells, while five automatic sensors have been sampling water depths since February 2023. Along with these measured data, a time series of the flooded areas in Nouakchott was reconstructed for the 2017-2023 period based on remote sensing data.

The goal of this project is to quantify the impacts of tree planting scenarios on lowering the groundwater table and potentially reducing the risk of flooding in the city.

Using the available geological and hydrogeological data, a 3D groundwater model was established using the FREEWAT software (Rosetto et al., 2018), which is built upon the MODFLOW code. The model was calibrated using groundwater level observations and the reconstructed time series of flooded areas. Additionally, five tree species were identified as suitable for such a long-term solution and are being monitored with sap flow meters since February 2023 to measure their transpiration. Based on the measured transpiration rates, a groundwater level-vegetation feedback routine is being implemented in order to formulate effective tree planting scenarios.

These scenarios aim to optimize the trees' impact on the water table while respecting local layout conditions, considering that trees are not yet abundant in public spaces and available space can be constrained.

REFERENCES

Rossetto, R., De Filippis, G., Borsi, I., Foglia, L., Cannata, M., Criollo, R., & Vázquez-Suñe, E. (2018). Integrating free and open source tools and distributed modelling codes in GIS environment for data-based groundwater management. Environmental Modelling & Software, 107, 210–230. https://doi.org/10.1016/j.envsoft.2018.06.007

P 13.32
Extreme water temperatures in mountain rivers

Amber van Hamel[1,2,3*], Manuela Brunner[1,2,3]

[1] WSL Institute for Snow and Avalanche Research SLF, Davos Dorf, Switzerland
[2] Institute for Atmospheric and Climate Science, ETH Zurich, Zurich, Switzerland
[3] Climate Change, Extremes and Natural Hazards in Alpine Regions Research Center CERC, Davos Dorf, Switzerland
**amber.vanhamel@slf.ch*

Human-induced warming, accompanied by more frequent extreme weather phenomena such as heat waves and prolonged drought, can result in extreme river water temperatures. Since water temperature is one of the main variables regulating physical, chemical and biological processes in streams, extreme water temperatures potentially result in severe impacts on both human resources and the survival of aquatic ecosystems. Despite the importance of extreme water temperatures, current research has mainly focussed on changes in mean water temperature. As there is little research on water temperature extremes, this project aims to improve our understanding of the spatial and temporal processes influencing the occurrence of current and future water temperature extremes in mountain rivers in Europe.

In this study, we analyze both temporal changes and spatial variability in the occurrences of water temperature extremes in mountain regions. First, to gain insights into the temporal variability of these extremes, we compare 30-year data series of water temperature in 18 catchments in the Alps. We apply trend analyses to extract information about the seasonality and long-term trends of these extremes. Second, to understand the frequency, severity and variability of extreme water temperature at a regional scale, we also compare 170 catchments spread over four different mountain regions in Europe. We use random forests to get insight into the importance of different contributing processes and the potential variations of water temperature extremes in both time and space.

Preliminary results of the trend analysis in the Alps show that extreme water temperatures, i.e. water temperature exceeding a locally varying threshold, have increased faster over the summer period 1991-2021 than mean water temperatures. Although the most severe extreme events can be mainly found at low elevations, the number of extreme events has increased over time at all elevations, with the strongest increase for catchments at high elevations. These first insights into the behaviour of water temperature extremes are already valuable for predicting future changes in extremes and the aquatic state of mountain rivers. Additional results on the spatial variation of extreme water temperature and the importance of different contributiong processes are expected soon.

P 13.33
Multiple-point geostatistics-based spatial downscaling of heavy rainfall fields

Wenyue Zou[1*], Guanghui Hu[1,3], Pau Wiersma[1], Shuiqing Yin[2], Grégoire Mariethoz[1], Nadav Peleg[1]

[1] *Institute of Earth Surface Dynamics, University of Lausanne, Lausanne, Switzerland (* wenyue.zou@unil.ch)*
[2] *State Key Laboratory of Earth Surface Processes and Resource Ecology, Faculty of Geographical Science, Beijing Normal University, Beijing 100875, China*
[3] *School of Geography, Nanjing Normal University, Nanjing, 210023, China*

High-resolution gridded rainfall products at sub-daily and 10^0 km scales are required for hydrological applications in mountainous and urban catchments. As most catchments are ungauged, gridded rainfall data are often obtained through remote sensing. However, their spatial resolution is often too coarse (at 10^1 km) and requires to be downscaled to a finer resolution. The challenge is not only to downscale the rainfall intensity to a finer scale by considering areal reduction factors, but also the spatial structure of the storm, as both elements are equally important to the assessment of the surface hydrological response. As a result of the lack of training data, the latter is difficult to obtain. Further development of the stochastic multiple-point geostatistics (MPS) [1] framework is presented to downscale long-term satellite-derived gridded rainfall series using only a few years of high-resolution rainfall observations. We demonstrate how the MPS framework can be used to downscale the satellite-derived CMORPH rainfall from 8 to 1 km resolution for 1998-2019, taking the city of Beijing as a case study, with a specific focus on extreme rainfall events. The high-resolution multisource-merged CMPAS dataset (1 km, hourly), available for 2015-2020, is used as the source of the training images. We show that the downscaling framework preserves the observed mean areal rainfall (with a bias of 2%), reproduces the spatial coefficient of variance (with a similar bias), and also retains extreme rainfall at the 99th percentile (with a bias of 6%). Furthermore, it adequately reproduces the rainfall spatial structure, preserving the variograms of the rainfall fields. Similarities were also observed comparing the 2- to 30-year return period maps of the downscaled rainfall extreme with ground observations, with half of the stations (10 out of 19) agreeing on the location and intensity of the extreme rainfall for all return periods**.** The results indicate that our framework downscales rainfall intensities and preserves the spatial structure well, especially for heavy rainfall, even if limited data is available. The proposed approach can be applied to other rainfall datasets and regions.

REFERENCES

[1] Gravey, M., Mariethoz, G., 2020. QuickSampling v1.0: a robust and simplified pixel-based multiple-point simulation approach. Geosci. Model Dev. 13, 2611–2630. https://doi.org/10.5194/gmd-13-2611-2020

P 13.34
Radiocarbon Inventories of Switzerland: Sources and cycling of dissolved organic carbon in Swiss lakes

Margot E. White[1], Benedict V.A. Mittelbach[1], Timo Rhyner[1], Negar Haghipour[1,2], Martin Wessels[3], Nathalie Dubois[1,4], and Timothy I. Eglinton[1]

[1] *Department of Earth Sciences, ETH Zürich, Switzerland (margot.white@erdw.ethz.ch)*
[2] *Laboratory for Ion Beam Physics, ETH Zürich, Switzerland*
[3] *Institut für Seenforschung der LUBW, Langenargen, Germany*
[4] *Department Surface Waters Research & Management, EAWAG, Dübendorf, Switzerland*

The Radiocarbon Inventories of Switzerland project (RICH) aims to establish a first-of-its-kind national inventory of radiocarbon for the country of Switzerland, emphasizing the role of aquatic systems as transporters, integrators, and processors of carbon. Delineating how environmental changes impact the carbon cycle requires a thorough understanding of reservoirs, fluxes, and processes - a task for which natural abundance radiocarbon is uniquely suited. Here, we focus on dissolved organic carbon (DOC) in Swiss lakes. DOC plays a crucial role in both nutrient transport and food web dynamics in aquatic ecosystems. By widely applying ^{14}C measurement of lake water DOC for the first time in ~15 lakes across Switzerland, we gain new insight into the sources and cycling of this important carbon pool. The ^{14}C signature of DOC produced by *in situ* primary productivity is constrained by concurrent measurements of dissolved inorganic carbon (DIC). In addition to radiocarbon and stable carbon isotope measurements, we use fluorescence and absorbance properties of dissolved organic matter to disentangle sources and understand the composition of lake water DOM. We find a range in the contributions of allochthonous DOC across lakes with different watershed characteristics and trophic states. Monthly measurements from Lake Constance and Lake Geneva further help to constrain seasonal changes in primary productivity and river influence, which impact the composition of DOC within these large oligotrophic lakes.

P 13.35
Reconstructing High-Resolution Snow Water Equivalent (SWE) Data for Improved Water Resource Management (1950-2100)

Fatemeh Zakeri [a,b] , Gregoire Mariethoz [a], Manuela Girotto [b]

[a] *Institute of Earth Surface Dynamics, Faculty of Geosciences and Environment, University of Lausanne, Lausanne, Switzerland*
[b] *Department of Environmental Science, University of California Berkeley, Policy, and Management, Berkeley, CA, USA*

Accurate knowledge of Snow Water Equivalent (SWE) is essential for water resource management, climate change insights, and hydrological studies. However, obtaining precise SWE data at high resolution remains challenging due to limitations in satellite, climate, and in-situ information. This research introduces an innovative method to derive daily SWE data spanning from 1950 to 2100 at a 500 m resolution. Utilizing the WUS–UCLA dataset, which offers daily 500 m SWE details for the years 1985–2021, this study seeks to bridge both the temporal and spatial resolution gaps.

Our methodology builds on recurring snow patterns and incorporates meteorological predictors from the low-resolution CMIP version 6 simulations with a 100 km resolution. We utilize the K-nearest neighbor algorithm paired with a specialized similarity metric to estimate SWE values. The approach selects days with available SWE data whose meteorological conditions match those of a query day lacking SWE, and then it estimates the SWE for that day.

To evaluate the effectiveness of our technique, we employed a leave-out cross-validation method and compared our results with the 1 km SWE Daymet and 4 km SWE datasets from the University of Arizona. In this validation, 80% of the days from the WUS–UCLA dataset were used as the learning set, while the remaining 20% were for validation. Our results reveal a strong alignment between our estimated SWE and actual observations, indicating this methodology's promise for enhancing water resource management and climate research.

14 Geoscience for Cultural Heritage

Giovanni Cavallo & Marta Caroselli

TALKS:

14.1 Antić A.: Enhancing Sustainable Cave Tourism Worldwide: The Show Cave Assessment Model (SCAM)

14.2 Cavallo G., d'Erme C., Cassitti P.: "Forgotten Colors". Tracing the Origin of Mineral and Artificial Early Medieval Pigments in Raetia Curiensis.

14.3 Muth X., Bosson A., Gressin A.: Matching fragmented lithic archaeological artefacts

14.4 Nistor D., Caroselli M., Correll S.: Charachterization of materials and techniques in the grotto-decorated chapel of the St Mary Magdalene Hermitage, Munich (Germany)

14.5 Oddsson B.: Folafótur Geopark in the Westfjords of Iceland

14.6 Pascucci S., Scioscia Santoro C., Caroselli M., Casocavallo B., Cerroni F., Piqué F.: The characterization of the painted plasters in the early roman Oceane tomb near Viterbo (Italy)

14.7 Peduzzi L.: Thermally induced modifications in different types of magnesian soft stones

POSTERS:

P 14.1 Rodier J., Berranger M., Serneels V.: Geochemical study of hammerscale, an overview. Implications for iron provenance and supply of an archaeological smith.

P 14.2 Spataro A., Primerano C.: CHIS4TI: Cultural Heritage Information System 4 Ticino

P 14.3 Bomou B., Adatte T.: Petrographic characterisation of molassic stones from Lausanne Cathedral

14.1

Enhancing Sustainable Cave Tourism Worldwide: The Show Cave Assessment Model (SCAM)

Aleksandar Antić[1]

[1] *Institute of Geography and Sustainability, University of Lausanne, Sion CH -1967, Switzerland (a.antic994@gmail.com)*

Geoheritage assessments play a pivotal role in preserving and understanding the natural and cultural attributes of geological sites. These assessments provide a foundation for sustainable land management and responsible tourism practices (Reynard & Brilha, 2017). By systematically evaluating geoheritage, we gain a comprehensive understanding of the ecological and historical significance of sites such as show caves (Cigna & Burri, 2000; Cigna, 2016; Cigna, 2019). This knowledge is essential for developing effective conservation strategies, supporting educational initiatives, and fostering lasting appreciation for the planet's geological phenomena.

This paper introduces the Show Cave Assessment Model (SCAM), a robust methodology designed to assess and improve sustainable cave tourism development. The main aim is to present SCAM as a practical tool applicable to show caves worldwide, with a specific focus on its assessment capabilities. Although initially developed and applied exclusively in Serbian show caves (Antić et al., 2022), SCAM's adaptability makes it suitable for global use. This paper provides insights into the methodology's versatility and its potential for broader application.

SCAM offers a comprehensive approach to identifying shortcomings in the protection of underground ecosystems and evaluating the speleological and tourist values of show caves. An essential aspect of SCAM involves collecting input from experts and tourists regarding the importance of specific value indicators. Authors intending to use the model will need to conduct two surveys—one with experts and another with tourists. The results from these surveys are then integrated into the SCAM matrix, providing a clear overview of speleological and tourist values for each examined show cave.

The vulnerability of karst terrain, which is often home to unique and delicate ecosystems (Daoxian, 2001; Li et al., 2021), underscores the urgency of responsible cave tourism practices. Karst landscapes are susceptible to environmental impacts, and improper tourism can exacerbate these vulnerabilities. Thus, safeguarding and conserving karst environments is not only an ecological imperative but also essential for ensuring the long-term viability of show cave tourism (Antić et al., 2020). By utilizing SCAM as a tool for sustainable development, we can strike a balance between the enjoyment of these natural wonders and their preservation for future generations.

Therefore, this paper advocates for the widespread adoption of SCAM as a pragmatic assessment tool for show caves globally, emphasizing the significance of protecting and preserving karst terrains and the unique underground ecosystems they host. By incorporating insights from experts, tourists, and authors, SCAM empowers stakeholders to implement sustainable practices, ensuring the preservation of speleological geoheritage for future generations.

REFERENCES

Antić, A., Peppoloni, S., & Di Capua, G. (2020). Applying the values of geoethics for sustainable speleotourism development. Geoheritage, 12, 1-9.
Antić, A., Tomić, N., & Marković, S. B. (2022). Applying the show cave assessment model (SCAM) on cave tourism destinations in Serbia. International Journal of Geoheritage and Parks, 10(4), 616-634.
Cigna, A. A. (2016). Tourism and show caves. Zeitschrift für Geomorphologie, 60(2), 217-233.
Cigna, A. A. (2019). Show caves. In Encyclopedia of caves (pp. 909-921). Academic Press.
Cigna, A. A., & Burri, E. (2000). Development, management and economy of show caves.
Daoxian, Y. (2001). On the karst ecosystem. Acta Geologica Sinica-English Edition, 75(3), 336-338.
Li, S. L., Liu, C. Q., Chen, J. A., & Wang, S. J. (2021). Karst ecosystem and environment: Characteristics, evolution processes, and sustainable development. Agriculture, Ecosystems & Environment, 306, 107173.
Reynard, E., & Brilha, J. (Eds.). (2017). Geoheritage: assessment, protection, and management. Elsevier.
Ruban, D. A. (2018). Karst as important resource for geopark-based tourism: Current state and biases. Resources, 7(4), 82.

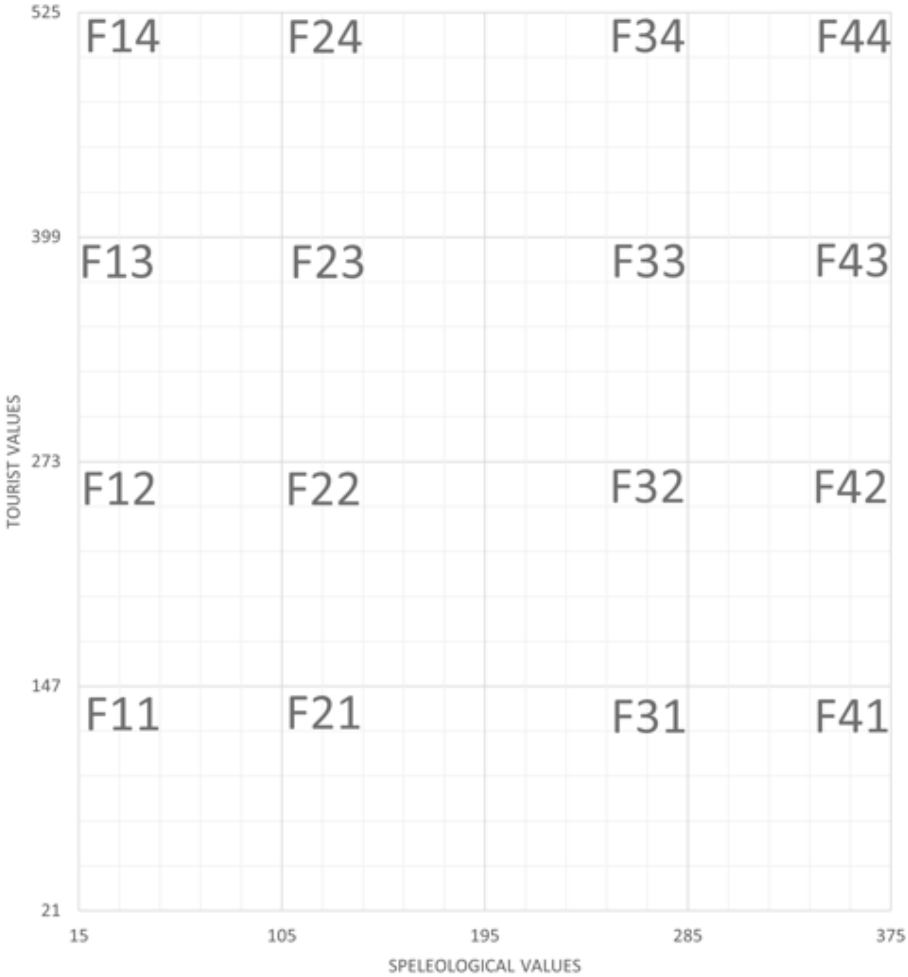

Figure 1. Structure of the SCAM matrix (Speleological and Tourist values).

14.2
“Forgotten Colors”. Tracing the Origin of Mineral and Artificial Early Medieval Pigments in *Raetia Curiensis*.

Giovanni Cavallo[1], Chiara d’Erme[1], Patrick Cassitti[2]

[1] *Institute of materials and constructions, University of Applied Sciences and Arts of Southern Switzerland, via Flora Ruchat-Roncati 15, CH-6850 Mendrisio (giovanni.cavallo@supsi.ch; chiara.derme@supsi.ch).*
[2] *Stiftung Pro Kloster St. Johann, CH-7537 Müstair (patrick.cassitti@muestair.ch).*

Only very few examples of Early Medieval wall paintings survive in Europe, the most well-known are mapped in Fig. 1. Half of the aforementioned sites are located in the historic region of *Raetia Curiens* corresponding to the present region of the Grisons Canton (Switzerland) and the Western part of South Tyrol (Italy).

This situation led to propose a research project funded by the Swiss National Science Foundation (SNSF) (https://data.snf.ch/grants/grant/201055) for comparative studies of wall paintings and painted fragments in the ancient *Raetia Curiensis* region using the same methodological approach at all sites, including non invasive (Technical Photography, TP; Hand-held X-ray Spectroscopy, HH-XRF; portable Infrared Spectroscopy, p-ATR/FTIR; Fiber Optics Reflectance Spectroscopy, FORS) and micro-invasive analysis (Optical Microscopy, PLM; Scanning Electron Microscopy coupled with Energy Dispersive X-ray Spectroscopy, SEM/EDX; Laser Ablation - Inductively Coupled Plasma Mass Spectroscopy, LA-ICP-MS; isotope analysis). The scope of the research is not only oriented towards the characterization of the painting materials and pictorial technique but also for understanding the provenance of the raw materials and the technological processes behind the production of artificial pigments.

The application of non-invasive analysis (Bläuer & Keller, 2020; Cavallo *et al.*, 2020; 2023) allowed for a preliminary identification of the materials used. Summarizing, Fe-bearing yellow and red mineral pigments (generally referred as ochre) and C-based pigment (presumibly charcoal black) were detected in all the studied sites. The presence of red lead (Pb_3O_4) is common though its presence in St. Peter in Mistail and St. Prokulus in Naturns is questionable. Remarkable is its extensive use in the painted stucco fragments from the St. Martin church in Disentis. The presence of lead white [cerussite and/or hydrocerussite, $PbCO_3$ and/or $Pb_3(CO_3)_2(OH)_2$] was confirmed in all the sites with the exception of St. Peter in Mistail and the monastery church of St. John. Blue pigments (natural ultramarine and Egyptian blue) were detected at Müstair and Mals. Green Cu-based pigments were found in Naturns A green Cu-based pigment was found also at Chur whilst the presence of Egyptian blue was clearly detected both on the Eastern wall of the crypt and on painted fragments.

The results of the non invasive campaign allowed for planning a well-disegned sampling strategy at the site of Disentis. About 40 micro-samples were analysed using microscopic techniques (PLM and SEM/EDX) in order to establish the tickness of the paint layer, the relationship with the preparation and/or the ground layer, the (inorganic) binder possibly used, the mix of different pigments. After this first analytical run, a further selection of samples was carried out for in-depth studies (LA-ICP-MS and lead isotope analysis) at the Department of Geosciences, University of Bern.

These first tests confirmed most of the results gathered using non invasive analysis. Extremely important is the presence of a Pb-Sn-(Si)-based pigment (lead-tin yellows type I and II?) always associated with minium in different proportions depending on the analysed microsample. This is important for better understanding the technical and technological process behind Pb-based pigments manufacture and use. In addition, the presence of V and As associated with ochre in a few samples may be an important marker for starting to establish the geological provenance of the raw materials.

REFERENCES

Bläuer, C., Keller, A. T. 2020. Mainly red and a hidden blue – Laboratory and MSI investigations on the Carolingian wall paintings in the Chapel of the Holy Cross of Müstair (Switzerland). Journal of Cultural Heritage, 42, 72-80.

Cavallo, G., Moretti, P., Piqué, F., Giraldo Ocampo, A.I., Aceto, M., Villa L., Cassitti, P. 2023. The non-invasive study of a group of Early Medieval wall paintings in the Raetia Curiensis region. Poster presented at Technart Conference, Lisbon (paper in preparation).

Cavallo, G., Aceto, M., Emmenegger, R., Keller, A.T., Lenz, R., Villa, L., Wörz, S., Cassitti P. 2020: Preliminary non-invasive study of Carolingian pigments in the churches of St. John at Müstair and St. Benedict at Malles. Archaeological and Anthropological Sciences 12(3). https://doi.org/10.1007/s12520-020-01024-2.

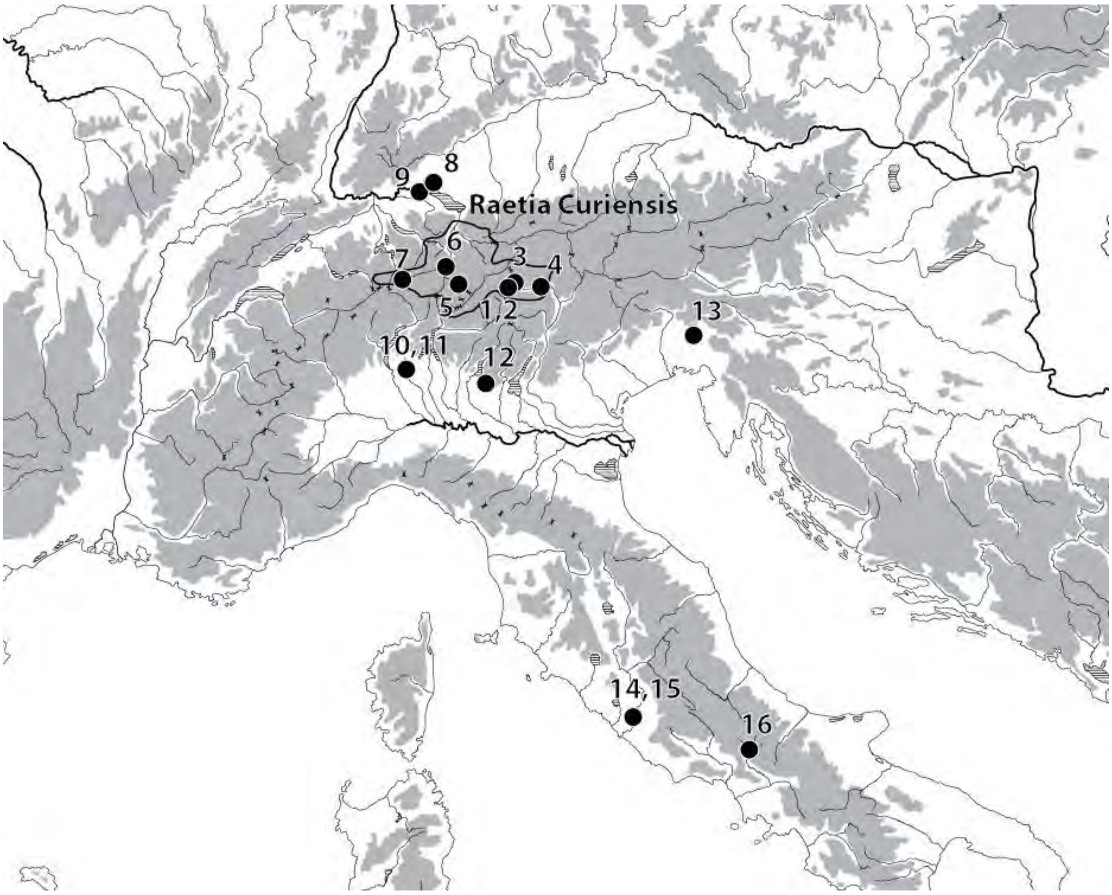

Figure 1. General map with indication of the Early medieval sites.
1, 2. Monastery church of St. John and the Holy Cross chapel in Müstair, Grisons, Switzerland, (late 8th); 3. The church of St. Benedikt in Mals/Malles, South Tyrol, Italy, (early 9th c.); 4. The church of St. Prokulus in Naturns/Naturno, South Tyrol, Italy, (10th c.); 5. The church of St. Peter in Mistail/Alvaschein, Grisons (late 8th c.); 6. The crypt church of St. Stephan in Chur, Grisons, (6th c.); 7. St. Martin church in Disentis/Mustér, Grisons (archaeologically recovered fragments of painted stucco decoration, late 8th c.); 8. The church of St. Georg in Reichenau-Oberzell, Baden-Württemberg (10th c.); 9. The Sylvester chapel at Goldbach, Baden-Württemberg (10th c.); 10, 11. The church of St. Maria Foris Portas at Castelseprio and the adjacent Torba Tower, Lombardy, Italy (8th-9th c.); 12. The church of Sta. Giulia, Brescia, Lombardy, Italy; 13. The Tempietto Longobardo at Cividale, Friuli, Italy; 14, 15. The churches of Sta. Maria Antiqua and San Saba in Rome, Italy.

14.3
Matching fragmented lithic archaeological artefacts

Xavier Muth[1,2], Adrien Bosson[1], Adrien Gressin[1]

[1] *School of Engineering and Management Vaud, HES-SO University of Applied Sciences and Arts Western Switzerland (xavier.muth@heig-vd.ch)*
[2] *Get in Situ Sàrl, CH1097 Bourg-en-Lavaux, Switzerland*

This “3D puzzles” problematic is widespread in various fields of the archaeological sciences. For every time periods, there are specific topics (e.g., pottery reconstruction in the neolithic, virtual 3D reconstruction of temples in the ancient Greece). Here we focus on prehistoric archaeology and more specifically on lithic artifacts refitting, when the 3D stratigraphic context of the artifacts is often more important than the artifact itself. Refitting fragmented prehistoric artifacts (Tixier 1978) not only provide lots of information about the original complete object, but also give valuable clues for qualifying the archaeological stratigraphy integrity (Bordes 2002).

The proposed methodology aims to gain efficiency when archaeologists test exhaustively the potential matches among large series of artifacts. Based on 3D digitized artifacts, the main idea is to transpose this 3D problem into a 2D one, enabling us the use of classical computer vision methodologies.

The algorithm involves the following main steps:
- decomposition of each object into faces
- generation of 2D shaded maps for each face
- matching of the 2D faces using SIFT algorithm (Lowe 2004)
- relative orientation of the objects when a match is found

The following lithic assemblage (Figure 1) has been successfully and automatically reassembled using the exposed method. It has now to be tested on a larger number of artifacts and various types of material.

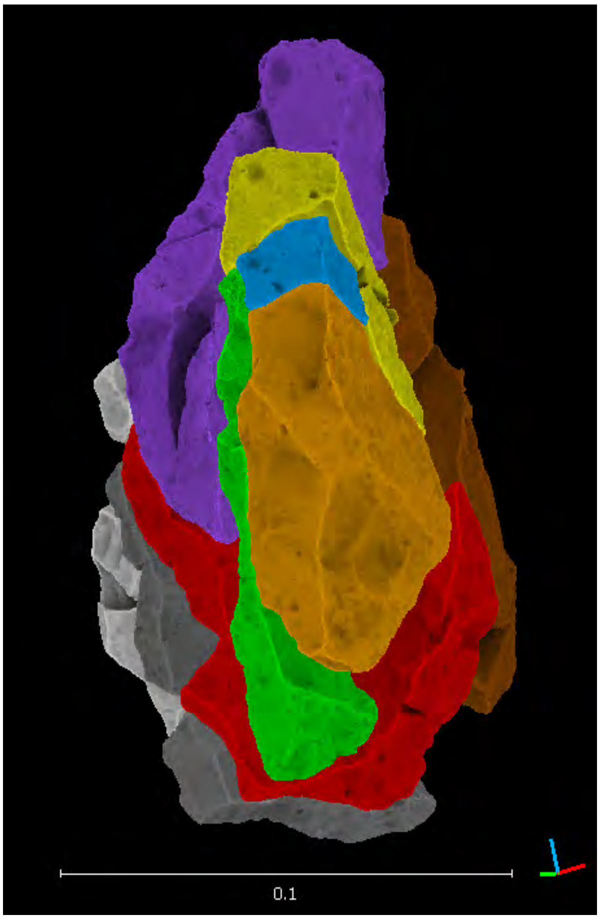

Figure 1 Example of a lithic assemblage that has been automatically refitted, based on the 3D photogrammetric digitizing of Lokalalei 2C assemblage provided by the Musée National de Préhistoire, Les Eyzies de Tayac, France. (Bosson 2022)

REFERENCES

Bordes, J.-G. 2002, Les interstratifications Châtelperronnien / Aurignacien du Roc-de-Combe et du Piage (Lot, France). Analyse taphonomique des industries lithiques : implications archéologiques. Phd thesis, University of Bordeaux I, 423 p.

Bosson, A. 2022: Appariemment 3D d'objets archéologiques, Master thesis, UNIGE - HES-SO.

Tixier, J. 1978: Notice sur les travaux scientifiques. Phd Thesis, University of Paris X, 117p.

Lowe, D. G. 2004: Distinctive Image Features from Scale-Invariant Keypoints, International Journal of Computer Vision. Band 60, Nr.2, p91-110.

14.4
Charachterization of materials and techniques in the grotto-decorated chapel of the St Mary Magdalene Hermitage, Munich (Germany)

Denise Nistor[1,a], Marta Caroselli[1], Stefanie Correll[2]

[1] *University of Applied Arts and Sciences of Southern Switzerland (SUPSI), Institute of Materials and Construction (IMC), Mendrisio, Switzerland.*
[a] *Conservation Restoration master's student (nistor.denise@gmail.com)*
[2] *Bayerische Verwaltung der staatlichen Schlösser, Gärten und Seen (Bavarian Palace Administration), Conservation Department, Munich, Germany.*

Figure 1. St Mary Magdalene Hermitage, Chapel.

Built in 1728, the St Mary Magdalene Hermitage (Magdalenenklause), is a park palace in the Nymphenburg Palace complex in Munich and is designed as an artificial ruin. The interior of the chapel is richly decorated with a variety of materials in imitation of a grotto and painted surfaces. The object had never been studied from a technical point of view before and was chosen as a case study for a Master's thesis in Conservation and Restoration at SUPSI. Well established multi-analytical investigations such as PLM (polarized light microscopy), XRF (x-ray fluorescence), FTIR (infrared spectroscopy) and SEM-EDS (Scanning electron microscope coupled with energy dispersive spectroscopy) were used with the aim of identifying the materials used, the execution techniques and the main deterioration phenomena with a view to its conservation. The results show that the grotto decoration was made of genuine rock formation limestone tufa and lime-gypsum mortar. The pebbles are elaborately decorated with paint layers and glass as well as metal glitter sprinkling technique, which is rarely preserved today. Possible identified pigments such as smalt, lead oxide red, copper-based green, orpiment, basic lead carbonate and yellow ochre contribute to the imitation of precious stones and minerals in the decorative scheme. This study provides a wide range of data, that allows to further improve the knowledge of the composition and manufacturing techniques of the grotto-decorated surfaces in the chapel.

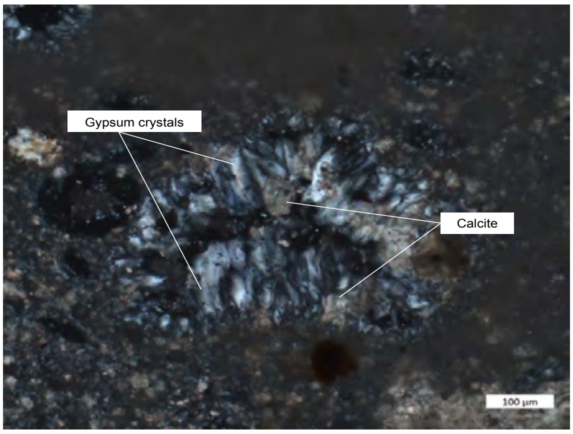

Figure 2. Mortar sample, PLM, 200x, XPL, gypsum crystals along the pore wall, partly extinct. Calcite on pore wall and in the middle.

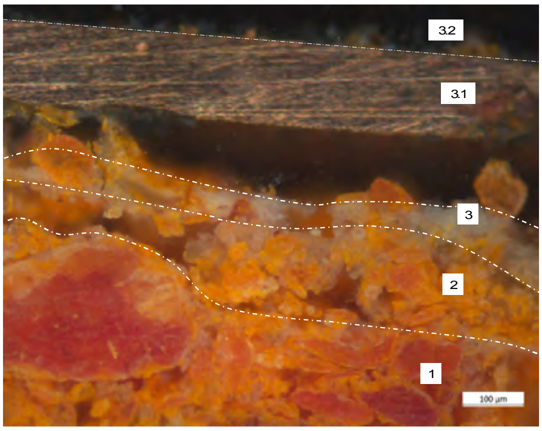

Figure 3. Paint layer sample, PLM, 200x, DF, two applications of lead-based red (1 and 2), followed by an organic layer of probably oil, wax and protein (3), copper platelet (3.1), green copper oleat formation (3.2).

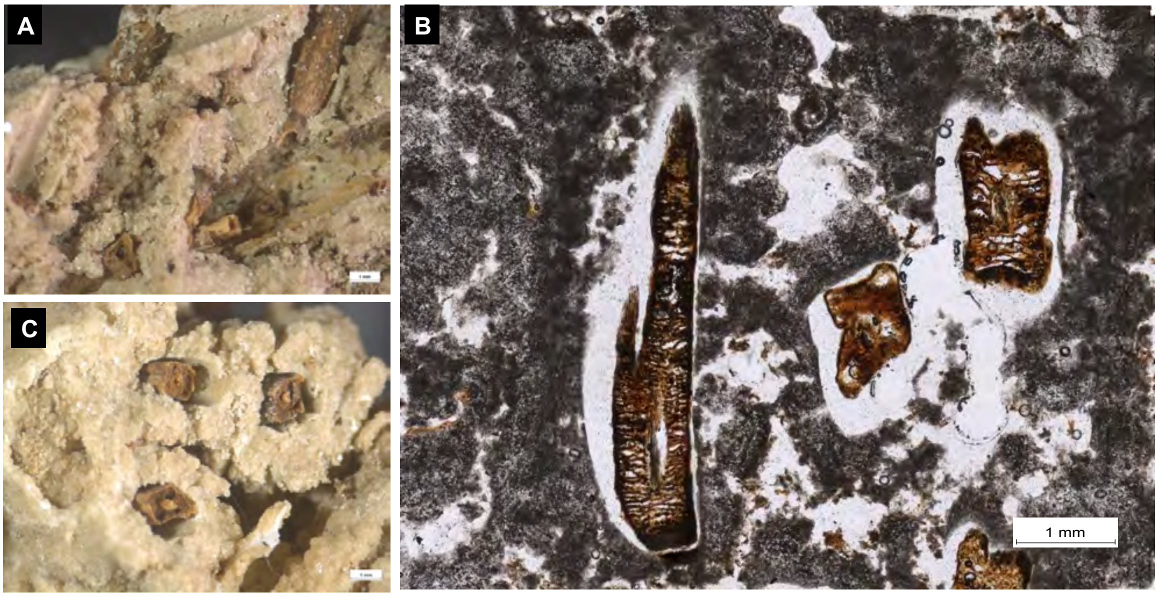

Figure 4. a) and b): Tufa application sample before embedding, probably needles of a coniferous tree, stereomicroscope. c) Thin section of calcareous tufa, PLM, 50x, PPL.

REFERENCES

Niehaus, F., & Poschlod K. 2018. Geologie und Naturwerksteine von Bayern. p. 125 – 144. In Grimm, W-D., and N. Ballerstädt. Bildatlas wichtiger Denkmalgesteine der Bundesrepublik Deutschland., Teil 1: Textband & Teil 2 Bildband. Ulm: Ebner. ISBN 978-3-87-188-247-0.

Schramm, H-P., & Hering B., 2000. Historische Malmaterialien und ihre Identifizierung. [Reprint] Bücherei des Restaurators Band 1. Stuttgart: Enke. ISBN: 3363008082.

14.5
Folafótur Geopark in the Westfjords of Iceland

Björn Oddsson[1]

[1] *Department of Earth Sciences ETH Zurich, Zurich, Switzerland, The Association Folafótur Geopark - Nature Reserve and Cultural Heritage, Reykjavik, Iceland*

The Westfjords constitute the large peninsula in the northwesternmost part of Iceland, facing the east coast of Greenland. Together with the Eastfjords they display the oldest rocks of Iceland, which resulted from the volcanic activity that took place in the Miocene and Lower Pliocene (Tertiary basalts) although now they are far from the active oceanic spreading ridge situated in the middle part of Iceland (Jóhannesson 2014).

The Westfjords provide dramatic landscapes characterized by a sequence of glacial fjords towered by mountain plateaus. The unspoiled natural beauty of this remote region of Iceland has been acknowledged worldwide. The Lonely Planet travel guide awarded the Westfjords as No. 1 region on the list for Best Travel 2022 (https://www.lonelyplanet.com/iceland/the-westfjords). Within the Westfjords, the Folafótur (Icelandic: foal's leg) peninsula, located midst in Iceland's greatest Fjord system, Ísafjarðardjúp, is renowned for its landscapes dominated by the imposing Mt. Hestur (Icelandic: horse. 536 m a.s.l.). Mt. Hestur is famous for its silhouette, and represents most prominent visual landmark for hikers walking in the region (Figure 1 and 2). It is Iceland's neatest example of the geomorphological process called glacial transfluence.

The Folafótur peninsula and the surrounding sea shelter extremely diverse and rich flora and fauna like the artic fox, a variety of birds, seals, whales, corals, molluscs, and other sea creatures in addition to the endemic arctic flora. Akin to other ecosystems, the wildlife on the Folafótur peninsula is likely to be increasingly affected by climate change in the future.

Finally, the peninsula is a history and literature landmark. The first mention can be found in the Landnámabók, a medieval Icelandic manuscript which describes the settlement of Iceland during 9th and 10th centuries (Pálsson & Edwards 1972). It includes the illustrious saga of Vébjörn Sygnakappi, Atli í Fljótum and Geirmundur Heljarskinn. With the exception of some traditional fairy tales the later history of the peninsula is hardly known. However, several archaeological sites, represented by ruins of historical fishing and farming settlements, document dense inhabitation from the centuries past until ultimate abandoned in the early forties. The Nobel price for literature winner, Halldór Laxness, uses the ambience of Folafótur for his autobiographic novel Heimsljós in 1937 – 1940 (Laxness 1955). It is just here where he had his moments of ephiphany and experienced the „Kraftbirtingarhljómur Almættisins", meaning 'The Explosive Sonics of Divinity'.

Since the new landowners were aware of the high value of biodiversity, geodiversity and cultural heritage of Folafotur peninsula in 2017, measures have been taken for its protection and conservation. First steps included participation in the regional planning for the community of Súðavík which was finalized in 2020 and therafter taking the lead in the following detail planning of the area. The latter resulted in a permission for building of an autarkic alpine-style hut inside the protected area. It is currently under construction and shall serve as accomodation and working place for scientists, volunteers and visitors. A non profit organization, the Association Folafótur Geopark - Nature Reserve and Cultural Heritage, was founded under Icelandic law in order to carry out the development of the geopark, to set up a research station and coordinate future scientific research and its dissemination.

The Association initiated a cooperation project with the Italian State CNR Institute of Geosciences and Earth Resources at the University of Pisa in 2020 which main objective is the establishment of a geopark following the criteria laid down by UNESCO›s International Geoscience and Geoparks Programme (https://en.unesco.org/global-geoparks/focus). The involved structural geologists are specialists of geotectonics with ample experience of geopark development and assessment mainly within the Global Geoparks Network. This presentation discusses the results of the first two missions carried out in summer 2022 and 2023 (Ellero et al. 2023). They include a detailed geological-geomorphological and tectonic mapping of the peninsula in the scale of 1:10.000 combining significant features of geology, illustrating Earth's geodynamics, and geomorphological processes related to climate change. Furthermore, the identification of diverse geodiversity and cultural sites and their symbolic representation on the map. The geodiversity sites were classified according to their primary interest in geomorphological, magmatic, tectonic, and lithological sites. They were carefully weighted for both the potential scientific significance for understanding the geological history of the area, and for their educational and aesthetic values. The cultural sites were distinguished according to their cultural value and connection with geological and geomorphological aspects and are subdivided according to their primary interest as archaeological, literature, and historic sites. The resulting geological geomorphological map thus highlights the main elements of geodiversity and cultural heritage of Folafótur. The study represents a starting point for the establishment of possible geosites and the quantitative and qualitative assessment of the geoheritage of Folafótur peninsula which is essential for a geoconservation strategy.

Past studies of Iceland's geology have mainly focussed on the active volcanism and the youngest regions of the country.

While careful mapping of Tertiary basalts including roots of extinct volcanoes in eastern Iceland revealed valuable insight to the early geological development, their counterpart in the Westfjords have almost been neglected. Actual global tectonic interpretation of Iceland's geology, with an active rifting zone migrating north-westwards above deep sitting stationary Mantle Plume / Hot Spot and repeated shifting of the active zones to synchronise with the Hot Spot, indicate the western part of Iceland and especially the Westfjords may encounter key information on earlier tectonic development of the Mid Atlantic Ridge. The striking abundance of geothermal energy in the Westfjords can be interpreted as a footprint of the Hot Spot. It is hoped for the studies in Folafótur may initiate further research of the interesting geology of the Westfjords.

REFERENCES

Ellero, A., Oddsson, B. & Ottria, G. 2023: Geology and geodiversity of the Folafótur peninsula (Westfjords, Iceland).

Jóhannesson, H. 2014: Geological Map of Iceland 1: 600.000. Bedrock geology (2nd ed.). Icelandic Institute of Natural History.

Laxness, H. K. 1955: Heimsljós I-IV. Helgafell.

Pálsson, H. & Edwards, P. 1972: The Book of Settlements: Landnámabók. Translation from the original of Ari Þorgilsson the Learned.

Figure 1. Panoramic view of Mt. Hestur from the north of the Folafótur peninsula looking towards south.

Figure 2. View to the north from top of Mt. Hestur on the isle of Vigur off the hoof of Folafótur in Ísafjarðardjúp and the mountains of Snæfjallaströnd in the background with glacier Drangjökull on the far right.

14.6
The characterization of the painted plasters in the early roman Oceane tomb near Viterbo (Italy)

Sara Pascucci[1], Chiara Scioscia Santoro[2], Beatrice Casocavallo[3], Federica Cerroni[3], Marta Caroselli[1], Francesca Piqué[1]

[1] *Scuola Universitaria Professionale della Svizzera Italiana (SUPSI), Conservation e Restoration, SUPSI, CH-6850 Mendrisio (sarapascucci@yahoo.com Marta.caroselli@supsi.ch, francesca.pique@supsi.ch)*
[2] *Funzionario restauratore, Soprintendenza Speciale Archeologia Belle Arti e Paesaggio di Roma (chiara.sciosciasantoro@cultura.gov.it)*
[3] *Soprintendenza Archeologia, Belle arti e Paesaggio per l'Area metropolitana di Roma, la provincia di Viterbo e l'Etruria meridionale. (beatrice.casocavallo@cultura.gov.it; federica.cerroni@cultura.gov.it)*

The *Oceane* Tomb is a hypogeous space located near Viterbo, in the area of the *Poggio Giudio* Necropolis (6th-1st century B.C.) in central (Italy). The tomb and its wall paintings suggests that it is a tomb of Roman origin dating back to the 1st-3rd century A.D. although this needs to be confirmed with further analysis.
The *Oceane* Tomb is a chamber tomb excavated in the tuffaceous cliff face characteristic of this area. The wall paintings are composed of two layers of the plaster: a rougher leveling one, the *arriccio,* and a smoother superficial one, the *intonachino*. These plasters cover the vertical walls but not the ceiling of the tomb. The wall paintings are executed over the *intonachino* with natural earth-based colors. The paintings suffer from severe detachment and disintegration of the mortars.To develop a compatible conservation intervention, it was necessary to characterize the making of the wall paintings and its plasters. The scientific techniques used inlcude HH-XRF, reflected and transmitted light optical microscope observation, FTIR- ATR, SEM-EDX.

The *arriccio* plaster layer is characterized by a purplish color very similar to that of the tuffaceous cliff face. It is rich of an amorphous-glassy compounds as binder and aggregates of volcanic origin. The *arriccio* plaster contains a predominance of silicate components while calcium carbonate is absent (Figs. 1 - 4)

The nature of the *arriccio* plaster is peculiar and the current hypothesis is that it may be a complete reaction of calcium hydroxide with the local tuff, geologically referred to as 'Vicano black-slag red tuff' composed of volcanic minerals and ash. The reduced presence of calcium is probably related to an extremely limited use of lime. The presence of a clay fraction is possible, but further studies are necessary.

The literature consulted reports only one case study with similar characteristics: the mortar of a conduit of the Trajan Aqueduct (109 AD) near Lake Bracciano, a few kilometers away (Botticelli 2021). Both case studies are located in the vicinity of the Latium Antiappennines consisting of series of mountain ranges of volcanic origin (Sabatini, Cimini and Volsini Mountains).

Even Vitruvius in the Book II of De Architectura (c. 15 B.C.) describes the quarries to extract aggregates that make strong and long-lasting plasters and writes that the best are those around Lake Bolsena, thus including the nearby Viterbo area.

The *intonachino* plaster is considerably different as it contains calcium carbonate and structures such as lime lumps in addition to a high silicate component. The aggregates consist of carbonate stone fragments with granulomentry up to 3 mm and cocciopesto particles, which imparts a hydraulic character to the mortar.

Currently, the hypotheses on the making of the *arriccio* plaster needs further confirmation and research, but the infromations obtained can certainly be considered the starting point for a study of this particular technique. The understanding of the relationship between the mineralogical phases of the *arriccio* and those of the rock cliff and the possible interaction with lime.

REFERENCES

Botticelli, M.; Calzolari, L.; De Vito, C.; Mignardi, S.; Medeghini, L. Aqua Traiana, a Roman Infrastructure Embedded in the Present: The Mineralogical Perspective. Minerals 2021, 11, 703. https://doi.org/10.3390/min11070703

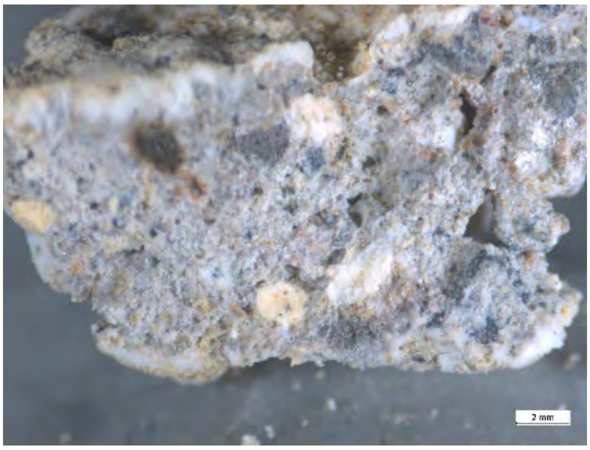

Figure 1: Fragment of A*rriccio* plaster

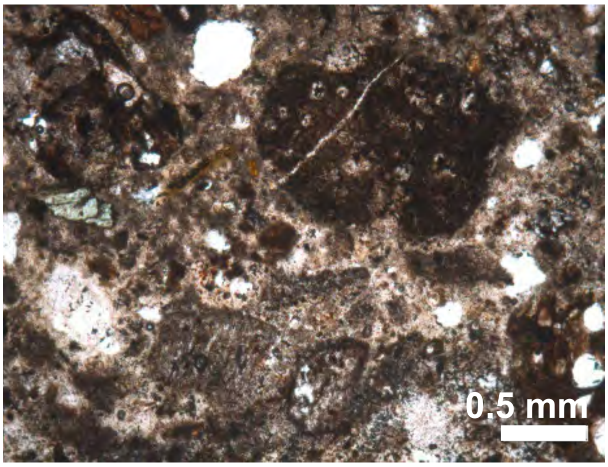

Figure 2. Transmitted light optical microscope, parallel polar image showing probable pozzolanic aggregate in the *arriccio*

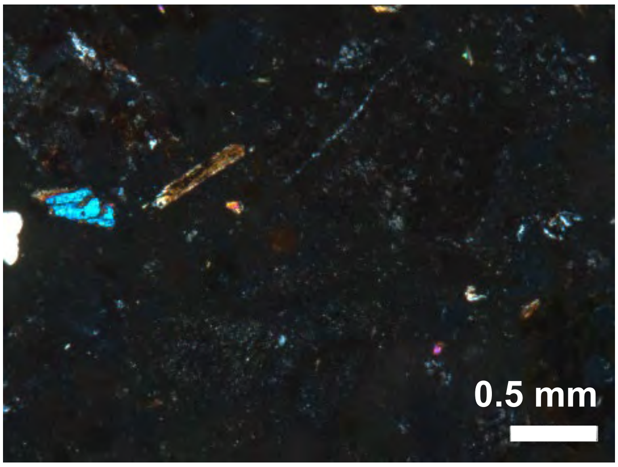

Figure 3. Transmitted light optical microscope, crossed polar image showing probable pozzolanic aggregate in the *arriccio*

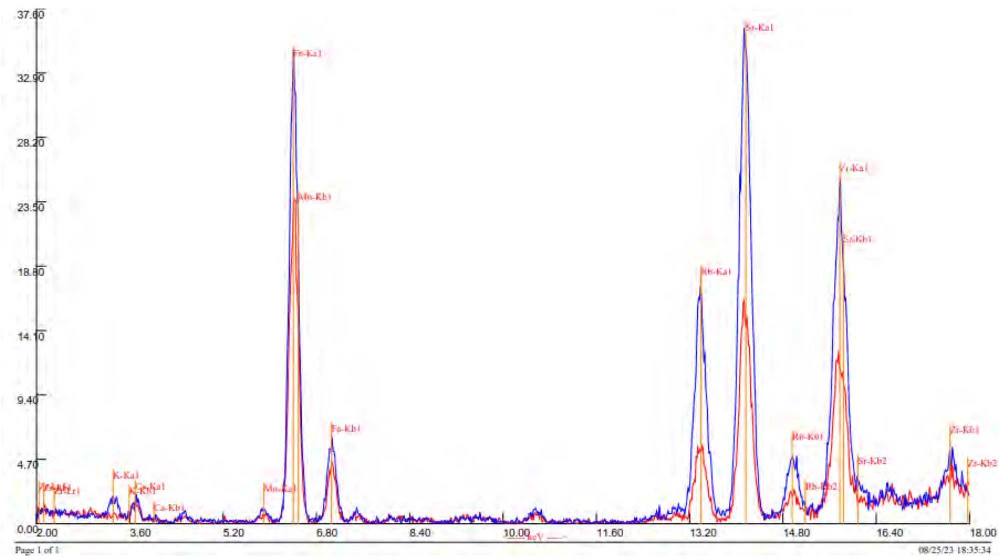

Figura 4. HH-XRF spectra of analyses performed in situ on the rock substrate (blue) and on the *arriccio* (red) showing the same elemental composition with chemical elements such as Sr, Fe, Zr, Rb, and traces of Ca, Mn. Notable the limited presence of calcium in both the rock and the *arriccio* plaster.

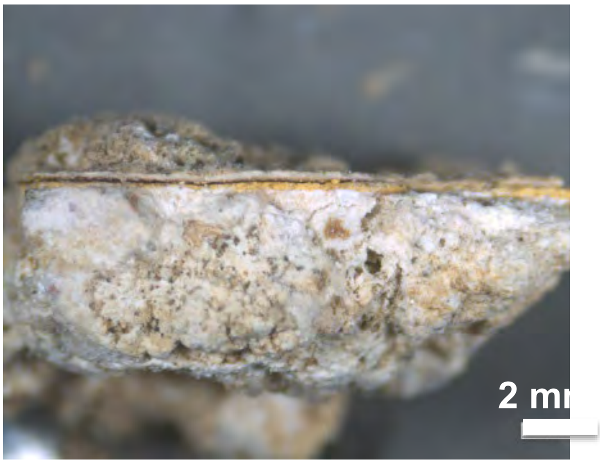

Figure 5. Cross-section of *intonachino.*

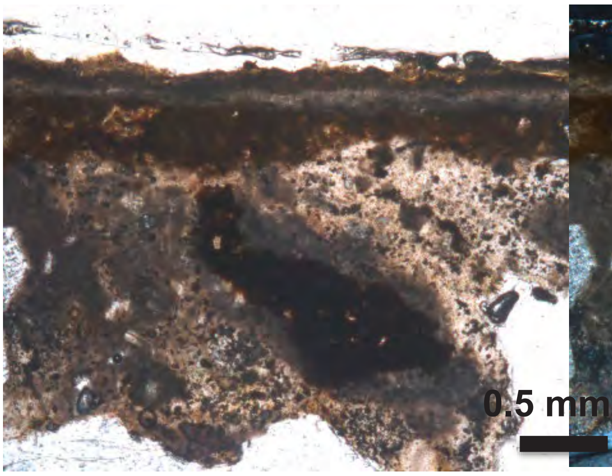

Figure 6. Transmitted light optical microscope (PPL) image showing a *cocciopesto* fragment

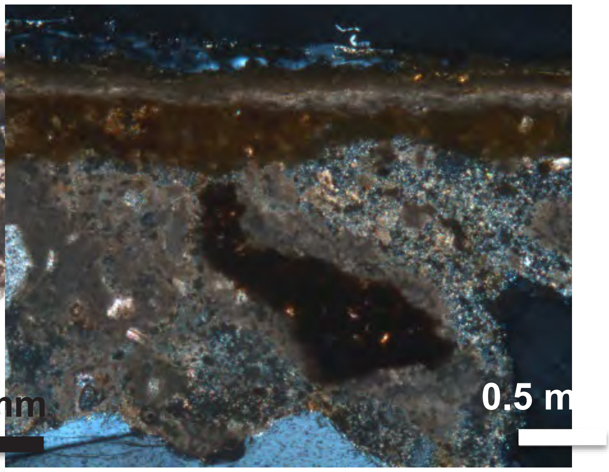

Figure 7. Transmitted light optical microscope (XPL) image showing a *cocciopesto* fragment

14.7
Thermally induced modifications in different types of magnesian soft stones

Lorenzo Peduzzi

Département des Géosciences, Université de Fribourg, Suisse

Archeological findings manufactured from various species of magnesian soft stone, mainly cooking vessels, have been observed to show modifications of color, texture and possibly mineralogy. It was hypothesized that these variations could be thermally induced and resulted from the cyclical exposition to heat during their use.

The rock species chosen for this study are a talc schist from the Bagnes Valley, a talc-carbonate rock from Chiavenna, a coarse-grained garnet-chlorite-chloritoid rock from the region of Valmeriana, and a fine-grained chloritoschist from the region of Zermatt.

In this work the hypothesis that the modifications observed in archeological findings might be thermally induced, is tested. Samples of four different species of magnesian soft stone were subjected to temperatures of 600°C, 800°C and 1000°C for 2 and 12 hours. Samples obtained from the untreated rocks underwent XRF and XRD analyses to determine their chemical and mineralogical composition. XRD and optical microscopy were used to identify the variations of mineralogy and structure that occurred in samples that underwent the heat treatment. For this work, only the samples that were heated at 600°C and 1000°C were considered.

The heat treatment resulted in multiple modifications, especially regarding the color, structure, and mineralogy of the samples. The variations that occurred in the samples that underwent heat treatment at 600°C were mostly related to the color and apparition of cracks. At this temperature carbonates, which were rich in magnesium, were devolatilized and turned into periclase. Clinochlore, talc, pyrope and chloritoid resisted the heat treatment at this temperature. The crystallinity of clinochlore, pyrope and chloritoid did in some cases increase following the heating at 600°C. The heat treatment at 1000°C resulted in radical changes regarding the mineralogy of the rocks. Clinochlore and talc were completely destabilized, they were replaced by enstatite and forsterite. The appearance of magnetite and spinel was observed in some samples. At this temperature the chloritoid grains were observed to have started melting, while the crystallinity of pyrope increased following the heating at 1000°C. The structure of the rock was strongly impacted by the heat treatment at 1000°C, the shape and arrangement of the grains were altered by recrystallization processes and by the change in mineralogy.

The crystallization of newly formed minerals, especially at 1000°C was of very low quality, given the short duration of the heat treatment. The presence of the newly formed minerals could only be observed through X ray diffraction. The results of this work could be regarded as surprising, given the short duration of the heat treatment, that still had a very strong impact on the mineralogy and structure of the rocks.

P 14.1
Geochemical study of hammerscale, an overview. Implications for iron provenance and supply of an archaeological smith.

Jean Rodier[1], Marion Berranger[2], Vincent Serneels[1]

[1] *Département des Géosciences, Université de Fribourg, Suisse*
[2] *CNRS, LMC-IRAMAT, UMR7065, Université de Technologie Belfort Montbéliard, CNRS, Montbéliard, France*

Knowing the diversity of worked iron and its origins in an archaeological forging context would allow a better understanding of iron circulation. However, this question remains difficult to address.

The first method, the study of smithing slags, make an interesting contribution. However, their chemical compositions result from the accumulation of various substances in the hearth. The second method, the study of slag inclusions in metallic fragments, makes it possible to establish such chemical signatures. Nevertheless, these debris are often scarce or absent. The representativity of the sampling is therefore difficult to assess.

A new approach is based on the study of the hammerscale which are the waste formed during the hammering of hot iron. Unlike metal objects, they are often found in large quantities. And, unlike smithing slags, each hammerscale is produced from a single piece of iron. Previous research on experimental hammerscale has shown that slag inclusions in the worked iron contribute to their formation. It is thus possible to distinguish between hammerscale produced from iron of different origins. Hammerscale from two archaeological sites (LTA 5e BC) have been studied. The first archaeological site, Weyersheim, is located in north-east of France. 350 Hammerscale have been chemically compared with 72 slag inclusions measured in 5 iron debris. Hammerscale and slag inclusions correlate well chemically in terms of major, minor and trace elements. In this case the addition of fluxes does not seem to be used by blacksmiths. The chemical nature of the iron that has been worked on the archaeological site of Weyersheim appears to be constant during the different forging operations. Highlighting either a continuous supply from the same producer or a seasonal work with one stock of the same metal.

The second archaeological site, Sévaz, is located in western part of Switzerland. The estimated quantity of iron worked on this site is 350 kg which makes it one of the most important for the time and the region. However, this raises many questions since out of more than 250 dated smelting sites in the region none have been dated from this period. The question of the origin of the iron worked is therefore central but no piece of uncorroded iron was found for slag inclusion analysis. 234 hammerscale have been chemically compared with 250 local iron ore samples that could have been used. The results show that the iron ores are not chemically compatible with hammerscale. The iron worked on the Sévaz archaeological site has been imported.

Despite the 400 km separating these two sites, the chemical signature of the worked iron is almost the same with strong anomalies in REE ($\sum$REE >1000 ppm) and an abnormal chemical partitioning between LREE and HREE (HREE/LREE>2). This specific signature is compatible with the bi-pyramid iron bar in circulation during this period and geographic area. The ore used to produce all this iron is geologically specific, indicating a potentially major production center at this period in western Europe.

P 14.2
CHIS4TI: Cultural Heritage Information System 4 Ticino

Alessio Spataro[1], Claudio Primerano[1]

[1] *Scuola universitaria professionale della Svizzera italiana (SUPSI), Institute of Earth sciences, Via Flora Ruchat-Roncati 15, CH-6850 Mendrisio (alessio.spataro@supsi.ch)*

There are many factors that put the cultural heritage of a territory at risk. To ensure its preservation over time, intelligent management is required, This, through innovative digital solutions, supports significant activities such as recording, and cataloging combined with the analysis and conservation of the collective heritage. This cultural heritage includes, for example, historical monuments like churches.

In this context, the Institute of Earth sciences at SUPSI is engaged in a project aimed at developing a web application for the semantic, temporal, and spatial management of information related to the cultural heritage of Canton Ticino. This application is capable of handling complex space-temporal queries and visualizations using point clouds as a fundamental data structure.
It's an open-source web platform that can evolve over time based on the needs of industry professionals. In fact, this application aims to satisfy the requirements of conservation and restoration specialists, as well as those managing cultural and architectural assets. The CHIS4TI application should also be interoperable to facilitate data exchange and consequently leverage the full potential of this information in various fields, including administrative, scientific, touristic, and educational domains.

Here are some relevant technical details about the capabilities of the CHIS4TI web platform:
- visualization and querying of Point Cloud data using Potree software.
- Visualization and querying of Mesh geometries using 3DHOP software.
- OpenLayer map integration for GIS-type usage of objects of interest and orthophotos.
- PostGIS database queried through GraphQL.

The CHIS4TI platform is being realized through a real-world case. In fact, for the project's development, a reference study area has been chosen: the Parco Scherrer in the municipality of Morcote. In this nice setting, SUPSI was already active with projects related to education, obviously in cooperation with local administrations.

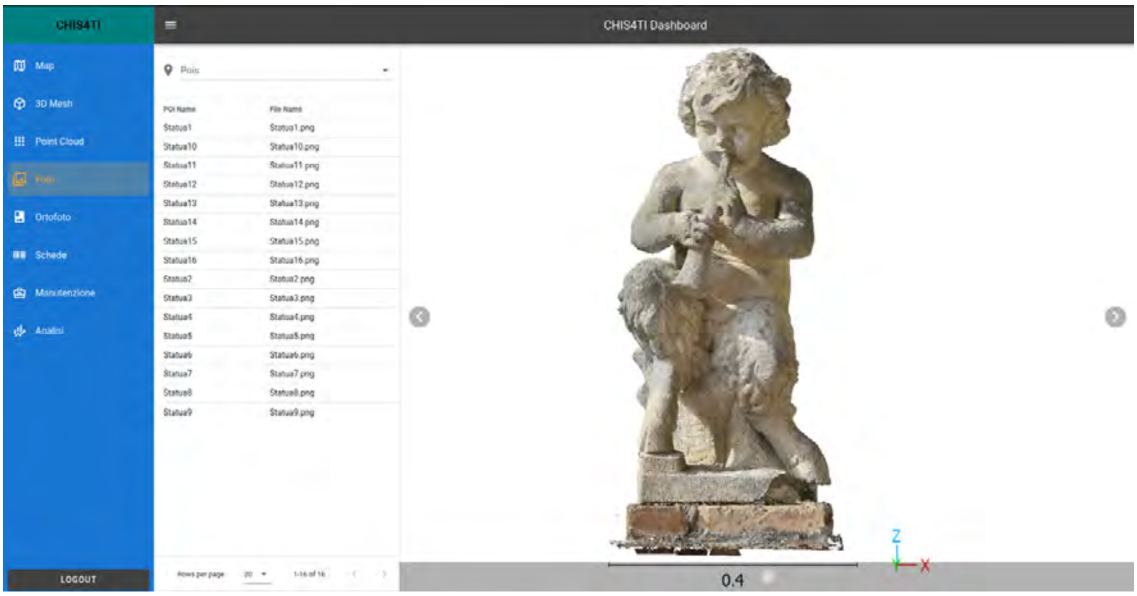

Figure 1. Detail of the CHIS4TI web application

P 14.3
Petrographic characterisation of molassic stones from Lausanne Cathedral

Brahimsamba Bomou[1], Thierry Adatte[1].

[1] *ISTE, University of Lausanne, Unil-Mouline, CH-1005 Lausanne (brahimsamba.bomou@unil.ch)*

As part of the restoration of Lausanne Cathedral, we were tasked with characterising its molassic stones using a petrographic, mineralogical and geochemical approach. This project focused on the petrographic study of the facings of the tower on the transept of Lausanne Cathedral, consisting firstly of mapping the surface of the stone elements of the tower, and secondly of sampling certain stones destined to be renewed. Mineralogical (X-ray diffraction) and geochemical (XRF analysis of major elements) analyses were carried out on these samples, helping to characterise and confirm the visual petrographic observations.

The mapped surfaces of the south tower of the transept show a wide variety of facies, but also several periods of restoration. According to the archaeological survey, several periods have been observed: Gothic I (12th century); Gothic II (13th century); an undetermined phase (14th-17th centuries); a restoration by Sinner (18th century); a restoration by Naef (1910-1916); and the restorations of the late 20th-early 21st centuries. For each of these periods, a certain type of facies and associated quarry were used.

In the Gothic I section, it is mainly grey molasse from Lausanne, with eight facies of medium to coarse grain size, and often variegated. This is the predominant type of stone on the south tower.

For the Gothic II section, a Cretaceous Rudist limestone, most probably from the Jura, was used at the base of the tower. This material is much more resistant to weathering than molasse and was added later to protect the base of the tower from erosion (the presence of molasse at the base of the tower can still be seen in some places). At the top of the tower, another type of facies was used, a carbonate sandstone that was used as a repair, probably following the fire of 1235.
For the period between the 14th and 17th centuries, two facies of grey molasse (facies 9 and 10) were used, particularly for the top of the north-east buttress. For the period of Sinner's restoration (1768-1774), it is essentially a facies of grey molasse of variegated Lausanne, medium to coarse grained.

Then, during the Naef restoration period (1910-1916), a wide variety of facies were used. For the foothills, another grey molasse facies was used for the most part and the Molière sandstone for the glacis of the latter, most probably because of its resistance. Granite molasse (highly indurated and resistant to alteration) can be found at intervals in the foothills. At the base of the south-east buttress, there is also a molasse that has been given the name Ursy molasse (according to archive informations). For the sacristy, we find Belmont molasse, but also Molière sandstone, which was used for the roof. Another facies used in abundance for the arcades and cornices on the south and east facades of the 2nd floor, as well as the columns on the 2nd floor of the south facade, is Obernkirchen sandstone, a fine grain showing good resistance to weathering. On the 2nd floor, it is worth noting that the 8 columns on the south and east facades of the tower, bearing the date 1916, are the only ones in the cathedral to use reconstituted stone.

During the last phase of work at the end of the 20th century and the beginning of the 21st century, the south-west buttress was mainly replaced with Burdigalian green marine molasse, and Bollingen sandstone was used for the glacis. This summarises the different types of stone used throughout the history of Lausanne Cathedral.

However, the great difficulty lies in describing these facies 'on the surface', as large areas are heavily weathered, and without the help of samples taken from stones destined to be renewed, it would have been difficult to draw any conclusions about their origin. However, the database that has been acquired will make it possible in the future to compare these data with non-destructive analysis (portable XRF) that can be applied to surfaces that cannot be sampled.

15 Cryospheric Sciences

Matthias Huss, Kathrin Naegeli, Nadine Salzmann, Theo Jenk, Andreas Vieli

Swiss Snow, Ice and Permafrost Society

TALKS:

15.1 Baccolo G., Di Stefano E., Bohleber P., Brügger S.O., Brütsch S., Jenk T., Eichler A., Maggi V., Schwikowski M.: What can we learn from ice cores drilled at temperate glaciers? First insights from the Adamello ice core (Rhaetian Alps)

15.2 Berg J.*, Reynolds D., Quéno L., Jonas T., Lehning M., Mott R.: A seasonal snowpack model forced with dynamically downscaled forcing data resolves hydrologically relevant accumulation patterns

15.3 Cook S.J., Jouvet G., Millan R., Rabatel A., Zekollari H., Dussaillant I.: Ice loss in the European Alps until 2050 using a fully assimilated, deep-learning-aided 3D ice-flow model

15.4 Cremona A.*, Landmann J., Huss M., Schwaizer G., Paul F., Farinotti D.: Glacier mass balance monitoring in the Swiss Alps by assimilating remotely sensed snow cover observations

15.5 Dadic R., Martin J., Pirazzini R., Anderson B., Cheng B., Schneebeli M., Blixt I., Chazan A., Dean S., Heil P., Hannula H-R., Hoppmann M., Horgan H., Jaggi M., Lehning M., Leonard G., Light B., Löwe H., Macfarlane A., Martin A., Mewes L-H., Rack W., Robinson N., Ryan K., Smith I., Vargo L., Webster M., Wigmore O., Wolfperger F.: Snow on Antarctic Sea Ice

15.6 Hannula H.-R., Pirazzini R., Dadic R., Brus D., Schneebeli M.: Arctic Ocean sea ice surface albedo during the fall freeze-up season: observations at different scales

15.7 Hosmann S.*, Fabbri S.C., Büchi M.W., Hilbe M., Bauder A., Anselmetti F.S.: Exploring below the retreating ice: Swath bathymetry reveals sub-to-proglacial processes and longevity of future glacial lakes

15.8 Jung S.*, Werder M., Damsgaard A.: Glacier basal movement drives the closure of channels incised in subglacial till

15.9 Morard S.*, Hilbich C., Mollaret C., Pellet C., Hauck C.: 20-year permafrost evolution documented through petrophysical joint inversion, thermal and hydrological data

15.10 Ogier C.*, Van Manen D-J., Maurer H., Hertrich M., Raess L., Bauder A., Farinotti D.: What causes GPR signal scattering in temperate ice?

15.11 Robson B., Lambiel C., Ravanel L., Irving J., Baron L., Gentizon J.: Investigating hanging glacier geometries in the Mont-Blanc Massif (France) and Pennine Alpes (Switzerland) using ground penetrating RaDAR

15.12 Schöttner J.*, Walet M., Walter B., Adam V., Rheinschmidt F., Schweizer J., van Herwijnen A.: Producing artificial snow samples with weak layers to determine mechanical properties for a variety of microstructural morphologies

15.13 Sedaghatkish A.*, Luetscher M.: Modeling the effect of free convection on permafrost melting-rates in ice-rich media

15.14 Van Tricht L., Paice C.M., Rybak O., Popovnin V., Satylkanov R., Huybrechts P.: Monitoring the annual geodetic mass balance of Bordu and Sary-Tor glaciers, Central Asia, using UAV data

15.15 Volery A.*, Barandun M., Naegeli K.: Importance of the sub-seasonal, spatio-temporal variability of bare-ice albedo of Abramov Glacier, Kyrgyzstan

15.16 Voordendag A.*, Goger B., Prinz R., Rutzinger M., Kaser G.: Glaciological applications of long-range permanent terrestrial laser scanning data at Hintereisferner, Austria

15.17 Walet M.*, Schöttner J., Adam V., Rheinschmidt F., Schweizer J., van Herwijnen A.: Fracture of weak snowpack layers: mixed mode fracture tests in the field

15.18 Wetter C., Schmelzbach C., Stähler S.C.: Seismo-acoustic sensing on ice: a new approach for continuous contact-free floating ice characterisation

POSTERS:

P 15.1 Lüthi M., Zaninetti A., Nap A., Wehrle A.: How to propel a floating iceberg 400 m up into the air

P 15.2 Barandun M., Hasler A., Belloni F., Hoelzle M.: Improved glacier monitoring using low-cost satellite communication service in Central Asia

P 15.3 Bramati G.*, Hardmeier F., Adams J.S., Vieli A., Naegeli K.: Hyperspectral thermal remote sensing of the Cryosphere: first application on a debris-covered glacier in the Swiss Alps

P 15.4 Navruzshoev H.*, Abdulhamid K., Saks T., Barandun M., Khusrav K., Smirnov A., Hoelzle M.: Glacier mass balance in the Gunt River Basin, Pamir, Tajikistan

P 15.5 Saks T., Rinterknecht V., Lavrentiev I., Béra G., Mattea E., Hoelzle M.”: Cosmogenic dating of Abramov glacier advances during the Little Ice Age and Last Glacial Maximum

P 15.6 von der Esch A.*, Huss M., van Tiel M., Farinotti D.: Investigating the sensitivity of the Glacier Evolution Runoff Model (GERM) towards input data quality

P 15.7 Mattea E.*, Barandun M., Saks T., Garbo A., Hoelzle M.: Monitoring daily flow velocities at Abramov glacier with low-cost, open-source GNSS loggers

P 15.8 Amschwand D.*, Tschan S., Scherler M., Hoelzle M., Haberkorn A., Kienholz C., Krummenacher B., Aschwanden L., Gubler H.: Depicting the water and ice cycle on rock glacier Murtèl

P 15.9 Gabriel L.*, Hertrich M., Ogier C., Maurer H., Farinotti D.: Exploring englacial hydrology with surface nuclear magnetic resonance

P 15.10 Klahold J.*, Racz G.C., Irving J.: What happens below the surface of the Otemma Glacier? Investigating Alpine glacier hydrology through multi-method geophysical analysis

P 15.11 Moradi H.*, Furrer G., Margreth M., Wolpert L., Mair D., Wanner C.: Fluxes of toxic elements mobilized from a rock glacier in Val Mustair: insights on ice melt dynamics

P 15.12 van Ginkel J., Walter F., Lindner F.: Iluminating the subglacial environment with passive seismic methods: Glacier de la Plaine Morte as case study

P 15.13 Worek M.*, Brütsch S., Stockinger I., Moser R., Schwikowski M., Jenk T.M.: Neoglaciation in the Alps: first results from Tödi ice cap

P 15.14 Conzett L., Kleiner C., Fischer M.: An inventory of formerly ice-covered, now ice-free passes in the Swiss Alps from 1850 to present

P 15.15 Louis C.*, Halloran L., Roques C., Molson J.: Hydrological significance and dynamics of active rock glaciers under climate change: a case study from the Val d’Ursé, Bernina Range, Switzerland

15.1
What can we learn from ice cores drilled at temperate glaciers? First insights from the Adamello ice core (Rhaetian Alps)

Giovanni Baccolo[1,2], Elena Di Stefano[3], Pascal Bohleber[4], Sandra O. Brügger[1,5], Sabina Brütsch[1], Theo Jenk[1], Anja Eichler[1], Valter Maggi[3], Margit Schwikowski[1,2]

[1] *Laboratory of Environmental Chemistry, Paul Scherrer Institut, Villigen, Switzerland (giovanni.baccolo@psi.ch)*
[2] *Oeschger Centre for Climate Change Research, University of Bern, Switzerland*
[3] *Environmental and Earth Sciences Department, University of Milano-Bicocca, Italy*
[4] *Department of Environmental Sciences, Informatics and Statistics. University of Venice, Italy*
[5] *Department of Environmental Sciences, University of Basel, Switzerland*

The cold portions of accumulation basins are usually the glacial areas that receive most attention for ice core drilling projects. This is because the limited impact of melting and the conservation of precipitation allow the best preservation of the stratigraphic signals used for paleoclimatic reconstructions.

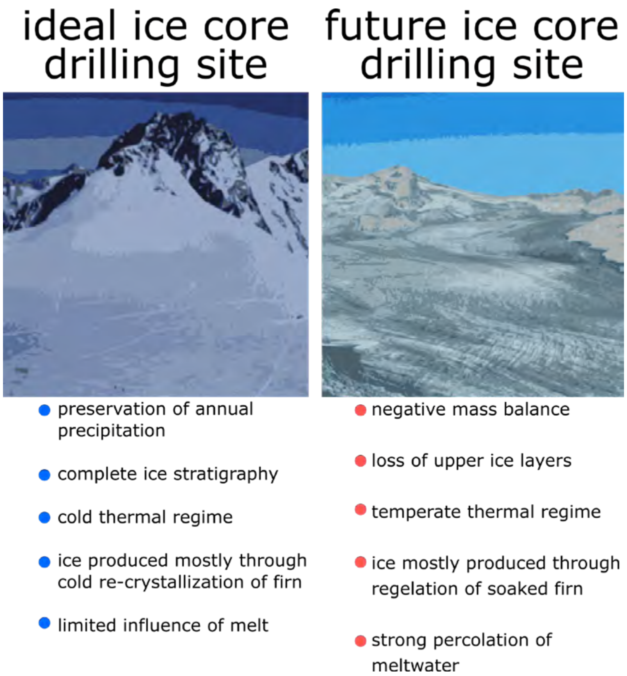

Figure 1. A comparison between sites that have been traditionally considered for ice core drilling activities on mountain glaciers (left) and what to expect for the near future due to the impact of climate change.

Because of climate change, sites with such glaciological features are rapidly shrinking or even disappearing across the mountain ranges of Earth. The thermal regime of accumulation basins of high-altitude glaciers is turning from cold to temperate and their mass balances are approaching negative values (Gilbert et al., 2015). This is posing issues on the ability of glaciers to preserve climatic and environmental signals (Zhang & Kang, 2023). The loss of upper ice layers exposes to the surface old ice, obliterating the most recent signals normally used for calibration with instrumental data. At the same time the increased presence of meltwater affects the preservation of signals in the temperate portions of glaciers.

The exploitation of mountain glaciers as paleoclimatic archives in the near future will only be possible if the ice core science community develops new methods and competencies to extract information from temperate ice addressing meltwater disturbances. To this aim, a 223 m long ice core was drilled in 2021 at the Adamello glacier, in the Rhaetian Alps. At the drilling site (3100 m a.s.l.) the glacier exhibits a negative mass balance and a temperate regime. Thus, the site is ideal to assess the ability of temperate glaciers having a negative mass balance to preserve climatic signals.

A set of paleoclimatic proxies has been investigated in the upper 26 m of the ice core. We present here preliminary results. They show that while most of the analytes are significantly affected by meltwater percolation and regelation, some of them, in particular the less soluble ones, still exhibit a detectable seasonality. This has allowed to develop a chronology, estimate the age of surface ice and identify what proxies are best preserved in temperate ice.

REFERENCES

Gilbert, A., Vincent, C., Gagliardini, O., Krug, J., & Bertier, J. K. E. 2015: Assessment of thermal change in cold avalanching glaciers in relation to climate warming, Geophysical Research Letters, 42, 6382-6390.

Zhang, Y, & Khang, S. 2023: Melting glaciers threaten ice core science on the Tibetan Plateau, Nature Geoscience, 16, 656-657.

15.2
A seasonal snowpack model forced with dynamically downscaled forcing data resolves hydrologically relevant accumulation patterns

Justine Berg[1,3], Dylan Reynolds[1,2], Louis Quéno[1], Tobias Jonas[1], Michael Lehning[1,2], Rebecca Mott[1]

[1] *WSL, Swiss Federal Institute for Snow and Avalanche Research, SLF Davos, Davos, Switzerland*
[2] *Laboratory of Cryospheric Sciences, School of Architecture, Civil and Environmental Engineering, École Polytechnique Fédérale de Lausanne, Lausanne, Switzerland*
[3] *Institute of Geography & Oeschger Centre for Climate Change Research, University of Bern, Bern, Switzerland*

Mountain snowpack stores months of winter precipitation at high elevations, supplying snow melt to lowland areas in drier seasons for agriculture and human consumption worldwide. Climate change is expected to negatively impact this vital resource, decreasing the volume of water stored for downstream ecosystem processes. Accurate seasonal predictions of the snowpack are thus of great importance, but such forecasts suffer from major challenges such as resolving interactions between forcing variables at high spatial resolutions. To test novel approaches to resolving these processes, seasonal snowpack simulations are run at different grid resolutions (50~m,100~m,250~m) and with variable forcing data for the water year 2016/2017. COSMO-1E data is either dynamically downscaled with the High-resolution Intermediate Complexity Atmospheric Research (HICAR) model or statistically downscaled to provide forcing data for snowpack simulations with the Flexible Snowpack Model (FSM2oshd). Simulations covering complex terrain in the Swiss Alps are carried out with the operational settings of the FSM2oshd model or with a model extension including wind- and gravitational-induced snow transport (FSM sntran). The simulated snow height is evaluated against observed snow height collected during LiDAR flights in spring 2017. Spatial snow accumulation patterns and snow height distribution are best matched with simulations using dynamically downscaled data and the sntran model extension, indicating the importance of both accurate meteorological forcing data and snow transport schemes. This study demonstrates for the first time the effects of applying dynamical downscaling schemes to snowpack simulations at the seasonal and catchment scales.

15.3
Ice loss in the European Alps until 2050 using a fully assimilated, deep-learning-aided 3D ice-flow model

Samuel J. Cook[1]*, Guillaume Jouvet[1], Romain Millan[2], Antoine Rabatel[2], Harry Zekollari[3,4,5] and Inés Dussaillant[6]

[1] IDYST, Faculty of Geosciences and Environment, Université de Lausanne, Lausanne, Switzerland
[2] Univ. Grenoble Alpes, CNRS, IRD, INRAE, Grenoble-INP, Institut des Géosciences de l'Environnement (IGE, UMR 5001), Grenoble, France
[3] Laboratory of Hydraulics, Hydrology and Glaciology (VAW), ETH Zürich, Zurich, Switzerland
[4] Swiss Federal Institute for Forest, Snow and Landscape Research (WSL), Birmensdorf, Switzerland
[5] Laboratoire de Glaciologie, Université libre de Bruxelles, Brussels, Belgium
[6] Department of Geography, University of Zürich, Zürich, Switzerland
**Corresponding author*

Modelling the short-term (<50 years) evolution of glaciers is difficult because of issues related to model initialisation and data assimilation. However, this timescale is critical, particularly for water resources, natural hazards, and ecology. Using a unique record of satellite remote-sensing data, combined with a novel optimisation and SMB-calculation method within the framework of the deep-learning-based Instructed Glacier Model, we are able to resolve initialisation issues. We thus model the evolution of all glaciers in the European Alps up to 2050 under present-day climate conditions, assuming no future climate change. We find that the resulting committed ice loss exceeds a third of the present-day ice volume by 2050, with multi-kilometre frontal retreats for even the largest glaciers. Our results show the importance of modelling ice dynamics to accurately retrieve the ice-thickness distribution and to predict future mass changes. Thanks to high-performance GPU processing, we also demonstrate our method's global potential.

15.4
Glacier mass balance monitoring in the Swiss Alps by assimilating remotely sensed snow cover observations

Aaron Cremona[1,2], Johannes Landmann[3], Matthias Huss[1,2,4], Gabriele Schwaizer[5], Frank Paul[6], and Daniel Farinotti[1,2]

[1] *Laboratory of Hydraulics, Hydrology and Glaciology (VAW), ETH Zurich, Zurich, Switzerland (cremona@vaw.baug.ethz.ch)*
[2] *Swiss Federal Institute for Forest, Snow and Landscape Research (WSL), Birmensdorf, Switzerland*
[3] *Federal Office of Meteorology and Climatology, MeteoSwiss, Zurich-Airport, Zurich, Switzerland*
[4] *Department of Geosciences, University of Fribourg, Fribourg, Switzerland*
[5] *ENVEO IT GmbH, Innsbruck, Austria*
[6] *Department of Geography, University of Zurich, Zurich, Switzerland*

Modelling glacier mass balance in real-time is of interest as it has the potential to provide information about water availability. However, one of the main challenges lies in the substantial uncertainties stemming from the scarcity of observational data. In this study, we investigate the potential of remotely-sensed observations of fractional snow coverage to constrain the spatial variability of modelled glacier mass balance in the Swiss Alps. The model we use in this investigation is CRAMPON, an operational glacier mass balance model able to calculate regional mass balance at the daily scale, which relies on the infrastructure provided by the Open Global Glacier Model (OGGM). In a first step, we derive the snow-covered fraction of glacier areas from Sentinel-2 observations and compare it with the corresponding snow-covered area fraction modelled with CRAMPON. The comparison between modelled and observed snow-covered fractions reveals an average mean absolute deviation of less than 12% for glaciers larger than 4 km². This benchmarks CRAMPON's capability to reproduce the evolution of the snow cover throughout the melt season for medium-sized to large glaciers. In a second step, we constrain the model parameters by integrating information from the snow cover observations during model calibration. In this calibration procedure, melt parameters are tuned to match ice volume changes that are computed from Digital Elevation Models spanning over the average period 2011-2019. As this period is relatively short and closely aligned with the one of the Swiss Glacier Inventory 2016, we run CRAMPON with constant glacier geometry, preventing uncertainties induced by geometry change parametrization, which would be necessary otherwise. To maximize the agreement between modelled and observed fractional snow coverages that are available over the melt seasons, we adjust a precipitation correction factor that controls the accumulation modelled by CRAMPON. The calibration is proven to be successful as (i) it leads to parameter convergence, and (ii) the so-calibrated model better reproduces both the ice volume change and the snow cover evolution. The workflow thus constrains the modelled mass balance with snow cover observations, showing potential for reducing the effect of parameter equifinality in the field of real-time glacier monitoring.

15.5
Snow on Antarctic Sea Ice

Ruzica Dadic[1,2] , Julia Martin [2], Roberta Pirazzini[3], Brian Anderson [2], Bin Cheng [3], Martin Schneebeli [1], Ian Blixt[2], Azrael Chazan[2], Sidney Dean[2], Petra Heil [4], Henna-Reetta Hannula [3], Mario Hoppmann [10], Huw Horgan[11,1,2], Matthias Jaggi [1], Michael Lehning [1], Greg Leonard [6], Bonnie Light [7], Henning Löwe [1], Amy Macfarlane [1], Andrew Martin[2], Lars-Hendrik Mewes[1], Wolfgang Rack [8], Natalie Robinson [9], Ken Ryan[2], Inga Smith [6], Lauren Vargo[2], Melinda Webster [7], Oliver Wigmore [2], Fabian Wolfperger [1]

[1] WSL Institute for Snow and Avalanche Research SLF, Davos, Switzerland (ruzica.dadic@slf.ch)
[2] Victoria University of Wellington, Antarctic Research Centre, Wellington, New Zealand
[3] Finnish Meteorological Institute, Helsinki, Finland
[4] Australian Antarctic Division, Hobart, Australia
[5] UiT The Arctic University of Norway, Tromso, Norway
[6] The University of Otago, Dunedin, New Zealand
[7] University of Washington, Seattle, USA
[8] University of Canterbury, Christchurch, New Zealand
[9] NIWA, Taihoro Nukurangi, Wellington, New Zealand
[10] AWI, Alfred Wegener Institute, Bremerhaven, Germany
[11] Laboratory of Hydraulics Hydrology and Glaciology (VAW), RTH Zürich, Zürich, Switzlerand

Snow cover affects the variability of the physical properties of sea ice. The snow’s unique thermal and optical properties govern the mass and energy fluxes in the sea ice system. They are essential for sea ice evolution, energy exchanges between the ocean and the atmosphere, and light availability for ecosystems below the sea ice. Furthermore, snow significantly impacts remote sensing retrievals, especially for sea ice thickness. Yet, data on the physical properties of snow and its effects on sea ice are extremely limited, especially in Antarctica. This leads to significant uncertainties in the coupling of climate feedback and results in significant biases in model representations of the sea ice cover.
During our field campaign from October to December 2022 in McMurdo Sound, we quantitatively investigated the physical properties of snow on Antarctic sea ice, following the same protocols used during the MOSAiC expedition. The season’s unique sea ice conditions provided the ideal laboratory to study a range of snow conditions and to differentiate between sea ice and snow drivers for the atmosphere-sea ice-ocean system. Our set of snow measurements on sea ice, unprecedented in Antarctica, includes ground snow/ice measurements, automatic weather and radiation stations, drone-based measurements, and measurements of primary production beneath the sea ice. These extensive measurements made it possible to capture snow’s physical properties and spatial variability and simultaneously measure the different components of the energy balance at varying spatial scales and their implications for primary production. This dataset will improve our understanding of snow’s role in the Antarctic sea ice system.

15.6
Arctic Ocean sea ice surface albedo during the fall freeze-up season: observations at different scales

Henna-Reetta Hannula[1,2], Roberta Pirazzini[1], Ruzica Dadic[2], David Brus[1], Martin Schneebeli[2]

[1] *Finnish Meteorological Institute, Erik Palménin aukio 1, 00560 Helsinki, Finland (henna-reetta.hannula@fmi.fi)*
[2] *WSL Institute for Snow and Avalanche Research, Flüelastrasse 11, CH-7260 Davos Dorf, Switzerland*

Sea ice albedo governs the Earth's energy absorption and is critical to climate change. Here, we present albedo measurements at different scales and discuss the implications of our results for climate models and satellite retrievals of sea ice. We carried out broadband albedo observations over sea ice from different platforms: a) unmanned aerial vehicle (UAV) -based platform, b) on-ice transects, and c) fixed station, during the MOSAiC expedition in August-September 2020. This period represents the transition from summer melting to winter freezing. The albedo observations are supported by UAV-based photo-mosaics of the sea ice surface to infer relevant surface information. The hemispherical albedo observations have a footprint of about 6 m when collected at ~1 m above the surface and footprints from 30 to 180 m when taken from a UAV flying 5m to 30m above the surface (footprints representing ~90 % of the upwelling flux).

The spatial heterogeneity of the sea ice surface albedo observed at different scales is compared for the time series, and the height to reach the areal average albedo, which is represented in satellite and climate model retrievals, is defined during the different phases of the sea ice freeze-up. The study improves our understanding of the uncertainties that arise from satellite validation over heterogeneous Arctic sea ice when point-to-pixel comparisons are made between in-situ and remotely sensed datasets representing different scales.
Furthermore, the study will help in characterizing the statistical distributions of various surface features (melt ponds, leads, ridges and scattering ice) during the progress of the freeze-up and their impact on the areal averaged albedo. Such understanding will contribute to develop statistically-based surface descriptors that will better represent the sea-ice albedo in coarser scale climate models, which are used to understand and predict the forthcoming changes in the new Arctic.

15.7
Exploring below the retreating ice: Swath bathymetry reveals sub-to-proglacial processes and longevity of future glacial lakes

Siro Hosmann[1], Stefano C. Fabbri[1,2,3], Marius W. Büchi[1], Michael Hilbe[1], Andreas Bauder[4,5], Flavio S. Anselmetti[1]

[1] Institute of Geological Sciences and Oeschger Centre for Climate Change Research, University of Bern, Switzerland (siro.hosmann@unibe.ch)
[2] Université du Québec à Rimouski, Institut des sciences de la mer de Rimouski (ISMER), Rimouski, Canada
[3] Laboratoire EDYTEM, Université Savoie Mont Blanc, Le Bourget du Lac, France.
[4] Versuchsanstalt für Wasserbau, Hydrologie und Glaziologie (VAW), ETH Zürich, Switzerland
[5] Swiss Federal Institute for Forest, Snow and Landscape Research (WSL), Birmensdorf, Switzerland

The formation of subglacial overdeepenings is widely debated, yet essential for understanding glacial systems and their geomorphic processes. Knowledge of how glaciations formed landscapes is particularly important as receding glaciers currently uncover subglacial landscapes that are prone to a series of natural hazards. We present high-resolution (1x1 m) swath bathymetric data of a proglacial lake in front of the Rhonegletscher (Swiss Alps) that started to form in the early 2000s allowing an unprecedented look into a freshly uncovered glacier bed in an overdeepened setting. The lake floor is characterized by a series of subaquatic moraines that exhibit various sedimentary features, such as delta fans and subaquatic delta channels. The data allow us to correlate the succession of these moraines with the glacier's retreat history as seen on aerial photos, providing critical understanding of when, where and how such subaquatic moraines form. Sub- and englacial conduits control the location of active and inactive lake-inflow channels. These conduits carry large amounts of sediments that rapidly infill the inherited subglacial landscape produced by the deglaciation. Comparing two surveys from 2015 and 2021 allows a quantification of the accumulation and erosion processes in the central lake basin. A backscatter-intensity map differentiates between fine- and coarse-grained sediment and bedrock, and short gravity cores allow quantifying recent sedimentation. Towards the glacier front, which still extends subaquatically into the lake, our high-resolution data visualizes how the submerged ice front is interacting with its proglacial lake. This highly dynamic environment is characterized by iceberg calving (as observed in September 2021), fluctuating outflow conduits, rapid sedimentation due to particle-laden meltwaters and dumped glacial debris. Assuming constant sediment yield, the Rhone Lake will persist for ~300 years. However, as intense glacier retreat will lead to new overdeepened lakes in the next decades that efficiently trap sediments upstream, this and similar chains of proglacial lakes will persist much longer with implications for natural hazards as well as opportunities for hydropower, water resources and tourism.

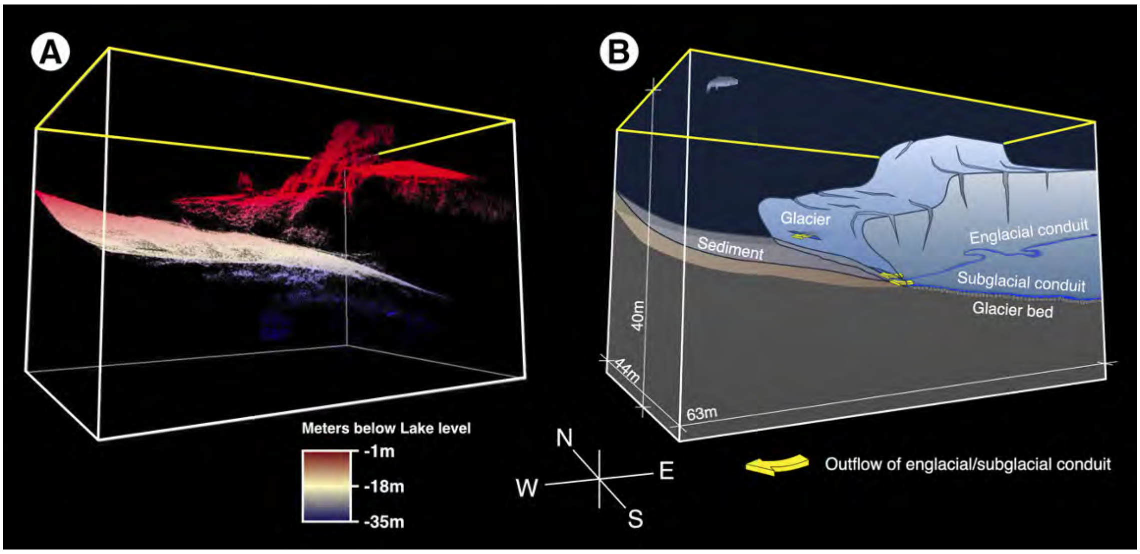

Figure 1. Left: Ungridded point cloud of swath-bathymetry data of proglacial Rhonesee with the submerged glacier front. Yellow rectangle on top represents lake level. Right: 3D-interpretation of the data in Fig A. Model shows morphological features contributing to the formation of a subglacial overdeepening.

15.8
Glacier basal movement drives the closure of channels incised in subglacial till

Simon Jung[1,2], Mauro Werder[1,2], Anders Damsgaard[3]

[1] *Laboratory of Hydraulics, Hydrology and Glaciology (VAW), ETH Zurich, Hönggerbergring 26, CH-8093 Zürich (sijung@ethz.ch)*
[2] *Swiss Federal Institute for Forest, Snow and Landscape Research (WSL), Zürcherstrasse 111, CH-8903 Birmensdorf*
[3] *Geo (Danish Geotechnical Institute), Sødalsparken 12, DK-8220 Brabrand*

Many of Antarctica's ice streams reside on deformable beds. The description of their basal conditions is a major source of uncertainty in modeling studies attempting to predict their response to a changing climate (Kazmierczak 2022). The mechanics at the glacier bed, often divided into glacier sliding and deformation of the subglacial sediments (so-called till), depend on the subglacial water pressure and thus on the subglacial drainage (Clarke 2005). To understand the drainage system at the ice-till interface, past works modelled the stability of channels incised in the till. Such channels open due to erosion by water flow and close due to till erosion and fluvial deposition. Till rheology is a central point of discussion in these models. The first major modelling approaches assumed a viscous rheology of the subglacial till (Walder & Fowler 1994; Ng 2000). Lab and field experiments show the subglacial till to be better described by a plastic rheology (Clarke 2005). A later study using a plastic rheology showed that till does not deform near channels at low enough effective pressures but at higher effective pressures the till then rapidly deforms to reduce the channel to a stable size (Damsgaard et al. 2017).

The presented research builds on this study by Damsgaard et al. (2017) by extending the model used there to include the effect of basal till deformation due to glacier sliding on the dynamics of such channels. Our results show that the glacier sliding leads to non-zero channel closure rates at all effective pressures. This closure rate is shown to increase with both the applied glacier sliding rate and the effective pressure and decrease with the channel size. This feedback between basal sliding and channel closure could potentially be a mechanism leading to high sliding speeds, such as found in ice streams, by increasing basal water pressure due to decreased channel size.

REFERENCES

Kazmierczak, E. et al. 2022: Subglacial hydrology modulates basal sliding response of the Antarctic ice sheet to climate forcing. The Cryosphere 16.10, 4537–4552.

Clarke, G. K. C. 2005: SUBGLACIAL PROCESSES. Annual Review of Earth and Planetary Sciences 33.1, 247–276.

Walder, J. S. & Fowler, A. 1994: Channelized subglacial drainage over a deformable bed. Journal of Glaciology 40.134, 3–15.

Ng, F. S. L. 2000: Canals under sediment-based ice sheets. Annals of Glaciology 30, 146–152.

Damsgaard, A. et al. 2017: Sediment behavior controls equilibrium width of subglacial channels. Journal of Glaciology 63.242 , 1034–1048.

15.9
20-year permafrost evolution documented through petrophysical joint inversion, thermal and hydrological data

Sarah Morard[1], Christin Hilbich[1], Coline Mollaret[1], Cécile Pellet[1], Christian Hauck[1]

[1] *Department of Geosciences, University of Fribourg, Fribourg, Switzerland (sarah.morard@unifr.ch)*

This study investigates the ground characteristics of the high altitude (3’410 m a.s.l.) permafrost site Stockhorn in the Swiss Alps using a combination of surface and subsurface temperature, soil moisture, electrical resistivity and P-wave velocity time series data including a novel approach to explicitly quantify changes in ground ice content. This was motivated by the clear signal of permafrost degradation visible in the full available dataset at this long-term monitoring site within the PERMOS (Permafrost Monitoring Switzerland) network. First, we assess the temporal and spatial evolution of the ground ice and water content by combining and analysing all available in situ thermal (borehole and ground surface temperature), hydrological (soil moisture) and geophysical (geoelectric and seismic refraction) data over two decades (2002-2022) regarding the driving factors for the spatially different warming. Secondly, we explicitly quantify the volumetric water and ice content and their changes in the subsurface from 2015 to 2022 using a time-consistent petrophysical joint inversion scheme using the open-source library pyGIMLi. The petrophysical joint inversion scheme has been improved by constraining the rock content to be constant in time for six subsequent inversions. This allows us to obtain consistent changes in ice and water content over the monitoring period based on jointly inverted resistivity and traveltime data. All the different data show a warming trend of the permafrost. The ice content calculated from the petrophysical joint inversion has decreased by about 15 vol.% between 2015 and 2022. Changes in ice content are first observed in the lower, south-facing part of the profile. As a result, resistivity and P-wave velocity have been decreasing significantly. Permafrost temperatures measured in the boreholes have increased between 0.5 and 1°C in 20 years. Our study shows the high value of joint and quantitative analysis of datasets comprising complementary subsurface variables for long-term permafrost monitoring.

15.10
What causes GPR signal scattering in temperate ice?

Christophe Ogier[1,2], Dirk-Jan Van Manen[3], Hansruedi Maurer[3], Marian Hertrich[3], Ludovic Raess[1,2], Andreas Bauder[1,2], and Daniel Farinotti[1,2]

[1] *ETHZ, D-BAUG, Zurich, Switzerland (ogier@vaw.baug.ethz.ch)*
[2] *Swiss Federal Institute for Forest, Snow and Landscape Research (WSL), Birmensdorf, Switzerland*
[3] *Institute of Geophysics, ETH Zurich, Zurich, Switzerland*

Ground penetrating radar (GPR) has been extensively used in glaciology to characterize englacial and subglacial properties such as ice thickness, liquid water content or water drainage pathways.
However, GPR radargrams in temperate ice often appear blurred by undesirable noise, mostly appearing as highly scattered signal and strong attenuation. It is often suggested that this noise
originates from englacial water inclusions, since water and ice have a large contrast in their dielectric permittivity. Here, we use the open-access software gprMax to forward-model a GPR signal in temperate ice and to quantitatively assess the role that water scatterers have as noise source. In particular, we explore how different liquid water contents (LWC) and water-inclusions size affect the GPR signal, and show that their effect is much larger than the potential presence of a wet snowpack or a heterogenous distribution of ice permittivity. This confirms previous hypotheses suggesting that water inclusions within the ice are the main factor for the typical noise seen in GPR data for temperate ice. For simulations referring to 25 MHz GPR antennas, we find that a bulk LWC equal or superior to 0.2 %, associated to decimeters-scale water inclusions, already constitute a limit in bedrock detectability for ice thicknesses larger than 100 m. These values of LWC and water-inclusion size are typical for Alpine field settings, clarifying why noisy signals are often encountered in such environments. Our numerical simulations for different LWC values also suggest than distinguishing between cold and temperate ice based on GPR scattering might be more difficult than previously assumed.

15.11
Investigating hanging glacier geometries in the Mont-Blanc Massif (France) and Pennine Alpes (Switzerland) using ground penetrating RaDAR

Ben Robson[1], Christophe Lambiel[1], Ludovic Ravanel[2], James Irving[3], Ludovic Baron[3], Jérémie Gentizon[1]

[1] *Institut des dynamiques de la surface terrestre (IDYST), Université de Lausanne, Mouline - Géopolis, 1015 Lausanne (ben.robson@unil.ch)*
[2] *Environnements, Dynamiques et Territoires de la Montagne (EDYTEM Lab.), Université de Savoie, CNRS, F-73376, Le Bourget-du-Lac, France*
[3] *Institut des sciences de la Terre (ISTE), Université de Lausanne, Mouline - Géopolis, 1015 Lausanne*

By the end of this century, all glaciers below 4000 m altitude in the European Alps are projected to transition from cold-based to a temperate-based state due to climate forcing (Gilbert et al., 2015)the primary driver of avalanching glacier instability on steep slopes. Prediction of future potential instability therefore requires appropriate modeling of the thermal evolution of these glaciers. Application of a state-of-the-art model to a glacier in the French Alps (Taconnaz. This evolution carries substantial implications for hanging glaciers as they are particularly sensitive to thermal change (Gilbert et al., 2014). Given the high density of human settlements, infrastructure and access for recreation seen in the European Alps, where unstable hanging glaciers already threaten villages, transport routes and ski infrastructure (Margreth et al., 2011; Pralong & Funk, 2006), it is critical their evolution is well understood. Modelling hanging glaciers is difficult because of their complex geometries (Maggioni et al., 2018)because of the climate change and the related transition from cold to warm based ice in high elevation glaciers, avalanches due to the collapses of hanging glaciers have raised importance and interest. In this work, we present the case study of Palòn de la Mare, a mountain glacier with a secondary hanging snout, which frequently breaks off producing ice and mixed ice/snow avalanches. We analysed the evolution of this portion of the glacier in the last 30 years also with respect to its mass balance and snow and weather data. Among the recorded nine glacier collapses, we gave a special focus on 5 avalanche events: three pure ice avalanches in 1999, 2002, 2006 and two mixed ice/snow avalanches in 1986 and 2017. For reproducing the ice/snow avalanche events, we used the model RAMMS-Extended. This model allows the simulation of an avalanche from the release to the runout by taking into account: i, of which little is known owing to the difficult nature of data acquisition. Our study utilised ground-based ground-penetrating radar techniques - long established in glaciology – in a novel application in the challenging topographical environments of hanging glaciers to investigate the bedrock geometries (Fig. 1). With the addition of unmanned aerial vehicle photogrammetric surveys, we assessed the current condition of four hanging glaciers at two sites at the Pointes du Mourti (3563 m a.s.l.), Pennine Alps, Switzerland, and the Aiguille du Midi (3842 m a.s.l.), Mont-Blanc Massif, France. Our approach was particularly successful at the Pointes du Mourti, Switzerland, where we were able to extract subglacial bedrock geometry covering an area of 9791 m^2, representing 16.2 % of the glacier area in 2022. We demonstrated that this hanging glacier, with mean inclination angle 43°, resides in a concave feature on the mountain slope, where bedrock amplitudes are high, indicating a rugged subglacial surface. We further demonstrated that the surface topography of hanging glaciers underwent substantial changes during the unusually hot summer of 2022, which followed the very dry winter of 2021/2022, far surpassing historical norms. The Pointes du Mourti hanging glacier lost 1.17 m of height in average and more than 7 % of its surface area between October 2021 and September 2022. The Jumeau Ouest hanging glacier, at the Aiguille du Midi, lost 1.3 m between June and September 2022. Our findings affirm that ground-based GPR can be successfully employed in challenging topographical environments to determine sub-glacial geometries. This research contributes valuable insights for both scientific and administrative communities invested in comprehending the consequences associated with the evolution of hanging glaciers.

Figure 1: GPR survey, Pointes du Mourti, CH, September 2022. Photo: Loïc Perez

REFERENCES

Gilbert, A., Vincent, C., Gagliardini, O., Krug, J., & Berthier, E. (2015). Assessment of thermal change in cold avalanching glaciers in relation to climate warming: COLD AVALANCHING GLACIERS INSTABILITY. *Geophysical Research Letters*, *42*(15), 6382–6390. https://doi.org/10.1002/2015GL064838

Gilbert, A., Vincent, C., Six, D., Wagnon, P., Piard, L., & Ginot, P. (2014). Modeling near-surface firn temperature in a cold accumulation zone (Col du Dôme, French Alps): From a physical to a semi-parameterized approach. *The Cryosphere*, *8*(2), 689–703. https://doi.org/10.5194/tc-8-689-2014

Maggioni, M., Cola, G., Scotti, R., Freppaz, M., & Monti, F. (2018, October 12). *Ice/snow avalanches from the hanging snout of the Palòn de la Mare glacier (Central Italian Alps)*.

Margreth, S., Faillettaz, J., Funk, M., Vagliasindi, M., Diotri, F., & Broccolato, M. (2011). Safety concept for hazards caused by ice avalanches from the Whymper hanging glacier in the Mont Blanc Massif. *Cold Regions Science and Technology*, *69*(2–3), 194–201. https://doi.org/10.1016/j.coldregions.2011.03.006

Pralong, A., & Funk, M. (2006). On the instability of avalanching glaciers. *Journal of Glaciology*, *52*(176), 31–48. https://doi.org/10.3189/172756506781828980

15.12
Producing artificial snow samples with weak layers to determine mechanical properties for a variety of microstructural morphologies

Jakob Schöttner[1], Melin Walet[1], Benjamin Walter[1], Valentin Adam[1,2], Florian Rheinschmidt[2], Jürg Schweizer[1], Alec van Herwijnen[1]

[1] WSL Institute for Snow and Avalanche Research SLF, Flüelastrasse 11, CH - 7260 Davos Dorf (jakob.schoettner@slf.ch)
[2] Institute for Structural Mechanics and Desig, Technische Universität Darmstadt, Franziska-Braun-Str. 3, D - 64287 Darmstadt

Slab avalanches result from the failure of a weak snowpack layer buried underneath a cohesive slab. Determining the material properties of different weak layer morphologies is therefore necessary to better understand and model slab avalanche formation. However, mechanical experiments on weak layers are difficult due to seasonal availability and the need to transport the fragile samples to the laboratory. These problems can be circumvented by using artificially created weak layers. Here we present methods for producing snow samples that contain two different weak layers and can be used to measure the mechanical properties in a testing machine.

First, we grow weak layers consisting of depth hoar. In nature, depth hoar forms when the snowpack is subjected to strong temperature gradients over longer periods of time (days or weeks). We mimic this process by sieving low density snow between two dense slabs and subjecting it to a temperature gradient between 100 K/m and 300 K/m for up to 7 days. Depth hoar then grows in the low density snow layer with grain sizes up to 5 mm. Computer tomography analysis shows a clear trend of decreasing specific surface area (SSA) over time as the depth hoar develops. Mechanical experiments show that the compressive strength of the artificial specimens is between 3 MPa and 8 MPa, comparable to natural depth hoar weak layers. Second, we grow weak layers consisting of surface hoar. In nature, surface hoar grows due to deposition of atmospheric moisture on the snow surface that is colder than the air due to long-wave radiative cooling. In the laboratory, we artificially grow surface hoar in a ring wind tunnel. For this purpose, the snow surface is cooled from below with a cooling plate that can reach temperatures as low as -50 °C. The required humid air is supplied from a water basin that is maintained between 5 °C and 30 °C. The parameters surface temperature, air temperature, wind speed and humidity allow to influence the resulting surface hoar crystal shape in good agreement with the Nakaya diagram. Several methods of covering the surface hoar with a cohesive layer of snow, required for the mechanical testing procedure have been evaluated and first strength experiments support the feasibility of this method.

By controlling the growth of weak layers in the laboratory, we now have the necessary experimental basis to start collecting data on the influence of weak layer morphology on the mechanical properties.

15.13
Modeling the effect of free convection on permafrost melting-rates in ice-rich media

Amir Sedaghatkish[1,2], Marc Luetscher[1]

[1] *Swiss Institute for Speleology and Karst Studies (SISKA), CH-2300, La Chaux-de-Fonds, Switzerland*
[2] *Center for Hydrogeology and Geothermics (CHYN), University of Neuchâtel, CH-2000 Neuchâtel, Switzerland*

Predicting the melting rate in ice-rich permafrost contexts is key to study the stability of infrastructures built on frozen ground, hydrological processes, ecosystem dynamics and greenhouse gas releases from ice-filled aquifers due to global warming. Accurate modeling of heat transfer during the thawing of permafrost in ice-rich media yields melting rates that differ from those predicted by conventional conduction-based models. This research entails the development of a conceptual model of a karst aquifer subject to mountain permafrost, supported by a numerical simulation incorporating meltwater free convection. The methodology relies on the the Apparent Heat Capacity method and the Darcy approach for energy and momentum equations. Notably, the anomalous behavior of water between 0 and 4 ^{o}C causes warmer meltwater to flow downwards, leading to an acceleration of the melting process and a melting rate approximately one order of magnitude higher than that predicted by conventional models that disregard free convection. The outcomes of the model are compared qualitatively with field data from Monlesi cave in Switzerland, thereby confirming the close agreement of the proposed model with real-world observations in contrast to purely conduction-based models.

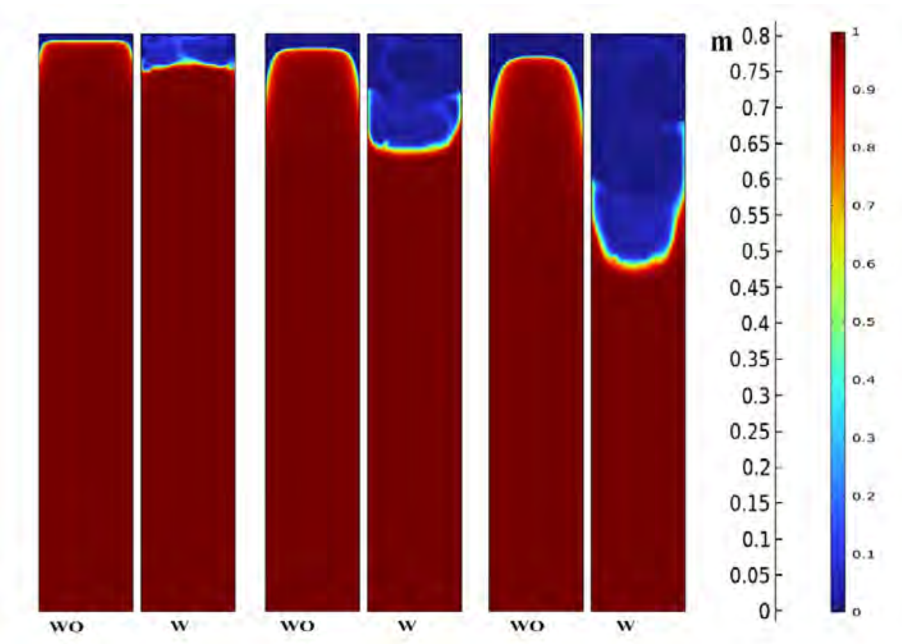

t=3 hr t=6 hr t=9 hr

Figure-1 ice fraction contour inside an ice cleft melting from top. The aperture is 10 cm. Two different scenarios are considered: without free convection (WO) and with free convection (W). (zero (blue) and one (red) in legend show the fraction of the water and ice domains, respectively)

15.14
Monitoring the annual geodetic mass balance of Bordu and Sary-Tor glaciers, Central Asia, using UAV data

Lander Van Tricht[1], Chloë Marie Paice[1], Oleg Rybak[1,2,3], Victor Popovnin[4], Rysbek Satylkanov[5,6], Philippe Huybrechts[1]

[1] *Earth System Science & Departement Geografie, Vrije Universiteit Brussel, Pleinlaan 2, B−1050 Brussels, Belgium*
[2] *Water Problems Institute, Russian Academy of Sciences, ul. Gubkina 3, Moscow 119333, Russia*
[3] *SSC RAS, ul. Ya. Fabritsiusa 2/28, Sochi 354002, Russia*
[4] *Department of Geography, Lomonosov Moscow State University, 1 Leninskie Gory 119991 Moscow, Russia*
[5] *Tien Shan High Mountains Scientific Center at the Institute of Water Problems and Hydropower of the National Academy of Sciences of Kyrgyz Republic, ul. Pionerskaya 9, Kyzyl Suu 722000, Kyrgyzstan*
[6] *Scientific Research Center of Ecology and Environment of the Central Asia, Erkindik blvd, Bishkek 720040, Kyrgyzstan*

The geodetic mass balance of a glacier corresponds to glacier-wide volume changes, converted to mass changes using density assumptions. It is typically calculated by differencing multi-temporal digital elevation models. In this study, we show how the annual geodetic mass balance of a glacier can be derived from Uncrewed Aerial Vehicle (UAV) data. The presented workflow is applied to two small to medium-sized glaciers in the Kyrgyz Tien Shan (Central Asia): Bordu glacier and Sary-Tor glacier. The obtained geodetic mass balance of 2021/22 and 2022/23 is compared with the glaciological mass balance derived from ablation stakes and snow pits. A previously calibrated mass balance model is used to correct for the difference in acquisition dates. The results show that the determined geodetic mass balance matches closely with the glaciological mass balance. Besides, for both glaciers the geodetic mass balance does not seem to be particularly sensitive to the assumptions regarding volume-to-mass conversion. Therefore, our results demonstrate that UAVs can serve as a valuable instrument to quantify the annual geodetic mass balance and to validate the glaciological mass balance. The conventional glaciological mass balance estimation often relies on interpolation and extrapolation methods, whereas UAVs offer the potential for direct data acquisition over the entire glacier surface.

15.15
Importance of the sub-seasonal, spatio-temporal variability of bare-ice albedo of Abramov Glacier, Kyrgyzstan

Anouk Volery[1], Martina Barandun[1], Kathrin Naegeli[,2]

[1] *Department of Geosciences, University of Fribourg, Chemin du Musée 4, CH-1700 Fribourg (anouk.volery@unifr.ch)*
[2] *Remote Sensing Laboratories, Department of Geography, University of Zurich*

The retreat of glaciers in Central Asia jeopardizes the reliability of local populations on water supplies provided by glacial melt during warm and dry seasons (Armstrong et al., 2019). The development of adequate measures to adapt to such impacts first requires an extensive understanding of the variables governing glaciers' mass balance. One of those variables is bare-ice albedo which controls the absorption of solar radiation at the surface of the glacier's ablation area – where most of net mass loss occurs (Benn and Evans, 2010). Bare-ice albedo has been understudied so far despite its influence on melting rates (Naegeli et al. 2015). This gap in research is problematic for Central Asia, considering that glaciers' ablation areas are exposed to radiation for extended periods (Zhou et al. 2017). Moreover, glaciers around the world, including in Central Asia, are becoming darker (Zhang et al. 2021).

Considering such circumstances, this contribution presents the sub-seasonal and interannual spatio-temporal variability of bare-ice albedo of Abramov glacier, Kyrgyzstan for the month of July, August, and September from 1999-2022. The bare-ice variable is investigated and linked to air temperature and mass balance data over multiple timescales. The results provide insights into 1) the sub-seasonal spatio-temporal variations of bare-ice albedo, 2) the evolution of bare-ice albedo under changing climatic conditions, 3) the influence of air temperature on variations of bare-ice albedo, 4) the relationship between bare-ice albedo and glacier mass balance.

REFERENCES

Armstrong, R.L. et al. (2019). Runoff from glacier ice and seasonal snow in High Asia: separating melt water sources in river flow, Regional Environmental Change, 19(9), 1249-1261.

Benn, D. and Evans, D. (2010). Glaciers and Glaciation, 2nd edition. London, Routledge.

Naegeli, K., Damm, A., Huss, M., Schaepman, M. and Hoelzle, M. (2015). Imaging spectroscopy to assess the composition of ice surface materials and their impact on glacier mass balance. Remote Sensing of Environment, 168, 388-402, doi:10.1016/j.rse.2015.07.006.

Zhang, Y et al. (2021). Albedo reduction as an important driver for glacier melting in Tibetan Plateau and its surrounding areas, Earth-Science Reviews, 220, 103735.

Zhou, H. et al. (2017). Seasonal snow cover regime and historical change in Central Asia from 1986 to 2008, Global and Planetary Change, 148: 192-2016.

15.16
Glaciological applications of long-range permanent terrestrial laser scanning data at Hintereisferner, Austria

Annelies Voordendag[1,2], Brigitta Goger[1,3], Rainer Prinz[1], Martin Rutzinger[4], Georg Kaser[1]

[1] *Department of Atmospheric and Cryospheric Sciences (ACINN), Universität Innsbruck, Innrain 52, 6020 Innsbruck, Austria (annelies.voordendag@uibk.ac.at)*
[2] *Institute of Geodesy and Photogrammetry, ETH Zürich, Stefano-Franscini-Platz 5, 8093 Zürich, Switzerland*
[3] *Center for Climate Systems Modeling, ETH Zürich, Universitätstr. 16, 8092 Zurich, Switzerland*
[4] *Department of Geography, Universität Innsbruck, Innrain 52, 6020 Innsbruck, Austria*

Glacier mass change has crucial impacts on hydrology, sea level rise, and climate change. Geodetic and glaciological mass balance observations so far have insufficient resolution to capture processes occuring on small spatial and/or short temporal scales. However, a permanent Terrestrial Laser Scanning (TLS) station adjacent to Hintereisferner (HEF, Ötztal Alps, Austria) provides daily Digital Elevation Models (DEMs), which allow closing spatiotemporal gaps in established glacier monitoring methods. An uncertainty assessment showed that smaller-scale processes, such as snow deposition and redistribution with a vertical spatial scale >0.10 m can be investigated with the TLS setup at HEF.

In this presentation, we show applications of the TLS data in glaciology. First, the glacier loss day (GLD), which is the day in the hydrological year when the glacier irrecoverably loses mass, is determined for three hydrological years with the TLS data. An extremely early GLD and a strong ablation season led to a record mass loss for HEF in 2022. This GLD is an expressive indicator of the glacier's imbalance with the persistently warming climate and can be measured or modelled on other mountain glaciers as well.

Second, a case study of wind-driven snow redistribution at HEF is studied with three DEMs from the TLS data before, shortly after, and 15 hours after snowfall. The DEMs are complemented with weather station data and large-eddy simulations using the Weather Research and Forecasting (WRF) model with a novel snow drift module. The TLS data shows a detailed overview of small-scale snow drift paterns at a horizontal spatial scale of 1 m at the glacier and can also be utilized for detailed model evaluation, leading to improved process understanding.

The TLS station in this harsh environment measures operationally since 2020. It enables the observation and quantification of surface changes such as glacier melt and snow redistribution at a high spatiotemporal resolution.

15.17
Fracture of weak snowpack layers: mixed mode fracture tests in the field

Melin Walet[1], Jakob Schöttner[1], Valentin Adam[1,2], Florian Rheinschmidt[2], Jürg Schweizer[1], Alec van Herwijnen[1]

[1] *WSL Institute for Snow and Avalanche Research SLF, Flüelastrasse 11, 7260 Davos Dorf, Switzerland (melin.walet@slf.ch)*
[2] *Technical University of Darmstadt, Institute of Structural Mechanics and Design, Darmstadt, Germany*

Dry-snow slab avalanches release due to crack propagation in a weak layer inside the snowpack. Understanding the fracture characteristics of the weak layer is essential for describing the onset of crack propagation and hence for predicting avalanche release. Avalanches release on steep slopes, thus crack propagation is a mixed mode fracture problem. Multiple fracture modes therefore play a role ranging from mode I, describing loading normal to the crack surface, to mode II, which describes loading parallel to the crack surface and normal to the crack front. Of particular relevance is the interaction between the fracture modes.

Until now, experiments focussed on estimating fracture toughness values for weak layers, a material property describing the resistance to crack growth. Yet, a full interaction range between mode I and mode II fracture toughness is still lacking. Here we present the results of mixed mode fracture experiments on snow specimen with a weak layer consisting of faceted crystals. Our results show a quadratic interaction law between mode I and mode II and indicate that the specific fracture energy is larger for mode II than for mode I. This agrees with the behavior observed in other materials. With the use of high-speed photography, we also obtain a high-resolution displacement field during fracture, allowing us to retrieve the elastic properties of the slab and the weak layer.

This detailed interplay between the full range of fracture modes for a weak layer of faceted crystals marks the start for a series of experiments, that will investigate the fracture properties of numerous weak layer microstructures. Since the snow microstructure most likely controls the mechanical properties, a characterization of the microstructure is essential. The connection between weak layer fracture and the microstructure of weak snowpack layers can be used to ultimately improve slab avalanche forecasting.

15.18
Seismo-acoustic sensing on ice: a new approach for continuous contact-free floating ice characterisation

Christoph Wetter[1], Cédric Schmelzbach[1], Simon C. Stähler[1,2]

[1] *Institute for Geophysics, Department of Earth Sciences, ETH Zurich (cedric.schmelzbach@erdw.ethz.ch)*
[2] *Space Science and Technology, Department of Earth Sciences, ETH Zurich*

Seasonal ice on Alpine lakes has a substantial influence on local weather, climate, ecology and economy. Therefore, the investigation of the thickness and ice properties such as the elastic parameters of floating ice on lakes and likewise the sea is critical to understand the impact of rising temperatures on Alpine and Arctic environments. Additionally, ice properties are important for the safety on ice for both recreational activities and engineering purposes.

Today, a multitude of remote sensing and geophysical methods exist for the surveillance of sea and lake ice. Although optical and microwave remote sensing serve as key tools for ice cover monitoring, accurately estimating the ice thickness remains challenging. In contrast, geophysical methods like ground penetrating radar and seismic techniques, akin to manual drilling, can provide direct observations but require contact with the ice and are typically laborious and potentially dangerous.

In this study, we explored the possibility of deploying microphones on frozen lakes in the Swiss Alps to track the lake ice evolution using acoustic signals originating from frequently occurring ice quakes. Recording acoustic signals coupled to the propagation of seismic waves in floating ice introduces new avenues for non-contact and continuous monitoring of ice thickness, quality, and dynamics. We show how off-the-shelve microphones can be used to record audible signals above the ice.

An example recording of sound signals generated by ice quakes recorded at Lake Oeschinen is displayed in Figure 1. Frequent ice quakes excite seismic waves that are characterised by strong dispersion (frequency-dependent propagation velocity). Wave components traveling through the ice at the speed of sound in air couple particularly well into the air and manifest themselves as distinct monochromatic sound signals. The frequency of the sound observation is directly correlated with the ice thickness.

To monitor the ice growth with time using seismo-acoustic signals, we deployed three sensors on frozen Lake St. Moritz in a three-month-long field campaign in winter 2021/22. Figure 2 shows the ice thickness evolution starting from around 40 cm thickness in mid-January, peaking to a maximum of around 58 cm mid-March and subsequently decaying to around 54 cm by the end of March 2022. These measurements bear an uncertainty of 2 cm. The ice thickness was confirmed by manual drilling.

We demonstrate with our experiments that seismo-acoustic recordings present a novel economical means of contact-free and continuous monitoring of ice evolution with potential applications to climate change impact monitoring and ensuring safety on ice for transportation and recreation. Furthermore, contact- free floating ice monitoring potentially carries relevance for studies of Arctic and Antarctic sea ice shelve dynamics.

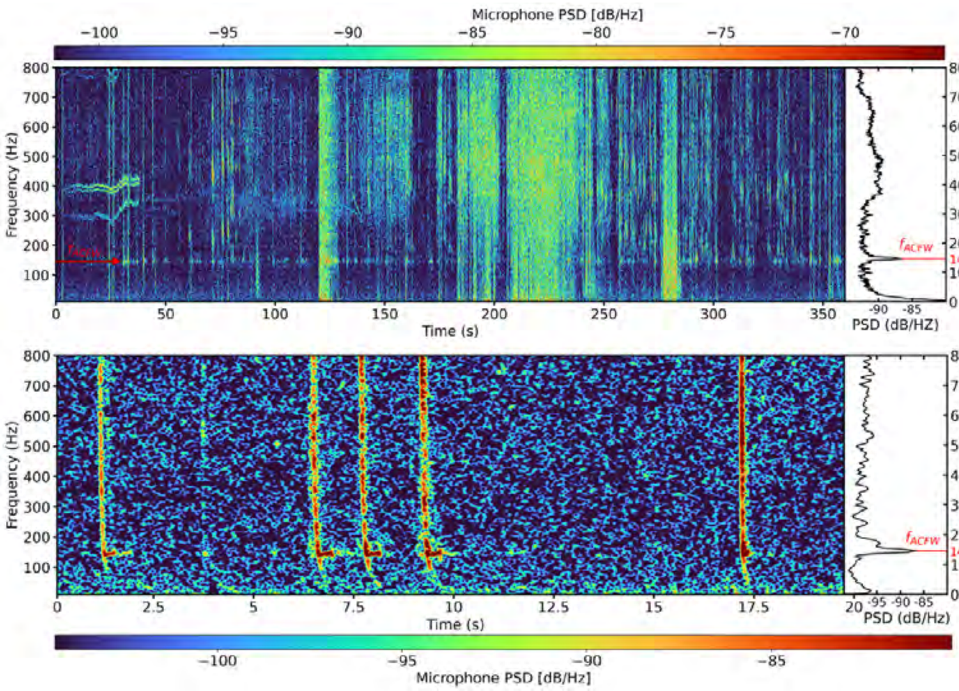

Figure 1. Microphone recording of ice quakes at Lake Oeschinen. Top: six-minute recording of hundreds of ice quakes visible as vertical lines in the spectrogram. Bottom: Zoom-in on five ice quakes showing typical mono-chromatic air-coupled waves at 146 Hz.

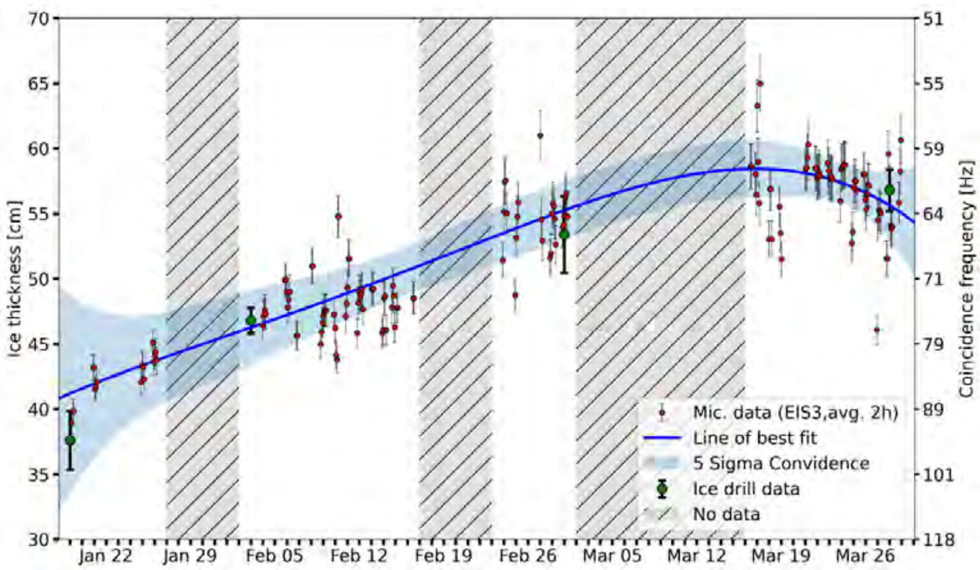

Figure 2. Ice-thickness curve from Lake St. Moritz in the winter season 2021/22. Roughly 2'000 individual ice quake recordings were utilized. Ice-drill data are shown as ground-truth.

P 15.1
How to propel a floating iceberg 400 m up into the air

Martin Lüthi, Antoine Zaninetti, Ana Nap, Adrien Wehrlé

[1] *Department of Geography, University of Zurich, 8057 Zurich (martin.luethi@geo.uzh.ch)*

During fieldwork at Greenland fastest glacier (Sermeq Kujalleq in Kangia or Jakobshavn Isbrae) we observed an iceberg shooting some 400 m up before rotating sideways and plunging into the water. Several similar events were captured with time-lapse photography, seismometers and terrestrial radar interferometry. Here, we analyze such events with theoretical considerations and detailed numerical modeling. The process is clearly buoyancy-driven, but the rates of uplift and the height above the water line allow us to constrain the proportions of the iceberg under water as compared to the visible part. Also, the question how the iceberg can obtain a submerged position priming the up-shooting leads to interesting conclusions with regard to iceberg release through fracturing.

P 15.2
Improved glacier monitoring using low-cost satellite communication service in Central Asia

Martina Barandun[1], Andreas Hasler[2], Federico Belloni[3] and Martin Hoelzle[1]

[1] *Departement of Geosciences, University of Fribourg, Fribourg, Switzerland (martina.barandun@unifr.ch)*
[2] *SensAlpin GmbH, Davos, Switzerland*
[3] *Astrocast SA, Chavannes-près-Renens, Switzerland*

Glacier monitoring has been (re)established over the last two decades in the Central Asian Tien Shan and Pamir. Annual glacier mass balances are now regularly reported to the World Glacier Monitoring Service and serve as the baseline to observe climate change in a sparsely documented region since the mid 1990's. Several sites within the Central Asian monitoring network have been appointed with modern automatic weather stations and terrestrial cameras. The monitoring of cryosphere in Central Asia has undergone several updates in recent years, with the inclusion of hydrological and permafrost observations. However, current efforts are restricted to only one field visit per year and the transmission of data is limited to a select number of sites and datasets.

While satellite communication is a promising technology for transmitting data from remote stations, it remains prohibitively expensive and power-intensive. As a consequence, this provision is frequently restricted to projects of a certain length or to establishments with ample financial means. For distant stations such as those in the Central Asian Tien Shan and Pamir, data retrieval relies heavily on field accessibility.

Here, we report on updates regarding the current monitoring sites during the 2023 field season. A low-cost, low-power satellite communication system has been used to monitor stations observing changes in snow, glaciers, and permafrost in the Tien Shan and Pamir regions. The monitoring stations have been integrated with the Astrocast SA communication technology at three locations. The engineering firm, SensAlpin GmbH, has established a protocol between the Astronode S+ satellite trasnceiver and the Campbell Scientific data logger system. Astrocast SA configured the Astronode S+ for cold and high-altitude environments. The project is financed by a Technogrant from the Swiss Polar Institute (SPI).

The satellite communication described above now enables us to retrieve the borehole temperatures on an hourly basis from a recently drilled permafrost borehole in the Inner Tien Shan at 3600 m above sea level. The second site is transmitting data from automated weather station situated in the upper ablation area of the Batysh Sook glacier in Inner Tien Shan, at an elevation of 4100 m above sea level. The third station gathers near-real-time meteorological information at 4800 m above sea level in East Pamir for the first time in history. The Eastern Pamir is an area with extremely limited data available relating to meteorology, glaciology and hydrology. In addition, and independently to the above outlined system, glacier ablation is now measured in 30-minute intervals at a minimum of one location for each glacier with long-term observation.

As well as offering swift accessibility to data stored in far-off and unreachable regions, the satellite communication system will also furnish insights into the condition of the station and facilitate identification of station malfunctions. This is critical for the monitoring sites to curtail data loss. Over the next couple of years, our low-priced satellite communication system, employing Campbell Scientific data loggers, will be fitted-out across all cryosphere monitoring sites in Central Asia. This scheme enables affordable and unrestricted close-to-real time data transfer to all.

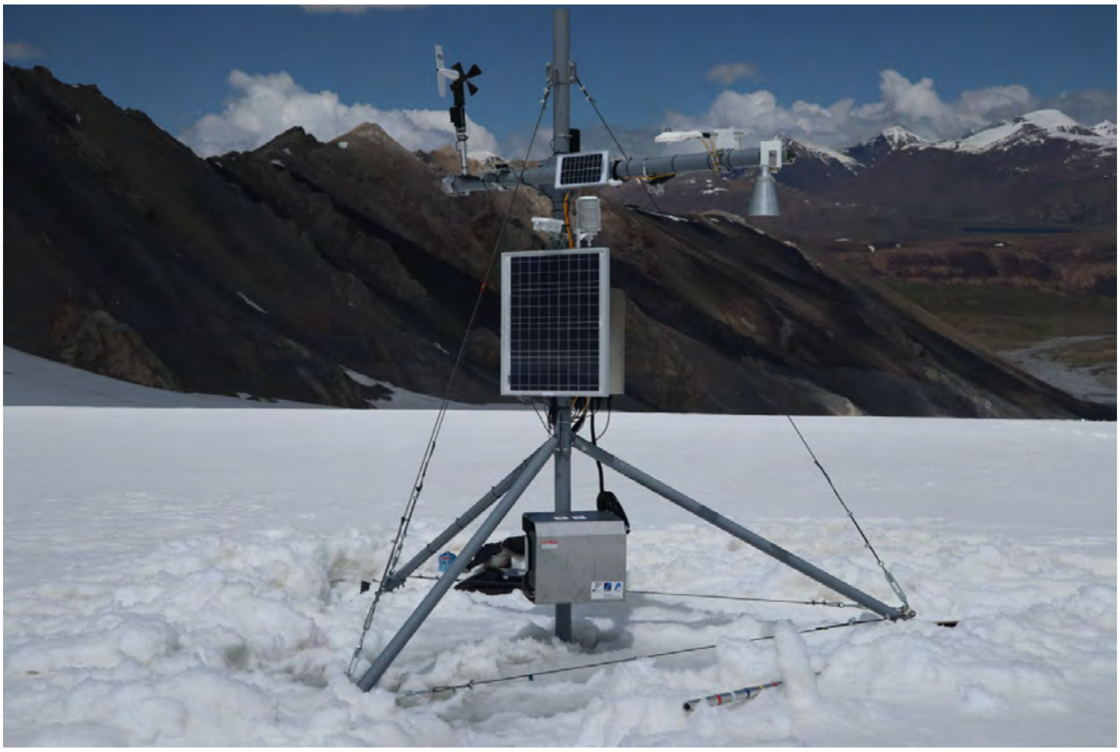

Figure 1: Implemented system on an automatic weather station at Batysh Sook Glacier in the Inner Tien Shanat 4100 m a.sl. (source: M. Barandun, 2023-07-12)

Figure 2 Left: Astronode S+ satellite trasnceiver at the test station connected to the monitoring system by SensAlpin GmbH; Right: the Astronode S+ in a sealed housing with sealing compound (source: SensAlpin GmbH)

P 15.3
Hyperspectral thermal remote sensing of the Cryosphere: first application on a debris-covered glacier in the Swiss Alps

Gabriele Bramati[1], Florian Hardmeier[2], Jennifer Susan Adams[1], Andreas Vieli[2], Kathrin Naegeli[1]

[1] *Remote Sensing Laboratories, Department of Geography, University of Zurich, Zurich, Switzerland (gabriele.bramati@geo.uzh.ch)*
[2] *Glaciology and Geomorphodynamics Group, Department of Geography, University of Zurich, Zurich, Switzerland*

Debris-covered glaciers are characterised by variable surface features strongly altering their melt behaviour in a diverse and heterogeneous manner. Despite their extensive occurrence and source of freshwater in many mountaineous regions, their response to climate change is diverse and still poorly understood (Kääb et al. 2012). Thus, an improved understanding of surface characteristics, such as debris-cover thickness, and linked processes, for instance sub-debris melt dynamics, is urgently needed.

Monitoring the characteristics of debris coverage is a challenging task. So far, direct measurements, energy balance models, digital elevation model differencing and the use of remote sensing data have been used to investigate its thickness, spatial heterogeneity, and the evolution over time. In particular, thermal infrared (TIR) remote sensing offers a great potential for the estimation of debris thickness, thanks to the known coupling of surface temperature and thickness of the debris (Gök et al., 2023). However, TIR datasets are scarce and often lack the necessary spatial and temporal resolution. In addition, TIR instruments feature strong limitations being uncooled or equipped with single broadband sensors. Airborne hyperspectral TIR data offers the potential to capture entire landforms at a detailed spatial resolution, and the high spectral resolutions allow for more advanced debris thickness estimations. This is of particular importance in sight of the upcoming multispectral thermal missions TRISHNA (Thermal infraRed Imaging Satellite for High-resolution Natural resource Assessment), SBG (Surface Biology and Geology), and LSTM (Land Surface Temperature Monitoring).

In this contribution we present an overview of our extensive across-scale data collection on Zmuttgletscher located at the northwestern side of Matterhorn in Summer 2023. The first ever hyperspectral airborne TIR survey of a debris-covered glacier was acquired with NASA's JPL Hyperspectral Thermal Emission Spectrometer (HyTES). It is an airborne sensor featuring 256 bands in the 7.5 – 12 µm spectral wavelength region (Hook et al., 2013). Concurrently with the airborne survey on 7th July 2023, an extensive set of ground instruments has been installed. An Automatic Weather Station was placed on the glacier recording air temperature, humidity, windspeed, wind direction, precipitation, incoming shortwave radiation, and atmospheric pressure, together with a full four-components radiation sensor. Debris thicknesses were measured manually and ablation stakes were drilled. Four TIR radiometers were installed to acquire additional point information of the debris skin temperature. Several ground surface temperature loggers in different debris settings (i.e. rock grain size, shade, ridge, furrow) recorded the near surfce temperature continuously. For calibration purposes, a TIR radiometer, as well as two water temperature sensors at different depths were deployed in a proglacial lake.

This across-scale TIR data collection will be the basis for our future investigations that aim at (i) characterising the influence of scale on the surface temperature retrieval in such enviroment and (ii) exploring the hyperspectral thermal data (radiometric temperatures and emissivity spectra) in order to improve spatial debris thickness estimation. Feeding our results into a numerical model will substantially improve estimates of the glacier-wide sub-debris melt and shed light on the influence on its dynamics.

REFERENCES

Gök, D. T., Scherler, D., & Anderson, L. S. (2023). High-resolution debris-cover mapping using UAV-derived thermal imagery: limits and opportunities. The Cryosphere, 17(3), 1165-1184.

Hook, S., Johnson, W., and Abrams, M.: NASA's Hyperspectral Thermal Emission Spectrometer (HyTES), in: Thermal Infrared Remote Sensing – Sensors, Methods, Applications, edited by: Kuenzer, C. and Dech, S., Springer, Dordrecht, the Netherlands, 2013

Kääb, A., Berthier, E., Nuth, C., Gardelle, J., & Arnaud, Y. (2012). Contrasting patterns of early twenty-first-century glacier mass change in the Himalayas. Nature, 488(7412), 495-498.

P 15.4
Glacier Mass Balance in the Gunt River Basin, Pamir, Tajikistan

Hofiz Navruzshoev[1,2], Kayumov Abdulhamid[1], Tomas Saks[2], Martina Barandun[2], Kabutov Khusrav[1], Andrey Smirnov[3], Martin Hoelzle[2]

[1] Center for Research of Glaciers of the National Academy of Sciences of Tajikistan, 33, Rudaki Avenue, Dushanbe, Tajikistan (hofiz.navruzshoev@gmail.com)
[2] Department of Geosciences, University of Fribourg, Switzerland
[3] Institute of Geography RAS, Russia

Glacier monitoring and research are of great importance both for predicting the state of water resources and their use in various economic sectors, including agriculture and energy. Glaciers are furthermore very important indicators for climate change, especially in data sparse regions such as High Mountain Asia. Most glaciers around the world are retreating (WGMS, 2018). Mass loss has accelerated in recent decades. The responses of glaciers in High Mountain Asia, including the Tien Shan and Pamir, are spatially and temporally very heterogeneous (Barandun et al., 2021). Continued glacier retreat will have serious implications for freshwater resources in Central Asia, especially under high-emission scenarios (Holzle et al., 2019). The Gunt River basin is the second largest tributary of the Panj (Amu Darya) River basin. It covers a significant area of the South-West Pamir (13700 609 km^2) out of which 609 km^2 is glacierized (Varnakova and Rototaeva, 1979). In the past non of its glaciers have been monitored.

Since 2020, the mass balance of glacier # 457 using direct glaciological (Østrem et al., 1969) and other methods, which is located in the upper Tokuzbulak River, has been measured in situ. The establishment of a long-term monitoring in the Gunt River basin is an important step forward to improve glacier monitoring in the Eastern Pamir and to better understand the heterogeniouse glacier response to climate change in the region. According to the obtained data it was revealed that the glacier in the period from 2020-2021 -0.35 m w.e. yr^{-1} and in the period from 2021-2022 lost -0.44 m w.e. yr^{-1} of its mass. To complement the mass balance observation, in summer 2023, an automatic weather station (AWS) has been installed and extensive ice thickness measurements were performed. This additional measurements in combination with mass balance surveys will help to better understand the processes governing the glacier mass balance and provide the baseline to better predict future glacier response to climate change and its impacts on the water resources of the region.

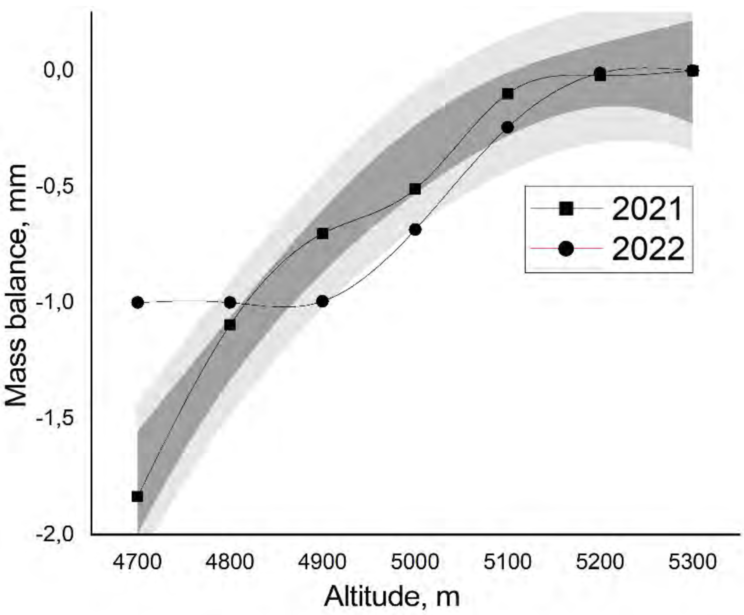

Figure 1. Mass balance of glacier #457 for 2020-2022.

REFERENCES

Hoelzle, Martin; Barandun, Martina; Bolch, Tobias; Fiddes, Joel; Gafurov, Abror; Muccione, Veruska; Saks, Tomas; Shahgedanova, Maria (2019). The status and role of the alpine cryosphere in Central Asia. In: Xenarios, Stefanos; Schmidt-Vogt, Dietrich; Qadir, Manzoor; Janusz-Pawletta, Barbara; Abdullaev, Iskandar. The Aral Sea basin: water for sustainable development in central Asia. Abingdon (UK): Routledge, 100-121. DOI: https://doi.

org/10.4324/9780429436475-8
World Glacier Monitoring Service (2018): Global Glacier Change Bulletin No. 2 (2014-2015). Zemp, M., Nussbaumer, S. U., Gärtner-Roer, I., Huber, J., Machguth, H., Paul, F., and Hoelzle, M. (eds.), ICSU(WDS)/IUGG(IACS)/UNEP/UNESCO/WMO, World Glacier Monitoring Service, Zurich, Switzerland, 244 pp., based on database version: doi:10.5904/wgmsfog-2018-11.
Varnakova G.M., Rototaeva O.V. Catalog of glaciers of the USSR. T. 14 (Central Asia), vol. 3 (Amu-Darya river basin), part 15 (Gunt river basin). Leningrad: Gidrometeoizdat. -1979. -128 p.
Østrem Gunnar et al. Glacier Mass-Balance Measurements. a Manual for Field and Office Work. Rev. ed. 1969. P. 66.
Barandun, M., Pohl, E., Naegeli, K., McNabb, R., Huss, M., Berthier, E., et al. (2021). Hot spots of glacier mass balance variability in Central Asia. Geophysical Research Letters, 48, e2020GL092084. https://doi.org/10.1029/2020GL092084

P 15.5
Cosmogenic dating of Abramov glacier advances during the Little Ice Age and Last Glacial Maximum

Tomas Saks[1], Vincent Rinterknecht[2], Ivan Lavrentiev[4], Gabriel Béra[2,3], Enrico Mattea[1], Martin Hoelzle[1]

1 Department of Geosciences, University of Fribourg, Fribourg, 1700, Switzerland (tomas.saks@unifr.ch)
2 Aix Marseille Univ, CNRS, IRD, INRAE, CEREGE, Aix-en-Provence, France
3 Department of Geography, Paris 1 Panthéon-Sorbonne Univ, LGP CNRS, UMR 8591, 94320 Thiais, France
4 Institute of geography, Russian Academy of Sciences, Moscow, Russia,

The Koksu river valley in the Pamir-Alay range, southern Kyrgyzstan, hosts 25 glaciers larger than 1 km^2 and numerous smaller glaciers. The largest glacier in the catchment is the Abramov glacier covering 21.35 km^2. The glacier has been extensively monitored since 1965 to 1999, and since 2011 long-term observations have been resumed. The long and detailed mass balance time series provide a benchmark climate variable, among other information, for the Pamir-Alay range.
We present cosmogenic ^{10}Be exposure dating results of glacier moraines directly deposited by the Abramov glacier. Additionally, we present a 24 km long Ground Penetrating Radar survey (conducted with a 20 MHz VIRL-7 monopulse radar), allowing a detailed reconstruction of the glacier changes since the Little Ice Age (LIA) combined with historical mass balance observations.

The obtained radar data shows predominantly a temperate ice structure of Abramov with a maximal measured thickness reaching to a depth of 220 m.

The dating results suggest a LIA glacial advance at around 271±74 years ago.
The second part of dating results suggest a Late Glacial advance of the Abramov glacier at 17.1 ± 1.0 (0.5) ka. This data provides a robust constrain for the Last Glacial Maximum in the Pamir-Alay.

Secular mass balance reconstruction suggests a gradually more negative mass balance since the LIA advance. The mass balance is becoming increasingly negative since the last quarter of the 20th century. The results of the glacier reconstruction estimates the Equilibrium Line Altitude (ELA) was around 80 m lower during the LIA, a time period when the glacier covered roughly 35 km^2.

P 15.6
Investigating the sensitivity of the Glacier Evolution Runoff Model (GERM) towards input data quality

Alexandra von der Esch[1,2], Matthias Huss[1,2], Marit van Tiel[1,2], Daniel Farinotti[1,2]

[1] *Laboratory of Hydraulics, Hydrology and Glaciology (VAW), ETH Zurich, Zurich, Switzerland (vonderesch@vaw.baug.ethz.ch)*
[2] *Swiss Federal Institute for Forest, Snow and Landscape Research (WSL), Birmensdorf, Switzerland*

Glacier response to climate change and expected long-term decrease in volume is leading to changes in meltwater runoff, which can significantly impact downstream populations. To understand this development, and thereby assess future implications for alpine environments, it is essential to model both the ongoing as well as future glacier evolution and catchment runoff. High quality reference data is fundamental for creating these predictive models. However, especially for remote areas, data is often missing, or its temporal and spatial resolution is low.
In this study, we investigate the sensitivity of the Glacier Evolution Runoff Model (GERM) towards input data quality. The input data consists of meteorological data and digital elevation models of the glacier surface. Measured discharge and glacier massbalance data are used for calibration and validation. We aim to calibrate and validate the model using different data sets, and to optimize the model to make it applicable for areas where fewer data is available.
GERM is applied to the Rhone headwater catchment at Gletsch, Switzerland, an area where high-resolution data is available. We calibrate the model using the high-resolution data, and subsequently purposefully reduce the quality of the input data set. The results based on decreasing data quality are then compared to model results using the reference data. Understanding the limits of the model when working with different quality data and assessing its accuracy will allow us to evaluate possible implications when modeling areas with limited data availability.

P 15.7
Monitoring daily flow velocities at Abramov glacier with low-cost, open-source GNSS loggers

Enrico Mattea[1], Martina Barandun[1], Tomas Saks[1], Adam Garbo[2], Martin Hoelzle[1]

[1] *Department of Geosciences, University of Fribourg, Chemin du Musée 4, CH-1700 Fribourg (enrico.mattea@unifr.ch)*
[2] *Department of Geography and Environmental Studies, Carleton University, Colonel By Drive 1125, Ottawa, Canada*

Glacier instabilities such as surges constitute a serious natural hazard and a challenge to accurate estimation of mass balance. Glaciers of surge-type are clustered in several regions of the world including Central Asia: there, difficult logistics hamper the collection of long-term, year-round field measurements, especially since the end of most resident monitoring programs of the Soviet Union. So far, international efforts towards re-establishing local measurements have focused on meteorological and mass balance data. Thus, glacier dynamics are usually observed only with satellite-based methods, without ground control.

Here, we present results from one year of *in situ* monitoring of surface ice flow velocities at Abramov, a valley glacier covering 21 km^2 in the Pamir-Alay range of Kyrgyzstan. The glacier is known to be unstable, with a strong dynamic pulsation in 1972/73 and another speed-up event over 2000-2005. We installed four multi-constellation, open-source GNSS receivers in the ablation area between 3700 and 4000 m asl, logging daily raw data; then, we processed the measurements with the Precise Point Positioning technique to a typical accuracy of 1-3 cm.

Preliminary analysis of the displacements shows a marked annual cycle: large and highly variable velocities during the melt season are followed by a regular slowdown, starting at the first autumn snowfall and reaching minimum velocity in early May. Snow cover starting in October appears to fully decouple flow velocities from the surface melt rates, until about two months before full snow melt: then, we observe a new speed-up with multiple velocity peaks (> 100 % increase), in some cases associated with significant surface uplift. Mean monthly velocities (up to 100 m/yr in August) are similar to those measured just before the 1970s pulsation, in spite of multi-decadal glacier thinning (by > 25 % of the total ice thickness at the two lower investigated sites).

Beside a better understanding of local ice dynamics, our results provide ground truth to remote sensing methods of estimating glacier velocity. The achieved 3D accuracy suggests an additional application of our setups to measure ablation at daily resolution.

P 15.8
Depicting the water and ice cycle on rock glacier Murtèl

Dominik Amschwand[1], Seraina Tschan[1], Martin Scherler[1] , Martin Hoelzle[1], Anna Haberkorn[2], Christian Kienholz[2], Bernhard Krummenacher[2], Lukas Aschwanden[3], Hansueli Gubler[4]

[1] *Department of Geosciences, University of Fribourg, Chemin du Musée 4, CH-1700 Fribourg (dominik.amschwand@unifr.ch)*
[2] *GEOTEST AG, Bernstrasse 165, CH-3052 Zollikofen*
[3] *Institute of Geology, University of Bern, Baltzerstrasse 1+3, CH-3012 Bern*
[4] *ALPUG GmbH, Richtstattweg 3, CH-7270 Davos-Platz*

Rock glaciers store, alter, and release water and ice over different time scales: Liquid water on short-term (sub-monthly) scale, ground ice in the coarse-debris active layer on intermediate term (seasonal), and “old” permafrost ice on long-term scale (over millennia). Different views emerged from different investigation approaches. One the one hand, remote senser and geophysicists tend to see huge ground ice reservoirs in ice-rich mountain permafrost landforms like rock glaciers or talus slopes. On the other hand, permafrost hydrologists struggle to detect the ice melt contribution to the rock-glacier outflow. Hence, the “hydrological significance” of rock glaciers is unresolved and a topic of ongoing research (Arenson et al., 2022).

Here, we estimate the water and ice fluxes on rock glacier Murtèl (Upper Engadine) and represent the fluxes in a novel way, emphasizing the different flux magnitudes and time scales (Fig. 1). The fluxes are drawn in a space-time polar diagram (Arènes et al., 2018) developed to represent the carbon or water cycles in the so-called critical zone, Earth’s climate-sensitive skin where the transformation of energy and matter (e.g., water) occurs. Short-term water and ice fluxes are from our hydrological measurements, ground-ice “ablation” measurements with a wildlife camera, and indirectly from energy balance estimates of the available melt energy. Long-term (decadal to millennial) information are drawn from 50+ years of research on Murtèl. A concise graphical representation of the processes and water-ice fluxes that includes the time dimension may help to grasp the debated “hydrological significance” of rock glaciers in the periglacial critical zone.

REFERENCES

Arènes, A., Latour, B., & Gaillardet J. 2018: Giving depth to the surface: An exercise in the Gaia-graphy of critical zones, The Anthropocene Review, 5(2), 1–16.

Arenson, L., Hoelzle, M., & Springman S. 2002: Borehole deformation measurements and internal structure of some rock glaciers in Switzerland, Permafrost Periglac. Process., 13, 117–135.

Arenson, L., Harrington, S., Koenig, C.E.M., & Wainstein P.A. 2022: Mountain permafrost hydrology—a practical review following studies from the Andes, Geosciences, 12(2), 48.

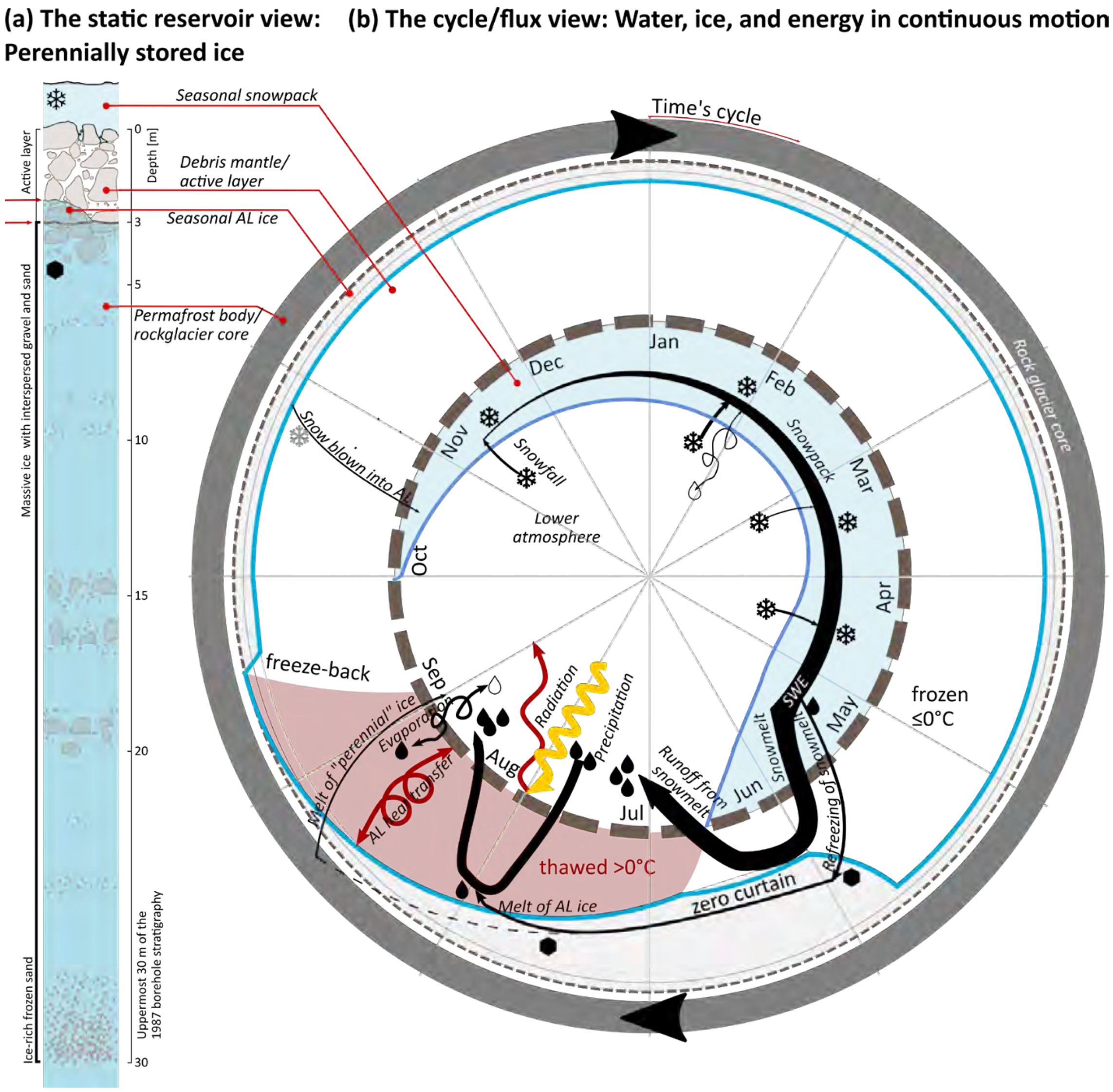

Figure 1. Two representations of water and ice on the seasonaly snow-covered rock glacier Murtèl, (a) as static storage and (b) as fluxes. The borehole stratigraphy is drawn after Arenson et al. (2002).

P 15.9
Exploring englacial hydrology with surface nuclear magnetic resonance

Laura Gabriel[1,2], Marian Hertrich[3], Christophe Ogier[1,2], Hansruedi Maurer[4], Daniel Farinotti[1,2]

[1] *Laboratory of Hydraulics, Hydrology and Glaciology (VAW), ETH Zurich, Hönggerbergring 26, CH-8093 Zürich (lagabrie@ethz.ch)*
[2] *Swiss Federal Institute for Forest, Snow and Landscape Research (WSL), Zürcherstrasse 111, CH-8903 Birmensdorf*
[3] *Bedretto Underground Laboratory for Geosciences and Geoenergies, ETH Zurich, Sonneggstrasse 5, CH-8092 Zürich*
[4] *Institute of Geophysics, ETH Zurich, Sonneggstrasse 5, CH-8092 Zürich*

Glaciers enclose a complex hydrological system transporting meltwater within the ice. Potential geometries of the glacial drainage network include channels, lakes, moulins, crevasses or streams. A particular case represents the so-called water pocket. The best-known water pocket was located at Tête Rousse in France, consisting of a subglacial reservoir filled with around 55 000 m^3 of water (Vincent et al., 2012). Due to the associated risk of an outburst flood, the cavity was artificially emptied in 2010.

Here, we test the potential of Surface Nuclear Magnetic Resonance (SNMR) for characterizing the englacial drainage system. Since SNMR is the only non-invasive geophysical method that allows direct detection of the liquid water content, it has the potential to deliver information complementary to Ground Penetrating Radar (GPR), a surveying technique often applied in the glaciological context (Church et al., 2021).

The specific goal of our study is to develop novel strategies that allow for a rapid scanning and iterative refinement of SNMR field surveys. Indeed, detecting englacial water bodies through SNMR with conventional survey designs would require unacceptable long survey times. The aim is to detect potential water bodies with the highest possible probability and an optimum field effort. Aspects to investigate include optimized loop geometries, pulse protocols, excitation sequences and the clever combination of SNMR with GPR data.

As a first step, we investigate different loop geometries based on previous works considering separate transmitter and receiver loops (Hertrich et al., 2009; Lehmann-Horn et al., 2011). We designed an SNMR field survey on Rhonegletscher, Swiss Alps, where part of the englacial drainage system has already been investigated using GPR (Church et al., 2021). Knowing the approximate position and extension of the channel allowed us to define measurement configurations covering different parts of the area where we expect significant amounts of water (see Fig. 1). By combining the obtained experimental data with 3D forward and inversion modelling, we aim at characterizing the current state of the channel system and learn about the sensitivity and resolution of our approach. In addition, we performed GPR measurements in the same area to further constrain the SNMR data. Through this first study, we aim at learning about the potential of deploying various loop configurations, and to devise strategies to efficiently detect and map englacial water by using SNMR.

REFERENCES

Church, G. et al. 2021: Ground-penetrating radar imaging reveals glacier›s drainage network in 3D, The Cryosphere, 15, 3975–3988
Hertrich, M. et al. 2009: High-resolution surface NMR tomography of shallow aquifers based on multi-offset measurements, GEOPHYSICS 74: G47-G59
Lehmann-Horn, J. A. et al. 2011: Imaging groundwater beneath a rugged proglacial moraine, GEOPHYSICS 76: B165-B172
Vincent, C. et al. 2012: Detection of a subglacial lake in Glacier de Tête Rousse (Mont Blanc area, France), Journal of Glaciology, 58(211), 866-878

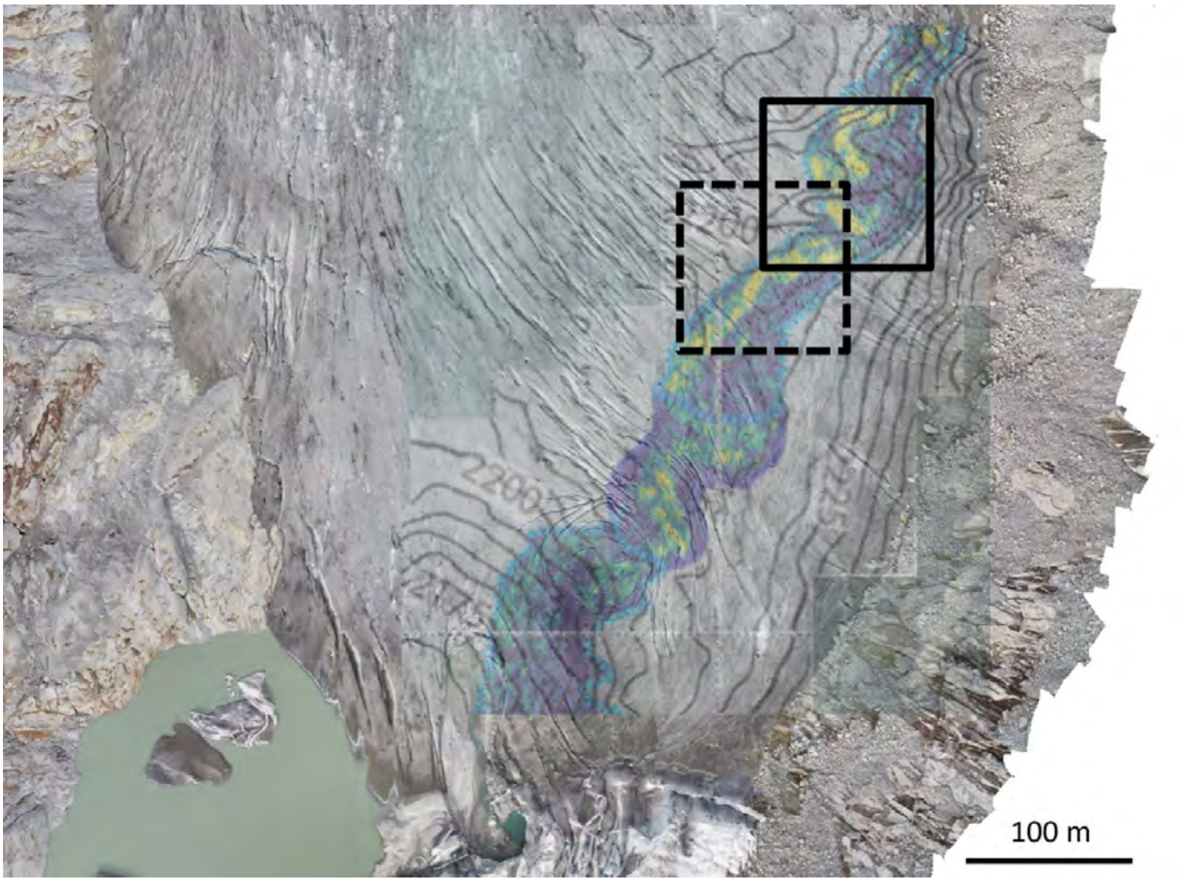

Figure 1. Aerial view of the lower part of Rhonegletscher (image provided by Elias Hodel) overlaid with the water channel system (in blue, green and yellow) investigated by Church et al. (2021). The black squares mark one of the deployed loop configurations comprising a transmitter (solid) and a receiver (dashed) loop.

P 15.10
What happens below the surface of the Otemma Glacier? Investigating Alpine glacier hydrology through multi-method geophysical analysis

Johanna Klahold[1], Gabriela Clara Racz[1], and James Irving[1]

[1] *Institute of Earth Sciences, University of Lausanne, Switzerland (johanna.klahold@unil.ch)*

Glacier dynamics are governed by interactions between ice, meltwater, and the surrounding hydrological system. To understand these complexities and their implications, advanced numerical models of glacier hydrology have been developed. These models require information about conditions inside the glacier and at its base for calibration and validation. Acquiring such data poses substantial challenges due to the restricted access to these sites. Indeed, conventional methods like borehole measurements offer limited point-scale insights, whereas direct exploration via subglacial conduits and moulins carries significant risk. Ground-penetrating radar (GPR) has much potential to address these challenges as it allows for surface-based and nowadays even drone-based high-resolution 3D imaging of internal glacier structures and properties.

In this study, we combine high-resolution drone-based 3D GPR data of the Otemma Glacier (Valais, Switzerland) with photogrammetry surveys, dye tracing experiments, and hydrological modeling, to investigate the structure of the englacial and subglacial drainage system. The analysis of GPR reflection amplitudes at the ice-bedrock interface indicates that the Otemma glacier has two main subglacial discharge pathways, which align with surface moulin locations and the position of the outlet stream. These findings are in agreement with preliminary modeling results. Further analysis of the GPR data also suggests the presence of a well-developed englacial drainage system. Currently we are developing a detailed processing workflow to account for the air-based nature of the data acquisition, which will allow for characterization of small-scale englacial and subglacial features.

P 15.11
Fluxes of toxic elements mobilized from a rock glacier in Val Mustair: insights on ice melt dynamics

Hoda Moradi[1], Gerhard Furrer[2], Michael Margreth[3], Louisa Wolpert[1], David Mair[1], Christoph Wanner[1]

[1] *Rock-Water Interaction Group, Institute for Geological Sciences, University of Bern, Baltzerstrasse 3, CH-3012 Bern (hoda.moradi@unibe.ch)*
[2] *Institute of Biochemistry and Pollutant Dynamics (IDP), Department of Environmental Systems Science, ETH Zurich, CH-8092 Zurich*
[3] *Swiss Federal Institute for Forest, Snow and Landscape Research WSL, Mountain Hydrology and Mass Movements, Zürcherstrasse 111, CH-8903 Birmensdorf*

In the Central Alps, an increasing number of high-altitude streams show distinctively white colored streambeds. The white color originates from the precipitation of nanocrystalline basaluminite [$Al_4OH_{10}(SO_4)x5(H_2O)$] sticking to the bed load of the streams (Bigham et al. 2000; Carrero et al. 2015). The phenomenon is triggered at the source of the streams where pyrite oxidation occurs in ice-rich permafrost bodies, i.e. in rock glaciers. This leads to the production of sulfuric acid and the subsequent dissolution of aluminum from the paragneiss host rocks. Owing to its pH-dependent solubility, basaluminite eventually precipitates when the acidic and aluminum-rich streams are neutralized along their flow paths (Wanner et al. 2018). Acidic conditions in the affected streams are also accompanied by elevated concentrations of other toxic elements such as Ni, Mn, Zn and F mobilized from the host rock and strongly exceeding the drinking water limits. The ongoing retreat of permafrost in mountainous terrain might expose more fresh sulfide-rich bedrock to aerobic waters and will change the hydrogeological conditions. Therefore, the mobilization of toxic elements is expected to increase with ongoing climate change and to cause environmental problems on the regional scale (Todd et al. 2012; Wanner et al. 2023).

To assess the hazard of permafrost retreat in areas with pyrite-containing host rock for the regional water quality, in 2021 we have initiated a detailed monitoring of the Val Costainas catchment, in Val Mustair, Eastern Switzerland. The monitoring includes monthly sampling and discharge measurements at the rock glacier outlet to track element fluxes being mobilized from the permafrost area. In addition, we continuously track these fluxes about 5 km downstream, at the Prasüra gorge, using a combined pressure and conductivity probe. These data are used to apply the determined correlations between electric conductivity and element concentrations. In accordance with the same procedure, correlation between water table and discharge measurements is applied.

Our monitoring for 2021, 2022, and 2023 shows that the fluxes of toxic elements (Mn, Ni, Zn, F) at the two sampling locations are very similar, demonstrating that all elements are mobilized from the rock glacier. Considering that the mobilized elements are enriched in rock glacier ice (Nickus et al., 2023; Wanner et al, 2023), this further suggests that the recorded fluxes can potentially be used to estimate ice melt production in rock glacier systems. The recorded annual fluxes of Mn, Zn, Ni, and F elements were surprisingly high, between 1 and 10 t. Moreover, the fluxes show a strong seasonal variation. In each year, more than 50 % of the annual fluxes are measured during the warm summer months (June-August), confirming their close relationship to ice melt production in the rock glacier. Interestingly, the fluxes also show considerable variations between the different years. The lowest fluxes were recorded in 2022 despite the very high summer temperatures. In 2021 and 2023, the fluxes were about 45 % higher. In these two years, the annual discharge of the stream was much higher than in 2022, which was a very dry year in the Central Eastern Alps. Accordingly, there is a strong positive correlation between discharge and toxic element mobilization from the rock glacier. This is further confirmed by the observation that in each monitoring year the peaks in element fluxes correlate with high discharges caused by snowmelt in May and June and heavy rainfall events in July and August. It follows that, unlike atmospheric temperature variation, the subsurface water flux in rock glacier systems (controlled by snowmelt and rainfall) has a strong control on ice melt production. The same applies for the toxic elements mobilized from the host rock because they are temporally stored in the permafrost ice before they are eventually exported during ice melt production in summer.

Monitoring in the upcoming years will track the evolution of annual toxic element fluxes and assess whether they will increase in the future in response to climate change. This will also provide more insights into the coupled interaction between water percolation through the permafrost body, the host rock minerals and the rock glacier ice.

REFERENCES

Bigham, J.M., & Nordstorm, D.K. 2000: Iron and aluminum hydroxysulfates from acid sulfate waters, *Rev. Mineral. Geochem*, 40, 351-403.

Carrero, S., Pèrez-Lopez, R., Fernandez-Martinez, A., Cruz-Hernandez, P., Ayora, C., & Poulain, A. 2015: The potential role of aluminium hydroxysulfates in the removal of contaminants in acid mine drainage, *Chem. Geol*, 417, 414-423.

Nickus, U., Thies, H., Krainer, K., Lang, K., Mair, V., Tonidandel, D. 2023: A multi-millennial record of rock glacier ice chemistry (Lazaun, Italy), Frontiers in Earth Science.
Todd, A.S., Manning, A.H., Verplanck, P.L., Crouch, C., McKnight, D.M., & Dunham, R. 2012: Climate-change-driven deterioration of water quality in a mineralized watershed, *Environ. Sci. Technol.* 46, 9324-9332.
Wanner, C., Pöthig, R., Carrero, S., Fernandez-Martinez, A.,Jäger, C., & Furrer, G. 2018: Natural occurance of nanocrystalline Al-hydroxysulfates: Insights on formation, Al solubility control and As retention, *GCA*, 238, 252-269.
Wanner, C., Moradi, H., Ingold, P., Cardenas Bocanegra, M.A., Mercurio, R., Furrer, G. 2023: Rock glaciers in the Central Eastern Alps-How permafrost degradation can cause acid rock drainage, mobilization of toxic elements and formation of basaluminite, Global & Planetary Change 277, 104180.

P 15.12
Iluminating the subglacial environment with passive seismic methods: Glacier de la Plaine Morte as case study

Janneke van Ginkel[1,2], Fabian Walter[2] , Fabian Lindner[3]

[1] *Swiss Seismological Service SED, ETH Zürich, Sonneggstrasse 5, CH-8092 Zürich, (janneke.vanginkel@sed.ethz.ch)*
[2] *Swiss Federal Research Institute WSL, Mountain Hydrology and Mass Movements, Zürcherstrasse 111, CH-8903, Birmensdorf*
[3] *Geophysical Observatory, Ludwig-Maximilians-Universität (LMU) München, Ludwigshöhe 8, 82256 Fürstenfeldbruck, Germany*

Hydraulic fracturing, flowing water, crevasse formation and basal slip generate elastic waves, which can be used to study the subglacial environment with relatively cheap and easy-to-install seismic equipment (Podolski & Walter 2016). In earthquake seismology, a well-established methodology to investigate subsurface properties is the horizontal-to-vertical spectral ratio (H/V) of ambient seismic vibrations. This approach was recently adopted in cryoseismological contexts to invert for velocity profiles of ice or firn (Jones et al., 2023), establish ice thickness and detect the presence of basal sediments (Picotti et al., 2017). Until now, these investigations have relied on seismic vibration records spanning only a few hours. Yet in such short time records, biases in H/V spectra interpretation may arise because of the dynamic character of the glacier, resulting in significant transient and changing local seismic sources.

This study aims to characterize the spatial and temporal variation in H/V spectra to test the sensitivity of the method to subglacial processes and changing seismic wave fields. Since the glacier geometry and subglacial conditions of Glacier de la Plaine Morte (Switzerland) are well constrained (Lindner et al., 2020; Preiswerk et al., 2019), this glacier is used as a benchmark. On Plaine Morte, a seismic array was deployed for four months in summer of 2016 and during this time, an ice-marginal lake formed and suddenly drained through and under the glacier (day 240, figure 1A), making this seismic record ideal for our purposes. This drainage event, drainage-related hydraulic tremors and moulin resonances are well recorded (figure 1B) and documented with the draining water. Based on changing H/V amplitudes and resonance frequencies (figure 1C), one can determine changes in subglacial conditions of the glacier like basal water flow. However, when using H/V to invert for thickness, it is imperative to carefully pick the data time window and to examine the seismic source beforehand.

The lessons learned from Plaine Morte will be applied to larger-scale glacier dynamics using seismic measurements on Sermeq Kujalleq in Kangia (also known as Jakobshavn Isbræ), one of Greenland's largest outlet glaciers. This approach offers glaciologists a valuable instrument to explore the often-difficult-to-reach subglacial environment and is pivotal for enhancing our understanding of ice flow dynamics.

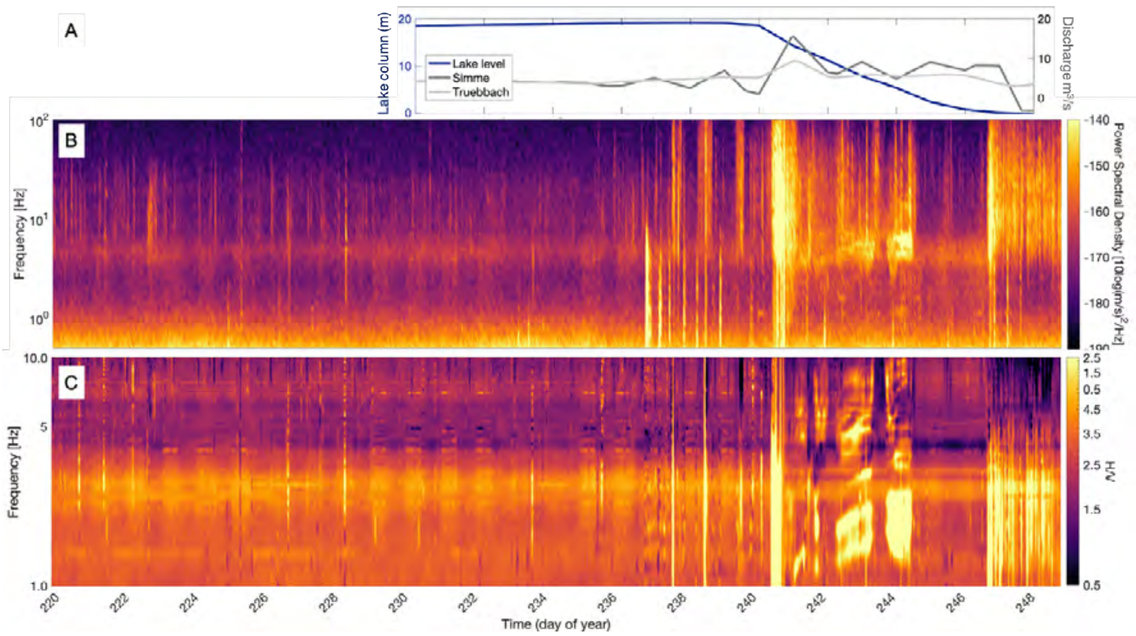

Figure 1. A) Lake level and river discharge curves. B) Power spectrum of seismic station PM02 on Glacier de la Plaine Morte, showing the amount of energy recorded on the vertical component over frequency and time. C) Hourly H/V curves plotted as a function of frequency over time showing H/V spectra variations in relation to hydraulic tremor and lake drainage.

REFERENCES

Jones, G. A., Ferreira, A. M. G., Kulessa, B., Schimmel, M., et al., 2023: Constraints on the cryohydrological warming of firn and ice in Greenland from Rayleigh wave ellipticity data. *Geophysical Research Letters*, *50*(15)

Lindner, F., Walter, F., Laske, G., & Gimbert, F. 2020: Glaciohydraulic seismic tremors on an Alpine glacier. The Cryosphere, 14(1), 287-308.

Picotti, S., Francese, R., Giorgi, M., Pettenati, F., & Carcione, J. M. 2017: Estimation of glacier thicknesses and basal properties using the horizontal-to-vertical component spectral ratio (HVSR) technique from passive seismic data. Journal of Glaciology, 63(238), 229-248.

Podolskiy, E. A., & Walter, F. 2016: Cryoseismology. Reviews of Geophysics, 54(4), 708-758.

Preiswerk, L. E., Michel, C., Walter, F., & Fäh, D. 2019: Effects of geometry on the seismic wavefield of Alpine glaciers. Annals of Glaciology, 60(79), 112-124.

P 15.13
Neoglaciation in the Alps: first results from Tödi ice cap

Michelle Worek[1,2], Sabine Brütsch[1], Inge Stockinger[1], Raphael Moser[3], Margit Schwikowski[1,2,4], Theo Jenk[1,2]

[1] *Laboratory of Environmental Chemistry, Paul Scherrer Institute, Forschungstrasse 111, 5232 Villigen PSI, (michelle.worek@psi.ch)*
[2] *Oeschger Centre for Climate Change Research, University of Bern, Hochschulstrasse 4, 3012 Bern*
[3] *Laboratory of Hydraulics, Hydrology and Glaciology, ETH Zürich, Hönggerbergring 26, 8093 Zürich*
[4] *Department of Chemistry, Biochemistry and Pharmaceutical Sciences, University of Bern, Freiestrasse 3, 3012 Bern*

About 3500 glaciers exist today in the European Alps. Modelling studies of glacier extent project around 50% of this present day volume to be lost by 2050. Up to 70-95% will be lost by 2100, depending on the assumed greenhouse gas emission scenario. Such a major loss of freshwater will have downstream consequences, also with regards to renewable energy production as glacial river runoff supplies hydropower plants. Projections into the future come from knowledge of past and present glacier behaviour, and while maximum Holocene glacier extents are well recorded by moraines, little information is available about minimum ice cover and ice-free conditions at high elevations. Few available data suggest a strong altitude gradient of Neoglaciation at high-elevation sites in the Alps. The question remains open of whether the current and projected low volume glaciation state is unprecedented through the Holocene.

Using a micro-radiocarbon dating technique with accelerator mass spectrometry, we aim to obtain the ages of the oldest ice from the base of three Alpine glaciers in the altitude range between around 3500 to 4200 m asl – Tödi, Mont Collon, and Alphubel. These study sites are characterized by low ice flow dynamics due to their summit ice cap-like geometry. The ages of the basal ice, in combination with other glacio-chemical tracers and glacial flow modelling, will help to infer the timing of past glacier coverage and glacier formation at higher elevations, providing additional constraint for validation of models used for the projected deglaciation in the European Alps. Projections with reduced uncertainty will help ensure sustainable development and adaption through the changing climate of the 21st century.

We will present preliminary results from the first ever ice core drilled on Tödi (Glarner Alps, 3570 m asl). There, in May 2023, two parallel cores to bedrock (~ 20 m depth) were successfully extracted. The ice was found to still be frozen to bedrock, thus persistent since its formation. Further, the cold ice temperatures raise hope of an undisturbed (by melt and melt-water percolation) paleo-archive. The ice thickness on this small ice cap decreased by roughly 30 m since the Little Ice Age. Considering the observed absence of firn, this decrease in the more recent past is most likely due to a negative mass balance at the drilling site. As a consequence, the age of ice at the current glacier surface is not modern (i.e. not equal to the year of drilling). Results from the analysis of black carbon, stable water isotopes, and major ions provide us first insight about signal preservation in the archive as well as an estimate of the average accumulation rates at the site. A first estimate of the surface age, based on radiometric dating with ^{210}Pb, ^{3}H, and potentially ^{39}Ar, is presented in addition.

P 15.14
An inventory of formerly ice-covered, now ice-free passes in the Swiss Alps from 1850 to present

Livio Conzett[1], Christian Kleiner[1], Mauro Fischer[1,2,*]

[1] *Institute of Geography, University of Bern, Hallerstrasse 12, CH-3012 Bern*
[2] *Oeschger Centre for Climate Change Research, University of Bern, Hochschulstrasse 4, CH-3012 Bern*
** presenting and corresponding author (mauro.fischer@unibe.ch)*

The Swiss glaciers have lost about 50% in area between 1850 (LIA maximum) and today (Linsbauer et al., 2021), and it is likely that by the end of the 21st century the majority of Swiss glaciers will have completely disappeared (Huss and Fischer, 2016; Zekollari et al., 2019).

Many glacial geomorphological phenomena associated with the observed rapid glacier shrinkage during past decades (e.g., growing rock outcrops, disintegration, collapse structures, tongue separation) are well known and documented (e.g., Paul et al., 2007; Fischer et al., 2021). To our knowledge, however, a detailed inventory and analysis of formerly (i.e. 1850) ice-covered, now ice-free passes is still missing for the Swiss Alps. Indeed, ice passes in the former accumulation area of glaciers, which topologically and topographically separate two neighbouring glaciers (at ice divides), or ice passes at glacial transfluences, seem to become increasingly ice-free. This happened, for instance, in the western Swiss Alps end of summer 2022, when Col de Tsanfleuron became ice-free for the first time in at least several millenia, physically separating the two glaciers Tsanfleuron (VS) and Sex Rouge (VD). Passes that are becoming ice-free are not only a further indication of climate change and associated rapid changes in high mountain landscapes, but are also of great interest, for example, for glacial archaeological research (e.g., Rogers et al., 2015; Hafner and Schwörer, 2018).

Through combination of time series of topographical maps (“a journey through time – maps”), historical to recent aerial images (“a journey through time – aerial images”) and Swiss glacier inventories (all data available through map.geo.admin.ch), we manually mapped formerly ice-covered but now ice-free passes in the entire Swiss Alps (including passes at the national border). In addition, the following parameters were compiled for each pass: i) pass name (if available), ii) coordinates (in CH1903+/LV95), iii) elevation (m a.s.l.), iv) IDs and aspect of adjacent glaciers (SGI-IDs for Swiss glaciers), and v) the year for which a pass can be described as ice-free for the first time. For completeness, we also mapped passes that are still ice-covered today.

The resulting dataset contains several hundred passes that became ice-free in the Swiss Alps between 1850 and today, of which the large majority concerns passes at former ice divides. Well over a hundred passes are still ice-covered today. For passes located at the borders with neighbouring countries, the complete ice melt may result in slight shifts of the national borders. Spatially, now ice-free passes are distributed relatively evenly across the entire Swiss Alps. The spread in elevation of now ice-free passes is large (>2’200 to >4’200 m a.s.l.), with a mean (and median) elevation around 3’000 m a.s.l. In accordance with the general evolution of Swiss glaciers since 1850, the majority of the passes got ice-free between 1950 and today. However, due to the varying spatiotemporal resolution, quality and uncertainty in the different source data used, uncertainty in the years during which passes got ice-free is considerable, especially further back in time.

REFERENCES

Fischer, A., Schwaizer, G., Seiser, B., Helfricht, K. and Stocker-Waldhuber, M. 2021: High-resolution inventory to capture glacier disintegration in the Austrian Silvretta. The Cryosphere, 15, 4637-4654, doi: 10.5194/tc-15-4637-2021.

Hafner, A. and Schwörer, C. 2018: Vertical mobility around the high-alpine Schnidejoch Pass. Indications of Neolithic and Bronze Age pastoralism in the Swiss Alps from paleoecological and archaeological sources. Quat. Int., 484, 3-18, doi: 10.1016/j.quaint.2016.12.049.

Huss, M. and Fischer, M. 2016: Sensitivity of very small glaciers in the Swiss Alps to future climate change. Front. Earth. Sci., 4:43, doi: 10.3389/feart.2016.00034.

Linsbauer, A., Huss, M., Hodel, E., Bauder, A., Fischer, M., Weidmann, Y., Bärtschi, H. and Schmassmann, E. 2021: The New Swiss Glacier Inventory SGI2016: from a topographical to a glaciological dataset. Front. Earth. Sci., 9:704189, doi: 10.3389/feart.2021.704189.

Paul, F., Kääb, A. and Haeberli, W. 2007: Recent glacier changes in the Alps observed by satellite: Consequences for future monitoring strategies. Glob. Plan. Change 56, 111-122, doi: 10.1016/j.gloplacha.2006.07.007.

Rogers, S. R., Lugon, R., Huss, M., and Fischer, M. 2015: Morphologie, Entwicklung und archäologisches Potenzial des Theodulgletschers:

gestern, heute und morgen, in: Providoli, S., Curdy, P. and Elsig, P. (eds.). 400 Jahre im Gletschereis – Der Theodulpass bei Zermatt und sein «Söldner», Hier und Jetzt Verlag, Baden.
Zekollari, H., Huss, M. and Farinotti, D. 2019: Modelling the future evolution of glaciers in the European Alps under the EURO-CORDEX RCM ensemble. The Cryosphere, 13, 1125-1146, doi: 10.5194/tc-13-1125-2019.

P 15.15
Hydrological significance and dynamics of active rock glaciers under climate change: a case study from the Val d'Ursé, Bernina Range, Switzerland

Cyprien Louis[1], Clément Roques[1], Landon Halloran[1], John Molson[2]

[1] *Centre for Hydrogeology and Geothermics, University of Neuchâtel, Rue Emile-Argand 11, CH-2000 Neuchâtel (cyprienlouis@bluewin.ch)*
[2] *Department of geology and geological engineering, Laval University, av. de la Médecine, CA-G1V Québec*

As a consequence of global warming, rock glaciers (RGs) and freeze/thaw cycles have an increasing influence on the hydrology and water chemistry of alpine environments. We continuously monitored the electrical conductivity and sampled springs and streams in the Val d'Ursé (Bernina Range, Switzerland), with the goal of understanding the importance of the Canfinal rock glacier within the hydrogeological context of this catchment. Using digital image correlation techniques (Bickel et al., 2018) with remote sensing imagery, we determined spatio-temporal variations in the active RG's creep velocity. Creep has been accelerating since 1990 as a result of rising temperatures and the most active regions are currently moving at a horizonal velocity of ~1 m year^{-1}.

The springs influenced by discharge from the RG have a distinct geochemical signature, reflecting the lithology of the debris it contains. Their discharge undergoes a diurnal dilution/enrichment cycle, the amplitude and phase of which are strongly influenced by the dynamics of the hydraulic head of the fractured aquifer. According to a FFT-based analysis of diurnal variations, this more mineralized water is the main component of springs at the foot ot the RG. Furthermore, the seasonal evolution of the phase lag and amplitude gap of the electrical conductivity in relation to the air temperature indicates that this dilution, which begins in the afternoon, can be largely attributed to a diurnal freeze/thaw cycle of the rock glacier ice. However, no isolated and significant contribution of the rock glacier at the catchment scale was found. We also propose a first step toward incorporating geochemical parameters into coupled cryo-hydrogeological models using the finite element HEATFLOW-SMOKER code (Molson and Frind, 2019). Our results aid in predicting current and future solute fluxes in mountain areas, as well as better understanding the role and future evolution of rock glacier freeze/thaw cycles in the context of climate change.

REFERENCES

Bickel, V. T., Manconi, A. & Amman, F. 2018: Quantitative assessment of digital image correlation methods to detect and monitor surface displacements of large slope instabilities, Remote Sensing, 10, 865.

Molson, J. & Frind, E. 2019: HEATFLOW-SMOKER user guide, Density-dependent flow and advective-dispersive transport of mass, thermal energy or residence time in 3D fractured porous media, Version 5.0.

16 Atmospheric Composition and Biosphere-Atmosphere Interactions +

17 Climatology

Martin Steinbacher, Christof Ammann, Mana Gharun, Ulrich Krieger
+
Stefan Brönnimann, Jörg Franke, Sven Kotlarski, Martine Rebetez

Commission on Atmospheric Chemistry and Physics (ACP)
Swiss Commission for Phenology and Seasonality (CPS)
Verband Geographie Schweiz (ASG)

TALKS:

16.1 Brugnara Y., Steinbacher M., Emmenegger L.: Towards an automated quality control tool for atmospheric composition time series

16.2 Brunamonti S., Emmenegger L., Tuzson B.: ALBATROSS: A balloon-borne spectrometer for water vapor measurements in the upper atmosphere

16.3 Filippini E., Hirte J., Volk M.: Will greener grass mitigate greenhouse gas increases?

16.4 Garner N.M., Top J., Mahrt F., El Haddad I., Ammann M., Bell D.M.: Impact of iron on the aging of biogenically-derived secondary organic aerosol

16.5 Krebs L., Gharun M., Scapucci L., Buchmann N.: 25 years of net ecosystem CO_2 exchange in a subalpine spruce forest

16.6 Manoharan Y., Artiglia L., Ammann M., Bartels-Rausch T.: The role of water's hydrogen bonding network in interfacial acid-base chemistry on ice and other environmental surfaces

16.7 Miller A., Ramelli F., Spirig R., Omanovic N., Fuchs C., Zhang H., Hervo M., Kanji Z.A., Ohneiser K., Rösch M., Seifert P., Lohmann U., Henneberger J.: Glaciogenic seeding of supercooled low stratus clouds by UAV to investigate microphysical ice processes: An introduction to the CLOUDLAB project

16.8 Scherrer S.C., de Valk C., Begert M., Gubler S., Kotlarski S., Croci-Maspoli M.: Estimating trends and the current climate mean in a changing climate

16.9 Schuppenhauer M.R., Chan S.W., Biraud S.C.: Beyond CO_2: Don't Measure – Don't Worry

16.10 Senoner A.E., Rajczak J., Kotlarski S.: A ranking-based CH2018 ensemble reduction for climate impact studies

16.11 Werner N., Zhang Q.: The Impact of the East African Uplift on Miocene Ecosystems – Insights from Earth System Modelling

POSTERS:

P 16.1 de Bonfioli Cavalcabo G., Stagakis S., et al.: Developing a high resolution 3D ecophysiology model for urban areas

P 16.2 Emberger S.: Observation and Modeling of Carbon and Water Fluxes across Urban Green Areas

P 16.3 Fernández-García V., Santín C., Strydom T., Natolojanahary M., Randrianiadanarivo H.M., Masango E., Mkansi N., González C., Otero X.L., Kull C.A.: Contrasting legacy of fire regimes on soil carbon stocks in open ecosystems in South Africa and Madagascar

P 16.4 Geissbühler D., Laemmel T., Gautschi P., Wacker L., Szidat S.: Radiocarbon Inventories of Switzerland (RICH) : Atmospheric $^{14}CO_2$ monitoring across space and time

P 16.5 Kohonen K.-M., Wang Y., Hörtnagl L., Buchmann N.: Reduced summertime peak CO_2 uptake following a reduced winter snowpack in an alpine grassland

P 16.6 Laemmel T., Geissbühler D., Henne S., Brunner D., Haghipour N., Leuenberger M., Szidat S.: Radiocarbon Inventories of Switzerland (RICH): Atmospheric $^{14}CH_4$ monitoring and modeling across space and time

P 16.7 Magyar P.M., Prokhorov I., Brunamonti S., Chénier N., Emmenegger L., Tuzson B., Mohn J.: Advances in clumped isotope measurements of nitrous oxide by laser spectroscopy

P 16.8 Mahrt F., Bilde M., Glasius M., Elm J., Christiansen O., Weidner T., Thomsen D.: Unravel the Secrets of Clouds

P 16.9 Scapucci L., Shekhar A., Aranda-Barranco S., Bolshakova A., Hörtnagl L., Gharun M., Buchmann N.: When soil is so dry that it cannot breath: effects of combined drought-heatwave on forest floor and soil respiration in a mixed deciduous forest in Switzerland

P 16.10 Waldner P., Kirchner T., Hilgers C., Verstraeten A., Schmitz A., Marchetto A., Thimonier A., Schmitt M., Raspe S., Nicolas M., Zolles A.: Longterm trends in atmospheric bulk and throughfall deposition of sulfur and nitrogen to forests in Central Europe

P 16.11 Bauer V., Scherrer S.C.: Observed heavy precipitation trends in Switzerland: an update and extension

P 16.12 Verard C.: On greenhouse and icehouse climate regimes over the Phanerozoic

16.1
Towards an automated quality control tool for atmospheric composition time series

Yuri Brugnara[1], Martin Steinbacher[1], Lukas Emmenegger[1]

[1] *Empa, Laboratory for Air Pollution and Environmental Technology, Ueberlandstrasse 129, CH-8600 Dübendorf (yuri.brugnara@empa.ch)*

The Global Atmosphere Watch (GAW) Programme of the World Meteorological Organization coordinates a worldwide network of ground-based in-situ monitoring stations (Fig. 1) that provide reliable scientific data on the chemical composition of the atmosphere. In the framework of the GAW Programme, the Quality Assurance/Scientific Activity Centre at Empa is developing a tool to support station operators in timely detecting issues in their measurements of atmospheric trace gases concentrations.

Once deployed, the quality control tool will allow station operators to upload the latest measurements to a server and receive an automatic report on data quality. It will initially focus on the mole fraction time series of the four trace gases most commonly measured in the GAW network: carbon monoxide (CO), carbon dioxide (CO_2), methane (CH_4), and surface ozone (O_3).

The tool makes use of different machine learning-based approaches aiming at identifying artefacts occasionally present in atmospheric time series at various time scales. This is achieved by exploiting historical time series as well as physics-based numerical forecasts provided by the Copernicus Atmosphere Monitoring Service. The latter involved the development of a downscaling algorithm based on random forest, which produces a debiased and more reliable forecast for each station. Anomalous deviations of the measurements from the forecast are then flagged as suspicious using unsupervised anomaly detection methods.

Given the current limited possibilities for near-realtime quality control, which can lead to erroneous data being delivered for long periods of time (see Fig. 2 for an example), this new tool will represent a valuable contribution towards reliable, comparable and traceable world-wide datasets in the field of air quality and greenhouse gases.

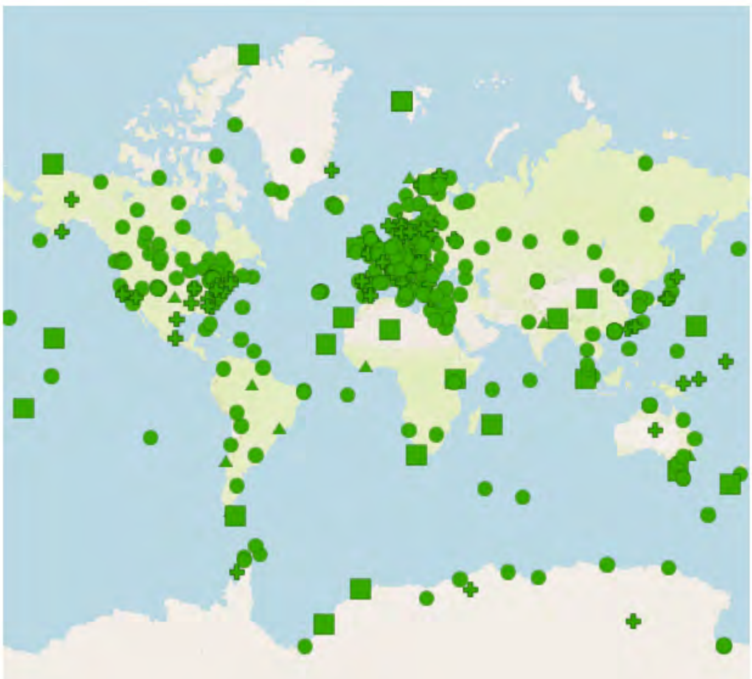

Figure 1. Map of GAW stations (source: GAW Station Information System, https://gawsis.meteoswiss.ch).

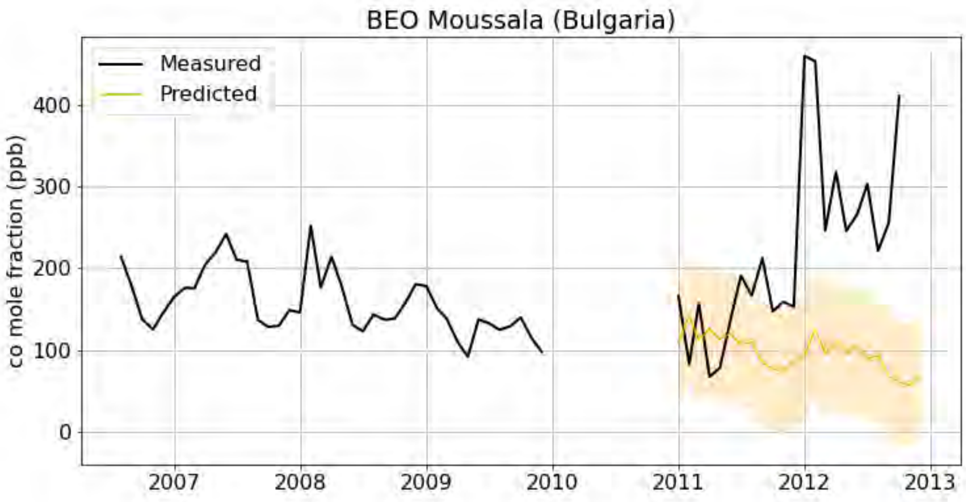

Figure 2. Example of time series (monthly averages of CO mole fractions) with prolonged erroneous measurements starting from summer 2011 as being available in the official GAW repository (World Data Centre for Greenhouse Gases). The prediction is made using a SARIMA model (the shading indicates the 95% confidence interval).

16.2
ALBATROSS: A balloon-borne spectrometer for water vapor measurements in the upper atmosphere

Simone Brunamonti[1], Lukas Emmenegger[1], Béla Tuzson[1]

[1] *Empa, Laboratory for Air Pollution/Environmental Technology, Ueberlandstrasse 129, CH-8600 Dübendorf (simone.brunamonti@empa.ch)*

Water vapor (H_2O) is the strongest greenhouse gas in the Earth's atmosphere, and its abundance in the upper troposphere-lower stratosphere (UTLS) is critical for the radiative balance. Yet, accurate measurements of H_2O in this region are notoriously difficult. Moreover, the reference method based on cryogenic frostpoint hygrometry is currently at a critical stage owing to its use of fluoroform (HFC-23) as cooling agent, which must be phased out due of its high global warming potential. Therefore, there is an urgent need for alternative, reliable technologies for the long-term monitoring of UTLS H_2O.

Here, we present ALBATROSS, a compact (< 3.5 kg) mid-IR laser absorption spectrometer for balloon-borne measurements of UTLS H_2O. The spectrometer relies on a specially designed segmented circular multipass cell to extend the optical path length to 6 m, while meeting stringent requirements in terms of mass, size, and temperature resilience (Graf et al., 2018; 2021).

The accuracy and precision of ALBATROSS at UTLS-relevant conditions were assessed using SI-traceable reference gases generated by a dynamic-gravimetric permeation method. The results show that the instrument achieves an accuracy better than ±1.5 % at all investigated pressures (30–250 mbar) and H_2O amount fractions (2.5–35 ppm) and a precision better than 0.3 % at 1 s resolution (Brunamonti et al., 2023). Such performance, unprecedented for a balloon-borne hygrometer, demonstrate the exceptional potential of mid-IR laser absorption spectroscopy for in-situ measurements of UTLS H_2O.

Further laboratory-based validation activities included the AquaVIT-4 International Intercomparison of Atmospheric Hygrometers, held at the AIDA cloud simulation chamber (Karlsruhe, Germany). Here, the performance of six atmospheric airborne hygromenters, including ALBATROSS, was evaluated under a wide range of challenging environmental conditions (pressure 15–500 mbar, temperature 185–245 K, H_2O amount fraction 1–1000 ppm).

Currently, ALBATROSS participates in the first measurement campaign of the "Swiss H_2O-Hub" project (2023-2026), a field intercomparison of state-of-the-art methods for in-situ (laser spectroscopy, frostpoint hygrometry) and remote sensing (Raman lidar, microwawe radiometry) measurements of UTLS H_2O, taking place at the MeteoSwiss Observatory Payerne. The results of this project will allow characterizing the performances of the spectrometer under real atmospheric conditions, as well as to investigate interannual variability and trends in UTLS H_2O over Switzerland.

REFERENCES

Graf, M., Emmenegger, L., and Tuzson, B., 2018: Compact, circular, and optically stable multipass cell for mobile laser absorption spectroscopy, Opt. Lett., 43, 2434–2437, https://doi.org/10.1364/OL.43.002434.

Graf, M., Scheidegger, P., Kupferschmid, A., Looser, H., Peter, T., Dirksen, R., Emmenegger, L., and Tuzson, B., 2021: Compact and lightweight mid-infrared laser spectrometer for balloon-borne water vapor measurements in the UTLS, Atmos. Meas. Tech., 14, 1365–1378, https://doi.org/10.5194/amt-14-1365-2021.

Brunamonti, S., Graf, M., Bühlmann, T., Pascale, C., Ilak, I., Emmenegger, L., and Tuzson, B., 2023: SI-traceable validation of a balloon-borne spectrometer for water vapor measurements in the upper atmosphere, Atmos. Meas. Tech. Discuss., https://doi.org/10.5194/amt-2023-83 (accepted 10 August 2023).

16.3
Will greener grass mitigate greenhouse gas increases?

Elisa Filippini[1,2], Matthias Volk[1], Juliane Hirte[3]

[1] Agroscope Zurich, Climate and Agriculture, Reckenholzstrasse 191, CH 8046 Zurich
[2] University of Zurich, Department of Geography, Soil Science & Biogeochemistry, Winterthurerstrasse 190, CH 8057 Zurich
[3] Agroscope Zurich, Water Protection and Substance Flows, Reckenholzstrasse 191, CH 8046 Zurich

We investigated the effect of grassland aboveground productivity (yield) on soil C stock in a field experiment, that was under the same management for 32 yrs. Using non-N mineral fertilizer applications, we generated six distinct productivity levels in a hay meadow at 1200 m asl. in the Alps.

Fertilization promotes plant growth and plant growth provides the organic matter (OM) that may become stabilized in the soil. We hypothesized that harvested yields are a valid proxy for the amount of plant derived organic C that enters the grassland ecosystem. Everything else being equal, this would result in larger soil organic C (SOC) stocks, increase the terrestrial sink for CO_2 and thus reduce the [CO_2] increase rate in the atmosphere.

Paralleling a 1.5°C warming (mean annual temperature), we found mean grassland yields to have consistently decreased by ca. 25% over the 32 yrs. period, while the yield was reduced further in years with pronounced summer heat, despite the high altitude of the site. During the same time, SOC stocks decreased by 15% on average.

Between fertilization categories grassland yields differed by factor 1.4- 2.0, depending on the reference period (30 yr. mean vs. single year). Surprisingly, SOC stocks did not differ between fertilization categories, no matter whether long-term means or single years were compared.

Analysis of ecosystem assimilation/respiration-ratios, from year-round CO_2 gas exchange measurements, suggests proportionally higher respiration rates in high yield fertilization treatments. Thus, in high yield grasslands the higher ecosystem OM input is apparently driving a higher decomposition rate, rather than increasing the SOC stock.

We conclude, that yield increases of agricultural grasslands do not serve as good proxies for a concomitant increase in SOC stock. Analogously, agricultural management practices, aiming at increased soil C sequestration rates, may focus rather on lower OM decomposition rates (C output) than on higher OM production rates (C input).

16.4
Impact of iron on the aging of biogenically-derived secondary organic aerosol

Natasha M. Garner[1], Jens Top[1], Fabian Mahrt[1], Imad El Haddad[1], Markus Ammann[1] and David M. Bell[1]

[1] *Laboratory of Atmospheric Chemistry, Paul Scherrer Institut, Forschungsstrasse 111, CH-5232 Villigen PSI (natasha.garner@psi.ch)*

Atmospheric aerosols play a key role for air pollution, health and climate. Secondary organic aerosol (SOA), which form through the oxidation of volatile organic compounds originating from sources such as emission by vegetation, often make up the majority of submicron particles by mass (depending on location and season; Jimenez et al. 2009). They can become internally mixed with other particles such as salts, termed secondary inorganic aerosol, mineral dust or particles emitted from combustion and industrial processes. When these particles contain transition metals, such as iron, they can initiate aging processes that can alter physical and chemical SOA properties (Al-Abadleh 2021). Furthermore, they can facilitate dissolution of minerals and form iron-organic complexes (Deguillaume et al. 2005), which are common in atmospheric particles (Tapparo et al. 2020). They can further generate reactive oxygen species within the condensed phase through dark peroxide and photochemical reactions (Fenton chemistry), leading to further aging of SOA by functionalization or fragmentation of organic species (Deguillaume et al. 2005; Daumit et al. 2016). Given the chemical complexity of SOA, a detailed understanding of these aerosol-aging processes and the subsequent impact they have on air quality, health and climate is lacking.

Here, we present data on the chemical composition of iron-containing SOA and how it evolves over time. Particles were produced by forming SOA via α-pinene (molecular formula, $C_{10}H_{16}$) ozonolysis on both ammonium sulfate or iron-containing seed particles in an atmospheric simulation chamber under dark conditions at low and high relative humidities (RH). This allowed us to probe the impact of dark e.g., peroxide, reactions on aerosol aging with varying aerosol mixing states. Aerosol bulk composition was determined using extractive electrospray ionization mass spectrometry, allowing for high chemical and temporal identification of oxidation products, i.e., monomers and dimers. Monomers (e.g., C8 to C10 species) are degradation products formed from the oxidation of α-pinene, whereas dimers (e.g., C18 to C20 species) are formed via the subsequent reaction of monomers.

At low RH, all particles were found to contain a higher fraction of monomers, compared to dimers. In contrast, at high RH the monomer/dimer ratio was smaller when iron was present. Furthermore, when iron was present in the seed particles the lifetimes of monomers and dimers varied greatly, where the signal for some organic species (e.g., C19s and C20s) was observed to decrease rapidly ($\tau_{1/2} \sim 25$ min.) following SOA formation under high RH conditions, while only slow decay was observed under low RH conditions ($\tau_{1/2} \sim 110$ min.). This suggests that iron-catalyzed reactions affect the composition of SOA, particularly at higher RH, as is common in many regions of the troposphere.

Overall, our results elucidate the key role of iron in altering the chemical composition of SOA particles during atmospheric transport. Such aging effects are also expected for other transition metals and need to be considered when predicting the role of SOA for air pollution and climate in chemistry-climate models.

REFERENCES

Jimenez, J.L. et al. 2009: Evolution of organic aerosols in the atmosphere, Science, 326, 5959, 1525-1529.

Al-Abadleh, H.A. 2021: Aging of atmospheric aerosols and the role of iron in catalyzing brown carbon formation, Environ. Sci.: Atmos., 1, 6, 297-345.

Deguillaume, L. et al. 2005: Transition Metals in Atmospheric Liquid Phases: Sources, Reactivity, and Sensitive Parameters, Chem. Rev. 105, 9, 3388–3431.

Tapparo, A. et al. 2020: Formation of metal-organic ligand complexes affects solubility of metals in airborne particles at an urban site in the Po valley, Chemosphere, 241, 125025.

Daumit, K.E. et al. 2016: Effects of Condensed-Phase Oxidants on Secondary Organic Aerosol Formation, J. Phys. Chem. A, 120, 1386−1394.

16.5
25 years of net ecosystem CO_2 exchange in a subalpine spruce forest

Luana Krebs[1], Liliana Scapucci[1], Mana Gharun[2], Nina Buchmann[1]

[1] *Institute of Agricultural Sciences, Department of Environmental Systems Science, ETH Zurich, Universitätstrasse 2, CH-8092 Zürich (luana.krebs@usys.ethz.ch)*
[2] *Institute of Landscape Ecology, Department of Geosciences, University of Münster, Heisenbergstrasse 2, D-48149 Münster*

Terrestrial ecosystems, and more specifically forests, act as an important carbon (C) sink by sequestering about 30% of global anthropogenic CO_2 emissions. However, we observe large inter-annual variabilities in C uptake rates which could be due to a diverse range of biotic and abioitic drivers. Therefore, it is crucial to advance our understanding of forest CO_2 fluxes in response to changes in climate. Long-term time series of measured net ecosystem CO_2 exchange (NEE) and its component fluxes, i.e., ecosystem respiration (R_{eco}) and gross primary production (GPP), are available from eddy covariance (EC) sites. They can be used to assess long-term trends of fluxes and C sequestration rates in response to changing climatic conditions. Such assessments allow an evaluation of the vulnerability of forests to future environmental changes, and thus form the basis for an improved understanding of the land-atmosphere ecosystem exchange.

In this study, we used 25 years of EC fluxes as well as environmental data of a subalpine coniferous forest in Davos, Switzerland (CH-Dav; an ICOS RI Class 1 station). CH-DAV belongs to the oldest ecosystem EC flux sites globally and has been delivering EC data since 1997. Measured high-quality CO_2 flux data were used to investigate functional relations between the fluxes and environmental variables while gap-filled CO_2 fluxes were used to calculate annual budgets. We employed time series and regression analyses to detect trends and anomalies in the CO_2 flux data. Furthermore, we investigated the climatic conditions to understand the driving factors behind these patterns. Our objectives were to 1) identify long-term trends and variabilities in the seasonal and annual NEE budgets and climatic conditions, 2) assess the carbon phenology of the forest e.g., the net carbon uptake period in response to environmental variables, and 3) compare the summer flux rates among the 25 years.

16.6
The role of water's hydrogen bonding network in interfacial acid-base chemistry on ice and other environmental surfaces

Yanisha Manoharan[1], Luca Artiglia[1], Markus Ammann[1], Thorsten Bartels-Rausch,[1]

[1] *Laboratory of Atmospheric Chemistry, Paul Scherrer Institut, Forschungstrasse 111, CH-5032 Villigen PSI (thorsten.bartels-rausch@psi.ch)*

Cloud formation, atmospheric chemistry, and human health are influenced by multiphase chemistry at the air-substrate interface of atmospheric particles and ground surfaces (Pöschl and Shiraiwa 2015). All of these impacts are affected by acidity (Angle et al. 2021). A conceptional understanding of interfacial acid-base character has not yet been reached (Saykally 2013). Using X-ray photoemission spectroscopy at near ambient pressure, we have suggested that the dissociation of acids adsorbed to ice is governed by the availability and mobility of water molecules to stabilize the dissociated ions and that the degree of dissociation at the air-ice interface differs from that predicted based on dissociation behavior in aqueous bulk solutions (Bartels-Rausch et al. 2017, Kong et al. 2017). Ice and snow host chemistry of relevance for the atmosphere and are of importance in cold regions of the Earth (Thomas et al. 2019).

Here, we present additional results of fundamental studies on the structure of the hydrogen bonding network of interfacial water and the dissociation of acidic trace gases upon adsorption. We show a wider temperature range of the acid-base interfacial chemistry at -50°C and -20°C addressing the impact of the increased liquid-like character of ice at the air-ice interface at temperatures approaching the melting point. This increased flexibility of water molecules at the air-ice interface has also been called the pre-melting or quasi-liquid layer. By comparing the interfacial dissociation of HCl, HNO3, and acetic acid gives insights into the role of the acidic strength on the interfacial dissociation. Taken together, the data indicate a dominating role of the water availability on dissociation rather than the acidic strength or its temperature trend.

We discuss how the limited availability of water may also be applied to other interfaces to explain the dissociation of acidic adsorbates there.

REFERENCES

Angle, K. J., D. R. Crocker, R. M. C. Simpson, K. J. Mayer, L. A. Garofalo, A. N. Moore, S. L. Mora Garcia, V. W. Or, S. Srinivasan, M. Farhan, J. S. Sauer, C. Lee, M. A. Pothier, D. K. Farmer, T. R. Martz, T. H. Bertram, C. D. Cappa, K. A. Prather and V. H. Grassian (2021). «Acidity across the interface from the ocean surface to sea spray aerosol.» Proc Natl Acad Sci U S A 118(2).

Bartels-Rausch, T., F. Orlando, X. Kong, L. Artiglia and M. Ammann (2017). «Experimental evidence for the formation of solvation shells by soluble species at a nonuniform air-ice interface.» ACS Earth and Space Chemistry 1(9): 572-579.

Kong, X., A. Waldner, F. Orlando, L. Artiglia, T. Huthwelker, M. Ammann and T. Bartels-Rausch (2017). «Coexistence of physisorbed and solvated HCl at warm ice surfaces.» Journal of Physical Chemistry Letters 8(19): 4757-4762.

Pöschl, U. and M. Shiraiwa (2015). «Multiphase chemistry at the atmosphere–biosphere interface influencing climate and public health in the anthropocene.» Chemical Reviews 115(10): 4440-4475.

Saykally, R. J. (2013). «Air/water interface: Two sides of the acid-base story.» Nature Chemistry 5(2): 82-84.

Thomas, J. L., J. Stutz, M. M. Frey, T. Bartels-Rausch, K. Altieri, F. Baladima, J. Browse, M. Dall›Osto, L. Marelle, J. Mouginot, G. M. Jennifer, D. Nomura, K. A. Pratt, M. D. Willis, P. Zieger, J. Abbatt, T. A. Douglas, M. C. Facchini, J. France, A. E. Jones, K. Kim, P. A. Matrai, V. F. McNeill, A. Saiz-Lopez, P. Shepson, N. Steiner, K. S. Law, S. R. Arnold, B. Delille, J. Schmale, J. E. Sonke, A. Dommergue, D. Voisin, M. L. Melamed and J. Gier (2019). «Fostering multidisciplinary research on interactions between chemistry, biology, and physics within the coupled cryosphere-atmosphere system.» Elementa 7.

16.7
Glaciogenic seeding of supercooled low stratus clouds by UAV to investigate microphysical ice processes: An introduction to the CLOUDLAB project

Anna Miller[1], Fabiola Ramelli[1], Robert Spirig[1], Nadja Omanovic[1], Christopher Fuchs[1], Huiying Zhang[1], Maxime Hervo[3], Zamin A. Kanji[1], Kevin Ohneiser[2], Michael Rösch[1], Patric Seifert[2], Ulrike Lohmann[1] and Jan Henneberger[1]

[1] *Institute for Atmospheric and Climate Science, ETH Zurich, Zurich, Switzerland (anna.miller@env.ethz.ch)*
[2] *Leibniz Institute for Tropospheric Research (TROPOS), Leipzig, Germany*
[3] *Federal Office of Meteorology and Climatology MeteoSwiss, Payerne, Switzerland*

Ice formation and growth processes have an essential role in cloud evolution and precipitation initiation. However, these processes are still not well understood, resulting in weather forecasts and climate projections. The ice phase is often explored only by field measurements of natural clouds or controlled experiments in the laboratory. In the CLOUDLAB project, we combine the two: we induce controlled aerosol perturbations in real clouds and thereby use them as a natural laboratory to investigate nucleation and ice crystal growth. Specifically, we utilize persistent supercooled low stratus clouds in the Swiss Plateau to conduct targeted glaciogenic seeding experiments with a suite of in situ and remote sensing instrumentation to observe the induced microphysical changes (Henneberger and Ramelli, et al., 2023).

The supercooled low stratus clouds are injected directly with approximately 20 g of ice-active seeding particles containing silver iodide, emitted from flares mounted on a multirotor Uncrewed Aerial Vehicle (UAV; Miller et al., 2023). 3 to 15 minutes downwind of the seeding location (Fig. 1), a tethered balloon system equipped with a holographic imager (Ramelli et al., 2020) measured the local changes in the cloud droplet and ice crystal properties while vertical and scanning cloud radars captured the vertically and horizontally resolved microphysical changes to the cloud structure. We are able to perform repeated and frequent seeding experiments with similar and well-constrained environmental conditions because of the persistent nature of stratus clouds and our novel application of seeding with a multirotor UAV.

Here we present successful seeding experiments from our field campaigns from the winters of 2022 and 2023. Our observations reveal an increase in radar reflectivity (> 20 dBZ) caused by a concurrent increase in ice crystal number concentrations by hundreds per liter with a simultaneous decrease in liquid water content. Furthermore, we demonstrate how the ice crystal sizes and radar reflectivities increased with increased time between seeding and measurement. Finally, we also show that our field observations can be qualitatively confirmed and contextualized with large eddy simulations (ICON-LES).

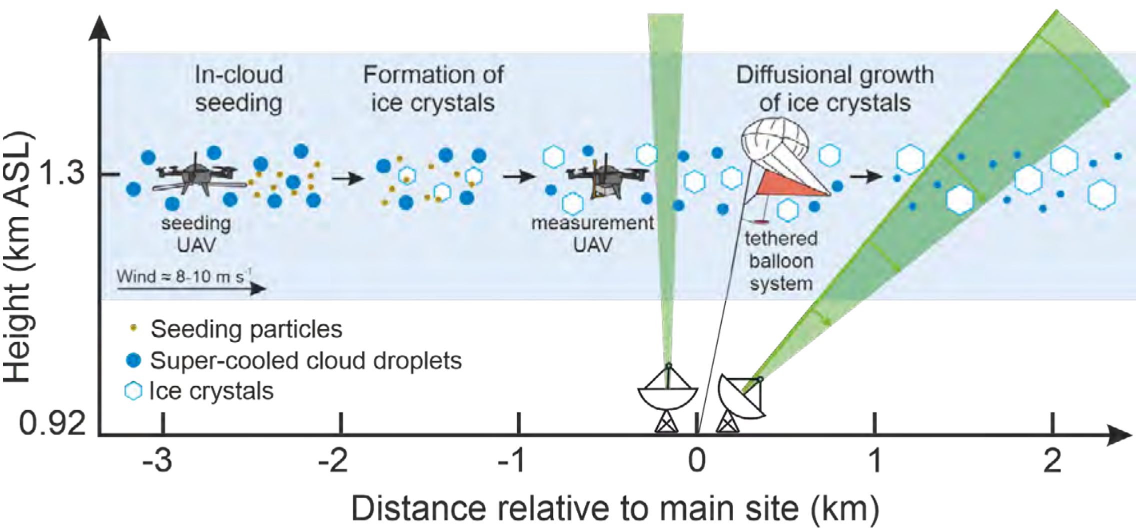

Figure 1. Schematic of a glaciogenic seeding experiment using a UAV for seeding, in situ measurements with a second UAV and a tethered balloon system, and remote sensing measurements with vertical and scanning cloud radars. From Henneberger and Ramelli, et al., 2023.

REFERENCES

Henneberger, J., Ramelli, F., Spirig, R., Omanovic, N., Miller, A. J., Fuchs, C., Zhang, H., Bühl, J., Hervo, M., Kanji, Z. A., Ohneiser, K., Radenz, M., Rösch, M., Seifert, P., Lohmann, U. 2023: Seeding of supercooled low stratus clouds with a UAV to study microphysical ice processes – An introduction to the CLOUDLAB project. Bulletin of the American Meteorology Society, *in press.*

Miller, A. J., Ramelli, F., Fuchs, C., Omanovic, N., Spirig, R., Zhang, R., Lohmann, U., Kanji, Z. A., Henneberger, J. 2023: Two new multirotor UAVs for glaciogenic cloud seeding and aerosol measurements within the CLOUDLAB project. Atmospheric Measurement Techniques Discussion, https://doi.org/10.5194/amt-2023-157, *in review.*

Ramelli, F., Beck, A., Henneberger, J., Lohmann, U. 2020: Using a holographic imager on a tethered balloon system for microphysical observations of boundary layer clouds. Atmospheric Measurement Techniques, 13, 2, 925-939, https://doi.org/10.5194/amt-13-925-2020.

16.8
Estimating trends and the current climate mean in a changing climate

Simon C. Scherrer[1], Cees de Valk[2], Michael Begert[1], Stefanie Gubler[3], Sven Kotlarski[1], Mischa Croci-Maspoli[1]

[1] *Federal Office of Meteorology and Climatology MeteoSwiss, Zürich-Flughafen, Switzerland (simon.scherrer@meteoswiss.ch)*
[2] *Royal Netherlands Meteorological Institute KNMI, De Bilt, The Netherlands*
[3] *Swiss Academy of Sciences SCNAT, Bern, Switzerland*

Monitoring the current state of the climate and the effectiveness of climate protection measures are a central task of MeteoSwiss and of great importance to society. Due to the intensifying climate change, classic standard values and linear trend estimators for temperature and other strongly changing variables are becoming less and less suitable for this purpose. Although several alternatives are available and in use, there are hardly any quantitative assessments of them. We review existing approaches that use past climate data to estimate the current mean climate. We apply these to the Swiss mean temperature over the period 1864-2099, which is composed of observations and climate scenarios. It turns out that several approaches work well for the entire period. In order to ensure broad applicability, additional criteria such as the flexibility of the method, broad applicability to a large number of climate variables and simplicity in terms of calculation and communication were taken into account. In the overall assessment, a climate trend line based on local linear regression for describing the climate evolution and determining the current climate mean proved to be particularly promising (cf. Fig. 1). The results lead to adjustments in the climate monitoring of MeteoSwiss.

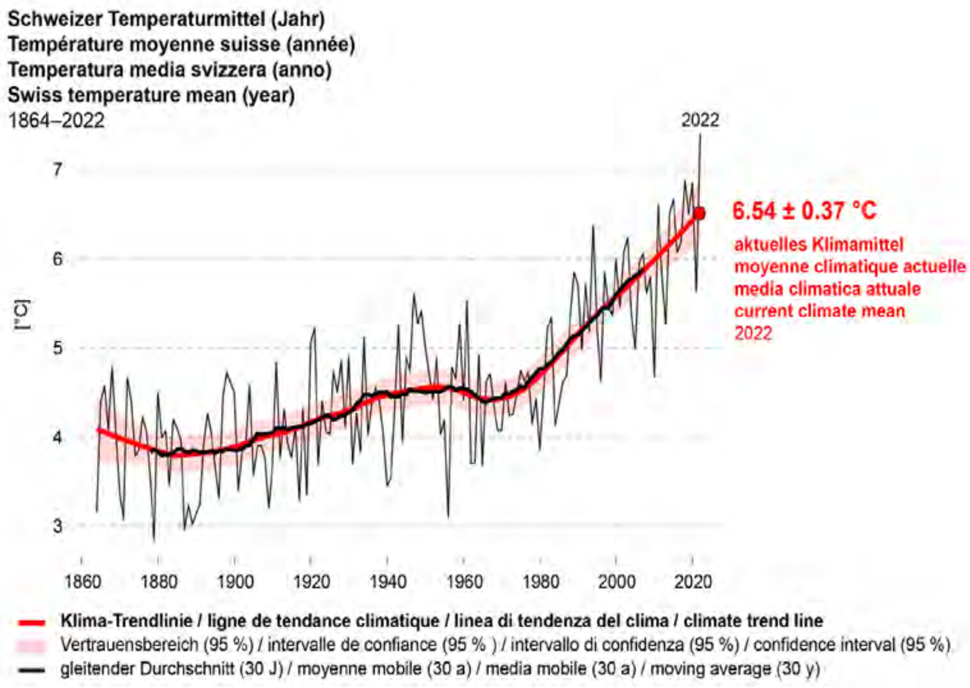

Figure 1. Evolution of the annual Swiss mean temperature since 1864 (thin black line), the moving 30-year mean (bold black line) and the new climate trend line (red) including 95 percent confidence interval (light red).

16.9
Beyond CO_2: Don't Measure – Don't Worry

Michael R. Schuppenhauer[1,2], Stephen W. Chan[3], Sebastien Biraud[3]

[1] Lawrence Berkeley National Lab, Biological Systems & Engineering One Cyclotron Road MS 978, Berkeley, CA 94720, (mschuppenhauer@lbl.gov)
[2] ARVA Intelligence Corp., 10 AR-152, Humphrey, AR 720733
[3] Lawrence Berkeley National Lab, Earth & Environmental Sciences, One Cyclotron Road MS 084, Berkeley, CA 94720

Globally half of habitable land is used for agriculture, for the U.S. 17% of land is used for crops, with an additional 44% for forests, grasslands and pastures, and 5% for wetlands. These manageable lands, the agroecosystems, as well as wetlands have an outsized potential for impact on the non-CO_2 greenhouse gas inventory, which acounts for more than 25% of greenhouse gases, namely through methane (CH_4) and nitrous oxide (N_2O). While plant growth typically serves as a carbon sink, agroecosystem emissions of nitrous oxide and methane counteract the sink in an outsized fashion, with 78% of all N_2O emissions and 38% of all CH_4 emissions in the US stemming from agriculture, which though otherwise is only responsible for 9% of all US GHG emissions.

Given the emissions as well as the daily and annual opportunity to impact change and drive carbon sequestration, accurate tools for and in flux research in agroecosystems at scale are critically needed. Indeed the sustainable production of biogenic carbon for food, fiber and fuel hinges significantly on the field-to-gate carbon intensity (CI) of the resulting commodity, and specifically there the emissions profile from the key agricultural GHGs methane and nitrous oxide. Yet, there is only limited continuous, year-round flux data available in agroecosystems at scale, and if generated those typically surprise conventional assumptions by orders of magnitude.

As part of the U.S. DOE SMARTFARM program, we established since 2021 six measurement sites on commercial fields that grow corn, rice and forage to assess the full sustainability of crop and residue production. Sites feature year-round real-time eddy covariance monitoring for carbon dioxide, methane, and nitrous oxide, are integrated with soil heat flux, temperature, and moisture measurements, and are monitored for agronomical input and outputs, and complemented with high-intensity grid soil, plant and forage composition analysis at multiple time points per year.

Initial data confirms significant spatio-temporal heterogeneity in all sites originally assumed to be homogenous. Further, diurnal patterns of the trace GHGs at all sites challenge conventional chamber measurements techniques that historically supplied inputs for model parameterization, and thus challenge emission factor estimations such as those used by the IPCC. Finally, other suprising results include nitrous oxide sinks in wetlands, methane peaks in winter wetlands, and inventory blowing nitrous oxide emissions in typical dairy farming. We therefore advocate for a significant expansion of spatial-temporal resolved measurement systems in agroecosystems to ground-truth climate smart agronomy approaches on reliable and replicated real-world data – moving beyond models with actual ground-based measurements.

16.10
A ranking-based CH2018 ensemble reduction for climate impact studies

Anna E. Senoner[1,2], Jan Rajczak[1], Sven Kotlarski[1]

[1] *MeteoSwiss, Zürich, CH-8058 Zürich-Flughafen (anna.senoner@meteoswiss.ch)*
[2] *Center for Climate Systems Modeling, ETH Zürich, Universitätstrasse 16, 8092 Zürich*

The CH2018 climate scenarios for Switzerland provide users with 68 transient and bias-corrected simulations of climate model chains (products DAILY-LOCAL and DAILY-GRIDDED). These scenarios take into account three emission scenarios (representative concentration pathways, RCPs), for which 12 (RCP2.6), 25 (RCP4.5) and 31 (RCP8.5) simulations are available at a daily resolution for the period 1981 to 2099, respectively. These projections build a CH2018 esemble which serves as a basis for all subsequent climate impact studies. Currently, major products of the CH2018 scenarios are communicated as climate change signals in terms of the median and the upper and lower estimate. Because these statistics are calculated as change signals and for each scenario time slice seperately, it is not possible to assign them consistently to a specific climate model chain. While some reduction of the ensemble is desired by the CH2018 users due to computational limitations, a structural way of sub-selecting model chains is missing at this point.

In this work, we present a new ensemble reduction method which navigates CH2018 users with a structured way of selecting climate model chains according to users' needs. This selection is case and emission scenario (RCP) specific. For each RCP, three representative climate model chains are selected that cover the spread of the climate change signal. This includes one chain correspodning to the upper, middle and lower bound of the ensemble spread, respectively. The selection of climate model chains is based on the climate change signals seen of multiple climate indicators (e.g., mean temperature, number of hot days) that are calculated for each climate model chain as a difference between the end-of-century (2070-2099) and the CH2018 reference period (1981-2010). The method builds further on the core statements of the CH2018 climate scenarios. For each application case, the most important climate indicators are specified and are ranked for all climate models according to their climate change signal. Next the indicators are split into three terciles which should represent the upper, lower and middle bound of the ensemble. For each bound one climate model chain is selected that best meets the selection criteria. Figure 1 presents results of the method application for one case (heat waves) and RCP 2.6. Three model chains marked in the figure that are selected as terciles 1, 2, 3 would be recommended for CH2018 users to be applied in praxis focusing on heat waves if a reduced ensemble is desired.

Currently the method is developed for the entire Switzerland and CH2018 users will be able to select from three emission scenarios (RCP2.6, RCP4.5 and RCP8.5) and eight application-cases (temperature, precipitation, temperature & precipitation, droughts, heat waves, heavy rainfalls, snow-scarce winters, and an expert case), to receive a set of three representative climate model chains. A further extension to Swiss sub-regions is planned to better represent regional climate patterns. The developed method is very flexible and can be easily adapted for an extended climate model ensemble or for new cases of applications.

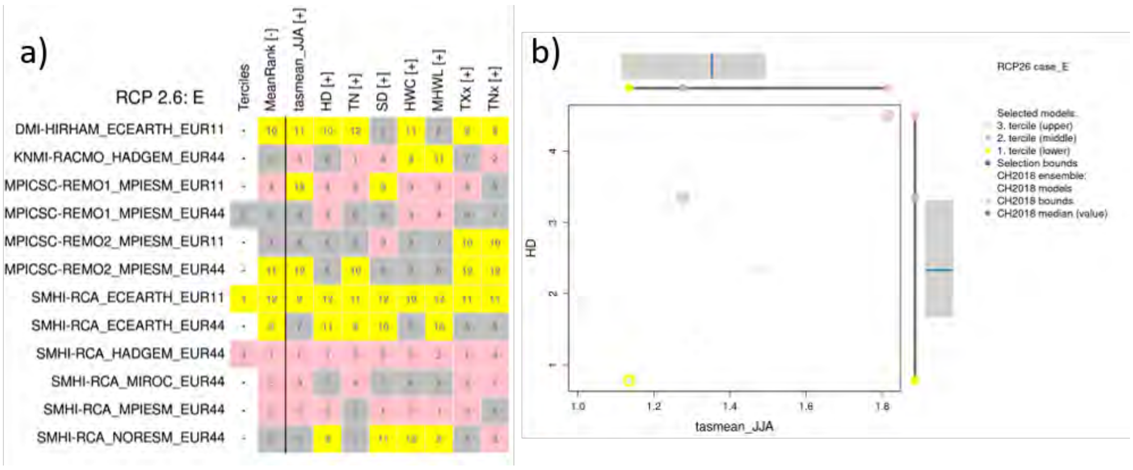

Figure 1. Example of the method application to the case E (heat waves) and the emission scenario RCP2.6. a) Ranking of the climate model chains for climate indicators according to their climate change signal. Climate indicators important for this case are: mean summer temperature (tasmean_JJA), hot days (HD), tropical nights (TN), summer days (SD), heat wave counter (HWC), mean maximum heat wave length (MHWL), hottest day of the year (TXx), and hottest night of the year (TNx). The sign in the squared brackets indicates the desired direction of the climate change signal to be ranked as the most extreme. MeanRank indicates the mean model rank over all important climate indicators. Terciles stand for the representative model chains selected for the 1st, 2nd and 3rd tercile. The climate model chain names follow the nomenclature from CH2018. b) The spread of the climate change signal represented by the sub-selection (three terciles) versus the spread of the full CH2018 ensemble presented here for HD vs. tasmean_JJA.

REFERENCES

CH2018 technical report: CH2018 (2018), CH2018 – Climate Scenarios for Switzerland, Technical Report, National Centre for Climate Services, Zurich, 271 pp. ISBN: 978-3-9525031-4-0, https://www.nccs.admin.ch/nccs/en/home/climate-change-and-impacts/swiss-climate-change-scenarios/technical-report.html

CH2018 dataset: CH2018 Project Team (2018): CH2018 - Climate Scenarios for Switzerland. National Centre for Climate Services. doi: 10.18751/Climate/Scenarios/CH2018/1.0.

Fischer A.M., K.M. Strassmann, M. Croci-Maspoli, A.M. Hama, R. Knutti, S. Kotlarski, C. Schär, et al. (2022) Climate Scenarios for Switzerland CH2018 – Approach and Implications, Climate Services, 26, 100288, https://doi.org/10.1016/j.cliser.2022.100288.

16.11
The Impact of the East African Uplift on Miocene Ecosystems – Insights from Earth System Modelling

Niklas Werner[12], Qiong Zhang[23]

[1] *Institute for Geophysics, Swiss Federal Institute of Technology (ETH Zürich), Sonnegstraße 5, 8092 Zürich (nwerner@student.ethz.ch)*
[2] *Department of Physical Geograp hy, Stockholm University, SE-106 91 Stockholm*
[3] *Bolin Centre for Climate Research, Stockholm University, SE-106 91 Stockholm*

The onset of early hominid evolution in the Late Miocene is intricately tied to the transition from forest ecosystems to vast grasslands in Central and East Africa. This shift has been linked to changes in the African hydroclimate due to the East African uplift. Using the Earth System Model EC-Earth3, we examine Miocene ecosystem changes at key time points (25, 15, and 5 Ma) by using high-resolution paleo-topography data from geophysical modelling (Moucha and Forte 2011). Our findings highlight the substantial influence of lower topography, particularly at 15 and 25 Ma, in altering the spatial rainfall distribution, resulting in a significantly drier Central Africa. Further, we reaffirm the significant impact of lowered East African topography on atmospheric conditions, including the weakening of the Hadley Cell, that has been proposed in prior research. These conditions may have supported savanna-like ecosystems at the Horn of Africa until at least 15 Ma. Our simulations consistently depict a humid East Africa until the Late Miocene, even with Miocene CO_2 levels, emphasizing the pivotal role of the East African uplift in regional aridification. While topography seems to govern the distribution of precipitation across Africa, our results stress the complementary role of elevated CO_2 levels for grassland expansion. In summary, this study shows the intricate interplay between topography, CO_2 levels, and ecosystem dynamics, offering insights into the factors shaping the African landscape during this pivotal time period.

REFERENCES

Moucha, R., Forte, A. 2011: Changes in African topography driven by mantle convection. Nature Geosci 4, 707–712. https://doi.org/10.1038/ngeo1235

P 16.1
Developing a high resolution 3D ecophysiology model for urban areas

Guido de Bonfioli Cavalcabo› *, Stavros Stagakis*, Christian Feigenwinter*, Dominik Brunner[1], Alexander Damm[2], Nina Buchmann[3], Roland Vogt*, Markus Kalberer*.

** Department of Environmental Sciences, University of Basel*
[1] Empa - Swiss Federal Laboratories for Materials Science and Technology
[2] Department of Geography, University of Zurich
[3] Department of Environmental Systems Science D-USYS, ETH Zurich

Adresses of authors:
guido.cavalcabo@unibas.ch, stavros.stagakis@unibas.ch, christian.feigenwinter@unibas.ch, dominik.brunner@empa.ch, alexander.damm@geo.uzh.ch, nina.buchmann@usys.ethz.ch, markus.kalberer@unibas.ch, aroland.vogt@unibas.ch .

Urbanization is one of the many markers of humanity›s impact on the Earth›s systems. An observable consequence of this urban growth is the notable rise in variables, such as temperature (Urban Heat Island or UHI) and CO2 emissions, experienced within urban centers compared to their suburban and rural surroundings. UHI, in particular, has gained significant attention due to its far-reaching implications on urban climate, energy consumption, air and water purity and human health. These elevated temperatures result from a complex interplay of factors such as urban morphology, land cover changes, anthropogenic heat emissions and altered energy balance.

Urban climate mitigation and adaptation strategies necessitate a thorough understanding of the micro-climate present in cities. But the sparse distribution of in situ weather stations, combined with their restriction to localized conditions and the uncertainty related to future climatic predictions renders relying solely on this data a challenge. In this context, urban climate modeling is a highly useful tool as it allows researchers and urban planners to explore various scenarios and interventions in a controlled environment providing insights into underlying mechanisms, future trends and possible effectiveness of adaptation and mitigation strategies.

In pursuit of this understanding, we are developing a 3D ecophysiological model that aims to simulate CO2, water and energy exchanges between plants and the urban atmosphere at the micro scale. The ecophysiology model will integrate a 3D multi-layer radiation module, a leaf-level process simulation module and a multi-layer soil water-energy balance module to generate canopy-level fluxes of energy, water and CO2. As a first step, we are presenting the 3D algorithm that assesses radiation interception across the urban canopy. This algorithm hinges on various inputs, including meteorological data such as incoming radiation, Digital Surface Models (DSMs) such as building, tree and terrain morphology, land cover information and Leaf Area Index (LAI). The geospatial information is used to develop a 3D representation of the study areas, using voxels of 5x5x5m volume which are characterized as buildings, trees, terrain or empty space. Using the meteorological inputs, we run a simple simulation for radiation exchange between atmosphere and street level in the 3D urban canyons we generated. The method is based on the creation of look-up tables (LUTs) tailored to the site-specific individual vegetation, building and terrain voxels.

The radiation interception model is tested within specific urban canyons featuring street-level radiation measurements in Basel and Zurich. As a first result, we show how the monthly and daily patterns of the modeled shortwave radiation agrees with the reference measurements during summer (full tree canopies) and winter (without tree canopies).

P 16.2
Observations and modeling of carbon dioxide and water fluxes across urban green areas

Sophie Emberger

Institute for Atmosphere and Climate Sciences, ETH Zurich, Rämistrasse 101, 8092 Zurich (sophiee@student.ethz.ch)

Cities show growing interest in reducing their greenhouse gas emissions and are currently voluntarily developing local emissions inventories; Nonetheless, prevailing methods employed by diverse cities frequently overlook biogenic fluxes (Decina et al. 2016). This underscores a pressing need for appropriate modeling tools, capable of separating and quantifying the anthropogenic and biogenic components of carbon dioxide (CO_2) dynamics within the unique urban environment. Given the inherent interconnection between anthropogenic and biogenic processes in urban ecosystems (Churkina 2012), along with the unique ecophysiology of urban vegetation, the modeling of surface exchange processes of water and carbon presents unique challenges.

In this work, the urban land surface model SUEWS (Surface Urban Energy and Water Balance Scheme) (Järvi et al. 2011) is used to simulate CO_2 and water fluxes across urban green areas in Zurich, Switzerland. The model performance is evaluated against measured transpiration and soil moisture. Additionally, the model sensitivity to maximum conductance (g_{max}) and leaf area index (LAI) is examined. Site-specific g_{max} for trees is obtained from sap flow observations, and LAI is optimized according to observed stand-level LAI.

Using these optimized parameters, the model performance in simulating soil moisture improves noticeably, showing a higher correlation with observations. However, despite the optimization of g_{max}, transpiration is greatly overestimated during summer, indicative of the models' incapability of simulating stomatal regulation by the trees. Turbulent heat fluxes emerge to be highly sensitive to changes in g_{max}. Conversely, only a minor influence of changes in g_{max} on CO_2 fluxes has been observed. The optimization of the LAI parameters, on the other hand, is found to significantly modify simulated CO_2 flux from photosynthesis, whereas turbulent heat fluxes only show minor sensitivity to the LAI parameters.
Soil respiration is overestimated during winter months, leading to substantial contributions to the biogenic CO_2 flux. As a consequence, this results in a positive annual net ecosystem exchange from biogenic processes across all parks, ranging from 275 to 723 g C m^{-2} yr^{-1}.

Given the high sensitivity of the simulated surface fluxes to the biogenic parameters employed in the simulation, we emphasize the importance of selecting optimal vegetation-related parameters when utilizing SUEWS for examining surface exchange processes within urban green areas. Moreover, it is imperative to recognize the ongoing necessity for ecophysiological measurements, specifically focusing on grass LAI and grass photosynthesis in order to improve the model performance for Zurich, specifically. A representative choice of these parameters is crucial to ensure an accurate representation of biosphere - atmosphere interactions in urban areas.
Overall, SUEWS is a promising tool in quantifying the relative contribution of the anthropogenic and biogenic components of urban heat and CO_2 fluxes and can therefore assist local stakeholders in mitigating urban heat islands, and CO_2 emissions.

REFERENCES

Churkina, G. 2012: Carbon Cycle of Urban Ecosystems. In: Carbon sequestration in urban ecosystems (Ed. R. Lal & B. Augustin). Springer Netherlands. 315–330.

Decina, S. M., Hutyra, L. R., Gately, C. K., Getson, J. M., Reinmann, A. B., Short Gianotti, A. G., & Templer, P. H. 2016: Soil respiration contributes substantially to urban carbon fluxes in the greater Boston area. Environ. Pollut. 212, 433–439.

Järvi, L., Grimmond, C., & Christen, A. 2011: The Surface Urban Energy and Water Balance Scheme (SUEWS): Evaluation in Los Angeles and Vancouver. J. Hydrol. 411(3-4), 219–237.

P 16.3
Contrasting legacy of fire regimes on soil carbon stocks in open ecosystems in South Africa and Madagascar

Víctor Fernández-García[1,2], Cristina Santin[3], Tercia Strydom[4], J. J. Maminiaina Natolojanahary[5], H. Miakoampo Randrianiadanarivo[5], Elijah Masango[6], Ndzalama Mkansi[7], Cintia Gonzalez[7], Xosé L. Otero[8], Christian A. Kull[1].

[1] *Institute of Geography and Sustainability, University of Lausanne, Géopolis, CH-1015 Lausanne (victor.fernandezgarcia@unil.ch)*
[2] *Ecología, Faculty of Biology and Environmental Sciences, Universidad de León, 24071 León*
[3] *Research Institute of Biodiversity, CSIC-University of Oviedo-Principality of Asturias, 33600 Asturias*
[4] *Scientific Services, Skukuza, 1350, South African National Parks*
[5] *Faculty of Letters and Human Sciences, Université d'Antananarivo, BP 566 Antananarivo*
[6] *SAEON – South African Environmental Observation Network, Colbyn, 0083 Pretoria*
[7] *Independent collaborator*
[8] *Department of Edaphology, Faculty of Biology, Universidade de Santiago de Compostela, 15782 Santiago de Compostela*

The storage of carbon in soils and vegetation of terrestrial ecosystems is a hot research topic. Carbon storage is an essential part of the global carbon cycle and, thus, a major influencer on climate regulation. Natural and human-driven disturbances modify ecosystems and their carbon storage capacity. Among the most important disturbances across the globe are landscape fires, whose emissions have been estimated to 2.2 Pg per year (van der Werf et al., 2017). However, the emissions caused by fires are partially compensated by charcoal production and storage, and the by the post-fire regeneration of vegetation. Thus, the net effect of fire on carbon stocks is controversial, and comprehensive approaches beyond comparing burned versus unburned areas are needed to better understand the role of fire on carbon stocks.

In this work we explored the influence of fire regimes on carbon stocks in soil, litter, ground vegetation (woody vegetation with <0.5 m height and herbaceous vegetation), and large vegetation (woody vegetation with ≥0.5 m height) in open ecosystems in South Africa and Madagascar. We selected three study sites in each region, three major savanna-type ecosystems were represented in South Africa (*Terminalia sericea*, *Combretum* and *Colophospermum mopane* dominated savannas) with fire regimes controlled for about 70 years; and three open ecosystems characteristic of central Madagascar, including two grassy ecosystems -dominated by *Loudetia simplex* and *Aristida rufescens*- and one woodland dominated by *Uapaca bojeri*. In each site, we identified five fire regimes (annual burning, biennial burning and triennial burning within the peak fire season, triennial burning out of the peak fire season and unburned areas for at least seven years). At each site, we set 20 plots of 20 m × 20 m (total of 120 plots) across the afore-mentioned fire regimes. In each plot, we collected soil samples from the uppermost 3 cm, from which we measured the bulk density, total carbon and carbonates. In addition, we collected, dried and weighed the litter and ground vegetation including root samples, and we took dasometric measurements of the large vegetation.

Results showed contrasting patterns in soil carbon, which is the major carbon reservoir in open biomes. Overall, in South Africa we found the highest soil carbon stocks in the unburned plots, but the differences were clear only in the site dominated by *Terminalia sericea*, where soil C stocks in the unburned plots were 26.8% higher than in the annually burned plots. In contrast, in Madagascar, the annually burned plots exhibited soil carbon stocks 27.3% higher than the unburned plots. We also found higher litter biomass in the unburned plots than in the areas affected by burning in both regions, as the annually burned plots have litter biomass near to zero in South Africa and in Madagascar. The results for the ground vegetation showed a pattern of higher biomass in the unburned and in the triennial burning than in the annually burned plots, particularly in the open ecosystems of Madagascar. We also found detrimental effects of frequent burnings on the biomass storage in large vegetation in South Africa and Madagascar. In the grassy ecosystems in Madagascar, we found that large vegetation is only present under triennial regimes or absence of burning.

The results of this work provide a comprehensive overview on the influence of fire regimes on ecosystem carbon storage in major open ecosystems, and thus might be considered when developing fire management strategies aimed at mitigating climate change. However, in view of the variability of effects on carbon stocks, we advocate for additional investigation to untangle the factors underlying these differing patterns. Specifically, we encourage the study of the potential influence of fire regimes and the time since the last fire on the recalcitrance of soil carbon.

REFERENCES
van der Werf, G. R., Randerson, J. T., Giglio, L., van Leeuwen, T. T., Chen, Y., Rogers, B. M., Mu, M., van Marle, M. J. E., Morton, D. C., Collatz, G. J., Yokelson, R. J., & Kasibhatla, P. S.: 2017. Global fire emissions estimates during 1997–2016, Earth System Science Data, 697–720.

P 16.4
Radiocarbon Inventories of Switzerland (RICH) : Atmospheric $^{14}CO_2$ monitoring across space and time

Dylan Geissbühler[1,2], Thomas Laemmel[1,2], Philip Gautschi[3], Lukas Wacker[3], Sönke Szidat[1,2]

[1] *Department of Chemistry, Biochemistry and Pharmaceutical Sciences, University of Bern, Bern, Switzerland (dylan.geissbuehler@unibe.ch)*
[2] *Oeschger Centre for Climate Change Research, University of Bern, Bern, Switzerland*
[3] *Laboratory of Ion Beam Physics, Institute for Particle Physics and Astrophysics, Federal Institute of Technology Zurich (ETHZ), Zurich, Switzerland*

The Radiocarbon Inventories of Switzerland project (RICH) aims to build the first database of radiocarbon (^{14}C) and model of the distribution and cycling of this radionuclide at a national scale across all major pools of the carbon cycle. Here we present our work to collect atmospheric $^{14}CO_2$ data based on complementary monitoring approaches in a representative manner for Switzerland over a multi-year period.

Radiocarbon measurements of atmospheric CO_2 provide unique information on its sources and subsequent transport. It allows the apportionment between biogenic and fossil-fuel derived sources, which are close to the contemporary atmospheric background and ^{14}C-free, respectively. The determination of the fossil CO_2 fraction in air samples, combined with atmospheric modelling efforts, can be used to identify fossil-fuel emission patterns from a local to a regional scale. These efforts can then be used to plan and enforce future CO_2 emissions mitigation steps (Turnbull et al. 2009).

Two $^{14}CO_2$ monitoring methods are presented here: direct air sampling at tall tower sites and collection of tree leaves. The air sampling is performed at a total of six sites across Switzerland, including one background site at the Jungfraujoch high altitude research station (JFJ), four tall towers at rural sites (SOT, ULM, BRM and ELG) and an urban site in Bern (BER) (Fig.1). Samples are collected every second week at all these sites, in a simultaneous manner, except for JFJ where two-weeks integrated night samples are collected as a background signal. In the second approach, tree leaves sampled over two consecutive growing seasons (2022-2023), at locations representing the different ecoregions of Switzerland, which are investigated for their different ecosystemic and anthropogenic characteristics of CO_2 emissions (Nussbaum et al. 2014) (Fig.1).

Preliminary results of the atmospheric monitoring show a clear seasonality of the CO_2 concentration and $^{14}CO_2$ content, with JFJ being a consistent background in terms of ^{14}C (Fig.2). ^{14}C values of tree leaves show that average differences between ecoregions seem to be small, however, more measurements are needed to make a full assessment.

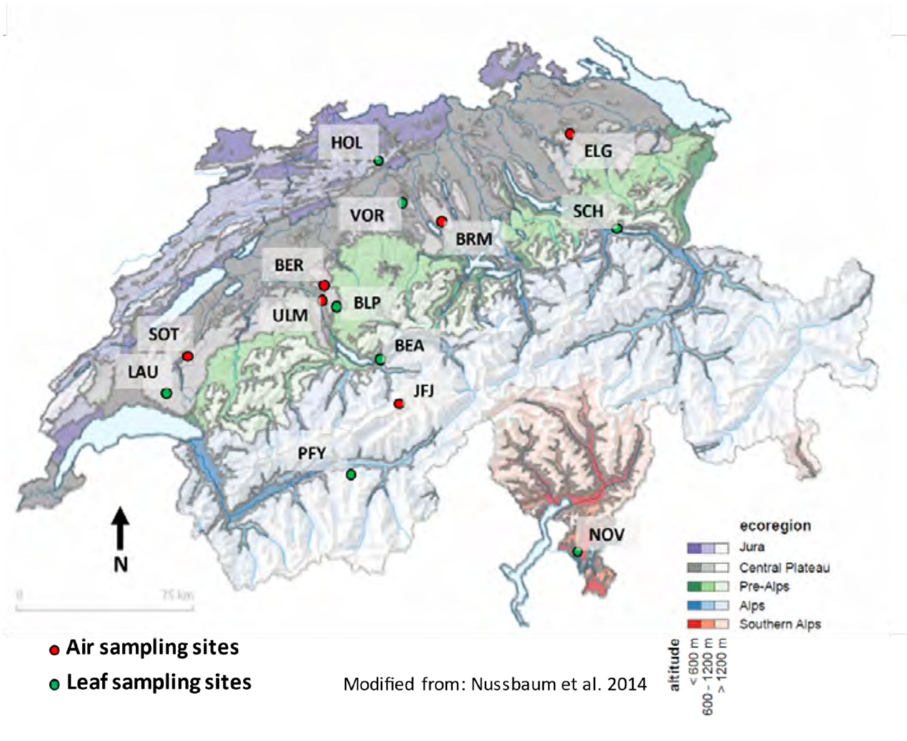

Figure 1. Map of Switzerland showing the locations of our air and leaf sampling sites and their relation to defined ecoregions and altitudes.

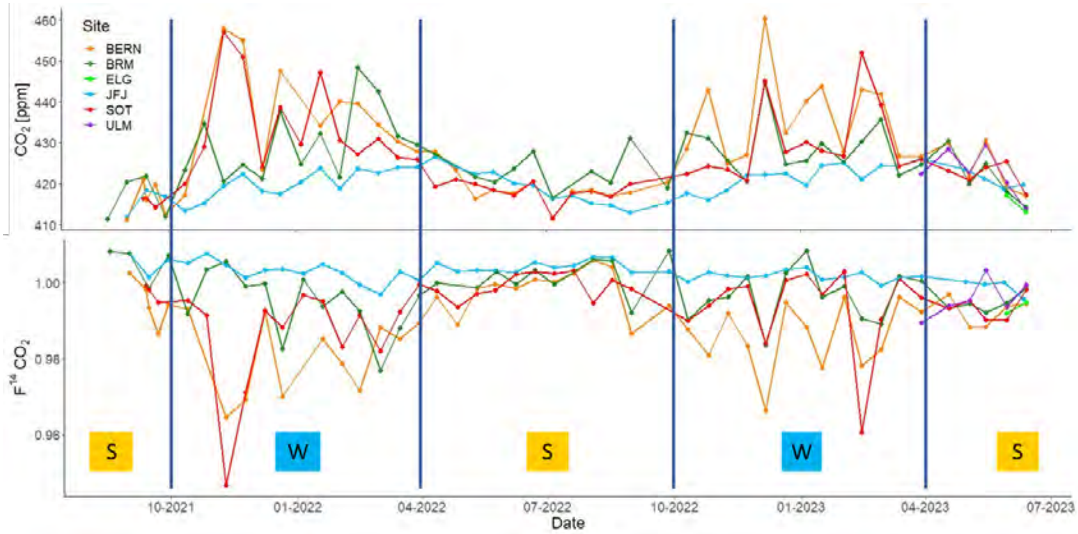

Figure 2. Air sampling CO_2 concentration and $F^{14}CO_2$ data from our 6 sites, with JFJ (blue) as background. Seasonality between summer signal (S) and winter signal (W) is indicated.

REFERENCES

Nussbaum, M., Papritz, A., Baltensweiler, A., Walthert, L., 2014. Estimating soil organic carbon stocks of Swiss forest soils by robust external-drift kriging. Geosci. Model Dev. 7, 1197–1210. https://doi.org/10.5194/gmd-7-1197-2014

Turnbull, J., Rayner, P., Miller, J., Naegler, T., Ciais, P., Cozic, A., 2009. On the use of 14CO2 as a tracer for fossil fuel CO2 : Quantifying uncertainties using an atmospheric transport model. J. Geophys. Res. 114, D22302. https://doi.org/10.1029/2009JD012308

P 16.5
Reduced summertime peak CO_2 uptake following a reduced winter snowpack in an alpine grassland

Kukka-Maaria Kohonen[1], Yi Wang[1], Lukas Hörtnagl[1], Nina Buchmann[1]

[1] *Institute of Agricultural Sciences, ETH Zürich, Universitätstrasse 2, CH-8092 Zürich (kukkamaaria.kohonen@usys.ethz.ch)*

Grasslands play a crucial role in Switzerland, covering up to 70% of the agricultural area, including many (sub)alpine elevations. Over the past decades, snow cover has been decreasing due to climate warming, particularly affecting the alpine region. However, the impact of climate warming on grasslands is not uniform. While reduced snow cover can lower grassland soil carbon stocks, increased temperatures may lead to higher productivity overcompensating respiration.

In this study, the biosphere-atmosphere carbon dioxide (CO_2) exchange was measured with the eddy covariance technique over an extensively managed alpine grassland (at 2000 m asl) in the Canton of Grisons, Switzerland. The grassland serves as a summer pasture for cattle for approximately three months each year. Measurements were carried out during the summers 2006 to 2014 as well as during the full years of 2015 to 2022. The grassland acted as a net CO_2 sink in all years. While a decreasing snowpack resulted in an earlier onset of the growing season, it also affected the capability of the ecosystem to fix CO_2. We show that the summertime maximum CO_2 uptake depends on the amount of snow in the previous winter, with a higher CO_2 uptake after a winter with a high snowpack. The peak uptake (cumulative uptake from the start of the growing season in late April/ early May until the maximum CO_2 uptake in mid June) contributed up to 60% to the whole growing season CO_2 uptake, indicating the high importance of the early summer uptake, and thus the snowpack of the previous winter. Moreover, we observed variations in the importance of radiation, soil moisture and temperature on the biosphere-atmosphere CO_2 exchange throughout the year.

P 16.6
Radiocarbon Inventories of Switzerland (RICH): Atmospheric $^{14}CH_4$ monitoring and modeling across space and time

Thomas Laemmel[1,2], Dylan Geissbühler[1,2], Stephan Henne[3], Dominik Brunner[3], Negar Haghipour[4], Markus Leuenberger[2,5], Sönke Szidat[1,2]

[1] *Department of Chemistry, Biochemistry and Pharmaceutical Sciences, University of Bern, Bern, Switzerland (thomas.laemmel@unibe.ch)*
[2] *Oeschger Centre for Climate Change Research, University of Bern, Bern, Switzerland*
[3] *Empa, Laboratory for Air Pollution/Environmental Technology, Dübendorf, Switzerland*
[4] *Laboratory for Ion Beam Physics, Department of Physics, ETH Zurich, Switzerland*
[5] *Climate and Environmental Physics, Physics Institute, University of Bern, Bern, Switzerland*

Methane (CH_4) is the second most important anthropogenic greenhouse gas after carbon dioxide (CO_2). Main CH_4 sources are linked to the use of fossil fuels (oil, gas, coal) and human-related or natural processes such as agriculture, waste management or wetlands. While biogenic emissions of CH_4 contain present-day atmospheric radiocarbon (^{14}C) levels, CH_4 derived from fossil sources is ^{14}C-free so that $^{14}CH_4$ measurements can be used for source apportionment to distinguish fossil from biogenic CH_4 sources.

A dedicated setup to analyze $^{14}CH_4$ was developed at the Laboratory for the Analysis of Radiocarbon with AMS (LARA), University of Bern (Espic et al., 2019). Typical samples are 60L of atmospheric air collected in bags, which, after extraction, result in about 60 µg carbon in CH_4-derived CO_2 form, enough for a ^{14}C gas measurement on a MICADAS (Mini Carbon Dating System) accelerator mass spectrometer equipped with a gas interface system (GIS).

Since 2019, biweekly air samplings have been conducted at three sites in Switzerland: the high-altitude research station Jungfraujoch (BE/VS) (3580 m asl) considered as a European continental background station, a tall tower in Beromünster (LU) and an urban site in Bern (BE). Three more tall towers have been visited in Sottens (VD), Ulmizberg (BE) and Elgg (ZH) since June 2021, March 2023 and Mai 2023, respectively.

Besides these *in situ* measurements, an atmospheric $^{14}CH_4$ transport model was developed to simulate $^{14}CH_4$ values for each sampling. It is based on the Lagrangian transport and dispersion model FLEXPART (Pieber et al., 2022), two CH_4 emission inventories (Meteotest EKAT for Switzerland, TNO-CAMS v4.2 for the rest of Europe), *a priori* $^{14}CH_4$ signatures for each emission type and the weather model COSMO. $^{14}CH_4$ emissions from nuclear power plants equipped with a pressurized water reactor (PWR) in Switzerland and neighboring countries are also taken into consideration.

This contribution will show the *in situ* $^{14}CH_4$ measurements as well as corresponding simulations and emphasize that the sporadic transport of $^{14}CH_4$ emitted from PWRs is greatly influencing the overall signal measured over the Swiss Plateau making CH_4 source apportionment for this region very challenging.

This work is part of the ongoing project RICH (Radiocarbon Inventories of Switzerland) aiming to develop a national radiocarbon inventory in the atmospheric, terrestrial and aquatic carbon pools.

REFERENCES

Espic, C., Liechti, M., Battaglia, M., Paul, D., Röckmann, T. & Szidat S. 2019: Compound-specific radiocarbon analysis of atmospheric methane: a new precontration and purifcation setup, Radiocarbon, 61, 5, 1461-1476.

Pieber, S. M., Tuzson, B., Henne, S., Karstens, U., Gerbig, C., Koch, F.-T., Brunner, D., Steinbacher, M. & Emmenegger, L. 2022: Analysis of regional CO_2 contributions at the high Alpine observatory Jungfraujoch by means of atmospheric transport simulations and $\delta^{13}C$, Atmospheric Chemistry and Physics, 22, 10721-10749.

P 16.7
Advances in clumped isotope measurements of nitrous oxide by laser spectroscopy

Paul M. Magyar[1], Ivan Prokhorov[1], Simone Brunamonti[1], Noémy Chénier[1], Lukas Emmenegger[1], Béla Tuzson[1], Joachim Mohn[1]

[1] *Laboratory for Air Pollution / Environmental Technology, Empa, Überlandstrasse 129, CH-8600 Dübendorf (paul.magyar@empa.ch)*

Environmental nitrogen cycling leads to the conversion of anthropogenic nitrogen pollutants to nitrous oxide (N_2O), which is accumulating in the atmosphere, where it acts as a potent greenhouse gas and ozone-depleting molecule. Stable isotopic measurements of $\delta^{15}N$, $\delta^{18}O$, and ^{15}N site preference have successfully been used to constrain the microbial processes responsible for nitrous oxide emissions in many settings, but given the complex array of nitrogen cycle processes and their overlapping isotopic signatures, these constraints are often not sufficient for a complete deconvolution of the history of a sample of N_2O. The 'clumped', or multiply-substituted, isotopologues $^{14}N^{15}N^{18}O$, $^{15}N^{14}N^{18}O$, and $^{15}N^{15}N^{16}O$ provide three additional independent constraints on N_2O sources and processing. These rare isotopologues are challenging to measure, but recent studies have demonstrated their potential for source partitioning and also for garnering insight into N_2O generation mechanisms by denitrifying bacteria, ammonia oxidizing bacteria, and abiotic reactions (Magyar 2017; Kantnerová et al. 2020; 2022).

We present a revised approach to laser spectroscopic measurement of seven singly- and doubly-substituted isotopologues of N_2O for the purpose of source determination, including sample introduction using an automated inlet system and catalytic equilibration of N_2O isotopologues. With these advances we aim for robust approaches to standardization and repeated measurements. In addition, we present hypotheses for possible clumped isotopic effects induced by bacterial denitrification.

REFERENCES

Kantnerová K. et al. 2022: Clumped isotope signatures of nitrous oxide formed by bacterial denitrification. Geochim. Cosmochim. Acta 328, 120–129.

Kantnerová K. et al. 2020: First investigation and absolute calibration of clumped isotopes in N_2O by mid-infrared laser spectroscopy. Rapid Commun. Mass Spectrom. 34, e8836

Magyar P.M. 2017: Insights into pathways of nitrous oxide generation from novel isotopologue measurements. Doctoral dissertation, California Institute of Technology.

P 16.8
Unravel the Secrets of Clouds

Fabian Mahrt[1], Merete Bilde[2], Marianne Glasius[2], Jonas Elm[2], Ove Christiansen[2], Tobias Weidner[2], Ditte Thomsen[2]

[1] *Laboratory for Atmospheric Chemistry, Paul Scherrer Institute, Forschungsstrasse 111, 5232 Villigen (fabian.mahrt@psi.ch)*
[2] *Department of Chemistry, Aarhus University, Langelandsgade 140,8000 Aarhus C*

Clouds in their various forms cover about 71% of the sky in the global annual mean. They affect weather and the hydrological cycle. Clouds also play a key role for climate by interacting with solar and terrestrial radiation, thus impacting the Earth's energy budget.

The formation of clouds has fascinated researchers for centuries. It is now well established that aerosol particles, small liquid or solid suspensions in air, can act as nuclei for clouds. However, despite considerable progress over the past, aerosol-cloud interactions still pose the largest uncertanties in climate projections. This is because our understanding how aerosol chemical composition drives cloud formation and affects cloud microphysical and radiative properties remains incomplete. Recent findings, showing that the chemical composition of aerosol particles itself is impacted by the atmospheric conditions of temperature and relative humidity under which they form, further complicate this challenge and are largely unexplored.
In addition, while previous research has often focused on understanding the impact of aerosol particle chemical composition on clouds, the reversal process how processing of aerosols in clouds affects their composition and properties has received less attention and denotes an another important aspect to be addressed by future work.

The novel Center for Chemistry of Clouds (C3) at Aarhus University, a Center of Excellence recently funded through the Danish National Research Foundation, seeks to study the fundamental processes at the interplay between aerosol particles and clouds. In collaborations with international partners, the mission of C3 is to address these challenges. Specifially, C3 aims to contribute to the understanding of key processes driving cloud formation and to unravel how aerosol surfaces and chemistry affect the processes leading to cloud formation. Another focus will be to gain a better understanding of aerosol transformation associated with cloud processing and other atmospheric aging mechanisms. This will be achieved through a combination of experimental and theoretical methods.

Here, we will present an overview of the forthcoming research projects and objectives of C3, as well as the analytical tools and methods available. This will help to identify synergies and shared interests with other researchers and promote possibilities for future collaborations with scientists in Switzerland, that has a strong and long standing tradition in both aerosol and cloud research.

P 16.9
When soil is so dry that it cannot breath: effects of combined drought-heatwave on forest floor and soil respiration in a mixed deciduous forest in Switzerland

Liliana Scapucci[1], Ankit Shekhar[1], Sergio Aranda-Barranco[2], Anastasiia Bolshakova[3], Lukas Hörtnagl[1], Mana Gharun[4], Nina Buchmann[1]

[1] *Department of Environmental Systems Science, ETH Zürich, Switzerland*
[2] *Department of Ecology, University of Granada, Granada, Spain*
[3] *University of Natural Resources and Life Sciences, Vienna (BOKU), Austria*
[4] *Department of Geosciences, University of Münster, Germany*

liliana.scapucci@usys.ethz.ch

Climate change is increasing frequency and intensity of heatwaves and droughts across Europe, with major consequences for forest ecosystems. Often drought and heatwaves occur simultaneously, resulting in combined drought-heatwave (CDH) conditions, as in 2022. CDH effects should thus be evident in forest CO_2 fluxes, with forest floor respiration (Rff) and soil respiration (SR) being major components. 2022 was the warmest year on record in Switzerland, and the summer was characterized by a two-week CDH between 14th of July and 4th of August. Due to low soil water availability and elevated temperatures, we expected that during the CDH period in 2022, both Rff and SR in a mixed deciduous forest were lower compared to normal years and showed altered physiological responses to environmental conditions. Therefore, we (1) compared the CDH period of 2022 with the CDH of 2018 (another extremely warm year recorded in Switzerland) with the reference period of 2019-2021, in terms of meteorological conditions and respiration, (2) assessed the main drivers of Rff and SR, and (3) contrasted the physiological responses of respiration during the CDH periods to non-CDH conditions. The study took place in the Lägeren (CH-Lae) forest, where data from subcanopy eddy covariance measurements (Rff; since 2018) and from a SR survey campaign (2022) were available. We compared data from 2018 and 2022 with the reference period of 2019-2021, in which we did not observe any CDH periods at CH-Lae.

We found a significant decrease in Rff during the CDH in 2018 and 2022 compared to the reference period of 2019- 2021, with a deviation from the mean 2019-2022 of -23 μmol m^{-2} s^{-1} in 2018 and -32 μmol m^{-2} s^{-1} in 2022. Temperature sensitivities (E_0) of Rff in 2018 (E_0 = 252.17) and 2022 (E_0 = 203.21) were significantly lower than the joint period of 2019-2021 (E_0 = 313.77). In addition, the SHAP analysis revealed that during the CDH periods low soil water content (SWC) played a key role in reducing Rff, while soil temperature (TS) effect on Rff declined compared to the rest of the year. Likewise, we found an altered effect of SWC and TS on SR during the 2022 CDH compared to the rest of the year. Thus, we attested that Rff decreased during the CDH periods and that both SR and Rff had altered physiological responses to TS and SWC during the CDH periods.

P 16.10
Longterm trends in atmospheric bulk and throughfall deposition of sulfur and nitrogen to forests in Central Europe

Peter Waldner[1], Till Kirchner[2], Char Hilgers[2], Arne Verstraeten[3], Andreas Schmitz[4], Aldo Marchetto[5], Anne Thimonier[1], Maria Schmitt[1], Stephan Raspe[6], Manuel Nicolas[7], Anita Zolles[8].

[1] WSL, Swiss Federal Institute for Forest, Snow and Landscape, Zürcherstrasse 111, CH-8903 Birmensdorf (peter.waldner@wsl.ch) (anne.thimonier@wsl.ch) (maria.schmitt@wsl.ch)
[2] TI, Thünen Institute of Forest Ecosystems, Alfred-Möller-Strasse 1, D-16225 Eberswalde, Germany (till.kirchner@ti.bund.de) (char.hilgers@ti.bund.de)
[3] INBO, Research Institute for Nature and Forests, Kliniekstraat 25, BE-1070 Brussels, Belgium (arne.verstaeten@inbo.be)
[4] State Agency for Nature, Environment and Consumer Protection of North Rhine-Westphalia, Leibnizstraße 10, D-45659 Recklinghausen, Germany (Andreas.Schmitz@lanuv.nrw.de)
[5] CNR-Istituto per lo Studio degli Ecosistemi, Largo Tonolli 50, I-28922 Verbania Pallanza (VB), Italy
[6] LWF, Bavarian State Institute of Forestry, Hans-Carl-von-Carlowitz-Platz 1, D-85354 Freising, Germany (stephan.raspe@lwf.bayern.de)
[7] ONF, Office National des Forêts, Département Recherche et Développement, Bâtiment B, Boulevard de Constance, F-77300 Fontainebleau, France (manuel.nicolas@onf.fr)
[8] BFW, Federal Research Centre for Forests, Seckendorff-Gudent-Weg 8, A-1131 Vienna, Austria (anita.zolles@bfw.gv.at)

Atmospheric deposition of air pollutants, such as sulfur dioxide and nitrogen oxides effect nutrition and biogeochemistry of forests. Clean air measures at European scale in the frame of the UNECE convention successfully reduced emissions (Waldner et al. 2014, Marchetto 2021). Focussing on Central Europe, we will show updated result of two or more decades of continuous monitoring of sulfur (S) and nitrogen (N) inputs to forests at selected sites of the International Coopeation Programme on Assessment and Monitoring of Air Pollution Effects to Forests. We see decreasing trends in both, bulk and throughfall deposition of S (about -60%) and N (about -30%). Selected effects on forest tree nutrition and biogeochemistry will be discussed (see also Schmitz et al. 2019).

REFERENCES
Waldner et al. 2014. Atmospheric Environment 95, 363-374.
Marchetto et al. 2021. Frontiers in Environmental Science 9.
Schmitz et al. 2019. Environmental Pollution 244, 980-994.

P 16.11
Observed heavy precipitation trends in Switzerland: an update and extension

Victoria Bauer[1], Simon C. Scherrer[1]

[1] *Federal Office of Meteorology and Climatology MeteoSwiss, Zürich-Flughafen, Switzerland (simon.scherrer@meteoswiss.ch)*

Heavy precipitation is an important natural hazard in the Alpine region. As predicted by theory and climate models, Scherrer et al. (2016) found a clear tendency for increases in the intensity and frequency of observed Swiss daily heavy precipitation in the period 1901–2014. In this study, we present an update until 2022, including several day precipitation aggregates and additional precipitation thresholds. The results broadly confirm those by Scherrer et al. (2016). For most stations, the trends are slightly smaller than in the period 1901–2014 but the general tendency towards increases is still valid. We also find increases for several-day heavy precipitation intensities and frequencies. In addition, the relative trends in the frequency of heavy precipitation increase more strongly for more extreme thresholds. There are seasonal differences with larger-scale positive trends along the northern slope of the Alps in the summer half-year. We also extended the analysis to a set of subdaily precipitation sums for the period 1981–2022. The interannual variability is very large and trends are hard to dectect. At the majority of stations, however, a small tendency towards an increase in intensity is found, especially in the summer half-year.

REFERENCES

Scherrer, S. C., Fischer, E. M., Posselt, R., Liniger, M. A., Croci-Maspoli, M. & Knutti R. 2016 Emerging trends in heavy precipitation and hot temperature extremes in Switzerland, J. Geophys. Res. Atmos., 121, https://doi.org/10.1002/2015JD024634

P 16.12
On greenhouse and icehouse climate regimes over the Phanerozoic

Christian Vérard*

** Department of Earth Sciences, University of Geneva (Switzerland).*

Throughout the Phanerozoic and more, the Earth has experienced cold and warm periods, which are typically associated with long-lasting (hundreds of million years, Myrs) greenhouse and icehouse climate regimes. Now, most published sea-level curves report two main maxima in the Cretaceous and Ordovician superimposed on a multitude of short-term fluctuations. The big humps are shown to be predominantly the results of the plate tectonic configuration, not icehouse and greenhouse regimes, suggesting that the small oscillations are related to continental ice variations. From this point of view, it can be inferred that polar ice caps are present almost all the time, and climate regime changes appear much more frequent and shorter than usually considered and are not well-documented from glaciogenic deposits. Relying on short-term oscillations, the volume of continental ice can be retrieved over the Phanerozoic.

18 Tackling the Climate Crisis: Interdisciplinary Perspectives on Climate Change Education and Communication

Moritz Gubler, Petra Bättig-Frey, Christina Colberg, Andreas Linsbauer, Matthias Probst

TALKS:

18.1 Baumann T., Probst M., Romppainen-Martius O., Sturny R., Schwierz C., Staub B.: Developping a hail learning module for secondary schools

18.2 Bhattacharya S., Shome A., Datta A.: Socio-Environmental survey of Yakten, an ecotourism hamlet situated in the eastern Himalayas in Sikkim, India

18.3 Di Tommaso M.: Adaptation and mitigation strategies of the construction sector towards the impact of climate change on infrastructure: review of an educational tool developed for the engineering community of emerging economies of Central Asia

18.4 Forrer C., Veith C.: Tackling Climate Change through Global Learning – Experiences and Learnings from an International Virtual Course

18.5 Hepner S. Ifejika Speranza C., Agonvonon G., Tabi Eckebil P., Mintah F., Iheaturu C.: Video documentation and insights from field research in forest-agricultural landscapes of West Africa

18.6 Höhnle S., Velling H., Schubert J.C.: Students' Attitudes on Climate Change – Results of a quantitative questionnaire-based study in Germany

18.7 Kastrup U., Bircher K., Eglinton T., Grün G., Hedrich H., Jefferson I., Sleigh J.: KEEP IT CO_2OL – an exhibition on CO_2 and us

18.8 Linsbauer A., Jouvet G., Heeb N., Chow N., Christen J., Finley B., Buetikofer M., Bucheli S.: IceAgeCam – an interactive view on ice ages and climate change

18.9 Perga M.E., Sarrasin O., Steinberger J., Lane S., Butera F.: The climate change research that makes the front page: Is it fit to engage societal action?

18.10 Pretet C., Perron S., Castelltort S., the project team: ClimatiZENs – Past climates for tomorrow's citizens

POSTERS:

P 18.1 Deisenrieder, V., Heitmann I., Schäffer L., Hüfner K., Marke T., Keller L.: Young people empower themselves and their communities through future-oriented projects in a valley affected by climate change

P 18.2 Volery A., Weber H., Barandun M., Imanalieva P.: 5 years of breaking the ice in Central Asia: Addressing Climate Change and Gender Inequality in STEM

18.1
Developping a hail learning module for secondary schools

Tamara Baumann[1], Matthias Probst[2], Olivia Romppainen-Martius[1], Rouven Sturny[1], **Cornelia Schwierz**[3], Benno Staub[4]

[1] Mobiliar Lab für Naturrisiken und Geographisches Institut, Universität Bern, Schweiz
[2] Geographisches Institut, Universität Bern; PH Bern; Gymnasium Burgdorf, Schweiz
[3] Bundesamt für Meteorologie und Klimatologie MeteoSchweiz, Zürich-Flughafen, Schweiz (cornelia.schwierz@meteoschweiz.ch)
[4] Vereinigung Kantonaler Gebäudeversicherungen VKG, Bern, Schweiz

After floods, hail is the most damaging natural hazard that regularly strikes Switzerland in summer. Although hailstorms are often small-scale events, millions of dollars worth of hail damage occur in Switzerland every year. Usually in combination with heavy precipitation, hailstorms cause damage to buildings, infrastructure, vehicles, agriculture and also to people.

In recent years, the knowledge and availability of data on hail in Switzerland have been greatly developed. Among other things, the Mobiliar Lab for Natural Risks at the University of Bern has established a research focus on hail. Furthermore, within the framework of the NCCS thematic priority “Hail Climate Switzerland”, a uniform national reference on hail hazard has been developed, so that current hail climatologies are freely accessible, and are continuously updated by MeteoSwiss.

The great importance of the natural hazard hail and these new scientific developments formed the ideal prerequisite for being able to create a learning module on hail. Current research and practical knowledge on hail and the risk posed by hail in Switzerland is conveyed in four learning modules. The content is aimed at secondary level II and ties in with topics from the subject of geography.

These learning modules can be worked on independently of each other. The central questions and learning tasks build on the learners’ existing knowledge and encourage them to think and research independently. The knowledge acquired in each module can be applied and deepened with practical examples in subsequent tasks. The contents are freely accessible at: www.risikoportal.ch (Figure 1a).

The development of the learning module followed an existing example from the field of flood risk. It was also able to benefit from existing generally understandable communication measures of the project “Hail Climate Switzerland” (Figure 1b), in particular from the brochure with the core statements. The development of the new hail learning modules involved experts, practical partners from the building insurance company and educators.

The presentation gives an insight into the development process of the learning module on hail and briefly introduces the resulting learning content. It shows how science, practice and education can work together to transfer new climate expertise into communication and teaching for young people.

Figure 1. Landing page for the newly developped hail module (top) and from the NCCS-site for the new Swiss hail climatology[1] (bottom).

1 Hail brochure «Hail climate Switzerland» available in DE, FR, IT and EN from www.hagelklima.ch.

18.2
Socio-Environmental survey of *Yakten*, an ecotourism hamlet situated in the eastern Himalayas in Sikkim, India

Sayan Bhattacharya[1*], Arkajyoti Shome[1], Avirup Datta[2]

[1] *School of Ecology and Environment Studies, Nalanda University, Rajgir, Bihar, India. (sayan.evs@gmail.com, sbhattacharya@nalandauniv.edu.in)*
[2] *Department of Environmental Science, University of Calcutta, Kolkata, West Bengal, India.*

The Himalayan landscapes have significant impacts on the climatic conditions and biodiversity in the Indian Subcontinent. Many villages are situated in the Eastern part of the Himalayas and some of them are proximate to the Himalayan forests (Bhattacharya, 2019). *Yakten* (27.2407 N, 88.5824 E) is one of the emerging ecotourism hamlets of the Eastern Himalayas, situated at an altitude of 1615 meters ASL, with incredible biodiversity and spectacular views of the Himalayan ranges. Environmental survey of the village was conducted by visiting *Yakten* village in Pakyong district, East Sikkim, India. The survey work focuses on an interdisciplinary understanding of the bio-cultural landscape and human-nature interactions, and addresses both natural and anthropogenic pressures on *Yakten* village. Primary data were collected using a mixed-methods approach, collecting background baseline information, scheduling interviews with local villagers and field observations. Most of the questions involved in the study were descriptive, and one-on-one interviews were used for collecting data. The length of each interview was about 40–50 minutes (by using both structured and semi-structured questionnaires) and was supplemented by field notes. Biodiversity of the region was documented by visiting the adjacent forest areas. Survey data was collected based on the attributes like demography, agriculture (production of cash crops and food crops), livestock management, management of local springs, waste management, disaster management, climate change and its possible impact on agriculture and water resources, local perceptions on climate change, status of local biodiversity, ecosystem services, conservation initiatives and development of ecotourism in the village. Applications of sustainable agricultural techniques like composting, vermicomposting, organic farming were studied and documented. Traditional ecological knowledge were explored by documenting diverse uses of medicinal plants, food and fodder collected from the forest areas by the local community. Photographic documentation accompanied every phase of the survey. Policy proposals for sustainable development of the hamlet were discussed for conserving the biodiversity and socio-ecological status of the village. Extensive study is needed in other mountain areas of the Eastern Himalayas to explore the socio-ecological conditions in the context of climate change. Bringing local populations into protected area management will also have a significantly positive impact on long-term conservation of the Eastern Himalayan landscape (Bhattacharya et al., 2019).

REFERENCES

Bhattacharya, S. 2019: Environmental crisis in the Eastern Himalayan landscapes in India. Consilience, 21, 66-85.

Bhattacharya, S., De, S., Shome, A., & Dutta, A. 2019: Socio-environmental survey of a forest hamlet proximate to Neora Valley National Park in the Eastern Himalayas, India. Indonesian Journal of Environmental Management and Sustainability, 3 (1),1-13.

Shrestha, A.B. & Devkota, L.P. 2010: Climate change in the Eastern Himalayas: Observed trends and model projections; Climate change impact and vulnerability in the Eastern Himalayas – Technical report 1. Kathmandu: ICIMOD.

18.3
Adaptation and mitigation strategies of the construction sector towards the impact of climate change on infrastructure: review of an educational tool developed for the engineering community of emerging economies of Central Asia

Michel Di Tommaso[1]

[1] *General manager of Istituto Meccanica dei Materiali SA (IMM SA), Via al molino 55, CH-6916 Montagnola (ditommaso@imm.ch)*

We present one tool, developped by us for a major international donor institution, as an example of promoting education on the subject of climate change. The tool - a technical manual on the impact of climate change in Central Asia infrastructure (figure 1) – is currently being circulated to government offices, contractors etc. working in the construction sector. The impact of climate change on our infrastructure is tangible with catastrophic financial, social and human losses. Whether the additive effects of the current interglacial period are considered or not, it appears undeniable that humans have strongly contributed, since the industrial revolution, to the growth of CO_2 and Green-House-Gases (GHG) to the point that their concentration is causing: 1) a sharp rise in the *rate of increase* of global temperaures and, 2) the intensification of extreme weather events. Construction is the second largest contributor to GHG among all industrial activities.Thus, any action towards making this sector sustainable, will have a tangible impact on global GHG emissions. Managing the transition to sustainable construction policies, requires therefore that also the engineering communities and policy makers of emerging economies become conscious players, considering the global perspective of the problem. Emerging economies, though, often struggle to implement effective environmental policies due to lack of funding and knowledge. Here we only focus on examples of tools to reduce the gap in the knowledge. The manual discussed in this paper is built around two main topics: *mitigation* and *adaptation*. The first topic discusses the ISO 14067 standard and the University of Bath's (UK) database for the calculation of carbon footprint of construction materials and processes, because it's only by knowing how much CO2 is produced by construction (which is the second largest global emitter of GHG) that we can think of how to reduce emissions with sustainable engineering and construction solutions. *Adaptation* strategies are discussed next by introducing environmental and climate stressors and how these combine during extreme events to cause infrastructure failure and damage, with emphasis on the multi-disciplinary aspect of this topic including: engineering, materials science, forestry, applied geology etc. We move on to discuss the strategies to increase the resiliency of construction against climate change, with the mitigation aspect in mind (sustainable bio-engineering solutions). We end the paper by presenting a tool (annexed to the manual) to estimate the impact of afforestation on CO_2 sequestration in road and railway projects (figure 2).

REFERENCES

Asian Development Bank, 2022: Manual for Climate Change Adaptation Measures for Transport Infrastructure in Central Asia with a Focus on Uzbekistan

Asian Development Bank, 2021: A Practical Guide to Concrete Pavement Technology for Developing Countries

Fares, A. 2021: Climate Change and Extreme Events. Elsevier

ISO 14067: Greenhouse gases — Carbon footprint of products — Requirements and guidelines for quantification

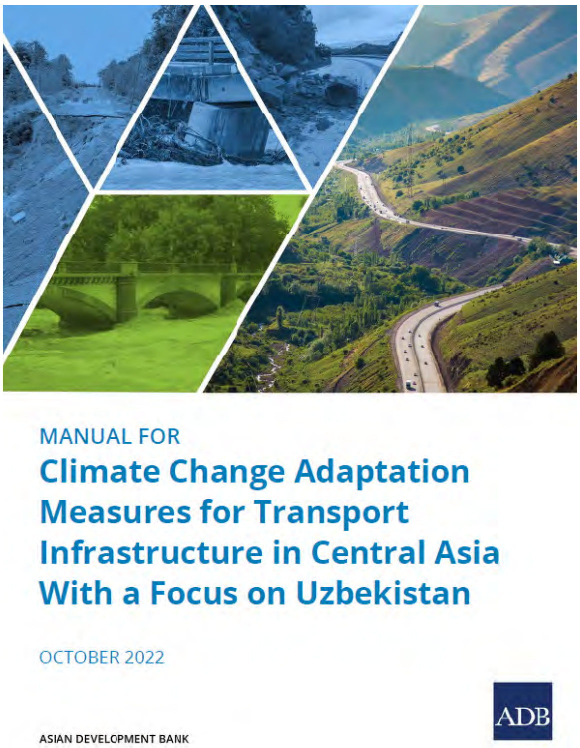

Figure 1. Front cover of the manual discussed in the paper

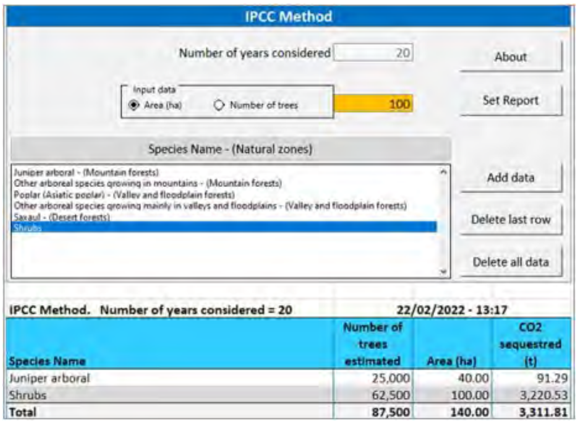

IPCC Method. Number of years considered = 20 22/02/2022 - 13:17

Species Name	Number of trees estimated	Area (ha)	CO2 sequestred (t)
Juniper arboral	25,000	40.00	91.29
Shrubs	62,500	100.00	3,220.53
Total	**87,500**	**140.00**	**3,311.81**

Figure 2. Example of the output of the CO2 calculator to estimate the impact of afforestation on transport infrastructure (roads and railways)

18.4
Tackling Climate Change through Global Learning -
Experiences and Learnings from an International Virtual Course

Carmen Forrer[1], Claudia Veith[1]

[1] *Institut für Umwelt und Natürliche Ressourcen, ZHAW Life Sciences und Facility Management, Grüentalstrasse 14, CH-8820 Wädenswil (carmen.forrer@zhaw.ch)*

Global learning, intercultural communication and virtual teamwork are at the heart of the programme called *International Virtual Course: Tackling Climate Change through Global Learning*. Students learn together and from each other about the challenges and strategies for coping with climate change in the agrifood system and test new forms of virtual collaboration. The international exchange enables insights into different realities and encourages a change of perspective.

Both, in the global North-South understanding as well as in the didactic setting, classic role understandings are broken down in order to enable collaboration at eye-level between all students and also supervisors, enabling joint learning.
The importance of climate change, the understanding of its complexity as well as learning about mitigation and adaptation strategies in education is also confirmed by literature (Reimers, 2021). In addition, the newest IPCC report (2023) states, climate change actions need to be based on equity and inclusivity in order to achieve long-term solutions and sustainable development.

To combine the aspects of equity and inclusivity in climate change education, four universities from four continents - the Universidade Federal da Grande Dourados (UFGD), the University of Agricultural Sciences, Bangalore (UASB), the University of Nairobi (UoN) and the Zurich University of Applied Sciences (ZHAW) - developed this programme. Students learn about climate change in the agrifood system in different contexts and countries and develop intercultural communication skills. Due to its online format and low costs, the course is very climate friendly and socially inclusive.

Since 2020, the course was carried out four times with a total of 143 students at the level of Bachelor/Undergraduate, Master, and PhD. The programme was concipated as a pilot-project and is constantly being improved.
The course is structured in four phases with different events and communication tools. The structure with the responsible university for each phase and the description of tasks is shown in Figure 1.

Strengths
The main strengths of this course are: the opportunity to participate with low costs and resources and that it is almost climate neutral but still allows for international experiences. To analyse and reflect on North-South-South collaboration on climate change, the course promotes mutual understanding of different backgrounds and realities.
In addition, the course has a strong focus on social competences in intercultural and virtual collaboration. Through daily meetings and small group works, students learn and experience the importance of communicating at eye level.
An overarching strength is the combination of the four participating universities, bringing together different expertise and a diverse knowledge base.

Figure 1: the four phases of the International Virtual Course with the responsible university and tasks.

Challenges
At the same time, the format faces different challenges: working together across different time zones, with sometimes poor internet connections, and cultural and language barriers.
Therefore, continuous reflection on communication skills are needed and implemented.
In our experience, these are the most challenging points:

- Communication is more complex and time-consuming than expected. Especially in online settings it is important to talk about the expected communication and to allow enough time for it.
- Commitment is more difficult in online settings. It is therefore even more important than in offline settings to create a personal and comfortable atmosphere in order to get students engaged.
- Coaching sessions, where coaches interact with students on a personal level, are particularly important.
- Conclusions and future perspectives

In conclusion, we would like to emphasise that the learning and inclusion of social skills is essential for intercultural exchange in this course goes beyond technical skills. The emphasis on respect, tolerance, and building personal connections remains key, allowing personal topics to be explored and meaningful relationships to be cultivated over time.
The use of online meetings during the pandemic has undoubtedly brought familiarity with virtual platforms, however on some occasions we could also identify aspects of corona fatigue.
This innovative approach for international and intercultural learning experiences can be seen as a model for future courses in different settings. Publishing the concept as part of Open Educational Resources will make it widely accessible, contributing to inclusive and climate-friendly education.

REFERENCES

Calvin, K., Dasgupta, D., Krinner, G., Mukherji, A., Thorne, P. W., Trisos, C., Romero, J., Aldunce, P., Barrett, K., Blanco, G., Cheung, W. W. L., Connors, S., Denton, F., Diongue-Niang, A., Dodman, D., Garschagen, M., Geden, O., Hayward, B., Jones, C., … Péan, C. (2023). *IPCC, 2023: Climate Change 2023: Synthesis Report. Contribution of Working Groups I, II and III to the Sixth Assessment Report of the Intergovernmental Panel on Climate Change [Core Writing Team, H. Lee and J. Romero (eds.)]. IPCC, Geneva, Switzerland.* (First). Intergovernmental Panel on Climate Change (IPCC). https://doi.org/10.59327/IPCC/AR6-9789291691647

Reimers, F. M. (2021). The Role of Universities Building an Ecosystem of Climate Change Education. In F. M. Reimers (Ed.), *Education and Climate Change* (pp. 1–44). Springer International Publishing. https://doi.org/10.1007/978-3-030-57927-2_1

18.5
Video documentation and insights from field research in forest-agricultural landscapes of West Africa

Samuel Hepner[1], Chinwe Ifejika Speranza[1], Georges Agonvonon[1], Pamela Tabi Eckebil[1], Frank Mintah[1], Chima Iheaturu[1]

[1] *Institute of Geography, University of Bern, Hallerstrasse 23, CH-3012 Bern (samuel.hepner@unibe.ch)*

Fieldwork is a critical component that can determine the success or failure of social-ecological research. We use the medium of a documentary video to illustrate aspects of a six-month field research conducted on nine forest patches in agricultural landscapes of Togo, Benin, Nigeria, and Cameroon. We show qualitative and quantitative methods of data collection, how we worked with local stakeholders and collected ecological data in forests, the challenges and surprises of fieldwork in such social-ecological settings, and discuss issues presented in the 15min-video. This presentation thus provides the opportunity to share and discuss fieldwork experiences, and how to achieve research objectives in the midst of constraining conditions and emerging opportunities.

Figure 1. Field research team in front of a huge *Ceiba pentandra* in the sacred forest patch of Koui, Togo.

REFERENCES

Wingate, V. R., Akinyemi, F. O., Iheaturu, C. J., & Ifejika Speranza, C. 2022: A Remote Sensing-Based Inventory of West Africa Tropical Forest Patches: A Basis for Enhancing Their Conservation and Sustainable Use. Remote sensing, 14(24), 6251.

18.6
Students' Attitudes on Climate Change – Results of a quantitative questionnaire-based study in Germany

Steffen Höhnle[1], Hanna Velling[1], Jan Christoph Schubert[1]

[1] Lehrstuhl für Didaktik der Geographie, FAU Erlangen-Nuremberg, Regensburger Strasse 160, D-90428 Nürnberg (steffen.hoehnle@fau.de)

In addressing climate change as one of the key problems of humanity (IPCC 2023), the school subject of geography is of particular importance, as it is a leading subject for Education for Sustainable Development with a pronounced systemic character (DGfG 2020). In this highly relevant area, on the one hand, the attitudes of students are considered decisive prerequisites for the success of learning processes. On the other hand, the change of students' attitudes is also regarded as an important goal of (geography) lessons (see e. g. Reinfried 2015) - yet there are hardly any differentiated, systematic findings on their characteristics on the level of the dimensions of the attitude construct regarding the important topic of climate change.

Against this background, in a quantitative, questionnaire-based study N = 10356 students in the federal state of Bavaria in Germany were surveyed about their attitudes on climate change, and the data were analyzed both descriptively and interference-statistically. Overall, there are remarkable differences regarding the different dimensions of the attitude construct in relation to climate change, as well as between genders and between students attending different types of schools. Aspects related to actions against climate change as well as to concerns and fears were rated much lower than aspects related to knowledge on climate change. Furthermore, students attending grammar school ("Gymnasium") show more positive attitudes than students attending secondary school ("Realschulen"), and these in turn than students attending lower-level secondary school ("Mittelschule"). These and the results of further analyses of the survey will be presented.

REFERENCES

Deutsche Gesellschaft für Geographie (DGfG) 2020: Bildungsstandards im Fach Geographie für den Mittleren Schulabschluss mit Aufgabenbeispielen. Bonn: DGfG.

Intergovernmental Panel on Climate Change (IPCC) 2023: Climate Change 2023. Synthesis report.

Chaiken, S. & Stangor, C. 1987: Attitudes and attitude change. In: Annual Review of Psychology 38, 575-630.

Reinfried, S. 2015. Werthaltungen und Einstellungen, In: Reinfried, S., & Haubrich, H. Geographie unterrichten lernen, 70-73

18.7
KEEP IT CO_2OL – an exhibition on CO_2 and us

Ulrike Kastrup[1], Kerstin Bircher[1], Timothy Eglinton[2], Gillian Grün[1], Natascha Hedrich[1], Isabel Jefferson[1], Joanna Sleigh[1]

[1] *focusTerra, ETH Zürich, Departement Erdwissenschaften, Sonneggstrasse 5, CH-8092 Zürich (ulrike.kastrup@erdw.ethz.ch; kerstin.bircher@erdw.ethz.ch; gruen@erdw.ethz.ch; natascha.hedrich@erdw.ethz.ch; isabel.jefferson@erdw.ethz.ch; joanna.sleigh@hest.ethz.ch)*
[2] *Geologisches Institut, Departement Erdwissenschaften, ETH Zürich, Sonneggstrasse 5, CH-8092 Zürich (timothy.eglinton@erdw.ethz.ch)*

‚I'm not allowed to fly anymore! – I should give up my car! – And I shouldn't eat meat anymore either!' That should not be all that comes to our mind when we want to protect the climate by reducing CO_2 emissions. Many new technologies and methods are being developed that will allow us to continue flying, driving cars and eating meat in the future. Unlike today, however, airplanes will fly on sustainable fuels made from solar energy; cars will run on renewable energy; and meat will be grown in the lab. Utopia or realistic scenario?

Where we stand and what options we have in coping with our excessive CO_2 emissions we want to discuss in *focus*Terra, the Earth & Science Discovery Center of ETH Zurich. *focus*Terra works at the intersection between science and the public and invites visitors to discover Earth in all its diversity and fascination. With our exhibitions and activities, we convey exciting, interesting and fascinating information on socially relevant scientific topics to the public. The upcoming exhibition KEEP IT CO_2OL will bring together the public and experts from science, industry and politics to inform and discuss the role of CO_2 in and for our lives, how it affects climate and what its sources of emission are, how technologies can achieve a reduction of CO_2 in the atmosphere and how we as individuals and society must contribute towards a more sustainable way of life. We want to raise awareness of the urgency to take immediate action, foster critical thinking and show what needs to be done. We want to inspire and empower people to create together a future where both humans and nature can thrive. Through our unique proximity to cutting-edge research and by teaming up with ETH and other experts from different fields, we are able to present state-of-the-art technologies and provide the public with the latest knowledge in CO_2-related research. It also allows us to highlight different perspectives (social, economic, environmental, political etc.), address misconceptions, challenges and opportunities, and to provide a platform for an engaging dialogue with society in which both critical and controversial issues can be addressed in a safe environment.

The exhibition's intended long-term impact is to increase understanding and further raise awareness for the need to act against climate change, to contribute to our visitors' science proficiency and to strengthen the importance of permanent dialogue platforms and extracurricular learning venues at universities. The exhibition includes intriguing hands-on and interactive exhibits which are designed to promote the engagement of visitors during and after their visit to the exhibition. Furthermore, the exhibition is designed to be accessible to visitors of all ages and backgrounds, also addressing people with impairments. School materials for teachers visiting the exhibition with their classes are developed as well as accompanying activities and events including guided tours, workshops, meet-a-scientist events and public science talk series to engage and enhance the communication and exchange between scientists and the public. The exhibition concept has won the Agora Optimus Prize 2023 by the Swiss National Science Foundation for its communication potential.

REFERENCES

Eglinton, T., Seneviratne, S., Kastrup, U. & Bircher, K. 2022: Ausstellung: Keep it CO2OL, SNF Agora Proposal 2022, https://data.snf.ch/grants/grant/215865.

Figure 1. A key visual for the exhibition. Source: *focus*Terra / ETH Zurich.

18.8
IceAgeCam – an interactive view on ice ages and climate change

Andreas Linsbauer[1], Guillaume Jouvet[2], Niklaus Heeb[3], Noemi Chow[3], Jonas Christen[3], Brandon Finley[2], Marco Buetikofer[3], Samuel Bucheli[4]

[1] *Department of Geography, University of Zurich, 8057 Zürich (andreas.linsbauer@geo.uzh.ch)*
[2] *Institute of Earth Surface Dynamics, University of Lausanne, 1015 Lausanne*
[3] *Knowledge Visualization, Zürcher Hochschule der Künste, 8031 Zürich*
[4] *Samuel Bucheli illustrations, www.samuelbucheli.ch, 6032 Emmen*

Over the last million years, cyclical changes in Earth›s orbital parameters have been responsible for climate fluctuations and ice ages that have shaped our landscape. Current climate change, on the other hand, is caused by human greenhouse gas emissions. The actual CO_2 content in the atmosphere exceeds the maximum value of the last 800,000 years by far and is the main cause of current global climate change. While public awareness of climate change has increased massively in recent years, many misconceptions are still widespread. In order to increase awareness about the impact from humans versus natural processes, we designed an interactive «IceAgeCam», which will be showcased starting October 2023 at Felsenegg (near Zurich), a popular and easy accessible vantage point.

The «IceAgeCam» consists of a display and two pumps to attract visitors and encourage them to interact with it. The amount of greenhouse gas (CO_2) in the atmosphere can be controlled playfully by using the two pumps. In this way, the audience experiences the changes in the landscape caused by ice ages over the last million years due to natural climate fluctuations. This experience contrasts with the recent and strong anthropogenic increase in the CO_2 concentration in the atmosphere within a very short time, and the resulting global warming.

Figure 1. Prototype visualization of the «IceAgeCam» at the vantage point Felsenegg near Zurich, in front of the view that overlooks the Lake of Zurich towards the Alps.

The interactive station will allow groups of users to actively experience past ice ages as well as the corresponding environmental changes thanks to an innovative design and new visualization techniques based on artificial intelligence. As it will be present at popular vantage points, the «IceAgeCam» intends to reach a broad and possibly not very informed audience to initiate discussions. A built-in camera takes pictures of the users in action in front of the ice age landscape. These images are available to the public for further communication and dissemination, e.g. via social media. The project is accompanied by activities on Instagram (@iceagecam), as well as events with the presence of researchers and public events on site. The direct connection to social media channels and website of the «IceAgeCam» (www.iceagecam.ch) aims to strengthen the engagement and dissemination of the project.

In this presentation we will present the IceAgeCam and describe the process from project idea to implementation. We will provide information on the scientific content and give insights into the communication activities. Furthermore, we are interessed to discuss how interactive and palyful visualisation tools can be used to reach a wide audience with messages about climate change.

18.9
The climate change research that makes the front page: Is it fit to engage societal action?

Marie-Elodie Perga[1], Oriane Sarrasin[2], Julia Steinberger[3], Stuart Lane[1], Fabrizio Butera[2]

[1] *Faculty of Geosciences and Environment, Institute of Earth Surface Dynamics, University of Lausanne, Geopolis, Mouline, CH-1015 Lausanne, Switzerland (marie-elodie.perga@unil.ch)*
[2] *Faculty of Social and Political Sciences, Institute of Psychology, University of Lausanne, Geopolis, Mouline, CH-1015 Lausanne, Switzerland*
[3] *Faculty of Geosciences and Environment, Institute of Geography and Sustainability, University of Lausanne, Geopolis, Mouline, CH-1015 Lausanne, Switzerland*

By growing awareness for and interest in climate change, media coverage enlarges the window of opportunity by which research can engage individuals and collectives in climate actions. However, we question whether the climate change research that gets mediatized is fit for this challenge. From a survey of the 51,230 scientific articles published in 2020 on climate change, we show that the news media preferentially publicizes research outputs found in multidisciplinary journals and journals perceived as top-tier. An in-depth analysis of the content of the top-100 mediatized papers, in comparison to a random subset, reveals that news media showcases a narrow and limited facet of climate change knowledge (i.e., natural science and health). News media selectivity reduces climate change research to the role of a sentinel and whistleblower for the large-scale, observed, or end-of-century consequences of climate change for natural Earth system components. The social, economic, technological, and energy aspects of climate change are curtailed through mediatization, as well as local and short-term scales of processes and solutions. Reviewing the social psychological mechanisms that underlie behavioral change, we challenge the current criteria used to judge newsworthiness and argue that the consequent mediatization of climate change research fails to breed real society engagement in actions. A transformative agenda for the mediatization of climate change research implies aligning newsworthiness with news effectiveness, i.e., addressing the extent to which communication is effective in presenting research that is likely to produce behavioral change.

18.10
ClimatiZENs - Past climates for tomorrow's citizens

Chloé Pretet[1], Séverine Perron[2], Andreas Müller[2,3], Sébastien Castelltort[4], the project team

[1] *AniMuse, Genève*
[2] *IUFE, Université de Genève, 40 boulevard du Pont d'Arve, 1205 Genève*
[3] *Section de physique, Université de Genève.*
[4] *Département des Sciences de la Terre, Université de Genève, 13 rue des maraîchers, 1205 Genève*

The ClimatiZENs project offers secondary I and II teachers a range of activities for their pupils on the theme of climate, from an Earth science perspective.
In the wake of the 2019 youth climate protest, it seems essential to provide teachers with the tools they need to convey complex concepts and facts about the Earth's past climates. In this way, pupils will be better able to grasp current environmental issues and consolidate their commitment: understanding the planet and how it works, is at the heart of action to combat climate change.

The project is made up of playful classroom module (evaluated), field trip, workshops at the University and in-service training for teachers.

The classroom module of this project deals with the climate of the past in relation to the dispersal of populations in the Sahara around 10,000 years ago. Using documents and rock samples from a published study, the pupils have to carry out an archaeological-geological investigation to reconstruct the climate at that time.

The field trip offers classes the chance to discover a renatured river, in a context of increased flooding due to climate change, and take measurements of sediment dynamics and water quality.

The workshop invites pupils to consider how past climates can be reconstructed using different proxies (tree slices, lake sediments and microfossils).

This presentation outlines the project and how it was conceived, as well as what is needed to involve teachers and their pupils in themes that go beyond their usual disciplines.

REFERENCES

https://www.unige.ch/climatizens

P 18.1
Young People Empower Themselves And Their Communities Through Future-Oriented Projects In A Valley Affected By Climate Change

Veronika Deisenrieder[1], Irina Heitmann[1], Lena Schäffer[2], Katharina Hüfner[3] Thomas Marke[2,] Lars Keller[1]

[1] *Institute of Subject Didactics, University of Innsbruck, Innrain 52, A-6020 Innsbruck (Veronika.Deisenrieder@uibk.ac.At)*
[2] *Institute of Geography, University of Innsbruck, Innrain 52, A-6020 Innsbruck*
[3] *Institute of Psychosomatic Medicine, Medical University of Innsbruck, Christoph-Probst-Platz 1 Innrain 52, A-6020 Innsbruck*

Paznaun in Tyrol (A) and its communities have been affected by a number of challenges in the past, such as financial poverty and epidemics in the early 19th century, the avalanche winter of 1999 and the flooding in Galtür in 2005, and more recently the village Ischgl as a hotspot of the C-19 pandemic, which received much media attention. At present, well-known peaks in the high alpine region are breaking off due to permafrost thaw (Land Tirol 2023) and well-known glaciers are melting more and more each year (ÖAV 2023). These and other effects of climate change will continue to be felt in the future.
Over time, the valley›s inhabitants have learnt to cope with various challenges: a strong sense of community, short communication channels and easy access to influential actors have a positive effect, as do the proximity to nature and direct access to leisure, exercise and recreational activities, which enable personal well-being and the experience of self-efficacy and community (apa 2022). At the same time, there is a lack of established structures and theoretically based concepts in the valley to make individuals and communities aware of and strengthen their self-efficacy and resilience in times of climate change.

Young people and adolescents are already the most affected by climate anxiety (Sanson et al. 2019). They are also experiencing the consequences of climate change more than any generation before them. At the same time, as future decision-makers, this group should help shape society towards climate-friendly and sustainable development. At present, however, this group is often excluded from decision-making processes (Kutalek et al. 2015), although they have already shown and still are showing great potential for transformation processes (Huth 2020; Holfelder et al. 2021). All the more these groups have to be empowered by appropriate educational initiatives for a socio-ecological transformation in mountain regions. Raising awareness, self-efficacy and the ability to act and adapt to the effects of climate change in Paznaun is the goal of the inter- and transdisciplinary research-education cooperation KIDZ PAZ-NOWN (k.i.d.Z.21 2023).

By combining the sciences of hydroclimatology, psychosomatic medicine and education for sustainable development (ESD), an intergenerational exchange at eye level is promoted between students and various partners from society and science. For most of the school year, the pupils work independently on questions from their own lives in the sense of inquiry-based learning (Mutlu 2020; Fassbender 2021). In the second year of the project, the cooperation network is expanded to include partners from the arts, and artistic projects are increasingly implemented.

The example of phenomena that can be seen and experienced on the spot makes it possible to perceive, act, experience, reflect and remember as a unit - thus attributing transformative educational processes and a crucial role in ESD to art (Zacharias 2014). As part of the creative process, crises can be overcome, adaptation processes can take place and even health-promoting effects can be achieved (Zander 2023). In a broader sense, kidz partsz-nown is about raising awareness of climate change and its effects, where constructive action and learning skills take on artistic forms in the sense of ‚learning through the arts‘ (Halverson und Sawyer 2022). What are major challenges and potentials of such a year-round educational concept at the nexus of society, science & art, in order to expand the scientific and social competences of the partners involved?

REFERENCES
APA (2022): Resilience. Hg. v. American Psychological Association. Online verfügbar unter https://www.apa.org/topics/resilience, accessed in February 2022., zuletzt geprüft am 24.09.23.
Fassbender, William J. (2021): The potential for (more-than-)representational video in education research. In: *International Journal of Research & Method in Education* 44 (3), S. 241–256. DOI: 10.1080/1743727X.2020.1772743.
Halverson, Erica; Sawyer, Keith (2022): Learning in and through the arts. In: *Journal of the Learning Sciences* 31 (1), S. 1–13. DOI: 10.1080/10508406.2022.2029127.
Holfelder, A.-K.; Singer-Brodowski, M.; Holz, V.; & Kminek, H. (2021): Erziehungswissenschaftliche Fragen im Zusammenhang mit der Bewegung Fridays for Future. In: *Zeitschrift Für Pädagogik* 1, S. 120–139. Online verfügbar unter https://www.beltz.de/fachmedien/erziehungswissenschaft/zeitschriften/zeitschrift_fuer, zuletzt geprüft am 24.09.23.
Huth, Tecla (2020): Fridays For Future – Die Veränderung unserer Gesellschaftsstrukturen durch Kommunikations- und Handlungsmacht. In: Jan Rommerskirchen (Hg.): Die neue Macht der Konsumenten. Wiesbaden: Springer Fachmedien Wiesbaden, S. 137–145.

k.i.d.Z.21 (2023): KIDZ PAZ-NOWn. Unter Mitarbeit von k.i.d.Z.21 - kompetent in die Zukunft. Hg. v. Climate Change Center Austria. Online verfügbar unter https://kidz.ccca.ac.at/kidz-paz-nown/, zuletzt geprüft am 24.09.23.

Kutalek, Ruth; Wang, Shiyong; Fallah, Mosoka; Wesseh, Chea Sanford; Gilbert, Jeffrey (2015): Ebola interventions: listen to communities. In: *The Lancet. Global health* 3 (3), e131. DOI: 10.1016/S2214-109X(15)70010-0.

Land Tirol (2023): Nach Felssturz auf Fluchthorn: Messergebnisse stehen fest. Sicherheit / Geoinformationen & Karten. Hg. v. Amt der Tiroler Landesregierung. Online verfügbar unter https://www.tirol.gv.at/meldungen/meldung/nach-felssturz-auf-fluchthorn-messergebnisse-stehen-fest/, zuletzt geprüft am 24.09.2023.

Mutlu, Ayfer (2020): Evaluation of students' scientific process skills through reflective worksheets in the inquiry-based learning environments. In: *Reflective Practice* 21 (2), S. 271–286. DOI: 10.1080/14623943.2020.1736999.

ÖAV (2023): Gletscherbericht 2020/2021: «Ewiges Eis» weiterhin auf dem Rückzug. Hg. v. Alpenverein Österreich. Online verfügbar unter https://www.alpenverein.at/portal/service/presse/2022/2022_04_01_gletscherbericht-2020-21.php, zuletzt geprüft am 24.09.2023.

Sanson, Ann V.; van Hoorn, Judith; Burke, Susie E. L. (2019): Responding to the Impacts of the Climate Crisis on Children and Youth. In: *Child Dev Perspectives* 13 (4), S. 201–207. DOI: 10.1111/cdep.12342.

Zacharias, W. (2014): Ästhe- tisches Lernen 2.0. Kulturelle Bildung in einer technisch-medialen Welt. In: Stefan Faas und Mirjana Zipperle (Hg.): Sozialer Wandel: Herausforderungen für Kulturelle Bildung und Soziale Arbeit: Springer VS, S. 113–126.

Zander, Ute (2023): Lust am Gestalten. Hg. v. Kultur Agenda 2030. Online verfügbar unter https://www.kulturagenda2030.de/, zuletzt geprüft am 24.09.23.

P 18.2
5 years of breaking the ice in Central Asia: Addressing Climate Change and Gender Inequality in STEM

Anouk Volery[1], Helga Weber[2], Martina Barandun[1], Perizat Imanalieva[3]

[1] Department of Geosciences, University of Fribourg, Chemin du Musée 4, CH-1700 Fribourg (anouk.volery@unifr.ch ; centralasia@inspiringgirls.org)
[2] Oeschger Centre for Climate Change Research and Institute of Geography, University of Bern, CH-3012 Bern
[3] Central Asian Institute for Applied Geosciences, KG-720027 Bishkek.

Central Asia faces a growing number of climate change-related risks and hazards (Xenarios et al, 2018). The development of mitigation and adaptation measures relies on the acquisition of extensive environmental data turned into relevant information for policy-makers and policy-enactors (Xenarios et al. 2018). This calls for activists in STEM fields and researchers to fill data and information gaps. The inclusion of women in STEM fields reinforces the quality of research and the diversity of perspectives (Salmon, 2015). It also reduces gender inequalities by providing women with well-paid positions in society (Almukhambetova and Kuzhabekova, 2021). However, the involvement of women in STEM has declined in Central Asia since the dissolution of the Soviet Union, and women must increasingly navigate contradicting discourses regarding their role in society (Almukhambetova and Kuzhabekova, 2021).

The project “Adventure of Science: Women and Glaciers in Central Asia” addresses this inequality, by proposing tuition-free glaciological expeditions to young women (18-25) of Kazakhstan, Uzbekistan, Tajikistan, Turkmenistan, and Kyrgyzstan. Ten participants are taught by professionals on environmental sciences, mountaineering and artistic exploration. The 10-day expedition fosters the interest of women in environmental and outdoors fields and strengthens confidence in physical and intellectual abilities. By involving participants from all countries of Central Asia, the project promotes the exchange of knowledge and experience across borders and builds up a transnational network of women researchers and activists. The expedition is led by a women-only team of instructor and mountain guide to offer a space which is free of stereotypical and traditional gender roles, still at play in regions of Central Asia.
After three programs in the field and two rounds of online programs (COVID-related), the Adventure of Science is fast growing. This development and increasing popularity demonstrate the demand to promote gender equality in STEM and environmental science across Central Asia.

REFERENCES

Almukhambetova, A. and Kuzhabekova, A. 2021: Negotiating conflicting discourses. Female students’ experiences in STEM majors in an international university in Central Asia. International Journal of Science Education, 43(4), 570-593.
Salmon, A. 2015: A Complex Formula: Girls and Women in Science, Technology, Engineering and Mathematics in Asia. Bangkok: UNESCO.
Xenarios, S. et al. 2018: Climate change and adaptation of mountain societies in Central Asia: uncertainties, knowledge gaps, and constraints. Regional Environmental Change, 19, 1339-1352.

19 Thinking the future of geoscience education in Switzerland to meet the challenges of sustainable development and exploration for resources and energy

Sebastien Castelltort, Stefan Heuberger, Nathalie Andenmatten Berthoud

Swiss Association of Geologists, CHGEOL
Swiss Geological Society, SGS

TALKS:

19.1 Schmelzbach C., Maurer H.-R., Robertsson J., van Manen D.-J., Slob E., Draganov D., Drijkoningen G., Ghose R., Wellmann F., Wagner F., van der Kruk J., Klitzsch N.: Joint Master in Applied Geophysics: a unique international study programme to educate tomorrow's geoscientists to solve global challenges for a sustainable future

19.2 Feucht C., Buckingham T.: "Adventure Geology"

19.3 Gilli A.: Why do students choose Earth Sciences? How do graduates view our study programme in retrospect?

19.4 Le Bec A.: Enhancing Fundamental Geological Education for Optimal Mineral Resource Utilization in a Context of Climate Change and Global Environmental Concern.

19.5 Meyer M.: Geoscientists, guarantors of sustainable management of subsoil resources

19.6 Vogel M., Schürch P.: Results from two surveys with employers of geologists and individual professional geologist in Switzerland – Suggestions to make the job we're passionate about more attractive for everybody.

19.7 Wyss, M.: Geoscience Education in Switzerland – is there Potential for Improvement?

19.1
Joint Master in Applied Geophysics: a unique international study programme to educate tomorrow's geoscientists to solve global challenges for a sustainable future

Cédric Schmelzbach[1], Hansruedi Maurer[1], Johan Robertsson[1], Dirk-Jan van Manen[1], Evert Slob[2], Deyan Draganov[2], Guy Drijkoningen[2], Ranajit Ghose[2], Florian Wellmann[3], Florian Wagner[4], Jan van der Kruk[3], Norbert Klitzsch[3]

[1] *Institute of Geophysics, ETH Zurich, Sonneggstrasse 5, CH-8092 Zürich, Switzerland (cedric.schmelzbach@erdw.ethz.ch.ch)*
[2] *Faculty of Civil Engineering and Geosciences, Delft University of Technology, Stevinweg 1, 2628 CN Delft, The Netherlands*
[3] *Computational Geoscience and Reservoir Engineering, RWTH Aachen University, Mathieustr. 30, DE-52074 Aachen, Germany*
[4] *Geophysical Imaging and Monitoring, RWTH Aachen University, Wüllnerstr. 2, 52062 Aachen*

Applied Geophysics involves the advancement and application of exploration and monitoring techniques for investigating the Earth›s subsurface, from a few meters to several kilometres depth. This depth range is crucial for various issues that are highly relevant to our society. Applied Geophysics entails developing and applying tools to image the subsurface for geo-energies and natural resources to address the energy transition, to characterise the subsurface for engineering and archaeological investigations, to monitor geohazards and the impact of climate change on the environment as well as to manage the underground.

To meet the rising demand for highly qualified Earth scientists, three leading European technical universities – ETH Zurich (Switzerland), TU Delft (The Netherlands), and RWTH Aachen University (Germany) – collaboratively established the *Joint Master in Applied Geophysics* in 2006 (Green et al., 2007; IDEA League, 2023). Our mission is to educate students in geophysical methodologies for exploring and monitoring the subsurface of the Earth to solve global challenges for a sustainable future.

A cohort of typically 20 students moves as a class from Delft to Zurich and finally to Aachen to follow courses for one semester at each university. During the fourth semester, students undertake their thesis work at one of the partner universities within the program, an approved external university, research centre, or company.

The Joint Masters programme offers a unique international and multifaceted education leading to an outstanding qualification in Applied Geophysics for career paths in industry and academia. The international programme provides the students an exceptional experience to study in cross-cultural teams and to live and learn in three European cities. The curriculum covers methodological aspects in the physical, mathematical, computational as well as data analysis and signal processing foundations of Applied Geophysics. Theoretical and methodological aspects are translated into practice in hands-on exercises and field work. The Joint Masters Programme is run in close collaboration with industry. Companies support the programme by providing grants for scholarships and opportunities for research projects. Experts from industry and governmental agencies deliver special lectures and are involved in the co-supervision of master thesis projects.

As of today, 350+ students and alumni are studying or have completed the programme. Around 50% of our current students are female. After completing the Master›s, about 40% pursue PhDs, 27% work in the engineering/energy sector, and about 29% in other sectors. The program attracts students from Europe (80%), the Americas (10%), Asia (6%), and Africa (4%).

Like many other Earth science study programs, student enrolment has experienced a decline over recent years. The figures have dropped from a peak of 39 students (cohort beginning in 2014) to 19 students (cohort beginning in 2022). In order to maintain the attractiveness of our program to future generations of students, we consistently review, modify, and reconsider both our curriculum and promotional approaches. Regular exciting feedback from our alumni underscores the comprehensive education of our programme that integrates theory and practice, along with a unique international atmosphere.

REFERENCES

Green, A. G., Maurer, H., Slob, E., Wapenaar, K., Clauser, C., & Littke, R. 2007: Joint MSc programme in applied geophysics: a new concept in geophysics education, First Break, 25(4), https://doi.org/10.3997/1365-2397.25.1106.27417
IDEA League 2023: Joint Master in Applied Geophysics, https://idealeague.org/geophysics/

Figure 1. Students and teaching staff at the graduation ceremony in Delft in August 2022.

19.2
Adventure Geology

Christa Feucht, Thomas Buckingham

The association “Adventure Geology” (www.erlebnis-geologie.ch) promotes general public awareness of the importance of geosciences and geodiversity for our society.

It is only thanks to knowledge of the underground that drinking water can be obtained, geothermal energy can be used, buildings can be constructed or warning and protection systems against landslides and floods can be developed.
The main activity of “Adventure Geology” is the operation of the interactive trilingual website www.erlebnis-geologie.ch (DE, FR, IT), where geo-offers and geo-events of Switzerland are currently linked: Whether excursions, guided tours, visits to mines, hikes, exhibitions, geological trails, lectures - (almost) everything is available on the website.

Our goal for the future is not only to reach out to the general public, but also to guides and rangers of the growing number of Swiss geoparks as well as to teachers. Geology is mostly forgotten, as covered under the biosphere. However, it is the the base of all life and it is important to educate not only about biodiversity but also geodiversity.

Our supporting members and partners are:

- Swiss Association of Geologists (CHGEOL)
- Swiss Academy of Natural Sciences (SCNAT)
- Federal Office of Topography (swisstopo)
- Swiss Geological Society (SGG)

19.3
Why do students choose Earth Sciences? How do graduates view our study programme in retrospect?

Adrian Gilli[1]

[1] *Department of Earth Sciences, ETH Zurich, Sonneggstrasse 5, CH-8092 Zurich (adrian.gilli@erdw.ethz.ch)*

Continuous curriculum revision is a fundamental process in higher education institutions. An important input is feedback from students frequently gathered through surveys.

For the past 10 years, prospective students in the Earth and Climate Sciences programme at ETH Zurich have completed a questionnaire about the sources of information used for their study selection and their reasons for studying Earth Sciences. Classic information sources such as the department's website and the study guide are of great importance. Also the ETH study information days for prospective students and geography teachers are often stated. The incoming students frequently mentioned the broad study programme and the excursions/field courses as decisive for choosing Earth Sciences.

An ongoing survey among graduates of the study programme will provide valuable feedback on our Master's programme. Questions regarding aspects that were either insufficiently covered or overly detailed during their studies will aid in improving our MSc Earth Sciences curriculum.

19.4
Enhancing Fundamental Geological Education for Optimal Mineral Resource Utilization in a Context of Climate Change and Global Environmental Concern.

Arnaud Le Bec

Head of Competence Center Geology, OMYA International AG. Switzerland.

Geology, a branch of the natural sciences centered on observation, plays a pivotal role in modern society. It is instrumental in addressing two key challenges: the acquisition of new mineral resources and the understanding of climate change impacts. Geologists are tasked with discovering essential resources while optimizing extraction methods to mitigate ecological consequences. Simultaneously, they analyze rock records to glean insights into past climatic shifts.
Utilizing tools such as hammers, magnifying glasses, and data from geophysics, geochemistry, mineralogy, and geomorphology, geologists survey outcrops to decipher Earth's history and dynamics. This interdisciplinary approach combines foundational scientific principles with advanced technology, facilitating precise interpretations of Earth's processes. The practice of geological interpretation thrives on meticulous attention to detail, encompassing both micro and macro perspectives. Geologists also play a critical role in education, imparting fundamental geoscience principles and technological advancements. A tangible illustration of these responsibilities is evident in the mineral industry, exemplified by OMYA, where geologists contribute their expertise to resource management and technological innovation.

19.5
Geoscientists, guarantors of sustainable management of subsoil resources

Michel Meyer[1]

[1] *Services Industriels de Genève, 2 Château-Bloch, CH-1219 Vernier (michel.meyer@sig-ge.ch)*

When we look around us, and throughout our day, geologists are everywhere! From the mineral materials that make up our homes to the metals that transport us whether we're cycling or driving a car, from the plastic bags we use to the computer components we surf on, from the waterproof coat we wear in the rain to the sunglasses we wear when the weather's fine, in our light bulbs or candles, whether we light up with electricity or the glow of a small flame, in our rechargeable batteries or our internal combustion engines - everything is geology! Indeed, in most of the objects that surround us, mineral resources have been used and have therefore had to be the subject of preliminary work to locate and characterize them, before they can be exploited and made available. Geoscientists are among the most essential professions in the supply of raw materials required by our societies. Despite this fundamental role, fewer people are interested in geoscience training today than a few decades ago. And yet, never more than today are the skills of those trained in the Earth sciences required to find solutions to today's climatic, environmental, meteorological, energy and even geopolitical challenges. Knowledge of the mechanisms that drive our planet and of the resources available to us is of the utmost importance, and all the more so if we are to meet the imperatives of sustainable, coordinated resource management.

Subsoil as a substrate for ecological transition
The ecological transition will need the subsoil and its local resources to take place. The current paradigm of transporting all the resources required to satisfy any need anywhere in the world, in infinite quantities, is untenable. In the space of a few centuries, we have gone from a situation where development was only possible if resources (notably water, wood and rock) were available directly on the territory concerned, to a situation where cities are built in deserts and all the resources required are imported. In the future, local and regional resources will be given priority, in short, virtuous circuits where they can be recycled. We can no longer be satisfied with a situation where our knowledge of the subsoil is poor, because in any case the required resources will be imported, or those that are exploited locally can be exploited ad infinitum without concern for their sustainability. We need to re-anchor ourselves, and to do this we need to know which resources are available locally and which ones we'll have to dispose of, or else assume the risks of dependence on third parties.

Regional geology is set to regain its credentials as an answer to these questions, and universities in particular need to step up their teaching on this topic and on local issues related to the subsoil. In the future, geologists will no longer be mainly mercenaries sent around the world on successive missions to go from one finished deposit to another, but rather the guarantors of sustainable management and exploitation of the underground world, in a given territory. The Deep-City concept developed some fifteen years ago (Parriaux, A. et al. 2010) proposed a simplified methodology for integrating the subsoil and its resources into land-use planning. The Canton of Geneva drew on these principles to draw up its new law on subsoil resources and to create a new tool called the “subsoil resource management plan - PGR” (Etat de Genève 2022), which aims to protect and ensure the sustainable management of resources while creating a framework conducive to their efficient exploitation.

Job trends for geoscientists
In addition to the renewed role that geoscientists will play in our more sustainable societies, the number of geoscientists in countries with no mining, gas or oil traditions will increase. This dynamic was already set in motion some twenty years ago with the introduction of legislation on the identification of polluted sites and the remediation of contaminated sites. Indeed, alongside the historical themes of mining, oil and gas, geotechnics, natural hazards, hydrogeology, quarries and gravel pits, other environmental themes such as polluted sites and landfills, remediation work and management of polluted materials, recycling of mineral materials, renaturation of watercourses, environmental impact studies and, of course, geothermal energy issues have already gained considerable ground. Universities and other research institutes are training professionals in the specifics of geothermal energy, providing the market with people who have the skills required to carry out projects (Meyer 2021). As far as research is concerned, there is of course a need to develop innovative technologies for future generations, but there is also a need for research projects to enable know-how that exists elsewhere to be transferred to Switzerland. As a result, academia not only has a fundamental research role to play, but must also provide the foresight and feedback on which public and industrial strategies can be built. The academic world must regain the legitimacy to carry out research on very concrete and local elements, such as improving knowledge of regional geology, to encourage the recognition and implementation of best practices. This means not only continuing to develop training programs, but also carrying out communication initiatives to show that geoscience professions can be a way of getting directly and concretely involved in solving the current climate crisis. To reinforce this local anchoring and the potentially highly applied side of geology studies, links between universities and local professional players (industries, authorities, design offices, companies) should be strengthened and student involvement in local projects sought.

REFERENCES

Etat de Genève 2020 : Plan de gestion des ressources du sous-sol. https://www.ge.ch/dossier/gestion-durable-ressources-du-sous-sol/gerer-proteger-ressources-du-sous-sol/plan-gestion-ressources-du-sous-sol

Meyer, M. 2021 : Collaboration entre l'industrie, l'académie et la politique :L'expérience genevoise. Swiss Bull. angew. Geol. Vol. 26/1, 43-46.

Parriaux, A., Blunier, P., Maire, P., Dekkil, G.& Tacher, L. 2010 : Projet Deep City. Ressources du sous-sol et développement durable des espaces urbains. Lausanne, 100p.

P 19.6
Results from two surveys with employers of geologists and individual professional geologists in Switzerland – Suggestions to make the job we’re passionate about more attractive for everybody.

Monica Vogel, Peter Schürch

Swiss Association of Geologists CHGEOL, Dornacherstrasse 29, 4500 Solothurn (info@chgeol.ch)

CHGEOL represents around 400 professional geologists and 30 companies employing geologists in Switzerland. This year we have conducted two surveys. The first survey addressed our member companies regarding the job market and particular needs with respect to the training of geologist at Swiss universities. The second survey addressed our individual members with questions also regarding the job market and employee satisfaction in general.

Hence, we feel competent to raise the voice for those employing young professionals leaving Swiss universities with a degree in Earth sciences or geology, but also for those who work as geologists in Switzerland. We will present findings from these surveys and will draw conclusions for employers but also for institutions training geologists.

Switzerland is a small job market for geologists, but still there is a considerable thematic breadth in potential jobs. This is a challenge with respect to adequate training. The cohort of international students at Swiss universities not intending to work in Switzerland has increased. Some university programs have deviated from the specific needs of the Swiss geological consulting companies. In addition, some expertise needed to address future challenges faced in Switzerland, is not taught at Swiss universities. Some geologists quit their employment in geological jobs to move elsewhere, why? With our presentation we hope to shed light on these issues with the intent it may be useful for decision makers at company, university, or government level.

P 19.7
Geoscience Education in Switzerland – is there Potential for Improvement?

Martin Wyss

No Abstract submitted...

20 Earth Observation and Remote Sensing

Alex Damm, Dominik Brunner, Othmar Frey, Claudia Röösli, Stefan Wunderle

Swiss Commission on Remote Sensing

TALKS:

20.1 Ammar A.: Assessing GEDI LiDAR data for mangrove canopy height and aboveground biomass mapping in Indus Delta, Pakistan

20.2 Bernhard P., Haener D., Frey O.: Persistent Scatterer Interferometry to Assess Railway Track Conditions Using TerraSAR-X Observations

20.3 Cannata M., Strigaro D., Pozzoni M., Salvetti A.: Toward an event-driven infrastructure for in-situ monitoring systems

20.4 Fernández-García V., Franquesa M., Kull C.A.: Characterising fire regimes in Southeast Africa at 20 m spatial resolution

20.5 Ghiggi G., Berne A.: The GPM-GEO Archive: A Multimodal Remote Sensing Dataset for Clouds and Precipitation Research

20.6 Graf L.V., Aasen H.: Time matters: Investigating calendar days, growing degree days and phenological stages as temporal reference for vegetation productivity estimation from space

20.7 Irani Rahaghi A., Naegeli K., Bouffards D., Odermatt D.: Cal/Val of high-resolution lake surface water temperature remote sensing in support of Swiss lakes temperature monitoring and modeling activities

20.8 Oriani F., Aasen H., Schneider M.: Monitoring mountain pasture habitats based on satellite image analysis in response to different drought conditions.

POSTERS:

P 20.1 Czerski D., Del Siro C., Spataro A., Hofmann-Lanter H., Eicher M.: Monitoring of slopes exposed to superficial erosion after the application of biodegradable geotextiles: two case studies in Canton Ticino, Southern Switzerland

P 20.2 Fawcett D., D'Odorico P., Ginzler C., Gessler A.: The Forestward Observatory to Secure Resilience of European Forests (FORWARDS): Linking Ground Based and Remote Sensing Data on Tree Vitality

P 20.3 Ghiggi G., Berne A.: GPM-API : A Python Interface to Access the Global Precipitation Measurement Mission Satellites Open Data Archive

P 20.4 Mas Sanz E., Stefko M., Hajnsek I.: DEM generation and cryospheric investigations with KAPRI, a ground-based fully polarimetric interferometric radar

P 20.5 Vleghe P.L., Shiyi Li, Hajnsek I.: Revealing the recent height changes of the Great Altesch Glacier using TanDEM-X DEM series

20.1
Assessing GEDI LiDAR data for mangrove canopy height and aboveground biomass mapping in Indus Delta, Pakistan

Ahmad Ammar[1]

[1] *Geospatial Research and Education Lab, Institute of Space Technology, Islamabad, Pakistan (ahmadammargeo@gmail.com)*

Mangrove ecosystems are of critical importance, providing valuable ecological benefits such as coastal protection, biodiversity conservation and carbon sequestration. Accurate mapping of canopy height (CH) and aboveground biomass density (AGBD) of these forests is essential for understanding their structural characteristics and carbon storage potential. We develop a wall-to-wall mapping approach for CH and AGBD estimation in the threatened Indus Delta mangroves (Pakistan) while assessing the Global Ecosystem Dynamics Investigation (GEDI) Light Detection and Ranging (LiDAR) data which provides high-resolution three-dimensional insights into the structure of forested lands, improving our ability to assess overall ecosystem health. GEDI mission provides footprints spaced apart along the satellite track, resulting in a sampling approach that captures a representative subset of the forests. Using Random Forest (RF) Machine Learning (ML) models, representative samples from GEDI L2A RH98 and L4B AGBD data are separately predicted against remotely sensed features and indices calculated and selected from a fusion of ALOS PALSAR-2, Sentinel-1 SAR and Sentinel-2 optical imagery. The resulting continuous surfaces are assessed against in-situ plot-level CH averages and AGBD measurements, i.e., min, max and mean of 1.63, 8.93 and 3.42m, and 0.71, 134.73 and 22.13 Mg/ha respectively. The validated maps after applying regression yield R2, RMSE, min, max and mean of 0.662, 0.5m, 1.68m, 9.06m and 2.84m respectively for CH, and 0.57, 17.47 Mg/ha, 3.78 Mg/ha, 208.23 Mg/ha and 17.35 Mg/ha respectively for AGBD which are comparable with in-situ measurements. However, the initially produced wall-to-wall AGBD map based on GEDI observations is shown to significantly underestimate AGBD in our study area, with min, max and mean of 0.82, 17.81 and 1.84 Mg/ha compared to the respective in-situ measurements. Nonetheless, these results indicate the usefulness of GEDI mission for cost-effective large-scale mapping by exploiting the potential of geo-computing cloud platform of Google Earth Engine (GEE) and contributes towards national inventorial mapping, facilitating efforts to protect and restore these endangered habitats.

20.2
Persistent Scatterer Interferometry to Assess Railway Track Conditions Using TerraSAR-X Observations

Philipp Bernhard[1], David Haener[2], Othamr Frey[1,3]

[1] *Earth Observation and Remote Sensing, ETH Zürich, Laura-Hezner-Weg 7, 8093 Zürich (bernhard@ifu.baug.ethz.ch)*
[2] *Swiss Federal Railways, SBB AG, Bern*
[3] *Gamma Remote Sensing AG, Bern*

The Swiss railway network is one of the most heavily used railway networks in the world. The planning, construction, operation, and maintenance of the infrastructure require considerable resources. Increasingly, new approaches and technologies are required to maintain the condition of the railway network and installations at a standard which meets operational safety requirements while keeping costs at a minimum. Remote sensing techniques using spaceborne radar systems are of particular interest for the inspection of railway infrastructure components, potentially, with high efficiency. If deterioration processes can be detected at an early, measures can be undertaken to improve the drainage situation and thus extend the service lifetime of the track. Current operational methods for measuring the railway track conditions rely on measurements from track geometry vehicles (chord and inertial measurement methods) and in-situ track condition evaluation methods (geotechnical investigations, visual inspection, excavation of sub-ballast, among others) (Landgraf 2018).
Spaceborne synthetic aperture radar (SAR), and SAR interferometry (InSAR) in particular, are promising to monitor the railway infrastructure due to its all-day, all-weather imaging capabilities and its relatively high temporal resolution. While radar interferometry as a technique is quite mature, critical factors, are i) sufficient temporal coherence ii) sufficient radar data acquisitions and temporal sampling rates and iii) temporal behavior of surface displacement (constant velocity, vs. abrupt changes). In this study we are using a time-series of TerraSAR-X observations to performed a persistent scatterer interferometry (PSI) analysis (Wegmuller 2009) to estimate surface deformations along 75km of railway track in the region around Basel, Switzerland. To analyze the PSI result, we applied a 2-meter buffer around the center of the track line and project the PSs on the closest point on the track. Drawing motivation from the chord-based measurement principle, we utilized the PSI deformation rates to extract several statistics within different sizes of moving windows along the track (50m, 200m). These statistics include the moving standard deviation of surface displacements, the number of PSI points with significant deformation values and the fraction of points excluded by employing quality thresholds in the regression-based deformation estimation. We use time-series data of chord-based measurements for comparison and validation.
To explore the hypothesis that the variability of PSI deformation measurements can be related to the longitudinal height measurements obtained from track geometry measurement vehicles we employ simple thresholding approaches. Preliminary results show a correlation between the PSI-derived quantities and problematic track parts indicated by the chord-based measurements. We furthermore investigate similarities and differences between the two approaches. A satellite-based measurement method to evaluate the railway track condition that is applicable on the network level has a high potential to significantly reduce the required resources of the railway infrastructure maintenance.

REFERENCES
Landgraf, M. (2018), Smart data for sustainable Railway Asset Management, Monographic Series TU Graz / Railway Research, Issue 3, 10.3217/978-3-85125-569-0.
Wegmuller, U., Walter, D., Spreckels, V. and Werner, C.L, (2009) Nonuniform ground motion monitoring with TerraSAR-X persistent scatterer interferometry, IEEE Transactions on Geoscience and Remote Sensing 48.2: 895-904.

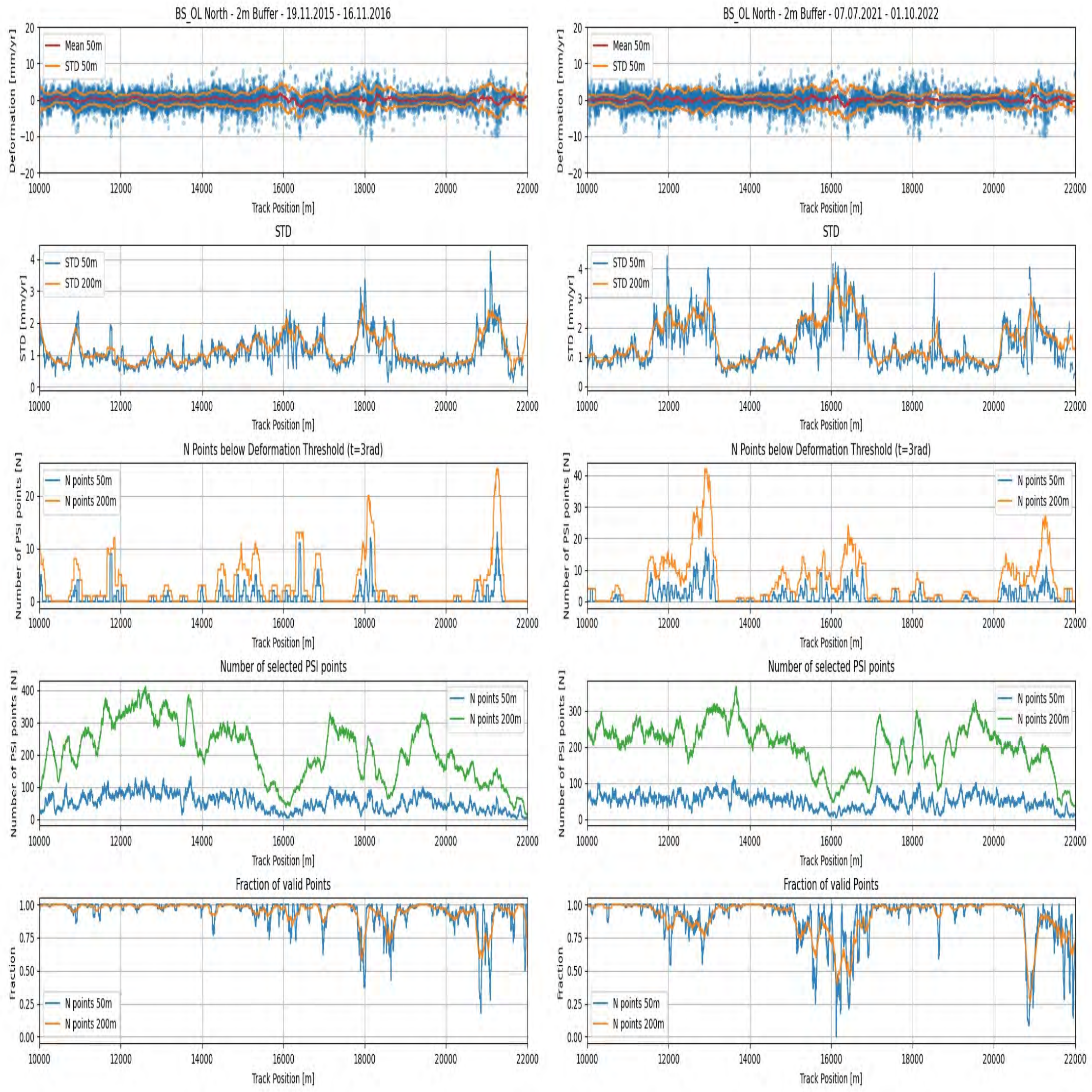

Figure 1 Example of computed PSI-based features along the railway track. The top row shows the deformation rates of PSs projected to the closed point on the track. The second row shows the standard deviation inside a 50m and 200m moving window. The third row shows the number of PS points above a threshold t. The fourth and the fifth tow show the number of selected PS points and the fraction of these with an accepted solution. Several parts of the track show an increase in these properties which could potentially indicate problematic track conditions.

20.3
Toward an event-driven infrastructure for in-situ monitoring systems

Massimiliano Cannata[1], Daniele Strigaro[1], Maurizio Pozzoni[1], Salvetti Andrea[2]

[1] *SUPSI, Istituto scienze della Terra, DACD, Canobbio, Switzerland (massimiliano.cannata@supsi.ch)*
[2] *Canton Ticino, Divisione delle costruzioni, Ufficio corsi d'acqua, Bellinzona, Switzerland*

Microservice architecture reflecs the cutting-edge approach in cloud application development (used by Amazon, Netflix and Twitter i.e.). In this approach a number of lightweight services (microservices), each designed to serve a specific domain, are virtualized in containers (such as Docker i.e.) and deployed, interconnected, in the cloud. This approach offers a large number of advantages like lower costs, faster innovation, isolated risk, flexibility and agility, local performance optimization, and unlimited value-add [1]. Due to these advantages, this architecture has been adopted also in the management of Hydromet-TI, the hydro-meteorological monitoring networks of the Canton Ticino where a number of processes activated at predefined time intervals (cron-jobs) and following a cascading logic are executed to collect data from FTP servers, archive them in a structured database accessible trough standard services, aggregate raw data to lower resolutions, perform data quality validations, deliver data to authorized partners, and check system health status [2]. While benefiting from microservice architecture, the cascading and time-based approach may pose some limitations for data-intensive real-time data processing due to latency problems and concentrated resource usage. The adoption of an event-driven and choreographed approach could greatly contribute to reduce those issues and realize a more flexible, efficient and reactive system [3]. Nevertheless, this change in architecture to be effectively exploited requires the redesign and development of several procedures. In this work we presents the provisional results of the on-going Hydromet-TI transition toward a event-based micro-service choreographed architecture discussing the network nodes adaptation, the designed architecture, the adopted technologies and logics and the implemented processes and services.

REFERENCES
[1] Blinowski, Grzegorz, Anna Ojdowska, and Adam Przybyłek. «Monolithic vs. microservice architecture: A performance and scalability evaluation.» IEEE Access 10 (2022): 20357-20374.
[2] Pozzoni, Maurizio, Andrea Salvetti, and Massimiliano Cannata. «Retrospective and prospective of hydro-met monitoring system in the Canton Ticino, Switzerland.» Hydrological Sciences Journal 67.16 (2022): 2386-2400.
[3] Khriji, Sabrine, et al. «Design and implementation of a cloud-based event-driven architecture for real-time data processing in wireless sensor networks.» The Journal of Supercomputing (2022): 1-28.

20.4
Characterising fire regimes in Southeast Africa at 20 m spatial resolution

Víctor Fernández-García[1,2], Magí Franquesa[3], Christian A. Kull[1]

[1] *Institute of Geography and Sustainability, University of Lausanne, Géopolis, CH-1015 Lausanne (victor.fernandezgarcia@unil.ch)*
[2] *Ecology, Faculty of Biology and Environmental Sciences, Universidad de León, 24071 León*
[3] *Instituto Pirenaico de Ecología, Consejo Superior de Investigaciones Científicas (IPE-CSIC), 50050 Zaragoza*

Burned area and fire regimes can be characterised across the globe using global burned area products. Those products are traditionally based on coarse-resolution imagery such as MODIS (or Moderate Resolution Imaging Spectroradiometer) which provides information at 250 and 500 m spatial resolution. Recently, other alternatives have been developed such as those based on Sentinel-3 (300 m) and Landsat imagery, with much finer pixel sizes but a lower revisit period (16 days). However, validation exercises (Franquesa et al., 2022) and recent advances in remote sensing (Ramo et al., 2021) have revealed large deficiencies in these global burned area products suggesting that the global burned area might be much higher. The burned area underestimations from global products in Africa have been quantified at >60%, and might be even larger in those regions where there is a high number of small fires, a rapid fade of burn scars, or where cloudiness limits the proper retrieval of land surface reflectance (Fernández-García & Kull, 2023). Within this context, Sentinel-2 imagery, available since 2015, reaches a better balance between spatial (20 m) and temporal resolutions (5 days combining the Sentinel-2 twin sensors) compared to other non-commercial satellites. One major challenge of using Sentinel-2 higher quality data is the need for high computational capacities, which nowadays can be addressed thanks to cloud computing platforms such as Google Earth Engine.

In this work we show how we developed and validated a burned area database for Southeast Africa (Madagascar, southern Mozambique, Eswatini and eastern South Africa) (Fernández-García et al., 2023). In addition, we used this database to characterise recent fire regimes in these four regions using fire recurrence and burning seasonality data for the period 2016-2022.

A total of 165,833 Sentinel-2 images were used to build the database, resulting in 25 GB of product data. The validation process in Madagascar revealed an accuracy much higher than global burned area products, with around four times more burned area every year. In general 57% of Sentinel-2 pixels burned at least once in Madagascar, 61% in southern Mozambique (Fig. 1), 43% in Eswatini and 23% in eastern South Africa between 2016 and 2022. The characterization of fire regimes in those four regions showed a large spatial heterogeneity, with well represented fire recurrence categories (annual, biennial, triennial burnings) and seasonalities (burnings out of the fire season and within the fire season).

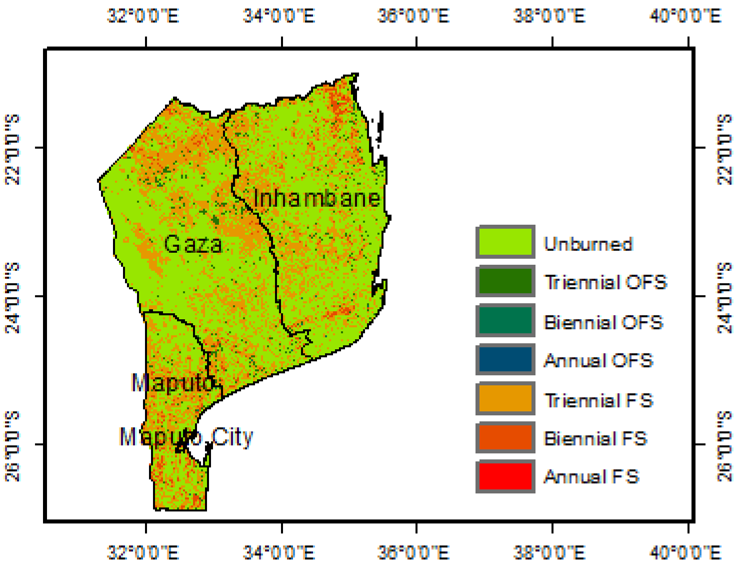

Figure 1. Spatial patterns of the fire regimes identified in southern Mozambique. OFS: Out of the fire season, FS: fire season.

Our work demonstrates the need of using imagery at similar or higher spatial and temporal resolution than Sentinel-2 to address burned area mapping and characterizations of fire regimes. Likewise, our dataset provides updated burned area estimates for these four regions that can be used to improve national statistics, as well as to implement environmental and social studies about fire.

REFERENCES

Fernández-García, V., Franquesa, M., Kull, C. A. 2023: A burned area database from Sentinel-2 imagery (2016-2022) for Madagascar, southern Mozambique, Eswatini and Eastern South Africa, submitted to PANGAEA.

Fernández-García, V., & Kull, C. A. 2023: Refining historical burned area data from satellite observations, International Journal of Applied Earth Observation and Geoinformation, 120, 103350.

Franquesa, M., Lizundia-Loiola, J., Stehman, S. V., & Chuvieco, E. 2022: Using long temporal reference units to assess the spatial accuracy of global satellite-derived burned area products, Remote Sensing of Environment, 269, 112823.

Ramo, R., Roteta, E., Bistinas, I., van Wees, D., Bastarrika, A., Chuvieco, E., & van der Werf, G. R. 2021: African burned area and fire carbon emissions are strongly impacted by small fires undetected by coarse resolution satellite data, Proc. Natl. Acad. Sci. U.S.A., 118, e2011160118.

20.5
The GPM-GEO Archive: A Multimodal Remote Sensing Dataset for Clouds and Precipitation Research

Gionata Ghiggi[1], Alexis Berne[1]

[1] *Environmental Remote Sensing Laboratory (LTE), EPFL, Lausanne, Switzerland (gionata.ghiggi@epfl.ch)*

The GPM-GEO archive is a unique analysis-ready dataset that combines third-generation geostationary (GEO) satellite multispectral VIS/IR imagery, precipitation and clouds products, with precipitation measurements acquired by the Global Precipitation Measurement Mission (GPM) Dual-frequency Precipitation Radar (DPR).

The archive was created to encourage synergistic and collaborative use of multiple data sources, to enable a broad range of studies in clouds and precipitation research and to support the development of new GEO precipitation products. One key application of the GPM-GEO archive is in the development of new artificial intelligence algorithms for GEO precipitation monitoring. At the global scale, the GPM DPR gives the best available precipitation estimates, hence providing a valuable reference for synthesizing precipitation latent heating profiles assimilable by numerical weather prediction models. It also enables the training of convection or hail detection algorithms. Unlike previous approaches, which most often relied on selecting regional representative data samples, the GPM-GEO archive provides the largest global sample database, allowing for the development of data-driven algorithms that can compensate for the lack of physical understanding and theoretical description of the relationship between the GEO-sensed VIS/IR radiances and the precipitation geophysical quantities of interest.

The GPM-GEO dataset is made up of 5 products currently produced using the GOES and HIMAWARI satellites data. The RAD product provides calibrated radiances for the 16 bands of the ABI and the AHI sensors. The QPE product includes the precipitation rate estimates derived from the GEO L2 RRQPE products, while the CLOUDS product provides the Cloud Mask, Cloud Top Phase, Cloud Top Temperature, Cloud Top Height (CTH), Cloud Effective Radius and Cloud Optical Depth derived from the respective GEO L2 products. The ANGLES and AUX products contain variables that facilitate the analysis of the dataset: these include the viewing angle of the GEO satellite and the sun, as well as the local solar time of each pixel acquisition. Auxiliary information on the surface land cover, elevation, as well as the top-of-the-atmosphere incoming solar radiation is also provided.

The GPM-GEO dataset, available from April 2019 to present, is generated when GEO Full Disc acquisitions occur every 10 minutes, resulting in a temporal mismatch of less than five minutes between satellite pixel acquisitions. For each GPM overpass within the GEO Field Of View (FOV), the GPM-GEO dataset includes the GEO data acquired between -40 to +20 minutes from the GPM DPR scanning time. These GEO data are remapped onto the GPM DPR swath scans, enforcing a swath image spatial resolution of 1km. To limit the effects of parallax, the GPM-GEO collocation is performed only on a reduced portion of the GEO FOV where the maximum parallax displacement is below 20 km (when considering a 10 km CTH in the mid-latitudes).

To facilitate the analysis of the dataset, the GPM-GEO software provides utilities for dataset manipulation, interactive exploratory analysis, visualization and the creation of meteorological composites that enable the overlay of the various products. Additionally, the GPM-GEO software code is modularized in a way that can be easily adapted and reused for the collocation of other sensors such as IR sounders and LEO VIS/IR sensors.

In summary, the GPM-GEO archive provides a valuable resource for researchers interested in clouds and precipitation studies and facilitates the development of new data-driven algorithms for precipitation monitoring and forecasting.

20.6
Time matters: Investigating calendar days, growing degree days and phenological stages as temporal reference for vegetation productivity estimation from space

Lukas Valentin Graf[1,2], Helge Aasen[1,2]

[1] *Crop Science, Institute of Agricultural Science, ETH Zürich, Universitätstrasse 2, CH-8092 Zürich (lukasvalentin.graf@usys.ethz.ch)*
[2] *Earth Observation of Agroecosystems Team, Division Agroecology and Environment, Agroscope, Reckenholzstrasse 191, CH-8046 Zürich*

Tracking vegetation productivity is pivotal to mitigate climate change effects, the simultaneous steady increase in demand for food and biomass and ensure more sustainable use of limited resources in a more resilient way. Time series of optical satellite data are an essential source to derive plant traits related for vegetation productivity.

Previous research has mainly focused on the detection of outliers and the filling of temporal gaps to understand spatio-temporal vegetation dynamics to reconstruct reliable time series data from satellite data. But so far, little attention has been paid to an essential part of time series analysis: The “timing” of the signal – or in other words – the “time axis” to which the signal is related. Obviously, time can be expressed as calendar dates. However, this neglects the mutual dependence of plant characteristics on phenological development.

Phenological development stages, in turn, are closely linked to environmental influences, such as the annual cycle of day length, precipitation patterns, and temperature curves. In our contribution, we highlight different time axis representation options for time series of satellite-based plant traits and what implications these have for the study of plant-environment interactions. The claim is that only with a sound understanding and, hence, representation of phenological development the potential of remotely sensed time series to quantify ecosystem productivity at larger spatial scales can be fully exploited. In addition, climate change requires conscientious consideration of phenological shifts to avoid misinterpretation of changes in vegetation dynamics.

To support this claim, we will use an in-situ data set collected in the Swiss agricultural landscape, as well as Sentinel-2 time series of the Green Leaf Area Index from winter wheat field parcels in Switzerland. In this course, we will present examples of how the interplay of environmental covariates, phenology, and vegetation traits can be used to advance remotely sensed vegetation time series reconstruction and interpretation.

20.7
Cal/Val of high-resolution lake surface water temperature remote sensing in support of Swiss lakes temperature monitoring and modeling activities

Abolfazl Irani Rahaghi[1,2], Kathrin Naegeli[2], Damien Bouffard[3,4], Daniel Odermatt[1,2]

[1] *Eawag, Swiss Federal Institute of Aquatic Science & Technology, Surface Waters – Research and Management, 8600 Duebendorf, Switzerland (abolfazl.irani@eawag.ch)*
[2] *Department of Geography, University of Zurich, 8057 Zurich, Switzerland*
[3] *Eawag, Swiss Federal Institute of Aquatic Science & Technology, Surface Waters – Research and Management, 6047 Kastanienbaum, Switzerland*
[4] *Institute of Earth Surface Dynamics, Department of Geosciences and Environment, University of Lausanne, 1015 Lausanne, Switzerland*

Lake Surface Water Temperature (LSWT) is often considered as the reference essential climate variable for climate changes. Satellite thermal imagery has been one of the key sources of LSWT monitoring. However, accurate LSWT satellite retrieval remains challenging. In particular future high-resolution thermal Earth Observation (EO) missions, such as TRISHNA with a large viewing zenith angle and a high revisit, requires adequate in situ measurements, as well as algorithm calibration and validation. The ultimate goal of this research, conducted under the Swiss TRISHNA – Science and Electronics Contribution (T-SEC) project funded by ESA Prodex, is to improve the thermal products of upcoming TRISHNA mission and similar EO sensors for inland and coastal waters. In this study, we specifically aim at (i) assessing the effect of morphological and meteorological features on LSWT retrievals, and (ii) investigating and improving existing LSWT algorithms (e.g., Acolite-TACT, USGS-L2) based on those features. Here, we report on our existing and planned study sites in the Swiss Alps, and present the instrumentation and preliminary results for four pre- and high-alpine lakes: (1) Lake Geneva (deep large lake; 372 m a.s.l.), (2) Ägerisee (mid-size lake; 724 m a.s.l.), (3) Steinsee (small glacier lake; 1934 m a.s.l.), and (4) Rhonesee (small glacier lake; 2200 m a.s.l.). Our preliminary matchup analysis between in situ measurements and Landsat 7/8/9 LSWT products looks promising. The results indicate a Mean Absolute Error (MAE) of < 1.5 °C, and a correlation coefficient of > 0.95. On the regional scale, our research will complement and profit from the ongoing lake monitoring and modeling activities in Switzerland, such as (i) Swiss Lake temperature monitoring network (https://www.bafu.admin.ch/bafu/en/home/topics/water/wasser--dossiers/swiss-lakes-new-stations-monitor-water-temperature-in-real-time.html), which is a pilot project conducted by eawag and the Federal Office for the environment (FOEN/BAFU) for continuous Swiss lakes temperature monitoring and assessment, (2) real-time 1D numerical modeling of several Swiss lakes using Simstrat (www.simstrat.eawag.ch), and (3) real-time 3D numerical modeling of selected pre- and high-alpine lakes (https://www.alplakes.eawag.ch).

20.8
Monitoring mountain pasture habitats based on satellite image analysis in response to different drought conditions.

F. Oriani [1,2], H. Aasen[2], M. Schneider[1]

[1] *Forage Production and Grassland Systems, Agroscope, Zurich (CH).*
[2] *Water Protection and Substance Flows Group Agroscope, Agroscope, Zurich (CH).*

Mountain pastures host rich plant biodiversity organized in various distinct habitats. An accurate long-term monitoring, going beyond the sole ground survey, is of primary importance for nature conservation and forage production planning. Within the GrassSense project, we develop a novel analytical framework to identify and monitor plant communities in mountain pastures based on the joint statistical analysis of ground data and satellite imagery. The driving research questions are whether it is possible to distinguish mountain pasture communities using commonly available satellite imagery and which analytical workflow and satellite products are suitable to track spatial and temporal changes.

We developed a workflow to monitor the greening of plant habitats, consisting of the following steps:

1) We considered as study zone the mid-to-high elevation mountain pastures surrounding the Swiss National Park in the Grisons canton, mapped over approx. 100 sq. km for pasture vegetation associations, including fertile pastures, wetlands, dry plant communities, and shrubs.

2) We coupled the ground classification to the reflectance signal measured in satellite images of the public product Sentinel-2 (European Space Agency): in particular, we computed the NDVI spectral index, which is a proxy for living vegetation and detects greening activity. The retrivial of a large amount of images for the extentive study zone was possible using the Eodal platform, recently developed at Agroscope [Graf et al. 2022].

3) To obtain a consistent signal, the dataset was preprocessed: i) to remove images which show less than 10% of the data in the vegetation parcels, ii) to exclude pixels in the mountain or cloud shadow, and iii) to consider only south-facing parcels, in an azimuth range of 90-270 degrees.

4) Then we analyzed the statistical distribution of NDVI in the greening season for the different habitat units and different elevation. Moreover, the response of the units to different drought conditions is analysed by considering a particularly dry and wet years respectively.

The results show that pasture habitats present different annual seasonality of the NDVI, linked to their phenological cycle. In particular, mesic fertile, infertile, and wet fertile pasture show an NDVI peak above 0.75 while, in the other units, it tends to be lower, with tall shrubs mainly below 0.5. Moreover, drought conditions seem to affect the beginning of the greening season, which occurs 40 to 50 days earlier in a wet year (Figure 1, 2020 blue color) than in a dry year (Figure 1, 2019 orange color).

The workflow developed in this study suggests that remote sensing imagery of mid-to-high resolution is a valid auxiliary tool to monitor the vegetation variability in mountain pastures, and to characterize, spatiotemporally and for different habitats, the changes in the phenological cycle due to different water availability conditions. Future studies will be devoted to refine this type of analysis with a link to plant physiology indicators, which are physically measurable on the field.

REFERENCES

Graf, L.,V., Perich, G., Aasen, H., 2022: EOdal: An open-source Python package for large-scale agroecological research using Earth Observation and gridded environmental data, Computers and Electronics in Agriculture, Volume 203, https://doi.org/10.1016/j.compag.2022.107487

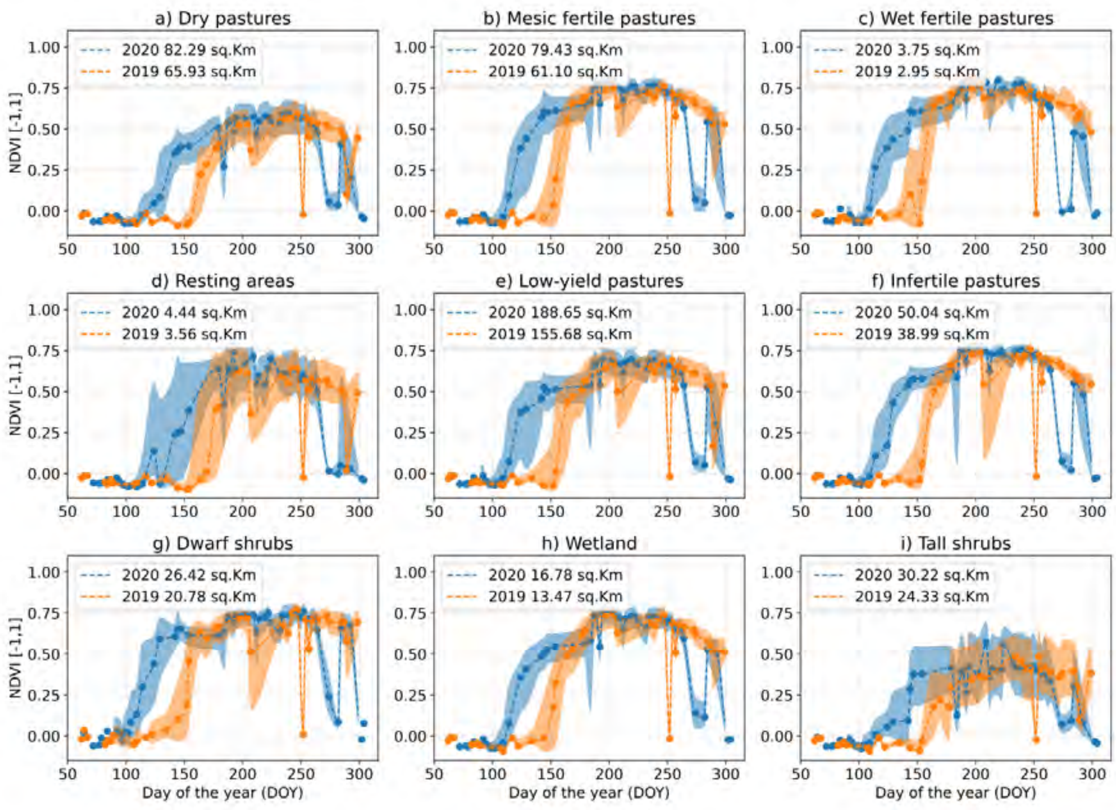

Figure 1. Annual NDVI Curve estimated on the bases of submonthly Sentinel-2 images in a relatively wet (blue color) and dry (orange color) years, with indicated the total surface analyzed. For every habitat unit (subfigures from a to i), the dashed line indicated the median NDVI value in time and the shaded area indicates the 25th - 75th percentile interval. The total surface analyzed in the two years is indicated in the legend.

P 20.1
Monitoring of slopes exposed to superficial erosion after the application of biodegradable geotextiles: two case studies in Canton Ticino, Southern Switzerland

Dorota Czerski[1], Chantal Del Siro[1], Alessio Spataro[1], Helene Hofmann-Lanter[2], Manuel Eicher[2]

[1] *Scuola universitaria professionale della Svizzera italiana (SUPSI), Institute of Earth sciences, Via Flora Ruchat-Roncati 15, CH-6850 Mendrisio (dorota.czerski@supsi.ch)*
[2] *Geobrugg AG, Aachstrasse 11, CH-8590 Romanshorn*

Research in the field of erosion prevention and slope stabilization, whether of natural or artificial origin, is continually advancing. Emerging techniques, aside from providing an answer from an engineering perspective, are focused on reducing environmental impacts and providing more sustainable solutions. This research project involves the application and monitoring of a bio-based, biodegradable geotextile intended for helping revegetation and erosion control on slopes facing a combination of unfavorable conditions. Importantly, this approach aims to avoid long-term environmental traces such as microplastics.

The mechanical properties of the geotextile and its degradation rate have already undergone laboratory testing. The current project aims to test the material on the field, under real environmental and climatic conditions. To achieve this, two large-scale 1:1 field tests were established in Canton Ticino, Southern Switzerland. These two study sites, located one in Maroggia and one in Chiasso, differ in slope exposure, steepness, and microclimatic conditions.

Following the installation of the geotextile in spring 2022, a comprehensive seasonal monitoring initiative spanning two years was launched. Scientific dataloggers are used to continuously measure soil temperature and humidity. Erosion levels are quantified through geodetic surveys combined with detailed 3D scanning of the slope using a laser scanner (LS Riegl VZ-4000). The rate of revegetation is assessed using UAV multispectral imagery to determine the NDVI (Normalized Difference Vegetation Index) with a DJI P4 Multispectral drone.

Moreover, soil physical-mechanical parameters, including grain size, permeability, and shear strength, were determined through both field and laboratory tests. In this contribution, we present the characteristics of the two study sites and combine them with the initial results obtained from the monitoring.

P 20.2
The Forestward Observatory to Secure Resilience of European Forests (FORWARDS): Linking Ground Based and Remote Sensing Data on Tree Vitality

Dominic Fawcett[1], Petra D'Odorico[1], Christian Ginzler[1], Arthur Gessler[1]

[1] *Eidgenössische Forschungsanstalt für Wald, Schnee und Landschaft (WSL), 8903 Birmensdorf, Switzerland (dominic.fawcett@wsl.ch)*

Environmental stresses exacerbated by climate change create increasing pressure on forest ecosystems, challenging their resilience and functioning. Remote sensing of leaf/canopy reflectance information allows estimation of tree functional traits linked with forest health, acclimation and adaptation. Through spectral data it is possible to detect element concentrations linked with the nutritional status of trees and pigments associated with the regulation of photosynthesis and photoprotection (D'Odorico et al., 2021). This allows mapping visible damage to leaves but also pre-visual vulnerability symptoms (e.g. downregulation). As part of the Forestward Observatory to Secure Resilience of European Forests (FORWARDS), we will develop methods to link ground-based measurements of tree vitality (leaf sampling and continuous measurement of tree water deficit) to reflectance data. We make use of multiple scales of remote sensing observations, from drone, aircraft and satellite data, to investigate and demonstrate how signals derived from reflectance scale and how they can eventually be used for European-wide forest monitoring.

A pilot phase of this project focused on three intensively monitored sites in Switzerland. For these sites, leaf and tree-level data in the field as well as multi- and hyperspectral acquisitions by drone and airborne instruments were acquired in August 2023. We will present early results from multispectral drone data of this pilot campaign as well as our concept and further plans in developing methodologies and extending our work to multiple sites across Europe in 2024.

REFERENCES

D'Odorico, P., Schönbeck, L., Vitali, V., Meusburger, K., Schaub, M., Ginzler, C., Zweifel, R., Velasco, V. M. E., Gisler, J., Gessler, A., & Ensminger, I. 2021: Drone-based physiological index reveals long-term acclimation and drought stress responses in trees. Plant, Cell & Environment, 44(11)

P 20.3
GPM-API : A Python Interface to Access the Global Precipitation Measurement Mission Satellites Open Data Archive

Gionata Ghiggi[1], Alexis Berne[1]

[1] *Environmental Remote Sensing Laboratory (LTE), EPFL, Lausanne, Switzerland (gionata.ghiggi@epfl.ch)*

Since the launch of the Tropical Rainfall Measuring Mission (TRMM) satellite in 1997, the follow-up satellites part of the Global Precipitation Measurement Mission (GPM) have generated till present a 26-year long precipitation data records. Over this period, the GPM constellation has been composed of two orbiting spaceborne radars and a fleet of 26 passive microwave (PMW) sensors. The GPM data archive is composed of various product levels, ranging from raw and calibrated measurements (L1) to intermediate geophysical retrieval products (L2), and multi-satellites merged datasets (L3).

Application programming interfaces (APIs), are intermediary tools for exchanging data between computer programs. APIs simplify software development and innovation by enabling applications to exchange and retrieve data fast and easily in a common standard format. Researchers and developers are not requested to know how an API is implemented; they simply use the interface to communicate and retrieve the products they need.

The presented GPM-API software is a python interface designed to simplify the download, processing, manipulation, and visualization of such a heterogenous data archive which sizes several petabytes.

The GPM-API offers a user-friendly interface that enables researchers and developers to (1) download the GPM products of interest (i.e. over desired region and/or time period) from the NASA servers, (2) search for the GPM files on the local disk, (3) open the products with a single line of code in an analysis-ready-data format and making it Climate and Forecast (CF) conventions compliant, (4) facilitate on-disk (lazy) and distributed processing of the archive, (5) display the product variable(s) of interest according to their intrinsic specifications, (6) identify customly-defined precipitation events and precipitating systems across the dataset temporal record, as well as (7) extract spatial (and temporal) data patches for the design of new physical retrievals and/or the training of new machine learning algorithms.

GPM-API aims to increase scientist productivity by simplifying coding tasks associated with data download, reading, manipulation and visualization design. This will accelerate model prototyping and development, will promote the improvement of precipitation retrieval algorithms and will foster research reproducibility. These simplifications will also widen the GPM users' community, enabling for example students and people with limited programming skills or remote sensing/meteorology background to engage with global precipitation data, making the GPM archive easily exploitable also for educational purposes.

The GPM-API software is available at https://github.com/ghiggi/gpm_api .

P 20.4
DEM generation and cryospheric investigations with KAPRI, a ground-based fully polarimetric interferometric radar

Esther Mas I Sanz[1], Marcel Stefko[1], Irena Hajnsek [1,2]

[1] *Institute of Environmental Engineering, ETH Zürich, Laura-Hezner-Weg 7, CH-8093 Zürich, Switzerland (esmasi@ethz.ch)*
[2] *Microwaves and Radar Institute, German Aerospace Center, Germany*

Radar remote sensing is a commonly used technique for Earth Observation and studying the natural environment. Mainly, two techniques are used to extract the information contained in the radar signal: polarimetry and interferometry. Polarimetry provides information on the different scattering mechanisms that take place within the resolution cell and describe how the signal interacts with the natural medium. On the other hand, interferometry exploits the information resulting from the phase differences between two signals. This might be the phase differences from two acquisitions retrieving data at the same time slightly from different observation angles (single-pass interferometry) or the phase difference between observations across time (differential interferometry). In the first case, the resulting phase can be converted to height and is commonly used for digital elevation model (DEM) generation. The latter allows to monitor displacements in the direction of the line-of-sight (LOS) of the radar, proving to be specially useful when targeting dynamic processes in nature which involve the motion of the terrain, such as soil settlements, glacier displacements, thermal dilation, etc.

Radar systems are extremely versatile and can be installed in a wide range of platforms, varying from ground-based sensors to air and space-borne ones. While radar sensors used in satellites offer vast coverage swaths, they are only capable of retrieving new information in a few days span, at best. In case of aircraft-based sensors, revisit times can be shortened to tens of minutes but still the time series span is limited. In contrast, ground-based systems offer the advantage of high-density repetition times for prolonged durations, hence, providing extended time series while reducing time decorrelation. It must be noted, at the expense of reduced coverage. This is particularly useful when observing natural phenomena within a limited spatial extent that presents variations in a matter of hours or even minutes, for instance, in glacier monitoring, the focus of our current investigations. A common approach in glacier monitoring is obtaining DEMs at different seasons and comparing the height differences to assess the volume loss of the glacier (Gardelle 2012). However, variations in the snow properties resulting from, for example, a snowfall or an increase in water content due to a temperature rise, have a direct impact on the received radar signal changing its penetration depth and eventually yielding different heights on the DEMs (Guneriussen 2001). How can these variations be accounted when generating DEMs? Furthermore, based on these alterations of the interferometric phase, is it possible to retrieve the properties of the snowpack by combining with other techniques such as polarimetry and tomography?

To address these questions, KAPRI (Ku-band Advanced Polariemtric Radar Interferometer), a ground-based portable, frequency-modulated continuous-wave (FMCW) radar is used. This radar is based originally on the GPRI (Gamma Portable Radar Interferometer) and modified to be able to acquire fully-polarimetric measurements (Baffelli, 2018). Moreover, the system was further upgraded together with the development of a new processing pipeline to operate in bistatic mode by making use of two independent KAPRI devices, one functioning as the primary transmitter/receiver and the other as the secondary receiver (Stefko, 2022a). KAPRI's bistatic capabilities were recently applied to characterize the coherent backscatter opposition effect (CBOE) in dry snow (Stefko, 2022b).

In this poster, preliminary results of the DEMs from the monostatic data at two different seasons (summer of 2021 and winter of 2022) as well as bistatic acquisitions are presented. The current research with KAPRI focuses on DEM generation at the Aletsch Glacier (Switzerland) using the seasonal monostatic data. The aim is combining the monostatic data with the bistatic acquisitions in order to reconstruct 3D deformation vectors that describe the glacier flow. Moreover, the data of these campaigns (in addition to future ones) constitutes a seasonal dataset that will be further investigated to characterise snow parameters by exploring scattering phenomena in the bistatic configuration featured on the polarisation matrix as non-symmetries.

REFERENCES

Baffelli, S., Frey, O., Werner, C., & Hajnsek, I. (2018). Polarimetric calibration of the ku-band advanced polarimetric radar interferometer. IEEE Transactions on Geoscience and Remote Sensing, 56(4), 2295–2311. https://doi.org/10.1109/TGRS.2017.2778049

Gardelle, J., Berthier, E., & Arnaud, Y. (2012). Impact of resolution and radar penetration on glacier elevation changes computed from DEM differencing. Journal of Glaciology, 58(208), 419–422. https://doi.org/10.3189/2012JOG11J175

Guneriussen, T., HЈgda, K. A., Johnsen, H., & Lauknes, I. (2001). InSAR for estimation of changes in snow water equivalent of dry snow. IEEE Transactions on Geoscience and Remote Sensing, 39(10), 2101–2108. https://doi.org/10.1109/36.957273

Stefko, M., Frey, O., Werner, C., & Hajnsek, I. (2022a). Calibration and Operation of a Bistatic Real-Aperture Polarimetric-Interferometric Ku-Band Radar. IEEE Transactions on Geoscience and Remote Sensing, 60, 1–19. https://doi.org/10.1109/TGRS.2021.3121466

Stefko, M., Leinss, S., Frey, O., & Hajnsek, I. (2022b). Coherent backscatter enhancement in bistatic Ku- and X-band radar observations of dry snow. Cryosphere, 16(7), 2859–2879. https://doi.org/10.5194/tc-16-2859-2022

P 20.5
Revealing the recent height changes of the Great Altesch Glacier using TanDEM-X DEM series

Pierre-Louis Vleghe[1], Shiyi Li[1], Irena Hajnsek[1]

[1] *Institute of Environmental Engineering, ETH Zurich, Stefano-Franscini-Platz 5, CH-8093 Zurich (pvlieghe@ethz.ch ; shiyi.li@ifu.baug.ethz.ch ; irena.Hajnsek@dlr.de)*

Monitoring glacier mass balance is essential for understanding glacier-climate interactions and predicting water resources management. As the largest glacier in the Alps, the Great Aletsch Glacier has a length of 22 km and covers about of 78 km^2 [1]. It contains 20% of the entire Swiss ice mass, and thus plays significent role in understanding the dynamics of glacier mass change in this region [1]. Because of its significance, the TanDEM-X satellite mission has selected the Great Aletsch Glacier as a super-testsite and has collected abundant single-pass bistatic Synthtetic Aperture Radar (SAR) data over the glacier since 2011. Leveraging these TanDEM-X satellite data, we generated 124 digital elevation models (DEMs) from the Coregistered Single-look Slant Range Complex (CoSSC) data product, calculated glacier elevation changes between 2011 and 2020, and quantified the temporal dynamics of the mass balance of the Great Aletsch Glacier.

The DEMs were generated using an iterative approach. We initially used an external DEM (swissALTI3D [2]) as the reference for geocoding and interferogram simulation. The simulated interferogram was subtracted from the interferogram between the CoSSC data pairs to generated a differential interferogram. The unwrapped phase in the differential interferogram corresponds to the height difference between the TanDEM-X measurements and the reference DEM, and thus we converted the phase into differential height to update the reference DEM. At this point, the updated reference DEM was accepted as the final product if the mean and standard deviation of the differential height met with the convergence criteria, otherwise it was used as the new reference in the subsequent iteration.

Following the DEM generation, we used xDEM python package [3] to analyze the DEM series. We first measured the elevation change by differencing two DEMs, then used a local hypsometric interpolation method to fill the DEM voids within the glacier outline, and finally integrated the elevation difference over the glacier to calculate the ice volume and mass change.

Our results revealed a consistent glacier-wide height loss of 1 $m.a^{-1}$ on average between 2011 and 2022, corresponding to a cumulative volumetric ice loss of 0.8 km^3 and mass loss of 699 Mt (assuming a mean ice density of 873.5 $kg.m^{-3}$ [4]). Notably, the glacier tongue experienced an accelerated recession, with an average height loss of 5.1 $m.a^{-1}$ for the period 2011-2016 and 6.5 $m.a^{-1}$ for the period 2017-2022.

In summary, our results have provided valuable insights into the dynamic changes of the Great Aletsch Glacier by analyzing the abundant TanDEM-X data. The detailed spatio-temporal of our work advanced our understanding of glacier recession in the Alps under the climate change.

REFERENCES

[1] Farinotti, D., Huss, M., Bauder, A., & Funk, M. 2009, An estimate of the glacier ice volume in the Swiss Alps, *Glob. Planet. Change*, vol. 68, no. 3, pp. 225–231.
[2] Swisstopo, SwissALTI3D. [Online]. Available: https://www.swisstopo.admin.ch/en/geodata/height/alti3d.html
[3] Dehecq, A. Accessed: Nov. 8, 2020, xDEM. [Online]. Available : https://xdem.readthedocs.io/en/stable/index.html
[4] Van Wyk de Vries, M., Carchipulla-Morales, D., Wickert, A.D. *et al.* Glacier thickness and ice volume of the Northern Andes. *Sci Data* 9, 342 (2022). https://doi.org/10.1038/s41597-022-01446-8
[5] Linsbauer, A., Huss, M., Hodel, E., Bauder, A., Fischer, M., Weidmann, Y., Bärtschi, H. & Schmassmann, E. 2021, The new Swiss Glacier Inventory SGI2016: From a topographical to a glaciological dataset. Frontiers in Earth Science, 22, doi:10.3389/feart.2021.704189.

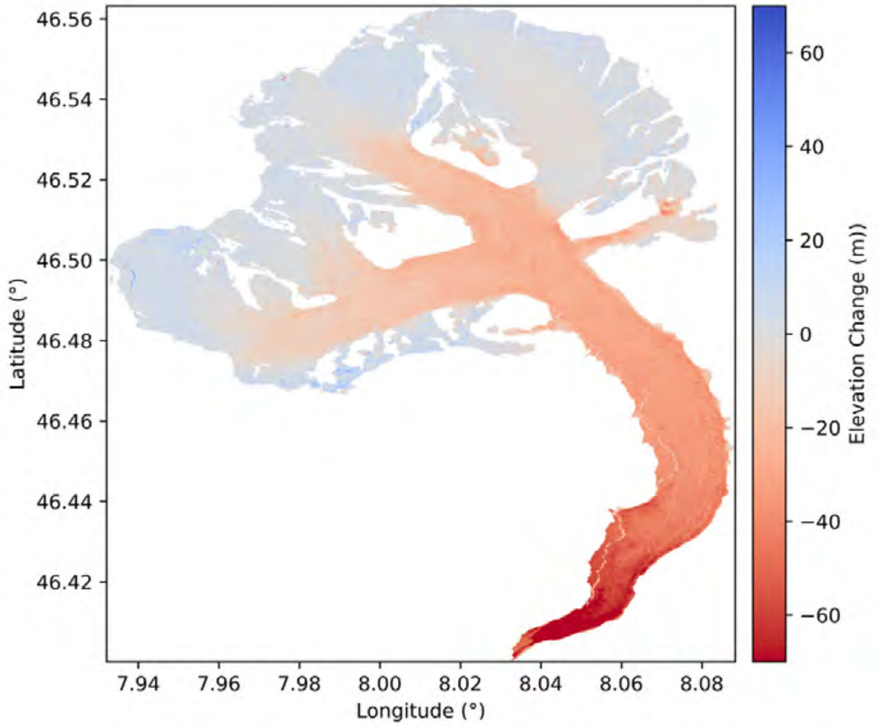

Figure 1. Elevation change map of the Great Aletsch Glacier between 2011 and 2022. The colormap shows the negative elevation changes in red and the positive elevation changes in blue. The glacier outline was selected from GLAMOS [5]. Coordinate Reference System (CRS): Latitude (°)/Longitude(°) in World Geodetic System 1984 (WGS 84).

21 Spatial data science: extracting knowledge from geo-environmental data

Massimiliano Cannata, Marj Tonini , Cédric Métraux, Philip Wehrens

Swiss Geocomputing Centre

TALKS:

21.1 Brandon Finley, Guillaume Jouvet: GlacierGan: Visualizing the Alps during the Last Ice Age

21.2 Daniele Strigaro, Massimiliano Cannata: Comparison between Open Standards adoption in environmental data management: SOS vs SensorThings API

21.3 Iram Parvez, Giorgio Boni, Rossella Bovolenta, Eva Riccomagno, Bianca Federici: Statistical Analysis and Forecasting Model of Groundwater Fluctuation due to Rainfall

21.4 Jürg Hunziker, Niklas Linde: Towards ground penetrating radar full-waveform inversion using an optimal-transport distance

21.5 Loïc Gerber, Grégoire Mariethoz: Synthetic hydrological data consistent with climate reanalysis to enable long-term hydrological modelling

21.6 Lucas Schmutz, Soulivanh Thao, Mathieu Vrac, Grégoire Mariethoz: Improved global predictions by considering the local performance of general circulation models

21.7 Luiz Gustavo Rasera, Jeff Boisvert, Shaun Barker: Implicit modeling of non-linear geological structures

21.8 Massimiliano Cannata, Daniele Strigaro, Gregory Giuliani, Jens Ingensand, Olivier Ertz, Maxime Collombin: OSiRES: Open geospatial standards and reproducible research

21.9 Reto De Paoli, Christian Buser, Maria Ponzio, Salome Schindler, Vincent Thöni: GIS based natural hazard management of Swiss Rail-way (SBB) power grid

POSTERS:

P 21.1 Jason Bula, Adrien Gressin, Jean-Christophe Loubier, Dominique Fumeaux: Combining AI and photogrammetry to secure bicycle races in Switzerland

P 21.2 Antoine Carreaud, Adrien Gressin: Back to the FLAIR one challenge

P 21.3 Gionata Ghiggi, Kim Candolfi, Jacopo Grazioli, Régis Longchamp, Charlotte Weil, Christine Unal, Marc Schleiss, Remko Uijlenhoet, Tim Raupach, Alexis Berne: DISDRODB: a global data base of raindrop size distribution observations

P 21.4 Alessio Poloni, Marj Tonini, Christophe Lambiel: Advanced spatial learning technique for automatic mapping of geomorphological features in alpine periglacial environment

P 21.5 Vladimir R. Wingate, Giulia Curatola Fernández, Chinwe Ifejika Speranza: Spatio-temporal changes across very small West African forest remnants

21.1
GlacierGan: Visualizing the Alps during the Last Ice Age

Brandon Finley[1], Guillaume Jouvet[1]

[1] *Institute of Earth Surface Dynamics, University of Lausanne, Lausanne, Switzerland (brandon.finley@unil.ch)*

In this work, we develop a deep-learning generative model to offer a new visualization for the Alps and its glaciation over the last 120'000 years as if a satellite had passed over and taken high resolution images. This visualization relies on a new coupled climate-glacier evolution model, which uses the latest paleo-climate and ice thickness field reconstructions. The ultimate goal is for it to be used in the “IceAgeCam”, which is an interactive machine developed by the ZHDK, UZH and UNIL that aims to better inform the public about the cause of climate change in a long-term climatic context.

For that purpose, we use image-2-image translation models, namely Pix2PixHD (Wang et al., 2018). Similar to how one can use an image-2-image translation model to map images of winter to summer, or zebras to horses, we will map relevant fields of multi-band climatic images into artificial satellite images. Each multi-band image is composed of predictors such as ice thickness, ice velocity, precipitation, surface temperature, etc. A key challenge here is the lack of data due to limited visualization research in this area. To overcome this problem we employ techniques such as Adaptive Discriminator Augmenter (ADA) (Karras et al., 2020) and transfer learning to aid the model in its convergence. Overall, this produces results with a low Kernel Inception Distance (KID) value of ~10, which is acceptable when comparing it to other popular image-2-image translation models such as Pix2PixHD. As a result, we produce reconstructed paleo satellite images of the Alps in high-resolution based on the latest glaciological and climatic research with an unprecedented level of realism. These new visualizations embedded into the “IceAgeCam” are essential to help disseminate climate research results to a large audience and provide them with a long-term context of climate warming.

Figure 1. An artificial satellite image over the Alps (24'000 years ago).

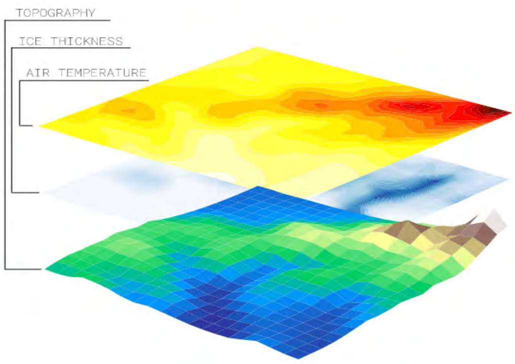

Figure 2. An illustration of the different variables used and how they are encoded as a multi-band image.

REFERENCES

Karras, T., Aittala, M., Hellsten, J., Laine, S., Lehtinen, J., & Aila, T. (2020). Training generative adversarial networks with limited data. *Advances in neural information processing systems*, *33*, 12104-12114.

Wang, T. C., Liu, M. Y., Zhu, J. Y., Tao, A., Kautz, J., & Catanzaro, B. (2018). High-resolution image synthesis and semantic manipulation with conditional gans. In *Proceedings of the IEEE conference on computer vision and pattern recognition* (pp. 8798-8807).

21.2
Comparison between Open Standards adoption in environmental data management: SOS vs SensorThings API

Daniele Strigaro[1], Massimiliano Cannata[1]

[1] *Institute for Earth Sciences, SUPSI, Via Flora Ruchat-Roncati 15 CH-6850 Mendrisio*

The rapid growth of environmental monitoring and data collection has led to the need for effective and standardized methods of managing and sharing environmental data. In this context, the Open Geospatial Consortium (OGC) defines the adoption of open standards for ensuring interoperability, accessibility, and efficient utilization of data across diverse platforms and applications to facilitate the exchange of sensor observations and related metadata in a standardized manner. The first generation of standards was mostly based on SOAP in XML format. However, due to the innovations that the field of informatics has undergone in the last decade, in 2016, the OGC began implementing a new generation of standards based on the OpenAPI specifications. This move aimed to facilitate the integration of geospatial data into modern web applications and systems. The Sensor Observation Service (SOS) and the SensorThings API (STA) represent these two approaches but with some differences.

This study presents a comparison between SOS and STA. While SOS is a recognized standard that enables real-time and historical data retrieval through XML standardized web services, the SensorThings API focuses on simplifying the management and retrieval of Internet of Things (IoT) sensor data, providing a RESTful interface for data access. This study examines key aspects of both standards, including data modeling, communication protocols, data querying methods, interoperability and the software implementation available (Kostev et al., 2018; Cannata et al., 2015). Furthermore, SOA and STA are evaluated in terms of adoption and community support. SOS shapes a substantial user and developer community, resulting in numerous implementations and tools that adhere to the standard. The SensorThings API, though relatively newer, benefits from its alignment with IoT trends, contributing to its growing adoption in various domains.
As the landscape of environmental data management continues to evolve, understanding the strengths and limitations of these open standards enables informed decision-making for adopting the most suitable approach to data management and sharing.

REFERENCES

Cannata, M.; Antonovic, M.; Molinari, M.; Pozzoni, M. IstSOS, a New Sensor Observation Management System: Software Architecture and a Real-Case Application for Flood Protection. Geomatics, Natural Hazards and Risk 2015, 6 (8), 635–650. https://doi.org/10.1080/19475705.2013.862572.

Kotsev, A.; Schleidt, K.; Liang, S.; Van der Schaaf, H.; Khalafbeigi, T.; Grellet, S.; Lutz, M.; Jirka, S.; Beaufils, M. Extending INSPIRE to the Internet of Things through SensorThings API. Geosciences 2018, 8 (6). https://doi.org/10.3390/geosciences8060221.

21.3
Statistical Analysis and Forecasting Model of Groundwater Fluctuation due to Rainfall

Iram Parvez[1], Giorgio Boni[1], Rossella Bovolenta[1], Eva Riccomagno[2], Bianca Federici[1]

[1] *Department of Civil,Chemical and Environmental Engineering (DICCA), Università degli Studi di Genova, Via Montallegro 1, 16145 Genoa, Italy (iram.parvez@edu.unige.it, giorgio.boni@unige.it, rossella.bovolenta@unige.it, bianca.federici@unige.it)*
[2] *Department of Mathematics, Università degli Studi di Genova, Via Dodecaneso 35, 16146 Genova, Italy (riccomag@dima.unige.it)*

Groundwater oscillations play a crucial role in triggering landslides, affecting slope stability. Groundwater fluctuation could be associated with rainfall and/or due to subsurface flow, depending on the site-specific hydrological and geotechnical properties. The present study focuses on Mendatica, a small village in the Liguria region, Italy. Firstly, research analyses time series data from eleven piezometers and one rain gauge distributed over the study area, to identify correlations between groundwater levels and rainfall. The methodology consists of two main parts: the use of time lag correlation (Rahmani, F. & M.H. Fattahi, [2021]) to determine the groundwater responsive behavior to rainfall and the use of clustering technique (Naranjo-Fernández, N., et al. [2020]) to group piezometers. Grouping piezometers with similar behavior helps to reduce the input feature selection process for groundwater forecasting models. The information obtained from time lag correlation helps in pre-processing the input data by improving accuracy of forecasting models.

Secondly, the present study uses machine learning forecasting approach, including ANN with GRU (Zhang et al 2017, Lin et al 2022), as well as general forecasting methods (Shirmohammadi et al 2013), to predict groundwater oscillation due to rainfall. The preliminary results indicate how the general forecasting methods present limited performance, whereas ANN with GRU shows more favourable outcomes.

The final objective of the present research is the development of a web-based decision-support system based on-site sensor data and machine learning to help technicians make data driven decisions.

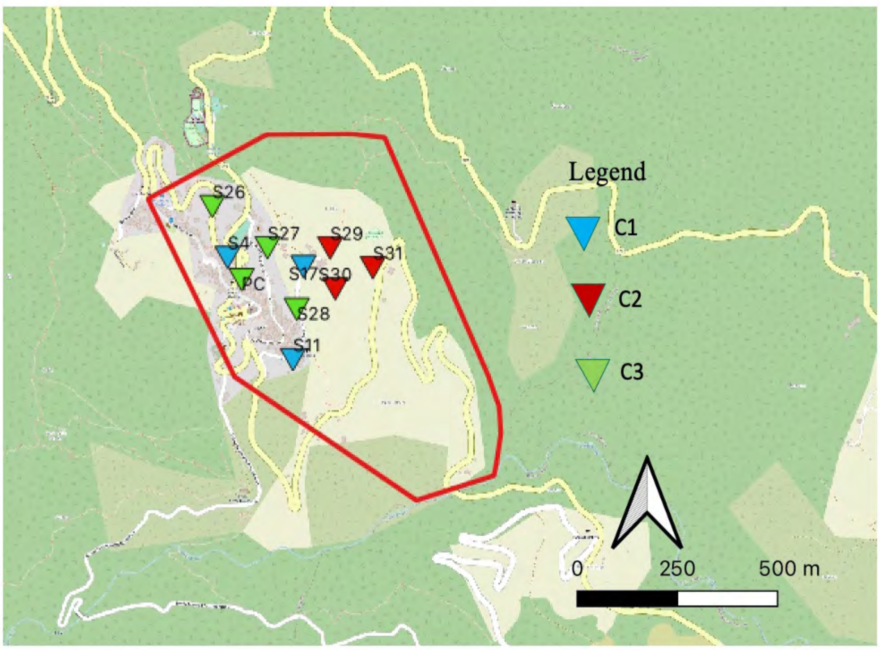

Mendatica site and piezometer position, grouped in 3 classes based on K-mean cluster analysis.

REFERENCES
Lin, H., Gharehbaghi, A., Zhang, Q., Band, S. S., Pai, H. T., Chau, K. W., & Mosavi, A. 2022. Time series-based groundwater level forecasting using gated recurrent unit deep neural networks. Engineering Applications of Computational Fluid Mechanics, 16(1), 1655-1672.
Naranjo-Fernández, N., et al. 2020, Clustering groundwater level time series of the exploited Almonte-Marismas aquifer in Southwest Spain. Water. 12(4): p. 1063

Rahmani, F. and M.H. Fattahi, 2021 A multifractal cross-correlation investigation into sensitivity and dependence of meteorological and hydrological droughts on precipitation and temperature. Natural Hazards. 109(3): p. 2197-2219.

Shirmohammadi, B., Vafakhah, M., Moosavi, V., & Moghaddamnia, A. 2013. Application of several data-driven techniques for predicting groundwater level. Water Resources Management, 27, 419-432.

Zhang, X., Shen, F., Zhao, J., & Yang, G. 2017. Time series forecasting using GRU neural network with multi-lag after decomposition. In Neural Information Processing: 24th International Conference, ICONIP 2017, Guangzhou, China, November 14–18, 2017, Proceedings, Part V 24 (pp. 523-532). Springer International Publishing.

21.4
Towards ground penetrating radar full-waveform inversion using an optimal-transport distance

Jürg Hunziker[1], Niklas Linde[2]

[1] *Institute of Earth Sciences, University of Lausanne, Lausanne, Switzerland (jurg.hunziker@unil.ch)*
[2] *Institute of Earth Sciences, University of Lausanne, Lausanne, Switzerland (niklas.linde@unil.ch)*

In deterministic full-waveform inversion (FWI) of ground penetrating radar (GPR) data, the optimisation algorithm usually gets stuck in a local minimum if the predicted data corresponding to the starting model are shifted by more than half a period compared to the observed data. This phenomenon is called cycle-skipping (Virieux and Operto, 2009).

Métivier et al. (2016) have shown for seismic reflection data that cycle-skipping can be avoided by performing optimization on the optimal-transport distance instead of the least-squares distance. Here, we implement a full-waveform inversion algorithm using the optimal-transport distance for crosshole GPR data. The optimal-transport distance assumes (1) mass conservation between the observed and the predicted signal and (2) no negative values in the signal. Both assumptions are violated when it comes to GPR data. Different to Métivier et al. (2016), we avoid both of these issues by using the approach described by Sambridge et al. (2022) for seismic data. This approach can be used to convert each GPR trace into a 2D probability density function (PDF) and, subsequently, reduce the PDF to two marginal distributions in order to have two 1D problems instead of one 2D problem. These marginal distributions of the observed data are then compared with those from the predicted data using the optimal-transport distance.

In an initial numerical experiment, we aim to invert a synthetic crosshole dataset consisting of four sources in one borehole and five receivers in the second borehole. The model domain is six meters deep and four meters wide and subdivided into eight rectangles to obtain an inversion problem with eight unknowns. The true simulated subsurface features a homogeneous relative electric permittivity of twelve and we start our inversion with a homogeneous model of a relative electric permittivity of four.

The observed data and predicted data corresponding to the starting model are shown in the left column of Figure 1 for the second source and all five receivers. The shift of the two datasets is clearly larger than half a period. Thus, FWI based on a least-squares distance would not be able to find a model that can explain the data as it would end up in a local minimum. Inversion based on the optimal-transport distance, however, is able to fit the data well, as can be seen from the comparison of the observed data and the predicted data based on the final model in the right column of Figure 1.

Figure 2.a shows the evolution of the optimal-transport distance as a function of iterations. We see that the data-fit is improved by 2.5 orders of magnitude during the inversion. In Figure 2.b the final model after 17 iterations is plotted. The values of the eight unknowns are not exactly twelve, but, averaged over the raypaths, come very close.

In conclusion, we have shown that using the optimal-transport distance to invert GPR data deterministically considering the full waveform allows to overcome the cycle-skipping problem common in FWI. The next step will be to include model regularization and apply this algorithm to more complex problems featuring more unknows, a heterogeneous subsurface and, eventually, real data.

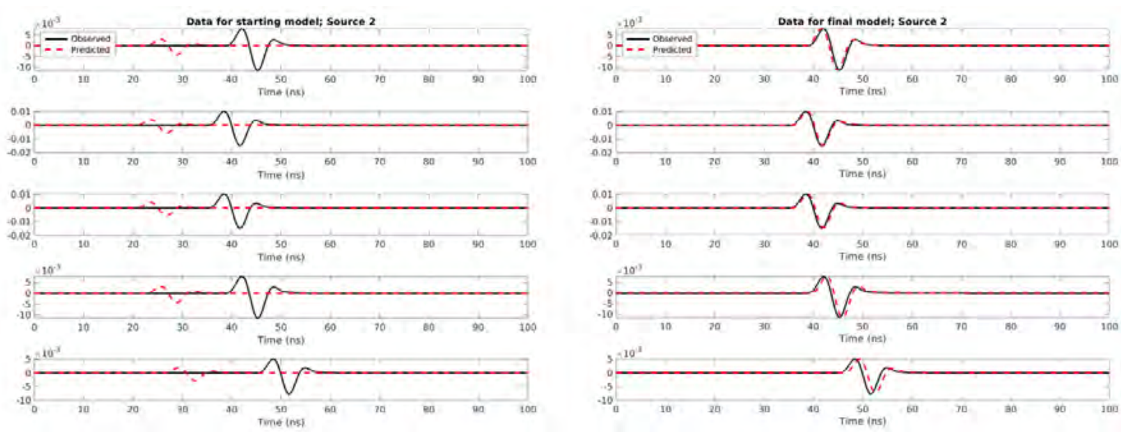

Figure 1. Comparison of the observed data (solid black line) with the predicted data (dashed red line) for the second source and all five receivers. Left column: Predicted data for starting model. Right column: Predicted data for final model.

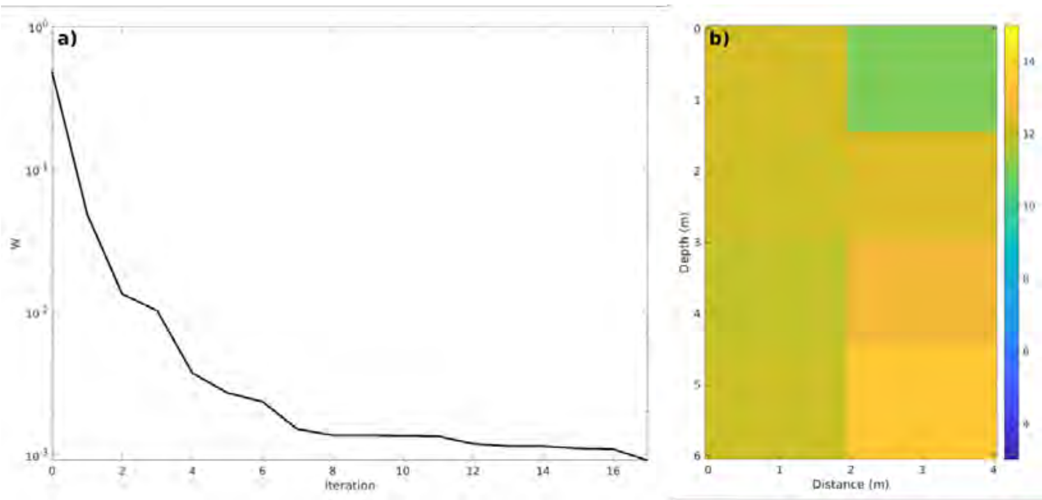

Figure 2. a) The optimal-transport distance as a function of iterations. b) The final model obtained after 17 iterations.

REFERENCES

Métivier, L., Brossier, R., Mérigot, Q., Oudet, E. & Virieux, J. 2016: Measuring the misfit between seismograms using an optimal transport distance: application to full waveform inversion, Geophysical Journal International, 205, 345-377.

Sambridge, M., Jackson, A. & Valentine, A.P. 2022: Geophysical inversion and optimal transport, Geophysical Journal International, 231, 172-198.

Virieux, J., & Operto S. 2009: An overview of full-waveform inversion in exploration geophysics, Geophysics, 74, WCC127-WCC152.

21.5
Synthetic hydrological data consistent with climate reanalysis to enable long-term hydrological modelling

Loïc Gerber[1], Grégoire Mariéthoz[1]

[1] *Institute of Earth Surface Dynamics (IDYST), UNIL-Mouline, Geopolis, University of Lausanne, 1015 Lausanne, Switzerland (loic.gerber.2@unil.ch)*

The creation of synthetic images of evapotranspiration, soil moisture, and terrestrial water storage is proposed to address the gaps in satellite data availability prior to the year 2000 and extend the data to pre-satellite periods. This is necessary to model and manage water resources and evaluate the impact of climate change on hydrological processes in regions with limited data. The synthetic images should closely resemble real satellite images.

The approach is based on the relationship between meteorological factors and existing satellite images and the idea that, under similar weather conditions, patterns of specific processes may repeat over time. The ERA5 reanalysis data is used as the meteorological predictor, and a *K*-Nearest Neighbor algorithm with a process-specific similarity metric is applied to generate the synthetic images.

The method is tested in the Volta River Basin in West Africa where water resources are critically impacted by climate change. The synthetic images are input into a spatially-distributed hydrological model for calibration and validation, and their quality is assessed by their ability to reproduce historical streamflow time series. The goal of this testing phase is to improve the generation technique and produce synthetic images that closely approximate unobserved processes and improve the accuracy of the modeling.

21.6
Improved global predictions by considering the local performance of general circulation models

Lucas Schmutz[1], Soulivanh Thao[2], Mathieu Vrac[2], Grégoire Mariethoz[1]

[1] *Institute of Earth Surface Dynamics (IDYST), UNIL-Mouline, Geopolis, University of Lausanne, 1015 Lausanne, Switzerland (lucas.schmutz@unil.ch)*
[2] *Laboratoire des Sciences du Climat et l'Environnement (LSCE-IPSL) CNRS/CEA/UVSQ, UMR8212, Université Paris-Saclay, Gif-sur-Yvette, France*

The utilization of General Circulation Models (GCMs) plays a crucial role in forecasting future climate changes and is heavily relied upon by policymakers in managing responses to human-induced global warming and climate change. To attain a robust global signal and assess uncertainties, GCMs are often combined in Multi-Model Ensembles (MMEs) using various approaches such as the Multi-Model Mean (MMM) or its weighted variants.
Recently, Thao et al. (2022) proposed a new model comparison approach that is based on graph cut optimization. This optimization method, originally developed in computer vision for tasks like image segmentation, is used for selecting the best-performing model at each gridpoint for a given variable, resulting in a patchwork of models that maximizes performance while avoiding spatial discontinuities. In contrast to methods like MMM that use global weights, this approach considers the local performance of individual models, resulting in improved global predictions.
Here we present a new combination approach of GCMs that utilizes graph cuts. Compared to the univariate method, this approach ensures that the relationships between variables are locally preserved while producing coherent spatial fields. Furthermore, we replace the use of distances between multi-decadal means with statistical distances between multi-decadal distributions, enabling the combined model to represent not only the average behavior (e.g. mean temperature or precipitation) but the entire multivariate distribution, including extreme values that have substantial societal and environmental impacts.

REFERENCES

Thao, S., Garvik, M., Mariethoz, G., & Vrac, M. (2022). Combining global climate models using graph cuts. Climate Dynamics, February. https://doi.org/10.1007/s00382-022-06213-4.

21.7
Implicit modeling of non-linear geological structures

Luiz Gustavo Rasera[1], Jeff Boisvert[2], Shaun Barker[1]

[1] *Department of Earth, Ocean and Atmospheric Sciences, University of British Columbia (UBC), 2020-2207 Main Mall, Vancouver, BC, Canada V6T 1Z4 (lgrasera@eoas.ubc.ca)*
[2] *Department of Civil and Environmental Engineering, University of Alberta, 6-241 Donadeo Innovation Centre for Engineering, Edmonton, AB, Canada T6G 2G7*

Implicit modeling enables rapid generation of numerical geological models directly from measured data, allowing geologists to create and evaluate multiple models quickly and efficiently. However, in many subsurface applications, accurately inferring and modeling complex non-linear geological structures, such as folds, veins, and channelized systems, from sparse data presents significant challenges. These challenges arise because most implicit modeling techniques rely on a single global anisotropy model to perform interpolation, often employing the Euclidean norm to calculate distances between data points and grid nodes, or stationary covariance functions to measure spatial autocorrelation. In sparse data settings, this approach fails to interpolate non-linear geological features, which requires significant human intervention in the implicit modeling process to achieve the desired results. To overcome these challenges, we propose an implicit modeling algorithm capable of generating non-linear geological structures from relatively sparse data sets. Our approach leverages an integrated artificial intelligence system to detect and infer local anisotropy patterns from data and utilizes a pathfinding algorithm to compute non-linear anisotropic distances between data points and grid nodes. We demonstrate the approach with illustrative examples of multiple-category geological models.

21.8
OSiRES: Open geospatial standards and reproducible research

Massimiliano Cannata[1], Daniele Strigaro[1], Gregory Giuliani[2], Jens Ingensand[3], Olivier Ertz[3], and Maxime Collombin[3]

[1] *SUPSI, Istituto scienze della Terra, DACD, Canobbio, Switzerland (massimiliano.cannata@supsi.ch)*
[2] *University of Geneva, Institute for Environmental Sciences/enviroSPACE, geneva, Switzerland*
[3] *HEIG-VD, Yverdon-les-Bains, Switzerland*

In the era of cloud computing, big data and Internet of things, research is very often data-driven: based on the analysis of data, increasingly available in large quantities and collected by experiments, observations or simulations [1]. These data are very often characterised as being dynamic in space and time and as continuously expanding (monitoring) or change (data quality management or survey). Modern Spatial Data Infrastructures (e.g. swisstopo or INSPIRE), are based on interoperable Web services which expose and serve large quantities of data on the Internet using widely accepted and used open standards defined by the Open Geospatial Consortium (OGC) and the International Organization for Standardization (ISO) [2]. These standards mostly comply with FAIR principles [3] but do not offer any capability to retrieve a dataset how it was in a defined instant, to refer to its status in that specific instant and to guarantee its immutability. These three aspects hinder the replicability of research based on such a kind of services.
OSIReS is a project, co-financed by swissuniversities in the frame of its Programme Open Science I, Phase B, that aims at tackle this issue. In this work, after presenting the project, ***We specifically discuss the issue, present the state of the art and propose a possible solution to fill this gap.***

REFERENCES
[1] Hamdi, A., Shaban, K., Erradi, A., Mohamed, A., Rumi, S. K., & Salim, F. D. (2022). Spatiotemporal data mining: a survey on challenges and open problems. Artificial Intelligence Review, 55(2), 1441-1488p
[2] Simoes, J., and A. Cerciello. “Serving Geospatial Data Using Modern and Legacy Standards: a Case Study from the Urban Health Domain.” The International Archives of the Photogrammetry, Remote Sensing and Spatial Information Sciences 48 (2022): 419-425.
[3] Giuliani, G., Cazeaux, H., Burgi, P. Y., Poussin, C., Richard, J. P., & Chatenoux, B. (2021). SwissEnveo: A FAIR national environmental
data repository for earth observation open science. Data Science Journal, 20(1)

21.9
GIS based natural hazard management of Swiss Rail-way (SBB) power grid

Reto De Paoli[1], Christian Buser[1], Maria Ponzio[1], Salome Schindler[1], Vincent Thöni[2]

[1] AFRY Svizzera SA, via Cantonale 109, CH-6537 Grono, (reto.depaoli@afry.com)
[2] SBB Energy Swiss Railway, Industriestrasse 1, CH-3052 Zollikofen

In the framework of a project commissioned by the Swiss Federal Railways (SBB), AFRY Switzerland Ltd. developed a partially automated GIS-based method to sub-ject a large number of infrastructure objects to the identification of their exposure to natural hazards. The methodology was developed in cooperation with SBB Energy, based on SBB's need to specifically identify infrastructures (pylons, substations, switching stations) and transmission lines which are endangered by gravitative nat-ural hazards and could therefore jeopardise the stable operation of the railway net-work.

Due to the large amount of asset data (1,800 km of transmission lines, 9,500 py-lons, 80 substations and frequency converters), an analytical and automated GIS approach based on ESRI ArcGIS Pro was developed to identify the risk, using can-tonal hazard maps for natural hazard processes and Aqua- and SilvaProtect modelled hazard maps. Outside the settlement areas in Switzerland, generally hazard maps aren't available, only local natural hazard index map can be available. To assess the degree of danger on SBB infrastructures, the AquaProtect and SilvaProtect maps were integrated as an interpretative basis. As a result, it was possible to obtain a first automatic classification of infrastructure hazards for gravitative processes (floods - debris flows, landslides, avalanches, rockfalls).

In addition to the assessment of the degree of hazard on individual assets, object-specific financial parameters were also analysed, such as capital / construction costs, asset value and potential financial loss upon occurrence. The financial dam-age is related to the degree of hazard, i.e. the intensity of the event and the type of process. Analysis was carried out primarily using specific ArcGIS Pro scripts and reviewed by natural hazards specialists.
Based on this initial classification of the degree of hazard for each asset, specific risk analyses and assessments were carried out for homogeneous sectors differentiat-ed by process with the aid of geomorphological and geological maps as well as technical infrastructure data and, where required, site inspections.

The planning of the hazard mitigation measures was carried out with integration of necessary mitigation structures on the map and using further geospatial analyses to calculate the costs of the measures and the ratio of building substance to measures based on a construction cost matrix including planning and access costs (pre-feasibility study phase, ±20%).
In a final step, all available and compiled data were collected in an ESRI WebApp, which is available to life cycle and asset managers, project engineers and mainte-nance resposables for daily use. This interactive web app serves as a platform on which to collect, combine, process, and visualise all relevant natural hazard man-agement information for the respective stakeholders. Thanks to the interactive and intuitive visualization of the results of complex analyses and evaluations, this tool serves non-natural hazard specialists as a support for technical and economic plan-ning in the context of projects for the renewal and expansion of the existing SBB power grid.

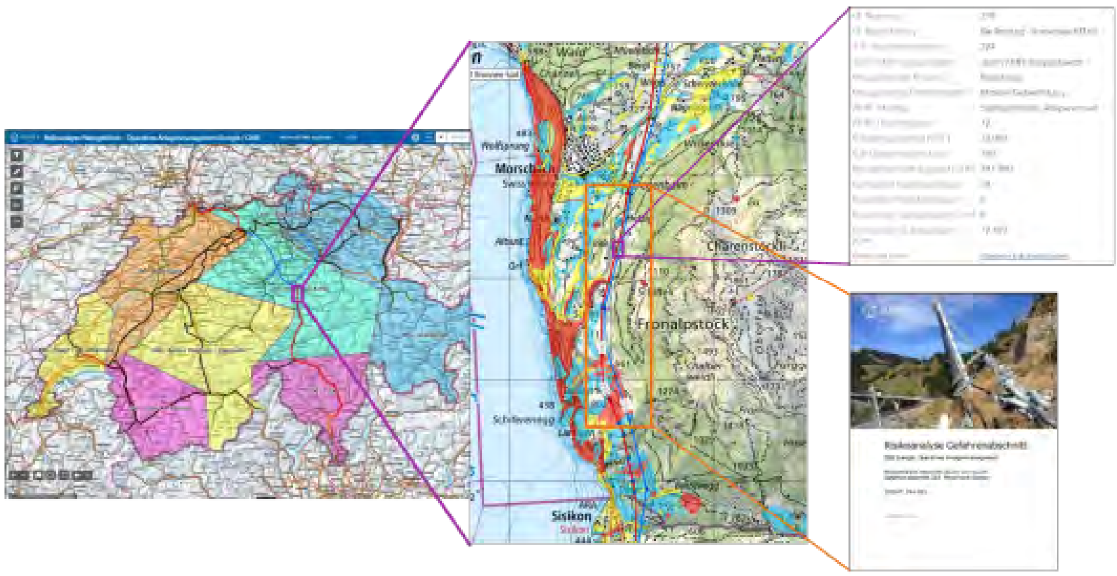

Figure 1. Example of the content searchable via ESRI WebApp

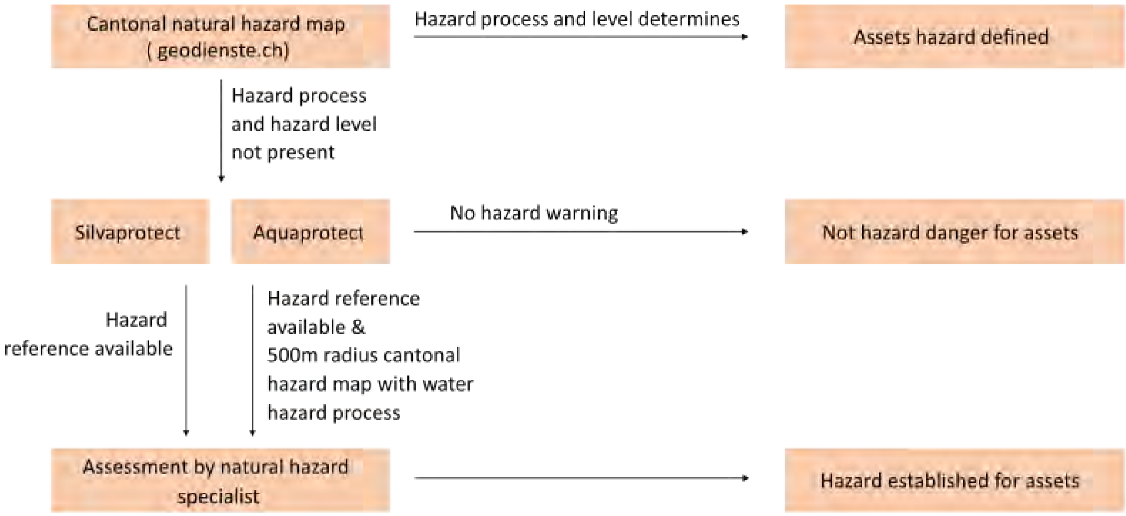

Figure 2. Outline of the analytical approach employed

REFERENCES

BAFU, Schutzwald in der Schweiz – Vom Projekt SilvaProtect-CH zum harmonisierten Schutzwald, 2013
BAFU, Übersicht der potenzielle Hochwassergefährdung in der Schweiz, Vom Projekt Aquaprotect, 2008 swisstopo, geo.amin.ch

P 21.1
Combining AI and photogrammetry to secure bicycle races in Switzerland

Jason Bula[1], Adrien Gressin[1], Jean-Christophe Loubier[2], Dominique Fumeaux[2]

[1] *University of Applied Sciences Western Switzerland (HES-SO / HEIG-VD), Insit Institute – (jason.bula, adrien.gressin)@heig-vd.ch*
[2] *University of Applied Sciences Western Switzerland (HES-SO Valais) Institute of Tourism – (jchristophe.loubier, dominique.fumeaux)@hevs.ch*

The safety of participants in bicycle races is a major concern for organizers and racers. Stage routes can include many obstacles such as road narrowings, traffic islands or road entrances and exits. Detecting these obstacles is essential to prevent accidents and prepare for the race.
The safety methods currently used in bicycle races are often manual, requiring tedious work to recognize and identify obstacles. The aim of this research project is to automate obstacle detection using photogrammetry combined with artificial intelligence.

The first stage of the methodology adopted in this project is based on the use of a system combining a vehicle-mounted stereo pair and an RTK GPS receiver (Figure 1 left). Once the mobile system has been calibrated (boresight and camera calibration), the route can be accurately modelled. This enables the construction of a precisely georeferenced 3D model over the entire race route.

The second step consists in using a pre-trained neural network to perform a semantic segmentation of the camera images (Chen et al., 2022). This segmentation produces masks corresponding to different classes of objects of interest, some of which represent potential obstacles (Figure 1 left). These masks are then projected onto the georeferenced 3D model for classification (Carreaud et al., 2022). In this way, the objects detected in the images are associated with the corresponding 3D points in model, resulting in a classified point cloud, where each point is assigned to a specific class, including the different obstacle categories (Figure 2).

This methodology for detecting and securing obstacles was successfully applied on the prologue stage of the Tour de Romandie 2023. However, some obstacles require detection based on geometry in the point cloud rather than image segmentation, for example, we have developed an algorithm to extract sidewalks and curb cut (see white and green lines on Figure 2). Moreover, by increasing the number of classes in the neural network and training it on specific labelled data, it would be possible to add more obstacle categories for more accurate and complete detection.

We would like to thank *Orbis 360* for providing acquisition equipment and assistance in the field.

Figure 1. Left: stereo pair coupled in red with RTK positioning placed on a car (Orbis 360), right: inference using the pre-trained model (Chen et al., 2022)

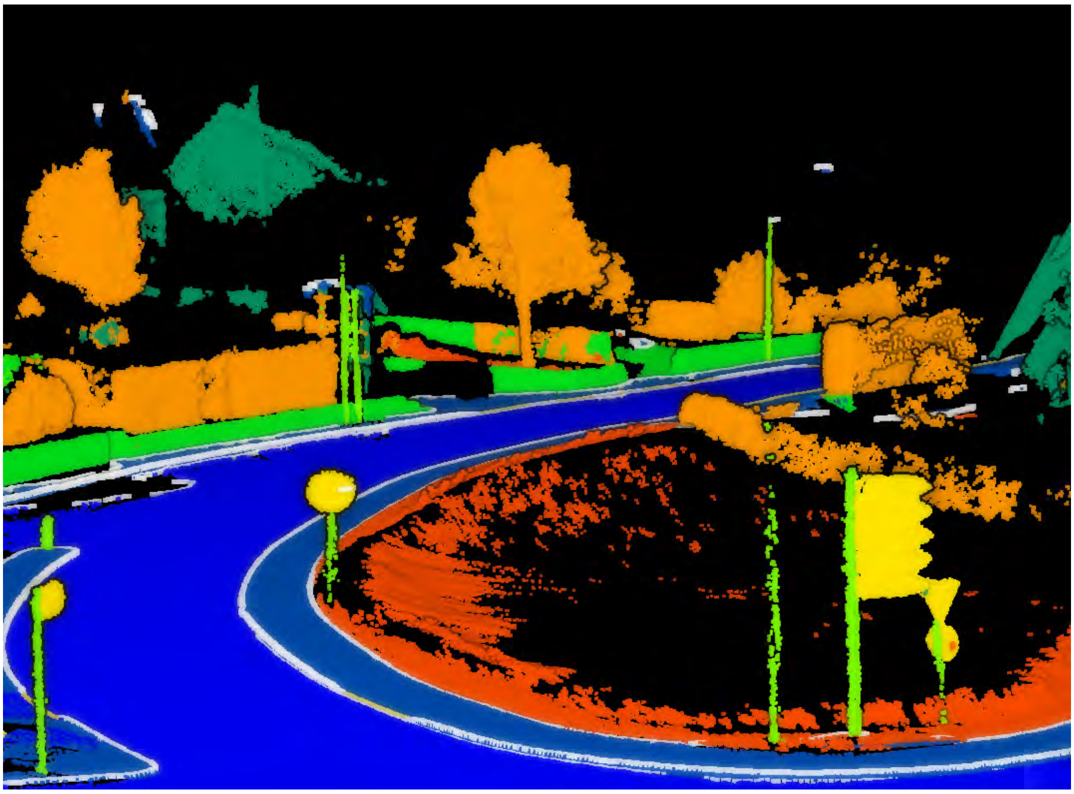

Figure 2. Reprojection of the classification in the 3D model and highlighting of white sidewalks and green curb cut by extraction in the geometry

REFERENCES

Chen, Z., Duan, Y., Wang, W., He, J., Lu, T., Dai, J., & Qiao, Y. (2022). Vision transformer adapter for dense predictions. *arXiv preprint arXiv:2205.08534*.

Carreaud, A., Mariani, F., & Gressin, A. (2022). Automating the underground cadastral survey: a processing chain proposal. The International Archives of the Photogrammetry, Remote Sensing and Spatial Information Sciences, 43, 565-570.

P 21.2
Back to the FLAIR one challenge

Antoine Carreaud[1], Adrien Gressin[1]

[1] *University of Applied Sciences Western Switzerland (HES-SO / HEIG-VD), Insit Institute - (antoine.carreaud, adrien.gressin)@heig-vd.ch*

Context
The FLAIR 1 (French Land cover from Aerospace ImageRy) challenge was organized by IGN France in March 2023 and consisted in classifying a dataset distributed throughout all France territory. The dataset is made up of 20 cm RGB-IR aerial images along with a DEM. The 12 land use classes of this challenge range from buildings to crops (see Figure 1).

Interest
The availability of a high-quality, specialized land cover dataset such as FLAIR 1 represents a significant opportunity for the geosciences AI community. This dataset allowed us to explore numerous approaches, utilizing it as a sandbox for experimentation. We provide in this contribution a short feedback on our participation in this challenge.

Method
Introduced in 2017, transformers revolutionized the world of NLPs, in 2021 this innovative concept was adapted for images (Vision-Transformer - ViT) and showed significant improvements over different CNN-based architectures such as U-Nets.
To obtain our results, we decided to re-train an existing ViT network, using only the RGB data provided by IGN. Initial tests to include IR and DEM data, as well as available metadata, didn‘t bring any significant improvements, so we decided to discard them for the time being.

Results and perspectives
After training our model on French aerial data and thanks to ViT‘s adaptability, we have successfully applied it to other data sources such as UAV-based ortho-image (on Fribourg city center), and swisstopo aerial images SwissImage (on Morat city), both ortho-image have a GSD of 10 cm (see results on Figure 2).

Such great results presented a significant opportunity to tackle important concerns, including the monitoring of vegetation, especially in urban areas to mitigate the effects of heat islands, or the tracking of soil artificialization to manage the impact of urbanization. These results also open up new opportunities for sustainable development project like the monitoring of soil pollution, efficient control of energy transport infrastructures, etc.

	Class	MSK	Pixels	%
	building	1	1,670,300,028	8.23
	pervious surface	2	1,636,681,162	8.07
	impervious surface	3	2,836,695,330	13.98
	bare soil	4	741,261,583	3.65
	water	5	1,034,960,677	5.10
	coniferous	6	540,883,511	2.67
	deciduous	7	3,061,129,298	15.08
	brushwood	8	1,408,504,416	6.94
	vineyard	9	665,099,230	3.28
	herbaceous vegetation	10	3,798,549,882	18.72
	agricultural land	11	2,061,788,310	10.16
	plowed land	12	720,090,325	3.55
	other	**>13**	117,147,576	0.58

Figure 1. Semantic classes of the flair-one dataset with their distribution.

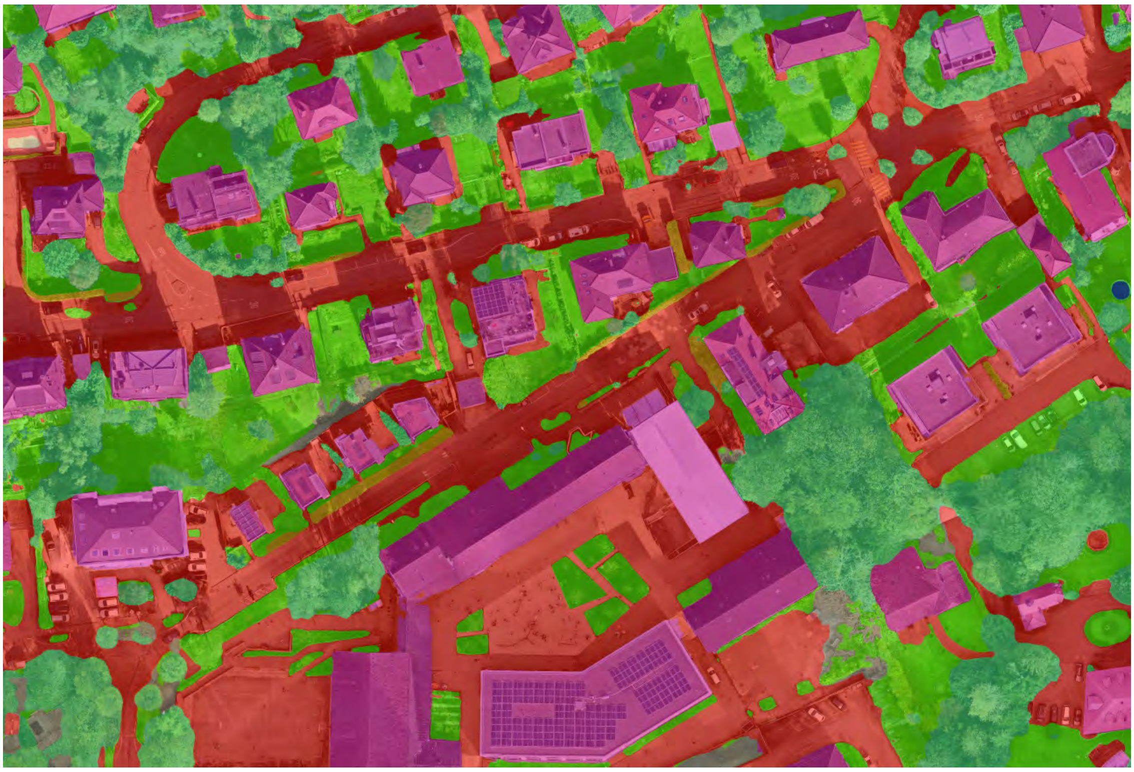

Figure 2. Result of the AI trained during the challenge on an ortho image of Friburg with a ground pixel of 10 cm.

P 21.3
DISDRODB: a global data base of raindrop size distribution observations

Gionata Ghiggi[1], Kim Candolfi[1], Jacopo Grazioli[1], Régis Longchamp[2], Charlotte Weil[2], Christine Unal[3], Marc Schleiss[3], Remko Uijlenhoet[4], Tim Raupach[5], Alexis Berne[1]

[1] *Environmental Remote Sensing Laboratory, LTE, EPFL, Lausanne, Switzerland (gionata.ghiggi@epfl.ch)*
[2] *ENAC-IT4Research, EPFL, Lausanne, Switzerland*
[3] *Geoscience & Remote Sensing Department, TU-Delft, Netherlands*
[4] *Department of Water Management, TU-Delft, Netherlands*
[5] *Climate Change Research Centre and ARC Centre of Excellence for Climate Extremes, UNSW Sydney, Australia*

The raindrop size distribution (DSDs) describes the number and size distributions of raindrops in a volume of air. It is key to model the propagation of microwave signals through the atmosphere (crucial for telecommunication and radar remote sensing), to improve microphysical schemes in numerical weather prediction models, and to understand rain-related land surface processes (rainfall interception, soil erosion). Despite its importance, the spatial and temporal variability of the DSD remains poorly understood. This has motivated scientists all around the globe to deploy DSD recording instruments known as disdrometers, in order to collect DSD observations in various climatic regions. However, only a small fraction of these data is easily accessible. Data are stored in disparate formats with poor documentation, making them difficult to share, analyze, compare and re-use. Additionally, very limited software is currently publicly available for DSD processing.

This abstract descrive the DISDRODB project, which aims to create a global archive of DSD measurements and to establish a global standard for DSD observation sharing. To this end, we undertook an inital effort to index, collect and homogenize many already public DSD data sets across the globe from various institutions, including NASA, NCAR, ARM, NCEP, NERC, INPE, EPFL, DELFT (...), and we currently maintain data and metadata from over 400 stations.

The DISDRODB metadata repository on GitHub, accessible at https://github.com/ltelab/disdrodb-data, allows the community to track changes and collaborate in refining station metadata using best open-source practices.
The DISDRODB archive follows a decentralized structure, in which data contributors upload station raw files to their preferred data repository (such as Zenodo or Figshare) and add the station metadata to the DISDRODB metadata repository, including the URL where the raw data are uploaded. This allow authors and contributors to retain autorship on their raw data, and it removes the need of maintaining a centralized data infrastracture.
In order to process their data, the data contributors need to specify the content of the raw data (i.e. the logged variables) into a reader template function that they add to the disdrodb Python package.
The open-source disdrodb package (available at https://github.com/ltelab/disdrodb) provides tools for interactions with the DISDRODB metadata repository and the user-side disdrometer data retrieval, standardization and homogenization.
The data processing of new disdrometer sensors can be easily incorporated into the DISDRODB system by utilizing modular configuration files. This allows for seamless integration of additional sensors alongside the currently supported ones, such as the OTT Parsivel 1 and 2, Thies LPM, and RD80.
In future, we plan to expand the disdrodb package to also include algorithms and utility for data preprocessing, analysis, and visualization of disdrometer measurements.

By adopting this framework, DISDRODB aims to promote the mobilization of data archives currently scattered across various institutions and foster international collaborations.

The DISDRODB group is actively seeking new data/code contributors and aims to create a thriving DSD community around the project, with the ultimate goal of accelerating and advancing reproducible precipitation research.

P 21.4
Advanced spatial learning technique for automatic mapping of geomorphological features in alpine periglacial environment

Alessio Poloni[1], Dr. Marj Tonini[1], Dr. Christophe Lambiel[1]

[1] *Institut des Dynamiques de la Surface Terrestre (IDyST), University of Lausanne, Batiment Geopolis, CH-1015 Lausanne (alessio.poloni@unil.ch)*

Permafrost corresponds to unconsolidated sediments or bedrock that remains frozen for at least two consecutive years (Rogger et al. 2017). This phenomenon is difficult to observe because it occurs in the sub-surface and is therefore invisible to the naked eye. Permafrost is an important component of high mountain regions, and its investigation is of current interest, especially with regard to its evolution in relation to ongoing climate changes. The main controlling factors are the mean annual air temperature, the solar radiation, the characteristics of the ground surface and of the active layer, and the snow duration and depth.

In mountainous regions such as the Alps, characterised by highly variable micro-climatic, topographical and terrain roughness conditions, the spatial distribution of permafrost is very heterogeneous. This complex pattern makes it difficult to map at the local scale. Several permafrost distribution models, based on physical, empirical or statistical approaches, have been developed, but these models tend to overestimate the actual extent of permafrost. In recent years, interest about prediction of the presence or absence of permafrost determined through the use of machine learning algorithms has grown.

Machine learning methods are increasingly applied in geo-environmental applications to predict the occurrence of a phenomenon based on the observations of its presence in a given area and on a set of predictive factors. The Machine learning domain includes algorithms capable of learning from data, by modelling the hidden relationships linking a set of input and output variables. For permafrost distribution, models based on Random Forest (RF) have proven to be efficient and accurate (Deluigi et al. 2017), but the algorithm is generally applied in a “non-spatially” way, and it cannot consider the spatial relationships between variables.

In this research, an advanced classification algorithm is developed with the aim of determining the occurrence of permafrost at the local scale with high accuracy. This algorithm is based on two methods derived from RF, which additionally allow a spatial analysis of the phenomenon: Geographical RF (Georganos et al. 2019) and Spatial RF (Benito 2021). One of the novelties of this approach consists in the addition of a new approach for short-range roughness computation (Trevisani et al. 2023). The input dataset includes twelve permafrost control variables (altitude, northness, eastness, terrain roughness, slope, direct solar radiation, ndvi, granulometry, plan curvature, profile curvature, combined curvature, lithology). The final output is an high-precision permafrost susceptibility map of the selected study area, which also consider the spatial contiguity among the pixels.

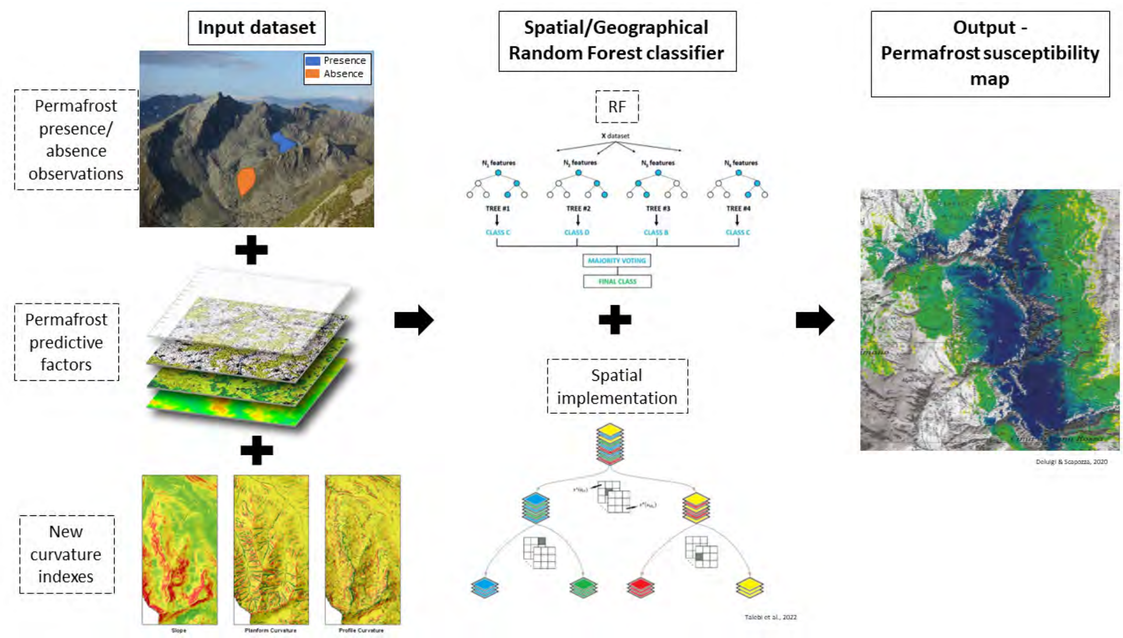

Figure 1. Methodology workflow diagram.

REFERENCES

Blas M. Benito. 2021. R package spatialRF: Easy Spatial Regression with Random Forest. doi: 10.5281/zenodo.4745208. https://blasbenito.github.io/spatialRF/

Deluigi, N., Lambiel, C., & Kanevski, M. 2017. Data-driven mapping of the potential mountain permafrost distribution. Science of The Total Environment, 590-591, 370-380. https://doi.org/10.1016/j.scitotenv.2017.02.041

Georganos, S., Grippa, T., Niang Gadiaga, A., Linard, C., Lennert, M., Vanhuysse, S., . . . Kalogirou, S. 2021. Geographical random forests: A spatial extension of the random forest algorithm to address spatial heterogeneity in remote sensing and population modelling. Geocarto International, 36(2), 121-136. https://doi.org/10.1080/10106049.2019.1595177

Rogger, M., Chirico, G. B., Hausmann, H., Krainer, K., Brueckl, E., Stadler, P., & Bloeschl, G. 2017. Impact of mountain permafrost on flow path and runoff response in a high alpine catchment. Water Resources Research, 53(2), 1288-1308.

Trevisani, S., Teza, G., & Guth, P. 2023. A Simplified Geostatistical Approach for Characterizing Key Aspects of Short-Range Roughness. CATENA, Volume 223, 106927, ISSN 0341-8162. https://doi.org/10.1016/j.catena.2023.106927.

P 21.5
Spatio-temporal changes across very small West African forest remnants

Vladimir R. Wingate[1], Giulia Curatola Fernández[1], Chinwe Ifejika Speranza[1]

[1] *Land Systems and Sustainable Land Management, Institute of Geography, University of Bern, Hallerstrasse 12, 3012, Bern, Switzerland*

Tropical forests are a fundamental component of the Earth System. In West Africa, vast tracts of tropical forests are being lost to deforestation; the remnant forest fragments provide a wealth of ecosystem services including biodiversity habitat connectivity, yet they are still to be mapped and their dynamics and ecosystem services quantified. Moreover, small forest fragments and remnant forest patches are disproportionately impacted by deforestation and fragmentation. It follows that such patches present a high probability of disappearing and therefore constitute an important research and conservation priority. Very small forest patches in the region have not been widely mapped or catalogued before; indeed, previous work has focused on inventorying remnant forest patches ranging in size from 100-1000 ha, and forest fragments at continental scales. Hence, for the first time, this study maps very small forest patches and quantifies both their cumulative forest cover loss and gain, as well as the annual cumulative forest change across all mapped patches, for the period 2000-2022, to quantify how quickly they are changing. Here, we leverage the Global Forest Watch tree cover dataset and an object-based forest fragment mapping method, to measure the area of forest change for individual forest patches outside of protected areas. We then differentiated them as either primary or secondary forests, and examined the area, rate, and trend of forest change, as well as identified the year when the most important change events took place. We found that very small forest patches (0.5 – 100 ha) lying outside of protected areas are present extensively throughout the West African Guinean and Guineo-Congolian biomes, which span the four countries of Togo, Benin, Nigeria, and Cameroon. Additionally, we identified that the smallest primary forest patches are losing on average almost half of their area over the 22-year study period - twice as much as for secondary forests, and a significant positive trend in the rate of forest loss was identified. Moreover, forest loss impacted particularly the smaller forest patches and accelerated over the analyzed period. Our results show that forest loss impact particularly very small remnant forest patches, is taking place at an increasing rate, and was particularly pronounced during the period 2020-2021.

22 Geodesy

Adrian Jäggi, Benedikt Soja, Daniel Willi

Swiss Geodetic Commission

TALKS:

22.1 Aichinger-Rosenberger M., Aregger M., Kopp J., Soja B.: Detection of convective storm signatures in GNSS-SNR: two case studies from the summer of 2021 in Switzerland

22.2 Behzadpour S., Gou J., Kiani Shahvandi M., Öhlinger F., Mayer-Gürr T., Soja B.: Machine learning-based GRACE accelerometer transplant

22.3 Benedikt M., Garayt B., Koch J., Mainaud-Durand H., Marti U., Rothacher M., Ryf A., Soja B., Varga M., Weyer B., Wieser A., Willi D.: Ongoing and futur geodetic studies for the CERN Futur Circular Collider

22.4 Borlat E., Deillon Y., Willi D.: Modernisation of the Swiss Vertical Reference System

22.5 Calero-Rodríguez E.J., Dach R., Jäggi A.: Advanced use of GNSS for geodesy: Estimability of the C20 gravity coefficient

22.6 Christ H., Jeiziner G., Villiger A., Biberstein-Pedroni C., Willi D.: Current status and futue developments of the Swiss Positioning Service swipos

22.7 Dach R., Schaer S., Arnold D., Brockmann E., Kalarus M., Prange L., Stebler P., Jäggi A.: GNSS Products Made in Switzerland

22.8 Geisser L., Meyer U., Arnold D., Jäggi A.: Scientific Potential of the Geodetic Technique of Satellite Laser Ranging

22.9 Jospin L.V., Layahe J., Skaloud J.: From Probability Graphical Models to Dynamic Networks — A Bayesian perspective on Smooth Best Estimate of Trajectory with applications in Geodetic Engineering

22.10 Kobel C., Arnold D., Jäggi A.: Advancing global GNSS network determination by the integration of Low Earth Orbiters

22.11 Lasser M., Meyer U., Arnold D., Jäggi A.: Time-variable gravity field determination from GRACE Follow-On data using empirical noise modelling

22.12 Mao S., Kłopotek G., Soja B.: Machine learning-based global ionospheric modeling using multi-GNSS data

22.13 Miller A., Arnold D., Jäggi A.: Modelling Non-Gravitational Forces for a more Dynamical Spire Orbit Representation using the Bernese GNSS Software

22.14 Müller L., Rothacher M., Soja B.: Formation of a GNSS network in space based on the Spire CubeSat constellation

22.15 Pan Y., Kłopotek G., Crocetti L., Weinacker R., Sturn T., See L., Dick G., Rothacher M., McCallum I., Navarro V., Soja B.: Tropospheric Delay Estimation with Crowdsourced Smartphone GNSS Data

22.16 Schmid L., Medic T., Wieser A.: Towards improved alignment of TRI and TLS data for geomonitoring with increased resolution

22.17 Shehaj E., Geiger A., Frey O., Moeller G., Strozzi T., Soja B., Rothacher M.: Evaluation of tropospheric delays in the Swiss Alps Region from GNSS, Persistent Scatterer Interferometry and the Numerical Weather Prediction Model COSMO

22.18 Shehaj E., Leroy S., Cahoy K., Geiger A., Crocetti L., Moeller G., Soja B., Rothacher M.: Mapping GNSS radio occultation climatologies using machine learning

22.19 Varga M.: Concept Development of the Swiss National Geomagnetic Networks

22.20 Xingjun L., Nicolas O., Wenbin X., Joël R.: Episodic events of oblique rifting using InSAR time series and seismicity (2016 – 2022), Reykjanes Peninsula (Iceland)

POSTER:

P 22.1 Behzadpour S., Soja B.: Exploring Thermospheric Neutral Density Solutions Based on GRACE/GRACE-FO

22.1
Detection of convective storm signatures in GNSS-SNR: two case studies from the summer of 2021 in Switzerland

Matthias Aichinger-Rosenberger[1], Martin Aregger[2,3], Jerome Kopp[2,3], Benedikt Soja[1]

[1] Institute of Geodesy and Photogrammetry, ETH Zürich, Zürich, Switzerland
[2] Institute of Geography, University of Bern, Bern, Switzerland
[3] Oeschger Center for Climate Change Research, University of Bern, Bern, Switzerland

Observations from Global Navigation Satellite Systems (GNSS) have become an important data source for atmospheric science over the last decades. Commonly derived parameters like signal path delays and integrated water vapor can be utilized for data assimilation, showing beneficial impacts on precipitation forecasts. In recent years, other meteorological phenomena and parameters, such as soil moisture variations, snow properties, or foehn winds have been studied by means of GNSS remote sensing.

Since their signals are broadcasted on L-band carrier frequencies, GNSS act as an all-weather-operation system, offering substantial benefits compared to e.g., optical remote sensing systems. Nevertheless, severe weather events can still impact the strength of signals received at a ground station, as we showcase in our study.

We investigate GNSS Signal-to-Noise Ratio (SNR) observations collected during two severe convective storm events over the city of Zurich in early summer [2021]. In order to detect storm signatures in SNR time series we utilize a simple statistical algorithm, originally developed for detecting hail particles from volcanic eruptions. Our results indicate that severe convective storms are visible in GNSS-SNR observations. During the exact event periods, which are determined by weather radar observations, SNR values of affected satellites show significant drops compared to normal weather conditions.

22.2
Machine learning-based GRACE accelerometer transplant

Saniya Behzadpour[1], Junyang Gou[1], Mostafa Kiani Shahvandi[1], Felix Öhlinger[2], Torsten Mayer-Gürr[2], and Benedikt Soja[1]

[1] *Institute of Geodesy and Photogrammetry, ETH Zurich, Robert-Gnehm-Weg 15, CH-8093 Zurich (sbehzadpour@ethz.ch)*
[2] *Graz University of Technology, Institute of Geodesy, Graz, Austria*

In the context of gravimetry satellite missions, specifically GRACE (Gravity Recovery and Climate Experiment) and GRACE-FO (GRACE Follow-On), the recovery of the gravity field relies on crucial measurements from accelerometers onboard both satellites. These accelerometers play a vital role in accurately assessing non-gravitational forces affecting the spacecraft's orbit, such as atmospheric drag, solar radiation pressure, and albedo. The quality of data from these accelerometers, referred to as ACC products, significantly determines the precision of the resulting gravity field models.

We investigate the potential of machine learning (ML) algorithms for recovering the ACC data of GRACE-B using measurements from GRACE-A and relevant model computations. We focus on the application of a Long Short-Term Memory (LSTM) architecture for predicting GRACE-B accelerometer data. The performance evaluation entails the utilization of Root Mean Square Error (RMSE) as a metric, coupled with a comprehensive comparison between the projected data and actual calibrated data. Additionally, a thorough comparative analysis will be conducted between the ML-based ACC products and the official transplant products and their impact on the gravity field will be discussed.

22.3
Ongoing and futur geodetic studies for the CERN Futur Circular Collider

Michael Benedikt[1], Bruno Garayt[2], Julia Koch[3], Helene Mainaud-Durand[1],Urs Marti[4], Markus Rothacher[3], Adrian Ryf, Benedikt Soja[3], Matej Varga[3], Benjamin Weyer[1], Andreas Wieser[3], Daniel Willi[4]

[1] *CERN, Esplanade des Particules 1, Geneva, 1211, Geneva 23, Switzerland*
[2] *Institut national de l'information géographique et forestiere, 73 avenue de Paris, 94165 Saint-Mandé Cedex*
[3] *ETH Zürich, Institute of Geodesy and Photogrammetry, Robert-Gnehm-Weg 15, 8093 Zürich*
[4] *Federal Office of Topography swisstopo, Seftigenstrasse 264 (P.O. Box), 3084 Wabern*

The Future Circular Collider (FCC) study is developing designs for a new research infrastructure to host the next generation of higher performance particle colliders to extend the research currently being conducted at CERN. The particle accelerator will be installed in a dedicated 91km long circular tunnel at around 200 m underground.

Building the FCC tunnel, installing and aligning each component and experiment of the machine at the intended location will be a challenging task relying notably on the quality and accuracy of the geodetic infrastructure. A solid geodetic foundation for the planning, construction, alignment and operation of the FCC will be implemented to support the different levels of accuracy required, from the initial decametric coarse placement study to the final and perpetually refined submillimetric alignment.

Studies are ongoing to update the CERN geodetic infrastructure making it ready for the FCC and compatible with each phase of the project. The definition of the local coordinate system is beeing updated, a new surface geodetic network will be materialized and a new local geoid model is under development.

22.4
Modernisation of the Swiss Vertical Reference System

Elisa Borlat[1], Yves Deillon[1], Daniel Willi[2]

[1] Institute of Territorial Engineering INSIT, School of Engineering and Management HEIG-VD, Route de Cheseaux 1 (CP-521), CH-1401 Yverdon-les-Bains (swiss_hieght_system@heig-vd.ch)
[2] Federal Office of Topography swisstopo, Seftigenstrasse 264 (P.O. Box), 3084 Wabern

The concept of altitude is not solely based on geometry, as a typical user of altimetric data might initially perceive. Instead, it is also based on physical definitions. A GNSS (Global Navigation Satellite System) measurement results in an ellipsoidal altitude, which is purely geometric. However, only physical heights which take into account the Earth's gravitational field, meet practical requirements, and allow measurements from different techniques to be combined, such as levelling with GNSS measurements. For several years, the quantity and utilisation of 3D geodata are surging, heavily driven by the rapid technological advancements in satellite-based GNSS, which allow a centimeter-level accuracy. This evolution underscores the constraints of the current swiss vertical reference system LN02, a century-old legacy built upon leveling measurements, which struggles to meet the contemporary requirements for absolute altimetric determination. The differences between LN02 and a rigorous height system is currently from 30 up to 40 centimetres (Schlatter, 2007).

In this context, the School of Engineering and Management HEIG-VD, in close collaboration with the Federal Office of Topography swisstopo, has launched a study on the modernisation of the height reference system and frame in Switzerland. This study covers the technical and normative aspects to be defined to allow a system change, including international comparison. An initial report has been published on this matter (Willi and al., 2022).
Part of this study consists of establishing the main characteristics of existing altimetric information (analog and digital) by drawing up a technical questionnaire targetting all users of altimetric data in Switzerland. The results show that over 90% of altimetric data is managed in the official swiss reference frame LN02, but that around 40% of data is first acquired by GNSS before being transformed into LN02, leading to a deterioration in data accuracy.
The study should also raise awareness among professionals and users of altimetric data, so that they can better anticipate any transition. Several videos were produced for this purpose, and the questionnaire helped identify the kind of problem expected by data managers. The main concern related to the risk of confusion between the old and new height references. The second main concern is the lack of communication between the various professions and understanding the new height system.

Investigations related to an altimetric system change will continue. This includes defining the new height system, creating and evaluating transformation tools. For the definition, the current choice is to use normal heights. The new altimetric system will be compatible with higher-level systems, such as global measurement systems like GNSS, and will have a kinematic component, allowing to take into account movements of the Earth's crust.

REFERENCES
Schlatter A. 2007. Das neue Landeshöhennetz der Schweiz LHN95, Schweizerische Geodätische Kommission, 328.
Willi D. and al. 2022. Studie zur Modernisierung des Schweizer Höhenbezugssystems und -rahmens (Teil I – Grundlagen, Stand der Technik und internationaler Vergleich), Geodäsie und Eidgenössische Vermessungsdirektion, Report 22-07.

22.5
Advanced use of GNSS for geodesy: Estimability of the C_{20} gravity coefficient

Emilio J. Calero-Rodríguez[1], Rolf Dach[1], Adrian Jäggi[1]

[1] *Astronomical Institute of the University of Bern, Sidlerstrasse 5, 3012 Bern, Switzerland (emilio.calero@unibe.ch)*

Geodesy profits from space-borne missions, since satellite-based observations are essential to realize terrestrial reference frames (TRF) at global scales. Among the different satellite techniques that support the generation and maintenance of these frames, the GNSS (Global Navigation Satellite System) constellations early became a major contributor due to the dense network of dedicated stations that provide high-quality measurements, which are today exploited at the millimetre level by the analysts.

Whereas the GNSS capabilities to determine the Earth's orientation as well as the coordinates of ground stations, both of which are vital to realize TRF, have been demonstrated within the decades, little attention has been paid to the GNSS sensitivity to the Earth's gravity field, which is another fundamental pillar of geodesy. Consequently, we present some recent findings with special focus on the gravity coefficient C_{20} (i.e., Earth's flattening).

We discuss the problem from an instructive point of view, starting from the fundamental GNSS observable and its relationship with the geodetic parameters. It is noticed that the estimation of C_{20} gravitational signals become very challenging because of two factors: (1) the large orbital altitude of GNSS satellites, which results in a poor sensitivity to these signals, and (2) correlations between the many co-estimated parameters. Only after applying some constraints and accumulating a sufficient amount of data, these problems are partially overcome and the estimated parameters represent physical signals.

22.6
Current status and futue developments of the Swiss Positioning Service swipos

Hanspeter Christ, Gilbert Jeiziner, **Arturo Villiger**, Claudia Biberstein-Pedroni, Daniel Willi

Swiss Federal Office of Topography swisstopo (arturo.villiger@swisstopo.ch)

The Swiss Positioning Service (swipos) is a real-time correction service for GNSS-RTK applications covering GPS, Galileo, and GLONASS. The main focus area of the service is on the state territory of Switzerland and its backbone is the Automated GNSS Network Switzerland (AGNES) which provides 31 evenly distributed stations over Switzerland. Incorporating additional sites from partner institutions close to the Swiss boarder ensures the service quality not only within the country but also close to the boundary regions.

The main purpose of the swipos-service is to ensure the access to the Swiss reference systems using real-time kinematic applications (RTK). This is currently achieved by offering two different services (also known as mountpoints) including a multi-GNSS mountpoint and a legacy mountpoint which includes GPS and GLONASS only. While swipos was extended to multi-GNSS, the Beidou support remained restricted to Beidou 2 and stopped by the end of June 2023. We are currently working on the extension of swipos to support Beidou 3 aiming to offer full mutli-GNSS correction streams in late 2024.

22.7
GNSS Products Made in Switzerland

Rolf Dach[1], Stefan Schaer[1,2], Daniel Arnold[1], Elmar Brockmann[1], Maciej Kalarus[1], Lars Prange[1], Pascal Stebler[1], Adrian Jäggi[1]

[1] *Astronomical Institut, University of Bern, Sidlerstrasse 5, CH-3012 Bern (rolf.dach@unibe.ch)*
[2] *Federal Office of Topography swisstopo, Seftigenstrasse 264, CH-3084 Wabern*

Geodata usually is geo-referenced with respect to a global or regional reference frame. One of the most common, well established, and most efficient technologies to provide direct access to reference frames are GNSS (Global Navigation Satellite Systems). Monitoring the atmosphere using GNSS is another field of applications. Most of these applications require precise GNSS satellite orbits, satellite clock corrections based on a stable global reference frame, well defined conventions for antenna calibrations and the various GNSS system biases.

The International GNSS Service (IGS) was established exactly for this purpose about 30 years ago. Today the IGS is a global infrastructure providing several series of products where all of them follow the same principle: solutions from a number of analysis centers are compared and combined with different latency and accuracy levels.

CODE – the Center for Orbit Determination in Europe – is one of the leading analysis centers with a dedicated focus on rigorous multi-GNSS processing. It is a joint venture of the following four institutions:

- Astronomical Institute, University of Bern (AIUB), Bern, Switzerland
- Federal Office of Topography swisstopo, Wabern, Switzerland
- Federal Agency of Cartography and Geodesy (BKG), Frankfurt a. M., Germany
- Institute for Astronomical and Physical Geodesy, Technical University of Munich (IAPG, TUM), Munich, Germany

The operational computations are performed at AIUB.

The presentation will provide an inside in the activities of the IGS in general but highlighting the contributions from the CODE analysis center in particular. This includes which products are available with which latency and how they can be beneficial for your work.

22.8
Scientific Potential of the Geodetic Technique of Satellite Laser Ranging

Linda Geisser[1], Ulrich Meyer[1], Daniel Arnold[1], Adrian Jäggi[1]

[1] Astronomical Institute, University of Bern, Sidlerstrasse 5, CH-3012 Bern (linda.geisser@unibe.ch)

For more than half a century, the technique of Satellite Laser Ranging (SLR), which measures the round-trip time-of-flight of ultra-short laser pulses emitted by a station to an artifical Earth orbiter, e.g., a satellite, and back to the station, is widely-used in geodetic and geophysical research studies. With its indispensable contribution to the determination of geodetic parameters, e.g., the geocenter and station coordinates, SLR is essential for the realization of long-term stable terrestrial reference frames. Although nowadays the Earth's time variable gravity field is determined by dedicated satellite gravimetry missions, e.g., Gravity Recovery And Climate Experiment (GRACE) and GRACE Follow-on, some of the low-degree Spherical Harmonic (SH) geopotential coefficients are still better determined by SLR.
To investigate the scientific potential of SLR, weekly multi-satellite SLR solutions, where the orbits are determined in 7-day arcs simultaneously with station coordinates and other geodetic parameters, e.g., SH geopotential coefficients and Earth rotation parameters, are performed. These solutions will cover all 'three pillars' of geodesy, i.e., geokinematics, Earth rotation and the Earth's gravity field, and, therefore, ensure a highest possible level of consistency. The quality of the estimated parameters is validated by comparison with internal and external reference series.

22.9
From Probability Graphical Models to Dynamic Networks — A Bayesian perspective on Smooth Best Estimate of Trajectory with applications in Geodetic Engineering

Laurent Valentin Jospin[1], Jesse Layahe[1], Jan Skaloud[1]

[1] *École Polytechnique Fédérale de Lausanne, CRYOS, Station 2, 1015 Lausanne (laurent.jospin@epfl.ch)*

Bayesian statistics is concerned with the integration of new information obtained through observations with prior knowledge, and accordingly, is often related to information theory (Jospin 2022). Recursive Bayesian estimation methods, such as Kalman Filters, have long been the de facto approach for Smooth Best Estimate of Trajectory (SBET) computations (Aslan 2021). Recently, the robotics and geodetic engineering communities have proposed to use an alternative approach referred to as Dynamic Networks (Rouzaud 2011), to globally determine the SBET solution. Global approaches are generally more complex to compute but are better at propagating additional information to all unobserved variables (Buntine 1994).

In this presentation, we will outline the theoretical differences between recursive and global Bayesian models for SBET estimation from a probabilistic and information theoric perspective. We will show how prior knowledge can be integrated into the models and its effect on the accuracy of the SBET estimation in both cases. The theory will be illustrated with practical experimental results related to our recent work on line scanning Hyperspectral camera orientation. Line scanning sensor configuration is a good candidate to demonstrate the benefits of a Bayesian approach to sensor orientation, as each scan-line corresponds to a single pose of the platform, making them far less constrained as compared to pinhole cameras (Brell 2016). The traditional point estimate method for orientation estimation of pinhole cameras (i.e., Bundle Adjustment) is under-constrained in such a configuration. As such, the inclusion of a prior is necessary to make the solution unique.

REFERENCES

Jospin, L.V., Laga, H., Boussaid, F., Buntine, W. and Bennamoun, M., 2022. Hands-on Bayesian neural networks—A tutorial for deep learning users. IEEE Computational Intelligence Magazine, 17(2), pp.29-48.

Aslan, M.F., Durdu, A., Yusefi, A., Sabanci, K. and Sungur, C., 2021. A tutorial: Mobile robotics, SLAM, bayesian filter, keyframe bundle adjustment and ROS applications. Robot Operating System (ROS) The Complete Reference (Volume 6), pp.227-269.

Rouzaud, D. and Skaloud, J., 2011. Rigorous integration of inertial navigation with optical sensors by dynamic networks. Navigation, 58(2), pp.141-152.

Buntine, W.L., 1994. Operations for learning with graphical models. Journal of artificial intelligence research, 2, pp.159-225.

Brell, M., Rogass, C., Segl, K., Bookhagen, B. and Guanter, L., 2016. Improving sensor fusion: A parametric method for the geometric coalignment of airborne hyperspectral and LiDAR data. IEEE Transactions on Geoscience and Remote Sensing, 54(6), pp.3460-3474.

22.10
Advancing global GNSS network determination by the integration of Low Earth Orbiters

C.Kobel, D.Arnold, A.Jäggi

The Precise Orbit Determination (POD) of Low Earth Orbiters (LEO) is a fundamental aspect of today's Earth observation techniques, enabled by Global Navigation Satellite Systems (GNSS) data. Traditionally, this procedure relies on the utilization of separately established GNSS satellite orbits and clock corrections, determined by data collected from terrestrial GNSS stations, which are introduced as known. However, emerging insights from recent studies highlight the advantages of integrating data from Global Positioning System (GPS) collected by receivers onboard LEO satellites into the computation of global GPS network solutions. Through such integration, the quality of resulting GPS orbit solutions is improved, and specific geodetic parameters, including Earth's center-of-mass coordinates, are refined.

In this study, we process code and phase observations collected from spaceborne GNSS receivers of LEO satellites together with data from International GNSS Service (IGS) ground stations. Through this approach, an integrated GNSS-LEO solution is computed, encompassing the estimation of orbit parameters for both GNSS and LEO satellites, together with key geodetic parameters. To exploit the data, single-receiver ambiguity fixing will not only be adopted to the terrestrial GNSS data but also to the LEO GNSS data.

Within the scope of this investigation various configurations of integrated LEOs are investigated, putting particular emphasis on the diversity of their orbit characteristics. An important aspect of this study involves elucidating the influence of explicit modeling of non-gravitational forces in the determination of LEO orbits on the resulting LEO-integrated global network solution.

This study uses various quality metrics to determine the quality of the solutions, including the analysis of GNSS orbits. It also includes the rigorous assessment of the quality of the derived geodetic parameters, with special attention on Earth's center-of-mass coordinates and Earth rotation parameters. The goal of this study is a substantial contribution to the ongoing evolution of satellite-based Earth observation, positioning systems, and estimation of geodetic parameters.

22.11
Time-variable gravity field determination from GRACE Follow-On data using empirical noise modelling

Martin Lasser[1], Ulrich Meyer[1], Daniel Arnold[1], Adrian Jäggi[1]

[1] *Astronomical Institute, University of Bern, Sidlerstrasse 5, CH-3012 Bern (martin.lasser@unibe.ch)*

Over the last twenty years the satellite missions GRACE and its successor GRACE Follow-On have provided a unique insight into the time-variable components of the Earth's gravity field on a global scale. A lot of effort has been and is still put into understanding the measurement data but also different analysis concepts. In this contribution we study GRACE Follow-On satellite-to-satellite tracking using the inter-satellite K-band link and kinematic positions of the satellites as observations and pseudo-observations, respectively, to derive orbits and global gravity field models. A key component of any model is the accurate specification of its quality. In the case of gravity field modelling from satellite data typically a least-squares adjustment is performed to obtain model parameters representing the satellites' orbits and a snapshot of the Earth's gravity field. However, associated formal errors usually do not reflect the error level that could be expected, but provide much lower error estimates. We present an approach to come up with reasonable error estimates by empirically modelling the stochastic noise based on the post-fit residuals between the final GRACE Follow-On orbits, that are co-estimated together with the gravity field, and the observations, expressed in position residuals for the kinematic positions and in K-band range-rate residuals. We compare and validate the solutions that use empirical modelling with solutions which do not make use of any kind of empircal noise modelling by examining the stochastic behaviour of the respective post-fit residuals, by investigating areas where a low noise is expected and by inspecting the mass trend estimates in certain areas of global interest.

22.12 Machine learning-based global ionospheric modeling using multi-GNSS data

Shuyin Mao[1], Grzegorz Kłopotek[1], Benedikt Soja[1]

[1] *Institute of Geodesy and Photogrammetry, ETH Zurich, 8093 Zurich, Switzerland (shumao@ethz.ch)*

Accurately modeling the complex structures and variations within the ionosphere is an important yet challenging task. Traditional spatial modeling techniques, like spherical harmonics, can efficiently capture large-scale and global features of the ionosphere, but they tend to smooth out local variations and irregularities due to limited degrees and orders. As a result, this could lead to the potential loss of important small-scale details of the ionosphere. To address this challenge and achieve a more precise representation of the ionosphere, it becomes imperative to explore novel modeling approaches. As an effective tool to automatically uncover non-linear relationships between inputs and outputs, machine learning (ML) has shown great potential in various fields.

The goal of this study is to develop ML-based global ionospheric maps (ML-GIM) to capture essential local features better than traditional approaches. First, vertical total electron content (VTEC) from 350 global IGS stations was derived using carrier-to-code leveling through a Kalman filter. Next, the derived satellite-specific VTEC time series were used to train the chosen ML models. Several algorithms including neural network (NN), extreme gradient boosting (XGBoost) and random forest (RF) were compared. Finally, the performance of the ML models was evaluated by comparing the spatial predictions with the VTEC data processed by the Massachusetts Institute of Technology (MIT) and satellite altimetry data. The results indicate that the NN outperforms XGBoost and RF. ML-GIM also show superior performance compared to Chinese Academy of Sciences' GIMs based on spherical harmonics, reducing the average standard deviation with satellite altimetry-based VTEC from 4.91 TECU to 4.05 TECU.

22.13
Modelling Non-Gravitational Forces for a more Dynamical Spire Orbit Representation using the Bernese GNSS Software

Alexandra Miller[1], Daniel Arnold[1], Adrian Jäggi[1]

[1] Astronomical Institute, University of Bern, Sidlerstrasse 5, CH-3012 Bern (alexandra.miller@students.unibe.ch)

In recent years, the use of nano satellites, which weigh less than 10 kg, has increased substantially. Because they can be built and launched rather cost-effectively, mega-constellations made up of hundreds of such satellites have become more commonplace. A prominent example of such a megaconstellation are the Spire Lemur satellites, operated by Spire Global Inc. They are low earth orbiters (LEOs) equipped with dual-frequency GPS receivers, enabling precise orbit determination (POD) using GPS code and phase measurements.

From these measurements, reduced-dynamic orbit solutions can be calculated with the Bernese GNSS Software, using, e.g., piecewise-constant and constant accelerations as pseudo-stochastic parameters (PSPs).

Up until now, the Spire force modelling at the Astronomical Institute of the University of Bern was mainly confined to gravitational forces, with the accelerations caused by the unmodelled non-gravitational forces being largely absorbed by PSPs. As Spire satellites have a large area-to-mass ratio and are LEOs, non-gravitational forces, e.g., drag, solar radiation pressure and Earth radiation pressure play a large roll. In order to explore the possibility of a more dynamical orbit solution, these non-gravitational forces are introduced to the POD using different macro models, as well as a stricter constraining of the PSPs. Because of the lack of external orbit validation methods, mainly RMS, PSP and kinematic-to-reduced-dynamic orbit comparisons are used to determine the quality of the produced orbit solution. In addition, external solutions calculated using ESA’s NAPEOS software package, which also implemented non-gravitational forces, are reproduced as closely as possible and compared.

22.14
Formation of a GNSS network in space based on the Spire CubeSat constellation

Lukas Müller[1], Markus Rothacher[1], Benedikt Soja[1]

[1] *Institute of Geodesy and Photogrammetry, ETH Zürich, Zürich, Switzerland*

The number of Low Earth Orbit (LEO) satellites equipped with Global Navigation Satellite System (GNSS) receivers is growing rapidly. GNSS observations in space are no longer limited to a few Earth observation satellites, but large nanosatellite constellations enable the formation of a dense and homogeneous network of GNSS receivers around the Earth. An example is the Spire CubeSat constellation, which consists of more than 100 satellites equipped with dual-frequency GNSS receivers. In this study, we use data from the Spire constellation to investigate the feasibility of forming a GNSS network in space.

A space-based GNSS network has the potential to improve geodetic Earth observation, as it offers several advantages over a ground-based GNSS network and over GNSS observations on board single or formation-flying satellites. First, such a GNSS network can be processed in a double-difference mode without the need for ground observations, and thus, the GNSS signals are not affected by tropospheric refraction. Secondly, a dense and homogeneous GNSS network in space can improve the sensitivity to certain geodetic parameters by providing a better observation geometry than a few LEO satellites or a ground-based network. This study investigates the feasibility of forming such a space-based GNSS network for the estimation of various parameters, namely the orbit parameters of the LEO and the GNSS satellites, as well as low-degree coefficients of the Earth's gravity field, including the geocenter coordinates.

In a first step, we use simulated GNSS observations to develop the framework for the processing of a GNSS network in space and to get an impression of the required accuracy for the a-priori LEO and GNSS orbits. Based on the orbits of the Spire CubeSat constellation, we compute the number of possible GNSS single- and double-differences and the corresponding baseline lengths. Using these observations, we investigate how well carrier-phase ambiguities can be resolved and how this depends on the constellation geometry. By processing GNSS double-difference observations, we estimate parameters related to the LEO orbits and the Earth's gravity field. To assess the expected accuracy of these parameters, we examine their sensitivity to small errors resulting from, e.g., the force model or small acceleration errors like neglecting ocean tide or Earth albedo effects. Initial results indicate that an accuracy of the a-priori LEO orbits at the level of a few centimetres is required to take advantage of the double-difference processing and to successfully resolve the carrier-phase integer ambiguities.

In a further step, the methods developed on the basis of the simulated data set will be applied to real GNSS observations from 24 satellites of the Spire constellation over a period of one day. By comparing the results obtained from the simulated and real GNSS observations, we will assess the applicability of the network processing approach to LEO constellations and identify the main limitations. Based on this research, we will draw conclusions about the potential of large satellite constellations to complement the existing Earth observation missions and ground-based GNSS networks.

22.15
Tropospheric Delay Estimation with Crowdsourced Smartphone GNSS Data

Yuanxin Pan[1], Grzegorz Kłopotek[1], Laura Crocetti[1], Rudi Weinacker[2], Tobias Sturn[2], Linda See[2], Galina Dick[3], Markus Rothacher[1], Ian McCallum[2], Vicente Navarro[4], Benedikt Soja[1]

[1] *Institute of Geodesy and Photogrammetry, ETH Zurich, Zurich, Switzerland (yxpan@ethz.ch)*
[2] *International Institute for Applied Systems Analysis (IIASA), Laxenburg, Austria*
[3] *GFZ German Research Centre for Geosciences, Potsdam, Germany*
[4] *European Space Agency, European Space Astronomy Center, Madrid, Spain*

The monitoring of the troposphere is of significant importance for human activities. The Global Navigation Satellite System (GNSS) is an essential tool to conduct this task. Currently, GNSS tropospheric monitoring relies primarily on geodetic-grade stations. However, such stations are too costly to be densely deployed, which limits the contribution of GNSS to tropospheric monitoring. In 2016, Google released the raw GNSS measurement Application Programming Interface (API) for smartphones running Android 7.0 or later. Given that there are billions of Android smartphones worldwide, it is a great scientific opportunity to utilize these devices for atmospheric monitoring. The Application of Machine Learning Technology for GNSS IoT Data Fusion (CAMALIOT) project was launched in 2021 to investigate this idea. During a 9-month data crowdsourcing campaign in 2022, around twelve thousand smartphone users participated worldwide and more than 5 TB of data were collected.

In this study, we will demonstrate Zenith Total Delay (ZTD) estimation with smartphone data collected in Germany. First, the data of high quality were automatically selected by a machine learning (ML)-based classifier. Then, the GNSS observations were processed with Precise Point Positioning (PPP) with the ionospheric delays interpolated with surrounding SAPOS (Satellite Positioning Service of the German State Survey) GNSS stations. The ZTDs derived from ERA5 and an ML-based delay model served as benchmarks. The results reveal that an accuracy of about 10 mm can be achieved by utilizing the crowdsourced smartphone data of high quality. Furthermore, limiting factors, such as the minimal time span of the data collection, are also discussed. The results of this study demonstrate the potential of crowdsourced smartphone data for tropospheric monitoring and can serve as a reference for future GNSS data crowdsourcing campaigns.

22.16
Towards improved alignment of TRI and TLS data for geomonitoring with increased resolution

Lorenz Schmid[1], Tomislav Medic[1], Andreas Wieser[1]

[1] *Geosensors and Engineering Geodesy, Institut of Geodesy and Photogrammetry ETH Zürich, Stefano-Franscini-Platz 5, CH-8093 Zürich (lorenz.schmid@geod.baug.ethz.ch)*

Fusing Terrestrial Radar Interferometry (TRI) and Terrestrial Laser Scanning (TLS) offers a powerful tool for geomonitoring by leveraging their complementary strengths. While TLS provides high-resolution 3D point cloud data for comprehensive site mapping, it is limited to centimeter-level precision in many outdoor applications and thus often not sufficient to detect displacements in the millimeter range, even exploiting redundancy. In contrast, TRI has the potential of detecting sub-millimeter deformations but poses challenges in image distortion and interpretation. Combining the two enables precise localization and quantification of motion/deformation of small geological features, for example, related to landslides, rockfalls, or permafrost-induced debris flows, while also simplifying the interpretation through 3D mapping.

In a preliminary study (Schmid et al., 2023), we investigated the accuracy of TRI-to-TLS mapping using a common workflow. With height differences up to several hundred meters and distances up to about 1.5 km between the instruments and the monitored surfaces we found systematic misalignments on the order of several tens of meters. This level may be acceptable for globally monitoring deformation processes like the sliding of an entire slope, but is not adequate for precise localization of individual events or local variations of a deformation process. To tap into this unused potential, we are investigating methods for better alignment of TRI data with TLS point clouds.

We pursue two approaches: (i) a data-driven approach relying on corresponding features automatically detected within the point clouds and radar images of the monitored scene; (ii) a more controlled, but labor-intensive approach using in-house developed collocation targets. The data-driven approach is based on the co-registration of topography features with low angles of incidence (AOIs) from the TLS point cloud and high amplitude pixels from TRI observations. So far, we achieved a mapping uncertainty of TRI data onto a TLS point cloud on the level of the median projected TRI pixel resolution (4.8 m @ 900m) using this approach.

The uncertainty can be further reduced using the collocation targets each of which consists of a radar corner reflector and a glass prism. Estimating the center of these targets independently from the TRI and TLS observations provides well-defined tie points between the datasets, enabling accurate co-registration and georeferencing. Using data from a field experiment with such collocation targets, we show that the target centers can be detected with a resolution on the level of a few centimeters at the present distances between 1200 and 2300 meters using both technologies. Compared to the resolution of the TRI images used herein, this is approximately 36 times better than the range resolution of 0.75 m, and 20 times better than the cross-range resolution of 0.1°. For TLS, the above resolution of the target centers is better than the chosen point cloud resolution and equals 10 to 30% of the laser footprint diameter (0.15 mrad).

Herein, we demonstrate the successful application of both georeferencing methods to real-world datasets, compare their advantages and shortcomings, and discuss possibilities for future improvements. Moreover, we show the advantage of the technological synergy of TRI and TLS with improved alignment precision in a monitoring use case of detecting exfoliation sheets (Guerin et al., 2020).

REFERENCES

Guerin A., Jaboyedoff M., Collins B. D., Stock G. M., Derron M., Abellán A., Matasci B. 2020: Remote thermal detection of exfoliation sheet deformation, Landslides 18, 865-879, DOI: 10.1007/s10346-020-01524-1

Schmid L., Medic T., Collins B. D., Meier L., Wieser A. 2023: Georeferencing of Terrestrial Radar Images in Geomonitoring using Kernel Correlation (submitted for publication)

22.17
Evaluation of tropospheric delays in the Swiss Alps Region from GNSS, Persistent Scatterer Interferometry and the Numerical Weather Prediction Model COSMO

Endrit Shehaj[1], Alain Geiger[1], Othmar Frey[2,3], Gregor Moeller[1], Tazio Strozzi[3], Benedikt Soja[1], Markus Rothacher[1]

[1] *Institute of Geodesy and Photogrammetry, ETH Zürich, Robert-Gnehm-Weg 15, 8093 Zürich, Switzerland (eshehaj@ethz.ch)*
[2] *Institute of Environmental Engineering, ETH Zürich, Zürich, Switzerland*
[3] *Gamma Remote Sensing, Gümligen, Switzerland*

High spatio-temporal variations of atmospheric water vapor are reflected directly in observations of microwave signals. While tropospheric conditions are consistent across different microwave techniques, such as GNSS and radar, the estimated tropospheric delays contain differences due to factors like observation geometry, signal processing, wavelengths, or spatial sampling. These differences can become even more distinct in particular scenarios, such as the Swiss Alps, where complex atmospheric dynamics and strong changes in the terrain altitude lead to large variability in the vertical and horizontal refractivity fields.

In this work, we analyse (relative) tropospheric delays estimated by both GNSS and Persistent Scatterer Interferometry (PSI). To compare the two techniques, GNSS delays are interpolated to the PSI locations using the least-square collocation software COMEDIE (Collocation of Meteorological Data for Interpolation and Estimation of Tropospheric Path Delays). In addition, we compare the delays from both microwave techniques with tropospheric delays computed from the Numerical Weather Prediction (NWP) model COSMO (Consortium for Small-scale Modelling), employed for generating regional and local forecast products in the Alpine region.

For this investigation, we utilise GNSS Zenith Total Delays (ZTDs) observed from the AGNES and COGEAR networks in Switzerland, the latter of which boasts a relatively dense coverage in the Alpine area. We also incorporate PSI tropospheric estimates derived from an interferometric stack of Cosmo SkyMed X-band Synthetic Aperture Radar (SAR) data acquired between 2008 and 2013.

We focus on different factors affecting the relative GNSS delays obtained from the interpolation of zenith delays to the persistent scatterer locations. These factors encompass assumptions in the collocation method, GNSS network density, and size. Our findings indicate that the delays estimated from the different methods tend to have a different dependency on the terrain altitude, necessitating careful consideration of the assumptions, particularly those related to correlation lengths in the interpolation process. The PSI-derived tropospheric path delays obtained capture small-scale spatial variations very well, whereas GNSS can depict large-scale tropospheric variations.

This research aims to provide further insights into the question of whether tropospheric delays retrieved at GNSS permanent stations can aid in PSI processing. The ultimate objective is to enhance the processing of short-wavelength radar observations acquired in alpine regions, with spatial gaps in the SAR data due to layover and shadow, for which isolating the tropospheric phase, and phase unwrapping may be challenging. Furthermore, understanding the ability of these microwave techniques to sense small-scale structures in the lower atmosphere is also important in view of the combination of these methods for atmospheric monitoring in mountainous terrains.

22.18
Mapping GNSS radio occultation climatologies using machine learning

Endrit Shehaj[1], Stephen Leroy[2], Kerri Cahoy[3], Alain Geiger[1], Laura Crocetti[1], Gregor Moeller[1], Benedikt Soja[1], Markus Rothacher[1]

[1] *Institute of Geodesy and Photogrammetry, ETH Zürich, Robert-Gnehm-Weg 15, 8093 Zürich, Switzerland (eshehaj@ethz.ch)*
[2] *Atmospheric and Environmental Research (AER), USA*
[3] *STAR lab, AeroAstro, MIT, USA*

Radio occultation (RO) is a space-based remote sensing technique that measures the refractive bending of signals transmitted by the Global Navigation Satellite Systems (GNSS) satellites as they transect the Earth’s limb on their way to a GNSS receiver onboard a Low Earth Orbiting (LEO) satellite. The bending angle can be converted into profiles of key atmospheric properties such as microwave refractivity, temperature, pressure, and water vapour. Benefits of RO measurements include long-term stability, all-weather capability, and high accuracy. However, atmospheric sounding density is spatially and temporally non-uniform, which makes it difficult to incorporate the measurements into useful climatologies.

In this work, we use machine learning (ML) to address challenges in generating RO climatology maps. We apply a neural network algorithm to RO refractivity measurements. Then we compare ML-based RO climatologies with those resulting from Bayesian interpolation (BI), another state-of-the-art approach to climatology map creation that fits occultation data using spherical harmonics as basis functions. Finally, we train the ML models using the residuals of BI in a combined BI+ML approach.

For this work, we use observations from the COSMIC-2 constellation, which produces approximately 3500 RO soundings daily in the latitude interval [46°S, 46°N]. We map microwave refractivity on different constant geopotential height surfaces (2, 3, 5, 8, 15, 20 km), representing diverse atmospheric regimes, focusing our evaluation on the lowest layer (2 km), where RO is sensitive to boundary layer clouds and correlated variations in water vapor. Our findings indicate that the combined BI+ML approach delivers the best results. The posterior uncertainties in microwave refractivity at each iso-height surface for BI-only are 10.9, 9.1, 5.3, 1.6, 0.6 and 0.3 N-unit (ppm). Using BI+ML, these uncertainties are reduced to 8.7, 6.6, 3.6, 1.1, 0.3 and 0.2 N-units, respectively.

Using the forecasts of the operational numerical weather prediction system of the European Centre for Medium-range Weather Forecasts (ECMWF) as a nature run, we perform a closed-loop validation where ML-based and BI-based maps are compared to the gridded products of ECMWF. We project the maps from BI, BI+ML, and the original ECMWF grid onto spherical harmonics (up to degree 120) in order to discover the implicit spatial resolution of each mapping technique. By evaluating the explained variance, we were able to show an improvement in the horizontal resolution (at 2 km height), from degree 8 for BI-only to degree 14 for BI+ML. ML also enables the production of maps at hourly resolution, while BI is only able to provide RO-based maps of refractivity at a cadence of a few days. We apply our ML approach to a preliminary scenario to assess whether RO climatologies produced using ML can be used to detect specific atmospheric structures, such as atmospheric rivers.

22.19
Concept Development of the Swiss National Geomagnetic Networks

Matej Varga[1]

[1] *Geologisch Institut, University of Basel, Bernoullistrasse 32, CH-4056 Basel (vargam@ethz.ch)*

The temporal and spatial variability of the geomagnetic field mainly results from changes in the Earth's core field and the complex composition of the Earth's crust. To ensure reliable geomagnetic information across the national territory, regular measurements and geomagnetic models are required.

This work presents a conceptual design for the Swiss repeat station and mapping geomagnetic networks. Various aspects that were considered are outlined, including criteria for selecting station locations and determining the optimal distance. The conceptual design suggests re-observing the repeat stations every 2 years on 2 to 4 stations. Furthermore, as a long-term objective, enhancing the spatial resolution of geomagnetic models is recommended by first checking the geomagnetic points in the existing national geomagnetic database and then consistently increasing the number of points. Finally, the required measurement equipment needed to map the geomagnetic field, the measurement methodology of repeat stations, and the process of geomagnetic data reduction is presented.

All the results come from a project conducted from August 2022 to January 2023 in collaboration between the Federal Office of Topography (Swisstopo) and the Swiss Federal Institute of Technology Zurich (ETHZ). More detailed information may be found in the report "Concept Development of the Swiss National Geomagnetic Networks".

22.20
Episodic events of oblique rifting using InSAR time series and seismicity (2016 – 2022), Reykjanes Peninsula (Iceland)

Xingjun Luo[1,2], Nicolas Oestreicher[2], Wenbin Xu[1*], Joël Ruch[2]

[1] *Lab of Volcano and Earthquake Research, School of Geosciences and Info-Physics, Central South University, Changsha 410083, China (wenbin.xu@csu.edu.cn)*
[2] *Department of Earth Sciences, University of Geneva, Geneva, Switzerland*

Oblique rift zone and bookshelf fault structures in the Reykjanes Peninsula are part of the intricate boundary between the North American and Eurasian plates. Studying their evolution provides a deeper understanding of plate tectonic processes. Additionally, it can help to better assess volcanic activity, contributing to a better forecast of volcanic eruptions. After a period of dormancy lasting 800 years, the Reykjanes Peninsula has experienced strong episodic plate boundary motion since at least 2017 and preceding three eruptions in 2021, 2022, and 2023. These events have been accompanied by significant seismic activity and ground displacement, related to both strain release at the plate boundary and dike intrusions.

Here we employed D-InSAR and InSAR time series to investigate the deformation occurring on the Reykjanes Peninsula from June 2016 (i.e. before the first eruption) to December 2022. We divide the entire time series into two eruption events, five earthquake swarms with observable deformation, and five short time series separated by the above events. The discretization of the observation period allows us to improve the InSAR process for different events and to avoid confusing the deformations of different events. Using InSAR and seismicity, we identified ground displacement and earthquake swarms in the Fagradalsfjall volcano area from 26 July 2017, highlighting an activation of a portion of the plate boundary four years before the first eruption. The overall earthquake distributions aligned with the plate boundary (N070), composed of north-south alignments of fault ruptures suggesting a bookshelf structure. This activity represents the earliest discernible InSAR deformation documented in the area. Before the first eruption on March 19, 2021, an uplift occurred in Svartsengi for six months from January to July 2020. Subsequently, a west-to-east earthquake swarm sequence took place at Svartsengi, Fagradalsfjall, and Krysuvik from July to October 2020. We observed that the magnitudes of deformation gradually intensified during this sequence. This was followed by an M5.6 earthquake on 20 October 2020, 10 km away from the March 2021 eruption site. Then, the distribution of earthquakes before the eruption ($M_L \geq 4$, February 19-25, 2021) suggests a positive stress field change eastward and westward from Fagradalsfjall, which is favorable to a dike injection. Before the second eruption on July 31, 2022, multiple seismic swarms also occurred, primarily centered around the Svartsengi and Fagradalsfjall regions, again highlighting that the plate boundary was activated with an overall left-lateral sense of shear. Moreover, Svartsengi exhibited a second uplift episode similar to the one preceding the first eruption. However, this uplift lasted only two months (May to June 2022) and was observed just one month before the eruption. Our results suggest that the volcanic activity at Reykjanes Peninsula was enhanced after the first eruption, possibly increasing connectivity among the various volcanic systems. We also suggest that the ongoing rifting events that started in 2021 were preceded by recurrent tectonic strain releases that might have facilitated magma to rise up to the surface.

The transition of the Reykjanes Peninsula from dormancy to sustained tectonic activity and eruptions is a rare occurrence. The comprehensive observations of tectonic and volcanic activity on the Reykjanes Peninsula, utilizing both InSAR and seismic data over seven years, provide valuable insights to better understand the evolution of oblique rifting and bookshelf-type fault systems at divergent plate boundary worldwide.

P 22.1
Exploring Thermospheric Neutral Density Solutions Based on GRACE/GRACE-FO Accelerometer Data

Saniya Behzadpour[1] and Benedikt Soja[1]

[1] *Institute of Geodesy and Photogrammetry, ETH Zurich, Robert-Gnehm-Weg 15, CH-8093 Zurich (sbehzadpour@ethz.ch)*

The neutral mass density of the upper thermosphere can be deduced through the analysis of orbit and accelerometer data obtained from satellites in Low Earth Orbit (LEO). Particularly, the accelerometers on geodetic satellites play a crucial role as they capture non-gravitational accelerations experienced by these satellites. This valuable data serves as a precise means of estimating density, even within very brief time intervals. Presently, the most accurate approximations of atmospheric density rely on such datasets due to the absence of direct measurements.

In this contribution, we present our density estimation approach and compare our solution based on GRACE/GRACE-FO data to other published datasets. We focus on a comprehensive comparison of density variations, specifically during intervals of quiet geomagnetic activity and episodes characterized by geomagnetic events. By conducting this analysis, we also aim to explore the resulting orbital decay from these density fluctuations throughout the course of these events.

24 Human Geographies: Materials, Natures, Politics

Rony Emmenegger, Maaret Jokela-Pansini

Swiss Association for Geography (ASG)

TALKS:

24.1 Alain Müller, University of Basel: Handmade Relief Models as ontological Operations and ontological Operators

24.2 Anya Kaplan-Seem, University of Minnesota: Croplands, waterlands: subsurface drainage and ontological multiplicity in the US Midwest.

24.3 Carolyn Smith, University of Cambridge: Living in tune with volcanism: rhythms of indigeneity and risk across the Chile – Argentina border.

24.4 Georges-Henry, Laffont, Ecole Nationale Supérieure d'Architecture de Saint Etienne: Common goods, soil care and territorial reappropriation in Chanaleilles (Haute Loire): First analyses of a relational ecology under construction

24.5 Jueling Hu, University of Fribourg: A Flash of Silver Green: Urban Futures that Rainforests Speculate.

24.6 Katrin Hofer, ETH Zurich: Conflicting rationalities: diverting understandings and expectations of public participation in local development in South Africa

24.7 Kelvin Haule (University of Dodoma), Manoj Roy, Roger Pickup and Kirk Semple (University of Lancaster): Ways to improve the wellbeing of Tanzania's sanitation workers and their urban environment.

24.8 Maaret Jokela-Pansini and Beth Greenhough, University of Oxford: Co-creating knowledge with patients: exploring women's experiences with long covid through body mapping (UK)

24.9 Max-Peter Menzel, Alpen-Adria Universität Klagenfurt; Tina Haisch, Fachhochschule Nordwestschweiz, Basel: Geographies of Valuation

24.10 Nitin Bathla, ETH Zurich: Extended urbanisation and the wild: Feline intimacies in India's ruderal landscapes.

24.11 Robert Braun and Richard Randell, Institute for Advanced Studies (IHS) Masaryk University: Geological Theology: The Epoch of Sovereign Anthropos.

24.12 Susanne Boerner, University of Birmingham: Co-creating everyday understandings of climate change impacts with Brazilian youth: a critical reflection-action approach

24.1
Handmade Relief Models as ontological Operations and ontological Operators

Alain Müller[1]

[1] *Institute of Cultural Anthropology and European Ethnology, Departement of Social Sciences, University of Basel, Rheinsprung 9/11, CH-4056 Basel (alain.mueller@unibas.ch)*

In this paper, I present the main results of my ethnographic engagement with so-called “handmade relief models.” In a first step, I focus on what I call—based on Bruno Latour’s conceptualization of “modes of existence”—, the felicity conditions necessary to enact a relief model successfully. By drawing on the specialized literature on the subject, I show that what is considered a successful relief model looks confusingly similar to what it is supposed to *re-present* in miniature, that is, a “real” mountain; and thus pertains to an objectification of what “a mountain” *is*, and therefore to an ontological qualification. In a second step, I trace the socio-material trajectory of reliefs, which takes place at the intersection of heterogenous practices such as geomorphological and cartographic sciences, crafting, museography and conservation, and involves the reception by the public as well. I show that this trajectory is in fact marked by a succession of ontological operations and experiments: (1) defining the “real mountain” that serves as the “original” to be *re-presented* (2) assembling a set of “inscriptions” (Latour 1999) enabling it to be qualified and *re-presented* (topographic maps, photographs, sketches, etc.) (3) then modelling and later on repairing the relief model with a palette of materials that impose their own obligations (Stengers 2005) on the craftspersons as well as the restorers and conservationists, and finally (4) experiencing it as a viewer as a *re-enactment* of the “real mountain,” a final stage in which the relief itself therefore becomes what I call an ontological operator; that is, a full-fledged actor that acquires the agency to take part in the collective making of what is perceived as “reality.”

REFERENCES

Latour, B. 1999. *Pandora’s Hope: Essays on the Reality of Science Studies*. Cambridge Mass: Harvard Univ. Press.
Latour B. 2013. *An Inquiry into Modes of Existence: An Anthropology of the Moderns*. Cambridge Mass: Harvard Univ. Press.
Stengers, I. 2005. Introductory Notes on an Ecology of Practices, Cultural Studies Review, 11(1), 183-196..

24.2
Croplands, waterlands: subsurface drainage and ontological multiplicity in the US Midwest

Anya Kaplan-Seem[1]

[1] *University of Minnesota, 414 Social Sciences Building, 267 S. 19th Ave, Minneapolis, MN 55455 (kapla298@umn.edu)*

This paper investigates the ontological politics of subsurface drainage practices (drain tile) in the Red River Valley (RRV), an agricultural floodplain in the U.S. Upper Midwest. Characterized since the early 1920s by the near total dominance of commodity crop production, nearly all of it dependent on extensive drainage works, the RRV is today a site of contentious negotiations over how shallow subsurface water is measured, controlled, distributed, and imagined. The private agronomic interests of individual growers at the field scale pit neighbors against one another, while a multitude of regional public and not-for-profit actors work to balance drainage needs and desires against mandates to reduce future flood damage and ensure lasting water quality. Drawing on interviews with farmers, engineers, hydrologists, and conservationists throughout the region, the paper delves into the world-making capacities of subsurface drainage infrastructures and practices. It re-reads the standard definition of drainage — as a practice for removing excess water from land for crop production — as a description of the enactment of the Earth and asks: by whom, for whom, to what extent, and with what effects is the RRV made to be cropland?

At the same time, the paper thinks from within a different ontlogy: the RRV as a waterland whose seepages, evapo-transpirations, flows, and overflows persistently exceed the infrastructures and imaginaries designed to contain them. In the RRV, formerly a glacial lakebed, ground regularly ceases to be a reliable surface, becoming instead a register of the permeability and impermanence of ground as ground. And yet, the ontological stability of cropland as land is the basis upon which the RRV stakes its claims to identity, culture, and purpose: since the late 1800s, when it was violently appropriated by settler speculators and homesteaders, it has been hailed as a place of limitless agricultural potential and home of the American farmer who feeds the world.

As such, in this paper I develop an analysis of drainage that understands it to be at once a fulcrum on which cropland and waterland ontologies flicker into and out of presence, and a technical focal point for their coordination. Building on this analysis, I make three intertwined claims. First, I suggest that separation is a dominant mode of cropland relations. Second, I argue that drainage practices make commodity croplands cohere technically, discursively, and politically as settler geographies. Finally, I posit that a dichotomous understanding of water’s relation to land is a key ontological assumption of settler epistemologies, with implications for what might be required to undertake anticolonial scholarship in/on croplands.

24.3
Living in tune with volcanism: rhythms of indigeneity and risk across the Chile – Argentina border

Carolyn Smith[1]

[1] *Department of Geography, University of Cambridge, 20 Downing Place, CB2 3EL (cs932@cam.ac.uk)*

The Global South is disproportionately affected by disasters; it is perhaps unsurprising, therefore, that decolonial scholarship and disaster discourses are beginning to converge in their understanding of the underlying causes of slow onset emergencies: highlighting the role of persistent imbalances of power that perpetuate conditions of vulnerability at multiple scales (Atallah, 2016; Marchezini *et al.*, 2021, p. 4). Disaster risk reduction (DRR) processes are inherently (geo)political: a key element of contemporary statecraft, they actively maintain the colonial/modern logics from which they stem (Donovan, 2021).

As such, a risk-centred framework for understanding disasters – and volcanism more specifically – cannot be uncritically applied within (post)colonial territories. If we accept the need to decolonise DRR and, more specifically, the mitigation of volcanic risk, then we must move beyond rudimentary attempts to 'integrate' other ways of knowing within existing DRR frameworks and accept the inevitable partiality of knowledge (De la Cadena, 2010). The paper highlights the potential for political ontology to allow us to change 'not only the content but the terms of the conversation' (to paraphrase Mignolo, 2018, p. 124); the emerging discourse brings to the fore the power-laden processes of disagreement and negotiation that occur when particular realities are enacted, examining the con/disjunctures between multiple, partially connected worlds.

The research is empirically grounded in relation to a specific case study: the territory surrounding Copahue volcano, which is bisected by the border between Argentina (Neuquén) and Chile (Bio Bío), see Figure 1. The research findings are based on nine months of ethnographic fieldwork with two transhumant Mapuche communities – one on either side of the national border – who live with Copahue's persistent activity. The research situates Copahue volcano as a point of equivocation between worlds and is concerned with identifying opportunities for "symmetrical disagreement" without the need for a unified, or universal, system (De la Cadena, 2010, p. 352).

The paper contributes directly to the emerging debate that examines the implications of ontological difference in relation to our understanding of disasters, and volcanism. The key themes that emerged from the data were concerned with imaginaries of time and patterns of spatio-temporal movement; the paper outlines how rhythm analysis could provide a useful 'boundary object' to facilitate more symmetrical co-production of mitigation strategies in the future. Despite originating from urban analysis literature, the paper argues for the relevance and value of applying rhythm analysis within this context due to its potential to address longstanding issues of (mis)communication and trust, allowing ways of knowing and being in the territory to be woven together, rather than dissected. Here, the volcano is included within the framework, alongside both human and non-human actors, opening new avenues for more nuanced discussion and collaboration. The implications are considerable: an ontological shift for rhythm analysis as a research methodology, and a further step towards the decolonization of volcanic risk.

.

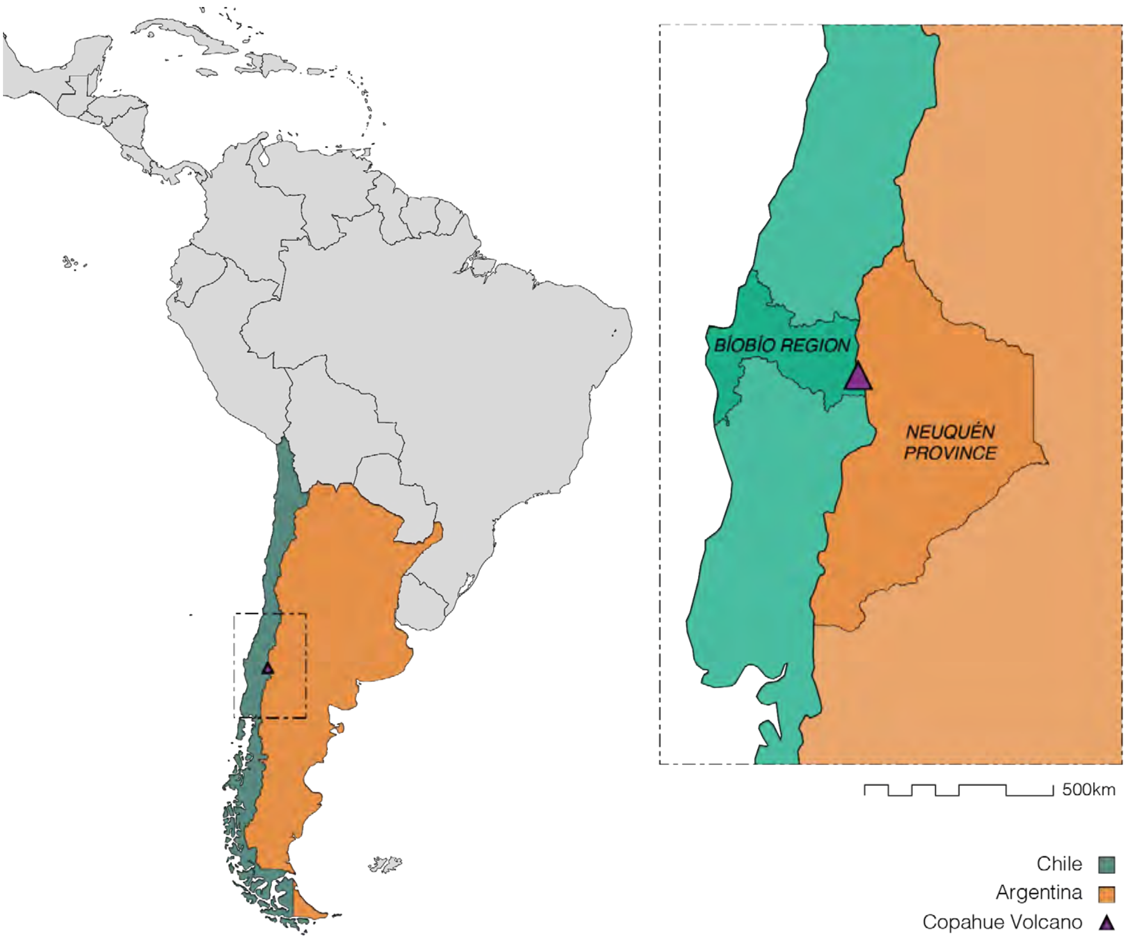

Figure 1: Location map for copahue volcano

REFERENCES

Atallah, D.G. (2016) 'Toward a decolonial turn in resilience thinking in disasters: Example of the Mapuche from southern Chile on the frontlines and faultlines', *International Journal of Disaster Risk Reduction*, 19, pp. 92–100.

De la Cadena, M. (2010) 'Indigenous Cosmopolitics in the Andes: Conceptual Reflections beyond "Politics"', *Cultural Anthropology*, 25(2), pp. 334–370.

Donovan, A. (2021) 'Colonising geology: Volcanic politics and geopower', *Political Geography*, 86, p. 102347.

Marchezini, V., González-Muzzio, C. and Rodas, A.M. (2021) 'Descolonización de la ciencia de los desastres: Enfoques desde Latinoamérica y Caribe', *REDER*, 5(2), pp. 1–4.

Mignolo, W.D. (2018) 'What Does It Mean to Decolonize?', in C.E. Walsh and W.D. Mignolo (eds) *On Decoloniality: Concepts, Analytics, Praxis*. Duke University Press, pp. 106–134.

24.4
Common goods, soil care and territorial reappropriation in Chanaleilles (Haute Loire): First analyses of a relational ecology under construction

Georges-Henry Laffont[1], Roméo Carabelli[2]

[1] EVS UMR 5600 University of Lyon & ENSA Saint-Etienne, France, georges-henry.laffont@st-etienne.archi.fr
[2] CITERES UMR 7324 University of Tours, France, romeo.carabelli@univ-tours.fr

Mankind has upset the great terrestrial balances (Berque, 2019) and liberalism has imposed itself through an existential narrative leading to enclosures, to the transformation of “everything” into a resource (Tsing, 2017). Reweaving links to physical, cultural and symbolic substratum (Carabelli & Laffont, 2022); refounding new relationships between human and non-human (Hache, 2012); making *milieu* (Younès & Goetz, 2010), such is the challenge! Some regions are renewing their ties with the care of the earth (Pattaroni et al., 2009), by working together through the ordinary, mobilizing technical, social and ecological know-how in a dynamic relationship with places and the living (Dewey, 2003). Chanaleilles[1] is a key focus of our attention. In this rural commune in the Haute Loire region (France), actions are aimed at opening up the field of possibilities by: defending an existing system based on the values of sharing, cooperation, mutual aid and support; overcoming the constraints and difficulties of the area’s situation (mid-range mountains, demographic decline, restrictive laws, etc.). By questioning the relationship with the land through the “uses” (grazing, cutting, cultivation, etc.), “living(s)” (human, animal, plant, water), “ transit “ (transhumance, nomadism, migration, pilgrimage, walking, etc.) entries, this proposal, part of axis 3, has two objectives. Firstly, to understand the brakes, levers and driving forces behind the environment, using a variety of survey methods (observations, interviews, surveys, residence). Secondly, based on Chanaleilles, to explore the potential for re-enchantment of the world of the commons (sectional[2] and communal), certainly beni communi attached to humans (Rodotà, 2016) but also “choses lieux” (Vanuxen, 2018), thought of and mobilized as co-ownership and co-activity of all living things and on the reciprocal principle of debt and gift (Faburel, 2019). It is these initial analyses and explorations that will be proposed for debate.

[1] https://chanaleilles-hautgevaudan.fr
[2] https://www.collectivites-locales.gouv.fr/institutions/administrer-les-sections-de-commune

REFERENCES
Berque, 2019, *Descendre des étoiles, monter de la terre : la trajection de l’architecture*, Bastia, Ed Eoliennes.
Carabelli et Laffont, 2022, « Vers des communs territoriaux en Val de Loire. Retours sur des expériences de caractérisation de ressources et de modalités d’action pour faire territoire autrement ». Dans Segapeli Silvana (dir), 2022, *Vous avez dit espace commun* ? Peter Lang, Bruxelles, pp :231-242
Dardot et Laval, 2014, *Commun, essai sur la révolution au XXI ème siècle*, Paris, la Découverte.
Deleuze et Guattari, 1980, *Mille plateaux*, Paris, Minuit, p.434-527
Dewey, (1927), 2003, *Œuvres philosophiques, Tomes 2, le public et ses problèmes*, Paris, Farrago
Faburel, 2019, *Les métropoles barbares*, Paris, Le Passager clandestin.
Hache, 2012, *Ecologie politique. Cosmos, communautés, milieux*. Paris, Amsterdam.
Hardin, 1968, “ The tragedy of the commons”, Sciences, vol.162, n°3 859.
Pattaroni, Vincent Kaufmann et Adriana Rabinovich, 2009, « L’habitat en question », Espacetemps.net. 29 octobre 2009
Rancière, 2000, *Le partage du sensible. Esthétique et politique*, Paris, La Fabrique éditions.
Rodotà, 2016, « Vers les biens communs. Souveraineté et propriété au XXI ème siècle », Tracés, n°16 -pp : 214-218
Tsing, 2017, *Le champignon de la fin du monde : sur la possibilité de vivre dans les ruines du capitalisme*, Paris, La découverte, coll. Les Empêcheurs de penser en rond.
Vanuxen, 2018, *Les sections de commune pour la protection des paysages ? : Le cas du Goudoulet, section du plateau ardéchois*. hal-03407755

24.5
A Flash of Silver Green:
Urban Futures that Rainforests Speculate

Jueling Hu[1,2]

[1] Department of Geosciences, University of Fribourg, Chemin du Musée 4, CH-1700 Fribourg (jueling.hu@unifr.ch)
[2] Amsterdam School of Cultural Analysis, University of Amsterdam, Turfdraagsterpad 9, 1012 XT Amstrerdam

Geographers and anthropologists have drawn attention to space and places as future-making resources (Bunnell 2022; Bryant and Knight 2019). While national-scale place references and physical experiences are considered key elements of urban imaginaries, much less attention has been afforded to speculative interventions. In this paper, I examine the speculations of Malaysian cities in the framework of eco-futurisms, which place rainforests prominently at the center of the imaginaries.

My project records rainforests as mediated and affective sites of urban future-making in Southeast Asia. Rainforests, in these works, are often addressed through their material features that invite the practitioners to respond (Ingold 2011). The humidity, smells, and sounds have been woven into the orientation of certain city experiences as futuristic in embodied manners. By tracing the theme of rainforests in the grid of sensations – in science fiction writing, speculative filmmaking, bio-art installations, and rainforest data visualization – I seek to understand how rainforests, in the forms of the cells, species, and ecosystems, are mobilized to produce aspirations of ecological urban futures. I also emphasize the significant role of digital technologies in imagining rainforest-themed urban futures, as visual and audio recorders, sensors, and computational modeling are increasingly used by creative practitioners (Gabrys 2022).

I focus on Malaysian creative organizations involving writers, artists, architects, and botanical initiatives on the island of Borneo. By conducting semi-structured interviews and doing ethnography, I aim to (a) provide ecological versions of imagining urban futures by sorting out the artistic and designing efforts in Sarawak and Sabah, in the 21st century Malaysia, (b) and unfold these versions in the networks of creators' talents, socio-political contexts, environmental challenges, technological innovations, and global climate change agenda.

REFERENCES

Bunnell, T. 2022: WHERE IS THE FUTURE? Geography, Expectation and Experience across Three Decades of Malaysia's Vision 2020. International Journal of Urban and Regional Research, 46(5), 885–895. https://doi.org/10.1111/1468-2427.13105

Bryant, R., & Knight, D. M. 2019: The Anthropology of the Future (1st ed.). Cambridge University Press. https://doi.org/10.1017/9781108378277

Ingold, T. 2011: Being Alive: Essays on Movement, Knowledge and Description. Routledge. https://doi.org/10.4324/9780203818336

Gabrys, J. 2022: The Forest That Walks: Digital Fieldwork and Distributions of Site. Qualitative Inquiry, 28(2), 228–235. https://doi.org/10.1177/10778004211042356

24.6
Conflicting rationalities: diverting understandings and expectations of public participation in local development in South Africa

Katrin Hofer[1]

[1] *Institute for Spatial and Landscape Development, ETH Zurich, Stefano-Franscini-Platz 5, CH-8093 Zürich (kathofer@ethz.ch)*

There are various ways in which institutional stakeholders and ordinary residents engage in the production of space in cities. While there is generally agreement in both theory and practice that citizens should be involved in decisions affecting the design and development of urban spaces, relatively little is known about how the public thinks about engaging with the state for the development of their neighbourhoods.

This paper takes an explorative stance and delves into residents' understandings and expectations of state-society engagements for the development of their city. It builds on the in-depth case study of Bramfischerville, a low-income residential area in the City of Johannesburg. Data was collected during several months of fieldwork through a mixed-methods approach, combining findings from a baseline survey, qualitative group interviews with residents of Bramfischerville, expert interviews with local leaders and selected city officials, and observations from the field.

Preliminary results indicate that people show overall strong support for (state-led) participation in local development. Yet, findings also reveal that residents of Bramfischerville largely feel disillusioned and neglected by the state, as they face many economic, social and infrastructural challenges. Rather than being involved in planning, residents moreover express a preference for contributing to local development through physical – and paid – labour. Thereby opportunities for local employment are portrayed as a way of feeling 'seen' by the state, and as a way of making an active contribution to the improvement of their areas. This exposes "conflicting rationalities" (Watson, 2003) between the people's perspective of participation and dominant views in the state discourse and (Western) planning theory. By foregrounding a resident-centric view, findings from this study thus reveal fundamental differences between how states and communities see participation in local development. This has important implications for both theory on public participation, and its practical application in any given context.

REFERENCES

Watson, V. 2003: Conflicting rationalities: Implications for planning theory and ethics, Planning Theory & Practice, 4(4), 395-407.

24.7 Ways to improve the wellbeing of Tanzania's sanitation workers and their urban environment

Kelvin Haule[1*], Manoj Roy [2], Roger Pickup[2], Kirk Semple[2]

[1] *University of Dodoma, Po Box 395, Tanzania*
[2] *Lancaster University, Lancaster Environment Centre*
** Lead author: oswinkelvin@gmail.com, Po Box 395, University of Dodoma, Tanzania*

SDG related policy makers are interested in transformative urban governance. Co-production is among of these transformative urban governance approaches (Watson, 2014). Co-production involves diverse stakeholders (government, non-business, Non-government organisations, civil society's organisations) working as partners in delivering development. It is a means of addressing gaps of resources in service provision (Pieterse, 2014). Arguably, inclusion and Co-production with/for marginalized communities (such as informal sanitation workers) are going to be challenging. The logic is rooted in Marxist Proletarianism that associates their poor wellbeing or value with capitalism. Capitalism has made marginalized communities unable to become neoliberal subjects. This paper analyses the Co-production with, for and by sanitation workers in Dar es Salaam, Tanzania. The city has multiple sanitation workers who performance various roles in the sanitation value chain. Their working conditions vary widely from manual scavenging being most precarious to least paid/secure. Conversely, their economic and socio-ecological value is undermined (WaterAid, 2022). Their payment, wages or salaries are very low (Table 1 and 2). Here, we estimate the value of their workforce by adopting the Contingent Valuation Method (CVM) especially willingness to pay (WTP) for sanitation work the beneficiaries. We compare the wellbeing of sanitation workers against others in the informal and or hazardous work spectrum. The analysis demonstrates a widening gap between their wellbeing and value of their work. By mapping systematically of relevant policies, we identify a systematic neglect of their rights and wellbeing. This helps to assess the nature of and practices of Co-production in sanitation services. Also, using a Shift Flow Diagram (SFD), we identify different types of sanitation workers (both private, public, households, and or commercial) in different stages of sanitation value chain (Figure 1). We conclude that unless the wellbeing and value of sanitation workers are uplifted, the city's approach towards realization of SGD 6.2 and target 3.9 will be incomplete and compromised. The implementation of Co-production governance will require development coalitions to uplift the wellbeing and value of sanitation workers.

Table 1: The amount (Tshs) paid to Sanitation workers in Dar es Salaam

Group skills and task	Income level per job
Informal skilled workers doing construction of new systems working in a group of 10 individuals. Completion on average in 10 days	1,500,000-2,500,000Tshs per contract (USD 650-USD1085)
Informal unskilled workers offering pit excavation or old latrine evacuation services in a group of 5 individuals. Completion on average in 1-2 days	150,000-250,000Tshs per contract (USD 65-USD 108)
Daily labour employed for assistance of a cesspit emptier	210,000Tshs per month (USD91)
Casual labour offering cleaning services (e.g maintenance of toilet, occasional cleaning of drains and sewers)	120,000Tshs per month (USD 52)

Source: WaterAid, 2022

Table 2: Sociological value of sanitation work

Names given to sanitation workers (frogs, Ninja, Wapagazi, Wadibuaji) Sanitation taboos (works done by poor and uneducated people) Working environments: poor and crude, no or low investment in working gears Stigmatized workers Workers are not free to inform friends or neighbours of the work they do Names the toilet myths (msalani, kujisaidia, kusalimia)

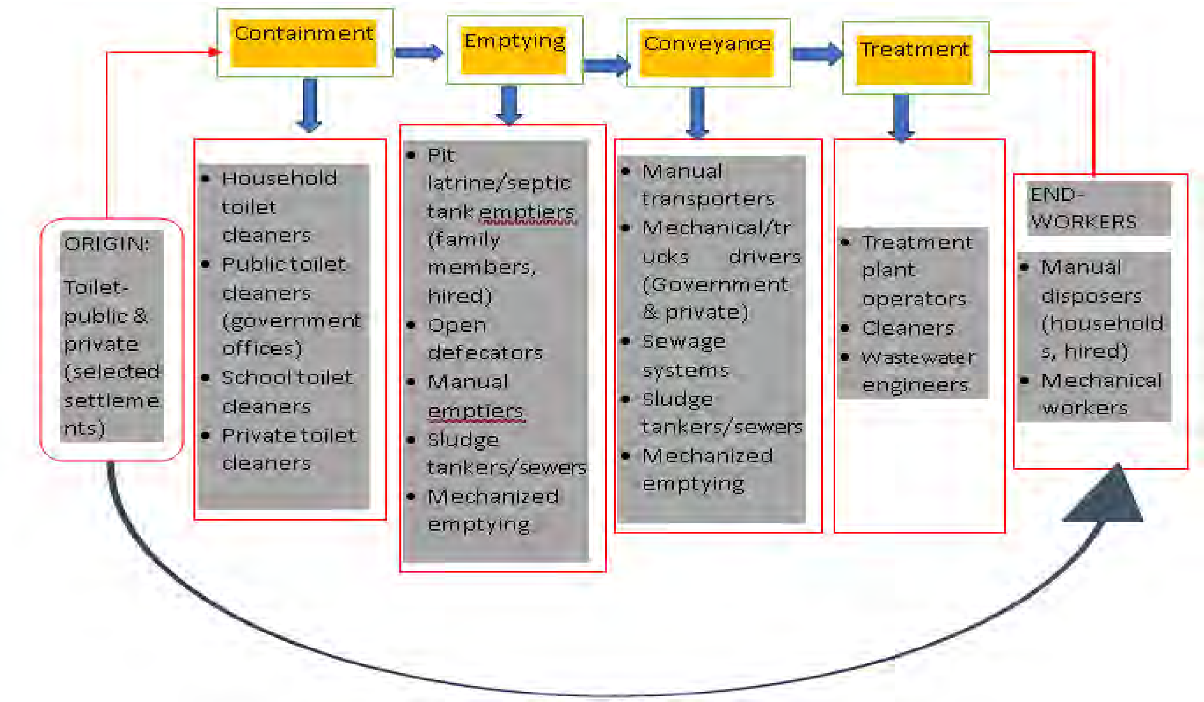

Figure 1: The Co-production of sanitation workers in SFD

REFERENCES

Pieterse, E. 2014: Filling the Void: An Agenda for Tackling African Urbanisation in *Africa's Urban Revolution.* Edited by Parnell, S. and Pieterse, E. Zed Books. London, pp 200 – 220

Watson, V. 2014: Co-Production and Collaboration in Planning –The difference.
Planning Theory and Practice 15(1): 62 – 76

Water Aid 2022: Assessment of the Health, Safety and Dignity of Sanitation Workers in Dar es Salaam, Dodoma and Arusha Tanzania. Water Aid.

24.8
Co-creating knowledge with patients: exploring women’s experiences with long covid through body mapping (UK)

Maaret Jokela-Pansini[1], Beth Greenhough[2]

[1] *School of Geography and the Environment, University of Oxford (maaret.jokela-pansini@ouce.ox.ac.uk)*
[2] *School of Geography and the Environment, University of Oxford (beth.greenhough@ouce.ox.ac.uk)*

This study uses body mapping to understand women’s diverse experiences with long covid in the UK. Long covid is a chronic illness in which the symptoms of the COVID-19 coronavirus continue over long time periods. It affects one in five COVID-19 patients. Recent studies have found that long covid particularly affects women (Sudre et al., 2020) and according to some studies, up to 70 % of the patients are female. In this study, we first aim to understand how women experience long covid and how these experiences differ depending e.g. on age, race, ethnicity, sexuality, (dis)ability and education. Second, we ask how women have adjusted to their new way of life and how this has changed how they view themselves.

We build on recent studies in geography using participatory and arts-based methods as a way of co-creation (Askins, 2018; Hawkins, 2019; McLean, 2022)queries and hesitations regarding articles drawing on participatory action research (PAR. Our participants used collage and drawing to respond to a series of prompts about their experiences of long-covid. We argue that body mapping as a creative method can bring new insights into people’s experiences with illness and also foster geographies of co-creation that can be further applied to benefit patients beyond academic spaces.

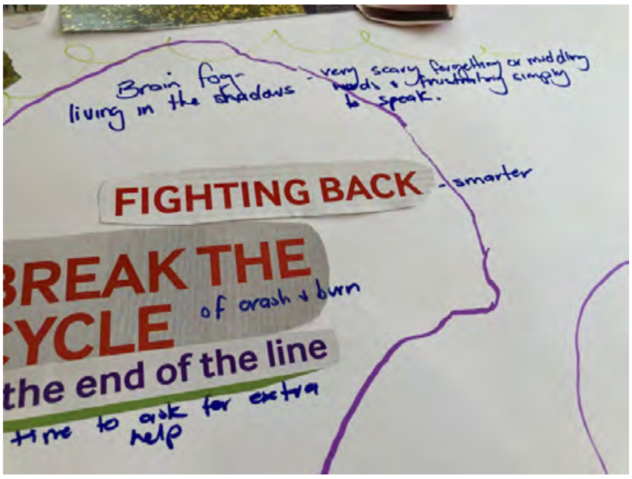

Figure 1. Image of a body map, June 2023

Our findings show that one of the patients’ key challenges was **language**: finding words and communicating their experiences to family, friends, and health professionals. Participants often highlighted their **gender**: they spoke about changes in their hormonal functions and doctors not taking them seriously due to being women. Finally, a shift in **identity** from ‘my former self’ to living in a shadow was strengthened by the temporal dimension of still living in the pandemic, thus living in a different time than others.

REFERENCES

Askins, K. 2018: Feminist geographies and participatory action research: Co-producing narratives with people and place. Gender, Place & Culture, 25(9), 1277–1294.
Hawkins, H. 2019: Geography’s creative (re)turn: Toward a critical framework. Progress in Human Geography, 43(6), 963–984.
McLean, H. 2022: Creative Arts-Based Geographies: Some Cautionary and Hopeful Reflections. ACME: An International Journal for Critical Geographies, 21(3), Article 3.
Sudre, C.H., Murray, B., Varsavsky, T. et al. 2021: Attributes and predictors of long COVID. Nature Medicine 27, 626–631.

24.9
Geographies of Valuation – a laboratory approach

Max-Peter Menzel[1], Tina Haisch[2]

[1] Department of Geography and Regional Studies, University of Klagenfurth, Universitätsstraße 65-67, A-9020 Klagenfurt (max-peter.menzel@aau.at)
[2] Institut for Nonprofit and Public Management, University of Northwestern Switzerland, Peter Merian-Strasse 86, CH-4002 Basel (tina.haisch@fhnw.ch)

We explain the phenomenon of recent urban growth and transformation in terms of the co-production of value and the need to collectively develop systems of valuation.
Classical contributions argue that urban growth is the result of the generation of novelty that occurs when different knowledge is combined and these combinations take place in diverse and densely populated cities (Jacobs 1969, Glaeser 1999, Storper and Venables 2004). However, we depart from this classical canon by arguing that it is not the creation of novelty per se that is crucial to the processes at hand. Instead, it is the valuation of knowledge. By negotiating which novelties, objects and events are of value, value is assigned to these entities (Hutter and Stark 2015). Valuations take place in all sectors. However, valuations require extensive forms of interaction and negotiation when there are no trajectories (Dosi 1982) or standards (Aspers 2009) to help define value. These conditions also exist in new and emerging industries where different technological approaches and designs compete (Dosi 1982, Abernathy and Utterback 1978, Audretsch and Feldman 1996). However, in industries that depend on the production of symbolic associations, this uncertainty is not limited to a particular phase. Instead, the evasion of clearly defined trajectories and the resulting uncertainty is the defining feature of these industries (Reckwitz 2013). We investigate these phenomenons using a laboratory setting: we analyse the processes at two art fairs in Basel as representatives of different urban settings.

REFERENCES

Abernathy, W. J. and Utterback, J. M. (1978): Patterns of Industrial Innovation. In: Technology Review 80(7), 40-47.
Aspers, P. (2009): Knowledge and valuation in markets. In: Theory and Society 38(2), 111-131.
Audretsch, D. B. and Feldman, M. P. (1996): Innovative clusters and the industry life cycle. In: Review of Industrial Organization 11(2), 253-273.
Dosi, G. (1982): Technological Paradigms and Technological Trajectories. In: Research Policy 11(3), 147-162.
Glaeser, E. L. (1999): Learning in Cities. In: Journal of Urban Economics 46254-277.
Hutter, M. and Stark, D. (2015): Pragmatist Perspectives on Valuation: An Introduction. In: Moments of Valuation: Exploring Sites of Dissonance1.
Jacobs, J. (1969): The Economy of Cities. New York: Vintage Books.
Reckwitz, A. (2013): Die Erfindung der Kreativität: Zum Prozess gesellschaftlicher Ästhetisierung. Berlin: Suhrkamp.
Storper, M. and Venables, A. J. (2004): Buzz: face-to-face contact and the urban economy. In: Journal of Economic Geography 4(4), 351-370.

24.10
Extended urbanisation and the wild: Feline intimacies in India's ruderal landscapes

Nina Bathia

ETH Zürich

There has been an emergent contradiction between environmental and developmental politics of the Indian state during the last couple of years. The population of state-protected animals such as leopards has has seen a rapid rise, all the while when the state is undertaking large-scale infrastructure projects such as urban corridors that are pushing extended urbanization and catalyzing extended urban natures that engender the territories of reproduction of these animals. According to the estimates published through the Status of Leopards in India report by the Government of India, the leopard (*Panthera pardus fusca*) population increased by 63% in the years between 2014 and 2018 to 12,852. The increase in feline population has been used by the Indian state to highlight its vibrant and successful conservation efforts. This increase however has come at a time when there have been overt attempts to dissolve environmental protections over forests while enclosing agrarian land for urbanization. This contribution is interested in exploring the conflict between state›s human and non-human biopolitical subjects amidst large-scale landscape change. Drawing upon recent scholarship on leopard-human conflict in India, and the author›s own fieldwork, this paper will discuss human-leopard conflict and multiscalar landscape change in the Aravalli region located between Delhi and Jaipur in northern India. The paper will survey how this conflict manifests at multiple scales in terms of road kills, leopard lynching, but also in a human-leopard coexistence around a diurnal-nocturnal rhythm in urban parks, and other unintentional landscapes. This multi-scalar analysis will discuss how sentient non-humans sense and adapt to large scale urban change, and the lessons this can offer for landscape and urban design. I will also attempt to draw parallels between the human-leopard conflict in India and the incipient wolf-human conflict here in Switzerland.

24.11
Geological Theology: The Epoch of Sovereign Anthropos

Robert Braun[1,2], Richard Randell[1,2]

[1] *Institut für Höhere Studien - Institute for Advanced Studies (IHS), Josefstädter Strasse 39, Vienna A-1080 (randell@ihs.ac.at)*
[2] *Department of Sociology, Masaryk University, Jostova 10, CZ-60200 Brno Czech Republic*

The term “the Anthropocene” has been contested on the grounds that its root term, “Anthropos,” implies all humans, Europeans and indigenous peoples, inhabitants of the Global North and the Global South, owners of coal-fired power stations and those living on less than one dollar a day, are all equally responsible for the planetary crisis we find ourselves in. Alternative terms such as “Capitalocene,” Thermocene, Plantationocene,” “Chthulucene” and Thanatocene have been floated (Bonneuil and Fressoz 2016).

What we understand the Anthropocene to be depends on whom we understand Anthropos to be. Anthropos is not “all humans” but the sovereign collective Being of the occident who “decides on the exception,” and who decides on the normal situation (Schmitt 2005). The Anthropocene is the epoch that is the exception, different from all the other epochs that the science of geology has inscribed as the normal situation, the *state of nature.* With the imminent decision by the International Commission on Stratigraphy regarding which event will mark the beginning of the Anthropocene, the official geological history of the planet will become a history of the exception and of the normal situation, located at the intersection of geography and historiography.

“All significant concepts of the modern theory of the state,” Carl Schmitt (2005), argued in *Political Theology,* are “secularized theological concepts.” As with the concepts of the modern state, so also the geological concept of “the Anthropocene” contains a secularized theology. It is a theology that exists not in the realm of ideas but is a metaphysics that is built into the very fabric of the world that Anthropos has constructed. The Anthropocene is primarily an ontopolitical epoch, not a geological epoch. This epoch is an ontology, a *nomos* (“order made visible”) created by the violence of sovereign power (Schmitt 2003; Agamben 2017; Braun and Randell 2022), the genealogy of which is documented in the book of Genesis: “In the beginning God said to Adam: ‘Be masters of the fish of the sea, the birds of heaven, and all the living creatures that move on earth… to you I give all the seedbearing plants everywhere on the surface of the earth, and all the trees with seed-bearing fruit; this will be your food’” (Gn 1:29-31 NJB). These verses articulate and reproduce the relationship of domination by Anthropos over all life and non-life (see, for example, Armstrong 2022, 11; Derrida 2002). “Adam” is not only a proper name, Adam signifies also “Man,” “Anthropos” (2 Th 2:3 NJB), who is not “all humans” but an onto-theological entity that has now expanded across and appropriated the entire planet. The term “the Anthropocene,” consequently, is the appropriate name for the epoch in which we live. Precisely for the reasons advanced by critics of the term.

With the death of God as sovereign of the earthly political order (Nietzsche 2001), a transformed political theology emerged. Anthropos is the secularized sovereign that no longer derives nor needs to derive sovereignty directly from God, but who has displaced God by designating *himself* as the origin of sovereign power (cf. Hobbes 2017). It is *nomos* in its most profound and political sense: appropriation, not just of land but the entire Earth and all that exists on it; an *ur-terra nullius,* with the entire world not only available for appropriation but as belonging to Anthropos. It is an ontology wherein the entirety of the human, non-human and the more-than-human (Abram 1996) belongs to Anthropos who, as proprietor and sovereign of the planet, exists both inside and outside of the more-than-human world, which has been constituted through the defining cut made between Anthropos and “animals” and “nature.” The Anthropocene is a political epoch constituted through anthropogenic violence, both over Anthropos and over all that is external to Anthropos. It is the ceaseless dialectic of sovereign power and bare life (Benjamin 1996; Agamben 2017), whereby the sovereign power of Anthropos creates “bare being”: that which may be destroyed without a crime being committed. The irony of the Anthropocene is that bare being now includes Anthropos himself.

All ontology, Johanna Oksala (2010) has argued, is “politics that has forgotten itself.” To adequately address the violence and destruction that goes by the name “the Anthropocene” requires engaging with the politics of transformative forgetting; how the authentically political has been transformed within the ontology of Anthropos by sovereign power.

REFERENCES

Abram, David. 1996. *The Spell of the Sensuous: Perception and Language in a More-Than-Human World*. 1st ed. New York: Pantheon Books.
Agamben, Giorgio. 2017. *The Omnibus Homo Sacer*. Stanford, California: Stanford University Press.
Armstrong, Karen. 2022. *Sacred Nature: How We Can Recover Our Bond With the Natural World*. London: Jonathan Cape.

Benjamin, Walter. 1996. „Critique of Violence." In *Walter Benjamin: Selected Writings*, edited by M. Bullock and M. W. Jennings, 236-52. Cambridge, MA: Harvard University Press. Original edition, 1921.

Bonneuil, Christophe, and Jean-Baptiste Fressoz. 2016. *The Shock of the Anthropocene: The Earth, History and Us*. London: Verso.

Braun, Robert, and Richard Randell. 2022. „The Vermin of the Street: The Politics of Violence and the Nomos of Automobility." *Mobilities* 17 (1):53-68.

Derrida, Jacques. 2002. „The Animal That Therefore I Am (More to Follow)." *Critical Inquiry* 28 (2):369-418.

Hobbes, Thomas. 2017. *Leviathan*. London: Penguin Classics.

Nietzsche, Friedrich Wilhelm. 2001. *The Gay Science*. Cambridge: Cambridge University Press.

Oksala, Johanna. 2010. „Foucault's Politicization of Ontology." *Continental Philosophy Review* 43 (4):445-466.

Schmitt, Carl. 2003. *The Nomos of the Earth in the International Law of the Jus Publicum Europaeum*. Edited by G L Ulmen. New York: Telos Press. Original edition, 1950.

Schmitt, Carl. 2005. *Political Theology: Four Chapters on the Concept of Sovereignty*. University of Chicago Press ed. Chicago: University of Chicago Press. Original edition, 1922.

24.12
Co-creating everyday understandings of climate change impacts with Brazilian youth: a critical reflection-action approach

Susanne Börner, Assistant Professor in Human Geography, s.borner@bham.ac.uk

School of Geography, Earth & Environmental Sciences, University of Birmingham

This contribution presents insights and reflections based on hybrid participatory research (using WhatsApp and in person youth-led activities) with approximately 30 marginalised young people in the urban periphery of Sao Paulo. Using a reflection-action design based on the critical pedagogy of Paulo Freire, I invited young people to reflect on climate change impacts, resource scarcity, everyday identities, and visions for change. Participant engagement was based on a multi-method approach for co-creating everyday understandings of climate change impacts, including group and individual WhatsApp chats, photovoice, videos and creative activities. Results showed that participatory action research is a powerful tool for critically exploring ‘everyday’ and ‘hidden’ knowledges and social practices of youth that are often excluded from public debates and policies. Experimenting with different asynchronous and synchronous methods showed the importance of giving participants ownership over choosing their preferred method of communication. This contribution therefore also invites a collective reflection on participant ownership and power relations in co-creation processes when engaging particularly with vulnerable groups. Young people often preferred to interact through written group chats rather than engage in more ‘participatory’ remote activities such as photovoice. As they decided on whether, when, and how to participate (or not), power relations shifted from the researcher to the participant (while also considering limitations such as internet access). Results also showed that when young people start perceiving themselves as subjects in the construction of their identity and their reality, they feel more empowered to critically question their realities and to develop new perspectives for more sustainable, healthy, and equal environments. Finally, I argue that ‘purposeful’ participation calls for inclusive and dialogical forms of knowledge co-production which take youth perspectives seriously and promote more symmetrical relations between researchers and participants.

25 Human Geographies: Bodies, Cultures, Societies

Nora Komposch, Devran Koray Öcal

Swiss Association for Geography (ASG)

TALKS:

25.1 Carolin Schurr, University of Bern: Geographies of Reproductive Justice

25.2 Claske Dijikema, Bern University of Applied Sciences: Of Chains and Doves, peace as an everyday experience for migrant women in Germany

25.3 Johanna Paschen, University of Bern: Transdisciplinary research in art and climate science collaborations: Investigating methodologies, procedures, practices, and underlying assumptions to reach epistemic justice in terms of knowledge co-creation between artists, climate scientists, society, and the more-than-human in the context of Switzerland

25.4 Nora Komposch, University of Bern: Reproductive and Climate Justice: Exploring the Nexus of Global Warming, Gendered Migration and Seasonal Agriculture

25.5 Rosa Philipp, University of Bern: “El Sur resiste, existe porque resiste!” – R-existencia at the Isthmus of Tehuantepec, Mexico

25.6 Surangika Jayarathne, University of Bern: “From Serendipity to Struggle”.

25.7 Yvonne Riaño, University of Neuchâtel: Resisting Closed Borders: Informal Cross-Border Mobilities of Colombian Migrants Deported from Venezuela to Colombia

25.1

Geographies of Reproductive Justice

Carolin Schurr

University of Bern

No Abstract...

25.2

Of Chains and Doves, peace as an everyday experience for migrant women in Germany

Peace is still predominantly thought within the context of nation-states. This approach does not integrate all those who physically extract themselves from (different forms of) violence. What does peace mean those persons, who are on the move and who stay shorter or longer periods of time in transit and destination countries? What does peace mean in a transnational context? An exploratory research project at the University of Basel posed this question to five women, coming from different countries (Nigeria, Cameroun and Afghanistan), and are at different stages in the asylum process, but have in common that they asked asylum in Germany. The methods used are photo elicitation and feminist Relief Maps. This research theoretically builds on Important contributions from feminist scholarship that challenge the idea of the nation-state as the dominant concept or context in which to think about peace. It helps to understand peace as an everyday experience, and a process in time and space, building on the temporal turn in geography.

25.3
Transdisciplinary research in art and climate science collaborations: Investigating methodologies, procedures, practices, and underlying assumptions to reach epistemic justice in terms of knowledge co-creation between artists, climate scientists, society, and the more-than-human in the context of Switzerland

Johanna Paschen[1,2]

[1] *Institute of Geography, University of Bern, Hallerstrasse 12, CH-3012 Bern (johanna.paschen@unibe.ch)*
[2] *Institute for Practices and Theories of the Arts, Bern Academy of the Arts, Fellerstrasse 11, CH-3027 Bern*

Transdisciplinary art and climate science research collaborations are not necessarily happening on eye-level, leading to marginalised knowledge. Establishing epistemic justice in knowledge co-creation between artists, climate scientists, societal actors, and the more-than-human is crucial since it strives to contribute to social justice in the context of Climate and EcoJustice. This study explores underlying assumptions in art and climate science collaborations and their root causes to further investigate emerging practices, methods, and processes that promote epistemic justice and are undoing assumptions and consequently implement them for improved outputs regarding Climate and EcoJustice. As a conceptual framework, the combination of the concepts and movements of Ecological Art, Transdisciplinarity, and Climate and EcoJustice will be applied. Using data acquired through participatory interviews, participant observation, focus group discussions, and the transdisciplinary methods of actor constellation and storywall, I will suggest emerging challenges, issues, and inspirations in transdisciplinary processes. In addition, I will discuss the priorities of some practices over others by adding reflections from which can be learned when creating future art and climate science transdisciplinary research projects. The research is significant as it addresses power dimensions present in collaborations and practices on a societal, political, and scientific level in the context of art, ecology, and the environment and marginalised knowledge.

REFERENCES

Jahn, T., Bergmann, M., & Keil, F. 2012: Transdisciplinarity: Between mainstreaming and marginalization. Ecological Economics, 79, 1–10. https://doi.org/10.1016/j.ecolecon.2012.04.017

Kagan, S. 2014: The practice of ecological art. 4. https://www.researchgate.net/publication/274719395_The_practice_of_ecological_art

Lehnerer, G. 2022: Ein ‚Sprung ins Trans‘: Widerständige Arbeitspraktiken zwischen den Wissenschaften und den Künsten. In G. Lehnerer, M. Fladerer, & R. Hiden (Eds.), *Welten im Wandel: Jenseits von Wissenschaft und Kunst* (1 ed., Vol. 1, pp. 1–31). [1] epodium Verlag.

Martusewicz, R. A., Edmundson, J., & Lupinacci, J. 2014: Ecojustice education: Toward diverse, democratic, and sustainable communities. Routledge.

25.4
Reproductive and Climate (In)Justice: Exploring the Nexus of Global Warming, Gendered Migration and Seasonal Agriculture

Nora Komposch[1]

[1] *Institute of Geography, University of Bern, Hallerstrasse 12, CH-3012 Bern (nora.komposch@unibe.ch)*

The SisterSong Women of Color Reproductive Justice Collective defines reproductive justice as not only the right to have or not have children but also the right to raise them in stable and sustainable communities. Various factors, such as environmental racism, climate change, or the lack of secure places for families, can infringe upon the right to raise children in safe and sustainable communities. As the social and environmental impacts of the climate crisis - including droughts, food shortages, forced migration - affect marginalized families disproportionately, the importance of considering climate (in)justice in conjunction with reproductive (in)justice increases. Within the realm of agricultural labor studies, the connection between environmental degradation and reproductive oppression has so far mainly been explored in terms of reproductive health risks resulting from pesticides or other environmental toxins. In this talk I present a case study of female Moroccan agricultural workers who annually migrate to work in the berry industry of Spain. The study shows how in the context of seasonal agriculture, reproductive oppression extends beyond the exposure to toxins in the berry fields. Drawing on multi-sited ethnographic research conducted in Spain and Morocco, I link drought-related unemployment – both in Spain and Morocco – with workers decision not to return home and their offspring's intentions to migrate over the Mediterranean Sea. The case study shows how the climate crisis, combined with harsh (circular labor) migration policies, leads to long-term separation of seasonal agricultural workers and their families, and compels their children to take dangerous migration routes. Recognizing these interrelations not only enhances our understanding of the everyday realities faced by migrant agricultural workers but is also crucial for tracing accountabilities for reproductive and climate injustice across multiple scales.

25.5
"El Sur resiste, existe porque resiste!"[1] – *R-existencia* at the Isthmus of Tehuantepec, Mexico

Rosa Philipp[1]

[1] *Institute of Geography, University of Bern, Hallerstrasse 12, CH-3012 Bern (rosa.philipp@unibe.ch)*

The paper analyses the resistance towards the Interoceanic Corridor mega-project in the South of Mexico, concentrating on the *r-existencia* by women* and the defence of their *cuerpo-territorio*. The mega-project's objective is to unite the Atlantic and Pacific Oceans through constructing at the Isthmus of Tehuantepec. By promoting regional development, the Interoceanic Corridor has engendered discontent and instigated protests among the indigenous and local communities. The resistance movement is an essential component of broader national and international initiatives aimed at safeguarding land and *territorio*, which are under threat from the proposed mega-projects. Using the decolonial concept of *r-existencia,* this study analyzes the idea of resistance and its connection to protests at the Isthmus of Tehuantepec. *R-existencia*, however, goes beyond mere resistance and describes the act of reproducing life and creating alternative ways of living on *territorio* (Gabbert and Lang, 2019). The paper explores resistance as *r-existencia*, whereby women* utilize practices of everyday life and protest against the mega-project. The observations, interviews, and participation with women* in resistance show how the mega-project jeopardize their lives and bodies. The aim is to achieve a more profound comprehension of the *cuerpo-territorio* of women* in the context of *r-existencia*.

Keywords: resistance, mega-projects, *r-existencia, cuerpo-territorio*

REFERENCES:
Gabbert, K.; Lang, M. 2019: A modo de introducción. In K. Gabbert; M. Lang (Eds.): **¿Cómo se sostiene la vida en América Latina? feminismos y re-existencias en tiempos de oscuridad**. Ediciones Abya Yala : Fundación Rosa Luxemburg, Quito.

1 Engl. The South resists, exists because it resists.

25.6

“From Serendipity to Struggle”
Decolonizing Intercountry Adoption through Postcolonial and Feminist Perspectives

Surangika Jayarathne, Ph.D. candidate, Social and Cultural Geography Unit,
University of Bern, Switzerland.
surangika.karandanalekamlage@unibe.ch

Abstract

This study critically examines the intercountry adoption practices between Sri Lanka and Switzerland from a postcolonial and feminist perspectives. Focusing on the experiences of the Sri Lankan adoptees live in Switzerland, it explores the complex power dynamics, socio-cultural implications, and gendered dimensions within the adoption process. By analysing the historical context of colonialism and its impact on Sri Lanka’s child adoption system, this research sheds light on the ways in which postcolonial legacies continue to shape the adoption landscape. Moreover, it focusses on the prevailing narratives and discourses surrounding intercountry adoption, questioning the portrayal of adoption as a “saving a child”, adoptive parents as “saviours” and first mothers as “victims”, while examining the agency and autonomy of these parties. Furthermore, this research critically assesses the social, cultural, and psychological implications experienced by adopted children. It explores the complexities of transnational identity formation and the challenges faced by these children in negotiating their dual cultural heritage. Through an interdisciplinary approach, this research aims to contribute to the existing literature on intercountry adoption, postcolonial studies, and feminist theory. By amplifying the voices and experiences of the Sri Lankan adoptees living in Switzerland, it seeks to challenge dominant narratives and promote a more nuanced understanding of the complexities surrounding intercountry adoption.

KEYWORDS: Intercountry Adoption, Postcolonialism, Feminism, Adoptees, First Mothers, Sri Lanka, Switzerland

25.7

Resisting Closed Borders: Informal Cross-Border Mobilities of Colombian Migrants Deported from Venezuela to Colombia

Yvonne Riaño
Institute of Geography
University of Neuchatel
yvonne.riano@unine.ch

Millions of migrants return to their places of origin every year, either voluntarily or forcibly. Addressing geopolitics in returnee contexts is important because territorial conflicts are becoming increasingly acute. In Latin America, tensions related to Venezuela's political regime — as well as its contiguity with Colombia's unresolved internal conflicts — currently present major geopolitical challenges. This raises the issue of how returnees exercise agency in different geopolitical contexts, how such contexts influence their re-integration projects, and what coping strategies they use. We still have insufficient knowledge on the subject, particularly in Latin America. I use a feminist geopolitics perspective to address these gaps. Rather than focusing on the state and supranational powers, I examine struggles over power, territory and security by Colombian migrants illegally and violently deported by Venezuela's government. They use their agency in everyday spaces to recast power politics, resist imposed spatial immobilities, and recreate international borders. This perspective is particularly suitable for studying border zones such as that between Colombia and Venezuela, where disputes over territorial control between guerrillas, paramilitaries and the Venezuelan army are severe. The 30 studied returnees have experienced repeated forced mobilities, ranging from internal displacement in Colombia, subsequent emigration to Venezuela, and deportation to Colombia, followed by the Venezuelan governments' closure of the international border. Returnees face intense difficulties in reintegrating despite their strong motivation, entrepreneurial spirit, and resistance strategies. The geopolitical context of armed struggle between illegal groups, an absent Colombian state, and territorial conflicts between Colombia and Venezuela create an unfavourable environment for them. However, they develop *transmobility* strategies to survive — including the informal movement of people, goods, and capital between Colombia and Venezuela — but at the risk of their own lives. Resistance strategies need to be critically examined as they not only encompass dangerous mobilities but also the violation of human rights.

26 Human Geographies: Cities, Regions, Economies

Ottavia Cima

Swiss Association for Geography (ASG)

TALKS:

26.1 Adrien Guisan, University of Bern: Housing as commons? A scoping review (1990-2023)

26.2 Deniz Ay, University of Bern: Is strong sustainability an impossible balancing act? Governance of urban densification and housing affordability

26.3 Ifigeneia Dimitrakou, University of Zurich: Gaming the system of regulation through temporary housing: real estate intermediaries' practices in Zurich's rental market

26.4 Johannes Herburger, University of Liechtenstein: In Densification we Trust

26.5 Lidija Honegger and Gabriela Debrunner, ETHZ: Urban transformation, flexible planning, and temporary use – A new symbiosis to effectively deal with scarcity of land and affordable housing? Experiences from Kloten, Switzerland

26.6 Luisa Gehriger, University of Zurich: Operationalizing the problem of political alienation for housing studies: Tenants experiencing mass cancellations of rental contracts in Basel

26.7 Mosé Cometta, Università della Svizzera Italiana: Protected areas as ecological commons?

26.8 Samuel Agyekum, University of Bern: Greening Cities: On the transformative role of the Commons

26.9 Sindy Baron-Blanco, Damien Marage, Université de Franche-Comté: Modelling holistic territory quality: a path to restructuring forest governance?

26.10 Tanja Herdt, IRAP, and Sybille Wälthy, ETHZ: Intensification of land use, the historical legacy of urban planning and its impact on housing in Zurich

26.11 Theurillat Thierry, HES-SO: The role of real estate in urban and regional development, towards territorial real estate and economic systems

26.1
Housing as commons? A scoping review (1990-2023)

Adrien O.T. Guisan[1]

[1] Geography Institute, University of Bern, Hallerstrasse 12, CH-3012 Bern (adrien.guisan@unibe.ch)

Initially restricted to the analysis of institutional arrangements regulating the use of common-pool resources (CPRs), the conceptual scope of the commons was considerably extended over the last decades. Translated to the housing field, the notion of commons is used to frame a wide range of phenomenon, from the management of collective amenities, co-housing and cooperative projects, to various forms of informal settlements and squatting movements. This heterogeneity results in a "fuzzy" concept with no clear boundaries, and ambiguity on its use as a conceptual tool or a normative ideal. Based on systematic retrieval and screening methods, this scoping review synthetizes the available literature (1990-2023) to clarify how the concept of commons is applied in housing research. In a first step, the various uses, definitions and applications of commons among the main corpus are analyzed and mapped using descriptive statistics, bibliometric analysis and narrative synthesis. In a second step, sub-corpuses are reviewed to synthetize the available evidence on the effects of commons arrangements on three salient housing characteristics identified within the corpus: (i) affordability, (ii) inclusivity, and (iii) sustainability. As the first of its kind, this review contributes to the conceptual development and clarification of the burgeoning commons' literature on housing.

26.2
Is strong sustainability an *impossible* balancing act? Governance of urban densification and housing affordability

Deniz Ay,

University of Bern

In the GoverDENSE project, we compare urban densification projects from Switzerland and the Netherlands to explore how and under what circumstances urban densification can contribute to (strong) sustainability (Næss et al. 2020). We are interested in understanding the social consequences that the residents and communities face as public planning authorities as well as private actors implement densification objectives through project-based planning. While densification or inner-city development has become a main planning objective for many cities around the world, it also presents a highly profitable business which potentially undermines the availability of affordable housing in attractive city centers (Cavicchia and Cucca 2021, Debrunner and Hartmann 2020). Planners, therefore, need to act proactively and strategically to reinforce housing policy objectives regarding affordability and quality. This often depends on implementation by private market-oriented actors such as large institutional landowners, (foreign) investors, and developers. At the same time, planning has become more entrepreneurial and growth-oriented (Gerber 2016). Flexible and project-based planning instruments increase the potential for collaboration between public and private actors, however, at the same time, these also undermine the implementation of public policy as everything becomes negotiable (Bouwmeester et al. 2023). In GoverDENSE, through quantitative analysis we have identified patterns for five types of densification taking place in the regions of Bern and Utrecht: Soft densification, large-scale transformations, small-scale individual interventions, high-rises in low-rise areas, and small apartments for senior residents (Götze and Jehling 2023). In this paper, we explore the sustainability challenges associated with these five types and ask: How much of the potential of densification is realized in actual implementations of densification in two case study regions of Bern and Utrecht? What are the obstacles to fulfilling densification that makes new living space available to meet diverse housing needs in terms of size, accessibility, and affordability (social mixing across income, age, migration background through bringing new people in without driving people out)? We discuss our main findings on five in-depth case studies by focusing on 1) investors' interests over social interests, 2) drivers of projects over plans, and 3) profit-driven over economically "unproductive" land uses that are essential to maintaining the societal capacity to reproduce itself while respecting the ecological concerns and limits.

REFERENCES

Bouwmeester, J., Gerber, J. D., Hartmann, T., & Ay, D. (2023). Non-compliance and non-enforcement: An unexpected outcome of flexible soft densification policy in the Netherlands. Land use policy, 126, 106525.

Cavicchia, R., & Cucca, R. (2021). Urban Densification and Its Social Sustainability. In The Palgrave Encyclopedia of Urban and Regional Futures (pp. 1-14). Cham: Springer International Publishing.

Gerber, J. D. (2016). The managerial turn and municipal land-use planning in Switzerland–evidence from practice. *Planning Theory & Practice*, *17*(2), 192-209.

Götze, V., & Jehling, M. (2023). Comparing types and patterns: A context-oriented approach to densification in Switzerland and the Netherlands. Environment and Planning B: Urban Analytics and City Science, 50(6), 1645-1659.

Næss, P., Saglie, I. L., & Richardson, T. (2020). Urban sustainability: is densification sufficient?. *European Planning Studies*, *28*(1), 146-165.

Verheij, J., Ay, D., Gerber, J. D., & Nahrath, S. (2023). Ensuring Public Access to Green Spaces in Urban Densification: The Role of Planning and Property Rights. Planning Theory & Practice, 1-24.

26.3
Gaming the system of regulation through temporary housing: real estate intermediaries' practices in Zurich's rental market.

Ifigeneia Dimitrakou[1]

[1] *Social & Cultural Geography, Department of Geography, University of Zürich, Winterthurerstrasse 190, CH-8057 Zurich (ifigeneia.dimitrakou@geo.uzh.ch)*

The paper contributes to emerging debates about the regulation of short-term rentals (STR) by delving into the socio-legal foundations of this housing market segment. Drawing on a qualitative study conducted between September 2022 and June 2023 focused on the governance for-profit temporary housing (i.e., serviced, furnished, interim housing) in Zurich, the analysis examines how professionalized real estate intermediaries that run the business of temporary housing interact with regulations and carve out niches in extremely tight conditions in the local rental market. The analysis shows that blind spots of regulation occur when intermediaries practice, translate, or substitute laws governing rent relations and transactions in these markets. In doing so, these actors promote tenure flexibilization to shape new pathways to rent extraction. The paper concludes that the gaming of the system of rental regulation lies centrally in the creation of these markets and constitutes a field of de-regulation and semi-formality that remains unseen. To put the corruption of rent relations into sharper focus, it is necessary to expand and move beyond debates about regulation and land use.

26.4
In Densification we Trust

Johannes Herburger[1]

[1] *Liechtenstein School of Architecture, Universität Liechtenstein, Fürst-Franz-Josef-Strasse, FL-9490 Vaduz (johannes.herburger@uni.li)*

Urban densification and urban containment have become central pillars of the planning policies of the western Austrian province of Vorarlberg. They have found their way into spatial planning legislation, municipal building and planning regulations as well as into business plans of private and social housing and property development companies. Besides containing urban sprawl and protecting the finite resource soil, urban densification is promoted to solve the provinces housing (price) crises.

Even though urban densification has become a hegemonic principle in planning, the housing production rate in Vorarlberg is lower than the Austrian average (Statistik Austria, 2023, p. 83). When it comes to the completion of social housing, Vorarlberg has the lowest rate of completed housing units per household in all of Austria (Österreichischer Verband gemeinnütziger Bauvereinigungen, 2022, pp. 7–8). At the same time, however, the population growth exceeds the Austrian average.

This contribution argues that the problem of urban densification in Vorarlberg has its roots in the distribution and parcellation of land in the province. Vorarlberg has the lowest proportion of unbuilt building plots over 2.000 m² plot size in Austria (Umweltbundesamt, 2016, p. 29). Furthermore, the century old practice of testamentary partition led to very fragmented ownership arrangements, thus complicating development processes.

Deriving from this structure of land tenure, I will illustrate the diverse practices of actors involved at the public-private nexus of urban densification implementation. These day-to-day politics of urban densification in Vorarlberg illuminate how land property, plot parcellations and density regulations are not merely objective and quantitative artifacts but form the geometric basis for social relations and interactions emerging around this specific form of abstract space.

REFERENCES

Österreichischer Verband gemeinnütziger Bauvereinigungen. 2022: Verbandsstatistik 2022: Die gemeinnützige Wohnungswirtschaft in Zahlen. Wien. https://gbv.at/Fakten_Analysen/

Statistik Austria 2023: Wohnen 2022: Zahlen, Daten und Indikatoren der Wohnstatistik. Wien. https://www.statistik.at/fileadmin/user_upload/Wohnen-2022_barrierefrei.pdf

Umweltbundesamt 2016: Gewidmetes, nicht bebautes Bauland: Erstellung von Auswertungen für Österreich. Technischer Bericht. Wien. https://www.oerok-atlas.at/documents/OEROK_Bauland_Mai_2016.pdf

26.5
Urban transformation, flexible planning, and temporary use – A new symbiosis to effectively deal with scarcity of land and affordable housing? Experiences from Kloten, Switzerland

Lidija Honegger[1], Dr. Gabriela Debrunner[2]

[1] *ETH RAUM, Netzwerk Stadt und Landschaft NSL, ETH Zürich, Stefano-Franscini-Platz 5, CH-8093 Zürich (lidija.honegger@ethz.ch)*
[2] *Institut für Raum- und Landschaftsentwicklung IRL, ETH Zürich, Stefano-Franscini-Platz 5, CH-8093 Zürich (gdebrunner@ethz.ch)*

For many years, residential temporary use – herein referring to an interim form of housing, deviating from their legally-binding permanent use, taking place in buildings or on land prior to demolition, reconstruction, or change of land use – has been utilised by municipal planners as an informal planning instrument to reactivate urban brownfields (Castells 1983; Bishop & Williams 2012). Temporary use has, however, recently changed its strategic function from being a catalyst for revitalization to testing new uses (Galdini, 2019), particularly in cities with high population growth, density dynamics, and housing shortages. Residential temporary use approaches (e.g., container or DIY-living, tiny houses) are increasingly applied by city councils and municipal planning authorities to transform industrial areas into mixed-use housing zones (Honeck 2017), providing a flexible planning solution to cope with affordable housing and land scarcity (Debrunner & Gerber 2021). In this paper, we investigate the following questions: *(1) How do municipal planning authorities apply temporary use as an approach to deal with scarcity of land and housing? (2) What actors are involved, and what strategies and objectives do they follow? (3) What challenges and recommendations result for sustainable land use and housing policy?* To answer these research questions, we follow a qualitative case study approach of the City of Kloten, Steinacker – a 50ha transformation area owned by approximately 35 landowners. This example stands representative for 122 industrial zones in Switzerland, aiming to be transformed into mixed-use housing. Results help us to reflect on effective land use planning approaches through the adaptation of flexible planning instruments, notably temporary use. We discuss the results in comparison with international case studies (e.g., London, Amsterdam, Helsinki), to elucidate prerequisites encompassing legal, planning, procedural, and other dimensions that must be satisfied to enable a sustainable transformation from an industrial area to a mixed-use zone.

REFERENCES

Bishop, P., & Williams, L. 2012: The Temporary City. London: Routledge.
Castells, M. 1983: The city and the grassroots. A cross-cultural theory of urban social movements. Berkeley: University of California Press.
Debrunner, G., & Gerber, J.-D. 2021: The commodification of temporary housing. *Cities*, *108*, 102998.
Galdini, R. 2019: Urban re-use practices in contemporary cities: Experiences in Europe. *Cities*, *87*, 103–105.
Honeck, T. 2017: From squatters to creatives. An innovation perspective on temporary use in planning. *Planning Theory & Practice*, *18(2)*, 268–287.

26.6
Operationalizing the problem of political alienation for housing studies
Tenants experiencing mass cancellations of rental contracts in Basel¨

Luisa Gehriger [1]

[1] *Social & Cultural Geography, Department of Geography, University of Zürich, Winterthurerstrasse 190, CH-8057 Zurich (luisa.gehriger@geo.uzh.ch)*

This paper adds to a revitalization of alienation as a political problem in the field of housing studies, pointing us to property relations that fragment tenants from acting together with other residents in similar positions. Analyzing ethnographic observations and interviews conducted in Basel with tenants facing mass cancellations of rental contracts, it operationalizes the problem of alienation to more closely examine the interplay of property relations and the subjective or collective experience of tenants: The consolidation of landlords' interests through complicit legal frameworks fragments tenants not only by producing insecurities within affected blocks. This consolidation also drives processes of individualization and conflict between fellow tenants and between tenants and their union, as well as harms tenants' belief in (local) political institutions. On the other hand, experiencing these fragmentations and the widespread inhibition of people to act together with others is, in some cases, the most sorrowful aspect for tenants facing rental contract cancellations in Basel. With the proposed understanding of alienation, the paper adds to two debates in housing studies: Outlining alienating property relations, it first foregrounds institutional constraints regarding the question of why many residents do not confront landlords' plans. Secondly, political alienation highlights the sorrow that can stem from the inhibition of collective action. Here the paper contributes to the debate around displacement and un-homing, showing them to be much more than the loss of original habitat.

26.7
Protected areas as ecological commons?

Mosè Cometta[1]

[1] *Institute of Urban and Landscape Studies, Università della Svizzera italiana (mose.cometta@usi.ch)*

In an attempt to combat the biodiversity crisis and climate change, several nations signed the Kunming-Montreal Global Biodiversity Framework in 2022. This document sets the creation of protected areas on 30 per cent of the earth's surface by 2030 as a key piece of a sustainability strategy. Protected areas thus become one of the main tools in the fight against climate change.

However, these institutions – modes of territorial governance – are controversial. While some praise them for their ability to reduce inequalities and offer economic development opportunities to marginalised communities (Fauchald & Gulbrandsen, 2012; Mcneely, 2020; Mose & Weixlbaumer, 2006; Vilela et al., 2022), others argue that they are a process of greenwashing/ not resolving the metabolic rift of our society and are actually initiating a large-scale commodification of nature (Apostolopoulou et al., 2021; Büscher & Arsel, 2012a, 2012b; Smith, 2007).

In this presentation we will quickly analyse two examples of failure in establishing two protected areas in Switzerland as a starting point for a broader theoretical reflection on the possibilities offered by this instrument in relation to the right to the city and the co-production of space. Can a protected area be conceived as a common and guarantee integration in the decision-making processes concerning it? What does the conflict between spatial justice and environmental justice, between economic development and nature conservation, between local and global interests imply for this type of governance? This paper will attempt to address these questions from a theoretical point of view by proposing a possible way forward.

26.8
Greening Cities: On the transformative role of the Commons

Samuel Agyekum

Institute of Geography, University of Bern, Hallerstrasse 12, CH-3012 Bern (samuel.agyekum@unibe.ch)

The growing scientific evidence of the collective environmental and social value of green spaces has made it one of the most sought-after climate adaptive interventions in the urbanising world. Despite the immense contribution to resolving burgeoning socio-environmental problems, the creation and maintenance of green spaces face fierce land use competition; in which capitalist (for-profit) urban development often prevails. New voices initiatives – conceptualised as the new/urban commons – that acknowledge humanity›s dependence on these resources are emerging to enact new forms of socio-political arrangements to 1) protect and 2) reclaim these resources (Colding et al., 2013; Follmann & Viehoff, 2015; Huron, 2015). While studies are proliferating in this direction, a clear understanding of how these initiatives emerge, organise, govern, and perpetuate in varying socio-political contexts is lacking. These research gaps stem partly from uneven geographical attention in the commons literature, namely an overwhelming number of case studies in industrialized economies in the global North. In response, this study seeks to empirically analyse different socio-political (planning) contexts (an advanced capitalist society – Switzerland – and Ghana with a mix of neoliberal policies and strong customary institutions): to know the extent to which public policies, property rights and customary institutions promote collective institutional arrangements in governing urban green commons. This will be approached through policy and qualitative content analysis methods. The research will, therefore, contribute, through the lens of urban commons, to increase knowledge regarding the promotion of urban greens in the dominant capitalist urban landscape.

REFERENCES

Colding, J., Barthel, S., Bendt, P., Snep, R., van der Knaap, W., & Ernstson, H. 2013: Urban green commons: insights on urban common property systems, Global Environmental Change, 23(5), 1039-1051.

Follman, A., & Viehoff, V. 2015: A green garden on red clay: Creating a new urban common as a form of political gardening in Cologne, Germany, Local Environment, 20(10), 1148-1174.

Huron, A. 2015: Working with Strangers in Saturated Space: Reclaiming and Maintenaning the Urban Commons, Antipode, 47(4), 963-979.Lanphere, M., & Pamic J. 1992: K-Ar and Rb-Sr ages of Alpine granite-metamorphic complexes in northern Croatia, Acta Geologica, 22, 5-22.

26.9
Modeling holistic territory quality: a path to restructuring forest governance?

Sindy Baron-Blanco[1], Damien Marage[2]

[1] PhD student, ThéMA, UMR 6049 CNRS, Université de Franche-Comté, Besançon, France. (sindy.baron_blanco@univ-fcomte.fr)
[2] Geography teacher, ThéMA, UMR 6049 CNRS, Université de Franche-Comté, Besançon, France (damien.marage@univ-fcomte.fr)

According to the FAO forecasts (FAO, 2022), the forestry ans wood-based industries will be key players in metting the increasing demand for renewables raw materials by 2050. Currently, the sector faces challenges of illegal logging and combating deforestation.
In response to these challenges, many governments have signed up numerous international commitments and implemented legally binding measures. A holistic territorial approach through the commons would enhance the sustainability of life as a whole.
In the framework of Elinor Ostrom's proposals, which consider forests as a common pool resource and their governance as part of *“Governing the commons”* (Ostrom, 1990), we explore the recomposition of forest governance by modelling the holistic quality of three forest territories in France, Romania and Colombia, based on the study of a rare forest resource such as that of lutherie wood.
A proposal for recomposing forest governance through the commons suggests reintroducing a shared sense of purpose in our representation and interactions with strategic forest resources. This “sense-making” is a prerequisite for collective resource management (Aubert & Botta, 2022, p. 57). To achieve this, it is necessary to examine both the connections between humans and other environmental elements, and also the interactions among humans through these elements. This approach, focused on the representation of relationships, leads us to shift from viewing the world as a set of objects to a world of subjects (Ibid.: 158). It prompts us to rethink our relationship with nature througt the commons, to question what kind of nature we want to live in (Descola, 2015), and our ways of being alive (Morizot, 2022).

REFERENCES

Aubert, S., & Botta, A. (2022). *Les communs. Un autre récit pour la coopération territoriale.* Éditions Quae. https://doi.org/10.35690/978-2-7592-3464-6
Descola, P. (2015). *Par-delà nature et culture*. Gallimard.
FAO. (2022). *Global forest sector outlook 2050 : Assessing future demand and sources of timber for a sustainable economy : Background paper for The State of the World's Forests 2022. Provisional*. FAO. https://doi.org/10.4060/cc2265en
Morizot, B. (2022). *Manières d'être vivant | Enquêtes sur la vie à travers nous* (1re éd.). Babel.
Ostrom, E. (1990). *Governing the commons : The evolution of institutions for collective action*. Cambridge University Press.

26.10
Intensification of land use, the historical legacy of urban planning and its impact on housing in Zurich

Tanja Herdt together with Dr. Sibylle Wälthy,

ETH Wohnforum, DARCH, ETHZ.

With the revised Swiss Federal Spatial Planning Act (SPA) coming into effect in 2014, inward settlement development became the main objective of urban design and planning. As the country copes with the rapid growth of residents and jobs, the revised SPA requires additional planning strategies, regulations, and implementation tools from the federal to the municipal level. These must consider the positive and negative effects of the intensification of land use processes for the housing situation of tenants and their impact on the quality of life e.g., increase in housing prices per m2 and shortage of public green spaces in redevelopment areas. Both are indicators for potentially growing spatial and environmental injustice. These trends open a discussion not only on the future ecological consequences of urban densification but on the economic and social vision of urban design and planning and the necessary policies to accomplish them.
Since urban design and planning policies in Switzerland go back to the ideas of Modern Architecture of the 1930s, reflecting on the needs of spatial organisation and supply of housing at that time, the change of strategy in urban design requires a rethinking of established planning instruments and policies. Based on the communal zoning plan of Zurich and analysing different areas of urban densification from the modernist past and present, the study tries to make visible the potential blind-spots of urban densification strategies and their effects on housing. We find that existing zoning laws as well as the common practice of small-scale areal development through master planning prevent an assessment of the often complex and sometimes contradicting interrelationships between the diverging goals of sustainable development (Campell, 1996), i.e., the green, the growing, and the just city.

REFERENCES

Campell S. (1996). ”Green Cities, Growing Cities, Just Cities? Urban Planning and the Contradictions of Sustainable Development”. American Planning Association. Journal of the American Planning Association; Summer 1996; 62, 3; ProQuest Central, p. 296 – 299.

26.11
The role of real estate in urban and regional development, towards territorial real estate and economic systems: evidence from the Swiss case

Thierry Theurillat[1], Olivier Crevoisier[2], Anaïs Merckhoffer[2], Mathias Rota[1], Alain Segessemann[1]

[1] *University of Applied Sciences and Arts Western Switzerland, HES-SO*
[2] *University of Neuchâtel*

Urban and regional development theories have long considered real estate as a local by-product of export activities. However, the real estate sector has been booming for the past twenty years and has generated very large amounts of money at the global and national levels. This globalization of real estate and connection to financial markets, particularly analyzed in the literature through the prism of the financialization of real estate, does not always allow us to understand the role and dynamics of real estate in the territorial economy.
Taking the case of Switzerland and questioning the perspective of a purely induced real estate sector and using these two fields of literature (regional development and the financialization of real estate), we assume that the role of real estate, its development and its implication in regional development are very variegated according to territories. We argue that this variegation is structured by economic specialization, their sociological structure, and the history of building and residential structures. We thus address the following research issue: *how and to what extent has real estate played a driving role in Swiss urban and regional development since the 2000s?*
To answer this question, we use a methodology combining cluster analysis (PCA and DHC) as well as qualitative knowledge based on previous research. We build a typology identifying 8 main clusters. We describe in each of them the more or less driving role of real estate. To catch these phenomena, we propose the concept of territorial real estate and economic systems (TREES).